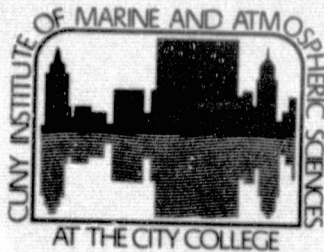


General Disclaimer

One or more of the Following Statements may affect this Document

- This document has been reproduced from the best copy furnished by the organizational source. It is being released in the interest of making available as much information as possible.
- This document may contain data, which exceeds the sheet parameters. It was furnished in this condition by the organizational source and is the best copy available.
- This document may contain tone-on-tone or color graphs, charts and/or pictures, which have been reproduced in black and white.
- This document is paginated as submitted by the original source.
- Portions of this document are not fully legible due to the historical nature of some of the material. However, it is the best reproduction available from the original submission.



THE UNIVERSITY OF KANSAS
SPACE TECHNOLOGY CENTER

REMOTE SENSING LABORATORY

NASA CR-

147487

E7.6-10187.

"Data available under NASA sponsorship
is the interest of early and wide dis-
semination of Earth Resources Survey
Program information and without liability
for any use made thereof."



THE MEASUREMENT OF THE WINDS NEAR THE OCEAN SURFACE
WITH A RADIOMETER-SCATTEROMETER ON SKYLAB

by

Vincent J. Cardone, James D. Young, Willard J. Pierson,
Richard K. Moore, J. Arthur Greenwood, Catherine Greenwood,
Adrian K. Fung, Robert Salfi, H.L. Chan, Mustafa Afarani,
and Mark Komen

FINAL REPORT ON EPN 550

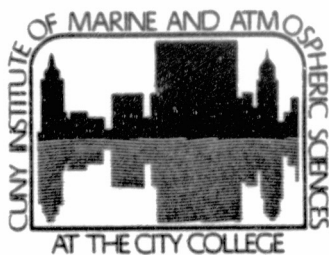
CONTRACT NO. NAS-9-13642

P.I. Willard J. Pierson

N76-18608

(E76-10187) THE MEASUREMENT OF THE WINDS
NEAR THE OCEAN SURFACE WITH A
RADIOMETER-SCATTEROMETER ON SKYLAB Final
Report, Jan. 1973 - Dec. 1975 (Kansas Univ.)
462 p HC \$12.00 /6.25
CSCL 04B G3/43
Unclas 00187

652



FINAL REPORT ON EPN 550

CONTRACT NO. NAS-9-13642

THE MEASUREMENT OF THE WINDS NEAR THE OCEAN SURFACE
WITH A RADIOMETER-SCATTEROMETER ON SKYLAB

by

Vincent J. Cardone, James D. Young, Willard J. Pierson,
Richard K. Moore, J. Arthur Greenwood, Catherine Greenwood,
Adrian K. Fung, Robert Salfi, H. L. Chan, Mustafa Afarani,
and Mark Komen.

Original photography may be purchased from:
EROS Data Center
10th and Dakota Avenue
Sioux Falls, SD 57193

Prepared jointly by: CUNY Institute of Marine and Atmospheric
Sciences at The City College and The
University of Kansas Remote Sensing
Laboratory

ORGANIZATIONS: CUNY Institute of Marine and Atmospheric Sciences
at The City College, Wave Hill 675 West 252 Street
Bronx, N.Y. 10471 (212) 796-8300 and
The University of Kansas Remote Sensing Laboratory
Raymond Nichols Hall, 2291 Irving Hill Drive,
Campus West, Lawrence Kansas 66045 (913) 864-9836

TITLE OF INVESTIGATION: A JOINT METEOROLOGICAL, OCEANOGRAPHIC AND SENSOR
EVALUATION PROGRAM FOR EXPERIMENT S193 ON SKYLAB.

TITLE OF REPORT: THE MEASUREMENT OF THE WINDS NEAR THE OCEAN SURFACE
WITH A RADIOMETER-SCATTEROMETER ON SKYLAB

PERIOD COVERED: January 1973 to December 1975

EREP INVESTIGATION: EPN 550

NASA CONTRACT: NAS 9-13642

PRINCIPAL INVESTIGATOR: Willard J. Pierson

CO-PRINCIPAL INVESTIGATOR: Richard K. Moore

CO-PRINCIPAL INVESTIGATOR: E. Paul McClain

DATE COMPLETED: January 21, 1976

MONITOR AND ADDRESS: Mr. Zack H. Byrns/TF6
PRINCIPAL INVESTIGATOR OFFICE
NASA LYNDON B. JOHNSON SPACE CENTER
HOUSTON, TEXAS 77058

TYPE OF REPORT: FINAL REPORT

ABSTRACT

The measurements over the ocean made by S193, a combination scanning pencil beam radar scatterometer and passive microwave receiver, in the noncontiguous modes during SKYLAB 2, 3, and 4 are analysed to show that the passive microwave measurements can be used to correct the radar measurements for attenuation and to eliminate areas of large cloud drops and rain and that the radar backscatter measurements can be used to compute the wind speed near the sea surface. The wind speeds so determined are at least as accurate as those that would have been reported by a weather ship located at each useable cell scanned by the instrument.

The total error variance,

i.e. $\sum_{i=1}^n \frac{1}{n} (U_{mi} - U_{ri})^2$, is stratified according to the methods used to obtain the surface truth, that is, the meteorologically determined wind speeds and directions at each cell. This total error variance is compared to estimates of the error variances from the meteorological analyses, which were independently obtained, and from intercomparisons of the radar determined winds. The above conclusion is a conservative interpretation of these results. The standard deviations of the errors in the radar measured winds may well be less than half that of the weather ships as shown solely by the SKYLAB data.

Chapter 1 outlines the chapters in this report, which describe how the experiment was planned and carried out, and how the data were analysed. It also gives some of the major conclusions. Chapter nine describes the application of the results of this final report to the measurements to be made by SEASAT-A.

Four appendices accompany this final report. Appendix A tabulates all of the useable data from the experiment and merges it with the meteorological and oceanographic surface truth. Appendix B gives the data for the analysis of surface truth errors. Appendix C is a report by A.K. Fung and H.L. Chan on the present status of radar backscatter theory. Appendix D by J.D. Young describes the methods he used to correct the backscatter data for various effects and gives his results on various methods for analysing the data.

ACKNOWLEDGEMENTS

Recently, one of us gave a paper on our results. When the long list of authors of the paper was read by the chairman of the session, the audience laughed. This program required the talents of many others as well as those listed as authors of this final report. Also much help was given by people not directly connected to the program.

At the CUNY Institute of Marine and Atmospheric Sciences, John Hayes and Walter Spring were most helpful in managing the data flow and carrying out the preliminary surface truth analyses. Emanuel Mehr began the development of some of the computer programs required in this study at the start of the theoretical phase of this study. At the Remote Sensing Laboratory, Arun Sobti and John Claassen respectively made fundamental inputs to data reduction problems and to the interpretation of the passive microwave data.

In oceanography, those who obtained the data are considered to have made as important a contribution as those who analysed it. The nine astronauts who manned SKYLAB, repaired the spacecraft and the instrument, and got the data should be listed as co-authors of this report.

The support given us by our co-principal investigator, E. Paul McClain and his associates of NOAA/NESS is very much appreciated. The data that they provided is described in Chapter 2.

The New York Regional Office of the National Weather Service of NOAA supported the data taking phase of this program. Our thanks are extended to Harold Gibson, the meteorologist in charge, and his helpful and cooperative staff. The Satellite Field Service also provided useful information.

Duncan Ross of the Atlantic Oceanographic and Meteorological Laboratory, NOAA, provided advance data on his SKYLAB aircraft underflight program so that, in particular, the NOAA C130 flight into AVA could be used in the analysis. Peter Black of the National Hurricane Center, NOAA, searched the archives and found the original records of some of the aircraft flights into Tropical Storm Christine.

Major James Sartor of the Sixth Weather Wing, Andrews AFB, provided the liason required to obtain the DAPP data.

Capt. E. A. Delaney and Cdr. Cromwell of the U.S. Coast Guard would have coordinated efforts to obtain surface truth with Weather Ship Hotel during a SKYLAB pass, but the opportunity never arose.

At the United States Naval Oceanographic Office, Jack J. Schule made possible the calculation of the wave spectral hindcasts, prepared as a back up for the interpretation of wave slope effects. Sheldon Lazanoff, the NAVOCEANO representative at the Fleet Numerical Weather Central, made the arrangements to provide the data files of sea surface analyses and reports from ships that provided the surface truth for this program.

The international effort to obtain special weather ship observations during SKYLAB passes was aided by John A. Ewing of the Institute of Oceanographic Sciences in Great Britain, and by J. R. H. Noble, Paul Johns, and Read Allen of Canada, J. Romer of France, M. W. F. Schregardus of the Netherlands, and Capt. G. A. White of England.

The continued interest in this program and the encouragement of Dallas Evans are very much appreciated.

These acknowledgements perforce omit the names of the many NASA scientists who supported this program both scientifically and administratively. Their help was nevertheless essential to the success of this program.

TABLE OF CONTENTS

	<u>Page</u>
ABSTRACT.....	1
ACKNOWLEDGEMENTS.....	iii
CHAPTER 1 OBJECTIVES, SUMMARY OF RESULTS AND MAJOR CONCLUSIONS.	1
OBJECTIVES.....	1
RESULTS.....	3
CONCLUSIONS.....	6
CHAPTER 2 THE EXPERIMENTAL DESIGN AND THE DATA TAKING PHASE....	8
THE INSTRUMENT.....	8
Description of S193.....	8
S193 as an Anemometer.....	11
SURFACE TRUTH STRATEGY.....	15
Plans.....	15
The AVA Pass.....	16
The Routine for a Particular S193 Pass.....	18
SUMMARY OF DATA USED AS SURFACE TRUTH.....	20
NASA.....	20
NOAA.....	21
DOD.....	21
UCAR.....	22
International Support.....	22
ERRORS IN THE MEASUREMENT OF THE WIND.....	24
CHAPTER 3 THE S193 RADSCAT MEASUREMENTS IN NONCONTIGUOUS MODES OVER THE OCEAN.....	29
INTRODUCTION.....	29
SKYLAB 2.....	29
SKYLAB 3.....	32
SKYLAB 4.....	32

PROBLEMS IN DATA REDUCTION.....	33
GENERAL DESCRIPTION OF THE PASSES.....	34
CHAPTER 4 THE ANALYSIS OF THE METEOROLOGICAL AND OCEANOGRAPHIC SURFACE TRUTH.....	38
Introduction.....	38
The Three Types of Meteorological Analysis that were used.....	39
ANALYSIS OF THE SURFACE WIND FIELD IN TROPICAL CYCLONES AVA AND CHRISTINE.....	43
A Tropical Cyclone Boundary Layer Model.....	43
Hurricane AVA.....	49
Tropical Storm Christine.....	64
SPECIFICATION OF THE WIND FIELD BY MANUSCRIPT SYNOPTIC ANALYSIS.....	77
Introduction.....	77
June 5.....	79
June 11.....	84
September 4.....	86
NORTHERN HEMISPHERE OBJECTIVE WIND FIELD ANALYSIS.....	91
The Objective Analysis Program.....	91
Planetary Boundary Layer Model.....	97
Comparison of Objective Winds and Special Aircraft and Weather Ship Measurements.....	102
ERRORS IN THE SPECIFICATION OF THE VECTOR WIND.....	109
A STUDY OF THE ACCURACY OF THE METEOROLOGICAL WINDS.....	114
A Further Analysis with Different Assumptions.....	123
Additional Considerations of Synoptic Wind Field Analyses.....	133
Documentation of Theory Used in the Error Analysis....	134
CHAPTER 5 THE MERGING OF THE METEOROLOGICAL, OCEANOGRAPHIC AND S193 DATA.....	139

RECAPITULATION.....	139
APPENDIX A.....	139
THE PURPOSE OF THE TABULATIONS.....	141
CHAPTER 6 BACKSCATTER THEORY, WAVE SPECTRA, BACKSCATTER MEASUREMENTS, AND WAVE MEASUREMENTS.....	142
Introduction.....	142
A First Attempt.....	143
A Model with Wind Speed Dependence.....	150
Fan Beam Doppler at K_u -Band.....	152
A Study of the Wave Spectrum.....	153
More on Equation (6.5).....	161
More Measurements of Backscatter and Capillary Waves..	164
The AAFE Program.....	173
Results of Fung and Chan.....	179
The Effects of the larger Gravity Waves on Backscatter.....	187
CHAPTER 7 PASSIVE MICROWAVE THEORY AND THE CALCULATION OF ATTENUATION AND DETECTION OF HEAVY RAIN WITH THE PASSIVE MICROWAVE DATA.....	191
PASSIVE MICROWAVE THEORY AND APPLICATIONS.....	191
THE USE OF PASSIVE MICROWAVE DATA FROM S193.....	192
Purpose and Theory.....	192
Theoretical Development.....	194
Attenuation results for SKYLAB 2 and 3.....	201
Elimination of Areas of Heavy Rain.....	205
CHAPTER 8 THE MEASUREMENT OF WINDS BY MEANS OF A RADAR ON A SPACECRAFT.....	210
INTRODUCTION.....	210
CORRECTIONS TO NOMINAL NADIR (OR INCIDENT) ANGLES FOR ALL OF THE DATA.....	212

GENERAL DISCUSSION OF CURVE FITTING AND REGRESSION TECHNIQUES.....	216
Principles.....	216
Comments on the scatter of plots of backscatter versus wind speed.....	220
Strategies for avoiding various problems.....	229
RESULTS ON LOG-LOG AND POWER LAW REGRESSIONS.....	229
Introduction.....	229
Referring the backscatter measurements to upwind.....	232
Tabulation of regression constants and examples of results.....	234
PREDICTIONS OF WIND SPEED GIVEN WIND DIRECTION AND BACKSCATTER VALUE.....	258
Introduction.....	258
Methods 5 and 6.....	259
Method 4.....	263
The Regression Constants for Methods 4, 5 and 6.....	266
Tabulation of the Predicted Radar Winds for each Observation and for each Method.....	268
Scatter Plots.....	268
Stratified root mean square difference analysis for Methods 4, 5 and 6.....	303
ERROR ANALYSIS OF THE DIFFERENCE BETWEEN THE METEOROLOGICAL WIND AND THE RADAR WIND.....	311
Introduction.....	311
Analysis.....	311
ERROR ANALYSIS OF THE RADAR WIND MAGNITUDES.....	317
Introduction.....	317
Analysis.....	317
COMPOSITE ERROR ANALYSIS.....	320

Ava and Christine.....	328
The Manuscript Synoptic Analyses.....	330
The Scatter Plots.....	330
SURVIVORS.....	331
CLOSING THE CIRCLE.....	331
Recapitulation.....	331
Simulated circle flights.....	331
CHAPTER 9 APPLICATIONS TO SEASAT-A.....	340
REVIEW.....	340
APPLICATIONS OF THE ERROR ANALYSIS.....	342
APPLICATIONS OF THE PLANETARY BOUNDARY LAYER MODEL.....	344
APPLICATIONS TO TROPICAL CYCLONES.....	346
REFERENCES.....	347

APPENDICES

APPENDIX A The merged SKYLAB Measurements and Meteorological and Oceanographic Surface Truth from SKYLAB 2, 3 and 4.

APPENDIX B The Data from the Withheld Weather Ship Analysis.

APPENDIX C Fung A. K. and H. L. Chan, 1975: A Theory of Sea Scatter at Large Incident Angles. The University of Kansas Space Technology Center, Remote Sensing Laboratory, RSL Technical Report 254-4, October.

APPENDIX D Young, J. D., 1975: Active Microwave Measurement of Sea Surface Winds from Space. The University of Kansas Space Technology Center, Remote Sensing Laboratory, RSL Technical Report 254-5.

(C and D furnished separately)

CHAPTER 1 OBJECTIVES, SUMMARY OF RESULTS AND MAJOR CONCLUSIONS

OBJECTIVES

"The principle objective of the use of the radar radiometer mode of S193 on Skylab [was] to prove conclusively that simultaneously measured values of the radar scattering cross section matrix and microwave temperature for two polarizations at 13.9 Ghz [would] provide data from which the winds in the planetary boundary layer over the ocean can be inferred. This principal objective of S193 [was] accomplished by operating the instrument over the oceans in appropriate scanning modes so as to measure the six quantities, σ_{HH}^0 , σ_{HV}^0 , σ_{VH}^0 , σ_{VV}^0 , T_{bVV} , and T_{bHH} , which are functions of $|\vec{V}|$, X , θ , sea surface temperature, wave conditions, the amount of foam on the sea surface, the intervening liquid water in the atmosphere, and other minor effects, for as wide a range as possible of these parameters."

The above paragraph, with the words in square brackets changed, is the opening paragraph, prepared in April 1971, describing the proposed procedures for the study of S193 data in the radar radiometer (radscat) mode. Details on the kinds of Z local vertical passes and on the techniques for processing the data followed. For example, the proposed program suggested that, "During the second manned period, there is the opportunity to obtain data from a tropical hurricane."-- "Also typical of a hurricane is a spiral pattern of thick clouds and rain."--"The gaps are just large enough for the beam to scan to the wind driven surface."

In 1971, the strong dependence of backscatter on wind direction relative to the pointing direction of the radar beam was not well recognized. Also the theories relating backscatter to sea surface properties were not well developed. As the program of measurements

with Skylab, S193, was accomplished, these theories were also refined so as to cover anisotropic effects and account for the variation of backscatter with wind direction at the same nadir angle and wind speed.

From the point of view of the analysis of the S193 data, the problem becomes one of inferring the properties of a vector from essentially one measurement. Various techniques were developed to solve this problem and to obtain results related primarily to the magnitude of the vector wind and to errors in the determination of the magnitude of the vector wind.

The original proposal for the study of S193 data did not say much about demonstrating the accuracy of the determination of the wind from the backscatter measurement. It only described how both special and conventional data on winds would be obtained and how the backscatter measurements would be compared with these winds. It was, of course, expected that good agreement would be found.

In support of instruments on SEASAT-A, which are four fan beam Doppler radars and a five frequency scanning passive microwave radiometer, quantitative results are required as to the accuracy of the radar determinations of the wind. These quantitative results will be presented in the chapters that follow.

In addition to the primary objective of this program, there were many other objectives that had to be attained in order to accomplish the primary objective. One was to demonstrate applicability of the measurement system to different kinds of weather systems such as tropical circulations, tropical storms and hurricanes (or typhoons etc.) and extra tropical cyclones and wind patterns. A second was to use the passive data to calculate attenuation so as to correct the backscatter measurements for attenuation. A third was to detect areas of heavy rain where backscatter measurements could not be used to

determine the wind. A fourth was to understand the effects of the spectrum of wind generated waves and swell, over all wave numbers, on backscatter. These objectives were attained as will be described in this final report.

RESULTS

During Skylab 2/3, there were 1563 measurements of σ_{VV}^0 , σ_{VH}^0 , σ_{HV}^0 , and σ_{HH}^0 for the three largest nadir angles at somewhere near 350 different cells. There were usually four measurements, one at each polarization combination, at each cell, but at times, some values could not be used. At each cell, there would be two measurements of the passive microwave temperatures, one for each polarization, for about 700 values. There were 1113 backscatter measurements at the two smallest nadir angles and about 556 passive microwave measurements. The sum of all measurements of backscatter and passive microwave temperatures during SL 2/3 was about 4000 values.

During SL 4, the passive microwave temperatures could not be used. There were a total of 1927 measurements of backscatter at the three highest nadir angles all in the cross-track noncontiguous mode representing about 482 separate cells on the sea surface scanned by the instrument. The total number of useful cells scanned by S193 was about 830 for SL 2/3 and SL 4 combined.

There were a total of twenty six passes in the ZLV mode that yielded useful data. Six were in the in-track noncontiguous mode. All others were in the cross-track noncontiguous mode. Nine passes were in tropical, or subtropical, areas. One pass scanned portions of a tropical hurricane. Another scanned a tropical storm. The remaining thirteen scanned northern hemisphere extratropical wind patterns.

The wind speed and direction as effectively determined in a neutral atmosphere at 19.5 meters above the sea surface was found for each cell scanned by S193 by one of three different meteorological

techniques. One technique was a streamline isotach analysis of the available data in the area of the scan, which was used in tropical and subtropical areas. The second technique was a theoretical numerical tropical cyclone model, which applied to the friction layer in the air over the sea surface. The last was a planetary boundary layer model for the northern hemisphere oceans. In each case the wind field over the entire area was found, and then the winds were interpolated to the cells that were scanned by Skylab.

Chapters 2 and 3 describe how the experiment was carried out and provide tables of the passes that were obtained.

Chapter 4 provides a description of how the meteorological and oceanographic "surface truth" was obtained and evaluates the accuracy of these determinations of the wind speed and direction. Meteorologists will not be particularly surprised by these results, but others may be. They need to be interpreted with great care. The data on which the analyses of the accuracy of the wind determinations is based are given in Appendix B.

Chapter 5 describes how the S193 data and the meteorological and oceanographic data were merged to provide the data base for the study of the variation of radar backscatter with wind speed and direction.

Appendix A of this report contains a listing of every pass that was found useful. The backscatter measurements and passive microwave temperatures that were measured, the wind speed and direction at each cell, as determined from meteorological data, the sea surface temperature, the location of each cell and the time of the measurement are tabulated.

The wind speeds at the cells scanned by S193 during SL 2/3 ranged from 2 or 3 knots to 51 knots as determined by the meteorological analyses. During SL 4, they ranged from 2 or 3 knots to 48 knots.

The higher winds during SL 2/3 tended to have a higher frequency of cross wind relative to the radar beam (aspect angle). The SL 4 data were somewhat more evenly distributed over aspect angle.

Chapter 6 reviews radar backscatter theory and brings the subject up-to-date with a theory that explains nearly all of the observed features of radar backscatter including differences between upwind and downwind and crosswind and the effects of the slopes of the larger waves. The details of this theory are given in Appendix C.

Chapter 7 shows how the passive microwave measurements were used both to compute the attenuation of the radar beam and to determine those cells where the backscatter measurement was suspect. There were only five cells in the entire analysis (all in tropical cyclones) that could not be used because of the presence of rain. The attenuations that were calculated were small for SL 2/3. These low values explain why it was possible to obtain useful results with the SL 4 data.

Chapter 8 describes how the radar data were corrected for the small variations in nadir angle so as to be able to use all measurements at a given nominal nadir angle. Six different regression schemes are described, five of which are actually applied to the data. Results are given in tabular and graphical form for five of the methods, and two of them are described in greater detail by Young (1975) in Appendix D. Additional methods may be contained in Appendix D that are not described.

The mean square errors representing the sums of the differences between the meteorological wind and the radar wind divided by the sample size are decomposed into the contributions from the errors in the meteorological data and the radar errors. The meteorological error contributions far exceed the radar error contributions. There is a strong relationship between the quality of the data used to obtain

the meteorological winds and the root mean square differences between the wind determined from meteorological data and the wind predicted from the backscatter data.

CONCLUSIONS

Given the direction of the wind from some independent source, with the typical accuracy of measurement by presently available meteorological methods, a backscatter measurement at a nadir angle of 50° , 43° or 32° can be used to compute the speed of the wind averaged over the illuminated area. This wind speed is at least as accurate as the wind speed that would have been obtained from weather ship data near that point in space and time. The error analysis strongly suggests that wind speeds from the radar measurements may actually have errors with standard deviations less than half that from nearby weather ships for winds greater than about 7 knots.

The measurements to be made by SEASAT-A will obtain not only the wind speed but also the wind direction with an accuracy equal to or better than a weather ship.

To calibrate SEASAT-A, it will be necessary to develop techniques that will reduce the error variances of conventional measurement and analysis procedures by at least a factor of 25 so that the standard deviations will be reduced by a factor of 5.

There are no marked differences between VV, HH and VH. Since VV is stronger, it is probably the best single backscatter value to measure. Cross polarized returns are to be preferred over HH because there will be no backscatter from large cloud drops and attenuation effects can be accounted for.

The effects of attenuation are very small and can be omitted without degrading the winds too much. This had to be done for SL 4, and the analysis was still successful.

The errors in the initial value specification of the winds in the planetary boundary layer over the oceans that presently exist for numerical weather prediction are large and differ substantially from one area of the ocean to another, depending on the density of ship reports. SEASAT-A will yield uniformly spaced vector winds of far greater accuracy and with a uniform error distribution. Since the data density will be from one to two orders of magnitude greater, further smoothing will define the planetary boundary layer to an even greater accuracy.

The winds in the tropical areas of the world ocean will be measured routinely by SEASAT-A with great accuracy. These areas are presently inadequately observed.

The winds in hurricanes and tropical storms can be measured to an accuracy comparable to that presently obtained from aircraft reconnaissance flights. The central pressure, radius of maximum wind, and area of gale force winds in a hurricane can probably be determined by inverting the procedures given in Chapter 4 that was used to specify the winds in Hurricane AVA and Tropical Storm Christine. A global capability for monitoring the winds in hurricanes and tropical storms can be developed with SEASAT-A.

CHAPTER 2 THE EXPERIMENTAL DESIGN AND THE DATA TAKING PHASE

THE INSTRUMENT

Description of S193. The radar radiometer part of S193, called Radscat for short, was a scanning pencil beam combination radar and passive microwave receiver.* It operated in a number of modes. The two modes used the most for this program were called the in-track non-contiguous mode and the cross-track non-contiguous mode. In these modes, the antenna was pointed at nominal angles corresponding to nadir angles of 50° , 40° , 30° , 15° , and 0° , and, in each of these positions, a pulse was transmitted by the radar. The duration of the pulse was such that the leading edge of the pulse could travel all the way to the sea surface and return almost to the antenna before the pulse was turned off. Then the receiver for the radar would be activated, and the entire backscattered signal for this transmitted pulse time would be received, passed through an appropriate Doppler filter, which depended upon the mode of operation, that is, whether it was in-track or cross-track, detected, and averaged. The result was a very stable measurement of the received power, which could be compared with the transmitted power measured with a small auxiliary bleeder circuit within the system, so as to calculate the radar backscattering cross section. Because of the long averaging time, it was calculated that the radar backscatter was measured to a sampling variability of ± 0.3 db. This sampling variability was caused by the Rayleigh fading of the return signal and was reduced to this very low value by the long averaging time. For each position of the antenna at these five different nadir angles, six measurements were made. They were σ_{HH}^0 , σ_{VH}^0 , and σ_{HV}^0 for the radar part of the instrument. Also the horizontally polarized and vertically polarized passive microwave

*For many more details see Moore, Ulaby, Sobti et. al. (1975).

temperatures were measured by converting the instrument to a radiometer after the four radar measurements. This was accomplished by increasing the bandwidth of the IF receiver system so as to be able to detect the very weak naturally radiated signals at these same frequencies.

In the in-track non-contiguous mode, as the antenna cycled through these five different angles, the sequences were so chosen that all the measurements would be obtained at the same spot on the sea surface. Sets of cells, with varying diameters, but all very close together, were measured such that a total of 30 measurements were obtained from nearly the same area of the ocean.

In the cross-track non-contiguous mode, the antenna would be pointed out to the side so that the nadir angle would be near 50° , the six measurements would be made, the antenna would drop to the next lowest angle, and six more measurements would be made, and so on, until vertical measurements were obtained. Depending upon which of the three cross-track non-contiguous modes was chosen, the antenna could return to the same side, either left or right, and repeat this sequence, or it could swing out to the other side and come back in to nadir. The result would be a checkerboard pattern of points with measurements at the intersections of corners of the checkerboard roughly on a square pattern with a very wide swath.

It was recognized in the design of the experiments with this instrument that these cross-track modes were very powerful for surveying the wind fields at the surface of the ocean of the dimensions of tropical cyclones, tropical storms, and even substantial portions of extra-tropical cyclones. The spacing of the points in the non-contiguous modes was much closer together than is achieved in typical synoptic analyzes of the wind field over the ocean, and the much larger density

of measurements, compared to that possible with conventional meteorological data sources, namely ships at sea, a very few aircraft measurements, and data buoy measurements, would be the data base for the program. The value of the instrument as an operational system is, of course, for the synoptic scale analysis of the wind fields over the ocean.

The experiment was designed in an attempt to obtain the widest possible range of wind speeds and wind directions relative to the pointing vector of the radar beam and the widest possible range of cloud thicknesses and drop size distributions within the clouds for nadir angles of 30° , 40° , and 50° . As a part of the theory of the combined use of passive and active systems in the same instrument, it had been demonstrated that the passive systems would respond very quickly to the thick wet clouds with large cloud drops that would be capable of affecting the radar return signal in the radar mode. The plan was to calibrate out the effect of these clouds on the radar signal by means of the data obtained with the passive system so as to obtain a better measure of the radar backscattering cross-section when there were clouds between the spacecraft and the cell at the sea surface being scanned.

As the experiment evolved, that is after SKYLAB was actually launched and after its repair during SKYLAB 2, it became apparent that the in-track non-contiguous mode had much less chance of recording backscatter for high winds. Also the in-track non-contiguous mode was lost at the conclusion of SKYLAB 3 (the second manned period). The scanning mechanism for the antenna was repaired at the beginning of SKYLAB 4 in such a way that only the cross-track non-contiguous mode could be used.

S193 as an Anemometer. To measure the winds, an anemometer is needed. The anemometer for the SKYLAB experiment is the roughened surface of the sea as the wind blows over the ocean. The sea becomes increasingly rougher, especially in the capillary wave region, as the speed of the wind increases. The capillary waves that are generated have a vector wave number spectrum that is a function of the speed and direction of the wind in the first few meters above the ocean surface. The backscatter measurements made with S193 provide a measure of the variation of the roughness of the sea surface caused by the wind. This measure has in turn been related to the wind over the ocean. By means of a planetary boundary layer theory developed by Cardone (1969), these measurements of the capillary waves have been related to the vector wind that would have been measured in a neutrally stratified atmosphere at an elevation above the sea surface of 19.5 meters.

The choice of 19.5 meters goes back to early work done on other programs where the ships that were used to relate wave parameters to wind speed had anemometers mounted at this height on their masts. Any other reference height, as long as it had been consistently employed, could have been used equally well.

Past research has indicated that wind reports from ships without anemometers more closely approximate winds at this elevation than they do at ten meters above the sea surface, as had been previously assumed. Reference is made to Pierson (1964) for some interesting points on this subject. The measurement at this height can be imagined to have been obtained by a ship at a fixed point on the ocean surface equipped with a well designed properly exposed cup anemometer and a wind vane. There are standard routines to correct the measurements made when the ship is under way that are applied by the transient ships equipped with anemometers for measuring the wind. One of the major problems, however, is that the anemometers on the ships that report the winds are installed

at many different heights, and the reports are not corrected to a standard height of 19.5 meters, or any other appropriate standard height, for the analysis of the wind field. This source of variability has been carefully removed whenever possible in the analysis of all of the meteorological data provided to this program.

The design of an anemometer is subject to many constraints, and anemometers have many different kinds of shortcomings. For example, if an anemometer is subjected to a step response gust, it has a start up time and it will generally overshoot the wind value given by the step response. If it responds to direction, it will oscillate about the mean value of the step response before it settles down to the correct value. Anemometers have a time lag, and anemometers can give erroneous readings if they are mounted or calibrated improperly. If the measurements are not averaged for a long enough time, the average wind can have errors because the turbulent components have not been properly filtered out. The radar backscatter measurements by S193 are subject to these same kinds of errors. They have to be discussed and interpreted in a way analogous to a discussion of the proper calibration of an ordinary anemometer.

The radar part of the S193 system can be considered to be the data link between the anemometer, which is the wind roughened sea surface, and the recording system, which is the spacecraft. The information transmitted on the data link is the strength of the back-scattered signal which is a function of how rough and how high the capillary waves (and larger waves) are on that portion of the sea surface illuminated by the radar. The waves, in turn, will vary as a function of the wind over the ocean.

The portion of the ocean illuminated by the radar varies in dimensions depending upon the nadir angle. Table 1.1 shows the

dimensions of the cell as a function of scan angle for SKYLAB. Many tens of square kilometers are illuminated by the radar beam during the process of making the measurement, which is accomplished in a fraction of a second. The area average due to the dimensions of the beam replaces the time average of a measurement made by a conventional anemometer, and, in fact, it is far superior to such a time average. The dimensions of the patch that is illuminated, especially at nadir angles of 30° , 40° , and 50° , effectively filters out all of the short period gusts and temporal fluctuations in the wind with periods shorter than twenty minutes, or so. The measurement made by the radar is thus analogous to having had 20 or 30 ships uniformly spaced over this area, each making a twenty minute measurement of the wind at the appropriate anemometer height, each averaging that measurement, and then averaging these averages to obtain, in principle, given well calibrated instruments, a very stable number to represent the wind for synoptic scale purposes.

Table 1.1 Dimensions and areas of the patch of sea surface scanned by S193 as a function of the angle of the antenna scan.
(as designed)*

Angle	0°	15.6°	29.4°	40.1°	48°
Approximate Length (KM)	11	12	15	21	29
Approximate Width (KM)	11	12	13	15	17
Area (KM) ²	95	108	151	236	385
Incremental Area (caused by movement of SKYLAB during measurement time)	21	39	68	97	142

The measurements made from SKYLAB should be expected to be much more stable and much more representative of the quantities required for synoptic scale meteorological purposes and global numerical weather predictions than those that are usually obtained from ships at sea. Only in scientific investigations is the wind typically averaged for a full twenty minutes. Most observers on ships do not average the winds

* These angles and areas were actually slightly different.

for this length of time, and an element of sampling variability represented by the residual effect of the gustiness is usually present even in the most carefully made observation of the wind by a ship.

The waves that respond to the wind and are the anemometer for this experiment have a time lag similar to the time lag of an anemometer. The time lag for the response of the capillary waves is negligible. Capillary waves can be shown to track the gustiness of the local winds within the illuminated spot. The most dramatic example of this effect is the so-called cats paws.

However, the larger gravity waves, on which the capillary wave ride, do have time lags, and these waves need not necessarily correspond to the local wind conditions. As the discussion of radar backscatter theory shows, in another section of this report, this one feature is probably the last problem of radar backscatter theory that needs to be resolved. In the work of Fung and Chan (1975), fully developed wind generated seas were assumed, and the probability density function for the slopes was based upon such an assumption. However, for actual ocean conditions, the gravity waves need not necessarily be lined up in the appropriate direction with reference to the local wind, they need not necessarily be either as high or as low as that wind speed alone requires they should be according to the fully developed spectrum described by Pierson and Moskowitz (1964). The effect of the tilts and the slopes of these larger gravity waves may cause, and probably do cause, fluctuations in the measurements of the backscatter of some as yet to be determined amount, perhaps a half db or so, that need to be corrected for.

Unfortunately, the wavelengths for most of the tilting mechanisms in these theories are of the order of perhaps 100 to 1000 times the length of the radar wavelength, which is two and a fraction centimeters, so that the slopes of pieces of the ocean of two meters to twenty meters in diameter are involved. These slopes are controlled by the local winds and probably reach equilibrium with the local winds within an hour or so even if the winds change abruptly. This part of the wave spectrum is not well understood.

Any additional contribution to the slopes that provide a tilting mechanism for a more adequate Bragg scattering theory due to the larger and longer gravity waves will cause small perturbations. It would be expected that these effects would be most pronounced for the lighter winds. If the winds are perhaps seven and a half meters per second, the theories for the generation of waves will indicate that the fully developed waves would be 1.2 meters high. The actual waves could be two, three, or four times higher than this, and have come from some other part of the ocean. They would be long gravity waves, but they could contribute enough to the slope variances that enter into the theory of Fung and Chan so as to change the theoretical value of backscatter measurement by an amount that would be sufficient to generate some error in the estimate of the wind speed.

SURFACE TRUTH STRATEGY

Plans. Extensive plans were made for underflights by aircraft to make measurements at some of the cells scanned by S193. However, it was recognized from the start of the program that this subset of cells would be an extremely small fraction of the total number of cells that would be scanned. Aircraft simply cannot keep up with spacecraft.

For this reason, plans were made to acquire data from the more conventional meteorological sources distributed over the oceans. At the time of SKYLAB, these conventional sources consisted mainly of the various on station weather ships and of the ships at sea that radio in weather reports every six hours for synoptic weather map analysis. Plans were also made to acquire whatever data might be useful from other types of spacecraft, such as the NOAA and Air Force spacecraft, which were then in operation.

The surface truth strategy for this part of the program was very simple. It consisted of contacting every available known source of meteorological and oceanographic data acquired over the oceans on a

routine basis and obtaining copies of these data before and after the pass of SKYLAB over a given portion of the ocean.

As a part of these data taking operations, plans were made to have the weather ships take special wind and wave observations at the time of passage of SKYLAB, starting ten minutes before and ending ten minutes after a pass. Special forms were distributed to the ships which were mailed back upon completion of each cruise. Ships from Canada, the Netherlands, France, and Great Britain participated in this program.

It took a number of months to acquire, collate, and utilize this large amount of conventionally obtained data, and the data were used not only for the times of the passes but during the entire second and third manned periods of SKYLAB, (SKYLAB 3 and SKYLAB 4). The synoptic data used for weather forecasts on a global basis, or on a northern hemisphere basis, is a transient kind of data. It exists at the time it is needed for the purpose of preparing meteorological forecasts. Shortly thereafter, some of it, but not all of it, becomes archived in the meteorological and oceanographic centers of various nations, and it is often very difficult to retrieve these data once they have been archived.

The AVA Pass. Some idea of the importance of getting data for S193, even in the presence of the many difficulties experienced with the spacecraft, can be obtained by a brief description of what happened when the pass over AVA was made. At this point in time, the solar shield, or umbrella, had been deployed on the spacecraft, but one solar panel for electrical power was still stuck in its undeployed position. A second solar panel had torn away from the spacecraft, and only the panels for the astronomical units were operational. A disturbance has formed over Mexico and had moved out over the North Pacific Ocean, as a back door tropical cyclone.

Predictions indicated that SKYLAB would pass near tropical cyclone AVA which would be just barely in range of the cross-track non-contiguous

mode, scanning off to the appropriate side. It was also indicated that the spacecraft would accidentally be nearly in the z local vertical mode. Usually, for all of the measurements with the EREP package, the spacecraft had to be rotated to a new position by means of three gyroscopes on the spacecraft so that the instrument package pointed straight down and a zero degree nadir angle could be achieved.

These facts were ascertained about six to eight hours before the spacecraft was due to pass the tropical hurricane and, in view of the importance of obtaining data for this program, only S193 was turned on during the time that SKYLAB was passing AVA, roughly from the moment it passed the southern tip of Baja, California until it had gone several hundred miles past the eye, which was off to the right of the direction of the spacecraft travel. No other instruments were turned on, and SKYLAB was not maneuvered to stay in z local vertical during the pass.

It was necessary to correct the measurements for slight deviations from the nominal design nadir angles and to correct for the effects of the Doppler filters for the extreme end of the pass. A good set of data was recovered from this one tropical cyclone, even with SKYLAB still in a crippled condition, without adequate electrical power. Two additional passes were made during this first manned period over the Gulf of Mexico that provided additional data for light winds, and an aircraft flight under the spacecraft in the Gulf of Mexico provided a cross calibration between the AAFE Langley radar on an aircraft and S193 on the spacecraft for wind near 13 knots.

Once the pass for AVA was decided upon, a NOAA aircraft operating under a different proposal, EPN 440, was dispatched. It arrived in Acapulco, Mexico at about the time of the spacecraft passage, and flew into the hurricane roughly two hours after the data were obtained by SKYLAB.

In all of the analyses that follow, it has been necessary to extrapolate and interpolate the measurements made by aircraft, ships, data buoys and other spacecraft to the time of the measurements made by S193 on SKYLAB. The details of this will be discussed later. However, the penetration of AVA by the NOAA aircraft, plus other penetrations by Navy and Air Force aircraft, both before and after the time of the SKYLAB pass, provided data that allowed the wind field for the hurricane to be reconstructed for the time of the pass according to theories that had been developed and tested on numerous other hurricanes in the Gulf of Mexico.

The Routine for a Particular S193 Pass. The events that transpired to acquire data for tropical hurricane AVA have already been described. For the other passes that were obtained, a routine was followed that should be described. When the SKYLAB spacecraft was manned and in operating condition, several, perhaps as many as four, candidate segments of different orbits would be selected at the Manned Spacecraft Center during which, for one of these orbits, SKYLAB would be put into the z local vertical mode and the various instruments of the Earth Resources Experiment Package would be operated. These candidate orbit sections were announced 48 hours in advance by telephone, and the principal investigators for the various programs could obtain a list of them. Some of these orbit segments would continue out over the ocean, or could be started over the ocean.

At the time of the data taking phase for SKYLAB, the group associated with the City University of New York had access to the complete facilities of the National Weather Service offices and data acquisition network. All of the numerical weather forecasting products produced by the National Weather Service, plus all of the analyses of the surface synoptic charts for the North Atlantic and North Pacific, plus information on hurricanes, plus teletype data, plus spacecraft cloud imagery were available on a real time operational basis. The 48 hour surface prognostic chart based on the

six level primitive equation model then operational at the National Weather Service was most helpful.

Given the candidate passes, the 48 hour forecasts for the northern hemisphere were used to obtain a forecast of what the wind speeds and directions would be for the different scanning modes for the different orbit segments. If the potential pass would yield wind speeds and directions that would help complete the range of values desired, it was requested along with concurrent operation of the cameras and the other instruments, with the exception of the high data rate multifrequency scanner. At times, optimum conditions for the operation of the other instruments would not occur when there were high winds, and the use of the other instruments was waived in order to obtain S193 data.

The pass would be confirmed, or denied, 24 hours prior to the time it would take place. Once the pass was confirmed, along with the scanning mode, numerous telephone calls were made, and, if needed, telegrams were sent. The telephone calls requested hemispherical surface charts prior to and after the pass, geostationary cloud imagery near the pass, VTPR data near the pass, sea surface IR temperature fields, and other useful material from our co-principal investigators at the National Environmental Satellite Center. They also requested the Air Force DAPP data prepared just before and just after the pass. Either a telephone call or a telegram alerted either European or Canadian weather centers, who then radioed the weather ships as to the time of the SKYLAB pass so that they could take special observations.

During the peak period of activity, the volume of mail of use to the analysis of the S193 SKYLAB data reached an amount such that a canvas lined cart roughly three feet deep by three feet wide by four feet long would be completely full when delivered during the day. These data were sorted according to the particular pass and used to define the cloud conditions, the atmospheric conditions, the sea surface temperatures, and the winds for each pass.

The swath width of S193 in the cross track non-contiguous mode was so great that the cameras and other sensors on SKYLAB could not cover the cells scanned in this mode. This was the main reason for the plan to gather cloud and sea surface temperature data from other sources. A second reason was that S193 could have stood by itself as an instrument even in the absence of any other instruments on SKYLAB, should such an eventuality have arisen. The conventional data base was sufficient to provide supplementary surface truth for sea surface temperature, clouds, and atmospheric structure. Ship reports of wind speed were acquired to supplement the aircraft underflights and special weather ship reports.

SUMMARY OF DATA USED AS SURFACE TRUTH

Meteorological and oceanographic data to be used as the surface truth in providing estimates of the wind in the planetary boundary layer and of the waves, cloud conditions, and atmospheric structure were obtained from NASA, NOAA, DOD, and UCAR and from international sources including the World Meteorological Organization. Some data were redundant; some data were not used for various reasons; but, at least, all data of any possible use were collected in near real time during the experiment.

NASA. The National Aeronautics and Space Administration provided surface truth in terms of aircraft underflights planned for several purposes. Winds were measured by means of the aircraft itself flying at a low altitude and comparing air speed with data from an inertial navigation system. The radar backscattering cross section was measured by means of a radar quite similar to S193 except for modifications needed so that it could be used on an aircraft. This area of NASA support was in part provided by the L.B. Johnson Manned Space Center and in part by the Advanced Applications Flight Experiment program base at the NASA Langley Research Center.

NOAA. The National Oceanic and Atmospheric Administration provided support at the Regional Office in New York City by permitting unlimited access to the NOAA data products and forecasting products. The schedules for the facsimile machines were changed so as to provide analysed fields and other data, depending on the potential swaths for SKYLAB.

The Atlantic Oceanographic and Meteorological Laboratory of NOAA provided additional aircraft underflights that obtained wind speeds and directions, wave heights, cloud data, microwave data and other data in a program called EPN 460. The aircraft data from AVA were most important for the analysis of the winds in that hurricane.

Copies of the reconnaissance reports and in-flight logs of the aircraft that penetrated tropical storm CHRISTINE were made available from the files of the National Hurricane Center. The data were for the six hour period up to the time of the pass and included dropsonde data, eye penetration reports and special low level wind measurements.

Our co-investigators at the National Environmental Satellite Center of NOAA intercepted the real time meteorological data that are obtained by NOAA for each SKYLAB pass that used S193. These data consisted of the six hourly surface synoptic chart analyses, the various NOAA satellite cloud images in both the visible and infrared, the atmospheric soundings from VTPR, and surface temperature fields.

DOD. The Department of Defense provided support in terms of magnetic tapes of ship reports, surface pressure fields, sea surface temperature and DAPP cloud data. The ship reports are collected

every six hours for the synoptic weather map times and maintained on a permanent file at the Fleet Numerical Weather Facility at Monterey, California, along with six hourly analyses for the northern hemisphere of the sea level pressure field, and 12 hourly analyses of the air temperature and vapor pressure field. These files were for the continuous period from 00 Greenwich Mean Time (GMT) July 15, 1973 to 12 GMT February 2, 1974. Approximately 300,000 ship reports were obtained. The reports were not homogeneously distributed in time. For example, for the North Atlantic Ocean there were typically 150 ship reports at 00 GMT, about a hundred reports at 06 GMT, about 250 reports at 12 GMT and 200 at 18 GMT.

Also made available were the DAPP cloud data from another source in DOD. These analyses describe the cloud structures as a function of height over the northern hemisphere. The plan was to use these data to supplement the passive microwave measurements for calculating attenuation effects.

UCAR. At the time of the passes over the North Pacific, the University Corporation for Atmospheric Research was conducting research with aircraft and buoys off the coast of the states of Washington and Oregon. Several SKYLAB passes during SKYLAB 3 were coordinated with aircraft flights made by UCAR. Unfortunately, the cells that might have been used also included some land, and the data from UCAR could not be used.

International Support. International support was provided by the Weather Ships operated by Canada, the United Kingdom, France, and the Netherlands. When a Weather Ship was at a location where

the CTNC mode scanning pattern would have points surrounding that ship, special observations starting ten minutes before and ending ten minutes after SKYLAB passage were made. Successive one minute averages of wind speed and direction entered on a special form and a wave record made with the Tucker Shipborne wave recorder were obtained and mailed to us.

Finally, the World Meteorological Organization collected data on all weather reporting ships and published the data in, "The International List of Selected, Supplementary and Auxiliary Ships", WMO Publication, No. 47 (1974). Included were the call letters of the ship, information on whether or not the ship had an anemometer, and, if it had one, what the height of the anemometer was above the sea surface, if it was known. The data in the tables of this document were also available on a magnetic tape which was purchased, reprocessed at the National Weather Records Center, and used in the analysis of the ship reports obtained from the Fleet Numerical Weather Center.

ERRORS IN THE MEASUREMENT OF THE WIND

A perfectly designed experiment is not easily achieved. Frequently, something will go wrong, or some essential component required for a complete understanding of the data obtained will have been overlooked in the description of the program to be carried out. In this program, there were two aspects of the problem that were missed in the planning and execution stages that have just been described.

The first aspect that was missed was that of the effect of wind direction on the backscatter measurements. A vector cannot be fully specified by one measurement. The other aspect of the experiment that was missed in the experimental design was that of being able to evaluate quantitatively the accuracy of the independently obtained wind speeds and directions against which the radar backscatter measurements were to be compared. These essential aspects of the experiment could have invalidated it if solutions had not been obtained during the analysis phase. One of the challenges of doing research is to be able to devise adequate solutions to unforeseen problems when they arise.

It was not particularly difficult to account for the effect of wind direction and to relate the backscatter measurement to the magnitude of the vector wind. This was done by means of two techniques, one being the equivalent upwind technique of Young using the AFFE data and the theory of Fung and Chan as given in Appendix D. The other was to treat the wind direction as known from the meteorological data and to correct the analysis for possible errors in this wind direction.

The second problem, namely that of the quality of the surface truth was not solved until the very end of the program. It was, in a sense, the crux of the entire experiment. In the various presentations

of the preliminary results of this program there was one persistent skeptic who kept asking the embarrassing question, "How did you measure the winds that provided the surface truth for this experiment, and how accurate were they?" Questions of this nature can be ignored, or answered with a cliché, or thought about, and eventually answered correctly.

It was not possible to measure the winds at every cell scanned by Skylab. In fact, three different methods had to be used to obtain the winds that were used as surface truth. These methods are described in Chapter 4. These methods had errors of a particular and rather peculiar nature associated with them. The last and very important part of this investigation was that of quantifying these errors and relating them to the basic objectives of remote sensing.

Three anemometers, side by side, at the same elevation above the sea surface each recording the wind speed and direction on a continuous recorder could, at a particular instant, record three completely different values of the wind speed and direction, and, yet, each could be properly designed and calibrated and each value would be correct. The time constant of the instruments would be different, and the instruments would then respond to different eddy scales in the wind. Although the three measurements would be different, the differences are not necessarily errors and can be explained in terms of the properties of the instrument and the nature of turbulence.

In this program, the problem is to compare wind measurements made by a radar on a spacecraft with wind measurements made by more conventional methods, and with winds computed from meteorological theory. Although the differences in the measurements made in these different ways have been treated as errors in Chapter 4 and 8, perhaps other terms

such as radar wind variability, meteorological wind variability and mean square wind magnitude difference might have been more apt.

The proper wind to use for a particular application depends on that application. High frequency fluctuations in the wind are important to study turbulence and Reynold's stresses. Other measures such as the peak five minute and two minute gusts in a one hour record are important in building design. The application of this method of remote sensing is the improved measurement of the synoptic scale winds in the planetary boundary layer so as both to define these winds more effectively over the global ocean and also to permit a more accurate initial value specification of the planetary boundary layer for numerical weather prediction methods.

For the second application, the wind needs to be averaged over an appropriate time and space scale that in part depends on the grid spacing of the meteorological prediction model. Spatial fluctuations with high wavenumbers need to be suppressed so that they will not alias into low wavenumbers and propagate, in turn, into forecast errors. Also to some extent the amount of smoothing, or averaging, of the wind depends on the particular theory used to parameterize the effects of turbulence in the equations of motion for the mean flow that are used for numerical weather prediction.

A goal of this particular remote sensing technique is to define the winds in the planetary boundary layer over a time, or space, average that will yield the best possible numerical prediction for appropriate forecast ranges for particular prediction models. It is here that the radar method has a clear superiority over other methods, not only because of the greater volume of data but also on a one to one comparison basis. It trades an extensive spatial average over an area for a time average at a point.

Although the wind could in principal be measured accurately and correctly by a ship or a data buoy, and the value reported could be an absolutely correct value for the wind at that point in space as averaged over a minute, or ten minutes, or twenty minutes, that measurement at a point far from a grid point of the numerical model is not the measurement that needs to be made.

In this sense, then, it is not that the wind measurements reported by ships have errors, since in one sense they are correctly made, but it is that these measurements are inadequate in that both the way they are made and their irregular spacing and low density over the oceans do not permit a definition of the full wind field for the purposes of modern meteorological theory.

The so-called errors in the meteorological winds described in Chapters 4 and 8 not only take into account such effects as the brief averaging time for most measurements but also the effects of trying to define a vector field from a limited amount of data irregularly and unevenly spaced over the oceans. From the point of view of specifying the vector wind field completely over the global ocean on a uniform grid of points to a required accuracy, ship reports introduce errors, and it is in this sense that the errors in the meteorologically specified winds will be discussed.

From the point of view of the goals of numerical weather prediction, other systems could be conceived that could, in principal, do as well. A weather ship, or a data buoy, at almost every five degree intersection of latitude and longitude might be almost as good, and would certainly, if it existed, improve weather forecasts. Inexpensive floating devices that would transmit sea level atmospheric pressure

have been suggested. Other ideas have undoubtedly also been put forth. None have the potential of one single instrument on a single platform capable of measuring the winds at about 320,000 points per day.

As the material in this report is presented, it will show that the errors, in the sense just defined, are surprisingly large, at least for the planetary boundary layer model that was used, and that the ability to specify the wind field in the planetary boundary degrades systematically as a function of whether or not a weather ship was nearby, or an aircraft underflight occurred, for a particular cell, or whether or not a ship report was available near the cell, or, as the last recourse, the isobaric field, extrapolated (or interpolated?) into the area of the cell that was scanned was used to compute the wind. The errors increase as the quality of the information used in the analysis degrades, but in each category, the errors still appear to be random.

The analysis, as carried out, has features that appear to be unique, and that have not been discussed in the meteorological literature (to our knowledge). With such large inherent errors in the analysis of the most complicated portion of the atmosphere for numerical prediction methods, it should be no longer surprising that certain kinds of errors consistently occur in numerical weather forecasts in the three to four day time frame. The errors in the initial value specification over the oceans have simply propagated and magnified to the point where consistent forecast busts occur.

CHAPTER 3 THE S193 RADSCAT MEASUREMENTS IN NONCONTIGUOUS MODES OVER THE OCEAN

INTRODUCTION

Between June 5, 1973 and February 1, 1974, SKYLAB made 26 passes in the z local vertical mode over the oceans during which useable S193 data in a non-contiguous scanning mode were obtained. For these 26 passes, the instrument was operated for a total of 140 minutes and 29 seconds, or the equivalent of 1.51 orbits of SKYLAB.

Information on these 26 passes is given in Table 3.1 in which the pass is identified and the general location, scanning mode, the beginning and ending time of the pass and the duration are tabulated. In the analysis and reduction of the data, the data from SKYLAB 2 and SKYLAB 3 were treated as one set, and the data from SKYLAB 4 were treated as a second set for reasons to be explained later.

SKYLAB 2

During SKYLAB 2, three useful passes were obtained on June 5, 6 and 11, 1973. The one on June 6 was the Hurricane AVA pass. Winds from 6 or 7 knots to over 40 knots were present in the various cells scanned by the instrument on these three different days. The back-scattering coefficient at 50° nominal nadir angle for σ_{HH}^0 varied by about 20 db. An AAFE Radscat underflight in the Gulf of Mexico on June 5 where 13 knot winds occurred demonstrated close agreement between the aircraft measurements and the spacecraft measurements as reported in Grantham et.al. (1975).

TABLE 3.1 S-193 RADSCAT NONCONTIGUOUS MEASUREMENTS OVER THE OCEANS

EREP No.	DOY	DATE 1973	LOCATION	MODE	TRACK	GMT START h / m/ s	GMT STOP h / m/ s	DURATION
5	156-1	June 5	Gulf of Mexico, Caribbean	ITNC	34	18/02/08	18/08/51	6m 43s SL 2
AVA	157-1	June 6	Hurricane Ava	CTNC-R	49	18/55/42	18/59/01	3m 19s
8	162-1	June 11	Gulf of Mexico	ITNC	48	15/20/21	14/24/08	3m 47s
13	216-1	Aug. 4	North Pacific	CTNC-L/R	48	17/08/12	17/11/51	3m 39s SL 3
13	216-2	Aug. 4	North Pacific	ITNC	48	17/12/04	17/14/45	2m 41s
16	220-1	Aug. 8	North Pacific	CTNC-L/R	34	15/51/22	15/54/40	3m 18s
16	220-2	Aug. 8	North Pacific	ITNC	34	15/54/52	15/58/40	3m 48s
16	220-3	Aug. 8	Gulf of Mexico	ITNC	34	16/04/42	16/07/18	2m 36s
16	220-4	Aug. 8	Gulf of Mexico	CTNC-L	34	16/07/39	16/09/40	2m 1s
23	245-2	Sept. 2	Tropical Storm Christine	CTNC-L	42	17/54/13	18/01/57	7m 44s
26	247-1	Sept. 4	N. of Venezuela	CTNC-R	70	18/02/24	18/09/44	7m 20s
29	252-1	Sept. 9	North Atlantic	ITNC	01	19/25/06	19/33/53	8m 47s

TABLE 3.1 (CONT'D.) S-193 RADSCAT NONCONTIGUOUS MEASUREMENTS OVER THE OCEANS

EREP No.	DOY	DATE	LOCATION	MODE	TRACK	GMT START h / m / s	GMT STOP h / m / s	DURATION
54	334-1	Nov. 30	Gulf of Mexico	CTNC-L/R	19	16/41/20	16/42/17	57s SL 4
60	338-1	Dec. 4 1974	North Pacific	CTNC-L/R	6	16/41/00	16/50/23	9m 23s
73	4-1	Jan. 4	North Atlantic	CTNC-L/R	29	19/32/00	19/42/00	10m
78	8-1	Jan. 8	North Atlantic	CTNC-L/R	14	16/37/27	16/43/00	5m 33s
79	9-1	Jan. 9	North Atlantic	CTNC-L/R	28	15/53/14	16/00/00	6m 46s
81	11-2	Jan. 11	North Atlantic	CTNC-L/R	58	17/43/52	17/53/00	9m 8s
89	24-1	Jan. 24	North Pacific	CTNC-L/R	33	17/47/06	17/51/20	4m 14s
90	25-1	Jan. 25	North Pacific	CTNC-L/R	47	17/03/30	17/08/00	4m 30s
92	27-1	Jan. 27	West of Mexico	CTNC-L/R	2	12/15/30	12/25/16	9m 36s
95	29-1	Jan. 29	North Pacific	CTNC-L/R	34	17/25/11	17/30/06	4m 55s
95	29-2	Jan. 29	Gulf of Mexico	CTNC-L/R	34	17/37/24	17/40/03	2m 39s
96	30-1	Jan. 30	North Pacific	CTNC-L/R	48	16/42/06	16/46/00	3m 54s
96	30-2	Jan. 30	Gulf of Mexico	CTNC-L/R	48	16/53/34	16/57/45	4m 11s
98	32-1	Feb. 1	North Pacific	CTNC-L/R	6	16/49/00	16/58/00	9m
SL 2 Total 13m 49s			SL 3 Total 41m 59s		SL 4 Total 84m 46s		GRAND TOTAL 140m 29s	

Data for DOY's 6-2 and 7-1 are also given in Appendix A as examples of faulty data.

SKYLAB 3

SKYLAB 3 obtained 9 data sets between August 4, 1973 and September 9, 1973. The North Pacific passes on August 4 and August 8 were over portions of weak extratropical cyclones, typical of mid-summer. Tropical storm Christine provided additional measurements during conditions of high winds. Two days after the pass over Tropical Storm Christine, a second pass made measurements north of Venezuela that yielded valuable data on tropical wind circulations after a decayed tropical storm.

Various reports and analyses of the SKYLAB 2 and SKYLAB 3 data (all labeled preliminary) have been published. The data and analyses contained in this final report represent all possible corrections to the original data. They supercede the previously published results since they contain various refinements of analysis not contained in the preliminary results.

Toward the end of SKYLAB 3, a malfunction occurred in S193 that caused the antenna to jam up against the stops and to be unable to scan in any mode. Had the instrument not been repaired during SKYLAB 4, this would have ended the data taking phase.

SKYLAB 4

At the start of SKYLAB 4, an EVA repaired the antenna scanning mechanism so that the CTNC mode could be used but not the ITNC mode. Unfortunately, the tip of the antenna was dislodged during the repair operation. By comparing before and after photographs of S193, the nature of the damage was ascertained, and a copy of the antenna, available on earth, was used to determine the antenna pattern of the damaged antenna. Roughly, the pattern was a hemisphere with a 12 db

main lobe in the middle (one way gain pattern).

About 20 db of gain was lost for the radar part of S193, and the backscatter from some of the weaker winds could not be detected. Fortunately, the square of the antenna pattern is needed for backscatter, and the antenna pattern could still be used to re-calibrate the measurements. However, the one way gain is involved in passive microwave measurements, and these were so badly degraded by the hemispherical part of the new antenna pattern, that the passive microwave measurements could not be used for SKYLAB 4.

PROBLEMS IN DATA REDUCTION

For some of the passes, SKYLAB was deliberately not put into the exact z local vertical mode, and roll angles were allowed. For other passes, the pitch of the spacecraft was also allowed to vary. Also during SKYLAB 4, one of the three control moment gyroscopes failed so that the spacecraft could not be easily maneuvered. Moreover, even if in the nominal z local vertical mode, the antenna did not scan to the desired command angles.

The compounded effects of different roll angles, pitch angles, and yaw angles, and different realized antenna scanning motions, as opposed to the commanded motions, produced variations in the nadir angle (or the incident angle), in the locations of the centers of the cells, and in the slant range. These effects complicate the problem of interpreting the data and require the calculation of each value of the backscattering cross section as corrected for all of these variations.

A great amount of effort went into refining and reprocessing the raw data from S193 so as to obtain the correct nadir angles, cell centers, backscatter values, and passive microwave temperatures.* This was necessary because the various variations could

* See Moore, Ulaby, Sobti et. al. (1975), pp. 501, 568 for example.

have a cumulative effect that would mask the results being sought.

On January 9, 1974, the left side CTNC scan mode failed, and, although the passes are indicated as CTNC-L/R in Table 3.1, only the right side scan achieved the nearly nominal desired nadir angles. The actual incident (or nadir) angles that were achieved for each of the S193 passes are given in Table 3.2.

For SKYLAB 4, approximately 160 different cells were scanned at each of the three largest nadir angles. With four different backscatter measurements at each cell, the data base for this period consisted of about 1920 values of radar backscatter and 482 wind speeds and directions. The data had to be treated separately because of other possible effects caused by the damage to the antenna.

GENERAL DESCRIPTION OF THE PASSES

The Sensor Coverage Summary Map for S193 found in the "Skylab Earth Resources Data Catalogue (JSC 09016)" shows the subsatellite tracks of SKYLAB when S193 was operated in the radiometer, scatterometer mode in purple. One group of passes begins over the North Pacific, reaches a maximum northward latitude near 155° W longitude and curves southward into the west coast. A second group of southbound passes occurred over the Gulf of Mexico. The two northbound passes leaving South America were for Christine and the wind field two days later as Christine was dissipating. The last group of passes were those over the North Atlantic starting off the East Coast of the USA, or Labrador, or Newfoundland and often extending all the way to Europe.

The time of the passes was controlled by the work/sleep schedule of the astronauts and thus by the precession of the orbit. In general,

SKYLAB 2, (the first manned period), data were obtained over the Gulf of Mexico, the Caribbean, and for AVA. SKYLAB 3 data were obtained over the North Pacific, and because of its importance, for Christine and her aftermath. SKYLAB 4 data were obtained over the North Atlantic at first and later over the North Pacific and Gulf of Mexico.

The hour to hour and day to day changes in the winds over the ocean made each pass a unique event, never to be duplicated in contrast, for example, to summertime passes over a city, which would not be expected to be very much different, if repeated a week later.

Table 3.2 Nominal incident angles (or nadir angles) for each
S-193 noncontiguous data segment over the oceans.

DOY-SEG. No.*	COMMAND ANGLE					
	1	2	3	4	5	
156-1	50.5	44	32	17	1	SL 2
157-1	50.5-52	44-46	34-36	20-23	4-10	
162-1	51	44.5	33	18	1.5	
216-1L	49	41.5	30.5	18	2	SL 3
216-1R	48	41.5	31.5	18	2	
216-2	50.8-51.8	44.3	33	17.6	1.6	
220-1L	49	41	30	15.6	0.5	
220-1R	49	42	32	17.7	1.6	
220-2	49.7	43	31.5	16.5	0.9	
220-3	49.6	43	31.5	16.5	0.7-1.5	
220-4	49	41.4	30.4	15.9	0.3	
245-2	49.5	42	31	16-20	1-10	
247-1	47	41	30.7	16.7	1	
252-1	50.7	44	32.5	17.5	1.3	
334-1L	50.1	42.4	31.3	16.7	0.7	SL 4
334-1R	48.3	41.6	31.0	16.7	0.7	
338-1L	50.2	42.4	31.3	16.7	1.1	
338-1R	48	41.5	30.9	16.7	1.1	
4-1L	50.5	42.8	32	16	1	
4-1R	47	40.6	30	17	0	

* L and R denote the left and right sides of a left/right cross track noncontiguous segment.

Table 3.2 (Cont.)

DOY-SEG. No.	COMMAND ANGLE				
	1	2	3	4	5
8-1L	50.7-52.3	43.1	31.5	17.3	1.5
8-1R	47	40.7	28.8	15.9	0.2
9-1R	47.6-48.9	40.8-41.4	30.2-30.4	16.0-17.4	0.2-9.7
11-2R	49	41	30	17	14
24-2R	50.0	42.3	31.8	23.1-24.3	10.3-13.0
25-1R	50	42	32	24	11
27-1R	49	42	31	23	15
29-1R	50.3	42.6	32.2	23.4-25.4	12.5-14.7
29-2R	50.5	42.9	32.3	24.3	12.3
30-1R	50	42.2	31.6	22.5-23.9	11.7-15.2
30-2R	49.9	42.4	31.8	23.1-23.9	11.7-14.5
32-1R	49.6-50.3	42.1-42.6	31.4-32.1	21.7-24.8	10.8-16.1

CHAPTER 4 THE ANALYSIS OF THE METEOROLOGICAL AND OCEANOGRAPHIC SURFACE TRUTH

Introduction. A famous statistician is quoted by Cramér (1946) as having remarked to the effect that, "Everybody believes in the law of errors, the experimenters because they think it is a mathematical theorem, the mathematicians because they think it is an experimental fact." The important feature of this quotation is that two different groups of people, one theoretically inclined and the other experimentally inclined, look at the same body of theory and data in two different ways. In the study of S193 as a potential anemometer, there were two different types of people. One type consisted of people who specialized in radar techniques and in the interpretation of radar backscatter theory; the other type consisted of meteorologists and oceanographers who specialize in the interpretation and analysis of meteorological and oceanographic data over the oceans. The radar theoretician would tend to think of the meteorologically provided values of the winds over the ocean as "the surface truth" whereas the meteorologists and oceanographers were fully aware of the difficulty of providing a value for the wind speed and direction at a point on the ocean a great distance from any kind of ship.

In carrying out this program, a great deal of care was exercised in keeping the two independent parts of the analysis separate. The radar data were corrected, processed, and edited, errors were removed, and so on, until such a time as the centers of the illuminated cells could be provided to those doing the meteorological and oceanographic analysis. Those doing the meteorological analysis, analysed the entire area involved and developed the capability to provide, given the coordinates of the cells, the vector wind at each cell. After the longitudes, latitudes, and times of the measurements were provided to the meteorologists, each of the fields, that had been analyzed by one of three different techniques,

was used to determine the winds at each cell. This information was returned to the scientists who studied the radar backscatter so that both groups could then proceed to analyze the jointly merged data.

The Three Types of Meteorological Analysis That Were Used. The nature of the SKYLAB passes over different types of weather systems for different parts of the northern hemisphere oceans necessitated three different kinds of analysis in order to produce the surface truth meteorological estimates of the winds at the cells that were scanned. The first kind of analysis was specifically developed for tropical storms and hurricanes. The second was the manuscript, or hand analysis of plotted weather data. The third was an objective analysis for the winds over the northern hemisphere oceans.

The first of the three analysis techniques was one for tropical storms and tropical cyclones that was developed as part of a program for forecasting waves in hurricanes in the Gulf of Mexico. This particular model for the winds in a hurricane has many features known to agree well with the observed wind fields in hurricanes and was calibrated against winds as hurricanes passed anemometers near the coastline in the Gulf of Mexico for a number of different tropical hurricanes and tropical storms of varying intensities and varying radii of maximum winds. One of the important features of this model of the wind field is that it makes a distinction between the radius of maximum wind and the parameter that describes the shape of the isobaric pressure profile as a function of distance from the center of the storm. The model also accounts for the effect of movement of the tropical hurricane, or tropical cyclone, in a rather unique way. The output of this model is a horizontal vector wind field that is uniquely defined by a number of parameters that serve as input to the model. Once these parameters are determined the winds throughout the entire field are given. At the outskirts of AVA, supplementary meteorological information was used to merge the numerically generated wind field with the observations from other sources.

The second type of procedure that was used to specify the winds at the locations scanned by S193 on SKYLAB was the procedure generally described as manuscript analysis of synoptic weather charts. This particular procedure is almost a lost art because of the computerization of these techniques at the larger centers for weather forecasting and analysis. However, it is still carried out in numerous places to obtain a description of what the weather is like over a portion of the world. In particular, manuscript analyses of the wind fields for the North Atlantic Ocean, North America and portions of Europe for the North Pacific and the Northern Hemisphere are produced by the National Weather Service and issued to those weather stations that have a need for them.

In the production of a manuscript analysis of a weather chart all of the available reports both from islands, continents, and ships are gathered, as of a certain synoptic map time, plotted on the chart as a coded set of symbols that contain information on the characteristics of the clouds, the horizontal visibility, the sea level pressure, the pressure tendency, the air temperature, the water temperature, the relative humidity, and the wind speed and direction. In particular, the winds are reported to the nearest knot and to the nearest 10° in direction by each of the reporting stations. Also at times some of the ships report wave conditions, but these observations of waves are the least reliable of all of the data provided by such a system.

Once all of the reports have been plotted, it is possible to carry out several kinds of analysis of the data. The one used in our study is called a streamline isotach analysis. Lines called streamlines, which are everywhere parallel to the reported wind directions are drawn. These lines can converge in areas where the air is rising. They can diverge from regions where the air is sinking. They can form peculiarly fascinating patterns in the subtropical regions of the oceans with cols and zones of convergence and divergence illustrated by the flow patterns. Superimposed

on the streamlines are the isotachs, which are lines connecting those points of constant reported wind speed. It is necessary to judge the quality of reports that are close together if one report differs by several knots from another nearby report. Such a technique, although subjective, can produce a field over the area scanned by the spacecraft that provides an estimate of the direction and speed of the wind at each of the cells of the particular pattern that occurred.

The manuscript analysis was carried out by V. J. Cardone, in all cases, after obtaining data from many different sources and using the techniques with which he had become proficient over the course of more than a decade of practical application of these procedures. Figures illustrating the manuscript analysis of several of the fields that were produced for this program are given when certain days are discussed. The most interesting manuscript analysis is the one of the wind field in the Caribbean several days after the pass over Christine after the storm had dissipated and yet in which there was a great deal of structure to the wind field in the area where the pass was obtained. Other examples of manuscript analyses are those that were done for two passes over the Gulf of Mexico in the first manned period.

The final type of analysis that was employed was an objective analysis in the same sense that the analysis of the wind fields for the tropical cyclone was objective. This technique was applied to the analysis of the winds over the entire Northern Hemisphere Oceans based on computer based procedures that were developed during past programs sponsored by various government organizations. In particular, this development, which goes back to Cardone (1969), was a part of the attempt to improve on numerical wave forecasting procedures, which are extremely sensitive to a correct analysis of the wind field in the planetary boundary layer.

The method applies the planetary boundary layer model developed by Cardone (1969) to ship observations of wind, pressure, sea temperature and air temperature to produce an analysis of the vector stress of the

wind on the sea surface, the vector wind at 19.5 meters above the sea surface and a measure of the atmospheric stability called the Monin Obukov stability length. A summary of this theory is given in a following section. The highlights of the theory are described briefly in what follows. It is not the only existing planetary boundary layer theory, but it does have many desirable features, and it has been tested extensively in the development of numerical wave prediction models and in other applications both by the group carrying the research for S193 and by others such as Elsberry et. al. (1974), Kaitala (1974), and Isozaki and Uji (1975).

The Cardone planetary boundary layer theory describes the mean wind, U , as a function of height, z , above the sea surface in terms of a vector that for the first several hundred meters above the surface does not change direction with height. Above a certain level, the wind vector begins to change direction so that the wind becomes the same as the gradient wind at an elevation of approximately 1 kilometer above the sea surface. The variation of the average wind with height for the first 20 or 50 meters above the sea surface is controlled by the stability of the atmosphere over the water, the friction velocity, and the roughness length z_0 . For all cases, if the stress of the wind on the sea surface, which when divided by the density of the air represents the square of the friction velocity, is specified, the wind increases with height for the first meter or so above the sea surface according to a prescribed rate. At an elevation of about 10 meters above the sea surface, the change of wind with height begins to be influenced by the stability of the atmosphere. For the same stress at the sea surface, if the air is colder than the water, the wind 10 meters above the surface will be less than it would be if the air temperature and water temperature were equal. Conversely, if the air is warmer than the water, the wind at 10 meters will be greater than it would be if the air had the same temperature as the water. Stated another way, the same wind speed measured 10 meters above the surface for cold air over warm water

would produce a stronger stress than that wind speed for warm air over cold water. At an elevation of 20 meters above the sea surface, the differences between the winds at 20 meters for the same wind stress but different stabilities at the sea surface can be substantial. This is especially true if the winds are fairly light; about five to ten meters per second.

The other important aspect of this boundary layer theory is the problem of defining the direction of the wind. This direction is generally defined in terms of the angle that the wind in the surface layer makes with the isobaric analysis of the pressure measurements reported by ships at sea. This cross isobar flow can vary from 20° to 45° depending upon the nature of the atmosphere around the point under consideration. This direction is particularly affected by a quantity called the thermal wind, which is a measure of the rate of rotation of the isobars with height in the first 50 to 100 meters above the sea surface. The Cardone boundary layer theory correctly accounts for this inflow angle and yields a very high quality estimate of both the magnitude and the direction of the wind in the first 20 to 50 meters above the sea surface. These theories in turn merge into the gradient winds at an elevation of about a kilometer.

ANALYSIS OF THE SURFACE WIND FIELD IN TROPICAL CYCLONES AVA AND CHRISTINE

A Tropical Cyclone Boundary Layer Model. Standard objective and subjective wind analysis techniques cannot be applied to the specification of the surface winds in strong tropical cyclones (tropical storms, hurricanes, typhoons etc.) since the required direct measurements of surface wind at sea simply are not available in the vicinity of such storms. Usually, for storms far out at sea, the only quantitative data available are what are gathered by aircraft that penetrate the storm at 5,000 - 20,000 feet, measure flight level pressure, wind and temperature and drop radiosondes in the eye to determine the minimum central pressure. Fortunately, the results

of a recently completed research program that developed ways to specify the winds in the boundary layer of hurricanes for application to numerical forecasting of waves could be applied to specify the winds in Ava and Christine (Cardone, Pierson and Ward, 1975).

The methods developed in the previous program are based upon a theoretical model (Chow, 1971) of the horizontal air flow in the boundary layer of a moving vortex. The model is initialized by a specification of the storm motion and the sea level pressure distribution and provides a specification of the wind speed and direction referred to an anemometer level of 19.5 meters on a high resolution grid of points about the storm.

The model is based upon the numerical integration of the equations of motion, vertically averaged over the depth of a boundary layer that is subject to horizontal and vertical shear stresses. In vector form, the equation of motion is written in coordinates fixed to the rotating earth as in equation (4.1)

$$\frac{d\vec{V}}{dt} + f\vec{k} \times \vec{V} = - \frac{1}{\rho} \nabla P + \nabla \cdot (K_H \nabla \vec{V}) - \frac{C_D}{h} |\vec{V}| \vec{V} \quad (4.1)$$

where \vec{V} is the vertically averaged horizontal velocity; f is the Coriolis parameter \vec{k} the unit vector in the vertical direction; ρ the mean density of air, P the pressure; K_H the horizontal eddy viscosity coefficient C_D the drag coefficient and h the depth of the boundary layer. This equation is resolved in a Cartesian coordinate system, whose origin is allowed to translate at constant velocity (V_F) with the center of the pressure field associated with the vortex, in this case the eye of the tropical cyclone. Variations in storm intensity and motion with time are represented by a series of steady states so that the pressure gradient becomes independent of time and may be simply prescribed. The nonlinear system of equations

is solved numerically on a fine mesh nested grid system as an initial value problem for the steady state solution of the horizontal component of the vertically averaged velocity; that is, until the wind field on the moving grid becomes approximately steady. A simple transformation then yields the wind field with respect to the fixed earth coordinate system.

To be able to prescribe the pressure field from the type of data provided by reconnaissance aircraft, a simple pressure field specification model was developed. The hurricane pressure field is considered to be composed of the sum of an axially symmetric part (\bar{P}) of a constant gradient, which can be interpreted as the gradient associated with the mean surface geostrophic flow (\vec{V}_g) in which the storm is embedded as determined from equation (4.2).

$$\vec{f}\vec{k} \times \vec{V}_g = -\frac{1}{\rho} \nabla \bar{P} \quad (4.2)$$

The symmetric variation of pressure with radius (r) away from the storm central pressure (P_0) is described as equation (4.3).

$$\bar{P} = P_0 + \Delta P \cdot e^{-R/r} \quad (4.3)$$

where R is a scale radius and ΔP is the pressure drop across the (symmetric) storm.

Typically, \vec{V}_g can be inferred from either large scale synoptic weather maps or climatology, and ΔP is obtained from P_0 , while R is either calculated from a pressure profile across the storm or can be inferred from a model derived relationship between R and the radius to maximum wind R_{max} .

The methods were tested against several hurricanes in the Gulf of Mexico, including intense hurricane Camille (1969), that passed near several instrumented oil rigs during a special industry sponsored program known as the Ocean Data Gathering Program (Ward, 1974).

As an example of the results of that study, Figure 4.1 shows the track of intense hurricane Camille with respect to the instrumented oil rigs, and the radial distribution of surface pressure as defined by a composite of pressure measurements from coastal sites in the path of the storm. Shown in the figure is the fit of equation (4.3) to the pressure variation with radius. In small but intense storms like Camille (and Ava) R , in this case 10 n.mi., is equal to the radius of maximum wind while in larger often less intense storms R is larger than the radius to maximum wind. Aircraft eye penetrations usually provide R_{\max} which then be converted to R for consistent model initialization.

A comparison of the modelled wind field and the measured winds at a site that experienced 30 minute average wind speeds at an elevation of 65 feet of over 100 knots is shown in Figure 4.2. Agreement is excellent overall but note the inability of the model to specify some of the fine structure apparent in the wind trace and that represents smaller scale variations in the storm circulation. This fine structure is associated with the spiral rain bands that show up so well on weather radar images of tropical cyclones. As shown in the figure, these bands can be associated with local wind anomalies of at least 10 knots. The relatively small footprint of S193 cells would allow such fine structure to be resolved so that these potential anomalies must be kept in mind when the model provided vector winds are compared to the Ava and Christine S193 measurements. Depending on its direction of movement, the effects of a spiral rain band passing a fixed point can last for a wide range of times. Instantaneously, as a function of two horizontal space coordinates the rain band effect may occupy a very small area compared to the area of the full cyclone. Since the storms were far out at sea when scanned it was not possible to define from the surface the particular rain band structure at the time of the pass.

A critical test of any marine wind specification program is its ability to produce accurate wave hindcasts when coupled to a state of the

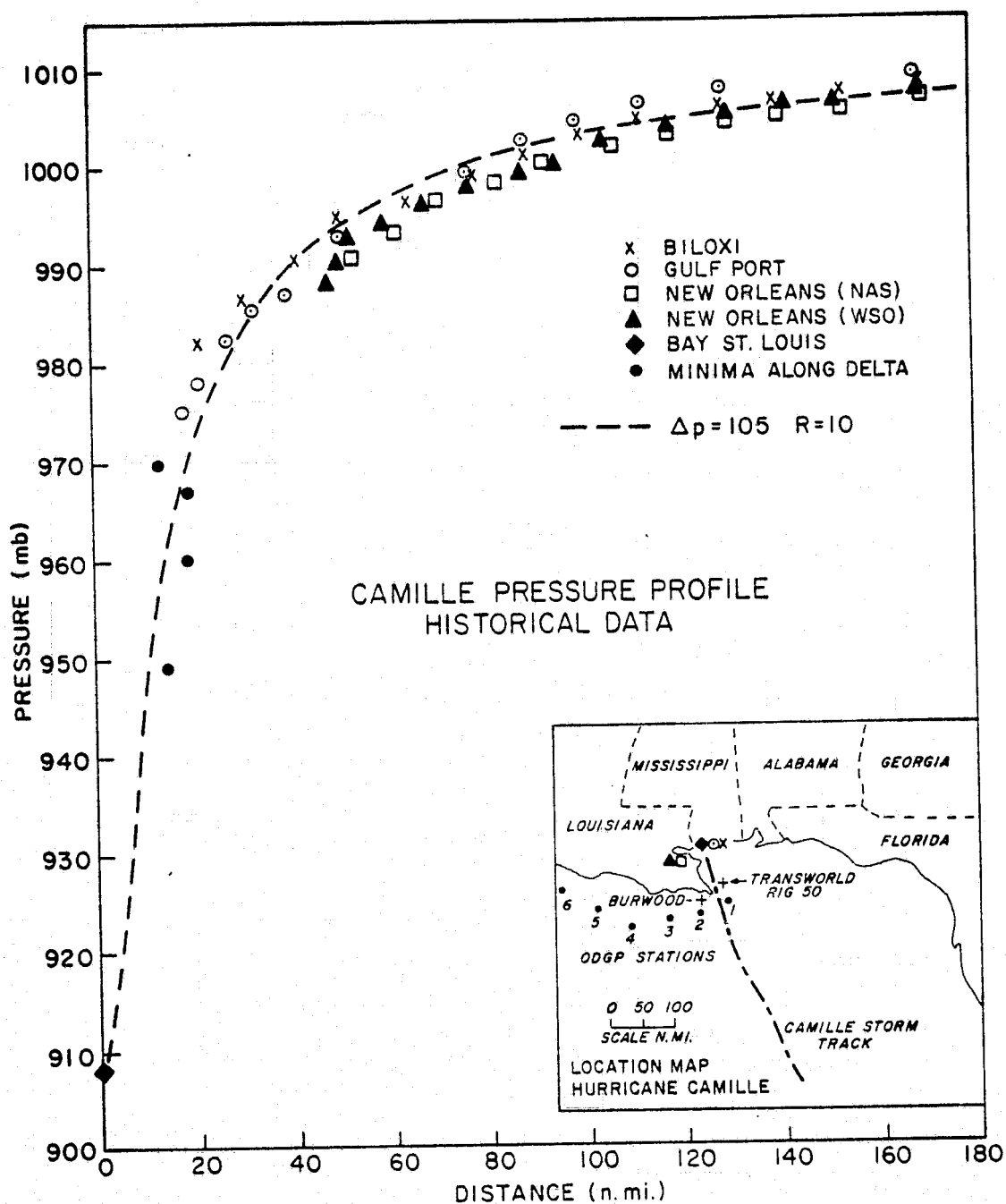


Figure 4.1 Pressure profile fitted to composite of coastal pressure measurements during approach of Hurricane Camille.

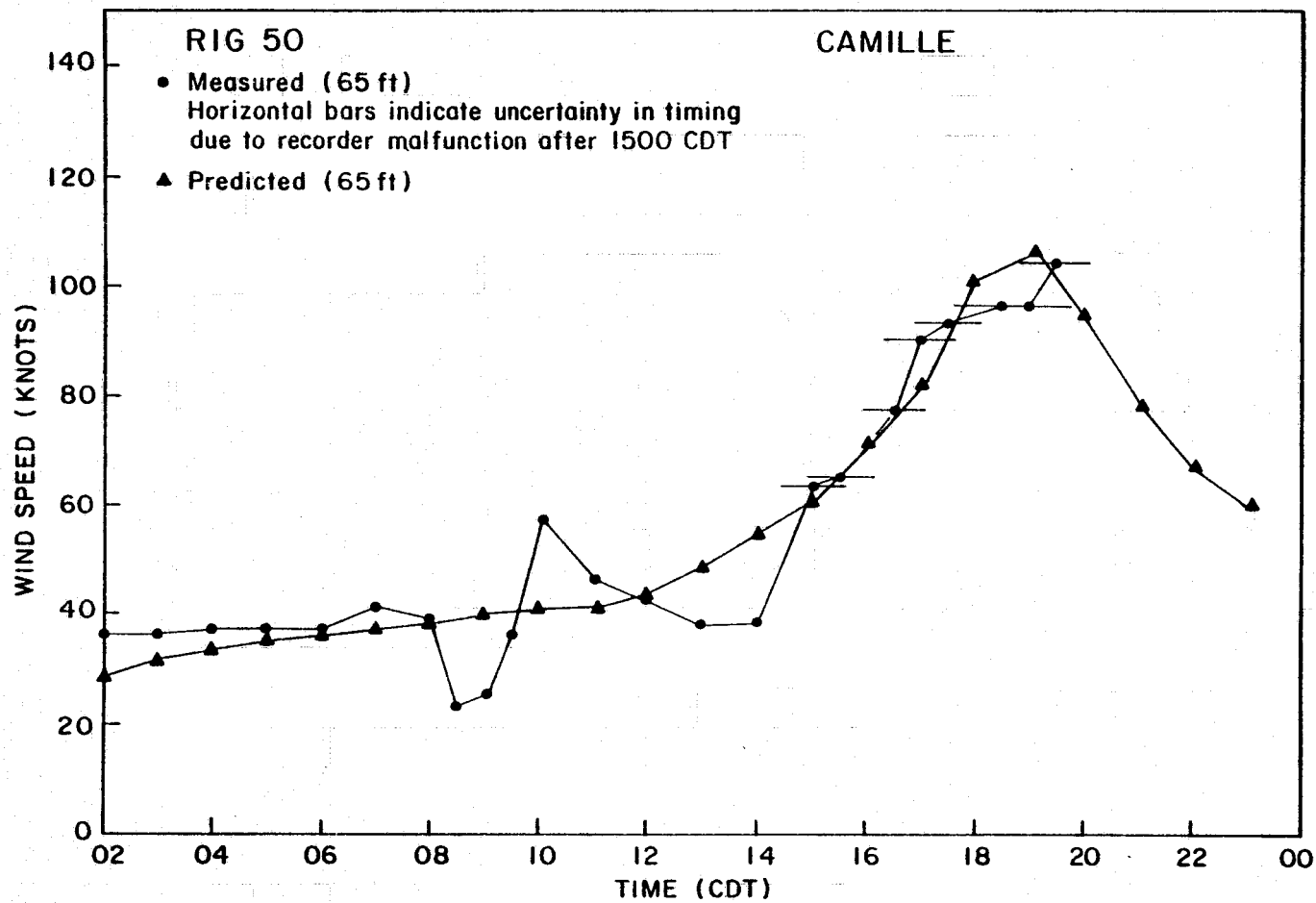


Figure 4.2 Comparison of wind speeds at Rig 50 during Camille.

art wave specification model. As shown by Cardone, Pierson and Ward (1974), these wind fields proved just such ability when tested against six Gulf of Mexico hurricanes of various sizes and intensities and verified against wave spectra calculated from wave records taken from carefully instrumented oil rigs.

Hurricane Ava. On the afternoon of June 6, 1973, Ava became the most intense hurricane of record in the eastern North Pacific Ocean and at the same time was observed by a unique complement of aircraft and satellite mounted remote sensors. The rather unusual set of circumstances that led to the S193 pass over Ava were reviewed in Chapter 2. This section presents the meteorological analysis that specified the surface wind distribution in and around Ava at the time of the pass and for the 30 hour period in its life history required to perform a numerical hindcast of wave conditions at the time of the pass.

Ava started as a weak tropical depression near the coast of Central America on June 1. It moved westward and strengthened slowly, becoming a hurricane on June 3 when Air Force reconnaissance observed maximum wind of 70 knots. Daily Air Force reconnaissance thereafter documented the explosive deepening observed between June 4 and June 6 as shown in Figure 4.3, which is a history of dropsonde measured minimum eye pressure. At the time of maximum intensity, Ava was a classical hurricane with a dense cirrus canopy, a banded cloud structure and a small circular clear eye. All of these features are visible in the NOAA-2 satellite visible and infrared images of Ava made on June 6 when she was about 500 miles southwest of Acapulco Mexico and shown in Figure 4.4. Figure 4.4a shows the full visible and infrared images from NOAA-2, and Figure 4.4b shows an enlargement of the visible image of Ava.

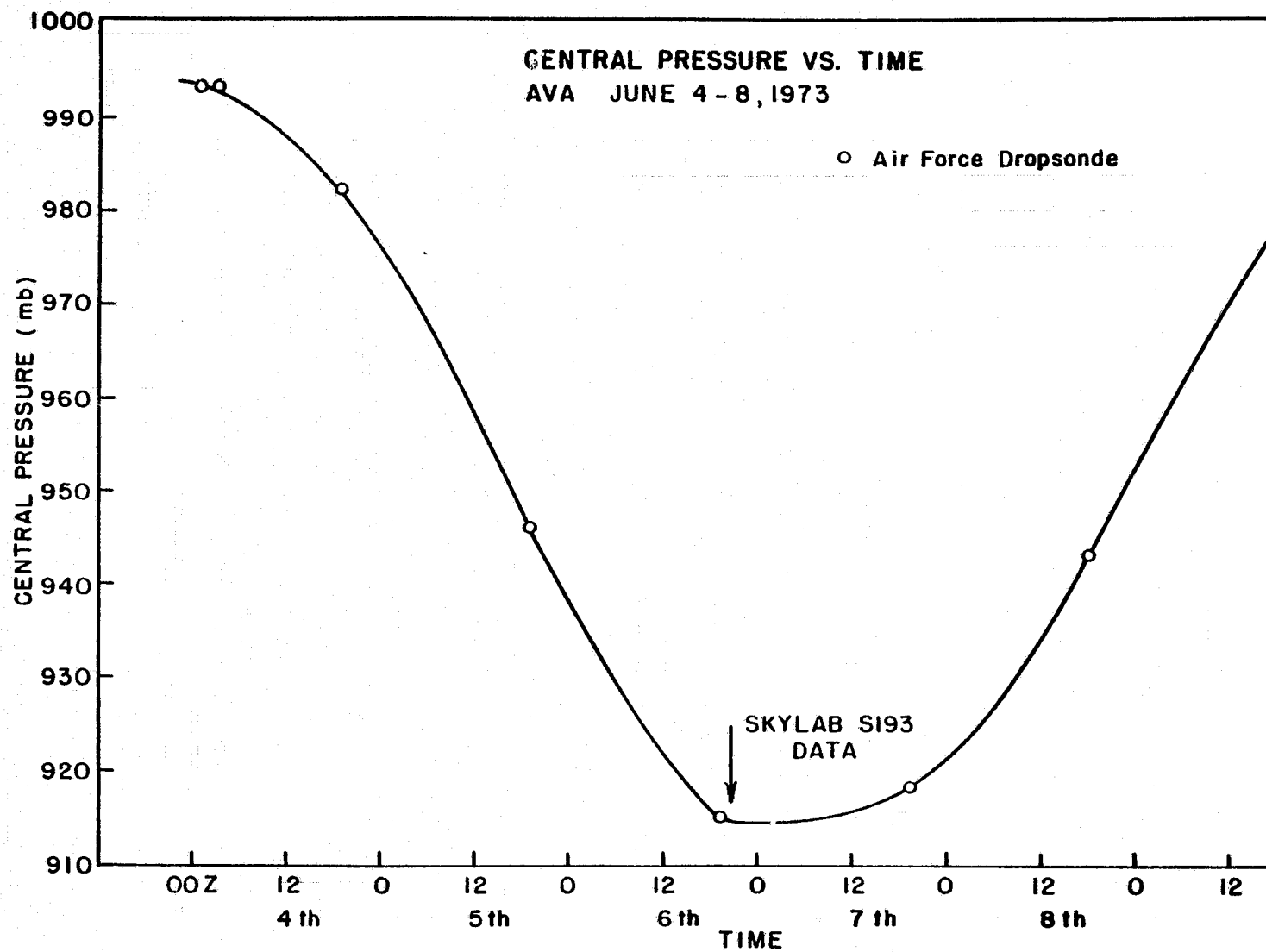


Figure 4.3 The variation of
central pressure with time in
Hurricane AVA.

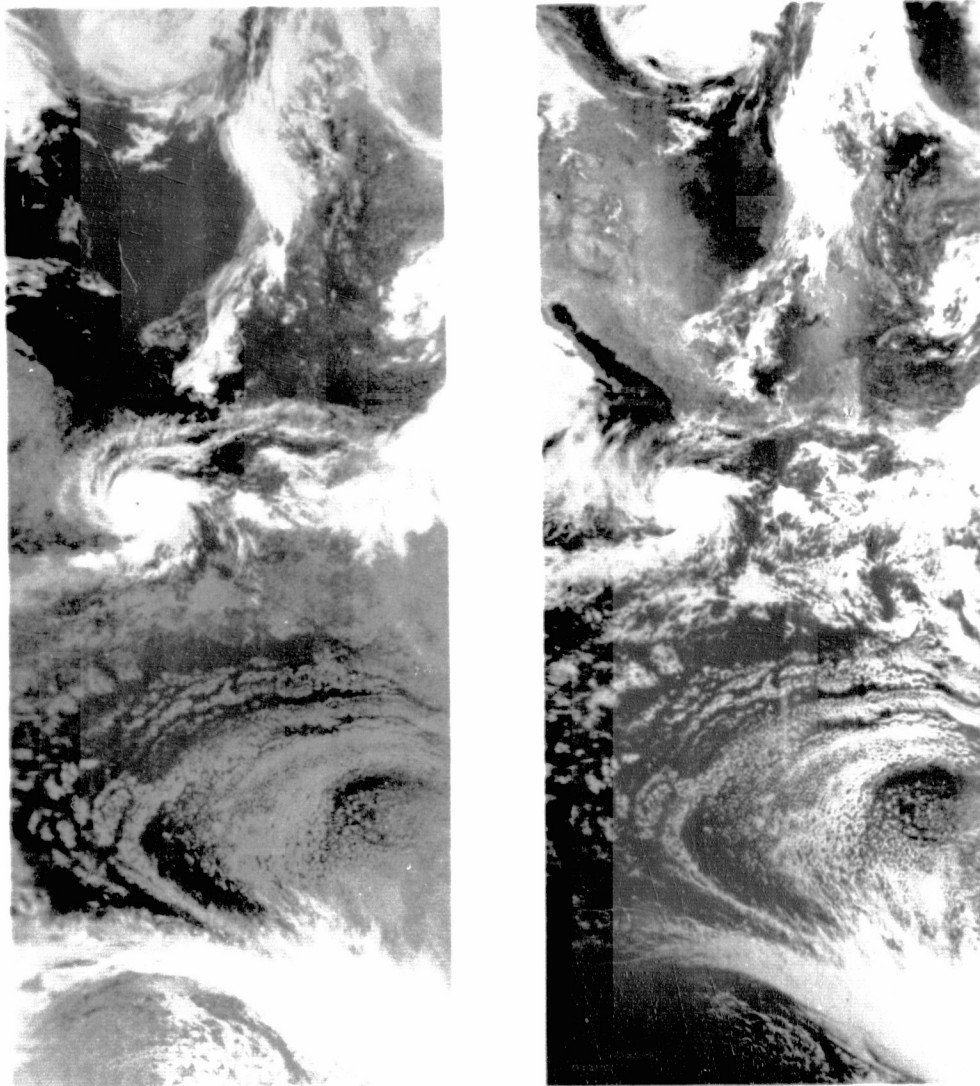


Figure 4.4(a) NOAA-2 (left infrared, right visible) images of Hurricane AVA on June 6, 1973.

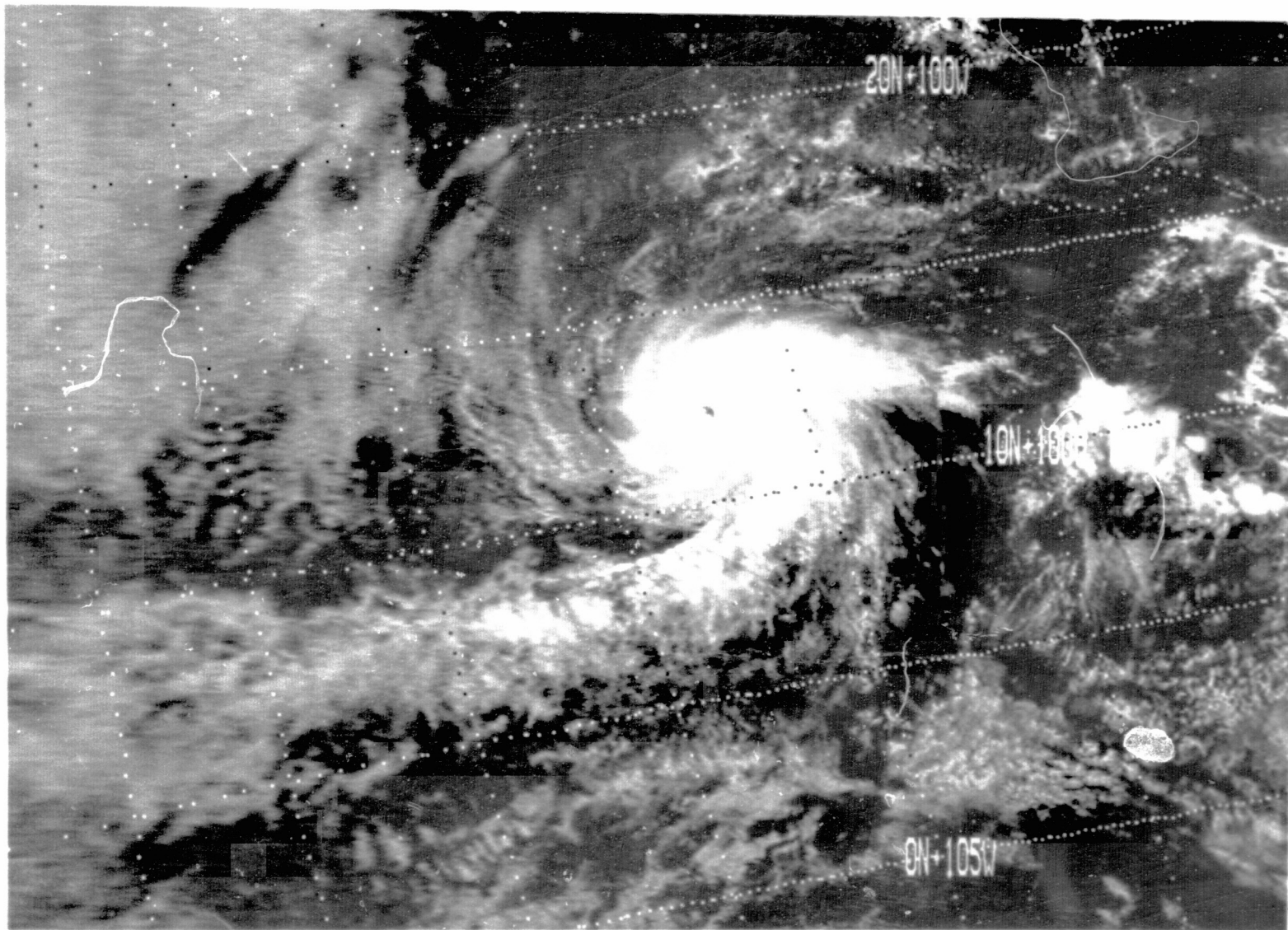


Figure 4.4(b) Enlarged view of
NOAA-2 visible image of
Hurricane AVA made at 1616 GMT,
June 6, 1973.

The track of Ava on June 5 and 6 is shown in Figure 4.5 and is reasonably well defined by satellite and aircraft fixes. Apparently Ava attained maximum intensity and minimum latitude on the day of the pass and began to weaken as it curved northwestward on June 7.

The Air Force and NOAA aircraft flights into Ava on June 6 consistently defined the basic structure of Ava. The Air Force aircraft penetration of Ava at 1930 GMT, June 6 provided the following quantitative information: minimum central pressure - 915 millibars; maximum flight level wind - 125 knots; radius of maximum winds - 10 nautical miles. An interesting account of the NOAA C130 mission into Ava is given by Davis (1973). The low level wind and laser profilometer wave data collected on this mission will be discussed in more detail below. Figure 4.6, taken from that paper shows the variation of the flight level winds and extrapolated surface pressure encountered in the penetration of Ava about four hours after the Air Force mission. Since this penetration was made at 10,000 feet, these profiles cannot be used to specify the boundary layer wind or pressure profiles directly. However, it is well established that the location of the radius of maximum wind does not vary with height in intense storms (Shea and Gray, 1973), which in the case of Ava was approximately 10 nautical miles.

The data provided by the aircraft were sufficient to prescribe the initial conditions of the boundary layer model described above reliably. That is, in equation (4.3), P_0 was set to 915 mb, Δp to 98 mb ($1013 - P_0$) and R to 10 nautical miles. The storm track defined an average westerly drift of 12 knots (\vec{V}_f) and on the basis of this track and climatology, the mean steering flow (\vec{V}_g) was specified to be westerly at 9 m/sec.

The numerical steady state solution of equation (4.1) subject to the above initial conditions is shown in Figure 4.7. The figure shows the wind distribution on an 800 x 800 kilometer square centered on the storm

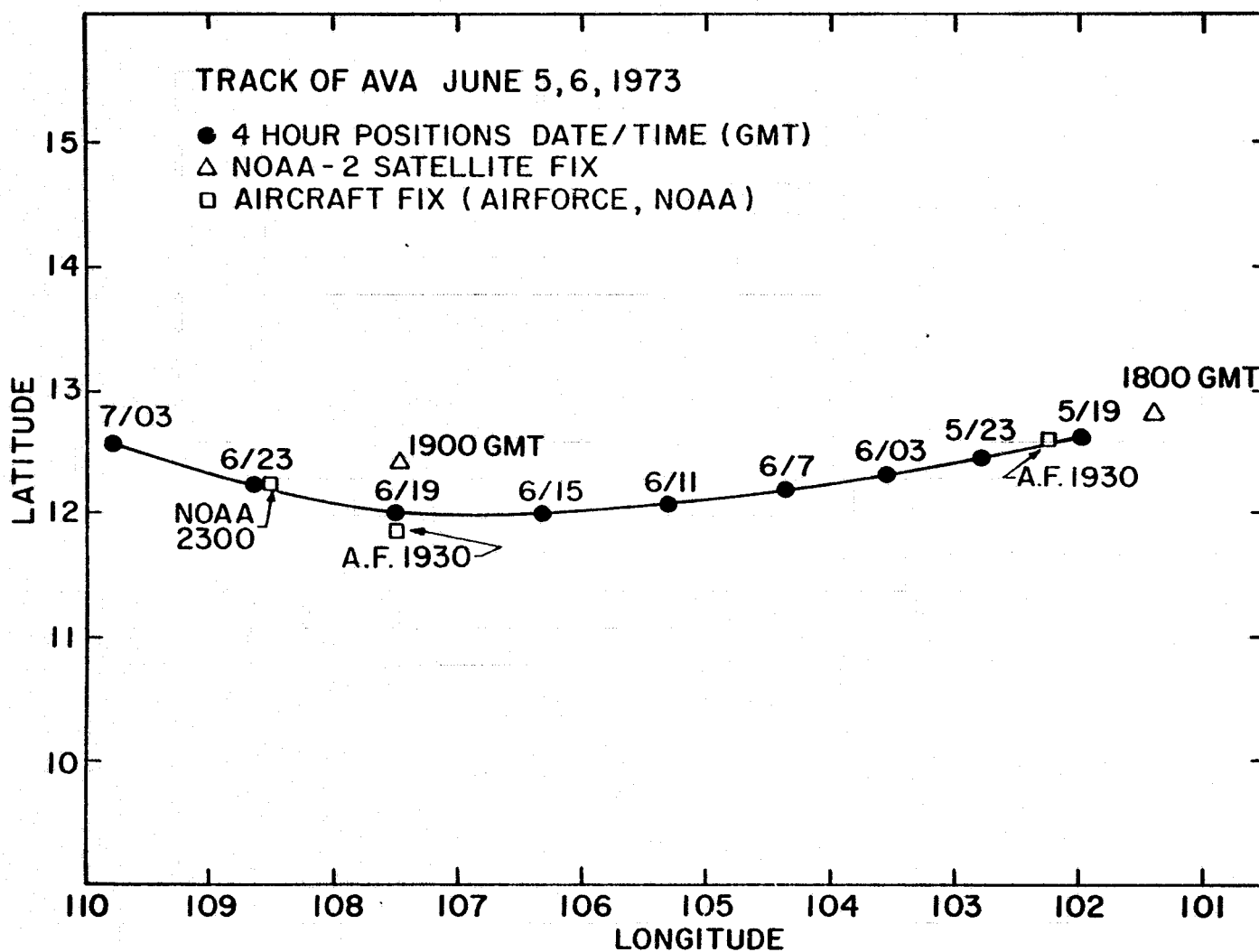


Figure 4.5 Track of Hurricane AVA.

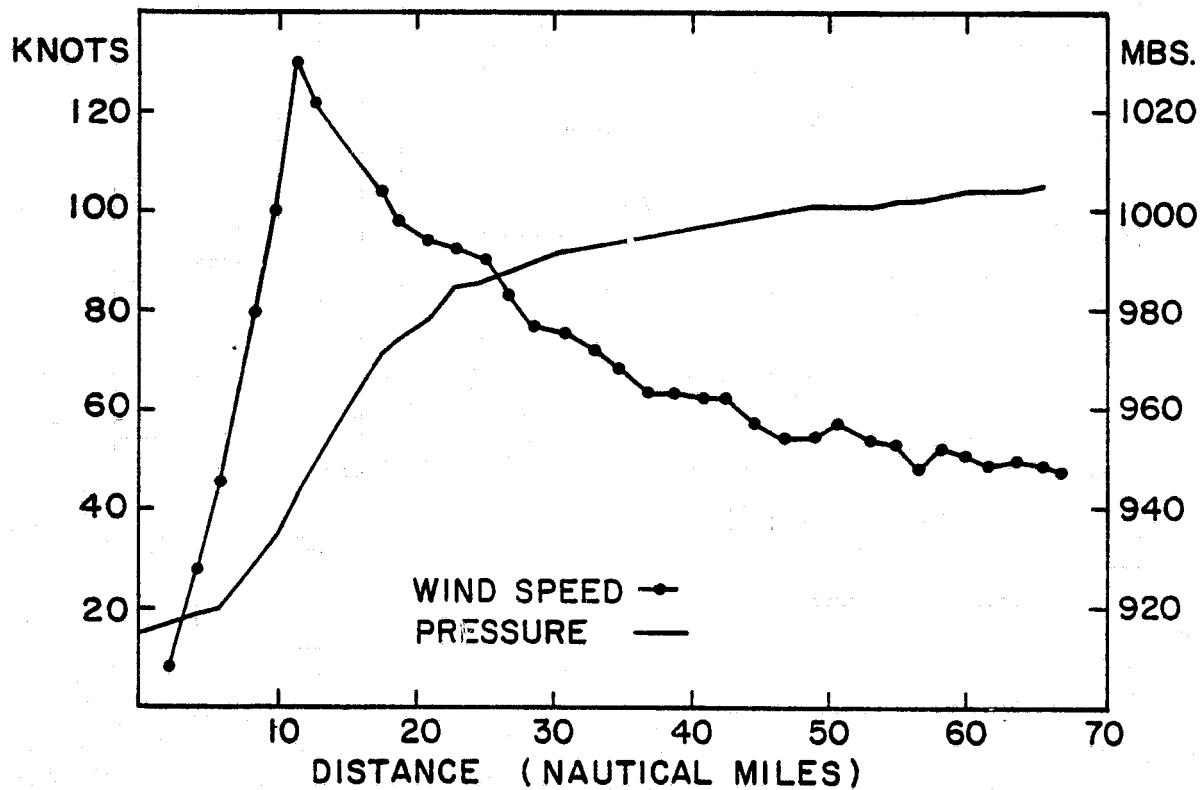


Figure 4.6 Variation of flight level wind and pressure (extrapolated to surface pressure) at 10,000 feet in the NOAA C130 penetration of Hurricane AVA, June 6, 1973 (from Davis, 1973).

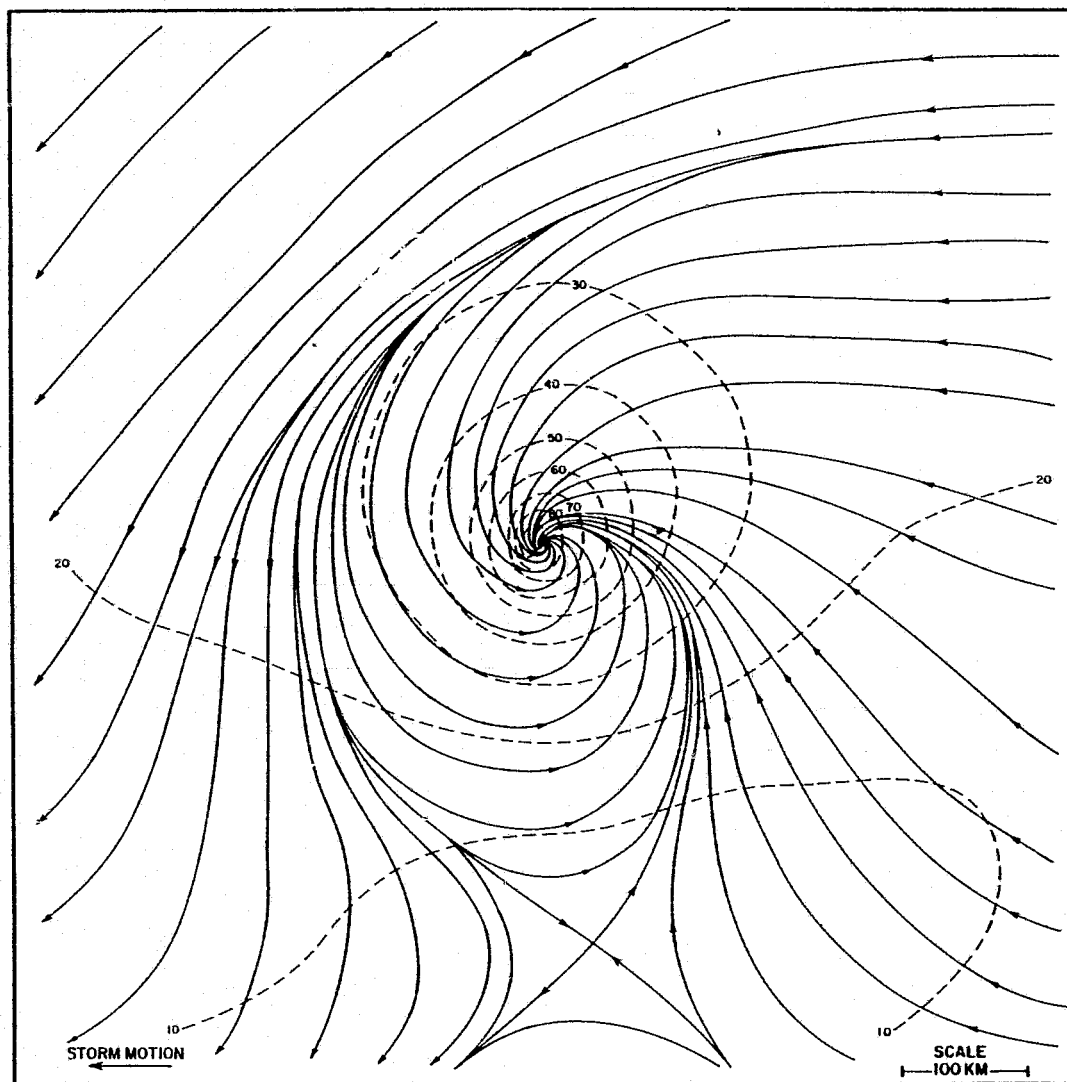
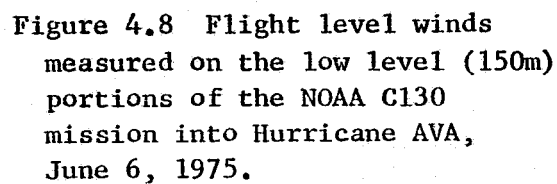


Figure 4.7 Theoretical boundary layer model solution for the surface wind distribution in AVA, shown in the form of streamlines and isotachs (knots).

center, in the form of streamlines drawn everywhere parallel to the wind direction and isotachs (in knots) of the integrated boundary layer wind speed after a scaling law has been applied that reduces the wind speed to anemometer (19.5 meters) level. That scaling law is part of the model itself and was developed in the prior research program cited above. Note the overall asymmetry in the modelled wind pattern with stronger winds in the northern half of the storm, the location of the maximum wind in the right front quadrant and greater inflow to the east of the storm than to the west.

All possible sources of data were sought in order to check and, if necessary, modify the modelled wind distribution prior to a final specification of surface winds at the locations of the S193 cells. The NOAA underflight provided flight level winds in the eastern sides of the storm as derived from the inertial navigation system. Part of the flight track is shown in Figure 4.8. Since this part of the mission spanned nearly four hours, the points are plotted with respect to the moving center of Ava. The winds measured along the low level portions of the flight are compared to the modelled winds in the eastern quadrant of Ava in Figure 4.9. The agreement is considered to be quite good, in view of the uncertainties associated with the location of the observations with respect to the eye. Particularly, for those points close to the eye, where the variation of wind with radius is extreme, the agreement is what should be expected. In the wind speed comparisons, the flight level winds, generally at 500 feet, are compared directly to the modelled winds which are considered to represent the 19.5 meter wind speed referred to neutral stability. While there are no direct measurements available in hurricanes to verify this procedure, a study will be presented in a later section that demonstrates that in a very unstably stratified boundary layer the winds speeds at 500 feet are very nearly the equivalent of the effective 19.5 meter wind speeds.



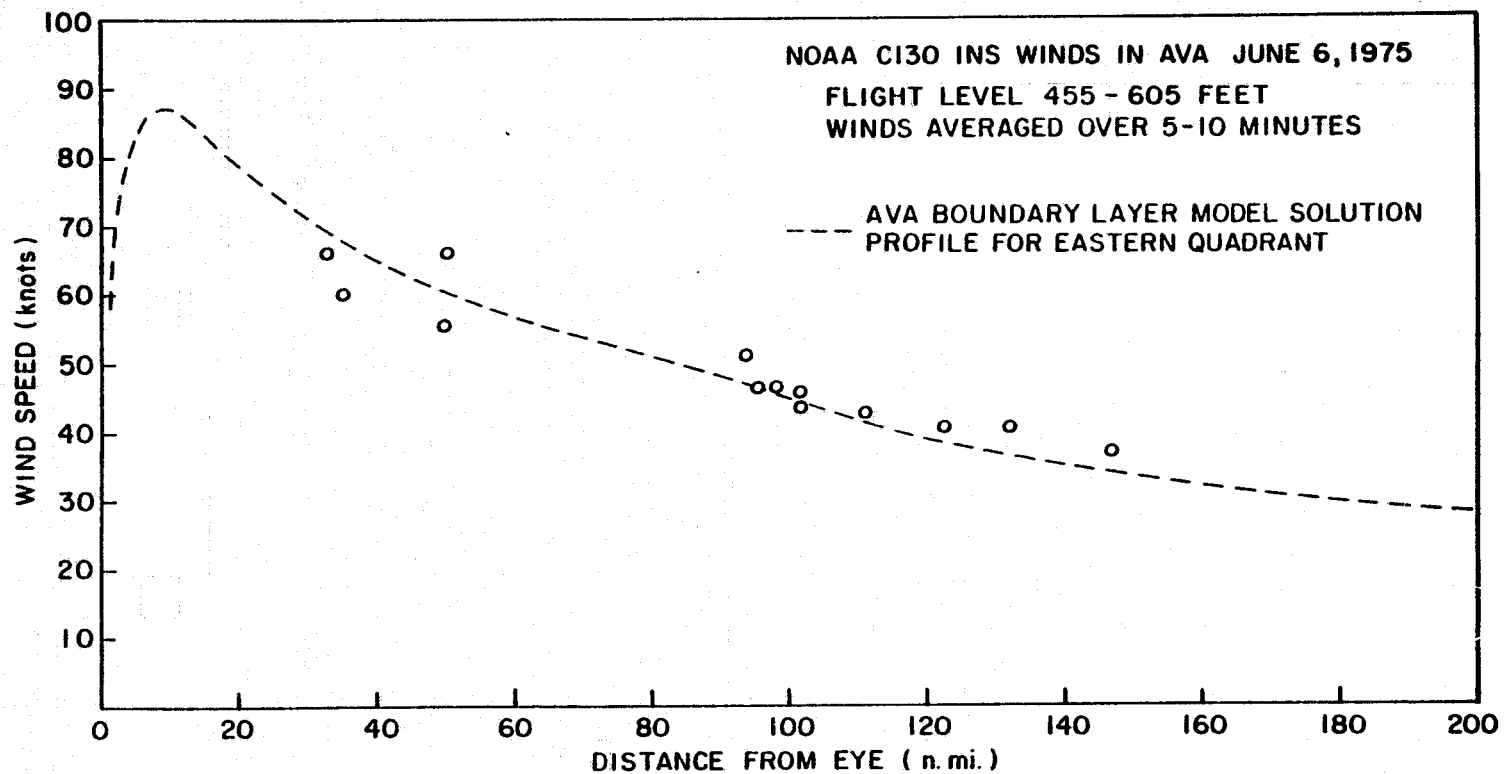


Figure 4.9 Comparison of averaged flight level (150m) wind speeds and model winds in the eastern (rear) quadrant of AVA.

While the aircraft data provided information inside the zone of gale force winds*, other sources of data were available for the outer region of the storm circulation in which most of the S193 cells were located. Figure 4.10 is a plot of all available surface ship weather reports near the time of the pass. The winds in this figure are encoded in a special way as proposed by Moskowitz (1966). The first digit gives the tens place of the wind direction and the second gives the unit place of the wind in knots. Each full barb means that the speed is close to a multiple of ten and a half barb means it is close to an additional five knots. For example, the southernmost ship reported a wind from 200° with a speed of 20 knots, the ship nearest the eye reported a wind from 190° and a speed of 44 knots, and the ship near 10° north reported a wind from 180° and a speed of 19 knots. The reports reveal a significant deficiency in the modelled winds in the upper half of the area scanned by S193. That is the actual winds are much weaker in speed and more northerly in direction than modelled, and this is attributable to horizontal variations in the sea level pressure gradient that are not well modelled by the simple steering flow specification used. The ship reports confirmed the roughness derived wind pattern provided by Strong (personal communication) from an analysis of the passage of the sunlint pattern across the area on ATS-3 photographs using methods given by Strong and Ruff (1970).

The final analysis of the surface wind field for Ava is shown in Figure 4.11 and is a simple smoothed composite of the modelled winds inside the 30 knot isotach and a hand produced streamline isotach pattern drawn closely to the sunlint derived and ship winds outside the area of high winds. The pattern of cells scanned by S193 is superimposed on the streamline isotach analysis in Figure 4.11.

* winds over 35 knots

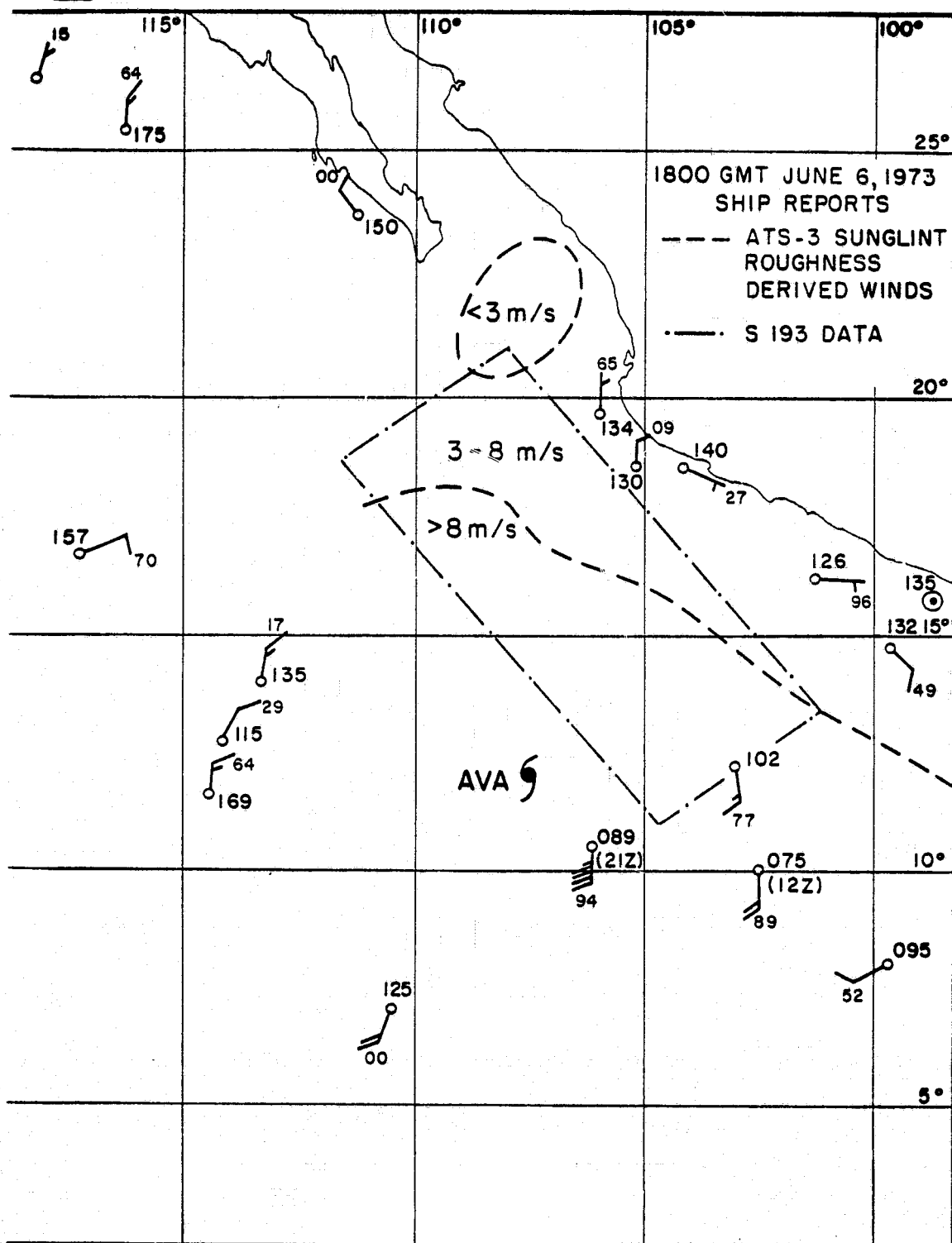


Figure 4.10 Conventional ship reports and sun glint derived wind information around AVA.

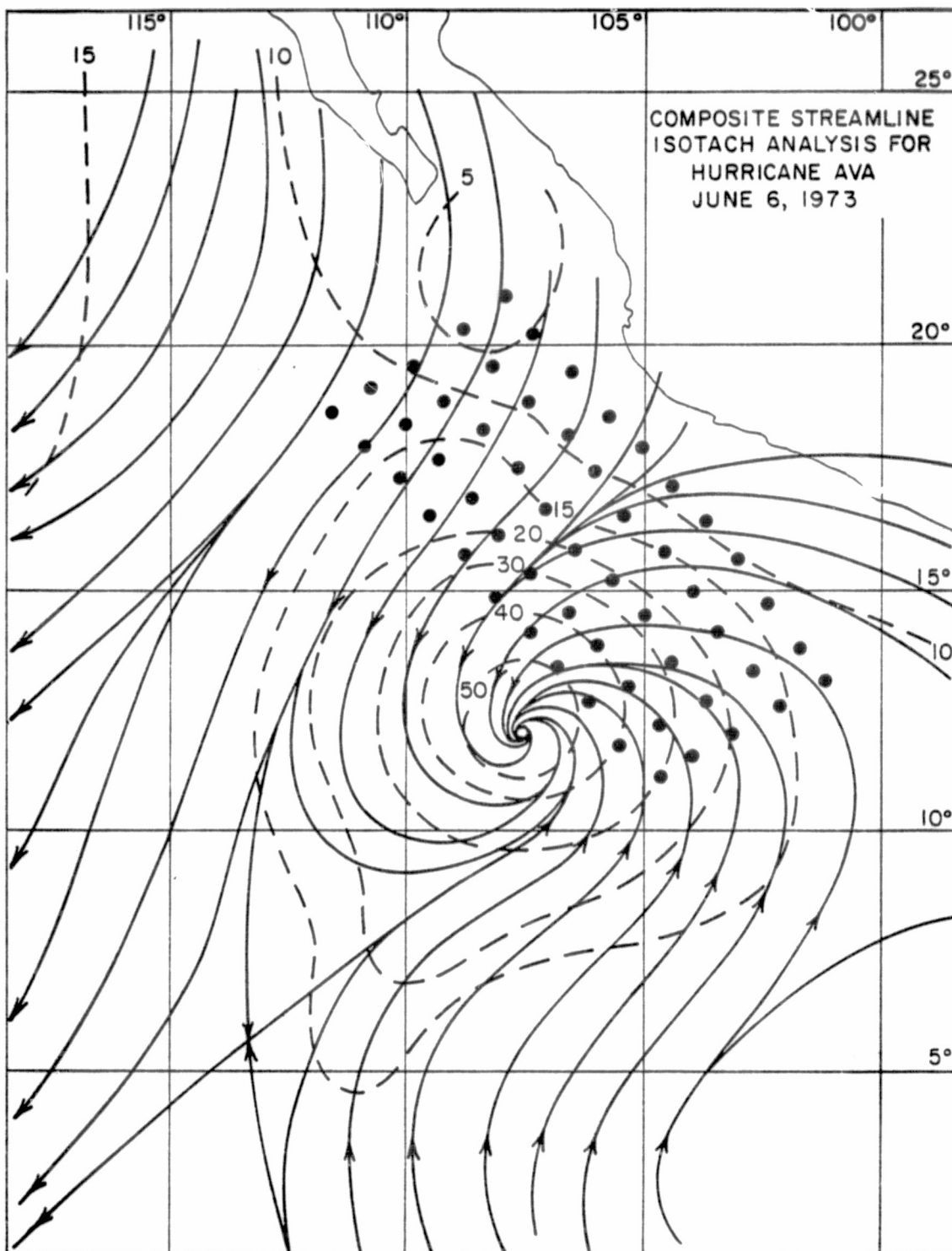


Figure 4.11 Composite analysis of
the surface wind field in AVA.

REPRODUCIBILITY OF THE
ORIGINAL PAGE IS POOR

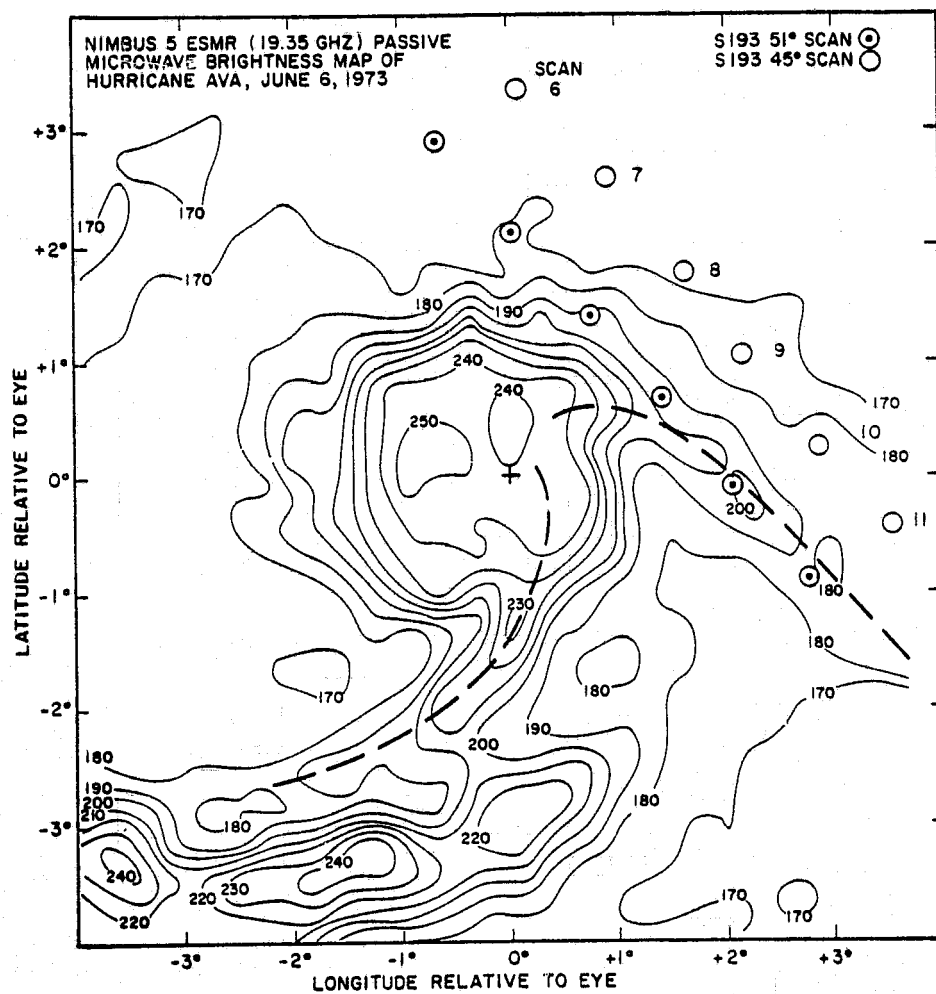


Figure 4.12 Composite of NIMBUS 5
ESMR brightness map and outer
incidence angle S193 scans in
AVA. All data plotted with
respect to moving eye of AVA.

It should be reemphasized at this point that some features of the hurricane surface wind field will be missed by this final analysis. The actual surface wind might be significantly higher or lower in the vicinity of spiral rain bands. While these bands cannot be precisely located in Ava some indication of those S193 cells that might be susceptible to such anomalies is provided by the passive microwave brightness pattern in Ava determined by the electrically scanned microwave radiometer (ESMR) on NIMBUS-5. This instrument operates at 19.35 GHz, has a field of view of 25 x 25 km at nadir and provides a pattern of brightness that can be transformed to categories of light, moderate or heavy precipitation averaged within the field of view (Allison et. al., 1974). The pattern of brightness temperature returned from Ava several hours before the Skylab pass is shown in Figure 4.12. The pattern has been shifted westward to account for the time difference, and some of the outer cells of the S193 scan of Ava have been superimposed. Because of uncertainties in position introduced by the shift in the pattern and possible changes in the precipitation pattern in the time between the NIMBUS and SKYLAB passes, Figure 4.12 should not be used to assign precipitation rates to the specific cells shown. However, it can be reliably stated that between scan 9 and 11, the 51° and 45° S193 cells were located either in or adjacent to one of the major bands feeding into Ava. Thus the backscatter at those cells could have been affected by the heavy rain itself associated with the band and by local increases and decreases in the wind speed.

Tropical Storm Christine. A tropical depression that was first noticed as it moved westward from the west African Coast on August 25, 1973, became a tropical storm in the central tropical Atlantic on August 30th and was named Christine. The storm was investigated by Air Force and Navy reconnaissance aircraft each day, thereafter, until it weakened

into a tropical wave on September 3. Christine never attained hurricane strength. However, it was intensifying toward hurricane strength late on September 1. At that time, the National Hurricane Center forecast continued strengthening to hurricane intensity and forecast it to continue moving westnorthwestward on a track that would bring the storm circulation within an S193 CTNC left scan pattern of a ZLV pass available the following day. In addition, a Navy reconnaissance aircraft was scheduled to investigate Christine on September 2. Thus, a nominal ZLV S193 pass was scheduled, and the Navy was requested to have its aircraft make low level wind observations and record them on their special in flight data logging system.

The general location of Christine at the time of pass and the region within which useful S193 data were taken is shown in Figure 4.13. This was a northbound pass and the instrument scanned only to the left of the track. Thus, the outer three rows of cells corresponding to the higher incidence angles scanned the most interesting part of Christine, that is the inner region of high winds around the center. In addition, the swath includes the wind gradient northeast of the storm where the trade winds are decreasing into the area of very light winds near the center of the subtropical high pressure system. The conventional surface wind data available from ships are shown in Figure 4.13. The almost total lack of such data within the area scanned is evident. This lack of surface wind data is also typical on a global scale of the information available about the winds in a tropical cyclone over most parts of the world ocean. The specification of the vector surface wind at the locations of the cells scanned therefore relied on the use of the tropical cyclone boundary layer model described above and applied to Ava.

The specification of the boundary layer model input parameters for Christine made use of the aircraft reconnaissance data almost exclusively. Unfortunately, the parameters are not as well defined as in the much more intense storm Ava. Christine was always a poorly organized cyclone, and

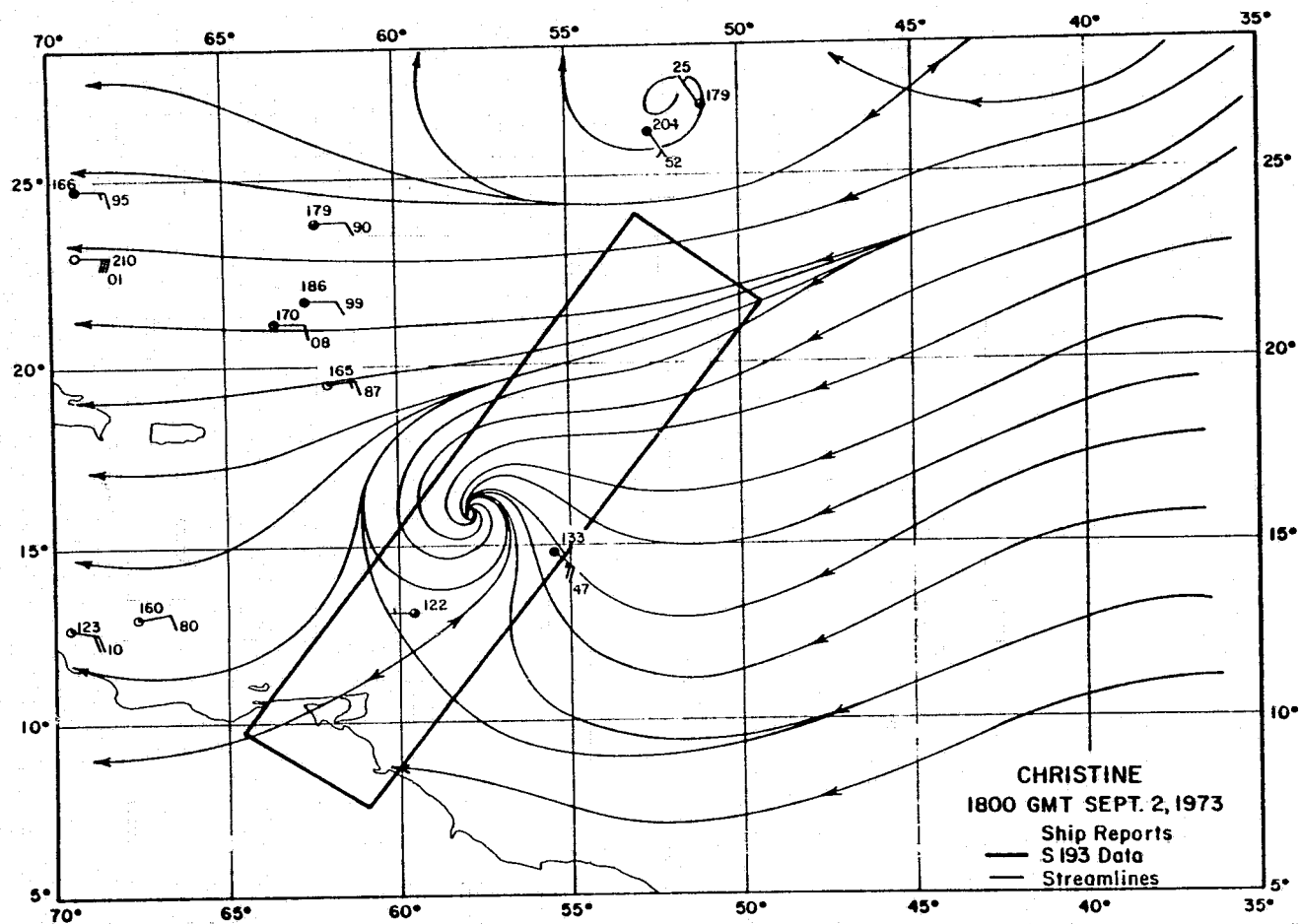


Figure 4.13 Location of S193
pass over tropical storm
Christine.

was apparently never in a steady state, particularly on the day of the pass. The track of the storm between September 1 and 3 and the variation of central pressure with time are shown in Figure 4.14. The storm reached maximum intensity about eight hours before the pass, at which time the Navy reconnaissance aircraft in the storm measured a central pressure of 996 millibars, maximum sustained winds of 62 knots at 10,000 feet, and estimated surface winds of about 65 knots. A dropsonde from the same aircraft made about an hour before the SKYLAB pass measured a central pressure of 1004 mb indicating that the storm had weakened considerably. This weakening was confirmed by similar observations from an Air Force reconnaissance aircraft that entered the storm center about six hours after the pass. From large scale pressure analyses at the time of the pass, the peripheral pressure was estimated at 1016 mb; thus the storm pressure anomaly at the time of the pass could be reliably fixed at 12 mb.

The determination of the characteristic scale of the storm, or R in equation (4.3), was not as simple. Christine was a large poorly organized storm, and the structure of its eye and eye wall was always poorly defined or non-existent. Indeed, Christine may never have had a well defined wind maximum at a single radius from the center. The data provided in the aircraft reconnaissance reports between September 1 and 3 were not consistent in this regard. Estimates of the radius to maximum wind ranged from 10 to 70 miles in this period. Greatest weight was given to the data in the "detailed vortex center messages" prepared by the observer on the Navy reconnaissance aircraft on the basis of penetrations at 0945 GMT and 1638 GMT on the day of the pass, which occurred between 1756 and 1801 GMT. In both penetrations, the maximum flight level wind was reported to be located 40 miles north of the center. This value was accepted since it was consistent with the low-level wind

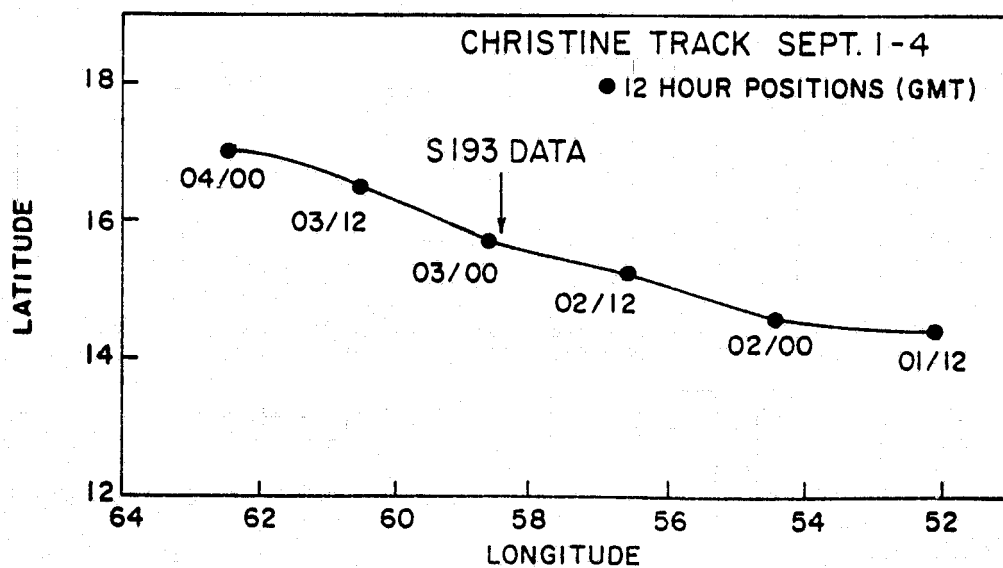
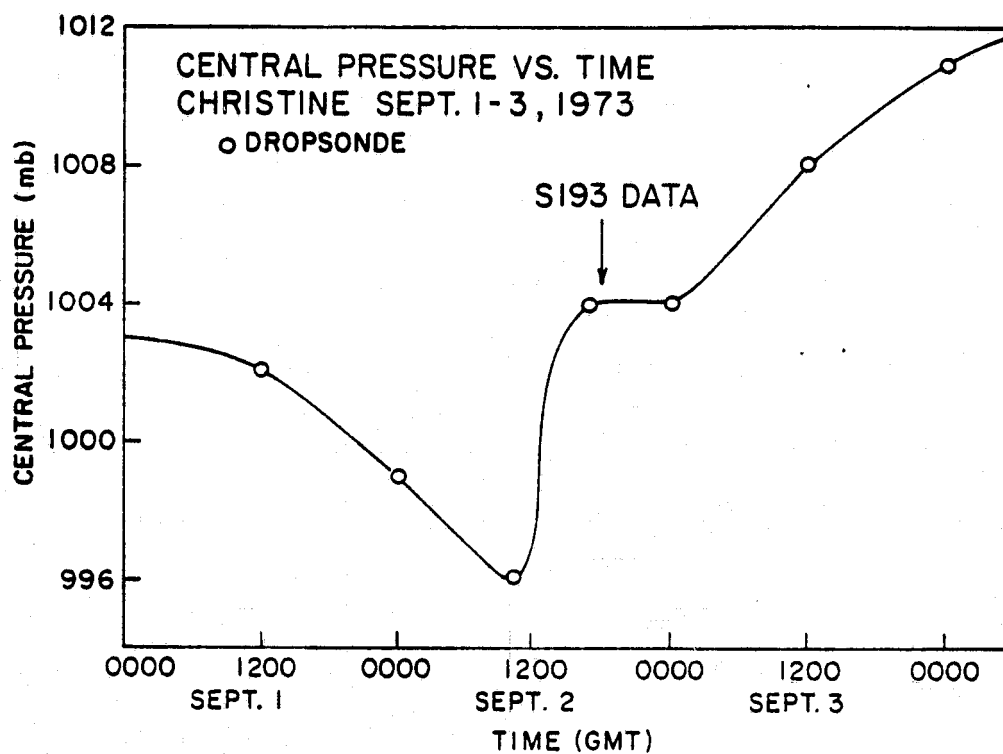


Figure 4.14 The track and variation of central pressure with time of tropical storm Christine.

measurements made by the aircraft as described below. Also, from the characteristics of the boundary layer model, it is known that for a slow moving storm like Christine, a radius to maximum wind of 40 nautical miles implies an exponential scale pressure (R) of about 60 nautical miles. The pressure profile corresponding to ΔP of 12 mb and R of 60 nautical miles. A pressure profile for $R_p = 60$ n.mi and $\Delta P = 12$ mb and $P_0 = 1004$ is shown in Figure 4.15 wherein it is compared to available observations.

The specification of the "steering flow" in Christine was complicated by the need to specify winds objectively from near the storm center and on into the subtropical high pressure cell. With regard to equation (4.2), the pressure pattern implies a variation of \vec{V}_g across Christine in a direction perpendicular to the track. This effect was modelled by a specification of a variable \vec{V}_g such that the magnitude of \vec{V}_g decreased exponentially with distance normal to the track away from a maximum value at the storm center. The direction, which is parallel to the storm track, did not change. In Christine, the large scale pressure field was close to the climatological pattern, and so \vec{V}_g was specified to be oriented along the track with a magnitude of 10 m/sec at the storm center, with half power points ($|\vec{V}_g| = 5$ m/sec) located 750 kilometers away from the center in a direction normal to the track.

The boundary layer model solution for the storm input parameters described above is shown in Figure 4.16. There is a pronounced asymmetry in the isotach pattern with maximum surface winds of 40-50 knots located 40 miles north and northeast of the center. The winds decrease to less than 10 knots in the northeast corner of the grid shown and to 2 knots on the outer most of the model nested grids (not shown). The location of the cells scanned by S193 and the vector winds specified by the model solution at those cells are shown schematically in Figure 4.17. The plot also shows the backscatter data for vertical polarization and identifies cells at which the passive microwave measurement indicated heavy precipitation.

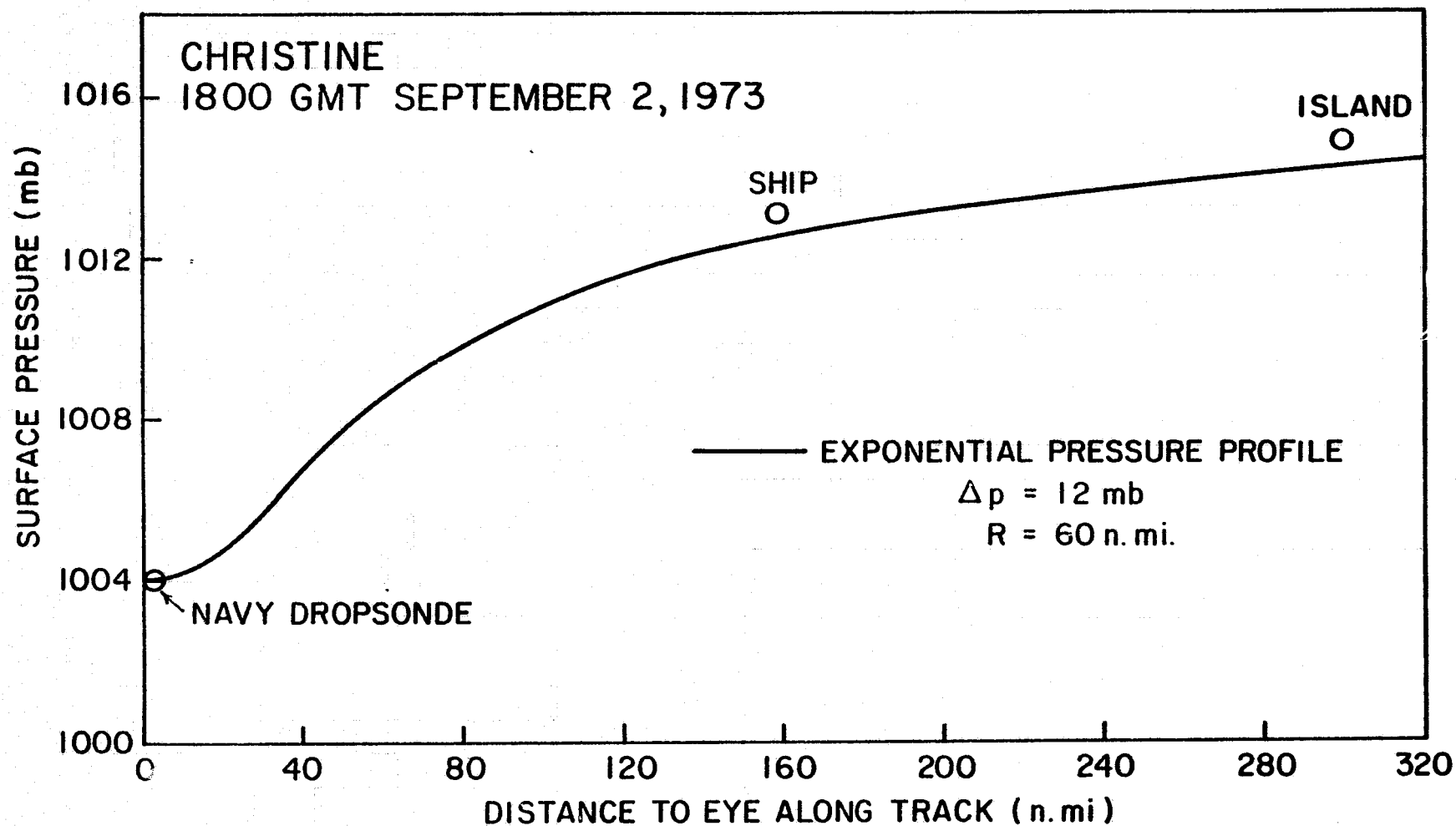


Figure 4.15 The variation of surface pressure with distance from the center of Christine in a direction along the track near the time of the S193 pass and the pressure profile used to initialize the boundary layer model.

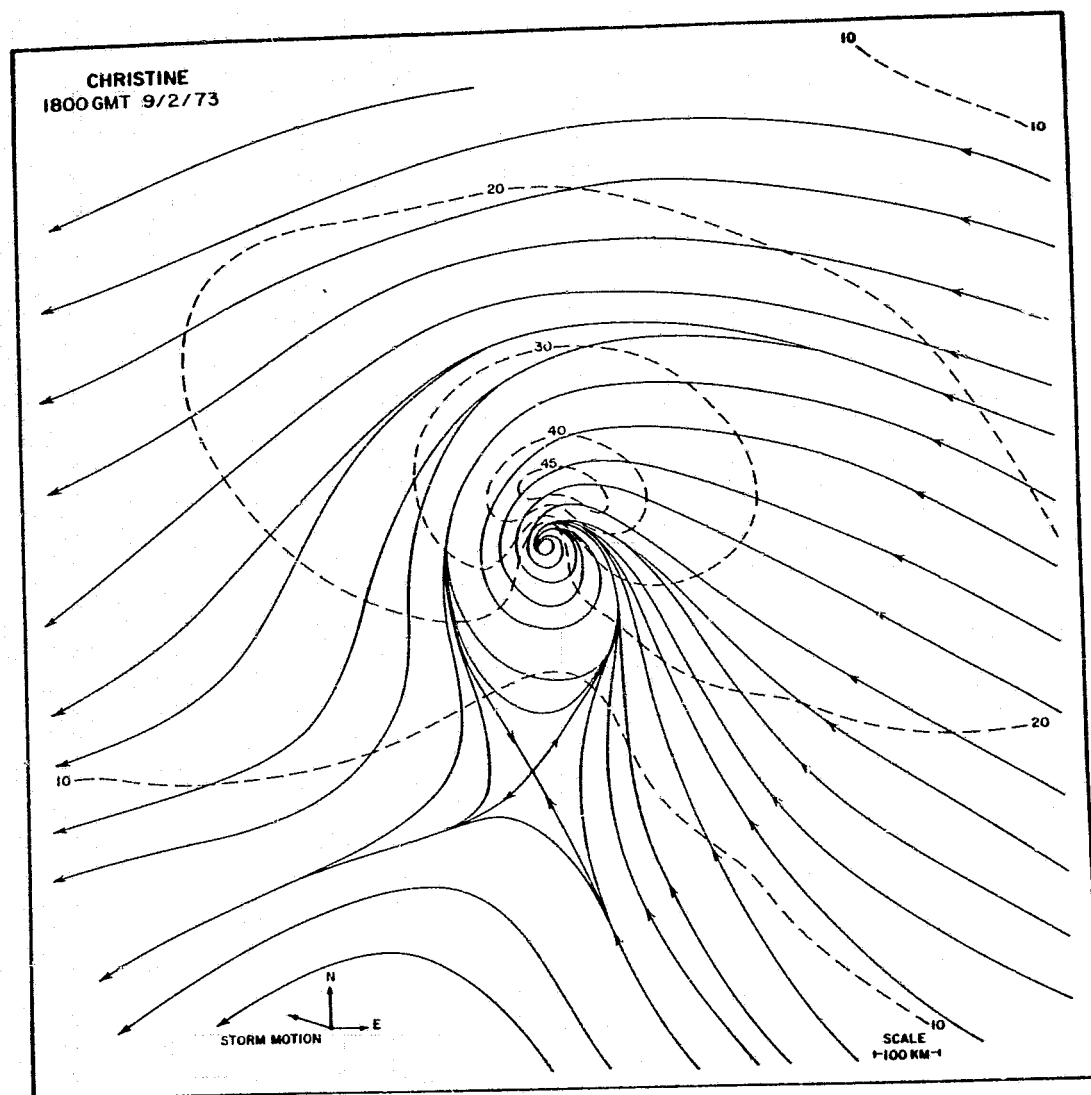


Figure 4.16 Boundary layer model solution for the effective 19.5 meter wind speed (isotach in knots) and direction (streamlines) in Christine.

σ_w vs Vector Wind
Christine
September 2, 1973
1800 GMT

Wind Speed Scale
0 10 20 30 40 50
Knots

σ_w (50°)

σ_w (42°)

σ_w (31°)

σ_w (20°)

σ_w (10°)

σ_w (0°)

σ_w (-10°)

σ_w (-20°)

σ_w (-30°)

σ_w (-40°)

σ_w (-50°)

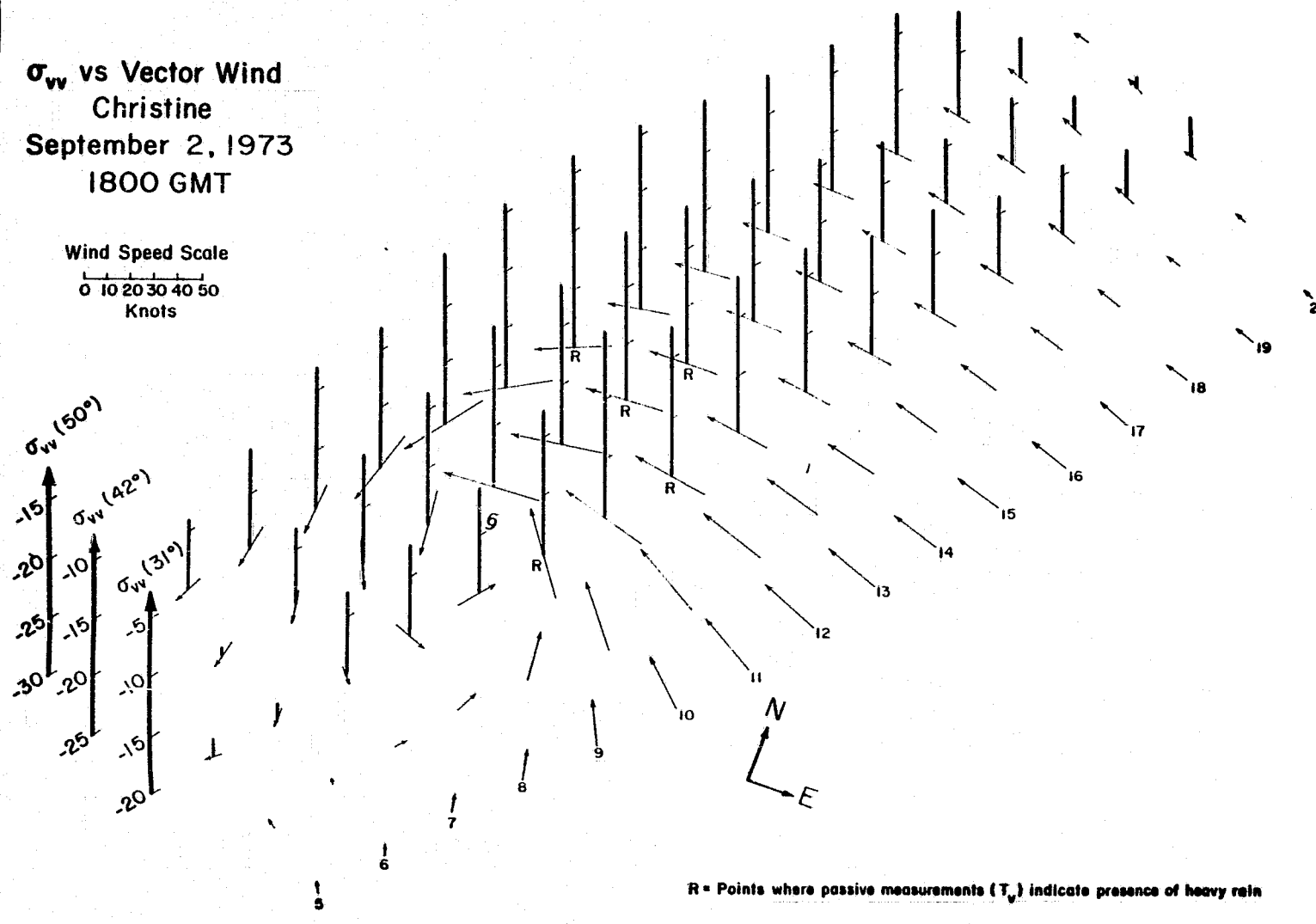


Figure 4.17 Comparison of the uncorrected backscatter measurements in Christine and the vector winds at the cells scanned.

It is not possible to determine the precipitation pattern in Christine precisely at the time of the pass. NIMBUS-5 ESMR data were not available for Christine on this day. An Air Force DAPP visible image made about 90 minutes before the S193 pass shows the overall cloud structure as given in Figure 4.18. The center of the storm is visible as a small relatively clear area surrounded by curved bands of moderately bright clouds. The dense cirrus canopy associated with Christine is seen to be displaced to the northeast of the low level circulation pattern of the storm and shields from view the cloud bands seen curving in from the south. That the banded cloud structure represents bands of heavy rain was verified by the Navy aircraft in its investigation of the northern and western parts of the storm. The following quote is taken from the remarks section of the 1638 GMT detailed vortex center message:

"RADAR PRESENTATION IMPROVED MARKEDLY, FIRST INDICATION HVY BUILD UP SW QUAD AROUND VORTEX. FEEDER ACTIVITY EXTENDS IN MULTIPLE HARD BANDS 150 NMI W SEMICIRCLE AND 100 NMI NE QUAD. SCTD TO BRKN CLOUDS IN EYE. TEMP PRESSURE AND WIND EYE COINCIDE."

This description is consistent with the DAPP image shown in Figure 4.18.

Some of the cells scanned in Christine were quite obviously affected by the rain bands. Additionally, it should be expected that the actual winds both at and near the cells affected will differ from those specified from the boundary layer model because of the characteristic anomalies in wind associated with the bands.

A study of the above description of how Christine was modelled for a SKYLAB pass between 1756 and 1801 shows that the central pressure was measured about eight hours before the pass, about one hour before the pass

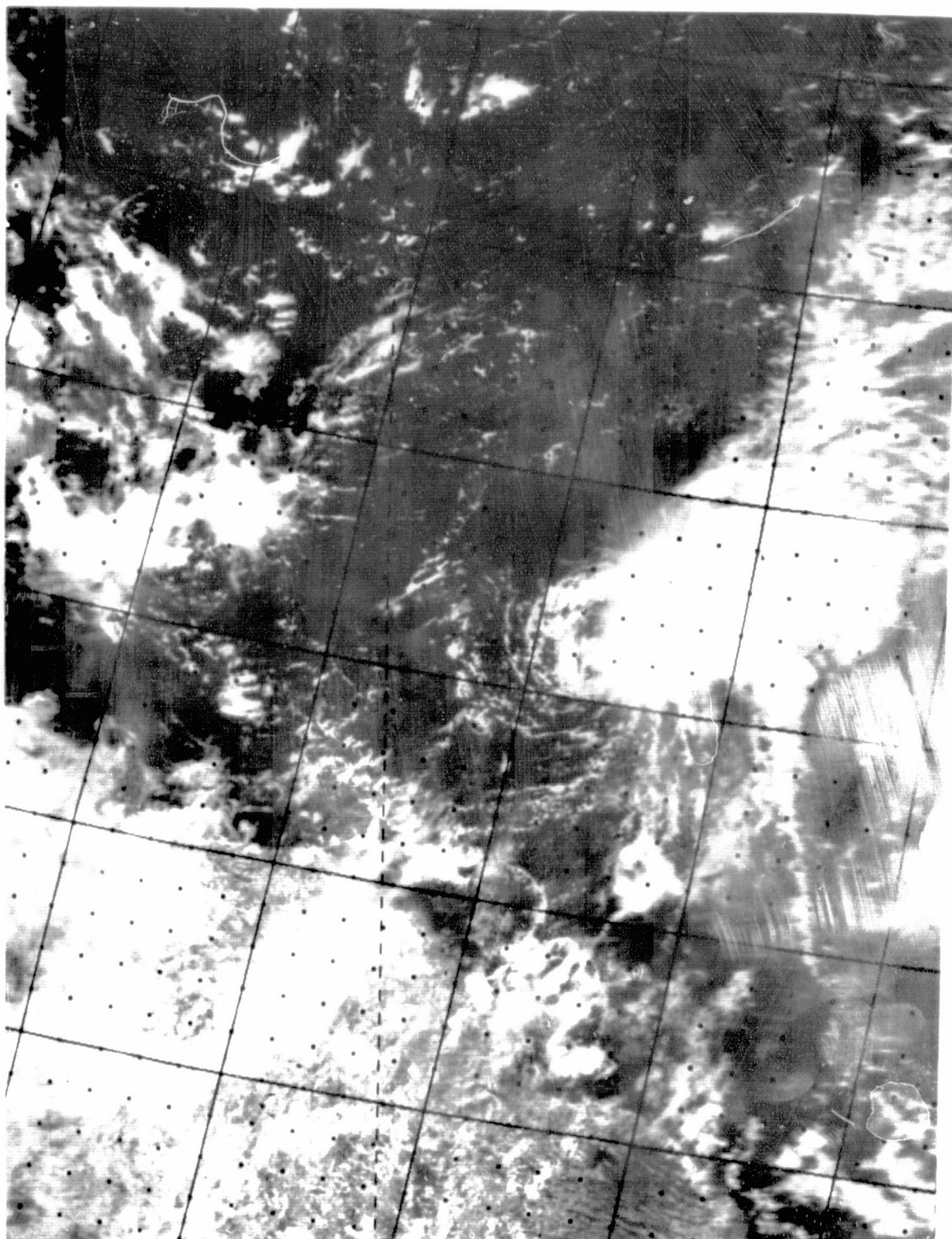


Figure 4.18 Air Force DAPP system
visible image of Christine at
1623 GMT, September 2, 1973.
(Thin straight streaks oriented
northwest to southeast were
introduced in the reproduction
and do not represent clouds).

and about six hours after the pass. The aircraft radar data were quoted for 1638 GMT and the DAPP pass was obtained at about 1630 GMT. Tropical storms and tropical hurricanes change in intensity with time over time scales of three to six hours and translate slowly at speeds of 5 to 10 m/s along a curved track. The universally applied technique for the study of these temporal and spatial changes is that of interpolation in space and time to bring all observations into agreement at a chosen time, which, in this situation, is the time of the SKYLAB pass. Because of the large scale coherency of the pressure and wind fields, these interpolation procedures yield reliable results.

A quantitative comparison of the modelled Christine winds with the low level winds measured by the Navy aircraft was not possible because the latter contained large systematic errors whose source has not yet been adequately explained. The winds measured by the aircraft at low flight levels around Christine between about 1200 GMT and 1700 GMT are shown in Figure 4.19. The points plotted represent 5 to 10 minute average flight level winds except for one detailed section south of the center where one minute averaged winds are plotted. The latter section particularly suggests a systematic error in one of the navigational parameters. The winds measured on the outbound leg appear to be too low in magnitude and exhibited too much inflow while the winds on the inbound leg appear to be too high in magnitude and exhibit too much outflow. The same can be said of the winds in the outbound and inbound legs measured north and west of the storm. Indeed, streamlines drawn parallel to the observed wind vectors would have anticyclonic rather than cyclonic curvature!

This type of error is reminiscent of the systematic error in winds derived from inertial navigation systems that is introduced by errors in the true air speed measurement. Ross^{*} developed a technique to remove

* personal communication

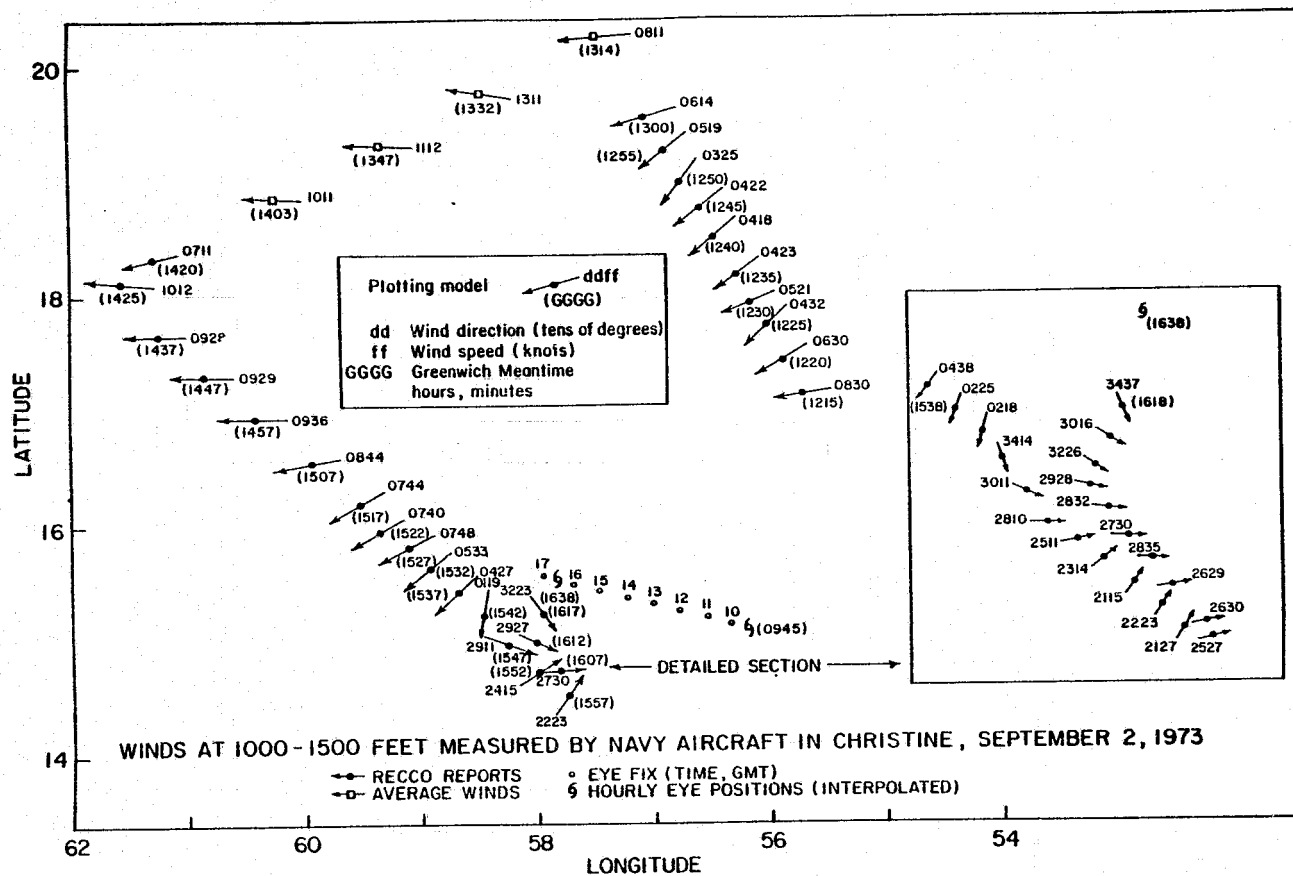


Figure 4.19 Flight level winds at 1000-1500 feet measured by a U.S. Navy reconnaissance aircraft in Christine on September 2, 1973.

this source of error from the measurements. The technique requires that on each aircraft mission, upwind and downwind runs be made in quick succession in a steady homogeneous wind field. In the case of Christine, the measurements were all made with the aircraft in a crosswind configuration. The large errors apparent in the data could, for example, occur from either a systematic error in the drift angle measurement or from a combination of true air speed and drift angle errors. It was not possible to correct the measurements since the source of the error is not precisely known and since the low level flight legs are all in regions of large wind variability.

SPECIFICATION OF THE WIND FIELD BY MANUSCRIPT SYNOPTIC ANALYSIS

Introduction. In a previous section, the subjective technique known as hand or manuscript synoptic analysis was described briefly. This section describes in detail the application of the method to the three passes for which it was used to specify the winds at the locations of all cells scanned by S193. The same technique was used to specify the winds at some of the cells scanned by S193 in the AVA pass as described in a previous section.

This technique was applied in favor of the objective techniques for several reasons. First, the three pertinent passes were all made over subtropical or tropical latitude - the passes of June 5 and 11 extended from the Gulf of Mexico southeastward into the Caribbean Sea and the pass of September 4 extended from the Caribbean northeastward into the subtropical North Atlantic. The analysis methods described in the previous section were inappropriate since tropical cyclones were not scanned in these cases. The objective technique to be described in the next section only works well in extratropical latitudes where the relationship between the sea level pressure distribution and the surface wind field is well defined and where the pressure field can be reasonably well defined by the available ship

reports. The pressure-wind relationship is more complex in the tropics and in addition the objective analyses of pressure that are possible in the tropics usually do not resolve the scales appropriate to the definition of the wind field. It is, therefore, generally accepted that the field of motion should be determined directly from the observations in the tropics. The basic problem, however, is that observations there, particularly over the tropical oceans, are very sparsely distributed. The observations that are available often do not represent the synoptic scale well because of local diurnal, orographic (in the case of land and coastal observations), or convective influences. As a result, the objective analysis programs that do extend to tropical latitudes usually define a field there that differs little from climatological persistence.

The subjective technique applied here allows the maximum utilization of available observations of the surface wind. The analyst is able to assess, at least qualitatively, the accuracy and representativeness of reports available at the synoptic observing time near the pass and to assimilate information from observations at adjacent observation times, say 6 to 12 hours on either side of the synoptic time near the pass.

The subjectivity in the analysis derived from the fact that the streamlines and isotachs are not drawn to fit the observations exactly, but to form a pattern that is the most likely a representation of the flow on the synoptic scale as deduced from all available information. The information includes the basic observations of surface winds from ships of various types, wind observations from island coastal land based stations, the large scale pressure pattern, and satellite photographs. Also, for the portions of two passes over the Gulf of Mexico that were underflown by NOAA C130 aircraft, the winds derived from the low level runs made by the aircraft were probably the most accurate data, and the

analysis could be made to fit these data most closely. The analyst also employs the concept of continuity in the process - that is, the pattern analyzed should be a logical evolution of the flow pattern in the recent past, say 24 to 48 hours.

A description of the data available and the analyses performed for each of these passes will now be provided.

June 5. The EREP made near 1800 GMT on June 5, 1973 in the ITNC mode, was the first pass in the Skylab experiment to provide S193 data. A preliminary analyses of the winds on this pass was reported in August, 1973 (Hayes et. al. 1973) at which time it was thought that S193 were taken only on the Gulf of Mexico portion track between the Texas and the Yucatan Peninsula. Actually, S193 data in the ITNC mode were acquired continuously until the track entered Panama. This final analysis, therefore, supercedes and extends the coverage of surface truth for this pass southeastward across the Caribbean Sea.

The general synoptic pattern in the vicinity of the June 5 pass and the surface data available near the pass time are shown in Figure 4.20. Since this was an ITNC pass, S193 data are available only very near the subsatellite track shown. Along this track, the data cluster into groups of five cells, one for each incidence angle, with the groups spaced about 60 miles apart along the track. Plotted in the figure are surface ship reports of weather, cloud cover, pressure and wind speed and direction and reports of pressure and occasionally wind at coastal stations. The reports at 1800 GMT were made within several minutes of the pass. Notice that there is not a single ship report within about 100 miles of the track for its entire length. Ship reports made at 1200 GMT June 5 and 0000 GMT June 6 are also plotted.

The pressure reports were used to draw the isobaric (lines of equal pressure) pattern over the region. This isobaric pattern is very much smoothed and is useful as an overall guide to the analysis of the winds.

Except within about 50 miles of the coast the synoptic scale winds over the sea should follow this pattern in that the flow should be nearly parallel to the isobars with the wind direction turned about 15 to 20° toward lower pressure and the speed of the wind inversely proportional to the spacing between the isobars. Even if the relationship between wind and pressure were known perfectly, it would not be possible to compute the surface flow from the pressure analysis shown since the gradients are too weak to be accurately defined by the sparse and error contaminated pressure measurements from the ships. Note the inconsistencies between the pressures reported by the cluster of four ships near 15°N 73°W and the smoothed analysis.

Within about 50 miles of a coast, the surface flow is strongly affected by the diurnal sea breeze circulation. That is, there is a component of the surface flow from sea to land from late morning through early evening and the reverse component at other times. The effect is particularly noticeable in Figure 4.20 in the reports from the northern, western and southern coasts of Cuba. While the sea breeze circulation is a mesoscale phenomenon, some of the S193 cells appear to have been affected by this effect, and the streamline isotach analysis was drawn to account for the expected influence of the sea breeze.

The final streamline-isotach analysis in the vicinity of the pass is shown in Figure 4.21. The surface wind measurements at 1800 GMT and winds derived from the low level portions of the NOAA C130 underflight are plotted in Figure 4.20. The aircraft measurements were useful in placing the 10, and especially the 13 knot, isotachs in the western Gulf of Mexico. The zone of 25 knot winds north of Panama is well defined by both on and off time ship reports. The report from Swan Island after adjustment to an equivalent over water wind was used to confirm the smooth increase in wind speed between Yucatan and Panama. The feature

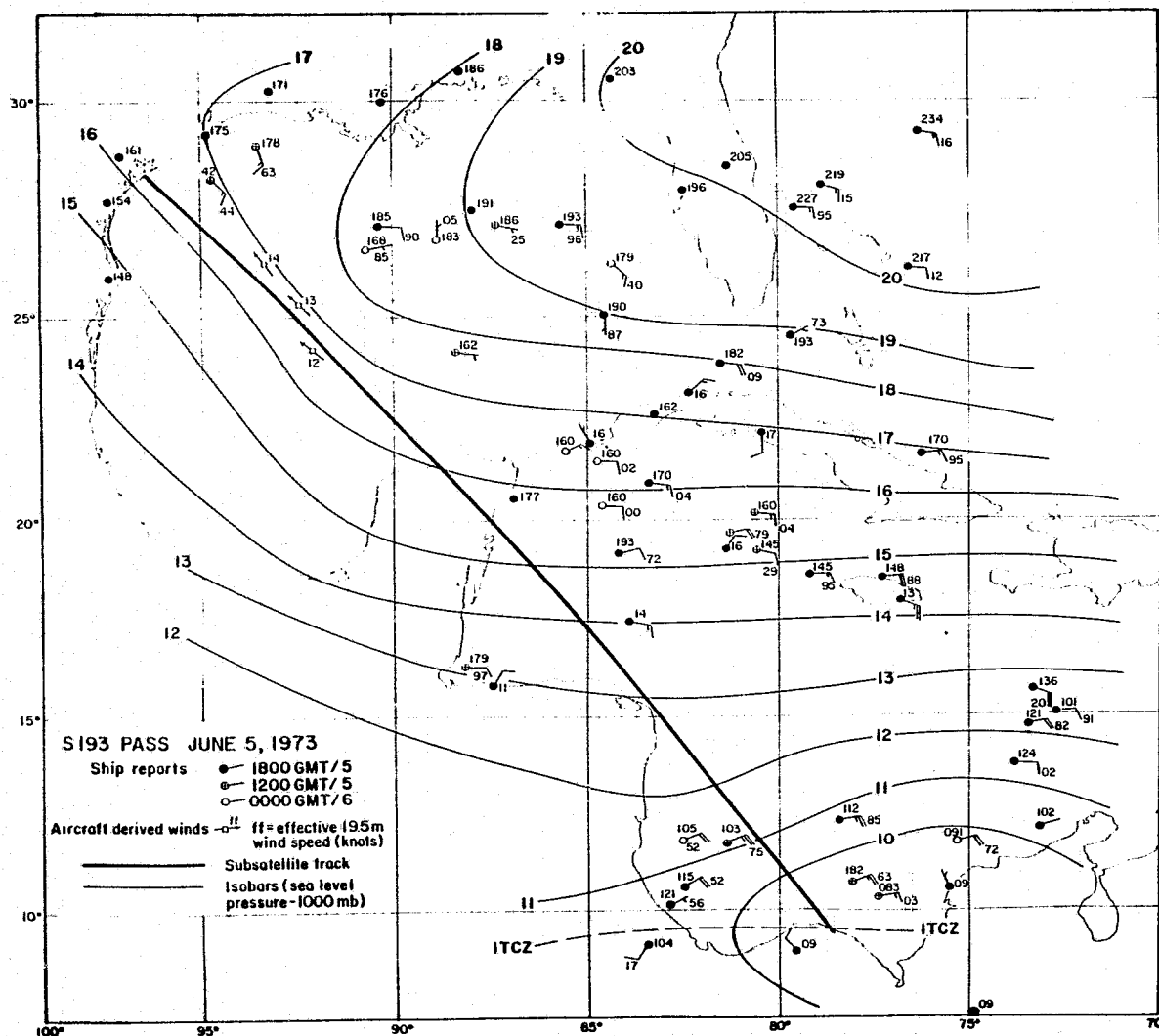


Figure 4.20 A composite of surface weather reports available in the region scanned by S193 on June 5, 1973, with a subjective isobaric analysis shown.

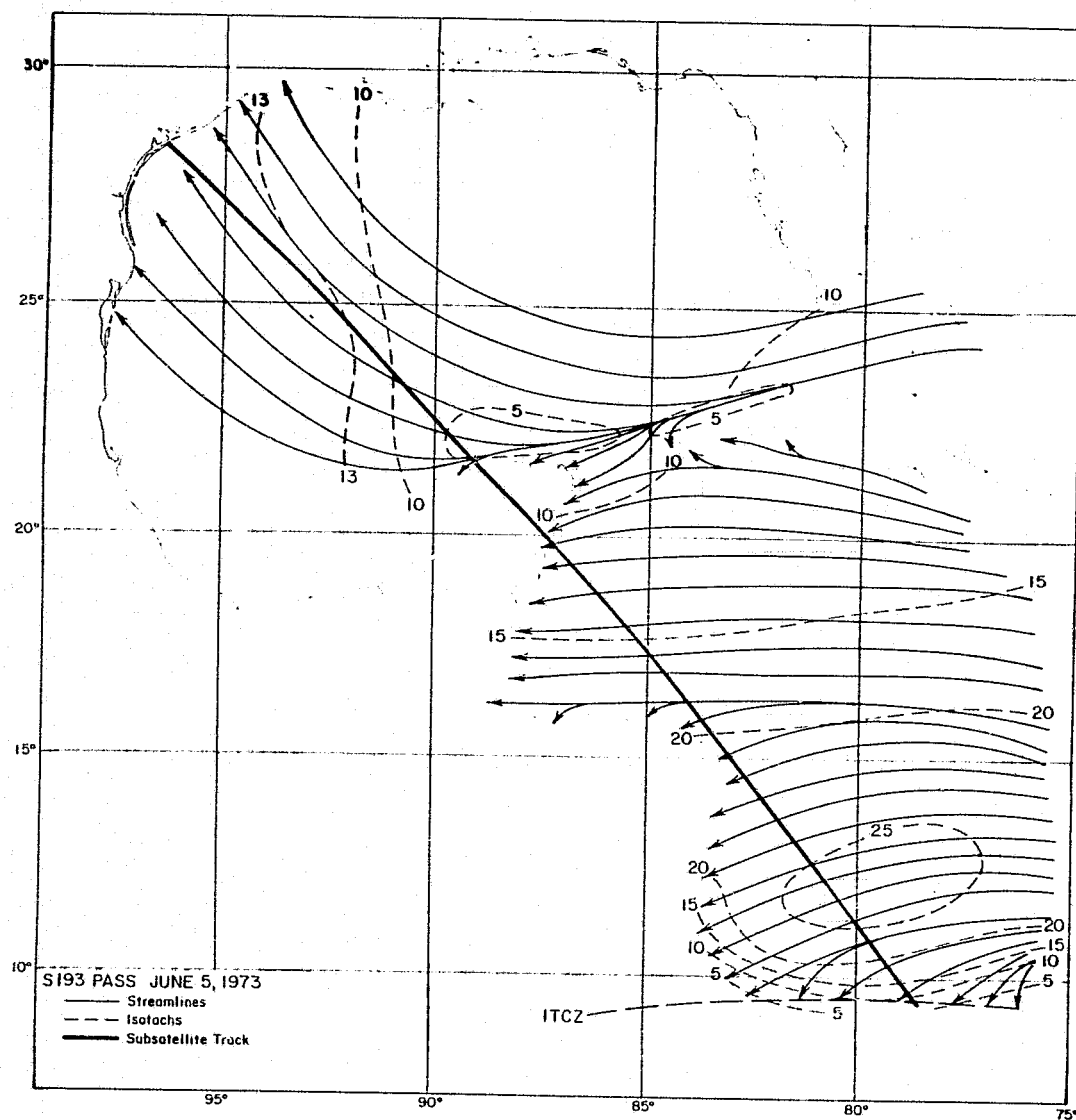


Figure 4.21 The surface wind streamline-isotach (knots) pattern in the vicinity of the area scanned by S193 on June 5, 1973.

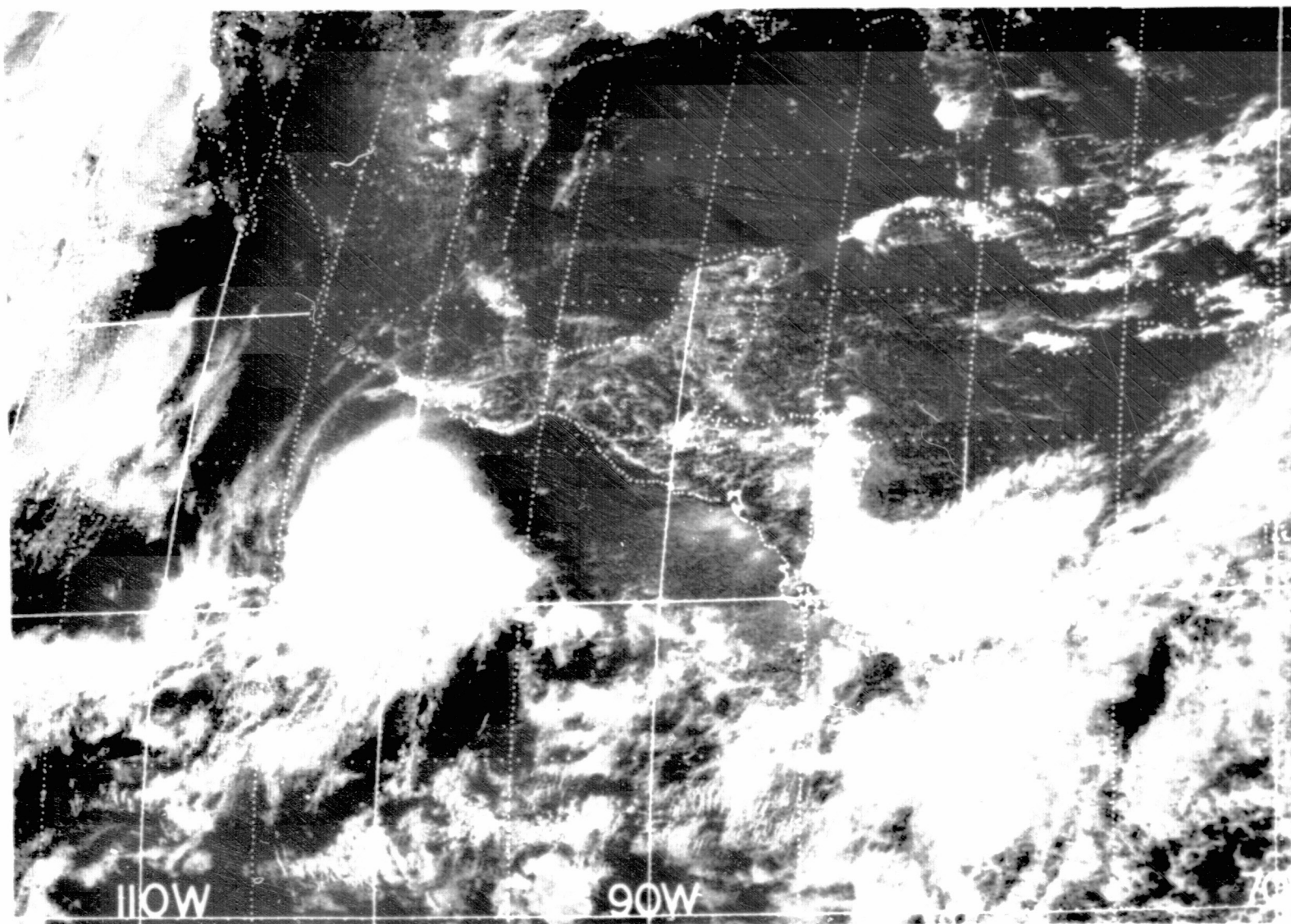


Figure 4.22 ATS-3 visible image
made at 1851 GMT of the area
scanned by S193 on June 5, 1973.

known as the intertropical convergence zone was positioned across the northern coast of Panama. This zone is accompanied by a trough of low pressure and near calm winds and thus caused the sharp gradient in the isotach pattern in that area. The wind speed and direction at each S193 cell was obtained by visual interpolation of values to the locations of the cells from the appropriate streamlines and isotachs in the vicinity of the cell.

Figure 4.22 is an ATS visible image of the area near the time of the pass. As verified also by the ship reports, and in great detail by a mosaic of photographs made from Skylab, most of the Gulf of Mexico and northern Caribbean were characterized by scattered patches and lines of shallow cumulus clouds. Dense patches of cloudiness covered the southwestern Caribbean. Several ships located beneath this cloud pattern indicate rain showers that are apparently widely scattered.

June 11. A nominal EREP pass was made on June 11, 1973 with S193 operated over water between 1520 GMT and 1524 GMT. In this pass over ocean S193 data were obtained continuously from just south of the Louisiana Coast southeastward across the Gulf of Mexico and on into the Caribbean Sea. The subsatellite track just touched the western tip of Cuba and some of the cells were apparently affected by that land mass.

Since the pass occurred almost midway between the standard six hourly surface weather reporting times, ship reports from 1200 GMT and 1800 GMT were examined to reveal the wind distribution. Reports from a then experimental data buoy located about 90 miles east of the track in the north central Gulf of Mexico were available at three hour intervals. A NOAA C130 low level underflight provided important wind measurements beneath the pass from near the northern coast of Cuba northwestward for about 300 miles along the track. Winds reported by the ships, the buoy and the aircraft after reduction to the 20 meter level are plotted in Figure 4.23.

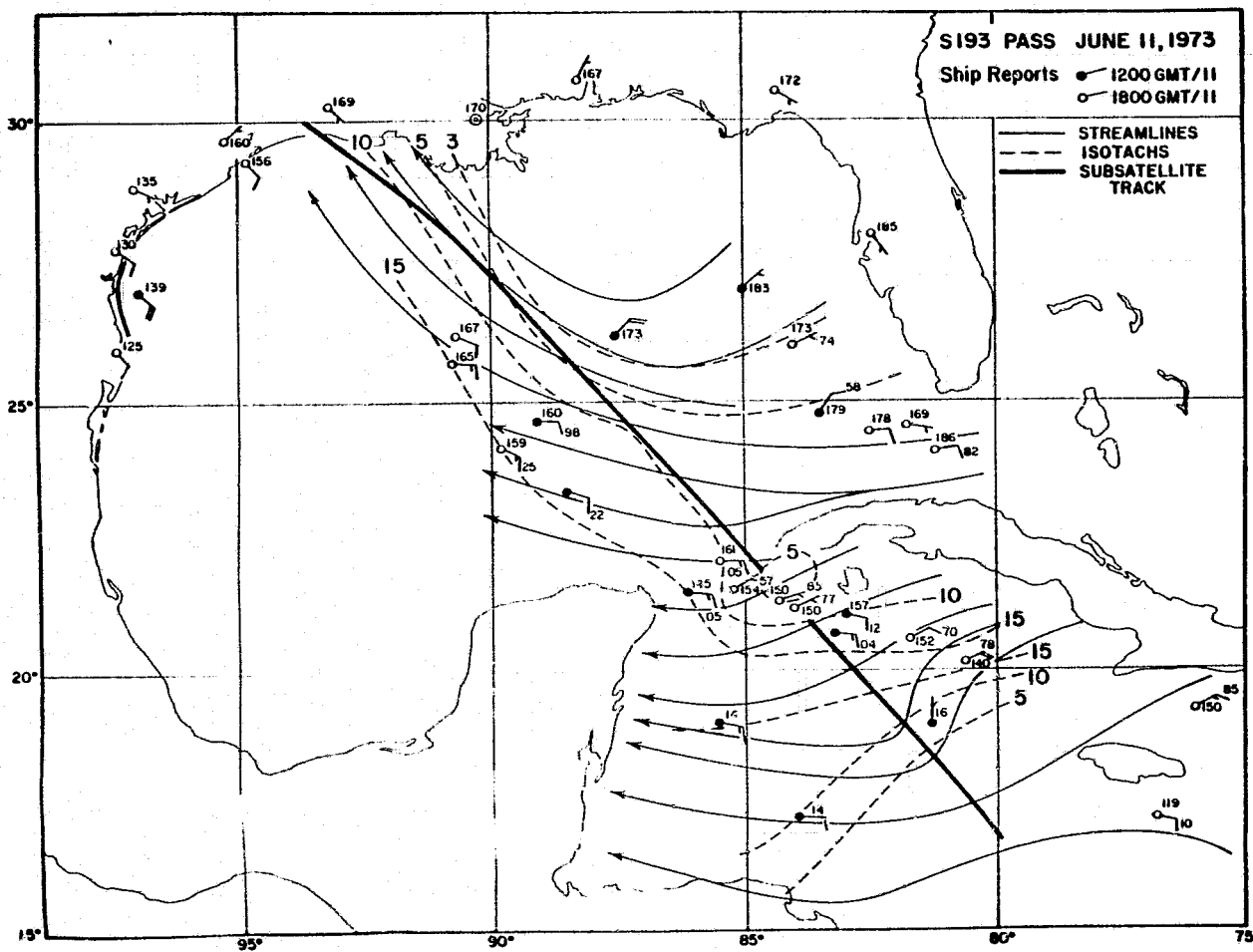


Figure 4.23 Surface wind streamline-isotach (knots) pattern in the area scanned by S193 on June 11, 1973, with the available surface wind reports shown.

The streamline-isotach analysis drawn to the available observations is superimposed on Figure 4.23. In contrast to the June 5 pass, there are quite a few reports in the immediate vicinity of the track, though except for the buoy and aircraft reports, the observations were made three hours before, or after, the pass. Nevertheless, the overall synoptic pattern should be quite stable in this area. The data allowed the resolution of the indicated detailed structure in the isotach pattern. The aircraft reports defined the gradual increase in wind speed southeastward along the track in the Gulf of Mexico along with the shift in wind direction from southeasterly west of the buoy position to easterly just north of Cuba. The numerous ship reports near and south of the western tip of Cuba define the area of very light winds there. In general, winds were quite light along the entire pass with maximum winds of about 15 knots indicated toward the end of the pass in the northern Caribbean Sea.

The cloud cover beneath the pass is shown in the ATS-3 visible image made at 1456 GMT (Figure 4.24). Only the northwestern end of the track is seen to be affected by the mass of cloudiness extending into the north central Gulf of Mexico from Louisiana. The nature of this cloud mass is shown in a high resolution visible DAPP image made at 1753 GMT (Figure 4.25). The image reveals numerous convective cloud clusters embedded in the cloud mass with more widely scattered convective elements east and south of the pass that were not resolved in the ATS image. The gray area in the DAPP image represents cirrus cloudiness formed at the tops of the cumulonimbus clouds that are present or have recently dissipated. Several active thunderstorms are evident, so that heavy rain could have affected some of the S193 cells in the northwestern portion of the pass.

September 4. Two days after the S193 pass over tropical storm Christine, S193 data were acquired on a northbound track that extended from northern Venezuela northeastward over Puerto Rico and on into the

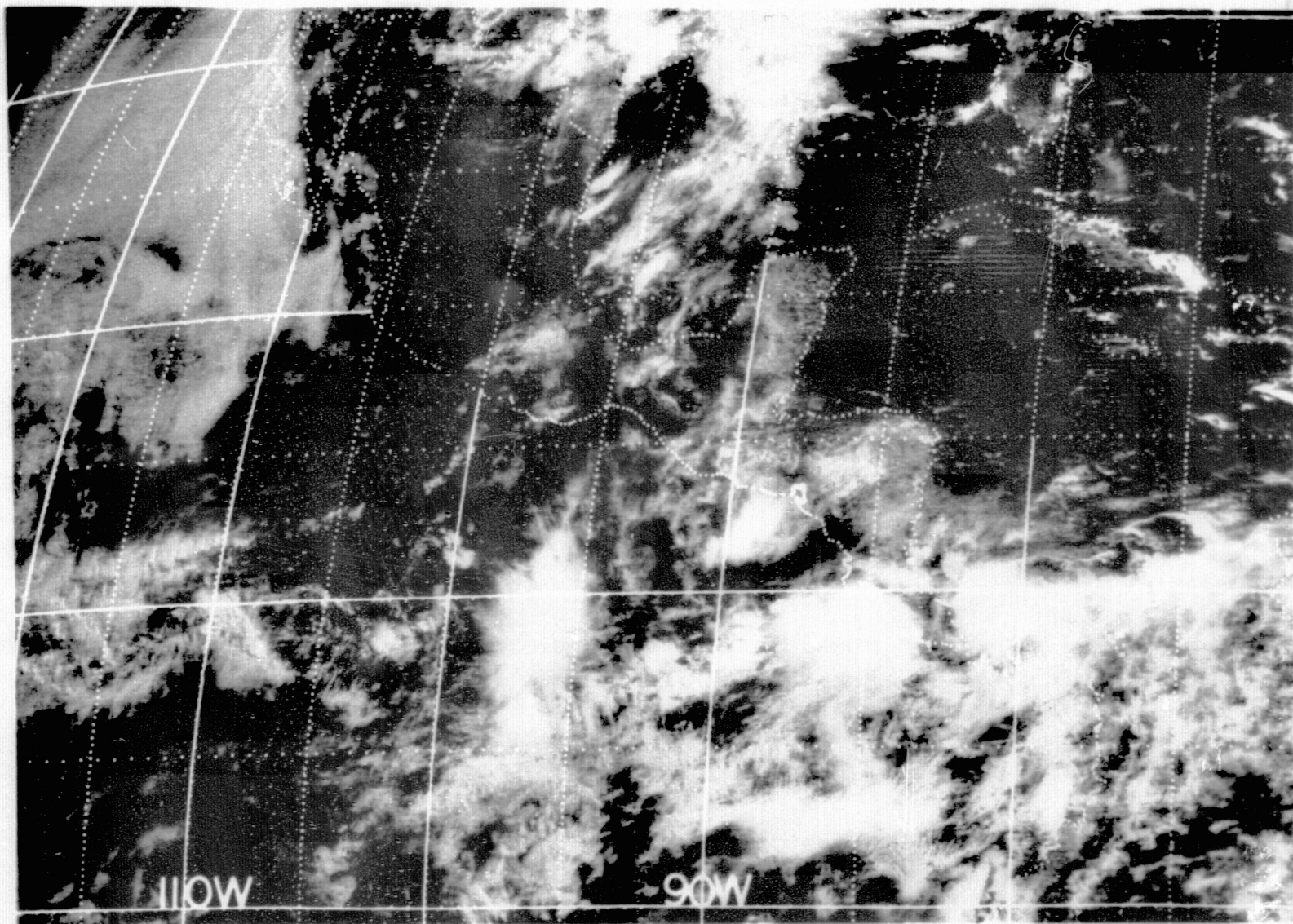


Figure 4.24 ATS-3 visible image
made at 1456 GMT of the area
scanned by S193 on June 11, 1973.

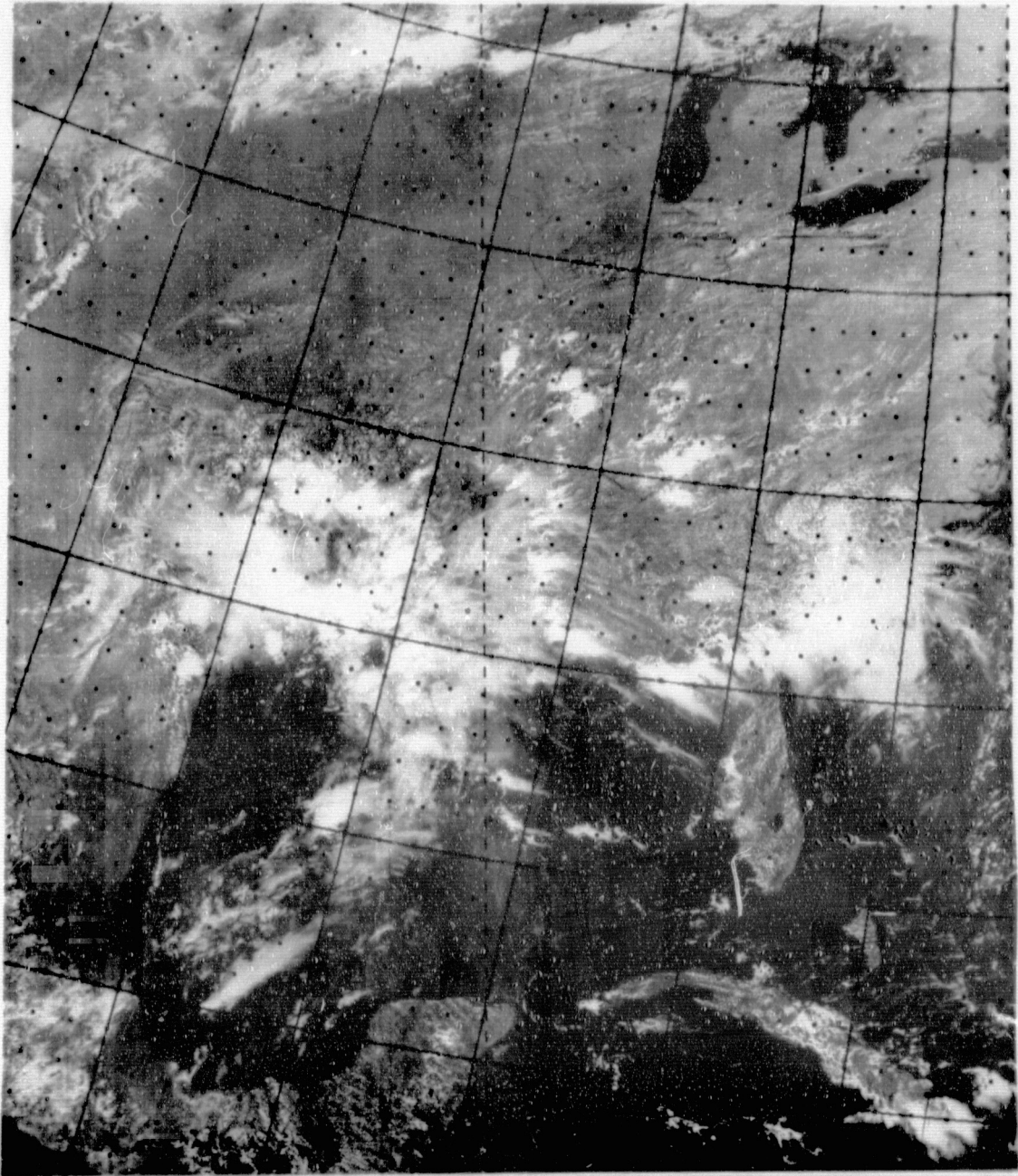


Figure 4.25 Air Force satellite
DAPP visible image made at 1753
GMT of the area scanned by S193
on June 11, 1973.

subtropical North Atlantic. The instrument scanned to the right of the track in the CTNC mode between 1802 and 1809 GMT. Of the 29 scans made, 22 were over water with the exception of a few cells that were affected by Puerto Rico and the Virgin and Leeward Islands.

Early on September 4, the NOAA National Hurricane Center had downgraded Christine to a tropical wave, which meant that a closed cyclonic circulation no longer existed and that peak winds were well below tropical storm strength. The wave progressed westward during the fourth and was positioned at about the longitude of central Puerto Rico at the time of the pass. Its passage across the eastern end of that island was accompanied by heavy squalls and gusty winds. San Juan experienced winds of 35 mph with gusts to 50 mph on the morning of the fourth but this heavy squall activity diminished considerably by the time of the pass.

Ship reports near the pass time (1800 GMT) and those at 1200 GMT and 0000 GMT, September 5 are plotted in Figure 4.26. The smooth streamline-isotach analysis drawn to the observations is based upon the assumption that Christine had completely degenerated into an easterly wave at the time of the pass. It is, however, quite possible that a small closed circulation was embedded in the wave just north of Puerto Rico as evidenced by the light southwesterly wind at San Juan at 1800 GMT. However, in the absence of over ocean measurements either from ships or aircraft in the area as well as along the axis of the wave over the Caribbean, it was not possible even to attempt to define such a feature. The complete absence of ship reports in the Caribbean within the scan pattern also makes the isotach analysis there suspect. The analysis is much more reliable northeast of the islands where the available observations define the smooth streamline pattern and fairly complex isotach pattern. In this portion of the pass the winds decrease from 20 to 25 knots just north of the Leeward and Virgin Islands to less than 5 knots very close to the center of the subtropical high pressure system.

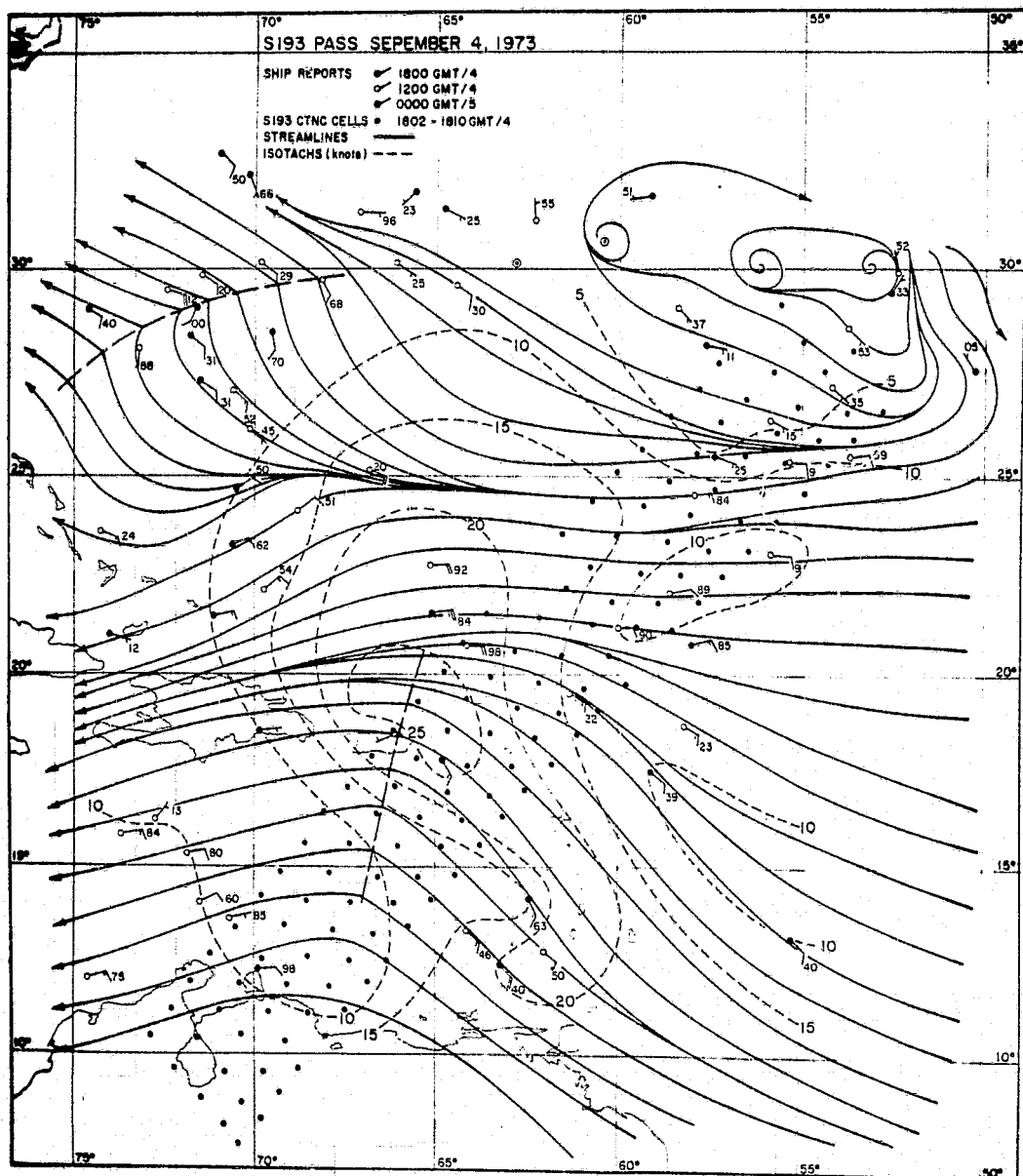


Figure 4.26 Streamline-isotach pattern in the vicinity of the tropical wave scanned by S193 on September 4, 1973. Surface wind reports are plotted.

At that time of the pass, the tropical wave was accompanied by considerable rain shower activity, particularly along and just east of the axis of the wave. The passive S193 measurements indicated that some of the cells were indeed affected by these heavy rain showers.

NORTHERN HEMISPHERE OBJECTIVE WIND FIELD ANALYSIS

The Objective Analysis Program. For all SL 4 passes and for those SL 2/3 passes not discussed previously, the surface winds at the S193 cells were calculated by linear interpolation in space and time from a file of surface (effective 19.5 meter) winds available at six hour intervals on a grid of points covering the oceanic parts of the Northern Hemisphere. This file of surface wind analyses was produced by the application of computer based procedures described by Cardone (1969) and since modified as described herein. The basic structure of the objective analysis scheme actually dates back to the study of Thomasell and Welsh (1963). In this section the overall objective analysis procedure will be outlined. The planetary boundary layer (PBL) model employed in the procedure will be outlined in the next section. Then the objective winds will be compared to special measurements made by aircraft and weather ships for certain passes. Finally the results of a study of the errors in the specification of the vector wind by the objective procedure will be presented.

The basic components of the analysis scheme and the flow of the computer procedure are shown in Figure 4.27. The basic input information available at six hour intervals consists of ship reports of the standard meteorological variables: wind speed and direction, sea level pressure, air temperature and sea surface temperature. The procedures either directly or indirectly use all of this information in the specification of the vector surface wind and stress. For the Skylab period, a file of all available Northern Hemisphere ship reports

was obtained from FNWC. In addition, the analyzed fields of sea level pressure and air temperature as produced objectively in the operational analysis-forecast cycle at FNWC were also obtained. These analyses are available at six hour intervals for pressure and twelve hour intervals for surface air temperature on a grid system known as the JNWP, or more recently the NMC grid, which consists of a rectangular array of grid points on a polar stereographic projection of the Northern Hemisphere, with a grid spacing in mid-latitudes of about 200 n.mi.

The first step in the analysis procedure at a given synoptic time is a calculation at each grid point of the wind distribution as a function of height in the boundary layer from the marine planetary boundary layer theory described by Cardone (1969), which was reviewed qualitatively in the introduction to this chapter. Basically, the sea level pressure field and air temperature field are used to compute the surface geostrophic wind speed and direction, the thermal wind speed and direction and the angle between the thermal wind and geostrophic wind. The pressure-vector wind relationship implied in the boundary layer model then provides an estimate of the vector wind and stress at each grid point that can be used even if no direct observations of the wind are available. The accuracy of this estimate will be limited both by the quality of the input fields, which can be quite in error over data sparse ocean areas and by certain theoretical limitations in the PBL theory as discussed below.

It is known that conventional ships observations of wind speed and direction despite their inherent errors can improve estimates of the wind derived from pressure wind relationships (see e.g. Thomasell and Welsh, (1963) more recently Lewis and Grayson, (1972)). Much of the procedure as shown schematically in Figure 4.27 involves the incorporation of these reports into the analysis. To allow a more accurate incorporation of

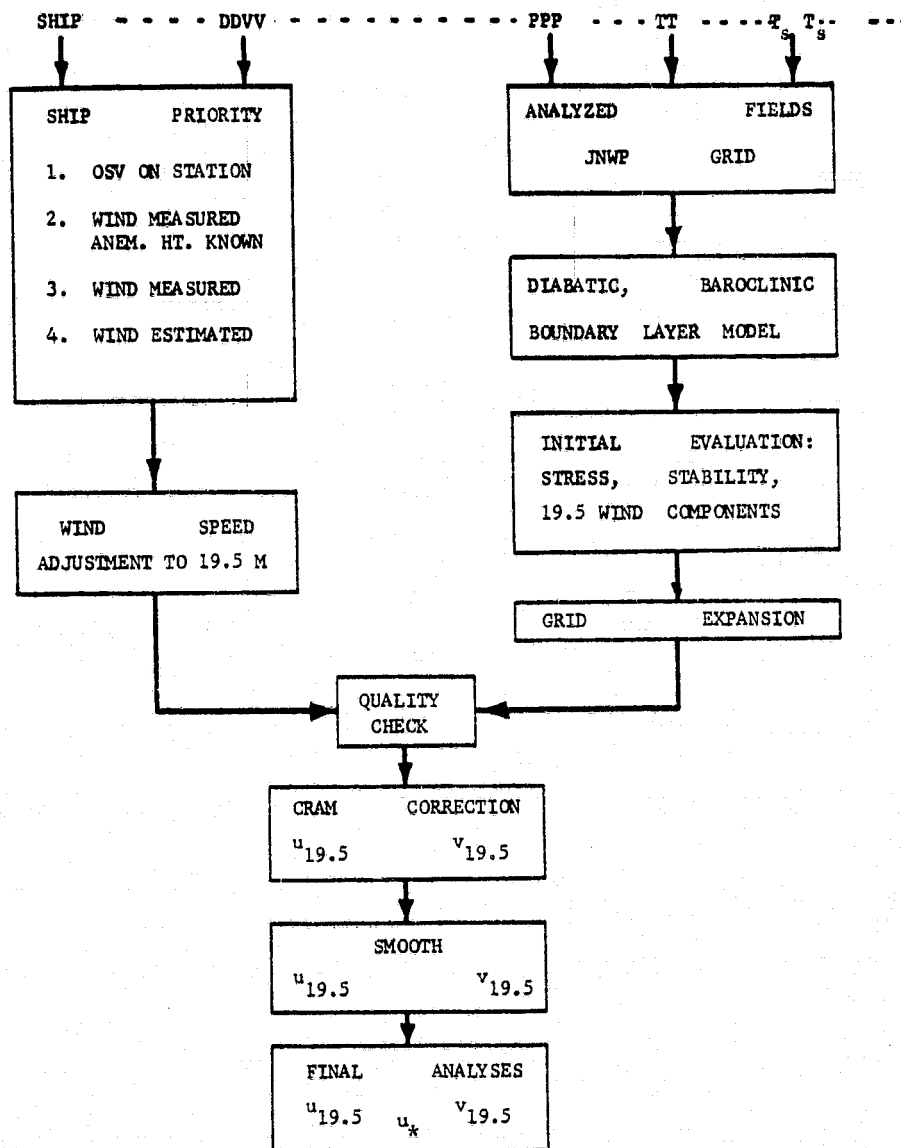


Figure 4.27 Generalized flow chart of the objective analysis program for surface winds in the planetary boundary layer in the Northern Hemisphere.

observations into the initial guess field and also to allow for the possibility of a smaller scale analysis where the data permit, the initial guess field is expanded to a grid system in which the JNWP grid spacing has been halved, creating four times as many grid points (125 x 125). The grid is shown in Figure 4.28 on which the land-sea distribution is shown. The analysis scheme is operative only on the "sea" grid points. In the procedure new grid point information is generated by fitting a curvilinear surface to the four grid points surrounding the generated grid point and interpolating the surface to the position of the grid point.

The objective analysis procedure incorporates ships' wind observations in a manner consistent with the nature and suspected accuracy of the observations. Observations from fixed weather ships are given highest priority, followed by winds from ships with anemometers at a known height, winds from ships with anemometer at some unknown height, and finally by winds estimated with the Beaufort scale. Each report is converted to the so-called effective 19.5 meter wind, that is, the wind that would exist at 19.5 m in neutral stability for the indicated surface stress.

Prior to incorporation into the analysis, the ship reports are individually checked for gross errors by comparing the reported wind speed and direction to that interpolated to the position of the ship from the initial guess field. If the difference of either exceeds a preset limit, the observation is discarded; otherwise, the ship report is used to correct the nearest grid point. For the analyses performed for the Skylab study, the limits on the wind were 30 knots for speed and 70° for direction.

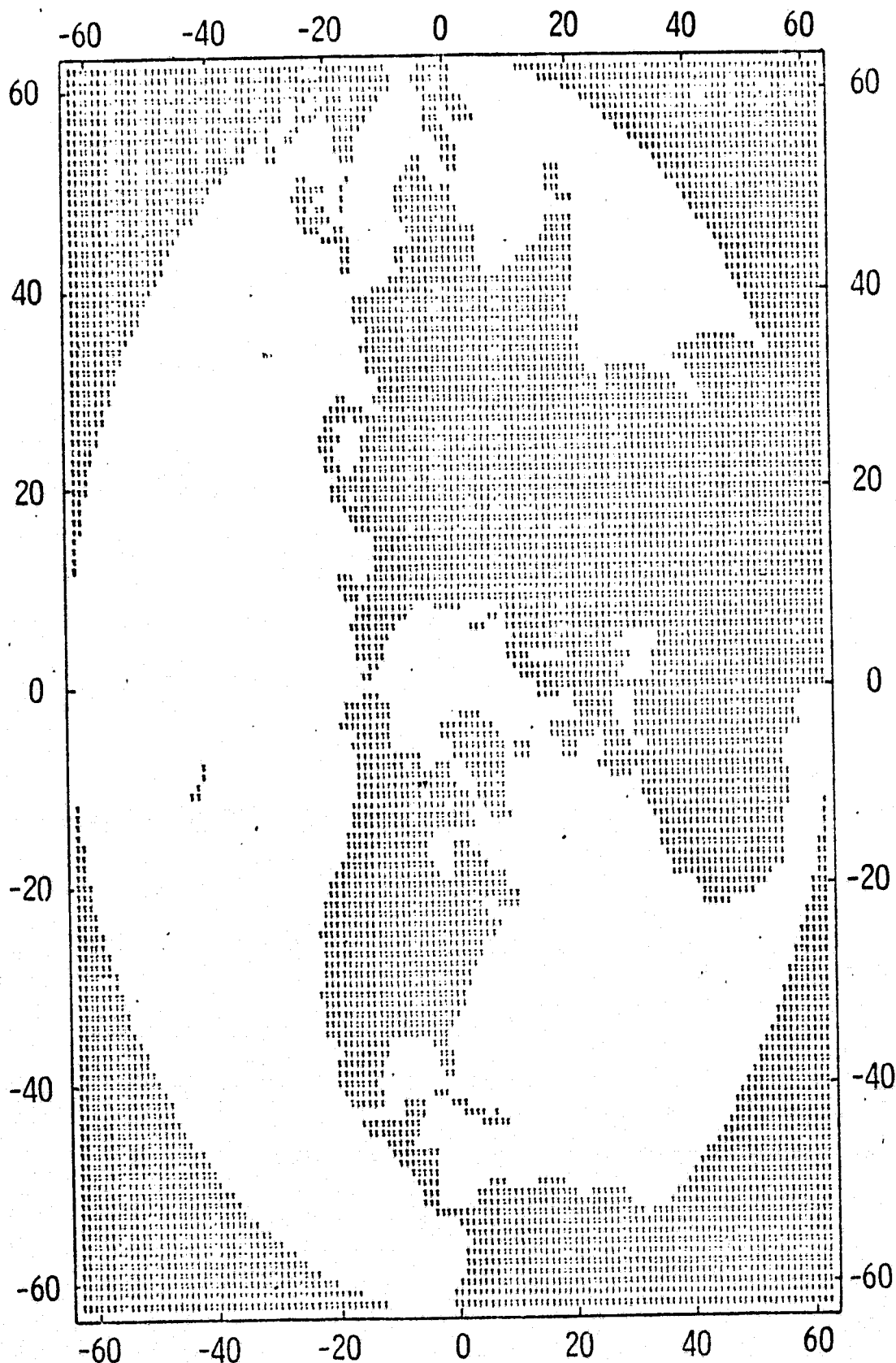


Figure 4.28 Expanded NMC grid used to specify the winds in the Northern Hemisphere objectively.

The influence of ship reports is expanded to portions of the grid not directly corrected by the observations by the application of the so-called Conditional Relaxation Analysis Method (CRAM) (see e.g., Harris, Thomasell and Welsh, (1966)). CRAM is applied to meridional and zonal effective 19.5 meter winds separately. The method requires grid point (i,j) values of the analysis parameter, say, $Q(i,j)$ to satisfy Poisson's equation

$$\nabla^2 Q(i,j) = F(i,j) \quad (4.4)$$

where ∇^2 is the two-dimensional finite difference Laplacian operator, subject to the constraints of the observations acting as internal boundary points and a set of perimeter boundary points. The forcing function $F(i,j)$ defines the shape of the Q field and is computed from the initial guess field of the parameter, $Q_g(i,j)$ as in equation (4.5).

$$F(i,j) = \nabla^2 Q_g(i,j) \quad (4.5)$$

The initial guess field determines the values of Q along the boundary of the grid system and may also be employed to translate observations to grid points prior to CRAM. If the grid spacing is small enough, this may be done accurately by interpolating the initial guess field to the position of the observation through curvilinear surface fitting to the four grid points surrounding the observation and translating the difference between the observed and interpolated values to the nearest grid point, thereby creating an internal boundary point.

After all observations have been translated to grid points, Poisson's equation is solved by a relaxation procedure. The small-scale noise in the resulting analysis due to fitting erroneous or unrepresentative data can be partially eliminated by applying a smoothing operator as given by Shuman (1957).

$$Q(i,j) = \frac{Q(i,j) + b\bar{Q}(i,j)}{1 + b} \quad (4.6)$$

where b is a parameter controlling the degree of smoothing, and

$$\bar{Q}(i,j) = \frac{1}{4} [Q(i+1,j) + Q(i-1,j) + Q(i,j+1) + Q(i,j-1)] \quad (4.7)$$

The current wind field analysis program actually applies CRAM twice. That is, after one pass through the ship observations and the application of CRAM, the final smoothed wind field is treated as an improved initial guess field, and the ship incorporation procedure is repeated with the complete (retained and discarded) file of observations. The procedure makes the error check on ships' observations less sensitive to gross errors in the pressure field, allows more "good" ship reports to be incorporated into the analysis and in general increases the influence of ships' wind observations in the final analysis.

The specification of the vector 19.5 meter effective wind at each S193 cell for a specific pass required the use of the two six hourly analyzed wind fields that straddled the time of the pass. For each cell, values of the meridional and zonal wind were calculated at the precise location of the cell by curvilinear surface fitting to the four grid points surrounding the cell. This was done for each wind field and a value obtained at the precise time of the pass by linear interpolation in time.

Planetary Boundary Layer Model. An important element of the objective analysis program just described is the calculation of an initial guess wind field from the analyzed pressure and temperature fields. In many parts of the grid, particularly outside the normal ship traffic lanes, the final analysis will "remember" entirely this initial guess field and even in the vicinity of ships' wind observations, the field serves as background for the incorporation of reports and

determines the shape of the field. In addition, as described by Pierson, Cardone and Greenwood (1974), a PBL will be needed to assimilate satellite derived winds into operational pressure analysis procedures when they become routinely available. In this section a brief summary of the PBL theory, as originally described by Cardone (1969), is presented.

The object of a PBL model is to describe the vertical variation of the vector wind and stress from the sea surface up to the height in the atmosphere at which the frictional forces caused by the earth's surface can be neglected. For an atmosphere in which time changes and horizontal gradients in the mean wind are small the flow at the top of the PBL will be in nearly gradient balance. Even under these assumptions, the problem is very complicated. Close to the ground, in the so-called surface boundary layer the wind variation with height is dominated by the physical processes associated with the lower boundary - namely the effective roughness of the surface and the heat flux across the interface. In this lower layer, the wind and stress vectors do not turn with height and the wind speed increases approximately logarithmically with height. In the surface boundary layer, the fluxes of heat and momentum vary little with height and are assumed to be constant thus simplifying the formulation considerably. Above the surface boundary layer, which is of the order of 10 to 100 meters in depth, the frictional forces decrease with height, coriolis forces become significant and the wind vector begins to turn to become more nearly parallel to the local horizontal gradient of pressure.

The PBL developed by Cardone (1969) is an extension of Blackadar's (1965) model in which the PBL is divided into two layers. However, Blackadar treated only an PBL that was neutrally stratified and in which the effective roughness of the lower boundary was externally prescribed

(a solid surface). Cardone (1969) extended the theory to include a realistic description of the effective roughness of the sea surface and the effect of non-neutral stratification as expressed in terms of the air sea temperature difference.

In the lower layer of the model, the mean wind speed varies with height according to equation (4.8).

$$U = \frac{u_*}{k} \left[\log (z/z_0) - \psi (z/L') \right] \quad (4.8)$$

where U is the wind speed, $u_* = (\tau/\rho)^{1/2}$, τ is the surface stress, ρ is the air density, $k = 0.4$, z is the height, z_0 is the roughness parameter, and L' is a modified form of the Monin-Obukov stability length. The wind profile stability dependence enters through the function, ψ , which is defined as equation (4.9),

$$\psi(z/L') = \int_0^{z/L'} \frac{1 - \Phi(\xi)}{\xi} d\xi \quad (4.9)$$

where $\Phi(z/L')$ is given as

$$\Phi(z/L') = 1 + B(z/L') \quad \text{stable}$$

$$\Phi^4 - (\delta z/L')\Phi^3 - 1 = 0 \quad \text{unstable}$$

$$\Phi(z/L') = 0 \quad \text{neutral}$$

with B' and δ' estimated at 7 and 18 respectively (Panofsky, 1963). Also, in this constant stress layer, the eddy viscosity, k_m , can be written as equation (4.10).

$$k_m = k u_* z / \Phi(z/L') \quad (4.10)$$

The upper layer of the two layer PBL model is a so-called Ekman layer in which the boundary layer is assumed to be a region in which the mean wind is steady and homogeneous and uniform at every level and in which the density may be considered to be independent of height. The equations of motion are then written as equations (4.11),

$$\begin{aligned} f(v - v_g) + \frac{d}{dz} \left[k_m \frac{d}{dz} (u - u_g) \right] &= 0 \\ -f(u - u_g) + \frac{d}{dz} \left[k_m \frac{d}{dz} (v - v_g) \right] &= 0 \end{aligned} \quad (4.11)$$

where u, v are the horizontal wind components, u_g, v_g are the corresponding geostrophic wind components and f is the coriolis parameter. The value of k_m is constant in this layer at a value defined by the height of the interface between the two layers, h ,

$$h = B_0 G/f \quad (4.12)$$

where G is the magnitude of the geostrophic wind, and B_0 is an assignable constant.

The solution for the boundary layer is determined from the equations for each layer by imposing the conditions of continuity of wind and its derivative at the interface.

For the situation in which the pressure field itself does not vary with height through the PBL, the solution is closed by the following four equations that are solved iteratively:

$$u_*/G = \left[zkB_0 \sin^2 \psi_0 / \phi (h/L') \right]^{1/3} \quad (4.13)$$

$$u_*/G = \sqrt{2} \ k \sin (\pi/4 - \psi_0) / \left[\ln B_0 R_0 - \psi (h/L') \right] \quad (4.14)$$

$$L' = u_*^2 \bar{\theta} \left[\ln (Z_a/Z_0) - \psi (Z_a/L') \right] / \left[k^2 g (\theta_a - \theta_s) \right] \quad (4.15)$$

$$z_0 (\text{cm}) = .684/u_* + 4.28 \times 10^{-5} (u_*^2) - 4.43 \times 10^{-2} \quad (4.16)$$

z_a is the height at which the air temperature θ_a is taken, $\bar{\theta}$ is the mean potential temperature of the boundary layer, $\theta_a - \theta_s$ is the air sea temperature difference and ψ_o is the angle between the surface isobars and the direction of the wind in the surface boundary layer. Thus, given the air sea temperature difference and the magnitude and direction of the surface geostrophic wind, which is computed from the sea level pressure field, the solution provides the magnitude and direction of the surface stress and L' . These quantities then define the vector wind at any height in the surface boundary layer according to equation (4.8) which usually is valid up to the 19.5 meter level.

The quantity R_o that appears in the equations is called the surface Rossby number:

$$R_o = G/fz_o \quad (4.17)$$

For neutral conditions, the solution obeys Rossby number similarity, that is

$$u_*/G = F_1(G/fz_o) \quad (4.18)$$

and

$$\psi_o = F_2(G/fz_o) \quad (4.19)$$

In the non-neutral barotropic case, an additional nondimensional number, G/fL' , describes the stability influence. Cardone (1969) describes a solution for the more general case in which the pressure gradient can vary with height. This variation depends on the horizontal air temperature gradient, which can be quite large near meteorological fronts.

Cardone (1969) compared the published empirical determinations of u_*/G , $U_{19.5}/G$ and ψ_0 over the sea with model predictions with excellent results. The model has also been evaluated at the Fleet Numerical Weather Central (Kaitala, 1974). It was concluded in that study that the model provided a good representation of the surface wind field. Elements of the model have been incorporated into the operational multi-level numerical weather prediction model at FNWC. Recently, the model was evaluated and tested by Isozaki and Uji (1975) in connection with the specification of marine boundary layer winds input to an Pacific Ocean spectral wave prediction model. They found that the PBL wind input provided better wave hindcasts than winds produced by synoptic analyses based upon ship observations.

Comparison of Objective Winds and Special Aircraft and Weather Ship Measurements. As described in Chapter 2, the real time aspects of the experiment included an effort to obtain special measurements of the surface wind beneath an S193 pass from the ocean station vessels and NOAA and NASA aircraft. Whenever an EREP pass was planned during which S193 could scan close to a weather ship, that ship was requested to make special wind and wave measurements at the expected time of the passage of Skylab. An example of the special observations made at Ocean Station "Papa" in SL 4 is shown in Figure 4.29. These special observations were available, typically, within several days of the pass and, for ships equipped with wave recorders, were accompanied by the actual wave record for the comparable 20 minute period. Summary wave information, however, was provided along with the winds.

Aircraft underflights were conducted for several passes in SL 2 and SL 3. These passes have already been described. In SL 4, the NASA JSC C130 conducted two underflights in the North Atlantic Ocean east of Newfoundland and the NOAA C130 provided data beneath a pass over

**SPECIAL METEOROLOGICAL OBSERVATIONS MADE AT
OCEAN WEATHER STATION "PAPA" IN CONNECTION
WITH SKYLAB PASSES ON JANUARY 24, 25, and 27, 1974**

Mean wind direction ($^{\circ}$ True) and speed (knots) over one minute intervals beginning at:

<u>January 24, 1974</u>	<u>January 25, 1974</u>	<u>January 27, 1974</u>
1740 Z - 278/40	1707 Z - 217/21	1840 Z - 253/29
1741 282/39	1708 220/20	1841 253/29
1742 282/42	1709 220/20	1842 256/26
1743 282/41	1710 221/20	1843 253/28
1744 282/40	1711 220/18	1844 257/25
1745 281/38	1712 222/20	1845 257/25
1746 281/40	1713 220/18	1846 257/26
1747 284/42	1714 222/20	1847 260/28
1748 281/36	1715 225/21	1848 257/26
1749 281/40	1716 226/20	1849 250/26
1750 278/39	1717 225/21	1850 254/29
1751 281/42	1718 231/22	1851 253/30
1752 281/43	1719 228/21	1852 255/29
1753 280/40	1720 230/19	1853 253/28
1754 278/40		1854 253/28
1755 274/44		1855 253/27
1756 274/46		1856 251/29
1757 278/40		1857 254/30
1758 281/43		1858 251/30
1759 278/42		1859 252/28

Waves: Average 23 ft.
Maximum 31 ft.

Waves: Average 10 ft.
Maximum 14 ft.

Waves: Average 8 ft.
Maximum 14 ft.

Position of ship:

50°00' N
145°00' W

Position of ship:

50°00' N
145°00' W

Position of ship:

49°51' N
145°20' W

Figure 4.29 An example of the special observations made at OSVP in the North Pacific in connection with actual or anticipated S193 passes.

the Eastern Pacific Ocean. Several additional flights were conducted beneath passes in which S193 was operated in the altimeter mode or in the CTC scatterometer mode and will not be discussed here.

The locations of the low level wind measurement runs made by the aircraft in SL 4 beneath the three pertinent CTNC passes are shown in Figures 4.30, 4.31, and 4.32. Shown in the figures are the locations of the nearby S193 cells and the winds at the cells calculated by the objective procedures just described. The flight level winds were generally representative of the 150 meter level. The surface boundary layer wind profile (that is equation 4.8) was assumed to be valid to this altitude, (see e.g. Ross and Cardone, 1974), and was used to reduce the winds to the 19.5 meter level on the basis of the observed air-sea temperature difference. The 19.5 meter winds were then converted to effective 19.5 meter winds to make them comparable to the objective winds. Even though the aircraft data were not used in the objective analysis procedure, the agreement between the aircraft derived winds and the objective winds is excellent in all three cases.

Many more special weather ship observations were made than were actually accompanied by S193 measurements since many planned S193 passes were cancelled on short notice. Table 4.1 summarizes all special aircraft and weather observations that were made within 150 miles of S193 cells at which good scatterometer measurements were made. The table includes the objective winds at the closest cell or cells and the distance between the special measurement and the cell. There are only 14 cases in which the special aircraft or ship observations are available to provide an independent check on the accuracy of the surface truth and only in five cases are the data near cells with incidence angles of 30° or greater! This high quality surface truth subset is obviously insufficient to evaluate S193 as a wind sensor. The difference between the objective winds and the special winds for the

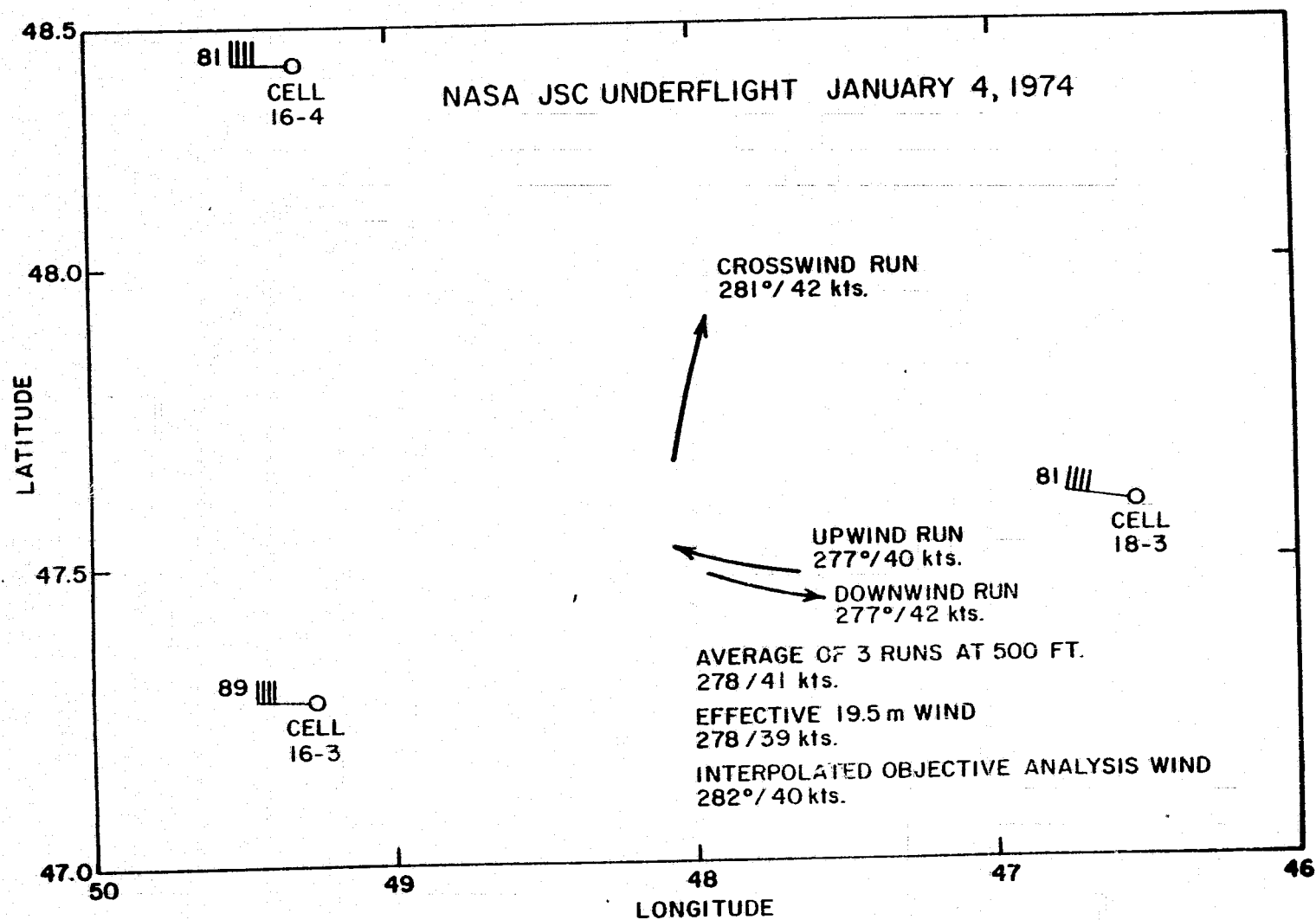


Figure 4.30 Winds measured by the NASA C-130 aircraft east of New Foundland beneath the S193 CTNC pass of January 4, 1974.

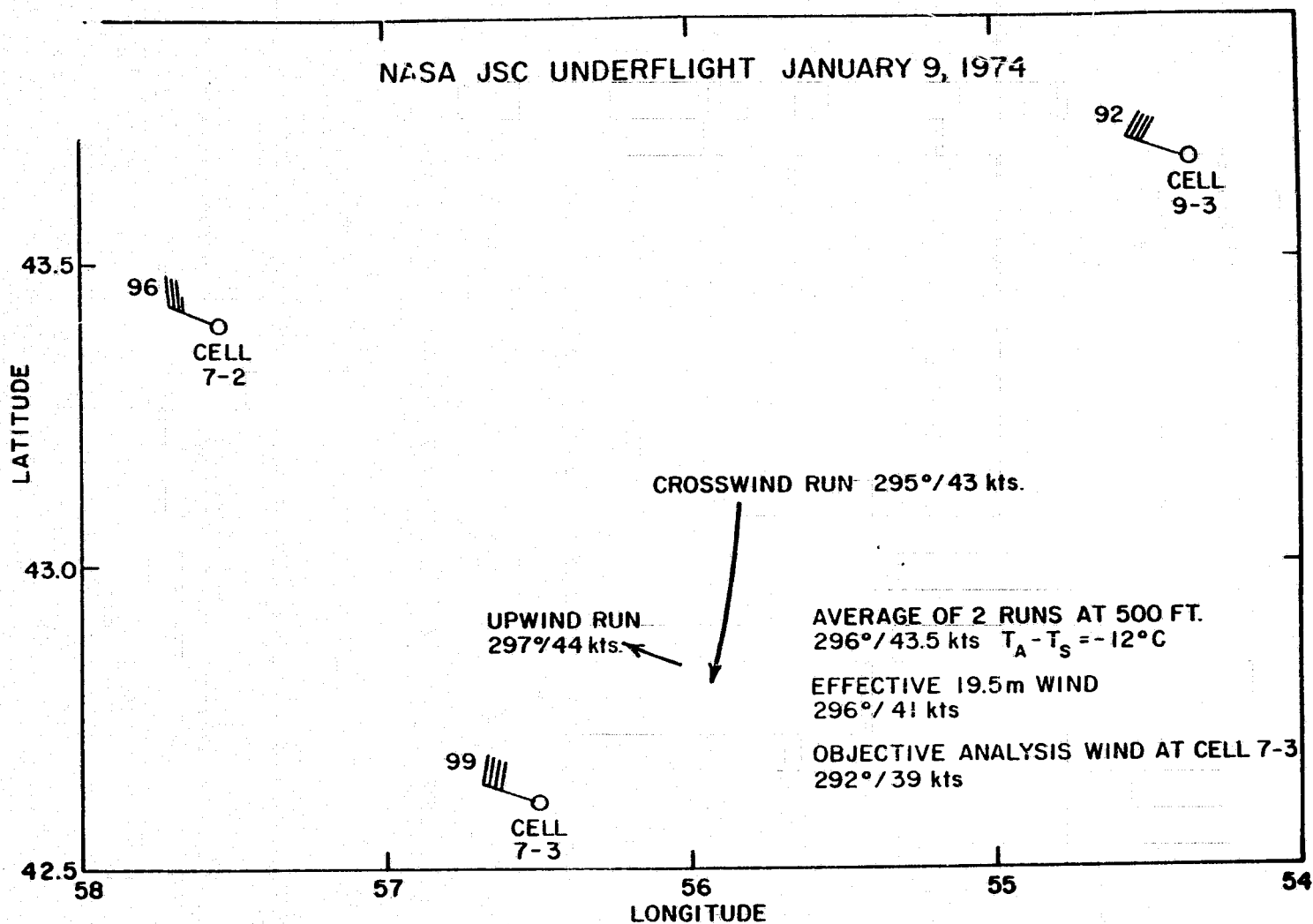


Figure 4.31 Winds measured by the NASA C-130 aircraft east of New Foundland beneath the S193 CTNC pass of January 9, 1973.

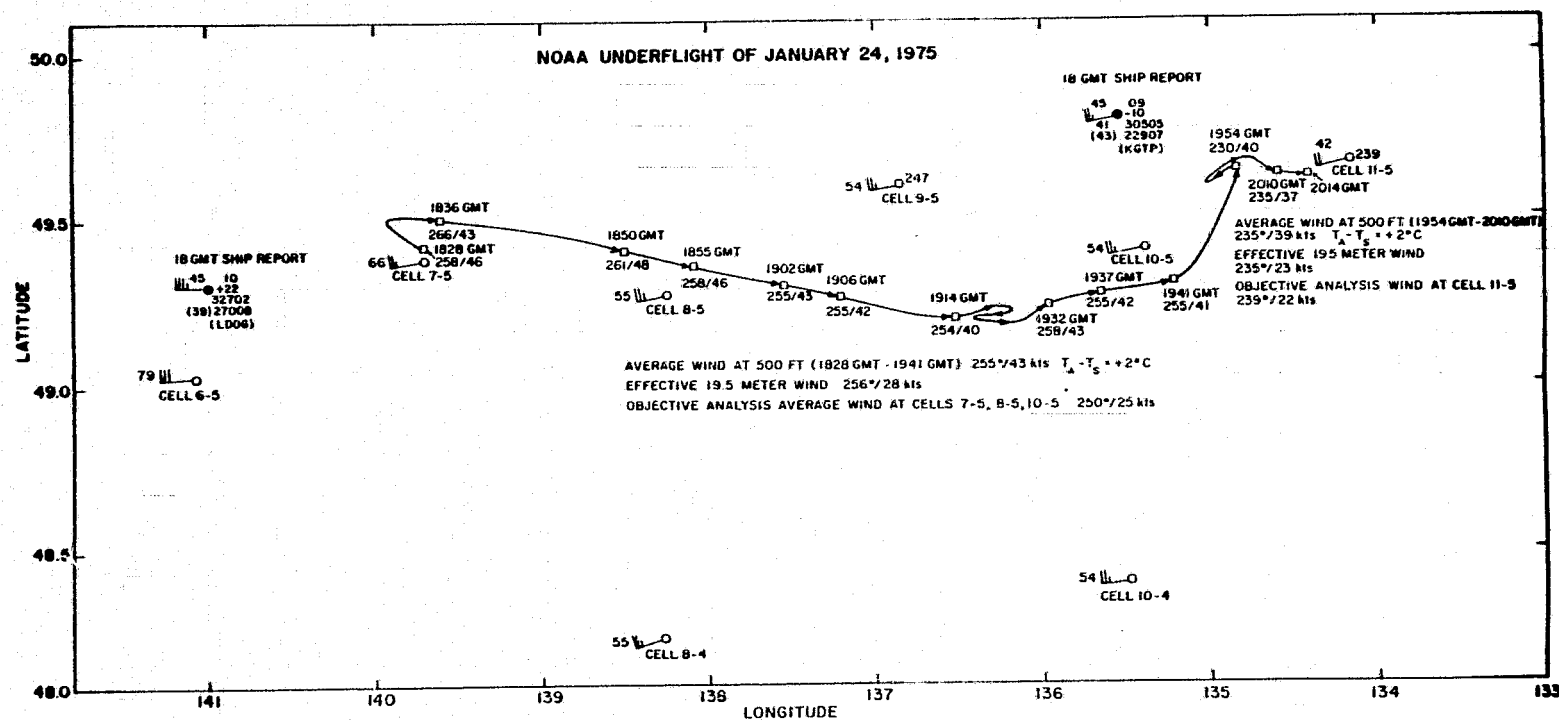


Figure 4.32 Winds measured by the NOAA C-130 aircraft in the eastern North Pacific Ocean beneath the S193 CTNC pass of January 24, 1973.

Table 4.1 Comparison of surface truth provided by objective analysis program and special wind observations from Ocean Station Vessels, the NASA C130 and the NOAA C130. Speeds are in knots, directions are in degrees, T_a = air temperature (degrees F), T_s = water temperature (degrees F), and distances are in nautical miles. $V_{19.5}$ is the observed wind speed referred to 19.5 meters elevation and neutral stability. The tabulated distance is the distance between the location of the special observation and the closest cell or cells.

No.	Day	Date	Site	SPECIAL OBSERVATION				$V_{19.5}$	OBJECTIVE ANALYSIS OF $V_{19.5}$			
				Time (GMT)	Dir/Speed	$T_a - T_s$			Cell	Time	Dir/Speed	Distance
1	216	8/4/73	OSV P	1700-1714	247/23	+ .4		22.4	14-5	1711	239/23	5
2	220	8/8/73	OSV P	1540-1559	239/9	- .7		10	13-5	1554	243/11	50
3	252	9/9/73	OSV K	1925-1935	90/5	- 1.9		6	29-3	1933	106/12	92
4	338	12/4/73	OSV P	1640-1659	267/26	- 2.0		27	3-4	1645	253/22	21
5	4	1/4/74	OSV J	1925-1935	230/26	- 2.8		27	35-2	1938	216/28	60
6	4	1/4/74	OSV K	1925-1935	220/31	- 2.8		32	40-2	1940	233/28	34
7	11	1/11/74	OSV K	1755-1805	220/53	+ .1		53	27-4	1750	235/49	53
8	24	1/24/74	OSV P	1740-1759	275/41	+ .5		40	3-5	1748	282/40	87
9	25	1/25/74	OSV P	1707-1720	223/20	$\pm 0.$		20	3-5	1704	228/18	130
10	32	2/1/74	OSV P	1710-1729	219/30	$\pm 0.$		30	17-5	1653	217/20	124
11	4	1/4/74	C130	1724-1747	278/41	-12.0		39	16-3/18-3	1911	282/40	30
12	9	1/9/74	C130	1740-1800	296/43	-12.0		41	7-3	1555	292/39	30
13	24	1/24/74	C130	1828-1941	256/43	+ 2.0		28	7-5/8-5	1749	250/25	5
14	24	1/24/74	C130	1954-2010	235/39	+ 2.0		23	11-5	1750	239/22	12

cases shown is 3.9 knots RMS in speed and 10° RMS in direction. A portion of this difference is attributable to the distance between the measurement and the cell.

ERRORS IN THE SPECIFICATION OF THE VECTOR WIND

The measurement of the winds involves the measurement of a vector quantity with both a magnitude and a direction. The specification of the winds in a wind field also involves magnitudes and directions. A value for the vector wind that has the correct magnitude but that has an error of 90° in direction has a much greater error than a value with the correct direction and an error in magnitude of 30%.

The measurement of light winds by ships at sea, even if the ship has an anemometer, is particularly difficult, except for weather ships hove to on their assigned positions, because the ship is under way at a speed that can vary from 7 to 10 meters per second. The cup anemometer then measures its own movement through relatively still air, where the air is moving at, say, 2 or 3 meters per second. If the light wind is blowing at right angles to the course of the ship, for example, then a correct vector difference must be obtained.

The measurement of high winds is also difficult because they can be very gusty and because, if the measurement is by anemometer on a ship, the ship motions in heave, pitch and roll because of the waves cause the anemometer to change elevation and to be swept through the air due to the motion of the mast. Winds are consequently best measured over a range of speeds from about 5 to 20 meters per second and the errors of measurement are greater for both lower and higher speeds.

The magnitude of the vector wind in the planetary boundary layer at a fixed elevation above the sea surface is essentially a linearly varying quantity that needs to be measured over a range from nearly

calm to about 50 meters per second. A range from zero to 35 meters per second would be adequate since 20 minute mean wind speeds much greater than this are rare and are found only near the centers of intense hurricane force tropical cyclones.

The User Agency Working Group for SEASAT-A has required that backscatter measurements capable of yielding wind speeds within ± 2 meters per second or $\pm 10\%$ of the true value, whichever is worse, and wind directions within $\pm 20\%$ of the true value be obtained by that spacecraft. The relaxation of the requirement for high winds is in recognition of the difficulty of measuring high winds. The accuracy of the direction measurement for light winds may also have to be relaxed because, in a vector sense, it is contradicted by the ± 2 meters per second specification. The User Agency Working Group did not, however, provide guidance as to exactly how it could be proved that the specifications have been met. The results that follow will provide a means to accomplish this objective.

Moreover, if the errors in measurement were truly random, they could be distributed about the true value in such a way that it would be (almost) correct in most meteorological applications to assume that the ± 2 meters per second requirement mentioned above represents the standard deviation of a normally distributed error in magnitude.

The only problem here is that when the magnitude of the wind vector is used as the defining parameter it is difficult to treat a ± 2 meters per second standard deviation for a 1 meter per second wind. A way out of this difficulty is to treat the vector wind and a vector error, which for light winds can mean that the true vector wind plus a typical vector error can be 180° away from the true wind.

All of these remarks are equally applicable to the problem of specifying the wind field on a grid of points. Errors caused by

interpolation and smoothing can produce marked changes in the direction of a light wind and, with strong gradients of the wind in areas of high wind, both the magnitude and direction of the wind can be altered. The techniques that have been used to specify the surface truth meteorological winds at the cells scanned by S193 are the best possible available procedures and are comparable in all respects to the procedures used in the major operational meteorological forecasting centers around the world. Nevertheless, errors in the original measurements exist and errors in the interpolation to a grid of points exist, and it is necessary to understand these errors before the errors in the S193 specification of the winds can be understood.

At a point in space and time, consider a true measurement of the wind given by $|V_T|$ and χ_T in the meteorological sense with winds from the north corresponding to $\chi = 0$ and winds from the east corresponding to $\chi = 90^\circ$. Also consider the reported wind, $|V_M|$ and χ_M . In vector form,

$$\vec{V}_M = \vec{V}_T + \vec{E} \quad (4.10)$$

where \vec{E} is an error vector that has been added to the true wind. In component form

$$\vec{V}_M = [|V_M| \cos \chi_M, |V_M| \sin \chi_M] \quad (4.11)$$

$$\vec{V}_T = [|V_T| \cos \chi_T, |V_T| \sin \chi_T] \quad (4.12)$$

and

$$\begin{aligned} \vec{E} &= [|E| \cos \delta, |E| \sin \delta] \\ &= [E_1, E_2] \end{aligned} \quad (4.13)$$

Without loss in generality, let $\chi_M = \chi_T + \Delta\chi$ and let $\chi_T = 0$, so that errors in direction are given as departures from the true direction. To simplify notation, let $|V_T| = V_T$ and $|V_M| = V_M$. It follows then that

$$\vec{V}_M = [V_T + E_1, E_2] \quad (4.14)$$

and that

$$V_M - V_T = [V_T^2 + 2V_TE_1 + E_1^2 + E_2^2]^{\frac{1}{2}} - V_T \quad (4.15)$$

$$= V_T \left[1 + \frac{2E_1}{V_T} + \frac{E_1^2 + E_2^2}{V_T^2} \right]^{\frac{1}{2}} - V_T \quad (4.16)$$

$$\cong V_T + E_1 + \frac{1}{2} \frac{E_2^2 - E_1^2}{V_T} - V_T$$

which represents the difference between the magnitudes of the true and meteorological winds. The last approximation is pretty good if the errors are about 10% of the true wind. Also

$$V_M \cos \Delta\chi = V_T + E_1 \quad (4.17)$$

$$V_M \sin \Delta\chi = E_2 \quad (4.18)$$

and

$$\tan \Delta\chi = \frac{E_2}{V_T + E_1} \quad (4.19)$$

which represents the difference in direction between the meteorological and the true wind.

Now suppose that E_1 and E_2 have a bivariate normal distribution, are independent, and have the same standard deviation as in

$$f(E_1, E_2) = \frac{1}{2\pi D^2} e^{-\frac{1}{2} \left(\frac{E_1^2 + E_2^2}{D^2} \right)} \quad (4.20)$$

From the other definition of E_1 and E_2

$$E = (E_1^2 + E_2^2)^{\frac{1}{2}} \quad (4.21)$$

$$\delta = \tan^{-1} E_1/E_2 \quad (4.23)$$

and

$$f(E, \delta) = \frac{1}{2\pi} e^{-\frac{1}{2} E^2 / D^2} \frac{E}{D} \frac{dE}{D} d\delta \quad (4.23)$$

The error vector has a Raleigh distribution in magnitude and a uniform rectangular distribution in direction under these assumptions. Also the expected value of E is given by equation (4.24).

$$\mathcal{E}(E) = D \int_0^\infty \frac{E^2}{D^2} e^{-E^2/2D^2} \frac{dE}{D} = \sqrt{\pi/2} D = 1.253 D \quad (4.24)$$

The expected value of E^2 is given by equation (4.25).

$$\mathcal{E}(E^2) = 2 D^2 \quad (4.25)$$

The effect of a vector error with components given by equation (4.13) on the true wind is markedly different as a function of V_T . For the situation where $D = 2$ and where $E_1 = \pm 2$ and $E_2 = \pm 2$ so that both errors are \pm one standard deviation, the errors in magnitude and direction are given below in Table 4.2. Other examples for $E_1 = 0$, $E_2 = \pm 2$ can also easily be calculated. Clearly $\Delta\chi$ can exceed 90° and be near 180° for a range of conditions.

If these assumptions correspond to reality, the errors in light winds can be two or three times the magnitude of the true wind and can have large direction errors. Errors in the magnitude of moderate and fairly high winds will depend on the variability of the component of the vector error in the direction of the true wind. The direction errors will be small.

Table 4.2 Errors in wind magnitude and direction for various values of the true wind and $E_1 = \pm 2$, $E_2 = \pm 2$.

True Wind Magnitude (meters per second)				
True Wind	1	3	10	20
Magnitude	2.61	4.39	2.17	2.09
Errors	1.24	-0.76	-1.75	-1.88
Direction	$\pm 33^\circ$	$\pm 26^\circ$	$\pm 9.4^\circ$	$\pm 5^\circ$
Errors	$\pm 63^\circ$	$\pm 45^\circ$	$\pm 14^\circ$	$\pm 6.3^\circ$

A STUDY OF THE ACCURACY OF THE METEOROLOGICAL WINDS

As described previously in this chapter, the meteorological surface truth was determined in three different ways. For the third way, the analysis technique spanned the entire ocean involved and used all available ship reports. These reports in order of accuracy came from weather ships [Type A] on station manned by professionals to record the weather and report it every six hours, from transient ships [Type B] equipped with anemometers at known heights, from transient ships [Type C] with anemometers at an unknown height, and from transient ships [Type D] that estimated the speed and direction of the wind. The grid points in the PBL model had their wind values set by using the above types of ships in descending order of priority. There were also points in the analysis where the winds were computed from the isobaric pressure gradients thus providing a fifth category [Type +].

The winds determined in this way were used to provide the wind speeds and directions at each of the cells scanned by S193 many of the passes in SL 2/3 and for all of SL 4. Early in the program, the important question of how good these meteorologically determined winds actually were arose, and it appeared to be a very difficult one to answer.

At the suggestion of Young (1975), a withheld data analysis of a set of wind fields was carried out using the same procedures that were used to specify the winds for the S193 cells. The wind fields were first calculated for the North Atlantic Ocean with the weather ship reports included in the data base. Then the weather ships were removed from the data base, the winds were recomputed, and the category of ship report, if one could be used, that replaced the weather ship was noted.

One of the hypothesis that can then be entertained is that wind speeds computed from backscatter measurements might be comparable to the quality of measurements of winds by weather ships on station, or by one of the remaining three ship categories. If the weather ships are thought of as making the best possible measurement of the wind, then the differences between the weather ship winds and the winds determined in their absence is a measure of how well, or how poorly, the winds were specified at the other cells scanned by S193.

The withheld data analysis used reports from the North Atlantic thirty hours apart beginning on July 15, 1973 and ending on February 2, 1974. Weather Ships A, B, C, I, J, K, and M were involved. Appendix B shows the results of these calculations sorted for winds from zero to ten knots, ten knots to twenty knots, twenty knots to thirty knots and over thirty knots. The date, time, ship and its position appear first.

Although, these are additional error sources both in the wind measurement by the weather ship and in the interpolation to the grid point, \vec{V}_{WS} will be equated to \vec{V}_T and \vec{V}_{SYN} to \vec{V}_M as in the

preceding analysis so as to learn about the kinds of "errors" present in the planetary boundary layer analysis. This assumption will be removed in the next section, and more realistic results will then be possible.

The values, VWS and CHIWS, represent the wind speed and direction interpolated to the nearest grid point of the NMC double resolution grid as obtained from a weather ship report. The values, VSYN and CHISYN, represent the winds at that same grid point following a complete reanalysis after the weather ship report was removed. VE and CHIE are the magnitude and direction of the vector difference between the weather ship wind and the synoptic wind. Since the weather ship report is probably the closest to the true wind and the synoptic wind represents the usual wind in areas away from the weather ships, these vector differences represent the kind of errors possible in computer based analyses of wind fields over the oceans.

The vector "error" is resolved both into east-west and north-south components and into components parallel and normal to the weather ship wind. The difference in direction between the weather ship wind and the synoptic wind is also shown.

The final column is the "Type" representing the nature of the data that replaced the weather ship that was used in the first analysis. Of course, there are no "Type A" values in this column since two weather ships are never on station simultaneously.

The data in Appendix B can be scanned to see some of the kinds of differences (which are akin to errors) that can result. For example, on 7/21/73 Weather Ship B yielded a wind magnitude of 10.7 knots, the synoptic analysis yielded 15.1 knots, but the vector error was 21 knots because of large differences in direction. Other large difference

values are found for Weather Ship A on 7/26/73, Weather Ship C on 8/14/73, Weather Ship B on 10/11/73, Weather Ship I on 10/21/73 (VE = 40 knots), Weather Ship M on 11/8/73, Weather Ship K on 1/28/74, and Weather Ship I on 1/31/74.

Tables 4.3 and 4.4 present various statistics calculated from this sample. The first group in the first table stratifies the data according to the type of information that replaced the weather ship, that is, one of three kinds of ships or the pressure field. The second group stratifies all data according to wind ranges and includes all types of replacement data in each range.

As described previously, the last step of the analysis consists of the application of a smoothing operator over the entire field. The final smoothed field was then interpolated to the position of the weather ship and compared to the weather ship report. The result is given in the third group called ANAL (BCD +). That these values are smaller than all the others is to be expected. They represent the base line error in attempts using present techniques for the analysis of wind fields over the ocean. The group labeled SHIP (BCD) compares the wind reported by the ship that replaced the weather ship with the weather ship wind without any corrections for the fact that the two ships are not at the same place in the field. These numbers are surprisingly large, and indicate the need for the various smoothing routines that are used in the synoptic analysis.

The last group in this first table is most instructive. The first step in the synoptic analysis is to compute the wind from the pressure gradient. This initial guess wind value is compared with the weather ship report. The initial guess compared as well with the weather ship as the full analysis using all of the available ship reports.

TABLE 4.3 STATISTICS OF THE VECTOR ERROR STRATIFIED ACCORDING TO TYPE,
WIND SPEED RANGES, AND OTHER EFFECTS*

BASE	TYPE	N	MEAN E	2ND MOM	SQ RT	E-W BIAS	N-S BIAS	NORM WIND BIAS	PAR WIND BIAS	E-W VAR	E-W STD	N-S VAR	N-S STD	NORM WIND VAR	NORM WIND STD	PAR WIND VAR	PAR WIND STD
SYN	B	21	8.7	111.6	10.6	-.64	-.37	-1.77	.75	80.5	9.0	31.1	5.6	70.4	8.4	41.2	6.4
SYN	C	32	8.0	87.6	9.4	-1.20	-1.29	-.80	1.75	39.0	6.2	48.7	7.0	57.2	7.6	30.4	5.5
SYN	D	100	8.3	109.2	10.5	-.45	.44	.00	.92	55.1	7.4	54.1	7.4	58.8	7.7	50.4	7.1
SYN	+	603	9.4	126.4	11.2	-.52	-.09	-.08	1.93	69.5	8.3	56.9	7.5	68.1	8.3	58.3	7.5
SYN	0-10	111	5.4	39.6	6.3	1.15	.19	.26	-3.02	18.7	4.3	20.9	4.6	12.6	3.5	27.0	5.2
SYN	10-20	284	7.5	76.0	8.7	.37	-.10	-.35	-.47	41.1	6.4	34.9	5.9	44.1	6.6	31.8	5.6
SYN	20-30	243	9.9	130.8	11.4	-.65	-.15	.12	3.27	73.8	8.6	57.0	7.5	75.8	8.7	55.0	7.4
SYN	GT 30	118	15.3	292.7	17.1	-4.11	-.11	-.57	8.46	158.1	12.6	134.5	11.6	151.8	12.3	140.8	11.9
ANAL	B	21	3.6	20.0	4.5	-.12	-.26	-.58	1.26	14.5	3.8	5.6	2.4	11.4	3.4	8.6	2.9
ANAL	C	32	3.9	21.5	4.6	-.68	-.72	-.34	1.68	10.0	3.2	11.4	3.4	11.0	3.3	10.4	3.2
ANAL	D	100	4.0	23.6	4.9	-.15	.13	-.12	1.59	11.6	3.4	12.0	3.5	11.8	3.4	11.8	3.4
ANAL	+	603	3.1	14.2	3.8	-.14	-.07	.02	1.56	7.6	2.8	6.5	2.6	5.3	2.3	8.9	3.0
SHIP	B	21	12.4	228.7	15.1	-1.27	-1.01	-.13	-4.18	140.8	11.9	87.9	9.4	152.4	12.3	76.3	8.7
SHIP	C	32	9.3	112.5	10.6	-.80	-.09	-1.62	-1.22	51.2	7.2	61.4	7.8	63.5	8.0	49.0	7.0
SHIP	D	100	10.8	188.8	13.7	.49	1.18	-.05	-2.53	98.1	9.9	90.7	9.5	88.3	9.4	100.4	10.0
IG	B	21	8.5	105.6	10.3	-2.56	.26	.27	4.56	82.4	9.1	23.3	4.8	54.4	7.4	51.2	7.2
IG	C	32	9.2	130.3	11.4	-1.95	-1.26	.25	4.26	47.6	6.9	82.7	9.1	66.4	8.2	63.8	8.0
IG	D	100	8.2	93.9	9.7	-1.59	1.26	.08	3.46	49.7	7.1	44.2	6.6	53.2	7.3	40.7	6.4
IG	+	603	8.8	108.5	10.4	-.84	.52	.05	3.75	56.3	7.5	52.3	7.2	47.2	6.9	61.4	7.8

*(assuming perfect weather ship winds)

TABLE 4.4 STATISTICS OF THE VECTOR ERROR IN A TWO-WAY STRATIFICATION
ACCORDING TO TYPE AND WIND SPEED RANGES*

TYPE	RANGE	N	MEAN	2ND	SQ	E-W	N-S	NORM	PAR	E-W	E-W	N-S	N-S	NORM	NORM	PAR	PAR
			E	MOM	RT	BIAS	BIAS	WIND	WIND					WIND	WIND	WIND	WIND
								BIAS	BIAS	VAR	STD	VAR	STD	VAR	STD	VAR	STD
B	0-10	2	4.4	19.4	4.4	-.31	-3.04	-3.40	-2.74	10.0	3.2	9.4	3.1	11.7	3.4	7.7	2.8
B	10-20	9	7.8	74.9	8.7	1.22	-2.17	1.34	-1.54	39.7	6.3	35.2	5.9	41.3	6.4	33.6	5.8
B	20-30	6	7.8	95.5	9.8	-3.88	1.70	-3.38	.22	53.2	7.3	42.3	6.5	79.7	8.9	15.8	4.0
B	GT 30	4	14.1	264.4	16.3	-.13	1.92	-5.54	8.45	248.4	15.8	16.0	4.0	151.3	12.3	113.0	10.6
C	0-10	7	5.4	32.5	5.7	-.32	1.47	-2.42	-3.25	22.7	4.8	9.8	3.1	13.3	3.6	19.2	4.4
C	10-20	10	5.7	38.3	6.2	.36	-.35	1.83	.37	15.2	3.9	23.1	4.8	23.9	4.9	14.5	3.8
C	20-30	10	8.4	89.0	9.4	.06	-.53	-2.92	2.77	55.4	7.4	33.6	5.8	66.4	8.1	22.7	4.8
C	GT 30	5	15.3	260.7	16.1	-8.08	-8.58	.43	9.44	76.4	8.7	184.3	13.6	167.2	12.9	93.5	9.7
D	0-10	18	4.0	24.4	4.9	1.25	-.72	1.08	-1.14	15.7	4.0	8.8	3.0	8.8	3.0	15.6	3.9
D	10-20	41	7.2	69.4	8.3	.29	.57	.21	-.13	35.6	6.0	33.8	5.8	41.3	6.4	28.1	5.3
D	20-30	30	10.2	167.6	12.9	-.61	.33	-.52	1.50	92.3	9.6	75.3	8.7	85.3	9.2	82.2	9.1
D	GT 30	11	14.1	237.4	15.4	-5.59	2.15	-1.09	6.61	90.8	9.5	146.5	12.1	133.3	11.5	104.0	10.2
+	0-10	84	5.7	43.9	6.6	1.29	.35	.39	-3.41	19.2	4.4	24.8	5.0	13.3	3.7	30.6	5.5
+	10-20	224	7.6	78.9	8.9	.35	-.13	-.61	-.52	43.3	6.6	35.6	6.0	45.7	6.8	33.2	5.8
+	20-30	197	10.0	128.4	11.3	-.60	-.26	.48	3.65	72.6	8.5	55.8	7.5	74.7	8.6	53.7	7.3
+	GT 30	98	15.5	301.6	17.4	-3.91	-.01	-.36	8.62	166.2	12.9	135.5	11.6	153.1	12.4	148.5	12.2

* (assuming perfect weather ship winds)

* The variances are computed about an assumed zero mean.

The second table (Table 4.4) stratifies the data from the first two groups in the first table into sixteen categories to see if there is a dependence between the type of ship and the different wind speed ranges. Some of the sample sizes are so small that the statistics are not very reliable.

For each classification, the sample size, the mean magnitude of the vector error, the second moment of the magnitude of the vector error and its square root are given. The next twelve columns provide statistics on the vector "error" resolved into east-west and north-south components and into components parallel and normal to the weather ship wind. Note that the sum of the E-W VAR plus the N-S VAR equals the second moment of E as do the NORM WIND VAR and PAR WIND VAR sums, as it should.

If the normal components of the vector "error" are normally distributed about a mean of zero, then the various biases are means of samples of size N from these populations. The expected value of the bias is zero. The standard deviation of the bias is given by the square root of the ratio of the appropriate variance and the sample size. A bias within plus or minus twice this value is not unusual. Values for the bias in Table 4.4 that do not lie within two standard deviations of the expected value of zero are those for E-W/BIAS for C GT 30, + 0-10, and + GT 30 and for PAR WIND BIAS for C GT 30, D GT 30, + 0-10, + 20-30, and + GT 30. With two sets of 16 pairs tabulated, these large biases are somewhat unusual. The biases for the synoptic analyses appears to be systematic.

The EW and NS vector components are essentially uncorrelated. For Type D, the range of wind speeds and the correlation coefficients were as follows: (0 - 10), -0.14; (10 - 20), -0.041; (20 - 30), -0.031; and (30+) , +0.12. For Type +, they were as follows: (0 - 10), +0.066; (10 - 20), -0.082; (20 - 30), -0.036; and (30+) , -0.009.

Table 4.4 shows that there is little to choose between types B, C and D. Small samples require caution in interpretation. However, ships with anemometers are better than no ship at all. The "errors" for winds greater than 30 knots are double the average of the "errors" for the lower winds. The sample sizes for Type D and Type + make it possible to conclude that a ship without an anemometer yields a better wind than the wind that can be computed from the pressure field.

An important result from these tabulations is obtained from the values of the variances and standard deviations of the vector "error" components normal to the weather ship and parallel to it. For all types in Table 4.3 (SYN BCD +). The variance of the normal component exceeds the variance of the parallel component. There is a 0.06 probability that this could happen by chance (one sided). For the pooled types stratified according to wind speed ranges, the same thing happens for the three highest ranges. For Table 4.4, of the sixteen categories, the normal wind "error" component variance exceeds the paralleled wind error component variance thirteen times. There is a 0.0106 probability that this could happen by chance (one sided).

This can only occur if the ship reports are poorer in reporting wind direction than in reporting wind speed. The variance of the normal component appears to exceed the variance of the parallel component by about 20%, say, for simplicity, by a factor of about 1.21. Equation (4.21) is therefore not quite correct and should be given by equation (4.26) where D^2 is the variance of the parallel component of the "error".

$$f(E_1, E_2) = \frac{1}{2\pi \cdot 1.1 D^2} e^{-\frac{1}{2} \left[\frac{E_1^2}{D^2} + \frac{E_2^2}{1.21 D^2} \right]} \quad (4.26)$$

All of the other equations that follow equation (4.21) are therefore not quite right and the magnitude of the vector error will have a probability density function that differs in some way from the Rayleigh distribution. Histograms of the magnitude of the vector error for Type + analyses are given in Figures 4.32, 4.33, and 4.34 for ranges of the weather ship winds of 10 to 20, 20 to 30 and greater than 30 knots.

The marginal distribution of δ can be found easily by transforming from cartesian to polar coordinates. It is given by equation (4.27),

$$f(\delta) = \frac{1.1}{2\pi} \frac{1}{[1 + 0.21 \cos^2 \delta]} \quad (4.27)$$

which shows that the directions of the vector error has a higher probability of being equal to $\pm 90^\circ$ than to zero or 180° . The magnitude and direction of the vector error are no longer independent. This result appears to be different from the error statistics in artillery shots at a distant target. The direction usually is very good and the range is poor so that for an equation similar to equation (4.26) the variance of E_1 exceeds the variance of E_2 .

The conditional distribution of the magnitude of the vector "error" is given by equation (4.28), which is a Raleigh distribution that depends on δ . The expected value of the magnitude of the vector "error" (given δ) is given by equation (4.29).

$$f(E/\delta) = \frac{(1 + 0.21 \cos^2 \delta)}{1.21 D^2} e^{-\frac{1}{2} \left(\frac{1 + 0.21 \cos^2 \delta}{1.21 D^2} \right) E^2} \quad (4.28)$$

$$e(E/\delta) = \sqrt{\pi/2} \frac{1.1D}{(1 + 0.21 \cos^2 \delta)^{1/2}} \quad (4.29)$$

A Further Analysis With Different Assumptions. Although weather ship observations of the wind, presently supplemented by an increasing number of data buoys, are undoubtedly the most accurate, these wind observations also undoubtedly have errors in them. The assumption that the weather ship wind represents the true wind, made in the preceding section, needs to be examined critically. A start toward a further understanding of the errors in the specification of the winds in the planetary boundary layer is given in this section.

Consider two ship reports of the vector wind made close enough together in space and time to represent the measurement of the same wind. Assume that each measurement consists of the true wind plus error components in the direction of the true wind and normal to the true wind with appropriate variances as in equations (4.30), (4.31), (4.32), and (4.33).

$$\vec{V}_1 = \vec{V}_T + \vec{E}_1 = (V_T + E_{11}, E_{12}) \quad (4.30)$$

$$\text{VAR } E_{11} = D_{11}^2; \text{VAR } E_{12} = D_{12}^2 \quad (4.31)$$

$$\vec{V}_2 = \vec{V} + \vec{E}_2 = (V_T + E_{21}, E_{22}) \quad (4.32)$$

$$\text{VAR } E_{21} = D_{21}^2; \text{VAR } E_{22} = D_{22}^2 \quad (4.33)$$

A linear combination of these two vector winds represents the best value of the wind to be used in a planetary boundary layer analysis as in equation (4.34).

$$\begin{aligned} \vec{V} &= \alpha \vec{V}_1 + (1 - \alpha) \vec{V}_2 \\ &= \vec{V}_T + \alpha \vec{E}_1 + (1 - \alpha) \vec{E}_2 \end{aligned} \quad (4.34)$$

The residual error of the linear combination can be called \vec{E}_{res} and is given by equation (4.35) in component form.

$$\vec{E}_{\text{res}} = (\alpha E_{11} + (1-\alpha) E_{12}, \alpha E_{21} + (1-\alpha) E_{22}) \quad (4.35)$$

The vector difference between \vec{V}_1 and \vec{V}_2 is defined as equation (4.36).

$$\vec{E}_{\text{diff}} = \vec{V}_1 - \vec{V}_2 = (E_{11} - E_{21}, E_{12} - E_{22}) \quad (4.36)$$

If the components of the error vectors are normally distributed independent random variables, the probability distribution functions for the error vectors would be given by equations (4.37) and (4.38). All of the data in Appendix B and the statistics in Tables 4.3 and 4.4 support these assumptions. For example, the normal and parallel components are both normally distributed and independent.

$$f(E_{11}, E_{12}) = \frac{1}{2\pi D_{11} D_{12}} e^{-\frac{1}{2} \left[\left(\frac{E_{11}}{D_{11}} \right)^2 + \left(\frac{E_{12}}{D_{12}} \right)^2 \right]} \quad (4.37)$$

$$f(E_{21}, E_{22}) = \frac{1}{2\pi D_{21} D_{22}} e^{-\frac{1}{2} \left[\left(\frac{E_{21}}{D_{21}} \right)^2 + \left(\frac{E_{22}}{D_{22}} \right)^2 \right]} \quad (4.38)$$

With all of these assumptions, the various expected values for the mean, the variance of the components, and the variance of the magnitude of \vec{E}_{res} and \vec{E}_{diff} can be found. They are given by the following equations.

$$\mathcal{E}(\vec{E}_{\text{res}}) = 0 \quad (4.39)$$

$$\mathcal{E}(\vec{E}_{\text{diff}}) = 0 \quad (4.40)$$

$$\mathcal{E}[(E_{\text{res}1})^2, (E_{\text{res}2})^2] = (\alpha^2 D_{11}^2 + (1-\alpha)^2 D_{21}^2, \alpha^2 D_{12}^2 + (1-\alpha)^2 D_{22}^2) \quad (4.41)$$

$$E[(E_{\text{diff1}})^2, (E_{\text{diff2}})^2] = (D_{11}^2 + D_{21}^2, D_{12}^2 + D_{22}^2) \quad (4.42)$$

$$E(|\vec{E}_{\text{res}}|^2) = \alpha^2 (D_{11}^2 + D_{12}^2) + (1 - \alpha)^2 (D_{21}^2 + D_{22}^2) \quad (4.43)$$

$$E(|\vec{E}_{\text{diff}}|^2) = D_{11}^2 + D_{12}^2 + D_{21}^2 + D_{22}^2 \quad (4.44)$$

The best linear combination of the two winds to use in a PBL analysis would be the one that would minimize the magnitude of the residual vector error in equation (4.43). This is obtained by setting the derivative with respect to α of equation (4.43) equal to zero and solving for α . The result is equation (4.45).

$$\alpha = \frac{\frac{D_{21}^2 + D_{22}^2}{2}}{D_{11}^2 + D_{12}^2 + \frac{D_{21}^2 + D_{22}^2}{2}} \quad (4.45)$$

Now suppose that the errors of measurement of the first ship, V_1 , are less than those of the second ship and that the variance of the magnitude of the vector error is some constant, R , where $0 < R < 1$, times the variance of the magnitude of the vector error of the second ship, \vec{V}_2 , as in equation (4.46).

$$D_{11}^2 + D_{12}^2 = R(D_{21}^2 + D_{22}^2) \quad (4.46)$$

Equation (4.45) then becomes equation (4.47) and equation (4.43) becomes equation (4.48).

$$\alpha = \frac{1}{1 + R} \quad (4.47)$$

$$E(|\vec{E}_{\text{res}}|^2) = \frac{R}{1 + R} (D_{21}^2 + D_{22}^2) \quad (4.48)$$

Since $1 - \alpha = R/(1+R)$, the weight factor in the linear combination of the two ship reports that represents the best wind estimate are $1/(1+R)$ and $R/(1+R)$, and the residual error variance of the linear combination is $R/(1+R)$ times the error variance of the poorer ship. The values of α and of $R/(1+R)$ are given as a function of R in Table 4.5.

Table 4.5 Values of α and $R/(1+R)$ as a function of R .

R	α	$R/(1+R)$
0	1	0
0.1	0.909	0.0909
0.2	0.833	0.167
0.3	0.769	0.231
0.4	0.714	0.286
0.5	0.667	0.333
0.6	0.625	0.375
0.7	0.588	0.412
0.8	0.556	0.444
0.9	0.526	0.474
1	0.500	0.500

From equation (4.44), the variance of the magnitude of the difference vector can be written as equation (4.49).

$$\mathcal{E} \left(\left| \vec{E}_{\text{diff}} \right|^2 \right) = (1+R) (D_{21}^2 + D_{22}^2) \quad (4.49)$$

The preceding withheld weather ship analysis started with the assumption that there were no errors in the weather ship winds. To emphasize this assumption, the word "error" has been put in quotation

marks in that section. This is a special case of the present analysis with R set equal to zero. For $R = 0$, $\alpha = 1$, and since \vec{E}_1 is zero, equation (4.34) yields the true wind with no error as the best linear combination. The difference vector is then a measure of the errors in the measurement of the second ship.

In contrast, for the other extreme, suppose that the errors of the weather ship measurements are equal to the errors of the second ship so that $R = 1$. The best estimate of the wind to use at the point in question is then the vector average of the two winds. The residual error variance is reduced to one half of that for either ship, and the variance of the magnitude of the difference vector is double the variance of the error for either ship alone. The errors in those parts of the synoptic analysis that used ships of types B, C or D would be reduced to one half of the tabulated values for variances and second moments and to $\sqrt{2}/2$ for Mean E and the standard deviations.

Neither of these two extremes is probably correct. The value of R is surely greater than zero and less than one, and the best answer lies somewhere between the values in Tables 4.3 and 4.4 and the values that would have been obtained by reducing all of the vector differences at the start of the withheld data analysis by $\sqrt{2}/2$.

For the purpose of the analysis of the S193 data to be carried out in Chapter 8, it is advisable to make a judgement on the value of R and to try to provide some idea of the size of the errors of the measurements of the wind provided by the five categories under discussion. This will be done next, subject to revision, if necessary, when the results of Chapter 8 are presented. Even on weather ships there are still many difficulties in measuring the wind. The speed is usually not averaged over a very long time so as to get a stable average, and the direction is not recorded continuously so as to get a true average value. The fact that the ship is not underway does make the measurement easier to carry out.

Some information on the variability of the winds as measured by a weather ship can be obtained from the tabulated one minute averages of wind speed and direction made during this program. Weather ships PAPA and CHARLIE provided these values whereas the other ships reported only the average for the longer than usual time interval.

Fifteen such special reports are summarized in Table 4.5. Depending on which of the 11 to 21 minutes happened to be the one chosen for the synoptic report, the values for some of the observations could have ranged over as much as 12 knots for some of the speeds and 61° for some of the directions.

Even twenty minute averages of the wind present problems in terms of the theories of turbulence and the periods and wavelengths that should be filtered out to obtain the best value for a numerical weather prediction model. Four of the special observations tabulated above were used to obtain the average wind speed and direction and then the variances of the vector components normal and parallel to the mean wind vector were computed. The results are given in Table 4.6. These values are small compared to, say, one half of the values given in Table 4.4 for corresponding wind speed ranges. Some part of the interpolation error given under ANAL BCD in Table 4.3 must also be involved in the use of a weather ship observation interpolated to a particular cell, which usually will not include the ship.

Also, the turbulent spectra of the horizontal wind components have spectral contributions that are substantial at frequencies corresponding to periods of 10 to 30 minutes with a gap in the 1 to 2 hour range. As shown by Pierson and Moore (1972) the size of the cells as in Table 1.1 at the three largest nadir angles are in one dimension

Table 4.5 Special Weather Ship Observations from PAPA and CHARLIE

DATE D / M / Y	GMT START	DIRECTIONS	RANGE	SPEEDS KNOTS	RANGE KNOTS	RECORD LENGTH MIN	SHIP
13/ 6/73	1333	276-301°	26°	18-24	7	20	P
4/ 8/73	1700	245-250°	6°	22-24	3	15	P
5/ 8/73	1615	225-230°	6°	12-14	3	20	P
8/ 8/73	1540	227-249°	23°	6-12	7	20	P
9/ 9/73	1920	100-160°	61°	4-7	4	21	C
17/ 9/73	1510	350- 10°	21°	10-13	4	11	C
4/12/73	1640	261-271°	11°	23-28	6	20	P
5/12/73	1550	328-336°	9°	38-46	9	20	P
10/12/73	1425	145-161°	17°	22-28	7	20	P
24/ 1/74	1740	274-284°	11°	36-46	11	20	P
25/ 1/74	1707	217-230°	14°	18-22	5	14	P
27/ 1/74	1840	251-260°	10°	25-30	6	20	P
29/ 1/74	1720	45- 58°	14°	9-11	3	20	P
31/ 1/74	1550	304-320°	16°	22-33	12	20	P
1/ 2/74	1710	215-223°	9°	29-32	4	20	P

Table 4.6 Selected statistics of special weather ship observations.
Units are knots and (knots)² and degrees.

DATE	\bar{V}	\bar{X}	NORM VAR	PAR VAR	TOTAL VAR
9/ 9/73	5.2	128°	1.8	0.6	2.4
7/12/73	25.1	153°	4.5	2.9	7.4
24/ 1/74	40.9	280°	3.6	4.0	7.6
31/ 1/74	26.6	312°	6.5	5.1	11.6

(neglecting the effects of area) the equivalent of 1.6 to 3 hour averages for 15 knot winds, of 19 to 38 minute averages for 25 knot winds and of 13 to 27 minute averages for 35 knot winds since this is the amount of time required for an eddy, based on Taylor's hypothesis, to be advected over a distance equal to a cell dimension at the wind speed indicated.

From Table 4.4, there is not much difference between the values tabulated for the three different types of ships. A much larger sample could probably show that they stratify according to the method of measurement. For the purposes here, the three types will be pooled into the category of transient ships, and weighted averages of the total variance using the sample size, N , for each wind speed range will be used. The weighted average for types B, C and D from 0 to 10 knots is 27; for 10 to 20 knots, it is 65; for 20 to 30 knots, it is 102; and for greater than 30 knots it is 237.

The variance total introduced by the analysis procedure is 14 to 23 (knots)² depending on wind speed ranges. One half of these values plus the variance totals from Table 4.6 yield 12.4 for the 0 to 10 knot range, 21.5 for the 20 to 30 knot range and 14 for the greater than 30 knot range. If the value of R is chosen to be 0.5, then the total variance of the formal and parallel error components for weather ships would be one third of the weighted averages for types B C and D as given in the preceding paragraph.

If, then, $R = 0.5$, the weighted B C D variances must be divided by 1.5 to obtain the variances of the transient ship wind errors. These transient ship variances in turn must be divided by two to get the variances of the weather ship wind errors. For the synoptic errors, the variances of the weather ship errors must be subtracted from the variances of the synoptic analysis errors.

Also since the tables showed that the normal wind error component variance was about 21% greater than the parallel wind error component variance, the totals must be divided by 2.21 to get the parallel error component and the normal component is then the total minus this amount.

The results of these assumptions, and of the calculations that they imply, are shown in Table 4.7. Additional tables for other values of R, say, 0.3, 0.4, 0.6, and 0.7 could easily be generated. These kinds of errors in the presently available meteorological techniques for specifying the winds over the ocean exceed the User Agency Working Group's requirements for SEASAT-A in that the standard deviations imply errors in directions exceeding $\pm 20^\circ$ for low winds and errors in speed exceeding ± 2 meters per second (± 4 knots) for winds under 40 knots for all but the weather ships. The requirement for SEASAT-A is thus for a remote sensing system for measuring winds as good as, if not better than, a weather ship near every cell scanned by the instrument.

Table 4.4 also shows that the inability to specify the direction of the wind in a PBL analysis produces larger normal components than parallel components to the error vector. The cross isobar flow, determined by the friction in the lower layers of the atmosphere is thus a source of difficulty in defining the wind field. The same proportions; namely 1.21 to 1.00 have been used in all three categories for Table 4.7.

The results of the withheld weather ship analysis and of the limited sets of one minute average winds over timed intervals from 11 to 21 minutes are not completely consistent. Effects such as the differences in anemometer exposure from one weather ship to another, of less than one minute averages in the reports, if they occur, and

of sample size all compound to make the estimation (in a statistical sense) of the errors in using a weather ship observation of the wind and interpolating it to a given cell in an S193 scanning pattern very difficult. The results of Chapter 8 suggest for example that the errors for light winds should be somewhat larger than those given in Table 4.7 for weather ships.

The histograms in Figures 4.33, 4.34, and 4.35 can be reinterpreted in terms of Table 4.7. If the variances of the errors in weather ship measurements are half those of transient ship, then the total variances for Type + must be reduced by the amounts given in the first column of Table 4.7. The magnitudes of the wind speed errors then scale according to $(5.73/78.9)^{\frac{1}{2}}$, $(94.4/128.4)^{\frac{1}{2}}$ and $(223.6/301.6)^{\frac{1}{2}}$ which equal 0.85, 0.86, and 0.86 respectively. The largest value in Figure 4.34 is then 38 knots.

Moreover, in the analysis of S193 data, the problem arises of whether or not the quality of the backscatter data can be demonstrated given these kinds of errors in the meteorologically determined winds that serve as the surface truth for this experiment. Strangely enough, this is still possible, and the results of the analysis of S193 data to follow are most encouraging.

Additional Considerations of Synoptic Wind Field Analyses. The above analysis provides a procedure for the immediate improvement of wind field analyses in the PBL. In the presently used procedure, if a weather ship is used at a grid point, no other ship is used. If a Type B is used, no other is used, and so on. Once the error statistics of weather ships are found, then properly weighted linear combinations of the vector winds reported by every ship that can influence a particular grid point can be computed and used at that grid point for

that wind. For two ships of the same quality, the error is reduced to 70% of that of one ship alone. For four ships, it would be reduced to one half that of one ship alone, and so on.

The withheld data analysis technique can be extended to Type C (or Type D or Type +), ships replacing Type B ships, Type D (or Type +) replacing Type C, and no ship (Type +) replacing Type D. The information gained would be particularly useful in defining the errors present in synoptic analysis procedures for less traveled parts of the ocean far from the locations of the weather ships. The error estimates in Table 4.6 will probably turn out to be the smallest that will be found and large areas of the ocean will have errors in the winds over them that are greater than those tabulated.

Documentation of Theory used in the Error Analysis. The statistical model used in the error analysis follows the theoretical developments of Rapp (1952), Crutcher (1957), Crutcher (1962) and Crutcher and Moses (1963). The techniques in these references will also allow the theory to be extended to include measurements by SEASAT-A of the vector wind. The application of these techniques is illustrated by the upper wind charts prepared by Crutcher and Bailey (1962), Crutcher (1959a), and Crutcher (1959b).

**TABLE 4.7 Estimates of the Errors of the Vector Wind for Weather Ships,
Transient Ships, and Synoptic Analyses for Various Wind Speed Ranges.**

Wind Speed Range Knots	WEATHER SHIP					TRANSIENT SHIP					SYNOPTIC				
	Total VAR	PAR VAR	PAR SD	NORM VAR	NORM SD	Total VAR	PAR VAR	PAR SD	NORM VAR	NORM SD	Total VAR	PAR VAR	PAR SD	NORM VAR	NORM SD
0 - 10	9	4.1	2	4.9	2.2	18	8.1	2.9	9.9	3.1	34.9	15.8	4	19.1	4.4
10 - 20	21.7	9.8	3.1	11.9	3.4	43.3	19.6	4.4	23.7	4.9	57.2	25.9	5.1	31.3	5.6
20 - 30	34	15.4	3.9	18.6	4.3	68	30.7	5.5	37.3	6.1	94.4	42.7	6.5	51.7	7.2
GT 30	79	35.7	6	43.2	6.6	158	71.5	8.5	86.5	9.3	223.6	101	10	122	11.1

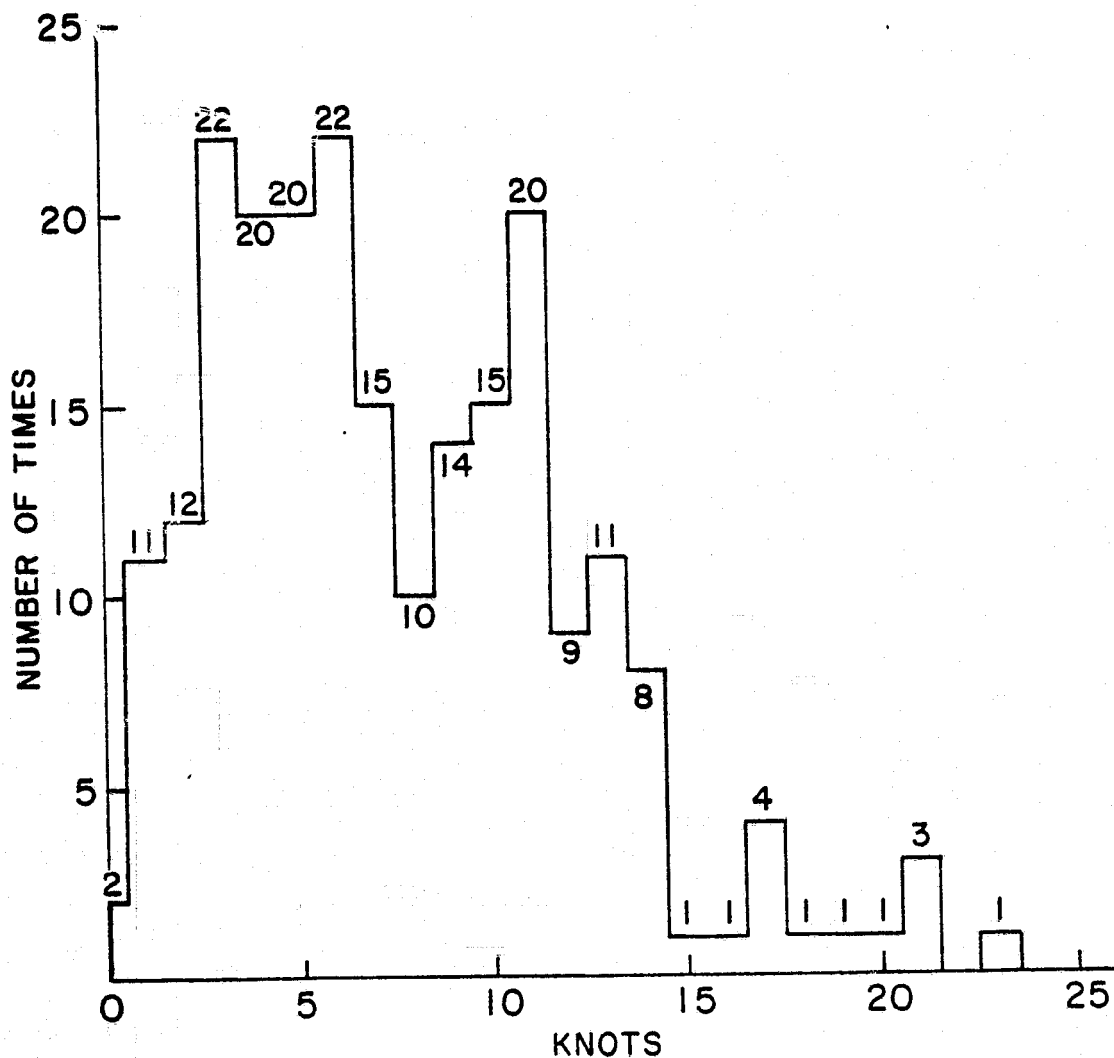


FIGURE 4.33 HISTOGRAM OF THE MAGNITUDE OF THE VECTOR WIND ERROR FOR TYPE +; 224 VALUES, 10 TO 20 KNOTS.

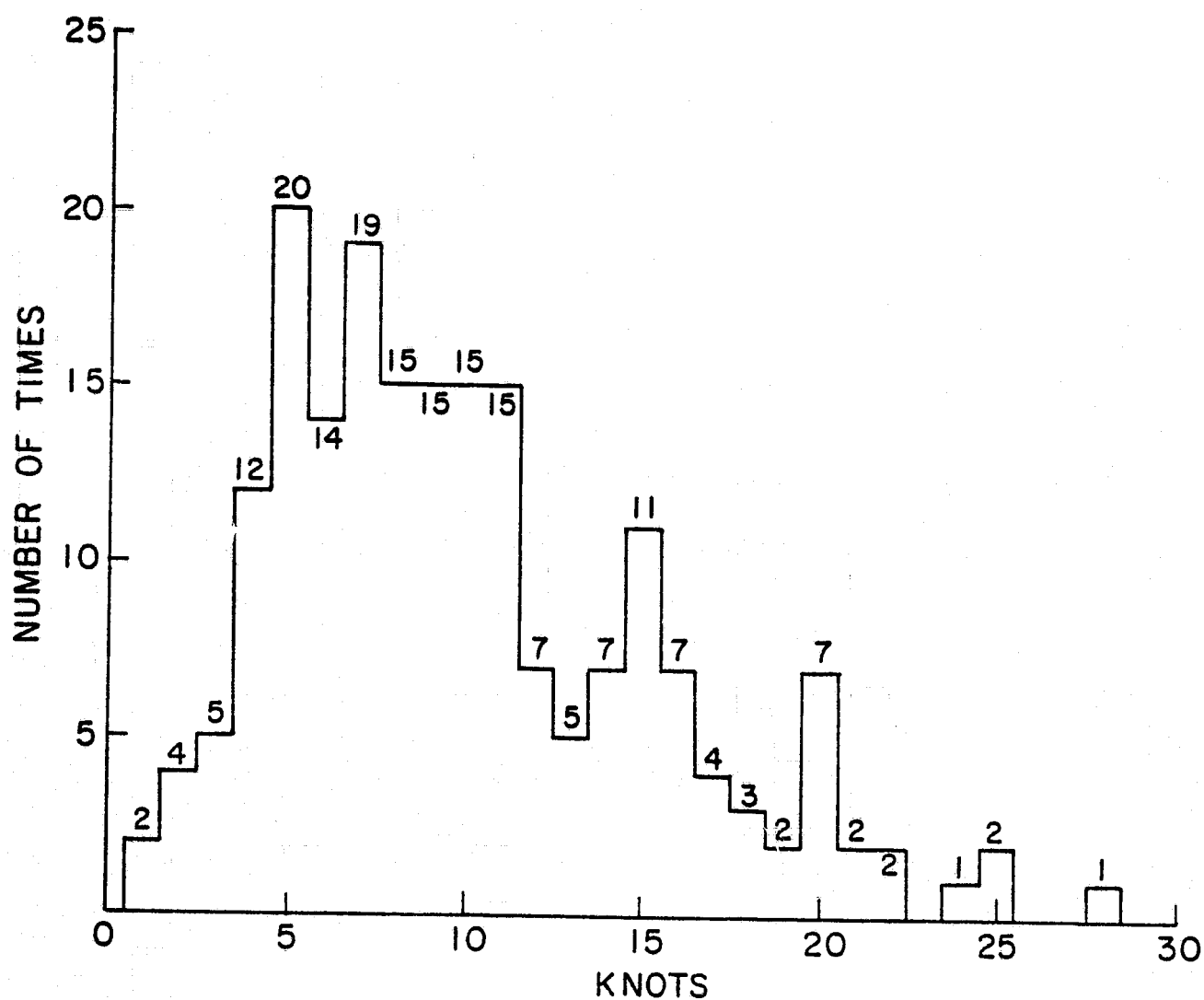


FIGURE 4.34 HISTOGRAM OF THE MAGNITUDE OF THE VECTOR WIND ERROR FOR TYPE +; 197 VALUES, 20 TO 30 KNOTS.

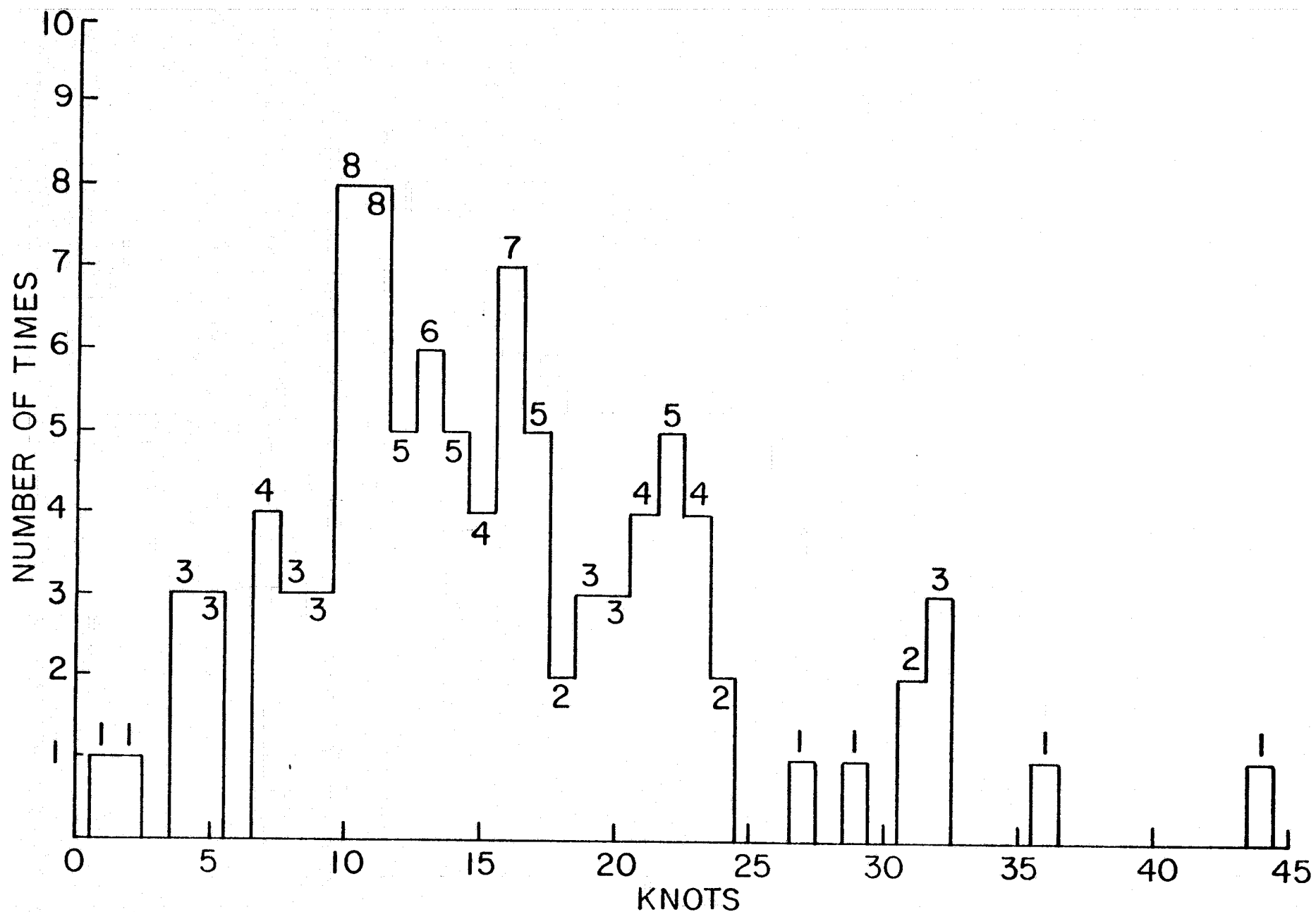


FIGURE 4.35 HISTOGRAM OF THE MAGNITUDE OF THE VECTOR WIND ERROR FOR TYPE + ; 98 VALUES, 30 OR MORE KNOTS

CHAPTER 5 THE MERGING OF THE METEOROLOGICAL, OCEANOGRAPHIC AND S193 DATA.

RECAPITULATION

As described in Chapters 2, 3, and 4, there eventually came a time when the S193 data were believed to be correct, and the meteorological and oceanographic data had been assembled and analysed. The next step was to merge the two data sets for the final data analysis steps that were still to come. At this stage of the analysis, the effects of variations of incident angle were still not corrected for. Also, attenuation had not been computed and the effects of wind direction relative to the pointing direction of the radar beam had not been treated.

APPENDIX A

Appendix A contains tables for every useful S193 pass during SKYLAB. The merged data for each pass are given in the order in which the pass is tabulated in Table 3.1. The data for both ITNC and CTNC passes are given in similar formats.

The heading on the page for the pass gives the DOY, the date, the type of pass and the location. The columns give the scan number, the incidence angle, the backscatter values in db for VV, HH, VH, and HV, the vertically and horizontally polarized antenna temperatures in degrees absolute, the aspect angle of the wind in degrees, the wind speed in meters per second, the sea surface temperature in degrees celsius, the time of the measurement, the latitude and longitude of the cell center (where - means west of Greenwich), and a data flag. Nearly all of the tabulated values are self explanatory except the values of the aspect angle, the azimuth angle and the data flag.

The azimuth angle and the aspect angle allow the wind direction to be referred to true north and to the pointing direction of the radar beam. The azimuth angle gives the direction toward which the radar beam was pointing at the time of the measurement. For example, on DOY 156-1 (June 5, 1973), scan numbers 2.1 through 8.5 show azimuth angles near 132° , which for a southbound in track noncontiguous pass is correct for a pass over the Gulf of Mexico. Zero degrees aspect angle is defined to be upwind, and positive angles are clockwise relative to upwind. The wind direction for scan number 2.1 (from which) is therefore 133.7° . The aspect angles vary from -179.9° to $+179.9^{\circ}$, where those near zero degrees are for upwind, those near $\pm 180^{\circ}$ are for downwind.

The data flag can be a (1), a (2), a (4), or a (-2). A (1) represents land in a portion of the cell; a (2) means the cell is near land, a (4) represents rain and a (-2) means that some undetermined local phenomenon is occurring. For most analyses, these points were excluded from further analysis.

For the ITNC passes, the cells for the different incidence angles form groups of five all at nearly the same point except for the 50° incidence angle, which is slightly displaced from the other four. For example for DOY 156-1, the latitudes and longitudes for scan numbers 3.2, 4.3, 5.4 and 6.5 are within 0.05 degrees latitude and 0.17 degrees longitude of each other, and scan number 2.1 is slightly displaced relative to the other four. For the CTNC passes, every cell is separate and distinct from all of the others.

As explained in Chapter 3, the passive microwave temperatures were not good for all SKYLAB 4 passes because of the damage to the antenna. These remaining data were nevertheless processed and useful results were obtained.

THE PURPOSE OF THE TABULATIONS

A study of this nature eventually reduces to the study of grouped sets of numbers obtained from various sources and manipulated according to the present theoretical understanding of what was measured. The data in Appendix A represent nearly all of the data needed for determining the relationship between winds and radar backscatter as measured by SKYLAB. The values tabulated are relatively untouched by theoretical manipulations at this stage of the presentation. The backscatter values have been corrected for the effects of the departure of the spacecraft from a local vertical, but the variability of the nominal incidence angles is still preserved.

In this form, it is possible for theories other than those actually used to be tested against the data, and should additional sources of meteorological data or other ways to analyse the meteorological data become available, these tables would be a good place to start in any reanalysis of the SKYLAB S193 data. These tables represent, by themselves, a significant achievement of EPN 550, since, of course, they are the only presently available measurements of radar backscatter from a spacecraft. Compared to the measurements that may eventually become available from SEASAT-A, they form a relatively small sample, but even this sample is much bigger than is available from many years of effort in remote sensing programs using various aircraft.

CHAPTER 6 BACKSCATTER THEORY, WAVE SPECTRA, BACKSCATTER MEASUREMENTS, AND WAVE MEASUREMENTS

Introduction. The measurement and theoretical understanding of the very short waves on the sea surface as a function of wind speed and direction and the measurement and theoretical understanding of radar backscatter as a function of wind speed and direction are strongly interrelated. Prior to the research of Wright (1968) there was not much of an effort to connect the properties of waves on water to the measurement of radar backscatter. In this section, the interaction of the above four aspects of the problem will be treated from 1968 to the present.

There are three different kinds of radar backscatter theories to be considered in this discussion. One applies for nadir angles near zero; that is with the antenna pointing straight down. The other two apply for nadir angles of about 30° , or more, and are called Bragg scattering theories, or Rayleigh-Rice theories, as given for example in Rice (1951). Although of great theoretical interest, those theories for radar backscatter for nadir angles near zero are not particularly important in efforts to study the data from S193 on Skylab. The response to wind speed of the radar backscattering cross section is strongest and most useful for nadir angles greater than about 30° . For this reason, the near nadir angle theories will not be treated in this discussion except to note that examples can be found in articles by Bass and Bacharov (1958), Chia (1968), Fung and Chan (1973, 1975a), and Jackson (1974).

Bragg scattering theory in its simplest form, as in Rice (1951), for example, involves only the spectrum of the waves evaluated at a specific value of the vector wave number spectrum where the vector component has the value, $2k_0 \sin \theta$ as evaluated in the direction of the pointing vector of the electromagnetic wave. In this expression, k_0 is the wave number of the electromagnetic wave; that is, $2\pi/\lambda$, where λ is the radio wavelength.

There are various extensions of the Bragg scattering theory. Some consider the higher order extensions of the theory involving sums and differences of the wave numbers involved, multiple reflections from the sea surface, and other effects. The extension that seems to have provided the most useful results is the composite theory that tilts the surface on which the shorter ocean waves are riding according to the probability density function of the slopes of the larger waves.

This review will concentrate on X-band and K_u -band radar backscatter, and in particular on backscatter for 8.9 and 13.9 GHz radio waves. For these two frequencies the radio waves are 3.37 and 2.15 cm long, and at a 30° nadir angle, $2k_0 \sin \theta = k_0$. It is, therefore, important to know about the spectrum of waves on the sea surface with lengths near these values. The slopes of portions of the sea surface of dimensions, say 10 to 100 times larger than these values, that is, about 20 centimeters to four meters are also important if slopes are to be considered in an improved theory. Of course, as the nadir angle, θ , varies from angles less than 30° , for example 25° or so, up to angles like 60° , the wave number given by $2k_0 \sin \theta$ varies, and values that correspond to the wavelengths from 4 cm to 1.25 cm are the result.

There are some differences in the definitions of the wave spectra involved between the oceanographic literature and the radar literature. In the radar literature a factor of π seems to be omitted, and the spectrum is treated as a double sided function, such as would arise from the inversion of a typical covariance function for the sea surface, instead of a single sided function. These features are usually thoroughly taken care of in exact derivations that use oceanographic representations for the wave spectrum.

A First Attempt. The work of Wright (1968) was strongly influenced by the work of O. M. Phillips (1966), as summarized in the book, "The Dynamics of the Upper Ocean". Phillips had derived a theory based on

dimensional analysis of the properties of waves from which it was concluded that an equilibrium range existed for gravity waves and for capillary waves. According to this theory, the wave number spectrum that should be used in radar theory would be given by equation (6.1) where the symbol, K , represents the magnitude of the vector wave number.

$$W(k) = BK^{-4} \quad (6.1)$$

If an isotropic spectrum is assumed, then K is given by equation (6.2).

$$K = (K_x^2 + K_y^2)^{\frac{1}{2}} \quad (6.2)$$

There are some semantic differences between the concept of an equilibrium spectrum and a saturation spectrum, but Wright interpreted Phillips' work to mean that over a large range of wind speeds the spectrum was of the form given by equation (6.1), and assumed that the spectrum was isotropic, that is completely independent of wind direction, so that the second equation could be substituted into the first equation.

The only remaining unknown constant in such an expression for the spectrum is the value of B , and on the basis of the material found in Phillips it was assumed that the value of B was 6×10^{-3} for gravity waves and 1.5×10^{-2} for the capillary waves.

The first order Bragg scattering equation for the normalized radar backscattering coefficient for vertical polarization is given by equation (6.3) where θ is the nadir angle and α_{vv} is a not-too-rapidly varying function of the dielectric constant, ϵ , and the nadir angle.

$$\sigma_{vv}^0 = 4\pi k_0^4 \cos^4 \theta \alpha_{vv} W(K_x, K_y) \quad (6.3)$$

In this context, then, once all of these assumptions are granted, and if the equilibrium range for what is loosely referred to as capillary waves with wavelengths such as those mentioned immediately above can be equated to a saturation range, then the problem of radar backscatter

would apparently be solved. The substitution of the equation for the wave spectrum into the equation for radar backscatter, with $K_x = 2k_0 \sin \theta$ in this particular case for σ_{vv}^0 , yields equation (6.4).

$$\sigma_{vv}^0 = 3.75\pi \times 10^{-3} \alpha_{vv} \cot^4 \theta \quad (6.4)$$

If the capillary spectrum saturates, and if it saturates for a relatively low wind speed, then this equation states that the radar backscattering cross section depends only upon the dielectric constant of sea water, and the nadir angle. In the above equation, the value of B is that that would be obtained for "saturated" capillary waves. Guinard (1969), for example, gives a similar equation (his equation 8) evaluated for gravity waves. Since the ratio of the saturation value for capillary waves to that for gravity waves, according to these assumptions, is 15/6, the constant 1.5×10^{-3} has been increased to 3.75×10^{-3} .

Both Wright (1968) and Guinard (1969) accepted the idea that the radar backscattering cross section at X-band saturated for a quite low wind speed and did not increase above this wind speed. At the time of the preparation of the second reference, Guinard (1969) concluded that:

"Lastly, the data collected with the X-band system at 30° grazing angle have been used to determine an optimistic estimate of the variation of RCS* with wind and a conservative estimate of the wind speed at which saturation occurs. The results have shown that the saturation condition, defined to hold in the region where the RCS varies as the square root of the wind, applies for winds in excess of ten knots. This is indicated by the fact that the increase in RCS for an increase of wind from the 10 knot to the 48 knot wind condition is approximately 3 dB. Further experiments are planned to further explore the critical region in the wind speed range from 5 to 20 knots."

(A grazing angle of 30° corresponds to a nadir angle of 60°).

The data and measurements at 8.9 gigahertz at the time of the presentation of this paper were a very strong indication that the measurement of radar backscattering cross section would not depend very

* Radar Cross Section (i.e. σ^0)

strongly on wind speed and did not depend on the direction of travel of the waves relative to the direction of the radar beam.

The status of the agreement between backscatter measurements at various wind speeds, the theory of radar backscatter, and the nature of the underlining waves that cause it, according to Guinard (1969), is summarized by Figures (6.1) and (6.2) from this report showing the range of wind speeds for which measurements were obtained, the back-scattering measurements and the theoretical curves for σ_{VV}^0 and σ_{HH}^0 for 8.91 GHz. Except for the 40 knot measurement in snow, the measurements for winds for 48 to 22 knots cluster close together, and the 5 knot measurements are well below the others for nadir angles from 30 to 60 degrees. The theoretical curve for saturation lies five to eight decibels above the cluster of points for winds between 22 and 48 knots for vertical polarization. For horizontal polarization, there is again very little spread and the fact that the observations lie 10 to 20 decibels above the theoretical curve was attributed by Guinard to the tilting effect of the large waves at high nadir angles.

The concept of a saturated, or equilibrium, or fully developed, wave spectrum in these wavelength regions was substantiated in Phillips (1966) by a number of other conclusions. These conclusions, which are pertinent to the properties of capillary waves, serve to reinforce the concept of a saturated, or a equilibrium, spectrum. For example, on page 117 the following statement can be found.

"It should be noted that an infinitesimal capillary wave cannot be in a state of stable equilibrium in which the energy flux from the wind balances the viscous dissipation. For according to the linear theory, these two energy fluxes are in fixed proportion, each being proportional to the square of the wave amplitude. A disturbance either dies away or grows until it is limited by one or the other of these finite amplitude effects."

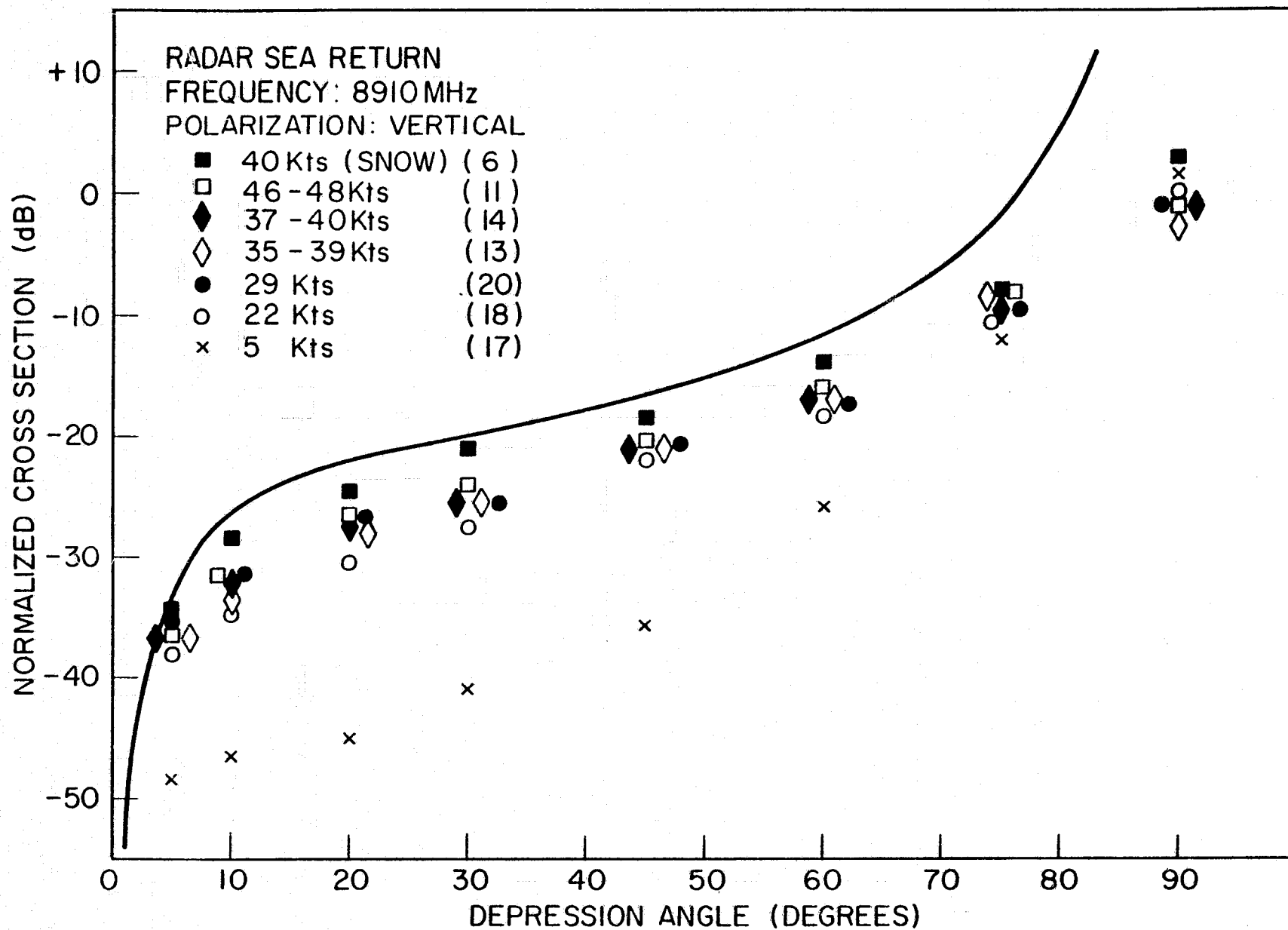


FIGURE 6.1 VERTICAL POLARIZATION BACKSCATTER AT 8.91 GHz ACCORDING TO GUINARD (1969).

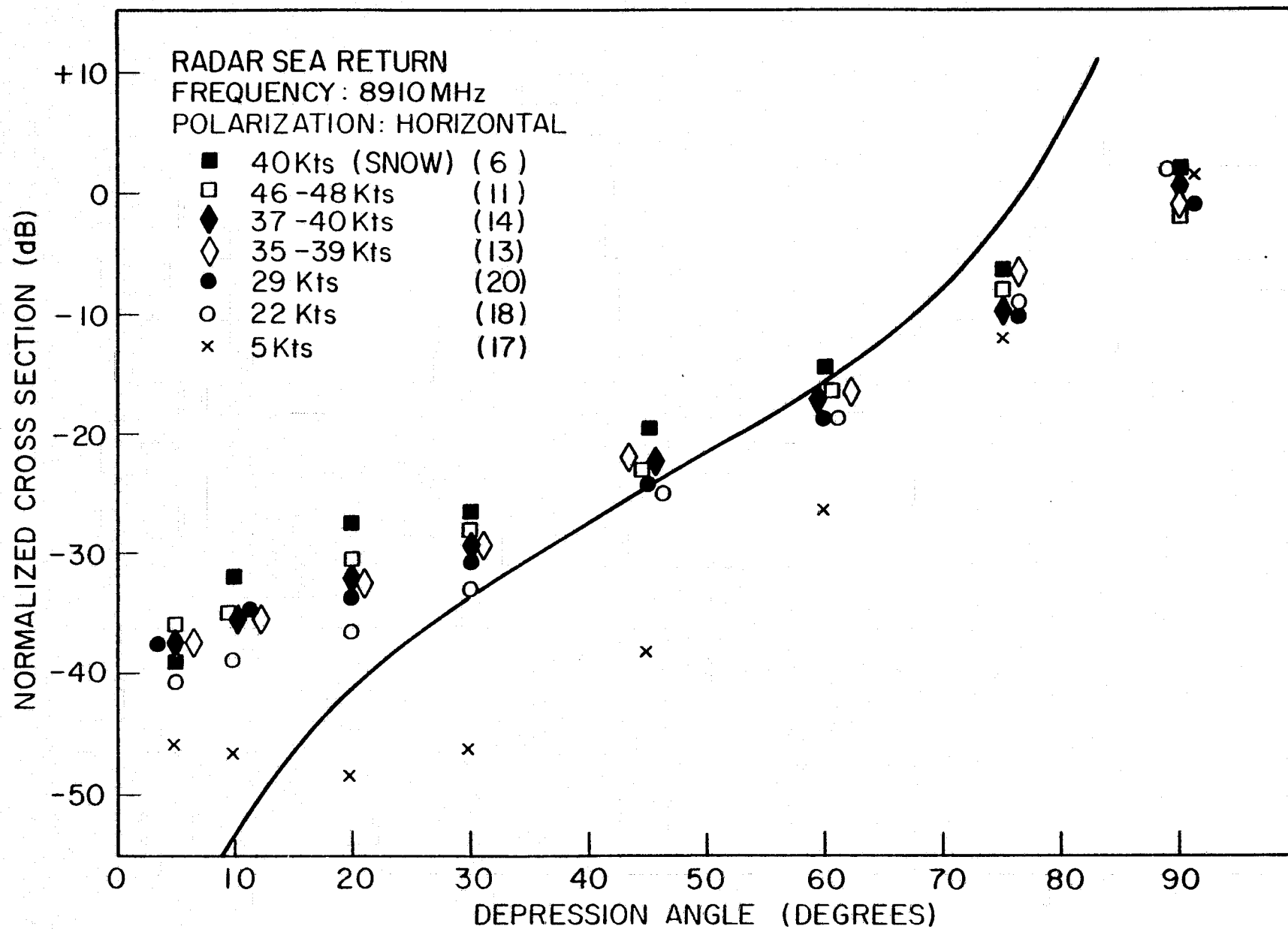


FIGURE 6.2 HORIZONTAL POLARIZATION BACKSCATTER AT 8.91 GHz ACCORDING TO GUINARD (1969).

Also a plausible explanation of an increase in the slope of the sea surface with wind speed as observed by Cox and Munk (1954) was obtained within the saturation theory by letting the high wave number part of the wave number spectrum grow toward higher wave numbers with increasing wind speed. The expression for the slope integrated over direction has a logarithmic singularity which allowed an explanation of an apparent increase in sea surface slope.

Additional efforts to measure radar backscatter had been initiated by NASA, and at the conference where the report by Guinard (1969) was given, an analysis of the larger gravity wave conditions and the winds that were observed over the oceans for a range of conditions encountered during a mission based at Shannon Ireland and called Mission 88, was given by Cardone (1969). Moore and Bradley (1969) reported on the analysis of the radar data obtained with a 13.3 GHz (K_u -band) fan beam Doppler radar on Missions 70 and 88 of this program.

The fan beam Doppler, which had calibration problems, had obtained the shape of the backscatter curve, σ_{vv}^0 as a function of θ for a fixed wind speed. However, the absolute level of the measurements fluctuated from one measurement set for one wind speed to another measurement set for a second wind speed by as much as 10 decibels. It had long been recognized that at nadir the backscattering cross section decreases with increasing wind speed and that at higher angles such as 30° , or greater, it increased with increasing wind speed. It was assumed that all the curves at different wind speeds crossed over at a nadir angle of about 10° and the relative shapes of these backscattering curves as normalized were compared for wind speeds varying from 12.5 to 49 knots for upwind for Missions 88 and 70 and for upwind and crosswind for Mission 88. The data that were available were for wind speeds of 49, 31, 26, 13, and 12.5 knots. For upwind measurements at a 35° nadir angle, Moore and Bradley reported a backscatter increase of 14 decibels, and for crosswind a backscatter increase of about 11 decibels over the range of wind

speeds from 12.5 to 49 knots. The upwind difference between 12.5 and 49 knots differed from the crosswind difference by 3 or 4 decibels with the upwind value exceeding the crosswind value. Since $49/12.5$ is 3.92, or 5.9 decibels, the 11 decibels in the backscatter suggest a backscatter dependence on the wind speed proportional to the 1.86 power.

The conclusions of Moore and Bradley (1969) are quoted below.

"1. At 13.3 GHz the shape of the scattering coefficient versus angle curve is truly dependent upon wind speed, with a difference in the ratio of 35° scattering coefficient to 10° scattering coefficient of more than 10 db for the wind speed range from 12 to 50 knots."

"2. Experimental error is sufficient that the absolute level of the curves must be established by better experiments. Hopefully, these can be conducted during the spring of 1970. Even with the error of measurement, however, the measured "absolute" value of scattering coefficient at 35° increases with increasing wind speed."

"3. The difference between the measurement made by the Naval Research Laboratory at 9 GHz and the NASA MSC aircraft at 13.3 GHz must be resolved. The Naval Research Laboratory measurements indicate a variation with wind speed of about 3 db over the same range where the NASA measurements indicate a variation of more than 10 db. Although it is possible that part of this may be due to differences in technique and calibration, a real difference due to this relatively small range of frequencies (a 50% increase over the 9 GHz) may exist."

A Model with Wind Speed Dependence. The next effort that tried to relate backscatter to the wave spectrum was that of Valenzuela, Laing and Daley (1971). The radar backscattering measurements as described by Guinard (1969), and available to these authors, covered nadir angles that ranged from 15° to 85° and included the angles, 30° , 45° , 60° , 70° , and 80° , in addition to the first two angles mentioned. There were four different frequencies available for the radars at 428 MHz, 1.228 GHz, 4.455 GHz, and 8.91 GHz. The radar wavelength are, for these frequencies, 70 cm, 24 cm, 6.73 cm, and 3.37 cm. By use of the Bragg scattering condition, namely $K = 2k_0 \sin \theta$, and with the variations in the angles

mentioned above, wavelengths from 135 cm to 1.7 cm can be sensed in the wave spectrum, if the assumption of the theory is correct; namely, that the first order Bragg scattering theory determines the radar backscatter completely.

Since the wave number spectrum has the dimensions of cm^{-4} , and isotropy is assumed, one can write equation (6.5). There is a constant needed that is assumed to be a universal constant. In this form, the quantity to be determined is ν , and it is assumed to be a constant that does not vary over the entire range of wave numbers in the spectrum. The dimensional analysis with L for length and T for time of the above equation is given below in equation (6.6). This shows that the analysis is dimensionally consistent.

$$W(K) = A g^{-\nu} U^{2\nu} K^{4-\nu} \quad (6.5)$$

$$\left(\frac{L^{-\nu}}{T^{-2\nu}} \right) \left(\frac{L^{2\nu}}{T^{2\nu}} \right) \left(\frac{L^{-4}}{L^{\nu}} \right) = L^{-4} \quad (6.6)$$

Valenzuela, Laing and Daley solved equation (6.3) to obtain equation (6.7)

$$W(K) = \frac{\sigma_w^0}{4\pi k_o^4 \cos^4 \alpha_v} \quad (6.7)$$

The backscatter measurements were used to determine the value of ν in equation (6.5). The spectrum that finally resulted was of the form given by equation (6.8).

$$W(K) = A U_{19.5}^{0.64} g^{-0.32} K^{-3.68} \quad (6.8)$$

This representation for the vector wave number spectrum still has no azimuthal angle dependence, and one would still use equation (6.2), given previously, in this equation in order to describe the variation of the spectrum as a function of two orthogonal wave numbers. With no azimuthal

angle dependence in this representation, it follows that the radar backscattering cross section grows slightly faster than $U^{0.5}$; that is,

$$\sigma^0 \sim U^{0.64} \quad (6.9)$$

where the wind is measured at about 19 or 20 meters above the sea surface.

A study of the data tabulated by Valenzuela, Laing and Daley (1971) suggests some interesting features. For example, the crosswind measurements provided a different constant than the upwind-downwind measurements. There are indications that the upwind-downwind values for the constants that were determined were nearly double the corresponding constants for crosswind for many of the data sets. This feature indicates the possibility of anisotropy in the data but it was not highlighted in the analysis carried out by the authors of the study.

Fan Beam Doppler at K_u -Band. Meanwhile, Bradley (1971) had completed an analysis of a much larger set of data obtained with the fan beam Doppler system, subject to the condition that the curves for σ_{vv}^0 could be normalized to an angle of 10° . He determined the constants A and B in equation (6.10) for several different values of θ over a range of wind speeds and for upwind and crosswind conditions. The winds were referred to a height of 19.5 meters, and the surface truth, in general, was provided by Cardone, who analyzed the wind data obtained at the time of the various flights. The range of wind speeds involved varied from 6 to 33 knots (3.08 to 17 meters per second). The values for A and B for different nadir angles and for upwind and crosswind conditions as obtained by Bradley are given in the following table.

$$10 \log_{10} \sigma_{vv}^0 = A + B \log_{10} U_{19.5} \quad (6.10)$$

Table 6.1 The values of A and B found by Bradley (1971) for different nadir angles and wind directions. (13.3 GHz)

Wind Direction	Incidence Angle	A	B	RMS Error
Upwind	15°	-7.51	3.30	0.717 dB
	25°	-24.56	11.21	0.892
	35°	-34.42	14.93	0.882
Crosswind	15°	-6.68	2.13	0.748
	25°	-22.84	7.51	1.196
	35°	-35.51	12.62	1.355

In antilog form, equation (6.10) transforms to equation (6.11).

$$\sigma_{VV}^0 = 10^{A/10} U^{B/10} \quad (6.11)$$

The results of Bradley are not in agreement with the results of Valenzuela, Laing and Daley (1971). If they are correct, they show that the higher the nadir angle, the stronger the power law. The table also shows that there is a difference between crosswind conditions and upwind conditions. These particular features cannot possibly be derived from a wave number spectrum such as the one assumed by equations (6.2) and (6.8). For these equations, if first order Bragg scattering is correct, the exact same power law should be observed with any frequency radar.

A Study of the Wave Spectrum. Pierson and Stacy (1973) undertook the study of wave data and the oceanographic literature in order to define the wave spectrum at high frequencies and high wave numbers, as well as the full range of the wave spectrum as might be observed on the open ocean. For their purposes, the wave number spectrum can be defined as equation (6.12).

$$S^*(k, \Phi) = \frac{S(k)}{\pi} \left[1 + \sum_{n=1}^{\infty} a_n \cos 2n\Phi \right] \quad (6.12)$$

for $0 < k < \infty$

and $-\frac{\pi}{2} < \Phi < \frac{\pi}{2}$, and zero otherwise

This spectrum has the property that its integral as given by equation (6.13) equals the total variance of the wavy surface.

$$m_0 = \int_0^{\infty} \int_{-\pi/2}^{\pi/2} S^*(k, \Phi) k dk d\Phi \quad (6.13)$$

Fully developed wind seas with no swell waves traveling in directions outside of 90° to the wind direction were assumed in the analysis. Under certain assumptions, it follows that equation (6.14) can be obtained,

$$S(k) = k S^*(k) = \int_{-\pi/2}^{\pi/2} S^*(k, \Phi) d\Phi \quad (6.14)$$

and this, in turn, if wave number and frequency can be related by the dispersion equation, can be calculated from records of the rise and fall of the wavy sea surface at a point. Also some idea of the total contribution to the slopes and curvatures of the sea surface can be obtained from $k^2 S(k)$ and $k^4 S(k)$.

As a part of this study, wave spectral data for waves measured in wind water tunnels were assembled and analyzed. The data were from a study conducted at NYU, from measurements by Toba (1973), and from a study by Sutherland (1967). These data were used to study that portion of the wave frequency spectrum from five hertz ($f = \omega / 2\pi$) upward to a viscous cut off frequency that was wind speed dependent. There were a total of 67 spectra available for values of u_* that ranged from 3.3 centimeters per second to 170.2 centimeters per second. These friction velocities correspond to winds at an elevation of 19.5 meters above the sea surface that would vary from 3.5 meters per second to over 28 meters per second. The lengths of the fetch in the various wind water tunnels varied from about 2 meters to over 18 meters.

At that time, it was believed that the gravity wave spectrum behaved like equation (6.15) at high frequencies.

$$S(\omega) = \alpha g^2 / \omega^5 \quad (6.15)$$

From the dispersion relationship for gravity waves, namely $\omega^2 = gk$, it follows that equation (6.16) can be obtained.

$$S(k) = \alpha / 2k^3 \quad (6.16)$$

In this equation, the constant α was given as $8.1 \times 10^{-3} *$.

The region of interest was called the capillary wave spectrum, although surface tension does not completely determine the dispersion relationship for these waves and Mitsuyasu and Honda (1974) questioned the terminology. But, nevertheless it was assumed that the capillary wave spectrum was given by equation (6.17) in wave number form.

$$S(k) = B/k^3 \quad (6.17)$$

The dispersion relation for all waves can be given by equation (6.18).

$$\omega = (gk + (\tau k^3 / \rho))^{1/2} \quad (6.18)$$

where τ is the surface tension, the ρ density and g the acceleration of gravity. The appropriate root of the cubic in k that results from the square of equation (6.18) yields an inverse solution for k as a function of ω suggested by equation (6.19).

$$k = k(\omega) \quad (6.19)$$

From $S(k)dk$ it is then possible to obtain equation (6.20) as a candidate for the frequency function for the wave spectrum.

$$S(\omega) = B (k(\omega))^{-3} \frac{dk(\omega)}{d\omega} \cdot d\omega \quad (6.20)$$

Given the estimate of the spectrum in this frequency range, as in $\hat{S}(\omega; u_*, F)$ for different friction velocities and fetches. The quantity given by equation (6.21) can be found.

$$H(\omega; u_*, F) = \frac{\hat{S}(\omega, u_*, F) (k(\omega))^3}{(\alpha/2) (dk(\omega)/d\omega)} \quad (6.21)$$

* α_{vv} in equation (6.3) has nothing to do with this α , nor with the α in Chapter 4.

If the assumptions are correct, $H(\omega, u_*, F)$ should be a constant over a range of ω from about 10π to 30π , or so. Finally from this quantity by integrating over a range of frequencies where the function appears to be constant, the quantity given by equation (6.22) can be computed.

$$D(u_*, F) = \frac{1}{\omega_n - \omega_1} \int_{\omega_1}^{\omega_n} H(\omega, u_*, F) d\omega \quad (6.22)$$

The quantity $D(u_*, F)$ is a number for each one of the 67 spectra available in the study.

Pierson and Stacy (1973) were making a mistake in the analysis at this point that was not realized until a year or so later. Nevertheless, the quantity, $D(u_*, F)$, was calculated and shown to be independent of the different fetches. The spectrum for this range of frequencies was then defined to be equation (6.23)

$$S(k) = \alpha D(u_*) / 2k^3 \quad (6.23)$$

with $D(u_*)$ defined to be equal to equation (6.24) for u_* greater than 12 cm per second.

$$D(u_*) = (1.247 + 0.268 u_* + 10^{-5} u_*^2)^2 \quad (6.24)$$

The results were plotted in a number of different ways and discussed in the report. One of these ways is shown here in Figure 6.3. The most interesting feature of this particular plot is probably the four order of magnitude increase in the value of $D(u_*)$ that occurs roughly as a friction velocity of 12 centimeters per second is reached. This was interpreted to be the onset of the generation of these high frequency waves. It indicates that backscatter measurement should drop off very sharply below a threshold wind speed of approximately 3.5 meters per second over the ocean since the Bragg scatterers will not be generated for wind speed less than this. The

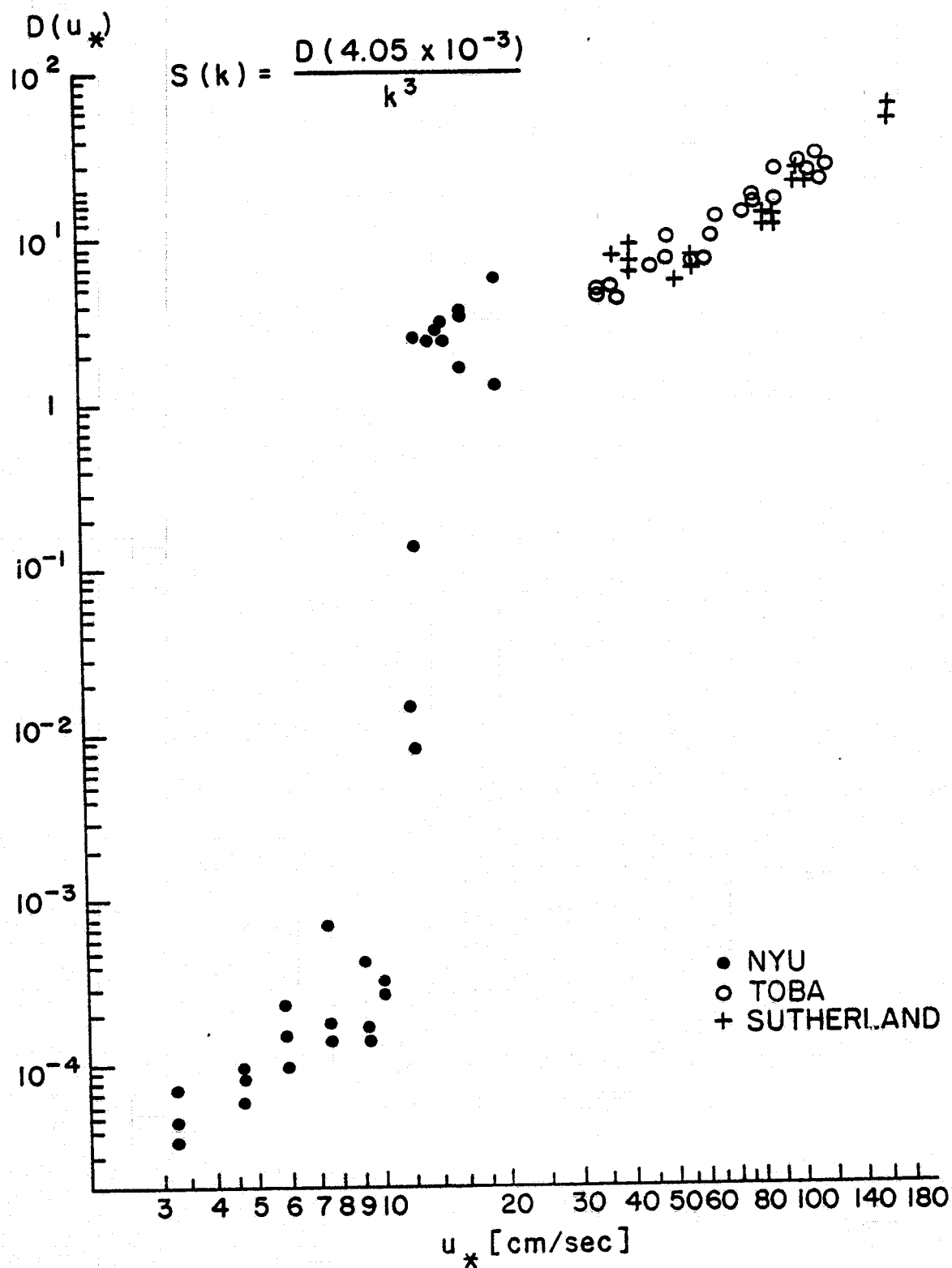


FIGURE 6.3 $D(u_*)$ VERSUS u_* (FROM PIERSON AND STACY (1973)). DATA FROM AN EARLIER BACKSCATTER THEORY HAVE BEEN OMITTED.

second important feature of this plot is that the quantity, $D(u_*)$, continues to increase by a considerable amount after the frictional velocity exceeds the value of 12 cm per second. For u_* ranging from 12 to approximately 190 cm per second, the quantity $D(u_*)$ varied from 2.5 to approximately 60. On a double log plot, the curve is not quite straight so that the analysis does not yield a straightforward power law. However, the range indicated yields an 11 db increase in U_* and a 14 db increase in $D(u_*)$ which imply, in a crude sense, a power law dependence of u_* to the 1.25 power.

In forming the function $H(\omega; u_*, F)$, the actual form of the function was graphed for a number of different values of u_* , and the result of this operation is shown in Figure (6.4) for values of the friction velocity ranging from about 57 to 169. The feature that was missed in the analysis was clearly shown in this set of plots. The curve for the lowest value of u_* slopes downward with increasing ω , and the curves in the middle lie half way between this downward slope and the decidedly upward slope of the values graphed for the highest value of u_* . If the function, $H(\omega; u_*, F)$, had been fitted by a straight line between ω_1 and ω_N as shown on this figure, its slope would have changed with an increase in u_* from a negative slope to a positive slope. The difficulty in seeing this feature, which is now obvious on the basis of the results of others, can in part be attributed to the high degree of sampling variability in the spectral estimates, as indicated by the length of the 90% confidence interval shown on the figure.

Pierson and Stacy were also concerned with the fact that the wave number spectrum had to be anisotropic. Stated in another way, equation (6.2) given much earlier, could not possibly hold at these frequencies, and an attempt was made to determine something about the coefficients, a_n , in equation (6.12). Even now, this particular Fourier series is not well known for waves with these wavelengths, and it is increasingly more important that more be learned about the anisotropy of the waves at these

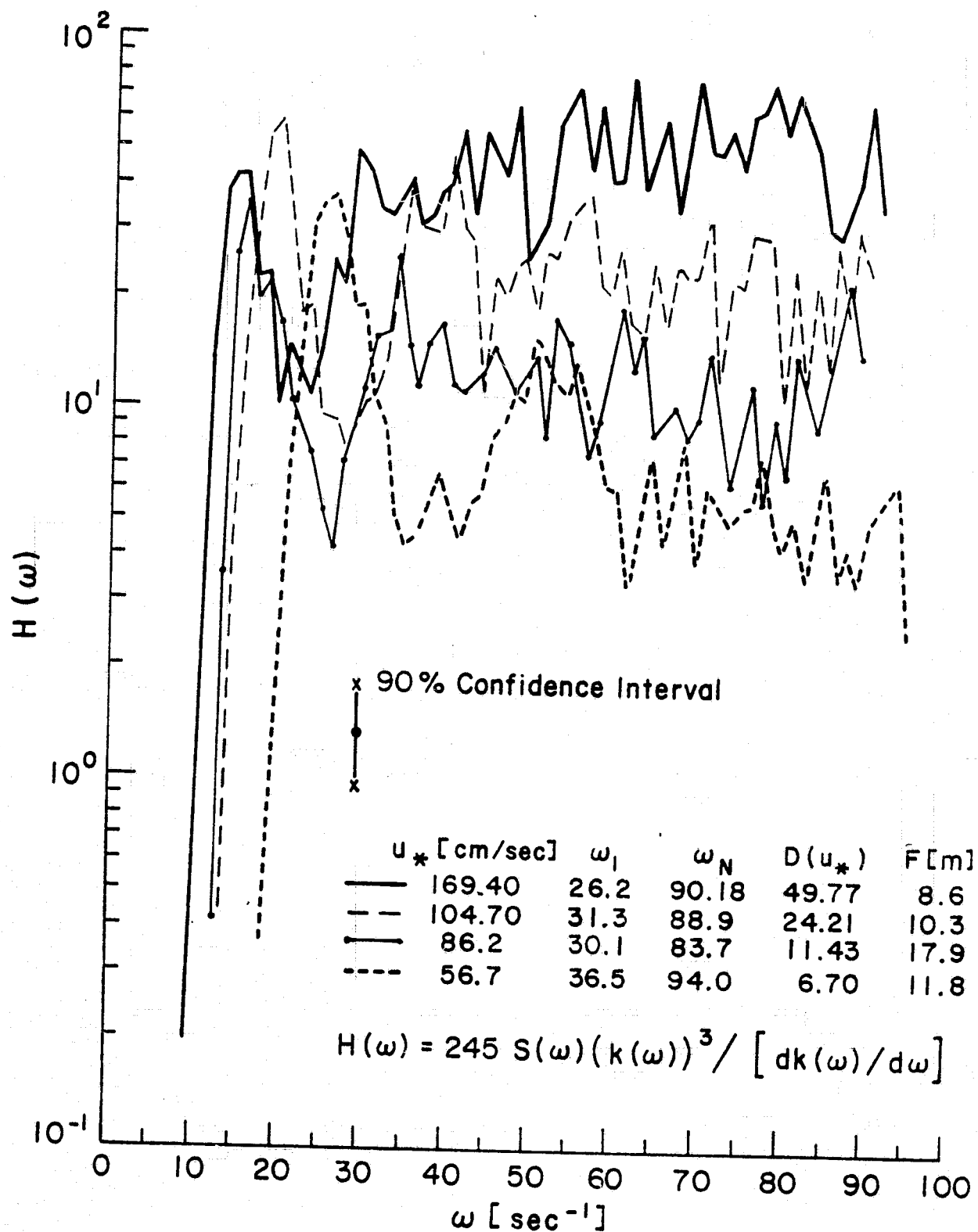


FIGURE 6.4 $H(\omega)$ VERSUS ω FROM PIERSON AND STACY (1973)

wave numbers and frequencies. However, from the study of the data obtained by Bradley and the Cox and Munk (1954) study of sea surface glitter patterns and probability distribution functions, it was possible to obtain two estimates of the coefficient a_1 in equation (6.12). The data from Cox and Munk are the result of certain integral operations on the spectrum given by equation (6.12) in which for upwind and downwind, it is multiplied by $k^2(\cos \Phi)^2$ and for crosswind, it is multiplied by $k^2(\sin \Phi)^2$. Similarly, for the upwind, downwind and crosswind values in the results obtained by Bradley to be different, the value of a_1 , at least, has to change. The results of this part of the analysis were that the quantity a_1 was wind speed dependent and increased from approximately 0.32 to 0.5 as u_* varied from 12 to 150 based on the data from Bradley. Based on the glitter measurements of Cox and Munk, a_1 increased from 0.1 near 12 cm per second to approximately 0.4 near 150 cm per second.

Even at this time, there were data available in the oceanographic literature, that, if interpreted properly, might have shed more light on the interrelationship between wave spectra and radar backscatter. Two reports of great importance are those of Leykin and Rosenberg (1970) and Kondo, Fujinawa, and Naito (1973). Both of these studies showed graphs of the frequency spectrum $S(\omega)$, or $S(f)$, as the case may be, for different wind speeds. The study by Kondo et. al. is more readily available, and reference to it shows, for example, in Figure 3 of that paper, that the frequency spectrum in the high frequency portion of the wind generated wave spectrum lies substantially above the proposed asymptomatic form given by $\alpha g^2 \omega^{-5}$. Moreover, the growth of the spectrum is greater at the higher frequencies than at the lower frequencies over the range of interest. In addition, both of these studies indicate that there is no saturation in this portion of the frequency spectrum. The study by Sutherland (1967) also indicated that there was no saturation in the spectrum. The conclusion of Kondo et. al. can be quoted as follows:

"However, our field results do not indicate the capillary saturation limit, at least within the range of winds encountered (about 1 to 16 meters per second measured at a height of 10 meters)."

The appropriate quote from Sutherland (1967) is:

"The present data do not show a true equilibrium range as predicted by Phillips (1958)."

More on Equation (6.5). Daley (1973) continued the analysis technique originally employed by Valenzuela et. al. (1971) using a much more extensive data set that employed the same four different radars and the same set of nadir angles. The data set consisted of the values used by Guinard (1969) obtained in 1969, values obtained in 1965, and a new set of values obtained in 1970 for wind speeds from 5.7 to 12.9 meters per second. The full range of wind speeds was from 5.7 to 24.2 meters per second. Still of the belief that radar backscattering could be explained by means of a first order Bragg scattering theory and the derivation summarized previously, Daley resolved these equations for the entire data set. However, a separate check was made of what the wind speed dependence of σ^0 would be as a power law function of the wind speed. The conclusions of Daley can be summarized in two tables, and by some general statements based on these tables. Only the results for the 8.91 GHz radar are discussed.

Table 6.2 based on the results of Daley (1973) gives the values of the power law that yields the best fit to the measured radar backscattering cross section in terms of a proportionality to the wind speed. Only values of wind speed greater than 5 meters per second were used. The limits of error, ± 2 standard deviations for the estimates of the mean values, that are given are ± 0.6 . The power law dependence of σ^0 on wind speed according to these results, and ignoring polarization for the moment, varies from 0.3 to 2.0 depending upon the entry in the table,

and if an error as large as two standard deviations is admitted as a possibility, the highest possible power law dependence would be 2.6 at 45° for crosswind cross polarized return. For co-polarized returns, of the 18 values of 2ν tabulated, half of them equal or exceed one, and the values are not too strongly in disagreement with Bradley (1971). The stronger dependence at crosswind compared with upwind is strange, and does not seem to check with other data.

Still under the assumption that the wave number spectrum had to be of the form given by equation (6.5), even these results were further averaged and smoothed to yield a value for 2ν in the equation for the spectrum which was supposed to hold over the full range of wavelengths and corresponding wave numbers mentioned above in the work of Valenzuela et. al. (1971). Table 6.3 gives these values, and again the power law dependence of radar backscatter is roughly, according to these results, proportional to the square root of the wind speed with very small deviations from this variation, depending upon whether the measurements were made upwind, downwind, or crosswind. The stronger wind speed dependence shown in Table 6.2 was probably lost in the scatter of the values for the constant A in equation (6.5).

Table 6.2 Values of 2ν from best fit of $\sigma^0 \sim U^{2\nu}$ for $U > 5$ m/s for X-band radar and for upwind (U), downwind (D), and crosswind (C) measurements. Limits of error equal to two standard deviations about the mean are ± 0.6 (from Daley (1973)).

Nadir Angle	Polarization								
	VV			HH			VH		
	U	D	C	U	D	C	U	D	C
30°	0.3	0.4	1.1	0.6	0.5	0.8	1.1	1.2	1.7
45°	0.8	1.0	1.2	1.2	1.3	1.8	1.7	1.8	2.0
60°	0.6	0.4	0.4	1.0	1.1	1.4	1.4	1.3	1.6

Table 6.3 Values for 2ν for equation (6.5)

Upwind	0.56 ± 0.3
Downwind	0.46 ± 0.3
Crosswind	0.39 ± 0.3

Although it was noted that the use of the power laws in the first of these two tables would give a better fit to the data, the final set of figures in Daley (1973) shows graphs of the predicted value of σ_{vv}^0 in db over a range of wind speeds from well under five meters per second to 24 meters per second for 8.91 gigahertz and for nadir angles of 30° , 45° and 80° . These results are plotted in figure 9 of that reference and are well worth studying in the light of the review being undertaken here. The theoretical curves, of course, show an increase of only about 3.5 db as the wind increases from 5 to 25 meters per second. The variation with wind speed is the same for all nadir angles and is obtained simply by displacing the same shaped curve up and down on the coordinate system. The data points scatter about the theoretical curves by as much as 20 db. In some places, some of the plotted values are 15 db higher than the corresponding point on the curve, and other plotted values are 20 db lower than the corresponding points on the curve. The measured values for upwind conditions at a nadir angle of 80° are plotted as small diamonds in the figure. There are 20 values plotted. Of these 20 values, only four lie on the line and touch it. None lie over the line and the remainder average five or six db below the line. One point at a wind velocity of six meters per second is 15 db below the theoretical curve.

Daley (1973) still believed in a theoretical upper bound to sea return and in an equilibrium spectrum. All of the wind speed power laws given have no indication of a wind speed above which they no longer apply. It is interesting to note that these weaknesses in the model show up in the tabulated data. The power law wind speed dependence is less and less as the radar wavelength increases, and becomes negligible for 428 MHz. Such a result is inconsistent with the model.

The data analyzed by Daley (1973) was made readily available in its original form, and Claassen and Fung (1972) analyzed the data taken during different years separately to see if a different power law could be obtained. The results of this study are also found in Claassen, Fung, et. al. (1972). A technique was developed to permit comparisons between two sets of data and to test the hypothesis that sets of data taken under different conditions such as, for example, a year apart, came from different populations. There were reasons to believe that Daley's results, especially those for upwind and downwind vertical polarization in Table 6.2, gave too low a power law. For the power law exponents of pooled sets of data, all but two of sixteen power laws exceeded one for four different nadir angles between 30° and 40° , and two polarizations and upwind and downwind. A further discussion of the matter can be found in Jackson (1974) and Daley (1973).

More Measurements of Backscatter and Capillary Waves. As these studies were under way and being carried out, SKYLAB was being planned, and an Advanced Application Flight Experiment Program was being initiated. The radar scatterometer passive microwave part of S193 on SKYLAB was also built for an aircraft version, with appropriate modifications, and independent observations of radar backscatter were obtained with this instrument as installed on an aircraft prior to, during, and after the SKYLAB experiment. Also new results on the high frequency part of the water wave spectrum as generated by the winds became available in papers by Mitsuyasu and Honda (1974, 1975). The wind tunnel used by Mitsuyasu and Honda was 80 centimeters high with available fetches from 105 to 825 cm. The water in the tunnel was 38 cm deep, leaving 42 cm for the air over the water.

Table 6.4 from Mitsuyasu and Honda shows the values of u_{*} measured for each reference wind at the wind tunnel entrance at the different fetches, and the corresponding 10 meter wind for the free atmosphere.

The friction velocity, u_* , increased with increasing fetch for the same reference wind speed in the wind water tunnel. The larger gravity waves grow down the fetch in such a tunnel, and the crests constrict the flow of the air between the top of the wind tunnel and the waves, thus, increasing the wind speeds over the waves and the stress of the wind on the water. It is very important to measure the profile of the wind over the wavy water surface at each fetch in order to correct for these effects in the analysis of the data. The various spectra that they published and the tabulated data about the different wave properties as a function of fetch clearly show that the capillary waves are growing as a function of the increase in u_* and can be correlated very well with the locally measured values of this parameter.

Table 6.4 Wind data (from Mitsuyasu and Honda (1974)).

U_r = reference wind tunnel wind at entrance.

U_r m/s	Station	F cm	u_* cm/s	z_0 cm	U_{10} m/s
5.0	1	105	14.9	2.24×10^{-4}	5.7
	2	225	22.2	2.40×10^{-3}	7.2
	3	345	21.6	2.94×10^{-3}	6.9
	5	585	21.6	3.05×10^{-3}	6.8
	7	825	25.9	1.47×10^{-2}	7.2
7.5	1	105	29.4	1.19×10^{-3}	10.0
	2	225	34.3	4.79×10^{-3}	10.5
	3	345	44.9	2.97×10^{-2}	11.7
	5	585	49.6	4.28×10^{-2}	12.5
	7	825	50.5	7.49×10^{-2}	12.0
10.0	1	105	36.9	4.07×10^{-5}	12.9
	2	225	51.2	1.06×10^{-2}	14.7
	3	345	66.9	4.95×10^{-2}	16.6
	5	585	64.5	3.99×10^{-2}	16.3
	7	825	66.9	4.19×10^{-2}	16.8

Continuation of Table 6.4

U_r m/s	Station	F cm	u_* cm/s	z_0 cm	U_{10} m/s
12.5	1	105	47.8	1.67×10^{-3}	15.9
	2	225	64.2	1.53×10^{-2}	17.8
	3	345	77.1	4.41×10^{-2}	19.3
	5	585	80.9	5.33×10^{-2}	19.9
	7	825	83.5	7.50×10^{-2}	19.8
15.0	1	105	79.6	1.00×10^{-2}	22.7
	2	225	109.0	8.76×10^{-2}	25.4
	3	345	126.4	1.63×10^{-1}	27.5
	5	585	157.2	3.83×10^{-1}	30.9
	7	825	179.6	6.15×10^{-1}	33.2

Figure 6.5 from Mitsuyasu and Honda show the frequency spectra of the waves at the longest fetch and for the largest u_* values for each reference wind. The spectra correspond to winds at 10 meters in the free atmosphere ranging from 7.2 to 33.2 meters per second. If the fetches had been longer and the waves for the gravity wave portion of the spectrum had continued to grow, it would be expected that some of the oscillations in these spectra in the range from 5 to 10 hertz, which are due to second order corrections to the larger gravity waves where the spectral peak is near two to four hertz would disappear and the nearly straight lines that go from 10 hertz out to 30 or 40 hertz on this graph would continue as nearly straight lines back into the range including these frequencies from 5 to 10 hertz.

As graphed, these spectra are extremely revealing. The frequency spectra on a double log plot are substantially straight lines, at least in the range from 10 to 30 hertz. This means that the spectrum can be expressed as a power law in frequency over this range. Also the spectra are closer together at 10 hertz than they are at 20 or 30 hertz. At 10 hertz, the spectra increase by approximately a factor of 10 for the five nominal wind tunnel speeds, and at 30 hertz the spectra increase by approximately a factor of 70.

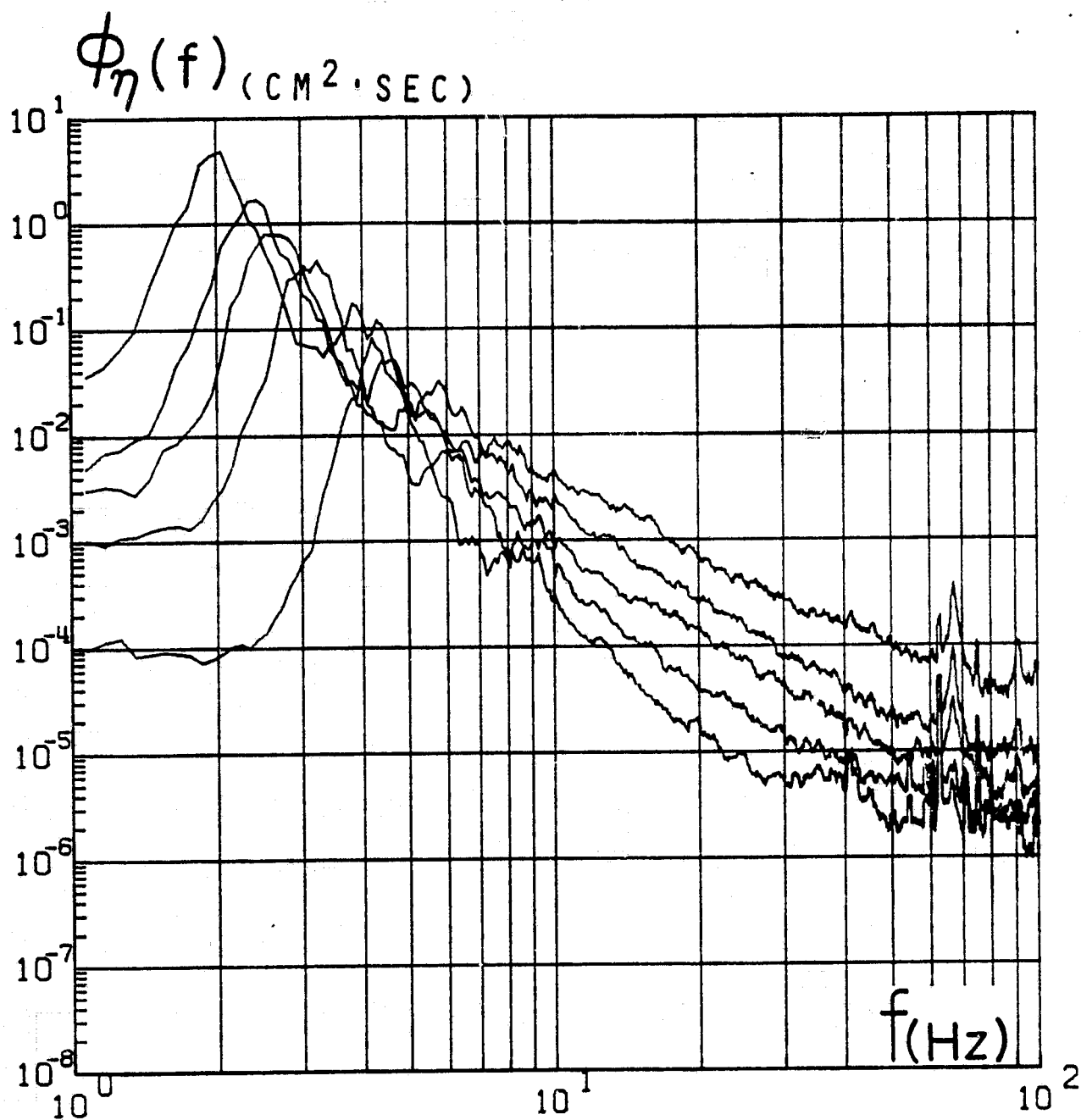


FIGURE 6.5 THE SPECTRA OF MITSUYASU AND HONDA (1974)
FOR THE FREQUENCY RANGE FROM 5 TO 30 Hz

The spectra proposed by Pierson and Stacy (1973) were modified in several ways by Pierson (1975), the most important being that the curves shown in Figure 6.5 were fitted in frequency space by equation (6.25).

$$S(\omega) = \frac{A}{2\pi} \left(\frac{2\pi f_0}{\omega} \right)^p \quad (6.25)$$

for $\omega > 10\pi$, and for $f_0 = 1$, $A = 0.875$, $u_* > 12$ and $p = 5 - \log_{10} u_*$

Given the spectrum in frequency form defined for frequencies greater than 5 hertz, the spectrum can be transformed to a wave number spectrum by means of equation (6.18) so as to obtain equation (6.26). The high frequency end of the spectrum was still cut off according to the results of Cox (1958). Also an additional modification of that spectrum are given in Pierson (1975).

$$S_4(k) = 0.875 (2\pi)^{p-1} \frac{(1 + 3\tau k^2/g\rho)}{g^{\frac{p-1}{2}} (k + \tau k^3/g\rho)^{\frac{p+1}{2}}} \quad (6.26)$$

for $k \gtrsim 1$, $u_* > 12$, and $p = 5 - \log_{10} u_*$

Two figures from Pierson (1975) are reproduced here for purposes of further discussion. Figure 6.6 shows the wave number spectrum for five different values of the friction velocity, u_* , corresponding to winds at 19.5 meters above the sea surface from 3.5 to 34.3 meters per second. The activity in the spectrum at the higher wave numbers corresponding to $k = 10^{-2}$ to $k = 10^1$ is quite evident. In this spectral plot, these changes would produce almost trivial changes in the height of the waves for problems in naval architecture, for example. For the interpretation of radar backscatter theory they are essential. The part of the wave number spectrum that is important in the calculation of radar backscatter using simple backscattering theories is that part that extends from $k = 1$ to $k = 10$, approximately, and $k = 1$ corresponds to a water wave length of 6.28 cm on this graph.

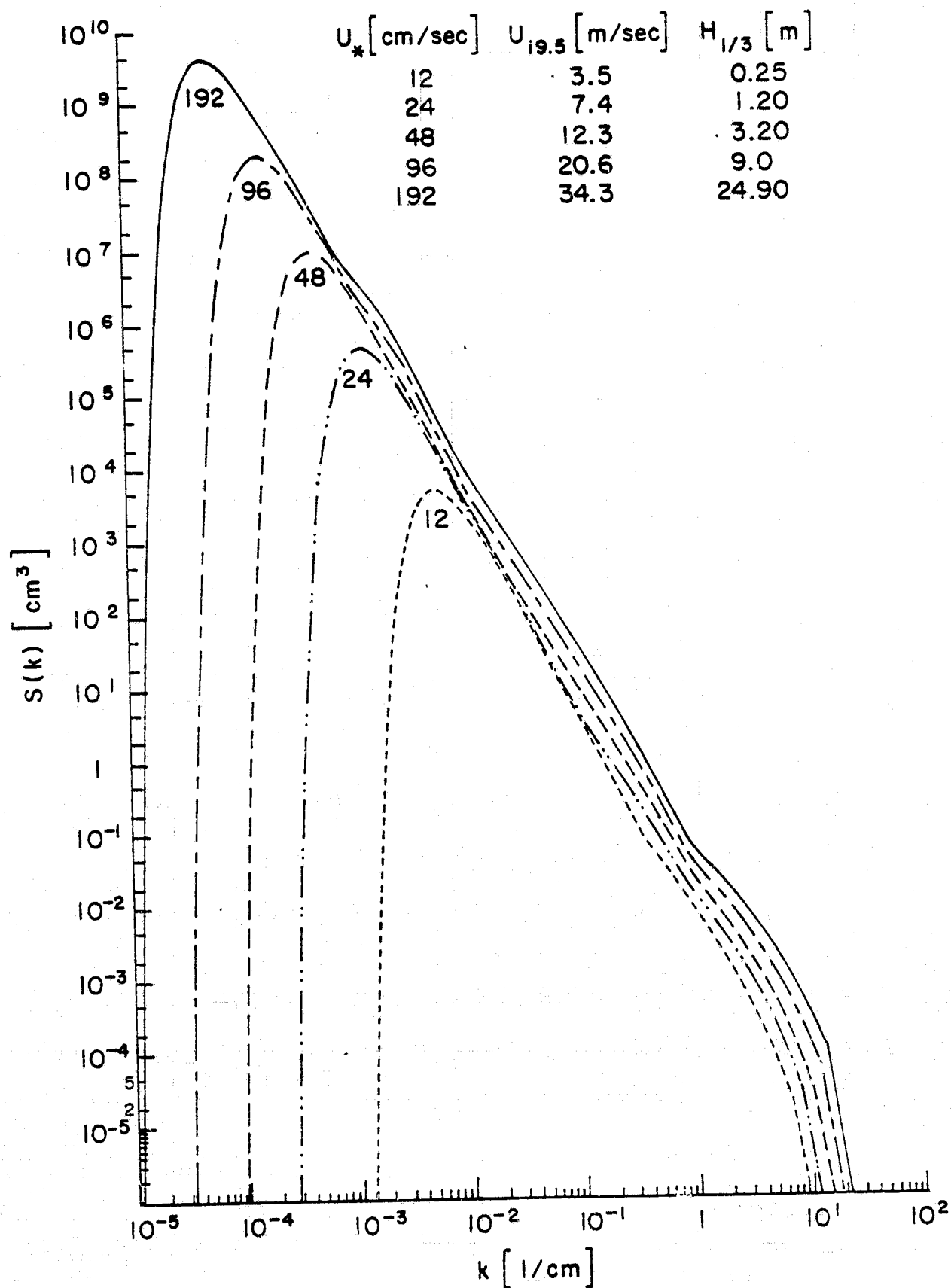


FIGURE 6.6 $S(k)$ versus k with both scales logarithmic for an extreme range of winds.

Figure 6.7 shows the graph of the slope spectrum plotted in a special way that is area preserving. The slope spectrum, strictly speaking, is given by $k^2 S(k)$, and it should be plotted on a linear wave number scale. However, since the contributions to the slope come from wave numbers ranging from 10^{-4} to 10^1 such a plot is not very practical. To compress the needed information onto one single figure, the slope spectrum has been multiplied by k and the resulting function has been plotted on a linear scale for the vertical axis and a logarithmic scale for the horizontal axis. Such a plot is area preserving and shows, for example, that the gravity wave contribution to the slope of the sea surface in the strict definition of slope, (for an infinitesimal change in the horizontal for the denominator and for an equally infinitesimal change in the vertical for the numerator) is very small compared to the contribution to the slope for waves with lengths from approximately 6 meters to waves with lengths of 0.6 cm.

The results of Mitsuyasu and Honda, which show that the wave number spectra spread further apart with increasing wave number and grows more rapidly at high wave numbers than at low wave numbers, begin to explain some of the differences in the power law derivations obtained by those who work at X-band and at K_u -band. The water wave number for say X-band could be indicated by the subscript, 1, and that for K_u -band could be indicated by the subscript, 2. The problem would then be to find the nadir angle that would be looking at the same water wave number on the sea surface. This is indicated by equation (6.27).

$$2k_{01} \sin \theta_1 = 2k_{02} \sin \theta_2 \quad (6.27)$$

If the appropriate values are substituted into this equation for the wave numbers, the result is equation (6.28), and it is possible to solve for the sine of θ_1 as some constant times the sine of θ_2 .

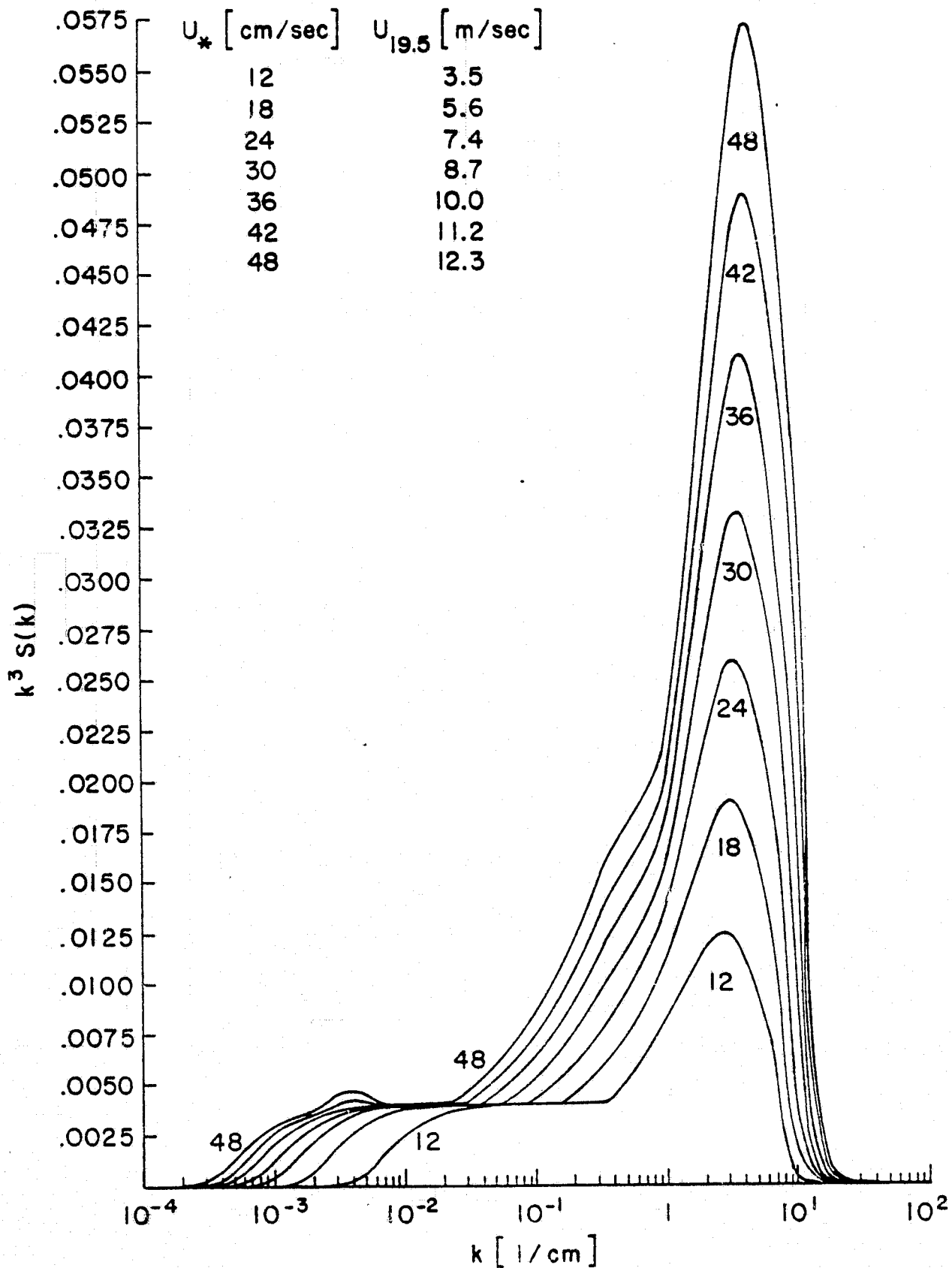


FIGURE 6.7 $k^3 S(k)$ versus $\log k$ for wind speeds up to 12.3 m/s. The graphs are area preserving.

$$\sin \theta_1 = 1.56 \sin \theta_2 \quad (6.28)$$

In essence, this result says that θ_1 has to be increased by some amount such that its sine is 1.56 times the sine of the nadir angle for the higher frequency radar. Clearly, for certain angles there exists no solution for this equation but solutions do exist for nadir angles of 20° , 30° , and 40° as given in Table 6.5 below.

Table 6.5 Nadir angle at 8.91 GHz (θ_1) required to yield same σ° as at tabulated nadir angle (θ_2) for 13.9 GHz.

θ_2	$\sin \theta_2$	$\sin \theta_1$	θ_1
20°	.342	.534	32°
30°	0.5	0.78	51°
40°	0.643	1.00	90°

This table shows that if one is probing the sea surface with a K_u -band radar at 13.9 GHz and at a nadir angle of 30° , it is necessary to use a nadir angle of 51° at 8.91 gigahertz in order to observe the same power law, under the assumption that the linear Bragg scattering theory presently under discussion is correct. At 20° , the corresponding angle for the X-band radar is 32° , and at a 40° nadir angle for a K_u -band radar the corresponding nadir angle for a X-band radar would have to be 90° .

The fact that the frequency spectra observed by Mitsuyasu and Honda spreads apart with increasing frequencies implies that the wave number spectra also spread apart with increasing wave number, and this means that the higher the nadir angle the greater the power law should be.

If sets of σ_0 versus θ curves for different wind speeds are all plotted on the same graph it would also follow that the different curves would come closer together with decreasing nadir angle. This has been a fact that was long observed. However, most attempts to explain it involve a transition to the theories of the Kirchoff type instead of theories of the Bragg type and begin to evoke an undefined region of these curves as a function of nadir angle somewhere near 30° where the Bragg scattering theory was thought to begin to fail. The results of Mitsuyasu and Honda, as confirmed at least in part by observations in the Black Sea and in the open ocean around Japan as described previously, all suggest that the convergence of the σ^0 curve with decreasing nadir angle is simply a function of the characteristics of the wave spectrum in the wave number region for the appropriate frequencies of the radar. These results also indicate a reason why the power law dependencies reported by Guinard (1969), Valenzuela et. al. (1971) and Daley (1973) are all lower than the power law dependencies detected with the radars being used in the various NASA programs that had frequencies of 13.3 and 13.9 gigahertz. The discrepancies, however, are larger than this simple explanation indicates and are partly due to the different techniques in smoothing and interpreting the data. The tables extracted from the work of Daley (1973) provide a partial explanation for this part of the discrepancy.

The AAFE Program. The work of the advanced application flight experiment program that used the same type of radar as the one used on SKYLAB began at this time to yield preliminary results concerning the

power law dependencies of the radar backscatter at 13.9 gigahertz. These results are summarized by Table 6.6 given by Grantham et. al. (1975) for nadir angles from 20° to 50° and for vertical and horizontal polarizations. These power laws are all close to one or greater. At 30° , they are very nearly equal to two, and at 50° , some of them are actually equal to two. These results are in much closer agreement to the work of Bradley (1971) than to the work of Daley (1973), and they indicate a very strong dependence of radar backscatter on wind speed. These results can be confirmed by both theoretical investigations and on the basis of the SKYLAB measurements with S193.

Table 6.6 Power law dependencies for AAFE Langley Radscat Program at 13.9 GHz (Preliminary) as in $\sigma^0 \sim U^N$.

Polarization	Direction	Nadir Angle				
		20°	25°	30°	40°	50°
VV	Upwind	1.0	1.53	1.9	1.9	1.9
	Downwind	.99	1.51	1.9	1.89	1.9
	Crosswind	.99	1.59	1.9	1.9	1.9
HH	Upwind	.94	1.48	1.9	2.0	2.0
	Downwind	.94	1.48	1.85	1.98	1.98
	Crosswind	.76	1.29	1.85	1.95	1.95

A new maneuver was developed for the airborne AAFE radar. It consisted of pointing the antenna straight down for level flight, and then banking the aircraft to a bank of 30° and flying around in a tight circle a great many times. The result was a graph of radar backscatter as a function of azimuth angle in degrees for a given wind speed. Figures 6.8 and 6.9 shows

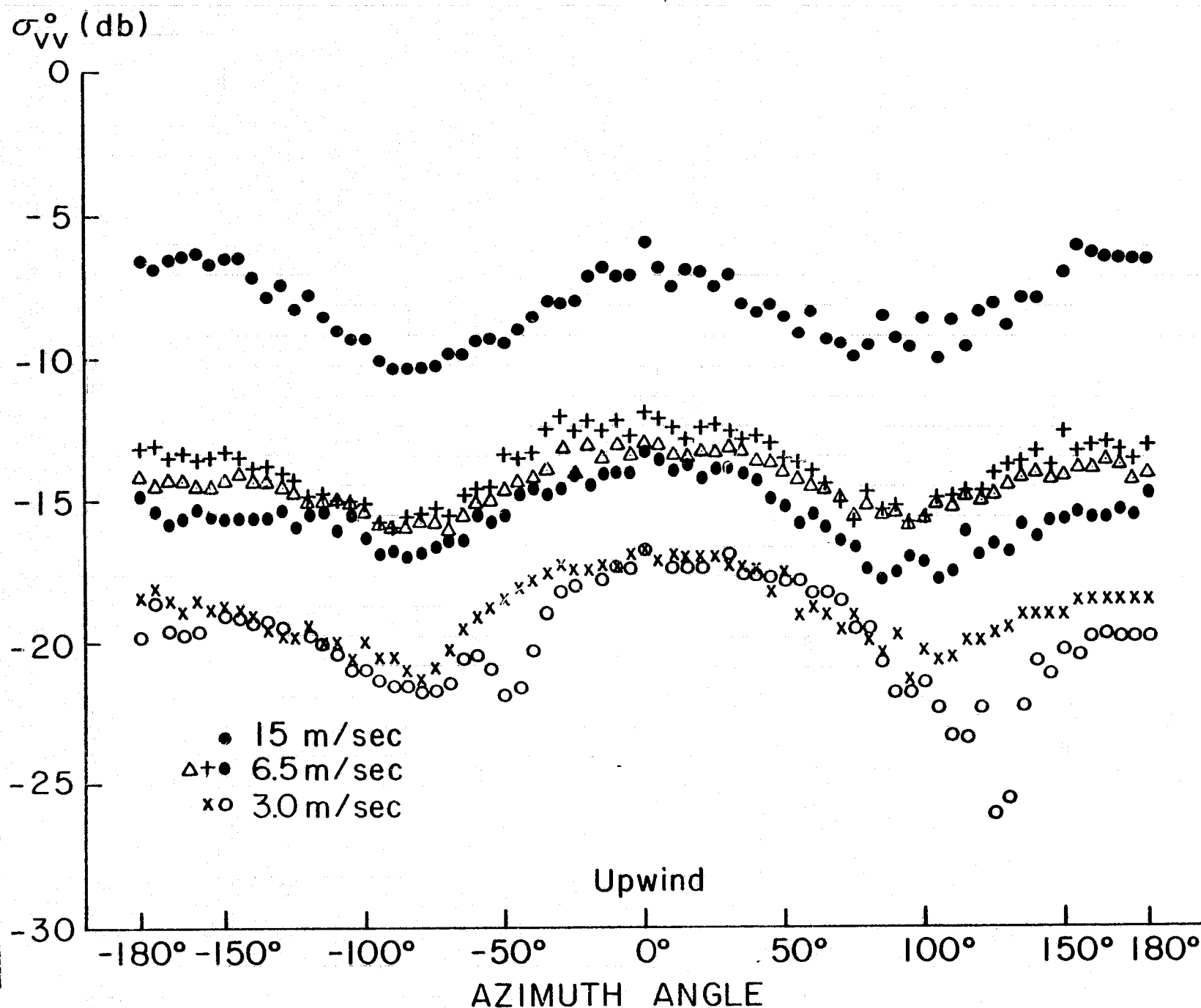


FIGURE 6.8 DATA FROM CIRCLE FLIGHTS WITH AAFE RADSCAT

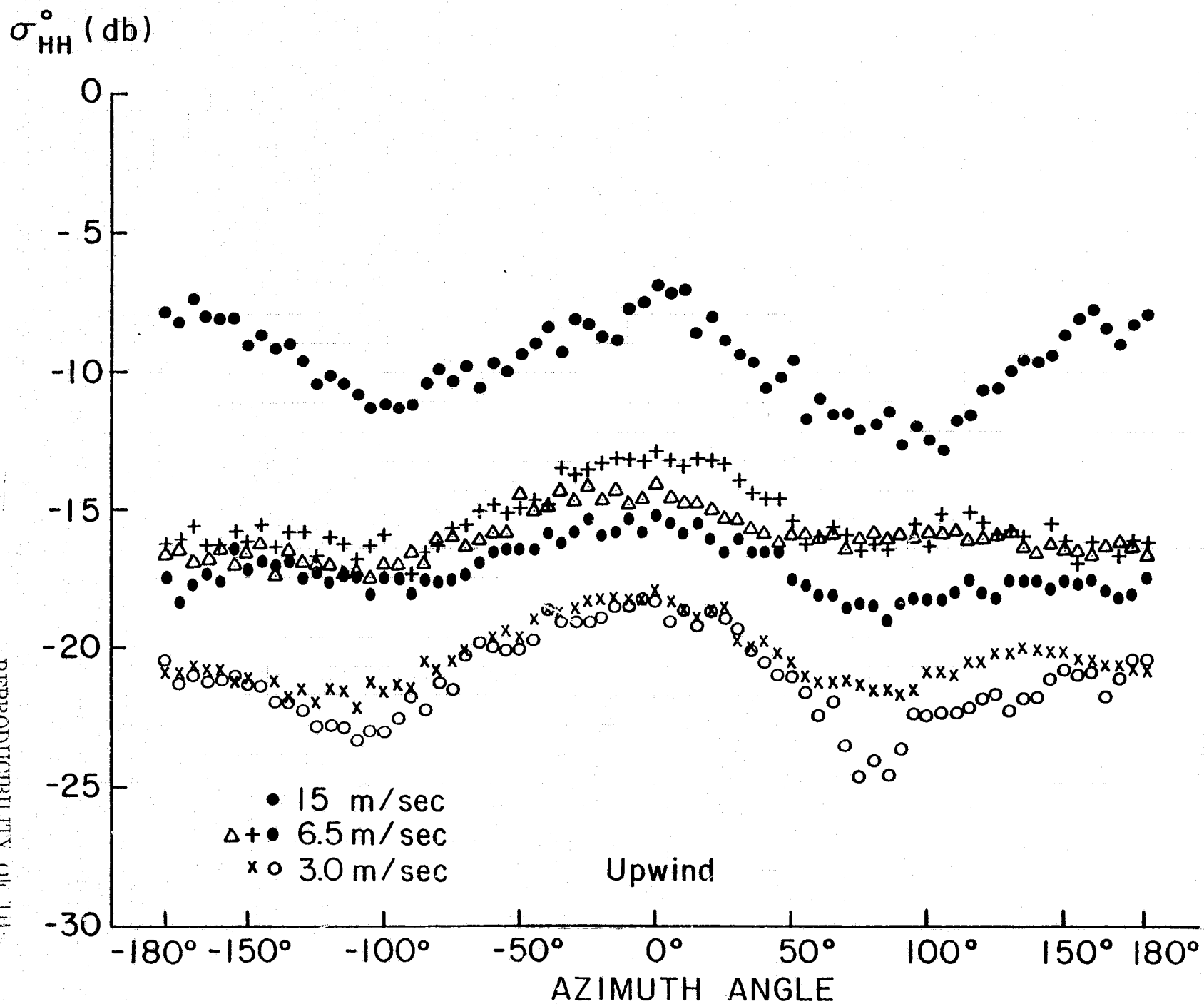


FIGURE 6.9 DATA FROM CIRCLE FLIGHTS WITH AAFE RADSCAT

a plot of the actual data obtained during these circle flights for wind speeds of 3, 6.5, and 15 meters per second. The only thing that has been done to these data is to have the upwind direction placed in the center and referred to 0° . Figure 6.10 shows a smooth version of these results as taken from Grantham et. al. (1975). In their smooth form, the curves show that upwind return is stronger than downwind return, and that crosswind is much lower than either upwind or downwind return for the same wind speed. For winds of 15 meters per second there is a 4 db difference between upwind and crosswind return, for 6.5 meters per second there is again about a 4 db difference, and for 3.0 meters per second there is almost a 6 db difference. From 3 to 6.5 meters per second there is a 4 db increase in backscatter, indicating a power law of 1.19. For upwind conditions for winds from 3 to 15 meters per second there is an 11 db increase in backscatter indicating a power law of 1.57, and at crosswind from 3 to 15 meters per second there is a 12 db increase in backscatter indicating a power law of 1.72. It is interesting to note that there is a range of 4 db for the same wind speed depending upon azimuth angle. These results should be contrasted with the quotation from Guinard (1969) where it was claimed that only a 3 db increase could be detected as the winds increased from 10 knots (approximately 5 meters per second) to 48 knots (approximately 24 meters per second) in measurements made at that time.

The reduction of these circle flight data had many difficulties and therefore the details of the last two figures may change upon further analysis. The roll angle of the aircraft did not remain constant but fluctuated about the nominal angle of 30° introducing trends caused by a changing nadir angle that had to be removed in the analysis. Details in the numerous problems that were encountered can be found in Afarani (1975).

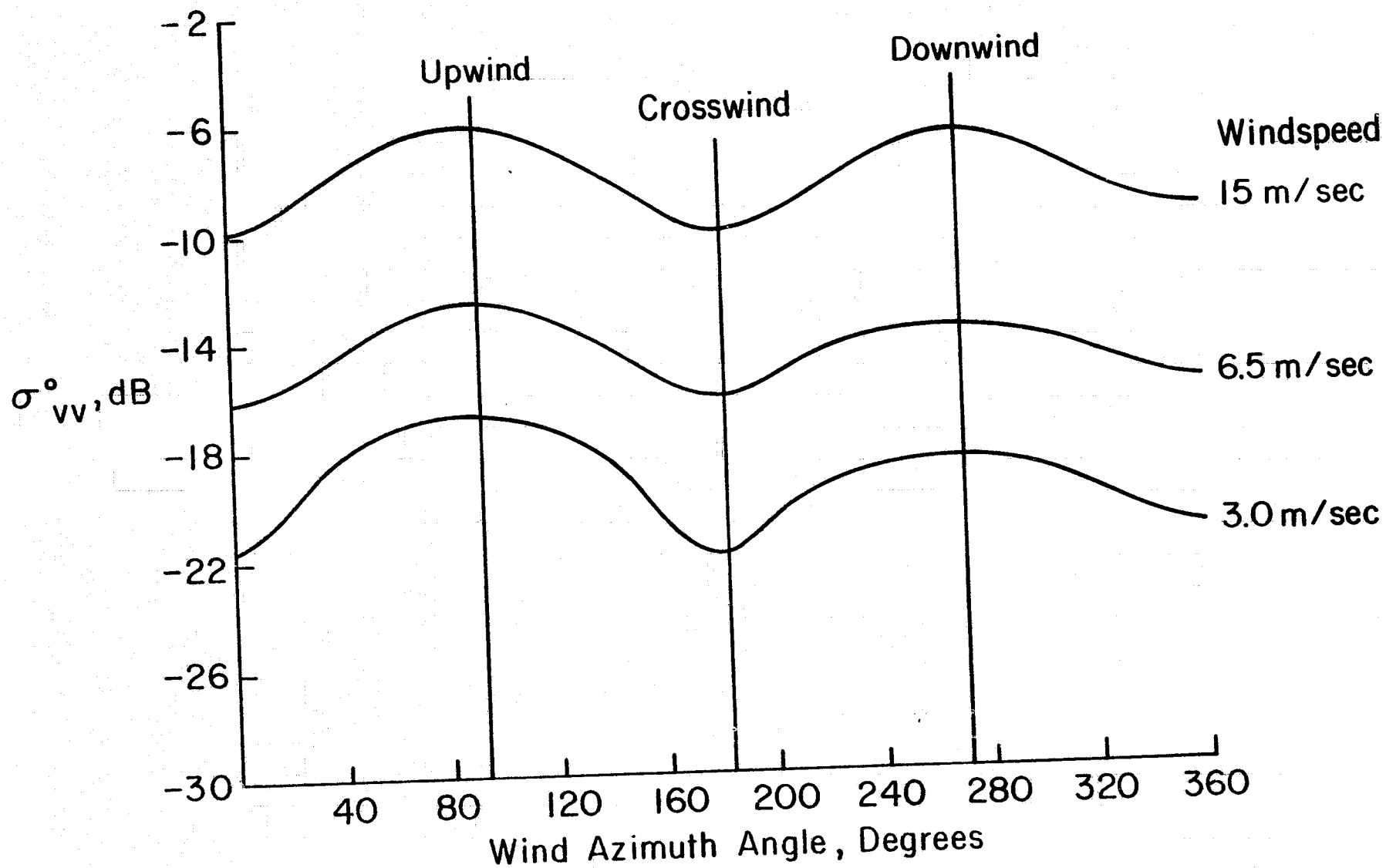


FIGURE 6.10 AAFE RADSCAT SCATTEROMETER WIND DIRECTION SENSITIVITY
(FROM W.L. GRANTHAM ET AL. 1975)

Results of Fung and Chan. There still remains the challenge of providing an adequate theory for radar backscatter for nadir angles from approximately 25° to 60° based on a more adequate Bragg scattering theory. The most questionable aspect of the various theories reviewed above was the fact that the effect of tilt on the capillary waves was not included in the calculation of the backscatter. The use of the spectra defined immediately above in wave number space as derived from the observations of Mitsuyasu and Honda would yield some very useful first order Bragg scattering theories that would be somewhat closer to reality than those obtained using equation (6.8) and the results of Daley (1973).

However, the most useful presently available theory for radar backscatter at these nadir angles is that due to Fung and Chan (1975 b), which is given as Appendix C to this report. This theory will be briefly reviewed here and some of its consequences will be described. The essence of the results of Fung and Chan can be summarized by equation (6.29)

$$\sigma_{pp}^o(\theta, u_*, \chi, \sigma_x, \sigma_y) = \int_{-\infty}^{\infty} \int_{-\cot \theta}^{\infty} \sigma_{pp}^o(\theta', \chi) P_{\theta}(z_{x'}, z_{y'}) dz_{x'} dz_{y'} \quad (6.29)$$

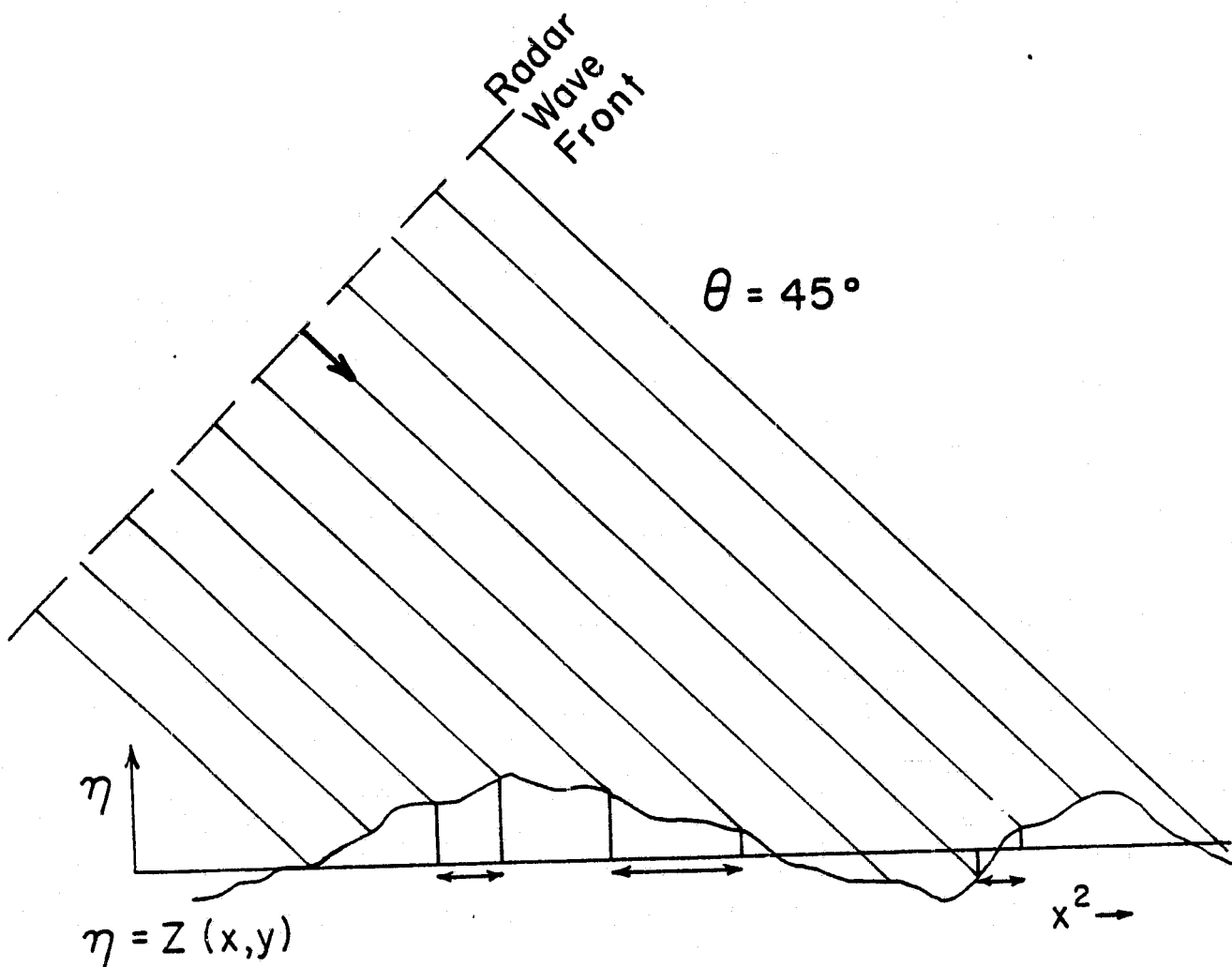
where

$$\sigma_{pp}(\theta, \chi) = 8 k_o^4 \sigma_1^2 |\alpha_{pp}| \cdot W(\theta, \chi) \quad (6.30)$$

and where $\sigma_1^2 W(\theta, \chi)$ is a modified two sided form of the spectrum given in equation (6.12) where $2k_o \sin \theta$ has produced the nadir angle dependence by introducing the Bragg condition into the spectrum. This equation shows that the radar backscattering cross section measured for VV, HH, or VH, depending upon the values of p and q used, is a function of the wind speed through the frictional velocity u_* , as defined by the variation of wind with height in the planetary boundary

layer, the nadir angle, the azimuth angle, χ , the slope of the sea surface in the x' direction, and the slope of the sea surface in the y' direction. This value for the radar backscattering cross section is computed by calculating the radar backscattering cross section for a range of different nadir angles, θ' , at a given wind speed, defined by u_* , and nadir angle, and summing the strength of these returns as a function of the probability density function of the tilts of small portions of the sea surface toward and away from the pointing direction of the radar beam. This operation is indicated by the function $P_{\theta}(Z_{x'}, Z_{y'})$, where the x' and y' axes are lined up so that x' is in the direction of the wind. The average tilt of the sea surface is near zero and these would correspond to the nominal nadir angle, but those portions of the sea surface that tilt toward the radar beam will have a smaller value of θ' and a larger backscatter and those that tilt away from the radar beam will have a larger value of the nadir angle and a smaller value for the backscatter. The integration over all possible tilts, properly weighted according to an appropriately derived probability density function, then yields the value of the radar backscatter.

The subscript, θ , in this equation for the probability density function for the slopes indicates that the probability density function must be calculated with reference to a plane normal to the direction of the radar beam. It is not the same probability density function that would be obtained by calculating the slopes that would be observed relative to a horizontal plane at the mean position of the sea surface. This point will be explained in greater detail below. However, the fact that the slope distribution of the sea surface was observed to be skewed toward the upwind direction by Cox and Munk, plus the consequences of an appropriate interpretation of this probability



$$P(Z_x, Z_y) = \frac{1}{2\pi\sigma_x\sigma_y} e^{-\frac{1}{2}\left[\left(\frac{Z_x}{\sigma_x}\right)^2 + \left(\frac{Z_y}{\sigma_y}\right)^2\right]}$$

slopes referred to a beam at zero nadir angle

$$P_\theta(Z_x, Z_y) = \frac{[1 + Z_x \tan \theta]}{2\pi\sigma_x\sigma_y} e^{-\frac{1}{2}\left[\left(\frac{Z_x}{\sigma_x}\right)^2 + \left(\frac{Z_y}{\sigma_y}\right)^2\right]}$$

slopes referred to a beam at a nadir angle of θ°

FIGURE 6.11 PROBABILITY DISTRIBUTION OF SLOPES CORRECTED FOR THE EFFECT OF NADIR ANGLE

density function allows for the explanation of the difference between the upwind and downwind measurements of backscatter, and the variation with λ of the wave number spectrum, assuming a very simple variation, when compounded with the effect of slopes, explains the observations of the circle flights made during the AAFE Langley Radscat Program.

Figure 6.11 illustrates a section along a wavy sea surface and a radar beam traveling toward the sea surface at a nadir angle of 45° . Equal sections normal to the radar beam are illustrated. Some of these sections reach the sea surface where the wavy surface is tilted toward the radar and other sections reach the sea surface where it is tilted away from the radar. The projection onto the horizontal plane of the portion of the sea surface tilted toward the radar is much shorter than the projection onto the horizontal plane of that portion tilted away from the sea surface. This means that the probability density function for the sea surface slopes, as typically derived, has to be corrected for the effect of nadir angle, except for the special case where the beam points straight down. Slopes toward the radar occupy more of the beam than slopes away from the radar and therefore have a higher probability of occurring. If the probability density function derived by the classical oceanographic procedures is given by equation (6.32), then the corrected probability density function for a radar beam approaching the sea surface at an angle θ is given by equation (6.33). Since the slopes of the sea surface can be represented in a more refined way in terms of a Gram Charlier series that puts the maximum slightly forward of zero slopes in the downwind direction, the combined effect of this, plus this correction, yields an enhanced return for upwind backscatter compared to downwind backscatter.

$$P(Z_x, Z_y) = \frac{1}{2\pi \sigma_x \sigma_y} e^{-\frac{1}{2} \left[\left(\frac{Z_x}{\sigma_x} \right)^2 + \left(\frac{Z_y}{\sigma_y} \right)^2 \right]} \quad (6.32)$$

$$P_{\theta}(Z_x, Z_y) = \frac{[1 + Z_x \tan \theta]}{2\pi \sigma_x \sigma_y} e^{-\frac{1}{2} \left[\left(\frac{Z_x}{\sigma_x} \right)^2 + \left(\frac{Z_y}{\sigma_y} \right)^2 \right]} \quad (6.33)$$

Fung and Chan have compared various observations from various sources such as the NRL data and the AAFE program data with the theory indicated by the above equation and found quite good agreement. They have also calculated the variation with azimuth angle of the radar backscatter based on different values of the first term in the Fourier series expansion of the angular variation of the wave number spectrum. Clearly if more can be learned about the angular variation of the vector wave number spectrum, this aspect of the theory can be improved.

Figure 6.12 shows the results of the application of this theory to conditions where the wind speed was 25 knots, the nadir angle was 30°, and VV polarization was used. The coded lines indicate that amplitude of the second harmonic of the Fourier expansion given in equation (6.12) as 0.35, 0.4, and 0.45 to show the variability due to this effect. The circles and squares indicate the values of backscatter normalized to zero at upwind for a full 360° circle. The differences between one part of the 360° circle from 0 to 180 and then back from 180 to 360 are a measure of the variability in the measurement system. The theory seems to fit the data quite well within half a db, or so, over the full range for a value of a_0 equal to 0.4.

Figure 6.13 shows a very important feature of this theory. The calculations for the Bragg scattering theory with tilt effects included for three different coefficients for the Fourier series expansion of the anisotropic behavior shows that the range of variability for these three different coefficients is not tremendously large. For comparison, the first order small perturbation theory for

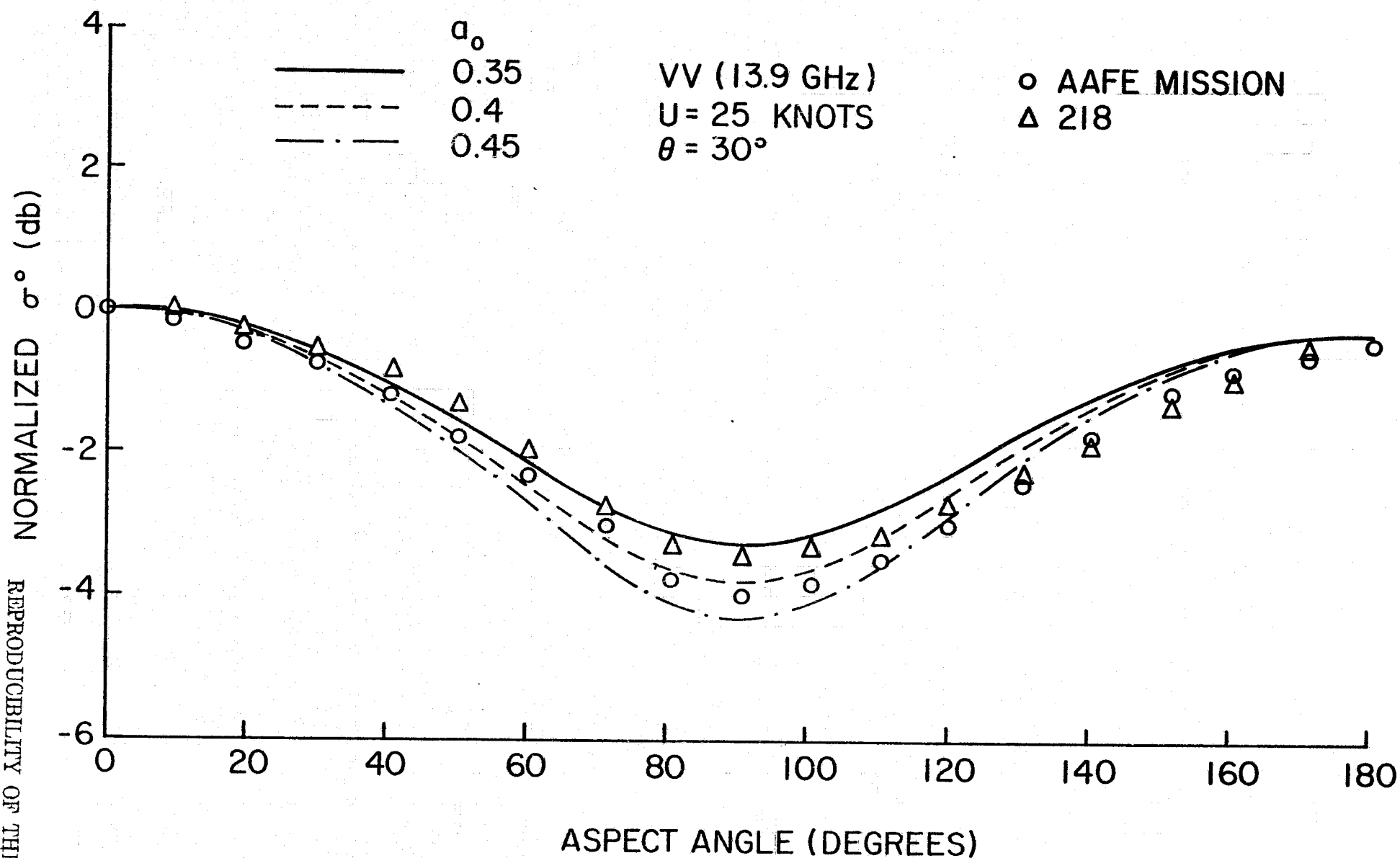


FIGURE 6.12 AZIMUTHAL DEPENDENCE OF σ^0 AT $\theta = 30^\circ$, U = 25 KNOTS AND 13.9 GHz FOR VARIOUS CHOICES OF q_0 FOR VV TOGETHER WITH AAFE DATA MISSION 218

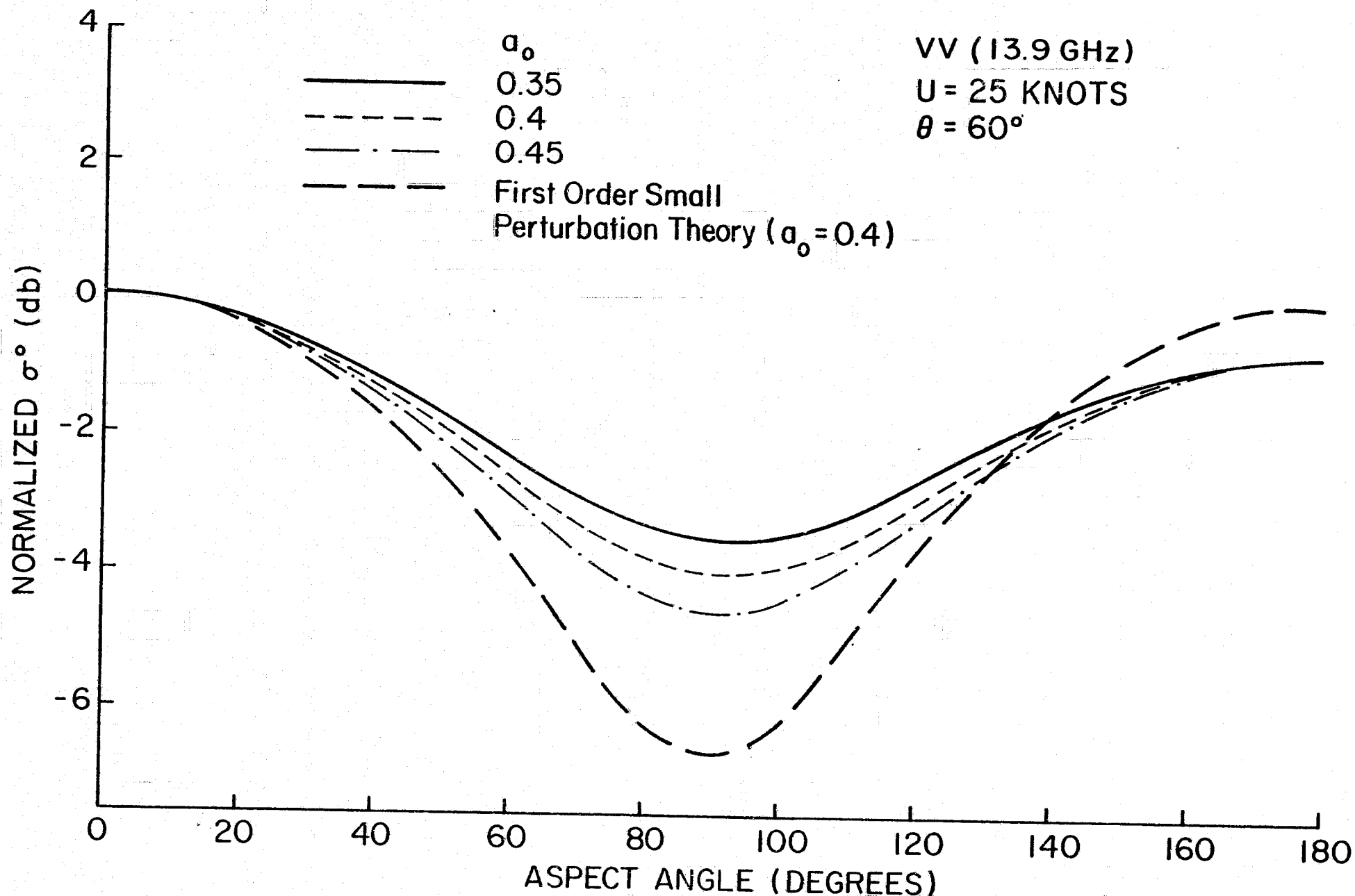


FIGURE 6.13 AZIMUTHAL DEPENDENCE OF σ^0 AT $\theta = 60^\circ$, U = 25 KNOTS AND 13.9 GHz FOR VARIOUS CHOICES OF a_0 FOR VV. THE FIRST ORDER SMALL PERTURBATION RESULTS ARE ALSO SHOWN FOR COMPARISON.

the middle value of these coefficients is shown. The first order small perturbation theory misses the difference between upwind and downwind and over predicts the minimum at crosswind. The effect of tilt tends to smooth out and reduce the effects of very strong angular variations in the capillary wave spectrum at the Bragg scattering wave number. This is a very important consequence of the theory. It will be necessary to understand both the slopes of the larger waves and the capillary wave spectrum thoroughly before a complete theory for backscatter will be possible.

Finally, equation (6.29), suggests a number of reasons why there may be more scatter in the comparisons of backscatter measurements with wind speed at low winds than at high winds. If the radar backscattering cross section depends upon the sea surface slope, it can be expected that this slope will differ from one place on the ocean to another when the winds are light simply because of the presence or absence of the larger gravity waves that contribute to that slope and that are not in instantaneous equilibrium with the local wind speed and direction. The radar backscatter from the ocean according to this theory is no longer uniquely a function of wind speed and direction. It will undoubtedly be possible in the future to account for these effects as wave forecasting models are improved because the sensitivity to the slope effect will not be too great.

In this connection reference is made to Figure 6.7 given earlier. Consider for example a u_z of 30 centimeters per second corresponding to an 8.7 meter per second wind at 19.5 meters above the sea surface. The part that contributes to the slopes of the sea surface near $k = 10^{-1}$ in this figure and that corresponds to waves with lengths of 60 cm or so will be present when the wind is blowing. However, the part toward low frequencies near $k = 10^{-3}$ might actually have some swell running,

produced by 20 or 25 meters per second winds a day or two earlier that would cause a large contribution in the region of the spectrum between $k = 10^{-4}$ and $k = 10^{-3}$. These numbers would never exceed a nominal value of .004 but they could occupy an area on such a plot over approximately a decade of wave number space. This would cause the parameters for the slope distribution needed in this theory to increase by 20 or 30%, and, in turn, this would produce a new value for the backscatter compared to the value that would be calculated under the assumption of a fully developed wind sea.

The effects of the larger gravity waves on backscatter. In planning a research program with a time span of many years (1971 to the present), the need to acquire certain kinds of supplementary data to permit a complete understanding of the primary quantities being measured is sometimes indicated. As an example, suppose that some of the theories available at the start of a program indicated that independent measurements of some property would be necessary to correct the primary measurements and interpret them properly. Suppose, also, that other theories indicated that the effects of this property were relatively insignificant. Suppose, also, that the data for this property could be recovered, or generated, either in time to be used in the analysis of the primary data, or at a much later time with an additional delay. Suppose finally, that there is a deadline for the submission of a final report on the experiment simply because the results are needed for further planning of new systems.

There are two decisions that can be made at the start of such a program, and there are two possible consequences of each decision. The process is similar to certain aspects of statistical decision theory, but much less quantitative. The two decisions are (1) to get the data or (2) not to get the data. If the first decision is

made, either the data will eventually turn out to be useful, and decision (1) will have been correct, or the data will turn out not to be useful and decision (1) will not have been correct, because money and effort had to be expended to get the data. If decision (2) is made, either the data will turn out not to be useful and decision (2) will have been correct, or the data will turn out to be needed and decision (2) will not have been correct. If decision (2) is made, and it is incorrect, there is always the (remote) possibility of an additional extension of the contract until the data can be obtained, or analyzed.

At the start of this program, the effects of the large gravity waves on backscatter, see Chapter 1, page 1, were not well understood. For example, simple Bragg scattering does not depend on the large waves, but the results of both Chia (1968) and Jackson (1974) required the full spectrum. Also the nature of the wave number spectrum for intermediate wavelengths was almost completely unknown.

The decision was made to acquire wave data from weather ships and to develop the ability to hindcast the wave spectrum over the Northern Hemisphere oceans. This was done by completing a program under development for many years; wave spectra were calculated from wave records and hindcasted for the Skylab passes over the North Pacific and North Atlantic and for AVA.

From the point of view of the theory of backscatter, the decision was correct because the results of Fung and Chan, discussed above, determine the slopes of the tilted pieces of the sea surface, in principal, from the full wave spectrum of waves longer than about 100 times the Bragg wave number.

There will be variations in the probability density function of the wave slopes that will be caused by the larger gravity waves and these variations are required for a complete evaluation of this theory

and for a complete calculation of backscatter values from first principles. However, these variations will probably only change the slope parameters by significant amounts for low winds in the range from 5 to 15 knots as explained in other parts of this text.

A working tool during this program has been plots of measured values of σ^0 in db versus the log of the wind speed as illustrated by Figure 8.7, as an example (one of hundreds). For a fixed low value of the wind speed, the range of the values of σ^0 is very large. When the winds are low, the background gravity waves are poorly correlated with the wind speed (see Moskowitz (1964) for example) and therefore it seemed plausible, until about a month ago, that the variations in backscatter at a low wind speed could be explained on the basis of the variations of the gravity waves.

This rationale collapsed after the error analysis given in Chapter 4 was completed and when Figure 8.3 was drafted and discussed. The large range of backscatter values in such plots for a given wind speed is primarily caused by the errors in the meteorological specification of the wind speed and secondarily caused by the variations in slopes of the larger gravity waves.

To study the secondary effect, it is necessary to control the primary effect by obtaining wind speed measurements such that the variances of the vector error components are at least a factor of 25 smaller than those achieved, so that the standard deviations are at least a factor of 5 smaller.

Therefore, at the very end of this program, the effort to refine the prediction of the wind speed based on a correction for the effects of the larger gravity waves had to be abandoned. The situation is somewhat like that of looking for a signal when the signal to noise ratio is - 10 db, except that radar designers do it easily by means

of long enough averaging times for both the signal and the noise and meteorologists do not know how to handle the similar problem.

The decision to obtain the wave data was correct from a theoretical point of view, but not from a practical point of view, since the data could not be used to achieve the major objective of this investigation. The major objective has been achieved, anyway.

In a larger sense, the time, effort and funds were not wasted. The U.S. Navy has a wave climatology, the Fleet Numerical Weather Facility at Monterey has an operational spectral wave forecasting program and hurricane wave forecasts are being actively tested at AOML in NOAA. These tools, if used properly, can play an important role in the analysis of GEOS-3 altimeter data this winter and SEASAT-A altimeter data and synthetic aperture wave imagery when SEASAT-A becomes SEASAT-1. Even now steps are being taken to improve the model at Monterey.

CHAPTER 7 PASSIVE MICROWAVE THEORY AND THE CALCULATION OF ATTENUATION AND DETECTION OF HEAVY RAIN WITH THE PASSIVE MICROWAVE DATA.

PASSIVE MICROWAVE THEORY AND APPLICATIONS

Passive microwave systems are currently used on spacecraft as illustrated by Figure 4.12, and a more elaborate system is being developed and studied for use on SEASAT-A. The SEASAT-A system is called SMMR and will scan a swath approximately 500 Km to each side of the subsatellite track with five frequencies ranging from about 500 megahertz to 20 gigahertz. Both theory and aircraft observations indicate that the combination of these ten measurements (two polarizations) will make it possible to determine the wind speed near the sea surface, the sea surface temperature even through clouds, the liquid water in the clouds, and the water vapor in the air at nearly all nadir angles. Pertinent references are Claassen and Fung (1973), Droppleman (1970), Fung and Chan (1975), Hollinger (1970, 1971), Moore and Pierson (1971), Nordberg et al. (1971), Ross et al. (1970), Ross and Cardone (1974), Stogryn (1967), Webster et al. (1974), Wentz (1975), Wu (1973) and Wu and Fung (1973).

The theories and presently available measurements using passive microwave systems all involve the determination of a matrix that removes the small effects of three of the four variables at a given frequency so as to recover the dominant effect of the remaining variable as in the following matrix equation, where U = wind speed, T_s = sea surface temperature, W = liquid water content, and e = water vapor content.

$$\begin{pmatrix} U \\ T_s \\ W \\ e \end{pmatrix} = \begin{pmatrix} a_{1,1} & a_{1,2} & \dots & a_{1,10} \\ a_{2,1} & a_{2,2} & \dots & a_{2,10} \\ a_{3,1} & a_{3,2} & \dots & \dots \\ a_{4,1} & a_{4,2} & \dots & a_{11,10} \end{pmatrix} \begin{pmatrix} T_{1H} \\ T_{1V} \\ T_{2H} \\ T_{2V} \\ \cdot \\ T_{5H} \\ T_{5V} \end{pmatrix} \quad (7.1)$$

The values of the a_{ij} , $i = 1$ to 4 , $j = 1$ to 10 , are nadir angle dependent. The values of U will probably turn out to be dependent on the full wave spectrum and on the percentage of foam so that fetch and duration effects will have to be removed. Also, there may prove to be a weak aspect angle dependence, but this is not expected to be anywhere near as strong as the aspect angle dependence of radar backscatter.

The Skylab EREP package did not carry the full complement of passive microwave sensors that these theories and measurements require. The way that the full complement of five sensors will function has yet to be demonstrated. However, measurements from other spacecraft have demonstrated the ability to determine liquid water and water vapor and measurements from aircraft have demonstrated the effect of wind speed on passive microwave temperatures at nadir. The microwave data during Skylab 2 and 3 at 13.9 GHz did not appear to show any clear correlation with wind speed.

THE USE OF PASSIVE MICROWAVE DATA FROM S193

Purpose and Theory. The passive microwave part of S193 on SKYLAB had two separate purposes compared to the planned uses of SMMR on SEASAT-A. One purpose was to correct the radar measurements for attenua-

tion effects as the radar beam propagated through the atmosphere and through clouds and rain drops to the sea surface and back. The other was to detect areas of heavy precipitation such that the co-polarized backscatter from the precipitation would be so strong that it would mask the return from the sea surface. The radar measurement cannot be used to find the wind speed under these conditions.

The physical reasoning and theoretical justification for this application of passive microwave measurements was given by Moore and Pierson (1971), and the design of a combination active radar and passive microwave radiometer was described by Moore and Ulaby (1969).

A slight paraphrase of the reasoning given by Moore and Pierson (1971) follows:

Although experiments show that the microwave radiometer response is proportional to windspeed, the experiments also show that a much greater effective temperature increase occurs when the radiometer flies over precipitation. Since precipitation is a cause of significant absorption of microwaves, and any absorber is also a radiator, this effect was to be expected as shown by Kreiss (1969) and Singer and Williams (1968). If the absorption is sufficiently strong, the effective temperature seen by the antenna is essentially the actual temperature of the absorbing medium. Since this temperature is always far above the effective temperature of the ocean surface, flying over a precipitating cloud causes large increases in the apparent temperature seen by the radiometer.

Although this increase in radiation from a precipitating cloud has been observed many times, the most significant measurements for our purpose relate the attenuation through the

precipitation, or cloud, with the emission from it. Wilson (1969) used an upward-looking radiometer to compare attenuation of microwave solar radiation with brightness temperature from the attenuating region. The agreement between attenuation computed on the basis of microwave emission from the precipitation and that measured for the solar radiation is excellent for attenuations less than about 10 db.

The accuracy of the calculations of attenuation based on measured microwave brightness depends on the stability of the model atmosphere used. The total emission is directly proportional to total absorption, but emission from the more distant parts of the atmosphere is attenuated itself, and the model must take this into account. Since Wilson's observations were in New Jersey, where most attenuation and radiation comes from rain, a different model is undoubtedly required in the wet tropics, where dense clouds may be a major source of attenuation and radiation. Furthermore, the model should account differently for absorption and scattering.

It might be added that the attenuations found by Wilson (1969) were quite high ranging from 1 to 12 db compared to those that were obtained from Skylab S193 measurements. The microwave frequencies were 16 and 30 gigahertz for this experiment.

Theoretical Development The most direct application of passive microwave temperatures is to measure them at a nadir angle near 50° , where sea surface roughness does not theoretically affect the value. It is then possible, given an independent measurement of the sea surface temperature and salinity, to calculate the two way attenuation of the

radar beam. This was done for all 50° measurements for SKYLAB 2 and 3. In the in track noncontiguous mode, it was then possible to calculate the attenuation for the other nadir angles since the attenuation is proportional to the total path length and can be calculated from appropriate ratios of the secant of the zenith angle.

Measurements by Hollinger (1971) and theories developed by Hollinger (1971), Stogryn (1967), Wu and Fung (1973) and Claassen et. al. (1971) made it possible for Claassen^{*} to develop a series of computer sub-routines to calculate the attenuation of the radar given apparent microwave temperature measurements at a 50° nadir angle. Figure 7.1 shows the results of various theories for the variation of the vertically polarized microwave temperatures and the measurements of Hollinger (1971). The variation with wind speed near 50° is very small. Komen (1975) put these programs into final form, and Young (1975) applied them to the Skylab 2 and 3 data.

Claassen also developed other algorithms for more complex situations that involve an iterative technique at nadir angles different from 50° . As illustrated in Figure 7.2, the surface brightness given by the sea surface temperature and wind speed was subtracted from the apparent temperature to yield an excess temperature, which then yielded an attenuation to correct the backscatter measurement. In principal, the new backscatter measurement yielded a new wind, that in turn changed the brightness temperature. The new excess temperature could then be used to obtain a new attenuation and so on. Successive over estimates and under estimates should converge to a true value for the wind and the attenuation.

The surface truth wind speeds and directions for the Skylab experiment had errors of such a magnitude that this degree of sophistication was not possible. Also, the passive microwave data were not good for SKYLAB 4.

* unpublished

The situation becomes much simpler at nadir angles near 50° because both theory and observation show as in Figure 7.1 that sea surface roughness no longer enters into the problem (except perhaps for thick foam). Actually, a slightly higher angle would be better and the curves suggest a small residual variation at 50° . At this angle, if the measured passive microwave temperature exceeds the amount radiated from the sea surface at a given temperature and salinity, the excess is caused only by the atmosphere (including clouds and rain) and can then be used to determine attenuation.

The first step is to calculate the vertically polarized brightness temperature. This is calculated from the water temperature and the emissivity, which in turn is calculated from Fresnel theory.

Thus according to Komen (1975), for example, for vertical polarization,

$$T_{Bv} = \epsilon_v(50^\circ, T_w) \cdot (T_w) \quad (7.2)$$

and

$$\epsilon_{rv}(\theta, T_w) = 1 - |R_v(\theta, T_w)| \quad (7.3)$$

and

$$R_v = \frac{\epsilon_r(T_w) \cos \theta - \sqrt{\epsilon_r(T_w) - \sin^2 \theta}}{\epsilon_r(T_w) \cos \theta + \sqrt{\epsilon_r(T_w) - \sin^2 \theta}} \quad (7.4)$$

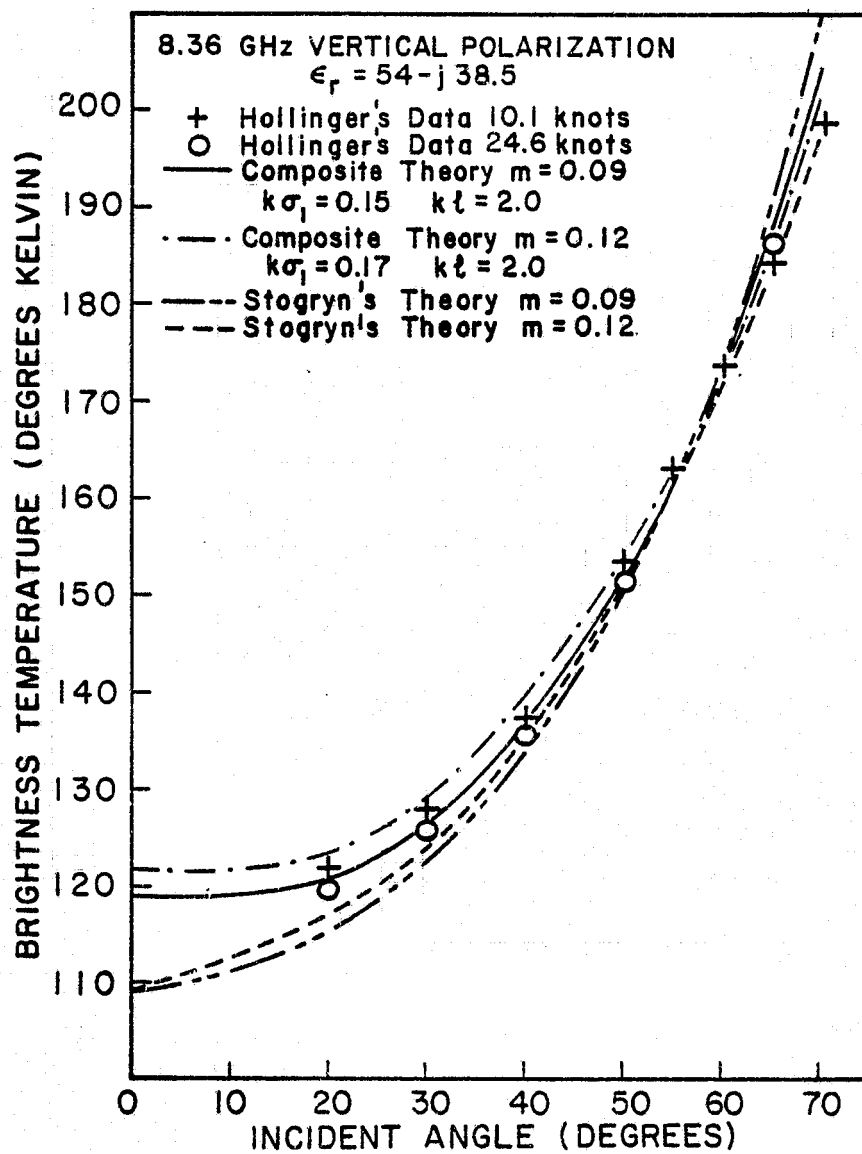


FIGURE 7.1 THE VARIATION OF BRIGHTNESS TEMPERATURE WITH INCIDENT ANGLE FOR TWO DIFFERENT THEORIES AND DATA FOR TWO DIFFERENT WIND SPEEDS.

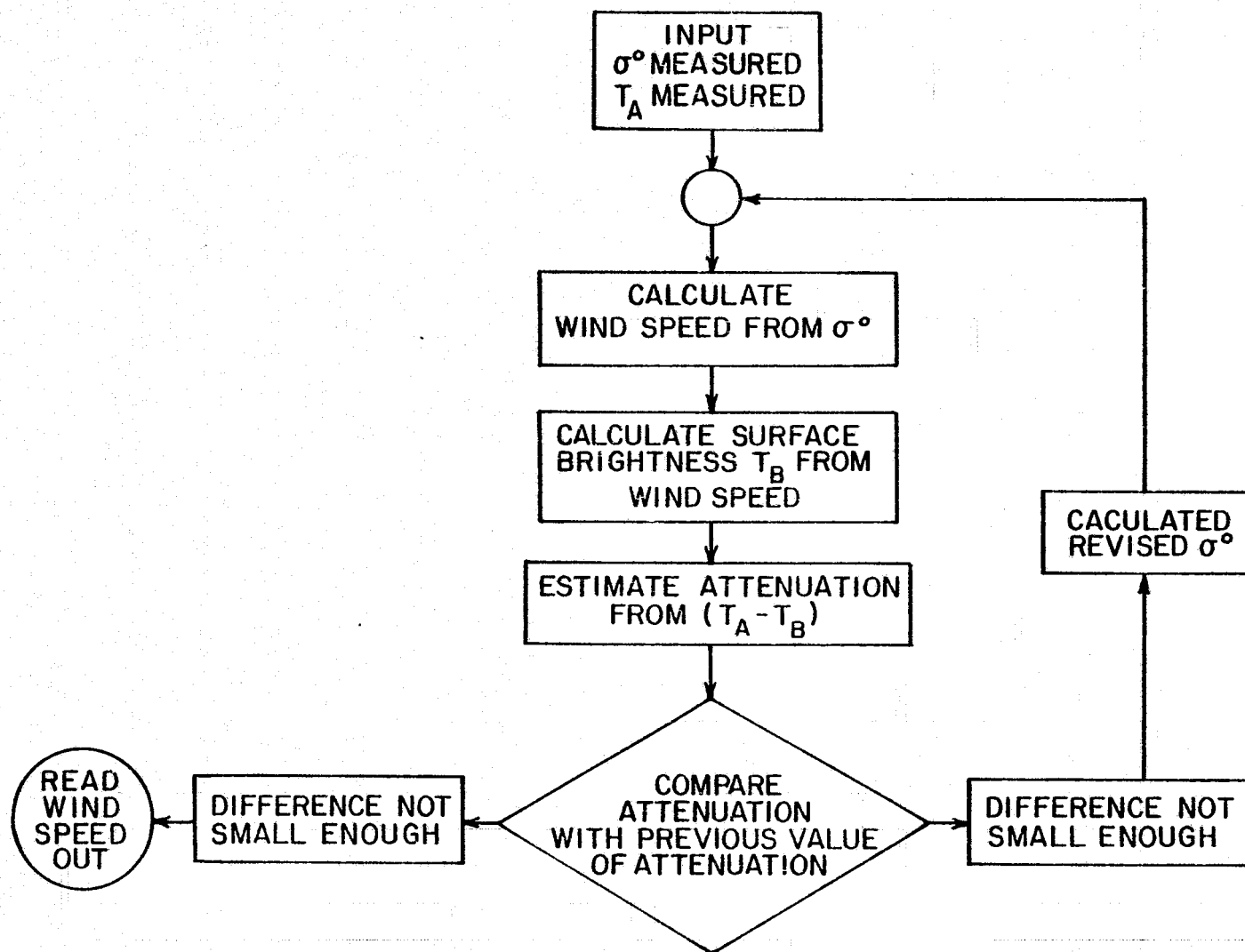


FIGURE 7.2 ALGORITHM FOR USING SCATTEROMETER AND RADIOMETER TOGETHER TO COMPENSATE FOR CLOUD / RAIN ATTENUATION AND PRODUCE IMPROVED WIND - SPEED ESTIMATE.

The notation, $\epsilon_r(T_w)$, represents the complex relative dielectric constant of sea water of temperature, T_w , and salinity, S . Climatological values for salinity, which does not vary much over the ocean (in this context), are sufficient. Given the sea surface temperature as provided by our NOAA colleagues at each cell, the value of T_{BV} could be found.

The measured microwave temperatures could exceed this value as in equation (7.5)

$$T_{ex V} = T_{app V} - T_{BV} \quad (7.5)$$

which defines the excess temperature.

The excess temperature is caused by the same effects that cause attenuation. The next step is to compute the theoretical values of excess temperature and electromagnetic wave attenuation so as to establish a relationship between the two.

Examples of such calculations are shown in Figure 7.3 for various model atmospheres and for atmospheres measured near various passes for Skylab 2 and 3 as determined from NIMBUS VTPR soundings. The theory of these calculations and the various computer programs involved are given by Komen (1975).

These curves yield a relationship between the excess temperature and the attenuation in db as given by equation (7.6) where $\alpha(50^\circ)$ is given in decibels.

$$\alpha(50^\circ) = 1.79 \times 10^{-2} (T_{ex V}) - 5.56 \times 10^{-5} (T_{ex V})^2 + 4.33 \times 10^{-6} (T_{ex V})^3 \quad (7.6)$$

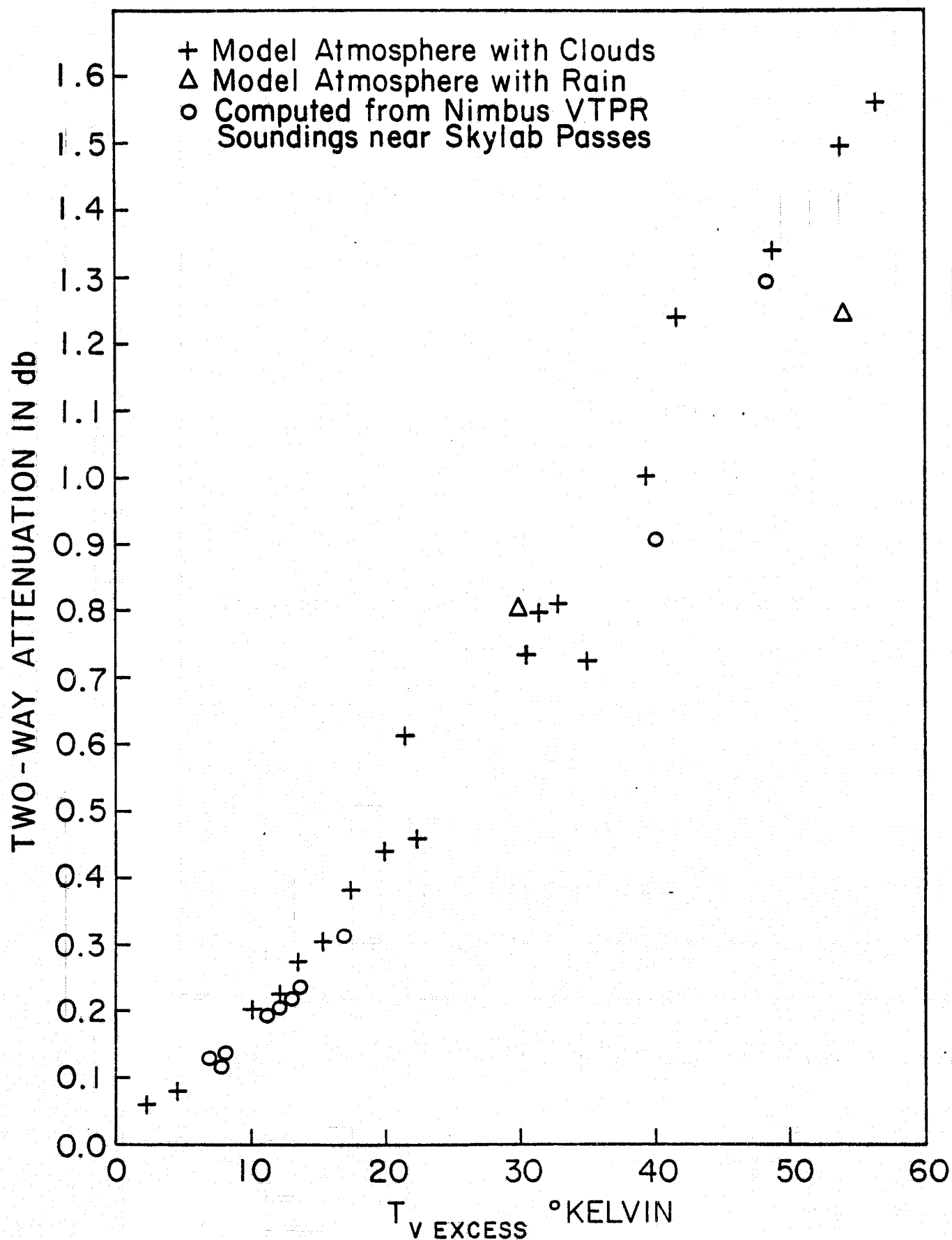


FIGURE 7.3 THEORETICAL VALUES OF TWO-WAY ATTENUATION
VERSUS EXCESS TEMPERATURE

It was also possible to relate the horizontally polarized excess temperature to the vertical excess temperature so as to check for internal consistency as in equation (7.7).

$$T_{\text{ex } H} = 1.531(T_{\text{ex } V}) + 4.47 \times 10^{-3}(T_{\text{ex } V})^2 - 8 \times 10^{-5}(T_{\text{ex } V})^3 \quad (7.7)$$

The correction to the radar backscatter measurement for the attenuation calculated from equation (7.6) is given by equation (7.8).

$$\sigma_c^0(\text{db}) = \sigma^0(\text{db}) + \alpha(\text{db}) \quad (7.8)$$

Once the attenuation at 50° is known, as $\alpha(50^\circ)$, the attenuation at other nadir angles can be found for the same area of the ocean as scanned by the in track noncontiguous mode as in equation (7.9).

$$\alpha(\theta) = \frac{\sec \theta}{\sec 50^\circ} \alpha(50^\circ) = \frac{\cos 50^\circ}{\cos \theta} \alpha(50^\circ) \quad (7.9)$$

The attenuation at 30° and 40° is therefore less than that at 50° .

Attenuation results for SKYLAB 2 and 3 The attenuation for each 50° nadir angle passive measurement during SKYLAB 2 and 3 was calculated. The results are given in Table 7.1. The minimum calculated value was 0.07 db [DOY 252-1 Scan 2.1] and the maximum was 0.62 [DOY 157-1 Scan 9.1] in AVA. A histogram of the number of times each attenuation value occurred is given in Figure 7.4 where 0.07 and 0.08 form one group, 0.09 and 0.10 the next, 0.11 and 0.12 the next, and so on. The average of the attenuation values (averaged as db), was 0.20 db.

TABLE 7.1*

ATTENUATION VALUES AT 50° NADIR ANGLE IN DB FOR SKYLAB 2 and 3 (TWO WAY)

	DOY	156-1 ,										
Scan No.	2. 1	3. 1	4. 1	5. 1	6. 1	7. 1	8. 1	19. 1	20. 1	21. 1	22. 1	
Atten.	0.18	0.18	0.20	0.20	0.15	0.15	0.16	0.25	0.23	0.24	0.24	
	DOY	157-1										
Scan No.	1. 1	2. 1	3. 1	4. 1	5. 1	6. 1	7. 1	8. 1	9. 1	11. 1		
Atten.	0.14	0.18	0.23	0.27	0.27	0.32	0.31	0.61	0.62	0.48		
	DOY	162-1										
Scan No.	3. 1	4. 1	5. 1	6. 1	7. 1	8. 1	10. 1	11. 1	12. 1	13. 1	14. 1	
Atten.	0.59	0.36	0.26	0.18	0.15	0.15	0.13	0.12	0.14	0.12	0.10	
	DOY	216-1										
Scan No.	3. 1	5. 1	7. 1	9. 1	11. 1	13. 1	14. 1	15. 1				
Atten.	0.24	0.43	0.20	0.17	0.18	0.17	0.18	0.20				
	DOY	216-2										
Scan No.	2. 1	3. 1	4. 1	5. 1	6. 1	7. 1	8. 1	9. 1	10. 1			
Atten.	0.12	0.17	0.11	0.12	0.10	0.11	0.15	0.19	0.49			
	DOY	220-1										
Scan No.	2. 1	3. 1	4. 1	5. 1	6. 1	7. 1	8. 1	9. 1	10. 1	11. 1	12. 1	13. 1
Atten.	0.21	0.31	0.17	0.16	0.18	0.12	0.15	0.14	0.20	0.15	0.18	0.17
	DOY	220-2										
Scan No.	2. 1	3. 1	4. 1	5. 1	6. 1	7. 1	8. 1	9. 1	10. 1	11. 1	12. 1	
Atten.	0.09	0.12	0.12	0.10	0.10	0.12	0.09	0.15	0.17	0.19	0.39	

REPRODUCIBILITY OF THIS
ORIGINAL PAGE IS POOR

* The DOY 247-1 data for the two largest nadir angles failed to pass the screening test imposed by Young (1975) as described in Chapter 8 so that these attenuation values were not used to correct the backscatter measurements. They are not included in the discussion, and the 19 values tabulated are not in the histogram given in Figure 7.4. The mean would change from 0.20 to 0.21 if these values were included. Note the high attenuation at Scan No. 16.1.

REPRODUCIBILITY OF THE
ORIGINAL PAGE IS POOR

TABLE 7.1 ATTENUATION VALUES AT 50° NADIR ANGLE IN DB FOR SKYLAB 2 AND 3 (TWO WAY) (Cont'd.)

DOY		245-2										
Scan No.	3. 1	4. 1	5. 1	6. 1	7. 1	8. 1	9. 1	10. 1	11. 1	13. 1	14. 1	15. 1
Atten.	0.24	0.29	0.18	0.22	0.24	0.22	0.27	0.28	0.30	0.23	0.20	0.19
		16. 1	17. 1	18. 1	19. 1	20. 1						
		0.17	0.22	0.17	0.18	0.16						
DOY		247-1										
Scan No.	9. 1	10. 1	11. 1	13. 1	14. 1	15. 1	16. 1	17. 1	18. 1	19. 1	21. 1	22. 1
Atten.	0.22	0.22	0.25	0.31	0.29	0.30	0.76	0.31	0.26	0.24	0.23	0.23
		23. 1	24. 1	25. 1	26. 1	27. 1	28. 1	29. 1				
		0.23	0.21	0.23	0.20	0.21	0.20	0.19				
DOY		252-1										
Scan No.	2. 1	3. 1	4. 1	5. 1	6. 1	7. 1	8. 1	10. 1	11. 1	12. 1	13. 1	14. 1
Atten.	0.07	0.11	0.14	0.13	0.11	0.11	0.11	0.19	0.15	0.11	0.09	0.14
		15. 1	16. 1	17. 1	18. 1	19. 1	20. 1	21. 1	22. 1	23. 1	24. 1	27. 1
		0.19	0.13	0.14	0.16	0.12	0.09	0.12	0.13	0.14	0.19	0.45
		28. 1	29. 1	30. 1	31. 1	32. 1	33. 1					
		0.30	0.21	0.22	0.18	0.14	0.21					

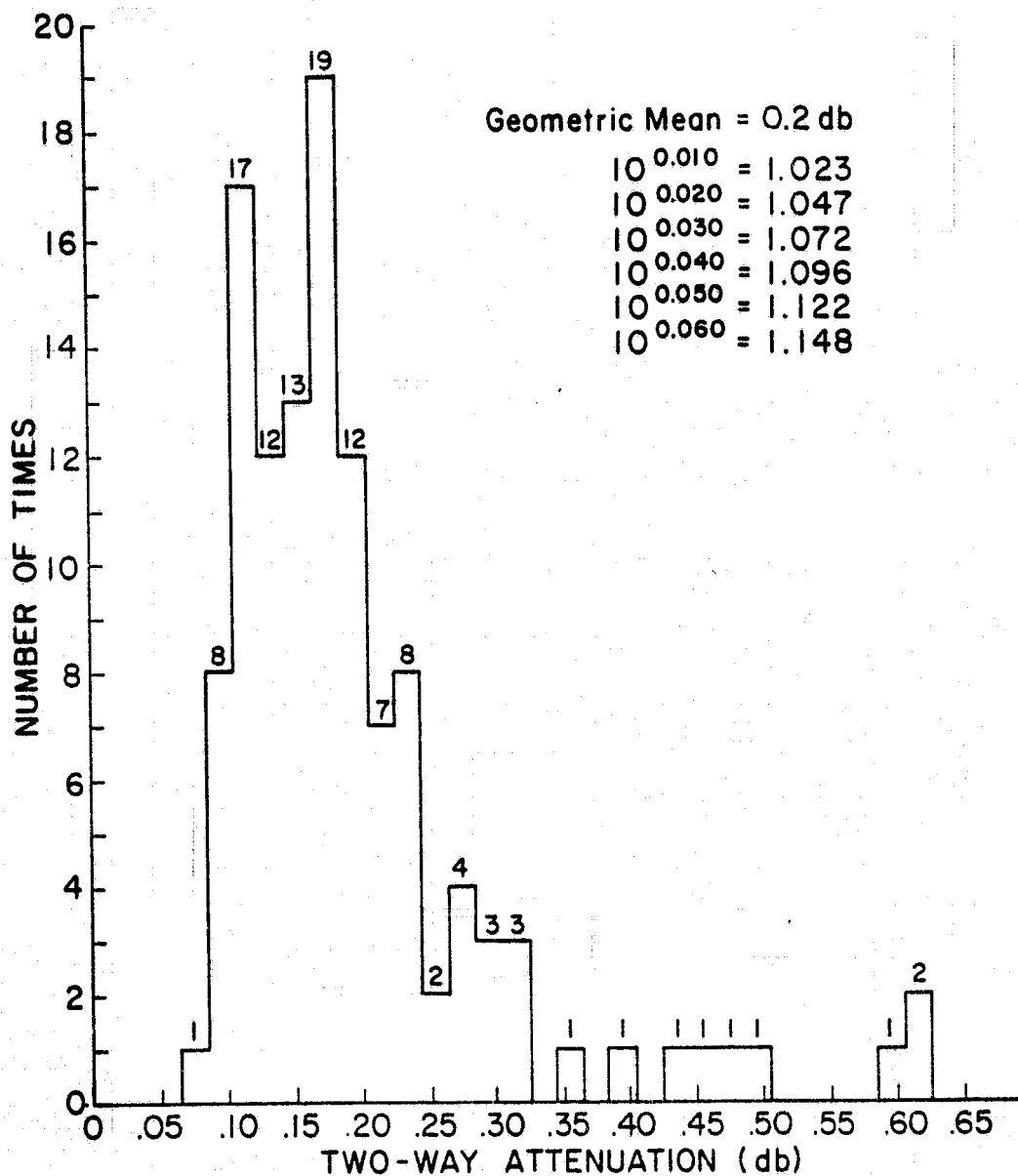


FIGURE 7.4 HISTOGRAM OF TWO-WAY ATTENUATION VALUES IN db AT 50° NADIR ANGLE FOR SKYLAB 2 AND 3. (118 VALUES)

The range of values for σ_{VV}^0 at 50° nadir angle was 43 db, and so these small increases to correct for attenuation had a very small effect on the analysis. It is clear that not correcting for attenuation at nadir angles other than 50° for the cross track mode would not have too serious an effect in attempts to relate wind speed to backscatter.

These results also explain, in part, why the use of backscatter data alone for SKYLAB 4 was possible. Effectively the average value of the attenuation can be thought to reduce the backscatter values by about 0.2 db. The return from clear areas might then be 0.1 db stronger than this reduced value and the return from cloudy areas from 0.2 to 0.4 db weaker. The net result would be to introduce an additional small error component in the wind determined from the radar measurement.

Elimination of Areas of Heavy Rain Very high excess temperatures indicate high attenuation values that can be caused only by large water drops as in heavy rain. Under these conditions the volume backscatter from the rain may be larger than the attenuated backscatter from the sea surface for the co-polarized return. High values of the passive microwave temperatures were used to locate those cells where effects would prohibit the use of the backscatter data to calculate wind speed. These high values occurred only in Hurricane AVA and in Tropical Storm Christine.

Graphs of the vertically polarized and horizontally polarized passive microwave temperatures for 50° and 44° nadir angles are shown for Hurricane AVA in Figure 7.5. The calculated attenuations from Table 7.1 are shown immediately above the appropriate value of T_V

for the 50° nadir angle. The value of T_v jumped to 238.5° K at scan 10 compared to 193.3° K at scan 9. From Figure 7.3, the excess temperature at scan 9 was about 28° K so that the excess temperature at scan 10 was about 73° . This yields an attenuation of about 2.7 db at scan 10. This attenuation is substantial and indicates that the measured backscatter probably did not come from the sea surface. Therefore the values for the backscatter at 50° scan 10 were not used to find the wind speed. The values for the attenuation are quite reasonable and increase toward the eye of AVA as the clouds thicken. The sharp jump at scan 10 probably corresponds to a rain band.

For scans 12, 13, and 14, the pitch of the spacecraft put the backscatter signals outside of the doppler pass band. These data also could not be used in the final analysis.

For a nadir angle of 44° in Hurricane AVA, the passive temperature suggests possible attenuation effects. However, no "hot spots" are evident so that scans 1 through 9 were used. Scans 10 through 14 had to be discarded for the same reasons as scan 12 to 14 at 50° nadir angle.

Similar graphs for Tropical Storm Christine and shown in Figures 7.6 and 7.7 for 50° , 42° and 31° nadir angles. For scan number 12 at 50° , the backscatter values were not used by Young (1975). However, a similar calculation as the one above shows that the attenuation was only about 0.6 db so that they might have been used. Clearly, the increases for scan 13 at 42° and for scans 10 and 12 at 31° require that these backscatter values be eliminated.

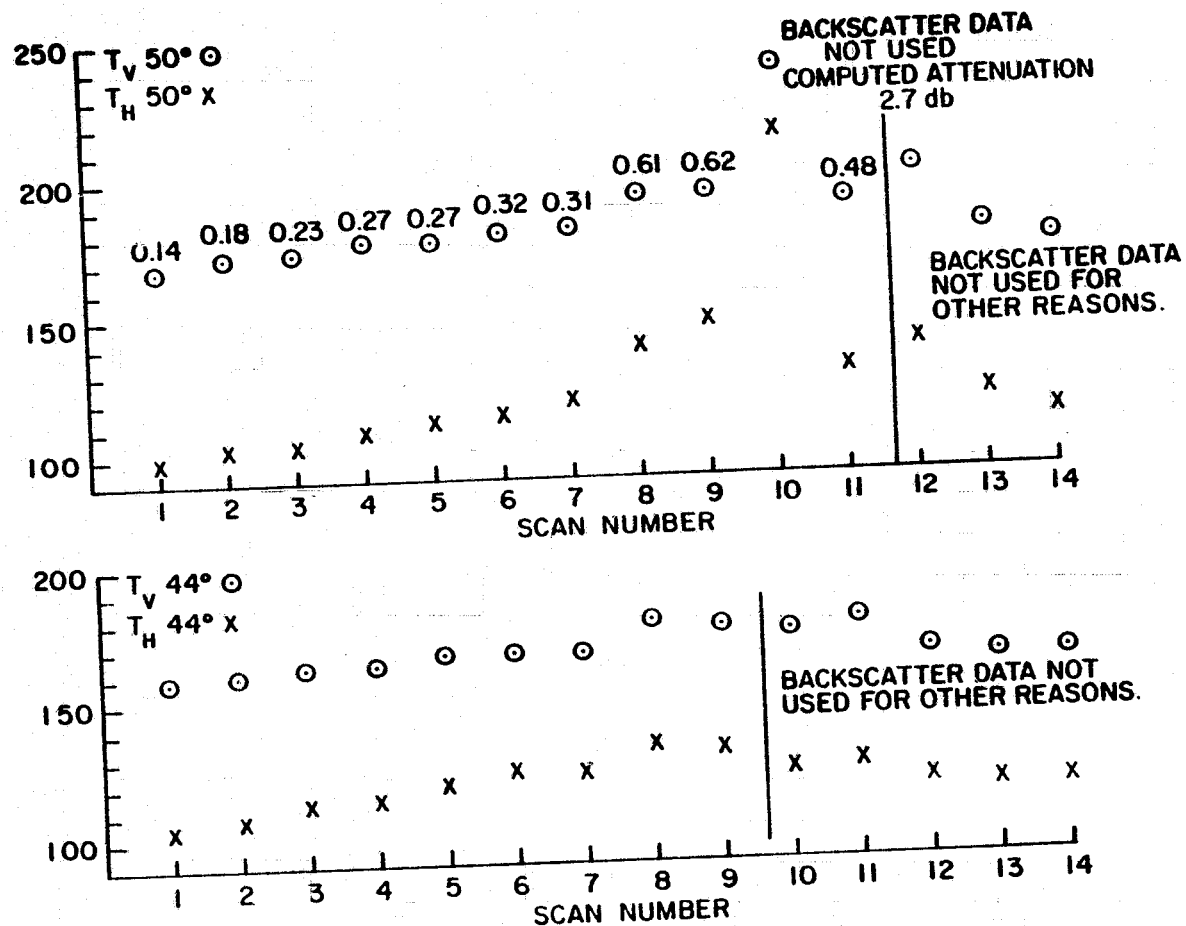


FIGURE 7.5 GRAPHS OF THE VALUES OF THE VERTICALLY AND HORIZONTALLY POLARIZED PASSIVE MICROWAVE TEMPERATURES FOR 50° AND 44° NADIR ANGLES IN HURRICANE AVA. VALUES FOR THE COMPUTED ATTENUATION ARE SHOWN IMMEDIATELY ABOVE EACH VALUE OF T_V FOR 50°.

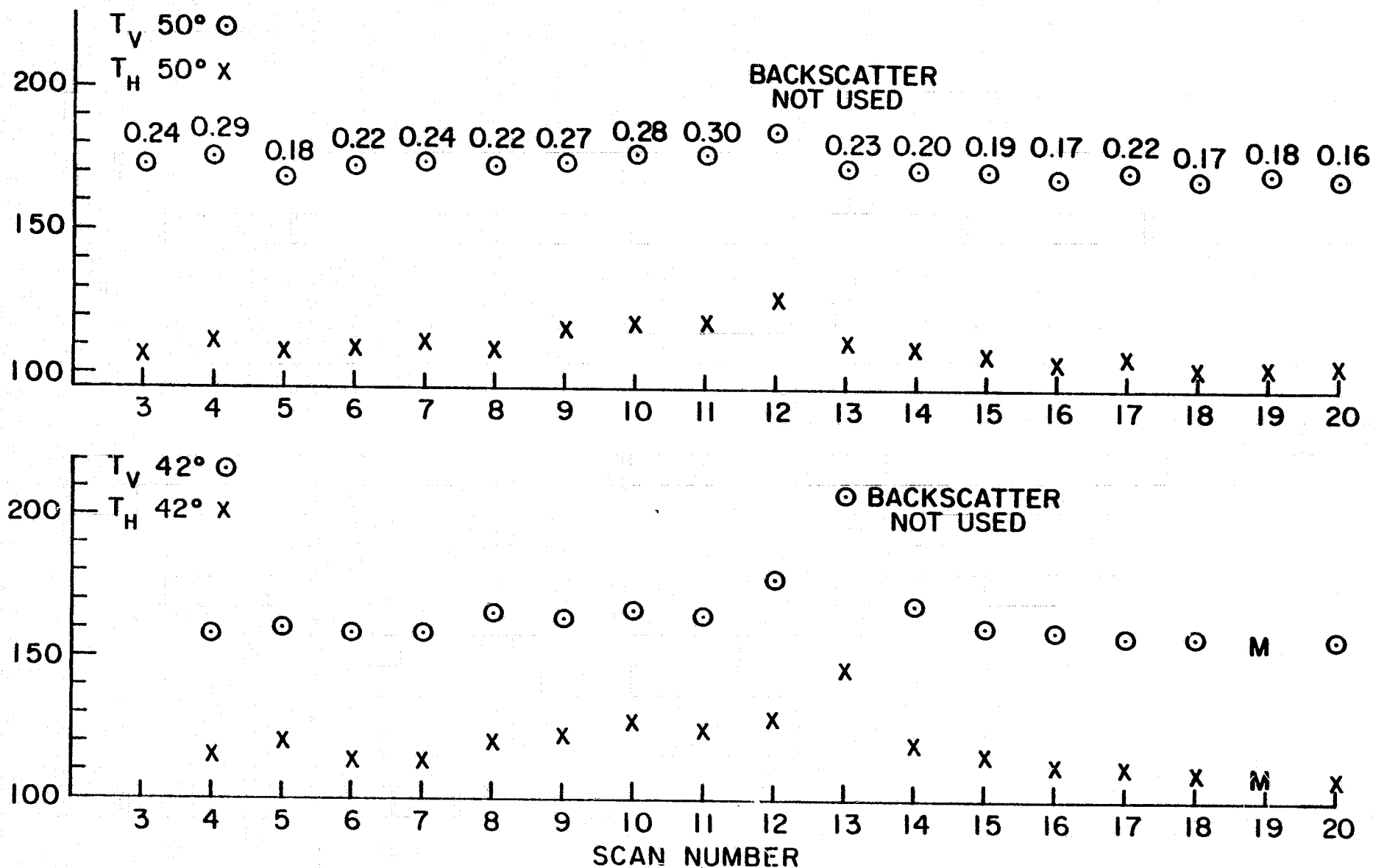


FIGURE 7.6 GRAPHS OF THE VALUES OF THE VERTICALLY AND HORIZONTALLY POLARIZED PASSIVE MICROWAVE TEMPERATURES AT 50° AND 42° FOR TROPICAL STORM CHRISTINE. VALUES FOR THE COMPUTED ATTENUATION ARE SHOWN IMMEDIATELY ABOVE EACH VALUE OF T_V FOR 50°.

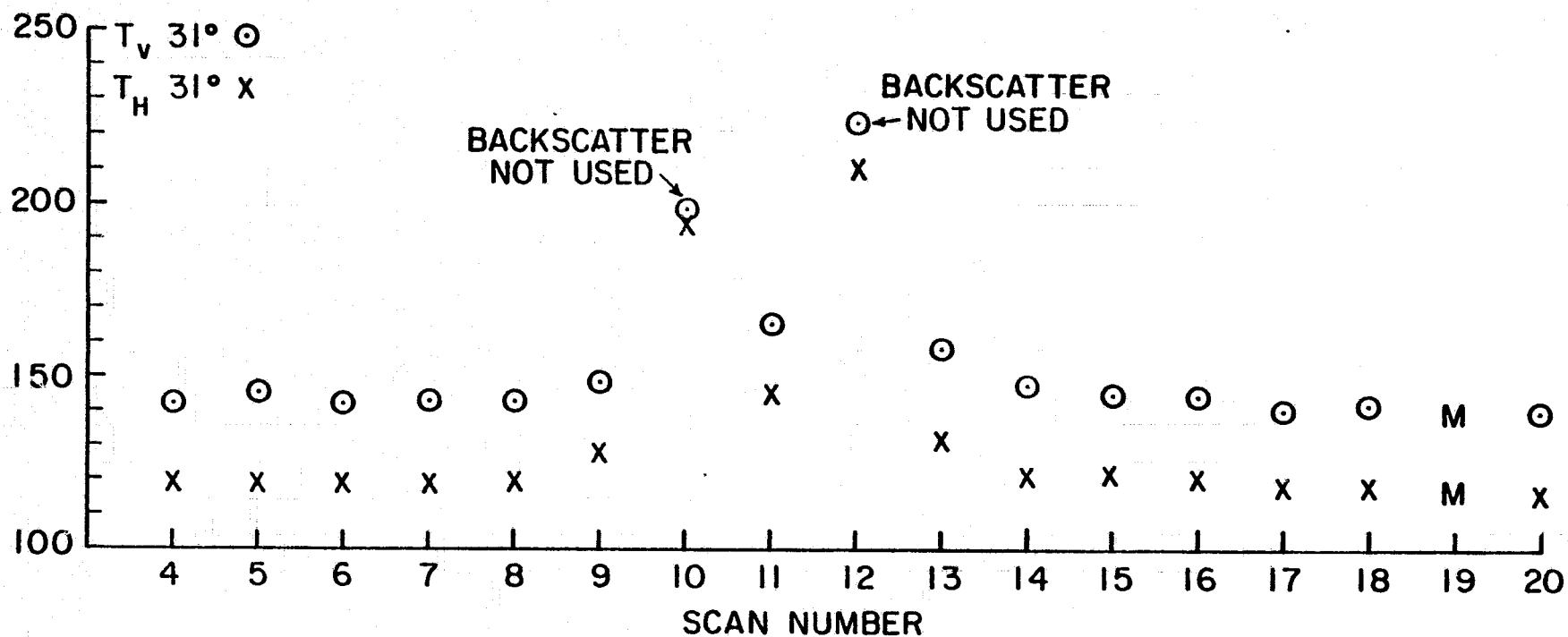


FIGURE 7.7 GRAPH OF THE VALUES OF THE VERTICALLY AND HORIZONTALLY POLARIZED PASSIVE MICROWAVE TEMPERATURES AT 31° NADIR ANGLE FOR TROPICAL STORM CHRISTINE.

CHAPTER 8 THE MEASUREMENT OF WINDS BY MEANS OF A RADAR ON A SPACECRAFT

INTRODUCTION

All that precedes is prelude. It might all have been put into one chapter entitled "Introduction". The actual page length of Chapters 2 through 7 is not an indication of the length of time required to accomplish the various stages of this investigation. Getting the data into the form described in Chapter 5 was the pacing item. The theories and procedures could be carried along in parallel, but the lengthy task of producing the data given in Appendix A was a very difficult part of the program. The results of all of the previous chapters is almost to have ready sets of number triplets of the form, $[U_m, \chi_m, \sigma^0]$, in which U_m is the meteorologically determined wind speed at a cell scanned by S193, χ_m is the wind direction relative to the pointing direction of the radar beam, and σ^0 is a backscatter measurement at one of five nadir angles and one of four different polarizations. The value of χ_m is a meteorologically determined variable given the geometry of the orbit and the position of the antenna.

To show that winds can be measured from a spacecraft, it is necessary to show that the values of σ^0 contain information on wind speed, given the wind direction, as in $U_r = U_r(\chi_m, \sigma^0)$, such that U_r predicts the meteorological wind, U_m , with the accuracy to be expected, given the difficulties in specifying the winds as discussed in Chapter 4. Since both the meteorologically determined wind speed and direction can have errors, it is also necessary to investigate the contributions to the difference between the radar wind and the meteorological wind caused by errors in the wind direction.

Six different techniques were used to investigate the interrelationships between the radar wind and the meteorological wind. Two

are described in greater detail by Young (1975) in Appendix D of this report, and three others are described here. The techniques of Young (1975) are also described in this chapter and are contrasted with the other two techniques that were used.

Also, Young (1975) obtained relationships for the power law dependence of σ^0 on wind speed, which is the inverse problem as far as a regression analysis is concerned. Before discussing the various regression techniques that were used, a general discussion of regression techniques is required to set the stage for the techniques that were actually used.

There was one last step of straight data correction required before the analysis could proceed. Because of various problems, the nadir angles for the five command angles were not always the same. So that larger sets of data for each nominal nadir angle could be studied as a unit, it was necessary to remove the small changes in backscatter expected because of the departure of the nadir angles from their nominal values. Once this was accomplished, the data sets could be studied by numerous methods to determine wind and backscatter interdependencies.

In summary, this chapter will first discuss the small corrections required to get all the nadir angles to five nominal values. This will be followed by a general discussion of curve fitting and regression techniques. Then the results of Young (1975) will be summarized. His suggestion of a withheld weather ship analysis as described in Chapter 4 has already had a profound effect on the final interpretation of the results. Then various efforts to eliminate some of the deficiencies in most regression technique will be described, and ways to determine the effects of wind direction errors will be derived and applied. Finally the results will be stratified

according to data quality and method of analysis and the conclusions on the validity of a radar system on a spacecraft for measuring the winds over the ocean will be presented.

CORRECTIONS TO NOMINAL NADIR (OR INCIDENT) ANGLES FOR ALL OF THE DATA

Young (1975) developed a set of formulas to correct the backscatter values to the nominal values of 1° , 17° , 32° , 43° , and 50° for all measurements. The corrections, in general, were quite small and done in such a way that if the actual nadir angle exceeded the nominal angle the correction was positive, and conversely. The technique, quoting Young (1975), with the notation and table numbers changed to conform to this report is described below.

"The S-193 noncontiguous data were taken at five command angle numbers having nominal incident angles of 1° , 17° , 32° , and 50° for SL2 and 3 and for part of SL-4. During most of SL-4 the incident angles deviated substantially from the 1° and 17° values for the right-side scans and remained near nadir for left-side scan. Table 3.2 gives a summary of the typical incident angles for each command angle within a particular data segment or for one side of a left/right data segment.

"Measurement fluctuations caused by incident angle variations were removed from the backscatter data by using Fung and Chan's (1975a) theoretical model. For each polarization, pq, and command angle number, j, a linear incident angle correction function $\Delta_\theta \sigma_{pqj}^0$ was estimated where

$$\Delta_\theta \sigma_{pqj}^0(\theta, U) = \frac{\partial \sigma_{pq}^0(U, \bar{\theta})}{\partial \theta} \bigg|_{\theta = \theta_j} (\theta_j - \theta) \quad (8.1)$$

and $\theta_j = 50^\circ, 43^\circ, 32^\circ, 17^\circ$, and 1° for $j = 1$ through 5 respectively. The wind speed dependent partial of σ_{pq}^0 with respect to incident angle can be approximated by equation (8.2).

$$\frac{\partial \sigma_{pq}^0(U, \theta)}{\partial \theta} \bigg|_{\tilde{\theta} = \theta_j} = a_{pqj} + b_{pqj} \log_{10} U \quad (8.2)$$

The values of a_{pqj} and b_{pqj} used to correct the backscatter data are given in Table 8.1, for U in meters per second.

"The incident angle correction was only used for $|\tilde{\theta}_j - \theta| \leq 2^\circ$. Data measured further than 2° from the nominal incident angles were not included in the regression analysis because of decreased accuracy of the correction for large incident angle variations."

Some examples of these corrections are given in Table 8.2 for Tropical Storm Christine on DOY-245-2 (9/2/73). Data for the first ten measurements have vanished because of the effects of the data flags shown on page A21 of the appendix. The entries in Table 8.2 should be compared with the uncorrected data in the table on page A21.

For scan number 3.1, the nadir (or incident) angle was 49.6° . The backscatter values tabulated on page A21 were corrected to a 50° nadir angle by adding the (negative) values in db given in columns 5 through 8 of Table 8.2 to the values in A21. Scan number 4.2 had a nadir angle of 42° which was corrected to 43° by adding -0.33, -0.63, -0.24 and -0.24 to the corresponding backscatter values. (In a sense, the spacecraft is moved and not the cell being scanned).

TABLE 8.2 DOY 245-2, 9/ 2/73 CTNC-L, TROPICAL STORM CHRISTINE (VERSION M3)

SCAN NUMB	CORRECTED SCAT COEFFICIENTS				INCID ANGLE CORRECTIONS				ASPECT ANGLE CORRECTIONS				ATTEN (DB)	TBM (DEG)
	VV (DB)	HH (DB)	VH (DB)	HV (DB)	VV (DB)	HH (DB)	VH (DB)	HV (DB)	VV (DB)	HH (DB)	VH (DB)	HV (DB)		
3.4	-32.16	-33.32	-36.76	-38.42	-0.11	-0.24	-0.10	-0.10	0.24	0.47	0.32	0.32	0.24	83.14
3.5														
3.6														
3.7	20.81	-1.35	-16.38	-14.25	-0.47	-0.46								
3.8	14.13	13.55	-3.18	-3.54	-0.03	-0.03								
4.1	-25.95	-23.91	-32.77	-34.59	-0.11	-0.24	-0.10	-0.10	1.16	1.50	2.07	2.07	0.29	82.74
4.2	-28.14	-29.62	-35.91	-41.75	-0.33	-0.63	-0.24	-0.24	0.35	0.57	0.40	0.40		
4.3	-18.11	-18.55	-33.49	-37.23	-0.37	-0.53	-0.22	-0.22	0.	0.	0.	0.		
4.4	0.32	0.09	-14.75	-15.38	-0.52	-0.51								
4.5		13.20	-3.94	-4.17		-0.02								
5.1	-26.83	-31.73	-34.21	-35.11	-0.11	-0.25	-0.10	-0.10	2.01	2.45	3.68	3.68	0.18	86.97
5.2	-23.69	-24.75	-32.00	-24.87	-0.31	-0.58	-0.22	-0.22	1.18	1.46	1.97	1.97		
5.3	-23.38	-19.28	-35.45	-44.03	-0.36	-0.51	-0.21	-0.21	0.	0.	0.	0.		
5.4	-0.28	-0.53	-15.41	-15.93	-0.43	-0.42								
5.5	13.05	12.91	-4.11	-4.15	-0.01	-0.01								
6.1	-21.69	-26.33	-32.18	-38.35	-0.10	-0.23	-0.09	-0.09	2.12	2.51	3.94	3.94	0.22	85.83
6.2	-23.71	-27.71	-36.24	-36.80	-0.30	-0.57	-0.21	-0.21	1.07	1.24	1.91	1.91		
6.3	-19.00	-20.13	-35.27	-35.27	-0.33	-0.48	-0.20	-0.20	0.11	0.13	0.18	0.18		
6.4	-1.23	-1.69	-16.38	-14.45	-0.48	-0.47								
6.5	14.00	14.01	-3.05	-3.54	-0.02	-0.02								
7.1	-19.52	-22.17	-29.84	-38.39	-0.11	-0.24	-0.09	-0.09	1.42	1.85	3.05	3.05	0.24	86.03
7.2	-17.98	-22.03	-34.83	-31.70	-0.30	-0.57	-0.21	-0.21	0.42	0.46	0.78	0.78		
7.3	-13.21	-15.23	-29.19	-28.63	-0.29	-0.42	-0.17	-0.17	0.80	0.88	0.81	0.81		
7.4	-0.32	-0.78	-15.53	-15.74	-0.41	-0.40								
7.5		13.54	-3.45	-3.66		-0.01								
8.1	-16.21	-21.33	-28.00	-24.68	-0.08	-0.19	-0.07	-0.07	1.54	1.73	2.94	2.94	0.22	87.14
8.2	-15.24	-17.90	-27.80	-29.50	-0.26	-0.51	-0.19	-0.19	0.14	0.15	0.27	0.27		
8.3	-12.56	-13.81	-28.51	-28.01	-0.27	-0.40	-0.16	-0.16	0.08	0.08	0.15	0.15		
8.4	0.24	-0.19	-15.85	-15.38	-0.45	-0.45								
8.5	12.90	13.21	-4.02	-4.09	-0.01	-0.01								

10/29/75

Table 8.1 Coefficients for incident angle correction
of backscatter measurements for wind speeds between
2 and 30 m/sec.

Pol. (pq)	Com. Angle (j)	θ_j	a_{pqj}	b_{pqj}
VV	1	50	-0.3351	0.0817
	2	43	-0.4235	0.1362
	3	32	-0.4657	0.2016
	4	17	-1.1466	0.1416
	5	1	-0.1549	0.0917
HH	1	50	-0.7216	0.1471
	2	43	-0.7892	0.2343
	3	32	-0.6609	0.2615
	4	17	-1.1241	0.1244
	5	1	-0.1555	0.0917
HV or VH	1	50	-0.3112	0.0946
	2	43	-0.3040	0.1015
	3	32	-0.2771	0.1207

The largest correction in this table for nadir angle effects is -0.63 db. All but 9 of the 86 corrections shown are under 0.50 db and 54 are under 0.25 db. The measured values for σ_{HH}^0 varied by 13 db for scans 4.2 to 8.2 so that these corrections are a small part of the total range of the signal. A review of all of the corrections for nadir angle effects made in the entire analysis shows that the largest single value was -1.16 db for HH on DOY 338-1 scan number 2.1 and that about 70% were between -0.25 and +0.25 db.

The columns labeled "aspect angle correction" are particular to the studies by Young (1975) and will be discussed later. The attenuation values were discussed and tabulated in Chapter 7.

GENERAL DISCUSSION OF CURVE FITTING AND REGRESSION TECHNIQUES

Principles It would be wonderful if the theories relating wave spectra, the winds, and backscatter measurements to each other were complete and perfect so that the theory could be used to compute the wind speed given a backscatter measurement and a wind direction. Despite the tremendous advances over the past few years in understanding the problem, as described in Chapter 6, there are gaps in the theory with reference to the full anisotropic properties of the capillary wave spectrum and to the details of the slope distribution that defines the tilting mechanism. The spectrum proposed by Pierson (1975) will undoubtedly be superseded as better data became available. The progress to date does provide a rational for and an explanation of the large variations of backscatter as a function of wind speed and of the variation of backscatter with aspect angle. In a few more years, it may be possible to close the gap, determine the larger scale slopes, z_x and z_y , that enter into the tilt theory, and compute backscatter for any nadir angle, wind speed, and slope spectrum from first principles.

With this in mind, it was necessary to use less sophisticated methods to determine the relationship between the number triplets, (U, χ, σ^0) , for the different polarizations and nadir angles. The goal of the program is to obtain winds from radar measurements and not radar measurements from winds. Once the attempt to use pure theory is abandoned, many possible techniques for obtaining a prediction of the wind from the radar measurement became available.

These techniques fall into the general category of multiple regression techniques of various degrees of complexity and ingenuity. They all have several things in common. One is that they try to minimize the sums of the squares of the differences between the values given by the "predictor" parameters (σ^0 and χ_m in this case) and the "predictand" which is the wind speed. Another is that they start by assuming a functional relationship between the "predictor" parameters and the quantity to be predicted. When all of the parameters in the set have errors, the choice of the proper function is often masked, and perhaps the greatest danger is the use of such techniques lies in having a preconceived notion of the appropriate function to be used. The data can often serve as a guide to the best functional form to be used.

Although the sums of the squares of the predicted and observed values will be a minimum for the particular functional form that was chosen, and although the bias over all values typically averages to zero, such curve fitting procedures frequently have biases over more restricted ranges of the data. For example in their application here, the radar predicted wind may be consistently high for low winds and consistently low for high winds.

A very simple example can be considered. Suppose that

$$y = x + x^2 \quad (8.3)$$

is the true equation relating y to x over the range, $0 < x < 1$. Also suppose that one insists that the data be fitted by a straight line of the form

$$y^* = b_0 + b_1 x \quad (8.4)$$

The requirement that

$$\int_0^1 (x + x^2 - b_0 - b_1 x)^2 dx = \min \quad (8.5)$$

yields, on setting the two partials with respect to b_0 and b_1 equal to zero, the result that

$$y^* = -\frac{1}{6} + 2x \quad (8.6)$$

which is the best least square prediction of y given the assumed form of y^* . Scatter in the basic data only obscures the fact that the best function was not chosen to start with.

The integral of $y - y^*$ over 0 to 1 is zero as in equation (8.7).

$$\int_0^1 (x + x^2 - 2x + \frac{1}{6}) dx = \left[\frac{x^3}{3} - \frac{x^2}{2} + \frac{x}{6} \right]_0^1 = 0 \quad (8.7)$$

However, the straight line underpredicts y for low values of x , overpredicts it for the middle range, and underpredicts it again for high values of x as shown in Figure 8.1. Much the same kinds of problems arise if too simple an assumption is made about the functional relationship between U , χ and σ^0 in this particular problem.

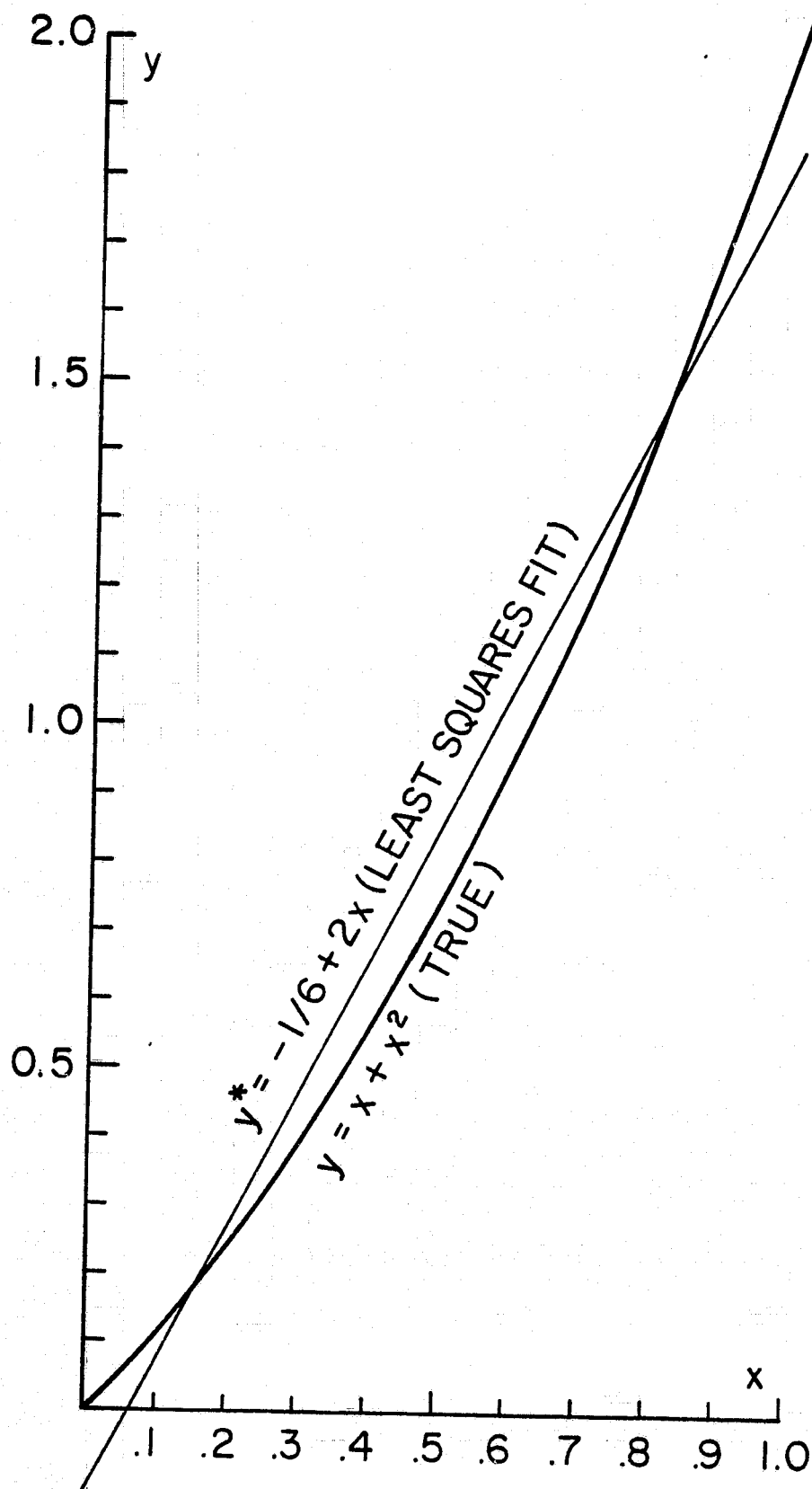


FIGURE 8.1 EXAMPLE FOR THE DISCUSSION OF LEAST SQUARES FITTING TECHNIQUES.

Comments on the scatter of plots of backscatter versus wind speed.

One of the corollaries to the legendary laws attributed to a scientist named Murphy as applied in meteorology and oceanography is the maxim; "If the data scatter, plot them on semilog scales, and if they still scatter, plot them on double log scales." This maxim is believed to produce scatter diagrams and groups of points that more clearly delineate power law relationships and to cluster the points into more easily discernable patterns. Like all such beliefs, exceptions occur, and the purpose of this section is to illustrate the problems that arise in the study of radar backscatter versus wind speed when semilog plots and double log plots are employed. Two alternatives are given for the more realistic interpretation of the data from S193.

It is almost a tradition that measurements of the normalized radar backscattering cross section be given in terms of decibels. If the variation of σ^0 for a given polarization combination as a function of nadir angle as that angle varies from zero to 80° is being graphed then decibels are the logical unit to use because the values can span 50 db, or more.

In the study of the variation of backscatter versus wind speed at a given nadir angle, σ^0 , for a given polarization, appears to increase by only about 20 db as the wind varies from about 5 knots to 50 knots. It is, therefore, not prohibitively difficult to plot σ^0 against wind speed on linear scales.

The decibel unit evolved from scientific notation via the bel to the decibel as a convenient measure of gain and loss in communication systems. Its use in the study of backscatter data in general, and S193 data in particular, needs to be questioned. A 3 db error in the prediction of radar backscattering cross section, given the wind

speed exactly, does not seem like much of an error. The re-location of the decimal point in going from bels to decibels is not much of an advantage when measurements are given to four or five significant figures. However, given an exact upwind measurement of σ^0 , a 3 db error in wind speed (with zero db equal to 1 knot) for a wind of 40 knots is not a trivial error.

The S193 experiment was designed without a full awareness of the impact of wind direction on the values of backscatter so that midway through the experiment, after the data were taken, it was necessary to devise a strategy to remove, or to treat, the variation in aspect angle. This problem will be treated in detail later on in this chapter.

For purposes of illustration, assume a nadir angle and a polarization that yields the relationship between backscatter and wind speed given in Equation 8.8 for measurements that are all upwind.

$$\sigma_{db}^0 = -46 + 20 \log_{10} U \quad (8.8)$$

An equally valid equation is then Equation 8.9

$$\sigma^0 = 2.5 \times 10^{-5} U^2 \quad (8.9)$$

Also assume, for purposes of illustration, either that all of the error of measurement lies in the wind speed and not the backscatter or that all of the error lies in the backscatter measurement and not the wind speed.

Figure 8.2 shows σ^0 in db versus wind speed on a linear scale. The "true" relationship is graphed. Errors of ± 4 knots and ± 8 knots

due entirely to the winds can be shown by simply displacing the "true" curve an appropriate distance to the left or right.

If the errors in the magnitudes of the winds scatter so that 65% of them are within ± 4 knots, 90% are within ± 8 knots and 10% are outside this range, then detecting the true curve within the scatter would be most difficult. Conversely backscatter errors of ± 3 db would totally mask the dependence of wind on backscatter above 20 m/s whereas for light winds ± 3 db lie within ± 4 knots.

Figure 8.3 shows the same curves as those on Figure 8.2 but now both scales are logarithmic. The "true" curve is a straight line. Were the same scatter of points on Fig. 8.2 plotted on this new figure, the pattern that they would produce would look quite different. Winds over 20 knots would bunch up into a very small narrow area in the upper right. Light winds would scatter over a much larger area. The kinds of errors in the wind vector discussed in Chapter 4 can produce points to the left of the true curve that are 20 db apart. If one were to believe the winds as being "exact", the plot would imply extreme variations in the measurement of the backscatter for the same light wind.

The difficulty with this form of presentation is that it assumes that the errors in the measurements of both the wind and the backscatter are percentage deviations from the true value. A 10% error in the measurement of the magnitude of a 50 knot wind is ± 5 knots, but a 10% error in the measurement of a 4 knot wind is ± 0.4 knots. For low winds, this is not within the capability of either measurement and reporting techniques or analysis techniques in meteorology. The scatter in plots such as these is a real unavoidable effect of the way winds are measured and analysed for synoptic meteorological purposes and for input to numerical weather prediction models.

Plotting the data in this form can do no particular harm (except, perhaps, confuse one's understanding), but the next step can yield poor results. The next step is usually to regress $\log_{10} U$ on σ^0 in db or σ^0 in db on $\log_{10} U$ so as to predict the least squares σ as a function of U or the least squares U as a function of σ . If there are many more points for low winds than for high, the errors in the low winds of factors of two and three are given much more weight than errors in high winds of 20 or 30% whereas both could be comparable in magnitude on a linear scale. The two regression equations can therefore produce lines on this plot that are markedly different in slope.

Still a third way to plot the data is shown in Figure 8.4 where both σ^0 and U are on linear scales. As U varies from 0 to 60 knots, σ^0 varies from 0 to 0.09 and the curve is a simple parabola. Errors in U are produced by simply translating the "true" curve an appropriate distance to the left or right. This plot shows the relative importance of winds above, or below, say 20 knots.

There is one additional way to use these equations. The stress of the wind in the sea surface expressed in terms of the drag coefficient at 19.5 meters is given by

$$\tau = \rho C_{19.5} U_{19.5}^2 \quad (8.10)$$

and so backscatter for this example on a linear scale would be a direct linear measure of the stress.

$$\tau = 4.10^4 \rho C_{19.5} \sigma \quad (8.11)$$

The equations of hydrodynamics do not involve the logarithm of the wind speed. The square of the wind speed is important in calculating the wind stress and the height of wind generated gravity waves. It seems therefore more appropriate to minimize scatter on diagrams such as Figure 8.4 than on diagrams such as Figure 8.3. Were it certain that the PBL theory used in this study was absolutely correct, then it might be advisable to regress $U_*^2 (= \tau/\rho)$ on σ and obtain the wind stress. However, the variation of wind with height also involves $z_0 = z_0(u_*)$ and the effects of stability so that the prediction of $U_{19.5}$ from σ^0 seems to be more appropriate.

The final graphical procedure is perhaps the best of all. From equation 8.8, if it were correct, it would be possible to calculate the wind speed that σ^0 implies and call it the radar wind, U_r , as in Equation 8.12.

$$U_r = 2 \cdot 10^2 \sigma^{\frac{1}{2}} \quad (8.12)$$

and plot U_r versus U_m on linear scales as in Figure 8.5. The horizontal and vertical distances are then a measure of the contribution to the discrepancy between U_r and U_m of the errors in the radar measurement and the errors in determining the magnitude of the vector wind. The problem that remains however is that U_r is not only a function of σ^0 but also a function of χ , and it is not as simple a problem as the one assumed for illustrative purposes above.

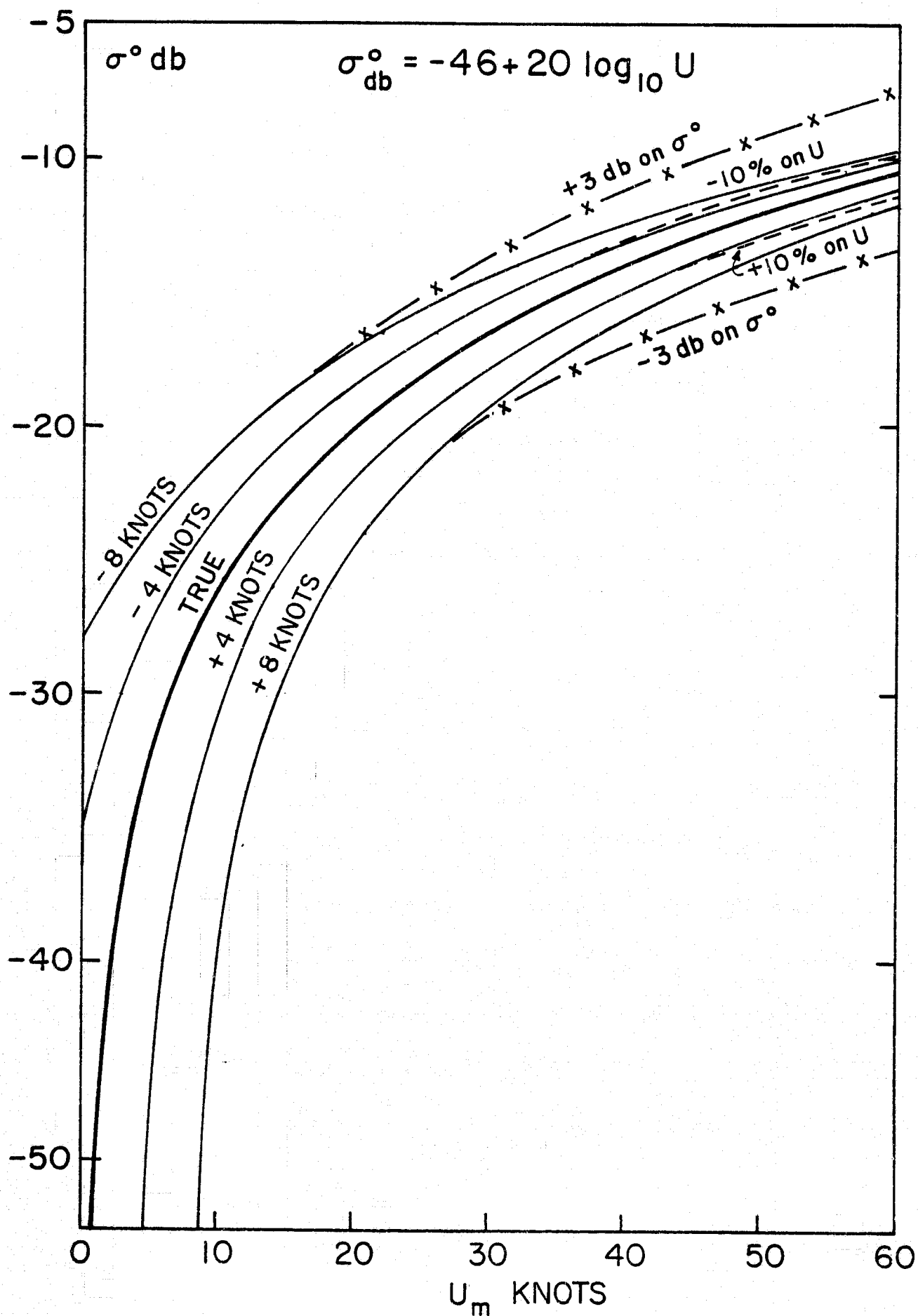


FIGURE 8.2 RELATIONSHIP BETWEEN U_m AND σ^0 ON A LINEAR AND A LOG SCALE.

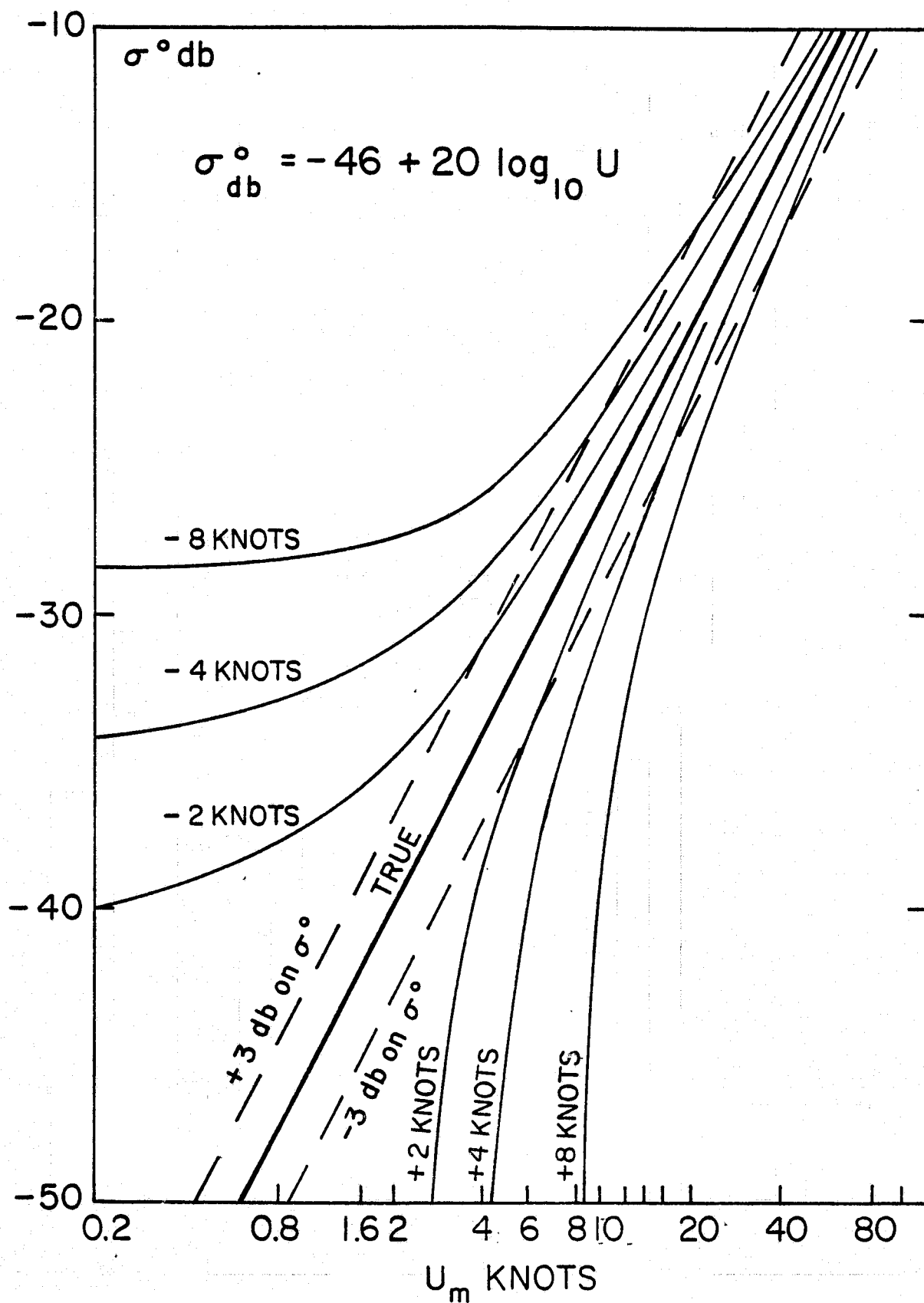


FIGURE 8.3 U_m VERSUS σ° ON DOUBLE LOG SCALES

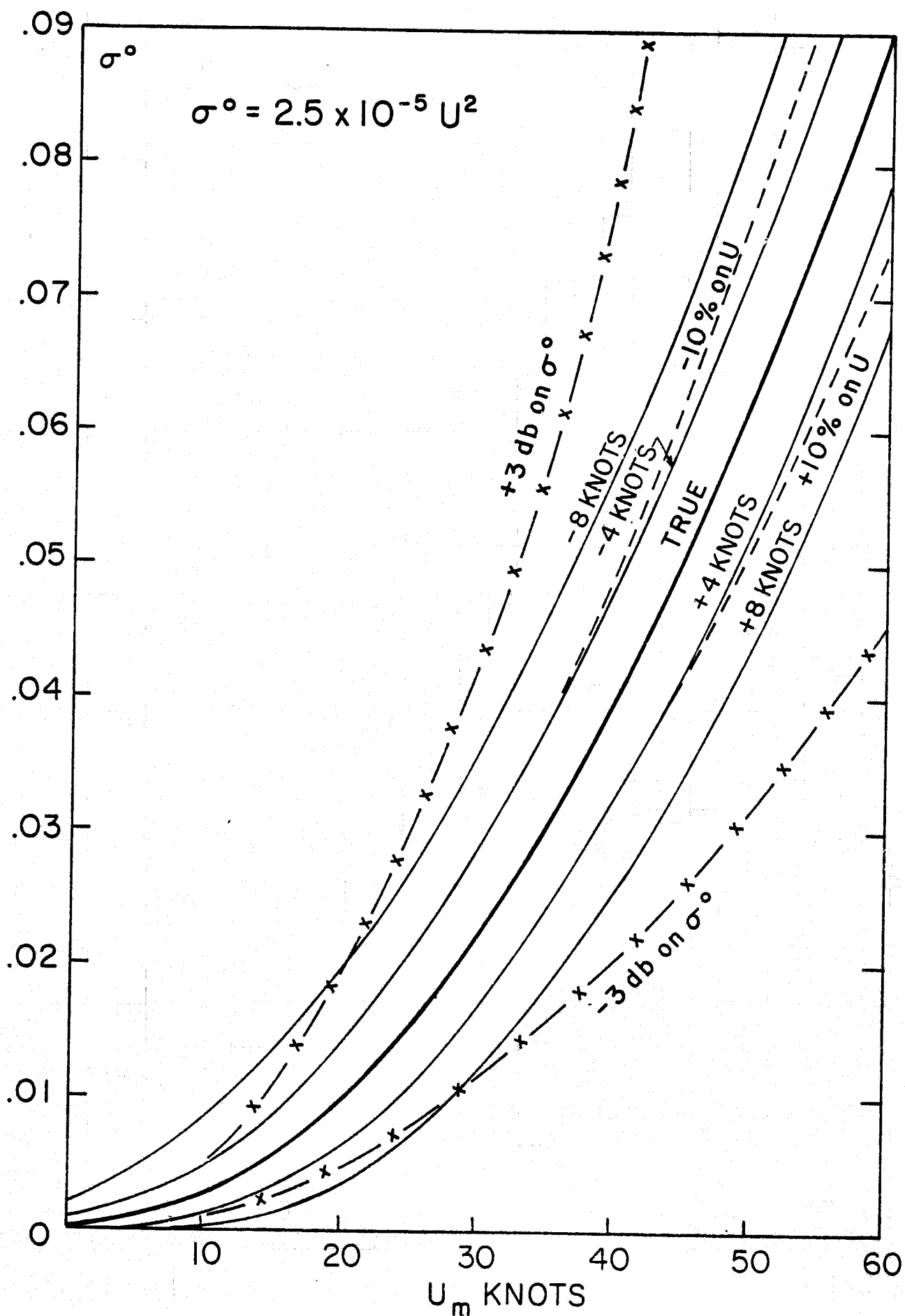


FIGURE 8.4 U_m VERSUS σ^o ON LINEAR SCALES

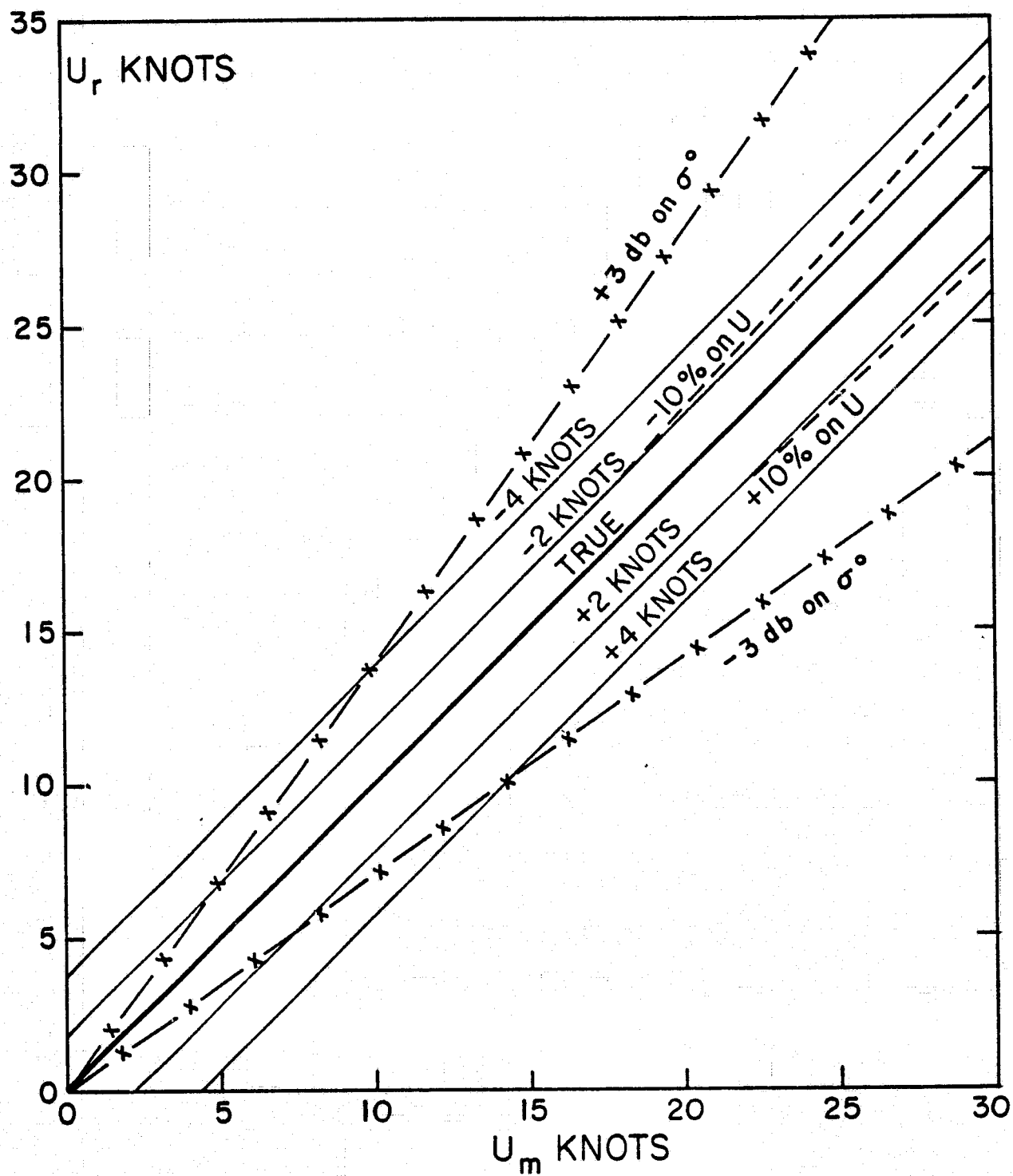


FIGURE 8.5 U_m VERSUS U_r

Strategies for avoiding various problems Multiple regression methods require care in their application. During the early stages of the study of radar backscatter versus wind speed with limited data sets, it makes sense to look for the various power law relationships that were discussed in Chapter 6. These methods can distinguish between say, $\sigma^0 \sim U^{0.5}$ and $\sigma^0 \sim U^{1.5}$. If x were the log of the wind and y the backscatter in db in Equation 8.3, with some additional constants, other than ones and zeros, then equation (8.5) would not be the best possible prediction of σ^0 , for example.

Although regressing $\log_{10} U_m$ on σ in db, either way, can yield a fit that may be useful, it is also necessary to regress the values of U_m on σ^0 in antilog form for an unknown power. Also, even the assumption of some simple power law relationship has to be looked at skeptically and eliminated, if possible, if the fit can be improved. It can be noted for example that the theoretical curves from Fung and Chan (1975b) in Appendix C are no longer straight lines on a double log plot.

There is no guarantee that what would appear to be systematic biases for various ranges of wind speed will be eliminated if too simple a set of regression equations is used to predict the winds from the radar measurements. For different ranges of wind speed the "apparent" power law may be quite different. With these introductory comments, the time has now arrived to see how well backscatter measurements predict the winds.

RESULTS ON LOG-LOG AND POWER LAW REGRESSIONS

Introduction Two of many possible ways to study the relationship between backscatter and the wind is to refer all the winds to upwind and then find (1) the best fit constants for the two log-log relationships, equations (8.13) and (8.14),

$$\sigma^0_{(db)} = a_0 + a_1 \log_{10} U \quad (8.13)$$

$$\log_{10} U = b_0 + b_1 \sigma^0_{(db)} \quad (8.14)$$

by finding the constants, a_0 , a_1 , b_0 and b_1 , that minimize

$$\sum_{i=1}^n (\sigma^0_i - a_0 - a_1 \log_{10} U_i)^2 \quad (8.15)$$

and

$$\sum_{i=1}^n \left(\log_{10} U_i - b_0 - b_1 (\sigma^0_{db})_i \right)^2 \quad (8.16)$$

and (2) the best fit constants for two power law relationships as in equations (8.17) and (8.18) where σ_0 is equal to $10^{(\sigma^0_{db})/10}$,

$$\sigma^0 = \alpha_0 U^{\alpha_1} \quad (8.17)$$

$$U = \beta_0 (\sigma^0)^{\beta_1} \quad (8.18)$$

by finding the constants α_0 , α_1 , β_0 and β_1 that minimize

$$\sum_{i=1}^n \left(\sigma^0_i - \alpha_0 U_i^{\alpha_1} \right)^2 \quad (8.19)$$

$$\sum_{i=1}^n \left(U_i - \beta_0 (\sigma^0_i)^{\beta_1} \right)^2 \quad (8.20)$$

This was done by Young (1975) as described in greater detail in Appendix D. Some of these results are summarized here.

The question might be asked of the radar designers as to whether or not the use of equation (8.13) (instead of 8.17) is really appropriate, even in radar design. Especially for high winds, the difference can be large.

The other two equations predict U , for upwind measurements only given an upwind measurement of σ^0 . The same comments can be made. Equation 8.14 minimizes $\sum (\log U_i - \log U_{pi})^2$ over the data set, and $E (\log U_i - \log U_{pi})$ will be near zero. Equation (8.18) minimizes $\sum (U_i - U_{pi})^2$ and $\sum (U_i - U_{pi})$ will be near zero.

In the situation where the wind is predicted from the backscatter measurement, of these two choices only equation (8.20) is useful. There is little, if any, practical use for a prediction of the logarithm of the wind speed.

Equations (8.13), (8.14), (8.17) and (8.18) all have a different meaning. In equation (8.13), a wind speed, U_1 is given, and the equation yields a value of σ^0 , say σ_{pi}^0 , in db. The sum, $\sum (\sigma_i^0 - \sigma_{pi}^0)^2$, will be a minimum over the particular set of observed data. Also, in general, the sum, $(\sigma_o^0 - \sigma_{po}^0)$, will be close to zero. If the value of σ^0 to be used in a radar design is desired, this equation may be the one to be used. Alternatively equation (8.17) might have been used and σ^0 obtained in antilog form. The sum $\sum (\sigma_i^0 - \sigma_{pi}^0)^2$, in antilog form will be a minimum, and the sum, $\sum (\sigma_i - \sigma_{pi})$ will be close to zero. If the values, of σ^0 are changed from db to antilog form or from antilog form to db after the use of the appropriate equation the sums of squares will not be a minimum and the sums of the difference will not be close to zero.

Referring the backscatter measurements to upwind The first step in this particular analysis is to refer to backscatter measurements to upwind by using the theoretical results of Fung and Chan for the three highest nadir angles. The technique, quoting Young (1975), is described below with appropriate changes as to chapters, figures and equations.

"The experimental measurements (Grantham et al. (1975); (Afarani, 1975) and a theoretical model (Fung and Chan) describing the wind direction dependence of backscatter measurements were discussed in Chapter 6. These measurements and [the corresponding] model reveal the basic shape and wind dependence of the anisotropic sea response, but the measurements include only a few wind conditions and some parameters in the model are still tentative.

An approximate wind-direction characteristic for the backscatter data was determined by finding a regression fit of the AAFE Radscat data shown in Figure 6.8 and scaling the amplitude of the variations to agree with the theoretical upwind/cross-wind ratio. The wind-direction correction to modify the backscatter measurements to that expected for upwind conditions is

$$\Delta_{\chi} \sigma_{pqj}^0(\chi, U) = (c_{pqj} + d_{pqj} \log U) \cdot (0.4980 - 0.1916 \cos \chi - 0.4042 \cos 2\chi + 0.0978 \cos 4\chi),$$

$$U \geq 3 \text{ m/sec}$$

$$= 0, \quad U < 3 \text{ m/sec} \quad (8.21)$$

where $\Delta_{\chi} \sigma_{pqj}^0$ is in dB, U is in m/sec, and $j = 1, 2$, or 3 correspond to the nominal incident angles 50° , 43° , and 32° respectively. The values used for c_{pqj} and d_{pqj} are given in Table 8.3.

No aspect angle corrections were applied to the backscatter measurements near 17° and 1° nor to any of the radiometric measurements. The

Table 8.3 Coefficients for aspect angle
correction of backscatter measurements

Polarization (pq)	Command Angle (j)	c_{pqj}	d_{pqj}
VV	1	-3.327	6.735
VV	2	-3.207	6.585
VV	3	-3.396	6.600
HH	1	-3.001	6.879
HH	2	-2.898	6.543
HH	3	-3.349	6.615
HV or	1	-6.823	13.268
VH	2	-6.821	13.200
	3	-6.868	13.139

direction of the wind should have little effect on microwave measurements near nadir and experimental measurements have thus far not revealed a wind direction effect on brightness temperature. Hence, not correcting these data for aspect angle should have little effect on the data analysis."

Tabulation of regression constants and examples of results The regression estimates for the constants given in equation (8.13) and (8.14) for SL 2/3 and SL 4 are given in Tables 8.4, 8.5, 8.6 and 8.7.

Scatter diagrams of σ_{vv}^0 in db versus wind speed in knots (SL 2/3), for 32° , 43° and 50° are shown in Figure 8.6, 8.7 and 8.8. The resemblance to Figure 8.3 is notable.

For SL 2/3 50° nadir angle, the best prediction of σ^0 in db, given U, is

$$\sigma_{vv}^0(\text{db}) = -33.4 + 16.9 \log_{10} U \quad (8.22)$$

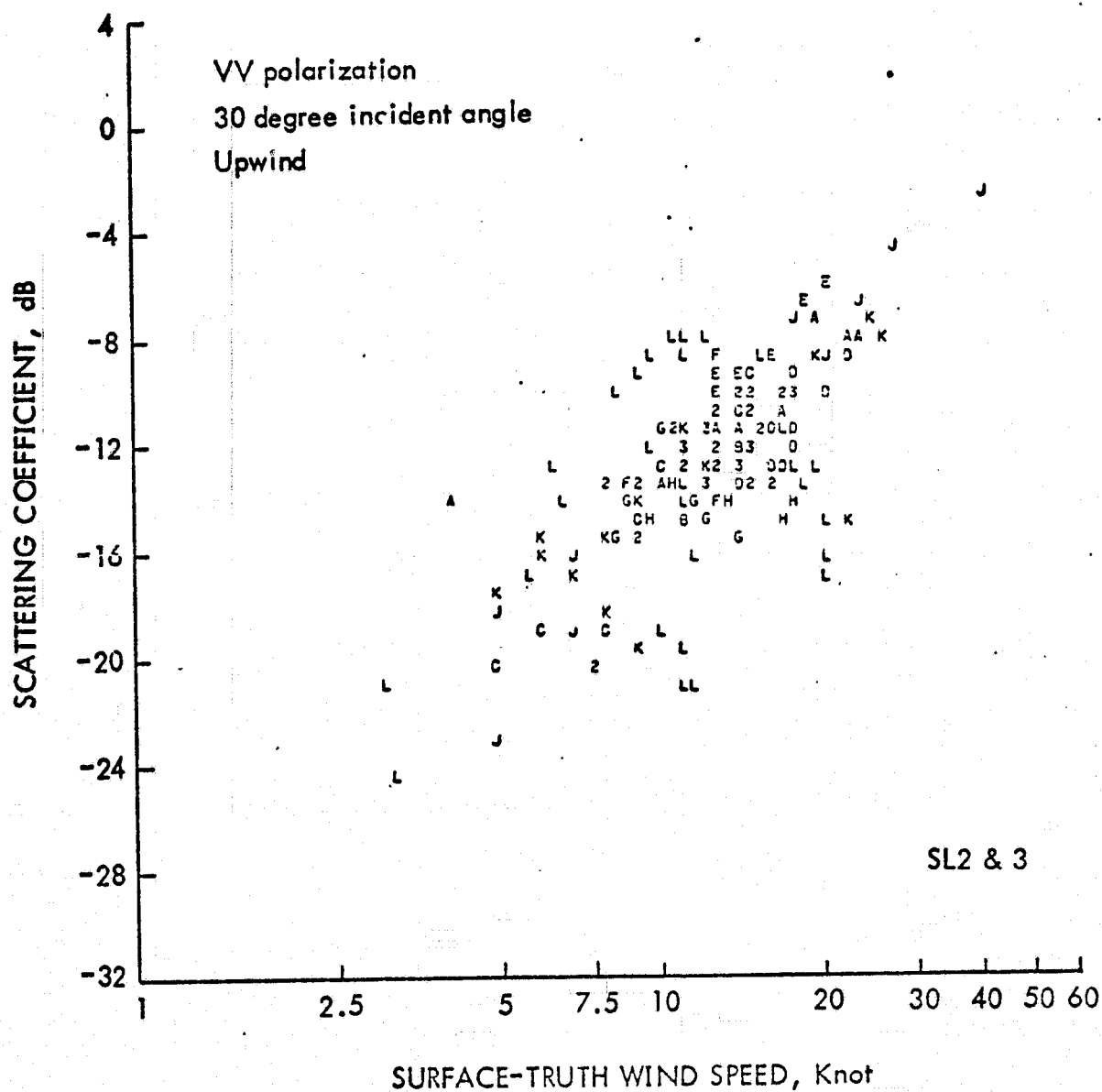
and the best prediction of U, given σ_{vv}^0 in db is

$$\log_{10} U = 1.387 + 0.029 \sigma_{vv}^0(\text{db}) \quad (8.23)$$

These two equations can be put into another form as in equation (8.24) and (8.25)

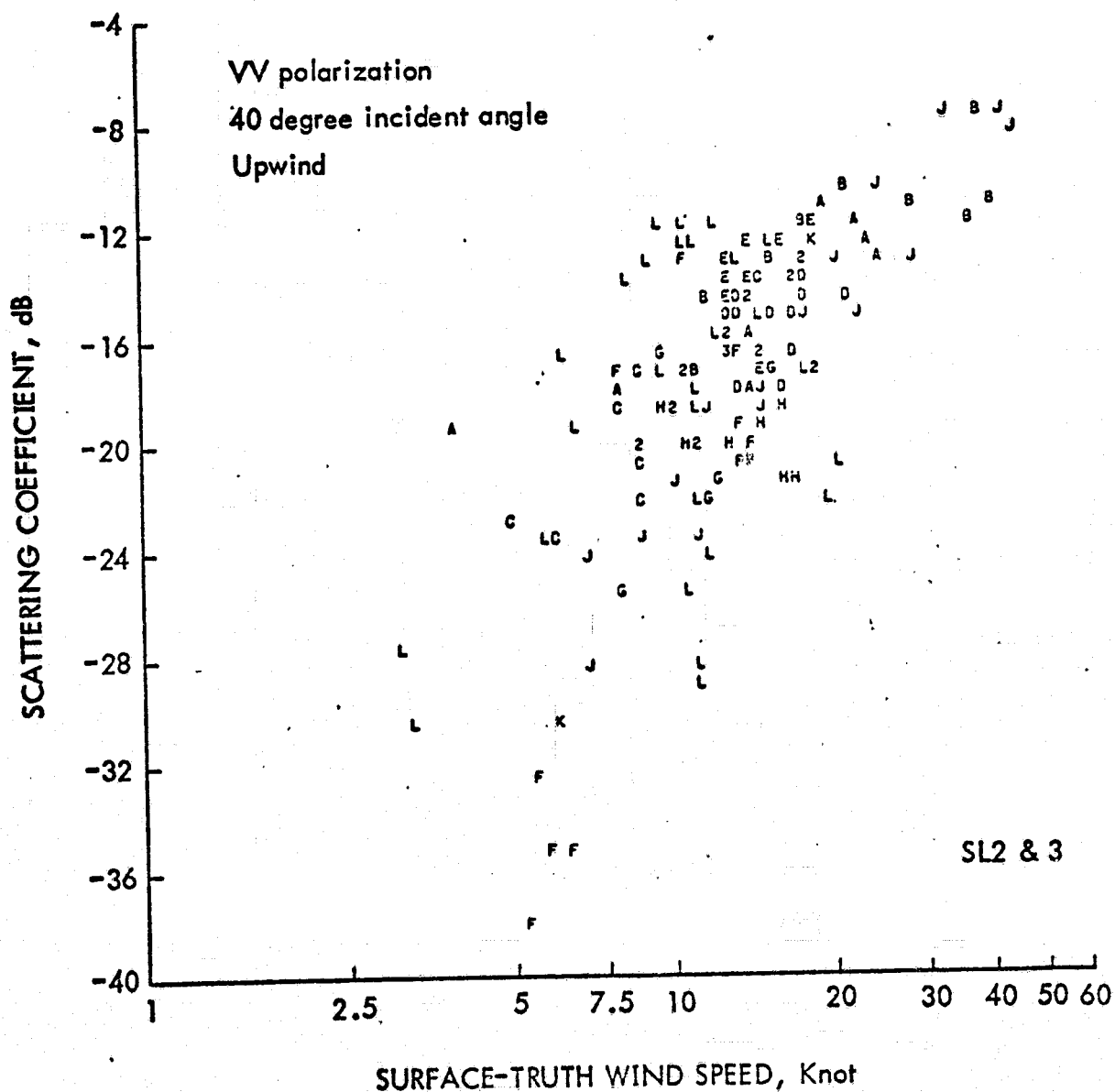
$$\sigma_{vv}^0 = 4.57 \times 10^{-4} U^{1.69} \quad (8.24)$$

$$U = 24.38 (\sigma^0)^{0.29} \quad (8.25)$$



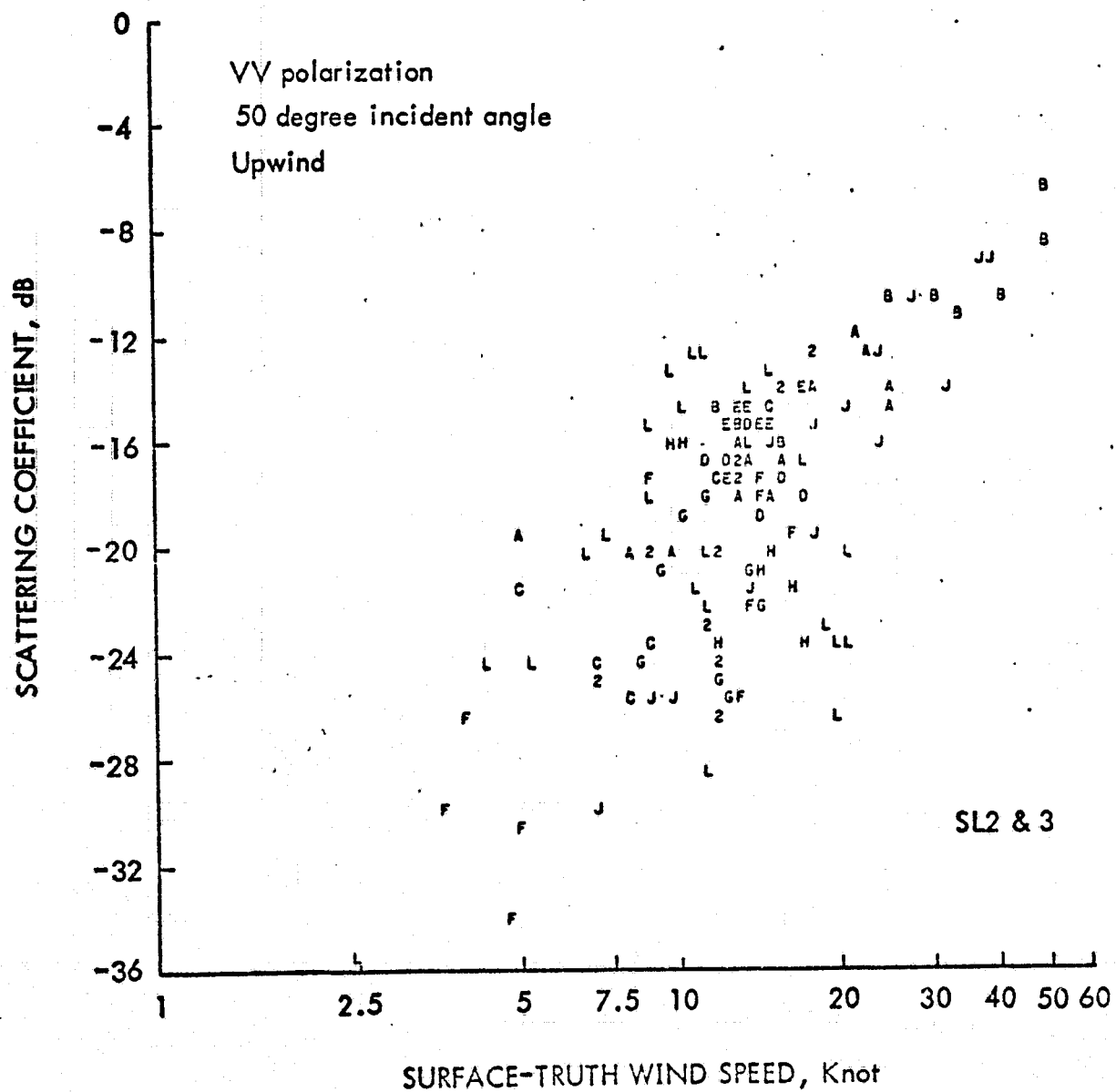
WIND SPEED DEPENDENCE OF
SCATTERING COEFFICIENTS

Figure 8.6



WIND SPEED DEPENDENCE OF
 SCATTERING COEFFICIENTS

Figure 8.7



WIND SPEED DEPENDENCE OF SCATTERING COEFFICIENTS

Figure 8.8

Table 8.4 Linear regression estimates of parameter in the model
 σ^0 (in dB) = $a_0 + a_1 \log$ (ground-truth wind speed in m/sec)
 for SL 2 and 3 data. The scattering coefficients were
 adjusted to upwind and to the nadir angles indicated
 before regression.

Nadir Angle	Pol.	a_1	Estimated Standard Error of a_1	a_0	Standard Error of a_0	No. of Observations
50°	VV	16.9	1.6	-33.4	3.85	124
	HH	18.1	1.5	-38.7	3.77	121
	VH	18.9	1.5	-46.4	3.69	110
	HV	18.0	1.4	-45.5	3.53	114
43°	VV	18.9	1.7	-33.1	4.02	134
	HH	18.9	1.6	-36.0	3.77	133
	VH	19.3	1.4	-45.5	3.28	126
	HV	19.3	1.5	-45.4	3.46	127
32°	VV	13.9	1.2	-23.9	2.70	147
	HH	13.2	1.2	-24.3	2.66	146
	VH	20.7	1.8	-43.7	3.94	141
	HV	19.5	1.5	-42.7	3.39	140
17°	VV	3.9	0.5	- 2.5	1.31	146
	HH	3.8	0.5	- 2.3	1.45	145
	VH	3.5	0.4	-17.9	1.21	136
	HV	3.5	0.4	-17.9	1.22	141
1°	VV	-2.1	0.3	15.2	0.92	134
	HH	-2.0	0.3	15.2	0.94	140
	VH	-2.5	0.3	- 1.6	0.87	136
	HV	-2.6	0.3	- 1.5	0.89	136

Table 8.5 Linear regression estimates of parameter in the model

σ^0 (in dB) = $a_0 + a_1 \log$ (ground-truth wind speed in m/sec)
for SL 4 data. The scattering coefficients were adjusted
to upwind and to the nadir angles indicated before regression.
Only data having ground truth wind speeds greater than 6 m/s
were used.

Nadir Angle	Pol.	a_1	Estimated Standard Error of a_1	a_0	Standard Error of a_0	No. of Observations
50°	VV	13.2	0.9	-19.8	1.51	115
	HH	11.5	1.2	-21.3	1.93	122
	VH	19.3	1.4	-27.7	2.32	116
	HV	16.2	1.7	-24.6	2.76	116
43°	VV	13.6	1.0	-19.1	1.63	121
	HH	13.1	0.9	-21.3	1.56	121
	VH	19.8	1.4	-27.3	2.28	119
	HV	19.7	1.5	-27.4	2.42	121
32°	VV	16.1	0.9	-19.1	1.71	166
	HH	16.5	0.9	-22.7	1.93	168
	VH	24.3	1.3	-30.9	2.53	164
	HV	24.3	1.3	-30.8	2.55	167

Table 8.6 Linear regression estimates of parameters in the model \log (ground-truth wind speed in m/sec) = $b_0 + b_1 \sigma^\circ$ (in dB) for SL 2 and 3 data. The scattering coefficients were adjusted to upwind and the nadir angles listed before regression.

Nadir Angle	Pol.	b_1	Estimated Standard Error of b_1	b_0	Standard Error of b_0	10^S	No. of Observations
50°	VV	0.0290	0.0027	1.387	0.159	1.44	124
	HH	0.0301	0.0025	1.541	0.154	1.43	121
	VH	0.0311	0.0025	1.786	0.150	1.41	110
	HV	0.0322	0.0026	1.811	0.149	1.41	114
43°	VV	0.0260	0.0023	1.279	0.149	1.41	134
	HH	0.0277	0.0023	1.389	0.144	1.39	133
	VH	0.0317	0.0023	1.762	0.133	1.36	126
	HV	0.0303	0.0023	1.721	0.137	1.37	127
32°	VV	0.0342	0.0030	1.236	0.134	1.36	147
	HH	0.0345	0.0031	1.271	0.136	1.37	146
	VH	0.0238	0.0021	1.445	0.133	1.36	141
	HV	0.0276	0.0022	1.545	0.128	1.34	140
17°	VV	0.0827	0.0100	0.731	0.190	1.55	146
	HH	0.0706	0.0098	0.737	0.198	1.58	145
	VH	0.0905	0.0116	2.164	0.195	1.57	136
	HV	0.0887	0.0112	2.131	0.195	1.57	141
1°	VV	-0.1163	0.0179	2.368	0.218	1.65	134
	HH	-0.1148	0.0177	2.349	0.223	1.67	140
	VH	-0.1425	0.0167	0.274	0.208	1.61	136
	HV	-0.1383	0.0158	0.291	0.206	1.61	136

Table 8.7 Linear regression estimates of parameters in the model \log (ground-truth wind speed in m/sec) = $b_0 + b_1 \sigma^0$ (in dB) for SL 4 data. The scattering coefficients were adjusted to upwind and to the nadir angles indicated before regression.

Nadir Angle	Pol.	b_1	Estimated Standard Error of b_1	b_0	Standard Error of b_0	10^S	No. of Observations
50°	VV	0.0622	0.0046	1.379	0.140	1.38	140
	HH	0.0406	0.0050	1.365	0.171	1.48	149
	VH	0.0406	0.0032	1.306	0.140	1.38	140
	HV	0.0369	0.0035	1.283	0.155	1.43	140
43°	VV	0.0593	0.0049	1.289	0.160	1.44	147
	HH	0.0560	0.0057	1.412	0.175	1.50	148
	VH	0.0435	0.0034	1.287	0.155	1.43	144
	HV	0.0416	0.0035	1.282	0.161	1.45	147
32°	VV	0.0551	0.0031	1.143	0.138	1.37	192
	HH	0.0516	0.0031	1.298	0.146	1.40	197
	VH	0.0367	0.0020	1.215	0.137	1.37	190
	HV	0.0366	0.0020	1.272	0.133	1.36	193

Equation (8.25) can be inverted to obtain equation (8.26)

$$\sigma_{VV}^0 = 1.65 \times 10^{-5} U^{3.448} \quad (8.26)$$

Equation (8.24) can be inverted to obtain equation (8.27)

$$U = 94.9 (\sigma^0)^{0.592} \quad (8.27)$$

These inverses are not very close together nor should they be expected to be close together. The heavy weighting of low winds and low values of σ^0 determines the fits, and they do not yield realistic results for high winds.

The regressions of σ^0 on U given in Tables 8.6 and 8.7 were used to predict the wind from the backscatter. The results were not good, because the log of the wind was actually predicted and when the meteorological wind was compared to the radar wind in antilog form, the high winds were missed by large amounts. This was to be expected for reasons given at the start of this chapter.

The power law regressions of the wind speed predicted from σ^0 as in equation (8.18) were much better. Tables 8.8, 8.9, 8.10, 8.11, and 8.12 summarize these results. One pair shows the result of predicting σ^0 from U for SL 2/3 and SL 4. The other three show the result of predicting U from σ^0 for SL 2/3 and SL 4. The last table given results for SL 4 for winds greater than 12 knots.

The root mean square differences (or errors) between the meteorological winds and the winds predicted from the backscatter measurements are given in Tables 8.10, 8.11, and 8.12. For SL 2/3 for all observations the largest root mean square difference was 5.5 knots and the smallest was 3.7 knots. For SL 4, for all observations, the largest

Table 8.8 Power law regression estimates of the parameter σ°
(in antilog form) in the model $\sigma^\circ = \alpha_0 U^{\alpha_1}$ (in knots)
for SL 2/3.*

		$\alpha_0 \times 10^{-5}$	α_1	Number of Cases	RMSD
50°	VV	22.67	1.635	124	0.0139
	HH	0.5991	2.456	121	0.0088
	VH	0.0111	3.262	110	0.0038
	HV	0.0133	3.212	140	0.0032
43°	VV	56.26	1.471	134	0.0202
	HH	15.74	1.672	133	0.0106
	VH	0.07741	2.759	126	0.0024
	HV	0.06589	2.805	127	0.0024
32°	VV	40.59	1.933	147	0.0227
	HH	54.41	1.739	146	0.0159
	VH	0.04778	3.169	141	0.0025
	HV	0.03534	3.268	140	0.0026
15°	VV	0.5209	0.3417	146	0.0228
	HH	0.5736	0.3084	144	0.0159
	VH	0.0138	0.3279	136	0.0072
	HV	0.0143	0.3133	141	0.0074
0°	VV	37.76	-0.1899	134	6.1
	HH	37.01	-0.1811	140	6.3
	VH	0.7939	-0.2306	136	0.115
	HV	0.7839	-0.2225	136	0.117

* α_0 to be multiplied by 10^{-5} except for 15° and 0°

Table 8.9 Power law regression estimates of the parameter σ^0
(in antilog form) in the model $\sigma^0 = \alpha_0 U^{\alpha_1}$ (in knots)
for SL 4.

		α_0	α_1	No. of Points = N	RMSD
50°	VV	0.00266	1.495	140	0.11
	HH	0.00701	0.973	149	0.08
	VH	0.00011	2.427	140	0.16
	HV	0.00014	2.329	140	0.17
43°	VV	0.00448	1.420	147	0.15
	HH	0.00548	1.170	148	0.09
	VH	0.00023	2.263	144	0.19
	HV	0.00028	2.189	147	0.20
32°	VV	0.00366	1.672	192	0.30
	HH	0.00189	1.655	197	0.16
	VH	0.000031	2.959	190	0.37
	HV	0.000038	2.895	193	0.36

Table 8.10 Power law regression estimates of the parameter U in the model $U \text{ (in knots)} = \beta_0 \sigma_0^{\beta_1}$ for SL 2/3.

		β_0	β_1	Number of Cases	RMSD
50°	VV	82.87	0.4196	124	5.5
	HH	102.5	0.3748	121	5.2
	VH	137.2	0.3263	110	4.4
	HV	140.9	0.3318	114	4.4
43°	VV	61.64	0.3881	134	5.2
	HH	84.40	0.4000	133	4.9
	VH	136.1	0.3414	126	4.1
	HV	134.0	0.340	127	4.2
32°	VV	36.41	0.3594	147	3.8
	HH	42.55	0.3847	146	3.9
	VH	75.90	0.2881	141	3.7
	HV	75.75	0.2878	140	3.7
15°	VV	11.82	0.6284	146	4.7
	HH	12.16	0.484	144	5.2
	VH	279.8	0.8778	136	4.9
	HV	206.4	0.7924	141	5.0
0°	VV	373.2	-1.070	134	4.7
	HH	529.3	-1.182	140	4.7
	VH	4.250	-1.345	136	4.7
	HV	3.571	-1.533	136	4.2

Table 8.11 Power law regression estimates of the parameter U (in knots)
in the model $U = \beta_0(\sigma^0)^{\beta_1}$ for SL 4.

		β_0	β_1	No. of Points = N	RMSD
50°	VV	45.24	0.5695	140	5.3
	HH	47.98	0.4019	149	7.4
	VH	38.90	0.3725	140	5.5
	HV	38.02	0.3496	140	6.3
43°	VV	37.98	0.5483	147	5.8
	HH	50.26	0.5220	148	6.6
	VH	36.64	0.3829	144	5.5
	HV	36.53	0.3657	147	5.8
32°	VV	27.65	0.5055	192	5.2
	HH	38.65	0.4767	197	5.6
	VH	31.75	0.3198	190	5.3
	VH	31.90	0.3200	193	5.2

Table 8.12 Power law regression estimates of the parameter U
(in knots) for $U \geq 12$ knots in the model $U = \alpha_0(\sigma^0)^{\alpha_1}$
for SL 4.

		α_0	α_1	No. of Points = N	RMSD
50°	VV	44.13	0.5008	115	4.5
	HH	53.13	0.4087	122	6.1
	VH	38.29	0.3226	116	4.9
	HV	37.13	0.2942	116	5.8
43°	VV	37.71	0.4731	121	4.9
	HH	51.03	0.4757	121	5.0
	VH	36.21	0.3242	119	4.8
	HV	36.09	0.3073	121	5.1
32°	VV	28.31	0.4431	166	4.8
	HH	37.82	0.4071	168	5.1
	VH	32.00	0.2800	164	4.8
	HV	32.08	0.2826	167	4.8

was 7.4 knots and the smallest was 5.2 knots. These values have to be studied in greater detail in terms of the type of surface truth that provides the meteorological wind.

All in all, the simple power law regressions, for upwind conditions only, do a creditable job of predicting the magnitude of the vector wind from a radar measurement when the wind speed is verified against the meteorologically obtained surface truth.

The three tables that yield regression coefficients for the prediction of the magnitude of the vector wind from the backscatter contain a total of 44 categories. Examples of scatter plots of the radar wind prediction of the meteorological wind are given in the next eight figures, four for SL 2/3 and four for SL 4. For SL 2/3, Fig. 8.9 is for VH 43° , Fig. 8.10 is for VH 50° , 8.11 is for HH 50° , and 8.12 is for VV 50° . An M represents either Hurricane AVA or Tropical Storm Christine. For SL 4, 8.13 is for VV 50° ; 8.14 is for HV 32° ; 8.15 is for 32° HH, and 8.16 is for 50° HH. The SL 4 plots are for all winds. The codes, A, B, C, D, and + were explained in Chapter 4. If several points fall on the same location the total number of points is printed, and the code is unfortunately lost.

These eight plots, as well as the others in the total set appear to have one common feature. They tend to give radar winds that are higher than the meteorological wind when the winds are low and to give radar winds that are lower than the meteorological wind when the winds are high. Figure 8.9 is a particularly good example of this tendency. Figure 8.12 is the clearest example of the under prediction of the high winds for SL 2/3. Similarly Figure 8.13 and Figure 8.16 are examples for SL 4.

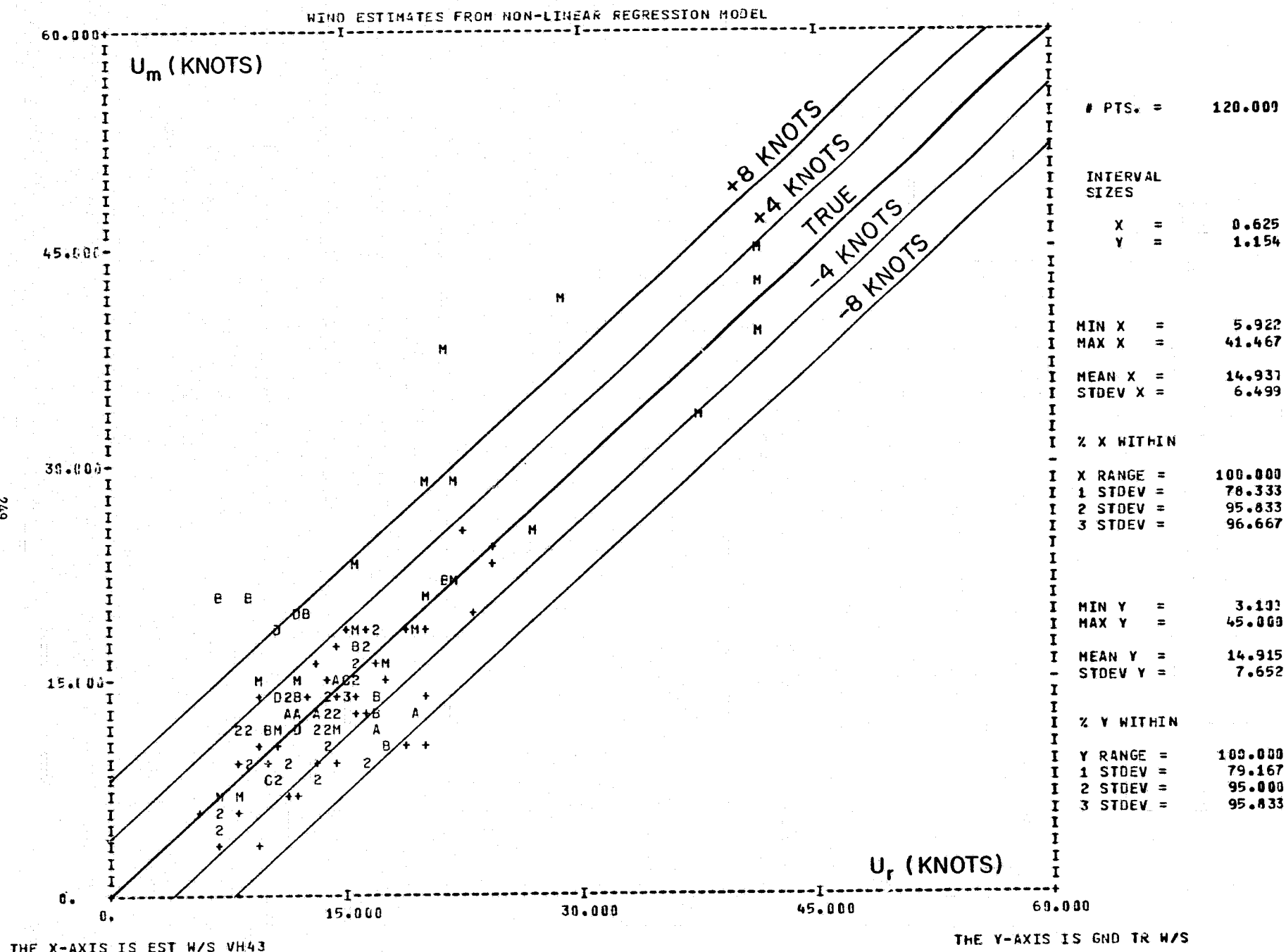


FIGURE 8.9 RADAR PREDICTED WIND VERSUS METEOROLOGICAL WIND FOR SL 2/3 VH 43°
(EQUIVALENT UPWIND ANALYSIS)

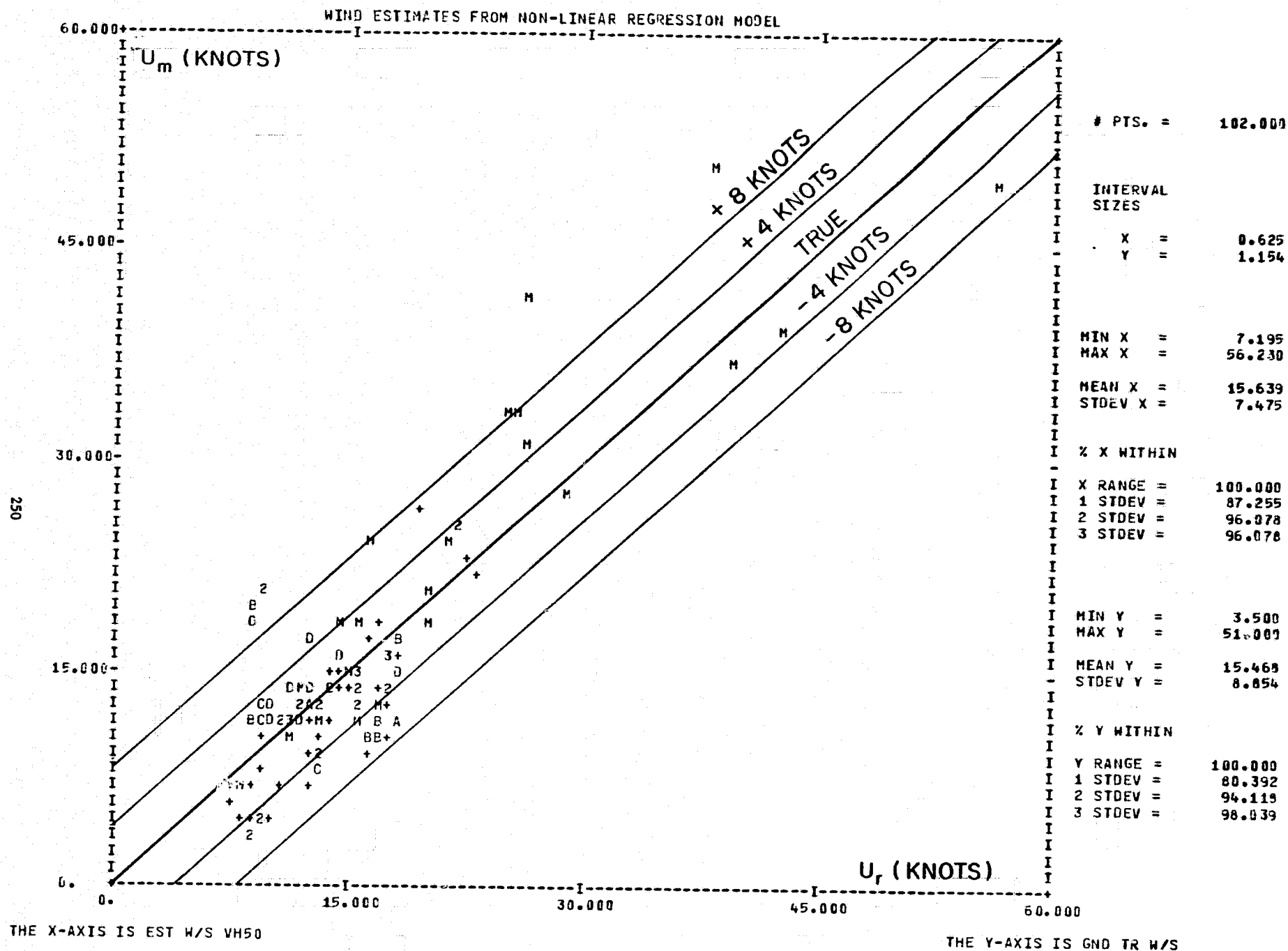


FIGURE 8.10 RADAR PREDICTED WIND VERSUS METEOROLOGICAL WIND FOR SL 2/3 VH 50°
(EQUIVALENT UPWIND ANALYSIS)

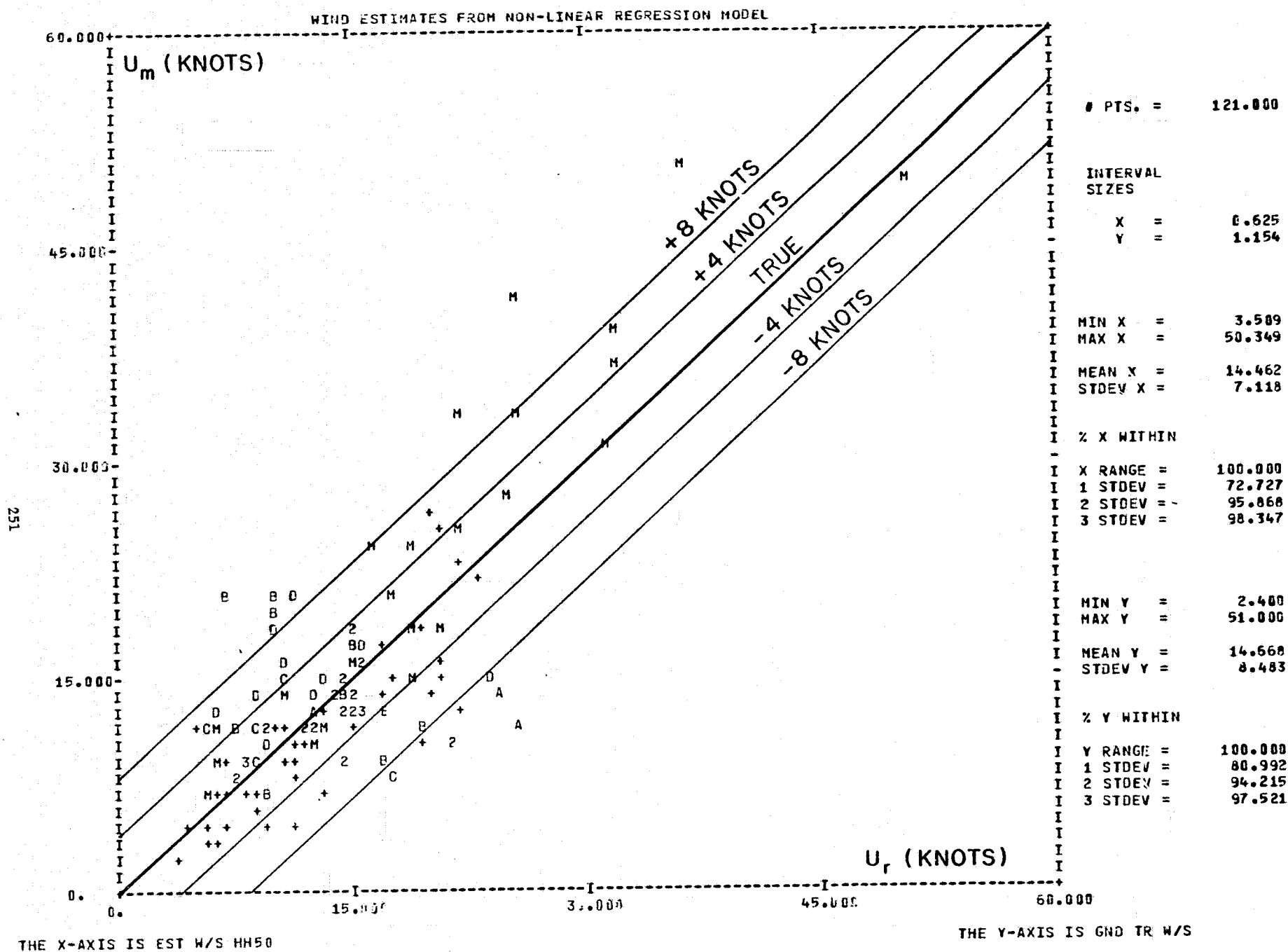


FIGURE 8.11 RADAR PREDICTED WIND VERSUS METEOROLOGICAL WIND FOR SL 2/3 HH 50°
(EQUIVALENT UPWIND ANALYSIS)

REPRODUCIBILITY OF THE
ORIGINAL PAGE IS POOR

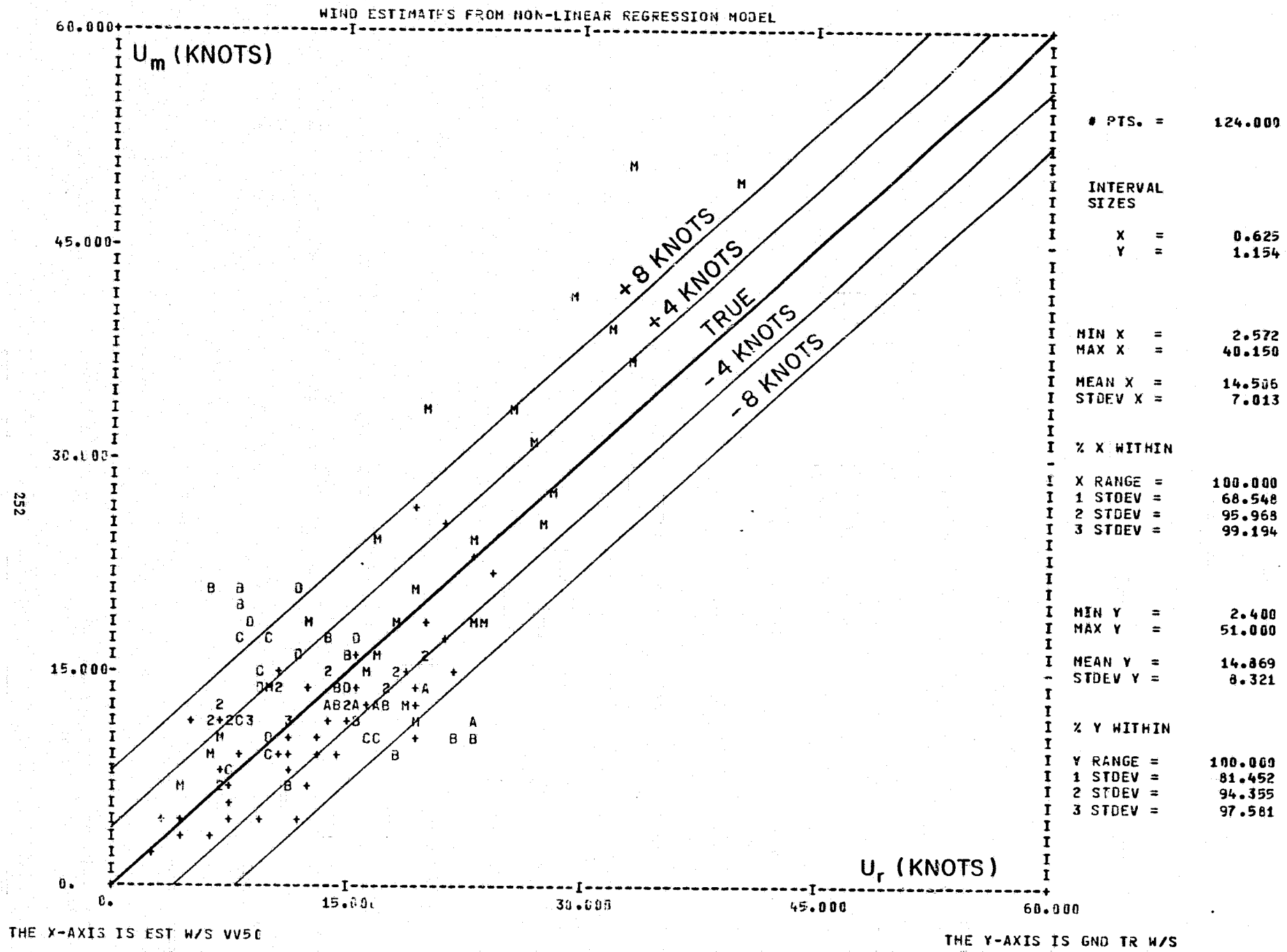


FIGURE 8.12 RADAR PREDICTED WIND VERSUS METEOROLOGICAL WIND FOR SL 2/3 VV 50°
(EQUIVALENT UPWIND ANALYSIS)

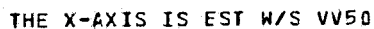


FIGURE 8.13 RADAR PREDICTED WIND VERSUS METEOROLOGICAL WIND FOR SL 4, VV 50°
(EQUIVALENT UPWIND ANALYSIS)

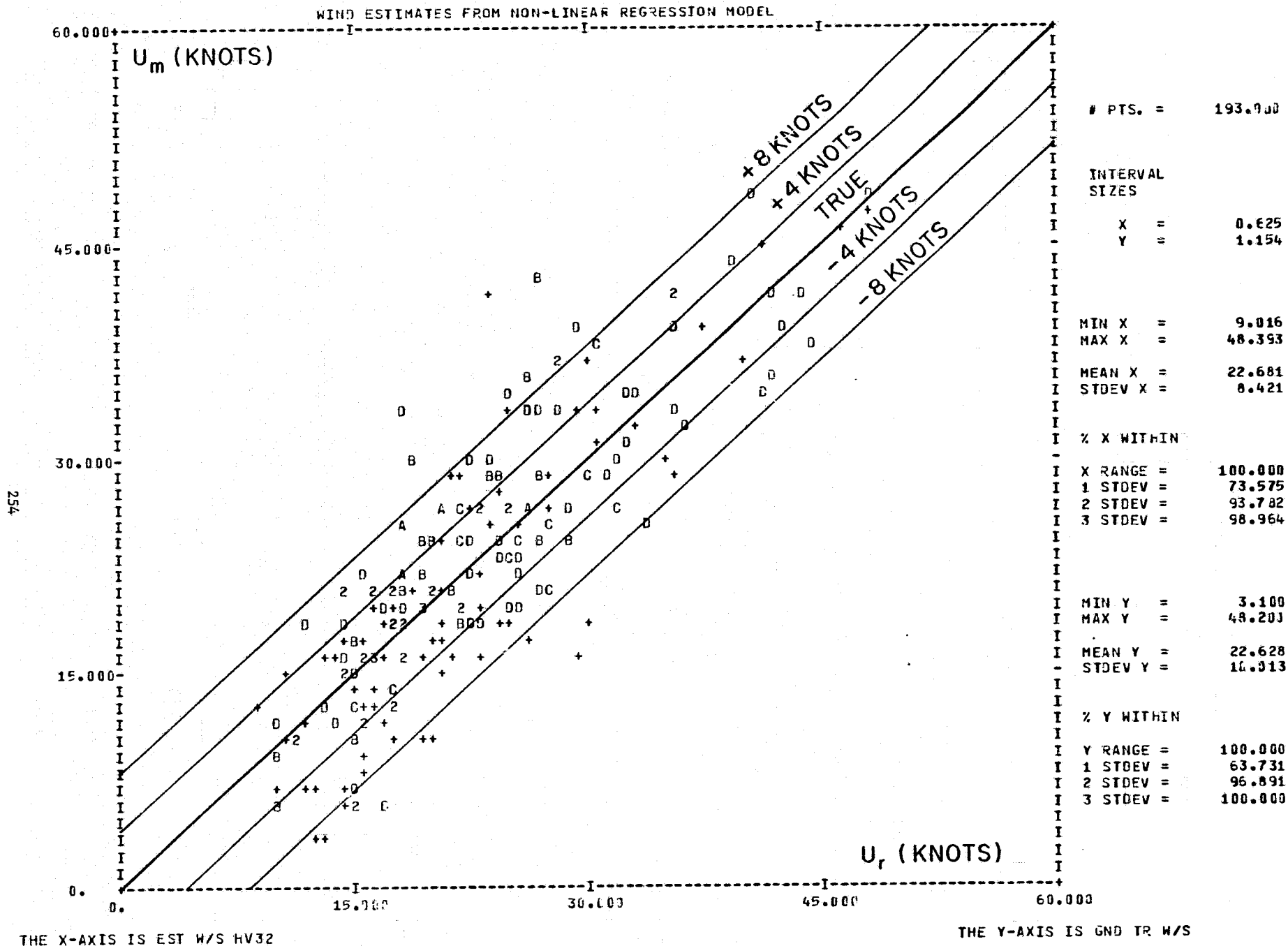
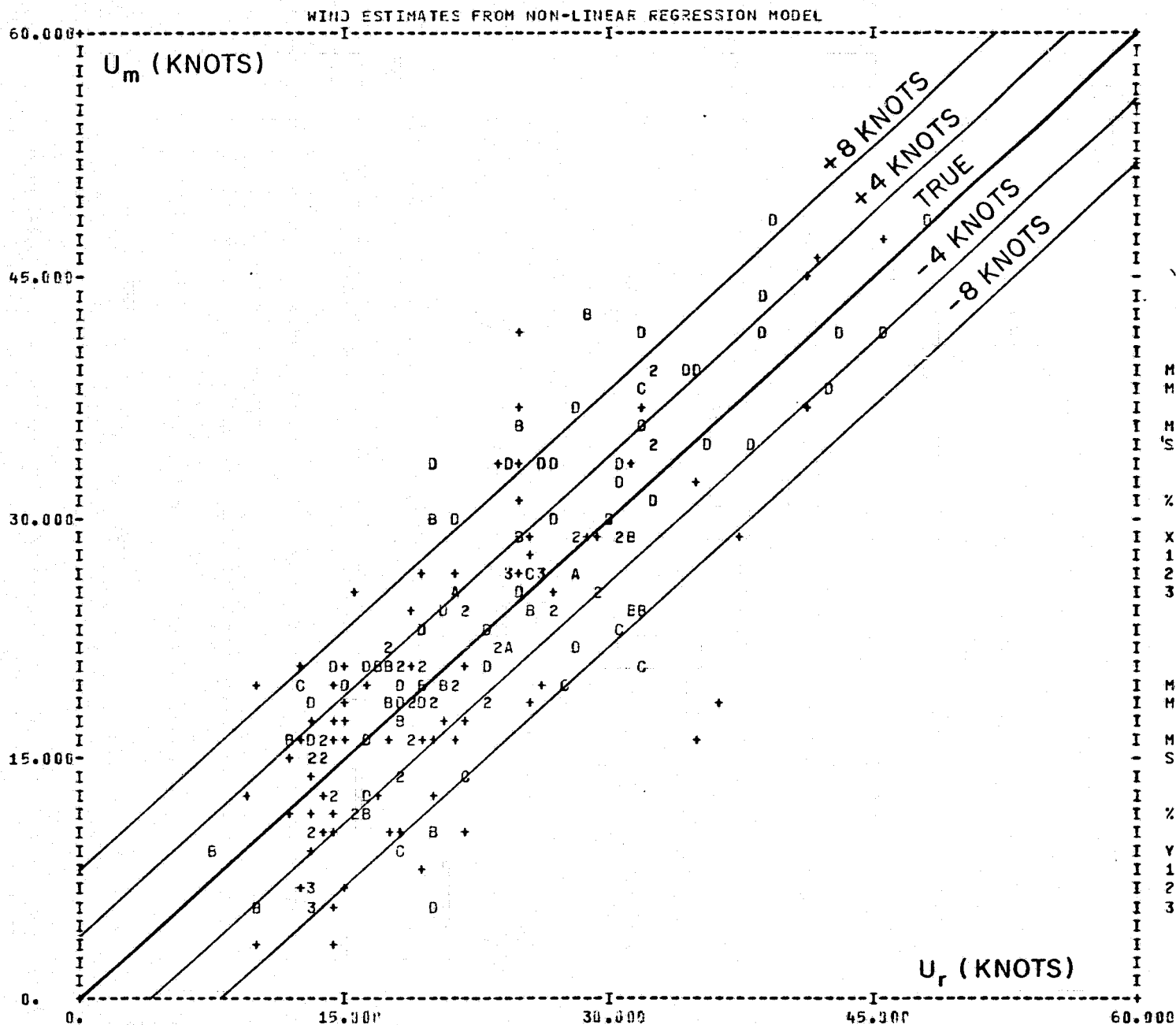


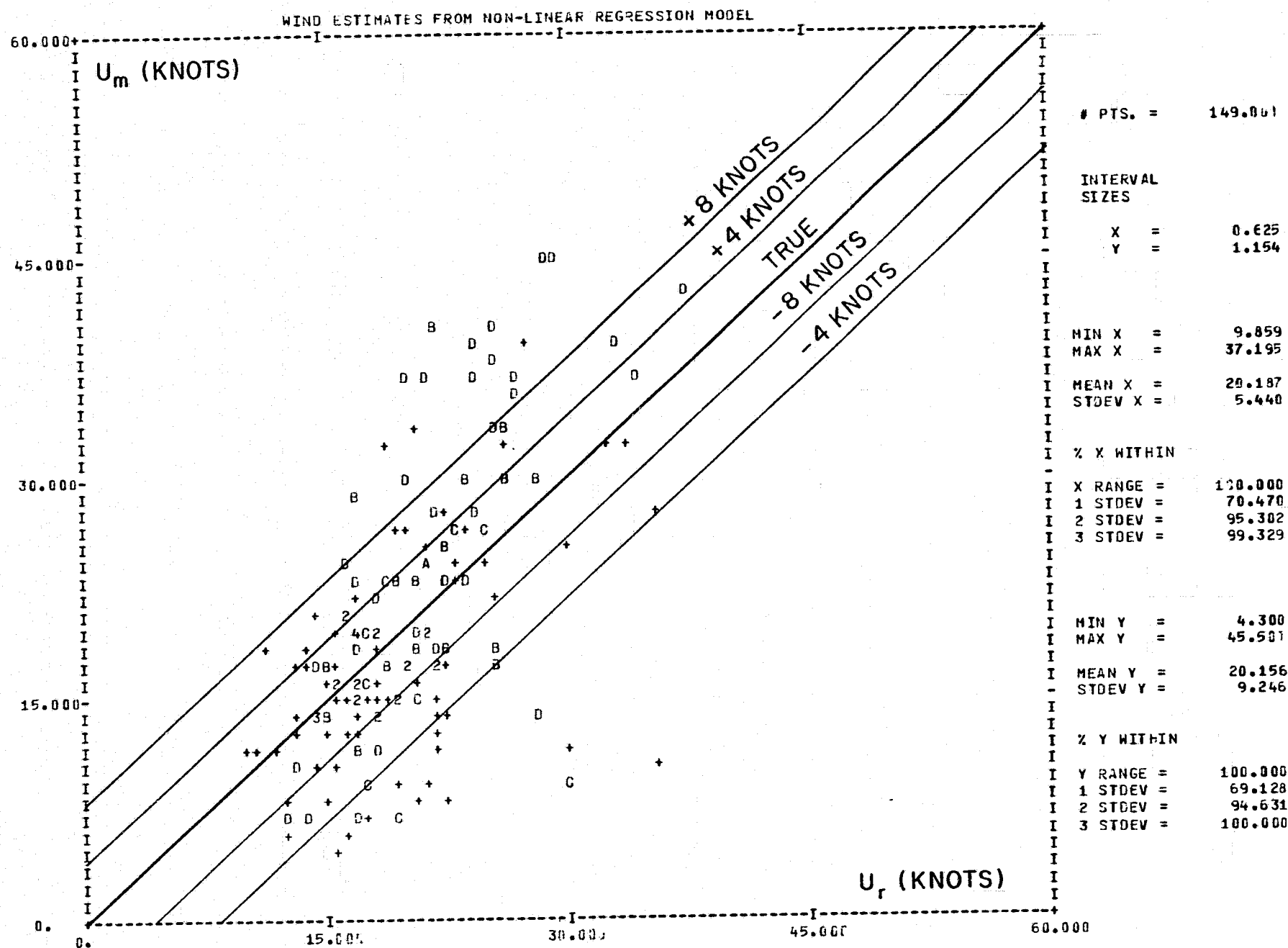
FIGURE 8.14 RADAR PREDICTED WIND VERSUS METEOROLOGICAL WIND FOR SL 4, HV 32°
(EQUIVALENT UPWIND ANALYSIS)



THE X-AXIS IS EST W/S HH32

THE Y-AXIS IS GND TR W/S

FIGURE 8.15 RADAR PREDICTED WIND VERSUS METEOROLOGICAL WIND FOR SL 4, HH 32°
(EQUIVALENT UPWIND ANALYSIS)



THE X-AXIS IS EST W/S HH50

THE Y-AXIS IS GND TR W/S

FIGURE 8.16 RADAR PREDICTED WIND VERSUS METEOROLOGICAL WIND FOR SL 4, HH 50°
(EQUIVALENT UPWIND ANALYSIS)

In general, the inverses of the power law relationships given in Tables 8.8 to 8.11 are closer together than the corresponding inverses from the log-log regressions. For example, Table 8.8 yields

$$\sigma^0 = 2.267 \times 10^{-4} (U)^{1.635} \quad (8.28)$$

and Table 8.10 yields

$$U = 82.87 (\sigma^0)^{0.4196} \quad (8.29)$$

for 50°VV. The corresponding inverses are

$$U = 169.4 (\sigma^0)^{0.6116} \quad (8.30)$$

and

$$\sigma^0 = 2.68 \times 10^{-5} (U)^{2.3832} \quad (8.31)$$

The corresponding values in equation (8.24), (4.57×10^{-4} and 1.69); equation (8.25) (24.38 and 0.29); equation (8.27) (94.9 and 0.592) and equation (8.26) (1.65×10^{-5} and 3.448) are much farther apart than these values based on power law regressions.

Tables 8.10 and 8.11 give values for the regression constants for both VH and HV polarizations. The differences are attributable in part to slightly different sample sizes and in part to slightly different measurements of σ_{HV}^0 and σ_{VH}^0 at each cell. The wind speeds can be treated as identical despite the few miles separating the cell centers. The values for 50° VH and 50° HV in Table 8.10, for $\sigma^0 = 0.01$. Yield wind speeds of 30.53 knots and 30.49 knots. At $\sigma^0 = 0.001$ they yield 14.4 and 14.6 knots. For practical purposes the two equations are identical. This conclusion is essentially the same for all cross polarized pairs in both SL 2/3 and SL 4 for the three highest nadir angles.

Table 8.10 also provides values for 15° and 0° nadir angles. For these angles, no corrections for wind direction effects were used. The dependence of wind speed on σ^0 is still evident. The wind speed still increases with increasing backscatter at 15° , and all but the HH polarization yields power laws close to one. At a nadir angle of 0° , the wind speed decreases with increasing backscatter according to a nearly linear relationship. For a 15° nadir angle, σ_{VH}^0 equal to 0.1 yields 37.7 knots and σ_{HV}^0 yields 40.86 knots, which are satisfactorily close together. With σ_{VH}^0 and σ_{HV}^0 equal to 0.02833, both equations yield 12.25 knots.

The signs of the exponent in Tables 8.8 and 8.10 change between 15° and 0° . The assumption made by Bradley (1971) that the backscatter data that were obtained during the early NASA aircraft program could be normalized to 10° is further substantiated by this result.

There is one possible objection to these results. It is that the meteorological wind was used to correct the backscatter to the equivalent upwind backscatter value. Then this backscatter value was used to predict the magnitude of the wind vector. The theory used is somewhat circular in that knowledge of the wind is used to get a result that is then used to predict the wind. This question and others of a meteorological nature are investigated in the next section.

PREDICTIONS OF WIND SPEED GIVEN WIND DIRECTION AND BACKSCATTER VALUE

Introduction. One way to avoid the step of correcting all backscatter values to the equivalent upwind values, as was done in the preceding section, is to try to represent the radar wind as a function of σ and χ as in equation 8.32.

$$U_r = U_r(\sigma^0, \chi) \quad (8.32)$$

This step assumes that the wind direction given by the meteorological analysis is correct, and assigns all error effects to the differences between the magnitudes of the meteorological wind and the radar wind.

Four procedures, referred to as methods three through six were devised to determine the relationship given by equation(8.32). Two were based on the preceding tables as a start and then applied successive corrections to the regressions that were obtained. Another started from first principles, obtained the desired function, and then corrected the magnitudes of the winds by an additional quadratic fit. The theory of three of the methods will be given first, and then the results will be analyzed.*

Methods 5 and 6. From Table 8.10, for example for VV 50°, equation (8.33) can be obtained where U_u represents an upwind measurement. To simplify notation, A_u and B_u have been used instead of β_0 and β_1 .

$$U_u = 82.87(\sigma^0)^{0.4196} = A_u(\sigma^0)^{B_u} \quad (8.33)$$

From the AAFE Langley program, it is known that at 15 m/s (29.16 knots) σ^0 is about 1 db down from upwind at downwind and about 4 db down from upwind at crosswind. From this information, four new coefficients A_c , B_c , A_d , and B_d can be calculated that will yield these values for U and σ^0 at this wind speed, subject to the additional restriction that all curves pass through the same point at $U = 1$ knot. The equations are derived for cross wind and changing one constant produces the equations for downwind.

From equation (8.33), it is possible to solve for σ^0 as in equation (8.34). **

$$\ln \sigma^0 = \frac{\ln U_u - \ln A_u}{B_u} \quad (8.34)$$

* Method three was an earlier version of methods five and six and did not give as good results.

** $\ln = \log_e$

This value for the backscatter must be reduced by 4 db at crosswind.

Let

$$K_c = \ln 10^{0.4} \quad (8.35)$$

The equation for crosswind

$$U_c = A_c (\sigma_0)^{B_c} \quad (8.36)$$

must yield the same wind speed at 29.16 knots (i.e. $U_u = U_c$) so that equation (8.37) must be satisfied.

$$\ln (29.16) = \ln A_c + B_c \left(\frac{\ln 29.16 - \ln A_u}{B_u} - K_c \right) \quad (8.37)$$

also for $U_c = U_u = 1$ knot, the requirements are that

$$\ln \sigma_0 = -\ln A_u / B_u \quad (8.38)$$

and hence that

$$\ln A_c = \frac{B_c}{B_u} \ln A_u \quad (8.39)$$

equation (8.37) can be put into the form given by equation (8.40) by means of equation (8.39).

$$B_c = B_u \left[\frac{\ln (29.16)}{\ln (29.16) - K_c B_u} \right] \quad (8.40)$$

The values of B_u and A_u are in the tables, and K_c is known so that B_c can be found from equation (8.40), and then A_c , from equation (8.39).

To find A_d and B_d , K_d is used instead of K_c as in equation (8.41)

$$K_d = \ln 10^{0.1} \quad (8.41)$$

For 50° VV SL 2/3, the three equations that result are given by equation (8.33) above and equations (8.42) and (8.43).

$$U_c = 146.78 \sigma^{0.4739} \quad (8.42)$$

$$U_d = 94.39 \sigma^{0.4320} \quad (8.43)$$

Given $A(= \beta_0)$ and $B(= \beta_1)$, for all polarizations and the three largest nadir angles, equations for U_u , U_c , and U_d can be found.

The first guess for the radar wind is then obtained as a Fourier series involving U_u , U_c , and U_d as in equation (8.44).

$$U_{r1} = A + B \cos X + C \cos 2X + D \cos 4X \quad (8.44)$$

For $X = 0$, upwind,

$$U_{r1} = U_u = A + B + C + D \quad (8.45)$$

For $X = 180^\circ$, downwind,

$$U_{r1} = U_d = A - B + C + D \quad (8.46)$$

For $X = 90^\circ$, crosswind,

$$U_{r1} = U_c = A - C + D \quad (8.47)$$

With $D = KA$, i.e. with the assumption that the fourth harmonic is linearly related to the constant term, these equations can be solved, and the radar wind expressed as a function U_u , U_c , and U_d and X .

$$\begin{aligned} U_{r1} = & \frac{1}{1+K} \left(\frac{1}{2} \right) [U_u + U_d + 2U_c] \\ & + \frac{1}{2} [U_u - U_d] \cos X \\ & + \frac{1}{4} [U_u + U_d - 2U_c] \cos 2X \\ & + \frac{K}{1+K} \left(\frac{1}{2} \right) [U_u + U_d + 2U_c] \cos 4X \end{aligned} \quad (8.48)$$

This equation was used to obtain values of the radar wind, U_{r1} . Various regression equations were then applied in sequence to U_{r1} to try to improve on this first estimate. Given $U_{r1}(\sigma^0, \chi)$ for a particular nadir angle and wind direction, the next step was to obtain

$$U_{r2} = A^* (U_{r1})^{B^*} \quad (8.49)$$

such that A^* and B^* would make

$$\sum_i (U_{mi} - U_{r2i})^2 \quad (8.50)$$

a minimum.

Method five used equation (8.49). Method six left it out.

The next step was to form

$$U_{r3}(\sigma^0, \chi) = U_{r2} [C_0 + C_1 \cos \chi + C_2 \cos 2\chi + C_3 \cos 3\chi + C_4 \cos 4\chi] \quad (8.51)$$

and to find C_0, C_1, C_2, C_3 , and C_4 to minimize

$$\sum_i (U_{mi} - U_{r3i})^2 \quad (8.52)$$

The next step was to form

$$U_{r4}(\sigma^0, \chi) = D_0 + D_1(U_{r3}) + D_2(U_{r3})^2 \quad (8.53)$$

and to find D_0, D_1 , and D_2 to minimize

$$\sum_i (U_{mi} - U_{r4i})^2 \quad (8.54)$$

The final result of this series of regressions is either equation (8.55a) or equation (8.55b) for methods five and six respectively.

$$U_{r4} = U_{r4}(U_{r3}(X, U_{r2}(U_{r1}(\sigma^0, X)))) \quad (8.55a)$$

$$U_{r4} = U_{r4}(U_{r3}(X, U_{r1}(\sigma^0, X))) \quad (8.55b)$$

If equation (8.48) were the best possible least squares fit to the data, the application of these additional steps would "do nothing". For example, both A^* and B^* would be one, C_0 would be 1 and C_1, C_2, C_3 , and C_4 would be zero. D_0 and D_2 would be zero, and D_1 would be 1. The successive regressions are not quite "do nothing" regressions as will be discussed when the results of their application to three different nadir angles, three polarizations and SL 2/3 and SL 4. It is difficult to see how all of the various operations interact. A simple power law equation vanishes along the way.

Method 4. Method 4 was a two step regression that assumed very little about a starting form for $U = U(\sigma, X)$ and corrected the first result by a quadratic improvement.

The first step was to find the constants $E_0, E_1, E_2, E_3, E_4, F_0, F_1, F_2, F_3$, and F_4 in equation (8.56) with σ^0 in db.

$$\begin{aligned} \ln U_{rs} = & E_0 + E_1 \cos X + E_2 \cos 2X + E_3 \cos 3X + E_4 \cos 4X \\ & + \sigma^0 [F_0 + F_1 \cos X + F_2 \cos 2X + F_3 \cos 3X + F_4 \cos 4X] \end{aligned} \quad (8.56)$$

so as to minimize

$$\sum_i U_{mi}^2 [\ln U_{mi} - \ln U_{rsi}]^2 \quad (8.57)$$

The minimization was carried out in such a way as to weight large values of U and σ^0 in antilog form more heavily than the usual techniques. For small values of the difference in equation (8.57) the weighting is exactly the right one. For large values, some bias is introduced, but this is mostly removed by the quadratic fit that follows.

Once the ten constants were found, U_{rs} , computed from σ^0 and χ , was used to find three more constants G_0 , G_1 and G_2 as in equation (8.58)

$$U_{rs} = G_0 + G_1 (U_{rs}) + G_2 (U_{rs})^2 \quad (8.58)$$

so as to minimize

$$\sum_i (U_{mi} - U_{rei})^2 \quad (8.59)$$

Given the constants E_j and F_j , equation (8.56) can be transformed to an interesting form as in equation (8.60)

$$U_{rs} = e^{(E_0 + \sum_1^4 E_j \cos j \chi)} e^{\sigma_{db}^0 [F_0 + \sum_1^4 F_j \cos j \chi]} \quad (8.60)$$

or

$$U_{rs} = e^{E(E_j, \chi)} e^{10 \log_{10} \sigma^0 [F_0 + \sum F_j \cos j \chi]} \quad (8.61)$$

or

$$U_{rs} = e^{E(E_j, \chi)} e^{4.343 [F_0 + \sum F_j \cos j \chi] \ln \sigma^0} \quad (8.62)$$

and finally

$$U_{rs} = \beta_0(\chi) (\sigma^0)^{\beta_1(\chi)} \quad (8.63)$$

where

$$\beta_0(X) = e^{[E_0 + E_1 \cos X + E_2 \cos 2X + E_3 \cos 3X + E_4 \cos 4X]} \quad (8.64)$$

and

$$\beta_1(X) = 4.343[F_0 + F_1 \cos X + F_2 \cos 2X + F_3 \cos 3X + F_4 \cos 4X] \quad (8.65)$$

For upwind,

$$\beta_0 = e^{(E_0 + E_1 + E_2 + E_3 + E_4)} \quad (8.66)$$

$$\beta_1 = 4.343[F_0 + F_1 + F_2 + F_3 + F_4] \quad (8.67)$$

For downwind,

$$\beta_0 = e^{(E_0 - E_1 + E_2 - E_3 + E_4)} \quad (8.68)$$

$$\beta_1 = 4.343[F_0 - F_1 + F_2 - F_3 + F_4] \quad (8.69)$$

For crosswind,

$$\beta_0 = e^{(E_0 - E_2 + E_4)} \quad (8.70)$$

$$\beta_1 = 4.343[F_0 - F_2 + F_4] \quad (8.71)$$

The quadratic correction in equation (8.58) has a particularly simple interpretation in this method. The exponents are simply doubled in the term involving G_2 .

The Regression Constants for Methods 4, 5 and 6. Five tables, Tables 8.13 through 8.17, give the values of the regression constants for methods 4, 5 and 6. Method 4 did not give good results for SL 2/3, because the distribution of wind directions for high winds was not uniform, and so it was only used for SL 4. The uneven distribution of wind directions for high winds caused problems for SL 2/3 even for methods 5 and 6, but they were not as severe.

Method 5 for SL 2/3 is given in Table 8.13. The values of A_u , B_u , A_d , B_d , A_c and B_c are listed first for each command angle and polarization. The cross polarized backscatter values were simply averaged and treated as one value. If either was missing the other was used alone. The numbers are what would be expected. The values of M and N are the A^* and B^* of equation (8.49). The P's are the C's of equation (8.51). The Q's are the D's of equation (8.53).

The power law transformation, equation (8.40) is difficult to interpret in terms of what it does to equation (8.48). The Fourier series, equation (8.51), undoes some of the effects of M in equation (8.49) because the constant term is less than one.

Except for the coefficient of the cosine of 4χ , the other trigonometric terms have small effects compared to that produced by requiring a 4 db difference between upwind and crosswind. The first harmonic strengthens the upwind downwind difference. The second harmonic weakens the upwind crosswind difference. The third harmonic was assumed to be zero and is non present with the same sign in all but command angle 1, HV+VH. The fourth harmonic is quite large and more or less knocks out the original fourth harmonic variation in equation (8.48).

The quadratic correction shows an important feature. The parabolas represented by these coefficients, except for one, have a minimum for U_{r3} greater than zero and predict a larger U_{r4} for values both smaller and larger than this.

This and other results demonstrate a difficulty with low wind speeds that appears to be caused by the sudden disappearance of capillary waves at wind speed near 5 or 7 knots, compounded with the inherent errors in measuring low winds discussed in Chapter 4.

Method 6 for SL 2/3 is given in Table 8.14. The values of A_u , B_u , and so on are the same. The power law transformation is omitted (equation 8.49). The P's represent the C's and the quadratic law is given by the S's.

The overall level is amplified by the constant term in the Fourier series. Upwind downwind is strengthened. Upwind crosswind is weakened except for 1-VV. Some third harmonic is present, and the fourth harmonic is greatly weakened. These are the effects that might be expected given the kinds of errors present in the meteorological values of the wind direction.

The quadratic correction for six of the nine terms has a minimum at $U_{r3} = 0$, given by S0. A wind speed less than this value cannot be predicted. These values are between 7.3 and 4.2 knots. The other three with negative values for S1 have minimums at 5.4 knots, 0.58 knots and 4.49 knots in the order shows and predict 9.98, 7.1 and 8.65 knots respectively.

All in all, method 6 gave somewhat better results than method 5 for SL 2/3. Scatter diagrams of the radar wind versus the meteorological wind will be given later. Despite an initial guess function that would have produced the required backscatter differences for upwind, downwind and crosswind, these effects are wiped out for SL 2/3 by the final results of the method.

Table 8.15 shows the values for method 4 for SL 4. The notations is back in phase with the theory. The first group of five numbers represents $B_0(X)$ as in equation (8.64) and the second group represents

$\beta_0(X)$ as in equation (8.65). The value of $\beta_0(X)$ is a minimum for upwind, somewhat larger for downwind (except 1-HH and 2-HV), and a maximum for crosswind. The same can be said for $\beta_1(X)$ except that F1 has the wrong effect twice, and F2 four times.

Nearly all of the quadratic corrections go through zero for U_{rs} when U_{rs} is near zero. The effect of the squared term is very small.

Table 8.16 shows the values for method 5 for SL 4. The same kinds of conclusions can be reached as with Table 8.13.

Table 8.17 shows the values of method 6 for SL 4. R0 through R3 are close to a "do nothing" transformation. The value of R4 greatly reduces the $\cos 4X$ term.

Tabulation of the Predicted Radar Winds for each Observation and for each Method. The wind speeds predicted by these three different methods are given in Table 8.18, which requires quite a few pages.* The DOY, scan number, meteorological wind speed and direction, backscatter value, as corrected, and radar wind speed for each regression method are tabulated.** These values are the "output" of this study and represent how well the wind speed can be predicted from a radar measurement, given the wind direction and a backscatter measurement of known nadir angle, polarization and instrument characteristics (i.e. the change from SL 2/3 to SL 4). Once in a while there are "busts" but the results for all three polarizations, all three nadir angles and all three methods are not very far apart.

Scatter Plots. Eleven scatter plots showing the results of method 6 for VV polarization for all three nadir angles and stratified according to "Type A" meteorological winds, "Type B" winds, and so on are given next. Figure 8.22 for SL 2/3 combines Hurricane AVA and Tropical Storm Christine. These scatter plots will be discussed later on in this chapter. Fig. 8.23 shows VH/HV for AVA and Christine.

*19 in fact

**Method 4 is tabulated for SL 2/3, for those who might wonder how well it did.

TABLE 8.13

SL 2-3: REDUCTION 5

COMMAND ANGLE POLARIZATION	1 VV	2 VV	3 VV	1 HH	2 HH	3 HH	1 HV+VH	2 HV+VH	3 HV+VH
AD	82.8700	61.6400	36.4100	102.5000	84.4000	42.5500	139.0500	135.0500	75.8250
BU	.4196	.3881	.3594	.3748	.4000	.3847	.3291	.3407	.2880
AD	94.3861	68.9480	39.8516	115.7350	95.5790	47.0743	155.7279	151.7650	82.6923
BU	.4320	.3987	.3684	.3846	.4112	.3951	.3366	.3488	.2937
AC	146.7770	100.4707	53.8416	173.7732	145.3981	66.0853	226.3386	223.3786	109.7085
BC	.4739	.4341	.3985	.4175	.4490	.4299	.3615	.3756	.3125
M	2.5174	2.8209	2.8609	2.0537	2.7059	3.2147	1.5143	1.9270	2.7338
N	.8061	.7695	.7102	.8833	.7859	.6647	1.0290	.9474	.7520
P0	.8138	.7684	.8409	.8270	.7777	.8365	.8410	.7818	.8421
P1	-.0544	-.0568	-.0291	-.0887	-.1032	-.0427	-.0055	-.0473	-.0264
P2	-.0127	.0550	.0832	.0175	.0714	.0991	.0633	.0936	.0836
P3	.0416	.0931	.0480	.0023	.0566	.0271	-.0020	.0610	.0415
P4	-.1083	-.2200	-.1565	-.0947	-.2268	-.1512	-.1553	-.2458	-.1631
Q0	14.4264	8.0514	6.0504	7.9465	7.3156	9.3188	8.9470	4.2561	5.1442
Q1	-1.0487	-.2697	-.1984	-.0704	-.1063	-.7245	-.3001	.3331	-.1065
Q2	.06359	.04431	.05346	.03065	.03665	.07390	.04132	.02279	.05163

REPRODUCIBILITY OF THE
ORIGINAL PAGE IS POOR

269

TABLE 8.14

SL 2-3: REDUCTION 6

COMMAND ANGLE POLARIZATION	1 VV	2 VV	3 VV	1 HH	2 HH	3 HH	1 HV+VH	2 HV+VH	3 HV+VH
R0	1.2477	1.2131	1.1837	1.2622	1.2318	1.1858	1.3666	1.3267	1.2795
R1	-.0673	-.0743	-.0072	-.1273	-.1545	-.0242	-.0144	-.0741	-.0079
P2	-.0188	.0938	.1166	.0333	.1248	.1496	.1000	.1622	.1274
R3	.0896	.1694	.0959	.0117	.0926	.0594	-.0052	.1038	.0848
R4	-.2359	-.4199	-.3284	-.1844	-.4328	-.3487	-.2412	-.4334	-.3469
S0	11.0508	7.2944	5.6343	6.7562	6.8707	7.2235	9.5305	4.1871	4.5560
S1	-.3938	.0649	.1832	.1972	.1508	-.0400	-.4096	.3886	.2639
S2	.03635	.02551	.02736	.01911	.02151	.03438	.04557	.01947	.02744

TABLE 8.15

SL 4 : REDUCTION 4

COMMAND ANGLE POLARIZATION	1. VV	2. VV	3. VV	1. HH	2. HH	3. HH	1. HV+VH	2. HV+VH	3. HV+VH
E0	4.2619	3.9283	3.6141	3.7888	4.1115	3.9460	4.3849	4.4798	4.1099
E1	-.1737	-.0540	-.0339	.0854	-.1193	-.1221	-.0871	.0569	-.0969
E2	-.3490	-.3057	-.2207	.1482	-.5343	-.2037	-.3855	-.4729	-.1531
E3	.0089	.1917	.0692	.2117	.4565	.1518	.6052	.3434	.1082
E4	-.0290	-.2051	-.0104	-.0196	-.4141	.0449	-.6862	-.4333	-.0015
F0	.15094	.12707	.12748	.06077	.10696	.11652	.11758	.13632	.11272
F1	-.01649	-.00144	-.00541	.01623	-.00286	-.01804	-.00166	.01095	-.00906
F2	-.01518	-.01279	.00761	.03010	-.03668	.00528	-.01905	-.02567	.01028
F3	.01413	.03556	.01639	.01556	.04852	.01109	.06281	.03843	.00989
F4	-.01159	-.03156	.00172	-.00483	-.04082	.01227	-.06781	-.04086	.00400
G0	1.3867	-1.2184	-1.2146	-7.1468	-4.6527	-5.2965	-6.7653	.4654	-.8024
G1	.7951	1.0625	1.0164	1.7751	1.3883	1.3810	1.5590	.9163	.9960
G2	.00378	-.00284	-.00023	-.02304	-.01063	-.00778	-.01343	-.00005	-.00005

SL 4 : REDUCTION 5

TABLE 8.16

COMMAND ANGLE POLARIZATION	1 VV	2 VV	3 VV	1 HH	2 HH	3 HH	1 HV+VH	2 HV+VH	3 HV+VH
AU	45.2400	37.9800	27.6500	47.9800	50.2600	38.6500	38.4600	36.5850	31.8250
BU	.5695	.5483	.5055	.4019	.5220	.4767	.3610	.3743	.3199
AD	52.7735	43.7432	31.1292	53.5096	58.0787	43.6997	42.1716	40.2024	34.3782
BD	.5925	.5696	.5235	.4132	.5413	.4927	.3702	.3841	.3270
AC	21.2843	72.0615	47.0518	77.3212	96.3912	66.7846	57.3289	55.1167	44.3211
BC	.6744	.6449	.5865	.4514	.6088	.5480	.4005	.4169	.3505
M	2.9285	3.5454	3.3212	4.7490	4.3475	3.7199	3.5616	3.5911	3.0985
N	.7430	.6837	.6999	.6032	.6259	.6668	.7359	.7373	.7787
PJ	.8658	.8491	.8858	.8004	.8248	.8714	.8236	.8261	.8687
P1	-.0106	-.0102	.0106	-.0368	-.0324	-.0009	-.0371	-.0319	-.0117
P2	-.0224	-.0379	-.0612	-.0531	-.0347	-.0581	-.0679	-.0682	-.0923
P3	-.0750	-.0194	.0110	.0075	.0200	.0575	-.0286	-.0062	.0235
P4	-.0800	-.1628	-.1686	-.0721	-.1743	-.1736	-.0921	-.1839	-.1948
QJ	12.0814	-5.1493	-3.4060	-34.8985	-18.4023	-7.3288	31.3459	22.3003	-.5446
Q1	-.4197	1.2966	1.0258	4.5327	2.6874	1.3902	-2.2496	-1.5933	.6291
Q2	.03811	-.00215	.00513	-.08589	-.03685	-.00263	.08077	.07059	.01656

REPRODUCIBILITY OF THE
ORIGINAL PAGE IS POOR

271

SL 4 : REDUCTION 6

TABLE 8.17

COMMAND ANGLE POLARIZATION	1 VV	2 VV	3 VV	1 HH	2 HH	3 HH	1 HV+VH	2 HV+VH	3 HV+VH
RJ	1.2222	1.2237	1.2242	1.2480	1.2491	1.2297	1.4525	1.4818	1.4726
R1	.0301	.0443	.0559	.0004	.0113	.0455	-.0295	-.0205	.0028
R2	.0255	.0169	-.0171	-.0135	.0265	-.0094	-.0746	-.0765	-.1187
R3	-.1342	-.0518	-.0041	.0212	.0381	.0769	-.0661	-.0259	.0279
R4	-.1835	-.3121	-.3086	-.2208	-.3707	-.3308	-.2545	-.4202	-.4057
SJ	8.4297	-7.2184	-3.5999	-14.0300	-15.5195	-5.2505	26.1577	8.0065	-4.3553
S1	.1155	1.7400	1.3058	2.6770	2.5833	1.5117	-1.6526	-.0302	1.1334
S2	.02111	-.01721	-.00582	-.04533	-.03701	-.01107	.06408	.02964	.00244

TABLE 8.18 (I)

SL2-3	COMMAND ASPECT ANGLE	ANGLE 1 MET. WIND	SIGMA, DB			REDUCTION 4			REDUCTION 5			REDUCTION 6			QUAL
			VV	HH	HV+VH	VV	HH	HV+VH	VV	HH	HV+VH	VV	HH	HV+VH	
156102	1.7	13.0	-17.50	-22.86	-32.72	12.02	12.81	13.37	13.37	13.16	12.89	13.69	13.40	12.82	A
156103	1.4	13.0	-17.12	-22.48	-32.46	11.89	12.72	13.23	13.80	13.50	13.14	14.13	13.75	13.07	A
156104	-4.0	13.0	-16.43	-22.28	-32.02	11.68	12.65	12.97	14.69	13.68	13.59	15.03	13.95	13.51	A
156105	-9.3	13.0	-18.64	-24.32	-36.48	12.34	12.86	15.01	12.24	11.97	10.32	12.59	12.18	10.32	A
156106	-19.7	10.0	-20.69	-25.72	-35.80	12.08	11.90	12.75	10.85	10.91	10.48	11.18	11.09	10.47	+
156107	-25.0	8.0	-20.52	-25.80	-37.81	11.64	11.27	11.30	10.81	10.71	9.55	11.16	10.89	9.59	+
156108	-35.3	5.0	-19.88	-25.79	-35.29	11.29	10.41	10.28	10.92	10.49	10.21	11.30	10.65	10.21	+
156112	-61.6	12.0	-21.61	-26.06	-35.12	10.45	10.50	9.43	11.21	11.90	11.22	11.48	12.05	11.20	+
156113	-56.8	14.0	-18.49	-23.79	-32.51	13.73	12.38	12.58	13.39	13.20	13.03	13.77	13.47	12.96	+
156114	-47.1	15.0	-19.45	-23.00	-32.52	11.61	11.66	12.08	11.44	12.14	12.05	11.84	12.43	11.99	+
156115	-47.4	16.0	-18.38	-19.78	-30.01	12.73	17.04	16.01	12.26	16.26	14.77	12.72	16.77	14.67	+
156116	-47.5	18.0	-15.69	-20.49	-29.79	17.33	15.71	16.47	15.74	15.30	15.09	16.37	15.77	14.98	+
156119	-68.1	22.0	-15.38	-20.38	-28.69	30.01	25.45	25.50	23.51	21.00	21.37	23.51	21.08	21.32	+
156120	-68.4	23.0	-16.11	-21.23	-29.56	25.62	21.82	21.83	21.15	19.23	19.26	21.09	19.31	19.20	+
156121	-63.6	25.0	-16.80	-21.52	-29.57	20.07	18.68	20.76	17.81	17.50	18.55	18.02	17.73	18.47	+
156122	-63.7	26.0	-17.60	-21.96	-30.62	17.37	17.45	17.46	16.15	16.80	16.55	16.34	17.03	16.47	+
157101	167.1	12.0	-15.77	-24.93	-29.67	18.28	12.18	16.83	18.66	14.51	18.46	17.51	14.25	18.59	M
157102	172.6	13.0	-16.37	-23.41	-29.30	16.60	14.70	17.86	17.16	16.76	19.38	15.97	16.28	19.57	M
157103	163.2	16.0	-15.88	-23.29	-29.46	17.88	14.43	17.19	18.54	16.29	18.64	17.63	16.01	18.74	M
157104	169.0	18.0	-14.02	-21.02	-27.71	25.68	20.67	22.41	23.53	20.81	23.20	21.71	20.12	23.43	M
157105	174.8	25.0	-12.93	-19.58	-26.84	33.46	27.94	26.07	27.30	24.73	25.99	24.68	23.61	26.33	M
157106	-179.7	34.0	-13.96	-18.01	-25.89	26.62	39.43	30.77	23.32	29.86	29.44	21.04	28.30	29.86	M
157107	-174.1	42.0	-12.90	-18.45	-25.68	33.58	34.98	31.67	27.43	28.11	30.24	24.84	26.76	30.65	M
157108	-153.3	51.0	-12.07	-14.88	-21.69	34.43	44.78	52.91	32.60	37.81	48.18	32.20	37.18	48.29	M
157109	-112.6	50.0	-12.78	-13.97	-22.16	41.82	47.87	46.06	51.14	58.42	57.69	53.27	58.56	57.47	M
157111	-46.1	31.0	-13.04	-15.44	-24.94	24.57	29.71	30.73	21.71	25.01	25.75	22.83	25.86	25.53	M
157113	-21.6	18.0	-13.26	-18.83	.00	12.38	12.75	.00	20.08	17.22	.00	21.02	17.77	.00	M
157114	-17.9	16.0	-16.56	.00	.00	12.00	.00	.00	14.15	.00	.00	14.66	.00	.00	M
162104	-28.8	7.0	-25.50	-29.80	-38.05	10.29	9.92	10.27	10.12	9.23	9.39	10.04	9.17	9.44	+
162105	-29.1	9.0	-24.36	-29.17	-41.54	10.45	10.02	9.21	10.10	9.39	8.73	10.14	9.36	8.86	+
162106	-34.5	9.0	-21.14	-25.72	-38.96	10.80	10.49	8.72	10.49	10.52	9.08	10.78	10.69	9.16	+
162107	-34.7	9.0	-21.12	-26.33	-32.19	10.80	10.25	12.27	10.49	10.26	12.15	10.78	10.39	12.08	+
162109	-75.3	5.0	-22.23	-27.79	-35.70	10.98	10.40	9.67	11.66	11.77	11.22	11.73	11.75	11.23	+
162110	-70.7	12.0	-19.36	-24.12	-33.30	14.51	14.38	12.48	14.35	14.94	13.31	14.35	15.00	13.29	+
162111	-75.9	15.0	-17.56	-23.08	-32.68	21.59	18.27	14.16	18.81	17.14	14.11	18.35	17.04	14.11	+
162112	-106.2	13.0	-19.70	-24.33	-34.51	18.18	17.71	12.94	16.97	16.44	12.30	16.70	16.39	12.29	+
162113	-106.5	7.0	-25.37	-31.82	-34.66	11.15	10.50	12.78	10.70	10.01	12.17	10.83	9.91	12.17	+
162114	-86.7	8.0	-26.97	-31.87	-37.85	9.32	9.12	8.73	10.17	9.91	9.96	10.19	9.75	10.01	+
216202	169.6	17.4	-15.23	-22.08	-30.48	20.25	17.55	15.16	19.90	18.77	17.04	18.46	18.21	17.17	+
216203	175.6	14.8	-16.65	-23.66	-31.76	15.86	14.36	12.94	16.48	16.54	15.14	15.28	16.03	15.27	+
216204	-167.5	13.3	-18.97	-23.81	-31.97	11.82	13.79	12.61	13.30	15.92	14.74	12.90	15.57	14.82	B
216205	-157.6	12.7	-18.81	-22.96	-32.49	12.30	14.60	11.96	13.58	16.15	13.60	13.41	15.99	13.62	B
216206	-145.7	12.6	-16.85	-22.12	-30.60	15.81	15.40	14.79	16.60	16.42	15.30	16.44	16.42	15.29	B
216207	-142.7	12.9	-16.03	-19.19	-29.11	18.11	20.15	17.51	18.72	21.18	17.10	18.67	21.23	17.06	+
216208	-138.8	13.7	-16.13	-20.24	-29.80	18.37	17.89	16.39	19.00	18.99	15.89	19.02	19.13	15.84	+
216209	-136.7	14.6	-16.96	-18.68	-29.22	17.01	20.68	17.49	17.40	22.59	16.92	17.46	22.73	16.86	D
220202	-114.5	14.0	-23.45	-26.99	-35.70	12.44	13.51	11.47	11.58	12.71	11.23	11.74	12.80	11.22	D
220203	-113.6	14.7	-24.53	-29.18	-33.49	11.66	11.95	13.73	10.96	11.14	13.22	11.13	11.17	13.19	C
220205	-123.8	12.4	-27.63	-23.77	-35.80	9.78	15.13	10.78	10.10	15.22	10.74	10.11	15.40	10.74	C
220206	-135.8	11.8	-26.78	-28.19	-36.28	9.40	10.63	9.53	10.10	10.63	10.09	10.09	10.66	10.11	+
220207	-142.9	11.4	-24.32	-31.04	-37.92	9.65	9.13	9.43	10.29	9.53	9.51	10.41	9.42	9.57	B
220208	-148.8	11.2	-19.40	-25.68	-33.56	12.16	11.42	11.00	12.91	12.47	11.99	12.97	12.50	11.99	+
220209	-145.8	10.2	-19.66	-25.69	-32.86	12.14	11.50	11.87	12.67	12.30	12.42	12.78	12.36	12.41	+

TABLE 8.18 (2)

220210	-135.7	9.2	-22.27	-29.29	-33.02	10.73	9.89	12.02	10.96	10.11	12.10	11.16	10.08	12.08	C
220211	-130.7	8.3	-25.15	-21.26	-32.15	10.16	10.91	13.67	10.27	17.98	13.26	10.40	16.18	13.21	C
220303	15.0	10.1	-16.77	.00	.00	11.94	.00	.00	14.00	.00	.00	14.46	.00	.00	C
220304	-5.4	9.9	-16.31	.00	.00	11.66	.00	.00	14.85	.00	.00	15.21	.00	.00	C
220305	-17.8	12.1	-24.36	.00	.00	12.51	.00	.00	10.12	.00	.00	10.20	.00	.00	C
220307	-15.5	17.7	-24.26	.00	.00	13.01	.00	.00	10.13	.00	.00	10.22	.00	.00	C
220308	-17.8	16.9	-22.09	.00	.00	12.35	.00	.00	10.43	.00	.00	10.68	.00	.00	C
220309	-23.2	15.2	-21.19	.00	.00	11.71	.00	.00	10.61	.00	.00	10.92	.00	.00	+
220310	-26.6	14.4	-21.61	.00	.00	11.30	.00	.00	10.45	.00	.00	10.72	.00	.00	+
220402	38.8	7.1	.00	-32.88	.00	.00	8.40	.00	.00	8.60	.00	.00	8.34	.00	+
220404	31.2	8.6	.00	-30.10	.00	.00	9.56	.00	.00	9.13	.00	.00	9.04	.00	+
220405	27.7	9.0	.00	-29.76	.00	.00	10.09	.00	.00	9.26	.00	.00	9.20	.00	+
220406	25.6	9.3	.00	-29.44	.00	.00	10.47	.00	.00	9.38	.00	.00	9.34	.00	+
220407	22.4	9.3	.00	-31.33	.00	.00	10.79	.00	.00	8.99	.00	.00	8.86	.00	+
245204	117.1	10.0	-27.41	-25.71	-36.05	10.11	14.34	11.04	10.15	13.75	10.90	10.21	13.87	10.90	M
245205	95.9	12.0	-28.99	-34.31	-38.47	9.25	8.93	9.02	10.10	9.21	9.74	10.04	8.98	9.80	M
245206	76.1	14.0	-24.00	-29.03	-35.39	9.82	9.63	10.09	10.72	11.00	11.44	10.82	10.96	11.45	M
245207	57.7	18.0	-21.41	-24.31	-33.47	10.42	11.85	11.22	11.06	12.84	12.20	11.35	13.08	12.16	M
245208	51.6	24.0	-18.04	-23.35	-30.62	13.69	12.28	15.49	13.10	12.84	14.53	13.55	13.15	14.44	M
245209	64.6	33.0	-18.04	-21.59	-28.99	16.35	18.88	23.25	15.52	17.63	20.05	15.69	17.84	19.96	M
245210	86.4	39.0	-15.19	-19.32	-25.51	39.85	40.51	46.58	30.24	28.06	33.10	28.87	27.25	33.31	M
245211	107.3	37.0	-14.36	-18.75	-25.96	37.15	31.78	31.43	39.61	30.91	32.52	39.83	30.54	32.52	M
245213	126.9	28.0	-14.03	-19.64	-26.78	27.00	19.95	23.40	31.77	22.28	24.54	32.41	22.47	24.44	M
245214	132.8	24.0	-15.62	-22.38	-28.85	20.65	15.32	18.42	22.03	15.92	17.98	22.15	16.11	17.91	M
245215	136.5	21.0	-16.86	-22.62	-29.41	17.24	14.73	17.17	17.67	15.30	16.60	17.72	15.46	16.54	M
245216	140.3	18.0	-17.43	-24.05	-31.32	15.65	13.08	14.02	15.97	13.59	13.82	16.02	13.71	13.78	M
245217	143.0	15.0	-18.02	-21.16	-31.73	14.40	16.53	13.35	14.78	17.37	13.42	14.83	17.46	13.39	M
245218	146.9	12.0	-21.34	-28.42	-33.39	10.72	9.87	11.25	11.36	10.64	12.02	11.52	10.63	12.02	M
245219	150.7	9.0	-26.73	-33.45	-38.93	8.98	8.32	7.22	10.10	9.06	9.37	10.06	8.84	9.44	M
245220	152.3	7.0	-30.43	-34.28	-38.51	8.91	8.16	7.35	10.41	8.92	9.53	10.00	8.67	9.60	M
252103	126.2	11.7	-28.01	-34.75	-37.94	9.58	9.14	9.18	10.11	8.77	9.66	10.05	8.52	9.70	C
252104	120.9	11.8	-26.52	-30.40	-35.84	10.28	10.84	10.96	10.21	10.17	10.86	10.31	10.15	10.86	C
252105	114.8	11.1	-24.48	-28.06	-36.81	11.64	12.63	10.57	10.95	11.83	10.53	11.13	11.89	10.54	+
252106	106.6	11.1	-24.87	-29.56	-35.77	11.48	11.84	11.64	10.91	11.14	11.28	11.04	11.11	11.29	D
252107	95.5	10.9	-23.36	-30.21	-38.49	12.12	10.77	8.98	11.68	10.80	9.73	11.67	10.69	9.79	D
252108	86.1	11.5	-30.71	-37.20	-40.01	8.90	7.97	7.31	10.27	8.59	9.23	9.99	8.23	9.32	+
252110	79.9	10.1	-16.50	-21.17	-29.76	28.50	27.16	22.63	22.87	21.58	19.03	22.00	21.22	19.07	+
252111	74.7	7.5	-20.32	-24.83	-34.81	13.39	13.93	10.66	13.48	14.51	11.90	13.42	14.50	11.90	+
252112	59.5	4.4	-24.96	-30.84	-39.01	9.09	8.30	6.64	10.15	9.44	9.35	10.24	9.36	9.41	+
252113	-11.6	2.4	-35.94	-39.11	-41.01	19.20	14.56	16.76	11.46	8.17	8.96	10.27	7.67	9.06	+
252114	-57.8	5.3	-24.60	-28.67	-37.84	9.15	8.88	7.27	10.16	10.11	9.67	10.27	10.15	9.70	+
252115	-63.8	8.7	-19.60	-23.82	-31.85	12.89	13.45	14.49	13.12	14.28	14.66	13.35	14.48	14.60	+
252116	-61.0	11.4	-21.58	-25.85	-35.87	10.44	10.63	8.70	11.19	11.99	10.71	11.46	12.15	10.71	D
252117	-52.1	13.5	-17.18	-22.26	-31.55	15.35	13.79	13.80	14.27	13.98	13.47	14.76	14.35	13.39	+
252118	-41.2	15.1	-14.46	-19.35	-29.57	17.40	15.79	15.56	16.97	15.98	14.85	17.76	16.52	14.74	+
252119	-28.3	17.7	-17.43	-22.27	-32.29	12.29	12.07	12.33	12.68	12.86	12.41	13.21	13.23	12.33	D
252120	-20.4	18.9	-23.27	-27.37	-36.86	11.97	11.64	12.60	10.20	10.15	9.99	10.37	10.24	10.00	D
252121	-14.5	20.8	-20.37	-25.63	-35.52	12.51	12.52	13.70	11.07	11.09	10.75	11.40	11.25	10.73	D
252122	-11.5	20.6	-24.28	-26.95	-36.54	13.89	13.00	14.63	10.14	10.48	10.28	10.23	10.58	10.28	B
252123	-11.5	20.5	-26.59	-31.21	-37.07	14.70	13.52	14.87	10.13	9.12	10.05	10.02	9.00	10.06	B
252124	-11.6	20.0	-24.15	-27.26	-37.06	13.82	13.03	14.84	10.15	10.35	10.05	10.25	10.43	10.06	B
252127	-6.6	13.4	-14.63	-16.64	-27.89	11.24	11.65	11.15	17.78	22.30	20.11	18.22	22.75	19.96	A
252128	.5	11.5	-13.12	-16.09	-26.85	10.77	11.43	10.57	21.59	23.73	22.66	22.13	24.15	22.50	A
252129	11.5	10.8	-13.21	-18.07	-27.97	11.18	12.06	11.51	21.05	19.18	19.81	21.77	19.64	19.65	B
252130	22.6	10.0	-13.92	-18.17	-28.49	12.49	12.98	12.93	18.37	18.20	17.85	19.20	18.79	17.69	B
252131	30.7	9.0	-15.87	-21.21	-30.91	13.14	12.58	13.00	14.36	13.71	13.58	15.00	14.15	13.48	B
252132	28.8	6.8	-20.87	-27.62	-40.18	11.27	10.41	9.66	10.62	9.87	8.93	10.95	9.93	9.03	B

TABLE 8.18 (3)

216103	-144.2	16.1	-16.13	-23.39	-29.57	17.74	13.62	16.63	18.34	14.38	16.40	18.27	14.48	16.37	+
216105	-143.3	14.0	-17.13	-23.78	-30.25	15.82	13.23	15.48	16.29	13.93	15.30	16.28	14.02	15.27	+
216107	-140.8	12.3	-17.94	-25.05	-30.96	14.78	12.20	14.49	15.06	12.67	14.25	15.12	12.77	14.21	+
216111	-122.3	14.4	-21.21	-25.54	-31.96	13.70	13.73	14.72	12.98	13.37	14.36	13.14	13.52	14.30	+
216113	-118.7	17.3	-20.94	-25.05	-31.74	14.54	14.72	15.40	13.74	14.30	15.08	13.85	14.44	15.02	B
216115	-124.0	16.0	-19.68	-24.25	-30.99	15.22	14.62	15.83	14.79	14.58	15.53	14.91	14.75	15.46	B
216114	56.1	11.4	-18.13	-20.35	-29.54	14.26	19.09	19.06	13.72	17.48	17.06	14.11	17.89	16.95	B
220103	-141.2	11.8	-25.74	-26.10	-36.22	9.37	11.43	9.22	10.13	11.86	10.12	10.17	11.93	10.15	+
220105	-140.8	13.1	-27.07	-33.96	-37.18	9.16	8.58	8.64	10.11	8.82	9.73	10.04	8.57	9.78	D
220107	-133.9	13.6	-23.72	-30.26	-35.13	10.50	9.92	10.51	10.54	9.78	10.70	10.73	9.73	10.70	D
220109	-108.3	16.6	-22.64	-29.10	-34.58	13.49	12.18	12.81	12.47	11.39	12.24	12.53	11.39	12.23	D
220111	-112.6	14.6	-20.87	-26.29	-32.17	15.46	14.36	15.48	14.47	13.53	14.94	14.48	13.60	14.89	D
220113	-120.8	14.3	-19.63	-25.48	-32.25	15.92	13.99	14.52	15.46	13.59	14.15	15.54	13.73	14.09	D
220102	106.0	9.1	-19.12	-24.07	-30.66	19.07	17.67	18.31	18.20	16.67	17.61	17.97	16.68	17.58	+
220104	114.7	6.9	-25.78	-29.37	-36.61	10.87	11.77	10.73	10.46	10.98	10.65	10.61	11.00	10.65	+
220106	106.4	4.8	-34.82	-37.10	-35.90	8.91	8.77	11.52	10.80	8.63	11.19	10.10	8.31	11.20	+
220108	79.4	3.5	-30.60	-34.05	-36.44	8.90	8.17	9.29	10.30	9.13	10.72	9.99	8.90	10.75	+
220110	44.7	4.0	-27.23	-32.42	-36.68	8.97	8.22	8.50	10.27	8.69	9.66	9.99	8.47	9.69	+
220112	40.4	5.0	-31.19	-34.06	-35.93	8.90	8.18	9.34	10.89	8.45	9.89	10.10	8.13	9.91	+

TABLE 8.18 (4)

SL2-3	COMP AND ASPECT	ANGLE 2 MET. WIND	SIGMA, DB			REDUCTION 4			REDUCTION 5			REDUCTION 6			QUAL
			VV	HH	HV+VH	VV	HH	HV+VH	VV	HH	HV+VH	VV	HH	HV+VH	
156102	6.6	14.0	-17.81	-20.37	-33.11	13.32	12.84	14.13	11.84	11.20	10.82	12.08	11.39	10.86	+
156103	1.4	13.0	-15.93	-18.93	-31.28	13.24	12.97	14.09	13.35	12.38	12.12	13.67	12.28	12.18	A
156104	1.0	13.0	-15.56	-18.92	-30.14	13.22	12.97	13.96	13.72	12.08	13.16	14.07	12.29	13.24	A
156105	-4.3	13.0	-16.28	-19.39	-31.09	13.28	12.94	14.06	13.06	11.79	12.34	13.36	11.99	12.40	A
156106	-14.7	12.0	.00	-21.22	.00	.00	12.74	.00	.00	11.09	.00	.00	11.27	.00	A
156107	-20.0	10.0	-18.85	-21.64	-33.41	13.11	12.60	12.79	11.50	11.10	11.00	11.65	11.27	11.02	+
156108	-25.4	8.0	-18.24	-21.12	-32.79	13.24	12.83	12.46	12.00	11.66	11.46	12.11	11.82	11.48	+
156109	-35.6	4.0	-19.19	-22.79	-33.74	12.31	11.51	10.42	11.20	10.71	10.53	11.25	10.80	10.53	+
156113	-61.8	13.0	-18.18	-23.91	-31.59	11.99	12.21	11.24	11.92	12.48	12.32	12.25	12.86	12.42	+
156114	-57.0	14.0	-17.31	-20.03	-30.84	12.94	13.25	12.48	12.87	13.48	13.18	13.15	13.85	13.27	+
156115	-47.4	15.0	-17.63	-20.19	-30.67	13.09	13.42	13.22	12.45	13.01	13.12	12.55	13.19	13.16	+
156116	-47.6	17.0	-14.51	-17.54	-28.17	16.67	16.82	18.01	16.21	16.35	16.19	16.46	16.75	16.28	+
156117	-47.8	18.0	-13.80	-17.27	-27.18	17.66	17.22	20.46	17.37	16.78	17.73	17.72	17.23	17.85	+
156118	-67.9	20.0	-13.16	-16.47	-27.10	16.47	16.92	18.68	17.84	17.89	17.42	18.96	19.04	17.70	+
156120	-68.4	23.0	-14.21	-17.44	-27.00	15.28	15.62	18.82	15.98	16.15	17.49	16.82	17.03	17.77	+
156121	-68.5	24.0	-15.23	-17.83	-27.52	14.27	15.13	17.70	14.50	15.54	16.64	15.15	16.33	16.90	+
156122	-63.8	25.0	-15.38	-17.84	-27.81	14.45	15.47	17.68	14.83	16.11	16.87	15.43	16.92	17.10	+
157101	161.7	11.0	-17.76	-22.36	-30.79	12.12	12.06	13.79	13.06	12.86	14.43	12.76	12.50	14.35	M
157102	172.6	12.0	-15.45	-21.51	-29.94	13.62	12.23	14.04	13.46	12.55	13.96	13.16	12.25	13.91	M
157103	163.5	16.0	-14.10	-19.59	-28.24	17.42	15.58	17.56	17.37	15.83	17.64	17.01	15.37	17.58	M
157104	164.3	18.0	-12.66	-18.12	-27.12	20.32	18.09	19.57	19.75	17.99	19.38	19.46	17.53	19.33	M
157105	-179.8	22.0	-11.95	-16.77	-25.95	18.98	19.19	20.24	17.39	18.16	19.06	16.95	17.75	19.02	M
157106	-159.1	29.0	-12.95	-16.19	-26.36	21.59	24.07	22.37	21.14	23.34	22.02	20.80	22.91	21.95	M
157107	-157.9	38.0	-13.73	-17.91	-27.57	20.04	19.85	19.87	19.87	19.66	19.79	19.43	19.08	19.70	M
157108	-140.1	41.0	-13.96	-15.05	-25.36	25.97	33.83	29.26	24.12	31.04	26.98	23.11	30.35	26.79	M
157109	-111.1	39.0	-11.98	-14.46	-24.32	24.74	25.02	24.21	33.38	33.80	31.27	35.41	35.50	31.52	M
162104	-28.7	6.0	-23.41	-26.08	-36.38	10.63	10.15	9.62	9.23	9.17	9.14	9.35	9.28	9.13	+
162105	-28.9	9.0	-22.15	-25.13	-37.09	11.15	10.58	9.17	9.69	9.52	8.79	9.81	9.63	8.77	+
162106	-34.4	9.0	-20.81	-23.20	-34.46	11.34	11.24	9.97	10.25	10.42	10.10	10.34	10.52	10.09	+
162107	-34.7	9.0	-17.48	-20.98	-31.71	13.61	12.89	12.55	12.54	11.94	12.13	12.58	12.05	12.15	+
162108	-34.9	9.0	-20.22	-22.81	-33.65	11.67	11.52	10.60	10.57	10.69	10.62	10.64	10.78	10.62	+
162110	-75.5	8.0	-19.44	-22.78	-33.94	11.20	10.83	9.08	10.18	10.15	9.37	10.49	10.41	9.43	+
162111	-70.9	14.0	-16.31	-19.17	-31.04	13.24	13.59	11.86	12.95	13.48	12.01	13.46	14.03	12.14	+
162112	-81.0	15.0	-15.90	-18.84	-29.94	13.54	13.82	13.23	12.55	12.75	11.77	12.93	13.06	11.87	+
162113	-106.5	10.0	-19.67	-22.25	-34.86	13.76	13.62	11.17	13.09	13.10	10.68	13.10	13.01	10.66	+
162114	-106.7	5.0	-22.71	-25.96	-37.66	11.66	11.09	9.40	10.61	10.21	8.93	10.65	10.19	8.91	+
216202	164.7	18.9	-12.56	-16.47	-26.41	20.42	21.74	20.98	19.80	21.16	20.63	19.51	20.78	20.59	+
216203	171.6	16.5	-13.76	-18.28	-28.22	16.32	16.79	16.62	15.69	16.43	16.24	15.33	16.01	16.19	+
216204	-177.5	14.2	-14.81	-19.35	-29.53	14.17	14.76	14.41	13.64	14.47	14.05	13.30	14.09	14.00	B
216205	-166.5	13.1	-17.12	-20.30	-30.72	12.23	14.16	13.45	12.82	14.47	13.87	12.56	14.07	13.81	B
216206	-155.6	12.7	-15.38	-20.46	-30.25	17.11	15.31	15.27	17.44	15.70	15.78	16.90	15.11	15.67	B
216207	-147.7	12.7	-14.95	-18.21	-28.34	20.59	21.40	20.00	20.01	20.51	19.37	19.18	19.63	19.21	B
216208	-141.8	13.1	-13.91	-18.62	-28.38	25.68	21.32	20.64	23.85	20.24	19.64	22.87	19.25	19.46	+
216209	-138.8	14.0	-13.92	-15.35	-26.39	26.41	28.61	26.07	24.57	26.70	24.34	23.54	25.76	24.14	+
216210	-137.8	14.8	-18.22	-18.89	-29.42	15.63	21.02	18.69	15.71	20.09	18.06	14.86	19.07	17.87	D
220202	-115.6	11.5	-21.23	-23.32	-33.52	12.83	13.61	12.78	13.03	13.71	13.30	12.65	13.28	13.21	D
220203	-113.6	15.4	-19.61	-22.18	-31.43	14.40	14.41	14.64	14.49	14.55	15.40	14.24	14.26	15.37	C
220206	-128.9	12.1	-22.95	-22.19	-32.13	10.56	15.10	14.43	11.33	15.09	14.73	10.95	14.38	14.58	C
220207	-138.8	11.6	-23.05	-26.25	-36.09	9.50	10.12	9.49	10.81	10.81	10.51	10.48	10.45	10.40	B
220208	-146.8	11.4	-20.78	-24.84	-36.09	10.78	10.79	9.01	12.06	11.62	10.41	11.63	11.20	10.30	B
220209	-148.8	10.8	-17.83	-21.29	-31.09	14.33	14.95	14.72	14.99	15.14	15.08	14.35	14.46	14.95	+
220210	-144.7	9.8	-17.27	-21.38	-31.11	16.15	15.31	15.11	16.30	15.25	15.20	15.49	14.51	15.05	+
220211	-137.7	8.9	-21.71	-24.96	-35.06	11.99	11.36	10.54	12.73	11.76	11.31	12.16	11.29	11.19	C

TABLE 8.18 (5)

220212	-127.6	8.0	-26.21	-22.39	-34.60	8.29	14.84	11.56	9.51	14.88	12.09	9.39	14.20	11.97	C
220304	3.5	9.6	-18.89	.00	.00	13.33	.00	.00	11.02	.00	.00	11.24	.00	.00	C
220305	-11.9	10.7	-19.76	.00	.00	13.17	.00	.00	10.70	.00	.00	10.90	.00	.00	C
220306	-18.4	13.3	-20.06	.00	.00	12.83	.00	.00	10.69	.00	.00	10.85	.00	.00	C
220307	-16.8	16.6	-21.38	.00	.00	12.65	.00	.00	9.99	.00	.00	10.16	.00	.00	C
220308	-16.0	17.7	-21.35	.00	.00	12.72	.00	.00	9.98	.00	.00	10.16	.00	.00	C
220309	-20.4	16.4	-18.99	.00	.00	13.06	.00	.00	11.41	.00	.00	11.56	.00	.00	+
220310	-24.8	15.0	-19.14	.00	.00	12.85	.00	.00	11.34	.00	.00	11.45	.00	.00	+
220402	48.8	9.2	.00	-29.85	.00	.00	7.15	.00	.00	8.22	.00	.00	8.32	.00	D
220403	44.7	9.5	.00	-26.06	.00	.00	8.99	.00	.00	9.24	.00	.00	9.34	.00	D
220404	40.3	9.9	.00	-21.85	.00	.00	12.04	.00	.00	11.38	.00	.00	11.48	.00	+
220405	37.1	10.2	.00	-24.33	.00	.00	10.42	.00	.00	9.90	.00	.00	10.00	.00	+
220406	32.7	9.9	.00	-23.79	.00	.00	11.02	.00	.00	10.14	.00	.00	10.24	.00	+
220407	25.5	9.6	.00	-24.14	.00	.00	11.03	.00	.00	9.95	.00	.00	10.06	.00	+
245204	119.0	7.0	-28.49	-30.19	-39.23	7.88	8.71	8.33	8.76	9.03	8.89	8.77	8.96	8.82	M
245205	91.0	9.0	-24.85	-26.18	-31.37	9.92	10.02	12.39	8.42	8.73	10.74	8.59	8.81	10.77	M
245206	62.7	11.0	-24.79	-28.96	-38.45	8.09	7.41	5.38	8.63	8.37	7.94	8.83	8.52	7.96	M
245207	37.7	15.0	-18.44	-22.54	-33.87	12.77	11.60	10.05	11.71	10.88	10.41	11.76	10.98	10.41	M
245208	22.8	23.0	-15.38	-18.05	-28.92	14.49	14.47	15.11	14.84	14.38	15.36	15.07	14.69	15.44	M
245209	42.5	29.0	-13.94	-16.95	-26.52	17.45	17.60	21.76	16.89	16.85	18.56	17.10	17.23	18.67	M
245210	134.1	45.0	-11.58	-13.87	-21.47	37.20	39.27	45.66	34.69	38.05	44.20	34.39	38.09	44.24	M
245211	128.0	43.0	-11.34	-13.88	-22.07	36.98	36.87	39.66	38.35	39.98	43.24	38.84	40.62	43.34	M
245212	131.9	34.0	-10.74	-13.39	-22.24	41.53	41.14	40.86	39.84	41.46	41.00	40.30	42.06	40.99	M
245214	138.5	25.0	-12.51	-15.09	-25.22	32.17	33.74	29.82	29.24	31.26	27.65	28.43	30.58	27.46	M
245215	142.4	21.0	-14.63	-18.99	-27.94	23.15	20.31	21.63	21.84	19.39	20.48	20.85	18.43	20.29	M
245216	144.2	18.0	-16.36	-21.06	-30.15	18.14	15.89	16.79	17.88	15.72	16.55	16.99	14.94	16.39	M
245217	148.0	15.0	-19.52	-24.65	-33.18	12.06	10.87	11.92	13.12	11.73	12.77	12.60	11.31	12.65	M
245218	150.7	12.0	-19.52	-24.36	-34.02	11.67	10.94	10.77	12.87	11.87	11.93	12.42	11.46	11.82	M
245219	153.6	10.0	-22.22	.00	-35.16	8.79	.00	9.47	10.59	.00	10.93	10.40	.00	10.84	M
245220	155.2	7.0	-24.14	-28.02	-38.31	7.44	8.00	7.03	9.56	9.58	8.96	9.49	9.43	8.89	M
247116	-12.2	19.0	-12.57	-15.65	-26.71	13.94	14.16	14.51	18.42	16.36	18.02	19.18	16.90	18.18	C
247128	-16.0	6.0	-30.56	-34.39	-42.12	11.16	9.48	11.26	7.90	7.59	7.02	8.00	7.62	6.99	C
252102	132.3	10.9	-26.77	-31.91	-41.09	7.56	7.21	6.43	9.21	8.52	7.95	9.11	8.44	7.87	+
252103	128.2	11.5	-29.61	-33.91	-41.01	6.60	6.71	6.74	8.47	8.11	8.04	8.47	8.06	7.96	C
252104	123.1	11.8	-25.41	-28.45	-37.21	9.19	9.46	9.48	9.94	9.80	10.12	9.79	9.63	10.03	C
252105	117.8	11.4	-19.75	-22.56	-32.39	14.43	14.33	13.90	14.73	14.53	14.55	14.31	14.11	14.48	C
252106	111.8	11.1	-19.62	-22.03	-32.58	14.27	14.38	13.35	14.20	14.44	13.68	14.02	14.21	13.65	+
252107	101.6	10.9	-18.61	-22.33	-32.01	13.99	13.03	12.91	13.06	11.98	12.13	13.19	11.97	12.15	D
252108	91.3	11.0	-23.46	-26.79	-36.25	10.47	9.79	9.00	8.77	8.57	8.00	8.95	8.65	8.00	+
252109	84.2	11.5	-31.04	-30.43	-40.68	7.56	7.99	6.06	7.71	7.79	6.50	7.72	7.85	6.47	+
252110	81.1	10.9	-13.70	-16.85	-27.19	15.10	15.63	16.84	15.15	15.12	14.74	15.76	15.62	14.91	+
252111	77.9	9.3	-14.06	-17.40	-28.63	14.85	15.13	14.92	14.86	14.68	13.43	15.51	15.25	13.59	+
252112	70.8	6.4	-16.67	-20.34	-31.29	12.96	12.54	11.54	12.60	12.31	11.79	13.07	12.74	11.92	+
252113	44.6	3.2	-31.11	-34.56	-40.41	6.44	5.98	4.90	7.89	7.60	7.31	7.96	7.63	7.29	+
252114	-38.6	3.1	-27.55	-29.99	-37.76	7.74	7.65	6.98	8.20	8.18	8.32	8.31	8.26	8.30	+
252115	-62.7	6.6	-19.66	-22.07	-32.34	10.87	11.20	10.29	10.78	11.46	11.59	11.07	11.78	11.69	+
252116	-63.9	9.7	-17.77	-20.33	-30.10	12.26	12.69	13.35	12.17	12.93	13.76	12.54	13.38	13.91	+
252117	-55.0	12.2	-16.99	-19.15	-31.11	13.14	14.15	11.99	13.16	14.51	12.88	13.50	15.01	12.98	D
252118	-49.0	13.9	-14.17	-17.64	-28.78	17.09	16.35	16.63	16.82	16.00	15.41	17.15	16.40	15.50	+
252119	-37.2	15.8	-12.88	-16.59	-28.44	18.42	17.64	17.04	18.61	17.07	15.62	18.93	17.45	15.68	+
252120	-26.3	18.0	-17.15	-20.31	-32.52	13.80	13.32	12.55	12.95	12.32	11.67	13.06	12.49	11.69	D
252121	-19.4	19.4	-17.15	-19.63	-31.37	13.63	13.43	13.71	12.87	12.57	12.66	13.06	12.80	12.71	D
252122	-14.3	21.0	-20.76	-23.87	-35.31	12.94	12.04	13.13	10.23	9.69	9.66	10.41	9.84	9.68	B
252123	-11.5	20.3	-22.11	-25.00	-36.69	12.98	11.92	13.48	9.57	9.17	8.89	9.76	9.32	8.89	B
252125	-12.6	19.2	-17.09	-19.12	-31.10	13.46	13.26	13.97	12.66	12.51	12.67	12.90	12.75	12.73	B
252126	-12.6	17.1	-13.51	-14.61	-27.08	13.88	14.52	14.52	16.91	18.06	17.48	17.47	18.80	17.63	B
252127	-10.5	14.9	-15.36	-15.25	-28.17	13.53	14.06	14.18	14.30	16.74	15.79	14.65	17.31	15.97	A

TABLE 8.18 (6)

252128	-4.4	12.5	-11.46	-13.71	-25.33	13.20	13.77	13.58	19.87	18.53	19.77	20.92	19.30	19.99	A
252129	3.6	11.2	-12.39	-14.69	-26.50	13.18	13.58	13.63	18.10	16.86	17.76	16.89	17.43	17.93	A
252130	14.7	10.5	-11.77	-14.52	-26.14	14.46	14.91	15.05	20.19	18.55	19.19	21.15	19.34	19.37	B
252131	25.8	9.7	-11.77	-15.44	-27.07	17.07	16.81	17.09	20.88	18.35	17.97	21.63	18.99	18.09	B
252132	32.9	8.5	-13.97	-17.68	-29.54	16.61	15.85	15.16	16.77	15.31	14.37	16.97	15.57	14.42	B
252133	23.0	5.7	-23.22	-27.28	-37.31	11.46	10.27	10.48	9.31	8.75	8.75	9.45	8.87	8.74	B
216103	-142.5	16.3	-18.94	-24.10	-32.18	13.72	11.89	13.68	14.26	12.34	13.96	13.57	11.82	13.82	+
216105	-139.7	14.3	-15.69	-21.53	-30.17	20.79	15.57	17.14	19.95	15.32	16.73	18.92	14.53	16.55	+
216107	-135.1	13.2	-16.55	-21.15	-30.02	19.38	16.54	17.64	18.95	16.20	17.28	17.92	15.35	17.10	+
216109	-128.4	13.5	-19.33	-22.69	-32.00	14.79	14.43	14.61	15.10	14.44	14.93	14.36	13.79	14.78	+
216111	-120.7	17.4	-18.45	-21.43	-31.33	16.18	15.87	15.30	16.80	16.35	16.12	16.21	15.78	16.02	B
216113	-118.0	22.1	-17.05	-20.25	-29.16	18.06	17.19	18.00	19.36	18.23	19.75	18.90	17.76	19.69	B
216102	43.9	17.9	-14.03	-17.85	-28.47	17.36	16.33	17.32	16.79	15.60	15.62	17.01	15.89	15.68	+
216104	45.8	18.1	-14.44	-18.37	-28.85	16.80	15.64	16.54	16.23	15.02	15.17	16.45	15.30	15.24	+
216106	47.3	18.3	-15.70	-19.87	-30.12	15.16	13.78	14.13	14.53	13.34	13.70	14.68	13.53	13.76	+
216108	49.1	17.4	-15.89	-19.81	-30.25	14.86	13.79	13.84	14.36	13.49	13.63	14.53	13.71	13.69	+
216110	50.8	15.9	-15.95	-19.41	-30.08	14.71	14.20	14.05	14.34	14.01	13.88	14.55	14.30	13.95	+
216112	51.3	13.5	-16.14	-19.98	-30.70	14.47	13.53	12.98	14.12	13.40	13.22	14.33	13.65	13.28	C
216114	55.0	13.8	-15.71	-18.62	-28.80	14.74	15.02	16.31	14.73	15.19	15.65	15.07	15.66	15.78	B
220103	-135.5	13.4	-18.12	-23.16	-32.62	16.12	13.54	13.53	16.13	13.54	13.74	15.25	12.89	13.58	+
220105	-138.9	14.2	-21.52	-25.46	-35.06	10.94	10.80	10.47	11.93	11.35	11.29	11.45	10.93	11.16	D
220107	-139.1	14.1	-21.59	-26.54	-35.25	10.84	9.87	10.26	11.86	10.62	11.13	11.39	10.29	11.01	D
220109	-112.6	15.0	-19.07	-23.44	-32.57	14.88	13.16	13.42	15.07	12.93	13.81	14.85	12.71	13.77	C
220111	-112.8	13.7	-22.89	-26.72	-35.34	11.56	10.77	11.08	11.15	10.36	11.12	11.05	10.26	11.08	B
220113	-116.0	13.7	-20.91	-25.28	-33.45	13.17	11.81	12.84	13.36	11.75	13.35	12.97	11.46	13.27	B
220102	94.6	10.5	-14.80	-18.77	-28.29	15.59	14.85	15.60	15.78	14.01	14.39	16.19	14.10	14.47	+
220104	96.4	8.2	-18.23	-21.76	-31.52	13.56	12.87	12.77	12.18	11.46	11.44	12.37	11.49	11.47	+
220106	91.0	6.2	-35.58	-35.74	-38.00	6.97	7.01	8.03	7.64	7.41	7.34	7.53	7.37	7.33	+
220108	71.8	5.1	-38.18	-40.22	-38.93	5.23	5.22	5.61	7.65	7.29	7.39	7.47	7.19	7.41	+
220110	46.3	5.4	-32.19	-32.15	-37.73	5.71	6.41	5.94	7.75	7.86	8.31	7.78	7.92	8.30	+
220112	45.0	5.7	-35.53	-35.44	-38.09	5.20	5.78	6.04	7.66	7.54	8.14	7.60	7.55	8.12	+

TABLE 8.18 (7)

SL2-3	COMMAND ASPECT ANGLE	ANGLE 3 MET. WIND	SIGMA, DB			REDUCTION 4			REDUCTION 5			REDUCTION 6			QUAL
			VV	HH	HV+VH	VV	HH	HV+VH	VV	HH	HV+VH	VV	HH	HV+VH	
156102	11.8	14.0	-12.86	-13.54	-27.76	13.67	13.61	14.17	13.19	13.05	13.51	13.03	12.84	13.42	+
156103	6.4	14.0	-13.01	-13.19	-28.15	13.65	13.83	14.09	13.06	13.37	13.18	12.82	13.06	13.00	+
156104	1.0	13.0	-11.83	-12.79	-26.95	14.25	14.08	14.62	14.30	13.77	14.28	14.05	13.41	14.09	A
156105	.7	13.0	-11.47	-12.59	-26.89	14.44	14.21	14.65	14.72	14.00	14.34	14.48	13.64	14.15	A
156107	-15.1	12.0	-13.46	-14.51	-28.41	13.22	12.89	13.73	12.56	12.13	12.90	12.44	11.98	12.84	A
156108	-20.3	10.0	-13.27	-13.91	-29.11	13.18	13.33	13.05	12.57	12.60	12.17	12.54	12.58	12.17	+
156109	-25.7	8.0	-13.70	-14.64	-29.03	12.60	12.62	12.75	11.92	11.79	11.94	11.95	11.83	12.00	+
156110	-36.1	4.0	-14.11	-15.14	-29.28	11.65	11.88	11.82	11.06	11.04	11.10	11.16	11.17	11.22	+
156114	-67.0	13.0	-13.80	-14.27	-27.67	11.22	12.12	12.37	11.52	12.03	12.40	11.91	12.57	12.84	+
156115	-57.3	14.0	-12.83	-13.70	-27.34	12.36	12.82	12.87	12.35	12.59	12.62	12.79	13.19	13.07	+
156116	-47.5	15.0	-13.04	-13.84	-27.79	12.38	12.96	12.75	11.83	12.13	11.96	12.10	12.51	12.24	+
156117	-47.9	17.0	-11.27	-12.10	-24.82	14.94	15.22	16.70	13.60	14.04	14.71	14.05	14.72	15.25	+
156118	-48.0	18.0	-10.70	-12.16	-24.87	15.92	15.13	16.62	14.27	13.97	14.66	14.80	14.64	15.20	+
156119	-68.3	20.0	-9.65	-10.61	-23.60	16.24	15.58	16.71	16.20	16.50	16.59	17.20	17.94	17.49	+
156121	-67.6	23.0	-10.60	-11.80	-24.27	14.84	14.27	15.84	14.84	14.64	15.72	15.58	15.59	16.49	+
156122	-67.0	24.0	-10.90	-11.65	-24.36	14.43	14.39	15.69	14.43	14.83	15.59	15.10	15.81	16.32	+
157102	157.9	11.0	-15.27	-17.83	-30.86	9.31	8.26	9.18	11.70	10.85	11.62	10.98	10.14	10.98	M
157103	159.0	14.0	-12.96	-15.02	-27.74	11.75	11.05	12.20	13.91	13.34	14.30	12.95	12.22	13.45	M
162102	-2.6	8.0	-18.97	-19.35	-34.43	11.18	10.40	11.82	8.97	9.16	9.15	8.88	9.03	9.00	+
162103	-8.0	5.0	-20.26	-21.80	-38.88	10.43	9.22	10.04	8.43	8.40	7.55	8.40	8.36	7.48	+
162105	-28.8	6.0	-18.94	-19.07	-34.88	8.67	9.23	8.64	8.62	9.11	8.55	8.70	9.16	8.57	+
162106	-28.8	9.0	-15.59	-16.23	-32.32	10.83	11.18	10.14	10.36	10.52	9.70	10.40	10.57	9.73	+
162107	-34.5	9.0	-15.51	-15.82	-31.18	10.46	11.30	10.37	10.16	10.61	10.02	10.24	10.71	10.10	+
162108	-34.8	9.0	-13.64	-13.55	-28.35	12.20	13.60	12.79	11.47	12.40	11.83	11.58	12.61	11.98	+
162109	-34.9	9.0	-14.71	-14.88	-30.79	11.13	12.17	10.63	10.67	11.27	10.22	10.76	11.40	10.30	+
162111	-75.5	8.0	-14.14	-14.95	-29.95	11.24	11.64	10.68	10.88	10.88	10.29	11.04	11.03	10.41	+
162112	-70.8	14.0	-12.65	-13.28	-27.29	12.41	12.82	12.59	12.38	12.68	12.47	12.75	13.18	12.83	+
162113	-81.0	15.0	-11.86	-12.66	-26.91	13.21	13.07	12.92	12.77	12.66	12.28	12.86	12.68	12.33	+
162114	-106.2	10.0	-13.65	-14.58	-29.64	13.45	13.16	12.71	13.39	12.78	12.19	13.51	12.83	12.24	+
216202	159.6	20.6	-7.19	-8.99	-21.89	24.67	25.15	21.96	23.49	24.09	22.50	22.57	22.89	21.53	B
216203	163.7	19.0	-7.89	-9.63	-22.65	21.94	22.78	19.90	21.51	22.25	20.83	20.10	20.44	19.54	+
216204	169.6	16.6	-9.71	-11.78	-24.63	16.58	16.26	15.80	17.58	17.51	17.35	15.80	15.35	15.81	+
216205	-179.5	14.3	-11.16	-12.99	-26.01	13.44	13.46	13.48	15.07	15.34	15.26	13.24	13.16	13.63	B
216206	-167.7	13.1	-12.92	-14.08	-27.25	11.21	11.88	12.23	13.51	14.23	14.41	12.24	12.61	13.20	B
216207	-156.8	12.7	-11.27	-13.49	-26.70	14.52	13.44	13.67	16.14	15.25	15.46	15.16	14.05	14.64	B
216208	-148.8	12.7	-10.84	-11.99	-25.22	16.03	16.61	16.72	16.95	17.50	17.26	16.29	16.65	16.69	B
216209	-143.9	13.1	-9.92	-11.69	-24.93	18.18	17.24	17.25	18.56	17.95	17.56	18.14	17.35	17.15	+
216210	-139.9	14.0	-10.25	-11.32	-23.90	17.70	17.82	19.04	18.16	18.67	19.10	17.84	18.33	18.88	+
220202	-131.6	8.2	-15.78	-15.86	-30.95	11.38	12.32	11.31	11.66	12.40	11.57	11.38	12.06	11.35	D
220203	-120.6	11.4	-14.03	-14.28	-28.47	13.51	13.85	13.74	13.92	14.48	14.22	13.90	14.53	14.24	D
220204	-114.9	15.4	-13.69	-13.75	-27.90	13.76	13.98	14.04	14.25	14.93	14.74	14.37	15.18	14.89	C
220205	-116.9	14.1	-17.10	-21.58	-33.40	11.60	10.29	10.76	10.91	8.77	10.19	10.87	8.79	10.16	C
220207	-130.1	12.1	-16.11	-16.47	-30.73	11.26	11.92	11.60	11.45	11.86	11.80	11.20	11.56	11.59	C
220208	-140.0	11.6	-14.70	-15.38	-30.69	11.54	12.15	10.81	12.36	12.75	11.60	11.92	12.20	11.26	B
220209	-147.0	11.4	-13.64	-14.40	-29.32	12.01	12.77	11.47	13.36	13.92	12.77	12.76	13.14	12.29	B
220210	-149.9	10.8	-12.21	-12.94	-26.56	13.64	14.81	14.45	15.01	15.97	15.60	14.71	14.79	14.93	+
220211	-145.8	9.9	-12.01	-13.16	-26.64	14.33	14.65	14.67	15.31	15.56	15.43	14.71	14.79	14.93	+
220212	-138.9	8.8	-14.42	-15.14	-29.94	11.94	12.49	11.57	12.67	13.02	12.19	12.24	12.48	11.84	C
220305	1.8	9.7	-14.95	.00	.00	12.78	.00	.00	11.38	.00	.00	11.13	.00	.00	C
220306	-12.7	10.8	-13.72	.00	.00	13.13	.00	.00	12.36	.00	.00	12.20	.00	.00	C
220307	-19.3	13.5	-14.29	.00	.00	12.47	.00	.00	11.72	.00	.00	11.66	.00	.00	C
220308	-17.4	16.8	-14.58	.00	.00	12.39	.00	.00	11.55	.00	.00	11.46	.00	.00	C
220309	-17.9	17.6	-14.24	.00	.00	12.59	.00	.00	11.81	.00	.00	11.73	.00	.00	C

TABLE 8.18 (8)

220310	-21.3	16.4	-13.62	.00	.00	12.87	.00	.00	12.21	.00	.00	12.19	.00	.00	+
220402	58.8	11.6	.00	-22.61	.00	.00	6.89	.00	.00	8.01	.00	.00	8.15	.00	D
220403	53.8	11.6	.00	-17.55	.00	.00	9.47	.00	.00	9.64	.00	.00	9.87	.00	D
220404	45.5	11.6	.00	-16.35	.00	.00	10.42	.00	.00	10.25	.00	.00	10.48	.00	D
220405	45.0	11.1	.00	-19.37	.00	.00	8.35	.00	.00	8.79	.00	.00	8.93	.00	+
220406	40.7	10.4	.00	-17.88	.00	.00	9.44	.00	.00	9.39	.00	.00	9.51	.00	+
245204	132.6	5.0	-18.11	-18.55	-35.36	9.57	10.19	8.30	9.91	10.23	8.93	9.71	9.98	8.77	M
245205	99.6	5.0	-23.38	-19.28	-40.74	9.18	11.32	8.27	7.20	8.91	6.69	7.34	8.89	6.68	M
245206	52.5	7.0	-19.12	-20.27	-35.45	7.20	7.80	6.57	8.26	8.54	7.94	8.47	8.71	8.07	M
245207	9.3	9.0	-13.20	-15.22	-28.89	13.51	12.47	13.69	12.87	11.53	12.56	12.67	11.28	12.41	M
245208	-22.5	14.0	-12.64	-13.89	-28.41	13.65	13.34	13.40	13.07	12.56	12.61	13.09	12.58	12.66	M
245209	-92.9	18.0	-10.32	-11.64	-24.45	14.59	13.63	14.74	15.34	14.24	15.29	15.41	14.06	15.30	M
245211	152.7	40.0	-4.46	-6.06	-16.35	37.46	38.42	40.75	31.94	34.00	37.02	33.13	35.91	38.38	M
245213	144.5	28.0	-6.72	-9.01	-20.46	26.70	23.57	26.21	25.54	23.99	25.51	26.01	24.19	25.68	M
245214	145.2	24.0	-7.91	-9.99	-22.41	23.03	21.02	21.73	22.57	21.51	21.58	22.52	21.23	21.34	M
245215	146.9	21.0	-10.37	-12.22	-24.92	17.08	16.21	17.09	17.72	17.06	17.63	17.15	16.28	17.13	M
245216	148.9	18.0	-11.43	-13.52	-26.21	14.98	13.90	15.00	16.08	15.10	15.99	15.40	14.22	15.42	M
245217	151.5	15.0	-13.29	-14.20	-28.48	12.00	12.71	11.97	13.71	14.26	13.61	13.00	13.32	13.00	M
245218	154.2	12.0	-14.31	-15.43	-29.66	10.56	10.90	10.53	12.63	12.89	12.58	11.91	11.98	11.96	M
245220	159.8	7.0	-16.60	-17.11	-32.86	8.10	8.75	7.56	10.64	11.39	10.28	10.01	10.54	9.72	M
247106	-50.0	9.0	-20.12	-20.69	-36.02	6.73	7.58	6.32	7.89	8.41	7.73	8.09	8.56	7.84	C
247107	-40.2	8.0	-18.54	-20.43	-35.61	7.92	7.89	7.02	8.48	8.48	7.92	8.62	8.59	7.99	C
247108	-40.6	7.0	-16.68	-17.89	-32.72	9.13	9.44	8.73	9.33	9.38	9.03	9.46	9.51	9.13	C
247109	-40.5	8.0	-15.53	-17.01	-31.95	10.06	10.10	9.29	9.98	9.81	9.40	10.11	9.94	9.50	C
247110	-20.9	9.0	-14.37	-15.59	-30.31	12.33	11.97	12.23	11.60	11.19	11.27	11.56	11.13	11.26	C
247111	-11.1	12.0	-11.36	-13.41	-26.43	14.61	13.70	14.88	14.84	13.18	14.81	14.74	12.96	14.75	C
247112	-11.0	16.0	-13.06	-13.84	-28.12	13.56	13.39	14.01	12.99	12.74	13.20	12.82	12.51	13.08	C
247113	-11.5	23.0	-14.58	-15.65	-30.17	12.69	12.17	13.00	11.65	11.21	11.58	11.48	11.01	11.45	C
247114	-11.6	26.0	-7.68	-9.04	-23.03	17.37	17.61	16.89	20.48	19.52	19.07	21.05	20.06	19.33	C
247115	-11.7	25.0	-7.09	-8.16	-21.88	17.89	18.60	17.64	21.65	21.37	20.87	22.43	22.32	21.33	C
247116	-22.0	20.0	-8.47	-9.84	-23.37	18.13	17.80	17.68	18.54	17.88	18.07	19.14	18.60	18.52	C
247117	-22.3	17.0	-9.85	-11.23	-24.56	16.48	16.08	16.57	16.39	15.68	16.51	16.69	16.02	16.80	C
247118	-22.6	15.0	-9.93	-11.51	-25.25	16.41	15.77	15.96	16.25	15.28	15.67	16.55	15.57	15.90	C
247119	-32.8	13.0	-11.02	-12.50	-26.31	15.49	14.88	15.00	14.09	13.56	13.68	14.34	13.86	13.92	C
247120	-43.1	12.0	-12.07	-13.61	-27.04	13.85	13.35	13.83	12.66	12.25	12.54	12.93	12.57	12.82	C
247121	-53.5	11.0	-12.27	-12.92	-27.26	13.21	13.86	13.11	12.77	13.32	12.57	13.22	13.99	12.97	C
247122	-53.6	11.0	-12.67	-14.33	-27.92	12.66	12.24	12.35	12.38	11.87	12.02	12.78	12.32	12.38	C
247123	-54.0	12.0	-13.68	-14.13	-28.88	11.43	12.45	11.33	11.48	12.07	11.30	11.80	12.55	11.61	C
247124	-54.5	12.0	-14.57	-15.63	-30.47	10.49	10.99	9.87	10.79	10.84	10.27	11.07	11.17	10.51	C
247125	-14.4	6.0	-15.26	-16.14	-31.50	12.16	11.78	12.16	11.09	10.86	10.67	10.97	10.72	10.58	C
247126	-25.1	6.0	-16.31	-17.01	-31.96	10.63	10.76	10.79	10.08	10.16	10.08	10.08	10.17	10.09	C
247127	-15.4	5.0	-17.77	-18.98	-34.73	10.77	10.10	10.60	9.51	9.33	8.99	9.46	9.27	8.92	C
252102	140.7	9.9	-19.35	-19.50	-34.43	7.93	8.64	8.02	9.09	9.66	9.32	8.90	9.39	9.07	+
252103	131.6	10.9	-20.30	-20.92	-35.38	8.43	8.91	8.40	8.75	9.64	8.94	8.66	8.92	8.79	+
252104	127.5	11.4	-22.40	-23.54	-36.85	7.94	8.25	8.08	7.97	8.24	8.39	7.98	8.23	8.29	C
252105	122.4	11.8	-17.79	-18.12	-33.29	10.82	11.42	10.47	10.39	10.62	10.25	10.29	10.50	10.16	C
252106	117.1	11.4	-14.61	-14.18	-28.99	13.13	13.82	13.35	13.24	14.48	13.66	13.25	14.63	13.72	C
252107	111.0	11.1	-13.70	-14.20	-28.55	13.64	13.56	13.49	13.93	13.88	13.74	14.08	14.06	13.86	+
252108	100.8	10.9	-13.52	-13.49	-28.55	13.20	13.27	12.97	12.74	13.15	12.37	12.77	13.11	12.38	D
252109	90.7	11.0	-15.77	-16.48	-31.53	11.33	11.65	10.91	9.84	9.74	9.38	9.78	9.61	9.29	+
252110	83.4	11.5	-22.39	-21.01	-39.19	7.84	9.44	7.18	7.10	8.08	6.68	7.24	8.11	6.67	+
252111	80.4	10.9	-10.04	-11.06	-24.43	14.85	14.11	14.83	14.96	14.66	14.72	15.24	14.90	14.93	+
252112	77.3	9.3	-10.33	-11.38	-25.16	14.68	14.06	14.33	14.69	14.45	14.10	15.08	14.88	14.39	+
252113	69.9	8.4	-12.87	-13.81	-27.77	12.19	12.41	12.18	12.20	12.19	12.11	12.58	12.65	12.46	+
252114	44.8	3.2	-24.29	-26.50	-50.67	5.35	5.46	2.44	6.86	7.60	5.49	7.06	7.60	5.42	+
252115	-39.4	3.1	-20.82	-20.47	-36.92	6.82	7.90	6.43	7.70	8.48	7.53	7.86	8.59	7.59	+
252116	-63.4	6.6	-13.89	-14.04	-28.47	11.14	12.31	11.57	11.44	12.23	11.74	11.82	12.80	12.12	+

TABLE 8.18 (9)

252117	-64.6	9.7	-13.17	-13.14	-27.00	11.87	13.14	12.99	12.07	13.16	12.97	12.50	13.88	13.46	+
252118	-59.7	12.2	-12.13	-12.75	-27.71	13.18	13.78	12.38	13.11	13.69	12.35	13.66	14.53	12.78	D
252119	-49.7	13.9	-10.51	-11.97	-25.46	16.20	15.33	15.65	14.58	14.29	14.11	15.19	15.07	14.61	+
252120	-37.8	15.8	-9.38	-10.79	-25.21	18.46	17.46	16.35	15.87	15.57	14.41	16.42	16.30	14.77	+
252121	-26.8	17.9	-12.79	-13.81	-28.90	13.41	13.39	12.78	12.67	12.48	11.96	12.73	12.57	12.03	D
252122	-20.1	19.4	-12.50	-13.28	-27.63	13.81	13.88	14.06	13.32	13.24	13.41	13.32	13.25	13.45	D
252123	-15.3	20.9	-14.62	-15.31	-31.32	12.48	12.31	12.17	11.56	11.46	10.77	11.44	11.32	10.69	B
252124	-12.1	20.3	-15.84	-16.64	-33.95	12.00	11.54	11.32	10.71	10.54	9.37	10.56	10.37	9.27	B
252125	-12.1	20.5	-16.66	-17.25	-32.31	11.59	11.19	12.00	10.18	10.18	10.22	10.06	10.03	10.11	D
252126	-13.4	19.1	-13.76	-13.46	-28.06	13.08	13.68	13.98	12.31	13.12	13.23	12.17	12.96	13.15	B
252127	-13.3	17.0	-11.05	-11.75	-25.11	14.87	15.09	15.69	15.18	15.13	16.27	15.15	15.09	16.34	B
252128	-11.1	14.9	-13.15	-13.45	-27.27	13.50	13.67	14.44	12.90	13.13	13.98	12.73	12.91	13.88	A
252129	-5.2	12.5	-7.73	-8.67	-22.43	16.72	17.51	16.79	20.42	20.17	19.99	20.78	20.55	20.18	A
252130	3.8	11.1	-8.16	-9.40	-23.20	16.37	16.78	16.35	19.61	18.73	18.82	19.83	18.82	18.88	A
252131	14.9	10.5	-7.60	-8.75	-22.52	17.93	18.30	17.58	20.53	20.11	19.77	21.23	20.96	20.20	B
252132	25.0	9.7	-8.46	-9.75	-23.90	18.63	18.24	17.43	18.28	17.86	17.09	16.93	18.70	17.50	B
252133	32.2	8.4	-10.38	-11.59	-26.24	16.43	16.09	15.09	14.89	14.69	13.86	15.22	15.13	14.03	B
252134	23.3	5.8	-16.74	-18.12	-34.23	10.53	10.13	9.73	9.89	9.63	9.02	9.89	9.63	9.02	B
216103	-140.3	16.6	-14.29	-14.71	-28.56	11.94	12.87	12.82	12.76	13.49	13.39	12.30	12.91	13.01	+
216105	-137.5	14.8	-11.39	-12.86	-25.75	15.89	15.34	16.32	16.46	16.02	16.54	16.10	15.57	16.26	+
216107	-132.8	14.0	-14.47	-14.83	-28.77	12.45	13.19	13.11	12.85	13.49	13.37	12.53	13.11	13.12	B
216109	-127.2	15.5	-13.03	-14.51	-27.50	14.23	13.67	14.53	14.90	14.08	15.01	14.75	13.89	14.91	B
216111	-122.5	20.3	-12.28	-13.57	-26.36	15.03	14.40	15.53	16.25	15.50	16.68	16.35	15.60	16.82	B
216113	-122.0	23.2	-11.49	-12.82	-25.34	15.79	14.98	16.46	17.54	16.74	18.15	17.80	17.02	18.42	B
216102	43.2	17.7	-9.93	-11.68	-25.03	17.48	16.00	16.53	15.07	14.39	14.42	15.62	15.02	14.85	+
216104	46.9	17.9	-10.84	-12.88	-25.69	15.70	14.17	15.45	14.05	13.08	13.79	14.53	13.58	14.22	+
216106	49.8	17.9	-12.37	-13.69	-27.48	13.20	13.07	13.01	12.52	12.35	12.26	12.89	12.80	12.60	+
216108	51.3	17.6	-13.51	-14.01	-28.73	11.69	12.65	11.58	11.54	12.09	11.34	11.84	12.53	11.62	+
216110	53.1	17.1	-13.86	-13.90	-28.46	11.26	12.72	11.79	11.31	12.26	11.59	11.61	12.75	11.91	+
216112	52.6	16.4	-12.84	-14.39	-27.60	12.48	12.21	12.74	12.18	11.79	12.24	12.55	12.21	12.61	C
216114	53.4	17.1	-10.95	-12.62	-25.24	15.24	14.25	15.76	14.24	13.67	14.50	14.86	14.40	15.10	A
220103	-130.8	14.8	-12.36	-14.79	-27.17	14.86	13.31	14.80	15.55	13.60	15.16	15.33	13.28	14.98	+
220105	-131.0	14.7	-14.92	-16.56	-30.99	12.18	11.79	11.33	12.50	11.76	11.56	12.21	11.45	11.35	D
220107	-124.4	15.0	-13.88	-14.33	-28.24	13.53	13.84	13.90	13.99	14.39	14.35	13.87	14.32	14.29	B
220109	-112.7	15.0	-12.71	-14.42	-27.32	14.35	13.53	14.33	15.38	13.79	15.25	15.65	13.95	15.47	B
220111	-115.2	12.8	-15.60	-15.37	-29.84	12.53	13.12	12.81	12.16	12.89	12.80	12.16	12.94	12.84	B
220113	-119.1	12.8	-14.58	-14.72	-29.21	13.12	13.54	13.21	13.30	13.86	13.48	13.27	13.90	13.49	B
220102	80.5	13.1	-10.30	-12.06	-23.92	14.59	13.45	15.26	14.61	13.36	15.31	14.84	13.46	15.56	+
220104	81.2	10.5	-12.93	-13.45	-27.02	12.38	12.61	12.85	11.73	11.87	12.18	11.76	11.85	12.23	+
220106	79.7	8.8	-14.06	-15.71	-29.61	11.50	11.35	11.11	10.81	10.17	10.34	10.87	10.18	10.38	+
220108	67.3	7.7	-21.00	-22.40	-36.03	6.80	7.44	6.75	7.62	8.00	7.74	7.85	8.14	7.88	+
220110	52.8	7.6	-20.57	-20.68	-34.93	6.51	7.60	6.85	7.76	8.43	8.13	7.97	8.59	8.27	B

TABLE 8.18 (10)

SL4	COMMAND ASPECT ANGLE	ANGLE 1 MET. WIND	SIGMA, DB			REDUCTION 4			REDUCTION 5			REDUCTION 6			QUAL
			VV	HH	HV+VH	VV	HH	HV+VH	VV	HH	HV+VH	VV	HH	HV+VH	
334103	-31.7	11.3	-7.82	-10.82	-12.11	17.29	18.29	14.66	15.86	17.87	16.02	16.31	18.88	15.98	D
334102	-164.6	14.4	-9.88	-11.67	-11.75	14.64	19.25	20.67	15.64	20.17	18.03	15.09	19.29	17.74	D
334104	-147.1	14.4	-4.89	-7.05	-8.30	30.55	24.91	29.52	25.88	24.71	22.48	27.18	25.38	23.54	D
338103	-138.0	19.2	-11.43	-11.20	-11.65	9.83	21.70	16.60	12.81	21.42	17.58	11.99	20.64	17.20	D
338105	-134.0	17.8	-10.44	-10.50	-12.61	11.62	22.85	12.55	13.81	22.76	17.01	13.13	22.37	16.55	D
338107	-150.9	18.1	-6.03	-10.06	-10.89	24.81	21.71	20.21	22.26	22.22	18.38	22.82	22.05	18.25	D
338109	175.0	22.9	-7.06	-9.73	-9.75	22.06	20.82	21.13	22.63	22.53	21.09	22.69	22.28	21.30	D
338111	162.1	23.1	-7.76	-11.96	-11.28	19.38	19.05	20.61	19.32	19.77	18.47	19.22	18.81	18.29	C
338113	158.2	19.5	-8.86	-12.30	-11.48	16.21	18.87	19.75	16.62	19.25	18.07	16.25	18.19	17.86	C
338115	148.4	15.1	-8.68	-11.49	-10.90	15.91	20.38	20.04	16.00	20.39	18.27	15.65	19.58	18.10	+
338117	114.6	9.7	-9.29	-12.37	-11.89	16.67	23.22	18.44	18.33	23.51	21.60	17.42	22.64	20.82	C
338121	132.4	4.4	-8.88	.00	.00	15.39	.00	.00	16.03	.00	.00	15.59	.00	.00	+
338102	32.4	17.6	-9.03	-12.43	-13.08	14.82	16.00	12.33	14.36	15.42	15.79	14.39	15.99	15.65	+
338104	46.2	19.4	-10.26	-12.06	-12.20	13.55	17.28	15.65	13.68	16.72	16.23	13.37	16.92	16.15	+
338106	49.1	19.2	-9.55	-11.73	-11.97	16.52	18.81	18.28	15.94	19.14	17.25	15.85	19.09	17.21	+
338108	61.1	16.7	-11.33	-12.65	-14.15	14.89	20.12	17.47	15.63	20.94	17.39	15.08	20.30	16.97	+
338110	68.2	13.5	-8.65	-12.61	-12.40	23.37	21.46	22.87	24.38	22.40	21.55	24.29	21.60	21.28	C
338112	28.4	8.6	-9.88	-12.64	-11.96	12.87	15.36	14.70	13.39	15.01	16.02	13.20	15.78	16.02	+
338114	-14.4	11.5	-7.67	-15.20	-11.52	15.70	10.31	14.95	15.35	10.86	15.99	15.93	11.80	16.04	+
338116	-23.3	14.5	-7.26	-11.63	-10.50	17.38	16.43	17.90	16.24	16.34	16.60	17.00	17.58	16.96	+
338118	-22.9	12.6	-8.12	-12.54	-12.35	15.51	15.20	13.47	15.03	15.22	15.86	15.43	16.30	15.82	+
338120	-16.3	7.0	-9.56	-14.41	-11.65	12.57	11.71	14.73	13.42	12.19	15.97	13.35	13.19	16.02	D
4115	-49.8	36.9	-6.59	-8.36	-9.84	25.59	22.14	24.38	23.65	23.57	20.04	25.07	24.54	20.89	D
4117	-40.0	27.7	-8.67	-9.55	-11.51	16.79	20.48	17.54	15.55	20.51	16.58	15.69	21.47	16.60	D
4119	-15.4	20.3	-7.66	-11.54	-11.74	15.78	16.79	14.54	15.39	16.84	15.94	15.98	18.44	15.96	D
4121	-23.6	23.2	-7.90	-11.62	-11.40	16.02	16.79	15.69	15.33	16.67	16.17	15.81	17.94	16.29	D
4123	-21.8	25.2	-5.59	-9.04	-10.44	21.41	21.30	17.87	19.31	20.47	16.60	21.08	22.39	16.98	+
4125	-18.3	23.4	-6.21	-9.29	-9.50	19.26	20.94	19.73	17.83	20.13	17.14	19.18	22.12	17.87	B
4127	-21.6	15.1	-5.89	-8.54	-10.43	20.54	22.14	17.88	18.64	21.11	16.60	20.19	23.10	16.99	+
4129	-58.9	7.8	-7.70	-9.86	-10.50	24.40	21.67	24.29	24.40	23.75	22.35	25.19	24.27	23.24	+
4131	-120.2	9.0	-7.73	-9.89	-10.98	20.93	24.63	21.24	21.22	24.74	21.90	20.84	25.08	21.55	+
4133	-143.5	15.2	-8.90	-10.62	-11.57	15.15	21.77	17.30	15.48	21.71	17.50	15.07	21.22	17.18	C
4135	-153.7	24.4	-8.00	-10.63	-11.33	18.08	20.90	19.32	17.68	21.52	18.02	17.51	21.14	17.81	A
4137	-155.9	28.2	-5.42	-9.29	-9.35	27.39	22.11	23.67	25.26	23.06	20.97	26.26	23.24	21.53	D
4139	-161.1	27.4	-6.54	-10.08	-10.77	23.12	20.98	21.05	22.48	22.21	19.07	22.85	22.06	19.03	+
4141	-175.2	26.4	-6.37	-9.26	-9.57	24.17	21.24	21.03	24.97	23.02	21.43	25.36	22.96	21.73	+
4143	174.5	26.7	-7.62	-11.53	-12.80	20.49	19.16	22.64	20.98	20.29	17.19	20.85	19.26	16.73	+
4145	165.7	29.7	-6.54	-8.52	-10.35	23.31	22.23	21.47	23.27	23.75	19.88	23.62	24.13	19.96	B
4147	156.9	33.7	-5.22	-8.66	-8.67	28.28	22.65	24.79	26.27	23.64	22.42	27.44	24.05	23.48	B
4149	153.1	29.7	-5.35	-7.86	-8.52	27.81	23.70	26.47	24.98	24.25	22.39	26.00	24.86	23.46	B
4151	159.3	27.5	-3.71	-5.18	-6.54	35.95	25.43	27.21	34.36	24.77	28.52	37.30	24.83	32.25	+
7103	-92.4	7.4	.00	-10.68	.00	.00	24.77	.00	.00	24.90	.00	.00	25.11	.00	C
7105	-84.0	9.7	.00	-6.77	.00	.00	25.45	.00	.00	21.21	.00	.00	21.06	.00	C
7107	-71.7	10.8	.00	-4.82	.00	.00	25.17	.00	.00	18.46	.00	.00	12.55	.00	+
7109	-58.7	16.8	.00	-8.06	.00	.00	22.47	.00	.00	24.57	.00	.00	25.30	.00	B
7111	-58.5	25.0	.00	-10.79	.00	.00	20.96	.00	.00	22.74	.00	.00	22.94	.00	B
7113	-60.5	30.3	.00	-10.45	.00	.00	21.47	.00	.00	23.47	.00	.00	23.79	.00	B
8105	-49.5	23.8	-8.47	-9.50	-12.64	19.34	21.05	16.68	18.10	22.32	16.80	18.38	23.04	16.65	+
8111	-88.9	16.5	-10.32	-12.45	-11.59	18.77	23.98	25.45	19.69	24.11	26.56	18.02	22.94	25.06	+
8113	-85.8	24.4	.00	-11.45	-11.95	.00	24.14	25.22	.00	24.66	25.44	.00	24.27	24.00	+
8117	-83.8	31.9	-11.88	-15.23	-14.31	15.27	22.63	22.47	16.44	20.69	19.95	15.06	17.65	18.45	+
8119	-82.8	32.5	-6.80	-9.28	-9.48	33.32	24.61	28.30	36.71	24.66	34.92	36.05	25.47	35.84	+
8121	-81.9	32.7	-7.46	-8.80	-10.44	29.99	24.68	27.12	32.42	24.39	30.50	31.48	25.26	30.36	+

TABLE 8.18 (II)

9110	151.9	33.5	-6.85	-11.52	-10.96	21.66	20.08	20.06	20.08	20.33	18.34	20.27	19.56	18.20	+
9112	140.3	36.7	-5.36	-12.24	-10.39	28.81	20.32	22.13	24.15	19.71	18.90	25.08	18.46	18.77	D
9114	127.8	40.6	-6.09	-12.31	-10.01	26.94	21.73	25.29	24.45	21.54	21.58	24.98	20.38	21.64	B
9116	120.2	45.2	-5.24	-10.13	-8.64	34.30	24.45	32.89	32.30	24.64	28.62	33.45	24.88	30.18	D
9118	117.5	45.5	-4.79	-10.53	-8.19	38.56	24.35	34.74	36.93	24.61	31.99	38.55	24.76	34.41	D
9120	114.5	43.0	-4.28	-7.95	-8.00	44.07	26.06	35.16	43.21	24.07	34.71	45.50	24.51	37.64	D
9122	105.5	39.1	-5.30	-9.54	-8.66	38.98	25.41	31.74	40.62	24.70	36.03	40.49	25.47	37.59	D
9124	94.6	37.5	-6.26	-9.35	-9.38	35.41	25.32	28.97	38.04	24.49	35.16	36.59	25.44	35.19	D
9126	84.5	36.3	-7.33	-11.72	-11.54	30.62	23.95	25.80	33.04	24.49	26.69	31.84	23.90	25.50	D
11202	111.0	11.3	-10.97	-13.11	-11.94	13.00	23.04	19.26	15.60	23.10	22.40	14.47	21.77	21.44	B
11204	102.8	18.6	-9.70	-11.71	-11.90	18.05	24.41	21.90	19.52	24.60	24.24	17.98	24.19	22.83	B
11206	98.5	26.0	-10.27	-14.04	-11.51	17.31	23.40	24.02	18.70	22.67	26.05	17.06	20.41	24.54	+
11208	96.1	32.8	-8.02	-11.83	-10.26	25.82	24.43	27.17	26.98	24.59	30.94	25.10	23.99	30.07	+
11210	95.8	38.1	-6.04	-12.68	-9.89	36.50	24.07	27.95	39.22	24.63	32.56	37.89	22.74	32.01	D
11212	93.7	39.6	-6.77	-13.31	-10.87	32.54	23.80	26.14	34.68	23.45	28.80	33.01	21.63	27.49	D
11214	90.4	37.5	-7.03	-12.93	-9.78	31.66	23.87	28.16	33.86	23.75	33.67	32.23	22.19	33.38	D
11216	88.3	33.3	-7.64	-12.03	-10.38	28.86	24.10	27.24	30.62	24.39	31.04	28.96	23.55	30.29	D
11218	91.1	30.0	-9.31	-14.71	-17.82	21.70	23.20	15.76	22.63	21.77	16.30	20.80	18.91	15.59	D
11222	74.3	39.2	-7.74	-10.89	-11.71	28.01	23.15	25.03	30.23	24.55	24.79	30.10	24.59	24.48	+
11224	62.4	40.8	-6.54	-10.40	-11.51	30.28	21.76	22.93	32.10	23.81	21.56	34.04	24.14	21.86	D
11226	52.5	37.4	-6.46	-11.09	-9.75	27.05	19.89	25.08	25.77	20.96	21.19	27.44	21.09	22.27	D
11228	60.8	29.4	-7.22	-14.43	-11.77	26.81	18.86	22.00	27.51	18.12	20.51	28.69	16.74	20.66	B
11230	29.2	24.1	-6.83	-11.88	-10.94	19.31	16.62	17.46	17.29	16.25	16.47	18.22	17.15	16.68	D
11232	2.6	22.7	-6.73	-9.88	-9.37	17.09	20.05	18.57	16.42	19.21	16.79	17.34	21.30	17.29	B
11234	-5.0	20.6	-7.16	-11.44	-9.75	16.27	16.95	17.93	15.81	16.91	16.59	16.54	18.66	16.97	B
11236	-13.3	14.4	.00	-13.15	-14.28	.00	13.76	10.06	.00	14.25	15.71	.00	15.53	15.51	C
24106	102.6	25.2	-6.66	-9.58	-9.47	30.98	25.40	29.02	32.33	24.67	33.02	30.99	25.48	33.21	+
24108	90.4	23.4	-7.28	-12.34	-10.67	30.34	24.09	26.74	32.27	24.23	29.82	30.56	23.15	28.72	+
24110	74.9	21.8	-8.70	-10.30	-11.30	24.27	23.45	25.62	25.60	24.81	26.15	24.94	25.14	26.06	+
24112	64.6	20.1	-8.26	-11.47	-10.30	23.96	21.46	25.66	24.75	23.12	25.51	25.06	22.98	26.82	+
25102	64.5	13.4	-9.26	-9.88	-10.31	20.67	22.34	25.64	21.15	24.44	25.46	21.00	24.92	26.76	+
25104	73.5	13.0	-11.53	-13.92	-13.93	15.98	21.78	22.08	16.94	21.49	19.75	15.96	19.74	18.83	+
25106	89.3	12.8	-8.78	-11.18	-12.06	23.87	24.46	24.70	24.90	24.80	25.09	23.10	24.63	23.42	+
25108	110.0	14.3	-6.96	-11.17	-10.64	27.13	24.40	24.48	27.84	24.67	26.21	27.04	24.62	25.77	+
25110	128.8	17.7	-7.47	-10.48	-10.29	20.42	23.41	23.64	19.64	23.50	20.74	19.54	23.27	20.66	+
25112	137.5	23.1	-7.16	-9.77	-10.10	20.74	23.24	23.75	18.97	23.15	19.52	19.00	23.06	19.47	D
25114	137.2	27.0	-7.65	-9.53	-10.53	18.95	23.50	21.68	17.87	23.42	18.93	17.74	23.44	18.75	C
25116	130.0	27.0	-6.75	-10.74	-11.23	23.27	23.04	18.72	21.43	23.07	18.96	21.61	22.67	18.59	C
27106	15.0	5.9	-7.53	-14.63	-12.56	16.02	11.27	12.96	15.56	11.82	15.76	16.21	12.81	15.67	+
27108	3.6	8.5	-10.56	-14.60	-14.10	10.94	11.00	10.75	12.56	11.79	15.72	12.19	12.92	15.53	+
27110	-4.7	10.1	-9.75	-11.97	-12.30	12.01	15.89	13.48	13.11	16.08	15.74	12.95	17.70	15.63	+
27112	-9.9	10.5	-9.00	-13.96	-11.15	13.19	12.23	15.52	13.78	12.90	16.04	13.86	14.09	16.12	D
27114	-14.4	10.5	-7.72	-12.80	-11.98	15.60	14.43	14.04	15.29	14.83	15.86	15.85	16.16	15.84	+
27116	-16.8	11.1	-8.41	-16.34	-13.10	14.62	8.87	11.88	14.58	8.95	15.72	14.89	9.69	15.59	+
27118	-23.2	12.3	-8.17	-13.86	-11.12	15.44	13.03	16.34	14.98	13.04	16.28	15.36	13.86	16.47	+
27120	-29.6	13.6	-8.63	-14.12	-13.09	15.24	13.21	12.10	14.66	12.55	15.76	14.83	12.97	15.64	+
27122	-38.3	14.9	-10.17	-12.49	-12.41	13.45	16.50	14.77	13.60	15.75	16.07	13.31	15.94	15.97	+
27124	-46.7	15.9	-8.94	-12.46	-10.61	17.49	17.69	21.54	16.41	17.36	18.17	16.50	17.15	18.51	C
27126	-54.5	16.1	-8.91	-12.42	-11.92	19.36	19.05	19.89	18.75	19.55	18.42	18.90	19.13	18.44	C
27128	-61.2	15.3	-9.84	-12.45	-12.11	18.35	20.27	21.43	18.59	21.24	20.05	18.35	20.68	20.05	+
27130	-71.9	15.0	-12.88	-12.35	-12.70	13.15	22.20	23.31	14.62	23.19	21.80	13.64	22.44	21.21	+
27132	-86.6	14.9	-9.19	-13.85	-12.59	22.66	23.34	24.30	23.60	22.68	23.65	21.92	20.45	22.01	+
27134	-109.4	13.4	-8.87	-13.95	-12.66	19.18	22.62	17.26	20.56	22.26	21.20	19.39	20.35	20.03	+
27136	-134.3	12.5	-9.56	-12.93	-13.40	14.80	20.24	9.69	15.56	19.45	16.46	15.09	17.89	16.02	+
27138	-155.4	11.4	-8.80	-18.01	-12.04	16.11	13.12	18.15	16.42	9.76	17.41	16.06	7.68	17.11	+
29102	10.9	16.8	-8.54	-12.70	-11.17	13.97	14.54	15.50	14.26	14.96	16.05	14.49	16.38	16.14	B
29104	22.4	14.3	-8.32	-13.21	-11.57	15.08	14.04	15.20	14.78	14.12	16.08	15.11	15.09	16.17	B

TABLE 8.18 (12)

29106	47.4	13.5	-4.24	-13.16	-14.51	15.59	15.92	10.98	14.83	14.92	15.69	14.79	14.83	15.51	B
29108	53.0	15.3	.00	-12.62	.00	.00	18.61	.00	.00	18.82	.00	.00	18.35	.00	D
29110	49.8	17.0	-8.05	-9.73	-10.97	20.62	20.85	21.16	19.18	22.10	18.42	19.66	22.74	18.69	B
29112	50.9	17.2	-8.92	-11.52	-11.37	18.48	19.27	20.33	17.58	19.93	18.20	17.70	19.92	18.35	B
29114	58.8	16.1	-9.95	-14.56	-13.18	17.58	18.29	18.47	17.68	17.33	17.95	17.46	15.99	17.67	+
29116	60.8	15.0	-8.89	-11.50	-10.82	20.95	20.82	23.97	21.07	22.38	22.44	21.18	22.27	23.17	+
29118	62.6	13.6	.00	-14.71	.00	.00	19.11	.00	.00	18.14	.00	.00	16.56	.00	+
29202	-140.2	11.0	-4.21	-5.05	-7.12	36.04	26.13	36.51	29.10	24.87	25.67	31.10	25.30	27.83	+
29204	-148.0	11.6	-8.01	-9.36	-12.30	17.74	22.67	15.61	17.12	23.01	16.95	16.93	23.11	16.60	+
29206	-159.5	7.1	-10.15	-11.12	-10.84	13.60	20.02	20.86	14.86	20.91	18.90	14.28	20.33	18.84	+
29208	-149.4	4.3	-11.21	-12.14	-11.98	10.76	19.59	16.85	13.14	19.44	17.23	12.39	18.37	16.91	+
30102	58.3	18.2	-8.38	-11.03	-11.44	21.92	20.76	22.04	21.71	22.42	20.24	22.09	22.52	20.52	B
30104	66.8	17.2	-8.72	-11.81	-10.18	22.87	21.63	26.17	23.71	23.10	26.94	23.67	22.76	28.40	B
30106	44.5	14.9	-6.73	-12.29	-11.49	23.34	17.56	18.52	20.69	17.14	17.00	21.79	17.06	17.04	+
30108	18.3	16.4	-8.56	-12.17	-12.40	14.31	15.68	13.28	14.40	15.84	15.81	14.65	17.20	15.76	+
30110	7.0	18.8	-7.69	-13.25	-10.41	15.32	13.47	16.78	15.14	14.04	16.28	15.65	15.38	16.50	+
30112	6.8	19.8	-6.75	-10.36	-10.40	17.16	19.07	16.80	16.46	18.55	16.29	17.40	20.52	16.50	+
30114	5.6	17.4	-8.88	-13.19	-11.43	13.28	13.56	14.93	13.83	14.13	15.91	13.92	15.49	15.91	D
30202	-17.0	8.1	-5.59	-8.18	-9.15	20.17	23.11	19.68	18.78	21.54	17.18	20.49	23.75	17.94	+
30206	-162.7	7.5	-11.02	-11.75	-10.54	12.38	19.24	21.34	14.10	20.07	19.47	13.39	19.19	19.50	D
30208	-158.6	9.0	-11.01	-10.58	-10.52	11.98	20.62	21.29	13.85	21.61	19.28	13.15	21.26	19.32	+
30210	-138.3	7.4	-10.61	-14.18	-11.88	11.26	18.36	15.64	13.48	16.84	17.35	12.78	14.85	16.95	D
30212	-112.0	6.2	-10.11	-12.16	-12.45	14.90	23.61	17.07	17.02	23.92	21.08	15.94	23.22	20.06	+
32102	41.2	19.4	-8.14	-11.99	-12.07	18.31	17.48	16.20	16.60	16.98	16.35	16.93	17.14	16.28	+
32104	31.0	20.0	-7.22	-11.53	-10.72	18.65	17.25	18.34	16.77	16.83	16.64	17.49	17.70	16.90	D
32106	23.8	19.3	-6.83	-11.45	-10.00	18.47	17.10	19.25	16.97	16.94	16.93	17.95	18.25	17.47	D
32108	22.5	18.3	-7.25	-11.40	-9.40	17.30	17.15	20.64	16.22	17.03	17.35	16.99	18.40	18.16	D
32110	24.9	16.6	-8.90	-11.39	-12.61	14.23	17.23	12.96	14.21	17.02	15.82	14.33	18.28	15.75	+
32112	24.8	16.2	-8.34	-12.34	-10.31	15.27	15.62	18.58	14.82	15.51	16.75	15.13	16.54	17.17	B
32114	21.4	18.2	-7.95	-10.49	-11.43	15.70	18.75	15.46	15.20	18.42	16.12	15.67	20.06	16.24	+
32116	18.3	20.1	-6.20	-8.95	-9.66	19.28	21.56	19.34	17.84	20.59	17.02	19.19	22.64	17.67	+
32118	17.1	21.7	-5.52	-11.17	-9.29	20.91	17.49	20.06	19.19	17.41	17.26	21.01	19.04	18.07	+
32120	16.1	21.7	-8.44	-10.67	-11.94	14.38	18.43	14.16	14.48	18.17	15.89	14.77	19.95	15.89	D
32122	20.9	20.7	-8.23	-12.99	-12.70	15.12	14.34	12.69	14.85	14.50	15.78	15.22	15.59	15.70	+
32124	35.1	19.4	-8.66	-12.58	-11.08	15.97	16.03	17.93	14.99	15.31	16.57	15.13	15.67	16.70	+
32126	49.1	18.2	-11.68	-16.91	-12.83	12.37	13.72	16.09	13.33	10.24	16.62	12.76	9.12	16.45	+
32128	64.3	17.3	-12.13	-11.87	-13.85	13.77	21.18	19.25	14.92	22.62	18.28	14.19	22.28	17.79	+
32130	77.6	17.0	-9.31	-16.84	-13.10	22.37	21.25	23.77	23.39	17.50	21.87	22.35	14.11	20.77	+
32132	90.2	17.4	-9.60	-16.83	-12.81	20.84	22.32	23.42	21.74	18.57	23.07	19.96	14.57	21.28	+
32134	96.4	18.1	-10.47	-10.39	-10.98	17.16	25.00	25.59	18.47	24.89	28.10	16.81	25.33	26.76	B

TABLE 8.18 (13)

SL4	COMMAND		ANGLE 2			SIGMA, DB			REDUCTION 4			REDUCTION 5			REDUCTION 6			QUAL
	ASPECT	MET.	WIND															
				VV	HH	HV+VH	VV	HH	HV+VH	VV	HH	HV+VH	VV	HH	HV+VH			
334103	-21.6	10.4		-9.76	-9.73	-10.99	10.82	16.16	14.79	11.14	16.07	14.98	10.36	17.08	15.15	D		
334104	-145.1	14.5		-4.23	-7.79	-8.41	28.31	26.63	26.48	26.57	25.26	24.31	27.13	26.09	24.70	+		
338103	-131.3	20.8		-8.47	-10.74	-11.20	14.77	18.22	17.53	18.40	22.07	20.51	16.84	20.71	19.79	D		
338105	-127.5	20.8		-7.93	-9.53	-12.39	16.75	23.25	13.98	20.36	25.05	18.94	19.15	25.04	18.01	D		
338107	-150.5	20.3		-4.62	-8.49	-8.79	25.08	23.05	23.43	24.62	23.05	22.27	25.44	23.52	22.91	D		
338109	172.6	24.3		-5.10	-7.59	-8.97	19.87	18.50	18.97	20.46	20.21	17.62	22.04	21.31	18.46	D		
338111	157.6	21.6		-6.90	-9.47	-10.62	18.20	19.96	18.31	18.39	19.78	17.70	18.45	19.54	17.93	C		
338113	153.7	18.8		-9.17	-10.71	-12.40	13.80	18.28	15.11	14.43	18.17	16.00	12.97	16.72	15.46	C		
338115	145.0	15.3		-10.00	-11.51	-12.44	11.34	16.06	14.14	13.64	18.10	16.63	11.41	15.70	15.87	D		
338117	117.2	10.5		-9.99	-10.12	-11.81	12.36	21.59	16.72	16.98	24.86	21.80	14.83	24.84	20.98	C		
338102	35.2	17.4		-7.04	-9.82	-11.73	17.64	17.88	14.90	17.48	18.13	15.66	17.84	18.10	15.47	B		
338104	42.2	19.8		-7.78	-10.73	-11.01	17.14	17.05	17.87	17.43	17.64	17.36	17.25	16.65	17.48	+		
338106	48.3	19.6		-8.89	-10.05	-12.48	15.82	19.41	15.22	16.58	20.30	16.55	15.83	20.16	16.19	+		
338108	55.2	16.2		-7.72	-10.66	-11.41	19.87	19.21	19.14	20.94	20.44	19.65	21.17	20.12	19.87	+		
338110	51.3	11.6		-9.53	-10.63	-12.01	15.14	18.67	16.87	15.98	19.76	17.73	14.95	19.24	17.62	+		
338112	3.5	9.6		-8.23	-12.14	-11.42	12.51	11.95	12.98	11.38	9.04	13.61	11.77	8.77	12.58	+		
338114	-25.4	13.6		-6.86	-9.50	-10.89	16.55	17.05	15.47	16.28	17.15	15.46	17.18	16.07	15.75	+		
338116	-32.1	15.3		-6.45	-9.48	-9.67	18.58	18.10	19.78	18.12	18.28	17.62	18.97	18.72	18.49	+		
338118	-32.9	12.2		-8.29	-11.32	-12.79	14.49	14.64	12.43	14.78	14.89	14.67	14.41	13.66	14.00	D		
338120	-29.5	6.7		-8.44	-9.68	-11.58	13.76	17.29	14.49	14.08	17.47	15.29	13.75	17.91	15.21	+		
4115	-51.9	39.8		-5.05	-7.39	-8.47	26.62	25.91	28.58	27.25	26.18	25.88	28.45	27.98	27.19	D		
4117	-50.3	30.4		-5.66	-7.09	-9.28	24.43	26.48	25.07	24.90	26.41	22.86	26.00	28.25	23.79	D		
4119	-47.6	24.7		-6.57	-9.97	-11.34	21.28	19.48	17.93	21.61	20.31	17.93	22.26	20.21	17.99	D		
4121	-40.8	25.2		-6.92	-9.37	-9.92	18.99	19.73	20.87	18.92	20.05	18.72	19.27	20.31	19.31	+		
4123	-32.1	26.2		-3.91	-7.27	-7.75	26.11	22.92	26.48	23.85	22.46	20.87	26.13	24.69	22.82	B		
4125	-26.4	24.2		-4.57	-6.53	-8.17	22.62	23.24	23.15	21.07	22.84	18.89	23.41	25.91	20.79	B		
4127	-45.8	14.7		-4.15	-6.64	-7.75	28.48	27.02	30.57	27.56	26.25	25.21	29.03	28.22	26.79	B		
4129	-90.0	10.8		-6.08	-7.97	-9.85	27.30	27.68	25.93	26.88	26.42	25.50	26.52	27.17	24.87	+		
4131	-123.2	13.3		-6.51	-9.98	-10.36	22.58	21.70	21.50	24.98	24.74	24.69	24.46	24.60	24.02	+		
4133	-142.7	18.1		-6.18	-10.70	-10.34	21.33	18.12	19.77	21.80	20.10	20.14	21.55	18.42	19.87	A		
4135	-154.8	28.2		-5.46	-9.39	-9.48	21.65	20.44	20.73	21.93	20.53	20.03	22.66	20.32	20.64	A		
4137	-161.1	28.1		-5.02	-7.10	-8.31	21.49	21.68	21.56	22.12	23.49	21.05	23.42	25.18	22.40	A		
4139	-166.1	26.0		-8.41	-9.86	-11.26	16.12	18.99	17.58	14.61	17.14	15.80	14.01	16.45	15.70	+		
4141	-175.4	24.6		-6.37	-8.70	-10.07	18.45	18.43	18.31	17.59	17.73	16.06	18.38	17.75	16.28	+		
4143	175.4	24.0		-7.30	-9.26	-11.20	17.59	18.56	17.84	15.83	16.66	15.07	16.01	16.17	14.73	B		
4145	168.6	27.1		-3.83	-6.86	-7.56	21.98	19.31	20.51	23.94	22.30	20.69	26.09	24.10	22.43	B		
4147	154.8	30.9		-3.52	-7.30	-8.02	27.03	24.00	24.18	26.97	24.43	23.27	28.35	25.85	24.51	B		
4149	149.9	28.5		-2.78	-4.52	-6.20	32.15	33.13	33.28	29.98	29.34	30.48	30.85	29.39	32.15	B		
4151	157.2	25.9		-2.78	-4.30	-5.65	28.08	27.41	29.07	28.68	28.66	30.00	30.25	29.54	32.72	C		
7105	-88.1	11.8		.00	-9.98	.00	.00	23.12	.00	.00	22.41	.00	.00	21.57	.00	C		
7107	-69.0	10.4		.00	-3.93	.00	.00	33.66	.00	.00	30.56	.00	.00	19.66	.00	+		
7109	-58.7	15.9		.00	-10.07	.00	.00	20.88	.00	.00	22.18	.00	.00	22.61	.00	C		
7111	-61.5	23.0		.00	-8.09	.00	.00	25.18	.00	.00	26.29	.00	.00	27.97	.00	B		
7113	-63.6	28.3		.00	-7.63	.00	.00	26.26	.00	.00	27.22	.00	.00	28.85	.00	B		
8103	-41.2	28.8		-5.21	-7.95	-9.23	23.96	23.08	23.30	23.04	22.89	20.03	24.36	24.35	20.93	+		
8105	-52.9	25.1		-5.79	.00	-10.40	24.52	.00	21.68	25.41	.00	21.09	26.47	.00	21.62	+		
8107	-71.5	18.5		-3.57	-7.13	-8.13	33.48	27.64	31.35	36.91	28.08	33.53	35.45	29.35	34.93	C		
8111	-93.0	18.5		-7.65	-10.74	-11.99	22.88	21.34	19.81	22.32	21.16	20.08	21.30	19.55	19.13	+		
8117	-84.8	29.5		-11.27	.00	-14.94	16.29	.00	14.78	14.27	.00	15.68	11.74	.00	14.33	+		
8119	-82.9	30.9		-6.52	-8.40	-10.21	26.11	26.07	25.00	25.89	25.52	24.58	25.89	26.30	24.34	+		
8121	-80.8	31.4		-5.75	-7.92	-8.96	27.99	26.82	28.68	28.46	26.44	29.09	28.69	27.58	29.30	+		
9110	147.7	34.8		-4.15	-8.09	-8.37	27.68	24.87	25.71	26.32	24.28	23.87	27.08	24.97	24.46	+		
9112	135.2	37.4		-4.83	-9.24	-8.69	27.40	23.09	27.02	26.03	23.59	24.88	26.17	23.32	24.83	D		

TABLE 8.18 (14)

9114	129.5	42.6	-4.65	-7.75	-7.74	30.60	30.88	35.41	29.15	27.83	31.98	28.95	28.60	31.69	B
9116	120.9	46.0	-3.37	-6.62	-6.99	39.74	36.33	42.64	36.06	29.94	40.13	34.27	29.24	39.87	D
9118	118.2	46.0	-3.73	-7.45	-8.36	37.52	32.87	32.55	35.18	29.16	33.73	33.69	29.54	33.25	D
9120	115.1	43.2	-4.21	-7.27	-8.59	34.75	33.43	31.15	33.78	29.40	33.19	32.68	29.55	32.67	D
9122	106.3	40.0	-3.96	-6.97	-7.56	35.74	33.31	36.71	34.87	29.39	38.18	33.38	29.55	37.69	D
9124	95.2	37.7	-4.57	-7.83	-7.96	32.22	28.72	32.95	31.94	27.08	33.42	31.15	27.90	32.78	D
9126	84.3	35.5	-5.98	-9.47	-9.53	27.53	24.04	26.97	27.47	23.39	26.68	27.46	23.23	26.46	D
11202	105.7	15.6	-10.21	-11.27	-12.59	13.33	18.19	15.55	16.71	22.27	20.24	14.44	21.15	19.30	B
11204	103.5	22.7	-8.02	-11.15	-11.79	20.30	19.34	18.81	21.74	21.76	21.53	20.51	20.41	20.62	B
11206	99.0	29.1	-6.55	-11.99	-9.93	25.43	17.73	25.33	25.63	19.28	26.21	24.95	16.73	25.41	+
11208	96.6	34.9	-6.62	-9.83	-10.66	25.41	23.47	23.08	25.31	23.49	23.61	24.62	22.97	22.76	D
11210	93.4	38.4	-5.21	-8.35	-8.93	29.93	27.13	29.00	29.65	25.98	28.99	29.16	26.53	28.31	D
11212	91.2	39.5	-4.64	-9.28	-8.40	31.71	24.74	30.87	31.64	24.03	30.95	31.02	23.83	30.41	D
11214	88.0	36.4	-6.21	-9.81	-9.39	26.96	23.46	27.39	26.54	22.75	27.01	26.27	22.08	26.54	D
11216	87.0	30.6	-7.11	-10.47	-10.32	24.65	22.12	24.62	23.93	21.35	24.04	23.45	20.06	23.51	D
11218	87.8	28.9	-6.25	-9.80	-9.73	26.85	23.49	26.34	26.42	22.77	25.87	26.15	22.12	25.36	+
11220	82.7	32.4	-5.84	-7.98	-10.24	27.84	26.87	24.93	28.02	26.28	24.52	28.13	27.29	24.29	+
11222	70.9	38.0	-8.28	-10.64	-10.36	21.37	21.18	24.20	21.60	21.52	24.91	21.61	21.34	25.46	+
11224	58.9	40.9	-6.39	-8.93	-9.76	23.95	23.20	24.73	25.45	24.46	24.72	26.37	25.78	25.63	+
11226	54.0	39.5	-3.76	-7.46	-7.98	31.33	25.95	31.04	32.27	26.43	28.63	32.90	28.21	30.24	D
11228	49.3	32.3	-5.65	-9.59	-9.23	24.27	20.57	25.04	24.59	21.46	22.59	25.68	21.81	23.52	B
11230	20.8	26.4	-5.59	-9.56	-9.48	18.84	16.34	18.07	17.92	16.23	16.17	19.93	17.46	17.23	B
11232	-9	24.9	-5.00	-7.76	-8.74	18.44	17.39	17.65	16.44	16.62	14.69	19.22	20.05	15.28	B
11234	6.7	20.0	-5.30	-8.60	-8.75	17.98	16.45	17.89	16.26	15.52	14.94	18.80	18.18	15.72	B
24102	115.8	27.3	-7.06	-9.67	-9.13	21.43	23.44	28.12	24.39	25.71	30.71	23.71	26.05	30.14	+
24104	110.6	29.6	-7.01	-10.28	-10.28	22.39	21.45	23.11	24.74	24.35	26.54	24.04	24.21	25.85	+
24106	101.3	27.8	-6.98	-9.66	-9.76	23.81	23.91	25.82	24.50	24.48	27.16	23.69	24.42	26.39	+
24108	87.0	24.4	-5.67	-8.54	-9.28	28.43	26.10	27.75	28.28	25.25	27.44	28.12	25.72	27.05	+
24110	73.7	22.5	-7.02	-9.67	-10.79	24.45	23.09	23.22	25.04	23.41	23.59	25.49	23.95	23.86	+
24112	64.3	20.1	-7.00	-9.74	-9.46	23.30	22.16	26.39	24.70	23.34	27.21	25.42	24.16	28.28	+
25102	66.5	15.0	-9.77	-12.35	-12.22	17.74	17.82	18.96	17.84	17.94	19.99	17.04	16.23	20.05	+
25104	73.4	14.9	-8.84	-11.33	-12.08	20.51	20.22	20.06	20.14	19.97	20.42	19.72	18.93	20.34	+
25106	86.1	15.0	-7.10	-10.41	-11.42	24.70	22.24	21.77	24.00	21.46	21.21	23.58	20.27	20.56	+
25108	109.0	15.6	-6.25	-9.85	-10.43	25.48	23.07	22.67	27.03	25.05	25.95	26.50	25.22	25.22	+
25110	129.7	18.5	-5.48	-9.60	-8.79	26.31	21.95	28.63	26.53	24.20	27.73	26.29	23.83	27.31	D
25112	137.5	24.0	-5.87	-10.52	-10.01	23.24	18.78	21.50	23.54	21.39	21.79	23.29	19.96	21.41	D
25114	137.1	27.2	-5.57	-8.78	-10.57	24.59	25.19	19.42	24.45	24.85	20.63	24.30	25.01	20.12	+
25116	131.7	25.4	-5.57	-9.94	-9.39	25.53	21.25	25.07	25.74	23.60	25.03	25.51	23.00	24.57	C
27104	24.3	3.3	-6.81	-12.13	-12.01	16.50	12.55	13.09	16.20	12.16	14.56	17.19	10.97	14.23	+
27106	4.0	5.8	-8.12	-12.00	-11.96	12.69	12.11	12.20	11.55	9.31	13.50	12.02	9.13	12.18	+
27108	-2.4	8.7	-10.10	-11.83	-11.84	9.88	12.30	12.35	8.92	9.50	13.50	8.18	9.47	12.21	+
27110	-6.7	10.3	-8.68	-10.33	-12.48	11.88	14.15	11.53	10.96	12.40	13.45	11.06	13.53	11.96	+
27112	-10.9	10.6	-7.50	-10.30	-11.16	13.94	14.38	13.62	13.09	13.07	13.95	13.98	14.15	13.47	D
27114	-14.1	10.7	-7.57	-9.70	-10.35	13.99	15.43	15.31	13.40	14.71	14.61	14.21	16.20	14.83	+
27116	-17.5	11.4	-7.55	-10.96	-12.48	14.27	13.85	11.85	13.92	13.07	13.87	14.66	13.30	13.04	+
27118	-20.1	12.6	-6.97	-10.92	-10.62	15.66	14.09	15.39	15.28	13.61	15.08	16.34	13.70	15.43	+
27120	-26.5	14.3	-6.82	-11.18	-11.37	16.78	14.23	14.56	16.50	14.21	15.18	17.37	13.59	15.21	+
27122	-35.3	15.7	-7.21	-10.49	-11.51	17.25	16.53	15.42	17.16	16.86	15.87	17.40	16.21	15.78	+
27124	-43.7	16.3	-8.17	-11.14	-12.01	16.51	16.45	15.56	16.97	17.13	16.38	16.56	15.78	16.10	C
27126	-50.3	15.9	-9.38	-11.80	-11.44	15.22	16.19	18.17	16.05	17.14	18.40	15.07	15.44	18.48	+
27128	-69.1	15.0	-8.09	-10.98	-11.21	21.53	20.43	21.75	22.05	20.85	22.47	22.21	20.42	22.81	+
27130	-71.8	15.2	-9.37	-11.79	-12.53	19.31	19.33	18.94	18.90	19.06	19.55	18.24	17.67	19.40	+
27132	-89.3	14.9	-8.65	-11.63	-11.33	20.87	19.70	21.81	19.77	18.97	21.40	18.39	16.42	20.63	+
27134	-115.4	13.5	-10.17	-11.73	-13.80	12.24	15.95	11.69	16.68	21.61	17.98	14.44	20.08	16.88	+
27136	-139.2	12.7	-7.50	-12.73	-11.21	17.28	12.35	17.17	19.24	16.61	19.03	18.21	13.09	18.45	+
27138	-155.2	11.1	-6.69	-9.61	-10.95	18.75	20.03	17.76	19.11	20.03	17.57	19.18	19.62	17.61	+
29102	8.8	15.3	-6.94	-9.51	-11.18	14.83	15.32	13.50	13.72	14.15	13.84	15.01	15.97	13.21	B

TABLE 8.18 (15)

29106	56.1	13.7	-7.54	.00	-10.29	20.49	.00	22.57	21.62	.00	22.35	21.98	.00	23.00	B
29108	67.7	17.6	-8.00	-10.87	-11.24	21.52	20.47	21.52	22.23	21.09	22.31	22.47	20.82	22.68	D
29110	60.7	18.4	-8.73	-10.08	-11.34	18.71	21.11	20.26	19.61	22.39	21.07	19.40	22.86	21.42	B
29112	62.3	18.0	-8.01	-10.93	-11.91	20.59	19.71	19.06	21.66	20.76	20.13	21.91	20.47	20.30	B
29114	65.4	17.5	-7.99	-10.07	-10.75	21.17	21.65	22.54	22.08	22.70	23.36	22.34	23.23	23.92	+
29116	63.7	16.4	-8.61	-10.76	-11.22	19.53	20.21	21.06	20.32	21.22	21.91	20.23	21.11	22.32	+
29118	61.5	15.1	-8.65	-11.64	-13.51	19.04	17.96	15.39	19.94	18.78	17.31	19.80	17.57	16.92	+
29202	-148.3	10.5	-3.28	-5.49	-6.85	30.94	31.79	31.61	28.75	28.37	28.52	29.58	29.44	29.72	+
29204	-170.2	10.9	-7.86	-10.00	-12.46	16.94	18.83	16.98	15.19	16.03	14.53	14.97	15.09	13.75	+
29206	-172.9	7.1	-9.27	-10.66	-11.04	15.72	18.86	17.88	12.64	14.34	15.34	11.59	12.74	15.14	+
29208	-145.4	3.7	-8.44	-9.94	-10.54	14.68	20.18	18.97	16.48	21.15	19.40	15.08	20.22	19.20	+
29210	-94.1	3.5	-9.39	-9.30	-11.14	18.58	24.79	21.89	18.02	24.25	22.07	16.06	24.10	21.20	B
30102	52.1	14.8	-7.66	-11.23	-12.33	19.37	17.59	16.24	20.26	18.67	17.43	20.41	17.61	17.23	B
30104	48.6	14.7	-7.55	-11.23	-11.31	18.94	17.03	18.21	19.56	17.97	18.21	19.66	16.71	18.30	B
30106	30.2	15.5	-7.05	-9.81	-11.38	16.80	17.16	15.02	16.64	17.35	15.52	17.17	17.62	15.54	B
30108	9.9	17.0	-8.04	-9.04	-9.72	12.97	16.04	16.17	12.16	15.17	14.59	12.68	17.38	14.93	+
30110	3.9	19.4	-6.93	-9.04	-9.62	14.67	15.73	16.01	13.31	14.44	14.27	14.60	16.73	14.35	D
30112	5.5	19.7	-8.00	-12.00	-10.12	12.91	12.12	15.15	11.82	9.42	14.10	12.37	9.24	13.93	D
30114	3.5	16.7	-6.93	-8.96	-9.68	14.67	15.83	15.88	13.29	14.56	14.23	14.59	16.93	14.26	D
30202	4.9	8.8	-4.02	-5.49	-6.47	20.80	20.89	23.24	18.49	21.03	16.87	22.00	25.96	19.26	+
30206	-177.8	6.7	-8.13	-9.08	-9.54	16.88	18.45	18.48	14.27	16.83	16.50	13.91	16.45	16.94	D
30208	-159.8	7.9	-9.46	.00	-13.56	14.10	.00	14.49	13.45	.00	14.61	12.08	.00	13.62	D
30210	-129.6	6.8	-10.56	-11.16	-12.84	9.74	16.78	12.70	14.37	21.50	17.86	11.74	19.82	16.84	D
30212	-100.1	6.4	-8.24	-10.81	-12.14	20.31	20.64	18.39	21.01	21.95	20.36	19.63	20.69	19.38	+
30214	-91.9	7.2	-8.08	-9.67	-10.21	21.92	23.84	24.78	21.18	23.29	24.48	19.98	22.73	23.75	+
30216	-95.4	6.6	-3.38	-7.07	-7.54	36.78	30.80	34.84	36.43	28.30	35.54	34.38	29.11	34.94	D
32102	35.1	18.9	-6.27	-10.79	-10.38	19.59	15.92	18.32	19.05	16.25	17.11	19.90	15.35	17.55	+
32104	26.8	20.4	-6.19	-10.68	-10.18	18.31	15.11	17.34	17.75	15.18	16.29	19.03	14.95	16.97	D
32106	22.3	20.2	-5.40	-9.28	-9.68	19.56	17.02	17.82	18.57	17.32	16.19	20.63	18.39	17.15	D
32108	24.1	18.8	-6.61	-9.84	-10.10	16.93	16.27	17.11	16.54	16.30	16.03	17.68	17.02	16.76	D
32110	26.7	16.7	-7.67	-9.76	-12.00	14.96	16.75	13.32	15.01	16.87	14.75	15.30	17.46	14.46	+
32112	28.5	16.2	-9.83	-11.33	-12.61	11.19	14.16	12.35	11.79	14.24	14.51	10.69	13.32	13.91	B
32114	26.3	17.1	-9.08	-9.81	-11.25	12.26	16.61	14.79	12.67	16.72	15.26	12.09	17.30	15.35	+
32116	21.3	18.5	-5.05	-9.16	-9.71	20.28	17.09	17.60	19.09	17.06	16.01	21.44	18.60	16.95	+
32118	15.9	20.8	-5.28	-9.01	-8.74	18.90	16.65	19.05	17.66	16.31	16.12	20.08	18.32	17.49	D
32120	9.9	21.4	-6.40	-8.85	-9.85	15.93	16.31	15.90	14.74	15.51	14.51	16.43	17.88	14.76	D
32122	16.9	20.6	-7.39	-10.80	-11.56	14.52	14.05	13.32	14.09	13.26	14.21	14.96	13.66	13.87	+
32124	33.7	20.0	-8.65	-14.33	-12.46	13.88	9.82	13.16	14.28	9.55	14.95	13.66	6.18	14.43	+
32126	49.0	19.5	-10.19	-11.66	-12.31	13.43	16.27	15.75	14.23	17.18	16.89	12.73	15.55	16.61	+
32128	61.2	18.8	-11.40	-10.76	-14.26	13.88	19.88	13.91	14.04	21.03	16.32	12.22	20.88	15.67	+
32132	83.9	18.2	-9.31	-11.55	-12.21	19.92	20.12	20.02	18.45	19.03	19.61	17.05	16.81	18.93	+
32134	92.1	18.5	-11.33	-9.97	-12.91	15.13	23.15	17.79	13.96	22.69	18.32	11.07	21.85	17.25	B

TABLE 8.18 (16)

SL4	COMAND ANGLE 3		SIGMA, DB			REDUCTION 4			REDUCTION 5			REDUCTION 6			QUAL
	ASPECT ANGLE	MET. WIND	VV	HH	HV+VH	VV	HH	HV+VH	VV	HH	HV+VH	VV	HH	HV+VH	
6202	106.0	17.5	-6.81	-8.48	-11.75	17.85	23.34	18.95	20.09	25.38	22.54	18.20	23.90	21.37	+
6203	102.5	18.5	-6.00	-8.91	-12.10	20.35	21.93	18.31	21.97	23.80	21.55	20.24	22.15	20.26	D
6204	113.5	21.0	-6.27	-7.99	-9.30	19.50	24.65	25.45	21.31	26.33	27.79	19.53	24.97	26.98	D
6205	104.5	24.3	-5.35	-7.01	-9.09	22.12	28.23	26.10	23.86	29.24	28.47	22.34	28.15	27.71	C
6206	118.6	26.6	-3.49	-7.34	-7.94	28.32	27.12	29.78	29.89	28.78	31.96	28.92	27.63	31.43	C
6207	110.6	28.7	-3.15	-5.99	.00	29.51	31.95	.00	31.07	33.00	.00	30.22	32.07	.00	C
6208	111.8	29.4	-3.34	-6.00	-7.43	28.58	31.88	31.44	30.33	33.01	33.45	29.46	32.08	33.02	D
6209	111.8	30.5	-3.69	-6.23	-7.86	27.17	31.02	29.85	29.10	32.28	32.15	28.15	31.33	31.67	D
6210	112.7	33.0	-4.57	-7.66	-10.61	23.80	25.94	21.32	26.15	28.03	25.03	24.99	26.80	24.13	D
6211	116.8	33.7	-5.37	-8.00	-10.20	20.67	24.58	22.05	23.39	26.86	25.51	22.05	25.52	24.69	D
6212	115.6	33.3	-5.42	-7.68	-9.59	20.14	25.37	23.48	22.82	27.37	26.40	21.49	26.11	25.69	+
334103	-7.6	11.0	-8.17	-8.11	-12.41	8.21	15.26	10.15	9.65	14.99	11.18	9.27	16.39	10.64	D
334102	-167.2	14.3	-5.97	-7.96	-11.94	13.11	14.28	11.55	13.86	15.66	13.61	13.75	16.15	13.22	+
338103	-126.3	22.2	-5.51	-6.71	-10.77	18.89	27.48	19.43	21.13	28.45	22.16	19.81	27.45	21.23	A
338105	-128.1	22.5	-4.20	-6.77	-9.08	22.67	26.91	23.71	24.15	27.75	25.15	23.25	26.75	24.55	D
338107	-156.2	21.6	-1.95	-4.20	-5.88	27.56	26.77	26.95	25.61	25.09	24.26	27.63	26.96	25.79	D
338109	171.9	24.0	-2.28	-4.80	-6.67	20.69	21.53	21.70	18.93	18.73	18.02	20.84	20.95	19.24	D
338111	154.9	19.9	-3.88	-6.99	-9.25	18.56	18.51	17.71	18.84	19.46	18.66	19.27	19.94	18.97	B
338113	151.1	18.6	-4.91	-7.68	-10.54	16.57	17.73	15.59	17.39	19.10	17.48	17.15	18.98	17.25	D
338115	142.2	16.1	-5.79	-8.04	-10.56	15.78	19.33	17.19	17.05	20.51	18.89	16.00	19.58	18.28	D
338119	116.9	8.3	-5.91	-6.82	-10.74	19.05	28.55	20.63	21.91	30.21	24.30	20.42	29.17	23.39	+
338102	40.5	17.2	-6.36	-7.59	-10.31	15.45	20.29	18.06	15.07	18.83	17.39	14.40	19.02	17.25	B
338104	45.6	20.6	-5.68	-7.29	-11.33	17.77	21.54	17.14	17.32	20.39	16.83	16.89	20.69	16.39	B
338106	46.5	20.3	-5.36	-8.29	-11.18	18.60	19.79	17.55	18.17	18.53	17.22	17.87	18.41	16.83	B
338108	43.3	15.8	-5.65	-7.93	-10.24	17.39	20.03	18.69	16.88	18.63	17.96	16.45	18.65	17.82	+
338110	25.4	11.0	-7.99	-9.05	-12.94	10.14	15.23	11.26	11.20	14.90	12.77	10.48	15.18	12.21	+
338112	-15.1	12.5	-3.45	-5.87	-7.88	18.07	21.34	19.17	17.16	19.55	17.16	18.68	21.90	18.29	+
338114	-33.2	16.0	-3.09	-6.38	-7.73	21.58	21.78	22.18	20.27	20.28	20.34	21.18	21.27	21.18	+
338116	-39.8	16.0	-3.89	-5.91	-9.03	20.72	23.57	20.45	19.77	22.19	19.19	20.11	23.16	19.44	+
338118	-40.4	12.1	-6.60	-8.68	-12.18	14.97	18.26	14.88	14.64	16.76	14.94	13.89	16.51	14.28	D
338120	-43.0	6.9	-8.27	-8.84	-14.82	12.62	18.35	11.69	12.39	16.85	12.36	11.10	16.51	11.04	+
4109	-49.0	25.1	-2.17	-4.75	-7.02	27.34	27.22	26.82	27.14	27.31	25.27	28.30	28.77	26.16	+
4113	-61.1	38.2	-1.98	-4.87	-6.23	30.42	28.90	31.10	32.43	30.33	31.77	33.75	31.82	33.08	C
4115	-56.2	39.7	-1.90	-4.25	-6.46	29.68	29.49	29.60	31.00	30.94	29.36	32.36	32.60	30.55	D
4117	-60.4	34.8	-1.93	-3.63	-5.50	33.88	31.84	33.18	36.41	34.00	33.71	38.00	35.66	35.23	D
4119	-69.6	34.9	-2.86	-5.29	-6.66	29.19	29.39	31.24	30.86	30.23	32.40	31.65	31.34	33.42	D
4121	-56.1	30.2	-4.33	-7.62	-10.27	22.76	22.17	20.66	23.34	22.08	20.99	23.65	22.44	21.03	D
4123	-47.3	28.6	-1.92	-3.94	-7.14	27.75	28.79	26.21	27.21	28.96	24.45	28.47	30.70	25.28	+
4125	-49.7	24.2	-1.49	-3.39	-4.90	33.08	30.39	32.98	33.17	31.33	30.74	35.01	33.20	32.31	B
4127	-70.9	18.0	-1.65	-2.92	-4.88	37.41	36.53	37.32	40.11	38.01	38.33	41.17	38.92	39.73	+
4129	-104.5	16.3	-1.08	-3.44	-5.53	40.02	41.93	39.64	39.57	41.10	39.51	38.64	39.56	39.15	+
4131	-123.6	18.2	-2.79	-5.86	-7.67	28.94	30.98	29.15	29.98	31.74	30.16	29.45	30.88	29.79	+
4133	-140.8	21.3	-1.55	-3.54	-5.01	34.26	34.39	35.27	31.25	32.32	30.86	32.06	32.70	31.58	C
4135	-155.1	26.2	-1.14	-4.47	-6.30	27.12	26.19	25.84	25.36	24.84	23.77	27.18	26.49	25.09	A
4137	-163.3	26.9	-3.14	-5.24	-7.69	19.27	21.56	20.05	18.75	20.38	18.85	19.99	22.22	19.85	C
4139	-169.8	24.0	-3.77	-5.21	-7.85	17.07	20.51	18.80	16.36	18.48	16.85	17.43	20.48	17.68	B
4141	-176.6	22.0	-2.60	-5.70	-8.06	19.58	18.39	17.83	17.77	16.34	15.44	19.51	18.05	16.03	+
4143	177.3	20.5	-4.47	-7.51	-8.95	15.23	13.55	15.83	14.42	13.36	14.33	15.17	14.20	14.60	B
4145	167.5	24.4	-1.42	-3.15	-4.66	27.07	27.86	28.80	24.07	23.38	22.61	27.08	26.48	24.79	B
4147	155.5	29.0	-1.88	-3.60	-5.42	28.00	29.12	28.78	25.98	26.81	25.46	27.98	28.87	27.12	B
4149	149.9	28.3	-1.51	-4.64	-7.06	27.16	27.27	24.75	25.61	26.16	23.64	26.81	27.21	24.39	B
4151	155.9	23.6	-2.02	-3.69	-6.28	23.84	28.67	25.69	22.87	26.44	23.56	24.30	28.51	24.93	C
4102	-119.2	9.7	-11.50	-16.18	-15.88	7.85	6.21	10.65	10.78	10.20	15.30	8.18	7.20	13.44	B

TABLE 8.18 (17)

4108	123.3	22.2	-5.44	-9.71	-12.29	19.53	18.91	16.38	22.00	21.57	20.07	20.69	19.66	18.86	B
4110	131.2	26.0	-3.22	-5.97	-7.52	25.55	28.80	28.11	26.03	28.91	27.74	25.51	28.19	27.49	B
4112	130.2	29.2	-3.90	-6.66	-8.70	23.27	26.76	24.45	24.35	27.36	25.31	23.58	26.42	24.81	B
4114	122.0	33.8	-3.46	-6.82	-8.61	26.48	27.89	26.17	28.14	29.29	28.19	27.40	28.24	27.65	D
4116	112.7	38.9	-2.59	-6.06	-6.95	31.57	31.54	33.18	32.96	32.79	34.80	32.26	31.86	34.45	+
4118	108.5	41.4	-2.60	-4.86	-7.00	32.14	36.32	33.30	33.20	36.57	34.84	32.38	35.59	34.41	D
4120	106.1	43.7	-2.12	-5.23	-7.10	34.62	34.88	32.98	35.11	35.03	34.35	34.28	34.13	33.87	D
4122	104.7	46.2	-1.25	-4.69	-6.00	39.08	36.96	37.50	38.78	36.63	37.82	37.89	35.67	37.43	+
4124	98.7	47.2	-1.01	-4.20	-5.78	40.36	38.45	38.23	39.29	37.02	37.47	38.32	36.10	37.04	+
4126	87.3	48.2	-.80	-3.72	-5.03	40.21	38.33	39.99	39.40	36.30	38.22	38.92	35.95	38.21	D
4128	81.0	41.9	-1.19	-3.54	-5.12	37.33	37.41	38.45	37.74	36.31	37.70	37.89	36.53	38.21	D
4130	74.7	36.9	-1.22	-3.72	-5.16	35.96	35.14	37.07	37.68	35.46	37.57	38.45	36.31	38.63	+
4132	68.4	32.7	-2.01	-4.36	-5.86	31.78	31.70	33.51	33.92	32.99	34.69	35.02	34.32	35.98	+
4134	59.9	29.2	-2.47	-5.26	-6.73	28.64	27.76	29.48	30.29	28.95	29.98	31.45	30.33	31.13	+
4136	51.9	26.2	-3.17	-5.55	-7.50	25.02	25.89	26.11	25.25	26.07	25.23	26.01	27.25	26.01	+
4138	41.9	24.2	-2.54	-5.99	-8.06	24.80	23.66	22.99	23.56	22.43	21.23	24.51	23.52	21.75	C
4140	29.7	25.5	-3.86	-5.73	-8.10	18.95	22.84	20.68	18.19	21.24	19.28	18.88	22.75	20.11	A
4142	20.6	26.4	-1.70	-4.31	-5.93	23.98	25.90	25.10	21.48	23.31	21.30	23.81	26.18	23.22	A
4144	4.5	30.3	-.01	-3.18	-4.59	29.60	29.45	28.45	23.04	24.00	20.11	26.85	28.15	22.35	D
4146	-2.4	34.6	1.16	-1.44	-2.92	35.28	35.81	35.33	25.82	27.89	22.78	30.45	32.90	25.77	D
4148	.7	33.3	-3.75	-5.84	-7.96	16.53	20.94	18.20	15.42	18.54	15.22	16.89	21.19	16.04	D
4150	9.2	29.2	-1.67	-3.60	-5.43	23.12	27.97	25.68	19.83	23.48	19.53	22.51	27.30	21.52	+
7103	-94.6	6.1	.00	-12.16	.00	.00	13.38	.00	.00	15.59	.00	.00	13.05	.00	B
7105	-80.2	10.5	.00	-7.39	.00	.00	25.04	.00	.00	24.81	.00	.00	24.39	.00	B
7107	-63.1	9.4	.00	-7.79	.00	.00	22.51	.00	.00	22.90	.00	.00	23.25	.00	C
7109	-57.6	14.3	.00	-6.30	.00	.00	25.08	.00	.00	25.62	.00	.00	26.59	.00	C
7111	-62.8	19.6	.00	-5.15	.00	.00	28.53	.00	.00	29.85	.00	.00	31.24	.00	C
7113	-65.6	25.0	.00	-5.13	.00	.00	29.08	.00	.00	30.33	.00	.00	31.65	.00	+
8105	-54.0	26.9	-3.09	-6.04	-8.44	25.64	25.15	24.23	26.22	25.40	23.93	27.06	26.41	24.47	C
8107	-71.8	25.3	-3.82	-5.71	-8.02	26.56	28.65	27.67	27.69	29.15	28.81	28.02	30.01	29.37	C
8109	-91.2	20.0	-3.82	.00	-9.02	27.88	.00	26.24	27.68	.00	26.81	26.61	.00	26.05	D
8111	-96.1	19.1	-5.02	-6.79	-10.00	23.74	28.50	23.58	24.25	28.29	25.12	22.75	27.24	24.14	+
8115	-89.9	23.7	-8.87	-10.30	-13.32	14.56	17.69	16.29	14.98	18.73	18.25	12.67	16.72	16.75	+
8117	-87.9	26.5	-7.49	-10.31	-13.12	17.53	17.62	16.72	17.74	18.49	18.48	15.80	16.55	17.07	+
8119	-84.1	28.4	.00	-4.41	.00	.00	35.11	.00	.00	33.62	.00	.00	33.61	.00	+
8121	-80.1	29.9	-3.15	.00	-6.75	29.59	.00	32.46	29.94	.00	32.46	29.85	.00	32.75	+
8104	165.4	18.8	-5.67	-7.94	-10.16	13.19	13.16	13.88	13.29	13.89	14.08	13.46	14.55	14.13	D
8106	121.4	18.7	-6.31	.00	-12.04	17.39	.00	17.12	20.21	.00	20.92	18.63	.00	19.76	D
8108	102.6	18.4	-5.57	-7.58	-10.75	21.60	26.18	21.49	23.13	27.30	24.31	21.52	26.06	23.26	D
8112	73.1	13.8	.00	-8.80	-11.73	.00	20.92	19.29	.00	21.23	20.75	.00	20.79	20.30	C
8114	50.3	12.2	-7.09	-9.60	-11.83	15.87	17.94	17.05	15.63	16.75	17.08	14.73	16.15	16.57	C
8116	56.4	12.6	-13.83	-14.01	-18.13	7.75	11.67	9.70	7.12	10.43	10.91	4.91	8.71	9.04	+
8118	77.3	15.1	-12.75	-13.14	-16.79	9.41	12.03	11.51	9.11	12.81	13.45	6.71	10.77	11.70	+
8120	95.4	18.8	-5.37	-7.71	-9.71	22.70	25.36	24.35	23.22	25.64	25.67	21.63	24.33	24.74	+
9102	-177.0	12.4	-6.14	-8.20	-10.33	12.12	11.95	13.19	11.93	12.35	12.87	11.96	12.91	12.70	+
9104	167.7	20.2	-3.85	-6.37	-8.27	17.06	17.40	18.00	16.56	16.91	16.79	17.56	18.28	17.52	+
9106	155.3	28.1	-2.80	-5.51	-6.80	21.52	22.75	24.17	21.14	22.43	22.73	22.12	23.61	23.88	+
9108	147.9	34.0	-.93	-4.01	-5.16	30.08	30.14	32.14	27.81	28.42	28.33	29.09	29.48	29.54	+
9110	143.4	36.4	-.84	-4.16	-5.49	31.96	31.17	32.34	29.39	29.55	28.81	30.31	30.09	29.58	+
9112	140.1	37.2	-1.60	-5.51	-6.75	29.72	27.65	28.54	28.04	27.08	26.70	28.44	26.93	26.94	D
9114	132.4	41.5	-.94	-4.96	-5.59	35.29	32.02	35.40	33.30	31.41	32.44	33.46	30.95	32.60	D
9116	120.7	48.0	-.59	-4.24	-5.18	40.65	37.57	40.19	39.87	37.82	39.11	39.42	36.78	39.03	D
9118	119.8	45.4	-.24	-3.69	-4.80	43.03	39.91	42.24	41.90	40.04	40.86	41.32	38.70	40.79	+
9120	115.8	42.0	-.15	-3.52	-4.83	44.44	41.16	42.65	43.54	41.40	42.01	42.69	39.77	41.87	D
9122	106.9	38.5	-.80	-3.90	-4.86	41.51	40.15	42.93	41.05	39.80	42.41	40.11	38.48	42.11	D
9124	95.8	34.9	-1.44	-5.05	-6.32	38.03	34.80	35.74	37.06	33.48	35.06	36.17	32.74	34.59	D
9126	83.0	31.2	-2.54	-5.85	-7.56	32.10	30.08	30.16	32.10	29.16	30.13	31.91	29.02	30.05	D

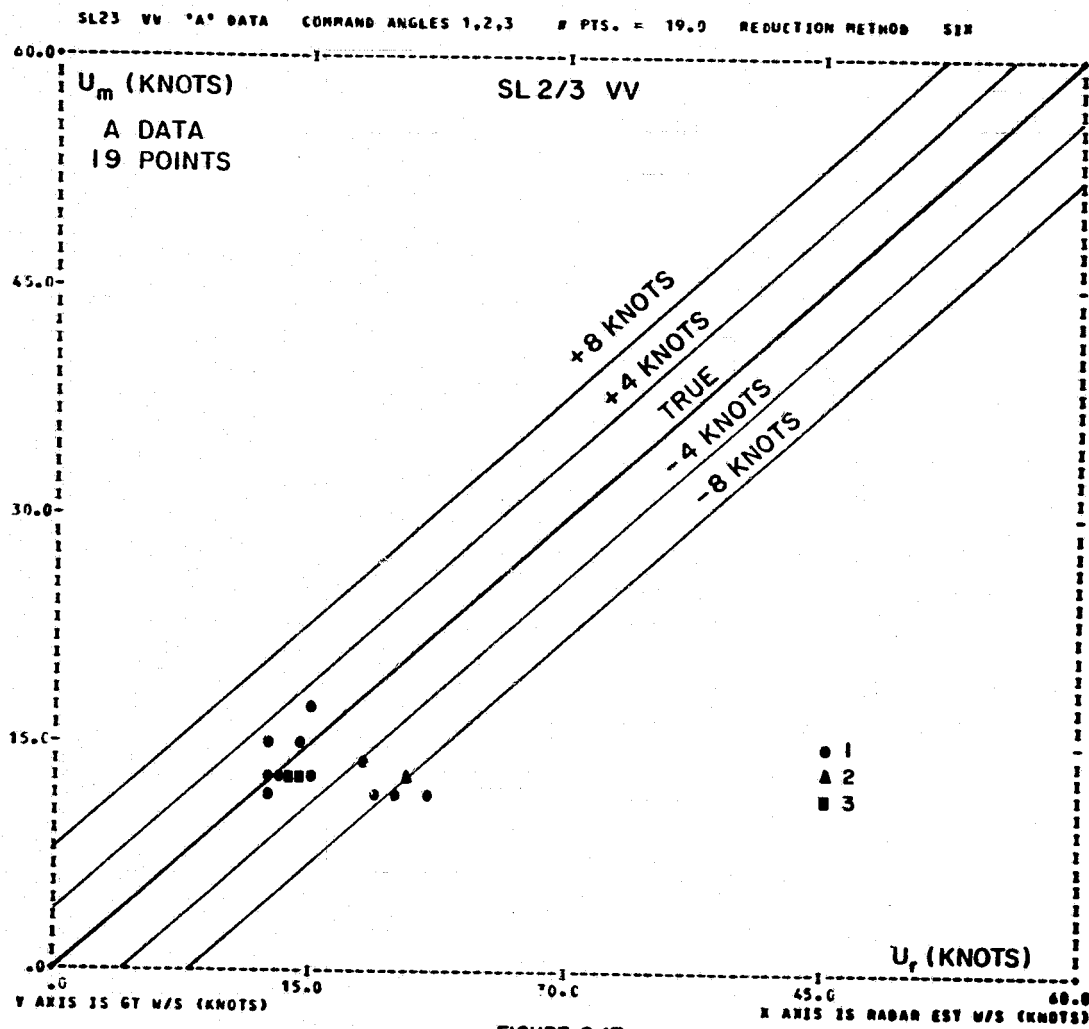
REPRODUCIBILITY OF THE
ORIGINAL PAGE IS POOR

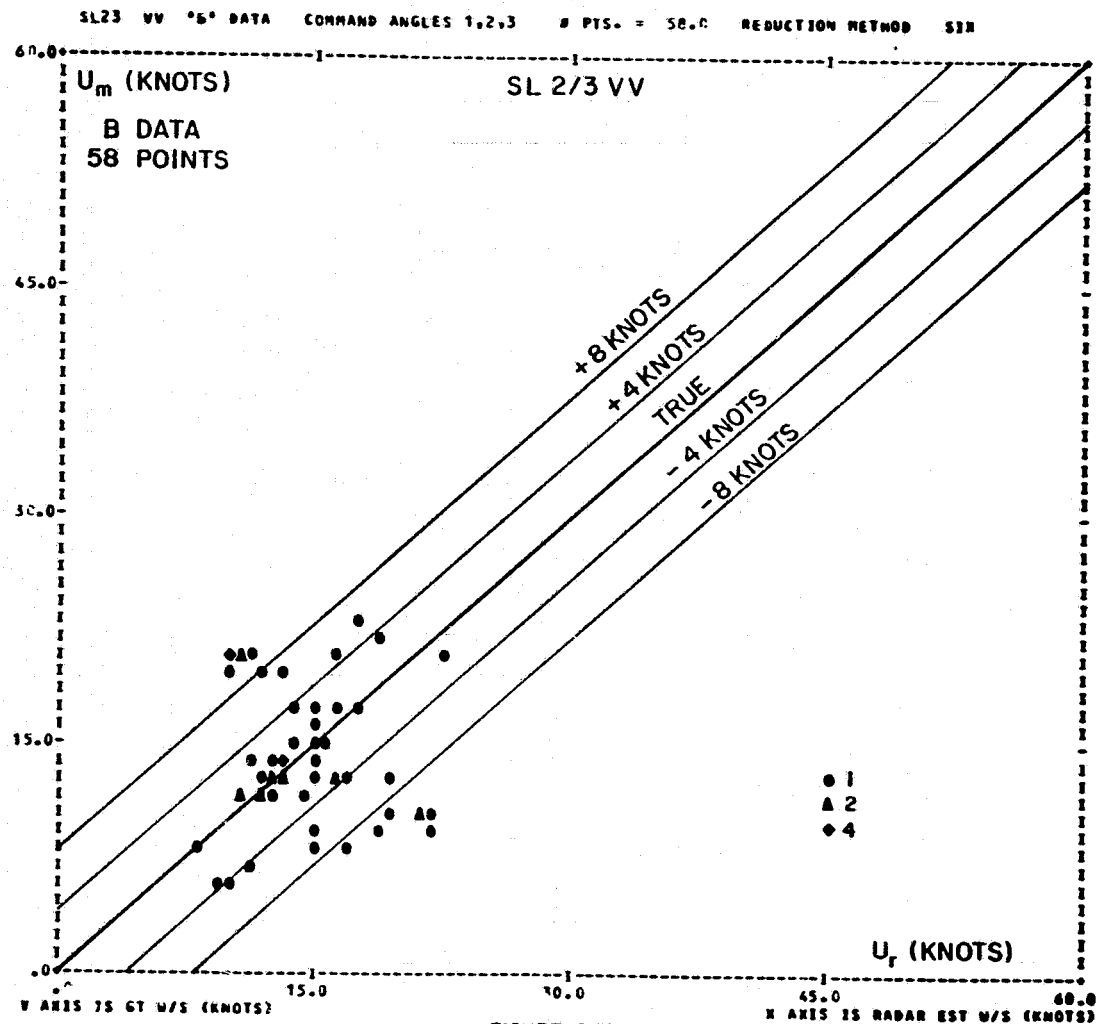
TABLE 8.18 (18)

11202	107.3	20.8	-5.83	-10.84	-13.92	20.39	16.63	14.49	22.61	19.85	18.68	21.01	17.67	17.15	B
11204	101.9	26.6	-5.11	-9.56	-10.42	23.08	20.02	22.35	24.39	22.14	24.94	22.89	20.28	23.94	+
11206	97.7	32.3	-2.90	-6.75	-7.15	31.43	28.77	32.64	31.36	28.72	32.82	30.34	27.68	32.25	D
11208	94.0	36.1	-2.20	-6.71	-6.70	34.36	28.60	34.10	33.70	28.12	33.53	32.84	27.13	33.04	D
11210	92.1	38.7	-1.91	-6.16	-6.10	35.55	30.30	36.25	34.74	29.36	35.12	33.98	28.56	34.75	D
11212	88.8	39.1	-2.88	-6.15	-7.68	31.29	29.90	30.24	30.85	28.85	30.04	30.13	28.20	29.58	D
11214	85.6	33.4	-3.25	-6.73	-7.63	29.71	27.59	30.16	29.50	26.87	30.00	28.92	26.25	29.72	D
11216	84.3	26.9	-4.63	-8.17	-9.23	25.07	23.15	25.39	25.04	23.05	25.93	24.15	22.01	25.43	D
11218	84.3	26.8	-5.18	-7.40	-10.03	23.45	25.39	23.32	23.45	24.98	24.13	22.39	24.22	23.47	+
11220	75.5	31.3	-4.43	-8.07	-9.09	25.46	23.10	25.50	25.75	23.08	26.25	25.30	22.46	26.09	+
11222	68.4	36.6	-5.35	-7.65	-8.45	22.06	23.29	26.17	22.90	23.77	27.43	22.75	24.06	28.01	+
11224	56.5	41.5	-3.84	-6.75	-8.42	24.10	23.98	24.66	24.84	24.23	24.77	25.38	24.98	25.36	+
11226	50.8	42.6	-1.36	-4.84	-5.99	30.28	27.27	29.93	30.55	27.61	28.36	32.08	29.05	29.60	B
11228	42.0	36.1	-1.65	-5.09	-5.16	30.95	25.59	30.76	29.05	24.53	27.16	30.90	25.84	28.65	B
11230	8.2	30.0	-1.66	-5.85	-6.66	23.14	21.05	21.84	19.75	18.89	17.54	22.44	21.46	18.99	B
11232	5.6	24.7	-1.06	-5.22	-6.13	25.23	22.83	23.28	20.74	19.88	17.91	23.84	22.86	19.51	B
11234	12.5	19.1	-2.68	-6.83	-7.01	20.06	18.66	21.17	18.25	17.53	17.85	20.27	19.47	19.27	D
24102	114.9	32.9	-3.36	-8.28	-8.14	28.06	23.83	28.63	29.94	26.26	31.06	29.13	24.85	30.57	+
24106	98.2	29.3	-2.47	-7.29	-7.15	33.24	26.95	32.67	33.01	27.31	32.91	32.05	26.12	32.34	+
24108	82.8	25.2	-2.67	-7.72	-6.69	31.60	24.32	32.98	31.62	24.07	32.62	31.42	23.32	32.71	D
24110	71.7	23.4	-3.79	-7.74	-8.42	26.61	23.34	26.60	27.76	23.70	27.78	28.10	23.78	28.24	D
24112	63.4	20.3	-5.24	-8.73	-11.11	21.72	20.56	19.87	22.56	20.75	21.04	22.55	20.67	20.94	+
25102	65.5	16.0	-6.91	-10.90	-13.29	18.30	16.46	16.25	18.75	16.46	17.67	18.03	15.49	16.99	+
25106	86.2	16.7	-4.07	-9.32	-9.46	26.92	20.10	24.84	26.78	20.49	25.43	25.92	18.94	24.79	+
25108	109.0	17.0	-2.63	-7.87	-8.18	31.95	25.34	28.89	33.08	27.33	31.26	32.27	26.04	30.70	+
25110	130.7	19.4	-2.34	-7.44	-6.94	29.18	24.16	30.35	28.98	25.16	29.41	28.72	24.00	29.28	D
25112	136.4	24.4	-2.20	-7.92	-7.76	28.25	21.30	26.04	27.37	22.32	25.46	27.36	21.15	25.30	D
25114	137.2	25.5	-2.18	-10.25	-8.18	28.14	15.12	24.51	27.18	17.24	24.32	27.22	15.38	24.10	+
25116	133.7	23.0	-2.51	-8.39	-8.07	27.72	20.64	25.69	27.35	21.99	25.60	27.13	20.57	25.30	D
27104	-7	3.1	-5.02	-9.11	-10.76	13.51	12.84	12.47	13.45	13.20	12.26	14.28	14.21	12.12	+
27106	-7.8	5.9	-6.16	-8.92	-10.45	11.42	13.48	13.24	12.14	13.75	13.02	12.47	14.78	13.08	+
27108	-8.9	8.7	-6.06	-9.90	-10.32	11.67	11.58	13.53	12.37	12.40	13.27	12.73	13.02	13.40	+
27110	-9.3	10.2	-6.51	-9.97	-12.99	10.89	11.48	9.47	11.80	12.34	10.86	11.98	12.92	10.19	+
27112	-11.7	10.7	-5.77	-8.87	-12.40	12.41	13.87	10.43	13.01	14.11	11.64	13.47	15.09	11.19	+
27114	-13.9	11.2	-3.64	-9.93	-8.83	17.45	11.98	16.88	16.66	12.73	15.71	18.11	13.21	16.47	+
27116	-16.4	11.9	-5.08	-10.64	-11.08	14.24	10.98	12.87	14.54	11.92	13.56	15.21	12.06	13.59	+
27118	-18.9	13.0	-4.80	-9.32	-9.92	15.15	13.76	15.22	15.28	14.03	15.25	16.01	14.56	15.67	+
27120	-25.3	14.9	-5.31	-9.46	-10.22	14.89	14.43	15.57	15.10	14.24	15.79	15.35	14.37	16.04	+
27122	-32.1	16.4	-5.04	-10.75	-10.68	16.58	13.39	15.87	16.26	12.67	15.92	16.32	12.02	15.85	+
27124	-39.6	16.6	-6.26	-10.10	-12.31	15.46	15.71	14.53	15.10	14.23	14.68	14.47	13.50	13.99	+
27126	-47.1	15.7	-5.54	-8.88	-9.31	18.33	18.81	21.18	17.95	17.50	20.27	17.57	17.14	20.42	D
27128	-43.9	15.9	-6.60	-10.70	-13.08	15.63	15.39	14.13	15.24	13.79	14.33	14.46	12.81	13.43	D
27130	-72.7	15.6	-7.38	-10.64	-16.28	17.84	16.91	12.22	18.10	17.28	14.03	17.01	16.15	12.52	+
27132	-93.4	15.1	-6.07	-12.26	-12.23	20.78	13.16	18.33	21.24	15.26	20.34	19.49	12.71	18.99	+
27134	-122.0	14.0	-6.18	-11.41	-13.01	17.65	14.79	15.10	20.42	18.10	19.12	18.87	15.74	17.78	+
27136	-141.0	13.1	-5.18	-9.94	-11.59	17.47	14.92	15.25	18.51	17.00	17.52	17.61	15.40	16.63	+
27138	-150.9	10.9	-4.14	-9.94	-9.29	18.52	12.45	18.38	18.98	15.03	19.41	19.04	14.08	19.54	+
29102	9.7	12.1	-4.34	-7.74	-8.80	15.36	16.24	16.59	15.00	15.73	15.05	16.14	17.28	15.72	B
29104	41.2	10.5	-2.79	-7.38	-7.36	23.93	20.78	24.53	22.70	19.35	22.35	23.54	19.63	23.10	+
29108	75.8	18.7	-6.74	-8.60	-12.99	19.32	21.51	17.05	19.58	21.73	18.61	18.56	21.18	17.74	D
29110	73.6	19.5	-6.22	-8.04	-9.42	20.40	22.75	24.28	20.84	23.01	25.48	20.12	22.85	25.59	B
29112	75.5	19.4	-4.83	-9.10	-9.89	24.06	20.31	23.29	24.63	20.59	24.45	24.34	19.87	24.34	B
29114	72.5	19.1	-5.50	-12.66	-11.59	22.07	13.15	19.53	22.70	13.57	20.99	22.32	11.86	20.59	C
29116	65.4	18.1	-5.11	-8.55	-10.87	22.29	21.06	20.50	23.22	21.37	21.78	23.24	21.34	21.74	+
29118	61.4	17.0	-5.86	-10.64	-10.57	20.04	16.88	20.71	20.64	16.58	21.68	20.35	15.74	21.71	+
29202	175.6	9.9	-6.26	-7.57	-12.48	11.89	13.35	9.83	11.70	13.17	10.80	11.68	13.98	9.98	+
29204	164.7	12.2	-6.25	-8.55	-11.72	12.43	12.46	11.64	13.06	14.05	13.34	12.92	14.38	12.99	D

TABLE 8.18 (19)

29206	176.3	6.9	-7.13	-9.74	-12.92	10.57	8.65	9.31	10.66	10.30	10.56	10.33	10.32	9.65	+
29208	-125.5	3.2	-7.69	-12.40	-12.94	13.63	12.15	14.84	16.42	15.45	18.52	14.49	12.85	17.17	+
29210	-89.0	5.5	-7.17	-9.68	-13.00	18.22	19.25	16.91	18.46	19.96	18.72	16.56	18.17	17.30	B
30102	31.0	10.8	-5.31	-10.17	-11.86	15.81	14.15	13.72	15.66	13.48	14.41	15.65	13.05	14.02	B
30106	13.9	16.6	-4.88	-10.77	-9.90	14.44	10.46	14.70	14.58	11.57	14.45	15.40	11.75	14.83	B
30108	.9	17.6	-4.28	-8.70	-8.97	15.21	13.73	15.90	14.58	13.82	14.08	15.78	15.00	14.53	+
30110	-1.2	19.2	-4.53	-8.66	-9.39	14.61	13.81	15.02	14.19	13.67	13.63	15.25	15.07	13.93	D
30112	2.2	18.9	-5.90	-9.82	-11.66	11.74	11.41	11.06	12.24	12.21	11.48	12.68	12.92	11.08	D
30114	-8.7	14.7	-5.84	-9.21	-10.80	12.07	12.93	12.68	12.65	13.36	12.77	13.10	14.27	12.74	D
30202	18.6	10.9	-3.42	-5.12	-6.11	18.50	23.58	24.33	17.65	21.41	20.55	19.09	23.99	22.41	+
30206	168.9	5.7	-2.64	-5.87	-9.18	19.97	18.64	15.84	18.68	17.49	15.33	20.35	19.12	15.71	D
30208	-161.8	6.2	-5.87	-9.89	-10.24	13.32	10.18	14.54	14.07	12.70	15.69	13.98	12.44	15.82	+
30210	-117.5	5.6	-5.85	-9.91	-10.83	19.15	18.87	20.36	21.99	21.96	24.03	20.52	20.04	23.10	D
30212	-85.5	6.5	-8.57	-10.10	-19.15	15.40	18.10	8.62	15.53	18.75	11.03	13.45	16.99	8.63	+
30214	-82.0	7.1	-6.75	-10.77	-12.36	19.38	16.54	18.23	19.45	17.21	19.65	18.04	15.47	18.62	+
30216	-90.8	6.9	-5.97	-10.03	-10.51	21.17	18.40	22.26	21.39	19.41	23.44	19.74	17.45	22.43	D
32102	27.7	18.5	-4.18	-6.91	-8.83	17.83	19.95	18.73	17.34	18.76	17.94	17.98	19.83	18.59	+
32104	23.6	20.6	-3.37	-7.17	-8.40	19.28	18.87	19.02	18.40	17.95	17.98	19.64	19.16	18.89	+
32106	22.3	20.9	-2.54	-7.15	-7.50	21.50	18.78	21.00	19.92	17.89	19.10	21.68	19.19	20.37	+
32108	25.9	19.2	-3.84	-7.99	-8.42	18.38	17.40	19.33	17.77	16.68	18.29	18.66	17.37	19.13	+
32110	30.6	16.8	-6.03	-10.31	-11.78	14.29	13.84	13.77	14.43	13.24	14.46	14.16	12.79	14.10	+
32112	32.6	15.8	-5.28	-9.60	-9.14	16.15	15.40	18.91	15.89	14.46	18.06	15.83	14.14	18.45	+
32114	30.2	15.2	-5.24	-10.27	-11.05	15.82	13.84	14.91	15.70	13.28	15.29	15.76	12.87	15.16	+
32116	23.0	16.3	-1.46	-6.35	-6.27	25.09	20.74	24.41	22.41	19.44	21.21	24.75	21.09	22.95	+
32118	13.8	20.2	-1.31	-7.91	-6.98	24.73	16.17	21.36	21.27	15.82	18.16	24.10	17.17	19.62	D
32120	7.8	21.9	-2.77	-7.30	-8.66	19.32	17.05	16.58	17.18	16.06	14.48	19.20	17.91	15.05	D
32122	11.7	21.0	-4.85	-9.16	-9.74	14.33	13.27	14.81	14.39	13.68	14.28	15.26	14.53	14.67	D
32124	32.8	20.9	-5.25	-10.58	-10.88	16.44	13.97	15.82	16.09	13.02	15.83	16.00	12.34	15.65	+
32126	46.0	20.7	-6.34	-9.76	-11.55	17.06	17.53	17.32	16.79	16.21	17.20	16.13	15.55	16.75	+
32128	59.1	20.1	-7.24	-13.95	-12.84	16.93	11.75	16.49	17.11	10.80	17.43	16.27	9.08	16.82	+
32130	65.4	19.3	-5.90	-11.41	-13.13	20.84	15.49	16.69	21.50	15.71	18.24	21.10	14.47	17.54	+
32132	70.6	19.0	-7.18	-11.36	-11.99	18.42	15.30	18.93	18.52	15.99	20.30	17.12	14.23	19.48	+
32134	90.2	19.0	-7.71	-10.51	-13.04	16.92	17.15	16.79	17.30	18.30	18.71	15.22	16.22	17.26	B





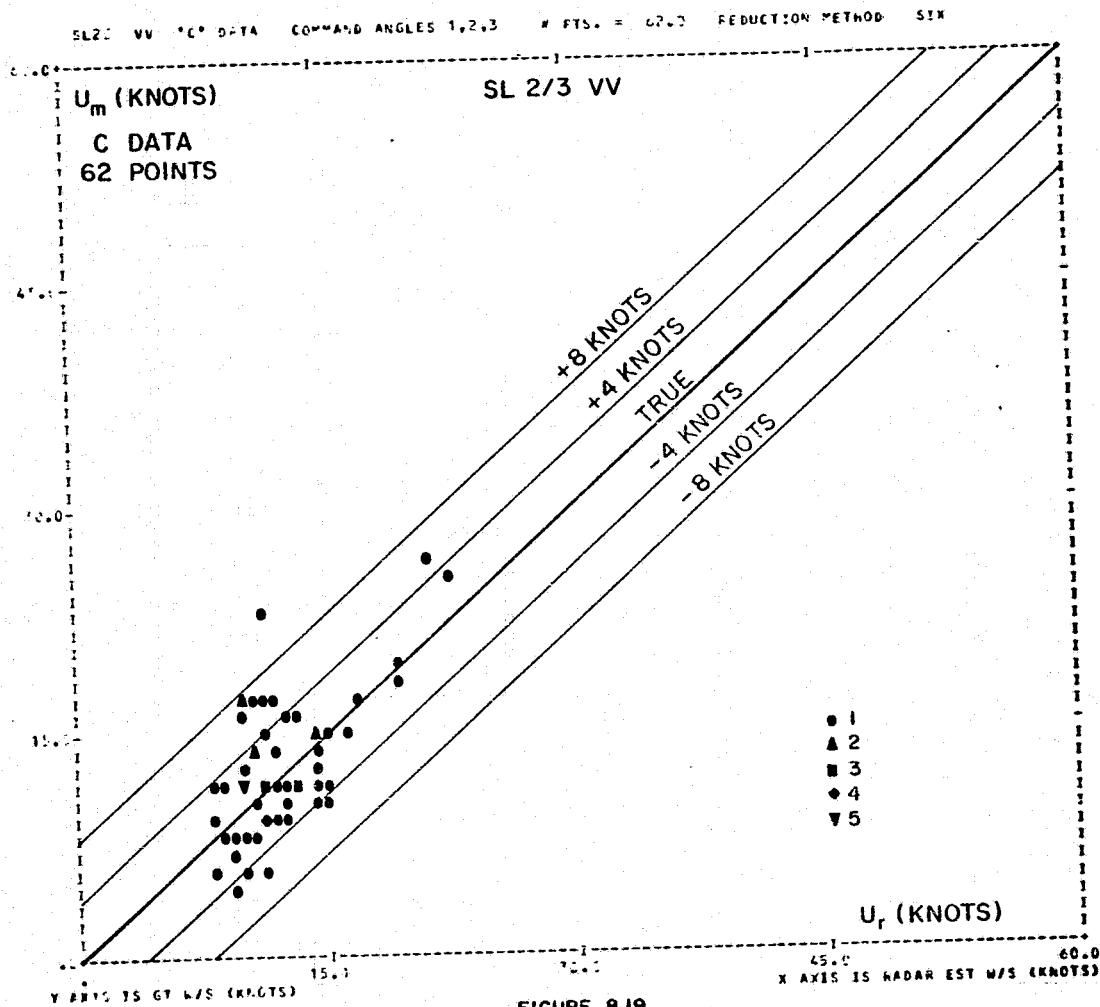
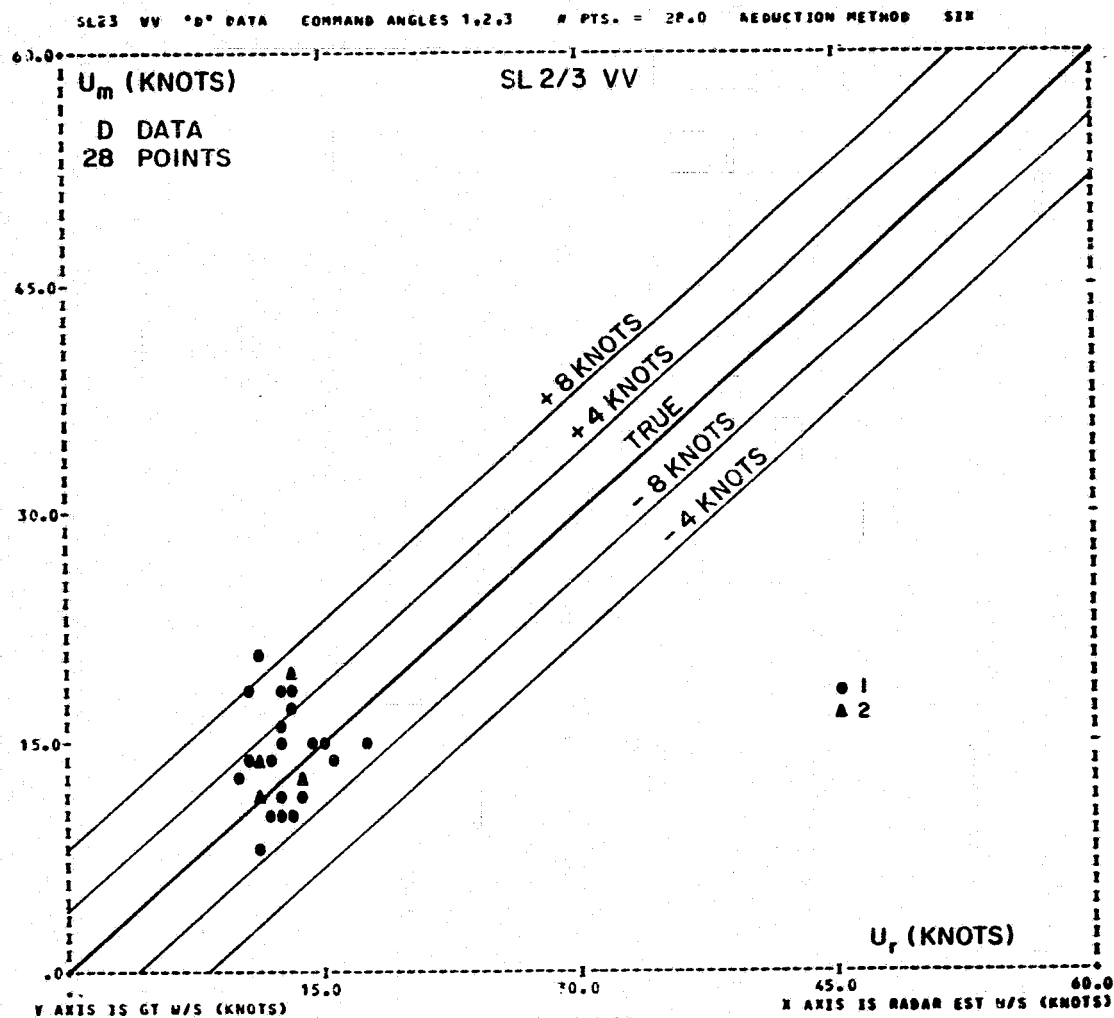
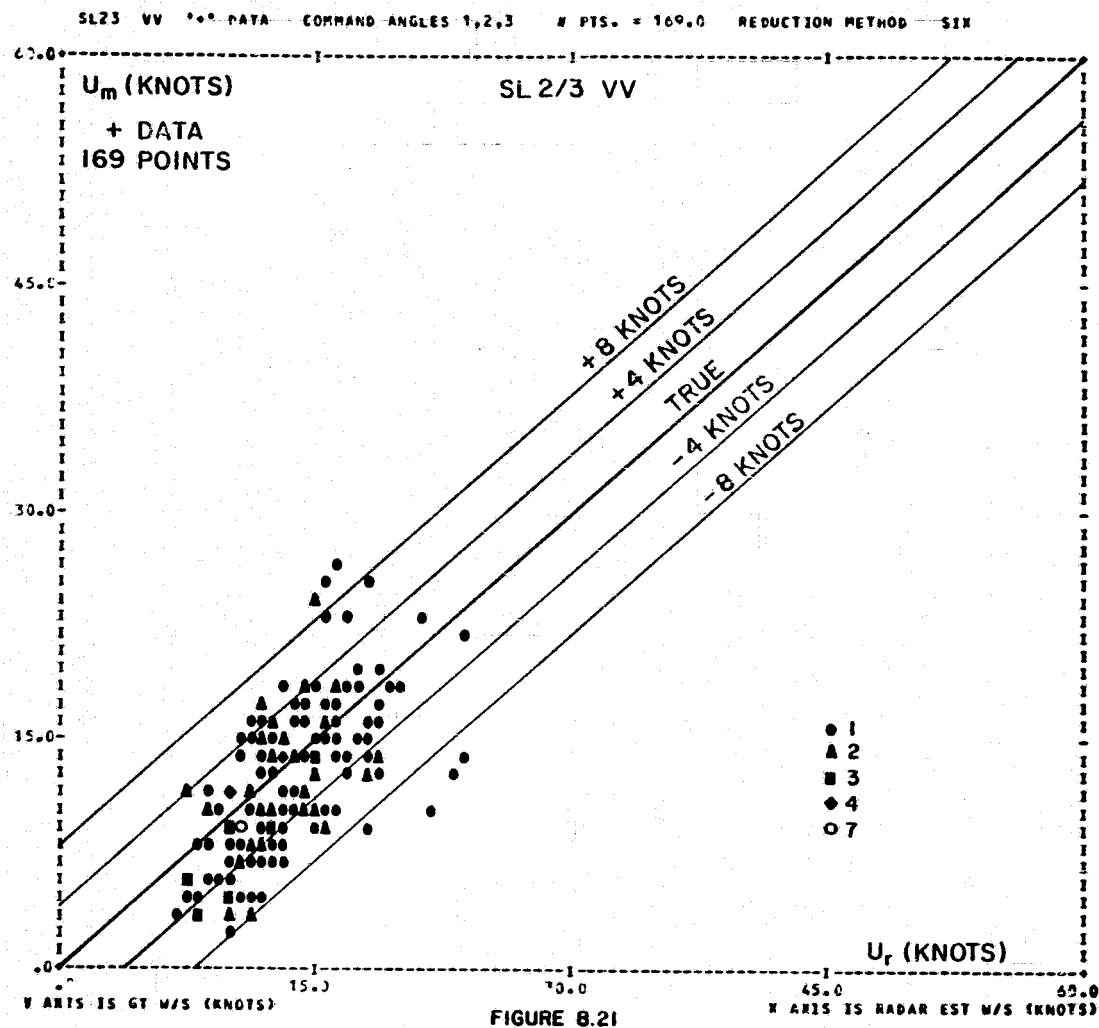
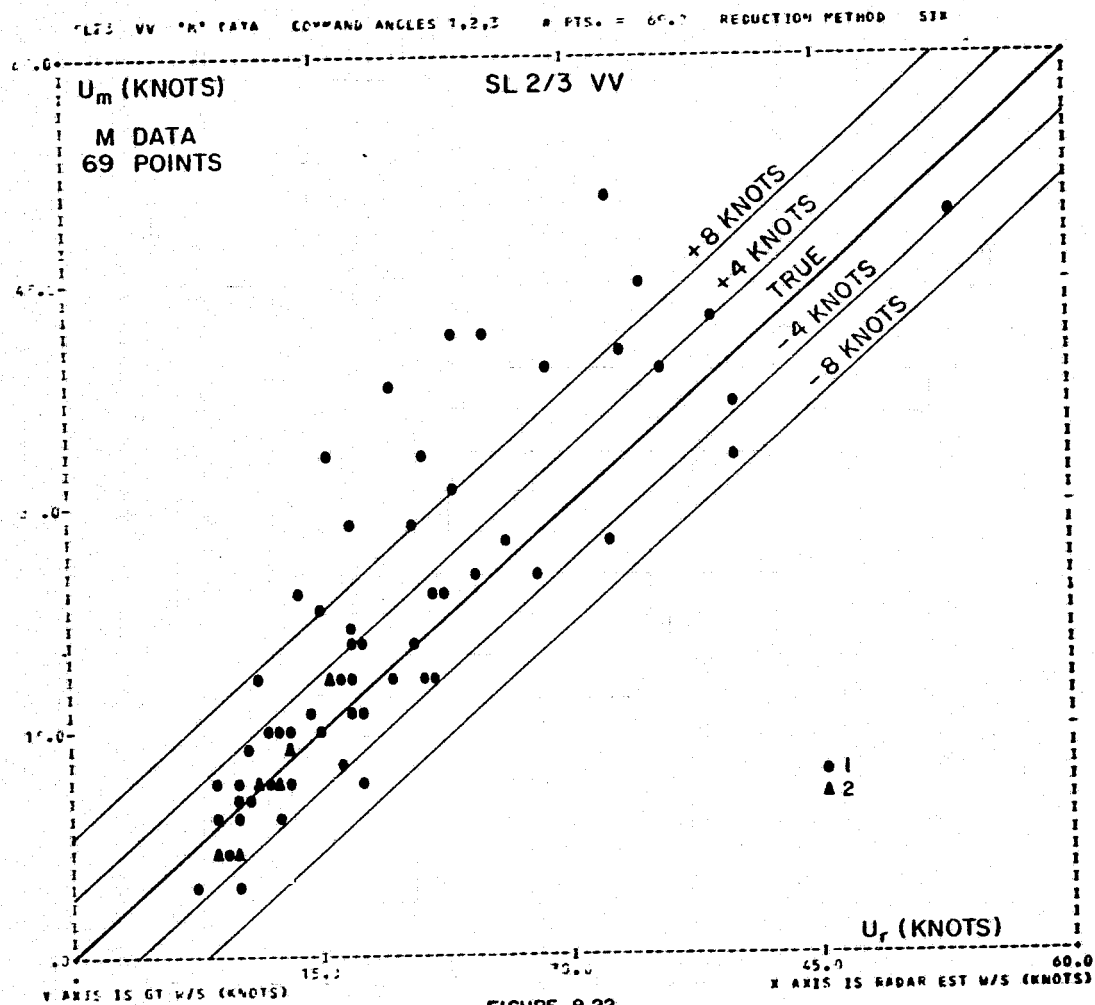


FIGURE 8.19





REPRODUCIBILITY OF THE
ORIGINAL PAGE IS POOR



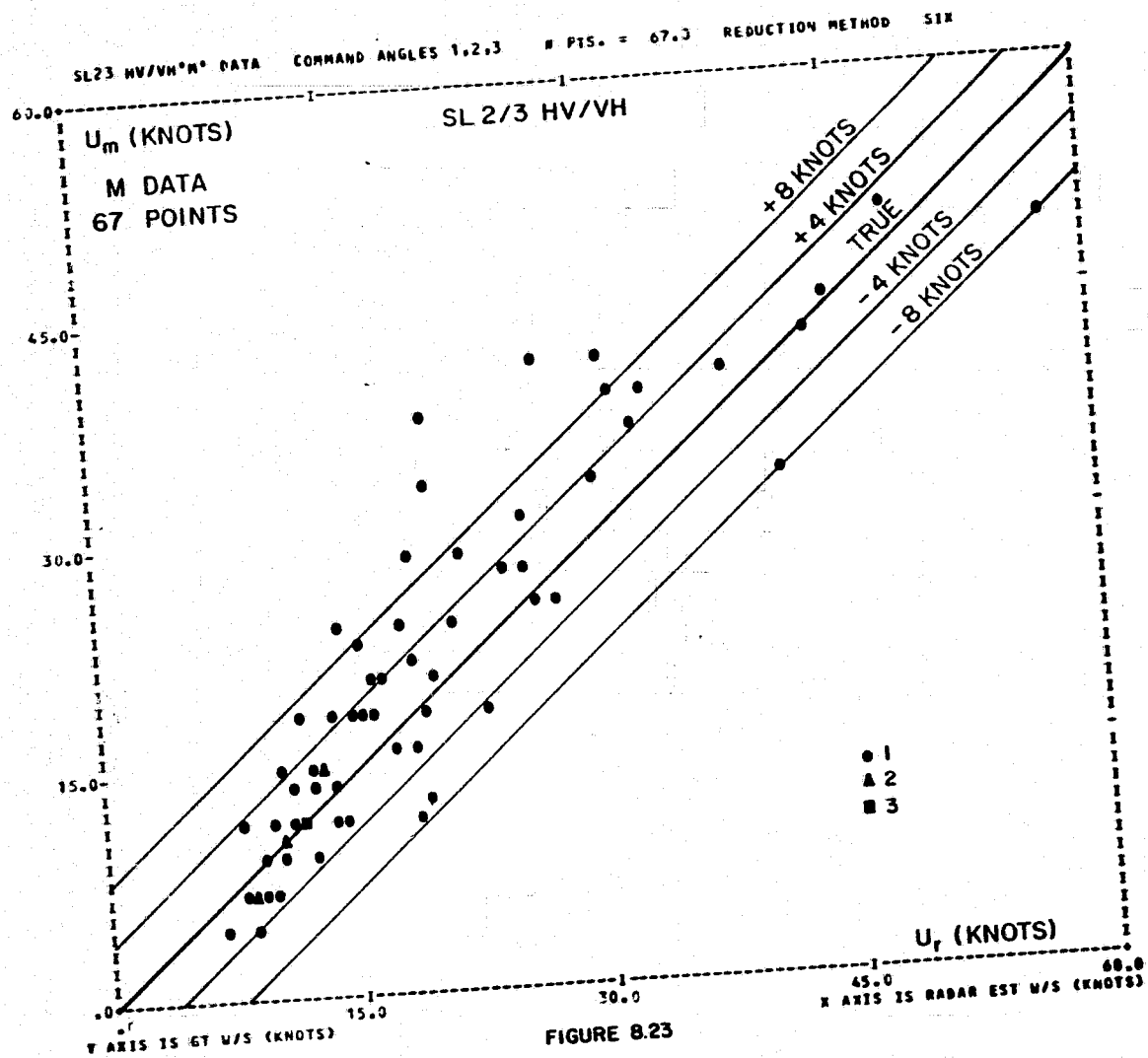


FIGURE 8.23

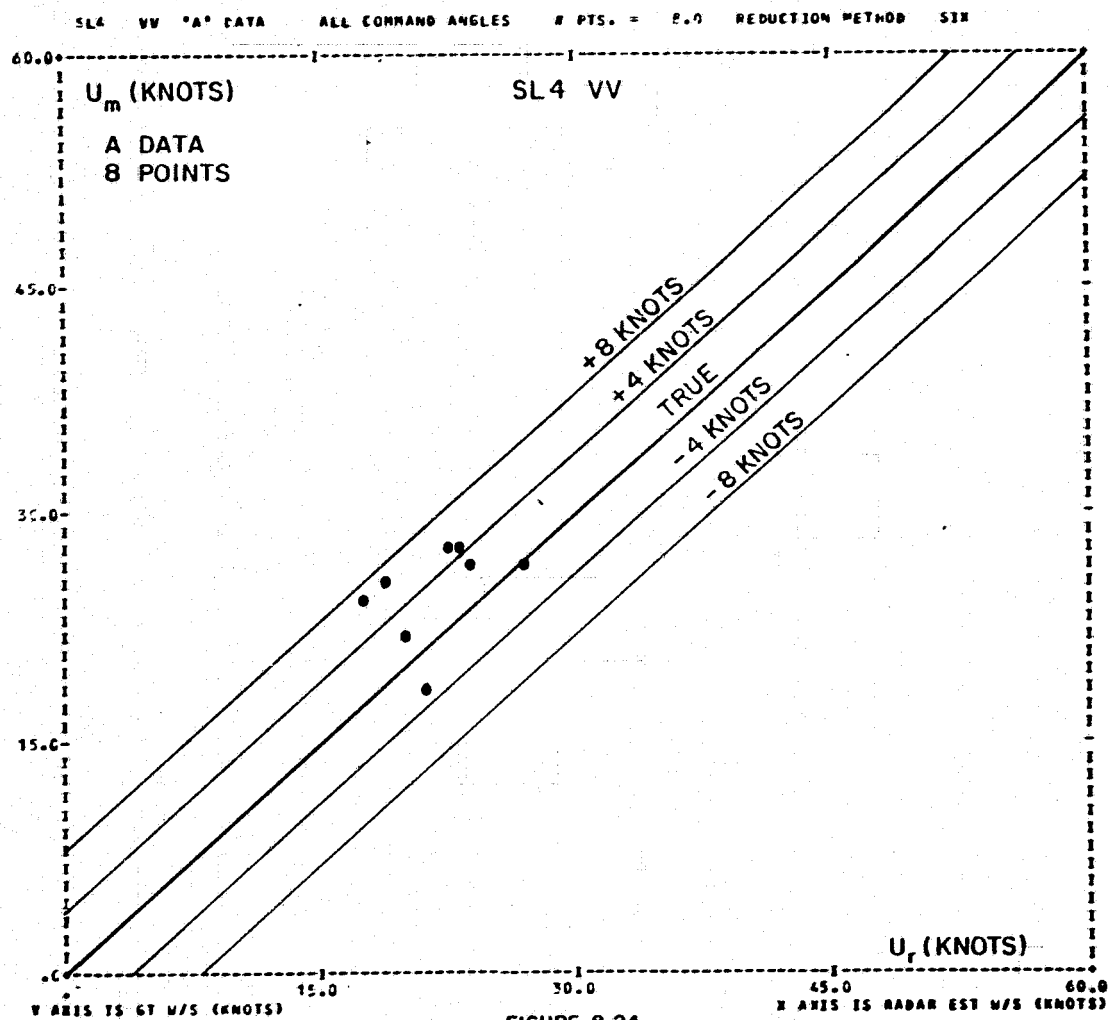
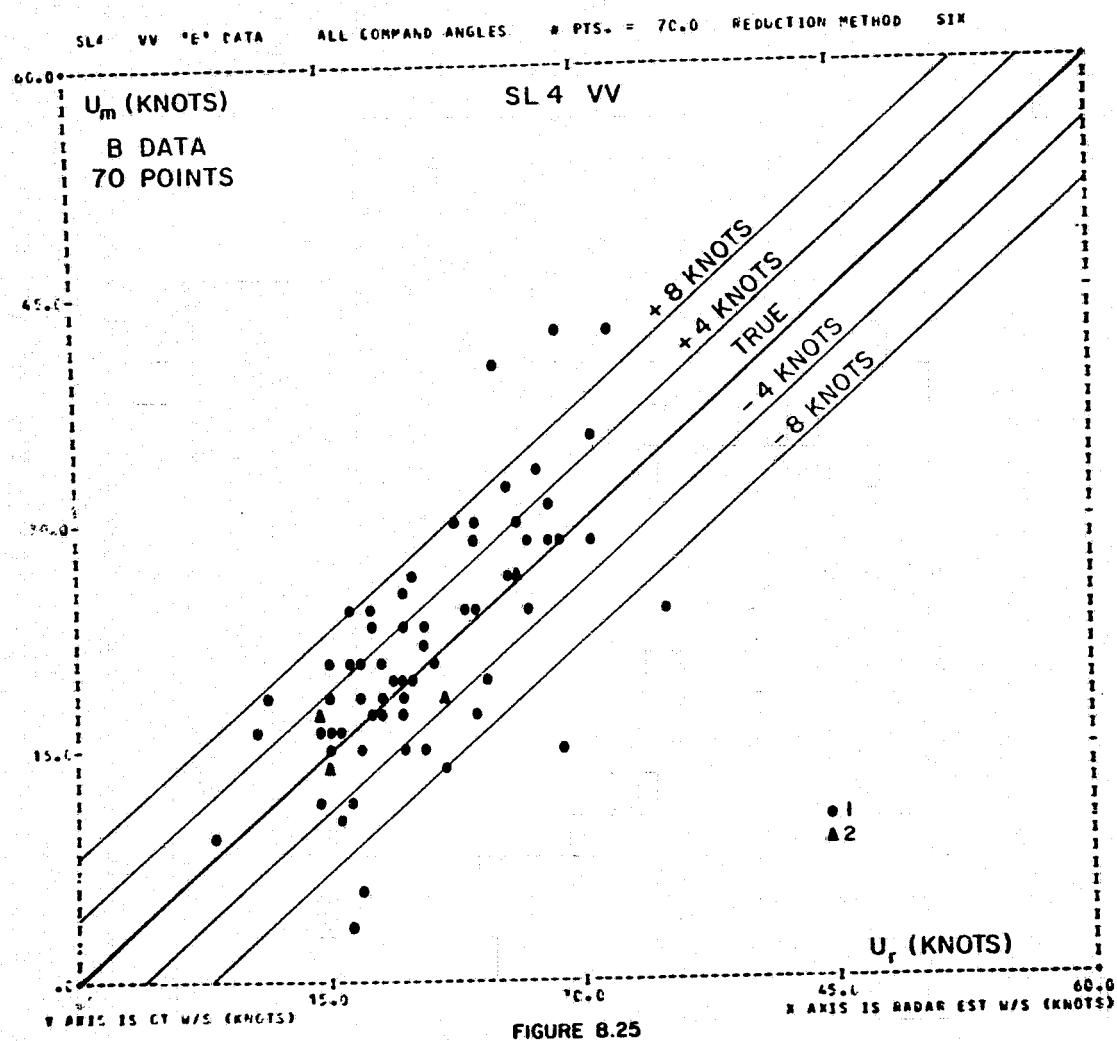


FIGURE 8.24



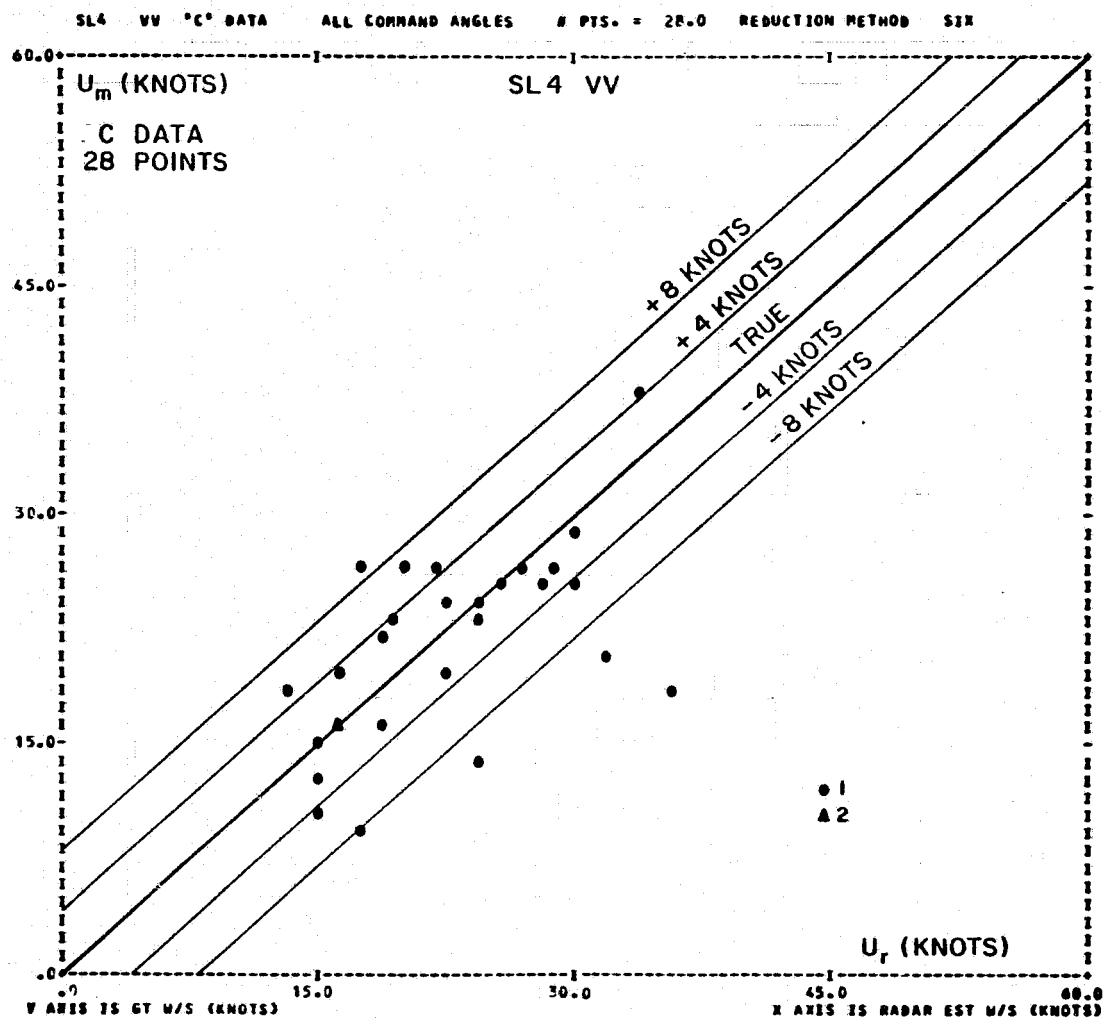
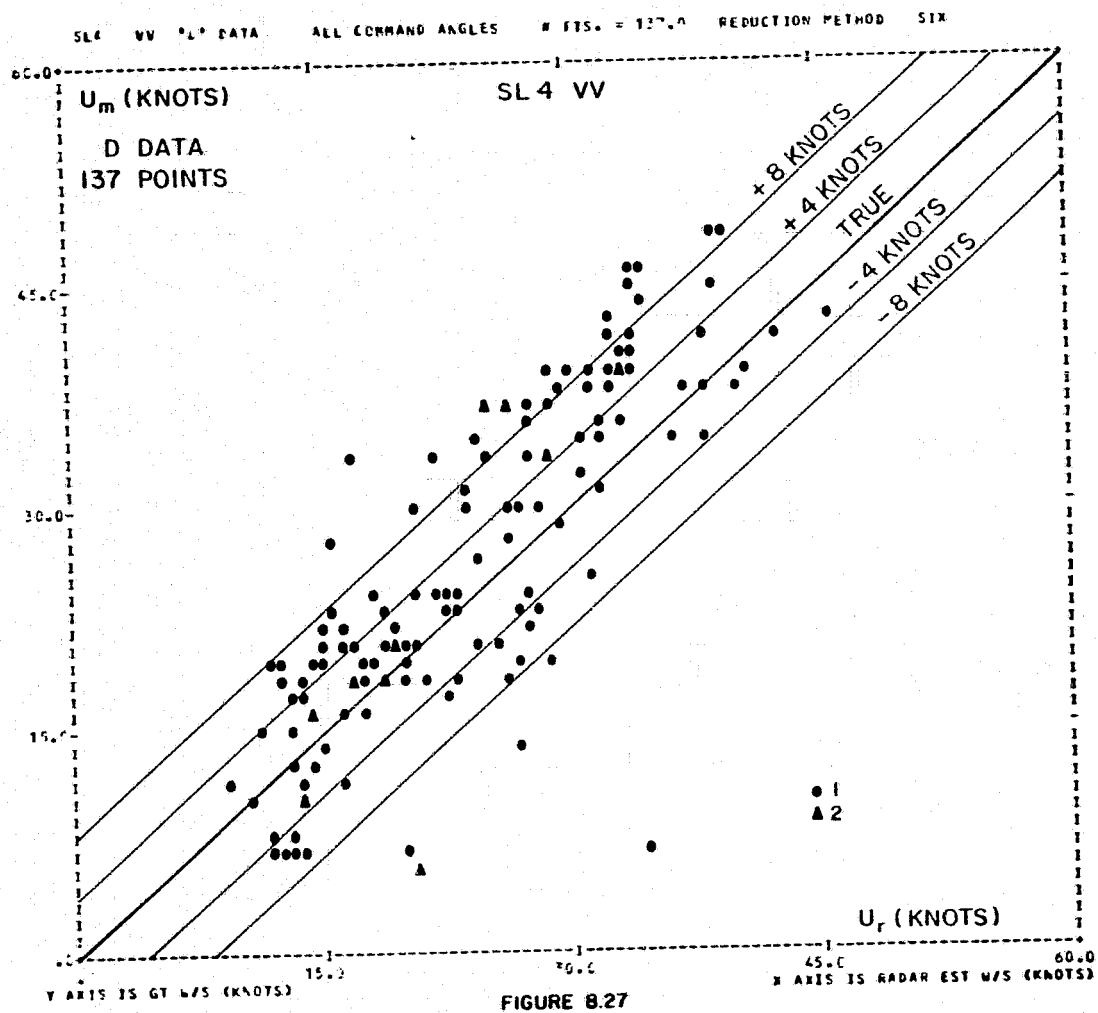


FIGURE 8.26



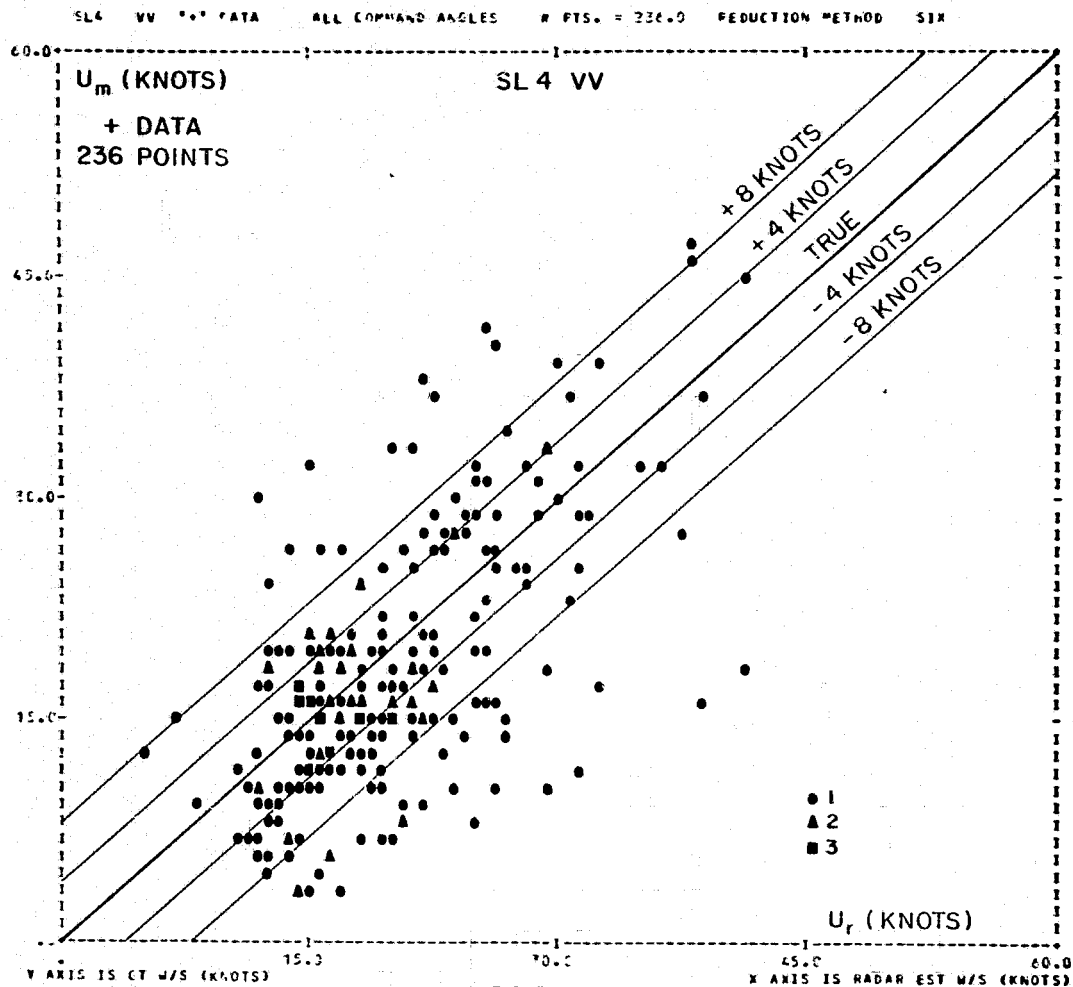


FIGURE 8.28

Stratified root mean square difference analysis for Methods 4, 5 and 6. The results of Table 8.18 are stratified according to wind speed, polarization, type of meteorological surface truth, and the regression method in Table 8.19, which again requires quite a few pages. For example, if the radar wind speed predicted from regression method 4 during SL 4 for VV was between 10 and 19.99 knots and it was verified by a "Type D" meteorological wind, it and all others like it were collected as a subsample. The mean meteorological wind, the mean radar wind, the difference (to show bias) and the root mean square difference are tabulated.

The number of observations in each class differs from method to method. For the same cell, for example one method might yield a radar wind of 18.7 knots and the other a radar wind of 20.2 knots. The values would then be grouped into different class intervals.

For SL 2/3, in addition to Types A, B, C, D and + (for synoptic analyses), two other categories are included. One stratifies the data for Hurricane AVA and Tropical Storm Christine. The other stratifies the data for the manuscript synoptic analyses described in Chapter 4. The points for the manuscript synoptic analysis were also coded as to Type A, Type B, and so on, so that this subset is also included in the totals for A, B, C, D and + in this and subsequent analyses.

Also, the NASA C130 underflight for DOY 156 was treated as a Type A report and accounts for eleven of the nineteen points in Figure 8.17. (Command angle 1, 4 points; angle 2, 4 points, and angle 3, 3 points). DOY 252 accounts for the other eight points.

TABLE 8.19 (I)

LAUT RMS

SL2-3 POLARIZATION VV

QUALITY A

REDUCTION 4

REDUCTION 5

REDUCTION 6

		19.	13.06	13.33	-.28	1.95	19.	13.06	15.51	-2.45	4.48	19.	13.06	15.82	-2.76	4.77
10.00	19.99	19.	13.06	13.33	-.28	1.95	17.	13.18	14.86	-1.68	3.56	16.	13.22	14.79	-1.57	3.35
20.00	29.99	0.	.00	.00	.00	.00	2.	12.00	21.00	-9.00	9.07	3.	12.17	21.27	-9.11	9.17

SL2-3 POLARIZATION VV

QUALITY B

REDUCTION 4

REDUCTION 5

REDUCTION 6

		58.	14.23	13.85	.38	4.63	58.	14.23	14.28	-.04	5.72	58.	14.23	14.22	.02	5.84
.00	9.99	3.	10.20	8.55	1.65	1.70	4.	9.85	9.13	.72	6.02	4.	9.85	9.27	.58	5.96
10.00	19.99	53.	14.37	13.82	.55	4.67	48.	14.82	13.86	.96	5.14	49.	14.78	13.86	.92	5.23
20.00	29.99	2.	16.65	22.63	-5.98	6.28	6.	12.47	21.03	-8.56	9.00	5.	12.42	21.67	-9.25	9.95

SL2-3 POLARIZATION VV

QUALITY C

REDUCTION 4

REDUCTION 5

REDUCTION 6

304

		62.	12.71	12.24	.48	3.46	62.	12.71	12.07	.65	3.47	62.	12.71	12.15	.56	3.43
.00	9.99	9.	10.09	8.35	1.74	2.67	12.	10.00	9.08	.92	3.71	9.	8.63	8.81	-.17	2.54
10.00	19.99	53.	13.16	12.89	.26	3.58	48.	12.86	12.44	.42	3.35	51.	12.93	12.36	.57	3.54
20.00	29.99	0.	.00	.00	.00	.00	2.	25.50	21.07	4.43	4.56	2.	25.50	21.74	3.76	3.94

SL2-3 POLARIZATION VV

QUALITY D

REDUCTION 4

REDUCTION 5

REDUCTION 6

		28.	14.34	12.87	1.47	3.58	28.	14.34	12.65	1.68	3.90	28.	14.34	12.67	1.66	3.83
.00	9.99	1.	13.10	9.16	3.94	3.94	0.	.00	.00	.00	.00	0.	.00	.00	.00	.00
10.00	19.99	27.	14.38	13.00	1.38	3.56	28.	14.34	12.65	1.68	3.90	28.	14.34	12.67	1.66	3.83

SL2-3 POLARIZATION VV

QUALITY M

REDUCTION 4

REDUCTION 5

REDUCTION 6

		69.	20.94	18.56	2.38	6.18	69.	20.94	18.70	2.25	6.37	69.	20.94	18.48	2.46	6.51
.00	9.99	14.	8.64	8.75	-.10	2.43	7.	7.29	8.68	-1.39	2.57	7.	7.29	8.74	-1.46	2.51
10.00	19.99	31.	16.77	14.28	2.50	5.31	39.	16.10	14.25	1.85	5.62	39.	16.10	13.98	2.12	5.53
20.00	29.99	13.	28.69	23.85	4.84	8.71	13.	27.69	23.83	3.86	7.99	14.	28.50	23.49	5.01	8.72
30.00	39.99	9.	38.56	35.81	2.75	7.98	9.	39.56	34.71	4.84	8.79	7.	40.43	35.17	5.26	9.03
40.00	49.99	2.	42.00	41.68	.32	7.86	0.	.00	.00	.00	.00	1.	34.00	40.30	-6.30	6.30
50.00	59.99	0.	.00	.00	.00	.00	1.	50.00	51.14	-1.14	1.14	1.	50.00	53.27	-3.27	3.27

SL2-3 POLARIZATION VV

QUALITY +

REDUCTION 4

REDUCTION 5

REDUCTION 6

REPRODUCIBILITY OF THE
ORIGINAL PAGE IS POOR

TABLE 8.19 (2)

169. 12.08 13.57 -1.49 4.54							169. 12.08 13.22 -1.14 4.22							169. 12.08 13.26 -1.18 4.06							
.00	9.99	25.	6.94	7.81	-.87	3.18	21.	7.30	8.30	-1.00	2.92	24.	7.18	8.54	-1.35	3.31	139.	12.72	13.69	-.98	3.96
10.00	19.99	133.	12.60	13.81	-1.21	4.23	142.	12.58	13.54	-.96	4.13	139.	12.72	13.69	-.98	3.96	6.	16.87	22.19	-5.32	7.47
20.00	29.99	10.	16.98	23.13	-6.15	8.87	6.	16.87	22.91	-6.04	8.19	6.	16.87	22.19	-5.32	7.47	0.	.00	.00	.00	.00
30.00	39.99	1.	22.00	30.01	-8.01	8.01	0.	.00	.00	.00	.00	0.	.00	.00	.00	.00	0.	.00	.00	.00	.00
SL2-3 POLARIZATION VV							MANUSCRIPT ANALYSIS														
REDUCTION 4							REDUCTION 5							REDUCTION 6							
103. 12.82 13.30 -.48 4.12							103. 12.82 12.89 -.07 3.68							103. 12.82 13.11 -.29 3.56							
.00	9.99	5.	7.60	8.35	-.75	1.92	11.	7.00	8.91	-1.91	2.44	10.	6.90	8.88	-1.98	2.50	89.	12.98	13.18	-.20	3.69
10.00	19.99	94.	12.73	13.09	-.36	4.12	88.	13.03	12.98	.05	3.82	89.	12.98	13.18	-.20	3.69	4.	24.00	22.02	1.98	3.04
20.00	29.99	3.	21.00	22.43	-1.43	4.99	4.	24.00	21.70	2.30	3.44	4.	24.00	22.02	1.98	3.04	0.	.00	.00	.00	.00
30.00	39.99	1.	22.00	30.01	-8.01	8.01	0.	.00	.00	.00	.00	0.	.00	.00	.00	.00	0.	.00	.00	.00	.00
SL2-3 POLARIZATION HH							QUALITY A														
REDUCTION 4							REDUCTION 5							REDUCTION 6							
20. 13.00 13.53 -.52 2.03							20. 13.00 15.16 -2.15 4.69							20. 13.00 15.39 -2.38 4.90							
10.00	19.99	20.	13.00	13.53	-.52	2.03	17.	13.10	13.94	-.84	2.99	17.	13.10	14.14	-1.04	3.14	3.	12.47	22.48	-10.02	10.20
20.00	29.99	0.	.00	.00	.00	.00	3.	12.47	22.07	-9.60	9.79	3.	12.47	22.48	-10.02	10.20					
SL2-3 POLARIZATION HH							QUALITY B														
REDUCTION 4							REDUCTION 5							REDUCTION 6							
58. 14.23 13.89 .34 4.87							58. 14.23 14.21 .03 5.64							58. 14.23 14.11 .13 5.73							
.00	9.99	2.	9.50	8.36	1.14	1.61	8.	12.39	9.27	3.11	7.23	8.	12.39	9.32	3.06	7.22	48.	14.49	14.58	-.09	5.34
10.00	19.99	54.	14.32	13.75	.57	4.85	47.	14.53	14.58	-.05	5.17	48.	14.49	14.58	-.09	5.34	2.	15.55	21.93	-6.38	7.57
20.00	29.99	2.	16.65	23.27	-6.62	6.94	3.	14.60	21.57	-6.97	7.43	2.	15.55	21.93	-6.38	7.57					
SL2-3 POLARIZATION HH							QUALITY C														
REDUCTION 4							REDUCTION 5							REDUCTION 6							
47. 12.45 12.49 -.05 3.76							47. 12.45 12.44 .01 3.61							47. 12.45 12.50 -.05 3.54							
.00	9.99	9.	9.51	8.65	.86	2.70	11.	9.41	8.79	.62	2.91	11.	9.41	8.79	.62	2.96	34.	12.66	13.18	-.52	3.64
10.00	19.99	38.	13.14	13.41	-.26	3.97	35.	13.05	13.33	-.28	3.81	34.	12.66	13.18	-.52	3.64	2.	25.50	21.19	4.31	4.61
20.00	29.99	0.	.00	.00	.00	.00	1.	25.00	21.37	3.63	3.63	2.	25.50	21.19	4.31	4.61					
SL2-3 POLARIZATION HH							QUALITY D														
REDUCTION 4							REDUCTION 5							REDUCTION 6							
33. 13.78 12.34 1.45 3.92							33. 13.78 12.25 1.54 4.23							33. 13.78 12.26 1.52 4.18							
.00	9.99	7.	11.81	8.69	3.12	3.45	6.	11.43	8.95	2.48	2.91	6.	11.43	9.00	2.44	2.92	26.	14.30	12.62	1.68	4.20
10.00	19.99	24.	14.28	12.69	1.59	3.81	25.	14.28	12.31	1.97	4.23	26.	14.30	12.62	1.68	4.20	1.	14.60	22.73	-8.13	8.13
20.00	29.99	2.	14.70	20.85	-6.15	6.15	2.	14.70	21.34	-6.64	6.78	1.	14.60	22.73	-8.13	8.13					

TABLE 8.19 (3)

SL2-3 POLARIZATION HH

QUALITY N

REDUCTION 4							REDUCTION 5					REDUCTION 6				
		67.	21.18	18.71	2.46	5.59	67.	21.18	18.68	2.50	5.94	67.	21.18	18.49	2.69	6.03
.70	9.99	11.	9.45	8.53	.92	2.39	9.	8.22	8.93	-7.0	2.28	10.	7.90	8.98	-1.08	2.66
10.00	19.99	36.	17.19	14.03	3.16	6.15	38.	16.89	14.39	2.50	5.77	37.	17.22	14.23	2.98	5.79
20.00	29.99	8.	26.87	24.04	2.84	5.77	10.	29.80	24.77	5.03	6.79	10.	29.80	24.27	5.53	7.25
30.00	39.99	8.	38.37	36.04	2.33	6.19	8.	40.12	34.61	5.52	7.66	7.	39.71	34.02	5.69	8.05
40.00	49.99	4.	43.50	43.58	-1.08	4.91	1.	34.00	41.46	-7.46	7.46	2.	38.50	41.34	-2.84	5.94
50.00	59.99	0.	.00	.00	.00	.00	1.	50.00	58.42	-8.42	8.42	1.	50.00	58.56	-8.56	8.56

SL2-3 POLARIZATION HH

QUALITY +

REDUCTION 4							REDUCTION 5					REDUCTION 6				
		175.	11.82	13.08	-1.26	4.11	175.	11.82	12.83	-1.01	3.86	175.	11.82	12.89	-1.08	3.73
.00	9.99	30.	7.00	8.09	-1.08	2.89	40.	7.44	8.74	-1.30	2.96	39.	7.30	8.65	-1.34	2.98
10.00	19.99	137.	12.59	13.55	-1.96	3.86	128.	12.97	13.60	-.63	3.78	130.	12.97	13.76	-.79	3.67
20.00	29.99	8.	16.62	23.63	-7.00	9.09	7.	15.71	22.02	-6.30	7.83	6.	16.15	21.75	-5.60	7.50

SL2-3 POLARIZATION HH

MANUSCRIPT ANALYSIS

306

REDUCTION 4							REDUCTION 5					REDUCTION 6				
		104.	12.81	13.13	-.33	3.83	104.	12.81	12.73	.08	3.54	104.	12.81	12.95	-.15	3.39
.30	9.99	8.	7.00	8.98	-1.98	2.70	14.	7.21	9.06	-1.85	2.27	15.	7.20	9.14	-1.94	2.33
10.00	19.99	94.	13.10	13.26	-.17	3.93	88.	13.45	13.12	.34	3.72	86.	13.38	13.33	.05	3.53
20.00	29.99	2.	22.50	23.63	-1.13	2.58	2.	23.50	21.18	2.32	2.66	3.	24.33	21.15	3.18	3.80

SL2-3 POLARIZATION HV/VH

QUALITY A

REDUCTION 4							REDUCTION 5					REDUCTION 6				
		19.	13.06	14.01	-.95	2.02	19.	13.06	15.39	-2.34	4.60	19.	13.06	15.42	-2.36	4.60
10.00	19.99	19.	13.06	14.01	-.95	2.02	17.	13.13	14.69	-1.56	3.70	16.	13.22	14.39	-1.17	3.23
20.00	29.99	0.	.00	.00	.00	.00	2.	12.45	21.38	-8.93	9.21	3.	12.17	20.89	-8.72	8.87

SL2-3 POLARIZATION HV/VH

QUALITY B

REDUCTION 4							REDUCTION 5					REDUCTION 6				
		58.	14.23	13.85	.39	4.38	58.	14.23	14.07	.16	5.44	58.	14.23	13.98	.25	5.45
.00	9.99	6.	9.10	8.81	.29	2.75	8.	12.36	9.03	3.33	7.13	8.	12.36	9.06	3.31	7.14
10.00	19.99	50.	14.75	14.16	.59	4.51	49.	14.41	14.73	-.32	5.16	48.	14.49	14.52	-.02	5.03
20.00	29.99	2.	16.65	20.98	-4.33	5.25	1.	20.60	22.50	-1.90	1.90	2.	15.55	20.87	-5.32	6.89

SL2-3 POLARIZATION HV/VH

QUALITY C

REDUCTION 4							REDUCTION 5					REDUCTION 6				
		47.	12.45	12.25	.20	3.56	47.	12.45	12.32	.13	3.10	47.	12.45	12.37	.08	3.07

TABLE 8.19 (4)

.30	9.99	9.	10.04	8.30	1.74	2.64	9.	8.62	8.46	.16	2.35	9.	8.62	8.48	.14	2.37
10.30	19.99	38.	13.02	13.18	-.16	3.74	37.	13.04	13.02	.02	3.23	37.	13.04	13.08	-.04	3.19
20.00	29.99	0.	.30	.00	.00	.00	1.	25.00	20.87	4.13	4.13	1.	25.00	21.33	3.67	3.67

SL2-3 POLARIZATION HV/VH QUALITY D

REDUCTION 4							REDUCTION 5					REDUCTION 6				
		28.	14.34	12.53	1.81	3.72	28.	14.34	12.33	2.00	4.15	28.	14.34	12.32	2.01	4.15
.00	9.99	3.	11.80	8.77	3.03	3.21	2.	12.00	9.73	2.27	2.52	2.	12.00	9.78	2.22	2.48
10.00	19.99	25.	14.64	12.98	1.66	3.77	26.	14.52	12.53	1.98	4.25	26.	14.52	12.52	2.00	4.25

SL2-3 POLARIZATION HV/VH QUALITY M

REDUCTION 4							REDUCTION 5					REDUCTION 6				
		67.	21.06	19.22	1.84	5.12	67.	21.06	19.36	1.70	5.26	67.	21.06	19.32	1.74	5.25
.00	9.99	12.	8.17	7.81	.36	2.43	9.	7.78	8.67	-.89	2.30	10.	7.70	8.77	-1.07	2.31
10.00	19.99	31.	16.29	14.34	1.95	5.00	36.	16.22	14.65	1.57	5.02	36.	16.94	14.80	2.15	5.48
20.00	29.99	13.	27.85	24.03	3.82	6.93	12.	28.08	24.43	3.65	6.59	11.	27.64	24.83	2.81	5.73
30.00	39.99	5.	37.40	32.85	4.55	5.65	5.	39.40	32.83	6.57	7.24	5.	39.40	33.28	6.12	6.93
40.00	49.99	5.	41.60	43.98	-2.38	4.92	4.	43.25	44.15	-.90	3.80	4.	43.25	44.21	-.96	3.77
50.00	59.99	1.	51.00	52.91	-1.91	1.91	1.	50.00	57.69	-7.69	7.69	1.	50.00	57.47	-7.47	7.47

SL2-3 POLARIZATION HV/VH QUALITY +

REDUCTION 4							REDUCTION 5					REDUCTION 6				
		164.	11.97	13.12	-1.15	3.89	164.	11.97	12.83	-.86	3.75	164.	11.97	12.87	-.89	3.70
.00	9.99	34.	7.40	7.85	-.45	2.96	35.	7.11	8.54	-1.43	3.23	34.	7.09	8.50	-1.41	3.27
10.00	19.99	122.	12.85	13.98	-1.13	3.82	125.	13.13	13.75	-.62	3.82	127.	13.13	13.82	-.69	3.74
20.00	29.99	8.	18.01	22.36	-4.35	7.08	4.	18.47	21.79	-3.32	5.33	3.	18.30	22.02	-3.72	5.95

SL2-3 POLARIZATION HV/VH MANUSCRIPT ANALYSIS

REDUCTION 4							REDUCTION 5					REDUCTION 6				
103. 12.82 13.16 -.35 3.52							103. 12.82 12.57 .25 3.35					103. 12.82 12.66 .15 3.27				
.00	9.99	16.	8.13	8.93	-.81	2.35	19.	7.37	8.84	-1.47	2.04	18.	7.33	8.80	-1.47	2.03
10.00	19.99	83.	13.28	13.55	-.27	3.73	82.	13.82	13.22	.59	3.59	83.	13.75	13.29	.45	3.50
20.00	29.99	4.	22.00	22.14	-.14	3.07	2.	23.50	21.12	2.38	2.95	2.	23.50	21.32	2.18	2.64

SL4 POLARIZATION VV QUALITY A

REDUCTION 4							REDUCTION 5					REDUCTION 6				
		8.	24.89	21.44	3.45	4.97	8.	24.89	21.21	3.68	5.17	8.	24.89	21.85	3.04	4.60
10.00	19.99	3.	24.03	18.64	5.40	5.59	2.	24.95	17.94	7.01	7.02	3.	24.03	18.73	5.30	5.69
20.00	29.99	5.	25.40	23.11	2.29	4.56	6.	24.87	22.30	2.56	4.37	5.	25.40	23.72	1.68	3.80

SL4 POLARIZATION VV QUALITY B

TABLE 8.19 (5)

REDUCTION 4							REDUCTION 5					REDUCTION 6				
		70.	21.53	20.56	.97	5.43	70.	21.53	20.27	1.26	5.89	70.	21.53	20.63	.90	5.52
.00	9.99	1.	9.70	7.85	1.85	1.85	0.	.00	.00	.00	.00	1.	9.70	8.18	1.52	1.52
10.00	19.99	37.	17.48	16.74	.73	4.78	38.	17.53	16.44	1.09	5.29	36.	17.41	16.51	.89	4.66
20.00	29.99	27.	25.07	24.25	.82	5.45	30.	25.80	24.34	1.46	6.16	29.	25.50	24.56	.93	6.13
30.00	39.99	5.	34.80	31.41	3.39	9.10	2.	33.40	31.86	1.54	10.62	4.	32.85	32.21	.64	8.06

SL4 POLARIZATION VV QUALITY C

REDUCTION 4							REDUCTION 5					REDUCTION 6				
		28.	21.47	22.16	-.68	5.52	28.	21.47	22.59	-1.12	5.98	28.	21.47	22.47	-1.00	5.71
10.00	19.99	13.	17.91	16.86	1.05	4.50	13.	17.91	17.23	.68	5.10	12.	17.16	16.55	.61	4.55
20.00	29.99	12.	24.21	25.26	-1.05	3.38	11.	23.80	25.18	-1.38	4.14	11.	23.89	24.44	-.55	4.48
30.00	39.99	3.	26.00	32.72	-6.72	12.29	4.	26.67	32.91	-6.24	10.92	5.	26.52	32.34	-5.82	9.42

SL4 POLARIZATION VV QUALITY D

REDUCTION 4							REDUCTION 5					REDUCTION 6				
		137.	26.11	24.07	2.04	6.87	137.	26.11	23.98	2.14	7.00	137.	26.11	23.97	2.14	6.80
.00	9.99	3.	12.33	9.26	3.07	5.89	1.	11.00	9.65	1.35	1.35	1.	11.00	9.27	1.73	1.73
10.00	19.99	51.	16.91	15.66	1.25	5.70	51.	16.95	15.31	1.64	5.67	50.	16.84	15.37	1.46	5.25
20.00	29.99	47.	27.86	25.50	2.37	6.97	47.	26.50	24.77	1.72	7.58	49.	26.45	24.92	1.53	7.24
30.00	39.99	31.	37.05	34.26	2.79	8.61	34.	38.06	34.16	3.90	8.33	33.	38.36	33.84	4.53	8.48
40.00	49.99	5.	43.94	42.17	1.77	5.18	4.	40.65	42.10	-1.45	1.68	4.	40.65	42.20	-1.55	1.68

SL4 POLARIZATION VV QUALITY +

REDUCTION 4							REDUCTION 5					REDUCTION 6				
		236.	18.40	19.90	-1.51	7.02	236.	18.40	20.00	-1.61	7.03	236.	18.40	19.89	-1.49	7.07
.00	9.99	3.	12.13	9.01	3.12	4.37	3.	12.13	8.38	3.75	4.69	3.	12.13	6.60	5.54	6.58
10.00	19.99	131.	14.57	15.67	-1.11	5.28	136.	14.84	15.88	-1.04	5.51	135.	14.53	15.71	-1.19	5.67
20.00	29.99	84.	22.24	23.73	-1.49	7.98	80.	21.86	24.21	-2.35	8.45	79.	22.26	24.00	-1.74	8.04
30.00	39.99	15.	27.97	33.37	-5.41	11.42	15.	31.61	34.46	-2.85	9.11	17.	30.68	33.78	-3.10	9.89
40.00	49.99	3.	36.30	41.13	-4.83	14.32	2.	31.70	41.01	-9.31	15.83	2.	31.70	41.25	-9.55	16.64

SL4 POLARIZATION HH QUALITY A

REDUCTION 4							REDUCTION 5					REDUCTION 6				
		8.	24.89	22.94	1.94	4.31	8.	24.89	22.94	1.95	4.49	8.	24.89	23.49	1.40	3.82
10.00	19.99	1.	18.10	18.12	-.02	.02	0.	.00	.00	.00	.00	1.	18.10	18.42	-.32	.32
20.00	29.99	7.	25.86	23.63	2.22	4.61	8.	24.89	22.94	1.95	4.49	7.	25.86	24.22	1.64	4.08

SL4 POLARIZATION HH QUALITY B

REDUCTION 4 REDUCTION 5 REDUCTION 6

TABLE 8.19 (6)

		76.	21.49	20.73	.76	6.84	76.	21.49	20.88	.62	6.99	76.	21.49	21.28	.21	6.69
.00	9.99	1.	9.70	6.21	3.49	3.49	0.	.00	.00	.00	.00	1.	9.70	7.20	2.50	2.50
10.00	19.99	32.	17.95	16.80	1.15	5.10	33.	18.09	16.71	1.39	5.58	29.	17.33	16.81	.52	4.84
20.00	29.99	40.	23.85	23.43	.42	7.93	42.	24.10	23.90	.19	7.93	45.	24.37	24.20	.17	7.66
30.00	39.99	3.	31.77	31.46	.30	8.11	1.	24.20	31.33	-7.13	7.13	1.	24.20	33.20	-9.00	9.00

SL4 POLARIZATION HH QUALITY C

REDUCTION 4							REDUCTION 5					REDUCTION 6				
		37.	19.39	23.10	-3.70	7.57	37.	19.39	23.31	-3.92	7.52	37.	19.39	23.30	-3.91	7.59
10.00	19.99	10.	17.70	17.42	.28	3.17	10.	17.70	17.56	.14	2.84	10.	17.70	16.89	.81	3.30
20.00	29.99	25.	19.62	24.56	-4.94	8.57	24.	18.85	24.64	-5.79	8.69	22.	18.52	24.34	-5.82	8.74
30.00	39.99	2.	25.00	33.17	-8.17	9.54	3.	29.40	31.88	-2.48	8.20	5.	26.62	31.57	-4.95	8.24

SL4 POLARIZATION HH QUALITY D

REDUCTION 4							REDUCTION 5					REDUCTION 6				
		135.	26.27	22.82	3.44	8.49	135.	26.27	22.70	3.57	8.85	135.	26.27	22.79	3.48	8.73
.00	9.99	0.	.00	.00	.00	.00	1.	19.70	9.42	10.28	10.28	1.	19.70	9.24	10.46	10.46
10.00	19.99	52.	16.57	16.49	.09	6.42	44.	17.15	16.05	1.10	6.22	48.	16.59	16.95	-.37	6.11
20.00	29.99	63.	30.51	24.34	6.17	9.82	76.	29.24	24.48	4.77	10.36	71.	30.23	24.45	5.78	10.46
30.00	39.99	18.	37.84	33.83	4.01	9.16	13.	39.03	34.40	4.63	6.77	15.	38.93	34.46	4.48	6.46
40.00	49.99	2.	40.25	40.65	-.40	1.31	1.	42.00	41.40	.60	.60	0.	.00	.00	.00	.00

SL4 POLARIZATION HH QUALITY +

REDUCTION 4							REDUCTION 5					REDUCTION 6				
		238.	18.34	20.03	-1.69	7.53	238.	18.34	20.02	-1.68	7.47	238.	18.34	19.82	-1.48	7.44
.00	9.99	3.	12.67	9.18	3.49	6.12	6.	11.10	9.35	1.75	4.65	9.	13.06	8.65	4.41	6.98
10.00	19.99	115.	15.00	15.64	-.63	4.85	116.	14.85	15.82	-.97	5.03	118.	15.10	15.83	-.73	5.34
20.00	29.99	106.	20.59	23.17	-2.58	8.78	103.	21.40	23.52	-2.12	8.70	97.	20.81	23.64	-2.83	8.95
30.00	39.99	13.	31.02	34.08	-3.07	11.89	11.	28.20	33.58	-5.38	12.65	14.	31.96	34.19	-2.24	10.65
40.00	49.99	1.	16.30	41.93	-25.63	25.63	2.	30.85	40.57	-9.72	17.94	0.	.00	.00	.00	.00

SL4 POLARIZATION HV/VH QUALITY A

REDUCTION 4							REDUCTION 5					REDUCTION 6				
		8.	24.89	21.56	3.33	4.47	8.	24.89	20.72	4.17	5.38	8.	24.89	21.30	3.59	4.71
10.00	19.99	3.	21.57	19.51	2.06	3.47	2.	24.95	18.65	6.30	6.30	2.	21.25	18.84	2.41	4.82
20.00	29.99	5.	26.88	22.79	4.09	4.97	6.	24.87	21.41	3.46	5.04	6.	26.10	22.12	3.98	4.67

SL4 POLARIZATION HV/VH QUALITY B

REDUCTION 4							REDUCTION 5					REDUCTION 6				
		70.	21.53	20.78	.75	6.12	70.	21.53	20.13	1.40	7.02	70.	21.53	20.37	1.16	6.69
10.00	19.99	36.	17.83	16.47	1.36	4.27	37.	18.78	16.67	2.11	5.50	38.	18.65	16.74	1.91	5.05

TABLE 8.19 (7)

20.00	29.99	29.	24.79	24.10	.70	7.27	30.	23.89	23.30	.59	8.51	29.	24.25	23.91	.34	8.24
30.00	39.99	5.	29.22	32.60	-3.38	9.29	3.	31.77	31.07	.70	7.29	2.	31.77	32.05	-.28	8.13

SL4 POLARIZATION HV/VH QUALITY C

REDUCTION 4							REDUCTION 5					REDUCTION 6				
		29.	20.72	22.10	-1.38	5.73	29.	20.72	22.28	-1.56	6.21	29.	20.72	22.40	-1.68	6.24
10.00	19.99	13.	16.48	17.36	-.89	4.81	13.	19.54	17.71	1.83	4.66	13.	19.54	17.62	1.92	4.60
20.00	29.99	13.	23.74	24.41	-.67	4.32	11.	19.66	23.43	-3.76	6.28	11.	19.66	23.34	-3.68	5.88
30.00	39.99	3.	26.00	32.57	-6.57	11.70	5.	26.10	31.63	-5.53	8.99	5.	26.10	32.75	-6.65	9.71

SL4 POLARIZATION HV/VH QUALITY D

REDUCTION 4							REDUCTION 5					REDUCTION 6				
		137.	26.11	23.65	2.46	7.66	137.	26.11	23.51	2.61	8.04	137.	26.11	23.53	2.58	7.83
10.00	19.99	51.	17.45	15.59	1.87	5.77	57.	17.78	16.10	1.68	6.59	59.	17.85	16.27	1.58	6.34
20.00	29.99	53.	27.28	24.69	2.59	8.65	46.	27.92	24.57	3.36	9.58	43.	27.75	24.66	3.09	9.21
30.00	39.99	29.	36.76	33.40	3.36	8.88	31.	37.17	33.80	3.37	8.24	33.	37.90	33.94	3.96	8.47
40.00	49.99	4.	43.77	42.10	1.67	4.92	3.	42.37	41.51	.85	4.37	2.	40.25	41.99	-1.74	2.56

SL4 POLARIZATION HV/VH QUALITY +

REDUCTION 4							REDUCTION 5					REDUCTION 6				
		236.	18.48	20.07	-1.59	7.09	236.	18.48	20.36	-1.88	7.11	236.	18.48	20.24	-1.76	7.07
.00	9.99	6.	9.77	9.44	.33	2.13	0.	.00	.00	.00	.00	4.	8.97	9.33	-.35	2.49
10.00	19.99	124.	14.86	15.86	-1.00	5.27	136.	15.16	16.25	-1.10	5.73	133.	15.18	16.27	-1.09	5.81
20.00	29.99	92.	22.04	24.11	-2.07	8.17	82.	21.23	24.08	-2.85	8.45	80.	21.35	24.02	-2.67	8.45
30.00	39.99	13.	29.79	34.94	-5.15	13.13	17.	30.24	34.01	-3.77	9.68	18.	30.69	33.99	-3.29	9.25
40.00	49.99	1.	45.40	42.24	3.16	3.16	1.	45.40	40.86	4.54	4.54	1.	45.40	40.79	4.61	4.61

ERROR ANALYSIS OF THE DIFFERENCE BETWEEN THE METEOROLOGICAL WIND AND THE RADAR WIND

Introduction. In Chapter 4, Table 4.6 gave estimates of the errors in the meteorological winds. These errors represent the kinds of errors presently existing in the description of the vector wind field in the planetary boundary layer over the oceans. Although the instantaneously measured wind direction and speed are determined with greater claimed accuracy than this by well designed and properly installed anemometers, these errors arise because of the lack of adequate temporal averaging procedures so as to obtain a stable estimate of the wind speed and direction truly representative of the desired synoptic scale and because of the need to interpolate to a grid of points in numerical analyses.

In the preceding sections of Chapter 8, regression techniques have yielded ways to determine the magnitude of the vector wind from a radar backscatter measurement under the assumption that the meteorological wind direction corresponds to the radar wind direction. In this section, an analysis is given of the difference between the magnitude of the meteorological wind and the magnitude of the radar wind subject to this constraint.

Analysis. As in an analysis paralleling the one in Chapter 4, when two ships were compared, let \vec{V}_m be the meteorological wind and \vec{V}_r be the radar wind.

$$\vec{V}_m = (V_T + E_{11}, E_{21}) \quad (8.72)$$

$$\vec{V}_r = (V_T + E_{12}, E_{22}) \quad (8.73)$$

The error vectors are E_{11} , parallel to the true wind for the meteorological wind, E_{21} , normal to the true wind for the meteorological wind, E_{12} parallel to the true wind for the radar wind, and E_{22} , normal to the true wind for the radar wind.

The difference between the meteorological wind and the radar wind is given by equation (8.74).

$$\vec{V}_m - \vec{V}_r = [E_{11} - E_{12}, E_{21} - E_{22}] \quad (8.74)$$

From Figure 8.29, the requirement that the radar wind be in the same direction as the meteorological wind imposes the constraint given by equation (8.75),

$$\tan \Delta X = \frac{E_{21}}{V_r + E_{11}} = \frac{E_{22}}{V_r + E_{12}} \quad (8.75)$$

which yields the condition that

$$E_{22} = E_{21} \left(\frac{V_r + E_{12}}{V_r + E_{11}} \right) \quad (8.76)$$

When this condition is imposed, equation (8.74) becomes equation (8.77).

$$\begin{aligned} \vec{V}_m - \vec{V}_r &= \left[E_{11} - E_{12}, E_{21} \left(1 - \frac{V_r + E_{12}}{V_r + E_{11}} \right) \right] \\ &= \left[(E_{11} - E_{12}), (E_{11} - E_{12}) \frac{E_{21}}{V_r + E_{11}} \right] \end{aligned} \quad (8.77)$$

There is a common factor in each component, and equation (8.77) can be written as (8.78).

$$\vec{V}_m - \vec{V}_r = (E_{11} - E_{12}) \left[1, \frac{E_{21}}{V_r + E_{11}} \right] \quad (8.78)$$

Since the two vectors are constrained to have the same direction, ΔX , the difference in the magnitudes can also be found in equation (8.79),

$$|\vec{V}_m| - |\vec{V}_r| = (E_{11} - E_{12}) \left[1 + \frac{E_{21}^2}{(V_r + E_{11})^2} \right]^{\frac{1}{2}} \quad (8.79)$$

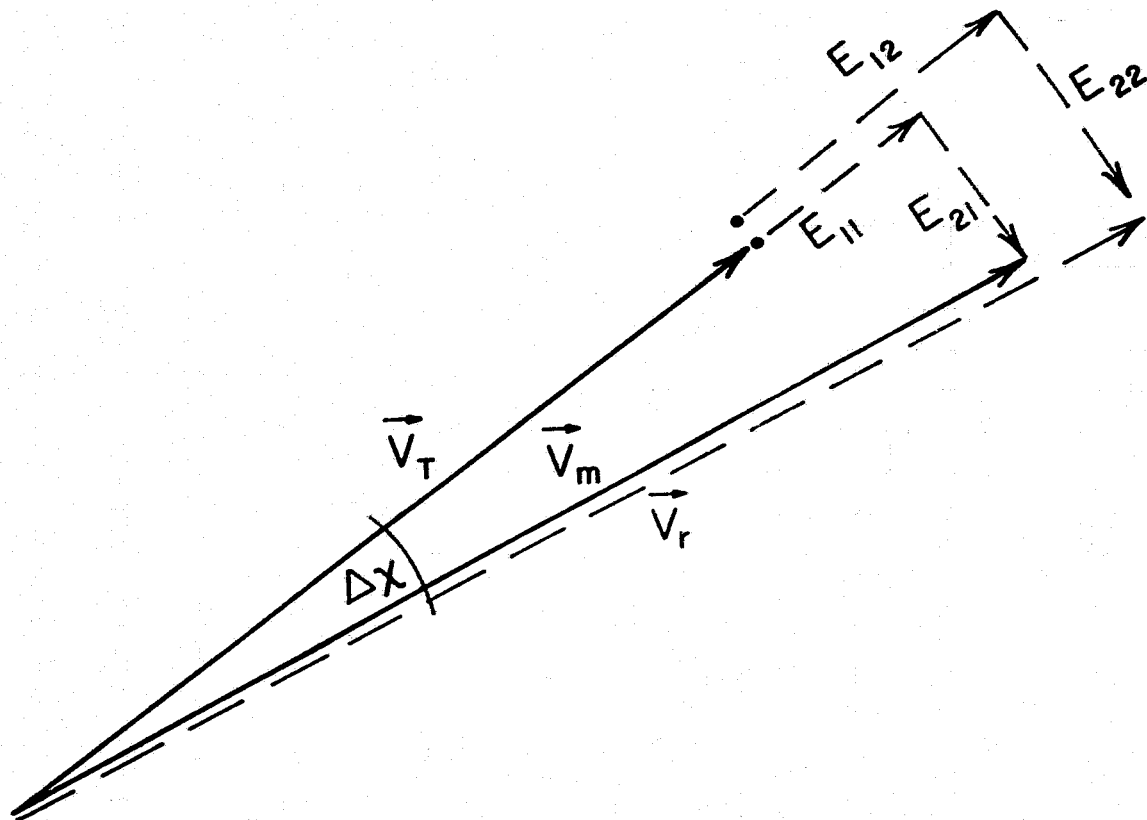


FIGURE 8.29 ERROR ANALYSIS OF THE METEOROLOGICAL AND RADAR WINDS SUBJECT TO THE CONSTRAINT THAT THEY BE PARALLEL.

or, in the notation of the preceding sections, as in equation (8.80).

$$U_m - U_r = (E_{11} - E_{12}) \left(1 + \frac{E_{21}^2}{(V_r + E_{11})^2} \right)^{\frac{1}{2}} \quad (8.80)$$

The calculation of $\mathcal{E}(U_m - U_r)$ and $\mathcal{E}(U_m - U_r)^2$ from equation (8.80) is not simple even under the further assumption that E_{11} , E_{12} , E_{21} , and E_{22} are normally distributed independent random variables as in Chapter 4. The term in the denominator and the square root cause difficulties. The second term in equation (8.80) will be approximated in a way not strictly correct but that probably suffices.

Consider the vector,

$$\vec{V}_m = (V_r + E_{11}, E_{21}) \quad (8.81)$$

The expected value of the variance is given by equation (8.82) and equation (8.83) for each component.

$$\mathcal{E}(V_r + E_{11})^2 = V_r^2 + D_{11}^2 \quad (8.82)$$

and

$$\mathcal{E}(E_{21}^2) = D_{21}^2 \quad (8.83)$$

If the approximation that equation (8.80) can be represented by equation (8.84) is made, the required expectations are easily calculated.

$$U_m - U_r \cong (E_{11} - E_{12}) \left[1 + \frac{D_{21}^2}{V_r^2 + D_{11}^2} \right]^{\frac{1}{2}} \quad (8.84)$$

For example

$$\mathcal{E}(U_m - U_r) = 0 \quad (8.85)$$

and

$$\begin{aligned} \mathcal{E}(U_m - U_r)^2 &= (D_{11}^2 + D_{12}^2) \left(1 + \frac{D_{21}^2}{V_r^2 + D_{11}^2} \right) \\ &= (D_{11}^*)^2 + (D_{12}^*)^2 \end{aligned} \quad (8.86)$$

The quantity represented by equation (8.86) was minimized in the regression techniques that were used to predict the meteorological wind from the radar wind. The root mean square difference between the meteorological wind and the radar wind is an estimate of the square root of the right hand side of equation (8.86). Equation (8.86) also shows that the differences between the two wind values, U_{mi} , and U_{ri} , are dominantly related to errors in the component parallel to the true wind and secondarily related to the tangent of the angle between the true wind and meteorological wind. The ratio, $D_{21}^2 / (V_T^2 + D_{11}^2)$ is an approximation to the variance of the tangent of the angle between the true wind and the meteorological wind.

From Table 4.6, this ratio can be computed for the ranges, 0 to 10, 10 to 20, and 20 to 30 knots by using the mid-value of each range for V_T . They are given in Table 8.20, along with the arctangent of the square root, and the factor by which the variances of the parallel component errors must be multiplied to account for errors in direction.

Table 8.20 Approximate values for the difference correction and the standard deviation of the angle between the true wind and the meteorological wind for mid-range values of 5, 15, and 25 knots.

	$D_{21}^2 / (V_T^2 + D_{11}^2)$	ΔX	$1 + (D_{21}^2 / (V_T^2 + D_{11}^2))$
Weather Ship			
0 - 10 knots	0.17	22°	1.17
10 - 20 knots	0.05	13°	1.05
20 - 30 knots	0.03	10°	1.03
Transient Ship			
0 - 10 knots	0.30	29°	1.30
10 - 20 knots	0.09	17°	1.09
20 - 30 knots	0.06	13°	1.06
Synoptic			
0 - 10 knots	0.46	34°	1.46
10 - 20 knots	0.12	19°	1.12
20 - 30 knots	0.08	16°	1.08

This factor ranges from 1.03 for weather ship observations between 20 and 30 knots to 1.46 for synoptic estimates between zero and 10 knots. The value of ΔX exceeds 20^0 for winds between zero and 10 knots for all classifications.

The values of $(D_{11}^*)^2$, which account for the effects of direction errors, are given in Table 8.21 for comparison with the estimates obtained from the regression analyses. For wind speeds greater than 30 knots, the additional effect of direction errors has been assumed negligible and $D_{11}^* = D_{11}$ from Table 4.6.

Table 8.21 Values of $(D_{11}^*)^2$ computed from Table 8.20 and Table 4.6.

Wind Range (knots)	Weather Ship		Transient Ship		Synoptic Analyses	
	$(D_{11}^*)^2$	D_{11}^*	$(D_{11}^*)^2$	D_{11}^*	$(D_{11}^*)^2$	D_{11}^*
0 to 10	5.7	2.4	12.9	3.6	27.9	5.3
10 to 20	12.5	3.5	25.8	5.1	35.1	5.9
20 to 30	19.1	4.4	39.5	6.3	55.8	7.5
GT 30	36	6	71.5	8.5	101	10

ERROR ANALYSIS OF THE RADAR WIND MAGNITUDES

Introduction. A question that demands an answer is: "How much of the mean square difference between the meteorological wind and the radar wind is caused by the errors in the meteorological wind and how much is caused by errors in the radar measurement?" This question is answered below under the assumption that the contribution of the radar wind to the total mean square difference is independent of the magnitude of the radar wind.

Analysis. Let U_V be the radar wind predicted by a given method for VV polarization, let U_H be the one for HH polarization, and let U_x be the one for cross polarization. Then

$$U_V = U_T + E_V \quad (8.87)$$

$$U_H = U_T + E_H \quad (8.88)$$

$$U_x = U_T + E_x \quad (8.89)$$

where E_V , E_H and E_x are the radar errors in the wind speed estimates.

The various expectations using the same assumptions as before about the distribution of errors are given below.

$$\mathcal{E}(U_V - U_H) = \mathcal{E}(E_V - E_H) = 0 \quad (8.90)$$

$$\mathcal{E}(U_V - U_x) = \mathcal{E}(E_V - E_x) = 0 \quad (8.91)$$

$$\mathcal{E}(U_H - U_x) = \mathcal{E}(E_H - E_x) = 0 \quad (8.92)$$

$$\mathcal{E}(U_V - U_H)^2 = \mathcal{E}(E_V^2) + \mathcal{E}(E_H^2) \quad (8.93)$$

$$\mathcal{E}(U_V - U_x)^2 = \mathcal{E}(E_V^2) + \mathcal{E}(E_x^2) \quad (8.94)$$

$$\mathcal{E}(U_H - U_x)^2 = \mathcal{E}(E_H^2) + \mathcal{E}(E_x^2) \quad (8.95)$$

The estimates of these quantities were calculated from the data and are given in Table 8.22. There were 382 values for SL 2/3 and 470 values for SL 4. The biases (equations (8.90), (8.91) and (8.92)) are satisfactorily small. The values for the left hand side of

equations (8.93), (8.94) and (8.95) are also tabulated for three different methods and for SL 2/3 and SL 4. The estimate of the mean square differences are larger for SL 4 than for SL 2/3.

Given the left hand side of equations (8.93), (8.94) and (8.95), the variances and standard deviations of E_v , E_H and E_x can be found. These are also given in Table 8.22. They are quite small for SL 2/3 and modestly noticeable for SL 4. The largest standard deviation is 3.24 knots for HH SL 4, method 6. Even with a damaged instrument, all values are under 2 meters per second. The increase in the radar error variance may have several explanations and be a combination of a number of factors such as the variability due to attenuation effects, which are not treated, increased cross polarization interactions, and raised thresholds. The covariances of the differences should be investigated. There may be information on additional radar effects in a more detailed analysis of these data.

It should be noted that Table 8.20 only finds the correction for D_{11}^2 to obtain $(D_{11}^*)^2$ as in equation (8.86). The value of $(D_{12}^*)^2$ for each polarization has been found in this section since $\mathcal{E} \begin{pmatrix} E \\ v v \end{pmatrix}^2 = (D_{12}^*)^2$ for VV polarization, and so forth.

Table 8.22 Cross comparisons between different polarizations for SL 2/3 (382 values) and SL 4 (470 values) and radar error variances derived therefrom. Units are knots and (knots)².

Method	4			5			6		
Polarization Combination	VV/HH	VV/HV	HH/VV	VV/HH	VV/HV	HH/HV	VV/HH	VV/HV	HH/HV
SL 2/3 Bias		not used		0.11	0.14	0.03	0.11	0.13	0.02
SL 2/3 MSD		not used		2.82	2.89	1.90	2.79	3.13	2.16
SL 4 Bias	.31	- .02	- .33	0.30	-0.01	-0.31	0.29	-0.00	-0.29
SL 4 MSD	15.52	6.97	9.30	14.14	5.76	9.18	16.65	7.29	11.70

Polarization	VV	HH	HV	VV	HH	HV	VV	HH	HV
Error									
SL2/3 Variance		not used		1.90	0.92	0.98	1.88	0.91	1.25
SL2/3 Stand.Dev		not used		1.38	0.96	0.99	1.37	0.95	1.12
Error									
SL4 Variance	6.59	8.93	0.38	5.35	8.78	0.40	6.12	10.53	1.16
SL4 Stand. Dev.	2.57	2.99	0.61	2.32	2.96	0.63	2.47	3.24	1.08

COMPOSITE ERROR ANALYSIS

Enough is now known to balance the error budget. Before doing so, the last step in the analysis needs to be derived. The problem is that neither the true meteorological wind, in the absence of substantial error, nor the true radar wind, which in a perfect theory ought to equal the meteorological wind, is known.

Consider equation (8.96), which is an identity.

$$U_m - U_r = (U_m - U_T) - (U_r - U_T) \quad (8.96)$$

This equation follows a technique of Lorenz (1971)*, given in a presentation accompanying the cited paper, but the paper does not contain these equations.

If the expectations of equation (8.96) and of its square are taken, and if the error structure is as has been assumed, the results are equations (8.97) and (8.98)

$$\mathcal{E}(U_m - U_r) = 0 \quad (8.97)$$

$$\mathcal{E}(U_m - U_r)^2 = \mathcal{E}(U_m - U_T)^2 - 2\mathcal{E}(U_m - U_T)(U_r - U_T) + \mathcal{E}(U_r - U_T)^2 \quad (8.98)$$

By means of the regression techniques that have been employed, equation (8.97) holds for the data sets. Also, the left hand side of equation (8.98) has been minimized for the particular technique used. This does not necessarily mean that the absolute minimum has been found. A better model might be discovered. Also for wind speed ranges with sparse data, the models may underestimate the contributions to the left hand side.

The first term on the right hand side of equation (8.98) was found for different wind speed ranges and different types of surface truth in Chapter 4 from essentially independent data. For the assumptions

* Lorenz, E.N. (1971) Fundamental Limitations in Ocean and Atmospheric Prediction. Eight U.S. Navy Symposium of Military Oceanography, Vol. 1, pp. 365-369 Naval Post Graduate School, Monterey, California.

that have been used, the middle term is zero. The various sources of error in the meteorological winds arise from factors that are different from the various sources of error in the radar winds. One possible coupling is through the very small corrections to the nominal nadir angles, and this effect must be small. The last term was found in the preceding section. Since the method for finding the first term on the right hand side could not detect a bias term, the bias in the meteorological wind, if one exists, must be balanced by an equal and opposite bias in the radar winds, and these biases can only be determined after the meteorological winds are measured much more accurately.

With equation (8.98), the balance can now be found. This is done in Tables 8.23 and 8.24. The results are stratified according to type and the range in knots of the radar wind predictions by pooling the three largest nadir angles for the three polarizations and method 6. The results are sufficiently different for different polarizations to require some interpretation. The ranges in knots are really 0 to 9.99 and so on.

The total variance comes from Table 8.19. It equals the sum of the squares of the differences between the meteorological wind and the radar wind for all pairs in the appropriate category. The meteorological variances for Tables 8.23 and 8.24 comes from Table 8.21 via Tables 8.20 and 4.6.

The total error variance should equal the meteorological error variance plus the radar error variance for each polarization combination within the effects of sampling variability which is large for small sizes. Equation 8.98 need not balance exactly because of the effects of sampling variability and sample size.

Table 8.23 Skylab 2/3 Component variance analysis for the three highest nadir angles (method 6).
Units are knots and (knots)².

RANGE	TYPE	TOTAL VAR			MET VAR	RADAR VAR			UNEXP VAR*			UNEXP SD**			NUMBER		
		VV	HH	HV/VH		VV	HH	HV/VH	VV	HH	HV/VH	VV	HH	HV/VH	VV	HH	HV/VH
0-10	A	11.2			5.7	1.9	0.9	1.2	3.6			1.9			16		
10-20	A	84	9.9	10.4	12.5	"	"	"	69.6	<u>3.5</u>	<u>3.3</u>	8.3	<u>1.9</u>	<u>1.8</u>	3	17	16
20-30	A		104.0	78.7	19.1	"	"	"		84.0	58.3		9.2	7.6		3	3
0-10	B	35.5	52.1	51.0	12.9	"	"	"	20.7	38.3	36.8	4.6	6.2	6.1	4	8	8
10-20	B	27.4	28.5	25.3	25.8	"	"	"	<u>0.3</u>	1.8	<u>1.7</u>	<u>0.5</u>	1.3	<u>1.3</u>	49	48	48
20-30	B	99	57.3	47.5	39.5	"	"	"	57.6	16.9	6.7	7.6	4.1	2.6	5	2	2
0-10	C	6.5	8.8	5.6	12.9	"	"	"	<u>8.3</u>	<u>5.0</u>	<u>8.5</u>	<u>2.9</u>	<u>2.2</u>	<u>2.5</u>	9	11	9
10-20	C	12.5	13.2	10.2	25.8	"	"	"	<u>15.2</u>	<u>13.5</u>	<u>16.8</u>	<u>3.9</u>	<u>3.7</u>	<u>4.1</u>	51	34	37
20-30	C	15.5	21.3	13.5	39.5	"	"	"	<u>25.9</u>	<u>19.1</u>	<u>27.2</u>	<u>5.1</u>	<u>4.4</u>	<u>5.2</u>	2	2	1
0-10	D		8.5	6.2	12.9	"	"	"		<u>5.3</u>	<u>7.9</u>		<u>2.3</u>	<u>2.8</u>		6	2
10-20	D	14.7	17.6	18.1	25.8	"	"	"	<u>13.0</u>	<u>9.1</u>	<u>8.9</u>	<u>3.6</u>	<u>3.0</u>	<u>3.0</u>	28	25	26
20-30	D		66.1		39.5	"	"	"		25.7			5.1			1	
0-10	BCD	15.4	22.6	27.5	12.9	"	"	"	0.6	8.8	13.3	0.8	3.0	3.7	13	25	19
10-20	BCD	18.7	21.1	18.6	25.8	"	"	"	<u>9.0</u>	<u>5.6</u>	<u>8.4</u>	<u>3.0</u>	<u>2.4</u>	<u>2.9</u>	128	107	111
20-30	BCD	75.1	44.6	36.1	39.5	"	"	"	33.7	4.2	<u>4.6</u>	5.8	2.1	<u>2.1</u>	7	5	3
0-10	SYN+	11	8.88	10.7	27.9	"	"	"	<u>18.8</u>	<u>19.9</u>	<u>18.4</u>	<u>4.3</u>	<u>4.5</u>	<u>4.3</u>	24	39	34
10-20	SYN+	15.7	13.5	14.0	35.1	"	"	"	<u>21.3</u>	<u>22.5</u>	<u>22.3</u>	<u>4.6</u>	<u>4.7</u>	<u>4.7</u>	135	130	127
20-30	SYN+	55.8	56.2	35.4	55.8	"	"	"	<u>1.9</u>	<u>0.5</u>	<u>21.6</u>	<u>1.4</u>	<u>0.7</u>	<u>4.6</u>	6	6	3
COUNTS									4/1/7	5/1/8	3/0/10	4/4	3/4	2/6	332	332	318

* Underlined numbers represent the amounts by which the sum of the meteorological error variance and the radar error variance exceed the total variance.

** Underlined numbers are the square roots of the corresponding values in the preceding columns.

Table 8.24 Skylab 4 component variance analysis for the three highest nadir angles (method 6). Units are knots and (knots)².

RANGE	TYPE	TOTAL VAR			MET	RADAR VAR			UNEXP VAR*			UNEXP SD**			NUMBER		
		VV	HH	HV/VH	VAR	VV	HH	HV/VH	VV	HH	HV/VH	VV	HH	HV/VH	VV	HH	HV/VH
10-20	A	32.4	0.1	23.2	12.5	6.1	10.5	1.2	13.8	<u>22.9</u>	9.6	3.7	<u>4.8</u>	3.1	3	1	2
20-30	A	14.4	16.6	21.8	19.1	"	"	"	<u>10.3</u>	<u>13.0</u>	1.5	<u>3.3</u>	<u>3.6</u>	1.2	5	7	6
0-10	B	2.31	6.2		12.9	"	"	"	<u>16.7</u>	<u>17.2</u>		<u>4.1</u>	<u>4.1</u>		1	1	
10-20	B	21.7	23.4	25.5	25.8	"	"	"	<u>10.2</u>	<u>12.9</u>	<u>1.5</u>	<u>3.2</u>	<u>3.6</u>	<u>1.2</u>	36	29	28
20-30	B	37.6	50.7	67.9	39.5	"	"	"	<u>8.0</u>	8.6	27.2	<u>2.8</u>	2.9	5.2	29	45	29
GT 30	B	65.0	81.0	69.4	71.5	"	"	"	<u>12.6</u>	<u>1.0</u>	<u>3.3</u>	<u>3.5</u>	<u>1.0</u>	<u>1.8</u>	4	1	3
10-20	C	18.9	10.9	21.2	25.8	"	"	"	<u>13.0</u>	<u>25.4</u>	<u>5.8</u>	<u>3.6</u>	<u>5.0</u>	<u>2.4</u>	12	10	13
20-30	C	20.1	76.4	34.6	39.5	"	"	"	<u>25.5</u>	<u>26.4</u>	<u>6.1</u>	<u>5.0</u>	<u>5.1</u>	<u>2.5</u>	11	22	11
GT 30	C	88.7	67.9	94.3	71.5	"	"	"	11.1	<u>14.1</u>	21.6	3.3	<u>3.8</u>	4.7	5	5	5
0-10	D	3	109.4		12.9	"	"	"	<u>16.0</u>	86.0		<u>4.0</u>	9.3		1	1	
10-20	D	27.6	37.3	40.2	25.8	"	"	"	<u>3.3</u>	1.0	13.2	<u>1.8</u>	1.0	3.6	50	48	59
20-30	D	52.4	109.4	84.8	39.5	"	"	"	6.8	59.4	44.2	2.6	7.7	6.7	49	71	43
GT 30	D	64.3	41.7	68.0	71.5	"	"	"	<u>13.3</u>	<u>40.3</u>	<u>4.7</u>	<u>3.6</u>	<u>6.3</u>	<u>8.2</u>	37	15	35
0-10	BCD	2.65	57.8		12.9	"	"	"	<u>16.4</u>	34.4		<u>4.0</u>	5.9		2	2	
10-20	BCD	24.4	29.7	32.9	25.8	"	"	"	<u>7.5</u>	<u>6.6</u>	5.9	<u>2.7</u>	<u>2.6</u>	2.4	98	87	110
20-30	BCD	43.6	87.6	72.2	39.5	"	"	"	<u>3.0</u>	37.6	31.6	<u>1.7</u>	6.1	5.6	89	138	83
GT 30	BCD	67	49.8	71.1	71.5	"	"	"	<u>10.6</u>	<u>32.2</u>	<u>1.6</u>	<u>3.3</u>	<u>5.7</u>	<u>1.3</u>	46	21	43
0-10	SYN+	43.2	48.7	6.2	27.9	"	"	"	9.1	10.3	<u>22.9</u>	3.0	3.2	<u>4.8</u>	3	9	4
10-20	SYN+	32.1	28.5	33.8	35.1	"	"	"	<u>9.1</u>	<u>17.1</u>	<u>2.5</u>	<u>3.0</u>	<u>4.1</u>	<u>1.6</u>	135	118	133
20-30	SYN+	64.6	80.1	71.4	55.8	"	"	"	2.7	13.8	14.4	1.6	3.7	3.8	79	97	80
GT 30	SYN+	116.6	113.4	82.2	101	"	"	"	9.5	1.9	<u>20</u>	3.1	1.4	<u>4.5</u>	19	14	19
COUNTS									5/2/10	8/1/8	7/0/8	4/1/5	5/1/4	5/0/4	479	494	480

*Underlined numbers represent the amounts by which the sum of the meteorological error variance and the radar error variance exceed the total variance.

**Underlined numbers are the square roots of the corresponding values in the preceding columns.

The sample sizes are sometimes misleading in meteorological and oceanographic data analysis because of spatial and temporal correlations between observations. Frequently an entire sequence of values can be too high or too low. The use of the F test and of fiducial confidence intervals on these estimates of the various variances involves fewer than the apparent number of degrees of freedom, and this correction has not been attempted.

There is little need for this degree of sophistication in the interpretation of these two tables except to note that the fiducial confidence intervals on samples of the size shown are quite broad and that F test of ratios of the various variances would lead in general to the conclusion that they may well have come from the same population.

The overall features of Tables 8.23 and 8.24 are what should dominate their interpretation. In general the total variance increases with wind speed. The exceptions are all for the zero to ten knot range, and plausible explanations for this fact were given in Chapter 4 and in the study of the regression methods.

The values for the unexplained variance represent the total variance minus the sum of the meteorological error and radar error variances where underlined values indicate that the estimates of the two error variances add up to more than the estimate of the total variance. If the independently obtained total variance estimates and meteorological variance estimates had been from much larger samples, say one hundred times larger, then these sums could have balanced much more closely. The unexplained standard deviations are the square roots of the corresponding variances.

There are several ways to interpret these tables. One is to note that, since the variances have been independently estimated, there is an even chance that the sums of the two error variances will be either larger or smaller than the total variance, if the choice of R was correct in Chapter 4.

With this criterion, the unexplained variances exceed the sums of the meteorological and radar error variances, for Types A, B, C, D and SYN+, 4 out of 12 times for VV, 5 out of 12 times for HH and 3 out of 13 times for HV/VH for SL 2/3, and 5 out of 17 times for VV, 8 out of 17 times for HH, and 7 out of 15 times of HV/VH for SL 4.

These values are shown in the row labeled counts along the bottom of the table in greater detail. For example 4/1/7 means that 4 of the values in the column above (excluding BCD) are positive, one required the radar error variance plus the meteorological error variance to make it negative, and 7 were such that the meteorological error variance exceeded the total variance.

For types A, (BCD), and SYN + the corresponding values are 4 out of 8 times for VV, 3 out of 7 for HH, and 2 out of 8 times for HV/VH for SL 2/3, and 4 out of 10 times for VV, 5 out of 10 times for HH and 5 out of 9 times for HV/VH in SL 4. The corresponding counts for A, (BCD), and SYN+ are under the unexplained standard deviations.

If the results for A, (BCD), and SYN+ are pooled for SL 2/3 and SL 4, the values are 8 out of 18 for VV, 8 out of 17 for HH and 7 out of 17 for HV/VH. The values of 8, 8, and 7 are within one standard deviation of the expected values of 9, 8.5 and 8.5 from binomial distributions with parameters $n = 18$ and 17 and $p = q = 0.5$. The balance is therefore as close as would be reasonable under the laws of chance.

Another way to interpret the table is to note how closely equation(8.98) nearly balances out category by category. That is, the terms that make up the balance are large compared to the amount of the imbalance. As examples, for SL 2/3 and SL 4 combined, and for A, B, C, D and SYN+, 37% of the sums balance to within ± 9 (knots²) and 62% to within ± 16 (knots²). For A, (BCD), and SYN+, the corresponding percentages are 40% and 67%. Since many of the terms from which the balances are computed range from 50 to 100 (knots²), the imbalances are small percentages of the totals involved.

An imbalance greater than 26 (knots²) in general is associated with a small sample size where 8 or fewer values were obtained. The notable exceptions are all for HH and HV/VH in Table 8.24.

For those wind speed ranges where all three polarizations yield a total variance, the lowest of the three can be given a score of one, the next lowest a score of two, and the highest, a score of three. For SL 2/3, and A, B, C, D, +, the scores for VV, HH and HV/VH are in order 24, 25, and 17 where the minimum possible (the best) would be 11 and the highest would be 33. For A (BCD) +, the scores for SL 2/3 are 17, 13, and 12 with the best equal to 7 and the poorest 21. Corresponding values for SL 4 are 23, 31 and 36 (best 15, worst 45) and 16, 18 and 20 (best 9, worst 27). Cross polarized total variances score somewhat better for SL 2/3 than either VV or HH and VV polarization has the best score for SL 4. The scores are not that much different to make any one polarization clearly and undeniably superior.

Although the above analysis does not indicate a clear superiority for a particular polarization combination, VV, all in all, seems somewhat better followed by HV/VH. As the strongest of the backscatter values, VV was able to yield radar predictions for winds in the 0 to 9.99 knot

range that had smaller errors. The weaker signal for SL 4 also appears to have affected the ability of HH and HV/VH to measure low winds.

There is little point in revising the value of R used to calculate the values of the weather ship and transient ship meteorological error variances. An increase of R to 0.6 would increase the estimates of the meteorological error variances for the weather ships and decrease the values for the transient ships and synoptic analyses. The number of underlined terms for the unexplained variance entries would then decrease for the transient ships and synoptic analyses. For the pooled SL 2/3 and SL 4 totals, the number of times the total variance would exceed the sum of the meteorological and radar error variances would become 10 out of 18, 10 out of 18 and 11 out of 18, thus tipping the balance to the other side. A value for R of 0.5 to 0.6 is therefore sufficiently close.

The conclusion is obvious. The radar backscatter measurements predict the winds to such an accuracy that the discrepancies between the radar prediction and the meteorological surface truth are almost entirely explainable by the inherent errors in both the way winds are either measured or determined from the pressure gradients and the way these values are smoothed and interpolated to a grid of points in a vector wind field. This conclusion is stated with proper reservations more formally in Chapter 1.

It is not possible to draw conclusions about how well radar backscatter can determine the vector wind on the basis of SKYLAB data. These results combined with circle flight data and the design features of the SEASAT-A system may make it possible to improve somewhat on the error analysis of Pierson, Cardone and Greenwood (1974) for SEASAT-A.

To be completely consistent with the theory used in this analysis, it would be necessary to conclude that the radar error variances completely account for the radar errors in measuring the magnitude of the vector wind. These were 1.9, 0.9 and 1.2 for SL 2/3 and 6.1, 10.5, and 1.2 for SL 4 with corresponding standard deviations all under 4 knots of 1.4, 0.95, 1.1, 2.5, 3.2 and 1.1. Except for VV and HH on SL 4 these are all under half of the standard deviations shown in Table 8.21 for Weather Ships for all wind speed ranges. A somewhat more conservative conclusion is that the radar measurements are at least as accurate as having had a Weather Ship near each of the cells scanned by S193 and that the standard deviations of the errors in the radar winds for all wind greater than 7 knots may well be half that of the errors in analyses based on weather ship reports.

AVA and Christine. The meteorologically determined winds for hurricane AVA and tropical storm Christine were not assigned a quantitative estimate of the errors in the winds determined by these theories. From the tabulated total error variances and standard deviations as given in Table 8.25, it can be noted that the values for tropical cyclones compare favorably with the total error variances from the combined PBL and manuscript analysis data. The wind model for the hurricane may well be almost as good as having had a transient ship at each of the cells scanned in these two cyclones. The few high winds in these cyclones are, of course, fitted in such a way as to minimize the error so that this conclusion requires some reservations.

The results for HV/VH are noticeably better than those for VV and HH for the 20 to 30 and greater than 30 knot ranges. The scatter photos in Figures 8.22 and 8.23 illustrate this improvement.

Table 8.25 Skylab 2/3 Total Variance and Standard Deviations for
Tropical Cyclones and Manuscript Analyses (Method 6).

Units are knots and (knots)²

RANGE KNOTS	TYPE	TOTAL VAR.			STAND. DEV.			NUMBER		
		VV	HH	HV/VH	VV	HH	HV/VH	VV	HH	HV/VH
0-10	TC	6.3	7.08	5.34	2.51	2.66	2.31	7	10	10
10-20	TC	30.6	33.5	30.0	5.53	5.79	5.48	39	37	36
20-30	TC	76.0	52.6	32.8	8.72	7.25	5.73	14	10	11
GT 30	TC	69.1	59.8	35.3	8.31	7.73	5.94	9	10	10
0-10	MS	6.3	5.4	4.1	2.50	2.33	2.03	15	15	18
10-20	MS	13.6	12.5	12.3	3.69	3.53	3.50	86	86	83
20-30	MS	9.2	14.4	7.0	3.04	3.80	2.64	4	3	2

Ten or twenty hurricanes from SEASAT-A should settle the question. The model can clearly be improved by iterating it with spacecraft data.

The Manuscript Synoptic Analyses. There were 103 cells involved in the manuscript synoptic analyses described in Chapter 4. The total error standard deviations are under four knots, and it almost pays to subtract the 1.9 to make them even smaller.* A skilled synoptic analyst can do as well, if not better than, sophisticated computer based procedures.

For these analyses, it was possible to code each cell as in the computer based analyses. Each cell was coded as to A, B, C, D or + on the basis of the nearby ship reports that were available for the analysis. Aircraft underflights were coded as type A. The details are given in Table 8.18. These data are a subset of the data in Table 8.23 and amount to about 32% of that data.

The Scatter Plots. The scatter plots of U_r versus U_m in Figures 8.9 to 8.16 and 8.17 to 8.28 can now be studied on a more rational basis. The rule is to interpret the scatter in the data by picking a zone of the U_r axis, perhaps 5 knots wide, and studying the scatter on the U_m axis by looking up and down only within this zone. The errors are dominantly in U_m and the scatter in these errors is shown by the data. Some care in interpretation is needed because the vertical and horizontal scales are not exactly equal. Also the seven, for example, in Figure 8.21 means that seven values all fall together at this point and are within a knot or two of being an exact prediction.

It is also necessary to retract the comment about the first set of scatter plots from Young (1975). The apparent bias is nonexistent when interpreted in this way, if due consideration is given of the fact that negative numbers cannot occur. Something must happen to the error structure for low winds that is not properly considered in this analysis since the errors can be so large.

*For VV and the corresponding value for other polarizations

SURVIVORS

For one reason, or another, although the cells that were listed in Table 4.1 seemed to be members of the useable data set, the various screening procedures used by Young (1975), and other problems, caused most of them to be eliminated. Data from DOY's 156, 252 and 4 survived. The results of the predictions for these cells are given in Table 8.25.

The Gulf C130 underflight on DOY 156 yielded the 13 knot wind speed tabulated, and method 6 missed it by 2.03 knots for cell 4 command angle 1. The others are all closer.

DOY 4 command angle 2 was missed by 5 knots. DOY 252 command angle 3 missed by 15 knots, DOY 4 command angle 3, cells 16 and 18 missed by 7 knots each.

This is hardly a large enough sample from which to draw any firm conclusions.

It is fortunate that contingency plans were made to obtain the routinely available meteorological data since the aircraft underflight program failed to provide an adequate data base for the verification of the potential of S193 and since the first level of back up based on special weather ship observations also led to little.

CLOSING THE CIRCLE

Recapitulation. In Chapter 6, the present status of the theory of radar backscatter and of other measurement programs was reviewed. The belief was stated that the theory was not quite good enough to permit the prediction of wind speed from backscatter measurements. However, these results provided a formulation for the first step of regression method 6.

Simulated circle flights. Simulated circle flights were carried out based on regression method 6 for SL 2/3 and SL 4, and the results are shown in Figure 8.30 and Figure 8.31. The steps that follow the "first guess" model which was based on the AAFE Langley data can destroy the model. For SL 2/3, this happened. The maximum was not at upwind.

Table 8.26 The survivors from Table 4.1 and DOY 156

Command Angle 1

DOY	CELL	ASPECT ANGLE	MET WIND	(SP MET WIND)	VV5	VV6
156	2	1.7	13	13ac	13.37	13.69
156	3	1.4	13	13ac	13.80	14.13
156	4	- 4.0	13	13ac	14.69	15.03
156	5	- 9.3	13	13ac	12.24	12.59

Command Angle 2

156	3	1.4	13	13ac	13.35	13.67
156	4	1.0	13	13ac	13.72	14.07
156	5	- 4.3	13	13ac	13.06	13.36
4	35	154.8	28.2	27*	21.93	22.66

Command Angle 3

156	4	1.0	13	13ac	14.3	14.05
156	5	.7	13	13ac	14.72	14.48
252	29	- 5.2	12.5	6**	20.42	20.78
4	16	113.7	38.9	39ac	32.96	32.26
4	18	08.5	41.4	39ac	33.20	32.38

* 60 nautical miles away at J

** 90 nautical miles away at K

REPRODUCIBILITY OF THE
ORIGINAL PAGE IS POOR

Downwind exceeded upwind. The output of the model can involve trigonometric terms up to $\cos 16^\circ$. Effectively the lack of an even distribution of the SL 2/3 data over angle forced the minimum to move from 90° to 120° .

For SL 4, method 6 saw no need in the data to destroy the first guess and the simulated circle flights for 3, 6.5 and 15 m/s compare favorably with corresponding figures in Chapter 6 except for absolute level, and this is explainable by what happened to the instrument, and the attempts to recalibrate it. Moreover, since the theory of Fung and Chan agrees with the AAFE circle flights, the time is drawing close when backscatter can be used to predict wind speed from first principles.

Tables 8.26 and 8.27 show the variation of backscatter for upwind, downwind and crosswind for SL 2/3 and SL 4 as predicted by regression method 6. For SL 2/3, the results do not agree to well with theory but for SL 4 they are quite good.

The values in Tables 8.27 and 8.28 are graphed in Figure 8.32. The re-calibration problem for SL 4 is illustrated by the rise of the backscatter curves by about 5 db. The sharp drop from 4 m/s to 3 m/s is considered to be, for SL 2/3, an effort of the regression analysis to fit the kind of sharp decrease in capillary wave heights and the sudden disappearance of backscatter predicted, for example, by Figure 6.3. The opposite curvature for SL 2/3 compared to SL 4 may also be the result of the regression methods trying to fit this sharp drop off.

The curves for downwind upwind and crosswind are all quite close together for SL 2/3. This is misleading since at 120° the points from Figure 8.30 would produce the curve so labeled. These features of the SL 2/3 curve on this figure and the corresponding features of Figure 8.30 are considered to be partially at least, an effect of the uneven distri-

bution of the wind directions and of the interaction of wind direction errors with the regression model.

For SL 4, downwind and upwind have essentially the same backscatter values, and the model has denied the existence of the 1 db difference built in at the start. Crosswind checks well with the results of Chapter 6. It is 2.3 db down for low winds and 4.93 db down for high winds. The shape of the backscatter curve versus wind speed agrees well with the results of Fung and Chan in Appendix C.

On the basis of these results, it may be possible to decrease σ^0 by about 5 db for SL 4 so that the various curves agree over the middle range of wind speeds and repeat the regression analyses using the entire sample. Some way to handle the sharp drop suggested by both theory and SL 2/3 might also be devised.

The two curves in Figure 8.32 yield quite different power laws depending on how the power law is computed. For the middle range of wind speeds since the slopes are the same, the power law locally is the same. For SL 2/3 from 3 to 30 m/s the power law would be 4.5. For higher speeds, it would be less. For lower winds, it would be higher. Conversely, for SL4, from 3 to 30 m/s the power law would be 1.9, and for low winds it would be less and for high winds greater.

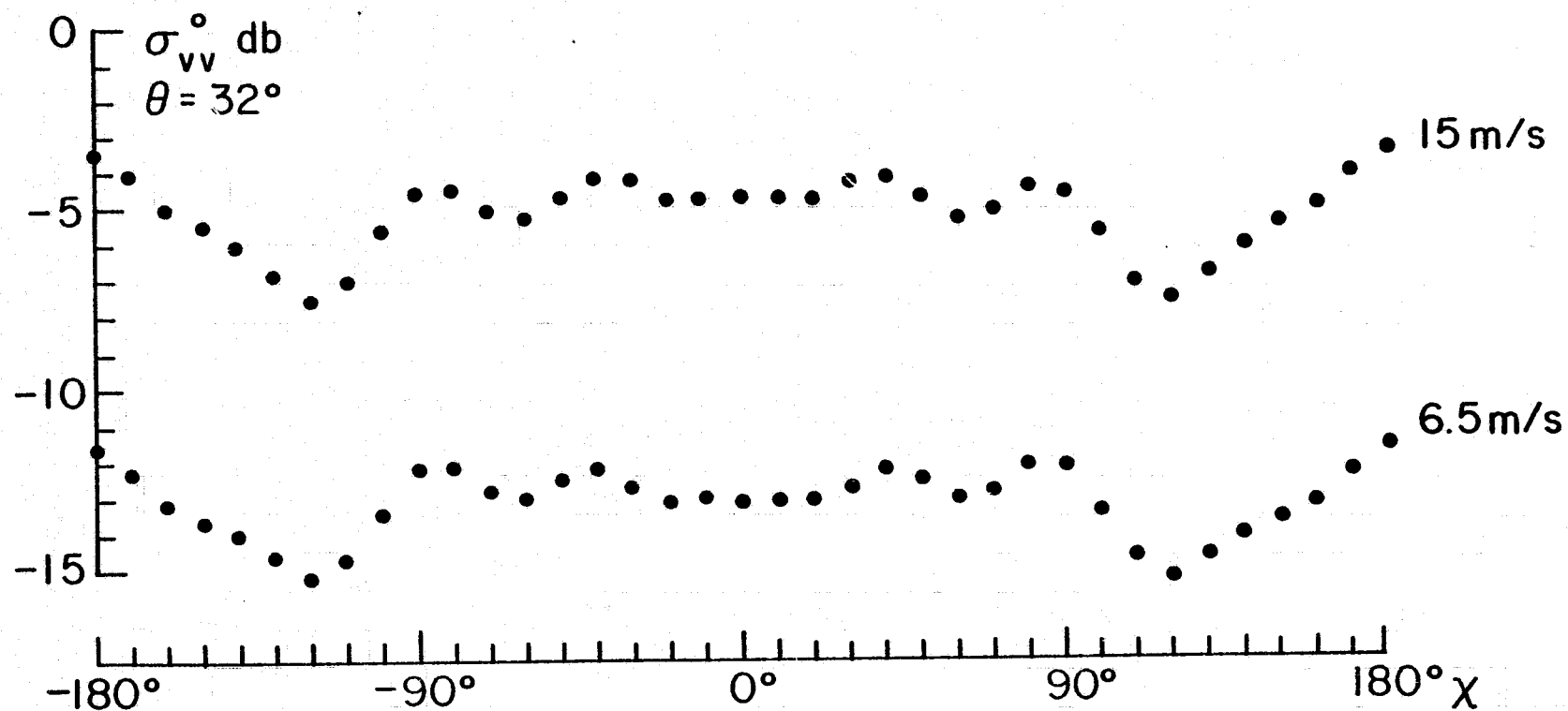


Figure 8.30 σ_{vv}^0 for 15 and 6.5 meters per second from Method 6 for SL 2/3.

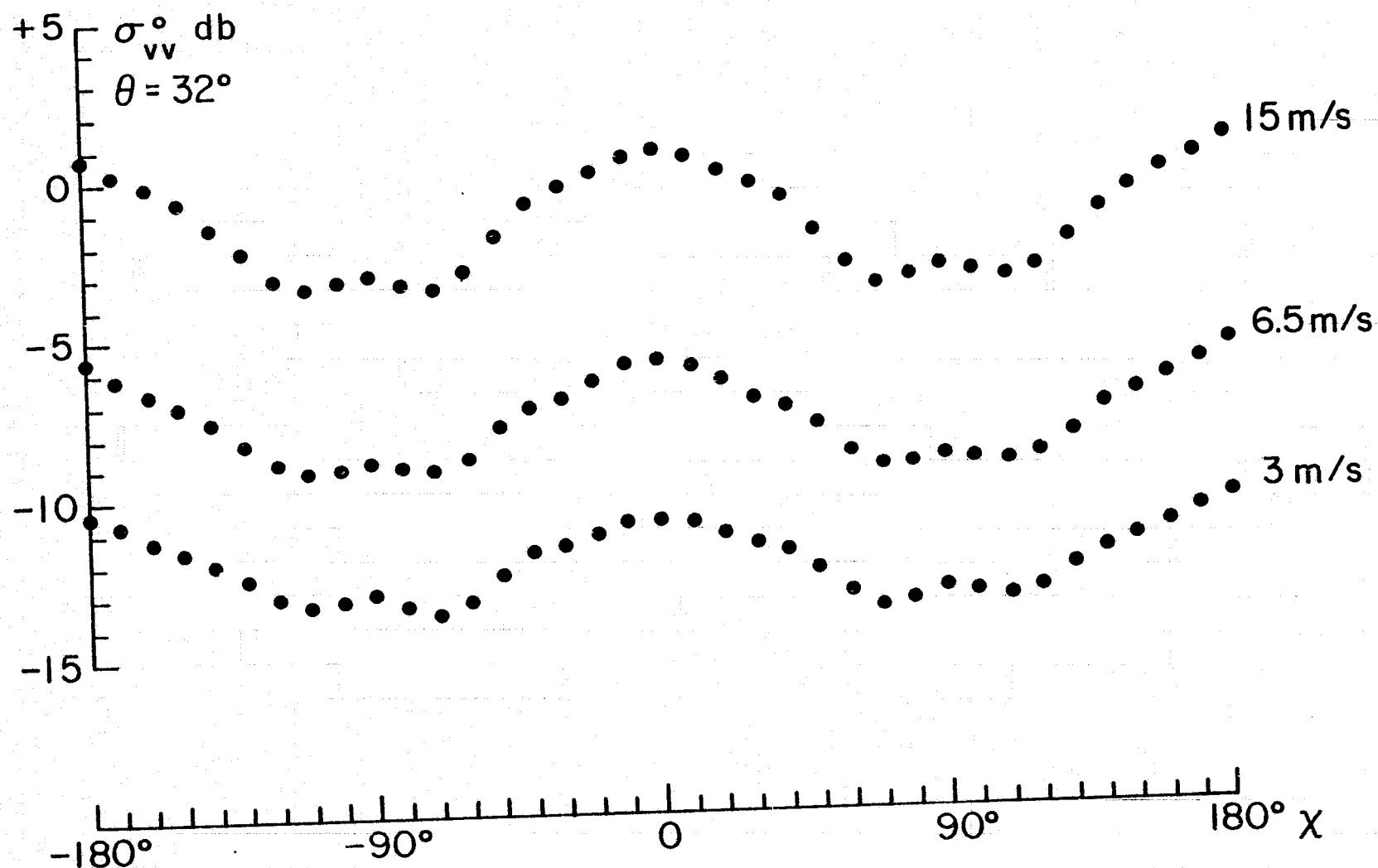


Figure 8.31 σ_{vv}^0 for 15, 6.5 and 3 meters per second from Method 6 for SL 4.

Table 8.27 Backscatter versus wind speed.

SL 23 POLARIZATION VV COMAND ANGLE 3

M/SEC	REDUCTION 5			REDUCTION 6		
	UPWIND	DOWNWIND	CROSSWIND	UPWIND	DOWNWIND	CROSSWIND
3.	-135.59	-132.52	-122.42	-44.85	-42.66	-40.77
4.	-22.22	-21.92	-20.18	-22.27	-20.64	-20.41
5.	-17.48	-17.30	-15.91	-17.17	-15.66	-15.81
6.	-14.58	-14.47	-13.29	-14.25	-12.81	-13.18
7.	-12.47	-12.41	-11.39	-12.22	-10.83	-11.34
8.	-10.81	-10.79	-9.88	-10.66	-9.31	-9.94
9.	-9.43	-9.45	-8.64	-9.40	-8.08	-8.80
10.	-8.26	-8.30	-7.59	-8.34	-7.04	-7.84
11.	-7.24	-7.30	-6.66	-7.43	-6.16	-7.02
12.	-6.33	-6.42	-5.84	-6.63	-5.38	-6.30
13.	-5.51	-5.62	-5.11	-5.92	-4.69	-5.66
14.	-4.77	-4.90	-4.44	-5.28	-4.06	-5.09
15.	-4.09	-4.24	-3.83	-4.70	-3.49	-4.56
16.	-3.46	-3.62	-3.26	-4.17	-2.97	-4.08
17.	-2.88	-3.06	-2.74	-3.68	-2.49	-3.64
18.	-2.34	-2.52	-2.25	-3.22	-2.05	-3.23
19.	-1.83	-2.03	-1.78	-2.80	-1.63	-2.84
20.	-1.35	-1.56	-1.35	-2.40	-1.24	-2.48
21.	-.89	-1.12	-.94	-2.02	-.88	-2.14
22.	-.46	-.70	-.56	-1.67	-.53	-1.82
23.	-.05	-.30	-.19	-1.33	-.20	-1.52
24.	.33	.08	.16	-1.01	.11	-1.23
25.	.70	.44	.50	-.71	.40	-.96
26.	1.06	.79	.82	-.42	.68	-.70
27.	1.40	1.12	1.12	-.14	.96	-.45
28.	1.73	1.44	1.42	.12	1.21	-.21
29.	2.04	1.75	1.70	.38	1.46	.02
30.	2.35	2.04	1.98	.62	1.70	.24

Table 8.28 Backscatter versus wind speed.

SL 4 POLARIZATION VV COMAND ANGLE 3

M/SEC	REDUCTION 5			REDUCTION 6		
	UPWIND	DOWNWIND	CROSSWIND	UPWIND	DOWNWIND	CROSSWIND
3.	-12.02	-11.80	-15.76	-10.80	-10.46	-13.11
4.	-9.77	-9.64	-13.83	-9.13	-8.84	-11.67
5.	-7.90	-7.84	-12.22	-7.71	-7.47	-10.44
6.	-6.31	-6.29	-10.84	-6.47	-6.27	-9.38
7.	-4.91	-4.95	-9.64	-5.37	-5.21	-8.43
8.	-3.68	-3.75	-8.57	-4.38	-4.26	-7.58
9.	-2.57	-2.68	-7.62	-3.48	-3.39	-6.80
10.	-1.57	-1.71	-6.75	-2.65	-2.58	-6.08
11.	-.65	-.83	-5.97	-1.88	-1.84	-5.41
12.	.19	-.02	-5.24	-1.15	-1.14	-4.79
13.	.97	.73	-4.57	-.47	-.48	-4.21
14.	1.69	1.43	-3.95	.17	.14	-3.65
15.	2.37	2.08	-3.36	.78	.73	-3.12
16.	3.00	2.69	-2.82	1.37	1.29	-2.62
17.	3.59	3.27	-2.31	1.93	1.84	-2.14
18.	4.16	3.81	-1.82	2.47	2.36	-1.67
19.	4.69	4.32	-1.36	2.99	2.86	-1.22
20.	5.19	4.81	-.93	3.50	3.35	-.78
21.	5.67	5.27	-.52	3.99	3.83	-.36
22.	6.13	5.71	-.12	4.47	4.29	.05
23.	6.56	6.13	.25	4.95	4.75	.47
24.	6.98	6.53	.61	5.41	5.20	.87
25.	7.38	6.92	.95	5.87	5.64	1.26
26.	7.76	7.29	1.28	6.33	6.09	1.66
27.	8.13	7.65	1.60	6.79	6.53	2.05
28.	8.48	7.99	1.91	7.25	6.97	2.45
29.	8.82	8.32	2.20	7.71	7.42	2.85
30.	9.15	8.64	2.48	8.18	7.87	3.25

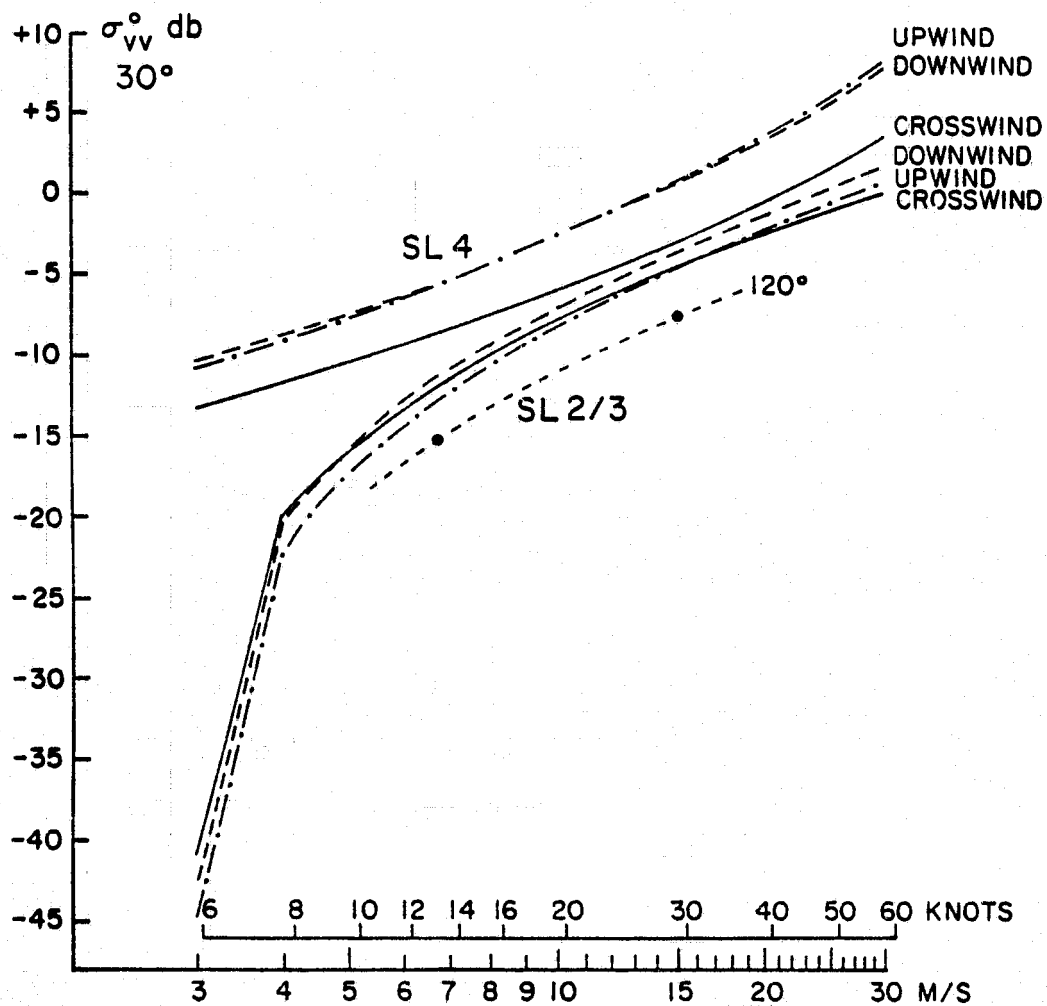


FIGURE 8.32 σ_{vv} (db) VERSUS WIND SPEED FOR METHOD 6

CHAPTER 9. APPLICATIONS TO SEASAT-A

REVIEW

Upon the completion of an investigation, it is advisable to review what has been accomplished before describing what still needs to be done. The suggestion for the use of a radar on a spacecraft to measure sea surface roughness appears in Ewing (1965) as a part of the report of the section chaired by W.J. Pierson in an article by R.K. Moore. The concepts were further refined by Moore and Pierson (1966), who described a Doppler radar for a spacecraft to measure winds, and later Moore and Pierson (1971) described the applications of an instrument called a radiometer-scatterometer to the measurement of the winds over the ocean. The design features of a radiometer-scatterometer were given by Moore and Ulaby (1969).

The use of aircraft to measure backscatter from the sea surface as a function of wind speed and wave conditions lead at first to results that disagreed with each other as described in Chapter 6. The results of this report on S193, of the AAFE Langley Program and of the fan beam Doppler program that preceeded the AAFE program all agree one with the other, and, in some respects, serve to cross check each other.

In 1969, the Commission on Marine Science, Engineering and Resources* pointed out the need for more and better measurements of environmental conditions over the oceans in Chapter 5 of their report. A figure on page 189 shows the global density of ship's reports in 1964 and cites Hanzana and Tourier (1968). Conditions have not changed very much since then.

*Our Nation and the Sea; a plan for National Action (1969). Report of the Commission on Marine Science, Engineering and Resources. J.A. Stratton, Chairman U.S. Government Printing Office, Washington, D.C. January 1969.

The Commission Report discussed both the satellite techniques tested on SKYLAB (page 193) and the development of a National Data Buoy Network. They commented that, "It is not yet possible, however, to envision the complete composition of a total system. The proper mix of platforms and instruments must be evaluated on the basis of performance and costs."

The papers by Moore and Pierson (1966) and Moore and Pierson (1971) discussed the problem of the initial value specification of the winds over the ocean and the input of this specification into numerical weather prediction methods. The study by Thomasell and Welsh (1964), who only compared weather ships with the calculation of winds from the pressure field, was mentioned in the 1966 paper and the possible sources of error in the specification of the wind in the planetary boundary layer were reviewed. Mentioned were different anemometer heights on the ships, incorrect isobaric analyses, variations of wind speed with elevation due to different temperature lapse rates and "the poor averaging time of two minutes for the wind that introduces considerable sampling variability in the estimate of a mean, which really ought to have been estimated for a longer time interval."*

Over the five year interval between the two papers, other concepts changed drastically, Much was learned in the interval, and much more has been learned since the 1971 paper.

This final report brings to an end the "proof of concept" phase of a program that will eventually lead to an operational system for measuring winds over the ocean from a spacecraft. It is part of the full program that has been in the planning stages since 1965. Preliminary reports on the results of Skylab and the AAFE Langley Radscat Program have already had an input to the design of a spacecraft called

*The model in Chapter 4 accounted for all but this last source of error. It proves to be still quite large.

SEASAT-A. In this last chapter, some of the ways the results of this study can be applied to SEASAT-A will be given.

APPLICATIONS OF THE ERROR ANALYSIS

The scatter in the plots of radar wind versus meteorological wind has been shown to be almost entirely due to the errors in the specification of the wind from meteorological sources. Except for low winds where special problems have been highlighted, the error increases with wind speed. There is a difference between winds from weather ships, transient ships and as calculated from synoptic isobaric patterns.

To be able to produce plots of radar wind versus meteorological wind with greatly reduced scatter based on forthcoming SEASAT-A data, the errors in the meteorologically determined winds must be greatly reduced compared to what they were during the SKYLAB period. There are three possible ways to do this and all should be developed in parallel. One would be to improve aircraft underflight techniques. This is well along.* A second would be to improve the accuracy of the weather ship reports of the winds and to carry out successfully and routinely what was attempted, with little success, for SKYLAB. A third would be to use the National Data Buoy network as a prime source for surface truth.

The data density from SEASAT-A, which will be a quasi-operational spacecraft, will be very high and the cells scanned by the spacecraft will be very close together. If the weather ship (or the data buoy) is within the swath, some cell will come within 25 km of the weather ship. If the weather ship data are based on a wind averaged for 10 or 20 minutes beginning prior to and ending after the spacecraft pass,

* W.L. Jones personal communication.

such measurements will eliminate error contributions from both spatial and temporal interpolation. The averaging time should be chosen so as to reduce the standard deviations by a factor of five compared to those determined in Chapter 4.

Shortly before SKYLAB, the United States withdrew its Weather Ships and the ones that remained were operated by the European nations and by Canada. Present plans are that the European nations will re-occupy most of the stations formerly occupied by the U.S. Coast Guard and that by the time SEASAT-A is launched, the number of weather ships will be substantially increased. If automatic weather stations* are used on the weather ships to record the meteorological parameters, and if the measurement of wind direction can be improved, the weather ships can play an important role in calibrating SEASAT-A. With about ten weather ships on station, and with about 70% probability that one will be in the SEASAT-A fan beam Doppler swath twice each day, about 1200 cells would become available during a three month period. In six months (October to March) a sufficient number of both low and high winds could be observed to demonstrate the instrument capabilities and to begin to understand the effects of wave slope as described in Chapter 6.

The National Data Buoy Network, plus data buoys from other nations, will be greatly increased in number by the time SEASAT-A is launched, providing potentially another 2000 observations during a three month period. Ten to fifteen minute averages of the wind speed and direction are presently obtained each hour. Perhaps it might be worthwhile to schedule the observations during the times of the SEASAT-A passes. The variability of these measurements has been studied by Adamo, Withee et al. (1971).

* Personal communication from L. Baer

SEASAT-A will make measurements that in principal can determine the vector wind, and, at most, three aliases. The regression equations in Chapter 8, are an improvement over three equations given by Pierson, Cardone and Greenwood (1974), and a search over χ and $\chi + 90^\circ$ with the two different backscatter values that are measured will locate the possible wind speeds and directions. All three equations, and perhaps variants of them, should be tried. With more accurate wind speeds and directions, this prime data set should converge quickly to very accurate regression equations for the determination of the vector wind at each cell scanned by SEASAT-A.*

APPLICATIONS OF THE PLANETARY BOUNDARY LAYER MODEL

By means of a model that yielded $\sigma^0 = \sigma^0(u, \chi)$, and from information on the design error structure of the SEASAT-A measurements, Pierson, Cardone and Greenwood (1974) have demonstrated in a completely independent analysis that SEASAT-A has very small wind speed and direction errors for moderate and high winds. The above error analysis would simply be used to obtain the best possible algorithm for the implementation of the techniques described in that reference. The algorithm can already be simulated quite well on the basis of present knowledge.

The PBL model described in Chapter 4 has a sound physical basis, but it can be improved by taking into account the errors in the different categories of ship reports. The method of Cressman (1959), and its current extensions, could perhaps be merged with this model to obtain a model with the best features of both. The domain of influence of a ship report needs to be expanded so that many ships will influence an entire area and the errors in the individual reports will average out.

*Alternatively, the errors in the meteorological winds can be accepted as they are. Based on a regression analysis, the radar winds would replace them at each cell and the improved meteorological measurements would never actually be required.

It would be useful even now to compare the results of other boundary layer models, and of any that may be derived in the future, with the SL 4 data and with each other.

There will always be, however, large areas of the oceans with poor ship coverage. It is also, we believe, evident that the number of data buoys required would be far too large to cover these areas adequately. The errors in the initial value specification of the PBL in such areas are much larger than those in the shipping lanes as demonstrated in Chapter 8. Moreover, they can easily be systematic instead of random over large areas. These errors must propagate into numerical weather prediction errors in the two, three and four day forecast range.

Efforts are underway to simulate the expected improvements in numerical weather prediction to be expected when SEASAT-A becomes operational. The error structure that has been modeled probably underestimates the present errors in the specification of the PBL and does not take into account their spatial variability and systematic features as caused by the variable density of ship reports from different areas of the ocean. SEASAT-A for example should make it possible for the first time to do numerical predictions for the southern hemisphere.

The data from SEASAT-A will have a known error structure. The data density will be somewhere between 80,000 and 320,000 points per day on a uniform grid depending on the final design. These measurements must clearly greatly improve the accuracy of the initial value specification of the planetary boundary layer.

The further reduction of any residual errors in the SEASAT-A data by means of spatial averaging techniques has not yet been estimated.

The smoothing technique would probably involve an area covered by N cells within some radius of definition, depending on the gradients in the field. A fit to these winds would then be required such that the differences between the fitted wind field and the SEASAT-A winds would exhibit the known error properties of the SEASAT-A measurements. The error variances would be reduced by $1/N$ and the standard deviations by $1/\sqrt{N}$. Over many ocean areas, the number of cells involved could easily be as many as 25 so that another factor of five would become available.

APPLICATIONS TO TROPICAL CYCLONES

One of the more impressive figures of this final report is the one for the Tropical Storm Christine pass. Had the pass been made by SEASAT-A the points would have been about half as far apart and part of the swath would have had SMMR data. Infrared and cloud imagery would also have been obtained. With so many more cells, more of them would be free from rain, the SMMR and other imagery would define the rain and wet cloud areas uniquely and the winds at the surface would be known for the full field. With such a data density, the tropical cyclone model can be integrated over a trial range of pressure fields and speeds of movement so as to find the values that give the best fit to the winds.

After a sufficient number of tests of this nature with simultaneous, but withheld, aircraft reconnaissance verification, this model and its inevitable successors, as more is learned, can be used to define these dangerous storms anywhere in the world on a routine basis. The improved measurements of the winds and atmospheric conditions around these storms may even make it possible to predict their movement in time to provide adequate warning to threatened landfall areas. These considerations are treated in additional detail by Pierson, Cardone, and Greenwood (1974).

REFERENCES

- Adamo, L. C., G. W. Wither, R. F. Erickson, and J. M. Syck, 1971: National Data Buoy Project: An Estimate of Temporal Variability. Lockheed Report No. 24274, Ocean Sciences Department.
- Afarani, M., 1975: Directional Properties of Ocean Radar Backscatter: A Harmonic Regression Analysis of AAFE Radscat Circle Experiment. CRES, University of Kansas, Tech. Report 186-15.
- Allison, L. J., E. B. Rodgers, T. Wilheit, and R. W. Fett, 1974: Tropical Cyclone Rainfall as Measured by the NIMBUS 5 Electrically Scanning Microwave Radiometer. Bull. Amer. Meteor. Soc., Vol. 55, pp. 1074-1090.
- Bass, F. G., 1961: Radiowave Propagation over Statistically Rough Surfaces. (In Russian) Radiofiz., 4(3), pp. 476-483. [A summary of this work can be found in Bass, F. G., I. M. Fuks, A. I. Kalmykov, and A. D. Rosenberg, 1968: Very High Frequency Radiowave Scattering by a Disturbed Sea Surface. IEEE Trans Antenna and Propagat. AP-16, pp. 554-559.]
- Bass, F. G. and V. G. Bocharov, 1958: On the Theory of Scattering of Electromagnetic Waves from a Statistically Uneven Surface. Radiotekhnika i elektronika, Vol. 3, pp. 251-258.
- Beckmann, P. and A. Spizzichino, 1963: The Scattering of Electromagnetic Waves from Rough Surfaces. Macmillan, New York.
- Blackadar, A. K., 1965: A Simplified Two-Layer Model of the Baroclinic Neutral Atmospheric Boundary Layer. Final Report: Flux of Heat and Momentum in the Planetary Boundary Layer of the Atmosphere. Penn. State University.
- Bradley, G. A., 1971: Remote Sensing of Ocean Winds using a Radar Scatterometer. Tech. Report 177-22, The University of Kansas Center for Research, 191 pp., MSC, NASA Contract NAS-9-10261.

- Cardone, V. J., 1969: Ground Truth for NASA Ireland Mission 88 March 1969. Microwave Observations of the Ocean Surface, SP-152, Analyses of the NASA/NAVY Review, pp. 51-66.
- Cardone, V. J., 1969: Specification of the Wind Distribution in the Marine Boundary Layer for Wave Forecasting. TR-69-1, Geophysical Sciences Lab., New York University, Bronx, New York.
- Cardone, V. J. and W. J. Pierson, 1975: The Measurement of Winds Over the Ocean from SKYLAB with Application to Measuring and Forecasting Typhoons and Hurricanes. Proceedings of the Eleventh International Symposium on Space Technology and Sciences, Tokyo.
- Cardone, V. J., W. J. Pierson, and E. G. Ward, 1975: Hindcasting the Directional Spectra of Hurricane Generated Waves. Paper No. OTC 2332, Offshore Technology Conference, Houston, Texas, May.
- Chan, H. L. and A. K. Fung, 1973: Backscattering from a Two-Scale Rough Surface with Application to Radar Sea Return. NASA CR-2327, Washington, D.C., November.
- Chia, R. C., 1968: The Theory of Radar Backscatter from the Sea. Univ. of Kansas, Center for Research, Tech. Report 112-1.
- Claassen, J. P., 1973: The Theory and Design of the Sky Attenuation Experiment. University of Kansas, Center for Research, Inc., CRES Technical Memorandum 237-1, NASA contract NAS 9-13356, May.
- Claassen, J. P., A. K. Fung, S. Wu, and H. L. Chan, 1971: Toward RADSCAT Measurements over the Sea and their Interpretation. University of Kansas, Center for Research, Inc., CRES Technical Report 186-6, NASA Contract NAS 1-10048, August.
- Claassen, J.P. and H.S. Fung, 1972: The Wind Response of Radar Sea Return and its Implication on Wave Spectral Growth. Technical Report 186-5, University of Kansas Center for Research, Inc., March.
- Claassen, J. P., H. S. Fung, R. K. Moore, and W. J. Pierson, 1972: Radar Sea Return and the Radscat Satellite Anemometer. IEEE Int'l Ocean '72 Conference, Newport, Rhode Island, September.
- Cressman, G. P., 1959: An Operational Objective Analysis System. Mo. Wea. Rev., Vol. 87, pg. 367.

- Cox, C. S., 1958: Measurements of the Slopes of High Frequency Wind Waves. J. Mar. Res., 16, pp. 177-225.
- Cox, C. S. and W. H. Munk, 1954: Statistics of the Sea Surface Derived from Sun Glitter. J. Mar. Res., 14 (2), pp. 198-277.
- Cramer, H., 1946: Mathematical Methods of Statistics. Princeton University Press.
- Crutcher, H. L., 1957: On the Standard Vector-Deviation Wind Rose. Journal of Meteorology, Vol. 14, No. 1, February pp. 28-33.
- Crutcher, H. L., 1959: Upper Wind Statistics Charts of the Northern Hemisphere. NAVAER 50-1C-535, Volumes I and II.
- Crutcher, H. L., 1962: Computations from Elliptical Wind Distribution Statistics. Journal of Applied Meteorology, Vol. 1, No. 4, December, pp. 522-530.
- Crutcher, H. L. and M. H. Bailey, 1962: Upper Wind Statistics Charts of the Northern Hemisphere. Office of the Chief of Naval Operations, NAVWEPS 50-1C-535, Volume III, March.
- Crutcher, H. L. and H. Moses, 1963: A Note on Ellipsoidal Wind Distributions. Argonne National Laboratory Radiological Physics Division Summary Report.
- Davis, H. W., 1973: An Airborne Research Mission into Hurricane AVA. Weatherwise, 26, pg. 208.
- Dropplemen, J. D., 1970: Apparent Microwave Emissivity of Sea Foam. Journal of Geophysical Research, Vol. 75, pp. 696-698.
- Elsberry, R. L., N. A. S. Pearson, and L. G. Corngati, Jr., 1974: A Quasi-empirical Model of the Hurricane Boundary Layer. Journal of Geophysical Research, Vol. 79, pp. 3033-3040.
- Ewing, G. C. (Ed.), 1965: Oceanography from Space. WHOI Ref. 65-10, 469 pages.
- Fung, A. K. and H. L. Chan, 1969: Backscattering of Waves by Composite Rough Surfaces. IEEE Trans. Antennas and Propagation, Vol. AP-17, No. 5, pp. 590-597.

- Grantham, W. C., E. Bracalente, W. C. Jones, J. H. Schrader
L. C. Schroeder, and J. L. Michell, 1975: An operational
satellite scatterometer for wind vector measurements
over the ocean. NASA TM X-72672. NASA Langley Research
Center, Hampton, Virginia.
- Guinard, N. W., 1969: The Variation of the RCS of the Sea with
Increasing Roughness. Microwave Observations of the Ocean
Surface, SP-152, Analyses of the NASA/NAVY Review, 11-12
June. Prepared by the Spacecraft Oceanography Project of
the Naval Oceanographic Office.
- Hanzana, M. and T. H. Tourier, 1968: System for the Collection of
Ships' Weather Reports. World Weather Watch Planning
Report No. 25. World Meteorological Organization, Geneva,
Switzerland.
- Harris, R. G., A. Thomasell, and J. Welsh, 1966: Studies of Techniques
for the Analysis and Prediction of Temperature in the Ocean.
Part III Automated Analysis and Prediction. Report 7421-213,
Travelers Research Center, Inc.
- Hayes, J., W. Spring, V. Cardone, and W. J. Pierson, 1973: A Preliminary
Analysis of the Surface Truth Data to be Correlated with the
SKYLAB II data obtained for the S193 Microwave investigators.
Report prepared for Johnson Spacecraft Center under Contract
NAS-9-13642, University Institute of Oceanography, CUNY,
43 pages.
- Hollinger, J. P., 1970: Passive Microwave Measurements of the Sea Surface.
Journal of Geophysical Research, Vol. 75, No. 27, pp. 5029-
5213, September.
- Hollinger, J. P., 1971: Passive Microwave Measurements of the Sea Surface
Roughness. IEEE Transactions, GE-9, No. 3, pp. 165-169, July.
- Isozaki, I., and T. Uji, 1974: Numerical Model of Marine Surface Winds
and its Application to the Prediction of Ocean Wind Waves.
Papers in Meteorology and Geophysics, 25, pp. 197-231.
- Jackson, F. C., 1974: A Curvature-Corrected Kirchoff Formulation for
Radar Sea Return from the Near Vertical. NASA CR-2406,
Washington, D.C., April.
- Kaitala, J. E., 1974: Heating functions and moisture source terms in
the FNWC primitive equation models. Printed lecture notes in
Continuing Education Program for Meteorological Specialists,
Naval Postgraduate School, Monterey, California.

- Komen, M., 1975: Methods for Correcting Microwave Scattering and Emission Measurements for Atmospheric Effects. University of Kansas Space Technology Center, CRES Technical Memorandum 254-6, August.
- Kondo, J., Y. Fujinawa, and G. Naito, 1973: High Frequency Components of Ocean Waves and Their Relation to the Aerodynamic Roughness. J. Phys. Oceanog., Vol. 3, No. 2, pp. 197-202.
- Kreiss, W. T., 1969: The Influence of Clouds on Microwave Brightness Temperature Viewing Downward over Open Seas. Proceedings of the IEEE, Vol. 57, No. 4, April, pp. 440-445.
- Lewis, J. M. and T. H. Grayson, 1972: The Adjustment of Surface Wind and Pressure by Sasaki's Variational Matching Technique. Fleet Weather Central Technical Note 72-1, 49 pages.
- Leykin, I. A. and A. D. Rosenberg, 1970: Study of the high frequency portion of the spectra of sea waves. Izv. AN SSSR, Fiziki Atmosfery i okeana, 6(12), pp. 791-794.
- Mitsuyasu, H. and T. Honda, 1974: The High Frequency Spectrum of Wind Generated Waves. J. of the Oceanographical Soc. of Japan, Vol. 30, No. 4, pp. 29-42.
- Mitsuyasu, H. and T. Honda, 1975: The High Frequency Spectrum of Wind Generated Waves. Research Institute for Applied Mechanics, Kyushu University, Vol. XXII, No. 71, March.
- Moore, R. K. and W. J. Pierson, 1966: Measuring Sea State and Estimating Surface Winds from a Polar Orbiting Satellite in Proceedings of the Symposium on "Electromagnetic Sensing of the Earth from Satellites", Ralph Zirkind, (Ed.), Copyright 1967 by the Polytechnic Press of the Polytechnic Institute of Brooklyn, Library of Congress, Catalog Card No. 67-28497, pp. R1 to R28.
- Moore, R. K. and G. Bradley, 1969: "Radar and Oceanography". Microwave Observations of the Ocean Surface, SP-152, Analyses of the NASA/NAVY Review, 11-12 June. Prepared by the Spacecraft Oceanography Project of the Naval Oceanographic Office.

- Moore, R. K. and P. T. Ulaby, 1969: The Radar Radiometer. Proceedings of the IEEE, Vol. 57, pp. 587-590.
- Moore, R. K. and W. J. Pierson, 1971: Worldwide Oceanic Wind and Wave Predictions Using a Satellite Radar-Radiometer. J. of Hydronautics, Vol. 5, No. 2, April, pp. 52-60.
- Moore, R. K., J. P. Claassen, A. K. Fung, S. T. Wu, and H. L. Chan, 1971: Toward RADSCAT measurements over the sea and their interpretations. Principal Investigators' Review, NASA Langley Research Center, October, pp. 115-140.
- Moore, R. K., F. T. Ulaby, A. Sobti, S. Ulaby, E. C. Davison, S. Siriburi, 1975: Design Data Collection with SKYLAB Microwave Radiometer-Scatterometer S-193. The University of Kansas Space Technology Center, Lawrence, Kansas. Remote Sensing Laboratory, Tech. Rept. 243-12. Final Report for NASA Contract NAS 9-1331, Volume 1.
- Moore, R. K., F. T. Ulaby, A. Sobti, S. Ulaby, E. C. Davison, S. Siriburi, 1975: Design Data Collection with SKYLAB Microwave Radiometer-Scatterometer S-193. The University of Kansas Space Technology Center, Lawrence, Kansas. Remote Sensing Laboratory, Tech. Rept. 243-12. Final Report for NASA Contract NAS 9-1331, Volume 2.
- Moskowitz, L., 1964: Estimates of the power spectrums for fully-developed seas for wind speeds of 20 to 40 knots. J. of Geophysical Research, Vol. 69, No. 24, pp. 5161-5179.
- Moskowitz, L., 1966: A modification of Agarwala's pictorial representation of wind velocity, 47, pg. 114.
- Nordberg, W., J. Conaway, D. B. Ross, and T. Wilheit, 1971: Measurements of microwave emissions from a foam covered wind driven sea. J. of Atmos. Sci., Vol. 28, No. 3, pp. 429-435.
- Panofsky, H. A., 1963: Determination of stress from wind and temperature measurements. Quart. J. Roy. Meteor. Soc., Vol. 88, 85.
- Pierson, W. J., 1964: The interpretation of wave spectra in terms of the wind profile instead of the wind measured at a constant height. J. Geophys. Res., Vol. 69 (24), pp. 5191-5203.

- Pierson, W. J., 1975: The theory and applications of ocean wave measuring systems at and below the sea surface, on the land, from aircraft and from spacecraft. Contractors Rept. for Goddard Space Flight Center, Greenbelt, Maryland, NAS-5-20041, June.
- Pierson, W. J., and L. Moskowitz, 1964: A proposed spectral form for fully developed seas based on the similarity theory of S. A. Kitaigorodskii. J. Geophys. Res., Vol. 69(24), pp. 5181-5190.
- Pierson, W. J., L. Tick, and L. Baer, 1966: Computer based procedures for preparing global wave forecasts and wind field analyses capable of using wave data obtained by a spacecraft. Sixth Symposium Naval Hydrodynamics, Office of Naval Research, Department of the Navy ACR 136.
- Pierson, W. J. and R. K. Moore, 1972: The extrapolation of laboratory and aircraft radar sea return data to spacecraft altitudes. In Proc. Fourth Annual Earth Resources Review, MSC, Houston, Texas.
- Pierson, W. J. and R. A. Stacy, 1973: The elevation, slope, and curvature spectra of a wind roughened sea surface. NASA contractor report CR-2247, Langley Research Center.
- Pierson, W. J., V. Cardone, and J. A. Greenwood, 1974: The Applications of SEASAT-A to Meteorology. The University Institute of Oceanography of the City University of New York. Prepared for the SPOC Group, Contract No. 04-4158-11.
- Phillips, O. M., 1958: The equilibrium range in the spectrum of wind generated waves. J. Fluid Mech., Vol. 4, pp. 426-435.
- Phillips, O. M., 1966: The Dynamics of the Upper Ocean. Cambridge University Press.
- Rapp, R. R., 1952: The effect of variability and instrumental error on measurements in the free atmosphere. New York University, College of Engineering, Bronx, New York. Meteorological Papers, Vol. 2, No. 1, June.

- Rice, S. O., 1951: Reflection of Electromagnetic Waves from Slightly Rough Surfaces. Commun. Pure Appl. Math., Vol. 4, pp. 351-378, June.
- Ross, D. B., V. J. Cardone, and J. W. Conaway, Jr., 1970: Laser and Microwave Observations of sea-surface condition for Fetch Limited 17- to 25 m/s Winds. IEEE Trans. on Geoscience Electronics, Vol. GE-8, No. 4, October.
- Ross, D. B. and V. J. Cardone, 1974: Observations of Oceanic Whitecaps and their relations to Remote Measurements of Surface Wind Speed. J. of Geophys. Res., Vol. 79, No. 3, January.
- Semenov, B. J., 1966: Approximate Computation of Scattering of Electromagnetic Waves by Rough Surface Contours. Radio Eng. Electron. Physics 11, No. 8, pp. 1179-87.
- Shea, D. J. and W. M. Gray, 1973: The hurricane's inner core, I, Symmetric and asymmetric. J. Atmos. Science, Vol. 30, pp. 1544-1564.
- Shuman, F. G., 1957: Numerical methods in weather prediction: II smoothing and filtering. Mo. Wea. Rev., Vol. 85, pp. 357-361.
- Singer, S. F. and G. F. Williams, 1968: Microwave Detection of Precipitation over the Surface of the Ocean. J. of Geophys. Res., Vol. 77, No. 10, May, pp. 3324-3327.
- Skolnik, M., 1969: A Review of Radar Sea Echo. Rept. 2025, July, U. S. Naval Research Lab., Washington, D.C.
- Smith, W. L. and W. M. Woolf, 1969: Synoptic Analysis of Satellite-Borne Temperature Profile Observations. Abstract EOS Transactions of the American Geophysical Union, Vol. 50, No. 11, p. 122.
- Stogryn, A., 1967: The Apparent Temperature of the Sea at Microwave Frequencies. IRE Transactions: Antennas and Propagation, Vol. AP-15, March, pp. 278-286.

- Strong, A. E. and I. S. Ruff, 1970: Utilizing satellite-observed solar reflections from the sea surface as an indicator of surface wind speeds. Remote Sensing of Environment, 1, pp. 181-185.
- Sutherland, A. J., 1967: Spectral measurements and growth rates of wind generated water waves. Tech. Rept. No. 84, Dept. of Civil Engineering, Stanford University, 64 pp.
- Thomasell, A. and J. G. Welsh, 1963: Studies of the specification of surface winds over the ocean. Travelers Research Center, Inc.
- Valenzuela, G. R., 1967: Depolarization of EM Waves by slightly rough surfaces. IEEE Trans. Antennas and Propagat., AP-15, pp. 552-557.
- Valenzuela, G. R., 1968: Scattering of electromagnetic waves from a tilted slightly rough surface. Radio Sci., 3, pp. 1057-1066.
- Valenzuela, G. R., M. B. Laing, and J. C. Daley, 1971: Ocean spectra for the high-frequency waves as determined from airborne radar measurements. J. Mar. Res., Vol. 29(2), pp. 69-84.
- Wark, D. Q., H. E. Fleming, and D. T. Hilleary, 1969: Measurements of Atmospheric Temperature Profiles with the Satellite Infrared Spectrometer. Abstract EOS Transactions of the American Geophysical Union, Vol. 50, No. 11, p. 122.
- Ward, E. G., 1974: Ocean Data Gathering Program-an overview. OTC Paper No. 210 8-B, Offshore Technology Conference, Houston, Texas, May.
- Webster, W. J., T. T. Wilheit, D. B. Ross, and P. Gloerson, 1974: Analysis of the Convair-990 Passive Microwave Observations of the sea states during the Bering Sea Experiment. Paper No. 6 in "Results of U.S. contribution to joint U.S./U.S.S.R. Bering Sea Experiment, May. Goddard Space Flight Center, Document X-910-74-141.

- Wentz, F. J., 1975: Computation of Theoretical Brightness Temperatures Corresponding to the Cape Cod Canal Radiometer Measurements. Part I of two parts, final report under contract L-24420A. Frank J. Wentz & Associates, Cambridge, Mass., August.
- Wentz, F. J., 1975: Radar Backscattering from a sea having an Anisotropic Large Scale Surface. Part II of two parts, final report under contract L-24420A, Frank J. Wentz & Associates, Cambridge, Mass., September.
- Williams, G. F., 1969: Microwave Radiometry of the Ocean and the Possibility of Marine Wind Velocity Determination from Satellite Observation. J. of Geophys. Res., Vol. 74, No. 18, August, pp. 4591-4594.
- Wright, J. W., 1966: Backscattering from Capillary Waves with Application to Sea Clutter. IEEE Trans. Antennas and Propag. AP-14, pp. 749-754.
- Wright, J. W., 1968: A new model for sea clutter. IEEE Trans. Antennas Propag., Vol. 16(2), pp. 217-233.
- Wu, S., 1973: The meteorological effects on microwave apparent temperature looking downward over a smooth sea. NASA CR-2325. The University of Kansas, Center for Research, Lawrence, Kansas, November.
- Wu, S. and A. K. Fung, 1973: A non-coherent model for microwave emission and backscattering from the sea surface. NASA CR-2326, The University of Kansas Center for Research, Lawrence, Kansas, November.
- Wilson, R. W., 1969: Sun-tracker measurements of attenuation by rain at 16 and 30 GHz. Bell System Technical Journal, Vol. 48, pp. 1383-1404.
- Young, J. D., 1975: Active Microwave Measurement of Sea Surface Winds from Space. University of Kansas, RSL Technical Report No. 254-5.

APPENDIX A

THE MERGED DATA SETS FOR SKYLAB 2,3, AND 4 AS DESCRIBED IN CHAPTER 5.

DOY	INDEX	PAGE
156 - 1	6 / 5 / 73	A 1 to A 4
157 - 1	6 / 6 / 73	A 5 to A 7
162 - 1	6 / 11 / 73	A 8 to A 9
216 - 1	8 / 4 / 73	A 10 to A 11
216 - 2	8 / 4 / 73	A 12 to A 13
220 - 1	8 / 8 / 73	A 14 to A 15
220 - 2	8 / 8 / 73	A 16 to A 17
220 - 3	8 / 8 / 73	A 18 to A 19
220 - 4	8 / 8 / 73	A 20
245 - 2	9 / 2 / 73	A 21 to A 24
247 - 1	9 / 4 / 73	A 25 to A 28
252 - 1	9 / 9 / 73	A 29 to A 33
334 - 1	11 / 30 / 73	A 34 to A 35
338 - 1	12 / 4 / 73	A 36 to A 39
4 - 1	1 / 4 / 74	A 40 to A 47
6 - 2	1 / 6 / 74	A 48 to A 49
7 - 1	1 / 7 / 74	A 50 to A 51
8 - 1	1 / 8 / 74	A 52 to A 55
9 - 1	1 / 9 / 74	A 56 to A 57
11 - 2	1 / 11 / 74	A 58 to A 60
24 - 1	1 / 24 / 74	A 61
25 - 1	1 / 25 / 74	A 62
27 - 1	1 / 27 / 74	A 63 to A 65
29 - 1	1 / 29 / 74	A 66 to A 67
29 - 2	1 / 29 / 74	A 68
30 - 1	1 / 30 / 74	A 69
30 - 2	1 / 30 / 74	A 70
32 - 1	2 / 1 / 74	A 71 to A 73

REPRODUCIBILITY OF THE
ORIGINAL PAGE IS POOR

ORGANIZATIONS: CUNY Institute of Marine and Atmospheric Sciences
at The City College, Wave Hill 675 West 252 Street
Bronx, N.Y. 10471 (212) 796-8300 and
The University of Kansas Remote Sensing Laboratory
Raymond Nichols Hall, 2291 Irving Hill Drive,
Campus West, Lawrence, Kansas 66045 (913) 864-9836

TITLE OF INVESTIGATION: A JOINT METEOROLOGICAL, OCEANOGRAPHIC AND SENSOR
EVALUATION PROGRAM FOR EXPERIMENT S193 ON SKYLAB.

TITLE OF REPORT: APPENDIX A THE MERGED SKYLAB MEASUREMENTS AND
METEOROLOGICAL AND OCEANOGRAPHIC SURFACE TRUTH FROM
SKYLAB 2, 3 and 4.

FOR: THE MEASUREMENT OF THE WINDS NEAR THE OCEAN
SURFACE WITH A RADIOMETER-SCATTEROMETER ON SKYLAB

PERIOD COVERED: January 1973 to December 1975

EREP INVESTIGATION: EPN 550

NASA CONTRACT: NAS 9-13642

PRINCIPAL INVESTIGATOR: Willard J. Pierson

CO-PRINCIPAL INVESTIGATOR: Richard K. Moore

CO-PRINCIPAL INVESTIGATOR: E. Paul McClain

DATE COMPLETED: January 21, 1976

MONITOR AND ADDRESS: Mr. Zack H. Byrns/TF6
PRINCIPAL INVESTIGATOR OFFICE
NASA LYNDON B. JOHNSON SPACE CENTER
HOUSTON, TEXAS 77058

TYPE OF REPORT: APPENDIX TO FINAL REPORT

DOY 156-1. 6/ 5/73 ITNG. GULF OF MEXICO/CARIBBEAN

DOY 156-1. 6/7 5/73										INSTR. GOLF OF MEXICO										S193 DATA									
SCAN NUMB	INCID ANGLE (DEG)	SCATTERING COEFFICIENTS				ANTENNA V (DEG)	TEMPS H (DEG)	ASPECT ANGLE (DEG)	WIND SPEED (M/S)	SEA TEMP (DEG)	GMT			CELL COORDINATES		S193 AZIMTH (DEG)	DATA FLAG												
		VV (DB)	HH (DB)	VH (DB)	HV (DB)						(HR MIN SEC)	LAT (DEG)	LONG (DEG)																
1.1	49.8					169.06	98.29	7.2	7.2	26.0	18	2	10.6	27.34	-94.63	132.8													
1.2	43.2					159.69	106.80	12.2	7.2	26.0	18	2	14.1	27.75	-95.12	132.8													
1.3	31.8					146.03	119.99	12.3	7.7	26.0	18	2	17.3	28.39	-95.89	132.7													
1.4	16.8					276.44	276.36				18	2	19.9	29.16	-96.72	133.1	2												
1.5																													
2.1	50.4	-17.65	-23.16	-32.79	-33.00	170.30	101.11	1.7	6.7	26.0	18	2	25.4	26.62	-93.85	133.3													
2.2	43.7	-18.07	-20.85	-33.94	-32.75	159.31	105.93	6.8	7.2	26.0	18	2	28.9	27.05	-94.36	133.2													
2.3	32.1	-12.91	-13.61	-28.19	-27.49	145.41	115.23	11.8	7.2	26.0	18	2	32.2	27.71	-95.14	133.2													
2.4	17.0	1.09	1.39	-14.62	-15.32	135.03	127.77	12.1	7.7	26.0	18	2	34.9	28.19	-95.97	132.9													
2.5	0.9	12.39	16.72	-5.23	-4.37	273.88	279.98				18	2	37.1	29.13	-96.76	134.2	2												
3.1	50.5	-17.29	-22.83	-32.80	-32.51	171.08	101.93	1.4	6.7	27.0	18	2	40.7	25.92	-93.12	133.6													
3.2	43.8	-16.22	-19.45	-31.71	-31.36	159.22	107.35	1.4	6.7	26.0	18	2	44.2	26.36	-93.64	133.6													
3.3	32.0	-13.05	-13.23	-28.01	-28.43	143.69	114.49	6.4	7.2	26.0	18	2	47.4	27.03	-94.41	133.6													
3.4	17.0	1.26	1.76	-14.45	-13.96	131.63	123.30	11.1	7.7	26.0	18	2	50.2	27.71	-95.22	133.9													
3.5	0.9	13.35	12.51	-3.86	-2.90	134.03	129.47	7.5	7.2	26.0	18	2	52.4	29.36	-96.00	137.5													
4.1	50.5	-16.62	-22.65	-31.93	-32.51	171.93	102.89	-4.0	6.7	26.0	18	2	55.9	25.23	-92.41	134.0													
4.2	43.8	-15.86	-19.45	-30.22	-30.57	159.68	107.33	1.0	6.7	27.0	18	2	59.4	25.67	-92.92	134.0													
4.3	32.1	-11.90	-12.87	-27.33	-26.75	142.32	114.17	1.0	6.7	26.0	18	3	2.7	26.34	-93.69	134.0													
4.4	17.0	0.90	1.46	-15.69	-14.04	131.32	121.44	6.1	7.2	26.0	18	3	5.4	27.03	-94.49	133.9													
4.5	0.9	12.96	13.40	-3.93	-3.18	131.09	126.47	5.5	7.2	26.0	18	3	7.6	27.68	-95.26	139.5													
5.1	50.5	-18.79	-24.64	-40.86	-32.43	172.12	103.46	-9.3	6.7	27.0	18	3	11.2	24.54	-91.72	134.3													
5.2	43.8	-15.55	-19.88	-31.30	-31.35	159.23	107.41	-4.3	6.7	27.0	18	3	14.7	24.98	-92.22	134.3													
5.3	32.2	-11.56	-12.70	-27.49	-26.49	143.16	115.65	0.7	6.7	27.0	18	3	17.9	25.65	-92.97	134.3													
5.4	17.0	1.42	1.39	-14.44	-14.84	131.28	122.47	0.5	6.7	26.0	18	3	20.7	26.35	-93.77	134.5													
5.5	0.9	13.67	13.75	-3.66	-2.79	129.17	127.16	-3.3	7.2	26.0	18	3	22.9	27.00	-94.53	140.3													
6.1	50.5	-20.83	-26.92	-36.22	-35.63	169.87	103.76	-19.7	6.1	28.0	18	3	26.4	23.84	-91.03	134.7													
6.2	43.8		-21.74					-14.7	6.2	27.0	18	3	29.9	24.28	-91.52	134.7													
6.3									6.7	27.0																			
6.4									6.7	27.0																			
6.5	0.9	13.21	13.22	-4.00	-3.35	129.12	128.17	-1.1	6.7	26.0	18	3	38.1	26.31	-93.81	136.1													
7.1	50.5	-20.67	-26.14	-42.97	-32.91	169.88	100.78	-25.0	4.1	28.0	18	3	41.7	23.13	-90.34	135.0													
7.2	43.8	-19.12	-22.14	-33.96	-33.25	158.45	105.64	-20.0	5.1	28.0	18	3	45.2	23.58	-90.83	135.0													
7.3	32.1	-13.51	-14.59	-28.55	-28.39	141.86	115.29	-15.1	6.2	27.0	18	3	48.4	24.26	-91.57	135.1													
7.4	17.0	1.01	1.57	-15.56	-14.70	131.82	122.46	-5.0	6.7	27.0	18	3	51.2	24.97	-92.36	135.0													
7.5	0.9	13.24	13.52	-4.21	-3.42	130.14	127.62	-5.5	6.7	27.0	18	3	53.4	25.63	-93.09	140.5													
8.1	50.5	-20.04	-26.14	-34.63	-36.24	170.27	101.71	-35.3	2.6	27.0	18	3	56.9	22.42	-89.67	135.3													
8.2	43.8	-18.52	-21.65	-32.61	-33.36	158.46	106.67	-25.4	4.1	28.0	18	4	0.4	22.87	-90.15	135.4													
8.3	32.2	-13.33	-14.00	-29.26	-29.04	140.93	115.41	-20.3	5.1	28.0	18	4	3.7	23.56	-90.88	135.3													
8.4	17.0	3.79	1.26	-14.72	-15.16	130.55	121.16	-15.3	6.2	27.0	18	4	6.4	24.27	-91.65	135.3													
8.5	0.9	13.39	13.30	-4.07	-3.24	129.27	127.26	-14.1	6.7	27.0	18	4	8.6	24.93	-92.39	144.1													

09/05/75

AI

REPR
ORIGINAL PAGE IS POOR

DOY 156-1, 6/ 5/73 ITNC, GULF OF MEXICO/CARIBBEAN

SCAN NUM3	INCID ANGLE (DEG)	SCATTERING VV (DB)	COEFFICIENTS HH (DB)	COEFFICIENTS VH (DB)	COEFFICIENTS HV (DB)	ANTENNA V (DEG)	TEMPS H (DEG)	ASPECT ANGLE (DEG)	WIND SPEED (M/S)	SEA TEMP (DEG)	GMT (HR MIN SEC)	CELL COORDINATES LAT (DEG)	CELL COORDINATES LONG (DEG)	S193 AZIMTH (DEG)	DATA FLAG
9.1	50.5	-26.89	-33.71	-39.76	-42.17	169.24	153.24	-75.7	2.6	28.0	18 4 12.2	21.72	-89.01	135.7	2
9.2	43.8	-19.50	-23.38	-34.64	-33.29	158.87	107.59	-35.6	2.1	28.0	18 4 15.7	22.16	-89.46	135.6	
9.3	32.1	-13.73	-14.69	-29.27	-26.81	142.37	115.28	-25.7	4.1	28.0	18 4 18.9	22.85	-90.21	135.7	
9.4	17.0	0.78	1.13	-14.90	-14.36	128.62	121.84	-20.8	5.1	28.0	18 4 21.7	23.57	-90.97	135.8	
9.5	0.9	13.35	13.56	-3.93	-3.18	129.17	129.22	-16.7	6.2	27.0	18 4 23.9	24.23	-91.69	136.7	
10.1	50.6	-9.03	-9.01	-15.34	-15.41	274.66	269.97				18 4 27.4	21.00	-83.33	135.9	1
10.2	43.8	-21.96	-17.16	-20.81	-29.99	199.76	127.32				18 4 30.9	21.46	-88.82	135.9	1
10.3	32.1	-14.16	-15.21	-29.78	-29.85	142.29	115.27	-36.1	2.1	28.0	18 4 34.2	22.14	-89.53	136.1	
10.4	17.0	0.93	1.19	-14.68	-15.43	130.01	120.72	-25.9	4.1	28.0	18 4 36.9	22.86	-90.29	135.9	
10.5	0.8	13.71	13.67	-3.80	-3.12	127.52	126.52	-26.1	5.1	28.0	18 4 39.1	23.54	-91.01	141.1	
11.1	50.5	-8.97	-8.66	-14.95	-15.12	269.62	269.99				18 4 42.7	20.28	-87.69	136.3	1
11.2	43.8	-8.25	-8.38	-14.29	-14.44	276.64	273.51				18 4 46.2	20.74	-88.16	136.3	1
11.3	32.2	-15.30	-13.93	-20.15	-27.87	193.12	133.05				18 4 49.4	21.43	-88.87	136.2	1
11.4	17.1	0.47	0.85	-15.38	-15.81	130.37	123.60	-36.0	2.1	28.0	18 4 52.2	22.15	-89.61	136.0	
11.5	0.9	13.58	13.63	-3.86	-2.64	128.97	125.89	-18.1	4.1	28.0	18 4 54.4	22.33	-90.33	138.1	
12.1	50.4	-21.72	-26.32	-35.30	-35.11	173.51	107.04	-61.6	6.2	29.0	18 4 57.9	19.57	-97.05	136.6	
12.2	43.8	-7.88	-8.44	-16.78	-15.23	254.47	211.38				18 5 1.4	20.02	-97.51	136.6	
12.3	32.2	-7.08	-6.96	-13.31	-13.53	276.70	274.49				18 5 4.7	20.71	-98.20	136.7	
12.4	17.1	-0.19	-0.15	-15.94	-15.46	164.97	135.94				18 5 7.4	21.44	-98.95	136.7	
12.5	0.9	13.52	13.86	-3.67	-3.18	132.45	128.38	-39.8	2.1	28.0	18 5 9.6	22.12	-99.66	136.8	
13.1	50.5	-18.59	-24.05	-32.61	-32.53	173.94	107.49	-56.8	7.2	29.0	18 5 13.2	18.84	-97.40	136.8	
13.2	43.7	-18.39	-21.32	-31.74	-31.72	163.76	115.08	-61.8	6.7	29.0	18 5 16.7	19.71	-98.87	136.8	
13.3	32.1	-6.74	-5.38	-13.38	-13.47	230.17	235.51				18 5 19.9	20.20	-97.56	137.0	1
13.4	17.1	-6.31	-6.19	-12.91	-12.77	276.21	277.14				18 5 22.7	20.72	-98.29	136.8	1
13.5	0.9	13.28	13.06	-5.20	-4.15	180.52	156.11				18 5 25.9	21.46	-98.99	144.1	
14.1	50.4	-19.52	-27.81	-32.36	-32.70	175.14	113.25	-47.1	7.7	29.0	18 5 28.4	18.12	-85.77	137.1	
14.2	43.8	-17.52	-20.46	-31.31	-30.62	163.12	112.37	-57.0	7.2	29.0	18 5 31.9	18.58	-96.22	137.0	
14.3	32.1	-13.80	-14.29	-27.64	-27.67	147.57	121.59	-62.0	6.7	29.0	18 5 35.2	19.28	-86.92	137.0	
14.4	17.0	-5.39	-4.48	-12.63	-12.49	252.92	263.65				18 5 37.9	20.00	-87.64	137.3	1
14.5	0.9	-4.42	-4.55	-12.51	-12.42	275.99	281.53				18 5 40.1	20.69	-88.33	145.1	1
15.1	50.6	-18.48	-20.06	-29.37	-30.72	179.91	113.53	-47.4	8.2	30.0	18 5 43.7	17.38	-85.13	137.4	
15.2	43.8	-17.83	-20.62	-30.89	-30.63	164.67	116.02	-47.4	7.7	30.0	18 5 47.2	17.95	-85.59	137.4	
15.3	32.1	-12.82	-13.70	-27.53	-27.37	146.25	123.73	-57.3	7.2	29.0	18 5 50.4	18.56	-86.28	137.3	
15.4	17.0	0.89	1.25	-15.84	-14.38	135.31	126.37	-63.0	6.7	29.0	18 5 53.2	19.29	-87.00	138.0	
15.5	0.9	-2.67	-2.51	-11.50	-11.27	269.01	269.48				18 5 55.4	19.97	-87.68	149.4	1
16.1	50.7	-15.80	-20.80	-29.73	-29.92	175.23	109.35	-47.5	9.3	28.0	18 5 58.9	16.65	-84.50	137.5	
16.2	43.8	-14.69	-17.93	-29.72	-27.75	163.73	121.74	-47.6	8.8	29.0	18 6 2.4	17.12	-94.95	137.6	
16.3	32.1	-13.03	-13.84	-28.39	-27.35	146.34	125.59	-47.5	7.7	30.0	18 6 5.7	17.83	-95.64	137.5	
16.4	17.0	0.89	1.26	-14.53	-15.44	133.10	126.36	-57.6	7.2	29.0	18 6 8.4	18.56	-96.35	137.6	
16.5	0.9	13.35	13.32	-1.22	-3.48	133.14	132.69	-71.6	6.7	29.0	18 6 10.5	19.25	-97.04	146.6	

09/05/75

DOY 156-1, 6/ 5/73 ITNC, GULF OF MEXICO/CARIBBEAN

SCAN NUMB	INCID ANGLE (DEG)	SCATTERING COEFFICIENTS				ANTENNA V (DEG)	TEMPS H (DEG)	ASPECT ANGLE (DEG)	WIND SPEED (M/S)	SEA TEMP (DEG)	GMT			CELL COORDINATES		S193 AZIMTH (DEG)	DATA FLAG
		VV (DB)	HH (DB)	VH (DB)	HV (DB)						(HR	MIN	SEC)	LAT (DEG)	LONG (DEG)		
17.1	50.5	-15.23	-16.63	-28.40	-27.60	181.65	143.31	-57.8	9.8	28.0	18	6	14.2	15.92	-83.89	137.8	1
17.2	43.8	-13.99	-17.67	-27.23	-27.26	165.10	116.49	-47.8	9.3	29.0	18	6	17.7	16.39	-84.34	137.8	
17.3	32.1	-11.25	-12.10	-25.00	-24.40	150.53	126.15	-47.9	8.8	29.0	18	6	20.9	17.10	-85.02	137.9	
17.4	17.1	0.63	1.16	-15.01	-14.53	134.55	131.99	-47.8	7.7	30.0	18	6	23.7	17.83	-85.72	137.9	
17.5	0.9	13.39	13.28	-4.30	-3.34	129.13	131.23	-59.9	7.2	29.0	18	6	25.9	18.53	-86.40	139.9	
18.1	50.5	-14.96	-19.57	-26.92	-26.77	185.45	118.64				18	6	29.4	15.19	-83.29	138.0	
18.2	43.8	-13.39	-16.91	-27.41	-27.12	166.88	117.27	-67.9	10.3	28.0	18	6	32.9	15.66	-83.73	137.9	
18.3	32.1	-10.68	-12.16	-25.61	-25.41	150.31	123.31	-49.0	9.3	28.0	18	6	36.2	16.37	-84.39	138.0	
18.4	17.0	1.21	1.54	-14.55	-14.14	137.26	127.41	-48.3	8.8	29.0	18	6	38.9	17.11	-85.10	138.3	
18.5									7.2	30.0							
19.1	50.6	-15.52	-20.69	-29.10	-28.52	175.76	109.90	-60.1	11.3	28.0	18	6	44.7	14.45	-82.67	138.1	
19.2	43.8	-12.14	-14.46	-24.85	-20.51	167.87	133.53				18	6	48.2	14.92	-83.12	138.1	1
19.3	32.1	-9.69	-10.66	-23.66	-23.61	151.13	124.69	-60.3	10.3	28.0	18	6	51.4	15.64	-83.78	138.3	
19.4	17.0	0.78	1.51	-14.43	-15.30	137.53	133.30	-48.5	9.3	28.0	18	6	54.2	16.38	-84.48	138.5	
19.5	0.9	12.83	12.67	-4.61	-4.28	134.55	133.03	-55.6	8.8	29.0	18	6	56.4	17.07	-85.14	145.6	
20.1	50.6	-16.25	-21.55	-29.76	-29.52	174.74	110.43	-60.4	11.8	28.0	18	6	59.9	13.71	-82.07	138.6	
20.2	43.8	-14.43	-17.87	-27.32	-27.03	164.87	114.24	-60.4	11.8	28.0	18	7	3.4	14.18	-82.51	138.4	
20.3	32.1	-9.46	-9.94	-21.95	-16.47	153.60	158.46				19	7	5.7	14.90	-83.17	138.4	1
20.4	17.0	1.59	1.66	-15.12	-14.66	139.41	130.60	-60.5	10.3	28.0	18	7	9.4	15.65	-83.87	138.5	
20.5	0.9	12.96	12.93	-4.70	-3.93	134.45	134.52	-52.3	9.3	28.0	18	7	11.6	16.34	-84.52	142.3	
21.1	50.5	-16.92	-21.80	-29.44	-29.95	175.16	110.88	-63.6	12.9	28.0	18	7	15.2	12.97	-81.47	138.6	
21.2	43.8	-15.46	-18.27	-27.67	-27.70	164.32	115.72	-68.5	12.4	28.0	18	7	18.7	13.45	-81.90	138.5	
21.3	32.1	-10.54	-11.95	-24.40	-24.11	149.57	121.53	-68.6	11.8	28.0	18	7	21.9	14.16	-82.56	138.6	
21.4	17.1	-3.78	-1.28	-14.46	-12.89	170.47	204.73				18	7	24.7	14.90	-83.25	139.1	1
21.5	0.9	12.61	13.00	-4.60	-4.30	145.61	139.57				18	7	26.9	15.61	-83.92	138.9	
22.1	50.5	-17.71	-22.24	-31.29	-30.10	175.07	112.30	-63.7	13.4	28.0	18	7	30.4	12.23	-80.87	138.7	
22.2	43.9	-15.60	-18.28	-28.01	-27.86	164.78	115.69	-63.8	12.9	28.0	18	7	33.9	12.70	-81.30	138.8	
22.3	32.2	-10.95	-11.71	-24.60	-24.11	148.68	122.66	-69.0	12.4	28.0	18	7	37.2	13.42	-81.96	139.0	
22.4	17.0	1.39	1.61	-15.77	-13.93	136.83	127.55	-69.1	11.8	28.0	18	7	39.9	14.17	-82.65	139.1	
22.5	0.8	15.26	16.81	-4.23	-0.40	184.33	201.08				18	7	42.1	14.88	-83.29	148.5	2
23.1	50.5	-18.19	-22.78	-30.27	-30.27	177.57	114.83				18	7	45.7	11.49	-80.29	139.1	
23.2	43.8	-15.47	-16.47	-28.05	-27.59	165.88	118.84				18	7	49.2	11.96	-80.71	139.0	
23.3	32.1	-10.96	-11.77	-24.58	-24.42	149.44	122.98				18	7	52.4	12.68	-81.36	138.8	
23.4	17.0	1.38	1.48	-14.11	-14.90	135.33	129.11				18	7	55.2	13.43	-82.04	139.5	
23.5	0.9	12.95	12.61	-4.53	-4.13	135.48	133.49				18	7	57.4	14.13	-82.69	147.4	
24.1	50.6	-20.84	-24.80	-34.45	-32.92	176.85	112.60				18	8	0.9	10.73	-79.68	139.1	
24.2	43.8	-16.42	-19.54	-28.62	-28.90	166.82	118.76				18	8	4.4	11.21	-80.12	139.1	
24.3	32.1	-11.19	-12.27	-24.67	-24.67	150.14	120.29				18	8	7.7	11.94	-80.77	139.2	
24.4	17.1	1.52	1.70	-14.29	-14.88	138.60	129.27				18	8	10.4	12.68	-81.44	139.6	
24.5	1.0	12.41	12.42	-5.03	-4.62	133.69	133.20				18	8	12.6	13.39	-82.03	157.3	

REPRODUCIBILITY OF THE
ORIGINAL PAGE IS POOR

09/05/75

DOY 156-1, 6/ 5/73 ITNC, GULF OF MEXICO/CARIBBEAN

SCAN NUMB	INCID ANGLE (DEG)	SCATTERING COEFFICIENTS				ANTENNA V (DEG)	TEMPS H (DEG)	ASPECT ANGLE (DEG)	WIND SPEED (M/S)	SEA TEMP (DEG)	GNT (HR MIN SEC)	CELL COORDINATES		S193 AZIMTH (DEG)	DATA FLAG
		VV (DB)	HH (DB)	VH (DB)	HV (DB)							LAT (DEG)	LONG (DEG)		
25.1	50.5	-19.78	-16.13	-27.20	-29.39	204.94	142.90								
25.2	43.8	-20.03	-22.31	-31.62	-34.03	169.34	121.32				18 8 16.2	9.99	-79.11	139.2	1
25.3	32.2	-12.43	-13.09	-25.83	-25.63	149.24	125.92				18 8 19.7	10.47	-79.53	139.2	2
25.4	17.1	1.25	1.55	-14.36	-15.00	136.66	130.46				18 8 22.9	11.19	-80.17	139.2	
25.5	0.9	12.37	12.40	-5.13	-4.78	137.06	137.59				18 8 25.7	11.94	-80.84	139.3	
											18 8 27.9	12.65	-81.48	153.2	
26.1	50.5	-6.80	-6.21	-14.13	-13.95	260.96	245.01								
26.2	43.8	-13.45	-12.78	-25.86	-24.50	197.39	180.55				18 8 31.4	9.25	-78.52	139.5	1
26.3	32.1	-13.53	-14.56	-27.97	-27.98	156.63	127.58				18 8 34.9	9.72	-78.94	139.3	2
26.4	17.1	1.04	1.23	-14.73	-14.34	139.92	131.73				18 8 38.2	10.45	-79.59	139.4	
26.5	0.9	12.30	12.17	-4.91	-4.40	135.42	135.44				18 8 40.9	11.27	-80.25	139.9	
											18 8 43.1	11.91	-80.89	147.9	
27.1	50.6	-7.35	-7.29	-14.47	-14.45	265.75	265.06								
27.2	43.8	-6.30	-6.51	-13.85	-13.75	266.37	263.14				18 8 46.7	8.49	-77.93	139.6	1
27.3											18 8 50.2	8.98	-78.36	139.5	1
27.4															
27.5															

JSC - 1/ 7/75

S. TRUTH - 1/21/74

LAST MOD - 8/28/75

THIS LISTING - 09/05/75

DOY 157-1. 6/ 6/73 CTNC-R, HURRICANE AVA

SCAN NUMB	INCID ANGLE (DEG)	SCATTERING COEFFICIENTS				ANTENNA V (DEG)	TEMPS H (DEG)	ASPECT ANGLE (DEG)	WIND SPEED (M/S)	SEA TEMP (DEG)	GMT			CELL COORDINATES		S193 DATA AZIMTH FLAG
		VV (DB)	HH (DB)	VH (DB)	HV (DB)						(HR MIN SEC)	(DEG)	(DEG)	LAT (DEG)	LONG (DEG)	
1.1	50.6	-15.96	-25.34	-30.37	-29.35	168.42	99.06	167.1	6.2	25.5	18 55 59.9	18.78	-111.61	227.9		
1.2	44.3	-18.19	-23.17	-30.64	-31.56	157.43	105.48	161.7	5.7	25.6	18 56 3.4	19.16	-110.82	228.3		
1.3	34.0	-17.26	-20.32	-33.95	-33.21	141.55	110.59	156.3	4.6	25.5	18 56 6.7	19.73	-109.87	228.7		
1.4	19.9	-6.45	-7.74	-22.11	-21.87	129.98	121.03	145.3	2.6	25.5	18 56 9.4	20.36	-108.87	229.7		
1.5	4.1	13.26	12.43	-3.19	-3.01	128.46	126.34	130.9	2.1	25.8	18 56 11.6	20.99	-107.93	239.1		
2.1	50.6	-16.57	-23.82	-29.66	-29.35	170.89	103.44	172.6	6.7	26.2	18 56 15.1	18.02	-110.90	227.4		
2.2	44.3	-15.88	-22.30	-30.24	-30.32	160.42	109.45	172.6	6.2	26.1	18 56 18.7	18.42	-110.12	227.4		
2.3	33.9	-15.88	-18.73	-31.43	-31.00	143.81	114.41	157.9	5.7	26.0	18 56 21.9	18.97	-109.16	227.1		
2.4	19.9	-3.06	-3.78	-18.45	-18.84	134.30	124.28	152.7	3.1	26.0	18 56 24.7	19.61	-108.17	227.3		
2.5	4.0	14.13	13.97	-2.90	-3.63	128.91	129.41	143.0	2.6	26.1	18 56 26.9	20.22	-107.22	222.0		
3.1	50.6	-16.06	-23.67	-29.68	-29.60	173.83	105.91	163.2	8.2	26.6	18 56 30.4	17.27	-110.19	226.8		
3.2	44.3	-14.50	-20.34	-28.52	-28.57	163.45	111.44	163.5	8.2	26.7	18 56 33.9	17.65	-109.41	226.5		
3.3	33.9	-13.53	-15.87	-27.86	-28.32	147.20	116.82	159.0	7.2	26.9	18 56 37.2	18.21	-108.46	226.0		
3.4	20.0	-1.94	-2.61	-17.04	-17.51	135.86	126.32	155.7	4.6	26.8	18 56 39.9	18.83	-107.47	224.3		
3.5	4.3	13.14	13.01	-3.98	-4.26	131.90	130.29	154.9	3.1	26.9	18 56 42.1	19.45	-106.53	210.1		
4.1	50.7	-14.24	-21.46	-28.17	-27.70	176.64	108.57	169.0	9.3	27.1	18 56 45.7	16.51	-109.51	226.0		
4.2	44.3	-13.05	-19.85	-27.32	-27.54	163.93	113.38	164.3	9.3	27.0	18 56 49.2	15.89	-108.71	225.7		
4.3	34.0	-12.22	-14.40	-26.34	-26.78	147.36	118.42	170.6	7.7	27.8	18 56 52.4	17.44	-107.77	224.4		
4.4	20.0	-2.11	-2.62	-17.53	-18.13	135.61	126.10	163.6	4.6	27.7	18 56 55.2	18.07	-106.77	221.4		
4.5	4.7	13.29	13.09	-3.76	-4.07	131.23	130.64	-174.0	3.6	27.8	18 56 57.4	18.68	-105.84	195.0		
5.1	50.7	-13.16	-20.04	-27.46	-26.77	176.75	111.27	174.8	12.9	28.0	18 57 0.9	15.74	-108.80	225.2		
5.2	44.4	-12.42	-17.61	-26.33	-26.39	166.44	115.88	-174.0	11.3	28.0	18 57 4.4	16.12	-108.04	224.8		
5.3	34.1	-14.74	-17.47	-30.22	-29.53	147.36	117.17	-174.3	8.2	28.0	18 57 7.7	16.68	-107.08	223.3		
5.4	20.2	-4.00	-4.11	-19.13	-19.80	137.56	125.42	-170.2	5.7	28.1	18 57 10.4	17.30	-106.09	219.2		
5.5	5.3	12.89	12.81	-4.34	-5.12	128.22	130.75	-153.0	4.1	28.2	18 57 12.6	17.91	-105.15	188.0		
6.1	50.7	-14.23	-18.51	-26.37	-26.35	179.95	114.92	-170.7	17.5	28.3	18 57 16.2	14.98	-108.13	224.7		
6.2	44.5	-13.36	-16.98	-26.79	-26.51	166.08	117.52	-159.1	14.9	28.3	18 57 19.7	15.35	-107.37	224.1		
6.3	34.2	-12.17	-14.41	-26.66	-26.99	148.35	120.44	-151.0	9.8	28.3	18 57 22.9	15.91	-106.40	221.8		
6.4	20.4	-2.89	-3.55	-18.19	-18.57	136.35	126.28	-141.6	6.7	28.4	18 57 25.7	16.52	-105.42	216.6		
6.5	6.0	11.72	11.70	-4.86	-5.54	128.58	132.09	-100.6	4.1	28.5	18 57 27.9	17.13	-104.48	180.8		
7.1	50.9	-13.20	-19.04	-26.50	-25.57	179.96	118.46	-174.1	21.6	28.4	18 57 31.4	14.20	-107.48	224.1		
7.2	44.6	-14.13	-18.68	-27.84	-27.84	165.98	117.33	-157.9	19.6	28.3	18 57 34.9	14.57	-106.68	222.9		
7.3	34.3	-12.92	-14.30	-26.50	-26.81	149.94	122.57	-140.6	11.3	28.4	18 57 38.2	15.13	-105.74	220.6		
7.4	20.6	-2.94	-3.32	-18.21	-18.71	136.90	128.94	-129.2	7.7	28.5	18 57 40.9	15.74	-104.75	214.2		
7.5	6.9	11.46	11.01	-5.39	-6.01	128.27	132.32	-90.2	4.6	28.5	18 57 43.1	16.34	-103.81	175.2		
8.1	50.9	-12.24	-15.32	-21.91	-21.57	192.85	138.91	-153.3	26.3	28.2	18 57 46.7	13.44	-106.80	223.3		
8.2	44.6	-14.27	-15.74	-25.33	-25.59	177.72	134.65	-140.1	21.1	28.1	18 57 50.2	13.80	-106.02	222.1		
8.3	34.4	-14.36	-14.78	-28.20	-28.19	149.91	121.45	-129.1	13.4	28.1	18 57 53.4	14.35	-105.07	219.1		
8.4	20.9	-2.46	-2.79	-18.02	-18.62	137.71	129.69	-116.0	8.8	28.5	18 57 56.2	14.95	-104.08	211.0		
8.5	7.7	10.52	10.37	-6.39	-6.92	129.10	131.63	-75.1	5.1	28.7	18 57 58.4	15.55	-103.14	170.1		

REPRODUCIBILITY OF THE
ORIGINAL PAGE IS POOR

09/05/75

A5

DOY 157-1, 6/ 6/73 CTNC-R, HURRICANE AVA

SCAN NUMB	INCID ANGLE (DEG)	SCATTERING VV (DB)	COEFFICIENTS HH (DB)	COEFFICIENTS VH (DB)	COEFFICIENTS HV (DB)	ANTENNA V (DEG)	TEMPS H (DEG)	ASPECT ANGLE (DEG)	WIND SPEED (M/S)	SEA TEMP (DEG)	GMT (HR MIN SEC)	CELL COORDINATES LAT (DEG)	CELL COORDINATES LONG (DEG)	S193 AZIMUTH (DEG)	DATA FLAG
9.1	51.1	-13.02	-14.53	-22.24	-22.47	193.26	147.48	-112.6	25.7	27.3	18 58 1.9	12.64	-106.14	222.6	
9.2	44.8	-12.45	-15.35	-24.64	-24.67	175.18	131.39	-111.1	20.1	27.8	18 58 5.4	13.01	-105.37	221.1	
9.3	34.7	-13.97	-15.12	-29.48	-29.27	150.66	122.71	-107.9	14.4	28.3	18 58 8.7	13.56	-104.41	217.9	
9.4	21.2	-2.98	-2.81	-18.43	-18.92	134.50	126.53	-99.0	9.3	28.8	18 58 11.4	14.17	-103.42	209.0	
9.5	8.5	11.20	11.96	-5.29	-5.90	130.63	139.97	-62.3	6.2	29.0	18 58 13.6	14.78	-102.48	167.3	
10.1	51.3	-12.51	-11.67	-21.32	-20.92	238.52	216.39	-76.9	19.6	28.5	18 58 17.2	11.85	-105.51	221.9	4
10.2	45.0	-11.82	-15.12	-24.96	-24.92	169.69	124.05	-80.2	16.5	29.0	18 58 20.7	12.22	-104.72	220.2	
10.3	34.8	-12.72	-14.88			156.02	130.64	-81.4	13.4	29.0	18 58 23.9	12.78	-103.76	216.4	
10.4	21.6	-2.96	-3.36	-17.40	-17.56	136.12	123.16	-81.6	8.8	29.0	18 58 26.7	13.38	-102.77	206.6	
10.5	9.5	11.68	11.16	-4.08	-4.64	127.98	131.53	-39.3	6.7	29.0	18 58 28.9	13.93	-101.83	164.3	
11.1	51.4	-13.29	-16.12	-24.86	-25.25	189.48	127.34	-46.1	16.0	29.0	18 58 32.4	11.05	-104.85	221.1	
11.2	45.1	-12.14	-15.09	-25.15	-24.43	172.25	125.10	-54.2	13.9	29.0	18 58 35.0	11.44	-104.05	219.2	
11.3	35.1	-11.16	-12.78			148.52	122.14	-60.2	10.3	29.0	18 58 39.1	11.99	-103.12	215.2	
11.4	22.0	-2.71	-3.48	-17.44	-18.21	145.62	133.46	-64.5	8.2	29.0	18 58 41.9	12.59	-102.12	204.5	
11.5	10.5	10.98	10.36	-3.16	-3.51	129.23	131.76	-26.8	6.7	29.0	18 58 44.1	13.20	-101.13	161.8	
12.1	51.6	-12.71	-14.48			200.50	138.79	-40.3	11.3	29.0	18 58 47.7	10.27	-104.20	220.3	4
12.2	45.3	-11.92	-16.63			165.80	118.68	-43.4	9.6	29.0	18 58 51.2	10.65	-103.42	218.4	
12.3	35.4	-10.29	-13.15			149.75	123.89	-58.8	8.8	29.0	18 58 54.5	11.18	-102.46	213.8	
12.4	22.5					138.90	132.47	-42.4	7.7	29.0	18 58 57.2	11.80	-101.48	202.4	
12.5	11.5					128.52	133.16	-14.8	6.2	29.0	18 58 59.4	12.40	-100.53	159.8	
13.1	51.8	-13.72	-19.87			179.37	118.27	-21.6	9.3		18 59 2.9	9.47	-103.58	219.6	
13.2	45.6	-13.06	-19.74			163.50	116.89	-27.6	8.8		18 59 6.4	9.84	-102.79	217.6	
13.3	35.7					146.02	121.20	-27.5	7.7		18 59 9.7	10.39	-101.83	212.5	
13.4	23.0					134.18	129.42	-25.1	6.7		18 59 12.4	11.00	-100.83	200.1	
13.5	12.4					128.39	133.50	1.0	6.2		18 59 14.6	11.60	-99.89	159.0	
14.1	52.0	-17.08				174.33	111.21	-17.9	8.2		18 59 18.2	8.67	-102.94	218.9	
14.2	45.8					162.18	115.06				18 59 21.7	9.04	-102.16	216.6	
14.3	36.0					145.97	120.64				18 59 24.9	9.59	-101.20	211.4	
14.4	23.5					135.11	129.25				18 59 27.7	10.23	-100.20	197.6	
14.5	13.5					142.51	152.70				18 59 29.9	10.80	-99.25	157.0	
15.1	52.1					172.88	110.26				18 59 33.4	7.87	-102.31	218.2	
15.2	46.1					160.64	115.05				18 59 36.9	8.24	-101.54	215.7	
15.3	36.3					148.34	124.62				18 59 40.2	8.79	-100.57	209.9	
15.4	24.0					195.00	188.24				18 59 42.9	9.40	-99.57	196.3	
15.5	14.5					131.49	137.56				18 59 45.1	10.00	-98.62	156.2	
16.1	52.4					172.85	110.22				18 59 48.9	7.45	-101.73	217.5	
16.2	46.4					160.98	115.89				18 59 52.2	7.43	-100.91	214.8	
16.3	36.8					145.28	121.90				18 59 55.6	7.97	-99.95	208.8	
16.4	24.5					161.32	155.44				18 59 58.2	8.60	-98.94	194.5	
16.5	15.5					129.81	135.43				19 0 0.4	9.19	-97.93	155.6	

09/05/75

DDY 157-1, 6/ 6/73 CTNC-R, HURRICANE AVA

SCAN NUMB	INCID ANGLE (DEG)	SCATTERING COEFFICIENTS				ANTENNA V (DEG)	TEMPS H (DEG)	ASPECT ANGLE (DEG)	WIND SPEED (M/S)	SEA TEMP (DEG)	GMT (HR MIN SEC)	CELL COORDINATES		S193 DATA AZIMTH FLAG (DEG)
		VV (DB)	HH (DB)	VH (DB)	HV (DB)							LAT (DEG)	LONG (DEG)	
17.1	52.7					171.72	111.13				19 0 4.1	6.22	-101.08	215.6
17.2	46.6					159.99	115.41				19 0 7.4	6.52	-100.30	213.9
17.3	37.1					143.72	120.50				19 0 10.6	7.13	-99.33	207.7
17.4	25.3					131.92	128.75				19 0 13.4	7.79	-98.32	192.7
17.5														
18.1	52.9					171.56	111.46				19 0 19.2	5.42	-100.47	215.8
18.2	46.9					158.93	115.40				19 0 22.7	5.81	-99.68	213.1
18.3	37.6					146.57	120.70				19 0 25.9	6.36	-98.71	206.4
18.4	25.9					135.61	130.25				19 0 28.6	6.99	-97.70	191.2
18.5	17.4										19 0 30.9	7.59	-96.74	153.5

JSC - 1/ 8/75

S. TRUTH - 4/11/75

LAST MOD - 8/28/75

THIS LISTING - 09/05/75

DOY 152-1, 6/11/73 ITNC, GULF OF MEXICO

SCAN NUMB	INCID ANGLE (DEG)	SCATTERING COEFFICIENTS				ANTENNA V (DEG)	TEMPS H (DEG)	ASPECT ANGLE (DEG)	WIND SPEED (M/S)	SEA TEMP (DEG)	GMT			CELL COORDINATES		S193 DATA AZIMTH FLAG
		VV (DB)	HH (DB)	VH (DB)	HV (DB)						(HR MIN SEC)			LAT (DEG)	LONG (DEG)	(DEG)
1.1						173.27	122.31	-2.5	3.1	28.0	15 20 25.8			27.51	-90.08	132.5
1.2	44.4					164.50	140.92	2.9	4.1	27.0	15 20 28.9			28.19	-90.89	132.1
1.3	32.6					153.05	143.22	4.0	5.1	27.0	15 20 31.6			28.88	-91.72	131.9
1.4	17.6								5.7	26.0						
1.5																
2.1	51.0	-19.40	-22.18	-33.49	-38.21	189.20	135.61	-13.0	2.1	28.0	15 20 37.0			26.42	-88.86	133.0
2.2	44.4	-27.21	-31.14	-38.15	-35.24	177.69	124.52	-8.0	2.6	28.0	15 20 40.6			26.84	-89.37	133.0
2.3	32.7	-19.22	-19.72	-35.42	-33.77	164.34	138.79	-2.6	4.1	27.0	15 20 43.8			27.52	-90.16	132.6
2.4	17.6	-0.87	-0.43	-16.25	-15.57	157.57	152.95	3.4	4.1	27.0	15 20 46.6			28.21	-90.93	131.5
2.5	1.5	15.16	15.16	-2.26	-1.57	153.38	159.95	23.5	5.1	27.0	15 20 48.8			28.86	-91.77	111.5
3.1	51.0	-29.20	-30.30	-37.43	-38.11	191.99	128.17	-23.3	2.6	28.0	15 20 52.3			25.73	-88.15	133.3
3.2	44.4	-22.62	-21.07	-36.47	-34.36	180.48	133.45	-18.2	2.6	29.0	15 20 55.8			26.16	-88.65	133.2
3.3	32.6	-20.50	-22.15	-35.44	-42.51	162.02	135.03	-8.0	2.6	28.0	15 20 59.1			26.84	-89.44	133.0
3.4	17.6	-1.45	-0.64	-16.16	-16.16	150.28	141.16	-1.8	4.1	27.0	15 21 1.8			27.54	-90.24	131.8
3.5	1.5	14.57	14.53	-2.11	-1.78	150.26	149.46	17.6	4.1	27.0	15 21 4.0			23.18	-91.02	117.4
4.1	51.0	-25.80	-30.44	-38.51	-38.11	182.93	118.22	-28.8	3.6	29.0	15 21 7.5			25.02	-87.44	133.8
4.2	44.3	-23.89	-26.97	-38.12	-35.38	172.76	123.61	-28.7	3.1	29.0	15 21 11.1			25.47	-87.95	133.7
4.3	32.7	-19.00	-17.66	-35.55	-32.49	154.96	127.93	-18.3	2.6	29.0	15 21 14.3			25.15	-88.71	133.3
4.4	17.7	-3.12	-2.56	-18.49	-17.84	139.76	132.01	-7.4	2.6	28.0	15 21 17.1			26.85	-89.51	132.4
4.5	1.6	15.38	15.26	-1.83	-1.93	138.08	136.19	23.1	4.1	27.0	15 21 19.3			27.51	-90.27	106.9
5.1	51.0	-24.64	-26.78	-42.99	-40.56	177.77	110.76	-29.1	4.6	29.0	15 21 22.8			24.33	-86.74	134.1
5.2	44.4	-22.62	-26.02	-36.44	-38.39	165.54	114.75	-28.9	4.6	29.0	15 21 26.3			24.77	-87.23	133.9
5.3	32.7	-19.21	-19.46	-34.58	-35.57	148.54	120.00	-28.8	3.1	29.0	15 21 29.6			25.46	-88.00	133.3
5.4	17.6	-2.44	-1.75	-16.98	-16.33	140.35	127.29	-17.7	2.6	29.0	15 21 32.3			26.17	-88.79	132.7
5.5	1.5	16.02	15.79	-1.40	-0.47	131.34	128.91	14.6	2.6	28.0	15 21 34.5			26.83	-89.55	110.4
6.1	51.0	-21.41	-26.33	-32.70	-45.67	173.51	105.84	-34.5	4.6	29.0	15 21 38.0			23.63	-86.05	134.5
6.2	44.3	-21.24	-24.11	-35.25	-34.26	162.41	110.30	-34.4	4.6	29.0	15 21 41.6			24.08	-86.55	134.4
6.3	32.7	-15.81	-16.57	-32.42	-32.47	145.29	117.70	-28.8	4.6	29.0	15 21 44.8			24.76	-87.29	133.8
6.4	17.6	-1.67	-1.35	-16.45	-16.45	132.76	124.08	-27.9	3.1	29.0	15 21 47.6			25.47	-88.08	132.9
6.5	1.5	16.26	16.47	-0.71	-0.37	131.94	128.44	-3.9	2.6	29.0	15 21 49.7			26.14	-88.83	118.9
7.1	50.9	-21.36	-26.88	-32.39	-32.39	171.73	106.16	-34.7	4.6	29.0	15 21 53.1			22.94	-85.39	134.7
7.2	44.4	-17.92	-21.92	-31.76	-31.76	159.08	109.30	-34.7	4.6	29.0	15 21 56.8			23.37	-85.86	134.7
7.3	32.7	-15.73	-16.16	-31.49	-31.09	141.92	115.00	-34.5	4.6	29.0	15 22 0.1			24.06	-86.60	134.5
7.4	17.7	-0.15	0.37	-15.50	-15.52	130.26	123.55	-28.2	4.4	29.0	15 22 2.8			24.78	-87.37	133.2
7.5	1.6	15.39	15.34	-1.74	-1.12	128.84	127.33	-5.3	3.1	29.0	15 22 5.0			25.45	-88.11	110.3
8.1	51.0	-23.99	-31.56	-43.00	-40.52	172.01	105.37	-45.1	4.1	29.0	15 22 8.5			22.22	-84.70	135.1
8.2	44.4	-20.65	-23.66	-33.50	-34.38	159.64	109.62	-34.9	4.6	28.0	15 22 12.1			22.67	-85.18	134.9
8.3	32.7	-13.86	-13.88	-28.92	-18.01	142.85	116.90	-34.8	4.6	29.0	15 22 15.3			23.36	-85.91	134.8
8.4	17.7	0.10	0.50	-15.46	-15.13	129.95	122.20	-33.9	4.6	29.0	15 22 18.1			24.08	-86.63	133.9
8.5	1.6	14.56	14.60	-2.62	-2.26	126.05	125.58	-5.7	4.6	29.0	15 22 20.2			24.75	-87.41	110.7

09/05/75

A8

REPRODUCIBILITY OF THE
ORIGINAL PAGE IS POOR

DOY 162-1. 6/11/73 ITNG. GULF OF MEXICO

SCAN NUMB	INCID ANGLE (DEG)	SCATTERING VV (DB)	COEFFICIENTS HH (DB)	VH (DB)	HV (DB)	ANTENNA V (DEG)	TEMPS H (DEG)	ASPECT ANGLE (DEG)	WIND SPEED (M/S)	SEA TEMP (DEG)	GMT (HR MIN SEC)	CELL COORDINATES LAT (DEG)	LONG (DEG)	S193 DATA AZIMTH FLAG (DEG)
9.1	50.9	-22.51	-28.41	-35.83	-35.08			-75.3	2.6	29.0	15 22 23.5	21.52	-84.05	135.3
9.2	44.3	-17.68	-11.83	-16.68	-21.47	207.72	142.59				15 22 27.3	21.96	-84.51	135.2
9.3	32.7	-14.92	-15.19	-31.49	-30.31	141.92	116.79	-34.9	4.6	28.0	15 22 30.6	22.05	-85.24	134.9
9.4	17.7	0.71	0.02		-14.39	129.59	122.28	-33.8	4.6	29.0	15 22 33.3	23.37	-85.99	133.8
9.5	1.6	14.51	14.55	-2.77	-2.13	125.81	124.79	-14.1	4.6	29.0	15 22 35.5	24.05	-86.72	114.1
10.1	51.0	-19.64	-24.73	-33.62	-33.48	170.75	104.89	-70.7	6.2	29.0	15 22 39.0	20.79	-83.38	135.7
10.2	44.4	-19.94	-23.71	-34.24	-34.35	158.63	107.06	-75.5	4.1	29.0	15 22 42.6	21.24	-83.84	135.5
10.3	32.8	-13.79	-9.63	-14.69	-16.84	198.26	154.54				15 22 45.8	21.94	-84.56	135.2
10.4	17.7	0.22	0.61	-15.49	-14.63	130.13	121.25	-33.9	4.6	28.0	15 22 48.6	22.67	-85.31	133.9
10.5	1.7	13.80	13.96	-3.44	-2.88	127.55	126.02	-17.1	4.6	29.0	15 22 50.8	23.34	-86.02	117.1
11.1	51.0	-17.85	-23.70	-33.48	-32.42	169.46	103.60	-75.9	7.7	28.0	15 22 54.3	20.37	-82.72	135.9
11.2	44.4	-16.77	-20.04	-31.79	-30.96	159.85	109.81	-70.9	7.2	29.0	15 22 57.8	20.52	-83.18	135.9
11.3	32.8	-14.42	-15.36	-30.62	-29.64	141.37	117.31	-75.5	4.1	29.0	15 23 1.1	21.22	-83.90	135.5
11.4	17.7	-1.16	-1.45	-13.34	-15.30	189.88	147.59				15 23 3.8	21.96	-84.64	134.8
11.5	1.7	14.46	14.39	-3.06	-2.65	128.55	124.97	-14.0	4.6	28.0	15 23 6.0	22.64	-85.35	114.0
12.1	51.1	-20.00	-24.98	-35.44	-34.14	170.79	103.92	-106.2	6.7	28.0	15 23 9.5	19.34	-82.07	136.2
12.2	44.4	-16.37	-19.71	-30.83	-29.82	159.85	109.31	-81.0	7.7	28.0	15 23 13.1	19.80	-82.53	136.0
12.3	32.8	-12.89	-13.63	-27.61	-27.28	144.58	118.95	-70.8	7.2	29.0	15 23 16.3	20.51	-83.24	135.8
12.4	17.7	0.54	0.65		-14.59	131.86	123.51	-74.9	4.1	29.0	15 23 19.1	21.24	-83.98	134.9
12.5	1.7	13.89	13.78	-3.44	-3.51	197.02	167.95				15 23 21.2	21.92	-84.68	116.3
13.1	51.1	-25.69	-32.52	-34.94		169.66	101.23	-106.5	3.6	28.0	15 23 25.0	19.60	-81.42	136.5
13.2	44.3	-21.13	-23.11	-35.06	-35.33	158.13	107.59	-106.5	5.1	28.0	15 23 28.3	19.38	-81.90	136.5
13.3	32.8	-12.12	-13.04	-27.09	-27.15	141.97	119.81	-81.0	7.7	28.0	15 23 31.6	19.79	-82.59	136.0
13.4	17.7	0.80	1.26	-14.77	-14.21	132.64	125.35	-69.9	7.2	29.0	15 23 34.3	20.53	-83.32	134.9
13.5	1.7	13.84	14.16	-3.25	-2.49	123.76	127.81	-57.8	4.1	29.0	15 23 36.5	21.21	-84.01	117.8
14.1	51.1	-27.29	-32.57	-36.88	-39.41	168.72	101.32	-86.7	4.1	28.0	15 23 40.0	17.89	-80.80	136.7
14.2	44.4	-23.21	-26.91	-37.89	-38.15	157.38	105.30	-106.7	2.6	28.0	15 23 43.6	18.35	-81.26	136.7
14.3	32.8	-13.93	-14.98	-30.28	-29.36	144.34	115.56	-106.2	5.1	28.0	15 23 46.8	19.06	-81.95	136.2
14.4	17.8	1.34	1.43	-14.33	-13.96	131.90	122.99	-80.6	7.7	28.0	15 23 49.6	19.80	-82.67	135.6
14.5	1.6	13.84	13.83	-3.54	-3.12	129.29	127.28	-51.0	7.2	29.0	15 23 51.7	20.50	-83.36	116.3
15.1	51.0	-27.82	-35.36	-33.28	-38.38	168.25	101.37				15 23 55.3	17.16	-80.17	137.0
15.2	44.4	-24.19	-27.75	-41.01	-38.33	158.11	107.56				15 23 58.8	17.63	-80.62	136.8
15.3	32.8	-16.72	-17.89	-33.62	-33.70	140.30	113.05				15 24 2.1	18.34	-81.31	136.4
15.4	17.7	0.59	1.12		-14.64	129.60	121.27				15 24 4.8	19.69	-82.03	135.4
15.5	1.5		-46.21	-41.17		129.21	128.22				15 24 7.1	19.77	-82.71	121.2

JSC - 1/ 7/75

S. TRUTH - 1/21/74

LAST MOD - 8/28/75

THIS LISTING - 09/05/75

DOY 216-1, 8/ 4/73 CTNC-L/R, NORTH PACIFIC

SCAN NUMB	INCID ANGLE (DEG)	SCATTERING COEFFICIENTS				ANTENNA V (DEG)	TEMPS H (DEG)	ASPECT ANGLE (DEG)	WIND SPEED (M/S)	SEA TEMP (DEG)	GHT (HR MIN SEC)	CELL COORDINATES		S193 DATA AZIMTH FLAG (DEG)
		VV (DB)	HH (DB)	VH (DB)	HV (DB)							LAT (DEG)	LONG (DEG)	
1.1	48.9					160.85	102.05	-146.9	9.0	9.5	17 8 14.4	53.24	-166.07	349.9
1.2	41.3					148.51	105.59	-145.3	9.1	10.0	17 8 17.8	52.40	-165.43	350.3
1.3	38.4					143.34	118.58	-145.0	9.2	11.5	17 8 21.0	51.41	-164.79	351.0
1.4	15.8					132.63	131.95	-144.9	9.2	12.5	17 8 23.7	50.35	-164.20	352.9
1.5														
2.1	47.7	-15.78	-20.62	-29.98	-30.08	160.05	103.73	44.0	9.2	15.3	17 8 29.1	45.49	-162.31	168.0
2.2	41.5	-13.54	-16.94	-27.85	-28.26	151.19	108.65	43.9	9.2	14.9	17 8 32.7	46.25	-162.20	168.1
2.3	31.3	-9.69	-11.34	-24.47	-25.16	139.30	116.39	43.2	9.1	14.4	17 8 35.9	47.25	-162.17	167.8
2.4	17.2	0.95	0.66	-16.01	-14.79	129.70	122.37	45.7	9.1	13.9	17 8 38.7	48.36	-162.20	166.3
2.5	1.7	13.05	12.52	-3.96	-4.25	125.19	124.11	79.8	9.1	13.0	17 8 40.6	49.43	-162.28	132.2
3.1	49.0	-15.82	-22.75	-29.06	-29.47	163.58	103.65	-144.2	8.3	9.5	17 8 44.4	53.63	-163.05	352.2
3.2	41.4	-18.43	-23.16	-31.98	-31.56	153.08	111.59	-142.5	8.4	10.2	17 8 47.9	52.77	-162.45	352.5
3.3	30.5	-13.82	-14.02	-27.80	-28.64	140.46	118.06	-140.3	8.5	11.0	17 8 51.2	51.77	-161.86	353.3
3.4	15.9	2.66	2.34	-13.79	-14.46	129.36	120.51	-140.5	8.8	12.0	17 8 53.9	50.70	-161.33	355.5
3.5	1.1	12.97	13.13	-3.89	-4.33	124.45	124.90	117.0	8.9	12.8	17 8 56.1	49.65	-160.87	98.0
4.1	47.8	-18.65	-22.33	-31.10	-32.70	160.28	101.84	44.8	9.3	15.0	17 8 59.6	45.77	-159.66	170.2
4.2	41.6	-13.96	-17.50	-28.21	-28.70	151.23	108.14	45.8	9.3	14.6	17 9 3.2	46.53	-159.53	170.2
4.3	31.3	-10.59	-12.53	-25.13	-25.82	138.61	113.50	46.9	9.2	14.0	17 9 6.4	47.54	-159.44	170.1
4.4	17.3	0.02	0.28	-14.73	-15.25	128.75	121.49	49.5	9.0	13.5	17 9 9.2	48.64	-159.41	168.5
4.5	1.7	12.99	12.56	-4.18	-4.41	126.41	125.97	85.6	8.8	12.7	17 9 11.4	49.72	-159.42	133.4
5.1	49.0	-16.84	-23.15	-29.63	-30.29	173.10	121.06	-143.3	7.2	9.5	17 9 14.9	53.94	-159.92	354.3
5.2	41.4	-15.17	-20.58	-30.04	-29.48	156.93	115.29	-130.7	7.4	10.0	17 9 18.4	53.06	-159.39	354.7
5.3	30.5	-10.90	-12.15	-24.84	-25.96	141.84	118.85	-137.5	7.6	10.7	17 9 21.7	52.05	-158.86	355.5
5.4	16.0	2.23	2.35	-14.11	-13.91	126.92	120.66	-136.3	8.1	11.5	17 9 24.4	50.95	-158.40	357.3
5.5	1.1	13.19	13.05	-3.69	-4.18	123.44	125.91	123.1	8.6	12.5	17 9 26.6	49.90	-158.00	98.9
6.1	47.8	-17.93	-22.53	-32.71	-32.05	159.02	100.47	46.5	9.3	14.7	17 9 30.1	45.99	-157.02	172.5
6.2	41.6	-15.23	-19.92	-29.69	-29.77	151.31	107.60	47.3	9.4	14.3	17 9 33.7	46.74	-156.82	172.7
6.3	31.3	-12.13	-13.36	-26.93	-27.61	136.74	112.70	49.8	9.2	13.8	17 9 36.9	47.75	-156.67	172.2
6.4	17.3	0.57	0.12	-15.13	-15.34	124.79	118.04	51.8	9.0	13.0	17 9 39.7	48.85	-156.59	171.2
6.5	1.7	13.01	12.93	-4.04	-4.55	122.44	122.97	89.9	9.5	12.2	17 9 41.8	49.93	-156.54	135.1
7.1	49.1	-17.65	-24.45	-30.55	-30.81	161.94	102.32	-140.9	8.3	9.5	17 9 45.4	54.16	-156.74	356.8
7.2	41.4	-16.03	-20.17	-29.44	-29.77	150.23	108.14	-135.1	8.8	9.9	17 9 48.9	53.27	-156.27	357.1
7.3	30.4	-13.97	-14.09	-28.42	-28.42	139.32	115.35	-132.8	7.2	10.5	17 9 52.2	52.23	-155.82	357.8
7.4	15.9	2.11	1.70	-13.43	-13.98	125.99	120.76	-132.8	7.7	11.2	17 9 54.9	51.14	-155.42	359.8
7.5	1.1	12.98	13.11	-3.96	-4.49	120.84	122.94	122.7	8.4	12.0	17 9 57.1	50.07	-155.09	104.3
8.1	47.9	-18.04	-22.91	-30.96	-31.78	159.67	104.67	49.0	8.8	14.2	17 10 0.6	46.12	-154.35	175.0
8.2	41.7	-15.44	-18.99	-30.00	-29.73	149.96	107.71	49.1	9.0	13.9	17 10 4.2	46.88	-154.10	174.9
8.3	31.4	-13.31	-13.73	-28.20	-28.88	134.80	113.34	51.3	9.1	13.4	17 10 7.4	47.88	-153.91	174.7
8.4	17.3	0.43	-1.10	-15.39	-15.52	125.27	119.47	54.9	9.0	12.8	17 10 10.1	48.98	-153.75	173.1
8.5	1.7	13.15	13.00	-3.90	-4.11	122.96	122.93	93.5	8.6	12.0	17 10 12.3	50.06	-153.63	136.4

09/05/75

A 10

REPRODUCIBILITY OF THE
ORIGINAL PAGE IS POOR

00Y 216-1, 8/ 4/73 CTNC-L/R, NORTH PACIFIC

SCAN NUMB	INCID ANGLE (DEG)	SCATTERING COEFFICIENTS				ANTENNA V (DEG)	TEMPS H (DEG)	ASPECT ANGLE (DEG)	WIND SPEED (M/S)	SEA TEMP (DEG)	GMT			CELL COORDINATES		S193 DATA AZIMTH FLAG (DEG)
		VV (DB)	HH (DB)	VM (DB)	HV (DB)						HR	MIN	SEC	LAT (DEG)	LONG (DEG)	
9.1	49.0	-24.40	-28.44	-35.66	-34.53	159.86	100.14	-133.1	6.1	9.4	17	10	15.9	54.29	-153.56	359.1 -2
9.2	41.4	-18.81	-21.72	-31.09	-32.09	148.93	107.25	-128.4	6.9	9.8	17	10	19.4	53.39	-153.14	359.4
9.3	30.5	-12.56	-13.82	-27.26	-27.27	138.73	116.79	-127.2	8.0	10.5	17	10	22.7	52.35	-152.76	0.2
9.4	16.0	2.17	1.77	-14.11	-13.71	126.61	113.28	-123.6	8.6	11.2	17	10	25.4	51.25	-152.44	1.6
9.5	1.1	13.26	13.15	-4.11	-4.41	125.26	125.76	134.9	9.2	11.8	17	10	27.6	50.17	-152.18	97.1
10.1	47.9	-20.18	-24.07	-32.51	-33.25	160.04	100.78	44.8	7.9	14.0	17	10	31.1	46.20	-151.66	177.2
10.2	41.7	-15.51	-18.61	-29.40	-30.84	150.07	106.74	50.8	8.2	13.5	17	10	34.7	46.94	-151.33	177.2
10.3	31.4	-13.64	-13.61	-28.17	-28.38	136.82	112.67	53.1	8.8	13.0	17	10	37.9	47.94	-151.12	176.9
10.4	17.4	0.04	0.07	-15.12	-15.43	123.62	115.75	56.3	9.5	12.2	17	10	40.7	49.43	-150.90	175.7
10.5	1.8	12.77	12.97	-4.05	-4.58	123.94	122.38	94.5	9.8	11.8	17	10	42.8	50.11	-150.71	139.5
11.1	49.0	-20.92	-24.91	-31.80	-31.56	160.75	100.92	-122.3	7.4	9.4	17	10	46.4	54.33	-150.35	1.3
11.2	41.4	-17.97	-20.52	-31.13	-30.78	149.29	108.54	-120.7	9.0	9.9	17	10	49.9	53.42	-150.00	1.7
11.3	30.4	-11.83	-12.92	-25.84	-26.24	138.40	115.37	-122.5	10.5	10.8	17	10	53.2	52.37	-149.69	2.5
11.4	15.9	2.35	2.17	-14.10	-13.60	125.44	121.25	-125.4	10.8	11.2	17	10	55.9	51.26	-149.44	4.4
11.5	1.0	13.05	12.87	-4.15	-4.74	121.90	121.42	133.0	10.8	11.7	17	10	58.1	50.18	-149.26	103.3
12.1	47.9	-19.62	-20.67	-30.76	-29.08	158.05	102.26	49.3	6.4	13.4	17	11	1.6	46.19	-148.97	179.7
12.2	41.7	-15.70	-19.17	-30.33	-30.37	150.10	125.69	51.3	6.9	13.0	17	11	5.1	46.93	-148.65	179.7
12.3	31.5	-12.64	-14.12	-27.80	-27.37	135.55	110.87	52.6	8.4	12.6	17	11	8.4	47.92	-148.33	179.4
12.4	17.3	0.74	0.27	-14.92	-15.10	124.38	117.55	57.1	9.9	12.0	17	11	11.1	49.81	-148.05	177.9
12.5	1.7	12.74	12.44	-4.26	-4.58	121.52	122.57	93.3	11.2	11.6	17	11	13.3	50.04	-147.80	143.7
13.1	49.0	-20.67	-24.46	-31.25	-31.71	160.13	102.76	-118.7	8.9	10.1	17	11	16.9	54.29	-147.13	3.7
13.2	41.5	-16.59	-19.40	-28.69	-28.93	149.30	108.49	-118.0	11.4	10.3	17	11	20.4	53.37	-146.86	4.0
13.3	30.5	-11.07	-12.19	-24.88	-25.18	137.69	117.75	-122.0	11.9	10.7	17	11	23.7	52.31	-146.62	5.0
13.4	15.9	2.16	1.80	-14.35	-13.43	128.65	122.85	-125.7	12.3	11.1	17	11	26.4	51.20	-146.45	6.7
13.5	1.0	12.80	12.51	-4.58	-4.70	119.81	122.92	128.4	11.7	11.5	17	11	28.6	50.11	-146.34	109.6
14.1	48.0	-17.56	-19.11	-28.83	-29.21	159.61	101.17	56.1	5.9	13.0	17	11	32.1	46.12	-146.28	181.9
14.2	41.7	-15.26	-17.80	-28.41	-28.48	149.79	105.28	55.0	7.1	12.7	17	11	35.7	46.86	-145.93	182.0
14.3	31.4	-10.74	-12.31	-24.74	-25.37	134.83	113.25	53.4	8.8	12.4	17	11	38.9	47.84	-145.55	181.6
14.4	17.3	1.07	0.79	-14.42	-14.90	127.60	119.17	56.4	10.5	12.0	17	11	41.7	48.91	-145.21	180.6
14.5	1.7	12.55	12.23	-4.66	-5.10	121.32	124.41	89.9	11.8	11.5	17	11	43.8	49.97	-144.89	149.1
15.1	49.1	-19.41	-23.67	-30.81	-30.62	162.28	105.35	-124.0	8.2	10.7	17	11	47.4	54.17	-143.92	6.0
15.2	41.4							-125.0	10.2	10.7	17	11	50.7	53.23	-143.76	6.0
15.3																
15.4																
15.5																

JSC - 2/ 9/75

S. TRUTH - 6/ 1/75

LAST MOD - 8/28/75

THIS LISTING - 09/05/75

All

DOY 216-2. 8/ 4/73 ITNC, NORTH PACIFIC

SCAN NUM	INCID ANGLE (DEG)	SCATTERING COEFFICIENTS				ANTENNA V (DEG)	TEMPS H (DEG)	ASPECT ANGLE (DEG)	WIND SPEED (M/S)	SEA TEMP (DEG)	GHT			CELL COORDINATES		S193 DATA AZIMTH FLAG (DEG)
		VV (DB)	HH (DB)	VH (DB)	HV (DB)						HR	MIN	SEC	LAT (DEG)	LONG (DEG)	
1.1	50.8					162.87	101.35	164.8	10.8	12.6	17	12	6.6	49.24	-136.15	99.2
1.2	44.4					152.46	105.54	161.8	10.6	12.0	17	12	10.1	49.35	-137.07	99.2
1.3	32.6					137.57	113.76	158.0	11.4	11.7	17	12	13.3	49.52	-136.59	99.0
1.4	17.6					125.86	118.08	151.9	10.8	11.4	17	12	15.9	49.67	-140.14	100.1
1.5																
2.1	50.8	-15.48	-22.61	-30.68	-30.80	162.37	102.26	169.6	9.0	13.4	17	12	21.4	49.05	-134.79	100.4
2.2	44.3	-12.96	-17.21	-27.02	-26.44	153.23	107.25	164.7	9.7	13.0	17	12	24.9	49.17	-135.73	100.3
2.3	32.7	-7.37	-9.26	-22.11	-21.99	138.98	113.57	159.6	10.6	12.0	17	12	28.2	49.35	-137.19	100.4
2.4	17.6	3.31	3.47	-13.43	-12.96	127.14	113.34	155.8	11.3	11.7	17	12	30.9	49.52	-138.73	101.2
2.5	1.7	12.66	12.48	-4.99	-4.34	124.23	123.21	122.4	10.8	11.4	17	12	33.1	49.66	-140.18	129.6
3.1	50.8	-16.92	-24.21	-31.96	-32.12	164.93	104.72	179.6	7.6	14.0	17	12	36.7	48.84	-133.40	101.4
3.2	44.4	-14.21	-19.10	-28.91	-28.28	152.83	106.75	171.6	8.5	13.8	17	12	40.2	48.97	-134.32	101.4
3.3	32.7	-8.09	-9.93	-22.95	-22.66	140.37	113.85	163.7	9.8	13.0	17	12	43.4	49.17	-135.79	101.3
3.4	17.7	3.64	3.82	-12.80	-12.51	128.49	119.64	157.4	10.7	12.0	17	12	46.2	49.35	-137.31	102.6
3.5	1.6	12.39	12.73	-4.78	-4.64	124.70	122.64	124.0	11.3	11.7	17	12	48.4	49.51	-138.76	133.0
4.1	51.8	-19.47	-24.89	-32.85	-32.02	164.16	103.31	-167.5	6.8	14.2	17	12	51.9	48.57	-131.83	102.5
4.2	44.4	-15.27	-20.19	-30.36	-29.45	154.00	109.36	-177.5	7.3	14.1	17	12	55.4	48.75	-132.94	102.5
4.3	32.7	-9.94	-12.18	-24.94	-24.69	137.64	112.64	169.6	8.5	13.8	17	12	58.7	48.97	-134.39	102.4
4.4	17.5	3.46	3.36	-13.20	-12.88	127.96	120.15	161.4	9.8	13.0	17	13	1.4	49.17	-135.91	103.6
4.5	1.7	12.03	12.21	-5.18	-4.59	127.02	121.89	123.8	10.7	12.0	17	13	3.6	49.34	-137.34	136.2
5.1	50.9	-19.07	-23.54	-32.87	-32.57	162.58	100.59	-157.6	6.5	14.2	17	13	7.2	48.35	-130.65	103.5
5.2	44.3	-17.56	-21.12	-31.04	-31.09	152.13	104.33	-166.5	6.7	14.2	17	13	10.7	48.51	-131.57	103.5
5.3	32.7	-11.40	-13.33	-26.26	-26.15	138.82	115.36	-179.5	7.4	14.1	17	13	13.9	48.74	-133.01	103.5
5.4	17.7	2.50	2.70	-14.18	-13.90	127.52	119.66	167.3	8.6	13.9	17	13	16.7	48.97	-134.50	104.7
5.5	1.7	12.22	12.44	-4.81	-4.73	125.79	125.29	129.3	9.8	13.0	17	13	18.9	49.16	-135.93	135.7
6.1	51.0	-17.09	-22.68	-30.57	-31.00	161.27	100.17	-149.7	6.5	14.1	17	13	22.4	48.08	-129.30	104.7
6.2	44.4	-15.81	-21.28	-30.67	-30.41	152.07	105.20	-155.6	6.5	14.2	17	13	25.9	48.25	-130.21	104.6
6.3	32.8	-13.18	-14.46	-27.43	-27.45	136.38	110.69	-167.7	6.7	14.2	17	13	29.2	48.50	-131.62	104.7
6.4	17.6	2.13	2.48	-14.84	-14.28	128.94	119.05	177.4	7.4	14.1	17	13	31.9	48.75	-133.12	105.6
6.5	1.6	12.34	13.23	-4.24	-3.87	123.78	121.18	142.0	8.6	13.8	17	13	34.1	48.96	-134.54	130.0
7.1	50.9	-16.24	-19.70	-29.29	-29.24	161.84	99.08	-142.7	6.6	13.7	17	13	37.7	47.79	-127.99	105.7
7.2	44.3	-15.33	-18.96	-28.46	-28.71	151.27	103.79	-147.7	6.5	14.1	17	13	41.2	47.98	-128.88	105.7
7.3	32.7	-11.48	-13.81	-26.97	-26.69	137.19	112.05	-156.0	6.5	14.2	17	13	44.4	48.25	-130.28	105.8
7.4	17.6	1.91	2.29	-15.06	-14.74	124.80	117.44	-173.8	6.8	14.2	17	13	47.2	48.51	-131.75	106.8
7.5	1.7	13.02	13.27	-4.09	-3.67	123.01	125.02	145.8	7.5	14.1	17	13	49.4	48.74	-133.15	137.2
8.1	50.9	-16.34	-20.75	-29.76	-30.12	163.50	101.61	-139.8	7.1	12.5	17	13	52.9	47.49	-126.66	106.8
8.2	44.3	-14.29	-19.38	-29.17	-28.06	152.63	104.05	-141.8	6.7	13.0	17	13	56.4	47.68	-127.55	106.8
8.3	32.7	-11.94	-12.29	-25.15	-25.47	136.63	110.58	-148.8	6.5	14.1	17	13	59.7	47.97	-128.94	106.8
8.4	17.5	2.09	2.37	-13.85	-14.31	125.25	116.76	-153.5	6.5	14.2	17	14	2.4	48.25	-130.40	107.5
8.5	1.7	13.33	13.39	-4.02	-3.88	120.49	120.48	155.7	6.8	14.2	17	14	4.6	48.49	-131.78	139.3

09/05/75

DOY 216-2, 8/ 4/73 ITNC, NORTH PACIFIC

SCAN NUMB	INCID ANGLE (DEG)	SCATTERING COEFFICIENTS				ANTENNA V (DEG)	TEMPS H (DEG)	ASPECT ANGLE (DEG)	WIND SPEED (M/S)	SEA TEMP (DEG)	GMT (HR MIN SEC)	CELL COORDINATES		S193 DATA AZIMTH FLAG (DEG)
		VV (DB)	HH (DB)	VH (DB)	HV (DE)							LAT (DEG)	LONG (DEG)	
9.1	50.9	-17.15	-19.15	-29.52	-29.16	165.20	102.81	-136.7	7.5	11.0	17 14 8.2	47.18	-125.37	107.7
9.2	44.3	-14.28	-17.07	-26.87	-26.32	152.85	107.25	-138.8	7.2	11.5	17 14 11.7	47.38	-126.25	107.8
9.3	32.6	-10.08	-11.94	-25.37	-24.60	136.52	103.62	-143.9	6.7	13.0	17 14 14.9	47.68	-127.62	107.9
9.4	17.6	1.97	2.67	-13.65	-14.19	122.52	115.63	-152.0	6.5	14.1	17 14 17.7	47.97	-129.06	109.0
9.5	1.6	13.06	13.17	-4.32	-3.81	124.10	121.49	165.1	6.5	14.2	17 14 19.9	48.24	-130.43	142.9
10.1	50.9	-33.11	-25.65	-30.18	-33.09	180.00	109.76	-136.8	8.0	11.0	17 14 23.4	46.84	-124.09	108.8 2
10.2	44.3	-18.56	-19.58	-30.62	-29.21	153.41	106.65	-137.8	7.6	11.0	17 14 26.9	47.05	-124.96	108.8
10.3	32.6	-10.40	-11.55	-23.89	-23.98	138.58	112.28	-139.9	7.2	11.5	17 14 30.2	47.37	-126.31	108.9
10.4	17.6	2.59	2.95	-14.40	-13.73	124.32	116.93	-146.1	6.7	13.0	17 14 32.9	47.68	-127.74	110.1
10.5	1.7	12.88	13.26	-4.33	-3.96	121.56	113.36	171.7	6.5	14.1	17 14 35.1	47.95	-129.09	145.3
11.1	50.9	-11.00	-11.09	-17.10	-17.31	261.92	260.76	-136.8	8.3		17 14 38.7	46.49	-122.82	109.8 1
11.2	44.3	-9.21	-8.68	-15.26	-15.41	248.82	233.02	-137.8	8.2		17 14 42.2	46.71	-123.67	109.8 1
11.3														
11.4														
11.5														

JSC - 2/ 9/75

S. TRUTH - 6/ 1/75

LAST MOD - 5/28/75

THIS LISTING - 09/05/75

DOY 220-1, 8/ 8/73 CTNC-L/R, NORTH PACIFIC

SCAN NUMB	INCID ANGLE (DEG)	SCATTERING COEFFICIENTS				ANTENNA V (DEG)	TEMPS H (DEG)	ASPECT ANGLE (DEG)	WIND SPEED (M/S)	SEA TEMP (DEG)	GMT (HR MIN SEC)	CELL COORDINATES		S193 DATA AZIMTH FLAG (DEG)
		VV (DB)	HH (DB)	VH (DB)	HV (DB)							LAT (DEG)	LONG (DEG)	
1.1	48.7					159.78	101.52	-141.1	5.4	7.4	15 51 24.5	53.81	-155.52	353.1
1.2	41.2					153.51	113.77	-135.2	6.5	7.9	15 51 28.0	52.95	-154.98	353.2
1.3	30.1					133.02	112.63	-129.4	7.6	9.0	15 51 31.1	51.93	-154.46	353.4
1.4	15.6					123.66	118.29	-123.3	8.4	10.5	15 51 33.8	50.86	-153.99	353.3
1.5														
2.1	48.6	-18.72	-23.17	-29.69	-30.93	162.18	100.37	109.0	4.7	13.5	15 51 39.3	45.81	-162.58	173.0
2.2	42.3	-14.59	-18.35	-28.04	-28.31	152.20	106.87	94.6	5.4	13.0	15 51 42.8	46.59	-162.38	173.4
2.3	31.8	-10.27	-12.01	-23.67	-24.22	141.40	118.29	80.5	6.7	12.3	15 51 46.0	47.63	-162.26	173.5
2.4	17.6	-0.75	-1.39	-16.10	-16.74	135.14	129.90	71.4	7.5	11.8	15 51 48.8	49.75	-162.19	173.6
2.5	1.6	13.01	12.75	-3.72	-4.44	122.46	122.43	70.2	8.0	11.2	15 51 51.0	49.84	-152.14	166.8
3.1	48.9	-25.40	-25.38	-35.47	-36.32	166.93	113.75	-141.2	6.1	7.4	15 51 54.5	54.07	-162.43	355.2
3.2	41.2	-17.53	-22.07	-32.14	-32.19	152.42	113.17	-135.5	6.9	8.0	15 51 58.0	53.19	-161.93	355.5
3.3	30.1	-11.78	-13.95	-26.70	-26.85	134.76	113.85	-138.8	7.6	9.0	15 52 1.3	52.15	-161.46	355.8
3.4	15.6	3.49	3.87	-12.90	-13.35	126.12	123.34	-124.0	8.0	10.1	15 52 4.9	51.07	-161.06	356.0
3.5	0.6	12.92	12.59	-4.61	-4.60	127.20	126.64	73.9	7.7	11.0	15 52 6.2	50.00	-160.71	164.1
4.1	48.6	-25.38	-28.47	-35.60	-35.89	160.39	99.11	114.7	3.6	13.5	15 52 9.8	45.98	-159.90	175.3
4.2	42.3	-18.01	-21.33	-31.16	-31.60	152.54	107.67	95.4	4.2	12.9	15 52 13.3	46.75	-159.68	175.6
4.3	31.8	-12.31	-13.40	-25.79	-27.29	139.82	114.39	81.2	5.4	12.2	15 52 16.5	47.79	-159.50	175.8
4.4	17.6	-3.75	-1.25	-15.94	-16.28	134.12	123.32	73.8	6.6	11.7	15 52 19.3	49.91	-159.35	176.2
4.5	1.6	13.98	12.64	-3.86	-4.69	130.63	131.34	69.6	7.4	11.0	15 52 21.5	50.00	-159.25	171.4
5.1	48.9	-26.73	-33.24	-35.58	-37.11	158.77	100.62	-140.8	6.7	8.0	15 52 25.3	54.24	-159.24	357.2
5.2	41.2	-23.01	-24.33	-34.04	-35.14	148.98	105.26	-138.9	7.3	8.5	15 52 28.5	53.33	-158.81	357.9
5.3	30.2	-14.35	-15.72	-30.42	-30.78	135.74	112.75	-131.0	7.6	9.5	15 52 31.8	52.29	-158.42	358.0
5.4	15.6	3.19	2.96	-13.25	-12.99	125.12	119.97	-122.8	7.6	10.0	15 52 34.5	51.20	-158.63	357.8
5.5	0.5	13.62	13.25	-3.41	-3.93	119.57	121.01	81.2	7.3	11.8	15 52 36.7	50.13	-157.80	161.8
6.1	48.6	-34.39	-36.16	-35.13	-35.90	160.58	90.27	106.4	2.5	13.5	15 52 40.3	46.08	-157.23	177.6
6.2	42.3	-25.21	-34.57	-35.95	-40.22	149.33	101.45	91.0	3.2	12.9	15 52 43.8	46.85	-156.96	178.0
6.3	31.8	-14.00	-15.62	-29.76	-29.43	136.65	111.02	79.7	4.5	12.3	15 52 47.0	47.39	-156.71	178.3
6.4	17.7	-1.00	-1.69	-16.51	-16.74	126.38	119.54	72.3	6.0	11.3	15 52 49.8	49.00	-156.51	178.7
6.5	1.7	13.37	12.75	-3.93	-4.37	123.21	123.19	70.7	7.3	10.7	15 52 52.0	50.08	-156.34	176.3
7.1	48.9	-23.38	-29.54	-35.46	-34.13	156.66	97.95	-133.9	7.0	8.7	15 52 55.5	54.32	-156.04	359.9
7.2	41.3	-21.02	-25.48	-33.30	-36.30	145.40	104.23	-133.1	7.3	9.2	15 52 59.0	53.41	-155.68	0.1
7.3	30.2	-13.32	-13.52	-27.69	-28.04	134.56	114.69	-124.4	7.7	9.5	15 53 2.3	52.35	-155.35	0.4
7.4	15.7	3.02	2.40	-13.44	-13.95	123.86	117.58	-114.5	8.4	10.0	15 53 5.0	51.25	-155.69	360.1
7.5	0.5	13.68	13.49	-3.29	-3.79	121.01	121.11	83.2	7.7	10.5	15 53 7.2	50.17	-154.88	161.8
8.1	48.6	-30.14	-33.04	-35.15	-35.89	159.16	95.99	79.4	1.8	13.5	15 53 10.8	46.12	-154.54	179.6
8.2	42.2	-27.89	-39.67	-37.42	-40.03	150.18	101.81	71.8	2.6	13.4	15 53 14.3	46.88	-154.23	180.2
8.3	31.9	-20.97	-22.36	-34.76	-37.26	134.92	108.72	67.3	4.0	12.0	15 53 17.5	47.89	-153.93	180.7
8.4	17.7	-1.62	-2.29	-16.62	-17.44	126.66	117.13	58.3	5.9	11.0	15 53 20.3	49.00	-153.66	180.7
8.5	1.6	13.44	13.30	-3.41	-3.93	120.55	120.54	71.7	7.4	10.5	15 53 22.5	50.09	-153.43	172.3

09/05/73

DOY 220-1, 8/ 8/73 CTNC-LAR, NORTH PACIFIC

SCAN NUMB	INCID ANGLE (DEG)	SCATTERING COEFFICIENTS				ANTENNA V (DEG)	TEMPS H (DEG)	ASPECT ANGLE (DEG)	WIND SPEED (M/S)	SEA TEMP (DEG)	GMT (HR MIN SEC)	CELL COORDINATES		S193 DATA AZIMUTH FLAG (DEG)
		VV (DB)	HH (DB)	VH (DB)	HV (DB)							LAT (DEG)	LONG (DEG)	
9.1	48.9	-22.36	-28.45	-34.59	-34.13	157.85	99.17	-118.3	8.5	9.3	15 53 29.0	54.33	-152.83	2.3
9.2	41.3	-18.55	-22.44	-31.65	-32.75	147.81	107.15	-112.6	7.7	9.4	15 53 23.5	53.39	-152.53	2.6
9.3	30.2	-12.20	-13.65	-26.85	-27.17	133.55	114.22	-112.7	7.7	9.6	15 53 32.8	52.33	-152.27	2.7
9.4	15.7	3.14	2.42	-13.63	-14.04	126.07	123.43	-109.7	9.6	9.8	15 53 35.5	51.21	-152.13	2.7
9.5	0.6	13.55	13.36	-3.47	-3.80	125.48	127.48	68.8	8.3	10.5	15 53 37.7	50.12	-151.96	181.2
10.1	48.5	-26.76	-31.40	-36.61	-35.90	161.88	130.64	44.7	2.1	13.5	15 53 41.3	46.68	-151.86	182.3
10.2	42.2	-31.91	-31.63	-37.43	-37.63	150.90	103.04	43.3	2.8	13.8	15 53 44.8	45.83	-151.51	182.7
10.3	31.8	-20.48	-20.56	-35.84	-33.90	145.16	120.99	52.8	3.9	12.1	15 53 48.0	47.84	-151.15	183.2
10.4	17.6	-3.10	-3.64	-18.18	-18.62	129.73	122.87	57.8	5.6	11.1	15 53 50.8	48.93	-150.82	183.2
10.5	1.5	13.44	13.43	-3.29	-4.15	124.57	126.60	67.6	7.7	10.6	15 53 53.0	50.31	-150.51	181.4
11.1	49.0	-20.60	-25.67	-32.67	-31.20	159.03	101.36	-112.6	7.5	9.8	15 53 56.5	54.22	-149.63	4.6
11.2	41.3	-22.36	-25.70	-34.91	-35.02	146.08	104.92	-112.8	7.1	9.8	15 54 0.0	53.28	-149.40	4.8
11.3	30.2	-15.05	-14.55	-29.22	-29.78	136.08	116.27	-115.2	6.6	10.0	15 54 3.3	52.21	-149.22	5.2
11.4	15.7	2.70	2.13	-13.63	-13.57	130.25	123.35	-115.0	7.7	10.5	15 54 6.0	51.15	-149.11	5.0
11.5	0.4	13.67	13.61	-3.20	-3.73	127.11	124.50	74.3	7.3	10.6	15 54 8.2	50.51	-149.05	172.7
12.1	48.5	-30.73	-33.05	-35.15	-35.90	160.65	97.85	40.4	2.6	14.0	15 54 11.8	45.96	-149.19	184.6
12.2	42.2	-35.23	-34.88	-39.67	-36.10	148.36	93.50	45.0	2.9	13.5	15 54 15.3	46.71	-149.79	185.0
12.3	31.8	-24.07	-28.46	-43.89	-43.89	135.05	110.43	50.0	3.8	13.0	15 54 18.5	47.70	-148.38	185.0
12.4	17.6	-3.31	-3.95	-13.63	-13.18	122.63	115.32	54.6	4.9	12.0	15 54 21.3	48.79	-147.98	185.4
12.5	1.6	13.96	13.75	-3.06	-3.80	120.72	121.74	60.2	6.4	11.5	15 54 23.5	43.85	-147.61	184.8
13.1	48.9	-19.32	-24.81	-32.01	-31.91	159.86	100.67	-112.8	7.4	10.5	15 54 27.0	54.02	-146.43	6.8
13.2	41.3	-20.36	-24.24	-33.95	-32.14	145.43	105.81	-113.0	7.1	11.0	15 54 30.5	53.59	-146.29	7.0
13.3	30.2	-14.03	-13.96	-28.50	-29.22	136.77	113.30	-112.1	6.6	11.1	15 54 33.8	52.62	-146.19	7.1
13.4	15.8	2.34	1.90	-14.27	-13.76	123.58	117.36	-120.3	6.2	11.5	15 54 36.5	50.91	-146.16	7.3
13.5	0.4	14.38	14.10	-2.58	-3.00	121.63	121.64	53.9	5.6	11.8	15 54 38.7	49.82	-146.16	183.1

JSC - 2/ 9/75

S. TRUTH - 6/ 1/75

LAST MOD - 8/28/75

THIS LISTING - 09/15/75

DOY 220-2, 8/ 8/73 ITNC, NORTH PACIFIC

SCAN NUMB	INCID ANGLE (DEG)	SCATTERING COEFFICIENTS				ANTENNA V (DEG)	TEMPS Y (DEG)	ASPECT ANGLE (DEG)	WIND SPEED (M/S)	SEA TEMP (DEG)	GMT			CELL COORDINATES		S193 AZIMTH (DEG)	DATA FLAG
		VV (DB)	HH (DB)	VH (DB)	HV (DB)						(HR MIN SEC)			LAT (DEG)	LONG (DEG)		
1.1	49.6					156.44	94.06	-121.4	5.3	14.1	15 54 54.2			48.83	-133.36	101.4	
1.2	43.1					145.23	97.24	-130.5	4.3	13.9	15 54 57.7			49.06	-139.25	101.5	
1.3	31.6					131.44	106.49	-157.4	3.3	13.7	15 55 0.8			49.20	-140.66	101.4	
1.4	16.5					120.11	112.27	-168.7	3.3	13.4	15 55 3.5			49.39	-142.16	102.3	
1.5																	
2.1	49.7	-23.35	-26.79	-35.44	-35.79	158.31	97.44	-114.5	7.2	14.4	15 55 9.0			48.66	-137.02	102.5	
2.2	43.2	-21.27	-23.41	-33.50	-33.56	148.29	102.63	-119.6	5.9	14.3	15 55 12.5			48.72	-137.89	102.6	
2.3	31.5	-15.61	-15.61	-31.18	-30.50	133.54	103.33	-131.6	4.2	13.9	15 55 15.7			49.01	-139.30	102.6	
2.4	16.5	-1.63	-0.58	-16.85	-16.52	120.96	111.54	-162.9	3.2	13.7	15 55 18.5			49.22	-140.78	103.9	
2.5	0.9	17.79	17.56	2.77	3.53	119.33	119.35	92.9	3.4	13.4	15 55 20.7			49.39	-142.22	177.1	-2
3.1	49.7	-24.46	-29.01		-33.42	159.99	97.57	-113.6	7.6	14.8	15 55 24.0			48.41	-135.65	103.6	
3.2	43.2	-19.65	-22.27	-31.82	-31.10	150.74	104.55	-113.6	7.9	14.6	15 55 27.7			48.56	-136.52	103.6	
3.3	31.5	-13.86	-14.02	-29.15	-28.54	134.12	110.20	-123.6	5.9	14.3	15 55 31.9			48.79	-137.92	103.6	
3.4	16.5	1.18	1.76	-14.39	-14.03	122.35	115.08	-136.3	4.2	13.9	15 55 33.7			49.01	-139.38	105.0	
3.5	0.9	14.98	15.10	-2.08	-1.66	118.11	119.73	121.7	3.2	13.7	15 55 35.9			49.21	-140.80	179.3	
4.1	49.6	-37.04	-29.01		-44.54	160.33	97.36	-115.8	6.8	15.2	15 55 39.3			48.15	-134.33	104.8	-2
4.2	43.1	-22.96	-28.16	-39.12	-34.99	148.53	101.80	-119.7	7.3	14.9	15 55 43.0			48.31	-135.18	104.7	-2
4.3	31.5	-13.53	-13.52	-27.78	-27.83	136.04	114.16	-114.9	7.9	14.6	15 55 46.2			48.56	-136.54	104.9	
4.4	16.5	1.69	2.05	-14.05	-14.42	124.50	116.15	-122.8	5.8	14.3	15 55 49.0			48.80	-138.00	105.8	
4.5	0.9	13.42	13.68	-3.77	-3.11	119.94	119.42	144.1	4.1	13.9	15 55 51.2			49.01	-139.41	134.9	
5.1	49.7	-27.52	-23.55	-37.92	-33.45	159.37	95.84	-123.8	6.4	15.0	15 55 54.7			47.85	-132.97	105.8	
5.2	43.2	-31.57	-29.81	-38.93	-39.44	149.33	101.51	-118.7	6.6	15.7	15 55 58.2			48.04	-133.82	105.7	-2
5.3	31.6	-16.97	-21.41	-35.06	-31.57	133.77	111.36	-116.9	7.3	14.9	15 56 1.5			48.30	-135.17	105.9	
5.4	16.5	1.78	2.23	-14.73	-14.32	123.59	119.41	-116.9	7.9	14.6	15 56 4.2			48.56	-136.62	106.9	
5.5	0.9	13.26	13.18	-4.32	-3.64	120.47	121.00	162.5	5.7	14.3	15 56 6.4			48.79	-138.01	180.5	
6.1	49.7	-26.65	-27.93		-36.14	159.64	97.53	-135.8	6.1	16.7	15 56 9.8			47.57	-131.67	106.8	
6.2	43.2	-22.96	-22.24	-32.34	-31.87	148.76	101.40	-128.9	6.2	16.2	15 56 13.5			47.75	-132.49	106.9	
6.3	31.5	-10.27	-29.19	-39.24	-39.50	134.60	110.64	-118.0	6.6	15.7	15 56 16.7			48.04	-133.83	106.8	-2
6.4	16.5	0.05	-0.49	-16.23	-15.23	123.65	117.37	-119.7	7.3	14.9	15 56 19.5			48.31	-135.26	108.0	
6.5	0.8	12.88	12.11	-4.47	-3.97	121.95	123.55	-179.4	7.8	14.6	15 56 21.7			48.56	-136.64	169.4	
7.1	49.7	-24.21	-32.81	-37.98	-37.62	160.87	97.76	-142.9	5.9	17.0	15 56 25.2			47.26	-130.34	107.9	
7.2	43.2	-23.07	-26.31	-34.87	-37.27	149.94	102.16	-139.3	6.0	16.9	15 56 28.7			47.45	-131.18	107.8	
7.3	31.5	-15.93	-16.21	-31.73	-25.42	134.51	110.49	-130.1	6.2	16.2	15 56 32.0			47.75	-132.51	109.1	
7.4	16.5	-13.25	-15.09	-29.71	-27.95	122.68	115.98	-120.8	6.6	15.7	15 56 34.7			48.04	-133.92	103.9	-2
7.5	0.8	14.45	14.82	-2.09	-2.22	119.20	121.40	172.6	7.3	14.9	15 56 36.9			48.31	-135.29	176.4	
8.1	49.7	-19.31	-25.49	-33.46	-33.47	159.30	98.24	-148.8	5.8	17.0	15 56 40.4			46.93	-129.05	108.8	
8.2	43.1	-20.79	-24.88	-36.00	-36.15	150.25	102.46	-145.0	5.9	16.9	15 56 44.0			47.14	-129.88	109.8	
8.3	31.5	-14.52	-15.13	-39.21	-30.49	134.42	109.89	-140.0	5.2	16.9	15 56 47.2			47.44	-131.19	109.0	
8.4	16.5	1.13	1.48	-15.96	-15.30	122.45	117.19	-130.9	5.2	16.2	15 56 50.6			47.75	-132.58	109.9	
8.5	0.8	17.78	17.55	3.16	3.48	121.90	121.43	187.8	5.6	16.7	15 56 52.2			48.04	-133.94	180.2	-2

REPRODUCIBILITY OF THE
ORIGINAL PAGE IS POOR

DOY 220-2, 8/ 8/73 ITNC, NORTH PACIFIC

SCAN NUMB	INCID ANGLE (DEG)	VV (DB)	SCATTERING HH (DB)	COEFFICIENTS VH (DB)	HV (DB)	ANTENNA V (DEG)	TEMPS H (DEG)	ASPECT ANGLE (DEG)	WIND SPEED (M/S)	SEA TEMP (DEG)	GMT (HR MIN SEC)	CELL COORDINATES LAT (DEG)	LONG (DEG)	S193 AZIMTH (DEG)	DATA FLAG
9.1	49.7	-19.56	-25.47	-32.35	-33.15	162.23	100.13	-145.8	5.3	15.4	15 56 55.7	46.58	-127.78	109.8	
9.2	43.3	-17.90	-21.43	-30.74	-31.50	150.02	103.67	-148.8	5.6	16.2	15 56 59.2	46.79	-128.58	109.8	
9.3	31.6	-13.48	-14.18	-28.95	-29.44	135.09	111.57	-147.0	5.9	16.9	15 57 2.5	47.12	-129.89	110.0	
9.4	16.5	1.59	2.12	-14.09	-14.86	122.82	116.52	-142.0	6.0	16.9	15 57 5.2	47.45	-131.27	111.0	
9.5	0.8	13.75	14.02	-3.24	-2.96	121.70	121.24	170.6	6.2	16.2	15 57 7.4	47.75	-132.60	168.4	
10.1	49.8	-22.19	-29.12		-32.93	162.85	102.25	-139.7	4.7	13.3	15 57 10.8	46.22	-126.53	110.7	
10.2	43.2	-17.31	-21.47	-31.07	-31.16	150.59	106.28	-144.7	5.0	14.0	15 57 14.5	46.44	-127.33	110.7	
10.3	31.5	-12.05	-12.70	-26.50	-26.39	136.67	113.66	-149.9	5.6		15 57 17.7	46.79	-128.61	110.9	
10.4	16.5	2.27	2.37	-14.96	-13.46	124.90	118.09	-148.5	5.9		15 57 20.5	47.13	-129.97	111.5	
10.5	0.8	13.19	13.67	-4.05	-3.35	122.13	120.59	152.5	6.0		15 57 22.7	47.44	-131.23	177.5	
11.1	49.7	-25.04	-21.03	-31.96	-32.12	163.20	102.06	-130.7	4.3	12.0	15 57 26.2	45.85	-125.33	111.7	
11.2	43.0	-20.70	-24.96	-35.88	-34.20	152.70	106.85	-137.7	4.6	12.9	15 57 29.7	46.08	-126.10	111.7	
11.3	31.5	-11.84	-12.91	-26.51	-26.51	137.45	113.92	-145.8	5.1		15 57 33.0	46.44	-127.35	111.8	
11.4	16.4	2.42	2.60	-14.54	-13.72	125.70	119.34	-151.7	5.6		15 57 35.7	46.80	-128.75	112.7	
11.5	0.9	13.30	13.31	-4.26	-3.72	121.42	121.98	147.6	5.9		15 57 37.9	47.12	-129.99	175.4	
12.1	49.6	-42.60	-32.64	-34.36	-39.46	172.91	105.15	-128.7	4.0	11.0	15 57 41.4	45.47	-124.09	112.7	2
12.2	43.1	-26.24	-22.44	-34.13	-35.10	152.70	105.29	-127.6	4.1	11.0	15 57 45.0	45.70	-124.86	112.6	
12.3	31.5	-14.24	-14.89	-29.94	-24.70	138.83	112.66	-138.9	4.5		15 57 48.2	46.07	-126.10	112.9	
12.4	16.5	2.21	2.41	-14.44	-13.97	125.91	119.62	-147.9	5.1		15 57 51.0	46.44	-127.43	113.9	
12.5	0.8	12.82	12.59	-4.64	-4.05	121.18	122.27	133.3	5.6		15 57 53.2	46.79	-128.72	187.7	
13.1	49.6	-12.18	-11.30	-17.86	-18.43	264.37	256.50	-129.6	3.7		15 57 56.7	45.06	-122.88	113.6	1
13.2	43.2	-9.14	-9.26	-15.94	-15.99	258.71	246.72	-127.7	3.9		15 58 0.2	45.30	-123.64	113.7	1
13.3	31.5	-24.12	-21.98	-32.97	-32.49	138.66	113.90	-138.7	4.1		15 58 3.5	45.69	-124.87	113.7	2
13.4	16.5	1.72	2.21	-14.86	-13.64	127.76	118.32	-140.7	4.6		15 58 6.2	46.07	-126.16	114.7	
13.5	0.8	12.88	12.83	-4.57	-4.27	123.70	124.71	150.9	5.1		15 58 8.4	46.43	-127.44	175.1	
14.1	49.8	-12.50	-12.18	-17.63	-17.53	266.83	265.13	-130.5	3.4		15 58 12.0	44.63	-121.68	114.5	1
14.2	43.1	-10.32	-9.95	-16.03	-16.55	265.96	264.26	-130.7	3.0		15 58 15.5	44.89	-122.46	114.7	1
14.3	31.6	-7.43	-7.04	-14.27	-14.31	259.13	253.65	-130.7	3.9		15 58 18.7	45.29	-123.66	114.7	1
14.4	16.5	-4.58	-5.19	-20.22	-20.33	127.68	117.69	-133.6	4.2		15 58 21.5	45.59	-124.95	115.6	1
14.5	0.9	13.59	13.51	-3.86	-3.73	124.68	122.15	146.8	4.6		15 58 23.7	46.06	-126.20	188.0	
15.1	49.6	-12.72	-12.12	-18.75	-18.76	268.80	262.51	-129.4	2.8		15 58 27.2	44.21	-120.54	115.4	1
15.2	43.1	-11.34	-11.06	-18.34	-17.38	269.38	266.67	-131.4	3.2		15 58 30.7	44.47	-121.29	115.4	1
15.3	31.4	-8.51	-8.14	-14.54	-14.77	266.14	265.42	-131.7	3.6		15 58 34.0	44.88	-122.48	115.7	1
15.4	16.4	-6.41	-6.08	-14.28	-13.74	255.18	257.65	-132.8	3.9		15 58 36.7	45.30	-123.75	115.8	1
15.5	0.9	16.71	17.18	0.84	1.02	123.96	122.50	149.5	4.2		15 58 38.9	45.63	-124.98	195.5	1

JSC - 2/ 9/75

S. TRUTH - 6/ 1/75

LAST MOD - 8/28/75

THIS LISTING - 09/05/75

DOY 220-3, 8/ 8/73 ITNC, GULF OF MEXICO (VERT POL)

SCAN NUMB	INCID ANGLE (DEG)	SCATTERING COEFFICIENTS				ANTENNA V (DEG)	TEMPS H (DEG)	ASPECT ANGLE (DEG)	WIND SPEED (M/S)	SEA TEMP (DEG)	GMT (HR MIN SEC)	CELL COORDINATES		S193 AZIMTH (DEG)	DATA FLAG
		VV (DB)	HH (DB)	VH (DB)	HV (DB)							LAT (DEG)	LONG (DEG)		
1.1	49.7					280.50		49.9	7.6		16 4 55.0	29.82	-96.47	132.1	1
1.2	43.2					281.79		55.7	8.2		16 4 58.4	30.21	-96.98	132.3	1
1.3	31.5					282.08		58.4	8.4		16 5 1.4	30.85	-97.80	132.6	1
1.4	16.3					280.99		57.0	8.1		16 5 3.9	31.51	-98.68	134.0	1
1.5															
2.1	49.7	-10.56				276.27		36.5	6.5		16 5 8.6	29.23	-95.79	132.5	1
2.2	43.1	-10.47				275.85		45.3	7.3		16 5 12.1	29.63	-96.29	132.7	1
2.3	31.4	-9.32				280.79		53.8	8.2		16 5 15.5	30.24	-97.09	133.2	1
2.4	16.5	-7.99				280.12		56.6	8.4		16 5 18.3	30.89	-97.92	134.4	1
2.5	0.8	2.50				282.24		-17.5	8.1		16 5 20.6	31.51	-98.73	208.5	1
3.1	49.5	-16.85				187.47		15.0	5.2		16 5 23.8	29.57	-95.05	133.0	
3.2	42.9	-8.97				268.21		27.8	6.0		16 5 27.4	29.97	-95.55	133.2	1
3.3	31.4	-9.21				272.95		44.5	7.3		16 5 30.7	29.59	-96.31	133.5	1
3.4	16.5	-8.39				278.83		52.2	8.2		16 5 33.6	30.24	-97.13	134.9	1
3.5	0.9	3.81				282.69		-20.3	8.4		16 5 35.8	30.36	-97.94	211.3	1
4.1	49.6	-16.21				197.52		-5.4	5.1		16 5 39.1	27.89	-94.30	133.4	
4.2	43.0	-18.90				170.96		3.5	4.9		16 5 42.6	28.30	-94.79	133.5	
4.3	31.4	-7.71				266.43		25.9	5.9		16 5 46.0	28.92	-95.55	134.1	1
4.4	15.5	-7.31				279.99		41.6	7.3		16 5 48.8	29.57	-96.35	135.4	1
4.5	0.8	7.64				279.70		-11.7	8.2		16 5 51.1	30.20	-97.14	200.3	1
5.1	49.5	-24.23				169.72		-17.8	6.2		16 5 54.3	27.22	-93.57	133.8	
5.2	43.0	-19.79				159.54		-11.9	5.5		16 5 57.9	27.62	-94.04	133.9	
5.3	31.5	-14.80				157.12		1.8	5.8		16 6 1.2	28.25	-94.79	134.2	
5.4	16.5	-6.50				267.51		24.1	6.0		16 6 4.1	28.91	-95.60	135.9	1
5.5	0.9	11.38				271.14		-29.3	7.3		16 6 5.4	29.53	-96.33	205.3	1
6.1	49.6	-23.15				167.22		-17.1	7.8		16 6 9.6	28.54	-92.84	134.1	1
6.2	43.0	-20.06				157.47		-19.4	6.8		16 6 13.1	28.94	-93.32	134.4	
6.3	31.4	-13.55				146.84		-12.7	5.6		16 6 16.5	27.57	-94.06	134.7	
6.4	16.4	1.44				143.61		0.2	5.0		16 6 19.3	28.24	-94.84	135.8	
6.5	1.0	2.32				255.47		-49.3	6.0		16 6 21.6	28.86	-95.62	207.3	1
7.1	49.6	-24.19				166.41		-15.5	9.1		16 6 24.8	28.85	-92.12	134.5	
7.2	43.0	-21.39				156.25		-16.8	8.5		16 6 28.4	28.25	-92.59	134.8	
7.3	31.4	-14.13				144.59		-19.3	6.9		16 6 31.7	28.89	-93.33	135.3	
7.4	16.4	1.69				133.21		-14.6	5.6		16 6 34.6	27.56	-94.11	136.6	
7.5	0.7	13.66				141.40		-69.4	5.1		16 6 36.9	28.20	-94.85	205.4	
8.1	49.7	-22.03				165.61		-17.8	8.7		16 6 40.1	28.15	-91.40	134.8	
8.2	43.0	-21.36				156.29		-15.0	9.1		16 6 43.7	28.57	-91.88	135.0	
8.3	31.4	-14.42				143.82		-17.4	8.6		16 6 47.0	28.21	-92.63	135.4	
8.4	16.5	1.86				131.52		-29.7	6.9		16 6 49.8	28.08	-93.37	136.7	
8.5	0.8	13.78				132.04		-82.5	5.7		16 6 52.1	27.52	-94.12	203.5	

09/05/75

DOY 220-3, 8/ 8/73 ITNC, GULF OF MEXICO (VERT POL)

SCAN NUMB	INCID ANGLE (DEG)	SCATTERING COEFFICIENTS				ANTENNA V (DEG)	TEMPS H (DEG)	ASPECT ANGLE (DEG)	WIND SPEED (M/S)	SEA TEMP (DEG)	GMT (HR MIN SEC)	CELL COORDINATES		S193 AZINTH (DEG)	DATA FLAG
		VV (DB)	HH (DB)	VH (DB)	HV (DB)							LAT (DEG)	LONG (DEG)		
9.1	49.7	-21.11				166.98		-23.2	7.8		16 6 56.8	24.39	-90.63	135.2	
9.2	43.0	-19.01				155.54		-20.4	8.4		16 6 58.9	24.87	-91.17	135.4	
9.3	31.4	-14.08				142.56		-17.9	9.1		16 7 2.2	25.52	-91.89	135.9	
9.4	16.4	1.56				131.61		-18.9	8.6		16 7 5.1	26.20	-92.65	136.9	
9.5	0.8	14.08				130.43		-93.1	7.1		16 7 7.3	26.84	-93.43	215.1	
10.1	49.6	-21.50				165.75		-26.6	7.4		16 7 10.6	23.76	-90.02	135.6	
10.2	43.1	-19.17				155.58		-24.8	7.7		16 7 14.1	24.16	-90.47	135.8	
10.3	31.4	-13.45				141.32		-21.3	8.4		16 7 17.5	24.82	-91.19	136.3	
10.4	16.5	1.32				132.12		-19.8	9.0		16 7 21.3	25.50	-91.94	137.8	

JSC - 2/16/75

S. TRUTH - 6/ 1/75

LAST MOD - 8/28/75

THIS LISTING - 09/05/75

DOY 220-4, 8/ 8/73 CTNC-L, GULF OF MEXICO (HOR POL)

SCAN NUMB	INCID ANGLE (DEG)	SCATTERING COEFFICIENTS				ANTENNA V (DEG)	TEMPS M (DEG)	ASPECT ANGLE (DEG)	WIND SPEED (M/S)	SEA TEMP (DEG)	GMT (HR MIN SEC)	CELL COORDINATES		S193 AZIMTH (DEG)	DATA FLAG
		VV (DB)	HH (DB)	VH (DB)	HV (DB)							LAT (DEG)	LONG (DEG)		
1.1	48.9						110.87	44.0	3.1		16 7 42.0	28.11	-88.45	46.0	
1.2	41.3						115.33	53.1	4.1		16 7 45.4	27.34	-89.85	45.9	
1.3	30.4						124.73	63.2	6.1		16 7 46.5	26.50	-89.74	45.8	
1.4	15.8						124.06	67.8	7.6		16 7 51.0	25.62	-90.50	46.2	
1.5															
2.1	49.0		-32.21				110.24	38.8	3.7		16 7 55.6	27.49	-87.83	46.2	
2.2	41.3		-28.78				115.14	48.8	4.7		16 7 59.2	26.71	-88.41	46.2	
2.3	30.3		-21.82				122.42	58.8	6.0		16 8 2.5	25.84	-89.10	46.2	
2.4	15.9		1.33				120.84	63.6	7.2		16 8 5.4	24.97	-89.84	46.6	
2.5	0.2		13.96				130.52	-84.8	7.7		16 8 7.7	24.13	-90.56	195.8	
3.1	49.0		-17.52				121.02	33.5	4.2		16 8 10.9	26.77	-87.14	46.5	-2
3.2	41.3		-24.97				114.48	44.7	4.9		16 8 14.5	26.00	-87.73	46.3	
3.3	30.5		-16.82				122.63	53.8	6.0		16 8 17.8	25.15	-88.41	46.2	
3.4	15.9		0.68				126.22	58.8	6.9		16 8 20.6	24.27	-89.15	46.2	
3.5	0.3		13.73				124.99	-106.5	7.2		16 8 22.9	23.42	-88.89	214.5	
4.1	49.0		-29.45				111.05	31.2	4.4		16 8 20.1	26.25	-86.46	46.8	
4.2	41.3		-20.79				117.21	40.3	5.1		16 8 29.7	25.28	-87.85	46.7	
4.3	30.4		-15.58				121.55	49.5	6.0		16 8 33.0	24.43	-87.73	46.5	
4.4	15.9		1.30				128.88	55.4	6.5		16 8 35.9	23.55	-88.47	46.6	
4.5	0.3		13.63				129.67	-79.6	6.5		16 8 38.2	22.71	-39.20	185.6	
5.1	49.0		-29.13				111.58	27.7	4.6		16 8 41.4	25.32	-85.78	47.3	
5.2	41.3		-23.28				115.15	37.1	5.3		16 8 45.0	24.55	-86.30	46.9	
5.3	30.4		-18.58				122.63	45.0	5.7		16 8 48.3	23.71	-87.06	47.0	
5.4	15.9		1.18				127.53	50.8	6.0		16 8 51.1	22.84	-87.79	47.2	
5.5	0.2		14.19				131.59	-85.5	5.8		16 8 53.4	22.01	-88.52	189.5	
6.1	49.1		-28.85				113.15	25.6	4.8		16 8 56.6	24.61	-85.11	47.4	
6.2	41.4		-22.79				117.19	32.7	5.1		16 9 0.2	23.84	-85.70	47.3	
6.3	30.5		-17.13				122.84	40.7	5.4		16 9 3.5	22.99	-86.38	47.3	
6.4	16.0		0.08				126.44	49.0	5.4		16 9 6.4	22.13	-87.13	47.0	
6.5	0.2		-1.21				268.32	-88.7	5.1		16 9 8.6	21.30	-87.86	190.7	1
7.1	49.1		-30.76				112.58	22.4	4.8		16 9 11.9	23.88	-84.45	47.6	
7.2	41.4		-23.10				116.54	29.5	4.9		16 9 15.5	23.11	-85.05	47.5	
7.3															
7.4															
7.5															

JSC - 2/15/75

S. TRUTH - 6/ 1/75

LAST MOD - 8/28/75

THIS LISTING - 09/05/75

DOY 245-2, 9/ 2/73 CTNC-L, TROPICAL STORM CHRISTINE (VERSION H3)

SCAN NUM3	INCID ANGLE (DEG)	SCATTERING COEFFICIENTS				ANTENNA V (DEG)	TEMPS H (DEG)	ASPECT ANGLE (DEG)	WIND SPEED (M/S)	SEA TEMP (DEG)	GMT			CELL COORDINATES		S193 DATA	DATA
		VV (DB)	HH (DB)	VH (DB)	HV (DB)						(HR MIN SEC)			LAT (DEG)	LONG (DEG)	AZIMTH (DEG)	FLAG
1.1	49.5					274.35	266.83	98.5	1.5	28.0	17 54 15.7	9.77	-64.51	311.5	1		
1.2	41.9					274.92	261.84	78.3	1.5	28.0	17 54 19.2	9.36	-63.71	311.7	1		
1.3	30.9					263.07	249.59	52.0	1.5	28.0	17 54 22.3	8.84	-62.81	312.0	1		
1.4	16.5					267.94	266.56	9.8	1.0	28.0	17 54 25.0	8.29	-61.89	313.2	1		
1.5																	
2.1	49.6	-12.72	-9.71	-17.13	-20.08	225.18	175.11	123.3	2.6	28.0	17 54 30.5	10.51	-63.96	311.7	1		
2.2	42.0	-5.85	-6.24	-12.93	-12.95	269.73	261.76	115.2	2.1	28.0	17 54 34.0	10.10	-63.15	311.8	1		
2.3	31.0	-4.92	-5.18	-12.07	-12.13	266.23	261.19	99.0	1.0	28.0	17 54 37.2	9.59	-62.24	312.0	1		
2.4	16.6	-3.41	-3.41	-11.35	-11.42	257.47	255.82	48.6	0.5	28.0	17 54 40.0	9.03	-61.33	313.4	1		
2.5	0.9	13.19	12.42	-4.49	-3.84	264.83	257.82	115.0	0.5	28.0	17 54 42.2	8.46	-60.45	8.0	1		
3.1	49.6	-32.53	-33.79	-37.23	-38.89	173.16	108.04	132.2	3.6	28.0	17 54 45.7	11.27	-63.40	311.8	2		
3.2	42.1	-21.92	-11.87	-21.66	-33.04	173.81	115.61	130.1	3.1	28.0	17 54 49.2	10.86	-62.58	311.9	1		
3.3	31.0	-15.97	-16.90	-29.69	-30.44	147.35	126.34	131.7	2.1	28.0	17 54 52.5	10.35	-61.67	312.3	1		
3.4	16.6	-0.34	-3.89	-16.38	-16.25	133.33	120.10	149.0	1.0	29.0	17 54 55.2	9.78	-60.75	313.0			
3.5	0.8	14.16	13.58	-3.16	-3.54	130.35	131.36	163.4	1.0	28.0	17 54 57.4	9.21	-59.87	5.6			
4.1	49.6	-27.29	-25.46	-35.04	-36.86	175.53	111.49	117.1	5.1	28.0	17 55 1.0	12.02	-62.82	311.9			
4.2	42.0	-28.16	-29.56	-36.08	-41.92	159.25	115.36	119.0	3.6	28.0	17 55 4.5	11.61	-61.99	312.0			
4.3	31.0	-17.74	-18.02	-33.27	-37.01	143.09	120.53	132.6	2.6	28.0	17 55 7.7	11.19	-61.09	312.4			
4.4	16.5	0.84	0.60	-14.75	-15.38	133.39	127.60	161.8	1.5	28.0	17 55 10.5	10.54	-60.16	313.2			
4.5	0.9		13.22	-3.94	-4.17	129.86	131.36	143.0	1.5	28.0	17 55 12.7	9.97	-59.29	8.0			
5.1	49.6	-28.91	-34.11	-37.98	-38.88	169.84	105.85	95.9	6.2	28.0	17 55 15.2	12.78	-62.23	312.1			
5.2	42.1	-24.56	-25.63	-33.76	-28.63	160.12	120.32	91.3	4.6	28.0	17 55 19.7	12.37	-61.41	312.0			
5.3	31.1	-23.82	-19.77	-35.24	-45.82	145.62	118.88	93.6	2.6	28.0	17 55 23.0	11.86	-60.50	312.4			
5.4	16.6	0.15	-0.11	-15.41	-15.93	132.72	123.52	170.2	1.5	28.0	17 55 25.7	11.29	-59.58	313.8			
5.5	0.9	13.06	12.92	-4.11	-4.15	139.25	131.76	146.6	2.1	28.0	17 55 27.9	10.72	-58.70	4.4			
6.1	49.6	-23.93	-28.83	-36.26	-34.43	171.98	108.94	76.1	7.2	28.0	17 55 31.5	13.53	-61.65	311.9			
6.2	42.1	-24.48	-28.38	-37.94	-31.50	158.47	113.36	62.7	5.7	28.0	17 55 35.0	13.13	-60.82	312.3			
6.3	31.1	-18.78	-19.78	-35.25	-35.25	143.21	118.57	62.5	3.6	28.0	17 55 38.2	12.61	-59.91	312.5			
6.4	16.6	-0.75	-1.22	-15.38	-16.45	131.13	125.35	155.7	1.0	28.0	17 55 41.0	12.74	-58.98	313.7			
6.5	0.8	14.02	14.33	-3.05	-3.54	126.65	129.23	165.1	2.6	28.0	17 55 43.2	11.46	-58.11	358.9			
7.1	49.6	-21.27	-24.03	-33.04	-33.59	173.11	111.11	57.7	9.3	28.0	17 55 46.7	14.29	-61.06	312.3			
7.2	42.0	-18.10	-21.92	-34.90	-32.27	158.39	113.49	47.7	7.7	28.0	17 55 50.2	13.67	-60.23	312.3			
7.3	31.1	-12.93	-14.81	-29.03	-28.47	143.03	113.96	9.3	4.6	28.0	17 55 53.5	13.37	-59.32	312.7			
7.4	16.6	0.39	-0.38	-15.53	-15.74	132.32	127.58	93.9	2.1	28.0	17 55 56.2	12.79	-58.39	313.9			
7.5	0.9		13.55	-3.45	-3.66	128.17	129.15	163.2	4.6	28.0	17 55 58.4	12.22	-57.51	9.3			
8.1	49.7	-17.89	-23.09	-31.09	-29.77	171.79	109.50	51.6	12.4	28.0	17 56 2.0	15.05	-60.47	312.4			
8.2	42.1	-15.12	-17.54	-27.82	-29.58	155.65	120.20	22.8	11.8	28.0	17 56 5.5	14.63	-59.64	312.2			
8.3	31.1	-12.37	-13.49	-23.51	-28.01	144.40	120.28	22.5	7.2	28.0	17 56 8.7	14.10	-58.73	312.5			
8.4	16.6	0.69	0.26	-15.05	-15.38	131.35	127.14	107.4	5.1	28.0	17 56 11.5	13.53	-57.80	313.4			
8.5	0.9	12.91	13.22	-4.62	-4.89	129.66	131.70	168.6	7.7	29.0	17 56 13.7	12.96	-56.92	1.4			

09/05/75

DOY 245-2, 9/ 2/73 CTNC-L. TROPICAL STORM CHRISTINE (VERSION H3)

SCAN NUMB	INCID ANGLE (DEG)	SCATTERING COEFFICIENTS				ANTENNA V (DEG)	TEMPS H (DEG)	ASPECT ANGLE (DEG)	WIND SPEED (M/S)	SEA TEMP (DEG)	GMT			CELL COORDINATES		S193 AZIMTH (DEG)	DATA FLAG
		VV (DB)	HH (DB)	VH (DB)	HV (DB)						(HR MIN SEC)			LAT (DEG)	LONG (DEG)		
9.1	49.6	-17.94	-21.37	-28.32	-29.46	174.51	115.52	64.6	17.0	28.0	17 56 17.2	15.80	-59.88	312.4			
9.2	42.1	-13.61	-16.39	-26.03	-26.36	163.96	122.59	42.5	14.9	28.0	17 56 20.7	15.38	-59.04	312.5			
9.3	31.1	-10.13	-11.33	-24.46	-24.35	149.34	128.32	-92.9	9.3	28.0	17 56 24.1	14.86	-58.13	312.9			
9.4	16.6	1.61	1.17	-14.16	-14.33	134.38	131.16	-141.1	11.3	28.0	17 56 26.7	14.28	-57.19	314.1			
9.5	0.8	12.79	12.62	-4.48	-4.63	131.30	133.85	150.8	10.8	28.0	17 56 28.9	13.70	-56.31	6.0			
10.1	49.7	-15.22	-19.26	-25.80	-25.48	175.11	118.20	86.4	20.1	28.0	17 56 32.5	16.55	-59.28	312.6			
10.2	42.1	-11.27	-13.36	-21.19	-21.35	166.36	127.40	134.1	23.2	28.0	17 56 36.0	15.14	-58.44	312.9			
10.3	31.0	-7.95	-8.64	-21.08	-21.38	199.10	199.13	-169.2	20.6	28.0	17 56 39.2	15.61	-57.52	313.2			
10.4	16.6	1.81	2.60	-14.02	-14.30	159.94	163.10	-172.1	16.5	28.0	17 56 42.9	15.03	-56.58	314.1			
10.5	0.9		12.25	-4.65	-4.73	134.40	131.29	130.8	13.9	28.0	17 56 44.2	14.45	-55.70	6.0			
11.1	49.7	-14.33	-16.65	-25.84	-26.11	176.41	119.98	137.3	19.0	28.0	17 56 47.7	17.30	-58.68	312.7			
11.2	42.1	-11.03	-13.35	-21.83	-21.56	164.66	124.29	128.0	22.1	28.0	17 56 51.2	16.88	-57.83	313.0			
11.3	31.1	-4.25	-5.73	-16.31	-16.06	165.76	146.69	152.7	20.6	28.0	17 56 54.5	16.35	-56.91	313.3			
11.4	16.6	2.51	0.50	-13.48	-13.25	189.50	135.69	163.6	17.0	28.0	17 56 57.2	15.77	-55.98	314.4			
11.5	0.9	12.04	12.01	-5.04	-5.40	134.88	135.35	113.6	14.4	28.0	17 56 59.4	15.19	-55.09	1.4			
12.1	49.7	-13.31	-16.05	-24.82	-25.63	184.92	127.92	120.1	17.0	28.0	17 57 3.0	18.05	-58.07	312.9			
12.2	42.1	-10.43	-12.95	-21.77	-22.96	176.41	128.35	131.9	17.5	28.0	17 57 6.5	17.63	-57.22	313.1			
12.3	31.1	-7.06	-6.85	-18.14	-18.92	224.57	212.49	145.7	17.5	28.0	17 57 9.8	17.10	-56.30	313.3			
12.4	16.6	1.85	1.50	-13.47	-14.13	160.74	164.19	154.3	15.4	28.0	17 57 12.5	16.52	-55.35	314.7			
12.5	0.9	12.05	11.85	-4.58	-5.03	133.11	133.60	112.2	13.9	28.0	17 57 14.7	15.93	-54.48	0.8			
13.1	49.7	-13.89	-19.41	-26.33	-26.86	172.82	111.84	126.9	14.4	28.0	17 57 18.2	18.80	-57.46	313.1			
13.2	42.1	-11.37	-11.87	-22.78	-23.11	207.50	145.53	135.8	14.9	28.0	17 57 21.7	18.37	-56.61	313.2			
13.3	31.1	-6.46	-8.63	-20.40	-20.84	157.47	132.22	144.5	14.4	28.0	17 57 25.0	17.84	-55.68	313.5			
13.4	16.7	1.82	0.88	-14.03	-14.27	161.75	144.31	150.1	13.4	28.0	17 57 27.7	17.26	-54.74	314.9			
13.5	0.9		13.09	-4.23	-4.70	132.71	132.66	102.4	12.9	28.0	17 57 29.9	16.67	-53.85	6.6			
14.1	49.7	-15.47	-22.13	-28.89	-28.41	171.16	109.68	132.8	12.4	28.0	17 57 33.5	19.54	-56.84	313.2			
14.2	42.2	-12.21	-14.57	-24.51	-25.33	167.44	119.43	138.5	12.9	28.0	17 57 37.0	19.12	-55.99	313.5			
14.3	31.1	-7.64	-9.61	-21.97	-22.41	146.38	122.77	145.2	12.4	28.0	17 57 40.2	18.59	-55.06	313.8			
14.4	16.7	2.05	1.59	-13.91	-14.13	138.55	130.60	149.9	12.4	28.0	17 57 43.9	17.89	-54.12	315.1			
14.5	1.0	12.90	13.18	-3.77	-4.55	129.21	129.71	112.1	11.3	28.0	17 57 45.2	17.40	-53.23	4.9			
15.1	49.8	-16.74	-22.43	-29.33	-29.16	170.87	107.82	136.5	10.8	28.0	17 57 48.7	20.30	-56.22	313.5			
15.2	42.1	-14.31	-18.44	-27.41	-27.89	160.24	115.85	142.4	10.8	28.0	17 57 52.2	19.85	-55.35	313.6			
15.3	31.2	-10.12	-11.86	-24.55	-24.88	144.94	122.38	146.9	10.8	28.0	17 57 55.5	19.33	-54.43	314.1			
15.4	16.7	-0.27	0.09	-14.19	-14.77	174.26	163.53	150.2	10.8	28.0	17 57 58.2	18.72	-53.49	314.8			
15.5	1.0	13.12	12.97	-4.27	-4.11	127.87	128.39	107.2	10.3	28.0	17 58 0.4	18.14	-52.59	359.8			
16.1	49.8	-17.33	-23.88	-31.53	-30.42	169.62	105.54	140.3	9.3	28.0	17 58 4.0	21.24	-55.60	313.7			
16.2	42.2	-16.08	-20.56	-29.87	-29.92	158.24	111.85	144.2	9.3	28.0	17 58 7.5	20.63	-54.74	313.8			
16.3	31.2	-11.17	-13.15	-26.10	-25.95	145.10	120.45	148.9	9.3	28.0	17 58 10.7	20.05	-53.80	314.1			
16.4	16.8	1.50	1.09	-14.36	-14.79	132.67	125.86	150.5	9.3	28.0	17 58 13.5	19.46	-52.85	315.5			
16.5	1.0		12.80	-4.54	-4.36	127.85	128.31	130.1	9.3	28.0	17 58 15.7	18.87	-51.95	7.9			

09/05/75

DOY 245-2, 9/ 2/73 CTNC-L, TROPICAL STORM CHRISTINE (VERSION H3)

SCAN NUMB	INCID ANGLE (DEG)	SCATTERING COEFFICIENTS				ANTENNA V (DEG)	TEMPS H (DEG)	ASPECT ANGLE (DEG)	WIND SPEED (M/S)	SEA TEMP (DEG)	GMT			CELL COORDINATES		S193 DATA AZIMTH FLAG (DEG)
		VV (DB)	HH (DB)	VH (DB)	HV (DB)						HR	MIN	SEC	LAT (DEG)	LONG (DEG)	
17.1	49.9	-17.94	-21.04	-31.52	-31.72	172.20	107.65	143.0	7.7	28.0	17	58	19.2	21.79	-54.96	314.0
17.2	42.1	-19.23	-24.11	-32.85	-31.03	156.82	111.93	149.0	7.7	28.0	17	58	22.7	21.33	-54.09	314.0
17.3	31.2	-13.03	-13.83	-27.56	-29.11	140.36	118.86	151.5	7.7	28.0	17	58	26.0	20.79	-53.16	314.5
17.4	16.7	1.50	1.23	-14.44	-14.65	133.09	126.22	153.3	7.7	28.0	17	58	29.7	24.19	-52.21	315.7
17.5	1.0	13.24	13.29	-4.09	-4.33	124.12	127.19	157.1	7.7	28.0	17	58	30.9	19.59	-51.31	2.9
18.1	49.8	-21.25	-28.24	-33.01	-33.57	169.29	103.65	146.9	6.2	28.0	17	58	34.5	22.51	-54.31	314.1
18.2	42.2	-19.23	-23.83	-33.75	-33.85	156.50	110.04	150.7	6.2	28.0	17	58	38.0	22.07	-53.45	314.3
18.3	31.2	-14.04	-15.04	-29.66	-29.32	140.99	117.37	154.2	6.2	28.0	17	58	41.2	21.52	-52.51	314.8
18.4	16.7	1.33	1.83	-14.49	-15.12	129.17	122.26	155.2	6.7	28.0	17	58	44.0	20.92	-51.56	315.8
18.5																
19.1	49.9	-26.69	-33.35	-40.88	-36.88	170.15	103.55	150.7	4.6	28.0	17	58	49.7	23.26	-53.67	314.3
19.2	42.1	-21.91		-34.94				153.6	5.1	28.0	17	58	53.5	22.80	-52.79	314.4
19.3																
19.4	16.7	0.16	0.10	-15.43	-15.79	129.03	122.22	158.7	5.1	28.0	17	58	59.2	21.65	-50.90	316.3
19.5	3.9		13.48	-3.44	-3.82	127.76	127.75	74.9	5.1	28.0	17	59	1.4	21.17	-49.89	42.1
20.1	49.8	-30.37	-34.14	-38.00	-38.91	169.13	104.05	152.3	3.6	28.0	17	59	5.0	23.99	-53.01	314.7
20.2	42.2	-23.86	-27.49	-37.97	-38.25	156.49	109.04	155.2	3.6	28.0	17	59	8.5	23.53	-52.15	314.8
20.3	31.1	-16.29	-16.66	-31.95	-33.42	140.88	117.39	159.8	3.6	28.0	17	59	11.7	22.97	-51.20	315.2
20.4	16.7	0.05		-16.09				161.4	4.1	28.0	17	59	14.5	22.37	-50.23	316.6
20.5																
21.1	49.7	-29.81	-35.09	-40.89	-35.78	168.43	101.77				17	59	20.2	24.73	-52.33	315.4
21.2	42.1		-30.28								17	59	23.7	24.28	-51.43	316.2
21.3	31.1	-15.94	-16.41	-31.95	-33.41	140.95	116.32				17	59	27.0	23.81	-50.39	325.6
21.4	16.7	0.28	-0.15	-15.94	-16.39	129.40	122.59				17	59	29.7	23.16	-49.44	322.9
21.5																
22.1	43.9	-37.12	-39.58	-37.29	-38.94	167.77	102.71				17	59	35.5	25.17	-51.11	317.9
22.2	41.5		-41.36								17	59	39.2	25.99	-50.56	319.7
22.3	26.5	-20.31	-21.44			138.92	116.91				17	59	42.2	24.34	-49.37	323.2
22.4	16.2	-1.91	-2.86	-17.64	-18.02	127.41	122.72				17	59	45.0	23.94	-48.62	332.9
22.5	5.4		12.91	-4.43	-5.30	124.10	125.15				17	59	47.2	23.32	-47.70	53.3
23.1	48.5	-37.21	-40.97	-38.08	-42.91	165.36	102.86				17	59	50.7	26.31	-50.56	321.6
23.2																
23.3	30.0	-27.09									17	59	57.5	25.34	-48.72	328.5
23.4	15.4	-7.64	-7.84	-23.23	-23.71	125.34	123.79				18	0	0.2	24.73	-47.75	343.7
23.5	8.4	6.84	7.47	-3.52	-9.23	125.19	126.46				18	0	2.4	24.11	-46.83	56.8
24.1	47.9	-35.43	-39.67	-37.38	-38.12	162.44	108.12				18	0	6.0	27.10	-49.63	325.0
24.2	40.4										18	0	9.3	26.67	-48.78	327.8
24.3	30.0		-44.11			136.71	118.90				18	0	12.8	26.16	-47.82	334.7
24.4	17.2	-23.25	-20.01	-39.44		125.31	123.75				18	0	15.4	25.52	-46.85	353.6
24.5	11.3	-8.05	-9.42	-23.22	-24.13	122.96	125.21				18	0	17.7	24.89	-45.94	58.9

09/05/75

DOY 245-2, 9/ 2/73 CTNC-L, TROPICAL STORM CHRISTINE (VERSION M3)

SCAN NUMB	INCID ANGLE (DEG)	SCATTERING COEFFICIENTS				ANTENNA V (DEG)	TEMPS H (DEG)	ASPECT ANGLE (DEG)	WIND SPEED (M/S)	SEA TEMP (DEG)	GMT (HR MIN SEC)	CELL COORDINATES		S193 DATA AZIMTH FLAG (DEG)
		VV (DB)	HH (DB)	VH (DB)	HV (DB)							LAT (DEG)	LONG (DEG)	
25.1	47.5	-38.82		-41.01	-42.98	159.31	119.64				18 0 21.5	27.91	-48.68	329.7
25.2	40.3	-38.31			-38.96	148.52	116.82				18 0 25.0	27.50	-47.83	332.5
25.3	38.2	-44.36			-44.10	135.61	121.36				18 0 28.3	26.97	-46.89	341.2
25.4	18.6	-27.88	-30.64		-39.41	123.61	126.26				18 0 30.8	26.33	-45.96	2.6
25.5	14.1										18 0 32.8	25.66	-45.04	61.2
26.1	47.2	-34.51		-41.03	-38.16	160.33	119.24				18 0 36.7	29.71	-47.74	332.4
26.2	40.3	-27.60	-28.80	-38.32	-38.05	147.73	119.65				18 0 40.0	28.29	-46.91	337.1
26.3	30.6	-37.30	-33.32	-44.07		137.34	126.78				19 0 43.1	27.74	-46.00	346.6
26.4	21.2	-39.58	-36.36			122.42	124.20				18 0 46.0	27.18	-45.03	10.8
26.5	21.1		-29.48								18 0 48.2	26.65	-43.89	62.3
27.1	47.3	-36.68	-39.71	-37.40	-38.15	153.23	115.23				19 0 51.7	29.51	-48.80	336.1
27.2	40.6		-29.22								18 0 55.2	29.10	-45.98	341.6
27.3	31.5		-44.07			137.59	129.65				18 0 58.4	29.55	-45.06	352.6
27.4	22.1				-39.31						19 1 1.4	27.91	-44.09	17.0
27.5	20.0	-39.23									18 1 3.4	27.19	-43.18	63.3
28.1	47.5	-43.22	-53.09	-53.07	-42.97	150.22	115.91				18 1 7.0	31.32	-45.84	340.0
28.2	41.0	-41.61	-42.00		-38.71	141.69	122.81				18 1 10.6	29.90	-45.01	346.0
28.3	32.5					129.67	131.19				18 1 14.1	29.36	-44.08	357.7
28.4	24.3	-39.50				119.23	130.27				18 1 16.7	28.69	-43.13	22.7
28.5	22.8	-35.26	-37.34		-53.48	121.21	133.10				18 1 18.7	27.95	-42.22	64.4
29.1	48.1	-38.35	-38.11	-40.97	-53.03	146.87	129.73				18 1 22.2	31.15	-44.87	343.8
29.2	41.9	-41.56	-41.34	-41.31	-37.96	138.35	127.62				18 1 25.7	30.72	-44.04	350.3
29.3	33.9	-44.21	-43.95	-43.93	-43.97	126.40	132.30				18 1 29.0	30.15	-43.14	2.4
29.4	26.7										19 1 32.4	29.50	-42.13	27.6
29.5	26.0					120.07	134.54				19 1 34.1	28.72	-41.21	64.8
30.1	43.7	-36.58	-38.06	-36.34	-36.04	153.33	127.08				18 1 37.5	31.98	-43.89	347.3
30.2	42.8	-41.50	-41.26	-41.26	-37.89	139.30	133.01				18 1 41.0	31.53	-43.07	354.3
30.3	39.0	-36.03	-45.62			123.53	132.96				19 1 44.2	31.27	-41.82	7.3
30.4	28.9		-36.09			124.38	141.62				18 1 46.9	30.23	-41.18	31.8
30.5	29.0	-34.28	-34.12	-41.95	-41.56	114.68	139.60				18 1 49.2	29.46	-40.21	65.5
31.1	49.6			-42.83	-37.99	159.30	129.09				18 1 53.0	32.84	-42.87	350.3
31.2	44.1										18 1 56.0	32.35	-42.07	357.8
31.3														
31.4														
31.5														

JSC - 5/ 2/75

S. TRUTH - 7/17/75

LAST MOD - 8/23/75

THIS LISTING - 69/05/75

DOY 247-1, 9/ 4/73 CTNC-R, NORTH OF VENEZUELA

SCAN NUMB	INCID ANGLE (DEG)	SCATTERING COEFFICIENTS				ANTENNA V (DEG)	TEMPS H (DEG)	ASPECT ANGLE (DEG)	WIND SPEED (M/S)	SEA TEMP (DEG)	GMT			CELL COORDINATES		S193 AZIMTH (DEG)	DATA FLAG
		VV (DB)	HH (DB)	VH (DB)	HV (DB)						(HR	MIN	SEC)	LAT (DEG)	LONG (DEG)		
1.1	46.7					271.69	258.02				18	2	26.5	6.78	-71.09	129.9	1
1.2	40.7					272.29	266.83				18	2	35.0	7.38	-71.48	129.9	1
1.3	30.5					269.25	266.24				18	2	33.2	8.14	-72.05	129.4	1
1.4	16.6					272.06	270.61				18	2	35.8	8.94	-72.74	128.6	1
1.5																	
2.1	46.9	-8.53	-7.46	-14.37	-16.84	267.22	263.21				18	2	41.3	7.49	-70.51	129.8	1
2.2	40.8	-7.67	-7.56	-13.55	-13.41	275.71	271.69				18	2	44.8	8.11	-70.89	129.7	1
2.3	30.6	-6.26	-5.63	-12.97	-12.91	272.80	269.26				18	2	48.1	8.87	-71.48	129.6	1
2.4	16.6	-5.00	-4.33	-11.55	-12.01	261.59	259.15				18	2	50.8	9.67	-72.16	128.8	1
2.5	1.0	-3.05	-1.57	-11.60	-11.67	259.46	261.70				18	2	53.0	10.45	-72.86	88.5	1
3.1	46.9	-7.73	-8.12	-14.21	-13.95	274.36	268.84				18	2	56.6	8.24	-69.92	130.0	1
3.2	40.9	-6.63	-7.64	-14.66	-13.17	269.25	266.31				18	3	0.1	8.85	-70.29	130.0	1
3.3	30.7	-6.83	-6.66	-13.54	-14.20	270.27	265.58				18	3	3.3	9.62	-70.88	129.6	1
3.4	16.7	-1.99	-1.52	-17.36	-18.37	142.91	143.82				18	3	6.1	10.42	-71.57	128.9	1
3.5	1.0	5.23	1.86	-9.31	-8.97	269.68	268.77				18	3	8.3	11.19	-72.27	92.6	1
4.1	46.9	-7.38	-7.41	-13.76	-13.80	275.99	271.47				18	3	11.8	8.98	-69.33	130.2	1
4.2	40.8	-6.21	-6.38	-12.94	-13.38	269.81	265.34				18	3	15.3	9.59	-69.70	130.0	1
4.3	30.6	-8.00	-7.60	-13.93	-13.87	277.68	273.59				18	3	18.6	10.36	-70.29	129.5	1
4.4	16.7	-2.62	-3.62	-18.49	-19.69	171.23	156.23				18	3	21.3	11.17	-70.97	129.0	1
4.5	1.0	10.03	6.47	-7.48	-7.63	269.27	263.24				18	3	23.5	11.95	-71.67	91.7	1
5.1	46.9	-8.09	-8.43	-14.27	-14.00	277.63	269.03				18	3	27.0	9.72	-68.72	130.2	1
5.2	40.8	-7.09	-7.67	-13.40	-13.14	275.40	270.40				18	3	30.6	10.34	-69.11	130.2	1
5.3	30.8	-7.51	-6.96	-13.33	-14.32	273.81	268.70				18	3	33.6	11.10	-69.68	130.1	1
5.4	16.7	-11.29	-8.39	-22.71	-24.59	133.67	135.10				18	3	36.6	11.91	-70.33	129.3	1
5.5	1.0	15.32	15.02	-1.55	-2.23	130.23	130.16				18	3	38.8	12.69	-71.07	91.1	
6.1	47.1	-6.81	-6.15	-13.09	-14.20	269.15	217.76				18	3	42.3	10.44	-68.12	130.5	1
6.2	40.8	-7.57	-7.00	-13.43	-13.61	273.72	245.30				18	3	45.8	11.67	-68.51	130.4	1
6.3	30.7	-19.67	-20.93	-36.43	-35.73	144.95	122.28	-50.0	4.5	27.0	18	3	49.1	11.84	-69.89	130.0	
6.4	16.7	-2.34	-2.86	-17.77	-18.49	131.78	125.37	-49.2	4.1	27.0	18	3	51.8	12.65	-69.78	129.2	
6.5	1.0	15.12	14.90	-1.81	-2.33	125.76	124.24	-19.0	3.1	27.0	18	3	54.0	13.43	-70.47	98.0	
7.1	47.1	-28.06	-35.12	-37.47	-38.14	167.81	111.46	-30.7	5.1	27.0	18	3	57.5	11.18	-67.51	130.7	
7.2	40.8	-30.36	-33.39	-37.90	-38.14	156.83	113.87	-39.5	4.6	27.0	18	4	1.1	11.81	-67.90	130.5	
7.3	30.7	-18.08	-19.77	-36.43	-34.22	143.84	113.61	-40.2	4.1	27.0	18	4	4.3	12.58	-68.48	130.2	
7.4	16.7	-1.09	-1.29	-15.85	-17.32	130.38	125.59	-49.0	3.1	27.0	18	4	7.1	13.47	-69.16	129.0	
7.5	1.1	15.25	15.21	-1.47	-2.08	127.48	132.03	-15.8	2.6	27.0	18	4	9.3	14.18	-69.86	96.8	
8.1	47.1	-22.62	-26.30	-32.75	-30.80	167.90	111.73	-10.8	4.6	27.0	18	4	12.8	11.91	-66.90	130.8	
8.2	40.9	-22.63	-25.45	-36.10	-35.36	156.38	113.93	-20.7	4.1	27.0	18	4	16.3	12.55	-67.29	130.7	
8.3	30.8	-15.25	-17.27	-32.18	-32.75	142.93	119.23	-40.6	3.6	27.0	18	4	19.6	13.31	-67.86	130.6	
8.4	16.7	-2.71	-3.56	-18.67	-18.77	130.45	125.14	-49.7	3.1	27.0	18	4	22.3	14.13	-68.56	129.7	
8.5	1.1	15.69	15.29	-1.43	-1.55	126.70	124.72	-10.2	2.6	27.0	18	4	24.5	14.92	-69.25	90.2	

09/05/75

DOY 247-1, 9/ 4/73 CTNC-R, NORTH OF VENEZUELA

SCAN NUMB	INCID ANGLE (DEG)	SCATTERING COEFFICIENTS				ANTENNA V (DEG)	TEMPS H (DEG)	ASPECT ANGLE (DEG)	WIND SPEED (M/S)	SEA TEMP (DEG)	GMT			CELL COORDINATES		S193 AZIMTH (DEG)	DATA FLAG
		VV (DB)	HH (DB)	VH (DB)	HV (DB)						(HR	MIN	SEC)	LAT (DEG)	LONG (DEG)		
9.1	47.1	-21.54	-26.42	-33.98	-34.26	165.87	108.00	-1.1	5.1	27.0	18	4	28.0	12.64	-66.29	131.1	
9.2	40.9	-19.46	-22.39	-34.03	-34.21	156.40	113.97	-10.9	4.6	27.0	18	4	31.6	13.28	-66.67	130.9	
9.3	30.7	-15.08	-16.36	-31.67	-31.67	142.96	119.26	-40.5	4.1	27.0	18	4	34.8	14.05	-67.25	130.5	
9.4	16.7	-1.75	-2.11	-17.44	-17.83	130.57	124.22	-50.0	4.1	27.0	18	4	37.6	14.87	-67.94	130.0	
9.5	1.1	17.05	16.92	0.19	-6.38	128.07	129.57	-12.6	4.1	27.0	18	4	39.8	15.65	-68.63	92.6	
10.1	47.1	-21.83	-25.99	-36.12	-36.59	166.28	108.91	-1.1	5.7	27.0	18	4	43.3	13.38	-65.66	131.1	
10.2	40.9	-18.16	-21.23	-37.36	-32.71	157.41	113.45	-10.8	5.1	27.0	18	4	46.8	14.01	-66.06	130.8	
10.3	30.7	-13.93	-14.95	-30.06	-30.77	142.88	129.24	-20.9	4.6	27.0	18	4	50.1	14.79	-66.63	130.9	
10.4	16.7	-1.16	-1.14	-16.56	-17.27	132.79	125.95	-50.0	4.1	27.0	18	4	52.8	15.61	-67.32	130.0	
10.5	1.1	17.83	18.20	0.69	0.33	128.52	129.56	-18.6	4.6	27.0	18	4	55.0	16.39	-68.01	98.6	
11.1	47.1	-18.44	-22.30	-32.44	-32.63	167.66	109.29	8.7	6.2	27.0	18	4	58.5	14.10	-65.04	131.3	
11.2	40.9	-16.18	-19.69	-31.18	-30.44	160.22	118.29	8.9	6.2	27.0	18	5	2.1	14.73	-65.42	131.1	
11.3	30.7	-11.02	-12.89	-26.27	-26.27	147.72	125.06	-11.1	6.2	27.0	18	5	5.3	15.50	-66.01	131.1	
11.4	16.7	-0.64	-1.29	-16.09	-16.54	131.93	125.57	-33.9	6.7	27.0	18	5	8.1	16.34	-66.69	129.9	
11.5	1.0	14.44	14.53	-2.63	-3.79	129.46	130.99	-8.2	7.2	27.0	18	5	10.3	17.13	-67.39	88.2	
12.1	47.3																
12.2	40.9	-14.12		-28.18	-27.07	162.06	129.25	8.4	7.2	27.0	18	5	13.2	14.77	-64.42	131.6	
12.3	30.7	-12.72	-13.31	-27.23	-28.69	146.97	123.26	-11.7	8.2	27.0	18	5	17.5	15.47	-64.79	131.4	
12.4	16.7	0.93	0.47	-14.97	-15.37	133.67	127.92	-20.2	9.3	27.0	18	5	20.6	16.25	-65.38	131.0	
12.5	1.1	12.70	12.65	-4.32	-4.91	146.01	149.95	-11.8	10.8	27.0	18	5	25.5	17.07	-66.06	130.2	
13.1	47.2	-14.46	-19.17	-29.36	-28.34	170.90	124.24	8.2	8.8	27.0	18	5	29.0	15.54	-63.77	131.8	
13.2	40.9	-12.35	-15.55	-26.94	-25.22	172.14	154.74	-1.8	10.3	27.0	18	5	32.6	15.18	-64.17	131.8	
13.3	30.7	-14.30	-15.20	-30.06	-30.37	145.97	128.55	-11.5	11.8	27.0	18	5	35.8	16.97	-64.74	131.5	
13.4	16.7	1.67	1.24	-14.12	-14.60	134.42	130.14	-20.6	12.9	27.0	18	5	38.6	17.79	-65.43	130.6	
13.5	1.0	12.67	12.62	-4.16	-4.73	136.10	143.13	2.0	13.4	27.0	18	5	46.8	18.59	-66.12	88.2	
14.1	47.2	-13.35	-17.65	-27.91	-27.74	169.72	112.84	8.1	11.8	27.0	18	5	44.3	16.26	-63.14	131.9	
14.2	40.9	-14.52	-13.35	-26.61	-28.45	183.10	129.37	8.1	12.4	27.0	18	5	47.8	16.90	-63.53	131.9	
14.3	30.7	-7.42	-8.63	-22.82	-23.37	151.58	125.79	-11.6	13.4	27.0	18	5	51.1	17.69	-64.10	131.6	
14.4	16.7	1.14	1.03	-14.13	-14.48	140.05	132.08	-20.6	13.9	27.0	18	5	53.8	18.52	-64.78	130.6	
14.5	1.1	11.64	11.76	-4.95	-5.46	134.02	137.54	3.6	13.9	27.0	18	5	56.0	19.32	-65.48	96.4	
15.1	47.1	-14.17	-19.51	-29.12	-27.67	170.09	113.80	7.8	11.3	27.0	18	5	59.5	16.97	-62.50	132.2	
15.2	41.0	-12.30	-13.92	-25.43	-25.56	166.20	139.95	-2.0	12.4	27.0	18	6	3.1	17.61	-62.87	132.0	
15.3	30.7	-5.81	-7.71	-21.66	-21.91	149.72	125.40	-11.7	12.9	27.0	18	6	6.3	18.41	-63.46	131.7	
15.4	16.7	2.91	2.57	-13.07	-14.24	140.04	132.10	-20.6	13.4	27.0	18	6	9.1	19.25	-64.13	130.6	
15.5	1.1	11.99	11.62	-4.72	-5.28	139.65	138.50	0.4	12.9	27.0	18	6	11.3	20.04	-64.83	89.6	
16.1	47.2		-17.13		-17.88	189.39	141.61	-2.3	9.3	27.0	18	6	14.9	17.70	-61.83	132.3	-2
16.2	41.0	-12.04	-14.59	-26.44	-26.13	160.98	116.50	-12.2	9.8	27.0	18	6	18.3	18.32	-62.21	132.2	
16.3	30.7	-8.13	-9.32	-23.14	-23.21	148.86	124.12	-22.0	10.3	27.0	18	6	21.6	19.12	-62.80	132.0	
16.4	16.8	2.41	2.19	-13.37	-13.83	137.29	139.42	-31.0	11.3	27.0	18	6	24.3	19.95	-63.48	131.0	
16.5	1.1	12.29	12.09	-4.53	-4.84	135.57	136.05	-5.9	11.8	27.0	18	6	26.5	20.76	-64.17	95.9	

DOY 247-1, 9/ 4/73 CTNC-R. NORTH OF VENEZUELA

SCAN NUMB	INCID ANGLE (DEG)	SCATTERING COEFFICIENTS				ANTENNA V (DEG)	TEMPS H (DEG)	ASPECT ANGLE (DEG)	WIND SPEED (M/S)	SEA TEMP (DEG)	GMT			CELL COORDINATES		S193 DATA AZIMTH FLAG
		VV (DB)	HH (DB)	VH (DB)	HV (DB)						(HR MIN SEC)	(DEG)	(DEG)	LAT (DEG)	LONG (DEG)	
17.1	47.1	-14.49	-18.90	-28.88	-29.54	170.84	111.46	-12.5	7.7	27.0	18 6 30.0			18.39	-61.19	132.5
17.2	40.9	-13.12	-15.37	-27.26	-27.45	158.64	116.26	-12.4	8.2	27.0	18 6 33.6			19.05	-61.56	132.4
17.3	30.7	-9.50	-10.71	-24.21	-24.49	146.05	123.43	-22.3	9.8	27.0	18 6 36.8			19.83	-62.13	132.3
17.4	16.7							-31.2	9.8	27.0	18 6 39.4			20.67	-62.82	131.2
17.5	1.1	12.73	12.71	-4.39	-4.55	130.41	131.85	1.0	11.3	27.0	18 6 41.8			21.49	-63.51	89.0
18.1	47.1	-13.89	-18.81	-28.67	-28.35	168.08	110.80	-13.0	6.2	27.0	18 6 45.3			19.10	-60.53	133.0
18.2	40.9	-12.92	-15.56	-25.88	-27.08	158.37	114.98	-12.8	6.7	27.0	18 6 48.8			19.74	-60.90	132.8
18.3	30.7	-9.55	-10.95	-24.86	-25.19	144.92	121.19	-22.6	7.7	27.0	18 6 52.1			20.54	-61.47	132.6
18.4	16.7	1.61	1.54	-13.97	-14.33	134.35	127.46	-31.6	8.8	27.0	18 6 54.8			21.39	-62.15	131.6
18.5																
19.1	47.1	-15.33	-20.39	-30.23	-30.05	167.33	109.56	-13.1	6.7	27.0	18 7 0.5			19.80	-59.85	133.1
19.2	40.9	-13.50	-16.51	-28.49	-28.78	157.06	114.15	-23.1	6.2	27.0	18 7 4.1			20.44	-60.23	133.1
19.3	30.7	-10.61	-11.89	-25.83	-26.24	145.85	121.57	-32.8	6.7	27.0	18 7 7.3			21.25	-60.79	132.8
19.4	16.8	1.35	1.09	-14.40	-14.79	133.10	125.70	-41.3	8.2	27.0	18 7 10.1			22.10	-61.46	131.3
19.5																
20.1	24.2										18 7 14.6			21.73	-60.64	133.5
20.2	40.9	-13.79	-17.30	-23.23	-29.00	157.76	113.37	-43.3	5.1	27.0	18 7 19.3			21.15	-59.54	133.3
20.3	30.7	-11.64	-12.99	-26.98	-26.50	144.71	120.06	-43.1	6.2	27.0	18 7 22.6			21.95	-60.11	133.1
20.4	16.7	1.35	1.14	-14.38	-14.74	133.39	124.40	-42.1	7.7	27.0	18 7 25.3			22.80	-60.79	132.1
20.5	1.0	13.18	13.11	-3.86	-4.00	125.67	129.22	-3.9	8.8	27.0	18 7 27.5			23.62	-61.49	93.9
21.1	47.2	-16.75	-21.49	-31.60	-31.36	166.76	107.48	-53.7	5.1	27.0	18 7 31.0			21.19	-58.49	133.7
21.2	40.9	-15.85	-18.13	-30.47	-31.29	156.08	111.70	-53.7	4.6	27.0	18 7 34.6			21.84	-58.86	133.7
21.3	30.7	-11.82	-12.27	-26.96	-26.96	144.26	123.07	-53.5	5.7	27.0	18 7 37.8			22.65	-59.43	133.5
21.4	16.7	0.08	0.79	-14.82	-14.77	150.32	148.03	-52.3	7.7	27.0	18 7 40.6			23.50	-60.09	132.3
21.5	1.0	13.57	13.32	-3.50	-4.07	126.28	128.27	-11.1	8.8	27.0	18 7 42.8			24.32	-60.79	91.1
22.1	47.1	-19.04	-23.70	-34.62	-33.47	166.86	106.58	-54.1	4.6	27.0	18 7 46.3			21.88	-57.79	134.1
22.2	40.9	-18.34	-21.12	-32.68	-32.26	156.33	113.99	-54.0	4.6	27.0	18 7 49.8			22.53	-58.16	134.0
22.3	30.8	-12.26	-13.74	-27.46	-27.24	144.66	121.00	-53.6	5.7	27.0	18 7 53.1			23.33	-58.72	133.6
22.4	16.7	0.96	0.36	-14.93	-15.19	131.42	125.07	-52.6	7.2	27.0	18 7 55.8			24.20	-59.39	132.6
22.5	1.1	13.72	13.54	-3.39	-3.65	126.89	126.87	-12.5	7.2	27.0	18 7 58.0			25.02	-60.08	92.5
23.1	47.1	-20.14	-24.79	-34.31	-34.15	166.35	107.10	-44.4	4.6	27.0	18 8 1.5			22.56	-57.09	134.4
23.2	40.9	-18.23	-21.15	-33.40	-31.68	157.37	113.02	-44.3	4.6	27.0	18 8 5.1			23.22	-57.45	134.3
23.3	30.7	-13.26	-13.51	-28.48	-28.71	142.03	118.41	-54.0	6.2	27.0	18 8 8.3			24.03	-58.02	134.0
23.4	16.7	0.75	0.47	-14.92	-15.33	130.83	124.73	-52.9	6.2	27.0	18 8 11.1			24.89	-58.69	132.9
23.5	1.1	14.13	13.81	-2.80	-3.51	126.39	127.38	0.5	5.1	27.0	18 8 13.3			25.72	-59.38	89.5
24.1	47.2	-22.02	-26.27	-35.13	-34.94	165.80	108.09	-44.7	4.6	27.0	18 8 16.8			23.23	-56.37	134.7
24.2	41.0	-18.03	-20.79	-33.40	-32.24	156.86	113.99	-44.6	6.2	27.0	18 8 20.3			23.89	-56.74	134.6
24.3	30.7	-14.14	-15.00	-29.84	-30.52	144.45	119.71	-54.5	6.2	27.0	18 8 23.6			24.71	-57.30	134.5
24.4	16.7	-0.07	-0.46	-15.51	-15.99	130.58	124.24	-23.1	3.6	27.0	18 8 26.3			25.58	-57.97	133.1
24.5	1.1	14.38	14.34	-2.37	-2.79	129.10	128.57	29.3	2.6	27.0	18 8 28.5			26.41	-58.66	90.7

09/05/75

DOY 247-1, 9/ 4/73 CTNC-R, NORTH OF VENEZUELA

SCAN NUMB	INCID ANGLE (DEG)	SCATTERING COEFFICIENTS				ANTENNA V (DEG)	TEMPS H (DEG)	ASPECT ANGLE (DEG)	WIND SPEED (M/S)	SEA TEMP (DEG)	GMT			CELL COORDINATES		S193 AZIMTH (DEG)	DATA FLAG
		VV (DB)	HH (DB)	VH (DB)	HV (DB)						(HR	MIN	SEC)	LAT (DEG)	LONG (DEG)		
25.1	47.2	-23.39	-25.49	-36.17	-37.15	166.47	106.22	-45.0	5.7	27.0	18	8	32.0	23.91	-55.66	135.0	
25.2	40.9	-20.28	-22.81	-35.22	-34.27	155.65	111.82	-45.1	5.7	27.0	18	8	35.6	24.57	-56.02	135.1	
25.3	30.9	-14.85	-15.54	-31.25	-31.26	143.38	119.76	-14.4	3.1	27.0	18	8	38.9	25.46	-56.50	134.4	
25.4	16.7	-0.87	-1.26	-15.55	-17.00	129.76	122.91	-13.5	2.1	27.0	18	8	41.6	26.26	-57.24	133.5	
25.5	1.1	15.13	14.97	-2.03	-2.13	127.85	127.32	25.3	1.5	27.0	18	8	43.3	27.10	-57.93	94.0	
26.1	47.2	-22.77	-26.76	-35.13	-34.61	165.25	104.52	-45.3	5.2	27.0	18	8	47.3	24.57	-54.93	135.3	
26.2	40.9	-19.88	-22.74	-34.16	-34.36	156.13	111.91	-45.3	5.1	27.0	18	8	50.9	25.25	-55.28	135.3	
26.3	30.8	-15.97	-16.36	-31.71	-31.71	143.54	118.31	-25.1	3.1	27.0	18	8	54.1	26.06	-55.84	135.1	
26.4	16.7	-1.95	-2.15	-17.43	-17.63	130.57	124.75	-23.7	2.1	27.0	18	8	56.8	26.94	-56.51	133.7	
26.5	1.1	15.70	15.54	-1.46	-1.94	127.69	129.18	17.3	0.5	27.0	18	8	59.0	27.78	-57.19	92.7	
27.1	47.2	-23.05	-26.89	-35.14	-37.16	165.59	105.89	-45.8	5.1	27.0	18	9	2.5	25.24	-54.19	135.8	
27.2	40.9	-21.58	-24.13	-33.31	-36.61	156.25	110.91	-35.5	3.6	27.0	18	9	6.1	25.91	-54.54	135.5	
27.3	30.7	-17.27	-18.25	-35.39	-33.47	142.58	118.45	-15.4	2.6	27.0	18	9	9.3	26.74	-55.10	135.4	
27.4	16.6	-3.82	-3.69	-19.17	-19.78	129.71	123.90	-14.3	1.5	27.0	18	9	12.1	27.62	-55.76	134.3	
27.5																	
28.1	47.1	-29.55	-33.26	-42.59	-44.61	164.75	105.06	-46.3	4.1	27.0	18	9	17.8	25.90	-53.45	136.3	
28.2	41.0	-29.85	-33.05	-41.51	-41.71	155.88	110.05	-16.0	3.1	27.0	18	9	21.3	26.56	-53.79	136.0	
28.3	30.7	-31.17	-33.67	-48.67	-48.67	141.58	119.02	-5.6	2.6	27.0	18	9	24.6	27.40	-54.34	135.6	-2
28.4	16.7	-22.60	-24.45	-33.98	-39.27	130.65	124.31	-4.7	1.5	27.0	18	9	27.3	28.28	-55.00	134.7	-2
28.5	1.1	10.86	11.09	-1.56	-2.46	128.86	127.30	34.7	0.5	27.0	18	9	29.5	29.13	-55.69	95.3	
29.1	47.3	-32.48	-37.22	-48.01	-44.08	164.42	103.74	-46.5	3.1	27.0	18	9	33.0	26.55	-52.68	136.5	
29.2	40.9	-33.19	-35.94	-45.38	-43.30	154.89	110.51	-16.3	2.6	27.0	18	9	36.6	27.23	-53.03	136.3	
29.3	30.7		-25.92	-49.37		144.16		14.0	1.5	27.0	18	9	39.3	28.04	-53.61	136.0	-2
29.4																	
29.5																	

JSC - 5/ 3/75

S. TRUTH - 8/26/75

LAST MOD - 8/28/75

THIS LISTING - 09/05/75

AUTHORITY OF THE
 ORIGINAL PAGE IS FOUR

DOY 252-1, 9/ 9/73 ITNG, NORTH ATLANTIC

SCAN NUMB	INCID ANGLE (DEG)	SCATTERING COEFFICIENTS				ANTENNA V (DEG)	TEMPS H (DEG)	ASPECT ANGLE (DEG)	WIND SPEED (M/S)	SEA TEMP (DEG)	GMT			CELL COORDINATES		S193 DATA AZIMTH FLAG (DEG)
		VV (DB)	HH (DB)	VH (DB)	HV (DB)						HR	MIN	SEC	LAT (DEG)	LONG (DEG)	
1.1	50.6					159.32	87.13	136.4	5.4	11.0	19	25	8.0	49.95	-52.07	80.6
1.2	44.1					149.90	96.51	141.5	5.1	10.7	19	25	11.5	49.76	-52.98	80.5
1.3	32.5					161.21	151.49	150.8	4.8	10.3	19	25	14.7	49.63	-54.41	80.2 1
1.4	17.5					230.97	229.50	162.3	5.0	10.3	19	25	17.3	49.48	-55.91	79.7 1
1.5																
2.1	50.6	-35.55	-39.70	-43.13	-46.23	158.26	88.60	130.3	5.8	12.0	19	25	22.6	49.95	-50.66	81.7 -2
2.2	44.1	-27.10	-32.55	-41.01	-41.57	148.10	96.18	132.3	5.6	11.8	19	25	26.3	49.89	-51.57	81.7
2.3	32.5	-19.48	-19.71	-34.49	-34.48	136.23	106.49	140.7	5.1	10.7	19	25	29.6	49.77	-53.01	81.3
2.4	17.4	-6.55	-7.10	-18.55	-15.97	148.35	165.24	151.1	4.8	10.3	19	25	32.3	49.63	-54.51	80.9 1
2.5	1.3	8.81	9.49	1.67	-4.82	234.55	236.75	159.1	5.0	10.3	19	25	34.5	49.48	-55.91	82.9 1
3.1	50.6	-28.14	-35.06	-38.55	-37.51	160.22	92.63	126.2	6.0	10.2	19	25	38.1	50.05	-49.20	82.9
3.2	44.1	-29.95	-34.57	-41.07	-41.36	149.37	96.99	128.2	5.9	11.8	19	25	41.6	49.99	-50.11	82.8
3.3	32.6	-20.45	-21.15	-35.44		134.79	106.61	131.6	5.6	11.8	19	25	44.9	49.89	-51.54	82.4
3.4	17.5	-2.56	-1.77	-18.13	-18.01	124.58	115.67	140.0	5.0	10.7	19	25	47.6	49.77	-53.06	82.0
3.5	1.2	18.76	17.99	4.09	6.83	144.97	157.92	139.5	4.8	10.3	19	25	49.8	49.63	-54.48	91.5 1.
4.1	50.6	-26.67	-30.75	-35.73	-36.17	162.96	97.92	120.9	6.1	13.5	19	25	53.3	50.11	-47.73	84.1
4.2	44.1	-25.72	-29.06	-39.15	-36.66	150.45	109.11	123.1	6.1	13.0	19	25	56.8	50.07	-48.66	83.9
4.3	32.4	-22.51	-23.71	-35.25	-38.52	134.32	106.12	127.5	5.9	11.8	19	26	0.1	49.99	-50.12	83.5
4.4	17.4	-2.87	-1.98	-17.81	-17.62	123.24	114.31	131.8	5.6	11.8	19	26	2.8	49.89	-51.63	83.2
4.5	1.3	14.58	14.87	-2.42	-2.37	122.14	120.51	133.9	5.0	10.7	19	26	5.0	49.78	-53.04	83.1
5.1	50.7	-24.66	-28.46	-35.74	-38.18	162.20	95.62	114.8	5.7	13.6	19	26	8.5	50.16	-46.25	85.2
5.2	44.1	-20.10	-23.24	-32.30	-32.96	151.59	101.36	117.8	5.9	13.4	19	26	12.1	50.13	-47.19	85.2
5.3	32.5	-17.94	-18.35	-33.68	-33.82	135.59	107.40	122.4	6.1	13.0	19	26	15.3	50.07	-48.64	84.6
5.4	17.3	-3.45	-3.26	-13.85	-18.43	122.30	113.89	126.7	5.9	11.8	19	26	18.1	49.99	-50.13	84.3
5.5	1.2	14.94	15.29	-2.42	-2.32	121.33	118.67	126.4	5.6	11.8	19	26	20.3	49.89	-51.60	88.6
6.1	50.6	-25.04	-29.93	-35.71	-36.16	161.29	95.26	106.6	5.7	14.0	19	26	23.8	50.19	-44.80	86.4
6.2	44.1	-19.97	-22.70	-32.83	-32.84	151.63	102.25	111.8	5.7	13.9	19	26	27.3	50.17	-45.72	86.2
6.3	32.4	-14.74	-14.37	-29.68	-29.45	137.22	110.50	117.1	5.9	13.4	19	26	30.6	50.13	-47.19	85.9
6.4	17.4	-1.19	-3.28	-16.39	-16.29	123.53	116.18	122.5	6.1	13.0	19	26	33.3	50.07	-48.71	85.5
6.5	1.3	15.11	15.52	-2.12	-2.07	118.55	118.48	118.9	5.9	11.8	19	26	35.5	49.99	-50.14	92.1
7.1	50.5	-23.54	-30.58	-43.04	-34.32	160.95	93.84	95.5	5.6	14.1	19	26	39.1	50.20	-43.34	87.5
7.2	44.0	-18.97	-22.99	-32.28	-32.30	151.28	100.43	101.6	5.6	14.0	19	26	42.0	50.20	-44.26	87.4
7.3	32.5	-13.87	-14.45	-28.86	-28.46	135.75	110.13	111.0	5.7	13.9	19	26	45.8	50.18	-45.71	87.0
7.4	17.5	0.51	0.93	-15.15	-15.14	125.75	117.36	116.4	5.9	13.4	19	26	48.6	50.13	-47.24	86.6
7.5	1.3	14.34	14.56	-3.41	-3.40	121.11	120.55	114.4	6.1	13.0	19	26	50.8	50.07	-48.67	92.6
8.1	50.8	-30.96	-37.73	-43.02	-37.50	161.92	92.77	86.1	5.9	14.1	19	26	54.3	50.19	-41.81	88.9
8.2	44.3	-23.90	-27.59	-37.93	-35.25	149.14	98.27	91.3	5.7	14.0	19	26	57.8	50.19	-42.76	88.7
8.3	32.6	-13.74	-13.81	-28.47	-28.94	135.49	104.74	100.8	5.6	14.0	19	27	1.1	50.19	-44.23	88.2
8.4	17.5	0.68	2.82	-15.03	-14.91	124.41	116.01	110.0	5.7	13.9	19	27	3.8	50.17	-45.77	88.0
8.5	1.3	13.42	13.66	-4.03	-4.27	123.35	120.76	112.2	5.9	13.4	19	27	6.0	50.13	-47.21	90.8

09/05/75

DOY 252-1, 9/ 9/73 ITNC, NORTH ATLANTIC

SCAN NUMB	INCID ANGLE (DEG)	SCATTERING COEFFICIENTS				ANTENNA V (DEG)	TEMPS H (DEG)	ASPECT ANGLE (DEG)	WIND SPEED (M/S)	SEA TEMP (DEG)	GMT			CELL COORDINATES		S193 AZIMTH (DEG)	DATA FLAG
		VV (DB)	HH (DB)	VH (DB)	HV (DB)						HR	MIN	SEC	LAT (DEG)	LONG (DEG)		
9.1	50.6	-17.50	-17.33	-29.88	-30.27	190.06	146.07	83.1	5.8	14.2	19	27	9.5	50.16	-40.39	89.9	4
9.2	44.1	-31.41	-31.12	-40.62	-41.35	157.64	105.79	84.2	5.9	14.2	19	27	13.1	50.17	-41.32	89.8	
9.3	32.5	-15.95	-16.74	-31.46	-31.89	134.04	107.92	90.7	5.7	14.0	19	27	16.3	50.20	-42.78	89.3	
9.4	17.4	1.09	1.43	-14.76	-14.56	123.94	115.54	101.0	5.7	14.0	19	27	19.1	50.19	-44.31	89.0	
9.5	1.2	13.48	13.46	-3.89	-4.19	122.28	122.24	102.1	5.7	13.9	19	27	21.3	50.16	-45.76	95.9	
10.1	50.6	-16.68	-21.55	-29.89	-30.00	165.60	103.08	79.9	5.2	14.3	19	27	24.8	50.11	-38.93	91.1	
10.2	44.1	-14.07	-17.52	-27.37	-27.58	159.58	115.39	81.1	5.6	14.3	19	27	28.3	50.14	-39.86	90.9	
10.3	32.5	-22.56	-21.26	-41.96	-36.72	140.36	110.61	83.4	5.9	14.2	19	27	31.6	50.17	-41.31	90.6	
10.4	17.3	0.60	0.54	-15.09	-14.98	123.52	114.59	90.6	5.7	14.0	19	27	34.3	50.19	-42.85	90.4	
10.5	1.3	13.54	13.67	-4.18	-3.95	120.97	120.91	95.7	5.7	14.0	19	27	36.5	50.19	-44.28	94.3	
11.1	50.6	-20.51	-25.25	-32.61	-37.35	163.53	99.98	74.7	3.9	14.3	19	27	40.1	50.03	-37.45	92.3	
11.2	44.1	-14.43	-18.10	-29.04	-28.80	153.01	105.72	77.9	4.8	14.3	19	27	43.6	50.08	-38.39	92.1	
11.3	32.4	-10.20	-11.29	-24.38	-24.74	144.23	120.27	80.4	5.6	14.3	19	27	46.8	50.13	-39.85	91.6	
11.4	17.5	-2.37	-1.89	-17.46	-17.80	127.87	118.44	82.7	5.9	14.2	19	27	49.6	50.17	-41.37	91.3	
11.5	1.2	13.58	13.71	-3.74	-3.74	121.47	119.89	85.1	5.7	14.0	19	27	51.8	50.19	-42.82	94.9	
12.1	50.6	-25.14	-31.23	-37.80	-40.55	161.31	93.14	59.5	2.3	14.4	19	27	55.3	49.94	-36.01	93.5	
12.2	44.1	-16.89	-20.67	-31.29	-31.32	151.90	102.04	70.8	3.3	14.3	19	27	58.8	50.00	-36.93	93.2	
12.3	32.4	-10.49	-11.61	-25.22	-25.32	139.11	113.54	77.3	4.8	14.3	19	28	2.1	50.07	-38.39	92.7	
12.4	17.5	1.13	1.37	-14.52	-14.37	133.25	127.00	80.6	5.6	14.3	19	28	4.8	50.13	-39.90	92.4	
12.5	1.2	15.05	15.04	-2.73	-2.56	126.14	124.50	81.0	5.9	14.2	19	28	7.0	50.17	-41.35	93.0	
13.1	50.7	-36.16	-39.59	-43.02	-39.42	160.51	91.30	-11.6	1.2	15.0	19	28	10.5	49.83	-34.53	94.6	
13.2	44.1	-30.55	-35.38	-40.45	-40.99	150.06	96.10	44.6	1.6	14.0	19	28	14.1	49.90	-35.47	94.4	
13.3	32.5	-13.04	-14.01	-28.02	-27.84	135.65	109.53	69.9	3.3	14.3	19	28	17.3	49.99	-36.92	94.1	
13.4	17.4	1.25	1.67	-14.42	-14.46	128.16	119.78	76.4	4.8	14.3	19	28	20.1	50.07	-38.44	93.6	
13.5	1.3	12.60	12.72	-4.75	-4.63	132.09	130.55	72.3	5.6	14.3	19	28	22.3	50.12	-39.88	100.7	
14.1	50.7	-24.80	-29.10	-39.41	-36.63	163.56	98.45	-57.8	2.7	15.0	19	28	25.0	49.70	-33.10	95.8	
14.2	44.0	-27.95	-30.75	-37.93	-38.17	150.72	98.80	-39.6	1.6	14.9	19	28	29.3	49.78	-34.04	95.6	
14.3	32.5	-24.48	-26.78	-63.17	-38.42	134.47	106.24	44.8	1.6	14.8	19	28	32.6	49.89	-35.47	95.2	
14.4	17.3	0.56	0.94	-15.31	-14.96	124.69	115.76	69.2	3.3	14.3	19	28	35.3	49.99	-37.00	94.8	
14.5	1.1	12.74	13.20	-4.85	-4.50	124.67	124.65	69.4	4.8	14.3	19	28	37.5	50.06	-38.44	101.5	
15.1	50.7	-19.78	-24.24	-32.44	-31.58	166.22	104.70	-53.8	4.5	15.6	19	28	41.1	49.55	-31.66	96.8	
15.2	44.0	-20.02	-22.75	-32.30	-32.91	153.85	105.00	-52.7	3.4	15.2	19	28	44.6	49.64	-32.59	96.7	
15.3	32.5	-21.02	-20.76	-35.44	-36.64	136.10	107.94	-39.4	1.6	14.9	19	28	47.8	49.77	-34.03	96.4	
15.4	17.4	-6.31	-6.52	-22.18	-21.45	121.61	112.66	46.1	1.7	14.8	19	28	50.6	49.89	-35.53	95.9	
15.5	1.3	13.61	14.01	-3.80	-3.90	121.30	120.22	62.5	3.3	14.3	19	28	52.8	49.98	-36.97	101.5	
16.1	50.7	-21.75	-26.25	-36.91	-35.11	163.53	97.89	-61.0	5.9	16.3	19	28	50.3	49.38	-30.23	99.3	
16.2	44.1	-19.13	-21.13	-38.48	-37.23	154.94	104.13	-53.9	5.0	15.9	19	28	53.8	49.44	-31.15	97.3	
16.3	32.4	-14.05	-14.28	-28.22	-28.33	138.63	111.99	-53.4	3.4	15.2	19	29	3.1	49.63	-32.59	97.4	
16.4	17.5	-2.44	-1.86	-17.51	-16.10	123.27	114.36	-49.5	1.5	14.4	19	29	5.8	49.77	-34.63	96.8	
16.5	1.2	16.58	16.75	-0.56	-1.77	118.32	117.17	41.7	1.7	14.8	19	29	8.0	49.88	-35.51	99.3	

REPRODUCIBILITY OF THE
ORIGINAL PAGE IS POOR

09/05/75

DOY 252-1.

9/ 9/73

ITNC. NORTH ATLANTIC

SCAN NUMB	INCID ANGLE (DEG)	SCATTERING COEFFICIENTS				ANTENNA V (DEG)	TEMPS H (DEG)	ASPECT ANGLE (DEG)	WIND SPEED (M/S)	SEA TEMP (DEG)	GMT			CELL COORDINATES		S193 DATA AZIMTH FLAG (DEG)
		VV (DB)	HH (DB)	VH (DB)	HV (DB)						(HR MIN SEC)	(DEG)	(DEG)	LAT (DEG)	LONG (DEG)	
17.1	50.7	-17.32	-22.62	-31.29	-32.00	163.86	99.23	-52.1	6.9	16.2	19 29 11.5	49.19	-28.02	99.1		
17.2	44.1	-17.31	-19.78	-30.87	-31.78	152.09	103.23	-59.0	6.3	16.1	19 29 15.1	49.31	-29.74	99.0		
17.3	32.4	-13.31	-13.35	-27.32	-26.84	139.27	115.25	-64.6	5.0	15.9	19 29 18.3	49.47	-31.16	98.6		
17.4	17.4	0.44	0.83	-15.08	-15.96	126.21	118.95	-64.6	3.3	15.2	19 29 21.1	49.63	-32.65	98.6		
17.5	1.2	14.93	15.00	-2.78	-2.19	120.79	119.73	-42.9	1.5	14.9	19 29 23.3	49.75	-34.07	100.9		
18.1	50.6	-14.57	-19.66	-29.87	-29.39	164.85	97.59	-41.2	7.8	16.3	19 29 26.8	48.99	-27.43	100.2		
18.2	44.0	-14.44	-18.39	-29.30	-28.55	154.64	105.28	-49.0	7.2	16.2	19 29 30.3	49.11	-28.34	100.0		
18.3	32.4	-12.24	-12.31	-27.67	-27.84	138.29	109.54	-59.7	6.3	16.1	19 29 33.6	49.29	-29.75	99.7		
18.4	17.4	0.74	1.06	-14.89	-14.79	128.74	121.93	-65.3	4.9	15.9	19 29 36.3	49.47	-31.22	99.3		
18.5																
19.1	50.7	-17.58	-22.64	-32.54	-32.25	162.71	95.51	-28.3	9.1	15.4	19 29 42.1	48.76	-26.03	101.3		
19.2	44.1	-13.15	-17.15	-28.80	-28.37	154.37	102.44	-37.2	8.1	16.3	19 29 45.6	48.90	-26.94	101.2		
19.3	32.4	-10.59	-12.11	-25.57	-25.35	140.74	113.58	-49.7	7.2	16.2	19 29 48.8	49.10	-28.34	100.7		
19.4	17.5	1.33	1.83	-14.31	-14.48	126.70	116.79	-60.4	6.2	16.1	19 29 51.6	49.29	-29.80	100.4		
19.5	1.3	13.28	13.05	-4.48	-4.56	125.62	124.42	-71.9	4.9	15.9	19 29 53.8	49.45	-31.20	104.9		
20.1	50.6	-23.44	-27.74	-36.71	-37.31	161.30	95.61	-20.4	9.7	16.6	19 29 57.3	48.52	-24.67	102.4		
20.2	44.1	-17.44	-20.89	-33.31	-32.10	151.30	100.37	-26.3	9.3	16.4	19 30 0.8	48.65	-25.56	102.3		
20.3	32.5	-9.49	-10.97	-25.70	-24.72	137.04	112.47	-37.8	8.1	16.3	19 30 4.1	48.88	-26.93	101.8		
20.4	17.5	1.37	1.74	-14.17	-1.21	128.40	119.47	-51.7	7.2	16.2	19 30 6.8	49.09	-28.39	101.7		
20.5	1.4	13.45	13.53	-3.98	-3.98	123.25	122.20	-60.7	6.2	16.1	19 30 9.0	49.27	-29.78	100.7		
21.1	50.7	-20.58	-26.05	-35.50	-35.96	162.72	94.50	-14.5	10.7	16.7	19 30 12.5	48.25	-23.29	103.5		
21.2	44.1	-17.47	-20.24	-31.10	-32.13	152.66	100.19	-19.4	10.0	16.6	19 30 16.1	48.41	-24.18	103.4		
21.3	32.5	-12.90	-13.98	-29.21	-28.68	137.24	109.52	-26.8	9.2	16.4	19 30 19.3	48.65	-25.56	102.8		
21.4	17.3	1.80	2.08	-14.98	-14.98	126.07	118.71	-39.6	8.1	16.3	19 30 22.1	48.88	-27.61	102.6		
21.5	1.2	13.33	13.68	-4.14	-4.14	124.40	121.80	-61.9	7.1	16.2	19 30 24.3	49.07	-28.39	111.9		
22.1	50.6	-24.48	-27.36	-36.21	-37.29	163.55	95.29	-11.5	10.5	17.2	19 30 27.8	47.98	-21.95	104.5		
22.2	44.1	-21.10	-24.50	-34.91	-36.27	152.17	100.20	-14.3	10.8	16.9	19 30 31.3	48.15	-22.63	104.3		
22.3	32.5	-12.65	-13.51	-27.24	-28.24	136.88	107.59	-28.1	10.0	16.6	19 30 34.6	48.41	-24.18	104.1		
22.4	17.5	0.98	1.03	-14.79	-14.73	124.25	117.41	-28.9	9.2	16.4	19 30 37.3	48.64	-25.62	103.9		
22.5	1.3	13.20	13.40	-4.65	-4.38	123.82	120.64	-42.6	8.1	16.3	19 30 39.5	48.86	-26.98	105.6		
23.1	50.8	-26.83	-31.70		-37.32	164.67	97.96	-11.5	10.6	17.3	19 30 42.9	47.63	-20.61	105.5		
23.2	44.2	-22.49	-25.70	-37.73	-36.29	152.98	101.02	-11.5	10.5	17.2	19 30 46.6	47.85	-21.47	105.5		
23.3	32.6	-14.81	-15.59	-31.70	-31.25	136.22	109.55	-15.3	10.8	16.9	19 30 49.8	48.12	-22.82	105.3		
23.4	17.6	1.06	1.33	-14.76	-14.62	124.35	115.87	-21.2	9.9	16.6	19 30 52.6	48.38	-24.24	105.2		
23.5	1.4	13.82	13.91	-3.53	-3.73	121.36	121.33	-29.2	9.2	16.4	19 30 54.8	48.62	-25.60	104.2		
24.1	50.7	-24.37	-27.72	-36.69	-37.92	167.33	98.59	-11.6	10.3	17.6	19 30 58.3	47.36	-19.30	106.6		
24.2	44.0							-12.5	10.6	17.4	19 31 2.9	47.53	-20.08	106.5		
24.3	32.4	-15.98	-16.84	-36.41	-32.77	136.59	110.43	-12.1	10.5	17.2	19 31 5.1	47.84	-21.51	106.1		
24.4	17.4	0.26	0.67	-15.37	-15.28	124.93	113.89	-15.8	10.8	16.9	19 31 7.8	48.12	-22.90	105.8		
24.5	1.3	13.61	13.49	-4.60	-3.78	120.46	120.90	-26.6	9.8	16.6	19 31 10.0	48.37	-24.24	110.6		

09/05/75

DOY 252-1. 9/ 9/73 ITNC, NORTH ATLANTIC

SCAN NUMB	INCID ANGLE (DEG)	SCATTERING COEFFICIENTS				ANTENNA V (DEG)	TEMPS H (DEG)	ASPECT ANGLE (DEG)	WIND SPEED (M/S)	SEA TEMP (DEG)	GMT			CELL COORDINATES		S193 AZIMTH (DEG)	DATA FLAG
		VV (DB)	HH (DB)	VH (DB)	HV (DB)						HR	MIN	SEC	LAT (DEG)	LONG (DEG)		
25.1	50.7	-14.60	-15.02	-27.30	-27.36	187.78	134.57	-12.6	9.2	17.9	19	31	13.5	47.04	-18.80	107.6	4
25.2	44.1	-17.45	-19.79	-30.65	-32.16	156.78	104.73	-12.6	9.9	17.7	19	31	17.1	47.23	-18.85	107.6	
25.3	32.5	-16.84	-17.49	-32.12	-32.80	139.40	110.16	-12.1	10.6	17.4	19	31	20.3	47.54	-20.17	107.1	
25.4	17.5	-0.26	-0.11	-15.97	-15.71	126.13	116.67	-14.1	10.4	17.2	19	31	23.1	47.83	-21.55	107.1	
25.5	1.4	13.95	13.98	-3.46	-3.32	121.85	121.77	-19.0	10.7	16.9	19	31	25.3	48.10	-22.88	109.0	
26.1	50.6	-15.44	-15.63	-28.61	-27.69	191.12	143.96	-11.6	8.2	18.6	19	31	28.8	46.69	-16.74	108.6	4
26.2	44.2	-13.89	-15.38	-27.92	-26.85	174.57	133.11	-12.6	8.8	18.1	19	31	32.3	46.90	-17.56	108.6	
26.3	32.4	-13.92	-13.68	-27.42	-28.98	140.48	113.86	-13.4	9.8	17.7	19	31	35.6	47.22	-18.87	108.4	
26.4	17.5	-0.48	-0.11	-16.18	-16.21	126.82	119.46	-13.1	10.5	17.4	19	31	38.3	47.53	-20.24	108.1	
26.5	1.4	14.46	14.55	-2.93	-2.99	122.17	122.59	-18.7	10.3	17.2	19	31	40.5	47.80	-21.54	112.7	
27.1	50.7	-14.84	-17.08	-27.61	-28.61	180.88	128.55	-6.6	6.9	19.4	19	31	44.1	46.33	-15.47	109.6	
27.2	44.2	-15.76	-15.99	-28.62	-28.36	175.54	138.47	-10.5	7.7	19.0	19	31	47.6	46.54	-16.27	109.5	
27.3	32.5	-11.23	-12.71	-25.70	-24.82	161.02	144.44	-13.3	8.8	18.1	19	31	50.8	46.88	-17.57	109.3	
27.4	17.5							-13.4	9.4	17.7	19	31	54.2	47.19	-18.83	108.3	
27.5	1.4	14.45	14.53	-2.47	-2.47	122.55	121.52	-19.5	10.4	17.4	19	31	58.5	47.51	-20.23	111.5	
28.1	50.8	-13.37	-16.62	-27.35	-28.86	174.42	117.43	9.5	5.9	19.7	19	31	59.3	46.45	-14.13	111.5	
28.2	44.2	-11.57	-14.47	-25.21	-25.11	167.01	122.38	-7.4	6.4	19.4	19	32	2.8	46.16	-15.32	111.4	
28.3	32.6	-13.35	-13.74	-27.43	-27.44	161.89	139.02	-11.1	7.7	19.0	19	32	6.1	46.52	-16.30	110.1	
28.4	17.5	-0.54	-0.37	-15.89	-15.71	153.02	149.49	-14.1	8.8	18.1	19	32	8.8	46.87	-17.64	110.1	
28.5	1.4	14.02	14.14	-3.59	-3.52	124.71	123.64	-20.7	9.8	17.7	19	32	11.0	47.18	-18.92	115.7	
29.1	50.7	-13.43	-18.53	-28.32	-28.73	169.41	105.23	11.5	5.6	20.0	19	32	14.5	45.56	-12.99	111.5	
29.2	44.2	-12.81	-15.48	-26.66	-27.01	159.36	110.47	3.6	5.8	19.8	19	32	18.1	45.79	-13.78	111.4	
29.3	32.5	-7.92	-8.94	-22.38	-22.90	153.95	126.31	-5.2	6.4	19.4	19	32	21.3	46.16	-15.05	111.2	
29.4	17.5	-1.82	-0.94	-17.12	-17.14	150.29	142.32	-11.9	7.7	19.0	19	32	24.1	46.52	-16.37	110.9	
29.5	1.3	12.68	13.03	-4.94	-4.83	150.86	154.65	-20.3	8.7	18.1	19	32	26.3	46.84	-17.64	116.3	
30.1	50.7	-14.12	-18.61	-28.51	-28.82	169.57	102.84	22.6	5.1	19.6	19	32	29.9	45.16	-11.78	112.4	
30.2	44.2	-12.17	-15.27	-26.51	-26.36	159.42	103.49	14.7	5.4	20.1	19	32	33.3	45.40	-12.57	112.3	
30.3	32.6	-8.36	-9.69	-23.25	-23.45	144.36	116.65	3.8	5.7	19.8	19	32	36.6	45.77	-13.81	112.2	
30.4	17.5	1.81	2.25	-14.65	-14.00	140.71	132.34	-5.8	6.4	19.4	19	32	39.3	46.15	-15.12	111.4	
30.5	1.3	13.45	13.79	-4.21	-3.79	149.71	145.68	-20.5	7.6	19.0	19	32	41.5	46.49	-16.37	119.5	
31.1	50.7	-16.07	-21.66	-31.62	-30.53	167.66	103.46	30.7	4.6	19.2	19	32	45.1	44.73	-10.58	113.3	
31.2	44.1	-12.14	-16.15	-27.32	-27.34	157.77	106.80	25.8	5.0	19.4	19	32	48.6	44.99	-11.37	113.2	
31.3	32.5	-7.77	-8.99	-22.72	-22.54	144.44	115.16	14.9	5.4	20.1	19	32	51.8	45.38	-12.60	113.1	
31.4	17.5	2.20	2.59	-13.71	-14.50	131.89	124.07	2.2	5.7	19.8	19	32	54.6	45.77	-13.89	112.8	
31.5	1.4	12.66	12.73	-5.03	-4.68	137.97	135.94	-12.0	6.3	19.4	19	32	58.8	46.12	-15.11	118.0	
32.1	50.8	-21.09	-28.11	-42.80	-37.95	165.36	97.55	28.8	3.5	19.3	19	33	0.3	44.30	-9.43	114.2	
32.2	44.1	-14.33	-18.37	-29.95	-29.63	155.51	105.10	32.9	4.4	19.4	19	33	3.8	44.57	-10.19	114.1	
32.3	32.6	-8.64	-10.01	-23.99	-24.01	141.64	114.45	25.0	5.0	19.4	19	33	7.1	44.96	-11.39	114.0	
32.4	17.5	2.42	2.62	-14.71	-14.35	132.05	121.57	14.1	5.4	20.1	19	33	9.8	45.37	-12.66	113.9	
32.5	1.4	12.59	12.93	-4.36	-4.41	128.44	127.40	-9.5	5.7	19.8	19	33	12.0	45.74	-13.88	116.5	

09/05/75

DOY 252-1. 9/ 9/73 ITNC, NORTH ATLANTIC

SCAN NUMB	INCID ANGLE (DEG)	SCATTERING COEFFICIENTS				ANTENNA V (DEG)	TEMPS H (DEG)	ASPECT ANGLE (DEG)	WIND SPEED (M/S)	SEA TEMP (DEG)	GMT (HR MIN SEC)	CELL COORDINATES		S193 DATA	
		VV (DB)	HH (DB)	VH (DB)	HV (DB)							LAT (DEG)	LONG (DEG)	AZIMTH (DEG)	FLAG
33.1	50.8	-33.10	-33.64	-39.16	-45.81	168.94	98.09	-4.1	2.6	19.1	19 33 15.5	43.85	-8.25	115.1	2
33.2	44.3	-23.67	-28.13	-40.39	-34.88	153.51	102.00	23.0	2.9	19.0	19 33 19.1	44.12	-9.01	115.0	
33.3	32.6	-10.57	-11.86	-26.49	-26.18	141.82	111.98	32.2	4.3	19.4	19 33 22.3	44.54	-10.21	114.8	
33.4	17.5	1.88	1.65	-14.06	-14.98	130.67	123.71	24.2	5.0	19.4	19 33 25.1	44.96	-11.47	114.8	
33.5	1.5	12.77	13.33	-4.47	-4.34	129.54	124.88	10.2	5.4	20.1	19 33 27.3	45.34	-12.66	117.8	
34.1	50.7	-11.04	-10.66	-16.61	-16.40	262.32	259.54	-36.9	3.0		19 33 30.8	43.40	-7.13	115.9	1
34.2	44.2	-11.71	-9.84	-15.46	-16.70	251.04	211.36	-17.9	2.7		19 33 34.3	43.67	-7.88	115.9	1
34.3	32.6	-16.97	-18.45	-33.32	-35.41	138.97	111.76	23.3	3.0	19.0	19 33 37.6	44.10	-9.04	115.7	
34.4	17.5	0.99	1.19	-14.97	-14.65	130.25	119.75	32.5	4.4	19.4	19 33 40.3	44.53	-10.28	115.5	
34.5	1.4	13.13	13.62	-4.29	-4.15	128.49	126.37	29.1	5.0	19.4	19 33 42.5	44.93	-11.46	118.9	
35.1	50.8	-11.92	-11.57	-17.99	-17.82	261.53	257.72	-47.8	2.9		19 33 46.1	42.93	-6.00	116.8	1
35.2	44.1	-10.39	-9.79	-15.88	-15.95	262.56	261.85	-42.7	3.0		19 33 49.6	43.21	-6.75	116.7	1
35.3															
35.4															
35.5															

JSC - 2/ 9/75

S. TRUTH - 5/31/75

LAST MOD - 8/28/75

THIS LISTING - 09/05/75

REPRODUCIBILITY OF THE
ORIGINAL DATA IS POOR

DOY 334-1, 11/30/73 CTNC-L/R, GULF OF MEXICO

(LEFT SIDE)

SCAR NUMB	IRCID ANGLE (DEG)	SCATTERING COEFFICIENTS				ANTENNA V (DEG)	TEMPS H (DEG)	ASPECT ANGLE (DEG)	WIND SPEED (M/S)	SEA TEMP (DEG)	GMT (HR MIN SEC)	CELL COORDINATES		S193 AZINTH (DEG)	DATA FLAG
		VV (DB)	HH (DB)	VH (DB)	HV (DB)							LAT (DEG)	LONG (DEG)		
1.1	30.1					130.29	95.32	-37.0	8.4		16 41 28.6	27.18	-68.20	46.0	
1.2	42.4					133.05	104.58	-31.0	8.5		16 41 32.1	26.36	-68.83	46.0	
1.3	31.2					133.61	113.50	-25.1	8.4		16 41 35.3	25.47	-69.55	46.1	
1.4	16.7					128.10	120.64	-17.8	8.2		16 41 37.9	24.56	-70.32	46.8	
1.5															
3.1	30.2	-7.86	-10.98	-13.15	-11.08	131.21	97.51	-31.7	5.8		16 41 58.7	25.78	-66.86	46.7	
3.2	42.4	-9.56	-9.35	-9.61	-12.11	135.24	104.65	-21.6	5.4		16 42 2.2	24.95	-67.49	46.6	
3.3	31.3	-7.97	-7.81	-8.74	-15.92	133.15	111.78	-7.6	5.7		16 42 5.4	24.07	-68.21	46.6	
3.4	16.7	3.31	1.47	-0.60	-0.73	127.24	120.65	2.8	6.2		16 42 8.2	23.16	-68.98	47.2	
3.5	0.7	17.12	15.17	13.24	13.24	128.32	126.58	-34.2	6.5		16 42 10.4	22.31	-69.72	92.2	

JSC - 7/31/75

S. TRUTH - 8/10/75

LAST MOD - 7/11/75

THIS LISTING - 10/21/75

DOY 334-1, 11/30/73 CTNC-L/R, GULF OF MEXICO

SCAN NUMB	INCID ANGLE (DEG)	SCATTERING COEFFICIENTS				ANTENNA V (DEG)	TEMP H (DEG)	ASPECT ANGLE (DEG)	(RIGHT SIDE)						
		VV (DB)	HH (DB)	VH (DB)	HV (DB)				WIND SPEED (M/S)	SEA TEMP (DEG)	GMT (HR MIN SEC)	CELL COORDINATES		S193 AZIMTH (DEG)	DATA FLAG
												LAT (DEG)	LONG (DEG)		
2.1	48.2	-9.42	-10.62	-11.17	-11.59	139.30	111.10	-104.6	7.4		16 41 43.4	20.68	-73.98	224.6	
2.2	41.6	-3.80	-5.95	-7.80	-7.40	149.22	126.12	-154.5	7.9		16 41 46.9	21.08	-73.23	224.5	
2.3	31.0	-5.68	-7.52	-11.79	-11.78	140.95	125.53	-162.2	7.4		16 41 50.2	21.66	-72.33	224.2	2
2.4	16.7	5.59	3.99	1.81	1.66	132.78	127.46	-171.8	7.1		16 41 52.9	22.31	-71.37	223.8	
2.5	0.7	17.13	15.20	13.17	13.15	126.26	127.86	-160.5	7.0		16 41 55.1	22.97	-70.45	186.5	
4.1	48.3	-4.43	-6.04	-8.48	-7.24	149.57	126.02	-147.1	7.4		16 42 13.9	19.28	-72.65	225.1	
4.2	41.6	-3.76	-6.93	-9.19	-6.89	153.91	135.05	-155.1	7.5		16 42 17.4	19.69	-71.89	225.1	
4.3															
4.4															
4.5															

JSC - 7/31/75

S. TRUTH - 8/10/75

LAST MOD - 9/11/75

THIS LISTING - 10/21/75

DOY 338-1; 12/ 4/73 CTNC-L/R, NORTH PACIFIC										(LEFT SIDE)				
SCAR NUMB	IRCID ANGLE (DEG)	SCATTERING COEFFICIENTS				ANTENNA V (DEG)	TEMPS H (DEG)	ASPECT ANGLE (DEG)	WIND SPEED (M/S)	SEA TEMP (DEG)	GMT (HR MIN SEC)	CELL COORDINATES		S193 DATA AZIMTH FLAG (DEG)
		VV (DB)	HH (DB)	VH (DB)	HV (DB)							LAT (DEG)	LONG (DEG)	
1.1	50.2					120.72	92.81	-149.7	7.7		16 45 19.9	53.22	-147.58	12.7
1.2	42.3						101.25	-141.1	9.3		16 45 24.0	52.23	-147.54	13.1
1.3	31.3					125.53	109.13	-157.7	10.0		16 45 26.6	51.16	-147.67	13.7
1.4	16.7					120.50	114.48	-158.9	9.9		16 45 29.2	50.04	-147.60	15.9
1.5														
3.1	50.2	-11.42	-11.23	-10.11	-13.04	124.55	95.74	-160.0	9.9		16 45 49.9	52.74	-144.60	15.0
3.2	42.5	-8.27	-10.39	-10.98	-10.98	128.17	103.70	-161.3	10.7		16 45 53.5	51.77	-144.68	15.3
3.3	31.3	-5.29	-6.41	-9.10	-12.05	127.68	112.92	-166.3	11.4		16 45 56.7	50.69	-144.82	16.3
3.4	16.8	6.24	4.21	2.26	2.26	122.64	115.75	-164.5	11.4		16 45 59.5	49.57	-145.01	17.5
3.5	1.2	15.25	13.46	11.26	10.94	117.77	118.30	175.7	11.2		16 46 1.7	48.51	-145.23	74.3
5.1	50.2	-10.42	-10.53	-12.03	-13.05	127.04	99.91	-164.0	9.2		16 46 20.4	52.18	-141.68	17.0
5.2	42.4	-7.71	-9.16	-12.18	-12.17	131.50	107.85	-167.5	10.7		16 46 24.0	51.21	-141.61	17.5
5.3	31.3	-3.97	-6.44	-8.55	-9.19	131.09	115.48	-168.1	11.6		16 46 27.2	50.13	-142.01	18.1
5.4	16.7	6.80	4.63	2.73	2.94	125.58	120.02	-162.7	11.7		16 46 30.0	49.02	-142.26	19.7
5.5	1.1	15.01	13.09	11.01	11.06	120.71	122.07	165.1	11.7		16 46 32.2	47.96	-142.53	77.9
7.1	50.2	-6.06	-10.14	-11.34	-10.42	129.95	104.00	-160.9	9.3		16 46 50.9	51.55	-138.81	18.9
7.2	42.5	-4.45	-8.19	-9.26	-8.03	133.98	112.00	-160.5	10.5		16 46 54.5	50.59	-138.99	19.5
7.3	31.3	-0.76	-3.92	-5.93	-5.61	133.64	118.93	-166.2	11.1		16 46 57.7	49.50	-139.26	20.2
7.4	16.7	7.64	5.52	3.80	3.57	127.25	123.86	-158.1	11.1		16 47 0.5	48.40	-139.57	22.1
7.5	1.0	14.93	13.03	10.73	10.87	123.59	123.29	143.3	10.3		16 47 2.6	47.34	-139.90	84.7
9.1	50.2	-7.19	-9.91	-9.41	-10.42	131.55	106.98	175.0	11.8		16 47 21.4	50.85	-136.03	21.0
9.2	42.4	-5.00	-7.34	-7.92	-10.04	136.04	114.05	172.6	12.5		16 47 25.0	49.88	-136.26	21.4
9.3	31.2	-2.15	-4.37	-5.87	-7.49	134.88	120.98	171.9	12.4		16 47 28.2	48.81	-136.58	22.1
9.4	16.7	7.81	5.69	3.99	3.81	128.92	122.41	174.2	10.9		16 47 31.0	47.71	-136.95	23.8
9.5	1.1	14.81	12.70	10.87	10.67	123.92	123.60	161.0	8.9		16 47 33.2	46.66	-137.32	84.0
11.1	50.2	-7.82	-12.08	-10.97	-11.75	129.77	106.86	162.1	11.9		16 47 51.9	50.07	-133.33	22.9
11.2	42.4	-6.74	-9.16	-10.98	-10.03	134.61	114.36	157.6	11.1		16 47 55.5	49.12	-133.62	23.4
11.3	31.3	-3.70	-6.72	-9.18	-9.07	133.42	120.43	154.9	10.2		16 47 58.7	48.06	-133.98	24.1
11.4	16.7	6.31	4.33	2.50	2.41	127.07	124.03	156.0	10.0		16 48 1.5	46.96	-134.40	26.0
11.5	1.1	14.93	13.61	11.41	11.37	123.42	126.48	16.7	0.8		16 48 3.7	45.92	-134.82	88.3
13.1	50.2	-8.92	-12.44	-11.33	-11.75	131.75	110.14	158.2	10.0		16 48 22.4	49.25	-130.72	24.8
13.2	42.4	-8.99	-10.38	-12.18	-12.33	135.38	117.62	153.7	9.7		16 48 26.0	48.29	-131.05	25.3
13.3	31.3	-4.69	-7.36	-10.84	-9.92	135.09	122.06	151.1	9.6		16 48 29.2	47.24	-131.47	25.9
13.4	16.8	6.49	4.48	2.84	2.60	128.71	124.40	166.2	9.9		16 48 32.0	46.16	-131.93	27.8
13.5	1.0	14.78	13.11	11.07	10.88	126.73	127.66	72.5	9.7		16 48 34.1	45.12	-132.40	98.5
15.1	50.1	-8.69	-11.54	-11.33	-10.42	134.66	115.13	148.4	7.8		16 48 52.9	48.35	-128.22	26.6
15.2	42.4	-9.79	-11.15	-12.17	-12.33	137.83	120.89	145.0	7.9		16 48 56.5	47.41	-128.57	27.0
15.3	31.4	-5.57	-7.73	-10.63	-9.92	136.30	124.12	142.2	8.3		16 48 59.7	46.37	-129.03	27.8
15.4	16.7	5.98	4.00	2.16	1.88	130.34	125.63	133.9	9.1		16 49 2.5	45.29	-129.54	29.1
15.5	1.0	15.70	14.10	11.70	11.57	125.77	124.59	68.0	9.7		16 49 4.6	44.27	-130.64	90.0

10/21/75

DOY 338-1; 12/ 4/73 CTNC-L/R, NORTH PACIFIC

(LEFT SIDE)

SCAN NUMB	INCID ANGLE (DEG)	SCATTERING COEFFICIENTS				ANTENNA V (DEG)	TEMPS H (DEG)	ASPECT ANGLE (DEG)	WIND SPEED (M/S)	SEA TEMP (DEG)	GHT (HR MIN SEC)	CELL COORDINATES		S193 AZIMTH (DEG)	DATA FLAG
		VV (DB)	HH (DB)	VH (DB)	HV (DB)							LAT (DEG)	LONG (DEG)		
17.1	50.2	-9.33	-12.46	-12.50	-11.34	139.28	122.71	114.6	5.0		16 49 23.4	47.41	-125.78	28.4	
17.2	42.4	-9.78	-9.73	-10.98	-12.33	144.58	130.96	117.2	3.4		16 49 27.0	46.47	-126.19	28.8	
17.3	31.3	-7.12	-10.40	-26.77	-16.13	143.68	134.07	122.4	6.1		16 49 30.2	45.44	-126.68	29.6	-2
17.4	16.6	4.59	2.92	1.17	0.73	137.25	134.23	121.9	6.8		16 49 33.0	44.37	-127.22	31.1	
17.5	1.1	16.26	14.66	12.81	12.72	130.88	130.06	80.7	7.5		16 49 35.2	43.36	-127.76	92.3	
19.1	50.1	-3.91	-5.51	-7.89	-7.60	166.97	157.46	104.0	3.3		16 49 53.9	46.41	-123.45	30.0	1
19.2	42.5	-3.54	-6.89	-7.88	-6.91	172.14	167.33	112.6	3.7		16 49 57.5	45.49	-123.88	30.4	1
19.3	31.2	-5.65	-6.44	-10.58	-10.58	166.72	160.48	116.9	4.3		16 50 0.7	44.45	-124.41	31.1	
19.4	16.7	5.76	3.69	1.93	1.69	160.36	158.93	117.9	4.6		16 50 3.5	43.40	-124.98	33.1	
19.5	1.1	17.56	15.65	13.51	13.50	150.56	150.95	76.5	4.8		16 50 5.6	42.41	-125.54	96.5	
21.1	50.1	-8.91				185.70		102.4	2.3		16 50 24.4	45.37	-121.20	31.6	
21.2															
21.3															
21.4															
21.5															

JSC - 8/ 1/75

S. TRUTH - 8/10/75

LAST MOD - 7/11/75

THIS LISTING - 10/21/75

DOY 338-1, 12/ 4/73 CYNC-L/R, NORTH PACIFIC

(RIGHT SIDE)

SCAN NUMB	INCID ANGLE (DEG)	SCATTERING COEFFICIENTS				ANTENNA V (DEG)	TEMP H (DEG)	ASPECT ANGLE (DEG)	WIND SPEED (M/S)	SEA TEMP (DEG)	GMT (HR MIN SEC)	CELL COORDINATES		3193 DATA AZIMTH FLAG (DEG)
		VV (DB)	HH (DB)	VH (DB)	HV (DB)							LAT (DEG)	LONG (DEG)	
2.1	48.0	-8.48	-11.23	-11.93	-13.20	125.86	93.64	82.4	7.2		16 45 34.7	43.05	-148.88	191.6
2.2	41.2	-6.47	-8.76	-10.13	-12.44	126.77	100.59	85.2	7.0		16 45 38.2	43.78	-148.36	191.8
2.3	30.8	-5.98	-7.05	-9.13	-10.91	125.33	106.19	80.5	8.9		16 45 41.5	46.69	-147.78	191.5
2.4	16.6	5.85	4.02	1.73	1.98	119.39	114.23	87.0	9.5		16 45 44.2	47.69	-147.18	190.0
2.5	1.1	15.25		11.42	11.36	117.36	116.17	152.2	10.2		16 45 46.5	48.69	-146.61	130.8
4.1	48.1	-9.73	-10.92	-11.49	-11.89	126.25	94.03	80.2	10.0		16 46 5.2	44.58	-146.34	193.8
4.2	41.4	-7.27	-9.80	-11.05	-10.11	128.48	100.98	82.2	10.2		16 46 8.7	43.29	-145.77	193.8
4.3	30.8	-5.31	-6.77	-12.07	-9.98	126.60	108.77	85.6	10.6		16 46 12.0	46.20	-145.14	193.4
4.4	16.6	5.99	4.17	2.19	2.02	122.82	115.46	89.9	11.3		16 46 14.7	47.19	-144.51	192.1
4.5	1.0	15.23	13.15	11.16	10.90	118.99	119.94	111.9	11.6		16 46 16.9	48.18	-143.91	136.1
6.1	48.2	-9.05	-10.64	-11.03	-11.88	127.02	95.23	89.1	9.9		16 46 35.7	44.05	-143.82	195.9
6.2	41.5	-8.40	-9.16	-9.99	-14.15	129.67	102.86	88.3	10.1		16 46 39.2	46.75	-143.23	195.7
6.3	30.9	-5.01	-7.79	-10.89	-10.89	128.28	109.57	86.5	10.5		16 46 42.5	45.65	-142.57	195.5
6.4	16.6	5.83	3.91	2.99	2.00	122.74	117.57	84.5	10.9		16 46 45.2	46.63	-141.86	194.5
6.5	1.0	14.54	12.89	10.83	10.35	121.94	122.44	102.0	11.0		16 46 47.4	47.60	-141.24	134.0
8.1	48.4	-10.88	-11.66	-11.46	-16.03	127.80	95.58	81.1	8.6		16 47 6.2	43.45	-141.37	197.9
8.2	41.5	-7.25	-9.78	-11.02	-11.03	130.46	102.95	85.2	8.3		16 47 9.7	44.15	-140.75	197.8
8.3	30.9	-5.29	-7.42	-9.97	-9.97	128.65	111.24	83.3	8.1		16 47 13.0	45.03	-140.05	197.7
8.4	16.7	6.43	4.51	2.73	2.67	126.62	119.24	82.0	8.5		16 47 15.7	45.99	-139.33	196.0
8.5	-1.2	14.18	12.55	10.42	10.26	124.02	126.18	79.4	9.4		16 47 17.9	46.95	-138.63	137.6
10.1	48.4	-8.22	-11.64	-12.61	-11.44	128.11	95.88	88.2	6.9		16 47 36.7	42.81	-138.97	199.8
10.2	41.6	-9.04	-9.71	-10.90	-12.37	131.62	104.10	81.3	6.0		16 47 40.2	43.49	-138.32	199.7
10.3	30.9	-7.66	-8.55	-11.84	-13.62	129.41	110.68	85.4	5.7		16 47 43.5	44.35	-137.58	199.6
10.4	16.7	5.68	3.82	1.79	1.86	126.51	120.44	7.2	6.8		16 47 46.2	45.30	-136.83	197.8
10.5	1.1	14.66	12.78	10.73	10.78	124.32	123.96	82.8	8.4		16 47 48.4	46.24	-135.10	141.2
12.1	48.4	-9.42	-11.63	-12.59	-10.51	128.86	97.88	88.4	4.4		16 48 7.2	42.10	-135.62	201.6
12.2	41.6	-7.79	-11.29	-11.13	-11.13	132.36	106.10	8.5	4.9		16 48 10.7	42.76	-135.95	201.3
12.3	31.0	-3.16	-5.44	-7.49	-7.99	131.93	114.50	-15.1	6.4		16 48 14.0	43.61	-135.19	201.1
12.4	16.8	5.71	3.98	1.90	1.69	127.70	121.20	-19.9	8.0		16 48 16.7	44.54	-134.40	199.9
12.5	1.2	14.91	13.19	10.83	11.10	125.07	123.86	87.8	9.2		16 48 18.9	45.47	-133.63	139.2
14.1	48.4	-7.26	-14.26	-11.84	-10.51	131.70	99.88	-14.4	5.9		16 48 37.7	41.34	-134.33	203.4
14.2	41.6	-6.40	-8.64	-9.98	-11.13	134.38	108.53	-85.4	7.0		16 48 41.2	41.99	-133.65	203.4
14.3	31.0	-2.77	-5.91	-7.99	-6.99	133.14	114.38	-83.2	8.2		16 48 44.5	42.83	-132.86	203.2
14.4	16.7	6.05	3.96	2.22	1.84	129.80	121.96	-86.0	9.4		16 48 47.2	43.74	-132.04	202.0
14.5	1.2	15.21	13.34	11.20	11.20	126.30	125.03	82.0	9.8		16 48 49.4	44.64	-131.24	144.0
16.1	48.4	-8.84	-10.88	-10.52	-9.74	132.53	100.81	-83.3	7.5		16 49 8.2	40.53	-132.11	203.3
16.2	41.7	-6.02	-8.68	-9.28	-9.37	134.67	108.03	-82.1	7.9		16 49 11.7	41.15	-131.41	203.1
16.3	31.0	-3.56	-5.43	-7.49	-10.06	132.63	114.27	-89.8	8.2		16 49 15.0	41.98	-130.59	204.8
16.4	16.7	5.61	3.93	1.95	1.69	127.09	119.70	-85.7	8.6		16 49 17.7	42.87	-129.75	203.7
16.5	1.1	16.30	14.14	12.29	11.95	126.61	125.40	8.8	8.8		16 49 19.9	43.76	-128.94	152.2

10/21/75

DOY 338-1. 12/ 4/73 CTNC-L/R, NORTH PACIFIC														(RIGHT SIDE)			S193 DATA	
SCAN NUMB	INCID ANGLE (DEG)	SCATTERING COEFFICIENTS				ANTENNA V (DEG)	TEMPS H (DEG)	ASPECT ANGLE (DEG)	WIND SPEED (M/S)	SEA TEMP (DEG)	GMT (HR MIN SEC)	CELL COORDINATES		S193 DATA AZIMTH FLAG (DEG)				
		VV (DB)	HH (DB)	VH (DB)	HV (DB)							LAT (DEG)	LONG (DEG)					
18.1	48.4	-7.70	-11.00	-12.56	-11.40	132.41	100.12	-22.9	6.3		16 49 38.7	39.66	-129.94	206.9				
18.2	41.6	-7.84	-10.48	-12.35	-12.53	135.46	107.88	-32.9	6.3		16 49 42.2	40.28	-129.23	206.9				
18.3	30.9	-6.24	-8.17	-12.01	-11.83	134.72	117.95	-10.4	6.2		16 49 45.5	41.09	-128.39	206.4				
18.4	16.8	3.63	2.03	-0.16	-0.57	132.69	124.80	-47.1	6.2		16 49 48.2	41.96	-127.53	205.1				
18.5																		
20.1	48.4	-9.12	-13.42	-12.30	-10.22	137.85	104.89	-16.3	3.6		16 50 9.2	38.75	-127.63	208.3				
20.2	41.7	-7.99	-8.84	-10.59	-11.92	142.62	115.84	-29.5	3.4		16 50 12.7	39.34	-127.12	208.5				
20.3	31.0	-7.92	-8.33	-15.88	-13.33	146.89	129.79	-43.0	3.6		16 50 16.0	40.14	-126.26	208.0				
20.4	16.8	3.27	1.24	-0.57	-1.14	153.67	146.57	-50.0	3.8		16 50 18.7	40.99	-125.39	207.0				
20.5	1.1	18.29	16.18	14.50	14.01	166.06	166.80	-1.9	3.9		16 50 20.9	41.85	-124.52	154.9				

JSC - 8/ 1/75

S. TRUTH - 8/10/75

LAST MOD - 9/11/75

THIS LISTING - 10/21/75

REPRODUCIBILITY OF THE
ORIGINAL PAGE IS POOR

DOY 4-1, 1/ 4/74 CTNC-L/R, NORTH ATLANTIC

(LEFT SIDE)

SCAR NUMB	INCID ANGLE (DEG)	SCATTERING COEFFICIENTS				ANTENNA V (DEG)	TEMPS H (DEG)	ASPECT ANGLE (DEG)	WIND SPEED (KTS)	SEA TEMP (DEG)	GMT (HR MIN SEC)	CELL COORDINATES		S193 AZINTH (DEG)	DATA FLAG
		VV (DB)	HH (DB)	VH (DB)	HV (DB)							LAT (DEG)	LONG (DEG)		
1.1	50.4					185.70	179.88	-62.9	3.2		19 29 39.2	48.29	-72.70	333.9	1
1.2	42.8					200.16	193.87	-67.1	3.5		19 29 42.6	47.55	-71.78	334.1	1
1.3	31.7					208.59	205.56	-71.1	3.4		19 29 45.8	46.68	-70.81	334.1	1
1.4	17.1					209.76	207.56	-64.8	3.2		19 29 48.4	45.76	-69.88	334.8	1
1.5															
3.1	50.6	-2.54	-4.01	-5.53	-5.80	184.87	177.78	-57.6	2.1		19 30 9.2	49.18	-70.26	335.6	1
3.2	42.9	-5.27	-4.82	-6.21	-9.03	191.25	182.04	-75.8	2.8		19 30 12.7	48.42	-69.33	335.8	1
3.3	31.6	0.60	-0.85	-2.82	-2.98	205.12	200.81	-73.1	3.2		19 30 16.0	47.54	-68.38	336.1	1
3.4	17.1	-0.01	-1.96	-3.69	-3.94	204.92	204.86	-55.4	3.1		19 30 18.7	46.59	-67.47	336.4	1
3.5	1.0	10.05	8.17	5.92	7.39	195.80	194.60	-36.6	2.2		19 30 20.9	45.68	-66.67	336.6	1
5.1	50.5	-0.35	-2.07	-4.12	-3.77	175.93	166.76	-57.5	3.0		19 30 39.7	50.01	-67.66	337.5	1
5.2	42.9	-4.72	-6.73	-6.99	-7.89	182.77	174.03	-75.5	4.2		19 30 43.2	49.24	-66.76	337.5	1
5.3	31.8	-1.05	-2.97	-4.75	-4.51	192.04	186.50	-57.6	5.0		19 30 46.4	48.34	-65.84	338.0	1
5.4	17.2	-1.88	-2.38	-4.51	-7.44	187.90	183.68	-55.1	5.5		19 30 49.2	47.37	-64.97	338.1	1
5.5	1.0					176.46	177.06	-49.1	5.8		19 30 51.5	46.44	-64.19	339.1	1
7.1	50.5	-0.61	-1.93	-3.84	-3.95	163.96	152.73	-48.5	7.3		19 31 10.2	50.79	-64.97	339.5	2
7.2	42.9	-0.84	-2.74	-4.54	-4.78	167.02	154.55	-43.7	7.9		19 31 13.7	50.00	-64.10	339.7	2
7.3	31.8	-2.32	-4.78	-6.84	-6.83	162.77	154.76	-47.7	8.7		19 31 16.9	49.07	-63.22	339.7	2
7.4	17.2	6.75	4.74	3.01	2.96	157.73	154.52	-41.2	9.5		19 31 19.7	48.09	-62.39	340.2	2
7.5	1.0	15.86	14.07	11.99	11.97	149.76	147.06	-53.6	10.2		19 31 21.9	47.14	-61.65	341.6	2
9.1	50.5	-1.23	-2.90	-5.06	-4.82	158.83	145.93	-48.5	11.9		19 31 40.7	51.51	-62.19	341.5	1
9.2	42.9	-0.86	-2.63	-4.11	-4.84	165.74	154.55	-43.4	12.4		19 31 44.2	50.69	-61.58	341.4	2
9.3	31.8	-2.04	-4.60	-7.25	-6.47	159.70	150.85	-49.0	12.9		19 31 47.4	49.75	-60.51	342.0	
9.4	17.2	7.18	5.42	3.46	3.60	155.97	152.54	-51.0	13.3		19 31 50.2	48.75	-59.72	342.0	
9.5	1.0	18.77	17.90	13.46	13.15	160.51	159.49	-59.7	13.5		19 31 52.4	47.78	-59.03	347.7	2
11.1	50.5	-1.10	-2.23	-3.88	-4.15	160.96	146.78	-45.4	16.0		19 32 11.2	52.14	-59.34	343.4	1
11.2	42.9	-3.59	-4.47	-6.22	-7.00	167.01	154.11	-51.7	16.6		19 32 14.7	51.32	-58.55	343.7	2
11.3	31.8	-2.48	-5.89	-8.30	-6.85	165.37	159.52	-44.8	16.5		19 32 18.0	50.35	-57.74	343.8	1
11.4	17.1	1.52	-0.94	-3.45	-3.45	173.02	172.35	-57.1	16.1		19 32 20.7	49.33	-57.00	344.1	1
11.5	1.0	21.34	21.75	17.48	15.74	168.68	168.47	-48.1	14.7		19 32 22.9	48.34	-56.36	340.1	1
13.1	50.5	-2.30	-3.58	-5.20	-6.10	157.11	139.11	-52.6	19.5		19 32 41.7	52.72	-56.39	345.6	1
13.2	42.8	-5.86	-7.65	-8.31	-8.91	158.06	139.72	-57.8	19.9		19 32 45.2	51.86	-55.65	345.8	2
13.3	31.8	-1.91	-4.78	-5.80	-6.47	157.10	143.92	-61.1	19.7		19 32 48.4	50.89	-54.90	346.1	
13.4	17.2	5.97	4.17	1.93	2.20	157.31	152.80	-58.2	18.6		19 32 51.2	49.85	-54.21	346.2	2
13.5	1.0	13.97	12.67	10.32	10.22	151.49	150.94	-58.0	17.6		19 32 53.4	48.85	-53.61	345.0	1
15.1	50.5	-6.62	-8.54	-8.82	-10.71	137.93	111.96	-49.8	19.0		19 33 12.2	53.21	-53.39	347.8	
15.2	42.9	-4.94	-7.26	-8.26	-8.31	141.94	119.87	-51.9	20.5		19 33 15.7	52.34	-52.69	347.9	
15.3	31.7	-1.78	-4.10	-6.47	-6.13	143.99	129.58	-56.2	20.4		19 33 19.0	51.34	-52.00	348.2	
15.4	17.2	6.65	5.03	3.17	2.99	141.12	134.09	-61.4	20.1		19 33 21.7	50.29	-51.36	348.4	
15.5	1.0	12.52	10.37	9.61	8.28	138.14	135.52	-61.1	19.9		19 33 23.9	49.27	-50.83	345.1	

10/21/75

A40

DOY 4-1, 1/ 4/74 CTNC-L/R, NORTH ATLANTIC											(LEFT SIDE)			
SCAN NUMB	INCID ANGLE (DEG)	SCATTERING COEFFICIENTS				ANTENNA V (DEG)	TEMPS H (DEG)	ASPECT ANGLE (DEG)	WIND SPEED (M/PS)	SEA TEMP (DEG)	GMT (HR MIN SEC)	CELL COORDINATES		S193 DATA AZIMUTH FLAG (DEG)
		VV (DB)	HH (DB)	VH (DB)	HV (DB)							LAT (DEG)	LONG (DEG)	
											19 33 42.7	53.62	-50.32	350.0
17.1	50.5	-8.71	-9.74	-10.57	-12.37	131.52	103.04	-40.0	14.3		19 33 46.2	52.74	-49.66	350.3
17.2	42.9	-5.56	-6.96	-7.75	-10.49	135.56	111.82	-50.3	15.6		19 33 49.4	51.72	-49.03	350.4
17.3	31.8	-0.84	-3.91	-5.53	-5.24	137.88	121.31	-08.4	17.9		19 33 52.2	50.66	-48.46	350.9
17.4	17.2	6.97	4.91	3.06	3.16	134.57	128.44	-68.9	20.8		19 33 54.4	49.63	-47.98	353.8
17.5	1.0	12.62	10.61	8.61	8.36	131.68	133.56	-76.8	21.4					
											19 34 13.2	53.96	-47.18	352.4
19.1	50.5	-7.83	-11.86	-10.76	-13.06	129.38	100.48	-15.4	10.9		19 34 16.7	53.05	-46.59	352.6
19.2	42.8	-6.45	-9.81	-11.11	-11.25	133.85	108.85	-47.6	12.7		19 34 19.9	52.02	-46.03	352.6
19.3	31.7	-2.81	-5.22	-6.66	-6.65	136.56	119.56	-89.6	18.0		19 34 22.7	50.94	-49.53	352.6
19.4	17.2	6.92	4.98	3.26	2.86	133.25	127.12	-72.6	20.7		19 34 24.9	49.91	-45.11	344.9
19.5	1.0	12.83	10.51	9.66	8.33	130.81	132.50	-64.9	21.8					
											19 34 43.7	54.20	-44.01	354.6
21.1	50.5	-8.02	-11.89	-10.76	-12.22	125.91	96.22	-23.6	11.9		19 34 47.2	53.29	-43.48	354.8
21.2	42.9	-6.81	-9.23	-10.15	-9.36	132.57	105.47	-40.8	13.0		19 34 50.4	52.24	-42.98	353.1
21.3	31.8	-4.22	-7.47	-12.25	-8.00	133.50	116.52	-56.1	15.5		19 34 53.2	51.15	-42.55	353.0
21.4	17.2	6.92	4.91	3.18	3.10	131.05	123.20	-66.0	18.8		19 34 55.4	50.10	-42.20	0.4
21.5	1.0	13.06	11.04	9.19	8.98	130.80	130.56	-76.4	21.6					
											19 35 14.2	54.35	-40.81	356.8
23.1	50.4	-5.70	-9.29	-9.95	-11.13	128.09	97.07	-21.8	13.0		19 35 17.7	53.43	-40.34	357.1
23.2	42.8	-3.81	-7.13	-7.15	-8.11	132.14	106.30	-42.1	13.5		19 35 21.0	52.38	-39.92	357.3
23.3	31.8	-1.79	-3.79	-6.28	-7.64	132.61	116.08	-47.3	14.7		19 35 23.7	51.28	-39.56	357.2
23.4	17.2	7.48	5.67	3.84	3.65	130.61	122.77	-61.2	17.0		19 35 25.9	50.22	-39.27	353.2
23.5	1.0	14.71	12.70	10.64	10.45	129.08	128.20	-89.2	19.7					
											19 35 44.7	54.44	-37.55	359.3
25.1	50.5	-6.33	-9.61	-9.04	-10.25	129.75	99.58	-18.3	12.0		19 35 48.2	53.50	-37.18	359.4
25.2	42.9	-4.53	-6.47	-8.05	-8.18	134.61	107.93	-26.4	12.5		19 35 51.4	52.43	-36.83	359.7
25.3	31.8	-0.37	-3.24	-5.39	-4.08	133.90	117.35	-49.7	12.5		19 35 54.2	51.32	-36.55	359.6
25.4	17.2	7.81	5.93	4.38	4.13	130.15	123.60	-67.6	14.6		19 35 56.4	50.26	-36.33	359.3
25.5	1.1	13.82	12.18	9.56	10.16	129.48	129.94	-79.3	17.8					
											19 36 13.2	54.41	-34.33	1.6
27.1	50.5	-6.02	-8.83	-9.96	-11.13	130.15	99.55	-21.6	7.8		19 36 18.7	53.47	-34.01	1.8
27.2	42.9	-4.07	-6.53	-7.62	-7.68	135.47	109.22	-45.8	7.6		19 36 22.0	52.40	-33.74	1.9
27.3	31.8	-0.60	-2.84	-4.34	-5.40	136.02	119.07	-70.9	9.3		19 36 24.7	51.28	-33.54	1.9
27.4	17.2	7.56	5.62	3.94	3.82	132.73	126.61	-66.9	12.5		19 36 26.9	50.22	-33.40	0.8
27.5	1.0	13.42	11.75	9.63	9.30	129.44	129.87	-92.8	18.2					
											19 36 45.7	54.32	-31.11	3.9
29.1	50.5	-7.84	-10.18	-10.46	-10.78	130.12	99.10	-58.9	4.0		19 36 49.2	53.36	-30.86	4.0
29.2	42.9	-6.07	-7.93	-9.47	-10.28	134.60	107.96	-90.0	5.6		19 36 52.4	52.28	-30.67	4.5
29.3	31.8	-1.05	-3.37	-5.08	-6.02	135.62	117.33	-104.5	8.4		19 36 55.2	51.16	-30.54	4.1
29.4	17.2	7.21	5.02	3.15	3.15	132.75	125.76	-107.1	11.7		19 36 57.4	50.09	-30.46	1.4
29.5	1.0	13.52	11.17	9.21	9.17	130.32	129.44	-103.4	14.8					
											19 37 16.2	54.12	-27.91	6.2
31.1	50.5	-7.86	-10.18	-11.38	-10.80	128.42	96.99	-120.2	4.6		19 37 19.7	53.16	-27.75	6.2
31.2	42.8	-6.44	-9.86	-11.15	-9.41	132.47	106.22	-123.2	6.8		19 37 22.9	52.08	-27.62	6.6
31.3	31.8	-2.68	-5.72	-7.55	-7.55	135.12	116.39	-123.6	9.4		19 37 25.7	50.96	-27.57	6.4
31.4	17.2	7.55	5.40	3.57	3.68	129.21	123.55	-121.4	11.7		19 37 27.9	49.69	-27.55	4.8
31.5	1.0	13.23	11.18	9.12	8.96	131.56	129.83	-136.8	13.9					

10/21/75

DOY 4-17 1/ 4/74 CTNC-L/R, NORTH ATLANTIC

(LEFT SIDE)

SCAN NUMB	INCID ANGLE (DEG)	SCATTERING COEFFICIENTS				ANTENNA V (DEG)	TEMP H (DEG)	ASPECT ANGLE (DEG)	WIND SPEED (MPS)	SEA TEMP (DEG)	GMT (HR MIN SEC)	CELL COORDINATES		S193 AZIMUTH (DEG)	DATA FLAG
		VV (DB)	HH (DB)	VH (DB)	HV (DB)							LAT (DEG)	LONG (DEG)		
33.1	50.5	-8.98	-10.85	-11.39	-11.81	127.52	95.25	-140.5	7.8		19 37 46.7	53.84	-24.75	8.5	
33.2	42.8	-6.07	-10.54	-10.21	-10.21	132.43	104.50	-132.7	9.3		19 37 50.2	52.88	-24.64	8.7	
33.3	31.8	-0.43	-3.38	-4.60	-5.11	134.67	115.97	-140.0	11.0		19 37 53.4	51.80	-24.60	8.8	
33.4	17.1	8.46	6.47	4.64	4.45	131.35	123.95	-136.2	12.0		19 37 56.2	50.67	-24.62	9.2	
33.5	1.0	12.68	11.12	8.77	8.85	130.66	128.95	-125.5	13.0		19 37 58.4	49.61	-24.68	9.3	
35.1	50.4	-8.09	-10.86	-10.50	-12.29	128.76	97.76	-134.7	12.6		19 38 17.2	53.48	-21.64	10.7	
35.2	42.9	-5.41	-9.39	-9.42	-9.43	132.39	105.72	-134.8	14.3		19 38 20.7	52.52	-21.60	10.6	
35.3	31.7	-1.07	-4.36	-6.78	-5.69	134.19	114.61	-135.1	13.5		19 38 24.0	51.43	-21.63	11.1	
35.4	17.1	8.60	6.68	4.67	4.76	129.12	122.17	-131.2	12.7		19 38 26.7	50.31	-21.71	11.2	
35.5	1.0														
37.1	50.5	-5.53	-9.54	-8.97	-9.90	127.86	97.29	-135.9	14.5		19 38 47.7	53.03	-18.58	12.9	
37.2	42.8	-5.00	-7.04	-8.57	-8.06	132.76	106.53	-131.1	14.5		19 38 51.2	52.07	-18.61	13.1	
37.3	31.7	-3.11	-5.17	-7.96	-7.45	132.83	115.44	-135.3	13.8		19 38 54.4	50.99	-18.71	13.3	
37.4	17.1	7.66	5.66	3.71	3.66	125.98	119.84	-131.2	12.8		19 38 57.2	49.87	-18.87	13.2	
37.5	1.0	15.44	13.52	11.23	11.42	122.82	123.71	-130.3	11.9		19 38 59.4	48.82	-19.04	10.3	
39.1	50.4	-6.66	-10.35	-10.72	-11.08	128.70	99.40	-131.1	14.1		19 39 18.2	52.51	-15.59	15.1	
39.2	42.8	-8.39	-9.78	-10.12	-12.49	133.17	107.79	-136.1	13.4		19 39 21.7	51.54	-15.68	15.1	
39.3	31.7	-3.76	-5.15	-6.55	-9.26	132.81	115.44	-134.8	12.4		19 39 25.0	50.47	-15.84	15.0	
39.4	17.1	7.77	5.97	4.12	3.93	127.31	120.38	-138.2	11.1		19 39 27.7	49.36	-16.06	15.2	
39.5	0.9	15.18	13.50	11.27	11.09	125.82	123.29	-130.5	10.9		19 39 29.9	48.30	-16.31	10.5	
41.1	50.4	-6.54	-9.56	-9.65	-9.92	131.27	104.51	-135.2	13.6		19 39 48.7	51.90	-12.63	17.2	
41.2	42.8	-6.40	-8.69	-10.12	-10.22	136.59	112.33	-135.4	12.7		19 39 52.2	50.96	-12.82	17.4	
41.3	31.8	-2.60	-5.67	-9.28	-7.02	137.19	120.65	-136.6	11.3		19 39 55.4	49.88	-13.05	17.6	
41.4	17.1	7.46	5.30	3.54	3.47	129.08	124.74	-132.8	10.5		19 39 58.2	48.78	-13.33	17.8	
41.5	1.0	15.40	13.37	11.55	11.17	125.84	126.29	-137.0	10.5		19 40 0.4	47.73	-13.62	28.0	
43.1	50.5	-7.80	-11.86	-13.04	-13.03	135.98	110.85	-134.5	13.7		19 40 19.2	51.24	-9.63	19.5	
43.2	42.8	-7.30	-9.21	-12.33	-10.24	140.65	120.91	-135.4	12.4		19 40 22.7	50.28	-10.04	19.6	
43.3	31.7	-4.44	-7.44	-10.06	-7.96	142.44	130.21	-137.3	10.6		19 40 25.9	49.22	-10.32	19.7	
43.4	17.1	8.27	4.21	2.23	2.02	142.64	136.91	-138.7	10.6		19 40 28.7	48.13	-10.66	19.3	
43.5	1.0	14.50	12.72	10.74	10.28	134.02	134.91	-135.4	11.6		19 40 30.9	47.09	-11.00	16.4	
45.1	50.4	-6.69	-8.81	-9.94	-11.10	143.66	122.36	-135.7	15.3		19 40 49.7	50.50	-7.09	21.3	
45.2	42.8	-3.82	-6.80	-7.60	-7.65	148.51	129.35	-138.6	14.0		19 40 53.2	49.55	-7.35	21.4	
45.3	31.7	-0.38	-3.07	-4.31	-5.09	151.59	137.62	-137.5	12.6		19 40 56.4	48.49	-7.68	21.5	
45.4	17.1	7.81	5.50	3.93	3.84	147.01	143.01	-135.2	12.7		19 40 59.2	47.41	-8.07	21.8	
45.5	1.0	12.52	10.74	8.40	7.92	142.20	142.16	-134.4	15.1		19 41 1.4	46.38	-8.47	13.6	
47.1	50.3	-5.30	-8.63	-8.17	-9.28	147.95	127.85	-136.9	17.3		19 41 20.2	49.68	-4.44	23.1	
47.2	42.8	-3.44	-7.17	-8.18	-7.72	154.47	139.54	-134.8	15.9		19 41 23.7	48.75	-4.73	23.2	
47.3	31.7	-0.80	-3.40	-5.06	-5.67	153.37	141.96	-135.5	14.9		19 41 26.9	47.71	-5.11	23.5	
47.4	17.1	8.61	6.47	4.81	4.82	148.33	144.76	-130.7	16.4		19 41 29.7	46.63	-5.56	23.3	
47.5	1.0	14.09	12.29	10.16	10.26	147.82	148.15	-132.3	16.9		19 41 31.9	45.62	-5.99	18.7	

10/21/75

DOY 4-1, 3/ 4/74 CTNC-L/R. NORTH ATLANTIC

(LEFT SIDE)

SCAN NUMB	INCID ANGLE (DEG)	SCATTERING COEFFICIENTS				ANTENNA V (DEG)	TEMP H (DEG)	ASPECT ANGLE (DEG)	WIND SPED (MPS)	SEA TEMP (DEG)	GMT (HR MIN SEC)	CELL COORDINATES		9193 DATA	
		VV (DB)	HH (DB)	VH (DB)	HV (DB)							LAT (DEG)	LONG (DEG)	AZIMTH (DEG)	FLAG
49.1	50.4	-5.41	-8.03	-8.18	-8.91	160.33	146.16	185.1	15.3		19 41 50.7	48.83	-1.88	24.9	
49.2	42.8	-2.68	-4.35	-6.45	-5.70	174.69	163.66	149.9	14.7		19 41 54.2	47.90	-2.21	25.1	
49.3	31.7	-1.39	-4.48	-6.73	-7.13	165.65	157.16	149.9	14.6		19 41 57.4	46.86	-2.64	25.1	
49.4	17.1	8.03	5.77	4.03	4.06	162.80	161.32	153.9	13.7		19 42 0.2	45.79	-3.11	25.1	
49.5	1.0	15.23	13.56	11.38	11.47	163.35	163.18	152.8	13.2		19 42 2.4	44.79	-3.58	25.2	
51.1	50.3	-3.80	-5.38	-6.57	-6.69	183.00	174.96	159.3	14.2		19 42 21.2	47.90	0.60	26.7	
51.2	42.8	-2.71	-4.17	-5.75	-5.45	194.02	186.97	157.2	13.3		19 42 24.7	46.98	0.24	26.8	
51.3	31.7	-1.93	-3.55	-6.42	-6.02	202.32	199.80	155.9	12.1		19 42 27.9	45.95	-0.23	27.1	
51.4	17.1	-3.23	-5.84			203.89	207.43	159.4	11.1		19 42 30.7	44.90	-0.74	26.6	

JSC - 7/25/75

S. TRUTH - 6/19/75

LAST MOD - 7/11/75

THIS LISTING - 10/21/75

REPRODUCIBILITY OF THE
ORIGINAL PAGE IS POOR

DOY 4-1, 1/ 4/74 CTNC-L/R, NORTH ATLANTIC

(RIGHT SIDE)

SCAN NO	INCID ANGLE (DEG)	SCATTERING COEFFICIENTS				ANTENNA V (DEG)	TEMP H (DEG)	ASPECT ANGLE (DEG)	WIND SPD (M/S)	SEA TEMP (DEG)	GHT (HR MIN SEC)	CELL COORDINATES		S193 AZIMTH (DEG)	DATA FLAG
		VV (DB)	HH (DB)	VH (DB)	HV (DB)							LAT (DEG)	LONG (DEG)		
2.1	46.9	-8.36	-12.59	-11.47	-10.59	140.86	110.62	-112.9	9.0		19 29 53.9	41.44	-66.59	154.9	
2.2	40.5	-8.74	-14.24	-13.12	-11.61	147.76	121.36	-114.1	7.2		19 29 57.4	42.20	-66.73	155.1	
2.3	30.0	-10.86	-15.24	-14.10	-16.89	156.53	138.97	-119.2	5.0		19 30 0.7	43.16	-67.01	155.2	
2.4	16.0	0.48	-1.66	-2.90	-3.11	168.62	150.81	-139.4	2.5		19 30 3.4	44.20	-67.40	155.4	2
2.5	0.1	21.07	15.42	13.08	14.19	196.25	193.75	170.9	1.8		19 30 5.6	45.21	-67.85	159.1	1
4.1	47.1	-8.90	-13.67	-12.55	-11.46	143.44	113.20	-125.6	7.0		19 30 24.4	42.18	-64.28	155.6	
4.2	40.7	-9.43	-10.88	-11.60	-11.61	149.49	124.79	-126.6	6.3		19 30 27.9	42.95	-64.40	156.6	
4.3	30.0	-12.08	-10.54	-12.23	-14.09	158.35	141.17	-141.8	4.5		19 30 31.2	43.94	-64.65	156.8	2
4.4	16.0	-2.78	-4.24	-6.18	-6.65	180.95	171.93	177.2	2.9		19 30 33.9	44.98	-65.00	156.8	1
4.5	0.1	7.89	5.73	3.69	4.03	190.24	191.20	-134.6	3.6		19 30 36.1	46.01	-65.40	85.6	1
6.1	47.2	-8.04	-11.41	-11.09	-13.07	141.34	111.53	-122.6	6.2		19 30 54.9	42.88	-61.92	158.6	
6.2	40.6	-7.05	-10.81	-9.69	-9.60	147.39	121.01	-113.7	5.4		19 30 58.4	43.66	-62.01	158.7	
6.3	30.1	-7.03	-11.52	-17.53	-14.43	151.32	133.75	135.3	5.7		19 31 1.7	44.65	-62.23	158.7	2
6.4	16.0	1.80	-1.54	-2.91	-1.81	163.37	154.88	145.3	7.3		19 31 4.4	45.71	-62.53	158.7	1
6.5	0.1	15.68	14.01	11.84	11.97	157.50	157.56	139.1	7.9		19 31 6.6	46.73	-62.90	117.9	2
8.1	47.3	-8.35	-11.71	-12.56	-12.55	137.06	106.00	104.7	7.2		19 31 25.4	43.53	-59.52	160.3	
8.2	40.7	-8.14	-10.81	-11.48	-11.62	140.14	112.94	102.4	8.5		19 31 29.0	44.32	-59.57	160.6	
8.3	30.2	-4.93	-8.95	-12.64	-11.22	142.55	126.70	123.3	11.4		19 31 32.2	45.30	-59.74	160.7	
8.4	16.0	6.15	3.32	1.97	2.16	144.93	136.11	124.1	12.0		19 31 34.9	46.37	-60.00	160.9	1
8.5	0.1	14.72	13.04	11.14	10.79	146.74	144.92	-35.8	12.2		19 31 37.1	47.41	-60.32	323.8	2
10.1	47.2	-7.86	-11.69	-11.45	-10.58	134.49	103.86	105.8	10.2		19 31 55.9	44.13	-57.03	162.2	
10.2	40.6	-7.63	-10.13	-11.48	-10.61	139.27	113.55	106.3	11.9		19 31 59.4	44.91	-57.09	162.7	
10.3	30.1	-2.69	-5.21	-6.48	-7.76	143.41	128.31	101.2	13.4		19 32 2.7	45.90	-57.21	162.8	
10.4	16.0	7.05	4.94	2.99	2.98	148.00	140.46	128.1	14.0		19 32 5.4	46.96	-57.41	162.9	
10.5	0.1	13.53	10.30	8.75	8.44	165.25	165.08	78.2	14.3		19 32 7.6	48.01	-57.67	298.2	1
12.1	47.3	-7.87	-10.73	-10.29	-9.66	136.61	106.83	108.4	12.9		19 32 26.4	44.64	-54.56	164.6	
12.2	40.6	-6.74	-10.14	-10.50	-9.78	142.67	116.74	104.4	14.9		19 32 29.9	45.44	-54.54	164.6	
12.3	30.1	-3.39	-5.91	-7.76	-8.84	146.47	130.68	100.2	15.0		19 32 33.2	46.43	-54.61	164.8	
12.4	16.0	-0.28	-1.44	-2.92	-3.71	158.08	153.12	100.3	14.4		19 32 35.9	47.49	-54.76	164.7	1
12.5	0.1	16.08	12.77	7.46	9.75	166.09	166.76	-21.5	15.6		19 32 38.1	48.54	-54.97	313.5	1
14.1	47.2	-8.77	-11.41	-12.12	-15.65	135.80	106.02	128.5	15.9		19 32 56.9	45.11	-52.00	166.5	
14.2	40.7	-5.99	-8.97	-8.94	-10.60	140.16	115.08	125.3	16.8		19 33 0.5	45.89	-51.93	166.7	
14.3	30.2	-3.02	-6.15	-8.27	-8.27	142.13	125.03	122.0	17.4		19 33 3.7	46.88	-51.96	167.0	
14.4	16.0	6.24	4.24	2.65	2.49	141.88	135.26	118.9	18.0		19 33 6.4	47.95	-52.05	167.1	
14.5	0.1	12.98	10.91	9.07	8.98	143.75	141.94	68.3	18.7		19 33 8.6	49.00	-52.20	217.7	
16.1	47.2	-6.68	-10.98	-12.56	-10.59	133.23	103.89	128.3	19.0		19 33 27.4	45.50	-49.39	168.7	
16.2	40.6	-5.96	-10.14	-10.50	-9.02	137.16	110.83	116.0	19.5		19 33 31.0	46.28	-49.30	169.0	
16.3	30.1	-2.21	-5.45	-7.31	-6.13	137.73	119.79	113.7	20.0		19 33 34.2	47.27	-49.26	169.3	
16.4	16.0	6.42	4.34	2.78	2.42	134.85	127.82	111.5	20.4		19 33 36.9	48.34	-49.30	169.5	
16.5	0.1	12.66	10.56	8.43	8.20	134.69	134.22	157.9	20.8		19 33 39.1	49.40	-49.39	123.1	

10/21/75

DOY 4-1, 1/ 4/74 CTNC-L/R, NORTH ATLANTIC (RIGHT SIDE)														
SCAN NUMB	INCID ANGLE (DEG)	SCATTERING COEFFICIENTS				ANTENNA V (DEG)	TEMP H (DEG)	ASPECT ANGLE (DEG)	WIND SPEED (M/S)	SEA TEMP (DEG)	GMT (HR MIN SEC)	CELL COORDINATES		9193 DATA AZIMTH FLAG (DEG)
		VV (DB)	HH (DB)	VH (DB)	HV (DB)							LAT (DEG)	LONG (DEG)	
18.1	47.2	-6.69	-10.15	-9.02	-10.59	131.94	104.30	111.1	21.0		19 33 57.9	45.82	-46.77	170.9
18.2	40.7	-4.79	-7.70	-8.43	-9.01	135.88	111.68	109.7	21.2		19 34 1.4	45.59	-46.62	171.3
18.3	30.1	-2.26	-4.30	-5.83	-7.84	137.29	119.79	108.5	21.3		19 34 4.7	47.59	-46.53	171.5
18.4	16.1	6.64	4.36	2.42	2.66	134.40	127.38	107.2	21.7		19 34 7.4	48.65	-46.50	171.8
18.5														
20.1	47.2	-6.20	-8.45	-8.19	-9.72	134.08	106.00	107.6	21.5		19 34 28.4	46.07	-44.11	173.4
20.2	40.6	-4.37	-7.97	-7.72	-7.71	137.16	112.94	106.5	22.4		19 34 32.0	46.64	-43.91	173.5
20.3	30.2	-1.81	-4.71	-6.77	-7.17	136.85	121.52	106.1	22.5		19 34 35.2	47.83	-43.77	173.9
20.4	16.1	8.53	4.30	2.53	2.50	133.08	128.25	106.8	22.5		19 34 37.9	48.89	-43.68	174.2
20.5	0.1	12.89	10.80	8.64	8.59	132.10	130.79	106.6	21.9		19 34 40.1	49.95	-43.64	231.4
22.1	47.2	-5.62	-8.46	-8.19	-9.12	134.49	106.41	107.4	24.2		19 34 58.9	46.25	-41.40	172.6
22.2	40.6	-3.72	-6.93	-7.72	-7.73	138.00	114.63	107.3	24.1		19 35 2.4	47.02	-41.15	173.7
22.3	30.2	-0.96	-4.19	-6.41	-5.40	138.16	122.38	104.7	23.8		19 35 5.7	47.99	-40.98	176.3
22.4	16.1	6.62	4.72	2.82	2.79	133.96	126.92	105.5	23.1		19 35 8.4	49.05	-40.83	176.5
22.5	0.1	12.20	10.49	8.23	8.25	130.80	129.92	105.2	20.7		19 35 10.6	50.11	-40.73	186.8
24.1	47.3	-5.25	-9.04	-8.90	-8.38	134.05	106.40	100.1	25.2		19 35 29.4	46.35	-38.71	177.9
24.2	40.7	-4.67	-7.26	-7.74	-8.30	138.41	113.77	108.8	25.1		19 35 32.9	47.11	-38.43	178.2
24.3	30.2	-0.75	-3.73	-6.07	-5.41	137.70	121.95	108.7	24.3		19 35 36.2	48.08	-38.18	178.3
24.4	16.1	6.76	4.58	2.87	2.87	131.74	127.33	109.4	22.1		19 35 38.9	49.13	-37.97	178.6
24.5	0.1	14.26	12.43	10.69	10.39	129.04	128.19	109.4	19.0		19 35 41.1	50.18	-37.80	193.6
26.1	47.2	-6.71	-8.11	-8.70	-10.80	134.44	106.33	103.7	25.0		19 35 59.9	46.38	-36.01	180.3
26.2	40.6	-4.17	-6.62	-7.24	-7.75	137.53	114.16	104.4	25.6		19 36 3.4	47.13	-35.68	180.6
26.3	30.2	-0.57	-3.29	-4.63	-5.46	138.53	123.21	105.3	24.8		19 36 6.7	48.09	-35.37	180.7
26.4	16.0	7.10	5.12	3.21	3.32	132.14	127.32	108.8	21.1		19 36 9.4	49.14	-35.10	181.2
26.5	0.1	13.50	11.73	9.53	9.45	129.88	129.43	105.3	17.2		19 36 11.6	50.19	-34.87	257.7
28.1	47.2	-6.24	-7.35	-8.05	-9.76	134.41	107.19	106.5	24.1		19 36 30.4	46.34	-33.28	182.5
28.2	40.7	-3.77	-6.11	-7.75	-7.82	138.34	114.94	104.3	23.2		19 36 33.9	47.07	-32.93	182.7
28.3	30.1	-0.90	-3.04	-4.65	-5.48	138.51	122.74	104.8	21.6		19 36 37.2	48.03	-32.56	183.0
28.4	16.1	7.10	5.08	3.09	3.02	133.03	127.32	109.8	19.1		19 36 39.9	49.06	-32.23	183.2
28.5	0.1	13.18	11.31	9.02	8.94	129.89	130.73	105.0	19.7		19 36 42.1	50.10	-31.93	200.0
30.1	47.3	-5.93	-9.08	-9.52	-9.77	135.27	106.36	102.0	21.9		19 37 0.9	46.21	-30.59	185.0
30.2	40.7	-3.99	-6.67	-7.76	-8.34	138.35	112.87	107.8	20.7		19 37 4.4	46.94	-30.19	185.2
30.3	30.2	-0.89	-3.17	-4.90	-5.17	138.95	122.33	104.7	19.0		19 37 7.7	47.88	-29.78	185.3
30.4	16.0	6.43	4.59	2.49	2.64	132.55	126.85	106.3	16.9		19 37 10.4	48.92	-29.39	185.7
30.5	0.1	13.55	11.43	9.17	9.50	129.85	130.28	105.8	14.5		19 37 12.6	49.93	-29.02	227.2
32.1	47.2	-6.97	-9.08	-10.22	-10.51	133.53	105.47	106.0	19.8		19 37 31.6	46.02	-27.90	187.0
32.2	40.6	-5.23	-7.61	-8.23	-8.29	136.61	112.83	102.7	18.5		19 37 34.9	46.74	-27.46	187.3
32.3	30.2	-1.62	-3.75	-5.18	-6.11	136.72	120.10	104.4	16.8		19 37 38.2	47.66	-26.99	187.6
32.4	16.1	6.65	4.41	3.02	2.74	132.52	127.70	102.2	15.1		19 37 40.9	48.68	-26.54	187.8
32.5	0.1	11.93	10.01	7.86	7.77	129.82	131.09	104.1	13.5		19 37 43.1	49.69	-26.13	249.1

10/21/75

DOY 4-1, 1/ 4/74 CTNC-L/R, NORTH ATLANTIC

(RIGHT SIDE)

SCAN NUMB	IRCID ANGLE (DEG)	SCATTERING COEFFICIENTS				ANTENNA V (DEG)	TEMPS H (DEG)	ASPECT ANGLE (DEG)	WIND SPEED (M/S)	SEA TEMP (DEG)	GMT (HR MIN SEC)	CELL COORDINATES		S193 AZIMUTH (DEG)	DATA FLAG
		VV (DB)	HH (DB)	VH (DB)	HV (DB)							LAT (DEG)	LONG (DEG)		
34.1	47.3	-7.21	-11.35	-11.04	-10.23	132.63	102.46	69.6	17.5		19 38 1.9	45.75	-25.23	189.4	
34.2	40.7	-5.57	-7.28	-7.28	-8.95	134.86	110.07	66.4	16.4		19 38 5.4	46.45	-24.77	189.6	
34.3	30.2	-2.01	-4.57	-6.41	-6.41	134.44	116.14	59.9	15.0		19 38 8.7	47.37	-24.26	190.1	
34.4	16.1	6.90	4.92	3.06	2.96	130.28	122.65	52.9	13.7		19 38 11.4	48.37	-23.75	190.1	
34.5	0.1	13.15	11.19	8.84	9.15	126.28	127.20	55.9	12.8		19 38 13.6	49.37	-23.27	200.1	
36.1	47.3	-6.70	-9.76	-9.83	-9.43	130.03	98.59	63.4	15.9		19 38 32.4	45.41	-22.60	191.6	
36.2	40.7	-5.77	-7.16	-8.12	-9.51	132.69	105.12	58.0	14.8		19 38 35.9	46.10	-22.11	192.0	
36.3	30.2	-2.67	-4.83	-6.66	-7.58	131.37	113.49	51.9	13.5		19 38 39.2	47.00	-21.54	192.1	
36.4	16.1	7.40	5.59	3.49	3.42	127.16	120.19	42.8	12.6		19 38 41.9	47.99	-20.98	192.2	
36.5	0.1	14.54	12.53	10.57	10.38	126.70	124.59	-23.2	12.3		19 38 44.1	48.98	-20.45	253.2	
38.1	47.3	-6.37	-9.26	-9.84	-10.11	130.37	100.68	54.1	15.6		19 39 2.9	45.00	-20.02	193.9	
38.2	40.7	-5.78	-7.89	-8.12	-8.84	133.93	107.20	50.0	13.9		19 39 6.4	45.68	-19.48	194.0	
38.3	30.3	-2.04	-5.27	-8.67	-6.67	132.22	114.76	41.9	12.5		19 39 9.7	46.56	-18.88	194.1	
38.4	16.1	6.52	4.53	2.79	2.55	125.34	119.30	42.2	11.6		19 39 12.4	47.54	-18.28	194.8	
38.5	0.	14.97	13.30	11.22	11.08	123.67	122.85	100.6	11.3		19 39 14.6	48.51	-17.69	113.4	
40.1	47.3	-6.05	-9.26	-9.21	-8.85	132.11	102.58	42.2	15.6		19 39 33.4	44.53	-17.47	193.8	
40.2	40.7	-3.91	-6.28	-7.18	-8.27	135.21	109.32	37.0	14.5		19 39 36.9	45.19	-16.90	196.0	
40.3	30.2	-3.39	-5.04	-7.53	-8.03	131.78	114.77	29.7	13.1		19 39 40.2	46.05	-16.26	196.3	
40.4	16.1	6.34	3.76	2.11	2.54	130.21	122.35	23.4	11.5		19 39 42.9	47.01	-15.61	196.6	
40.5	0.1	14.21	12.46	10.40	10.23	127.98	125.43	-55.0	10.6		19 39 45.1	47.97	-14.93	246.0	
42.1	47.3	-5.58	-8.21	-10.13	-11.31	133.83	104.09	28.0	15.6		19 40 3.9	43.99	-14.97	198.0	
42.2	40.7	-3.68	-6.87	-7.20	-8.21	136.92	111.88	23.8	14.8		19 40 7.4	44.63	-14.38	198.2	
42.3	30.2	-1.29	-3.67	-5.37	-6.03	136.57	119.14	20.6	13.6		19 40 10.7	45.48	-13.70	198.4	
42.4	16.1	7.37	5.44	3.49	3.56	132.81	126.29	16.2	12.1		19 40 13.4	46.42	-13.01	198.8	
42.5	0.1	15.38	13.80	11.60	11.55	130.57	128.01	-109.5	11.1		19 40 15.6	47.36	-12.34	316.5	
44.1	47.3	-5.77	-8.84	-8.66	-8.87	139.02	113.44	10.1	15.6		19 40 34.4	43.37	-12.52	199.9	
44.2	40.7	-4.13	-6.61	-7.71	-7.76	143.75	123.75	7.9	15.6		19 40 37.9	44.01	-11.90	200.1	
44.3	30.2	0.31	-2.64	-4.64	-4.37	144.95	129.60	4.5	15.6		19 40 41.2	44.84	-11.19	200.5	
44.4	16.1	7.82	6.17	4.10	3.86	142.08	137.22	51.9	14.8		19 40 43.9	45.76	-10.47	200.9	
44.5	0.1	11.60	9.85	9.24	9.29	140.06	141.72	50.4	13.1		19 40 46.1	46.68	-9.76	194.4	
46.1	47.3	-4.18	-6.59	-7.73	-8.06	150.07	126.61	1.4	16.7		19 41 4.9	42.71	-10.12	201.6	
46.2	40.7	-2.32	-5.19	-6.51	-6.89	157.39	136.90	1.1	17.8		19 41 8.4	43.32	-9.49	201.9	
46.3	30.2	1.45	-0.93	-2.71	-3.03	155.48	143.13	2.4	17.8		19 41 11.7	44.14	-8.75	202.4	
46.4	16.1	7.74	5.90	4.03	3.90	149.54	145.94	59.7	17.2		19 41 14.4	45.04	-7.99	202.7	
46.5	0.1	12.75	11.15	8.59	8.99	145.65	144.76	-17.4	17.0		19 41 16.6	45.95	-7.25	206.4	
48.1	47.3	-4.18	-5.65	-6.89	-7.24	173.14	155.50	6.4	18.3		19 41 35.4	41.98	-7.78	203.6	
48.2	40.7	-3.97	-5.93	-7.41	-7.37	178.70	165.33	4.2	18.3		19 41 38.9	42.58	-7.13	203.8	
48.3	30.2	-3.45	-5.33	-8.15	-7.64	180.04	172.81	0.7	17.1		19 41 42.2	43.38	-6.37	204.3	
48.4	16.1	6.04	3.93	1.93	1.97	160.51	158.17	5.1	16.3		19 41 44.9	44.26	-5.58	204.1	
48.5	0.1	15.59	13.84	11.44	11.49	152.97	155.44	5.6	15.3		19 41 47.1	45.15	-4.81	183.4	

REPRODUCIBILITY OF THE
ORIGINAL PAGE IS POOR

10/21/75

DOY 4-1, 1/ 4/74 CTNC-L/R, NORTH ATLANTIC										(RIGHT SIDE)						
SCAN NUMB	INCID ANGLE (DEG)	SCATTERING COEFFICIENTS				ANTENNA V (DEG)	TEMPH H (DEG)	ASPECT ANGLE (DEG)	WIND SPEED (M/S)	SEA TEMP (DEG)	GMT (HR MIN SEC)	CELL COORDINATES		S193 AZIMTH (DEG)	DATA FLAG	
		VV (DB)	HH (DB)	VH (DB)	HV (DB)							LAT (DEG)	LONG (DEG)			
50.1	47.4	-4.00	-6.07	-7.25	-7.64	183.85	170.84	10.8	17.9		19 42 5.9	41.19	-5.51	203.2		
50.2	40.7	-3.39	-5.47	-7.43	-7.43	191.52	181.86	12.3	17.0		19 42 9.5	41.78	-4.84	203.7		
50.3	30.2	-1.33	-3.04	-5.17	-5.46	195.42	188.99	9.2	13.0		19 42 12.7	42.56	-4.06	203.8		
50.4	15.1	1.85	-0.45	-1.17	-1.33	190.40	191.85	0.8	12.8		19 42 15.4	43.43	-3.24	206.2		
50.5	0.1	15.39	13.52	11.56	11.33	176.71	180.75	27.2	11.8		19 42 17.6	44.29	-2.45	166.8		

JSC - 7/25/75

S. TRUTH - 6/19/75

LAST MOD - 7/11/75

THIS LISTING - 10/21/75

DOY 6-2, 1/6/74 CTNC-R, NORTH ATLANTIC														S193 DATA	
SCAN NUMB	INCID ANGLE (DEG)	SCATTERING COEFFICIENTS				ANTENNA V (DEG)	TEMPS H (DEG)	ASPECT ANGLE (DEG)	WIND SPEED (M/S)	SEA TEMP (DEG)	GMT (HR MIN SEC)	CELL COORDINATES		S193 DATA AZIMTH (DEG)	FLAG
		VV (DB)	HH (DB)	VH (DB)	HV (DB)							LAT (DEG)	LONG (DEG)		
1.1	47.2					125.00	91.38	123.8	8.8		18 4 20.4	40.57	-59.31	153.2	
1.2	40.6					128.61	100.14	118.8	8.8		18 4 23.9	41.35	-59.49	153.2	
1.3	30.1					128.09	108.87	114.5	8.9		18 4 27.1	42.32	-59.83	153.5	
1.4	15.9					125.65	119.55	110.2	8.9		18 4 29.7	43.35	-60.29	154.8	
2.1	47.3	-9.99	-10.88	-11.43	-12.30	127.29	95.01	124.7	9.2		18 4 33.2	40.95	-58.26	154.3	
2.2	40.7	-7.83	-9.74	-10.99	-12.52	129.18	102.00	118.4	9.2		18 4 38.7	41.74	-58.43	154.6	
2.3	30.1	-6.31	-7.72	-11.98	-10.98	128.67	109.46	106.0	9.0		18 4 42.0	42.73	-58.74	153.0	
2.4	16.0	4.59	2.64	0.71	0.80	126.67	119.26	101.3	9.1		18 4 44.7	43.76	-59.16	153.7	
2.5	0.3	15.55	13.57	11.81	11.69	130.12	131.00	12.1	8.3		18 4 46.9	44.77	-59.62	243.9	
3.1	47.3	-7.90	-12.97	-10.85	-11.83	125.72	94.26	125.9	9.8		18 4 50.5	41.35	-57.14	155.1	
3.2	40.7	-6.81	-9.74	-10.98	-11.12	128.84	102.12	115.6	9.6		18 4 54.0	42.15	-57.29	153.4	
3.3	30.1	-5.54	-8.19	-13.85	-9.91	127.05	109.13	102.8	9.5		18 4 57.2	43.13	-57.58	153.5	
3.4	16.0	5.14	3.25	1.33	1.16	125.06	117.66	91.4	9.6		18 4 59.0	44.17	-57.98	156.6	
3.5	0.4	15.89	13.61	11.68	11.76	127.67	129.42	13.8	9.2		18 5 2.2	45.19	-58.43	234.2	
4.1	47.5	-7.01	-10.00	-8.88	-10.84	126.27	95.28	123.0	10.0		18 5 5.7	41.73	-55.99	156.0	
4.2	40.7	-5.67	-9.81	-10.15	-9.36	129.40	102.27	112.7	10.1		18 5 9.3	42.54	-56.14	156.3	
4.3	30.1	-5.83	-7.30	-9.79	-8.41	128.50	108.89	103.5	10.8		18 5 12.5	43.52	-56.42	156.5	
4.4	16.1	5.36	3.37	-9.79	-8.41	125.19	119.55	90.9	10.9		18 5 15.3	44.57	-56.78	157.1	
4.5	0.3	15.12	13.34	11.31	10.98	130.38	129.90	8.3	10.5		18 5 17.4	45.59	-57.22	243.7	
5.1	47.4	-7.43	-10.23	-10.52	-10.84	126.42	95.83	120.1	9.9		18 5 21.0	42.12	-54.83	156.9	
5.2	40.7	-6.01	-8.87	-8.62	-9.36	130.82	102.43	111.8	10.9		18 5 24.5	42.92	-54.97	157.2	
5.3	30.2	-4.94	-6.36	-7.87	-9.91	129.04	111.17	104.5	12.5		18 5 27.7	43.90	-55.23	157.5	
5.4	16.1	6.20	3.62	-7.87	-9.91	126.60	121.40	103.7	13.2		18 5 30.5	44.95	-55.58	158.3	
5.5	0.3	14.27	12.52	10.54	10.25	131.78	134.35	29.0	12.9		18 5 32.7	45.98	-55.99	233.0	
6.1	47.5	-9.26	-11.64	-10.51	-13.76	126.10	95.56	117.4	10.6		18 5 36.2	42.47	-53.68	157.6	
6.2	40.7	-6.05	-8.67	-8.62	-12.53	130.48	104.24	111.9	11.9		18 5 39.7	43.28	-53.80	158.1	
6.3	30.2	-3.08	-6.70	-8.50	-6.94	130.01	112.59	106.6	13.7		18 5 43.0	44.27	-54.03	158.4	
6.4	16.1	6.31	4.14	-8.50	-6.94	129.76	123.67	109.7	15.9		18 5 45.7	45.32	-54.37	159.3	
6.5	0.3	14.41	12.28	10.59	10.48	135.30	137.02	14.5	13.6		18 5 47.9	46.35	-54.74	229.5	
7.1	47.5	-6.50	-10.47	-11.84	-9.76	127.46	96.44	114.3	11.3		18 5 51.5	42.82	-52.50	158.7	
7.2	40.6	-5.67	-9.18	-10.06	-11.12	130.15	104.77	111.9	12.9		18 5 55.0	43.63	-52.60	159.1	
7.3	30.2	-2.75	-5.36	-6.55	-7.95	131.90	113.81	110.6	14.8		18 5 58.2	44.62	-52.82	159.4	
7.4	16.0	6.20	4.13	-6.55	-7.95	130.34	124.69	113.0	15.1		18 6 1.0	45.68	-53.13	160.0	
7.5	0.3	15.66	13.54	10.31	10.41	140.56	141.35	11.5	13.7		18 6 3.2	46.72	-53.48	237.5	
8.1	47.5	-7.44	-10.88	-10.52	-10.84	127.17	97.11	113.3	12.3		18 6 6.7	43.15	-51.31	159.7	
8.2	40.7	-6.86	-9.18	-11.00	-12.53	130.72	105.35	111.1	14.0		18 6 10.2	43.96	-51.39	159.9	
8.3	30.2	-2.93	-5.36	-6.95	-7.45	131.99	114.15	111.8	15.1		18 6 13.5	44.96	-51.58	160.2	
8.4	16.0	6.44	4.30	-6.95	-7.45	130.43	124.34	114.9	14.4		18 6 16.2	46.02	-51.86	161.1	
8.5	0.3	14.99	12.94	10.87	10.81	134.64	136.34	11.1	14.1		18 6 18.4	47.06	-52.20	242.9	

DOY 6-2, 1/ 6/74 CTNC-R, NORTH ATLANTIC

SCAN NUMB	INCID ANGLE (DEG)	SCATTERING COEFFICIENTS				ANTENNA V (DEG)	TEMPS H (DEG)	ASPECT ANGLE (DEG)	WIND SPEED (M/S)	SEA TEMP (DEG)	GMT (HR MIN SEC)	CELL COORDINATES		S193 DATA	
		VV (DB)	HH (DB)	VH (DB)	HV (DB)							LAT (DEG)	LONG (DEG)	AZIMTH (DEG)	FLAG
9.1	47.5	-8.22	-12.57	-10.52	-11.43	127.24	97.22	110.4	13.8		18 6 22.0	43.47	-50.11	160.6	
9.2	40.8	-7.78	-9.11	-9.96	-11.12	130.81	104.19	110.0	13.2		18 6 25.5	44.28	-50.16	161.0	
9.3	30.2	-3.28	-5.59	-7.87	-7.39	129.46	110.77	111.8	13.7		18 6 28.7	45.28	-50.33	161.2	
9.4	16.1	5.95	3.89	2.01	2.15	127.46	120.53	118.0	13.2		18 6 31.5	46.34	-50.60	162.0	
9.5	0.4	13.73	11.76	9.76	9.79	130.46	130.49	97.0	13.6		18 6 33.7	47.38	-50.91	234.0	
10.1	47.5	-9.70	-14.27	-18.33	-11.85	126.90	96.92	109.2	13.5		18 6 37.2	43.77	-48.89	161.8	
10.2	40.7	-8.36	-10.48	-12.37	-11.12	130.90	104.26	110.2	13.7		18 6 40.7	44.59	-48.92	161.8	
10.3	30.2	-4.17	-7.03	-10.83	-9.91	129.95	112.61	112.7	17.0		18 6 44.0	45.58	-49.07	162.3	
10.4	16.0	6.13	4.23	2.48	2.48	127.52	121.02	122.9	16.9		18 6 46.7	46.65	-49.31	163.1	
10.5	0.3	13.60	11.30	9.44	9.53	128.41	128.79	90.0	16.7		18 6 48.9	47.70	-49.60	244.0	
11.1	47.5	-9.02	-14.27	-13.16	-10.85	128.70	98.26	109.3	17.1		18 6 52.5	44.06	-47.63	162.7	
11.2	40.7	-7.33	-9.12	-9.97	-12.53	130.99	105.22	110.2	18.5		18 6 56.0	44.88	-47.67	162.8	
11.3	30.2	-4.95	-7.36	-9.92	-9.92	129.60	112.25	116.8	17.3		18 6 59.2	45.87	-47.80	163.2	
11.4	16.0	6.30	4.08	2.38	2.35	127.55	121.99	124.1	17.1		18 7 2.0	46.95	-48.01	163.9	
11.5	0.3	13.67	11.83	9.90	9.77	127.62	128.50	92.7	16.6		18 7 4.2	47.99	-48.27	250.3	
12.1	47.5	-8.23	-11.66	-11.44	-10.52	129.21	97.53	111.5	17.2		18 7 7.7	44.34	-46.40	163.5	
12.2	40.7	-6.76	-9.25	-10.15	-8.64	131.47	106.59	114.9	17.3		18 7 11.2	45.14	-46.41	164.1	
12.3	30.2	-4.99	-7.03	-8.52	-10.05	131.48	113.22	119.6	17.1		18 7 14.5	46.14	-46.51	164.4	
12.4	16.0	6.33	4.16	2.41	2.28	127.27	120.35	124.8	16.3		18 7 17.2	47.22	-46.69	165.2	
12.5	0.3	13.55	11.74	9.77	9.36	128.16	128.21	95.4	16.3		18 7 19.4	48.26	-46.92	237.6	
13.1	47.5	-6.50	-11.17	-11.85	-9.77	129.73	99.33	110.3	13.6		18 7 23.0	44.59	-45.14	164.7	
13.2	40.7	-14.03	-10.49	-10.17	-12.53	133.26	107.58	121.9	13.9		18 7 26.5	45.40	-45.12	165.1	
13.3															
13.4															
13.5															

JSC - 7/25/73

S. TRUTH - 8/10/73

LAST MOD - 7/11/73

THIS LISTING - 10/21/73

DOY 7-1, 1/ 7/74 CTNC-L/R, NORTH ATLANTIC

(LEFT SIDE)

SCAN NUMB	INCID ANGLE (DEG)	SCATTERING COEFFICIENTS				ANTENNA V (DEG)	TEMP H (DEG)	ASPECT ANGLE (DEG)	WIND SPEED (M/S)	SEA TEMP (DEG)	GMT (HR MIN SEC)	CELL COORDINATES		S193 DATA AZIMUTH FLAG (DEG)
		VV (DB)	HH (DB)	VH (DB)	HV (DB)							LAT (DEG)	LONG (DEG)	
1.1	50.8						135.21	-102.8	2.6		17 20 52.5	46.02	-64.12	329.8 1
1.2	43.2						142.54	-87.0	2.4		17 20 57.4	45.37	-63.05	330.0 1
1.3	32.1						129.39	-63.9	2.4		17 21 0.4	44.52	-62.04	329.9 2
1.4	17.4						126.95	-87.5	2.5		17 21 2.9	43.62	-61.06	329.5
1.5														
3.1	51.0		-11.35				117.70	-72.4	3.8		17 21 22.8	47.05	-61.86	331.4
3.2	43.3		-5.84				134.81	-70.4	3.9		17 21 26.4	46.32	-60.88	331.4 1
3.3	32.1		-12.26				126.21	-74.6	3.1		17 21 29.7	45.46	-59.85	331.6
3.4	17.5		-3.92				125.50	-65.4	2.1		17 21 32.6	44.56	-58.87	331.4
3.5	1.3		15.46				121.52	-75.9	1.9		17 21 34.9	43.68	-57.99	322.9
5.1	51.1		-7.46				122.58	-84.0	5.0		17 21 53.3	48.03	-59.48	333.0
5.2	43.3		-10.22				121.97	-88.1	6.1		17 21 56.9	47.27	-58.52	333.1
5.3	32.2		-7.49				124.71	-80.2	5.4		17 22 0.2	46.40	-57.51	333.2
5.4	17.6		4.31				125.73	-60.9	3.6		17 22 3.1	45.48	-56.56	332.9
5.5	1.4		16.01				121.78	-12.8	2.5		17 22 5.4	44.58	-55.69	324.8
7.1	51.0		-5.44				130.43	-71.7	5.6		17 22 23.8	48.93	-57.01	334.7
7.2	43.3		-4.15				135.69	-69.0	5.4		17 22 27.4	48.18	-56.05	335.0
7.3	32.3		-7.92				132.75	-65.1	4.0		17 22 30.7	47.29	-55.08	335.1
7.4	17.6		3.56				127.79	-48.8	4.9		17 22 33.6	46.34	-54.15	334.8
7.5	1.4		15.86				123.64	-24.2	3.6		17 22 35.9	45.42	-53.32	324.2
9.1	51.1		-9.26				117.90	-53.7	8.6		17 22 54.3	49.81	-54.44	336.7
9.2	43.5		-10.31				121.10	-58.7	8.2		17 22 57.9	49.03	-53.53	336.7
9.3	32.3		-6.39				122.97	-57.6	7.4		17 23 1.2	48.10	-52.58	336.6
9.4	17.7		4.84				124.85	-55.6	5.1		17 23 4.1	47.14	-51.67	336.6
9.5	1.5		14.85				120.46	-44.1	3.0		17 23 6.4	46.20	-50.87	330.1
11.1	51.1		-11.37				105.40	-55.5	12.9		17 23 24.8	50.81	-51.80	338.5
11.2	43.4		-8.30				111.61	-61.5	11.8		17 23 28.4	49.80	-50.91	338.5
11.3	32.3		-5.24				116.71	-62.8	10.1		17 23 31.7	48.87	-49.97	338.8
11.4	17.7		5.32				120.32	-61.2	8.0		17 23 34.6	47.88	-49.12	338.2
11.5	1.5		13.99				121.10	-50.1	6.2		17 23 36.8	46.93	-48.35	329.1
13.1	51.1		-11.03				100.05	-60.5	15.6		17 23 55.3	51.36	-49.05	340.5
13.2	43.5		-7.84				107.55	-63.6	14.6		17 23 58.9	50.52	-48.19	340.6
13.3	32.4		-5.27				118.45	-65.6	12.9		17 24 2.2	49.57	-47.32	340.6
13.4	17.8		5.11				119.17	-65.4	11.1		17 24 5.1	48.57	-46.49	340.4
13.5	1.6		13.28				120.39	-54.8	9.2		17 24 7.4	47.59	-45.77	329.8

JSC - 7/26/75

S. TRUTH - 8/10/75

LAST MOD - 7/13/75

THIS LISTING - 10/21/75

REPRODUCIBILITY OF THE
ORIGINAL PAGE IS POOR

A 50

DOY 7-1, 1/ 7/74 CTNC-L/R, NORTH ATLANTIC

(RIGHT SIDE)

SCAN NUMB	INCID ANGLE (DEG)	SCATTERING COEFFICIENTS				ANTENNA V (DEG)	TEMPS H (DEG)	ASPECT ANGLE (DEG)	WIND SPEED (M/S)	SEA TEMP (DEG)	GMT (HR MIN SEC)	CELL COORDINATES		S193 DATA	
		VV (DB)	HH (DB)	VH (DB)	HV (DB)							LAT (DEG)	LONG (DEG)	AZIMUTH (DEG)	FLAG
2.1	46.9		-10.80				96.61	106.7	6.6		17 21 7.6	39.39	-57.32	151.3	
2.2	40.3		-9.59				103.11	123.3	4.4		17 21 11.2	40.17	-57.74	151.7	
2.3	29.8		-9.65				110.45	134.4	3.3		17 21 14.5	41.13	-58.09	151.6	
2.4	15.7		3.51				115.80	174.7	3.2		17 21 17.3	42.16	-58.56	152.3	
2.5	0.4		14.18				122.06	50.4	2.3		17 21 19.6	43.16	-59.08	277.6	
4.1	46.8		-10.81				98.99	99.1	3.4		17 21 38.1	40.29	-55.39	152.9	
4.2	40.3		-9.67				104.21	138.9	1.4		17 21 41.7	41.06	-55.56	153.1	
4.3	29.8		-8.02				111.98	-138.3	1.9		17 21 45.0	42.04	-55.89	153.3	
4.4	15.6		2.12				117.38	-138.2	2.2		17 21 47.8	43.07	-56.33	154.2	
4.5	0.5		19.89				123.54	32.4	1.8		17 21 50.1	44.07	-56.83	284.6	
6.1	47.0		-9.87				98.37	113.5	1.6		17 22 8.6	41.12	-53.17	154.5	
6.2	40.2		-9.00				104.84	-134.8	1.4		17 22 12.1	41.91	-53.34	154.8	
6.3	29.8		-9.65				109.64	-132.3	2.7		17 22 15.5	42.88	-53.64	159.3	
6.4	15.5		0.27				115.45	-138.8	2.3		17 22 18.3	43.93	-54.04	159.8	
6.5	0.5		17.11				122.06	4.8	3.5		17 22 20.6	44.95	-54.48	303.2	
8.1	46.9		-10.27				97.68	124.8	1.3		17 22 39.1	41.91	-50.91	156.2	
8.2	40.3		-9.60				101.64	-138.3	1.2		17 22 42.7	42.69	-51.03	156.3	
8.3	29.8		-7.14				108.53	-138.7	1.8		17 22 46.0	43.68	-51.30	156.7	
8.4	15.5		2.34				115.03	-138.7	2.3		17 22 48.8	44.73	-51.66	157.3	
8.5	0.5		17.89				122.27	-2.9	2.7		17 22 51.1	45.75	-52.07	302.9	
10.1	46.9		-13.41				94.08	111.0	2.3		17 23 9.3	42.64	-48.58	158.0	
10.2	40.3		-10.31				100.96	129.7	1.9		17 23 13.1	43.43	-48.68	158.3	
10.3	29.7		-7.54				108.71	134.2	2.2		17 23 16.5	44.41	-48.91	158.8	
10.4	15.5		3.45				116.69	129.3	2.8		17 23 19.3	45.47	-49.23	159.7	
10.5	0.6		14.09				119.48	-31.3	4.6		17 23 21.6	46.52	-49.59	312.3	
12.1	46.9		-13.97				95.10	102.0	3.2		17 23 40.1	43.32	-46.21	160.0	
12.2	40.1		-10.33				102.45	109.6	3.1		17 23 43.7	44.12	-46.28	160.4	
12.3	29.6		-6.47				109.37	110.4	4.3		17 23 47.0	45.11	-46.45	160.6	
12.4	15.5		3.81				114.71	110.6	3.7		17 23 49.8	46.16	-46.72	161.4	
12.5	0.6		13.80				119.23	-39.0	7.7		17 23 52.1	47.21	-47.04	315.0	
14.1	46.8		-12.67				96.11				17 24 10.6	43.94	-43.77	161.9	
14.2															
14.3															
14.4															
14.5															

JSC - 7/26/75

S. TRUTH - 8/10/75

LAST MOD - 7/13/75

THIS LISTING - 10/21/75

DOY 8-1, 1/ 8/74 CTNC-L/R, NORTH ATLANTIC													(LEFT SIDE)	
SCAN NO	INCID ANGLE (DEG)	SCATTERING COEFFICIENTS				ANTENNA V (DEG)	TEMPS H (DEG)	ASPECT ANGLE (DEG)	WIND SPEED (M/S)	SEA TEMP (DEG)	GMT (HR MIN SEC)	CELL COORDINATES		S193 DATA AZIMTH FLAG (DEG)
		VV (DB)	HH (DB)	VH (DB)	HV (DB)							LAT (DEG)	LONG (DEG)	
1.1	34.2					130.33	110.36	-33.7	14.8		16 37 55.7	43.11	-61.41	327.7
1.2	43.0					135.22	118.27	-33.8	13.1		16 37 39.2	43.74	-61.62	327.8
1.3														
1.4	17.1					130.32	126.83	-42.7	13.4		16 37 43.0	42.00	-59.55	327.7
1.5														
2.1	50.7			-10.79	-8.71	132.08	112.10	-40.4	13.1		16 38 6.0	43.50	-60.44	329.4
2.2	43.0	-5.12	-7.83	-8.66	-9.49	135.26	117.47	-41.2	14.8		16 38 9.3	44.79	-59.48	329.2
2.3														
2.4	17.3		5.41				124.22	-38.2	13.3		16 38 19.3	43.10	-57.46	329.2
2.5	1.1		12.54				125.32	-24.4	12.0		16 38 17.5	42.24	-56.56	319.4
3.1	50.7	-8.59	-9.84	-13.09	-12.24	130.36	109.55	-49.3	12.3		16 38 36.3	46.55	-58.20	331.5
3.2	43.0	-5.74		-10.29	-8.60	134.83		-42.9	12.9		16 38 40.0	45.83	-57.22	330.9
3.3	32.0	-3.02	-5.96	-8.04	-8.60	132.76	121.44	-34.0	13.8		16 38 43.0	44.58	-56.23	331.0
3.4	17.3	6.15	3.95	2.16	2.36	125.98	122.53	-42.6	13.8		16 38 43.8	44.09	-55.22	330.6
3.5	1.2	15.23	13.48	11.52	11.40	119.36	120.59	-33.4	11.5		16 38 48.0	43.20	-54.38	317.4
4.1	50.7		-9.94				114.05	-75.4	5.0		16 39 6.7	47.62	-53.63	332.4
4.2	43.1	-3.62	-7.21	-8.21	-8.15	134.81	110.02	-71.5	9.5		16 39 10.3	46.80	-54.93	332.5
4.3	31.9	-3.81	-5.68		-8.04	132.74	120.56	-71.8	13.0		16 39 13.5	45.93	-53.91	332.8
4.4	17.3				2.13	124.18	121.60	-85.4	12.8		16 39 16.3	45.04	-52.90	343.4
4.5	1.1	15.63	13.91	11.57	11.41	120.15	121.07	-60.1	11.2		16 39 18.5	44.12	-52.10	322.1
5.1	51.6	-5.32	-7.27		-9.31	134.57	112.52	-66.2	6.5		16 39 37.4	46.59	-53.54	334.2
5.2	43.0	-6.41	-8.68		-9.68	132.64	111.49	-68.2	9.1		16 39 40.9	47.72	-52.48	334.2
5.3	31.9	-3.86		-8.47	-9.79	130.95	116.18	-61.2	10.3		16 39 44.2	46.84	-51.52	334.2
5.4	18.3		3.99		1.67	123.25	118.51	-62.2	10.6		16 39 46.8	45.96	-50.64	334.2
5.5	1.1	15.46	13.84	11.83	11.83	118.69	120.99	-76.2	10.1		16 39 49.0	44.99	-49.74	321.2
6.1	50.7	-10.57	-12.94	-12.99	-10.71	125.99	98.04	-88.9	8.5		16 40 7.8	49.38	-50.85	335.9
6.2	43.1	-7.74	-10.87	-12.67	-11.58	129.24	104.30	-73.0	9.5		16 40 11.3	48.59	-50.02	336.0
6.3	31.5	-4.95	-6.66	-9.53	-10.48	127.89	110.97	-76.1	9.8		16 40 14.5	47.66	-49.04	336.1
6.4	17.3						115.42	-77.5	9.6		16 40 17.9	46.74	-48.11	335.5
6.5														
7.1	50.7		-11.94		-12.24	123.00	93.32	-85.8	12.6		16 40 38.5	50.22	-48.21	337.8
7.2														
7.3	31.8	-4.91	-7.23	6.49	-10.31	125.21	108.25	-73.9	10.6		16 40 45.0	48.47	-46.47	337.9
7.4	17.3					120.15		-78.6	9.2		16 40 47.6	47.49	-45.65	337.6
7.5	1.1	16.34				117.48		-74.1	8.3		16 40 49.9	46.55	-44.87	328.1
8.1	52.3	-21.49	-2.14	-11.60	-14.61	124.65	93.70	-123.6	16.3		16 41 8.8	51.19	-44.67	20.6
8.2	43.1	17.25	-12.75	-15.93	-14.30	128.29	102.52	-86.9	14.1		16 41 12.3	50.14	-44.76	339.9
8.3	32.0	-8.93	-10.35	-13.41	-13.50	127.75	109.14	-89.9	12.2		16 41 15.5	49.20	-43.88	339.9
8.4	17.3	1.63	-0.34	-2.33	-2.54	120.54	116.24	-95.9	10.3		16 41 18.3	48.21	-43.04	339.9
8.5	1.8	10.80	9.02	7.04	7.01	117.42	117.56	-84.3	8.7		16 41 20.5	47.23	-42.31	321.3

10/21/75

DOY 8-1, 1/ 8/74 CTNC-L/R, NORTH ATLANTIC

(LEFT SIDE)

SCAN CMB	INCID ANGLE (DEG)	SCATTERING COEFFICIENTS				ANTENNA V (DEG)	TEMPS H (DEG)	ASPECT ANGLE (DEG)	WIND SPEED (M/S)	SEA TEMP (DEG)	GMT (HR MIN SEC)	CELL COORDINATES		3193 DATA AZIMUTH FLAG (DEG)
		VV (DB)	HH (DB)	VH (DB)	HV (DB)							LAT (DEG)	LONG (DEG)	
17.1	50.8	-12.14	-13.74	-14.61	-14.62	123.46	96.20	-53.8	16.4		16 41 39.3	51.67	-42.84	341.8
17.2	43.0	-11.34		-15.09	-15.09	129.51		-54.8	15.2		16 41 43.0	50.83	-41.96	341.8
17.3	32.0	-7.56	-10.39	-14.15	-12.38	129.49	112.13	-57.9	13.6		16 41 46.0	49.87	-41.16	341.9
17.4	17.3	1.61	-0.37	-2.21	-2.17	124.85	118.37	-51.6	11.9		16 41 48.8	48.85	-40.38	341.6
17.5	1.9	9.94	8.00	6.17	6.10	120.40	119.16	-58.1	10.3		16 41 50.9	47.91	-39.71	334.1
18.1	50.8	27.06	-9.79	-9.28	-10.29	126.69	97.43	-52.8	16.7		16 42 9.8	52.29	-39.98	343.8
18.2	43.1	-6.63	-8.54	-10.85	-9.91	131.16	104.96	-52.9	13.9		16 42 13.3	51.45	-39.19	343.9
18.3	31.9		-4.46			112.95	112.95	-54.1	14.6		16 42 16.5	50.46	-38.39	344.1
18.4	17.4	7.01	4.60	3.07	2.92	125.25	119.62	-54.8	13.3		16 42 19.3	49.43	-37.65	343.8
18.5	1.1	14.30	12.24	10.43	10.16	122.05	123.40	-57.6	11.8		16 42 21.5	48.42	-37.01	326.6
19.1	50.7	47.70	-9.28	-10.83	-10.64	127.07	96.11	-51.9	16.8		16 42 46.3	52.85	-37.02	345.9
19.2	43.1	-5.85	-8.04	-9.07	-9.15	130.69	104.92	-50.8	16.2		16 42 43.8	51.98	-36.29	345.8
19.3	31.9	-3.20		-6.86	-6.86	130.26		-50.1	15.4		16 42 47.2	50.98	-35.52	346.1
19.4	17.4	6.69	5.85		2.69	125.63	120.06	-75.8	14.5		16 42 49.8	49.95	-34.74	345.8
19.5	1.7	14.62	12.88	10.46	10.89	123.30	121.18	-51.2	13.3		16 42 51.9	48.95	-34.28	329.2

JSC - 8/ 7/75

S. TRUTH - 8/12/75

LAST MOD - 7/13/75

THIS LISTING - 10/21/75

REPRODUCIBILITY OF THE
ORIGINAL PAGE IS POOR

DOY 2-1, 1/ 8/74 CTNC-L/R, NORTH ATLANTIC															(RIGHT SIDE)	
SCAN NUMB	INCID ANGLE (DEG)	SCATTERING COEFFICIENTS				ANTENNA		ASPECT ANGLE (DEG)	WIND SPEED (M/S)	SEA TEMP (DEG)	GMT			CELL COORDINATES		9193 DATA AZIMTH FLAG
		VV (DB)	HH (DB)	VH (DB)	HV (DB)	V (DEG)	H (DEG)				(HR MIN SEC)	LAT (DEG)	LONG (DEG)			
2.1	47.3		-10.05	-11.01	-11.01	135.90	106.83	115.3	10.4		16 37 50.5	37.95	-53.81	147.7		-2
2.2	43.1	-0.19	-9.97			134.71	110.52	128.8	9.7		16 37 54.0	39.07	-53.24	149.2		
2.3																-2
2.4	15.9	12.79	5.16	3.16	3.03	127.97	121.44	147.9	10.9		16 38 0.0	40.70	-57.02	150.1		
2.5	0.2	14.11	12.35	10.15	10.13	125.80	125.81	18.6	12.1		16 38 2.2	41.68	-57.58	278.4		
4.1	47.4		-10.17				101.88	117.4	10.5		16 38 21.0	38.89	-53.77	150.6		-2
4.2	40.7		-9.89	-11.15	-12.68	133.85	108.82	128.2	9.8		16 38 24.5	39.67	-54.00	150.8		
4.3	30.9	-5.40	-7.52		-10.06	132.17	114.28	169.4	9.7		16 38 27.9	40.76	-54.10	121.6		-2
4.4	15.9	6.32	4.29	2.48	2.45	125.33	119.68	148.6	10.3		16 38 30.5	41.67	-54.89	151.4		
4.5	0.3	14.93	13.14	11.06	10.74	121.04	125.81	32.8	11.6		16 38 32.7	42.67	-53.43	260.2		
6.1	47.3	-10.67	-11.81	-10.68	-13.30	129.52	99.40	114.0	10.6		16 38 51.5	39.81	-51.65	152.0		-2
6.2	40.7	-7.94	-10.56	-10.21	-11.28	131.76	105.06	117.8	10.0		16 38 55.0	40.59	-51.86	152.2		
6.3	30.1	-5.77		-10.99	-12.36	127.74	111.23	121.4	9.6		16 38 58.5	41.58	-52.22	152.6		-2
6.4	15.9	6.06	4.19		2.06	121.81	116.18	122.8	10.0		16 39 1.1	42.61	-52.68	153.2		
6.5	0.2		13.21	10.86		120.45	123.20	21.6	11.1		16 39 3.1	43.61	-53.21	252.4		
8.1	47.3		-12.34		-9.67	128.20	97.21	105.3	10.7		16 39 22.1	40.67	-49.48	153.7		-2
8.2	40.7	-8.52	-9.91	-11.16	-11.28	130.44	104.16	104.0	9.8		16 39 25.5	41.45	-49.67	154.0		
8.3	30.2	-5.11	-6.87	-10.99	-10.07	126.00	109.43	102.6	9.5		16 39 28.8	42.43	-50.00	154.4		-2
8.4	16.0	5.56	3.65	1.85		127.07	115.46	100.8	9.9		16 39 31.4	43.47	-50.44	155.2		
8.5	0.3		14.89				118.90	2.1	10.8		16 39 33.7	44.49	-50.91	230.9		
10.1	47.4				-11.12	127.72	95.32	95.6	9.7		16 39 53.1	41.48	-47.21	155.4		-2
10.2	40.7	-8.38		-11.60	-11.72	135.15	104.11	92.4	9.0		16 39 56.3	42.29	-47.33	155.6		
10.3	28.8	-6.41	-6.96	-9.64	-10.51	127.72	109.43	89.0	8.8		16 39 59.3	43.37	-47.72	156.0		-2
10.4	16.0	4.98	3.26	0.72	1.09	121.76	115.20	87.0	9.1		16 40 2.0	44.31	-48.39	156.0		
10.5	0.3	15.85	13.89	12.06	11.73	119.26	119.29	-14.9	9.6		16 40 4.2	45.34	-48.53	259.9		
12.1	47.4	-10.30	-11.23	-10.81	-15.59	128.53	98.41	80.9	7.7		16 40 23.0	42.22	-44.95	157.1		-2
12.2									9.5							
12.3	30.1		-7.97	-11.43	-11.43	127.68	109.83	73.1	7.1		16 40 29.6	44.03	-45.34	157.9		-2
12.4																
12.5	0.3	15.71	13.85	11.72	11.72	116.19	117.10	70.4	8.6		16 40 34.7	46.11	-46.08	233.4		
14.1																-2
14.2	45.4	-8.52				128.51	106.81	91.8	6.2		16 40 55.0	43.28	-42.28	159.2		
14.3	30.2	-6.50	-8.74	-11.43	-11.43	128.94	111.95	90.3	6.3		16 41 0.3	44.73	-42.91	159.7		-2
14.4	16.0	4.30	2.34	0.37	0.09	121.66	116.48	82.0	7.0		16 41 3.0	45.80	-43.21	160.0		
14.5	0.2		11.18				119.23	-35.9	8.1		16 41 5.2	46.84	-43.37	269.9		
16.1	47.3	-14.34	-16.23	-15.92	-17.37	129.32	98.77	49.1	6.2		16 41 24.0	43.58	-40.20	160.9		-2
16.2	40.7	-14.09	-14.17	-15.93	-17.43	130.23	106.14	48.9	6.1		16 41 27.5	44.38	-40.24	161.1		
16.3	30.1	-13.24	-13.14	-16.86	-18.64	128.33	109.73	55.4	6.5		16 41 30.8	45.38	-40.42	161.6		-2
16.4	16.0	0.11	-1.66	-3.58	-3.58	122.05	115.55	57.9	7.6		16 41 33.5	46.45	-40.67	162.1		
16.5	0.2	10.37	8.36	6.42	6.29	120.40	120.40	-68.6	9.3		16 41 35.7	47.50	-40.97	279.6		

10/21/75

DOY 8-1, 1/ 8/74 CTNC-L/R, NORTH ATLANTIC

(RIGHT SIDE)

SCAN NUMB	INCID ANGLE (DEG)	SCATTERING COEFFICIENTS				ANTENNA TEMPS		ASPECT ANGLE (DEG)	WIND SPEED (M/S)	SEA TEMP (DEG)	GHT (HR MIN SEC)	CELL COORDINATES		S193 DATA AZIMTH FLAG (DEG)
		VV (DB)	HH (DB)	VH (DB)	HV (DB)	V (DEG)	H (DEG)					LAT (DEG)	LONG (DEG)	
18.1	47.3	-15.59	-19.36	-16.92	-18.22	129.28	99.15	55.1	6.2		16 41 54.5	44.16	-37.74	162.9
18.2	39.4	-10.08	-16.34	-19.17	-16.04	130.23	103.98	73.5	6.8		16 41 58.0	45.07	-37.78	162.3
18.3	30.2	-12.25	-12.38	-14.12	-18.95	129.68	112.74	77.3	7.8		16 42 1.3	45.96	-37.87	163.7
18.4	15.9	1.10		-2.58	-2.85	123.32	118.99	82.7	9.4		16 42 4.1	47.04	-38.06	164.3
18.5														
20.1	47.4		-10.61	-11.05	-10.49	128.38	97.83	70.0	7.5		16 42 25.0	44.66	-35.22	165.0
20.2	40.6	-6.76	-9.75	-11.00	-10.06	130.55	105.82	72.6	8.4		16 42 28.5	45.48	-35.21	165.4
20.3	30.2	-4.93	-7.02	-9.91	-9.15	130.12	113.12	75.4	9.7		16 42 31.8	46.47	-35.27	165.6
20.4	16.3	6.56	4.52		2.48	125.46	119.39	76.2	11.2		16 42 34.6	47.58	-35.27	166.8
20.5	0.3	14.35				123.34		-18.8	12.6		16 42 36.7	48.62	-35.62	281.8
22.1	47.4	-7.27	-11.32	-10.22	-9.76	129.60	97.75	177.8	10.0		16 42 35.5	45.12	-32.66	167.2
22.2	40.6	-6.07	-9.16	-10.06	-11.24	130.98	105.58	178.6	10.9		16 42 39.0	45.93	-32.60	167.4
22.3	30.2					129.19		178.1	11.7		16 43 2.1	46.91	-32.64	167.9
22.4														
22.5														

JSC - 8/ 7/75

S. TRUTH - 8/12/75

LAST MOD - 7/13/75

THIS LISTING - 10/21/75

DOY 9-1, 3/ 9/74 CTNC-L/R,-NORTH ATLANTIC

(RIGHT SIDE)

SCAN NUM	INCID ANGLE (DEG)	SCATTERING COEFFICIENTS				ANTENNA V (DEG)	TEMPS H (DEG)	ASPECT ANGLE (DEG)	WIND SPEED (M/S)	SEA TEMP (DEG)	GMT (HR MIN SEC)	CELL COORDINATES		S193 DATA AZIMTH FLAG
		VV (DB)	HH (DB)	VH (DB)	HV (DB)							LAT (DEG)	LONG (DEG)	(DEG)
2.1	47.5	-10.07	-12.04	-13.22	-13.85	126.59	93.00	-135.7	6.7		15 53 37.8	34.46	-57.41	144.7
2.2	40.8	-8.51	-9.26	-11.08	-11.32	127.52	99.96	-132.9	6.1		15 53 41.4	33.24	-57.75	144.9
2.3	30.2	-5.64	-7.44	-10.91	-9.24	127.39	106.41	-117.0	6.4		15 53 44.6	36.18	-58.23	145.0
2.4	16.0	6.44	4.45	2.49	2.70	122.29	115.34	164.7	7.8		15 53 47.4	37.16	-58.83	145.3
2.5	0.2	15.52	13.44	11.34	11.07	122.34	122.56	11.6	9.8		15 53 49.6	38.12	-59.47	211.4
4.1	47.6	-8.17	-10.55	-10.92	-12.38	128.23	95.09	-162.0	8.1		15 54 8.4	33.54	-55.55	146.0
4.2	40.9	-7.98	-10.84	-11.32	-11.46	130.46	102.52	-117.0	8.7		15 54 11.9	36.32	-55.86	146.0
4.3	30.3	-3.43	-5.72	-8.04	-8.12	128.72	111.66	167.7	10.4		15 54 15.1	37.28	-56.34	146.3
4.4	16.1	7.87	5.76	3.86	3.63	125.78	118.37	157.0	12.5		15 54 17.9	38.27	-56.92	147.0
4.5	0.2	14.06	12.32	10.22	9.86	124.93	124.52	11.3	14.4		15 54 20.1	39.24	-57.54	230.7
6.1	47.6	-6.36	-11.25	-10.92	-8.85	129.05	97.18	113.8	11.4		15 54 38.8	36.59	-53.64	147.2
6.2	40.8	-5.79	-8.35	-8.79	-9.53	132.14	105.08	164.5	12.8		15 54 42.4	37.38	-53.94	147.5
6.3	30.2	-2.38	-4.86	-6.33	-6.75	132.99	113.78	155.3	14.5		15 54 45.6	38.34	-54.39	147.7
6.4	16.1	8.57	6.43	4.68	4.53	128.34	121.79	168.0	16.5		15 54 48.4	39.35	-54.94	148.0
6.5	0.3	13.32	11.43	9.22	9.21	128.73	127.03	14.5	18.6		15 54 50.6	40.32	-55.55	236.5
8.1	47.6	-6.51	-10.57	-8.85	-11.30	129.87	99.71	160.4	15.6		15 55 9.4	37.60	-51.67	148.6
8.2	40.8	-4.92	-8.42	-9.54	-8.94	134.67	107.50	155.4	16.3		15 55 12.9	38.40	-51.94	148.6
8.3	30.3	-0.51	-3.38	-4.84	-4.84	134.28	116.36	167.9	17.5		15 55 16.1	39.36	-52.37	149.1
8.4	16.1	8.06	6.18	4.39	4.35	130.95	125.26	145.5	18.9		15 55 18.9	40.38	-52.91	149.5
8.5	0.3	12.85	11.40	9.16	9.06	128.27	128.71	11.6	20.1		15 55 21.1	41.36	-53.48	239.4
10.1	48.9	-6.56	-10.89	-9.76	-11.61	131.51	99.63	171.9	17.2		15 55 39.8	38.42	-49.54	150.1
10.2	41.4	-3.69	-7.24	-8.24	-7.73	135.87	108.27	147.7	17.9		15 55 43.4	39.32	-49.85	150.3
10.3	30.4	-0.43	-3.55	-5.14	-5.14	134.65	118.04	163.4	18.7		15 55 46.6	40.33	-50.29	150.6
10.4	17.1	7.79	1.60	2.88	3.81	131.31	123.87	161.0	19.5		15 55 49.4	41.30	-50.75	151.0
10.5	7.1	11.23	8.69	7.73	9.39	130.78	127.78	159.0	20.1		15 55 51.6	41.97	-51.04	153.0
12.1	48.8	-4.99	-11.49	-10.34	-9.64	131.86	101.73	160.3	18.9		15 56 10.3	39.36	-47.46	151.7
12.2	41.3	-4.33	-8.34	-8.77	-7.68	134.52	109.06	149.2	19.3		15 56 13.9	40.25	-47.74	151.8
12.3	30.4	-1.18	-4.89	-6.38	-6.39	135.01	117.53	160.1	19.2		15 56 17.1	41.27	-48.14	151.9
12.4	17.1	7.77	1.30	2.64	3.69	131.67	123.37	158.4	20.0		15 56 19.9	42.25	-48.57	152.6
12.5	7.2	11.41	8.50	7.80	8.19	129.42	131.14	162.5	20.6		15 56 22.0	42.90	-48.85	157.5
14.1	48.6	-5.69	-11.49	-10.37	-8.80	131.79	102.88	147.8	21.0		15 56 40.8	40.25	-45.32	153.2
14.2	41.3	-4.15	-6.85	-6.76	-7.79	137.43	112.37	149.5	21.9		15 56 44.4	41.13	-45.57	153.5
14.3	30.3	-0.52	-4.34	-6.05	-4.37	136.45	120.95	162.4	21.4		15 56 47.6	42.16	-45.93	153.6
14.4	17.0	7.18	1.48	2.51	3.42	132.08	127.23	162.8	21.4		15 56 50.4	43.15	-46.34	154.2
14.5	7.1	11.13	6.10	7.24	9.38	133.26	131.92	167.1	22.7		15 56 52.6	43.82	-46.58	157.9
16.1	48.7	-4.89	-9.40	-8.80	-7.81	135.18	105.83	120.2	23.3		15 57 11.4	41.06	-43.11	154.8
16.2	41.3	-2.92	-5.78	-6.39	-6.82	138.68	114.89	120.9	24.0		15 57 14.9	41.96	-43.32	155.1
16.3	30.4	-0.24	-3.70	-4.89	-4.89	140.17	123.54	120.7	24.7		15 57 18.1	42.99	-43.65	155.3
16.4	17.0	7.20	1.29	2.16	3.26	136.84	130.26	123.9	25.7		15 57 20.9	43.99	-44.02	156.1
16.5	8.0	10.56	7.71	6.89	8.91	134.92	134.04	124.9	23.2		15 57 23.1	44.61	-44.21	158.1

10/21/75

DOY 9-1, 2/ 9/74 CTNC-L/R,-NORTH ATLANTIC

(RIGHT SIDE)

SCAN NUMB	INCID ANGLE (DEG)	SCATTERING COEFFICIENTS				ANTENNA V (DEG)	TEMPS M (DEG)	ASPECT ANGLE (DEG)	WIND SPEED (M/S)	SEA TEMP (DEG)	GMT (HR MIN SEC)	CELL COORDINATES		S193 DATA AZIMTH FLAG
		VV (DB)	HH (DB)	VH (DB)	HV (DB)							LAT (DEG)	LONG (DEG)	
18.1	48.9	-4.51	-9.92	-7.38	-8.47	135.11	107.88	117.5	23.4		15 57 41.8	41.82	-40.81	158.5
18.2	41.3	-3.30	-6.63	-8.26	-7.75	140.32	116.52	118.2	23.7		15 57 45.4	42.73	-41.02	156.8
18.3	30.4	0.12	-3.15	-4.41	-4.65	139.66	125.22	119.8	23.4		15 57 48.6	43.77	-41.31	157.2
18.4	17.1	7.19	1.22	1.89	3.18	138.96	133.24	121.9	22.6		15 57 51.4	44.77	-41.64	158.1
20.1	48.6	-3.96	-7.20	-7.11	-8.33	137.18	110.96	114.5	22.1		15 58 12.4	42.57	-38.51	158.5
20.2	41.3	-3.79	-6.45	-7.09	-9.47	141.10	117.29	115.1	22.2		15 58 15.9	43.45	-38.67	158.9
20.3	30.4	0.19	-3.00	-4.50	-4.71	142.67	126.45	115.8	21.6		15 58 19.1	44.49	-38.91	159.2
20.4	17.2	7.14	1.36	1.74	3.19	140.22	134.50	117.2	20.3		15 58 21.9	45.50	-39.19	159.8
20.5	9.1	9.78	7.24	6.28	8.05	139.09	137.76	117.3	19.3		15 58 24.0	46.07	-39.30	161.7
22.1	48.5	-5.01	-8.80	-9.27	-7.68	137.10	109.44	105.5	20.1		15 58 42.8	43.23	-36.14	160.5
22.2	41.2	-3.56	-6.15	-7.05	-7.61	141.03	117.64	106.3	20.6		15 58 46.4	44.13	-36.24	160.7
22.3	30.3	-0.50	-3.40	-4.72	-4.75	142.60	125.51	106.9	19.8		15 58 49.6	45.17	-36.44	161.1
22.4	17.3	6.64	0.02	1.07	2.76	137.51	131.81	108.3	17.8		15 58 52.4	46.17	-36.68	161.7
22.5	9.2	9.63	6.91	6.04	7.93	136.86	136.41	107.6	16.4		15 58 54.6	46.73	-36.75	164.4
24.1	48.5	-6.00	-8.65	-9.03	-9.52	134.90	106.81	94.6	19.3		15 59 13.4	43.84	-33.71	162.4
24.2	41.3	-4.23	-7.08	-7.56	-8.13	138.41	115.46	95.2	19.4		15 59 16.9	44.72	-33.77	162.8
24.3	30.3	-1.17	-4.58	-6.64	-5.91	136.83	122.83	95.8	18.0		15 59 20.1	45.77	-33.92	163.2
24.4	17.3	6.72	-0.11	0.74	2.51	133.04	129.11	96.2	15.4		15 59 22.9	46.77	-34.11	163.8
24.5	9.5	10.04	7.98	6.32	8.57	131.19	131.21	95.4	13.4		15 59 25.0	47.32	-34.15	165.6
26.1	48.6	-7.09	-11.07	-11.76	-11.12	133.98	105.47	84.5	18.7		15 59 43.8	44.36	-31.21	164.5
26.2	41.2	-5.62	-8.68	-10.11	-8.65	136.64	111.99	84.3	18.3		15 59 47.4	45.26	-31.22	164.7
26.3	30.4	-2.26	-5.36	-6.98	-8.00	138.52	121.01	85.0	16.1		15 59 50.6	46.30	-31.32	165.0
26.4	17.4	6.22	-0.60	0.01	2.10	133.43	128.86	79.8	12.8		15 59 53.4	47.31	-31.46	166.2
26.5	9.7	9.57	6.72	5.79	8.37	130.27	130.70	76.3	11.1		15 59 55.6	47.85	-31.48	167.7

JSC - 7/26/75

S. IRUTH - 8/10/75

LAST MOD - 7/13/75

THIS LISTING - 10/21/75

DOY 11-2, 2/11/74 CTNC-L/R, NORTH ATLANTIC

(RIGHT SIDE)

SCAN NO	INCID ANGLE (DEG)	SCATTERING COEFFICIENTS				ANTENNA V (DEG)	TEMPS H (DEG)	ASPECT ANGLE (DEG)	WIND SPEED (M/S)	SEA TEMP (DEG)	GMT			CELL COORDINATES		S193 DATA AZIMUTH FLAG (DEG)
		VV (DB)	HH (DB)	VH (DB)	HV (DB)						(HR MIN SEC)	LAT (DEG)	LONG (DEG)			
2.1	43.7	-10.62	-12.31	-11.21	-12.06	132.47	100.53	111.0	9.8		17 44 15.3	46.13	-52.23	179.0		
2.2	41.3	-9.71	-10.29	-12.17	-12.33	136.41	108.76	109.7	8.0		17 44 18.9	47.01	-51.93	179.3		
2.3	38.4	-5.43	-10.22	-13.72	-13.71	137.38	117.65	107.3	10.7		17 44 22.1	48.04	-51.67	179.7		
2.4	17.2	6.08	-2.47	-0.59	2.23	134.49	126.55	106.2	12.4		17 44 24.9	49.05	-51.43	180.8		
2.5	9.2	10.23	7.56	6.73	8.61	133.91	131.27	103.9	13.2		17 44 27.0	49.59	-51.24	184.1		
4.1	48.9	-9.45	-11.09	-11.85	-11.60	127.77	95.02	102.8	9.8		17 44 45.8	46.12	-49.52	181.2		
4.2	41.3	-7.59	-10.29	-12.17	-10.93	130.86	104.52	103.5	11.7		17 44 49.4	47.01	-49.19	181.5		
4.3	30.3	-4.78	-9.01	-10.84	-9.75	132.55	112.41	101.9	13.7		17 44 52.6	48.04	-48.87	182.1		
4.4	17.3	6.52	-1.55	0.20	2.63	128.78	121.74	101.0	15.4		17 44 55.4	49.03	-48.57	183.0		
4.5	9.5	9.76	6.81	6.09	8.09	128.73	126.51	98.4	16.0		17 44 57.5	49.55	-48.34	184.6		
6.1	48.9	-10.07	-13.49	-10.26	-12.56	127.30	96.24	78.5	13.4		17 45 16.3	46.05	-46.84	183.5		
6.2	41.3	-6.17	-11.19	-11.05	-8.44	132.09	105.75	79.0	15.0		17 45 19.9	46.94	-46.46	184.0		
6.3	30.3	-2.60	-6.25	-6.84	-7.31	132.93	113.72	77.7	16.6		17 45 23.1	47.96	-46.06	184.3		
6.4	17.4	6.22	-1.30	0.19	2.50	130.52	123.05	75.9	17.5		17 45 25.8	48.92	-45.72	185.1		
6.5	9.8	9.61	6.62	5.84	8.21	128.72	126.98	74.3	17.9		17 45 28.0	49.43	-45.46	186.7		
8.1	49.1	-7.89	-11.42	-9.49	-10.99	129.86	98.37	76.1	16.9		17 45 46.8	45.89	-44.16	185.9		
8.2	41.3	-6.27	-9.07	-9.97	-11.07	133.79	107.02	76.6	18.0		17 45 50.4	46.79	-43.73	186.4		
8.3	30.4	-1.95	-6.27	-7.30	-6.04	133.37	116.73	74.0	18.6		17 45 53.6	47.79	-43.30	187.0		
8.4	17.5	6.07	-1.25	-0.10	1.96	130.03	124.31	73.4	19.2		17 45 56.4	48.74	-42.89	187.6		
8.5	10.0	8.92	6.39	5.58	7.84	128.68	127.78	70.7	19.4		17 45 58.5	49.24	-42.60	189.3		
10.1	49.2	-5.95	-12.34	-10.27	-9.55	130.22	100.02	77.8	19.6		17 46 17.3	45.67	-41.50	188.2		
10.2	41.3	-4.90	-7.65	-8.46	-9.20	135.02	109.51	73.4	19.8		17 46 20.9	46.56	-41.02	188.6		
10.3	30.4	-1.68	-5.73	-6.10	-6.09	135.07	116.67	72.1	19.9		17 46 24.1	47.55	-40.53	188.9		
10.4	17.7	6.01	-0.85	-0.29	2.17	130.43	125.13	70.1	19.9		17 46 26.9	48.48	-40.08	189.9		
10.5	10.3	10.15	6.21	5.33	7.57	128.63	126.83	67.4	19.8		17 46 29.0	48.96	-39.76	191.6		
12.1	48.8	-6.59	-12.78	-10.65	-11.01	130.61	99.97	73.7	20.5		17 46 47.8	45.43	-38.85	190.3		
12.2	41.4	-4.33	-8.59	-9.21	-7.41	134.54	108.62	71.2	20.3		17 46 51.4	46.26	-38.34	190.8		
12.3	30.4	-2.65	-5.74	-6.87	-8.48	133.71	116.64	68.8	20.1		17 46 54.6	47.24	-37.80	191.2		
12.4	17.7	5.67	-1.15	-0.62	2.09	127.31	122.03	65.9	19.0		17 46 57.3	48.16	-37.30	192.1		
12.5	10.5	10.28	6.27	5.02	7.70	126.43	122.98	63.6	18.4		17 46 59.5	48.62	-36.96	194.4		
14.1	48.8	-6.84	-12.38	-9.59	-9.86	129.71	98.23	70.4	19.3		17 47 18.3	45.09	-36.24	192.6		
14.2	41.4	-5.89	-9.11	-10.02	-8.56	133.65	106.45	68.0	18.7		17 47 21.9	45.90	-35.70	193.0		
14.3	30.4	-2.99	-6.28	-7.83	-7.34	131.47	113.97	65.6	17.2		17 47 25.1	46.86	-35.11	193.4		
14.4	17.9	5.95	-1.92	-1.35	1.75	126.38	119.81	63.6	15.8		17 47 27.9	47.75	-34.56	194.4		
14.5	10.8	9.29	6.29	5.23	8.35	125.96	121.21	61.5	15.0		17 47 30.0	48.19	-34.20	195.5		
16.1	48.8	-7.44	-11.46	-9.59	-11.04	128.80	96.91	68.3	17.1		17 47 48.8	44.67	-33.68	194.7		
16.2	41.3	-6.75	-9.70	-9.24	-11.12	131.47	105.98	67.0	15.8		17 47 52.4	45.46	-33.22	195.0		
16.3	30.4	-4.34	-7.68	-9.15	-9.15	130.11	111.74	64.3	13.8		17 47 55.6	46.40	-32.46	195.7		
16.4	17.9	5.64	-2.69	-2.24	1.89	125.02	118.01	61.3	11.8		17 47 58.4	47.28	-31.88	196.7		
16.5	10.9	9.67	6.72	5.71	8.29	123.32	119.89	57.3	10.7		17 48 0.5	47.71	-31.51	198.7		

10/21/75

DOY 11-2, 1/11/74 CYNCL/R, NORTH ATLANTIC

(RIGHT SIDE)

SCAN NUMB	INCID ANGLE (DEG)	SCATTERING COEFFICIENTS				ANTENNA V (DEG)	TEMP H (DEG)	ASPECT ANGLE (DEG)	WIND SPEED (M/S)	SEA TEMP (DEG)	GMT (HR MIN SEC)	CELL COORDINATES		S193 DATA AZIMUTH FLAG (DEG)
		VV (DB)	HH (DB)	VH (DB)	HV (DB)							LAT (DEG)	LONG (DEG)	
34.1	48.8	-6.92	-10.81	-9.70	-9.52	134.83	101.22	5.0	10.6		17 52 23.3	38.13	-12.90	211.0
34.2	41.4	-4.90	-7.77	-8.82	-8.24	141.74	113.26	5.7	10.3		17 52 26.9	38.78	-12.12	211.3
34.3	30.5	-2.32	-6.27	-6.17	-7.52	148.14	126.21	12.5	9.8		17 52 30.1	39.54	-11.25	211.5
34.4	18.4	6.06	-1.90	-1.35	2.62	154.48	146.02	5.5	9.2		17 52 32.8	40.24	-10.46	212.5
34.5	12.0	9.75	6.41	5.01	6.81	159.09	154.18	4.0	9.7		17 52 35.0	40.54	-10.02	213.0
36.1	48.7		-12.40	-14.03		145.45		-13.3	7.4		17 52 53.1	37.19	-10.93	212.3
36.2														
36.3														
36.4														
36.5														

JSC - 7/25/75

S. TRUTH - 6/19/75

LAST MOD - 7/13/75

THIS LISTING - 10/21/75

REPRODUCIBILITY OF THIS
 ORIGINAL PAGE IS POOR

DOY 11-2, 1/11/74 CTNC-L/R, NORTH ATLANTIC (RIGHT SIDE)														
SCAN NUMB	INCID ANGLE (DEG)	SCATTERING COEFFICIENTS				ANTENNA V (DEG)	TEMPS H (DEG)	ASPECT ANGLE (DEG)	WIND SPEED (M/S)	SEA TEMP (DEG)	GMT (HR MIN SEC)	CELL COORDINATES		S193 DATA AZIMTH FLAG (DEG)
		VV (DB)	HH (DB)	VH (DB)	HV (DB)							LAT (DEG)	LONG (DEG)	
18.1	48.8	-9.10	-14.13	-14.85	-20.62	127.06	97.34	71.1	13.4		17 48 19.3	44.18	-31.15	196.9
18.2	41.4	-5.91	-9.07	-9.94	-9.25	131.05	104.29	77.8	14.9		17 48 22.9	44.95	-30.54	197.2
18.3	30.5	-4.90	-6.93	-9.04	-10.89	130.56	110.44	84.3	13.8		17 48 26.1	45.88	-29.87	197.7
18.4	18.0	5.24	-3.32	-1.96	1.58	125.03	118.45	83.2	13.0		17 48 28.8	46.73	-29.25	198.8
18.5														
20.1	48.7	-5.57	-10.28	-7.98	-9.16	127.92	96.88	87.0	16.6		17 48 49.8	43.63	-28.68	199.0 -2
20.2	41.4	-5.51	-7.26	-9.51	-10.69	131.00	104.26	82.7	16.7		17 48 53.4	44.38	-28.04	199.3
20.3	30.5	-4.15	-7.61	-9.38	-8.64	130.52	111.27	79.5	16.1		17 48 56.6	45.29	-27.31	199.5
20.4	18.1	6.16	-2.62	-1.81	2.25	126.30	118.85	78.5	15.4		17 48 59.4	46.12	-26.66	200.5
20.5	11.3	9.30	6.71	5.74	7.75	125.44	122.42	76.4	15.0		17 49 1.5	46.51	-26.26	201.6
22.1	48.8	-7.51	-10.30	-9.95	-13.19	127.87	96.41	74.3	20.2		17 49 20.3	43.00	-26.25	200.7
22.2	41.4	-7.90	-9.87	-9.53	-10.71	130.54	104.64	70.9	19.6		17 49 23.9	43.75	-25.57	201.1
22.3	30.5	-5.04	-7.16	-7.91	-8.64	131.34	112.53	68.4	18.8		17 49 27.1	44.64	-24.83	201.6
22.4	18.1	6.38	-2.72	-1.36	2.87	128.01	120.98	64.4	18.1		17 49 29.8	45.45	-24.14	202.6
22.5	11.4	10.53	6.76	5.55	7.20	128.40	125.76	62.2	17.8		17 49 32.0	45.83	-23.74	203.8
24.1	48.7	-6.21	-9.68	-9.21	-13.19	127.82	96.78	82.4	21.0		17 49 50.8	42.34	-23.88	202.6
24.2	41.4	-5.93	-8.19	-8.03	-10.73	131.76	105.82	88.9	21.1		17 49 54.4	43.06	-23.18	203.1
24.3	30.5	-3.47	-6.20	-7.45	-8.77	133.48	116.85	86.5	21.4		17 49 57.6	43.93	-22.40	203.5
24.4	18.2	6.22	-2.14	-0.96	2.55	130.14	125.29	82.7	22.0		17 50 0.4	44.72	-21.69	204.3
24.5	11.6	9.72	6.50	4.95	6.44	131.36	130.46	80.9	22.7		17 50 2.5	45.08	-21.28	205.1
26.1	48.7	-6.08	-10.32	-9.22	-9.48	130.33	98.85	82.5	19.3		17 50 21.3	41.60	-21.56	204.5
26.2	41.4	-3.28	-6.59	-7.55	-7.55	135.11	106.64	84.0	20.3		17 50 24.9	42.31	-20.85	205.0
26.3	30.5	-0.97	-4.28	-5.09	-6.18	135.18	116.79	80.8	21.9		17 50 28.1	43.15	-20.05	205.2
26.4	18.3	6.54	0.10	0.45	2.78	132.71	127.43	84.7	23.7		17 50 30.8	43.92	-19.32	206.3
26.5	11.7	9.56	6.58	5.20	6.49	135.18	130.83	84.7	24.2		17 50 33.0	44.27	-18.89	207.3
28.1	48.8	-6.89	-13.72	-12.61	-10.30	130.27	98.79	80.8	15.1		17 50 51.8	40.80	-19.30	206.2
28.2	41.4	-5.14	-8.68	-8.79	-8.78	135.05	106.59	89.3	16.6		17 50 55.4	41.50	-18.57	206.7
28.3	30.5	-0.25	-4.50	-5.10	-4.50	137.31	116.29	82.0	18.6		17 50 58.6	42.33	-17.75	207.0
28.4	18.3	7.17	0.59	0.37	3.47	134.85	123.87	84.0	19.3		17 51 1.4	43.08	-17.00	208.0
28.5	11.8	10.20	7.11	5.89	6.96	135.11	130.30	80.1	19.6		17 51 3.5	43.42	-16.57	208.9
30.1	48.7	-6.48	-11.11	-10.92	-10.31	131.49	98.31	89.2	12.4		17 51 22.3	39.97	-17.11	207.8
30.2	41.3	-5.15	-8.70	-9.57	-8.81	137.55	107.39	80.8	13.6		17 51 25.9	40.65	-16.36	208.2
30.3	30.5	-1.39	-5.41	-6.13	-7.07	138.57	116.25	8.2	15.4		17 51 29.1	41.45	-15.52	208.8
30.4	18.3	7.00	-0.82	-0.12	3.31	134.80	124.74	2.3	16.3		17 51 31.8	42.18	-14.76	209.7
30.5	11.9	9.89	6.78	5.43	6.97	133.38	129.02	1.2	16.5		17 51 34.0	42.50	-14.32	210.2
32.1	48.8	-6.50	-9.28	-8.16	-10.33	131.05	97.04	2.6	11.7		17 51 52.8	39.07	-14.98	209.4
32.2	41.4	-4.62	-6.97	-8.16	-8.98	136.27	105.88	0.9	12.8		17 51 56.4	39.73	-14.21	209.9
32.3	30.5	-0.76	-4.73	-5.45	-6.63	137.68	115.80	5.6	12.7		17 51 59.6	40.52	-13.36	210.4
32.4	18.3	7.31	0.01	0.69	3.97	138.30	126.88	5.0	13.1		17 52 2.3	41.24	-12.57	211.0
32.5	11.9	10.42	7.46	6.00	7.29	140.22	132.00	0.7	13.5		17 52 4.5	41.55	-12.13	211.3

10/21/75

DCY 24-1, 1/24/74 CTNC-L/R, NORTH ATLANTIC										(RIGHT SIDE)				
SCAN NO	INCID ANGLE (DEG)	SCATTERING COEFFICIENTS				ANTENNA V (DEG)	TEMP H (DEG)	ASPECT ANGLE (DEG)	WIND SPEED (M/S)	SEA TEMP (DEG)	GMT (HR MIN SEC)	CELL COORDINATES		S193 DATA AZIMUTH FLAG (DEG)
		VV (DB)	HH (DB)	VH (DB)	HV (DB)							LAT (DEG)	LONG (DEG)	
2.1	49.9	-7.87	-12.00	-9.96	-10.30	125.65	92.56	118.1	11.3		17 47 36.0	44.64	-146.49	165.9 2
2.2	42.3	-6.84	-9.27	-8.15	-9.77	130.04	101.05	115.8	14.1		17 47 39.6	45.63	-146.49	166.2
2.3	31.7	-3.26	-8.15	-8.05	-8.08	130.89	113.02	114.9	16.9		17 47 42.8	46.69	-146.54	166.1
2.4	23.1	2.26	-3.44	-4.00	0.32	128.88	119.30	115.1	18.6		17 47 45.6	47.41	-146.53	165.9
2.5	13.0	9.91	6.87	5.53	6.01	127.09	124.14	114.9	19.9		17 47 47.7	48.15	-146.58	166.1
4.1	50.0	-7.35	-10.33	-9.97	-11.29	128.27	95.17	110.9	13.0		17 48 6.5	45.02	-143.91	168.1 2
4.2	42.3	-6.84	-9.93	-9.58	-10.76	133.49	106.37	110.6	15.2		17 48 10.1	46.01	-143.88	168.4
4.3	31.8	-3.33	-8.65	-8.05	-8.83	133.96	116.08	109.6	17.9		17 48 13.3	47.07	-143.86	168.4 2
4.4	23.8	1.95	-3.88	-4.71	-0.56	132.39	123.23	108.7	18.5		17 48 16.1	47.74	-143.80	168.3
4.5	10.8	9.33	7.62	6.50	7.19	131.83	131.43	109.8	19.7		17 48 18.2	48.69	-143.86	167.2 2
5.1	50.1	-6.72	-9.68	-9.97	-9.21	131.26	98.16	102.6	13.0		17 48 37.0	45.33	-141.32	170.4
5.2	42.3	-6.85	-9.36	-9.69	-9.79	134.77	107.23	101.3	14.3		17 48 40.6	46.32	-141.22	170.7
5.3	31.8	-2.50	-7.30	-7.48	-7.03	135.29	117.83	98.2	15.1		17 48 43.8	47.37	-141.17	170.8
5.4	24.0	1.64	-3.75	-4.50	-0.93	132.83	125.42	96.5	15.5		17 48 46.6	48.03	-141.05	170.5
5.5	10.3	9.43	7.50	6.27	7.15	132.70	130.58	96.7	15.2		17 48 48.7	49.03	-141.07	169.3
7.1	50.0	-7.36	-12.43	-11.32	-10.30	129.94	97.71	90.4	12.0		17 49 7.5	45.58	-138.69	172.6
7.2	42.3	-5.56	-8.26	-8.09	-9.69	134.30	107.25	87.0	12.6		17 49 11.1	46.56	-138.55	173.0
7.3	31.8	-2.69	-7.71	-6.99	-6.59	134.40	116.97	82.8	13.0		17 49 14.3	47.62	-138.42	173.2
7.4	24.3	1.40	-3.74	-5.31	-1.51	132.83	122.81	79.9	12.9		17 49 17.1	48.24	-138.27	173.1
7.5	10.3	9.72	7.69	6.35	7.62	129.68	128.87	77.4	12.7		17 49 19.2	49.27	-138.24	171.6
10.1	50.0	-8.74	-10.34	-12.06	-10.67	129.95	95.60	74.9	11.2		17 49 38.0	45.76	-136.05	175.1
10.2	42.3	-6.86	-9.35	-10.65	-10.78	133.46	105.94	73.7	11.6		17 49 41.6	46.73	-135.84	175.3
10.3	31.8	-3.78	-7.71	-8.05	-8.84	133.93	115.63	71.7	12.0		17 49 44.8	47.77	-135.66	175.3
10.4	24.3	1.19	-4.24	-5.32	-1.89	131.91	122.78	70.9	12.2		17 49 47.6	48.40	-135.47	175.1
10.5	10.5	9.82	7.82	6.59	7.72	131.36	127.56	71.9	12.6		17 49 49.7	49.41	-135.38	174.1
12.1	50.0	-8.24	-11.44	-11.32	-9.23	129.54	97.75	64.6	10.3		17 50 8.5	45.86	-133.40	177.4
12.2	42.3	-6.80	-9.37	-9.69	-8.91	133.90	107.24	64.3	10.3		17 50 12.1	46.82	-133.14	177.7
12.3	31.8	-5.19	-8.66	-11.53	-10.57	134.37	115.65	63.4	10.5		17 50 15.3	47.86	-132.89	177.6
12.4	24.3	-0.68	-5.98	-6.63	-3.38	133.24	122.35	61.4	10.5		17 50 18.1	48.49	-132.67	177.6
12.5														

JSC - 7/31/79

S. TRUTH - 8/10/75

LAST MOD - 8/13/75

THIS LISTING - 10/21/75

DOY 25-1, 1/25/74 CTNC-L/R, NORTH PACIFIC										(RIGHT SIDE)							
SCAN NUMB	INCID ANGLE (DEG)	SCATTERING COEFFICIENTS				ANTENNA V (DEG)	TEMPS H (DEG)	ASPECT ANGLE (DEG)	WIND SPEED (M/S)	SEA TEMP (DEG)	GMT			CELL COORDINATES		S193 AZINTH (DEG)	DATA FLAG
		VV (DB)	HH (DB)	VH (DB)	HV (DB)						HR	MIN	SEC	LAT (DEG)	LONG (DEG)		
2.1	49.8	-9.19	-9.73	-10.94	-9.53	122.34	88.95	64.5	6.9		17	4	18.5	43.91	-145.81	162.5	-2
2.2	42.1	-9.49	-11.81	-11.93	-12.11	126.24	97.54	66.5	7.7		17	4	22.0	44.89	-145.89	162.5	
2.3	31.4	-6.74	-10.65	-13.17	-13.21	125.54	105.11	65.5	8.2		17	4	25.3	45.95	-146.02	162.5	
2.4	23.0	-0.51	-6.90	-9.01	-1.77	123.54	113.08	64.0	8.6		17	4	28.0	46.65	-146.07	162.0	
2.5	12.5	10.26	7.36	6.02	6.96	122.31	116.76	61.8	8.9		17	4	30.2	47.43	-146.19	161.2	
4.1	49.7	-11.47	-13.76	-14.52	-13.28	124.19	90.76	73.5	6.7		17	4	49.0	44.41	-143.31	164.5	-2
4.2	42.1	-8.60	-10.85	-11.93	-11.94	128.09	99.35	73.4	7.7		17	4	52.5	45.37	-143.34	164.6	
4.3	31.6	-6.81	-10.65	-13.16	-26.38	127.45	107.86	72.5	8.5		17	4	55.8	46.43	-143.42	164.5	
4.4	23.6	-0.51	-7.63	-9.50	-2.36	125.41	114.93	71.8	8.9		17	4	58.5	47.10	-143.41	164.2	
4.5	10.9	11.18	8.41	7.35	8.82	121.14	119.84	72.9	9.4		17	5	0.7	48.03	-143.55	163.1	
6.1	49.9	-8.78	-11.14	-10.94	-13.28	126.04	92.51	89.3	6.6		17	5	19.5	44.82	-140.76	166.7	ORIGINAL
6.2	42.2	-6.90	-9.98	-10.57	-12.10	129.47	100.26	86.1	7.7		17	5	23.0	45.80	-140.75	166.9	
6.3	31.7	-4.03	-9.25	-9.49	-9.53	129.76	109.25	86.2	8.6		17	5	26.3	46.85	-140.77	166.8	
6.4	23.9	0.93	-4.70	-6.66	-1.38	126.41	116.34	87.6	9.0		17	5	29.0	47.51	-140.72	166.4	
6.5	10.3	11.25	8.95	7.66	9.05	125.97	120.39	83.0	9.4		17	5	31.2	48.50	-140.83	164.0	
8.1	49.9	-6.95	-11.14	-10.94	-10.35	126.97	93.85	110.0	7.4		17	5	50.0	45.16	-138.18	169.0	ORIGINAL
8.2	42.2	-6.02	-9.40	-9.73	-10.83	130.88	102.46	109.0	8.0		17	5	53.5	46.15	-138.11	169.0	
8.3	31.7	-2.56	-7.75	-8.74	-7.57	128.14	110.23	109.0	8.8		17	5	56.8	47.20	-138.08	169.0	
8.4	24.0	2.14	-4.03	-5.82	-0.82	128.72	116.89	111.2	9.1		17	5	59.5	47.85	-138.01	168.8	
8.5	10.3	11.09	8.62	7.79	8.74	124.80	121.79	115.1	9.7		17	6	1.7	48.85	-138.05	166.9	
10.1	49.9	-7.41	-10.39	-10.03	-10.35	128.74	96.00	128.8	9.1		17	6	20.5	45.45	-135.56	171.2	ORIGINAL
10.2	42.3	-5.21	-9.33	-8.21	-8.86	132.66	105.03	129.7	9.5		17	6	24.0	46.43	-135.44	171.3	
10.3	31.8	-2.22	-7.29	-6.96	-6.64	132.17	114.21	130.7	10.0		17	6	27.3	47.48	-135.36	171.3	
10.4	24.3	2.26	-3.79	-4.55	-0.06	130.61	120.02	131.0	10.6		17	6	30.0	48.11	-135.23	171.0	
10.5	10.5	10.75	8.65	7.46	8.57	129.19	126.98	132.1	11.4		17	6	32.2	49.12	-135.22	169.9	
12.1	30.1	-7.11	-9.74	-9.27	-10.71	129.68	98.15	137.5	11.9		17	6	51.0	45.65	-132.93	173.5	ORIGINAL
12.2	42.3	-5.61	-10.07	-9.74	-9.74	134.44	107.61	137.5	12.4		17	6	54.5	46.64	-132.75	173.5	
12.3	31.8	-2.08	-7.76	-7.53	-7.66	134.90	117.77	136.4	12.6		17	6	57.8	47.69	-132.61	173.6	
12.4	24.5	2.42	-3.68	-4.03	-0.74	133.73	123.59	136.9	12.8		17	7	0.5	48.30	-132.44	173.1	
12.5	10.7	10.77	8.42	7.21	8.36	133.57	130.50	138.2	13.0		17	7	2.7	49.31	-132.38	171.8	
14.1	30.1	-7.60	-9.51	-9.01	-11.81	132.80	102.86	137.2	13.9		17	7	21.5	45.79	-130.27	175.8	ORIGINAL
14.2	42.3	-5.30	-8.32	-9.74	-10.83	137.99	112.80	137.1	14.0		17	7	25.0	46.78	-130.05	175.9	
14.3	31.8	-2.06	-10.12	-8.95	-7.09	139.87	123.13	137.2	13.1		17	7	28.3	47.82	-129.84	175.8	
14.4	24.7	2.10	-3.68	-4.03	-1.04	141.35	130.72	137.5	12.9		17	7	31.0	48.41	-129.64	175.5	
14.5	11.2	10.53	8.13	7.10	8.53	146.65	141.37	137.9	12.1		17	7	33.2	49.41	-129.52	174.1	
16.1	30.0	-6.69	-10.67	-10.37	-11.82	141.45	116.17	130.0	13.9		17	7	52.0	45.87	-127.60	178.0	ORIGINAL
16.2	42.3	-5.30	-9.47	-9.65	-8.36	150.06	128.60	131.7	13.1		17	7	55.5	46.85	-127.34	178.3	
16.3	31.9	-2.41	-8.28	-8.19	-7.66	156.72	142.93	133.7	11.8		17	7	58.8	47.88	-127.07	178.3	
16.4	24.8	-21.38			-21.78	161.74	156.25	135.8	11.1		17	8	1.5	48.46	-126.83	178.2	
16.5																	

REPRODUCIBILITY OF THE
ORIGINAL PAGE IS POOR

-2

-2

10/21/75

DOY 27-1, 1/27/74 CTNC-L/R, WEST OF MEXICO

(RIGHT SIDE)

SCAN NUMB	INCID ANGLE (DEG)	SCATTERING COEFFICIENTS				ANTENNA V (DEG)	TEMPS H (DEG)	ASPECT ANGLE (DEG)	WIND SPEED (M/S)	SEA TEMP (DEG)	GMT (HR MIN SEC)	CELL COORDINATES		S193 DATA	
		VV (DB)	HH (DB)	VH (DB)	HV (DB)							LAT (DEG)	LONG (DEG)	AZIMTH (DEG)	FLAG
2.1	49.0	-7.77	-11.51	-10.41	-13.02	129.80	99.36	53.4	1.6		12 15 59.3	4.77	-144.55	129.6	-2
2.2	41.7	-6.32	-10.33	-12.13	-11.04	134.16	105.29	79.3	1.1		12 16 2.8	5.50	-145.39	129.7	-2
2.3	31.0	-6.23	-7.63	-9.00	-9.87	134.21	113.66	60.9	0.5		12 16 6.1	6.32	-146.04	129.1	-2
2.4	20.7	1.38	-7.04	-8.05	-0.22	130.87	119.06	-21.9	0.3		12 16 8.8	6.97	-146.55	128.9	-2
2.5	15.7	5.88	3.56	1.78	2.19	130.83	123.96	-44.7	0.5		12 16 11.0	7.31	-146.74	128.7	
4.1	49.1	-7.96	-12.83	-11.72	-12.17	133.19	99.17	40.2	2.0		12 16 29.8	6.25	-143.68	129.8	-2
4.2	41.7	-6.32	-11.20	-12.28	-11.04	136.71	108.72	24.3	1.7		12 16 33.3	6.99	-144.22	129.7	
4.3	31.0	-4.62	-8.53	-9.10	-11.95	136.06	115.44	-0.7	1.6		12 16 36.5	7.81	-144.08	129.7	
4.4	21.5	1.06	-5.53	-6.74	-0.58	133.97	123.89	-19.0	1.7		12 16 39.3	8.43	-145.35	129.0	
4.5	16.2	4.98	2.77	0.72	1.16	132.97	124.80	-29.7	1.9		12 16 41.5	8.78	-145.56	128.7	
6.1	49.2	-7.29	-14.11	-13.01	-11.69	134.89	101.29	19.0	3.0		12 17 0.3	7.72	-142.50	130.0	
6.2	41.8	-7.69	-11.19	-12.27	-11.03	138.01	111.25	9.0	3.0		12 17 3.6	8.47	-143.04	130.0	
6.3	31.1	-5.84	-8.45	-9.72	-10.78	133.63	118.91	-7.8	3.0		12 17 7.0	9.30	-143.70	129.8	
6.4	21.8	0.66	-6.03	-7.03	-0.83	135.28	123.44	-13.3	3.2		12 17 9.8	9.91	-144.16	129.3	
6.5	16.2	5.03	3.29	1.68	1.51	131.23	127.36	-19.3	3.3		12 17 12.0	10.28	-144.39	129.3	
8.1	49.2	-10.35	-14.11	-14.86	-12.99	134.03	102.55	5.6	4.4		12 17 30.8	9.20	-141.32	130.4	
8.2	41.8	-9.72	-11.08	-10.90	-12.26	137.96	110.76	-2.4	4.5		12 17 34.3	9.95	-141.86	130.4	
8.3	31.1	-5.78	-9.48	-10.61	-9.73	137.24	119.29	-5.9	4.5		12 17 37.6	10.78	-142.52	129.9	
8.4	22.0	0.57	-6.79	-6.42	-1.11	133.47	125.13	-12.5	4.5		12 17 40.3	11.38	-142.96	129.5	
8.5	16.1	5.47	3.60	1.57	1.59	132.46	124.73	-14.3	4.5		12 17 42.5	11.76	-143.20	129.3	
10.1	49.2	-9.54	-11.48	-11.29	-12.99	135.29	103.34	-4.7	5.2		12 18 1.3	10.67	-140.12	130.7	
10.2	41.8	-8.33	-9.65	-12.09	-12.42	138.34	111.13	-6.7	5.3		12 18 4.8	11.42	-140.66	130.7	
10.3	31.1	-6.25	-9.57	-11.91	-13.81	137.19	118.37	-9.3	5.3		12 18 8.0	12.25	-141.31	130.3	
10.4	22.2	0.90	-5.67	-6.44	-0.81	134.29	124.20	-10.8	5.2		12 18 10.8	12.85	-141.75	129.8	
10.5	15.9	5.64	3.92	1.85	2.03	131.99	125.82	-12.7	5.2		12 18 13.0	13.25	-142.01	129.7	
12.1	49.3	-8.83	-13.54	-10.36	-11.67	139.94	108.81	-9.9	5.4		12 18 31.8	12.11	-138.90	130.9	
12.2	41.9	-7.16	-9.63	-10.88	-11.01	140.41	113.67	-10.9	5.5		12 18 35.3	12.88	-139.44	130.9	
12.3	31.2	-5.53	-8.30	-10.74	-13.81	139.38	121.05	-11.7	5.5		12 18 38.5	13.71	-140.10	130.7	
12.4	22.3	1.02	-5.48	-7.29	-0.79	137.35	127.25	-11.3	5.6		12 18 41.3	14.31	-140.52	130.3	
12.5	15.7	6.28	4.00	2.23	2.22	135.84	128.96	-11.9	5.6		12 18 43.5	14.73	-140.80	129.9	
14.1	49.3	-7.54	-12.39	-12.42	-11.26	136.90	105.40	-14.4	5.4		12 19 2.3	13.56	-137.66	131.4	
14.2	41.8	-7.21	-9.00	-9.08	-11.13	141.26	114.04	-10.1	5.5		12 19 5.8	14.33	-138.21	131.1	
14.3	31.2	-3.39	-9.55	-9.86	-8.34	140.64	123.10	-13.9	5.0		12 19 9.0	15.17	-138.86	130.9	
14.4	22.4	2.39	-4.02	-4.36	-0.14	138.62	129.87	-13.3	6.0		12 19 11.8	15.77	-139.28	130.3	
14.5	15.7	2.68	0.28	-0.89	-0.67	144.42	137.05	-13.5	6.0		12 19 14.0	16.19	-139.57	130.5	
16.1	49.3	-8.24	-15.94	-12.96	-12.96	136.85	104.92	-18.8	5.7		12 19 32.8	14.99	-136.41	131.8	
16.2	41.9	-7.20	-10.23	-12.08	-12.41	140.78	114.83	-17.5	5.9		12 19 36.3	15.77	-136.95	131.5	
16.3	31.2	-4.85	-10.29	-12.09	-9.82	140.59	121.30	-16.4	6.1		12 19 39.5	16.61	-137.60	131.4	
16.4	22.5	0.73	-5.31	-6.41	-1.06	139.09	128.46	-15.8	6.3		12 19 42.3	17.21	-138.02	130.8	
16.5	15.4	6.31	4.45	2.61	2.77	136.61	131.85	-15.7	6.3		12 19 44.5	17.65	-138.33	130.7	

10/21/75

DOY 27-1, 1/27/74 CTNC-L/R, WEST OF MEXICO

(RIGHT SIDE)

SCAN NUMB	INCID ANGLE (DEG)	SCATTERING COEFFICIENTS				ANTENNA V (DEG)	TEMPS H (DEG)	ASPECT ANGLE (DEG)	WIND SPEED (M/S)	SEA TEMP (DEG)	GMT (HR MIN SEC)	CELL COORDINATES		S193 DATA AZIMTH FLAG (DEG)
		VV (DB)	HH (DB)	VH (DB)	HV (DB)							LAT (DEG)	LONG (DEG)	
18.1	49.4	-8.02	-13.51	-12.40	-9.56	135.99	102.31	-23.2	6.3		12 20 3.3	16.40	-135.13	132.2
18.2	41.9	-6.63	-10.27	-10.86	-9.92	139.03	111.39	-20.1	6.5		12 20 6.8	17.19	-135.67	132.1
18.3	31.2	-4.57	-8.97	-9.79	-9.81	137.95	119.11	-18.9	6.7		12 20 10.0	18.05	-136.32	131.9
18.4	22.4	1.24	-4.88	-5.27	-0.77	135.49	124.52	-19.2	6.8		12 20 12.8	18.65	-136.74	131.2
18.5														
20.1	49.4	-8.47	-13.77	-12.65	-13.19	132.53	99.75	-29.6	7.0		12 20 33.8	17.81	-133.82	132.6
20.2	41.9	-6.47	-10.52	-11.11	-11.11	136.46	108.83	-26.5	7.4		12 20 37.3	18.61	-134.37	132.5
20.3	31.3	-5.09	-9.14	-9.18	-10.97	134.82	116.88	-25.3	7.7		12 20 40.6	19.47	-135.01	132.3
20.4	22.5	0.70	-5.87	-7.21	-1.45	132.36	121.41	-24.7	7.9		12 20 43.3	20.07	-135.43	131.7
20.5	15.4	6.55	4.59	2.64	2.66	131.81	124.08	-25.0	8.0		12 20 45.5	20.52	-135.74	132.0
22.1	49.6	-10.03	-12.22	-12.13	-12.35	131.17	99.27	-38.3	7.7		12 21 4.3	19.19	-132.48	133.3
22.2	42.0	-6.86	-9.85	-12.30	-10.15	135.56	107.08	-35.3	8.1		12 21 7.8	20.00	-133.04	133.3
22.3	31.3	-4.80	-10.41	-10.95	-10.04	133.90	115.08	-32.1	8.4		12 21 11.0	20.86	-133.69	133.1
22.4	22.6	0.39	-6.37	-7.50	-1.60	131.43	120.92	-30.4	8.6		12 21 13.8	21.47	-134.10	132.4
22.5	15.4	6.57	4.23	2.58	2.70	130.47	123.17	-29.5	8.8		12 21 16.0	21.93	-134.41	132.5
24.1	49.7	-8.80	-12.20	-11.07	-9.79	130.28	96.66	-46.7	8.2		12 21 34.8	20.57	-131.13	133.7
24.2	42.0	-7.81	-10.50	-11.09	-12.29	133.79	105.75	-43.7	8.4		12 21 38.3	21.39	-131.68	133.7
24.3	31.3	-6.02	-9.76	-12.09	-12.12	131.66	112.84	-39.6	8.5		12 21 41.5	22.26	-132.32	133.6
24.4	22.6	0.17	-5.69	-6.92	-1.75	130.05	119.99	-36.2	8.5		12 21 44.3	22.97	-132.73	133.2
24.5	15.3	6.40	4.35	2.59	2.67	128.69	121.83	-35.1	8.5		12 21 46.5	23.34	-133.05	133.1
26.1	49.7	-8.79	-12.20	-12.11	-11.45	129.33	95.75	-54.5	8.3		12 22 5.3	21.92	-129.75	134.5
26.2	42.0	-9.63	-11.17	-12.13	-10.14	133.31	104.84	-52.3	8.2		12 22 8.8	22.76	-130.29	134.3
26.3	31.3	-5.30	-8.55	-9.05	-9.16	132.04	112.94	-47.1	8.1		12 22 12.0	23.64	-130.93	134.1
26.4	22.7	0.35	-6.01	-7.51	-1.83	128.69	118.19	-45.7	8.1		12 22 14.8	24.25	-131.33	133.7
26.5	15.2	6.58	4.54	2.63	2.75	126.91	119.62	-44.3	8.1		12 22 17.0	24.73	-131.65	133.3
28.1	49.6	-9.72	-12.20	-12.10	-11.87	128.46	95.69	-61.2	7.9		12 22 35.8	23.28	-129.34	135.2
28.2	42.0	-7.79	-10.40	-10.95	-11.07	131.56	102.66	-59.1	7.7		12 22 39.3	24.10	-127.06	135.1
28.3	31.3	-6.37	-10.38	-13.67	-12.09	129.79	110.10	-53.9	8.2		12 22 42.5	24.99	-132.33	134.9
28.4	22.8	-0.24	-6.00	-7.50	-1.99	127.76	116.38	-56.6	6.5		12 22 45.3	25.60	-110.43	134.6
28.5	15.1	6.58	4.42	2.70	2.59	126.86	119.57	-53.9	2.0		12 22 47.5	26.10	-98.74	134.1
30.1	49.7	-12.81	-12.18	-13.48	-11.85	127.98	93.08	-71.9	7.7		12 23 6.3	24.60	-126.88	135.9
30.2	42.0	-9.09	-11.24	-12.26	-12.43	131.07	100.90	-71.8	7.8		12 23 9.8	25.43	-127.42	135.8
30.3	31.3	-7.21	-10.38	-16.28	-16.22	129.29	110.48	-72.7	8.0		12 23 13.0	26.33	-128.05	135.7
30.4	22.7	-1.16	-8.14	-10.01	-2.85	125.94	115.45	-74.2	8.3		12 23 15.8	26.96	-128.44	135.2
30.5	15.0	6.54	4.57	2.75	2.61	125.07	118.66	-75.9	8.5		12 23 18.0	27.46	-128.76	134.9
32.1	49.7	-9.15	-13.71	-14.17	-11.05	126.21	91.75	-86.6	7.7		12 23 36.8	25.90	-125.40	136.6
32.2	42.8	-8.41	-11.13	-10.02	-12.41	130.17	109.85	-89.3	7.7		12 23 40.3	26.75	-125.92	136.3
32.3	31.3	-5.93	-12.03	-13.65	-10.76	129.24	108.24	-93.4	7.8		12 23 43.5	27.65	-126.55	136.4
32.4	22.8	-0.48	-5.98	-8.18	-2.33	125.89	112.40	-96.3	7.9		12 23 46.3	28.28	-126.93	136.3
32.5	15.1	6.56	4.66	2.59	2.80	123.73	117.32	-98.3	8.0		12 23 48.5	28.78	-127.26	136.3

10/21/75

DOY 27-1, 1/27/74 CTNC-L/R, WEST OF MEXICO

(RIGHT SIDE)

SCAN NUMB	INCID ANGLE (DEG)	SCATTERING COEFFICIENTS				ANTENNA V (DEG)	TEMPS H (DEG)	ASPECT ANGLE (DEG)	WIND SPEED (M/S)	SEA TEMP (DEG)	GMT (HR MIN SEC)	CELL COORDINATES		3193 AZIMTH (DEG)	DATA FLAG
		VV (DB)	HH (DB)	VH (DB)	HV (DB)							LAT (DEG)	LONG (DEG)		
34.1	49.6	-8.77	-13.71	-12.58	-12.59	126.63	91.74	-149.4	6.9		12 24 7.3	27.19	-123.88	137.4	
34.2	42.0	-9.86	-11.13	-10.01	-17.12	130.54	100.41	-115.4	6.9		12 24 10.8	28.04	-124.40	137.4	
34.3	31.4	-5.97	-11.11	-13.65	-12.06	128.79	109.54	-122.0	7.2		12 24 14.0	28.95	-123.00	137.0	
34.4	22.8	0.45	-5.65	-6.34	-1.38	126.73	116.70	-123.6	7.5		12 24 16.8	29.58	-125.38	136.6	
34.5	15.0	7.01	4.91	3.14	2.96	125.44	118.16	-124.4	7.7		12 24 19.0	30.09	-125.71	136.4	
36.1	49.7	-8.95	-12.72	-11.59	-14.94	126.58	92.95	-154.3	6.4		12 24 37.8	28.43	-122.31	138.3	
36.2	42.1	-7.16	-12.12	-10.99	-10.87	130.53	100.78	-139.2	6.5		12 24 41.3	29.30	-122.82	138.2	
36.3	31.4	-4.97	-9.66	-12.00	-10.85	129.18	110.80	-141.0	6.7		12 24 44.5	30.22	-123.42	138.0	
36.4	22.9	1.07	-5.75	-7.09	-0.82	128.02	115.33	-140.5	7.0		12 24 47.3	30.85	-123.80	137.5	
36.5	15.0	7.54	5.33	3.51	3.58	126.68	117.40	-139.3	7.3		12 24 49.5	31.38	-124.11	137.3	
38.1	49.6	-8.70	-17.78	-12.52	-11.36	127.81	94.01	-155.4	5.9		12 25 8.3	29.67	-120.71	139.4	
38.2	42.1	-6.39	-9.04	-9.11	-12.35	133.04	104.12	-155.2	5.7		12 25 11.8	30.54	-121.20	139.2	
38.3	31.4	-3.95	-9.65	-9.16	-9.17	133.51	112.93	-150.9	5.6		12 25 15.0	31.47	-121.79	138.9	
38.4	24.2					131.05		-146.8	5.7		12 25 17.7	32.03	-122.09	138.8	

JSC - 7/25/75

S. TRUTH - 6/18/75

LAST MOD - 4/13/75

THIS LISTING - 10/21/75

DOY 29-1, 1/29/74 CTNC-L/R, NORTH PACIFIC

(RIGHT SIDE)

SCAN NUMB	INCID ANGLE (DEG)	SCATTERING COEFFICIENTS				ANTENNA V (DEG)	TEMP H (DEG)	ASPECT ANGLE (DEG)	WIND SPEED (M/S)	SEA TEMP (DEG)	GMT			CELL COORDINATES		S193 DATA AZIMUTH FLAG (DEG)
		VV (DB)	HH (DB)	VH (DB)	HV (DB)						(HR MIN SEC)	(DEG)	(DEG)	LAT (DEG)	LONG (DEG)	
2.1	50.1	-8.60	-12.81	-9.80	-12.73	125.91	93.22	20.9	8.6		17 25 33.6			43.71	-149.30	184.1
2.2	42.6	-8.86	-9.32	-11.69	-10.64	129.43	101.46	8.8	7.9		17 25 37.3			46.64	-148.28	184.2
2.3	32.0	-4.35	-7.75	-8.09	-9.60	129.40	109.78	9.7	6.2		17 25 40.5			47.67	-148.47	184.3
2.4	23.4	-0.68	-5.09	-6.75	-3.03	126.49	113.18	12.6	3.0		17 25 43.3			48.35	-148.14	184.4
2.5	14.8	7.37	4.57	3.05	3.50	125.61	118.82	25.9	3.7		17 25 45.4			48.97	-147.85	184.1
4.1	50.1	-8.35	-13.30	-12.19	-11.01	127.21	93.08	42.4	7.4		17 26 4.2			45.52	-146.63	186.6
4.2																
4.3	32.0	-2.77	-7.36	-7.56	-7.07	129.38	111.07	41.2	3.4		17 26 10.9			47.46	-145.73	186.8
4.4	24.0	0.73	-4.01	-5.69	-3.67	129.11	117.78	55.2	4.6		17 26 13.8			48.09	-145.36	186.8
4.5	12.8	9.52	6.50	5.21	6.19	126.02	120.56	78.9	4.1		17 26 16.0			48.88	-145.00	186.1
6.1	50.3	-9.28	-13.30	-16.32	-12.70	126.34	92.82	40.4	6.9		17 26 34.7			45.24	-144.03	188.6
6.2	42.7	-7.43		-9.60	-10.77	129.43	101.05	26.1	7.1		17 26 38.5			46.15	-143.51	188.9
6.3																
6.4																
6.5																
8.1	50.4		-12.82				93.18	23.0	7.9		17 27 5.0			44.90	-141.47	191.0
8.2	42.8	-7.93	-10.73	-10.53	-11.85	129.38	101.41	67.7	9.1		17 27 8.8			45.81	-140.90	191.3
8.3	32.2	-6.81	-8.70	-10.34	-15.82	127.54	107.51	75.8	9.6		17 27 12.0			46.81	-140.32	191.2
8.4	24.5	-1.82	-7.21	-8.61	-3.95	125.99	113.27	79.9	9.8		17 27 14.8			47.39	-139.90	191.1
8.5	11.6	9.91	7.58	6.18	7.75	124.27	119.19	73.1	9.6		17 27 16.9			48.28	-139.42	189.9
10.1	50.5	-8.13	-9.95	-10.28	-11.69	126.69	92.32	49.8	8.8		17 27 35.8			44.50	-138.90	193.2
10.2	42.9	-8.67	-9.97	-10.53	-12.00	129.78	100.56	60.7	9.3		17 27 39.3			45.39	-138.31	193.3
10.3	32.2	-6.30	-8.15	-8.62	-10.38	127.52	109.68	73.6	10.0		17 27 42.5			46.38	-137.68	193.4
10.4	24.7	-0.99	-5.93	-7.08	-3.26	126.38	114.20	82.5	10.3		17 27 45.3			46.93	-137.24	193.5
10.5	11.5	9.81	7.74	6.66	7.64	124.19	119.02	75.8	11.2		17 27 47.4			47.84	-136.71	193.2
12.1	50.5	-9.00	-11.75	-10.63	-12.16	125.32	92.70	50.9	8.9		17 28 6.2			44.03	-136.38	195.1
12.2	42.8	-7.94	-10.83	-11.84	-11.86	128.45	100.93	62.3	9.3		17 28 9.8			44.91	-135.75	195.7
12.3	32.3	-4.94	-9.25	-9.45	-10.54	128.83	109.68	75.5	10.0		17 28 13.0			45.87	-135.09	195.3
12.4	24.9	-0.82	-6.29	-9.59	-3.53	126.37	113.94	82.3	10.5		17 28 15.8			46.42	-134.62	195.7
12.5	11.6	9.50	7.17	6.03	7.19	124.62	122.14	71.4	11.3		17 28 17.9			47.31	-134.05	194.6
14.1	50.6	-10.08	-14.87	-13.78	-12.72	126.63	93.54	58.8	8.3		17 28 36.7			43.49	-133.90	197.2
14.2	42.8	-7.94	-9.98	-11.70	-9.72	130.58	101.78	65.4	9.0		17 28 40.3			44.37	-133.25	197.6
14.3	32.3	-5.61	-12.82	-11.66	-11.71	128.78	110.50	72.5	9.8		17 28 43.5			45.31	-132.55	197.5
14.4	25.1	-0.58	-6.10	-8.15	-3.38	128.07	117.20	76.3	10.3		17 28 46.3			45.83	-132.06	197.7
14.5	12.0	8.87	3.84	5.60	7.04	126.73	123.37	79.6	11.0		17 28 48.4			46.69	-131.46	197.4
16.1	50.5	-9.00	-11.77	-11.69	-10.10	127.85	94.34	60.8	7.7		17 29 7.2			42.92	-131.49	199.2
16.2	43.0	-8.60	-10.74	-10.53	-11.85	132.22	103.00	63.7	8.4		17 29 10.8			43.75	-130.80	199.3
16.3	32.4	-5.22	-8.71	-10.36	-11.50	130.92	111.75	65.4	9.3		17 29 14.0			44.68	-130.06	199.6
16.4	23.8	-0.90			-3.38	130.21	119.77	67.4	10.0		17 29 17.0			45.28	-129.48	199.6
16.5	12.5	8.60	6.69	5.46	6.74	130.98	127.22	70.1	10.9		17 29 19.0			46.01	-128.93	198.9

10/21/75

DOY 29-1, 1/29/74 CTNC-L/R. NORTH PACIFIC										(RIGHT SIDE)			S193 DATA		
SCAN	INCID	SCATTERING COEFFICIENTS				ANTENNA	TEMPS	ASPECT	WIND	SEA	GMT	CELL COORDINATES		AZIMTH	FLAG
NUMB	ANGLE	VV	HH	VH	HV	V	H	ANGLE	SPEED	TEMP	(HR MIN SEC)	LAT	LONG	(DEG)	
	(DEG)	(DB)	(DB)	(DB)	(DB)	(DEG)	(DEG)	(DEG)	(M/S)	(DEG)		(DEG)	(DEG)	(DEG)	
18.1	50.4		-14.93				97.69	62.6	7.0		17 29 37.7	42.29	-129.13	201.4	
18.2	42.9	-8.61	-11.70	-16.25	-10.66	136.01	108.04	61.5	7.8		17 29 41.3	43.09	-128.40	201.5	
18.3	32.3	-5.93	-10.76	-11.66	-9.52	140.08	119.57	61.4	8.8		17 29 44.5	44.00	-127.63	201.6	
18.4	25.3	-1.72	-7.46	-8.16	-4.12	141.15	130.65	61.3	9.4		17 29 47.3	44.48	-127.12	201.7	
18.5															
20.1	50.7					143.14		75.1	6.6		17 30 8.0	41.54	-126.84	202.9	
20.2															
20.3															
20.4															
20.5															

JSC - 7/25/75

S. TRUTH - 6/18/73

LAST MOD - 4/13/75

THIS LISTING - 10/21/75

REPRODUCIBILITY OF THE
ORIGINAL PAGE IS POOR

DOY 29-2, 1/29/74 CTNC-L/R, GULF OF MEXICO

(RIGHT SIDE)

SCAR NO. 8	INCID ANGLE (DEG)	SCATTERING COEFFICIENTS				ANTENNA V (DEG)	TEMPS H (DEG)	ASPECT ANGLE (DEG)	WIND SPEED (M/S)	SEA TEMP (DEG)	GMT (HR MIN SEC)	CELL COORDINATES		S193 DATA	
		VV (DB)	HH (DB)	VH (DB)	HV (DB)							LAT (DEG)	LONG (DEG)	AZIMTH (DEG)	FLAG
2.1	50.4	-4.29	-6.26	-7.60	-6.74	185.75	171.53	-140.2	5.7		17 37 47.0	25.68	-98.73	222.2	
2.2	42.8	-3.20	-5.35	-7.23	-6.32	189.56	175.36	-148.3	5.4		17 37 50.5	26.25	-97.87	222.3	
2.3	32.2	-6.35	-7.69	-9.33	-15.81	173.70	165.70	179.6	5.1		17 37 53.8	26.88	-96.93	222.4	
2.4	23.9	0.17	-5.76	-7.40	-1.25	170.42	163.73	181.1	5.6		17 37 56.5	27.26	-96.29	232.9	
2.5															
4.1	50.3	-8.09	-9.55	-13.04	-11.65	154.15	132.89	-148.0	6.0		17 38 17.5	24.38	-97.25	223.0	
4.2	42.9	-7.85	-9.95	-13.27	-11.67	155.91	137.64	-170.2	5.6		17 38 21.0	24.92	-96.39	223.2	
4.3	32.3	-6.35	-8.69	-10.35	-13.26	152.21	139.09	164.7	6.3		17 38 24.3	25.54	-95.46	223.3	
4.4	24.4	-0.75	-5.59	-7.79	-3.41	147.59	137.53	150.8	7.2		17 38 27.0	25.89	-94.85	223.2	
4.5	12.6	8.80	7.20	6.00	7.00	142.00	138.12	148.3	6.4		17 38 29.2	26.41	-94.09	222.7	
6.1	50.4	-10.26	-11.38	-10.25	-11.64	143.85	119.05	-159.5	3.7		17 38 40.0	23.05	-95.80	223.5	
6.2	42.9	-9.25	-10.61	-10.38	-11.68	146.47	126.14	-172.9	3.7		17 38 51.5	23.58	-94.95	223.9	
6.3	32.3	-7.23	-9.88	-12.96	-13.01	143.38	128.13	176.3	3.6		17 38 54.8	24.19	-94.01	223.7	
6.4	24.5	-4.07	-8.37	-13.06	-6.11	140.07	130.04	178.2	3.0		17 38 57.5	24.52	-93.41	223.8	
6.5	12.3	9.63	5.72	4.80	6.52	133.76	129.54	-177.5	2.3		17 38 59.7	25.06	-92.64	223.5	
8.1	50.3	-11.31	-12.36	-12.48	-11.67	142.93	117.03	-149.4	2.2		17 39 18.5	21.71	-94.39	224.4	
8.2	42.9	-8.41	-9.89	-11.54	-9.50	145.98	123.51	-145.4	1.9		17 39 22.0	22.22	-93.54	224.4	
8.3	32.3	-7.80	-12.64	-12.99	-13.02	144.19	128.92	-125.5	1.6		17 39 25.3	22.83	-92.61	224.5	
8.4	24.7	-1.55	-7.23	-8.63	-3.84	141.74	129.97	-105.4	2.0		17 39 28.0	23.14	-92.02	224.4	
8.5	12.0	9.04	7.36	6.09	7.52	135.42	131.00	-85.5	2.8		17 39 30.2	23.68	-91.22	224.5	
10.1	50.5	-10.62	-10.59	-11.23	-12.12	149.25	126.50	-115.9	1.9		17 39 49.0	20.33	-93.02	224.9	-2
10.2	42.9	-9.36	-9.25	-10.41	-11.84	154.85	135.73	-74.1	1.8		17 39 52.5	20.85	-92.17	225.1	
10.3	32.4	-7.32	-9.89	-10.37	-15.81	155.51	142.57	-87.0	2.8		17 39 55.8	21.43	-91.24	225.0	
10.4	24.7	-3.29	-7.24	-9.69	-5.42	155.75	145.61	-87.9	3.6		17 39 58.5	21.74	-90.64	224.9	
10.5	12.0	9.09	7.18	6.30	7.44	149.58	147.81	-89.3	4.7		17 40 01.7	22.28	-89.85	224.3	

JSC - 7/25/75

S. TRUTH - 6/19/75

LAST MOD - 7/13/75

THIS LISTING - 10/21/75

DOY 30-1, 1/30/74 CTNC-L/R, NORTH PACIFIC

(RIGHT SIDE)

SCAN NO.	INCID ANGLE (DEG)	SCATTERING COEFFICIENTS				ANTENNA V (DEG)	TEMPS H (DEG)	ASPECT ANGLE (DEG)	WIND SPEED (M/S)	SEA TEMP (DEG)	GMT			CELL COORDINATES		S193 DATA AZIMUTH FLAG (DEG)
		VV (DB)	HH (DB)	VH (DB)	HV (DB)						HR	MIN	SEC	LAT (DEG)	LONG (DEG)	
2.1	49.7	-8.28	-10.84	-10.55	-12.10	125.65	92.52	28.3	9.4		16	42	35.1	45.87	-147.05	181.7
2.2	42.1	-7.34	-10.65	-10.44	-13.68	127.97	101.23	32.1	7.6		16	42	38.6	46.81	-145.71	181.9
2.3	31.4	-5.11	-9.88	-13.16	-10.28	126.50	109.93	31.0	5.6		16	42	41.8	47.85	-146.35	182.0
2.4	22.5	0.32	-6.26	-7.71	-1.41	125.35	115.33	11.7	5.3		16	42	44.6	48.56	-146.04	181.3
2.5	15.2	7.27	4.88	2.87	3.51	124.50	117.67	24.4	5.5		16	42	46.8	49.09	-145.80	181.4
4.1	49.8	-8.66	-11.68	-10.55	-9.71	126.57	95.57	66.8	8.9		16	43	5.6	45.75	-144.40	184.2
4.2	42.1	-7.23	-10.65	-11.62	-10.44	131.36	104.65	48.6	7.6		16	43	9.1	46.68	-143.99	184.4
4.3	31.5	-6.65	-12.92	-26.33	-11.40	131.34	113.44	26.6	7.2		16	43	12.3	47.70	-143.59	184.4
4.4	23.0	-0.14	-6.88	-10.16	-1.66	128.00	118.40	11.5	7.6		16	43	15.1	48.38	-143.26	184.5
4.5	14.3	8.16	5.71	3.80	4.62	127.52	121.64	21.5	7.6		16	43	17.3	49.00	-142.97	184.5
6.1	49.7	-6.61	-12.05	-12.11	-10.55	130.42	101.12	44.5	7.7		16	43	36.1	45.57	-141.77	186.5
6.2	42.2	-6.78	-9.31	-11.76	-10.56	134.86	110.23	30.2	8.0		16	43	39.6	46.47	-141.32	186.8
6.3	31.6	-4.80	-10.63	-10.40	-9.39	131.84	115.26	13.9	8.5		16	43	42.8	47.48	-140.85	187.1
6.4	23.1	1.50	-5.66	-7.31	-0.83	130.26	121.53	4.0	8.7		16	43	45.6	48.14	-140.48	187.0
6.5	13.5	8.96	6.65	5.02	5.76	129.31	124.63	25.8	8.5		16	43	47.8	48.82	-140.15	186.8
8.1	49.8	-8.52	-12.06	-12.10	-12.65	130.88	100.72	18.3	8.4		16	44	6.6	45.30	-139.14	188.7
8.2	42.2	-7.85	-8.63	-8.69	-10.57	133.53	108.94	9.9	8.8		16	44	10.1	46.19	-138.64	189.1
8.3	31.6	-4.23	-8.60	-8.63	-9.39	132.25	115.66	0.9	9.1		16	44	13.3	47.19	-138.12	189.1
8.4	23.5	0.76	-4.57	-5.85	-1.31	129.79	119.76	25.0	9.0		16	44	16.1	47.82	-137.73	189.0
8.5	12.9	9.74	6.98	5.70	6.27	128.00	125.02	15.1	9.0		16	44	18.3	48.56	-137.34	189.1
10.1	49.8	-7.71	-13.22	-10.03	-10.93	131.70	102.59	7.0	9.7		16	44	37.1	44.96	-136.55	191.0
10.2	42.3	-6.78	-8.69	-9.53	-9.62	135.63	109.76	3.9	10.0		16	44	40.6	45.84	-136.00	191.1
10.3	31.7	-4.51	-8.60	-10.25	-8.66	132.23	115.22	1.2	9.9		16	44	43.8	46.82	-135.44	191.2
10.4	23.5	0.52	-5.66	-7.31	-1.31	131.54	119.34	4.8	9.6		16	44	46.6	47.44	-135.00	190.8
10.5	12.4	8.94	7.24	5.80	6.66	128.02	122.02	15.0	8.8		16	44	48.8	48.21	-134.58	191.0
12.1	49.9	-6.78	-10.38	-10.03	-10.93	132.57	101.15	6.8	10.2		16	45	7.6	44.55	-134.01	193.2
12.2	42.3	-7.66	-11.69	-10.56	-9.62	132.67	106.40	2.5	10.1		16	45	11.1	45.42	-133.42	193.5
12.3	31.7	-5.88	-9.78	-10.26	-13.19	129.63	113.50	2.2	9.7		16	45	14.3	46.39	-132.81	193.8
12.4	23.7	-0.20	-5.32	-7.31	-2.35	129.80	119.78	25.7	8.5		16	45	17.1	46.99	-132.35	193.7
12.5	12.1	10.16	7.08	5.84	7.04	129.73	125.05	20.9	7.3		16	45	19.3	47.77	-131.85	192.9
14.1	49.9	-8.92	-13.22	-12.10	-10.94	130.44	99.02	5.6	9.0		16	45	38.1	44.08	-131.50	195.4
14.2	42.3	-6.78	-8.63	-8.70	-10.57	132.67	106.59	3.5	8.6		16	45	41.6	44.94	-130.87	195.5
14.3	31.8	-5.82	-9.16	-11.37	-10.29	132.25	113.93	8.7	7.6		16	45	44.8	45.89	-130.22	195.7
14.4	23.8	0.21	-6.88	-8.06	-2.80	131.98	122.38	14.7	7.1		16	45	47.6	46.47	-129.73	195.7
14.5	11.7	9.17	7.35	5.81	7.23	132.74	129.32	35.6	6.9		16	45	49.8	47.28	-129.19	195.6

JSC - 7/25/75

S. IRUTH - 6/19/75

LAST MOD - 7/13/75

THIS LISTING - 10/21/75

DOY 30-2, 1/30/74 CTNC-L/R, GULF OF MEXICO (RIGHT SIDE)														
SCAN NUMB	INCID ANGLE (DEG)	SCATTERING COEFFICIENTS				ANTENNA V (DEG)	TEMPS H (DEG)	ASPECT ANGLE (DEG)	WIND SPEED (M/S)	SEA TEMP (DEG)	GMT (HR MIN SEC)	CELL COORDINATES		3193 DATA AZIMTH FLAG (DEG)
		VV (DB)	HH (DB)	VH (DB)	HV (DB)							LAT (DEG)	LONG (DEG)	
2.1	49.9	+5.56	-8.12	-8.46	-9.81	200.45	189.91	-12.0	4.2		16 53 56.7	29.09	-95.07	220.0
2.2	42.3	-3.81	-5.07	-6.76	-5.91	209.83	199.71	4.9	4.5		16 54 0.2	29.66	-97.21	220.1
2.3	31.7	-3.34	-4.99	-5.48	-6.67	217.38	211.74	18.6	5.6		16 54 3.5	30.33	-96.28	220.4
2.4	23.1	-1.18	-3.71	-5.61	-4.56	222.92	224.27	21.0	5.8		16 54 6.2	30.75	-95.62	220.0
2.5	14.5	-1.11	-1.98	-4.20	-4.39	227.55	228.82	20.8	6.0		16 54 8.4	31.13	-95.04	220.2
4.1	49.9	-12.89	-11.11	-10.92	-15.49	169.59	149.00	-102.9	1.8		16 54 27.2	27.84	-96.49	220.9 -2
4.2	42.4	-10.33	-11.66	-10.55	-13.64	175.60	158.00	138.8	0.3		16 54 30.7	28.40	-95.62	221.2 -2
4.3	31.7	-15.36	-27.82	-26.67	-22.49	182.16	168.39	64.8	0.9		16 54 34.0	29.06	-94.69	221.2 -2
4.4	23.4	-7.84	-15.66	-21.71	-9.17	181.51	181.31	07.7	1.3		16 54 36.7	29.45	-94.05	221.3 -2
4.5	13.5	-2.85	-1.04	-6.04	-5.60	188.21	186.73	65.4	1.7		16 54 38.9	29.89	-93.40	221.6
6.1	49.9	-10.99	-11.67	-9.70	-11.31	149.06	124.26	-162.7	3.9		16 54 57.7	26.57	-94.93	221.7
6.2	42.4	-7.92	-8.68	-8.10	-10.69	153.39	130.38	-177.8	3.4		16 55 1.2	27.12	-94.05	221.8
6.3	31.8	-2.55	-5.75	-9.49	-8.78	154.47	138.22	168.9	2.9		16 55 4.5	27.76	-93.16	222.1
6.4	23.6	1.02	-2.63	-4.98	-1.59	153.36	146.72	160.8	2.8		16 55 7.2	28.13	-92.52	222.2
6.5	12.9	10.19	7.24	5.87	6.77	154.54	152.35	151.5	2.6		16 55 9.4	28.61	-91.83	222.5
8.1	49.9	-10.99	-10.53	-10.21	-17.80	138.76	110.66	-128.6	4.6		16 55 28.2	25.27	-93.43	222.6
8.2	42.5	-9.28			-13.43	148.42	117.61	-159.8	4.1		16 55 31.6	25.81	-92.59	222.8
8.3	31.8	-5.83	-9.80	-10.28	-10.30	140.39	122.45	-161.8	3.2		16 55 35.0	26.43	-91.65	222.8
8.4	23.7	-1.38	-7.96	-11.78	-3.62	138.37	128.76	-164.3	2.9		16 55 37.7	26.80	-91.03	223.3
8.5	12.6	10.03	7.01	5.68	6.78	137.69	132.25	-171.1	1.9		16 55 39.9	27.29	-90.32	223.1
10.1	49.9	-10.58	-14.12	-11.61	-12.09	135.74	108.10	-138.3	3.8		16 55 58.7	23.96	-91.97	223.3
10.2	42.4	-10.35	-10.76	-13.45	-11.93	138.82	114.62	-129.6	3.5		16 56 2.2	24.49	-91.12	223.6
10.3	31.8	-5.78	-9.81	-11.41	-10.16	136.85	120.25	-117.5	2.9		16 56 5.5	25.10	-90.19	223.5
10.4	23.8	-3.83	-8.62	-21.73	-7.50	134.84	125.24	-102.8	2.4		16 56 8.2	25.45	-89.57	223.8 -2
10.5	12.3	9.41	6.03	4.90	6.05	131.62	124.43	-81.0	2.1		16 56 10.4	25.94	-88.54	224.0
12.1	49.9	-10.01	-11.68	-10.58	-14.50	138.73	112.34	-112.0	3.2		16 56 29.2	22.63	-90.53	224.0
12.2	42.5	-7.86	-9.99	-13.43	-10.58	141.38	119.28	-100.1	3.3		16 56 32.7	23.13	-89.68	224.1
12.3	31.9	-8.46	-9.92	-22.43	-15.78	139.47	124.02	-85.5	3.3		16 56 36.0	23.74	-88.76	224.5
12.4	23.9	-2.95	-6.28	-10.99	-4.95	135.75	126.14	-74.3	3.5		16 56 38.7	24.08	-88.15	224.3
12.5	12.1	8.96	6.63	5.67	7.20	129.50	128.72	-60.0	3.8		16 56 40.9	24.58	-87.41	225.0
14.1	50.0	-3.69	-6.25	-7.14	-7.29	152.03	135.37	-98.9	3.5		16 56 59.7	21.27	-89.14	224.9 1
14.2	42.4	-7.87	-9.28	-10.49	-9.65	146.96	128.67	-91.9	3.7		16 57 3.2	21.78	-88.23	224.9
14.3	31.8	-6.70	-10.69	-13.21	-11.45	143.90	132.08	-82.0	3.7		16 57 6.5	22.37	-87.36	225.0
14.4	24.0	-2.12	-8.63	-10.21	-6.07	139.69	133.14	-77.1	3.7		16 57 9.2	22.69	-86.76	225.1
14.5	11.8	9.49	7.02	5.90	7.47	135.53	135.13	-70.4	4.0		16 57 11.4	23.20	-85.99	224.4
16.1	49.9	-2.44	-4.52	-5.72	-5.82	159.28	139.20	-102.3	3.7		16 57 30.2	19.90	-87.76	225.3 1
16.2	42.4	-3.16	-6.70	-7.66	-7.16	154.63	136.31	-95.4	3.4		16 57 33.7	20.40	-86.92	225.4
16.3	31.8	-5.92	-9.94	-10.47	-10.49	146.96	134.69	-90.8	3.6		16 57 37.0	20.98	-86.01	225.8
16.4	23.9	-0.80	-6.73	-8.60	-3.00	143.64	135.75	-90.2	3.8		16 57 39.7	21.30	-85.40	226.2
16.5	11.8	9.34	7.36	6.32	6.81	140.68	142.43	-88.4	3.8		16 57 41.9	21.80	-84.64	226.4

10/21/75

DOY 32-1, 2/ 1/74 CTNC-L/R, NORTH PACIFIC

(RIGHT SIDE)

SCAN NUMB	INCID ANGLE (DEG)	SCATTERING COEFFICIENTS				ANTENNA V (DEG)	TEMPS H (DEG)	ASPECT ANGLE (DEG)	WIND SPD (M/S)	SEA TEMP (DEG)	GMT (HR MIN SEC)	CELL COORDINATES		S193 DATA AZIMTH FLAG (DEG)
		VV (DB)	HH (DB)	VH (DB)	HV (DB)							LAT (DEG)	LONG (DEG)	
2.1	49.6	-7.97	-11.68	-13.18	-10.55	125.22	92.04	41.2	10.0		16 49 35.5	45.89	-167.43	176.8
2.2	42.1	-5.97	-10.24	-11.09	-9.13	127.88	99.43	35.1	9.7		16 49 39.0	46.82	-167.18	176.9
2.3	31.4	-3.98	-6.63	-8.32	-9.05	128.18	107.62	27.7	9.5		16 49 42.2	47.88	-166.96	177.3
2.4	21.7	1.42	-4.84	-5.94	-0.89	125.32	113.92	23.8	8.6		16 49 45.0	48.66	-166.75	177.2
2.5	16.1	5.54	3.47	1.35	1.94	124.48	116.32	21.9	8.3		16 49 47.2	49.08	-166.58	177.1
4.1	49.7	-7.10	-11.31	-10.21	-10.95	125.20	92.92	31.0	10.3		16 50 6.0	45.92	-164.75	179.0
4.2	42.2	-5.96	-10.24	-9.99	-9.99	128.77	101.15	26.8	10.5		16 50 9.5	46.85	-164.45	179.2
4.3	31.6	-3.25	-7.00	-8.31	-8.34	127.76	108.95	23.6	10.7		16 50 12.7	47.90	-164.16	179.4
4.4	22.3	2.06	-4.26	-5.43	-0.07	125.31	114.78	22.8	10.5		16 50 15.5	48.65	-163.91	179.2
4.5	15.8	6.42	4.43	2.46	2.79	123.59	117.15	21.8	10.4		16 50 17.7	49.13	-163.71	179.2
6.1	49.8	-6.76	-11.31	-11.21	-8.69	125.60	92.42	23.8	9.9		16 50 36.5	45.88	-162.07	181.2
6.2	42.3	-5.20	-8.89	-9.99	-9.11	129.55	101.13	22.3	10.4		16 50 40.0	46.81	-161.73	181.7
6.3	31.6	-2.44	-7.00	-7.70	-7.18	129.50	108.92	22.3	10.8		16 50 43.2	47.86	-161.38	181.7
6.4	22.8	1.01	-3.62	-4.01	-1.95	127.48	116.06	23.7	10.9		16 50 46.0	48.56	-161.09	181.3
6.5	15.2	6.59	4.30	2.37	2.63	126.17	118.84	23.8	10.9		16 50 48.2	49.12	-160.85	181.2
8.1	49.8	-7.21	-11.30	-9.38	-9.36	124.77	93.24	22.5	9.4		16 51 7.0	45.78	-159.41	183.5
8.2	42.3	-6.40	-9.44	-9.88	-10.00	128.24	100.25	24.1	9.7		16 51 10.5	46.70	-159.01	183.9
8.3	31.6	-3.72	-7.82	-8.32	-8.34	128.16	107.15	25.9	9.9		16 51 13.7	47.74	-158.61	184.1
8.4	22.9	0.34	-5.29	-7.48	-1.65	125.25	113.85	27.2	9.9		16 51 16.5	48.43	-158.28	183.8
8.5	14.7	7.00	4.73	3.15	3.45	123.98	117.10	28.3	9.9		16 51 18.7	49.02	-158.00	183.7
10.1	49.9	-8.86	-11.31	-11.21	-13.92	125.14	91.94	24.9	8.5		16 51 37.5	45.61	-156.77	186.1
10.2	42.4	-7.50	-9.43	-10.94	-12.77	128.23	100.18	26.7	8.6		16 51 41.0	46.51	-156.33	186.3
10.3	31.8	-5.93	-10.18	-12.40	-10.99	128.09	108.83	30.6	8.6		16 51 44.2	47.53	-155.87	186.4
10.4	23.0	0.	-6.71	-7.14	-2.16	125.19	114.66	34.2	8.6		16 51 47.0	48.22	-155.49	185.8
10.5	14.3	7.21	4.75	3.20	3.38	122.62	118.76	35.5	8.5		16 51 49.2	48.84	-155.17	185.5
12.1	50.0	-8.33	-12.32	-9.37	-11.20	125.49	93.15	24.8	8.3		16 52 8.0	45.35	-154.14	188.2
12.2	42.5	-9.65	-11.00	-12.36	-12.56	129.02	101.38	26.5	8.3		16 52 11.5	46.25	-153.65	188.5
12.3	31.8	-5.18	-9.46	-9.03	-9.06	128.46	108.76	32.6	8.1		16 52 14.7	47.27	-153.13	188.4
12.4	23.3	-0.22	-5.47	-6.48	-2.26	126.00	115.90	35.7	8.0		16 52 17.5	47.92	-152.73	188.3
12.5	13.7	7.92	5.41	3.66	4.16	124.72	119.54	39.1	7.8		16 52 19.7	48.60	-152.37	187.9
14.1	50.0	-7.96	-10.49	-11.21	-11.66	127.14	94.78	21.4	9.4		16 52 38.5	45.04	-151.54	190.6
14.2	42.4	-8.88	-9.44	-10.95	-11.24	130.56	101.31	26.3	8.8		16 52 42.0	45.94	-151.00	190.7
14.3	31.9	-5.18	-10.18	-10.97	-10.99	128.84	109.57	30.2	7.8		16 52 45.2	46.92	-150.44	190.8
14.4	23.5	0.	-5.84	-7.90	-2.15	127.25	115.40	34.4	7.2		16 52 48.0	47.56	-150.00	190.6
14.5	13.6	8.64	5.68	4.26	5.00	124.65	119.05	38.1	6.6		16 52 50.2	48.28	-149.59	189.9
16.1	50.0	-6.23	-8.99	-8.45	-10.95	126.65	93.42	18.3	10.3		16 53 9.0	44.65	-148.98	192.7
16.2	42.5	-4.91	-8.89	-9.12	-10.11	131.01	101.67	21.3	9.5		16 53 12.5	45.53	-148.39	192.7
16.3	31.9	-1.44	-6.31	-6.67	-5.83	132.33	111.72	23.0	8.4		16 53 15.7	46.51	-147.79	193.0
16.4	23.6	1.41	-3.27	-3.85	-1.27	129.39	118.87	25.2	8.1		16 53 18.5	47.13	-147.33	192.8
16.5	12.2	9.14	6.30	4.84	5.64	126.78	123.31	28.5	7.7		16 53 20.7	47.90	-146.85	192.5

REPRODUCIBILITY OF THE
ORIGINAL PAGE IS POOR

DOY 32-1, 2/ 1/74 CTNC-L/R, NORTH PACIFIC										(RIGHT SIDE)				
SCAN NUMB	INCID ANGLE (DEG)	SCATTERING COEFFICIENTS				ANTENNA V (DEG)	TEMP H (DEG)	ASPECT ANGLE (DEG)	WIND SPEED (M/S)	SEA TEMP (DEG)	GMT			S193 DATA AZIMTH FLAG (DEG)
		VV (DB)	HH (DB)	VH (DB)	HV (DB)						(HR MIN SEC)	LAT (DEG)	LONG (DEG)	
18.1	50.2	-5.58	-11.30	-9.37	-9.36	127.48	92.98	17.1	11.2		16 53 39.4	44.19	-146.46	194.9
18.2	42.6	-5.20	-8.82	-9.03	-8.39	131.43	100.80	15.9	10.7		16 53 43.0	45.08	-145.84	195.1
18.3	31.9	-1.32	-7.90	-7.79	-6.28	131.83	110.78	13.8	10.4		16 53 46.2	46.03	-145.18	195.2
18.4	24.0	2.30	-3.06	-4.18	-0.54	130.25	117.93	12.6	10.7		16 53 49.8	46.61	-144.71	195.4
18.5														
20.1	50.2	-8.53	-10.82	-11.54	-12.52	126.13	91.20	16.1	11.2		16 54 10.0	43.67	-143.98	196.9
20.2	42.5	-6.31	-8.64	-10.23	-9.47	138.08	99.45	9.9	11.0		16 54 13.5	44.54	-143.32	197.1
20.3	32.0	-2.82	-7.35	-8.04	-9.53	131.76	107.65	2.8	11.3		16 54 16.7	45.48	-142.62	197.2
20.4	24.2	1.32	-4.69	-5.08	-1.19	128.41	116.55	-1.8	11.7		16 54 19.5	46.04	-142.12	196.8
20.5	11.1	8.91	7.13	5.86	6.69	127.07	121.04	-1.1	12.5		16 54 21.7	46.90	-141.53	196.1
22.1	50.2	-8.29	-13.12	-13.51	-12.00	124.36	90.27	20.9	10.7		16 54 40.5	43.10	-141.56	199.1
22.2	42.6	-7.29	-10.59	-11.44	-11.59	128.73	98.53	16.9	10.6		16 54 44.0	43.94	-140.86	199.1
22.3	32.0	-4.89	-9.20	-10.23	-9.41	128.62	107.15	11.7	10.8		16 54 47.2	44.87	-140.14	199.3
22.4	24.3	-0.05	-5.80	-7.47	-2.70	127.04	114.30	9.8	11.0		16 54 50.0	45.40	-139.61	199.2
22.5	10.8	9.91	6.79	5.65	6.86	124.85	119.68	13.7	11.4		16 54 52.2	46.28	-138.95	198.3
24.1	50.2	-8.67	-12.66	-10.54	-11.54	125.13	89.78	35.1	10.0		16 55 11.0	42.46	-139.17	200.9
24.2	42.6	-8.48	-14.04	-11.45	-13.12	129.95	98.03	33.7	10.3		16 55 14.5	43.29	-138.46	201.3
24.3	32.0	-5.21	-10.54	-10.24	-11.35	128.11	107.51	33.8	10.8		16 55 17.7	44.19	-137.68	201.2
24.4	24.5	-1.57	-7.25	-8.66	-4.49	126.10	112.48	34.7	11.1		16 55 20.5	44.71	-137.15	201.3
24.5	10.8	8.98	6.54	5.69	7.04	123.07	119.61	34.7	11.9		16 55 22.7	45.58	-136.47	200.3
26.1	50.2	-11.67	-16.95	-13.52	-12.01	125.92	89.27	49.1	9.4		16 55 41.4	41.78	-136.84	202.9
26.2	42.6	-10.01	-11.36	-11.31	-12.92	128.60	97.53	49.0	10.0		16 55 45.0	42.58	-136.10	203.0
26.3	32.1	-6.30	-9.73	-10.10	-12.79	127.61	106.13	49.0	10.7		16 55 48.2	43.46	-135.30	203.0
26.4	24.5	-2.54	-7.53	-12.02	-5.05	125.13	112.84	49.3	11.0		16 55 51.0	43.97	-134.75	202.7
26.5	10.9	8.96	6.38	5.65	6.93	122.99	118.26	50.6	11.5		16 55 53.2	44.81	-134.04	202.4
28.1	50.3	-12.19	-12.02	-13.52	-14.27	124.59	89.19	54.3	8.9		16 56 12.0	41.01	-134.58	204.7
28.2	42.6	-11.26	-10.51	-12.73	-15.52	127.68	98.31	51.2	9.7		16 56 15.5	41.81	-133.80	204.8
28.3	32.0	-7.21	-13.92	-12.76	-12.80	126.66	106.06	59.1	10.3		16 56 18.7	42.68	-132.99	204.9
28.4	24.5	-2.31	-8.10	-9.19	-5.06	126.40	114.08	59.0	10.6		16 56 21.5	43.17	-132.43	205.0
28.5	11.0	8.80	6.45	5.62	6.99	123.36	118.19	58.8	11.0		16 56 23.7	43.99	-131.69	204.2
30.1	50.1	-9.38	-16.97	-15.85	-10.55	124.94	90.40	77.6	8.8		16 56 42.5	40.23	-132.36	206.4
30.2	42.6	-11.41	-12.58	-15.17	-22.89	128.90	98.66	72.4	9.3		16 56 46.0	40.99	-131.57	206.6
30.3	32.0	-5.91	-11.42	-14.92	-11.37	128.84	108.22	69.4	9.9		16 56 49.2	41.84	-130.73	206.6
30.4	24.5	-1.89	-7.54	-8.25	-4.03	127.26	114.94	67.3	10.2		16 56 52.0	42.32	-130.17	206.7
30.5	11.1	8.77	6.30	5.27	6.83	126.37	122.46	66.4	10.7		16 56 54.2	43.12	-129.41	206.6
32.1	50.1	-9.69	-16.97	-15.85	-10.03	126.20	91.66	90.2	9.0		16 57 13.0	39.38	-130.20	207.8
32.2	42.6	-9.24	-11.38	-11.32	-13.14	131.01	100.34	83.9	9.4		16 57 16.5	40.12	-129.40	208.1
32.3	32.0	-7.23	-11.42	-12.77	-11.38	131.86	109.90	79.6	9.8		16 57 19.7	40.95	-128.54	208.4
32.4	24.6	-2.32	-8.41	-11.09	-4.69	132.02	119.69	78.8	10.0		16 57 22.5	41.40	-127.97	208.2
32.5	11.2	9.89	6.24	4.93	6.56	133.64	150.13	77.5	10.5		16 57 24.7	42.19	-127.19	207.5

10/21/75

DOY 32-1, 2/ 1/74 CTNC-L/R, NORTH PACIFIC

(RIGHT SIDE)

SCAN NUMB	INCID ANGLE (DEG)	SCATTERING COEFFICIENTS				ANTENNA V (DEG)	TEMP H (DEG)	ASPECT ANGLE (DEG)	WIND SPEED (M/S)	SEA TEMP (DEG)	GMT (HR MIN SEC)	CELL COORDINATES		S193 DATA AZIMTH FLAG (DEG)
		VV (DB)	HH (DB)	VH (DB)	HV (DB)							LAT (DEG)	LONG (DEG)	
34.1	50.2	-10.58	-10.57	-10.22	-12.03	130.43	94.99	76.4	9.3		16 57 43.5	38.47	-128.12	209.6
34.2	42.6	-11.28	-9.81	-12.74	-13.15	136.93	107.92	72.1	9.9		16 57 47.0	39.20	-127.30	209.9
34.3	32.0	-7.77	-10.57	-14.93	-11.39	143.66	122.53	70.2	9.8		16 57 50.2	40.01	-126.41	209.8
34.4	24.8	-3.34	-8.12	-12.03	-6.43	147.38	138.90	70.0	10.0		16 57 53.0	40.45	-125.83	210.0
34.5	11.4	9.81	5.79	4.06	6.38	157.76	155.42	70.1	10.4		16 57 55.2	41.22	-125.05	208.9

JSC - 7/26/75

S. TRUTH - 8/10/75

LAST MOD - 7/13/75

THIS LISTING - 10/21/75

APPENDIX B

VECTOR ERROR VALUES FOR PLANETARY BOUNDARY LAYER MODEL
IN A WITHHELD WEATHER SHIP ANALYSIS
(STRATIFIED ACCORDING TO DATE AND WIND SPEED RANGES)

REPRODUCIBILITY OF THE
ORIGINAL PAGE IS POOR

ORGANIZATIONS: CUNY Institute of Marine and Atmospheric Sciences
at The City College, Wave Hill 675 West 252 Street
Bronx, N.Y. 10471 (212) 796-8300 and
The University of Kansas Remote Sensing Laboratory
Raymond Nichols Hall, 2291 Irving Hill Drive,
Campus West, Lawrence, Kansas 66045 (913) 864-9836

TITLE OF INVESTIGATION: A JOINT METEOROLOGICAL, OCEANOGRAPHIC AND SENSOR
EVALUATION PROGRAM FOR EXPERIMENT S193 ON SKYLAB.

TITLE OF REPORT: APPENDIX B THE DATA FROM THE WITHHELD WEATHER SHIP
ANALYSIS.

FOR: THE MEASUREMENT OF THE WINDS NEAR THE OCEAN
SURFACE WITH A RADIOMETER-SCATTEROMETER ON SKYLAB

PERIOD COVERED: January 1973 to December 1975

ERP INVESTIGATION: EPN 550

NASA CONTRACT: NAS 9-13642

PRINCIPAL INVESTIGATOR: Willard J. Pierson

CO-PRINCIPAL INVESTIGATOR: Richard K. Moore

CO-PRINCIPAL INVESTIGATOR: E. Paul McClain

DATE COMPLETED: January 21, 1976

MONITOR AND ADDRESS: Mr. Zack H. Byrns/TF6
PRINCIPAL INVESTIGATOR OFFICE
NASA LYNDON B. JOHNSON SPACE CENTER
HOUSTON, TEXAS 77058

TYPE OF REPORT: APPENDIX TO FINAL REPORT

DATE	DAY	YEAR	HOUR	SHIP	LAT	LONG	VWS	CHWS	VSYN	CHISYN	VF	CHIE	E:EW	F:NS	CW-CS	EPAR	ENORM	TYPE
7	15	1973	0	M	66.2	1.2	5.8	40.	7.3	33.	1.7	188.	-2	-1.7	7.	-1.5	-7	+
7	16	1973	6	A	62.7	-29.6	9.8	210.	11.3	228.	3.6	105.	3.5	-9	-18.	-2.0	3.0	C
7	16	1973	6	C	53.8	-35.5	7.6	240.	9.9	230.	2.8	21.	1.0	2.6	10.	-2.4	-1.3	+
7	16	1973	6	M	66.0	1.0	7.0	30.	9.5	4.	4.4	140.	2.8	-3.4	26.	-3.2	-3.1	B
7	17	1973	12	B	56.1	-51.4	9.0	240.	12.1	222.	4.5	4.	.3	4.5	18.	-3.5	-2.8	C
7	17	1973	12	M	66.1	1.2	8.3	20.	9.8	3.	3.1	131.	2.3	-2.0	17.	-1.9	-2.4	+
7	18	1973	18	A	62.2	-32.0	.0	0.	11.8	6.	11.8	186.	-1.2	-11.7	-6.	-11.8	-0	+
7	18	1973	18	M	66.4	1.5	9.8	30.	14.5	356.	8.4	135.	5.9	-6.0	-34.	-6.4	-5.5	+
7	20	1973	0	B	56.5	-51.0	5.5	210.	8.1	203.	2.7	9.	.4	2.7	7.	-2.6	-7	+
7	20	1973	0	M	66.5	1.8	8.3	320.	11.2	8.	0.4	236.	-6.9	-4.7	48.	-5.6	6.2	+
7	21	1973	6	J	52.3	-19.7	8.8	20.	9.5	338.	6.6	95.	6.6	-5	-42.	-3.0	-5.9	C
7	22	1973	12	I	59.0	-19.0	5.6	80.	4.9	84.	3.3	140.	2.1	-2.6	36.	-.4	-3.3	C
7	23	1973	18	I	56.8	-19.0	8.3	100.	16.8	98.	8.5	276.	-8.5	.9	2.	-8.5	-.3	C
7	25	1973	0	I	58.9	-19.3	.0	0.	5.6	25.	5.6	205.	-2.4	-5.1	-25.	-5.6	-0	+
7	25	1973	0	K	44.9	-16.0	7.7	300.	8.2	288.	1.7	41.	1.1	1.3	12.	-.7	-1.6	+
7	27	1973	12	I	58.8	-19.5	3.0	170.	11.9	228.	10.6	62.	9.4	5.0	-58.	-10.3	2.5	+
7	30	1973	0	A	62.0	-32.8	8.5	220.	9.6	200.	3.3	319.	-2.2	2.5	20.	-1.6	-2.9	+
7	30	1973	0	I	59.1	-18.3	9.5	210.	13.7	238.	6.9	98.	6.9	-1.0	-28.	-5.3	4.5	+
7	30	1973	0	J	52.5	-19.8	7.7	250.	10.2	250.	2.5	70.	2.3	.9	0.	-2.5	-0	+
7	31	1973	6	A	62.2	-33.0	7.7	60.	1.1	208.	8.7	56.	7.2	4.8	-148.	-7.6	4.1	+
8	1	1973	12	I	58.9	-18.4	9.6	290.	7.9	263.	4.4	344.	-1.2	4.2	27.	.7	-4.4	C
8	1	1973	12	J	52.5	-20.0	9.5	280.	12.0	292.	4.2	163.	1.2	-4.0	-18.	-3.0	2.9	+
8	2	1973	18	B	56.5	-51.0	5.5	210.	10.4	253.	7.4	103.	7.2	-1.7	-43.	-6.4	3.8	+
8	2	1973	18	J	52.5	-20.0	8.7	240.	15.0	253.	7.6	88.	7.6	.3	-13.	-7.3	2.0	D
8	5	1973	0	I	58.9	-19.2	5.7	200.	7.1	223.	2.4	93.	2.9	-.2	-23.	-1.9	2.2	+
8	6	1973	12	H	38.0	-71.0	8.7	30.	9.5	355.	5.5	110.	5.2	-1.9	-35.	-2.4	-5.0	+
8	6	1973	12	I	59.1	-18.9	9.5	10.	8.5	358.	2.1	66.	1.9	.9	-12.	.8	-2.0	+
8	7	1973	18	H	56.5	-51.0	8.5	250.	3.7	233.	5.1	262.	-5.0	-.7	17.	4.4	-2.5	+
8	9	1973	0	H	38.0	-71.0	4.4	100.	8.0	208.	6.0	61.	5.3	2.9	-48.	-5.1	3.3	+
8	9	1973	0	I	57.4	-15.9	8.3	80.	9.4	126.	8.4	11.	1.6	8.2	-56.	-4.8	6.9	+
8	11	1973	12	B	56.5	-51.0	6.8	270.	6.1	256.	1.7	329.	-.9	1.5	14.	.5	-1.6	+
8	11	1973	12	K	45.4	-16.2	7.7	140.	9.0	111.	4.4	232.	-3.5	-2.7	29.	-2.3	-3.7	B
8	12	1973	18	K	45.7	-13.7	7.7	80.	4.3	80.	3.9	38.	2.4	3.1	-20.	2.9	2.6	+
8	14	1973	0	B	56.5	-51.0	8.3	340.	6.9	345.	1.5	317.	-1.1	1.1	-5.	1.4	.7	+
8	16	1973	12	K	44.7	-15.1	8.7	260.	8.0	301.	5.9	197.	-1.7	-5.6	-41.	-1.4	5.7	D
8	17	1973	18	B	54.8	-52.8	4.7	160.	8.6	162.	1.1	145.	.7	-.9	-2.	1.1	.3	+
8	17	1973	18	K	45.0	-16.0	4.4	70.	4.9	99.	2.4	343.	-.7	2.3	-29.	-1.1	2.1	D
8	19	1973	0	H	56.1	-50.5	5.9	120.	8.4	132.	2.9	337.	-1.1	2.7	-12.	-2.6	1.2	+
8	20	1973	6	J	52.5	-20.0	5.8	170.	11.2	134.	7.0	292.	-6.5	2.6	32.	-6.3	-3.1	+
8	21	1973	12	J	52.5	-20.0	8.7	150.	15.0	164.	6.9	2.	.2	6.9	-14.	-6.6	2.1	+
8	22	1973	18	B	50.7	-50.7	7.6	340.	4.0	351.	3.9	329.	-2.0	3.4	-11.	3.7	1.5	+
8	22	1973	18	J	52.7	-19.8	7.7	238.	12.5	219.	5.2	22.	2.0	4.8	11.	-4.9	-1.5	+
8	22	1973	18	K	45.0	-15.9	9.8	250.	6.2	268.	4.3	224.	-3.0	-3.1	-18.	3.1	3.0	D
8	24	1973	0	K	45.0	-16.0	6.9	160.	6.7	224.	7.2	103.	7.0	-1.7	-64.	-3.7	6.2	+
8	25	1973	6	H	56.3	-50.6	8.8	320.	18.1	293.	11.0	92.	11.0	-.3	27.	-10.3	-4.0	+
8	25	1973	6	I	59.0	-19.0	9.8	200.	13.7	179.	5.7	321.	-3.6	4.5	21.	-4.6	-3.5	+
8	26	1973	12	B	56.3	-51.1	6.9	200.	10.2	251.	7.9	113.	7.3	-3.2	-51.	-5.9	5.4	+
8	27	1973	18	H	38.0	-71.0	6.7	240.	6.5	246.	.7	169.	.1	-.7	-6.	.2	.7	+
8	27	1973	18	M	66.0	2.1	6.8	150.	14.2	191.	10.1	37.	6.1	8.1	-41.	-9.1	4.5	+
8	30	1973	6	H	38.0	-71.0	4.4	220.	8.7	278.	7.4	120.	5.8	-4.6	-58.	-6.4	3.7	+

REPRODUCIBILITY OF THE
ORIGINAL PAGE IS POOR

DATE	DAY	YEAR	HOUR	SHIP	LAT	LONG	VWS	CHWS	VSYN	CHSYN	VF	CHIE	E:EW	F:NS	CW-CS	FPAR	ENORM	TYPE
8	31	1973	12	H	38.0	-71.0	4.4	260.	8.0	257.	3.6	73.	3.5	1.0	3.	-3.6	-0.2	0
8	31	1973	12	K	45.0	-16.0	4.3	190.	3.2	212.	1.8	148.	.9	-1.5	-22.	.8	1.6	+
9	1	1973	18	K	45.1	-16.0	9.8	250.	6.4	279.	5.2	214.	-2.9	-4.4	-29.	2.2	4.8	+
9	3	1973	0	J	52.4	-19.9	5.5	190.	15.0	225.	11.0	62.	9.7	5.2	-35.	-10.5	3.2	+
9	3	1973	0	K	45.3	-15.7	7.7	220.	9.9	200.	3.7	335.	-1.6	3.4	20.	-2.7	-2.6	+
9	5	1973	12	M	65.9	2.0	8.3	290.	19.5	345.	16.2	190.	-2.8	-16.0	-55.	-14.7	6.8	+
9	6	1973	18	H	56.2	-51.3	9.7	210.	5.9	220.	4.5	145.	-4	-4.5	-19.	3.7	3.2	+
9	10	1973	12	H	56.5	-51.0	9.7	160.	9.8	140.	3.4	242.	-3.0	-1.6	20.	-7	-3.3	+
9	10	1973	12	H	38.0	-71.0	8.4	30.	18.1	14.	10.3	181.	-2	-10.3	16.	-10.0	-2.3	+
9	10	1973	12	I	58.9	-19.6	7.7	150.	10.1	156.	2.6	354.	-3	2.6	-6.	-2.4	.8	0
9	10	1973	12	J	52.5	-19.2	9.8	90.	10.4	95.	1.1	328.	-6	.9	-5.	-6	.9	+
9	11	1973	18	I	59.0	-19.8	9.8	140.	9.0	161.	3.5	73.	3.4	1.0	-21.	.1	3.5	0
9	11	1973	18	K	45.1	-10.3	9.8	150.	11.3	166.	3.3	41.	2.2	2.5	-16.	-1.9	2.7	+
9	13	1973	0	C	52.7	-35.5	6.6	170.	8.7	209.	5.5	78.	5.4	1.1	-39.	-3.6	4.2	+
9	13	1973	0	I	59.1	-19.3	8.7	160.	7.4	162.	1.3	149.	.7	-1.1	-2.	1.3	.3	+
9	13	1973	0	K	45.3	-16.3	8.6	160.	3.7	171.	5.0	152.	2.4	-4.4	-11.	4.7	1.6	0
9	14	1973	6	J	52.5	-19.8	6.7	70.	13.8	57.	5.7	217.	-3.4	-4.5	13.	-5.3	-2.0	+
9	18	1973	0	C	52.7	-35.5	5.7	290.	12.1	316.	7.4	156.	3.0	-6.8	-26.	-7.0	2.5	+
9	19	1973	6	J	52.4	-20.0	8.3	150.	6.8	271.	13.2	124.	10.9	-7.3	-121.	-11.1	7.1	0
9	20	1973	12	A	62.1	-32.9	8.7	220.	14.0	223.	5.3	48.	4.0	3.6	-3.	-5.3	.5	0
9	20	1973	12	M	65.9	2.1	9.8	30.	8.9	61.	5.1	325.	-2.9	4.2	-31.	-5	5.0	+
9	30	1973	12	H	56.4	-50.0	6.8	280.	6.8	269.	1.8	2.	.1	1.8	15.	-2	-1.8	+
10	3	1973	0	J	52.4	-19.9	9.8	190.	8.6	172.	3.1	249.	-2.9	-1.1	18.	.7	-3.0	+
10	5	1973	12	K	45.1	-16.0	8.3	330.	6.6	316.	2.5	10.	.4	2.4	14.	1.5	-2.0	0
10	6	1973	18	K	45.2	-15.8	7.7	160.	7.7	159.	.1	245.	-1	-0	1.	-0	-1	0
10	9	1973	6	H	38.0	-71.0	10.0	30.	7.3	46.	3.4	91.	3.4	-1	14.	2.4	-2.4	+
10	9	1973	6	K	45.1	-15.6	6.5	120.	14.5	124.	6.0	310.	-4.7	3.9	-4.	-6.0	.6	+
10	10	1973	0	I	59.0	-18.7	9.7	280.	9.0	291.	1.9	217.	-1.2	-1.5	-11.	.5	1.9	0
10	18	1973	0	J	52.4	-19.9	9.8	260.	11.5	242.	3.7	8.	.5	3.7	18.	-2.2	-3.0	+
10	20	1973	12	B	55.5	-51.7	8.7	320.	3.6	311.	5.2	326.	-2.9	4.3	9.	5.0	-1.4	+
10	20	1973	12	K	45.5	-14.9	7.7	320.	7.5	313.	.9	34.	.5	.8	7.	.1	-9	0
10	21	1973	18	K	45.7	-14.0	9.8	280.	11.8	289.	2.6	145.	1.5	-2.1	-9.	-2.1	1.5	0
10	23	1973	0	K	44.8	-15.9	6.8	330.	1.7	60.	7.0	316.	-4.9	5.0	90.	-1.7	6.8	+
10	25	1973	12	K	45.0	-16.1	9.8	100.	9.0	96.	1.0	137.	.7	-8	4.	.8	-7	+
10	26	1973	18	K	45.1	-16.2	7.5	180.	10.4	173.	3.1	336.	-1.3	2.8	7.	-3.0	-9	+
10	28	1973	0	H	56.5	-51.0	5.7	310.	17.4	286.	12.4	95.	12.4	-1.1	24.	-12.2	-2.3	+
11	3	1973	6	H	56.5	-51.0	7.0	220.	11.1	234.	4.6	75.	4.5	1.2	-14.	-4.3	1.7	+
11	12	1973	0	M	65.6	2.4	6.1	160.	4.2	201.	4.0	117.	3.6	-1.8	-41.	.4	4.0	+
11	13	1973	6	A	63.1	-29.5	8.4	230.	9.4	312.	11.7	177.	.6	-11.7	-82.	-8.2	8.3	+
11	14	1973	12	M	65.9	1.9	9.8	290.	10.2	266.	4.2	13.	1.0	4.1	24.	-1.2	-4.0	+
11	15	1973	18	J	52.5	-19.6	8.7	290.	12.6	281.	4.2	82.	4.2	.6	9.	-4.0	-1.4	+
11	18	1973	6	J	52.7	-19.8	8.3	280.	11.2	250.	5.8	24.	2.4	5.3	30.	-4.0	-4.2	+
11	18	1973	6	M	65.8	1.0	5.8	200.	12.1	154.	9.1	307.	-7.3	5.4	46.	-8.1	-4.2	+
11	20	1973	18	J	52.5	-20.4	7.2	190.	12.4	162.	6.4	313.	-5.1	4.7	28.	-6.0	-3.4	C
11	22	1973	0	J	52.4	-20.2	8.3	210.	7.9	192.	2.6	282.	-2.5	.5	18.	-0	-2.6	+
11	23	1973	6	C	52.7	-35.5	7.8	190.	7.8	166.	3.2	268.	-3.2	-1	24.	-7	-3.2	+
11	25	1973	18	I	58.9	-18.7	8.8	20.	7.4	357.	4.2	64.	3.7	1.8	-23.	1.6	-3.8	+
12	2	1973	0	J	52.2	-19.9	9.8	30.	5.6	91.	8.6	355.	-7	8.6	-61.	-8	8.6	+
12	9	1973	12	K	45.0	-16.2	5.4	240.	2.1	150.	5.5	262.	-5.4	-7	81.	-1.3	-5.3	0
12	13	1973	6	C	52.8	-35.4	5.8	200.	13.9	215.	8.4	45.	6.0	5.9	-15.	-8.3	1.5	+

MONTH	DAY	YEAR	HOUR	SHIP	LAT	LONG	VWS	CHWS	VSYN	CHSYN	VF	CHIE	E:EW	F:NS	CW-CS	EPAR	ENORM	TYPE
12	15	1973	18	C	52.6	-35.3	9.1	20.	11.6	18.	2.5	191.	-1.5	-2.5	2.	-2.5	-0.3	+
12	24	1973	12	J	52.5	-20.1	9.7	240.	7.2	292.	7.7	193.	-1.7	-7.5	-52.	-1.2	7.6	+
12	25	1973	18	K	44.9	-16.2	8.4	40.	13.7	6.	8.2	151.	4.0	-7.2	34.	-6.7	-4.7	+
12	29	1973	12	H	38.0	-71.0	9.7	240.	7.0	241.	2.7	237.	-2.3	-1.5	-1.	2.7	.2	D
12	30	1973	18	I	59.1	-19.0	8.4	189.	10.0	190.	2.3	50.	1.7	1.4	-10.	-1.7	1.5	+
12	30	1973	18	K	45.2	-15.6	4.7	70.	7.2	59.	3.0	98.	2.9	-1.4	11.	2.3	-1.9	D
1	1	1974	0	H	38.0	-71.0	9.8	270.	6.1	233.	6.1	307.	-4.9	3.7	37.	1.7	-5.9	+
1	2	1974	6	J	52.4	-19.8	5.7	230.	22.0	201.	17.2	12.	3.5	16.9	29.	-17.0	-2.8	+
1	31	1974	0	H	38.0	-71.0	8.4	70.	3.8	290.	11.6	82.	11.5	1.6	-140.	-10.2	-5.4	+
1	31	1974	0	J	52.3	-19.9	5.7	130.	10.2	176.	7.5	29.	3.7	6.5	-46.	-6.2	4.1	+
2	1	1974	6	A	62.0	-32.6	8.3	80.	9.5	36.	6.8	157.	2.6	-6.2	44.	-3.5	-5.8	+

MONTH	DAY	YEAR	HOUR	SHIP	LAT	LONG	VWS	CHWS	VSYN	CHISYN	VF	CHIE	E:EW	E:NS	CW-CS	EPAR	ENORM	TYPE
7	15	1973	0	C	52.7	-35.5	10.6	260.	10.2	264.	.8	201.	-3.3	-3.8	-4.	.4	.7	+
7	15	1973	0	I	58.9	-18.9	11.0	50.	12.4	27.	4.9	145.	2.8	-4.0	-23.	-2.3	-4.3	+
7	16	1973	6	I	55.7	-18.9	12.3	10.	12.4	344.	5.6	88.	5.6	.2	-26.	-1.3	-5.4	+
7	17	1973	12	A	62.0	-33.0	10.4	230.	5.2	195.	6.8	256.	-6.6	-1.7	35.	3.3	-6.0	+
7	17	1973	12	C	54.2	-33.4	10.5	220.	13.7	227.	5.2	201.	-1.9	-4.8	-7.	4.7	2.3	+
7	17	1973	12	I	58.9	-19.2	14.1	290.	9.6	270.	6.0	323.	-3.6	4.8	20.	3.6	-4.8	+
7	17	1973	12	J	52.5	-20.0	10.3	340.	17.2	341.	.9	170.	.0	-1.9	-1.	-.9	.3	+
7	18	1973	18	D	50.0	-33.9	12.1	170.	11.7	230.	11.0	112.	11.1	-4.4	-60.	-5.6	10.5	+
7	18	1973	18	K	45.1	-18.0	10.6	300.	10.8	312.	4.1	242.	-3.6	-1.9	-12.	1.4	3.9	D
7	20	1973	0	I	59.0	-19.8	13.0	00.	11.8	6.	11.3	118.	10.0	-5.2	54.	-4.2	-10.5	+
7	21	1973	6	H	50.5	-51.0	10.7	330.	15.1	70.	21.0	287.	-20.1	6.1	108.	-18.4	10.2	+
7	21	1973	6	K	44.6	-15.3	13.2	230.	13.0	319.	2.4	50.	1.9	1.6	11.	-.0	-2.5	+
7	22	1973	12	A	62.1	-34.0	10.5	120.	13.9	136.	7.2	88.	7.2	.2	-10.	4.8	5.4	+
7	22	1973	12	H	50.5	-51.1	10.8	10.	17.6	325.	12.6	91.	12.6	-.1	-45.	-7.3	-10.3	+
7	22	1973	12	J	52.0	-13.0	14.1	290.	7.5	209.	7.6	311.	-5.8	5.0	21.	5.7	-5.1	D
7	22	1973	12	K	44.2	-15.8	19.0	270.	10.4	264.	3.2	303.	-2.7	1.7	0.	2.5	-2.0	+
7	23	1973	18	A	62.2	-34.2	15.1	110.	10.6	134.	6.0	71.	6.6	2.2	-24.	3.2	6.1	C
7	23	1973	18	J	52.5	-19.8	15.7	230.	8.4	249.	9.5	307.	-7.6	5.7	31.	5.1	-8.1	+
7	23	1973	18	K	44.7	-15.0	17.7	270.	24.6	274.	7.1	104.	6.8	-1.7	-4.	-6.9	1.2	D
7	23	1973	18	M	66.2	1.3	17.1	30.	11.5	337.	12.7	72.	13.0	4.2	-53.	-1.2	-13.7	+
7	25	1973	0	A	62.0	-33.0	13.5	120.	7.0	197.	13.7	90.	13.7	-.1	-77.	-4.0	13.2	+
7	25	1973	0	J	52.4	-19.6	17.2	300.	8.5	297.	8.7	303.	-7.3	4.7	3.	8.7	-.9	+
7	28	1973	6	M	65.9	1.2	10.8	360.	15.3	350.	4.5	173.	.5	-4.5	2.	-4.5	-.4	+
7	26	1973	6	B	50.3	-51.1	18.9	190.	8.4	197.	10.6	184.	-.8	-10.6	-7.	10.4	2.3	+
7	26	1973	6	J	52.5	-19.9	15.7	190.	16.7	208.	5.2	98.	5.1	-.7	-18.	-1.8	4.9	+
7	26	1973	6	K	41.9	-15.3	11.8	40.	12.8	26.	3.2	141.	2.0	-2.5	14.	-1.4	-2.9	+
7	26	1973	6	M	65.5	2.0	15.5	330.	15.3	350.	5.4	252.	-5.1	-1.6	-20.	-.7	5.3	+
7	27	1973	12	A	62.1	-32.9	15.0	180.	14.2	210.	9.8	133.	7.1	-6.7	-30.	2.3	9.5	+
7	27	1973	12	J	52.4	-10.9	13.5	190.	12.8	206.	3.7	119.	3.3	-1.8	-16.	.2	3.7	+
7	27	1973	12	K	45.0	-15.8	15.2	40.	17.4	42.	2.3	236.	-1.9	-1.3	-2.	-2.2	.5	D
7	28	1973	18	D	56.5	-51.0	10.6	140.	14.6	133.	2.3	226.	-1.9	-1.3	7.	-.5	-2.3	+
7	28	1973	18	I	58.9	-19.0	15.7	220.	10.2	219.	.6	10.	.1	.6	1.	-.5	-.3	+
7	28	1973	18	K	44.9	-15.9	10.2	20.	15.3	20.	.9	20.	.3	.8	0.	.9	.0	+
7	28	1973	18	M	65.6	3.0	13.5	200.	2.6	206.	10.0	199.	-3.5	-10.3	-6.	10.0	1.4	+
7	30	1973	0	B	50.5	-51.0	15.7	230.	14.4	250.	1.3	250.	-1.2	-.4	0.	1.3	.0	+
7	30	1973	0	K	44.8	-15.9	16.2	250.	15.5	30.	10.9	283.	-10.6	2.5	40.	-3.1	10.4	D
7	30	1973	0	M	65.0	3.8	14.0	240.	9.9	244.	4.2	230.	-3.2	-2.7	-4.	4.1	1.0	D
7	31	1973	6	C	52.2	-34.4	10.7	270.	19.1	260.	8.4	85.	8.4	.7	2.	-8.4	-.4	+
7	31	1973	6	J	52.6	-19.7	12.6	270.	16.5	268.	2.2	285.	-2.1	.6	2.	2.1	-.6	C
7	31	1973	6	K	44.8	-16.0	13.0	360.	14.4	11.	3.0	248.	-2.7	-1.1	11.	-1.6	2.5	D
8	1	1973	12	A	62.7	-33.0	15.2	270.	8.8	270.	6.6	259.	-6.5	-1.2	-8.	6.3	2.1	D
8	1	1973	12	H	50.5	-51.0	11.0	250.	10.5	205.	2.0	174.	.1	-2.8	-15.	.1	2.8	+
8	1	1973	12	C	52.7	-35.7	18.4	230.	11.8	252.	8.7	199.	-2.9	-0.2	-22.	5.3	6.9	+
8	1	1973	12	M	64.3	3.0	12.0	250.	10.0	234.	5.3	322.	-3.2	0.1	26.	.2	-5.3	C
8	2	1973	18	I	59.0	-18.6	10.5	250.	10.4	245.	3.5	274.	-3.5	.3	5.	3.0	-1.7	+
8	4	1973	0	J	52.4	-19.7	11.0	200.	11.3	248.	9.1	132.	6.7	-6.1	-48.	-3.9	8.2	C
8	4	1973	0	K	44.3	-15.9	10.5	280.	10.6	287.	1.3	109.	-.2	-1.3	-7.	-.2	1.3	+
8	4	1973	0	M	66.0	1.4	12.3	40.	10.5	86.	4.3	284.	-4.2	1.1	-6.	-4.1	1.3	C
8	5	1973	6	A	61.9	-33.1	10.0	350.	17.2	30.0	2.2	280.	-3.1	.5	-10.	.5	3.1	+
8	5	1973	6	B	56.5	-51.0	16.3	310.	15.6	206.	6.7	22.	2.5	6.2	24.	-.7	-6.6	+

MONTH	DAY	YEAR	HOUR	SHIP	LAT	LONG	VKS	CH14S	VSYN	CH15YN	VF	CH1E	E:EW	E:NS	CK-CS	EPAR	ENORM	TYPE
8	5	1973	6	H	38.0	-71.0	13.2	270.	10.4	304.	7.0	210.	-4.6	-5.8	-34.	.5	7.4	B
8	6	1973	12	K	45.1	-16.1	10.0	270.	12.1	278.	6.2	254.	-6.0	-1.7	-8.	5.7	2.5	D
8	7	1973	10	H	30.0	-71.0	13.0	80.	5.4	143.	11.6	55.	9.6	6.6	-63.	.5	11.6	D
8	7	1973	18	I	59.0	-18.5	13.1	290.	10.0	304.	4.2	255.	-4.0	-1.1	-14.	2.7	3.2	+
8	7	1973	18	J	52.4	-20.1	17.7	270.	15.2	264.	3.0	302.	-2.6	1.6	6.	2.4	-1.9	+
8	9	1973	0	A	62.0	-24.2	15.2	210.	8.7	186.	6.1	236.	-6.7	-4.5	24.	5.2	-6.2	+
8	9	1973	0	C	52.5	-37.4	16.2	270.	10.5	285.	5.1	161.	1.7	-4.8	-15.	-2.9	4.2	+
8	10	1973	6	B	56.5	-51.0	15.4	330.	13.6	321.	2.0	17.	.9	2.8	9.	1.6	-2.4	+
8	10	1973	6	H	70.0	-71.0	20.0	230.	13.4	228.	6.6	234.	-5.4	-3.9	2.	6.6	-.7	+
8	10	1973	6	J	52.5	-20.1	10.6	260.	9.3	225.	6.1	321.	-3.9	4.7	35.	-.6	-6.1	+
8	10	1973	0	K	45.0	-15.8	14.7	200.	4.8	234.	11.1	186.	-1.1	-11.0	-34.	7.4	8.2	+
8	10	1973	0	M	66.0	2.0	19.0	50.	10.1	77.	9.1	5.	.8	9.0	-27.	2.8	8.6	+
8	11	1973	12	C	52.4	-35.4	14.4	310.	8.3	279.	12.1	331.	-5.9	10.5	31.	7.5	-9.5	D
8	11	1973	12	J	52.4	-20.1	16.5	190.	25.0	175.	10.7	332.	-5.1	9.5	15.	-9.9	-4.3	+
8	11	1973	12	M	66.0	2.1	14.7	210.	15.0	209.	.4	349.	-.1	.4	1.	-.3	-.3	+
8	12	1973	18	B	56.5	-51.0	12.9	40.	14.8	347.	12.5	111.	11.6	-4.5	-53.	-7.0	-10.3	+
8	12	1973	18	C	52.6	-35.0	10.4	210.	15.7	245.	10.6	152.	5.0	-9.3	-35.	-.6	10.6	+
8	12	1973	18	J	52.7	-20.1	18.6	180.	16.5	173.	3.0	222.	-2.0	-2.2	7.	2.0	-2.3	+
8	12	1973	18	M	66.1	2.1	19.5	250.	25.8	223.	12.2	357.	-.7	12.2	27.	-8.4	-8.9	+
8	14	1973	0	I	59.1	-18.5	11.0	220.	16.4	206.	6.3	1.	.1	6.3	14.	-5.7	-2.7	+
8	15	1973	0	B	56.5	-51.0	10.9	260.	9.9	236.	4.4	325.	-2.5	3.6	24.	.1	-4.4	+
8	15	1973	6	C	52.6	-35.5	15.1	340.	12.5	17.	9.1	284.	-8.8	2.2	37.	-.4	9.1	D
8	15	1973	0	I	59.0	-19.4	17.7	190.	21.2	182.	4.4	328.	-2.3	3.8	8.	-3.7	-2.5	C
8	15	1973	0	M	66.0	2.0	16.7	230.	10.5	229.	6.2	232.	-4.9	-3.8	1.	6.2	-.3	+
8	16	1973	12	B	56.5	-51.0	17.8	180.	10.3	197.	8.5	159.	3.0	-8.0	-17.	6.7	5.2	+
8	16	1973	12	J	52.5	-20.1	12.3	330.	3.7	334.	8.6	320.	-4.5	7.3	-4.	8.6	.9	+
8	16	1973	12	M	66.2	1.9	16.7	180.	11.9	171.	5.3	201.	-1.9	-4.9	9.	4.6	-2.6	+
8	17	1973	18	I	58.9	-18.5	17.7	310.	19.0	308.	1.4	103.	1.4	-.3	2.	-1.3	-.6	+
8	17	1973	18	J	52.3	-20.2	16.7	110.	10.0	130.	8.1	85.	8.0	.7	-20.	5.7	5.7	+
8	20	1973	6	I	59.0	-19.1	15.3	100.	14.7	92.	2.2	170.	.4	-2.1	6.	.5	-2.1	+
8	20	1973	0	K	45.0	-16.1	15.7	190.	10.1	190.	5.6	190.	-1.0	-5.5	0.	5.6	.0	D
8	21	1973	12	B	56.1	-51.2	13.1	20.	17.5	352.	8.5	126.	6.9	-5.0	-28.	-5.9	-6.2	+
8	21	1973	12	I	59.1	-19.1	17.4	140.	18.0	120.	3.4	234.	-2.8	-2.0	11.	-.9	-3.3	+
8	21	1973	12	K	45.1	-16.0	18.6	170.	3.8	162.	9.9	176.	.7	-9.9	7.	9.7	-2.3	+
8	21	1973	12	M	65.9	1.8	20.0	310.	19.5	303.	2.5	25.	1.0	2.2	7.	.4	-2.4	+
8	22	1973	18	C	52.5	-35.5	15.7	250.	9.9	241.	6.1	265.	-6.1	-.6	9.	5.6	-2.5	B
8	22	1973	18	H	38.0	-71.0	13.0	180.	10.6	124.	11.3	231.	-8.8	-7.1	56.	-3.3	-10.8	+
8	22	1973	18	I	59.0	-19.0	13.5	150.	13.8	150.	.3	330.	-.1	.3	0.	-.3	.0	+
8	24	1973	0	B	56.3	-50.4	15.6	170.	4.9	190.	11.7	159.	4.3	-10.9	-28.	9.1	7.4	+
8	24	1973	0	C	52.7	-35.2	13.5	310.	17.8	303.	4.7	103.	4.6	-1.0	7.	-4.4	-1.6	B
8	24	1973	0	I	59.1	-19.1	12.5	130.	14.6	147.	4.3	34.	2.4	3.6	-17.	-1.7	3.9	+
8	24	1973	0	J	52.7	-20.0	15.9	160.	15.9	181.	7.6	111.	7.0	-2.7	-21.	2.6	7.1	D
8	24	1973	0	M	65.9	2.3	12.8	330.	16.2	349.	5.8	214.	-3.3	-4.8	-19.	-4.1	4.2	+
8	25	1973	6	H	38.0	-71.0	11.8	70.	1.1	193.	12.3	65.	11.1	5.1	-113.	-5.7	10.9	D
8	25	1973	6	J	52.4	-20.1	11.0	200.	10.3	207.	1.5	142.	.9	-1.2	-7.	.6	1.3	+
8	25	1973	6	K	45.0	-16.0	10.8	350.	8.0	329.	4.0	31.	2.2	3.8	21.	2.1	-3.9	D
8	26	1973	12	C	53.3	-39.0	15.7	260.	12.0	274.	4.5	217.	-2.7	-3.6	-14.	2.4	3.8	D
8	26	1973	12	I	59.2	-19.0	14.7	210.	21.1	175.	12.4	312.	-9.2	8.3	35.	-9.1	-8.4	D
8	26	1973	12	J	52.6	-19.4	11.0	150.	16.1	211.	14.4	73.	13.8	4.3	-61.	-10.8	9.6	+
8	26	1973	12	K	45.0	-16.0	17.2	180.	14.1	203.	16.6	131.	12.6	-10.8	-63.	-6.3	15.3	B

REPRODUCIBILITY OF THE
ORIGINAL PAGE IS POOR

MONTH	DAY	YEAR	HOUR	SHIP	LAT	LONG	VWS	CHWS	VSYN	CHISYN	VF	CHIE	E:EW	F:NS	CW-CS	EPAR	ENORM	TYPE
	27	1973	18	J	52.5	-20.0	12.3	220.	13.8	237.	4.1	117.	3.7	-1.9	-17.	-2.0	3.6	+
	29	1973	0	K	44.9	-15.9	16.7	220.	7.2	251.	11.2	201.	-3.9	-10.4	-31.	7.1	8.6	+
	29	1973	0	M	66.1	2.3	12.3	210.	12.3	193.	3.6	291.	-3.4	1.3	17.	-5	-3.6	+
	30	1973	6	J	52.5	-20.1	12.0	250.	14.2	252.	2.3	23.	.9	2.2	8.	-1.5	-1.8	0
	30	1973	6	K	45.0	-16.1	15.4	369.	15.4	2.	.5	271.	-.5	.0	2.	-.0	.5	0
	30	1973	6	M	65.1	2.5	15.7	130.	10.0	140.	6.9	103.	6.7	-1.6	-18.	4.9	4.9	+
	31	1973	12	I	59.1	-18.8	16.7	240.	19.7	206.	11.0	328.	-5.0	9.4	34.	-5.9	-9.3	+
	31	1973	12	M	64.3	2.9	12.0	200.	2.5	170.	10.7	207.	-4.8	-9.6	30.	8.6	-6.4	+
	1	1973	10	J	52.9	-10.1	17.7	240.	15.5	262.	6.7	180.	.0	-6.7	-22.	.9	6.6	0
	1	1973	10	K	65.6	2.2	12.8	190.	7.5	130.	10.0	226.	-7.1	-6.9	51.	.6	-9.9	+
	3	1973	0	C	51.2	-37.7	14.2	350.	12.0	331.	4.7	55.	3.8	2.7	19.	.5	-4.6	+
	3	1973	0	M	66.1	2.1	11.0	90.	8.3	152.	10.2	44.	7.1	7.3	-62.	-3.1	9.7	+
	4	1973	6	A	61.8	-32.4	16.3	50.	12.5	57.	4.2	29.	2.0	3.7	-7.	3.7	2.0	+
	4	1973	6	J	52.4	-19.7	13.2	360.	5.1	323.	9.6	19.	3.1	9.1	37.	5.4	-7.9	+
	4	1973	6	K	46.8	-13.0	11.0	170.	5.4	183.	5.9	158.	2.2	-5.4	-13.	5.3	2.5	C
	4	1973	6	M	65.9	2.0	16.7	206.	11.0	243.	11.5	159.	4.1	-10.7	-43.	1.2	11.4	+
	5	1973	12	A	62.6	-33.1	18.6	40.	19.9	54.	4.2	302.	-4.1	2.6	-14.	-1.9	4.5	+
	5	1973	12	C	51.5	-17.6	14.9	230.	18.4	260.	9.7	158.	3.6	-9.0	-30.	-2.0	9.4	C
	5	1973	12	I	58.5	-17.4	12.3	150.	21.5	137.	11.3	292.	-10.5	4.2	23.	-10.2	-4.8	+
	6	1973	12	A	62.1	-32.8	10.8	340.	10.9	1.	4.0	254.	-3.9	-.7	21.	-.8	3.9	+
	6	1973	18	C	51.7	-37.2	14.9	10.	20.1	38.	9.9	263.	-9.6	-1.2	-28.	-6.9	7.0	+
	8	1973	0	I	54.0	-13.0	14.7	100.	9.1	104.	6.8	90.	6.8	-.0	-8.	6.5	2.0	0
	8	1973	0	K	45.2	-15.3	14.9	170.	13.6	163.	6.6	185.	-.5	-6.6	7.	6.2	-2.4	+
	8	1973	0	M	65.5	2.3	17.3	290.	15.3	240.	11.3	350.	-2.0	11.1	40.	-1.9	-11.1	+
	9	1973	6	A	62.2	-32.4	16.4	210.	12.8	164.	9.3	291.	-8.7	3.3	46.	-5.6	-7.5	+
	9	1973	6	H	56.5	-51.0	15.6	190.	14.7	166.	6.8	260.	-6.3	-1.1	24.	-.4	-6.3	+
	9	1973	6	I	58.8	-19.6	13.0	60.	7.6	63.	5.4	56.	4.5	3.0	-3.	5.4	.7	+
	9	1973	6	J	52.6	-20.1	14.7	80.	13.9	102.	5.5	9.	.9	5.4	-22.	-.3	5.5	+
	9	1973	6	K	44.5	-13.6	14.0	200.	12.7	169.	7.2	265.	-7.2	-.7	31.	-.7	-7.2	+
	10	1973	12	M	65.0	2.0	15.5	320.	24.9	335.	10.7	177.	.6	-10.7	-15.	-9.9	4.0	+
	11	1973	18	A	62.1	-33.1	18.2	150.	14.8	145.	1.0	192.	-.4	-1.0	5.	1.3	-1.4	+
	11	1973	18	J	52.9	-20.3	13.5	100.	17.9	107.	4.8	307.	-3.8	2.9	-7.	-4.5	1.6	0
	13	1973	0	A	62.6	-33.1	12.3	180.	18.1	171.	6.3	333.	-2.8	5.6	9.	-6.0	-1.9	+
	14	1973	6	A	62.1	-32.8	17.7	190.	17.0	212.	6.7	117.	5.9	-3.0	-22.	-.6	6.6	0
	14	1973	6	M	66.0	1.9	19.0	190.	14.9	223.	16.4	139.	6.9	-7.8	-33.	1.0	10.3	+
	15	1973	12	I	55.2	-15.4	14.5	120.	14.2	121.	5.3	117.	4.7	-2.4	-1.	5.3	.3	0
	15	1973	12	M	65.9	2.4	13.2	320.	13.6	270.	11.3	27.	5.1	10.1	50.	-5.1	-10.1	0
	16	1973	18	A	62.6	-33.0	18.6	70.	10.5	37.	11.3	100.	11.2	-2.0	33.	5.1	-10.1	0
	16	1973	19	B	56.4	-50.7	13.0	310.	9.6	295.	4.5	304.	-1.3	4.3	15.	3.0	-3.4	+
	16	1973	18	I	59.1	-19.4	13.8	150.	13.4	140.	2.5	233.	-1.9	-1.4	10.	-.1	-2.3	0
	16	1973	18	M	65.9	2.0	14.4	110.	14.0	117.	1.0	26.	1.1	1.4	-7.	.3	1.2	+
	18	1973	0	I	58.8	-19.7	17.1	20.	5.7	344.	12.9	35.	7.4	10.6	-36.	8.1	-10.1	+
	18	1973	0	J	52.3	-20.3	14.1	320.	4.7	310.	10.5	323.	-8.7	11.6	10.	14.1	-3.3	+
	19	1973	0	M	66.2	1.6	14.7	120.	8.5	136.	7.1	98.	7.0	-1.0	-18.	5.5	4.5	+
	19	1973	6	A	61.9	-32.6	15.3	220.	16.6	240.	6.8	131.	5.1	-4.4	-24.	-2.6	6.2	+
	19	1973	6	B	56.5	-51.0	12.8	260.	12.7	237.	5.1	337.	-2.0	4.7	23.	-.9	-5.0	+
	19	1973	6	I	58.9	-19.7	14.2	209.	15.1	266.	3.7	17.	1.1	3.5	14.	-1.3	-3.4	+
	19	1973	6	M	65.9	2.0	15.1	146.	16.6	143.	1.9	348.	-.4	1.8	-3.	-1.7	.8	+
	19	1973	12	H	56.5	-51.0	19.9	270.	13.1	252.	7.7	362.	-6.5	4.0	18.	5.0	-5.9	+
	20	1973	6	B	56.5	-51.0	16.7	180.	18.2	188.	3.9	286.	-3.8	1.1	12.	-1.9	-3.5	+

MONTH	DAY	YEAR	HOVR	SHIP	LAT	LONG	VWS	CHWS	VSYN	CHISYN	VF	CHIF	F:EW	F:NS	CW-CS	EPAR	ENORM	TYPE
9	28	1973	0	I	59.0	-13.8	15.5	320.	9.5	316.	6.1	326.	-3.4	5.0	4.	6.0	-1.1	+
9	29	1973	6	C	52.7	-35.4	17.0	180.	17.3	172.	2.4	273.	-2.4	.1	8.	-.5	-2.4	+
9	30	1973	12	H	38.0	-71.0	16.5	50.	16.7	35.	4.3	135.	3.1	-3.1	15.	-.8	-4.3	+
9	30	1973	12	M	65.6	1.8	19.2	290.	14.0	342.	15.3	244.	-13.7	-6.7	-52.	-2.2	15.1	+
10	1	1973	18	H	38.1	-71.0	17.3	60.	21.2	71.	5.4	209.	-5.1	1.7	-11.	-4.2	3.3	0
10	1	1973	18	J	52.5	-29.0	12.3	220.	10.4	213.	2.3	253.	-2.2	-7.	7.	1.8	-1.5	+
10	1	1973	18	K	45.1	-15.4	19.2	40.	16.9	46.	3.0	4.	.2	3.0	-6.	2.2	2.0	+
10	3	1973	0	B	50.5	-50.8	15.4	210.	13.5	235.	6.5	149.	3.4	-5.6	-25.	.5	6.5	+
10	3	1973	0	C	52.7	-35.9	14.1	270.	9.3	288.	6.0	241.	-5.3	-2.9	-18.	4.1	4.4	+
10	4	1973	6	H	37.9	-71.0	13.0	270.	12.4	253.	3.8	343.	-1.1	3.6	17.	.0	-3.8	+
10	4	1973	6	I	59.0	-18.9	18.6	200.	12.1	158.	6.5	204.	-2.6	-6.0	2.	6.5	-.6	+
10	4	1973	6	K	45.0	-10.1	18.9	360.	18.4	10.	4.0	314.	-2.8	2.7	10.	2.2	3.3	+
10	5	1973	12	I	59.1	-19.2	13.5	140.	14.2	144.	3.2	44.	2.2	2.3	-13.	-1.0	3.0	+
10	5	1973	12	M	50.1	1.6	12.3	340.	5.1	343.	7.2	338.	-2.7	6.7	-3.	7.2	-.6	+
10	6	1973	18	H	55.1	-52.3	14.6	160.	15.6	121.	10.1	236.	-8.4	-5.7	39.	-4.3	-9.2	+
10	6	1973	18	J	52.4	-19.2	15.7	230.	17.5	255.	3.2	110.	3.0	-1.1	-9.	-2.0	2.5	+
10	6	1973	18	M	60.1	1.3	17.2	120.	7.6	129.	9.8	113.	9.0	-3.8	-9.	9.4	2.7	+
10	6	1973	0	C	52.7	-35.5	17.4	60.	5.2	242.	21.0	71.	16.9	6.8	-128.	-15.9	-13.7	+
10	8	1973	0	I	59.0	-19.0	12.9	220.	21.3	250.	12.0	102.	11.7	-2.6	-30.	-10.1	6.4	+
10	8	1973	0	J	52.4	-19.9	15.1	210.	11.4	260.	4.0	240.	-3.5	-2.0	10.	3.1	-2.6	+
10	8	1973	0	K	45.3	-15.6	16.5	120.	14.3	137.	5.2	353.	-.7	5.2	-17.	-4.3	3.1	+
10	9	1973	6	B	50.5	-51.3	14.6	30.	18.4	41.	4.9	255.	-4.8	-1.2	-11.	-4.1	2.8	+
10	9	1973	6	I	50.6	-19.0	11.0	20.	6.8	353.	5.8	52.	4.6	3.6	-27.	3.0	-5.0	+
10	9	1973	6	J	52.4	-20.0	18.6	220.	8.9	148.	18.8	248.	-16.7	-6.7	72.	-3.2	-17.7	+
10	10	1973	12	K	45.2	-15.7	12.3	170.	8.1	155.	4.9	195.	-1.3	-4.8	15.	3.8	-3.2	0
10	11	1973	18	I	59.0	-19.1	12.1	100.	13.5	47.	1.6	253.	-1.5	-.5	3.	-1.4	-.6	+
10	11	1973	18	K	45.1	-15.5	13.5	200.	6.9	241.	7.3	278.	-7.3	1.0	19.	5.9	-4.4	0
10	13	1973	0	H	38.0	-71.0	12.6	20.	1.2	321.	12.0	25.	5.1	10.9	-59.	5.3	-10.8	+
10	14	1973	6	B	50.5	-50.8	11.6	40.	6.9	32.	4.7	43.	3.2	3.4	2.	4.7	-.4	+
10	14	1973	6	J	52.4	-20.1	18.1	80.	5.7	67.	12.6	86.	12.6	.9	13.	11.9	-4.1	+
10	14	1973	6	M	65.9	2.2	15.7	330.	14.9	342.	7.3	260.	-3.2	-.6	-12.	.5	3.3	+
10	15	1973	12	I	59.0	-18.9	18.4	40.	18.0	49.	9.7	152.	4.5	-8.6	31.	-2.2	-9.5	0
10	18	1973	0	C	52.9	-35.2	12.3	210.	14.9	212.	1.2	55.	1.0	.7	-2.	-1.1	.5	+
10	18	1973	0	K	45.0	-16.3	13.4	19.	22.3	2.	8.9	185.	-.8	-8.9	2.	-6.9	-.5	0
10	19	1973	6	J	52.8	-18.4	14.7	280.	24.9	274.	10.2	95.	10.2	-.9	2.	-10.2	-.5	+
10	21	1973	18	J	52.5	-20.0	13.0	290.	17.3	239.	13.6	11.	2.6	13.4	51.	-9.1	-10.1	+
10	21	1973	18	M	65.4	1.5	10.1	360.	11.2	31.	5.8	275.	-5.8	.5	31.	-2.5	5.2	+
10	23	1973	0	B	50.5	-51.0	16.3	330.	13.5	352.	6.3	277.	-6.3	.7	-22.	1.6	6.1	+
10	23	1973	0	J	52.5	-20.2	16.7	200.	17.1	169.	9.0	277.	-5.0	1.1	31.	-2.8	-8.6	+
10	24	1973	6	C	52.4	-35.8	17.2	230.	24.0	245.	8.6	96.	8.6	-.9	-15.	-7.4	4.5	+
10	24	1973	6	K	45.0	-15.3	12.3	120.	12.0	113.	1.9	195.	-.4	-1.5	7.	.2	-1.5	+
10	25	1973	12	J	52.6	-20.7	13.5	208.	16.5	215.	4.0	60.	4.8	.8	-15.	-3.5	3.5	+
10	26	1973	18	I	58.9	-19.1	17.7	240.	18.5	258.	3.3	181.	2.1	-2.5	-10.	-1.1	3.1	+
10	28	1973	0	J	52.1	-20.3	11.0	200.	15.3	308.	11.4	174.	1.2	-11.3	-46.	-7.9	8.2	+
10	29	1973	6	J	52.1	-20.2	17.3	160.	16.1	166.	2.1	107.	2.0	-.6	-6.	1.1	1.8	0
10	30	1973	12	C	52.6	-25.3	12.4	270.	16.9	293.	7.5	184.	-1.0	-7.4	-23.	-2.0	7.2	+
10	30	1973	12	I	59.3	-18.7	14.7	160.	14.6	164.	8.0	90.	8.0	.0	-24.	-.6	8.0	+
10	31	1973	18	B	50.5	-51.0	12.8	240.	15.1	205.	6.4	147.	4.0	-5.1	-25.	-3.5	5.4	+
10	31	1973	18	I	59.0	-18.9	13.3	230.	11.8	204.	3.4	193.	-.8	-3.3	-14.	1.1	3.2	0
11	2	1973	0	B	50.5	-51.0	14.3	130.	22.0	120.	7.5	203.	-3.5	-.1	6.	-2.8	-2.0	+

REPRODUCIBILITY OF THE
ORIGINAL PAGE IS POOR

DATE	DAY	YEAR	HOUR	SHIP	LAT	LONG	VMS CHINS	VSYN CHISYN	VF	CHIF.	F:EW	F:NS	CW-CS	FPAR	ENCRM	TYPE	
11	3	1973	6	I	59.0	-19.0	14.4	310.	13.9	310.	2.0	238.	-1.7	-1.1	-8.	2.0	+
11	4	1973	12	A	61.7	-32.0	11.2	80.	4.8	84.	7.1	44.	4.9	-5.1	-24.	4.6	+
11	4	1973	12	M	65.3	-2.4	14.3	90.	5.8	229.	19.1	78.	18.7	3.8	-139.	9.4	+
11	5	1973	12	I	59.1	-19.0	19.8	320.	14.5	312.	5.8	340.	-2.0	5.5	8.	-2.8	+
11	5	1973	13	K	44.9	-16.3	17.1	40.	15.0	18.	6.5	100.	6.4	-1.2	22.	-6.4	0
11	7	1973	0	K	45.0	-15.9	14.5	150.	1.6	116.	13.2	154.	5.8	-11.9	34.	-8.1	+
11	8	1973	0	K	45.0	-15.3	10.7	180.	7.3	192.	5.9	119.	5.2	-2.9	-32.	5.7	+
11	9	1973	12	K	45.2	-15.9	15.2	220.	11.9	214.	3.6	240.	-3.1	-1.8	6.	-1.6	+
11	10	1973	18	A	62.6	-39.7	13.4	240.	2.2	146.	13.7	249.	-12.8	-4.9	94.	-13.4	+
11	10	1973	18	I	59.0	-18.9	13.5	320.	25.3	313.	12.0	125.	9.0	-6.9	7.	-1.6	+
11	10	1973	18	K	44.8	-16.2	17.3	40.	11.4	17.	9.0	70.	8.4	3.1	23.	-7.2	+
11	12	1973	0	C	52.7	-35.5	11.4	190.	12.8	250.	1.0	34.	1.1	1.6	4.	-1.3	0
11	12	1973	0	K	45.9	-16.0	15.3	20.	12.4	2.	1.2	62.	4.0	2.0	18.	-4.7	+
11	15	1973	18	M	64.0	-2.0	13.6	40.	24.2	346.	17.2	143.	10.4	-13.7	-44.	-9.4	+
11	18	1973	0	B	56.5	-51.0	10.2	190.	14.0	142.	14.0	239.	-12.3	-7.4	48.	-14.3	+
11	20	1973	10	I	59.1	-19.0	15.7	200.	10.1	198.	2.8	340.	-7.7	2.7	5.	-1.4	+
11	24	1973	12	C	52.7	-35.5	15.1	110.	15.6	104.	1.7	214.	-9	-1.4	6.	-1.6	C
11	24	1973	12	E	47.3	-14.3	11.8	60.	8.1	70.	2.2	35.	1.9	2.7	-10.	1.9	0
11	25	1973	18	K	45.1	-15.9	12.3	30.	12.7	62.	6.4	313.	-5.1	4.7	-32.	6.5	+
11	28	1973	0	K	44.6	-15.9	15.4	109.	16.2	11.	4.2	7.	5	4.2	-15.	4.0	+
12	3	1973	0	J	52.4	-20.0	10.5	230.	16.9	232.	8.4	57.	7.1	4.6	-3.	.5	0
12	4	1973	12	J	52.4	-20.0	14.5	180.	15.3	142.	4.4	139.	3.2	-3.6	-12.	3.9	+
12	4	1973	12	K	45.1	-16.0	13.3	130.	7.0	111.	6.4	152.	2.9	-5.4	14.	-4.3	+
12	5	1973	10	C	52.6	-35.5	10.7	190.	14.1	161.	0.1	247.	-7.5	-3.1	29.	-8.1	+
12	7	1973	0	K	44.9	-16.3	13.5	230.	8.0	277.	10.0	6.	1.2	10.7	53.	-10.8	+
12	7	1973	0	M	61.5	-2.0	14.9	90.	17.4	350.	21.5	110.	20.3	-7.2	-70.	-13.7	+
12	8	1973	0	C	52.7	-35.5	19.3	200.	21.2	226.	0.3	113.	8.6	-3.6	-26.	8.5	+
12	8	1973	0	M	66.0	-1.9	19.8	320.	9.7	350.	13.2	294.	-12.1	5.5	-36.	11.6	+
12	9	1973	12	M	56.5	-51.0	10.4	230.	21.5	222.	3.2	114.	2.4	-1.3	-2.	.6	+
12	10	1973	18	C	52.7	-35.4	15.5	230.	21.4	262.	10.6	39.	6.6	8.3	28.	-7.3	+
12	12	1973	0	K	45.3	-14.9	15.3	80.	5.6	10.	10.2	91.	10.2	-1	20.	-5.2	E
12	13	1973	0	K	45.0	-16.1	12.2	240.	5.3	302.	8.7	2.	.3	8.7	38.	-7.5	+
12	14	1973	12	C	52.8	-35.4	16.7	170.	7.8	220.	10.2	142.	8.7	-11.2	-58.	14.2	0
12	14	1973	12	I	58.0	-18.9	12.5	120.	5.3	165.	9.5	97.	9.5	-1.1	-45.	8.8	+
12	14	1973	12	K	45.1	-16.1	10.7	330.	3.5	101.	13.8	337.	-5.3	12.8	149.	-5.5	+
12	15	1973	18	K	44.8	-16.1	11.3	250.	17.9	211.	6.0	307.	-4.8	3.6	19.	-6.0	+
12	17	1973	0	A	62.1	-35.1	15.7	290.	5.7	334.	12.7	270.	-12.7	.0	-49.	11.8	+
12	17	1973	0	B	56.5	-51.0	16.0	60.	12.1	10.	12.4	108.	11.8	-3.9	50.	-12.3	+
12	17	1973	0	C	51.5	-37.1	19.9	120.	20.3	123.	1.1	11.	.2	1.1	-3.	1.0	+
12	19	1973	12	A	61.8	-32.9	13.7	60.	15.0	55.	2.5	207.	-1.2	-2.3	5.	-1.2	+
12	19	1973	12	B	58.0	-71.9	12.5	350.	14.2	353.	0.1	205.	-3.9	-8.2	-23.	4.9	0
12	22	1973	0	A	61.1	-30.1	10.4	60.	9.5	62.	11.2	95.	11.1	-1.0	14.	-6.1	+
12	25	1973	18	B	56.4	-51.0	14.5	290.	25.6	313.	13.5	158.	5.1	-12.5	-23.	5.7	+
12	25	1973	18	C	52.9	-35.9	14.9	220.	13.4	202.	8.3	250.	-7.8	-2.8	18.	-6.1	+
12	25	1973	18	H	34.0	-71.0	14.4	130.	19.0	123.	5.0	243.	-4.9	1.1	7.	-1.8	+
12	25	1973	18	I	58.4	-18.2	15.7	280.	15.6	244.	9.7	351.	-1.4	9.6	36.	-9.2	+
12	27	1973	0	K	45.2	-15.3	12.2	260.	5.0	226.	7.6	250.	-7.1	-2.6	14.	-3.1	+
12	28	1973	0	B	58.0	-71.0	12.2	250.	15.5	222.	8.7	357.	-4	8.2	28.	-5.7	H
12	28	1973	0	K	45.4	-15.5	16.2	220.	10.9	167.	13.0	242.	-12.9	-1.8	53.	-12.9	+
12	29	1973	12	B	58.0	-50.8	14.3	100.	13.3	152.	1.1	135.	.8	-1.8	-2.	.5	+

MONTH	DAY	YEAR	HOUR	SHIP	LAT	LONG	WLS	CHWS	VSYN	CHTSYN	VF	CHIE	E:EW	FINS	CW-CS	EPAR	ENORM	TYPE
12	29	1973	12	I	59.1	-17.4	11.0	300.	12.1	203.	7.6	39.	2.3	2.8	17.	-1.6	-3.2	+
12	29	1973	12	M	65.8	3.7	18.2	240.	36.9	218.	21.2	19.	7.0	20.0	22.	-20.0	-6.8	0
1	1	1974	0	M	65.5	2.2	19.8	200.	12.1	206.	10.4	160.	1.9	-10.2	-26.	5.7	8.7	+
1	2	1974	6	B	56.6	-50.5	15.4	260.	3.8	203.	11.6	279.	-11.5	1.8	-3.	11.6	.8	+
1	2	1974	6	F	33.0	-71.0	19.8	310.	18.7	200.	12.9	244.	-11.6	-5.6	-39.	-3.3	12.5	+
1	3	1974	6	I	56.4	-13.7	10.5	130.	15.2	162.	8.4	23.	3.3	7.7	-32.	-6.3	5.6	+
1	3	1974	12	J	52.4	-13.7	20.0	219.	21.5	219.	3.6	100.	3.5	-6	-9.	-1.7	3.1	+
1	4	1974	18	B	56.6	-50.8	15.0	320.	23.2	326.	4.7	171.	.8	-4.7	-6.	-4.3	2.0	+
1	4	1974	18	H	34.0	-71.0	17.6	360.	12.2	349.	6.1	22.	2.3	5.6	11.	5.1	-3.4	+
1	5	1974	12	I	58.9	-13.9	16.6	250.	17.6	245.	1.8	11.	.4	1.8	5.	-1.1	-1.4	+
1	9	1974	18	M	66.0	2.0	19.5	130.	22.1	130.	4.2	6.	.4	4.1	-9.	-2.8	3.1	+
1	12	1974	6	F	36.7	-71.0	19.2	340.	13.8	203.	16.0	23.	6.7	15.5	57.	-3.0	-16.6	+
1	12	1974	0	I	59.0	-19.1	17.7	290.	18.0	293.	13.1	180.	-.1	-13.1	-43.	-5.1	12.1	+
1	13	1974	12	I	59.8	-13.4	14.7	260.	15.2	211.	12.4	320.	-6.6	10.5	49.	-5.6	-11.1	0
1	14	1974	18	I	59.1	-19.0	16.7	230.	21.0	252.	8.3	121.	7.2	-4.2	-22.	-5.5	6.3	+
1	17	1974	6	F	56.4	-52.8	13.6	10.	26.5	323.	19.9	113.	18.3	-7.8	-47.	-17.2	-9.9	+
1	17	1974	6	K	43.0	-16.2	18.3	290.	18.5	239.	15.8	355.	-1.3	15.8	51.	-7.0	-14.2	+
1	18	1974	12	H	38.0	-71.0	19.7	40.	17.6	46.	2.9	0.	.0	2.9	-6.	2.0	2.1	+
1	18	1974	12	I	59.0	-19.2	20.0	236.	27.4	244.	9.3	95.	9.3	-8.8	-14.	-8.0	4.8	+
1	18	1974	12	K	45.0	-15.8	14.3	189.	13.9	159.	5.2	255.	-5.0	-1.3	21.	-.5	-5.1	0
1	22	1974	6	H	38.0	-71.0	19.0	310.	13.0	220.	23.5	346.	-5.7	22.8	90.	-13.8	-19.0	+
1	22	1974	6	M	65.9	2.1	19.2	290.	20.0	276.	4.0	22.	1.8	4.5	14.	-1.4	-4.6	+
1	24	1974	18	B	56.9	-52.7	14.6	270.	7.7	285.	7.4	254.	-7.2	-2.0	-15.	6.4	3.8	+
1	24	1974	18	K	44.8	-15.3	13.2	260.	12.0	270.	2.5	204.	-1.0	-2.3	-10.	1.0	2.3	+
1	24	1974	18	M	66.0	1.6	16.5	290.	10.5	215.	17.1	326.	-9.5	14.2	75.	-6.2	-15.9	+
1	26	1974	0	H	38.0	-71.0	14.8	10.	14.4	333.	9.3	79.	9.1	1.7	-37.	-2.6	-8.9	+
1	27	1974	6	J	52.3	-20.7	16.7	210.	14.6	230.	5.8	151.	2.8	-5.1	-20.	1.1	5.7	+
1	28	1974	12	I	56.9	-18.4	11.2	270.	23.1	315.	17.1	163.	5.1	-16.3	-45.	-15.2	7.9	+
1	28	1974	12	J	52.0	-19.7	18.3	270.	29.5	287.	13.1	131.	9.9	-8.6	-17.	-12.0	5.4	+
1	28	1974	12	M	65.8	1.0	16.7	130.	19.8	148.	6.5	21.	2.3	6.1	-18.	-3.9	5.2	+
1	29	1974	18	A	62.0	-32.7	16.5	320.	13.5	3.	11.3	266.	-11.3	-.8	43.	-1.4	11.3	+
1	29	1974	18	B	55.7	-50.2	15.8	270.	12.6	271.	3.2	266.	-3.2	-.2	-1.	3.2	.3	+
1	29	1974	18	H	38.0	-71.0	18.4	340.	14.5	299.	12.1	32.	6.4	10.3	41.	-.6	-12.1	0
2	1	1974	6	M	65.7	2.3	18.6	240.	6.2	236.	10.4	243.	-9.3	-4.7	4.	10.4	-1.3	+

REPRODUCIBILITY OF THE
ORIGINAL PAGE IS POOR

MONTH	DAY	YEAR	HOUR	SHIP	LAT	LONG	VWS	CHINS	VSYN	CHISYN	VF	CHIE	E:EW	F:NS	CW-CS	EPAR	ENORM	TYPE
7	15	1973	0	J	52.2	-17.8	21.5	360.	18.7	349.	4.8	49.	3.6	3.1	11.	2.4	-4.1	+
7	15	1973	0	K	45.1	-16.0	21.5	310.	17.8	321.	5.3	270.	-5.3	-0.	-11.	3.3	4.1	+
7	16	1973	6	J	52.3	-20.0	25.3	350.	23.6	356.	2.4	43.	1.6	1.8	4.	1.6	-1.8	0
7	17	1973	12	K	45.5	-15.6	23.0	340.	22.5	354.	5.6	262.	-5.5	-0.8	-14.	-0.2	5.6	0
7	18	1973	18	J	52.5	-20.5	23.9	290.	31.6	261.	8.8	76.	8.6	2.1	9.	-8.0	-3.7	+
7	20	1973	0	J	52.4	-20.2	22.3	310.	18.2	317.	4.8	262.	-4.7	1.0	-7.	3.9	2.7	+
7	20	1973	0	K	45.6	-14.0	23.7	280.	12.2	277.	11.5	203.	-11.2	2.6	3.	11.5	-1.2	+
7	21	1973	6	M	66.0	1.9	25.8	36.	18.6	27.	7.3	38.	4.5	5.8	3.	7.2	-1.4	+
7	22	1973	12	M	66.2	1.5	23.0	20.	15.3	42.	10.5	347.	-2.4	10.2	-22.	6.0	8.6	+
7	25	1973	6	A	62.1	-33.2	25.3	60.	10.9	132.	24.3	35.	13.8	19.9	-72.	-3.1	24.1	+
7	27	1973	12	C	52.6	-35.3	21.1	180.	13.4	232.	16.6	141.	10.6	-12.9	-52.	-4	16.6	+
7	28	1973	18	A	62.2	-32.6	25.3	210.	14.7	225.	11.7	191.	-2.3	-11.5	-15.	9.7	6.5	+
7	28	1973	18	C	52.7	-35.5	29.0	210.	17.6	223.	12.5	192.	-2.5	-12.2	-13.	10.7	6.5	+
7	31	1973	6	M	65.6	4.5	28.8	220.	21.7	245.	12.9	175.	1.2	-12.9	-25.	4.4	12.2	C
8	2	1973	18	A	61.9	-32.9	23.9	290.	12.9	294.	11.1	265.	-10.7	2.9	-4.	10.9	1.7	+
8	2	1973	18	C	52.3	-35.1	20.2	320.	14.2	280.	13.0	4.	1.0	13.0	40.	1.3	-13.0	+
8	2	1973	18	H	38.0	-71.0	27.8	200.	24.4	181.	9.2	259.	-9.1	-1.7	19.	1.9	-9.1	C
8	4	1973	0	B	56.5	-51.0	23.7	320.	15.8	309.	8.7	340.	-3.0	8.2	11.	7.5	-4.5	+
8	4	1973	0	H	38.0	-71.0	27.6	230.	19.3	223.	8.8	246.	-8.0	-3.6	7.	8.1	-3.4	0
8	5	1973	6	C	52.4	-35.1	29.8	280.	8.1	323.	24.5	267.	-24.5	-1.3	-43.	13.7	20.3	+
8	5	1973	6	J	52.5	-19.7	23.7	270.	14.2	275.	9.6	263.	-9.6	-1.2	-5.	9.4	2.1	+
8	5	1973	6	K	44.3	-15.7	20.5	230.	19.4	245.	5.3	159.	1.9	-5.0	-15.	.4	5.3	+
8	6	1973	12	A	62.0	-33.1	24.4	360.	23.4	8.	3.5	291.	-3.3	1.2	8.	.8	3.4	0
8	6	1973	12	J	53.2	-17.0	26.8	260.	18.6	301.	17.7	216.	-10.4	-14.2	-41.	1.6	17.6	0
8	9	1973	0	J	52.6	-13.6	22.3	230.	9.3	213.	13.7	241.	-12.0	-6.5	17.	12.0	-6.5	+
8	9	1973	0	M	65.9	2.1	21.4	280.	14.6	271.	7.3	298.	-6.5	3.5	9.	6.5	-3.3	+
8	10	1973	6	C	52.7	-35.5	28.9	200.	15.4	199.	13.5	201.	-4.9	-12.6	1.	13.5	-5	+
8	11	1973	12	H	38.0	-71.0	21.5	210.	16.4	209.	5.1	213.	-2.8	-4.3	1.	5.1	-4	0
8	11	1973	12	I	56.9	-19.0	22.3	220.	22.3	207.	5.0	303.	-4.2	2.0	13.	-6	-5.0	8
8	12	1973	18	I	59.1	-13.9	28.1	180.	23.0	179.	5.1	184.	-4	-5.1	1.	5.1	-5	+
8	14	1973	0	C	52.7	-35.7	29.9	360.	7.1	75.	24.0	344.	-6.9	24.1	75.	-4	25.0	+
8	14	1973	0	K	66.3	2.3	26.0	230.	20.4	214.	8.5	271.	-8.5	.2	16.	4.6	-7.2	+
8	15	1973	6	J	52.4	-20.0	20.5	170.	18.0	192.	7.7	109.	7.3	-2.6	-22.	1.0	7.7	+
8	16	1973	12	I	59.0	-18.9	20.5	290.	26.3	263.	6.5	80.	6.4	1.1	7.	-6.0	-2.5	+
8	17	1973	18	C	52.4	-35.0	23.1	50.	16.6	44.	6.8	65.	6.2	2.9	6.	6.4	-2.4	+
8	17	1973	18	M	66.2	2.0	24.6	160.	10.7	224.	22.1	134.	15.8	-15.4	-64.	.1	22.1	+
8	19	1973	0	C	52.2	-37.0	23.1	70.	12.2	76.	11.0	63.	9.9	4.9	-6.	10.8	2.4	+
8	19	1973	0	I	56.9	-18.7	20.8	180.	15.4	14.	5.5	359.	-1	5.5	-4.	5.3	1.5	+
8	19	1973	0	M	66.3	2.3	26.5	250.	8.3	272.	13.8	233.	-11.1	-0.3	-29.	9.6	9.9	+
8	20	1973	6	B	56.6	-51.2	20.8	50.	17.2	26.	8.6	104.	8.4	-2.1	24.	1.8	-8.5	+
8	20	1973	6	M	66.0	2.0	21.5	330.	17.9	335.	10.9	324.	-6.7	8.5	-5.	10.6	2.5	+
8	21	1973	12	C	52.7	-35.1	23.1	210.	3.5	232.	19.6	208.	-8.8	-17.9	-22.	17.9	8.7	+
8	26	1973	12	M	66.0	2.2	22.3	210.	20.1	215.	7.9	172.	.4	-2.8	-5.	2.1	1.9	+
8	27	1973	18	C	53.0	-24.9	26.0	360.	15.4	209.	20.2	246.	-18.1	9.0	51.	1.0	-20.2	+
8	29	1973	0	C	52.5	-35.7	21.3	270.	17.9	265.	3.8	244.	-3.5	1.6	5.	3.3	-1.9	+
8	29	1973	0	M	66.0	-71.0	25.9	250.	19.2	236.	8.6	263.	-8.4	1.9	14.	5.9	-6.3	+
8	29	1973	0	I	59.2	-12.7	20.3	200.	23.5	210.	8.7	28.	4.6	.8	-10.	-3.0	3.6	8
8	29	1973	0	J	52.4	-19.6	22.3	250.	17.2	249.	5.1	252.	-4.9	-1.5	1.	5.1	-4	+
8	30	1973	6	I	59.0	-19.1	26.5	270.	18.9	213.	8.1	287.	-7.7	2.3	7.	7.4	-3.2	0
9	3	1973	0	A	69.7	-30.0	23.0	350.	11.4	345.	11.7	355.	-1.0	11.6	5.	11.5	-2.0	+

MONTH	DAY	YEAR	POUR	SHIP	LAT	LONG	VWS	CHWS	VSYN	CHISYN	VF	CHIE	E:EW	F:NS	CW-CS	EPAR	ENORM	TYPE
9	4	1973	6	B	56.3	-50.7	23.6	260.	9.4	304.	18.1	239.	-15.4	-9.4	-44.	7.6	16.4	+
9	5	1973	12	J	52.6	-19.7	21.4	190.	13.9	215.	10.6	156.	4.3	-9.7	-25.	5.5	9.0	+
9	5	1973	12	K	45.5	-14.9	23.0	320.	16.9	320.	6.1	320.	-3.9	4.7	0.	6.1	.0	D
9	6	1973	18	I	52.9	-18.8	25.2	250.	15.2	215.	15.4	284.	-15.0	3.8	35.	5.4	-14.5	+
9	6	1973	18	J	52.7	-19.7	23.3	190.	19.7	174.	7.0	241.	-6.1	-3.4	16.	2.7	-6.4	+
9	8	1973	0	B	55.5	-52.4	26.1	190.	18.5	156.	7.8	200.	-2.6	-7.3	4.	7.5	-1.8	C
9	8	1973	0	C	52.6	-35.5	27.7	340.	15.0	339.	5.7	343.	-1.7	5.4	1.	5.7	-.4	+
9	11	1973	18	B	56.4	-50.4	22.9	150.	15.1	152.	7.8	146.	4.4	-6.5	-2.	7.8	.8	+
9	13	1973	0	B	56.5	-51.0	21.1	190.	12.7	158.	12.3	223.	-8.4	-9.0	32.	5.2	-11.2	+
9	13	1973	0	M	65.7	2.2	22.3	260.	12.5	260.	9.0	260.	-9.7	-1.7	0.	9.8	.0	+
9	14	1973	6	C	52.7	-35.5	20.1	150.	12.1	159.	9.5	126.	7.7	-5.5	-19.	6.9	6.5	+
9	15	1973	12	A	62.2	-33.1	22.3	150.	6.5	118.	16.0	135.	11.3	-11.3	12.	15.3	-4.6	+
9	15	1973	12	B	56.5	-51.0	23.0	310.	19.3	290.	8.2	4.	.5	8.2	20.	2.3	-7.9	+
9	15	1973	12	C	52.7	-35.5	25.5	270.	22.5	278.	4.5	226.	-3.2	-3.1	-8.	2.8	3.5	D
9	15	1973	12	K	45.2	-15.8	21.4	270.	19.3	251.	7.0	333.	-3.2	6.3	19.	.9	-7.0	+
9	16	1973	18	C	52.7	-35.5	21.9	280.	25.0	282.	3.2	116.	2.9	-1.4	-2.	-3.1	.8	+
9	16	1973	18	K	45.1	-15.9	22.2	290.	16.5	282.	4.7	324.	-2.8	3.7	8.	3.5	-3.1	+
9	18	1973	0	K	45.0	-15.6	25.9	240.	15.3	240.	10.5	240.	-9.1	-5.3	0.	10.5	.0	+
9	19	1973	6	C	52.7	-35.5	20.9	320.	20.6	309.	10.4	342.	-3.2	9.9	11.	8.8	-5.7	+
9	20	1973	12	K	44.6	-15.6	23.0	330.	29.9	301.	14.8	72.	14.1	4.5	29.	-9.8	-11.2	D
9	26	1973	0	K	45.8	-14.0	22.3	240.	23.7	252.	5.0	149.	3.2	-3.8	-12.	-1.9	4.6	C
9	28	1973	0	V	65.9	1.9	21.6	150.	17.0	147.	8.7	161.	1.5	-4.4	3.	4.6	-1.1	+
9	29	1973	6	I	50.1	-19.1	22.9	360.	22.0	341.	7.5	74.	7.2	2.1	19.	-.3	-7.5	+
9	29	1973	6	J	52.3	-19.3	20.8	310.	20.7	364.	2.2	34.	1.2	1.8	6.	-.0	-2.2	+
9	29	1973	6	K	45.4	-13.5	25.0	320.	25.2	320.	.2	140.	.1	-.2	0.	-.2	-.0	D
9	29	1973	6	M	65.8	1.8	23.0	30.	18.7	37.	5.0	3.	.2	5.0	-7.	4.1	2.8	+
9	30	1973	12	I	59.0	-18.5	24.6	230.	20.9	223.	4.6	263.	-4.6	-.5	7.	3.5	-3.0	+
10	1	1973	18	B	54.7	-52.6	26.6	360.	26.4	319.	18.6	69.	17.3	6.7	41.	-6.3	-17.5	C
10	1	1973	18	C	52.8	-35.3	29.5	190.	29.3	172.	9.2	270.	-9.2	-.0	16.	-1.2	-9.1	+
10	1	1973	18	I	52.9	-14.9	23.9	220.	23.7	232.	5.0	138.	3.3	-3.7	-12.	-.3	5.0	+
10	3	1973	0	K	45.0	-16.0	22.3	40.	18.4	34.	4.4	66.	4.0	1.8	6.	3.8	-2.3	+
10	3	1973	0	N	65.3	2.5	27.3	240.	22.8	226.	7.6	287.	-7.2	2.2	14.	3.7	-6.6	+
10	6	1973	18	C	52.7	-35.3	21.4	310.	18.9	203.	8.1	11.	1.6	7.9	22.	.9	-8.0	+
10	8	1973	0	H	56.5	-51.3	26.0	90.	20.2	75.	9.3	129.	6.5	-5.2	15.	4.9	-6.7	+
10	10	1973	12	P	56.5	-51.0	25.1	50.	27.8	6.	20.0	125.	16.3	-11.5	44.	-9.7	-17.4	+
10	10	1973	12	C	52.9	-35.4	20.4	100.	15.4	101.	5.0	97.	5.0	-.6	-1.	5.0	.4	+
10	10	1973	12	I	58.9	-13.9	24.4	90.	27.0	84.	3.7	221.	-2.5	-2.8	6.	-2.7	-2.6	+
10	10	1973	12	J	52.5	-19.9	22.3	110.	19.8	96.	5.7	167.	1.3	-5.6	14.	1.8	-5.4	D
10	10	1973	12	N	66.0	1.6	27.9	30.	24.9	19.	5.9	84.	5.8	.6	11.	2.5	-5.3	+
10	11	1973	18	H	37.9	-73.9	26.6	30.	21.6	25.	5.4	50.	4.2	3.5	5.	4.9	-2.3	C
10	11	1973	18	N	65.8	1.8	25.2	300.	25.3	322.	9.6	220.	-6.2	-7.3	-22.	-1.8	9.4	+
10	13	1973	0	B	56.5	-51.0	21.3	60.	13.0	47.	9.1	79.	8.9	1.8	13.	7.8	-4.8	+
10	13	1973	0	I	59.0	-19.8	20.7	90.	16.4	71.	7.4	136.	5.2	-5.3	19.	3.2	-6.7	+
10	13	1973	0	M	66.0	1.7	21.3	270.	13.0	240.	8.8	255.	-8.5	-2.3	-10.	8.0	3.7	+
10	14	1973	6	H	34.0	-70.9	27.9	240.	21.6	224.	9.3	289.	-9.2	1.6	16.	5.2	-7.7	C
10	15	1973	12	B	56.6	-51.3	25.2	120.	25.3	139.	9.3	39.	5.2	6.5	-19.	-1.5	8.2	+
10	16	1973	18	B	56.5	-51.0	22.2	171.	27.6	146.	11.5	274.	-11.5	.9	24.	-7.1	-9.0	+
10	16	1973	18	C	51.4	-37.3	24.5	140.	19.3	145.	5.5	122.	4.7	-3.0	-5.	5.1	2.1	+
10	16	1973	18	N	65.1	1.7	21.7	340.	27.6	346.	3.4	219.	-2.1	-2.6	-6.	-2.0	2.7	+
10	19	1973	6	I	54.2	-14.6	22.2	250.	14.9	277.	11.2	213.	-6.1	-9.4	-27.	4.9	10.1	+

BII

REPRODUCTION OF THE
ORIGINAL PAGE IS FORBIDDEN

MONTH	DAY	YEAR	HOUR	SHIP	LAT	LONG	VWS	CHWS	VSYN	CHISYN	VF	CHIE	E:EW	F:NS	CW-CS	EPAR	ENORM	TYPE
10	19	1973	6	M	65.9	1.8	21.2	350.	19.2	341.	2.0	341.	-7	1.9	-1.	2.0	.4	+
10	20	1973	12	I	58.6	-18.1	25.8	300.	25.3	308.	3.6	222.	-2.4	-2.7	-8.	.2	3.6	+
10	20	1973	12	M	65.7	1.7	25.4	290.	12.0	309.	14.6	274.	-14.5	1.1	-19.	12.0	8.3	+
10	21	1973	18	C	53.5	-34.6	27.6	270.	29.4	267.	2.3	49.	1.2	1.5	3.	-1.8	-1.4	+
10	21	1973	18	I	59.0	-18.5	25.2	260.	30.6	169.	40.0	310.	-30.7	25.7	91.	-31.0	-25.2	D
10	23	1973	0	A	61.9	-33.0	27.7	250.	23.9	247.	4.0	308.	-4.0	-1	3.	3.8	-1.4	+
10	23	1973	0	I	49.0	-18.9	23.0	250.	25.6	239.	5.3	4.	.3	5.3	11.	-3.0	-4.4	+
10	23	1973	0	A	61.0	-32.5	27.3	250.	21.7	241.	6.8	260.	-6.7	1.2	9.	5.3	-4.3	D
10	24	1973	0	B	56.4	-51.1	25.7	240.	9.8	251.	16.2	233.	-13.0	-9.7	-11.	15.4	4.9	+
10	24	1973	6	M	65.9	1.9	20.8	220.	20.3	223.	1.2	156.	.5	-1.1	-3.	.5	1.1	+
10	24	1973	12	I	58.9	-14.2	27.5	180.	24.8	190.	8.5	116.	7.7	-3.7	-18.	1.2	8.4	+
10	25	1973	18	B	56.5	-51.0	22.5	200.	18.2	210.	12.8	172.	1.7	-12.6	-19.	8.7	9.3	+
10	26	1973	18	C	52.6	-35.4	27.8	310.	27.1	303.	3.4	25.	1.4	3.1	7.	.5	-3.4	D
10	26	1973	18	M	66.0	1.8	22.3	190.	12.3	210.	11.5	169.	2.3	-11.3	-20.	8.7	7.6	+
10	26	1973	0	K	44.8	-16.1	23.0	50.	20.2	40.	4.7	98.	4.6	-7	10.	2.5	-4.0	+
10	29	1973	0	K	44.9	-10.3	24.6	110.	16.5	196.	8.2	118.	7.3	-3.9	4.	8.0	-1.7	+
10	30	1973	12	B	55.6	-51.2	23.6	230.	24.4	216.	14.0	155.	6.3	-13.5	-36.	-5.3	13.9	+
10	30	1973	12	J	52.6	-20.4	22.3	140.	17.7	155.	6.9	99.	6.9	-1.0	-15.	3.8	5.8	+
10	30	1973	12	K	45.0	-15.4	24.5	110.	18.9	175.	23.9	64.	21.5	10.4	-65.	-8.5	22.3	D
10	31	1973	12	M	65.9	1.3	27.3	210.	23.5	202.	5.2	244.	-4.8	-1.9	6.	3.5	-3.8	+
11	2	1973	6	A	62.5	-32.4	21.4	240.	8.9	7.	14.1	323.	-8.4	11.3	27.	10.2	9.7	+
11	2	1973	0	I	59.1	-18.7	21.5	180.	6.9	191.	14.8	175.	1.3	-14.7	-11.	14.2	4.1	+
11	2	1973	0	J	52.3	-20.1	22.9	20.	11.0	30.	12.2	11.	2.3	12.0	-10.	11.6	4.0	+
11	2	1973	0	K	44.9	-15.3	24.3	130.	22.8	225.	29.2	127.	16.1	-12.2	-45.	-2.8	20.0	+
11	3	1973	0	M	65.4	2.2	22.3	190.	10.7	164.	9.9	246.	-9.0	-4.6	26.	1.3	-9.8	+
11	3	1973	6	K	44.5	-19.4	24.4	220.	10.3	315.	6.4	334.	-2.7	5.8	5.	6.0	-2.1	+
11	4	1973	12	K	44.5	-19.4	24.4	220.	10.3	315.	6.4	334.	-2.7	5.8	5.	6.0	-2.1	+
11	5	1973	18	A	61.9	-32.9	29.6	150.	21.1	137.	10.2	172.	.4	-10.2	13.	7.7	-6.7	+
11	5	1973	18	B	55.4	-52.6	25.1	170.	19.9	153.	8.4	214.	-4.7	-7.0	17.	4.1	-7.3	+
11	6	1973	6	C	51.6	-37.8	25.4	250.	20.8	236.	7.2	244.	-6.6	2.9	14.	3.8	-6.1	+
11	9	1973	12	C	51.5	-37.5	22.3	270.	23.0	290.	5.6	0.	.0	5.6	14.	-1.4	-5.4	+
11	9	1973	12	M	65.9	2.2	23.5	240.	18.5	324.	5.5	1.	.1	5.5	6.	4.9	-2.5	+
11	10	1973	18	M	65.4	1.9	20.5	300.	7.9	245.	15.9	279.	-15.7	2.6	-45.	6.6	14.5	+
11	12	1973	0	J	52.9	-18.1	20.6	240.	20.9	252.	6.2	153.	2.8	-5.6	-12.	-9	6.2	+
11	13	1973	6	J	52.8	-18.0	20.8	260.	20.8	269.	3.3	188.	-5	-3.3	-9.	.5	3.3	+
11	15	1973	18	B	56.5	-51.0	22.3	120.	21.4	110.	3.0	192.	-8	-3.8	10.	.6	-3.9	+
11	17	1973	0	C	52.7	-35.5	21.1	83.	17.9	82.	4.2	72.	3.9	1.3	-2.	4.1	.7	C
11	17	1973	0	J	52.6	-20.1	24.6	170.	18.3	190.	6.3	170.	1.1	-6.2	0.	6.3	.0	+
11	17	1973	0	M	65.9	1.5	22.1	320.	15.1	347.	11.0	282.	-10.8	2.2	-27.	4.6	10.0	+
11	18	1973	6	I	59.1	-18.7	25.0	220.	13.7	221.	11.3	319.	-7.4	8.5	-1.	11.3	.4	+
11	20	1973	18	B	56.5	-51.0	20.8	270.	16.1	220.	4.3	223.	-3.0	-3.1	-10.	2.4	3.6	D
11	20	1973	18	C	52.7	-35.5	25.2	230.	27.2	246.	7.1	131.	5.3	-4.7	-15.	-2.9	6.5	C
11	22	1973	18	M	66.0	2.3	24.9	160.	21.0	202.	20.0	115.	18.1	-8.6	-42.	1.2	20.0	+
11	22	1973	0	J	59.1	-18.0	22.9	240.	24.5	230.	1.8	32.	.9	1.5	2.	-1.6	-.8	+
11	23	1973	6	J	52.5	-20.5	20.5	240.	17.2	234.	3.8	268.	-3.0	-1	6.	3.2	-2.1	+
11	24	1973	12	B	56.5	-51.0	24.4	100.	22.5	76.	9.9	167.	2.2	-9.7	24.	-.2	-9.9	+
11	24	1973	12	I	59.1	-18.0	21.4	310.	16.1	340.	13.5	261.	-13.3	-2.0	-39.	.5	13.5	+
11	25	1973	18	C	52.2	-37.1	25.4	130.	16.0	133.	7.5	123.	6.3	-4.1	-3.	7.4	1.3	D
11	27	1973	6	B	56.5	-51.0	21.3	50.	11.0	243.	10.9	83.	19.8	2.4	-67.	-3.5	-19.6	+
11	28	1973	0	I	59.2	-19.3	20.8	230.	18.5	260.	10.4	283.	-9.6	4.0	30.	-.5	-10.4	+

MO:YR	DAY	YEAR	HOOR	SHIP	LAT	LONG	VWS	CHWS	VSYN	CHSYN	VF	CHIE	C:EW	E:NS	CK-CS	EPAR	ENORM	TYPE
12	2	1973	0	K	45.1	-16.1	22.8	40.	20.9	31.	3.9	97.	3.9	-4	9.	1.6	-3.6	+
12	3	1973	6	K	45.1	-15.7	25.9	100.	22.7	96.	3.6	126.	2.9	-2.1	4.	3.1	-1.8	+
12	4	1973	12	I	59.1	-19.0	20.5	250.	13.4	249.	7.1	252.	-6.8	-2.2	1.	7.1	-4	+
12	5	1973	18	B	56.5	-51.0	20.7	250.	8.4	106.	27.9	260.	-27.5	-4.8	144.	-25.1	-12.2	+
12	7	1973	0	J	53.2	-17.1	27.3	258.	24.6	204.	3.8	292.	-3.5	1.4	6.	2.6	-2.9	C
12	8	1973	6	K	44.7	-16.1	21.5	330.	16.7	329.	4.9	333.	-2.1	4.3	1.	4.8	-4	+
12	10	1973	13	A	61.9	-32.4	27.1	300.	11.1	288.	11.5	312.	-8.6	7.6	12.	10.5	-4.6	+
12	10	1973	18	B	56.5	-51.0	22.3	230.	20.2	212.	7.0	294.	-6.4	2.8	18.	1.0	-6.9	+
12	10	1973	18	I	58.2	-18.1	27.7	300.	21.6	298.	7.2	306.	-5.8	4.2	2.	7.1	-1.0	+
12	10	1973	18	K	45.7	-14.4	20.8	210.	5.2	221.	15.7	206.	-7.0	-14.1	-11.	15.2	4.0	D
12	12	1973	0	A	61.6	-33.3	28.7	270.	15.1	252.	15.1	288.	-14.3	4.7	18.	12.2	-8.9	+
12	12	1973	0	J	52.4	-19.8	23.6	260.	16.0	266.	7.9	248.	-7.3	-3.0	-6.	7.5	2.5	D
12	13	1973	6	I	56.6	-12.5	27.6	300.	24.1	289.	6.1	349.	-1.1	6.0	11.	3.0	-5.3	D
12	13	1973	6	J	52.4	-20.1	23.0	280.	18.9	279.	4.1	265.	-4.0	1.0	1.	4.1	-4	+
12	13	1973	6	M	66.6	1.6	26.6	10.	20.5	27.	9.2	329.	-4.7	7.9	-17.	4.9	7.8	+
12	14	1973	12	A	61.8	-33.7	27.7	120.	19.4	156.	17.3	79.	17.0	3.4	-30.	3.8	16.9	+
12	15	1973	18	A	61.6	-33.2	21.4	310.	23.1	296.	5.7	50.	4.4	3.6	14.	-2.3	-5.2	+
12	15	1973	18	J	52.6	-19.4	21.5	350.	11.2	272.	20.1	20.	7.5	20.8	78.	-6.7	-21.0	D
12	15	1973	18	M	65.5	2.2	28.1	160.	26.3	151.	4.6	223.	-3.1	-3.4	9.	1.5	-4.4	D
12	17	1973	0	I	56.6	-19.6	28.1	320.	20.9	313.	8.7	337.	-3.4	8.0	7.	8.0	-3.5	+
12	17	1973	0	J	52.5	-20.2	20.7	310.	15.7	314.	5.2	290.	-4.6	2.4	-4.	4.9	1.4	+
12	18	1973	6	I	58.7	-19.3	26.5	30.	21.9	67.	13.5	313.	-9.9	9.2	-37.	-5.5	12.3	+
12	18	1973	6	J	52.6	-19.6	26.6	100.	9.4	149.	17.2	140.	11.1	-13.2	0.	17.2	.0	+
12	18	1973	6	K	45.2	-15.9	28.1	210.	22.5	223.	6.0	171.	1.4	-7.9	-13.	8.9	6.3	+
12	18	1973	6	M	65.7	1.2	25.9	280.	17.6	339.	22.3	238.	-18.9	-11.8	-58.	-3.9	22.0	+
12	19	1973	12	I	58.9	-19.8	27.6	30.	36.0	28.	8.5	201.	-3.1	-7.9	2.	-8.4	-1.0	+
12	20	1973	18	A	61.9	-33.3	24.7	130.	15.3	117.	15.2	143.	9.1	-12.1	13.	13.6	-6.7	+
12	20	1973	18	I	58.8	-18.8	24.4	40.	17.0	34.	7.7	53.	6.2	4.6	6.	7.3	-2.6	+
12	20	1973	18	J	52.4	-20.1	29.9	340.	20.1	310.	15.1	40.	11.3	10.0	30.	-2.2	-14.9	+
12	20	1973	18	M	65.7	1.4	22.8	50.	16.2	54.	4.8	35.	2.7	4.0	-4.	4.5	1.6	+
12	22	1973	0	M	65.6	.6	21.3	30.	8.1	50.	14.0	19.	4.4	13.2	-20.	11.9	7.3	+
12	23	1973	6	H	56.7	-51.1	22.0	190.	21.5	163.	10.2	264.	-10.1	-1.1	27.	-1.9	-10.0	+
12	23	1973	6	M	38.0	-71.0	21.5	290.	15.4	275.	7.7	321.	-4.9	6.0	15.	5.4	-5.6	C
12	23	1973	6	K	44.9	-15.9	21.4	320.	31.4	296.	14.7	80.	14.5	2.6	24.	-11.9	-8.7	D
12	23	1973	6	M	66.0	1.6	27.5	40.	14.8	41.	8.7	28.	5.4	6.8	-1.	8.7	.4	+
12	24	1973	12	H	78.0	-71.0	24.7	360.	21.0	344.	7.3	52.	5.8	4.5	16.	2.7	-6.8	+
12	25	1973	18	M	66.6	2.1	27.4	250.	24.8	203.	21.0	310.	-16.1	13.5	47.	-6.1	-20.0	A
12	27	1973	0	C	52.7	-35.5	22.9	240.	24.1	250.	4.3	139.	2.8	-3.2	-10.	-1.5	4.0	+
12	27	1973	0	I	56.9	-18.0	24.4	250.	29.2	239.	7.0	17.	2.1	6.7	11.	-5.2	-4.7	+
12	27	1973	0	M	65.8	2.6	20.7	130.	24.5	205.	10.5	82.	10.4	1.5	-25.	-5.7	8.7	+
12	28	1973	6	C	52.7	-35.5	25.9	330.	17.4	263.	18.9	12.	4.0	10.5	47.	.3	-18.9	+
12	28	1973	6	J	52.5	-19.9	28.2	220.	28.1	218.	1.0	363.	-8	.5	2.	.1	-1.0	+
12	29	1973	12	C	52.7	-35.5	25.1	290.	20.2	269.	9.6	339.	-3.4	8.9	21.	3.2	-9.0	+
12	29	1973	12	K	45.4	-14.7	26.0	200.	14.2	233.	16.1	171.	2.4	-15.9	-33.	7.6	14.2	+
12	30	1973	18	J	52.5	-19.7	22.3	180.	19.4	203.	8.8	120.	7.6	-4.4	-23.	1.1	8.7	+
1	1	1974	0	K	45.1	-16.1	23.6	180.	15.4	184.	8.3	173.	1.1	-8.2	-4.	8.1	1.6	+
1	2	1974	6	M	65.8	1.9	29.6	220.	21.1	204.	11.3	253.	-10.8	-3.3	17.	7.2	-8.7	+
1	3	1974	12	H	56.5	-50.0	23.0	30.	20.8	16.	16.3	116.	10.4	-7.7	44.	-3.5	-16.0	+
1	3	1974	12	H	38.0	-71.0	21.0	60.	16.2	45.	7.1	96.	7.1	-8	15.	4.5	-5.5	+
1	3	1974	12	I	59.0	-19.1	25.1	160.	6.0	211.	20.2	171.	3.1	-20.0	-31.	15.5	12.9	+

B13

REPRODUCIBILITY OF THE
ORIGINAL PAGE IS POOR

MONTH	DAY	YEAR	HOUR	SHIP	LAT	LONG	VWS	CHWS	VSYN	CHISYN	VF	CHIE	E:EW	E:NS	CW-CS	EPAR	ENORM	TYPE
1	3	1974	12	K	45.0	-16.5	27.5	240.	24.8	255.	7.3	179.	.1	-7.3	-15.	1.8	7.1	+
1	4	1974	18	I	58.9	-19.0	25.2	120.	17.8	167.	18.4	75.	17.8	4.7	-47.	-.6	18.4	+
1	4	1974	18	K	45.0	-16.2	26.6	220.	27.0	232.	5.6	132.	4.2	-3.8	-12.	-1.0	5.5	+
1	4	1974	18	M	64.8	2.2	21.4	170.	19.2	163.	3.3	215.	-1.9	-2.7	7.	2.0	-2.6	+
1	6	1974	0	J	52.5	-19.9	21.5	250.	21.1	233.	6.3	328.	-3.4	5.3	17.	-.5	-6.3	+
1	6	1974	0	K	44.9	-19.9	26.9	250.	28.9	237.	6.7	354.	-.7	6.7	13.	-3.1	-6.0	+
1	7	1974	6	H	38.0	-71.0	26.1	280.	14.0	269.	12.6	292.	-11.7	4.8	11.	11.6	-5.0	+
1	8	1974	12	B	54.7	-52.4	23.4	270.	22.7	267.	5.9	202.	-5.7	1.2	3.	5.7	-1.5	D
1	8	1974	12	K	45.0	-16.6	25.0	230.	26.7	240.	4.7	134.	3.4	-3.2	-10.	-1.3	4.5	D
1	9	1974	18	K	45.1	-15.8	26.2	220.	20.6	229.	6.7	191.	-1.3	-6.6	-9.	5.3	4.1	R
1	11	1974	0	H	56.5	-51.0	27.9	330.	29.4	297.	16.3	49.	12.2	10.0	33.	-6.0	-15.2	+
1	11	1974	0	H	38.0	-71.0	25.3	260.	19.7	237.	10.5	307.	-8.4	6.3	23.	3.6	-9.9	D
1	11	1974	0	M	65.9	1.9	28.1	130.	35.8	157.	16.7	27.	7.5	14.9	-27.	-10.8	12.8	+
1	12	1974	6	M	60.1	2.0	27.3	160.	30.8	130.	10.7	61.	9.3	5.1	-20.	-5.1	9.3	+
1	13	1974	12	H	38.0	-71.0	28.0	330.	23.7	333.	4.5	314.	-3.2	3.1	-3.	4.3	1.5	B
1	13	1974	12	J	52.0	-17.1	24.3	260.	30.7	267.	7.2	111.	6.7	-2.6	-7.	-6.6	3.0	+
1	14	1974	18	J	52.5	-19.9	25.8	260.	20.6	249.	6.8	205.	-6.2	2.9	11.	4.7	-4.9	+
1	14	1974	18	M	65.9	2.0	20.5	180.	15.1	161.	7.0	218.	-4.9	-6.2	19.	4.3	-6.7	+
1	16	1974	0	H	57.1	-51.0	28.2	110.	7.7	110.	21.1	110.	19.2	-7.2	0.	21.1	.0	+
1	16	1974	0	H	38.0	-71.0	26.5	250.	21.7	242.	5.9	281.	-5.7	1.1	8.	4.5	-3.7	+
1	16	1974	0	I	59.0	-18.6	25.3	240.	11.8	250.	13.8	231.	-10.0	-8.6	-10.	13.1	4.4	+
1	16	1974	0	M	66.0	1.9	24.3	280.	9.0	267.	15.4	256.	-14.9	-3.7	-7.	15.1	3.0	+
1	17	1974	6	H	38.0	-71.0	25.3	340.	17.4	305.	14.0	22.	5.6	13.8	35.	3.3	-14.3	+
1	17	1974	0	I	58.9	-19.1	29.6	230.	24.0	205.	12.8	282.	-12.5	2.7	25.	2.8	-12.5	+
1	17	1974	6	M	65.9	1.7	28.8	250.	21.2	244.	8.0	266.	-8.0	-.6	6.	7.4	-3.0	+
1	18	1974	12	B	54.6	-50.7	28.0	340.	32.5	343.	3.9	186.	-.4	-3.9	-3.	-3.6	1.5	+
1	19	1974	18	K	45.1	-15.9	26.8	170.	26.4	174.	5.8	8.	.9	5.8	-4.	-5.7	1.5	+
1	21	1974	0	B	56.1	-53.1	27.9	330.	28.1	310.	9.7	51.	7.6	6.1	20.	-1.9	-9.5	+
1	21	1974	0	H	38.0	-71.0	23.3	70.	9.2	72.	14.1	69.	13.1	5.1	-2.	14.1	.8	D
1	21	1974	0	K	45.3	-15.7	26.6	280.	8.0	270.	26.6	281.	-20.2	3.9	2.	20.6	-1.0	+
1	26	1974	0	M	66.0	2.4	22.9	220.	10.1	243.	9.4	171.	1.4	-9.3	-23.	3.0	6.9	+
1	27	1974	6	A	62.0	-31.0	29.1	220.	11.4	237.	16.5	210.	-9.1	-16.1	-17.	16.4	8.5	+
1	27	1974	6	H	38.0	-71.0	25.1	220.	15.9	204.	10.7	244.	-9.7	-4.7	16.	8.2	-6.9	+
1	27	1974	6	I	58.2	-13.7	20.5	220.	28.5	231.	9.2	76.	9.0	2.2	-11.	-8.4	3.9	+
1	27	1974	6	K	44.8	-15.9	20.6	190.	24.8	212.	10.0	121.	0.5	-5.2	-22.	-.1	10.0	D
1	27	1974	6	M	66.1	2.1	29.9	130.	14.5	157.	15.8	98.	15.7	-2.2	-27.	8.1	13.6	+
1	28	1974	12	A	62.1	-31.2	20.7	60.	8.9	93.	15.4	46.	11.0	10.7	-33.	10.5	11.3	+
1	28	1974	12	B	56.3	-49.9	27.1	320.	26.1	331.	5.2	247.	-4.8	-2.1	-11.	.5	5.2	+
1	31	1974	0	M	65.9	1.9	24.4	40.	15.6	127.	15.2	52.	11.9	9.4	-37.	3.9	14.7	+
2	1	1974	6	J	59.0	-18.6	25.2	340.	11.1	21.	10.3	317.	-12.6	13.3	41.	7.9	16.5	+
2	2	1974	12	A	61.9	-32.8	10.5	80.	14.2	48.	11.7	122.	9.6	-5.9	32.	3.2	-10.9	+
2	2	1974	12	B	56.0	-48.8	21.2	190.	31.4	107.	10.3	1.	.1	10.3	3.	-10.2	-1.1	+
2	2	1974	12	J	52.7	-19.0	20.7	290.	29.9	290.	9.8	135.	6.9	-7.0	-8.	-0.4	2.9	+

MONTH	DAY	YEAR	HOUR	SHIP	LAT	LONG	VMS CHIAS	VSYS CHISYN	VF CHIE	E:EW	E:NS	CH-CS	EPAR	ENORM	TYPE			
7	30	1973	0	C	52.7	-35.5	38.1	210.	17.7	219.	20.8	202.	-7.9	-19.2	-9.	19.9	6.0	+
8	6	1973	12	C	52.8	-35.6	39.6	290.	19.8	303.	20.8	278.	-20.6	2.8	-13.	18.8	8.9	D
8	22	1973	18	M	65.9	2.6	33.2	250.	23.6	260.	10.8	228.	-8.0	-7.3	-10.	9.1	5.8	+
8	30	1973	6	C	52.8	-35.1	38.3	200.	25.8	198.	12.5	204.	-5.1	-11.5	2.	12.5	-1.3	+
8	31	1973	12	C	52.0	-36.1	38.2	290.	27.8	280.	8.4	325.	-4.8	6.9	10.	5.9	-5.9	+
8	31	1973	12	J	52.7	-19.2	32.5	220.	28.3	235.	9.0	165.	2.3	-8.7	-15.	3.1	8.4	+
9	1	1973	18	I	58.8	-19.0	30.5	270.	32.0	270.	1.5	90.	1.5	.0	0.	-1.5	-7.0	+
9	16	1973	18	J	52.3	-20.1	36.8	260.	23.6	253.	13.7	272.	-13.7	.5	7.	12.9	-4.5	+
9	28	1973	0	J	52.6	-19.6	42.8	270.	22.7	278.	20.6	261.	-20.3	-3.2	-8.	19.7	6.0	+
9	30	1973	12	C	52.7	-35.3	33.0	170.	19.1	176.	14.1	162.	4.4	-13.4	-6.	13.7	3.4	D
10	4	1973	6	B	56.5	-51.0	46.6	280.	24.6	275.	22.2	286.	-21.4	5.9	5.	21.8	-4.1	+
10	9	1973	6	M	60.0	2.0	41.3	50.	44.5	35.	10.0	150.	5.5	-9.5	14.	-4.4	-10.0	+
10	11	1973	18	B	56.5	-51.0	34.2	50.	24.0	11.	24.7	88.	24.7	1.0	39.	5.7	-24.0	B
10	13	1973	0	K	41.9	-10.0	46.4	300.	25.3	283.	23.4	318.	-15.5	17.5	17.	19.1	-13.6	+
10	13	1973	12	J	52.4	-20.0	49.5	20.	25.1	34.	17.2	359.	-.2	17.2	-14.	14.2	9.8	+
10	15	1973	12	K	41.0	-16.1	35.2	380.	24.4	292.	12.4	256.	-12.0	-3.0	-12.	10.0	7.3	C
10	15	1973	0	B	55.7	-51.3	31.0	190.	20.2	217.	15.0	155.	6.8	-14.4	-27.	7.4	14.1	+
10	24	1973	6	I	59.1	-18.9	42.5	230.	32.7	220.	11.8	259.	-11.5	-2.3	10.	9.2	-7.4	+
10	25	1973	12	B	56.5	-51.0	40.7	320.	20.3	303.	17.3	346.	-4.1	16.9	17.	12.6	-11.9	+
10	25	1973	12	M	66.0	2.4	41.2	250.	23.4	263.	19.1	234.	-15.5	-11.2	-13.	16.7	9.3	+
10	29	1973	6	C	52.8	-35.5	30.4	220.	34.6	211.	6.6	345.	-1.7	6.4	9.	-4.6	-4.8	+
10	29	1973	6	I	58.9	-19.1	31.9	230.	39.5	223.	8.7	17.	2.5	8.4	7.	-7.8	-3.9	+
10	30	1973	12	A	61.1	-33.7	30.5	190.	30.4	211.	11.1	111.	10.4	-4.0	-21.	-1.9	10.9	+
11	3	1973	6	B	56.5	-51.0	31.6	110.	26.2	112.	5.5	100.	5.4	-1.0	-2.	5.4	1.1	+
11	3	1973	6	K	49.0	-16.0	31.0	203.	12.7	203.	18.3	198.	-5.6	-17.4	-3.	18.3	1.6	+
11	4	1973	12	B	56.5	-51.0	48.3	80.	22.8	112.	31.4	57.	26.4	16.9	-32.	18.2	25.6	+
11	5	1973	18	M	65.6	1.0	40.9	360.	25.1	351.	16.6	14.	3.9	16.1	9.	15.3	-6.4	+
11	7	1973	0	C	51.2	-37.5	31.0	259.	28.0	210.	20.4	312.	-15.1	13.6	40.	-4.3	-19.9	+
11	7	1973	0	I	59.1	-18.9	31.4	180.	32.4	210.	16.5	102.	16.2	-3.3	-30.	-5.2	15.7	+
11	8	1973	6	I	59.1	-18.9	37.4	250.	30.3	227.	15.2	301.	-13.0	7.9	23.	4.1	-14.6	+
11	8	1973	6	J	52.2	-20.6	30.2	210.	25.9	211.	4.3	204.	-1.8	-4.0	-1.	4.3	.5	+
11	8	1973	6	M	65.9	1.7	35.7	240.	10.6	178.	32.1	257.	-31.3	-7.3	62.	6.2	-31.5	+
11	12	1973	0	A	63.1	-31.0	23.0	270.	14.0	271.	19.0	269.	-19.0	-.2	-1.	19.0	.6	B
11	12	1973	0	B	56.5	-51.0	49.4	240.	28.0	266.	26.6	212.	-14.0	-22.7	-26.	15.5	21.7	+
11	12	1973	0	I	58.1	-15.8	33.2	250.	31.1	258.	5.0	189.	-.8	-4.9	-8.	1.8	4.6	+
11	13	1973	6	I	58.6	-18.1	36.3	270.	28.8	292.	14.4	222.	-9.6	-10.8	-22.	4.9	13.6	+
11	13	1973	6	M	65.9	2.2	31.8	360.	32.9	18.	10.2	273.	-10.2	.5	18.	-2.7	9.8	+
11	14	1973	12	I	59.1	-18.6	46.0	290.	24.7	287.	21.4	293.	-19.6	8.5	3.	21.2	-2.4	+
11	15	1973	18	I	59.1	-18.0	35.1	350.	20.6	2.	15.6	334.	-6.8	14.0	12.	13.7	7.3	+
11	22	1973	0	M	60.0	2.4	35.5	250.	19.6	222.	20.4	277.	-20.2	2.4	28.	11.7	-16.7	+
11	23	1973	6	V	65.9	2.2	30.2	310.	23.3	306.	7.1	323.	-4.3	5.7	4.	6.8	-2.1	+
11	25	1973	18	B	56.5	-51.0	37.2	100.	15.9	89.	21.8	108.	20.7	-6.7	11.	20.6	-7.1	+
12	2	1973	0	B	56.5	-51.0	36.8	220.	23.8	208.	14.4	240.	-12.5	-7.2	12.	12.2	-7.7	+
12	2	1973	0	V	65.5	1.9	30.6	230.	16.6	247.	15.5	212.	-8.2	-13.2	-17.	12.7	8.9	+
12	3	1973	6	V	65.6	2.7	37.0	270.	24.7	265.	12.6	280.	-12.4	2.2	5.	12.2	-3.2	+
12	4	1973	12	M	64.6	3.4	35.1	320.	33.2	327.	4.6	258.	-4.5	-1.0	-7.	1.6	4.3	B
12	5	1973	18	I	59.0	-18.9	37.7	310.	28.0	306.	10.0	321.	-6.2	7.8	4.	9.6	-2.6	+
12	7	1973	0	B	56.5	-51.0	30.4	180.	25.6	153.	13.9	237.	-11.6	-7.6	27.	1.5	-13.8	+
12	9	1973	12	M	66.3	2.1	42.4	190.	23.2	206.	21.1	172.	2.8	-20.9	-16.	17.6	11.7	+
12	10	1973	18	V	60.0	2.6	35.2	280.	27.0	257.	14.8	326.	-8.4	12.2	23.	5.4	-13.8	+

MONTH	DAY	YEAR	HOOR	SHIP	LAT	LONG	VWS	CHWS	VSYN	CHSYN	VF	CHIE	E:EW	E:NS	CW-CS	EPAR	ENORM	TYPE
12	12	1973	0	I	59.9	-19.3	40.4	200.	23.8	232.	23.2	168.	4.9	-23.3	-32.	10.5	21.4	+
12	12	1973	0	M	65.8	2.5	35.7	310.	22.6	317.	13.7	298.	-12.1	6.5	-7.	13.0	4.4	+
12	14	1973	12	H	56.5	-51.0	31.3	300.	21.6	265.	18.4	342.	-5.6	17.5	35.	4.0	-18.0	+
12	14	1973	12	M	65.7	2.0	36.3	10.	18.6	344.	20.1	29.	9.9	17.5	-21.	15.3	-13.0	+
12	15	1973	18	I	59.0	-19.7	40.8	300.	36.4	292.	6.9	347.	-1.6	6.8	8.	4.0	-5.7	+
12	18	1973	6	C	52.6	-35.3	42.6	330.	35.0	326.	0.1	348.	-1.7	7.9	4.	7.5	-3.0	B
12	19	1973	12	D	56.5	-51.0	30.1	170.	19.2	166.	11.0	177.	.6	-11.0	4.	10.8	-2.1	+
12	19	1973	12	J	52.8	-20.1	61.9	350.	42.4	1.	21.8	320.	-11.5	18.6	11.	18.4	11.8	+
12	19	1973	12	K	44.0	-16.1	51.7	240.	33.4	309.	28.8	17.	8.3	27.6	31.	10.9	-26.6	+
12	19	1973	12	M	65.6	2.0	46.4	310.	20.1	342.	31.2	290.	-29.3	10.7	-32.	19.2	24.6	+
12	20	1973	18	B	56.4	-51.0	46.6	250.	24.2	247.	16.6	254.	-15.9	-4.4	3.	16.3	-2.1	+
12	20	1973	18	H	38.0	-71.0	34.5	170.	20.8	131.	22.5	206.	-9.7	-20.3	39.	6.0	-21.7	C
12	20	1973	18	K	45.6	-17.0	46.0	350.	42.1	349.	4.0	1.	.0	4.0	1.	3.9	-.8	+
12	22	1973	0	H	38.0	-71.0	46.9	200.	21.0	212.	36.4	205.	-35.1	9.7	48.	10.4	-34.9	+
12	22	1973	0	J	52.3	-20.0	41.3	300.	25.7	293.	16.1	311.	-12.1	10.6	7.	15.3	-5.0	+
12	22	1973	0	K	44.9	-15.7	30.5	300.	29.4	265.	18.0	9.	2.9	17.8	35.	-4.4	-17.5	D
12	23	1973	6	I	59.4	-17.8	35.2	10.	22.7	10.	12.5	10.	2.2	12.3	0.	12.5	.0	+
12	23	1973	6	J	52.4	-19.9	35.8	330.	29.2	332.	6.7	321.	-4.2	5.2	-2.	6.6	1.2	+
12	24	1973	12	I	59.0	-18.5	30.4	190.	21.7	108.	8.7	195.	-2.3	-8.4	2.	8.7	-1.1	C
12	24	1973	12	K	44.8	-16.0	38.3	340.	34.0	359.	12.7	279.	-12.5	2.0	-19.	2.2	12.5	D
12	28	1973	6	D	56.5	-51.1	36.0	290.	26.2	295.	10.2	277.	-10.1	1.2	-5.	9.7	3.1	+
12	23	1973	6	I	59.2	-18.1	39.6	203.	24.2	193.	15.9	211.	-8.1	-13.6	7.	15.1	-4.8	+
12	28	1973	6	M	65.8	3.7	42.1	270.	33.7	278.	9.4	242.	-8.7	-4.7	-8.	8.0	5.9	+
12	29	1973	12	J	52.5	-20.0	35.3	270.	24.7	286.	13.8	241.	-12.1	-6.8	-16.	9.7	9.9	D
12	30	1973	18	C	51.8	-36.3	31.4	280.	26.2	284.	9.5	329.	-4.9	8.2	16.	4.0	-8.7	+
12	30	1973	18	M	65.9	3.0	35.2	230.	20.4	260.	20.3	200.	-6.9	-19.1	-30.	10.1	17.6	C
1	1	1974	0	E	56.5	-50.7	37.0	70.	7.5	29.	31.7	79.	31.1	6.1	41.	20.4	-24.3	+
1	1	1974	0	I	59.0	-15.0	36.7	190.	29.0	201.	9.9	156.	4.0	-9.1	-11.	7.0	7.0	+
1	2	1974	6	K	45.1	-16.1	34.1	190.	24.2	230.	22.0	145.	12.6	-18.0	-40.	1.9	21.9	+
1	4	1974	18	J	52.5	-20.0	31.3	220.	23.2	232.	9.9	191.	-1.8	-9.7	-12.	7.4	6.5	+
1	6	1974	0	D	56.4	-50.3	33.7	290.	18.8	335.	24.4	257.	-23.7	-5.5	-45.	5.0	23.8	+
1	6	1974	0	M	65.7	1.9	36.7	160.	25.1	157.	11.7	166.	2.7	-11.4	3.	11.5	-1.9	+
1	7	1974	6	H	56.6	-51.0	33.5	200.	26.3	287.	8.1	257.	-7.2	-1.9	-7.	7.0	4.1	+
1	7	1974	6	I	59.0	-19.2	30.3	180.	8.2	200.	22.8	173.	2.8	-22.6	-20.	20.3	10.4	+
1	7	1974	6	J	52.4	-19.3	32.3	270.	28.5	241.	15.7	332.	-7.4	13.8	29.	-.2	-15.7	+
1	7	1974	6	K	45.0	-16.4	45.9	260.	22.7	260.	23.2	260.	-22.8	-4.0	0.	23.2	.0	+
1	8	1974	12	H	33.0	-71.0	34.3	310.	20.6	306.	13.8	316.	-9.6	9.9	4.	13.6	-2.4	D
1	8	1974	12	J	52.6	-19.6	35.7	250.	37.4	269.	12.2	162.	3.2	-11.6	-19.	-3.6	11.6	+
1	9	1974	18	J	52.5	-19.7	33.0	160.	19.4	190.	18.0	129.	14.7	-11.9	-30.	9.2	16.5	+
1	11	1974	0	J	52.2	-20.4	44.9	260.	32.8	254.	12.7	276.	-12.7	1.2	6.	11.9	-4.7	+
1	11	1974	6	K	44.7	-16.7	42.5	200.	31.6	240.	16.4	300.	-14.5	8.4	20.	8.3	-14.5	+
1	12	1974	6	K	44.8	-16.2	30.1	220.	23.6	244.	12.8	172.	1.9	-12.7	-24.	3.9	12.2	+
1	13	1974	12	B	56.5	-51.9	30.2	280.	22.3	295.	10.4	246.	-9.5	-4.2	-15.	6.9	7.8	+
1	13	1974	12	M	66.4	2.0	34.3	203.	35.2	207.	4.3	102.	4.2	-.9	-7.	-1.2	4.2	+
1	14	1974	18	H	56.4	-49.8	54.4	310.	42.0	310.	12.4	310.	-9.5	8.0	0.	12.4	.0	C
1	14	1974	18	K	45.0	-15.9	31.8	220.	27.1	220.	4.7	220.	-3.0	-3.6	0.	4.7	.0	D
1	16	1974	0	J	52.6	-19.7	36.8	30.	11.8	267.	40.3	43.	30.2	32.5	-123.	-31.8	-30.9	+
1	16	1974	0	K	44.9	-16.1	45.8	200.	36.3	252.	11.1	287.	-10.6	3.3	8.	9.1	-6.4	D
1	17	1974	6	J	52.2	-20.3	32.3	230.	34.5	225.	4.9	267.	-4.9	-.2	5.	3.7	-3.3	+
1	19	1974	18	D	56.1	-51.6	35.0	310.	23.3	309.	11.7	312.	-8.7	7.8	1.	11.7	-.6	+

MONTH	DAY	YEAR	HOUR	SHIP	LAT	LONG	VWS	CHWS	VSYN	CHSYN	VF	CHIE	E:EW	E:NS	CW-CS	EPAR	ENORM	TYPE
1	19	1974	18	H	38.0	-71.0	39.7	250.	17.3	245.	22.5	254.	-21.6	-6.3	5.	22.2	-3.5	+
1	19	1974	18	I	59.0	-19.2	43.8	180.	40.8	194.	10.7	113.	9.9	-4.2	-14.	1.7	10.6	+
1	19	1974	18	J	52.3	-19.9	43.5	180.	38.8	191.	9.2	126.	7.4	-5.4	-11.	3.9	8.3	+
1	21	1974	0	M	66.0	2.2	35.7	210.	27.3	222.	10.6	178.	5.4	-10.6	-12.	7.6	7.4	0
1	22	1974	6	I	58.7	-18.1	30.2	170.	19.8	153.	12.7	197.	-3.7	-12.1	17.	9.1	-8.8	+
1	22	1974	6	K	46.1	-13.3	32.3	210.	25.2	208.	7.2	217.	-0.3	-5.7	2.	7.1	-1.1	0
1	23	1974	12	H	56.4	-52.4	33.0	10.	25.8	243.	15.4	59.	13.3	7.8	-27.	3.6	-15.0	+
1	23	1974	12	J	52.6	-20.2	30.4	280.	31.1	278.	1.3	42.	.9	1.0	2.	-7	-1.1	+
1	23	1974	12	M	66.0	2.0	31.0	150.	18.1	168.	14.9	128.	11.7	-9.1	-18.	11.4	9.6	+
1	24	1974	15	I	59.7	-17.1	41.5	200.	26.4	221.	19.3	171.	3.1	-19.1	-21.	12.3	14.9	+
1	24	1974	18	J	53.1	-17.4	33.2	210.	25.9	228.	11.7	167.	2.6	-11.4	-18.	5.7	10.3	+
1	27	1974	6	H	57.0	-52.2	41.3	310.	37.9	300.	7.7	9.	1.2	7.6	10.	2.8	-7.2	+
1	28	1974	12	K	45.1	-16.1	33.9	310.	30.2	258.	28.3	7.	3.6	28.1	52.	-9.3	-26.7	0
1	31	1974	0	I	59.9	-18.3	40.7	230.	6.4	278.	32.3	281.	-31.8	5.9	2.	32.3	-1.4	+
1	31	1974	0	K	45.3	-15.6	38.4	200.	34.3	217.	11.5	139.	7.5	-8.7	-17.	2.4	11.2	+
2	1	1974	6	H	38.0	-71.0	35.0	290.	24.8	284.	10.7	304.	-8.8	6.0	6.	10.0	-3.7	+
2	1	1974	6	J	52.7	-19.7	32.9	240.	22.2	336.	10.9	348.	-2.2	10.6	4.	10.6	-2.3	+
2	1	1974	6	K	45.2	-16.5	42.8	300.	40.8	270.	21.7	10.	3.7	21.4	30.	-3.7	-21.4	+

APPENDIX D

FORTRAN COMPUTER PROGRAMS

D.1 BRIEF DESCRIPTION OF THE FUNCTION OF EACH PROGRAM

D.1.1 Programs To Create or Modify Skylab Oceanographic Data Files

MERGE	Creates Skylab Oceanographic Data Files. Uses subroutine AAFEAC.
DIVIDE	Creates two Skylab Oceanographic Data Files, one of scans to the left and another of scans to the right, from one Skylab Oceanographic Data File whose data were taken in the CTNC Left/Right mode.
APPEND	Used to add components to the data vectors of Skylab Oceanographic Data Files.
SKEW	Creates from an ITNC Skylab Oceanographic Data File another Skylab Oceanographic Data File which has the data vectors together which contain measurements from one cluster of surface cells. The data vectors of the new file are arranged by surface-cell cluster rather than by scan.

D.1.2 Program To List Data From Skylab Oceanographic Data Files

Program List (LST)	Lists components of any function of the components of data vectors from Skylab Oceanographic Data Files. Uses Subroutine LIST
--------------------	--

D.1.3 Program To Create Skylab Oceanographic Temporary Data Files

Program TRNGEN	Creates a Skylab Oceanographic <u>Temporary Data File</u> (usually on disc) from a Skylab Oceanographic Data File (usually on tape). Uses Program Directive Interpreter
----------------	--

D.1.4 Programs To Analyze and Display Data From Skylab Oceanographic Temporary Data Files

For CTC data:

Program IMAGE

Produces images having 13 shades of gray by overprinting on the line printer (See Figure 5.1 for an example). The image may be of any component of the data vectors on the Skylab Oceanographic Temporary Data Files. The Program will also produce a histogram of the component imaged.

Uses Subroutine PITCHR and Subroutine DF (density function calculator).

For noncontiguous data:

Program SCATTERGRAM

Produces scattergrams of pairs of components from Skylab Oceanographic Temporary Data Files. Symbols for the scattergrams can also be stored in the data vectors.

Uses Subroutine SCAT.

Program REGRESS

Supervises linear regression of any components of the data vectors. REGRESS prepares the data files and command files for the UCLA Biomed program BMDO2R. The REGRESS activity must be followed by a BMDO2R activity.

Program Standard Deviation

Calculates the standard deviation of any component of the data vectors.

Uses Subroutine STDV and Subroutine FREEFORM.

Program Autocorrelation Function

Calculates the autocorrelation function of any component of the data vectors. The standard deviation program should be run first because this program requires an estimate of the standard deviation a priori.

Uses Subroutine AUTCOR and Subroutine FREEFORM

Program Maximum Likelihood Estimator

Used to find simultaneously the maximum likelihood estimates of linear regression coefficients and error covariance matrix.

Uses Subroutine FUNC1.

D.1.5 Subroutines Used To Remove Effects Other Than Wind Speed From Backscatter Measurements

Subroutine INCANG	Estimates the effects of incident angle variation on backscatter measurements.
Subroutine ASPCOR	Estimates the effects of aspect angle variation on backscatter measurements.
Subroutine ATM50	Estimates the attenuation at 50° incident angle.

D.1.6 Subroutines Used To Remove Effects Other Than Wind Speed From Radiometric Measurements

Subroutine ATM50	Removes effects of sea water temperature variations and excess temperature variations to estimate horizontal emissivity.
Subroutine TRANSREF	Removes effects of incident angle variations at all nominal incident angles and removes effects of sea water temperature variations and excess temperature variations at nominal incident angles other than 50°.

These subroutines use:

- Subroutine EPS
- Subroutine HEXCESS
- Subroutine TATM
- Subroutine ATTENV
- Subroutine FRESNEL

D.1.7 Other Utility Subroutines

Subroutine CATGOR	Assigns a category designation to each data vector.
Subroutine FFT	Calculates the Fast-Fourier Transform.

D.2 PROGRAM LISTINGS

The programs are listed in the following order (the order in which they are described in the previous section):

	<u>Routine</u>	<u>Programmer</u>	<u>Page</u>
Program	Merge	Young	206
Subroutine	AAFEAC	Young	212
Program	Divide	Sullivan	213
Program	Append	Sullivan	217
Program	Skew	Liang	223
Program	LST	Young	226
Subroutine	LIST	Young	229
Program	TRNGEN	Kahn	230
Program	Directive Interpreter	Kahn	242
Program	Image	Crooks	250
Subroutine	D ²		255
Program	Scattergram	Kahn	258
Subroutine	SCAT	Kahn	270
Program	Regress	Birrer	281
Program	Standard Deviation	Birrer	287
Subroutine	STDV	Birrer	290
Subroutine	FREEFORM	Birrer	292
Program	Autocorrelation Function	Birrer	294
Subroutine	AUTCOR	Birrer	297
Program	Maximum Likelihood Estimator		300
Subroutine	FUNC1	Birrer	306
Subroutine	INCANG	Hiang	311
Subroutine	ASPCOR	Hiang	312
Subroutine	ATM50	Komen	313
Subroutine	TRANSREF	Komen	315
Subroutine	EPS	Komen	316
Subroutine	HEXCESS	Komen	316
Subroutine	TATM	Komen	316
Subroutine	ATTENV	Komen	317
Subroutine	FRESNEL	Komen	317
Subroutine	CATGOR	Birrer	318
Subroutine	FFT	Young	319

CMERG

PROGRAM MERGE

DATE 5/30/74

PURPOSE TO READ JSC RADSCAT DATA CARDS (OR TAPE IF CONTIGUOUS DATA) PRODUCED BY DCOM AND CUNY SURFACE TRUTH CARDS AND TO WRITE STANDARD DATA VECTORS ON TAPE (FILE CODE 01). THE PROGRAM ALSO CALCULATES ASPECT ANGLE AND AN ASPECT-ANGLE CORRECTION.

DATA CARDS

- A) 1 CARD--- 15
NUMBER OF FILES TO BE SKIPPED ON OUTPUT TAPE
 - B) 1 CARD FOR EACH DATA SEGMENT --- 212
FILE CODE OF JSC DATA, FILE CODE OF CUNY DATA
(A FILE CODE OF ZERO FOR THE CUNY DATA DENOTES THAT NO SURFACE TRUTH IS AVAILABLE, SO ALL SURFACE TRUTH VALUES WILL BE SET TO DEFAULT)
 - C) 1 CARD FOR EACH DATA SEGMENT --- 412,14,10A6,412
HEADER RECORD INFORMATION AS FOLLOWS -
MODE, MONTH, DAY, AND YEAR OF PASS, NUMBER OF DATA RECORDS, TITLE, MONTH, DAY, YEAR OF CUNY DATA, IFMT
 - IFMT = 0 IF SURFACE TRUTH IS IN KU FORMAT, (13,11,12;
11,F2.0,F3.0,312,F4,1) WITH VARIABLES DOV,
SEQ,SCAN,CON,WSPD,WDIR,MO,DA,YR,SEATHP (DATE
OF SURFACE TRUTH)
 - = 1 IF SURFACE TRUTH IS IN CUNY FORMAT AND ONLY
WIND SPEED AND DIRECTION ARE TO BE INCLUDED IN
DATA VECTOR
 - = 2 IF SURFACE TRUTH IS IN CUNY FORMAT AND ALL
CUNY DATA IS TO BE INCLUDED IN DATA VECTOR

(SEE SEPARATE WRITE-UP FOR DESCRIPTION OF CUNY
FORMAT)
 - D) 1 BLANK CARD
SIGNALS END OF PROCESSING
- NOTE ••
CARDS B) AND C) SHOULD BE REPEATED ONCE FOR EACH
DATA SEGMENT

ORIGINAL PAGE IS
OF POOR QUALITY

2 ITNC
3 CTNC-L
4 CTNC-R
5 CTNC-L/R

OTHER INPUT DATA

JSC AND CUNY DATA ON FILES SPECIFIED BY DATA CARDS
ABOVE

OUTPUT

OCEANOGRAPHIC DATA FILES TO FILE CODE 1

LIST OF NUMBER OF DATA RECORDS WRITTEN TO FILE CODE 1
AND NUMBER OF RECORDS INDICATED IN HEADER RECORD

```

      INTEGER DOY
      DIMENSION IDATJS(3),IDATCU(3),IDATPS(3),ITITLE(10),SIG(4),THETA(3)
1     ,T(2),A(3),IDAT(3),X(18),IX(18),B(31),Y(31),IY(31)
      DATA A/3*.0377777777777/.B/31*.0377777777777/.C/0377777777777/
      EQUIVALENCE (A(1),II),(X,IX)Z(X(1),DOY),(X(2),NSEG),(Y,IY)

```

CHANGE TODAY'S DATE FROM BCD TO INTEGER

```
CALL CLOCCK1(IDAT(2),IDAT(1),IDAT(3))
DO 14 I=1:3
  IDAT(I)=IDAT(I)/64**4
  ID1=IDAT(I)/64
  ID2=IDAT(I)-ID1*64
14 IDAT(I)=ID1*10*ID2
```

READ NUMBER OF FILES TO BE SKIPPED ON
OUTPUT TAPE

```

      READ (5,107) NSKIP
107  FORMAT(I5)

```

ECHO DATA CARDS

```
WRITE(6,108) NSKIP
108 FORMAT(///' ECHO INPUT DATA CARDS',///I6)
```

```

C      SKIP NSKIP FILES
C
C      IF (NSKIP.EQ.0) GO TO 4
C      DO 7 I=1,NSKIP
C      8 READ (1,END=7)
C      GO TO 8
C      7 CALL FCLOSE(1)

C      READ FILE NUMBERS FOR JSC AND CUNY DATA
C
C      4 READ(5,100,END=30) IJSC,ICUNY
C      100 FORMAT(2I2)
C      WRITE(6,109) IJSC,ICUNY
C      109 FORMAT(1X,2I2)
C      IF(IJSC.EQ.0) STOP

C      REWIND FILE IJSC IF WE ARE TO USE IT
C      AGAIN
C
C      IF(IJSC.EQ.LASTJ) REWIND(IJSC)
C      IF(IJSC.NE.LASTJ.AND.LASTJ.NE.0) CALL FCLOSE(LASTJ)
C      LASTJ=IJSC

C      READ HEADER INFO FOR THIS FILE
C
C      READ(5,102)MODE,IDATPS,NUMREC,ITITLE,IDATCU,IFMT
C      102 FORMAT(4I2,I4,10A6,4I2)
C      WRITE(6,113) MODE,IDATPS,NUMREC,ITITLE,IDATCU,IFMT
C      113 FORMAT(1X,I2,I2,I4,10A6,4I2)
C      NWORDS=19
C      IF(IFMT.EQ.2) NWORDS=50
C      NITC=0
C      IF(MODE,GE,2.AND.MODE,LE,5) GO TO 20

C      CONTIGUOUS MODE, JSC DATA ON TAPE
C
C      ASSIGN 21 TO JGO
C      GO TO 23

C      NONCONTIGUOUS MODE, JSC DATA ON CARDS
C
C      20 ASSIGN 22 TO JGO
C
C      23 IF(ICUNY.EQ.0) GO TO 17

C      SURFACE TRUTH IS AVAILABLE
C
C      SET SWITCHES TO READ SURFACE TRUTH
C      WITH RIGHT FORMAT
C
C      IF(IFMT.NE.0) GO TO 40
C      ASSIGN 31 TO KGO

```

ORIGINAL PAGE IS
OF POOR QUALITY


```

      GO TO 41
40 IF(IFMT.NE.1.AND. IFMT.NE.2) GO TO 42
   ASSIGN 32 TO MGO
   GO TO 41
42 WRITE(6,110) IFMT
110 FORMAT(' IFMT=',I8,' WHICH IS ILLEGAL')
   STOP

```

C
C
C

SET SWITCH TO ADD DESIRED NUMBER OF
COMPONENTS TO DATA VECTOR

```

41 IF(IFMT.EQ.0.OR. IFMT.EQ.1) GO TO 36
   ASSIGN 34 TO LGO
   ASSIGN 38 TO MGO
   GO TO 39
36 ASSIGN 33 TO LGO
   ASSIGN 37 TO MGO

```

C
C
C

READ FIRST SURFACE TRUTH CARD

```

39 IF(IFMT.EQ.0) GO TO 35
   READ(ICUNY,112,END=105) IDOY,ISEG,ISCAN,ICOM,V,WNDANG,(Y(I),I=1,4)
   ,SEATMP,Y(7),IDATCU(3),(IDATCU(I),I=1,2),(Y(I),I=5,31)
112 FORMAT(I3,I1,I2,I1,28X,F3,1,F3,0,2F5,2,2(F3,1,F3,0),F4,1,4X,A1,2X,
   1 312,78X,8(F3,1,F3,0,1))
   GO TO 44
35 READ(ICUNY,103) IDOY,ISEG,ISCAN,ICOM,V,WNDANG,IDATCU,SEATMP
103 FORMAT(I3,I1,I2,I1,F2,0,F3,0,3I2,F1,1)
44 ISRL=((ICOM*10000+ISCAN)*10+ISEG)*1000+IDOY
   ASSIGN 6 TO IGO
   GO TO 18

```

C
C
C

NO SURFACE TRUTH

```

17 DO 19 I=173
19 IDATCU(I)=11
   ASSIGN 2 TO IGO
   ASSIGN 33 TO LGO

```

C
C
C

READ EACH JSC CARD

```

18 IREC=0
   GO TO JGO,(21,22)

```

C
C
C

READ JSC DATA FROM CARDS

```

22 READ(IJSC,101,END=5) DOY,NSEG,NSCAN,NCOM,NTIME,XLAT,XLONG,AZIM;
   THETA,SIG,T,DESCR,IDATJS
101 FORMAT(I3,I1,I2,I1,I8,F5,2,F6,2,F4,1,3F4,2,6F5,2,4I2)

```

C
C
C

CHANGE ALL DEFAULT VALUES TO
037777777777

```

C
  IF (SEATMP.EQ.0.) SEATMP=A(1)
  IF ( NTIME.EQ.99999900) NTIME=11
  IF ( XLAT.EQ.999.) XLAT=A(1)
  IF (XLONG.EQ.999.) XLONG=A(1)
  IF (AZIM.EQ.999.) AZIM=A(1)
  DO 11 I=1,3
11 IF (THETA(I).EQ.99.) THETA(I)=A(1)
  DO 12 I=1,4
12 IF (SIG(I).EQ.99.) SIG(I)=A(1)
  DO 13 I=1,2
13 IF (T(I).EQ.0.) T(I)=A(1)
  NSRL=((NCOM*10000+NSCAN)*10+NSEG)*1000+DOY
  GO TO 24

      READ JSC DATA FROM TAPE

21 READ(IJSC,END=5) IX
  DO 25 I=8,18
  IF (IX(I).NE.11) X(I)=FLOAT(IX(I))/1000,-200.
25 CONTINUE
  NSRL=((IX(5)*10+IX(4))*1000+IX(3)*10+IX(2))*1000+IX(1)
  IF (IX(6).NE.11) GO TO 26
  NTIME=11
  GO TO 27
26 NTIME=IFIX(X(8)*100.+0.5)*10000+((X(7)*100+X(6)))
27 XLAT=X(9)
  XLONG=X(10)
  AZIM=X(11)
  THETA(1)=X(12)
  DO 28 I=1,4
28 SIG(I)=X(I+12)
  DO 29 I=1,2
29 T(I)=X(I+16)

      COUNT THE NUMBER OF JSC RECORDS

24 IREC=IREC+1

      WRITE HEADER RECORD FIRST TIME THROUGH
  IF (IREC.EQ.1) WRITE(1) DOY,NSEG,MODE,NWORDS,NUMREC,1DATPS,1DATJS,
1 1DATCU,1DAT,ITITLE
  GO TO 1GO, (6,2)

      IF CUNY DATA IS MISSING WRITE RECORD WITH
      DEFAULT SURFACE TRUTH VALUES

6 IF (NSCAN*10+NCOM.LT.ISCAN*10+ICOM) GO TO 2

      IF JSC DATA IS MISSING SOMETHING IS WRONG
      STOP

```

ORIGINAL PAGE IS
OF POOR QUALITY

SUBROUTINE AAFEAC(RADANG,WNDANG,ASPANG,ASPCOR)

INPUT

RADANG INSTRUMENT ANGLE W.R.T. NORTH

WNDANG WIND ANGLE W.R.T. NORTH

OUTPUT

ASPANG ASPECT ANGLE, ANGLE OF WIND W.R.T. THE INSTRUMENT

ASPCOR ASPECT-ANGLE SCATTERING-COEFFICIENT CORRECTION

ASPANG=WNDANG-RADANG
 IF(ASPANG.GT.-180.) GO TO 3
 ASPANG=ASPANG+360,
 GO TO 2
 3 IF(ASPANG.LE.180.) GO TO 2
 ASPANG=ASPANG-360,
 2 ANGLE=ASPANG/57.296
 ASPCOR= 2.745-1.056* \cos (ANGLE)-2.228* \cos (2.*ANGLE)*0.539* \cos (4.*
 ANGLE)
 1 RETURN
 END

ORIGINAL PAGE IS
 OF POOR QUALITY

CDIVIDE

THIS PROGRAM TAKES AN INPUT FROM FILECODE 01
AND PRODUCES A MODIFIED TAPE ON FILECODE 07

WRITTEN BY M.L.SULLIVANT

THERE IS ONLY ONE SUPPORT SUBROUTINE, "LABLSS",
WHICH LISTS THE CONTENTS OF A LABEL ONTO FILECODE 6.

THE COMMANDS ARE READ FROM FILECODE 05.
THE THREE COMMANDS ARE "SKIP", "COPY", AND "DIVIDE",

THE COMMAND SHOULD BE IN COL. 1-6 LEFT-JUSTIFIED.
THE NUMBER OF FILES TO SKIP OR COPY SHOULD BE IN
COL. 8-9, RIGHT-JUSTIFIED. IF THE NUMBER IS BLANK,
ZERO, OR NEGATIVE, THEN ONE FILE IS ASSUMED.

THE COMMAND "DIVIDE" CAUSES THE FILE ON 01 TO BE SPLIT
INTO TWO FILES: IF THE MODE OF THE INPUT FILE IS 5,
IF THE MODE IS 5 THEN THE OPTION FIELD (COL 8-13)
IS EXAMINED TO SEE IF THE FILE SHOULD BE PROCESSED WITH
THE RIGHT SCAN RECORDS OR THE LEFT SCAN RECORDS FIRST,
IF THE FIELD IS BLANK THEN LEFT IS ASSUMED.
IF "RIGHT " OR "LEFT " OR " " IS NOT THERE THEN
AN ERROR OCCURS,
IF THE MODE IS NOT 5 THEN AN ERROR OCCURS,

FOR EXAMPLE, SUPPOSE YOU HAVE A TAPE WITH THE THIRD FILE
BEING MODE 5. ALSO, THE FIRST FILE SHOULD BE SKIPPED AND
THE SECOND FILE SHOULD BE COPIED WITH NO CHANGES,
THE THIRD FILE HAS LEFT RECORDS FIRST.

\$	IDENT	PROJECT-NUM,NAME-OF-USER
\$	OPTION	FORTRAN
\$	OBJECT	
\$	<OBJECT DECK>	
\$	ENDECK	
\$	EXECUTE	,11K
\$	TAPE	01,X1DD,,99999,,INPUT-TAPE
\$	TAPE	07,X2DD,,99999,,OUTPUT-TAPE,OUT
\$	FILE	11,A1RR,5L
\$	SKIP	01
\$	COPY	01
\$	DIVIDE	LEFT
\$	ENDJOB	

C	CHARACTER CARD=80,VERB=6	540
	INTEGER LABEL(27),IDATA(150)	550
	INTEGER OLDSIZE	560
	EQUIVALENCE (CAPD,VERB),(LABEL(4),NUMWPR),	570
	& (LABEL(5),NUMWIF),(MODE,LABEL(3))	580
	DATA ISIDE,ILEFT,IRIGHT/' SIDE'),' (LEFT','(RIGHT/'	590
C	100 READ(5,1,END=950) CARD	600
	WRITE(6,2) CARD	610
C		620
C	IS IT A VALID VERB,	630
C		640
	IF (VERB.EQ."SKIP ") GO TO 200	650
	IF (VERB.EQ."COPY ") GO TO 300	660
	IF (VERB.EQ."DIVIDE") GO TO 400	670
C		680
C	NOT IN LIST,	690
	WRITE(6,3)	700
	GO TO 900	710
C		720
C	PROCESS "SKIP" HERE.	730
C		740
	200 DECODE(CARD,4) NUMBER	750
	IF (NUMBER.LT.1) NUMBER = 1	760
	KOUNT = 0	770
	205 READ(1) LABEL	780
	CALL LABLSS(LABEL(1))	790
	KREC = 0	800
	210 READ(1,END=220)	810
	KREC = KREC + 1	820
	GO TO 210	830
	220 CALL FCLOSE(1)	840
	WRITE(6,12) KREC	850
	KOUNT = KOUNT + 1	860
	IF (KOUNT.LT.NUMBER) GO TO 205	870
	WRITE(6,5) KOUNT	880
	GO TO 100	890
C		900
C	PROCESS "COPY" HERE,	910
C		920
	300 DECODE(CARD,4) NUMBER	930
	IF (NUMBER.LT.1) NUMBER = 1	940
	KOUNT = 0	950
	310 READ(1) LABEL	960
	CALL LABLSS(LABEL(1))	970
	KREC = 0	980
	WRITE(7) LABEL	990
	320 READ(1,END=330) (IDATA(I),I=1,NUMWPR)	1000
	KREC = KREC + 1	1010
	WRITE(7) (IDATA(I),I=1,NUMWPR)	1020
		1030
		1040

ORIGINAL PAGE IS
OF POOR QUALITY

	GO TO 320	1050
330	CALL FCLOSE(1)	1060
	WRITE(6,12) KREC	1070
	CALL FCLOSE(7)	1080
	KOUNT = KOUNT + 1	1090
	IF (KOUNT.LT.NUMBER) GO TO 310	1100
	WRITE(6,6)KOUNT	1110
	GO TO 100	1120
C		1130
C	PROCESS "DIVIDE" HERE,	1140
C		1150
400	READ(1) LABEL	1160
	IF (MODE.NE.5) GO TO 480	1170
	NUM2 = NUMWIF/10*5	1180
	NUM1 = NUMWIF-NUM2	1190
	KREC = 0	1200
C		1210
	DECODE(CARD,8) VERB	1220
	IF (VERB.EQ."RIGHT ") GO TO 406	1230
	IF (VERB.EQ."LEFT ") GO TO 404	1240
	IF (VERB.EQ." " " " GO TO 404	1250
C		1260
C	ERR:	1270
C		1280
	WRITE(6,9)	1290
	GO TO 900	1300
C	LEFT SIDE IS FIRST,	1310
404	MODE=-3	1320
	NUMWIF=NUM1	1330
	LABEL(26)=ILEFT	
	LABEL(27)=ISIDE	
	WRITE(7) LABEL	1340
	CALL LABLSS(LABEL(1))	1350
	NUMWIF=NUM2	1360
	MODE=-4	1370
	LABEL(26)=IRIGHT	
	LABEL(27)=ISIDE	
	WRITE(11) LABEL	1380
	GO TO 410	1390
C	RIGHT SIDE IS FIRST,	1400
406	MODE=-3	1410
	NUMWIF=NUM2	1420
	LABEL(26)=ILEFT	
	LABEL(27)=ISIDE	
	CALL LABLSS(LABEL(1))	1430
	WRITE(7) LABEL	1440
	MODE=-4	1450
	NUMWIF=NUM1	1460
	LABEL(26)=IRIGHT	
	LABEL(27)=ISIDE	
	WRITE(11) LABEL	1470
	GO TO 420	1480

C	LEFT SIDE.	1490
410	DO 420 J=1,5	1500
	READ(1,END=450) (IDATA(I),I=1,NUMWPR)	1510
	KREC = KREC + 1	1520
	WRITE(7) (IDATA(I),I=1,NUMWPR)	1530
420	CONTINUE	1540
C	RIGHT SIDE,	1550
430	DO 440 J=1,5	1560
	READ(1,END=450) (IDATA(I),I=1,NUMWPR)	1570
	WRITE(11) (IDATA(I),I=1,NUMWPR)	1580
440	CONTINUE	1590
C	GO TO 410	1600
C		1610
450	CALL FCLOSE(1)	1620
	WRITE(6,12) KREC	1630
	CALL FCLOSE(7)	1640
	CALL FCLOSE(11)	1650
	REWIND 11	1660
	READ(11) LABEL	1670
	CALL LABLSS(LABEL(1))	1680
	WRITE(7) LABEL	1690
	KREC = 0	1700
C		1710
460	READ(11,END=470) (IDATA(I),I=1,NUMWPR)	1720
	KREC = KREC + 1	1730
	WRITE(7) (IDATA(I),I=1,NUMWPR)	1740
	GO TO 460	1750
470	CALL FCLOSE(7)	1760
	WRITE(6,12) KREC	1770
	CALL FCLOSE(11)	1780
	REWIND 11	1790
	GO TO 100	1800
C		1810
480	CALL LABLSS(LABEL)	1820
	WRITE(6,10)	1830
C		1840
900	WRITE(6,11)	1850
950	STOP	1860
1	FORMAT(A80)	1870
2	FORMAT(1H0,"DIRECTIVE = ".A80)	1880
3	FORMAT(1H0,"UNKNOWN DIRECTIVE")	1890
4	FORMAT(7X,12)	1900
5	FORMAT(1H0,12," FILES WERE SKIPPED")	1910
6	FORMAT(1H0,12," FILES WERE COPIED")	1920
8	FORMAT(7X,A6)	1930
9	FORMAT(1H0,"OPTION ON DIVIDE IS NOT RIGHT OR LEFT")	1940
10	FORMAT(1H0,"MODE NOT 5")	1950
11	FORMAT(1H0,"PROGRAM TERMINATED ABNORMALLY")	1960
12	FORMAT(1X,10X,"ACTUAL RECORD COUNT =",I5)	1970
	END	1980

ORIGINAL PAGE IS
OF POOR QUALITY

CAPPEND

THIS PROGRAM TAKES AN INPUT FILE FROM FILECODE 01,
AND PRODUCES A MODIFIED FILE ON FILECODE 07.
THE MODIFIED FILE CONSISTS OF THE ORIGINAL INPUT FILE
WITH SPECIFIED VALUES ATTACHED TO THE INDIVIDUAL
RECORDS.

THIS PROGRAM WAS WRITTEN BY M.L.SULLIVAN (OCT 1974)

FOR REMOTE SENSING LAB
THE CENTER FOR RESEARCH, INC. (CRINC)
UNIVERSITY OF KANSAS
LAWRENCE, KANSAS 66044

THERE IS ONLY ONE SUPPORT SUBROUTINE FOR THIS PROGRAM,
"LABLSS", WHICH PRODUCES A LIST OF THE CONTENTS OF
THE LABEL ONTO FILECODE 06.

THE COMMANDS, WHICH ARE READ FROM FILECODE 05,
ARE--"SKIP ", "COPY ", "FORMAT", "DEFAULT", AND
"APPEND".

THE COMMAND SHOULD BE IN COL. 1-6 LEFT-JUSTIFIED,
WITH TRAILING BLANKS. WITH THE COMMANDS TO SKIP
INPUT FILES OR WITH THE COMMAND TO COPY INPUT FILES
TO THE OUTPUT FILECODE, THE NUMBER OF FILES TO SKIP OR
COPY SHOULD BE IN COL. 8-9, RIGHT-JUSTIFIED. IF
THE NUMBER IS BLANK, ZERO, OR NEGATIVE, THEN ONE FILE
IS ASSUMED.

THE COMMAND "FORMAT" DECLARES THAT THE INPUT FORMAT FOR
APPEND PROCESSING IS IN COL. 8-67. IF BLANK,
THEN "(I15,I8,4F8.4)" IS ASSUMED.
THE FORMAT STAYS IN EFFECT UNTIL A NEW ONE IS GIVEN.

THE COMMAND "DEFAULT" DEFINES THE DEFAULT VALUE,
WHICH IS A REAL NUMBER IN COL. 8-16.
WHEN A VALUE TO BE APPENDED IS INPUT, IT IS CHECKED
AND IF IT IS WITHIN .01 OF THE DEFAULT VALUE THEN
THE OCTAL CONSTANT 377777777777 IS SUBSTITUTED.
THIS VALUE IS THE NOISE WORD FOR THE HONEYWELL
635 AND WILL BE PRINTED AS ALL BLANKS UNDER A F FIELD.

THE COMMAND "APPEND" CAUSES A GROUP OF DATA TO BE
APPENDED TO A FILE. ONE APPEND CARD WILL PROCESS
ONE INPUT FILE AND PRODUCE ONE OUTPUT FILE.
THE FIELDS ON THE APPEND CARD ARE COL. 8-10
HAS THE NUMBER OF DATA SETS FOLLOWING THE APPEND

10
20
30
40
50
60
70
80
90
100
110
120
130
140
150
160
170
180
190
200
210
220
230
240
250
260
270
280
290
300
310
320
330
340
350
360
370
380
390
400
410
420
430
440
450
460
470
480
490
500
510
520

CARD, EACH DATA SET IS OBTAINED BY EXECUTING A
 READ STATEMENT WITH THE INPUT FORMAT. EACH DATA SET
 CONSISTS OF THE SERIAL NUMBER TO START APPENDING TO
 FOLLOWED BY THE NUMBER OF RECORDS TO APPEND (WITH
 THE CONVENTION OF BLANK, ZERO, OR NEGATIVE NUMBERS
 EQUAL ONE), FOLLOWED BY THE DATA TO BE APPENDED.
 THE NUMBER OF VARIABLES TO BE APPENDED IS OBTAINED
 FROM COL. 16-17 OF THE APPEND CARD,

AS FILES ARE ENCOUNTERED THEIR LABELS ARE DISPLAYED
 FOR THE USERS INFORMATION. THE END OF PROCESSING A
 FILE IS INDICATED BY A MESSAGE TELLING THE ACTUAL
 RECORD COUNT OF THAT FILE (LESS LABEL RECORD),

SERIAL NUMBERS ARE CHECKED, AND IF THE NUMBER INDICATES
 THAT THE RECORD HAS ALREADY BEEN PROCESSED, THE
 MESSAGE "BAD SERIAL NUMBER" IS DISPLAYED AND PROCESSING
 STOPS.

IF A "HOLE" OCCURS IN THE APPENDED DATA (SERIAL
 NUMBER INDICATES SKIPPING INPUT RECORDS), THEN
 THE INTERVENING RECORDS ARE GIVEN DEFAULT (377777777777
 OCTAL) VALUES AND A MESSAGE IS DISPLAYED, TELLING
 THE USER THAT DEFAULT VALUES WERE INSERTED.
 THE SERIAL NUMBER OF THE FIRST AND LAST RECORD SO
 APPENDED WILL BE DISPLAYED FOR THE USERS INFORMATION.
 IF THE VALUES ARE IN THE LAST CONTIGUOUS BLOCK OF
 DEFAULT DATA, THEN ONLY THE STARTING MESSAGE APPEARS.

THE FOLLOWING DECK SET UP SHOULD BE USED AS A GUIDE.

```

$ IDENT PROJECT-NUH.NAME-OF-USER
$ OPTION FORTRAN
$ OBJECT
  <OBJECT DECK FOR MAINLINE
  AND SUBROUTINE>
$ ENDECK
$ EXECUTE
$ LIMITS ,11K
$ TAPE 01,X1DD,,99999,,INPUT-TAPE
$ TAPE 07,X2DD,,99999,,OUTPUT-TAPE,CUT
  <DIRECTIVES>
$ ENDJOB

```

FOR EXAMPLE, THE FOLLOWING DIRECTIVES WOULD
 SKIP 2 FILES, COPY 5 FILES, HAVE 2 VARIABLES
 APPENDED TO THE SIXTH FILE IN 3 DATA SETS WITH A
 REDEFINED FORMAT AND A DEFAULT VALUE OF -99.0,
 AND FINALLY COPYING 3 FILES.

C	COL 1	8	16	1050
C				1060
C		SKIP	02	1070
C		COPY	05	1080
C		DEFAULT	-99.0	1090
C		FORMAT	(I9,I3,F4.0,F8.2)	1100
C		APPEND	003 02	1110
C		20001156	02 0.0-145.14	1120
C		500021156	50 1.0 700.	1130
C		300531156	133-1.0 345.0	1140
C		COPY	03	1150
C				1160
C				1170
C				1180
C				1190
C				1200
C				1210
C				1220
C				1230
C				1240
C				1250
C				1260
		CHARACTER CARD*	80,VERB*6,FMAT*60,CHAR12*12	1270
		INTEGER LABEL(27),	DATA(150),IDEFAULT/037777777777/	1280
		REAL RVAL(99)		1290
		INTEGER OLDSIZE		1300
		LOGICAL FLAG		1310
		INTEGER IVAL(99)		1320
		EQUIVALENCE (CARD,VERB),(IDEFAULT,RDEFAULT),(LABEL(4),		1330
		& NUMWPR),(RVAL(1),IVAL(1))		1340
C				1350
		FMAT = "(I15,I8,4F8.4)"		1360
		DEFAULT = 999.0		1370
100		READ(5,1,END=950) CARD		1380
		WRITE(6,2) CARD		1390
C				1400
C		IS IT A VALID VERB,		1410
C				1420
		IF (VERB.EQ."SKIP ") GO TO 200		1430
		IF (VERB.EQ."COPY ") GO TO 300		1440
		IF (VERB.EQ."DEFAULT") GO TO 400		1450
		IF (VERB.EQ."FORMAT") GO TO 500		1460
		IF (VERB.EQ."APPEND") GO TO 600		1470
C				1480
C		NOT IN LIST.		1490
C				1500
		WRITE(6,3)		1510
		GO TO 900		1520
C				1530
C		PROCESS "SKIP" HERE.		1540
C				1550
200		DECODE(CARD,4) NUMBER		1560

	IF (NUMBER.LT.1) NUMBER = 1	1570
	KOUNT = 0	1580
205	READ(1) LABEL	1590
	CALL LABLSS(LABEL(1))	1600
	KREC = 0	1610
210	READ(1,END=220)	1620
	KREC = KREC + 1	1630
	GO TO 210	1640
220	CALL FCLOSE(1)	1650
	WRITE(6,12) KREC	1660
	KOUNT = KOUNT + 1	1670
	IF (KOUNT.LT.NUMBER) GO TO 205	1680
	WRITE(6,5) KOUNT	1690
	GO TO 100	1700
C	PROCESS "COPY" HERE.	1710
C		1720
C		1730
300	DECODE(CARD,4) NUMBER	1740
	IF (NUMBER.LT.1) NUMBER = 1	1750
	KOUNT = 0	1760
310	READ(1) LABEL	1770
	CALL LABLSS(LABEL(1))	1780
	KREC = 0	1790
	WRITE(7) LABEL	1800
320	READ(1,END=330) (IDATA(I),I=1,NUMWPR)	1810
	KREC = KREC + 1	1820
	WRITE(7) (IDATA(I),I=1,NUMWPR)	1830
	GO TO 320	1840
330	CALL FCLOSE(1)	1850
	WRITE(6,12) KREC	1860
	CALL FCLOSE(7)	1870
	KOUNT = KOUNT + 1	1880
	IF (KOUNT.LT.NUMBER) GO TO 310	1890
	WRITE(6,6) KOUNT	1900
	GO TO 100	1910
C	PROCESS "DEFAULT" HERE.	1920
C		1930
C		1940
400	DECODE(CARD,7) DEFAULT	1950
	GO TO 100	1960
C	PROCESS "FORMAT" HERE.	1970
C		1980
C		1990
500	DECODE(CARD,8) FMAT	2000
	IF (FMAT.EQ." ") FMAT = "(I15,I8,4F8,4)"	2010
	GO TO 100	2020
C	PROCESS "APPEND" HERE.	2030
C		2040
C		2050
600	DECODE(CARD,9) NUMBER,NUMVAR	2060
	IF (NUMBER.LT.1) NUMBER = 1	2070
	IF (NUMVAR.LT.1) NUMVAR = 1	2080

C	NUMBER = NUMBER OF SETS OF DATA.	2090
C	NUMVAR = NUMBER OF VARIABLES TO BE APPENDED.	2100
C	READ(1) LABEL	2110
C	OLDSIZE = NUMWPR	2120
C	NUMWPR = NUMWPR + NUMVAR	2130
C	CALL LABLSS(LABEL(1))	2140
C	WRITE(7) LABEL	2150
C	KOUNT = 0	2160
C	KREC = 0	2170
C	FLAG = .FALSE.	2180
C	WRITE(6,16)	2190
C		2200
C	610 READ(5,FMT) (ISTART,IKOUNT,(RVAL(J),J=1,NUMVAR)	2210
C	DO 615 J = 1,NUMVAR	2220
C	IF (ABS(RVAL(J)-DEFAULT).LT. 0.01) IVAL(J) = IDEFAULT	2230
C	615 CONTINUE	2240
C	WRITE(6,15) (ISTART,IKOUNT,(RVAL(J),J=1,NUMVAR)	2250
C	I1=ISTART/10000	2260
C	I2=I1/1000	2270
C	I1=I1-(I2*1000)	2280
C	I3 = I2/10	2290
C	I2 = I2 - I3*10	2300
C	I4 = I1*1000 + I2*100 + I3	2310
C		2320
C	620 READ(1,END=700) (IDATA(I),I=1,OLDSIZE)	2330
C	KREC = KREC + 1	2340
C	IF (ISTART.EQ.IDATA(1)) GO TO 640	2350
C	IS SEQUENCE NUMBER IN ASCENDING ORDER,	2360
C	I1=IDATA(1)/10000	2370
C	I2=I1/1000	2380
C	I1=I1-(I2*1000)	2390
C	I3 = I2/10	2400
C	I2 = I2-I3*10	2410
C	I5 = I1*1000 + I2*100 + I3	2420
C	IF (I4.LT.I5) GO TO 699	2430
C	IF FLAG NOT SET, THEN SET FLAG,	2440
C	AND PRINT MESSAGE TELLING USER THAT VALUES	2450
C	WERE INSERTED HERE.	2460
C	IF (FLAG) GO TO 625	2470
C	ENCODE(CHAR12,18) IDATA(1)	2480
C	DECODE(CHAR12,19) J1,J2,J3,J4,J5	2490
C	WRITE(6,13) " ",J1,J2,J3,J4,J5	2500
C	FLAG = .TRUE.	2510
C		2520
C		2530
C		2540
C		2550
C	NO MATCH, FILL WITH DEFAULT VALUES.	2560
C		2570
C	625 DO 630 J = 1,NUMVAR	2580
C	IDATA(I+OLDSIZE) = IDEFAULT	2590
C	630 CONTINUE	2600

	WRITE(7) (IDATA(I),I=1,NUMWPR)	2610
	NUMOLD = IDATA(1)	2620
	GO TO 620	2630
C		2640
C	MATCH.	2650
C	SET FLAG OFF	2660
640	IF (.NOT. FLAG) GO TO 645	2670
	ENCODE(CHAR12,18) NUMOLD	2680
	DECODE(CHAR12,19) J1,J2,J3,J4,J5	2690
	WRITE(6,17) J1,J2,J3,J4,J5	2700
	FLAG = .FALSE.	2710
645	K = 0	2720
650	DO 660 J = 1,NUMVAR	2730
	IDATA(J+OLDSIZE) = IVAL(J)	2740
660	CONTINUE	2750
C		2760
	WRITE(7) (IDATA(I),I=1,NUMWPR)	2770
	K = K+1	2780
	IF (K.GE.IKOUNT) GO TO 665	2790
	READ(1,END=700) (IDATA(I),I=1,OLDSIZE)	2800
	KREC = KREC + 1	2810
	GO TO 650	2820
C		2830
665	KOUNT = KOUNT + 1	2840
	IF (KOUNT.LT.NUMBER) GO TO 610	2850
670	READ(1,END=690) (IDATA(I),I=1,OLDSIZE)	2860
	KREC = KREC + 1	2870
	IF (FLAG) GO TO 675	2880
	ENCODE(CHAR12,18) IDATA(1)	2890
	DECODE(CHAR12,19) J1,J2,J3,J4,J5	2900
	WRITE(6,13) "0",J1,J2,J3,J4,J5	2910
	FLAG = .TRUE.	2920
675	DO 680 J = 1,NUMVAR	2930
	IDATA(J+OLDSIZE) = IDEFAULT	2940
680	CONTINUE	2950
	WRITE(7) (IDATA(I),I=1,NUMWPR)	2960
	GO TO 670	2970
C		2980
690	CALL FCLOSE(1)	2990
	WRITE(6,12) KREC	3000
	CALL FCLOSE(7)	3010
	GO TO 100	3020
C	SERIAL NUMBER IS IN DECREDING ORDER,	3030
C	MEANS AN ERROR HAS OCCURED,	3040
699	WRITE(6,14) ISTART	3050
	GO TO 900	3060
C		3070
700	WRITE(6,10)	3080
900	WRITE(6,11)	3090
950	STOP	3100
1	FORMAT(A80)	3110
2	FORMAT(1H0,"DIRECTIVE = ".A80)	3120

3	FORMAT(1H0,10X,"UNKNOWN DIRECTIVE")	3130
4	FORMAT(7X,12)	3140
5	FORMAT(1H0,10X,12," FILES WERE SKIPPED")	3150
6	FORMAT(1H0,10X,12," FILES WERE COPIED")	3160
7	FORMAT(7X,F8,4)	3170
8	FORMAT(7X,A60)	3180
9	FORMAT(7X,13,5X,12)	3190
10	FORMAT(1H0,10X,	3200
8	"ENCOUNTERED END OF FILE BEFORE FINISHING DIRECTIVE")	3210
11	FORMAT(1H0,10X,"PROGRAM TERMINATED ABNORMALLY")	3220
12	FORMAT(1H0,"ACTUAL RECORD COUNT =",15)	3230
13	FORMAT(11,T62,	3240
8	"DEFAULT VALUES INSERTED STARTING AT SERIAL NO.",5(4)	3250
14	FORMAT(1X,"BAD SERIAL NUMBER = ",115)	3260
15	FORMAT(1X,115,18,(T25,4F8.2/))	3270
16	FORMAT(1H0,"LIST OF APPEND DATA",	3280
8	/1X," SERIAL NO. COUNT VALUES")	3290
17	FORMAT(1X,T66,"STOPPING AT SERIAL NO.",5(4)	3300
18	FORMAT(112)	3310
19	FORMAT(14,11,13,11,13)	3320
	END	3330

CSKEW

PROGRAM SKEW

DATE 6/20/74

PURPOSE CHANGE THE ITNC DATA BY GROUPING TOGETHER THE DATA
WITH SAME CELL POINT ON THE SURFACE,
THE MODE OF SKEWED ITNC FILE IS 0,

DATA CARDS

A), 1 CARD --- 315
NO. OF FILES WANT TO SKIP ON THE INPUT TAPE, NO.
OF FILES WANT TO SKIP ON THE OUTPUT TAPE, NO. OF
FILES WANT TO SKEW ON THE INPUT TAPE
(INPUT TAPE MUST BE ITNC)
B), 1 BLANK CARD --- SIGNALS THE END OF PROCESSING
*** NOTE ***
CARD A) MAY BE REPEATED AS NECESSARY

DECK SET UP

```

$ IDENT 9999,USER
$ SELECT JYOUNG/SKEW
$ DATA CARDS
$ TAPE 01,A100,,20000,,TAPEIN
$ TAPE 02,A200,,00000,,TAPEOT,OUT
$ ENDJOB

```

VARIABLES DESCRIPTION

NFSKIP --- NO. OF FILES TO SKIP ON INPUT TAPE
MFSKIP --- NO. OF FILES TO SKIP ON OUTPUT TAPE
NFSKEW --- NO. OF FILES TO SKEW ON INPUT TAPE
IX --- DATA VECTOR
NCOH --- COMMAND ANGLE NUMBER
NSCAN --- SCAN NUMBER

```

7 READ(5,102,END=1) NFSKIP,MFSKIP,NFSKEW
102 FORMAT(3I5)

```

```

IF(NFSKEW.EQ.0) STOP
IF(NFSKIP.EQ.0) GO TO 6
DO 2 I=1,NFSKIP
3 READ(1,END=5)

```

ORIGINAL PAGE IS
OF POOR QUALITY

הנהלת המועצה

החברה

C

THE

הנהלת

© 2000 Blackwell Science Ltd

CCC

2

THE

100

PAGE 4

PUT DEFAULT VALUES IN DATA VECTOR AFTER NSCAN IS DONE

100

CLS

PROGRAM LST

DATE 5/22/74

PURPOSE TO LIST UP TO 150 FUNCTIONS OF THE COMPONENTS OF DATA VECTORS OF STANDARD DATA FILES. ONE WRITE IS EXECUTED FOR EACH DATA VECTOR. THE PROGRAM SEQUENTIALLY

- (1) READS A DATA VECTOR FROM FILE CODE 01
- (2) CALLS A USER PROVIDED ROUTINE TRNGN2 WHICH TRANSFORMS THE DATA VECTOR
- (3) WRITES THE TRANSFORMED VECTOR.

THE USER IS FREE TO SPECIFY ANY FUNCTIONS IN TRNGN2.

SUBROUTINE REQUIRED

THE USER MUST PROVIDE A SUBROUTINE OF THE FOLLOWING FORM

```

SUBROUTINE TRNGN1 (NCOM,NITC,NSCAN,IX,X)
  DIMENSION IX(150),X(150)
  DATA ..... (IF REQUIRED)
  RETURN
  ENTRY TRNGN2
  :
  :
  TRANSFORMATIONS
  :
  :
  RETURN
  END

```

NOTE --- NCOM, AND NSCAN ARE THE COMMAND ANGLE NUMBER AND SCAN NUMBER RESPECTIVELY AND ARE PROVIDED FOR THE USERS CONVENIENCE. IX AND X ARE BOTH THE DATA VECTOR.

DATA CARDS

ORIGINAL PAGE 13
OF POOR QUALITY

- 1 CARD --- 12
FILE CODE TO WRITE LISTING
- 1 OR MORE CARDS (AS NEEDED) --- 2613
NUMBER OF COMPONENTS OF TRANSFORMED VECTOR TO
LIST AND SUBSCRIPTS OF THESE COMPONENTS
- 6 CARDS --- 12A6 (COLUMNS 1 THROUGH 72 INCLUSIVE)
HEADER FORMAT WRITTEN AT TOP OF EACH PAGE
- 2 CARDS --- 12A6 (COLUMNS 1 THROUGH 72 INCLUSIVE)
FORMAT FOR SET OF COMPONENTS FROM ONE VECTOR
(USUALLY ONE LINE)
- 1 OR MORE CARDS --- 215
NUMBER OF FILES TO SKIP, NUMBER OF FILES TO
LIST. EACH CARD INDICATES BOTH NUMBERS
- 1 BLANK CARD
SIGNALS THE END OF LISTINGS

DECK SET-UP

```

$ IDENT 9999,USER
$ SELECT JYOUNG/LST
$ FORTRAN
$ INCODE IBMF
  SUBROUTINE TRNGN1 (NCOM,NITC,NSCAN,IX,X)
  DIMENSION IX(150),X(150)
  DATA .....( IF REQUIRED )
  RETURN
  ENTRY TRNGN2
  .
  .
  .
  RETURN
  END
$ EXECUTE
$ LIMITS 10,11K
$ INCODE IBMF
  .
  .
  .

```

PAGE 4

ORIGINAL PAGE IS
OF POOR QUALITY

SUBROUTINE LIST(N,NSUB,FMTD,FMTLN,L)

THIS SUBROUTINE LISTS DATA FROM ONE FILE

INTEGER DOY
DIMENSION FMTD(72),FMTLN(24),ITITLE(10),IDATJS(3),
1 IDATCU(3),IDATPS(3),IX(150),IDATMD(3),NSUB(100)
DATA BLANK/1H /

READ HEADER RECORD

READ (01) DOY,NSEQ,MODE,NWORDS,NREC,IDATPS,IDATJS,IDATCU,IDATMD;
1 ITITLE
ASSIGN 11 TO JGO
IF(MODE,EQ,0) ASSIGN 12 TO JGO
CALL CLOCK1 (IDA,IMO,IYR)
CALL TRNGN1(NCOM,NITC,NSCAN,IX,IX)
NLINE=1
MSCAN=0
IF(MODE,EQ,1) GO TO 2
ASSIGN 5 TO IGO
NITC=0
GO TO 8

ITC PASS

2 ASSIGN 6 TO IGO
GO TO 8

WRITE DATE AT BOTTOM OF PAGE

3 WRITE(L,103) IMO,IDA,IYR
103 FORMAT(/90X,A2,'/',A2,'/',A2)
NLINE=1
MSCAN = MSCAN - 1

WRITE HEADER FOR THIS FILE AT TOP OF
EACH PAGE

8 WRITE (L,101) DOY,NSEQ,IDATPS,ITITLE,BLANK
101 FORMAT (1H1, ///20X,'DOY',I4,'-',I,'-',I4X,I2,'/',I2,'/',I2,
14X,10A6, /A1)
WRITE (L,FMTD)

READ A DATA VECTOR

4 READ (1,END=1) (IX(I),I=1,NWORDS)
NCOM=IX(1)/100000000
GO TO IGO, (5,6)
5 NSCAN=(IX(1)-NCOM*100000000)/10000
GO TO 7

6 NITC=(IX(1)-NCOM*100000000)/100000000
NSCAN=(IX(1)-NCOM*100000000-NITC*100000000)/10000

SKIP A LINE BETWEEN SCANS (OH BETWEEN
CELLS IF MODE =0 INDICATING THIS IS AN
ITNC FILE THAT HAS BEEN SKEWED)

7 GO TO JGO, (11,12)
11 IF (MSCAN,EQ,NSCAN) GO TO 10
WRITE(L,102)
NLINE=NLINE+1
GO TO 10
12 IF(NLINE/6*6,NE,NLINE,AND,NLINE,NE,1) GO TO 10
WRITE(L,102)
NLINE=NLINE+1
102 FORMAT (//)

LET THE USER TRANSGENERATE IX BEFORE
LISTING IT

10 CALL TRNGN2
WRITE (L,FMTLN) (IX(NSUB(I)),I=1,N)
NLINE=NLINE+1
MSCAN=NSCAN
IF (NLINE,GE,49) GO TO 3
GO TO 4
1 WRITE(L,100) IDATJS,IDATCU,IDATMD,IMO,IDA,IYR
100 FORMAT (///10X,'ISC = ',I2,'/',I2,'/',I2, 8X,'S, TRUTH = ',I2,'/',I2,
1I2,'/',I2,8X,'LAST MOD = ',I2,'/',I2,'/',I2,8X,'THIS LISTING = ',
1A2,'/',A2,'/',A2)
RETURN
END

CTFNH TRANS-GENERATOR PROGRAM MAIN LINE

LANGUAGE -- HONEYWELL'S SERIES 6000 FORTRAN
SYSTEM RELEASE 8.

WRITTEN BY JAMES KAHN 17-FEB-75.

PURPOSE

THIS PROGRAM TRANSFERS DATA FILES FROM MAGNETIC TAPE TO DISK. IT IS CAPABLE OF MERGING TAPE FILES INTO ONE DISK FILE. PROGRAM OPERATION IS DETERMINED BY DIRECTIVES RETURNED BY THE 'READ' SUBROUTINE FROM FILE CODE 5. FILE CODES 6 AND 42 CONTAIN THE REPORTS ON THE DIRECTIVES AND THE DISK OUTPUT DIRECTORY. THE INPUT FILE CODE IS 1. OUTPUT FILE CODES ARE 2 AND 3 WHICH CONTAIN THE FILE HEADERS AND THE DATA, RESPECTIVELY. THE USER MUST SUPPLY A DATA PROCESSING ROUTINE FOR THIS PROGRAM. 'TRNGN1'. IT IS USED TO SET-UP SUBROUTINE LINKAGES. WHILE 'TRNGN2' IS THE NON-ARGUMENTAL ENTRY POINT USED BY THE MAIN LINE FOR DATA PROCESSING OF THE FILE. ON EACH ENTRY THROUGH 'TRNGN2' THE DATA AREA WILL CONTAIN THE DATA RECORD FROM THE MAG. TAPE FILE WITH THE REMAINDER OF THE AREA ZEROED OUT.

TRNGN1 ARGUMENTS

SCAN	SCAN NUMBER OF DATA RECORD(INTEGER).
ITC	ITC NUMBER OF DATA RECORD(INTEGER).
COM	COMMAND ANGLE NUMBER(INTEGER)
RECSIZE	MAXIMUM DATA ARRAY SIZE(INTEGER).
HEADER	INPUT FILE HEADER RECORD, SIZE - 27(INTEGER).
DATA	DATA RECORDS FROM THE INPUT FILE DIMENSIONED BY RECSIZE(INTEGER).
DATA	DITTO(REAL).

TRNGN007
TRNGN008
TRNGN009
TRNGN010
TRNGN011
TRNGN012
TRNGN013
TRNGN014
TRNGN015
TRNGN016
TRNGN017
TRNGN018
TRNGN019
TRNGN020
TRNGN021
TRNGN022
TRNGN023
TRNGN024
TRNGN025
TRNGN026
TRNGN027
TRNGN028
TRNGN029
TRNGN030
TRNGN031
TRNGN032
TRNGN033
TRNGN034
TRNGN035
TRNGN036
TRNGN037
TRNGN038
TRNGN039
TRNGN040
TRNGN041
TRNGN042
TRNGN043
TRNGN044
TRNGN045
TRNGN046
TRNGN047
TRNGN048
TRNGN049
TRNGN050
TRNGN051
TRNGN052
TRNGN053
TRNGN054
TRNGN055
TRNGN056
TRNGN057

ORIGINAL PAGE IS
OF POOR QUALITY

DIRECTIVES

REWIND NO VARIABLE FIELD. REWINDS INPUT FILE.

TITLE TITLES OUTPUT FILE, COLUMNS 16 - 76 CONTAIN THE NEW TITLE. IF NOT PRESENT, THE OLD TITLE IS RETAINED.

RECSIZE VARIABLE FIELD (COLUMNS. 16 - 73) CONTAINS THE NEW SIZE OF THE OUTPUT DATA RECORDS. ASSUMED NUMBER IS 50.

SELECT SELECTS INPUT FILES IDENTIFIED BY THE DAY OF YEAR AND SEGMENT NUMBER (I.E. 365-1). FILES TO BE MERGED MUST BE SEPERATED BY COMMAS. A *** FOLLOWED BY AN INTEGER NUMBER LESS THAN 10 INDICATES THAT THE NTH FILE IS TO BE PROCESSED. A BLANK IN THE VARIABLE FIELD WILL TERMINATE PROCESSING OF THE VARIABLE FIELD AND CLOSE THE OUTPUT MERGE FILE.

ETC ALLOWS THE VARIABLE FIELD FROM THE PRECEEDING DIRECTIVE TO BE CONTINUED. NO LIMIT IS ON THE NUMBER OF CONTINUATIONS OF THE VARIABLE FIELD. SCAN IS TERMINATED WHEN A CARD ENDS WITH A BLANK INSTEAD OF A COMMA.

CONTENTS OF TRANS-GENERATOR PROGRAM

..... (MAIN LINE)
 READ (LIEFARY)
 TRNGN1 (USER SUPPLIED)
 TRNGN2 (USER SUPPLIED)

TRNGN067
 TRNGN068
 TRNGN069
 TRNGN070
 TRNGN071
 TRNGN072
 TRNGN073
 TRNGN074
 TRNGN075
 TRNGN076
 TRNGN077
 TRNGN078
 TRNGN079
 TRNGN080
 TRNGN081
 TRNGN082
 TRNGN083
 TRNGN084
 TRNGN085
 TRNGN086
 TRNGN087
 TRNGN088
 TRNGN089
 TRNGN090
 TRNGN091
 TRNGN092
 TRNGN093
 TRNGN094
 TRNGN095
 TRNGN096
 TRNGN097
 TRNGN098
 TRNGN099
 TRNGN100
 TRNGN101
 TRNGN102
 TRNGN103
 TRNGN104
 TRNGN105
 TRNGN106
 TRNGN107
 TRNGN108
 TRNGN109
 TRNGN110
 TRNGN111

n n

SAMPLE PROGRAM

TITLE	EXAMPLE :
SELECT	4-1,4-5*2,5-1,
ETC	6-2
REWIND	
SELECT	2-1

SAMPLE PROGRAM EXPLANATION

THE TITLE OF THE MERGED OUTPUT FILE IS 'EXAMPLE A'. THE FILES MERGED ARE 4-1, THE SECOND OCCURRENCE OF 4-5, 5-1, AND 6-2. THE INPUT FILE IS THEN REMOVED. THE TITLE IS TAKEN FROM THE INPUT FILE 2-1, WHICH IS TRANSFERRED TO THE OUTPUT FILE.

TONGH 112
TONGH 113
TONGH 114
TONGH 115
TONGH 116
TONGH 117
TONGH 118
TONGH 119
TONGH 120
TONGH 121
TONGH 122
TONGH 123
TONGH 124
TONGH 125
TONGH 126
TONGH 127
TONGH 128
TONGH 129
TONGH 130
TONGH 131
TONGH 132
TONGH 133
TONGH 134
TONGH 135
TONGH 136
TONGH 137
TONGH 138
TONGH 139
TONGH 140
TONGH 141
TONGH 142
TONGH 143
TONGH 144
TONGH 145
TONGH 146
TONGH 147
TONGH 148
TONGH 149
TONGH 150
TONGH 151
TONGH 152
TONGH 153
TONGH 153
TONGH 153
TONGH 153
TONGH 153
TONGH 153
TONGH 153

ORIGINAL PAGE IS
OF POOR QUALITY


```

IMPLICIT INTEGER( A = Z )
PARAMETER CMDS = 4, MAXDATA = 150, X-SEC = 27, XDATA = 17,
COMMON /READC/ ENCLINE, INREC, EOF, PELL
1 COMMON /DATA( MAXDATA ), HEADER( X-SEC ), IDATE( 3 ),
INTEGER DATA( MAXDATA ), RECSIZE / 50 /, SUBFIELD( 3 ),
1 FILENAME( 2 ), RECSIZE / 50 /, SUBFIELD( 3 ),
2 TAB / 30 /, ITITLE( 1 ),
1 CHARACTER COMMAND, INPUT * 60, TITLE * 60 /,
2 COMMANDS ( CMDS ) /, TITLE, *HEADER*, *RECSIZ*,
1 *SELECT* /, DATE * 8, LOCATION * 3,
2 / 30H(T1, ***, T , 13, ***, I1, 42) /,
3 OLDNAME * 60
4 EQUIVALENCE( FILENAME, HEADER ),
1 ( MODE, HEADER( 3 ) ), ( SERIAL, DATA( 1 ) ),
2 ( TITLE, ITITLE ), ( INRECORD, HEADER( 4 ) ),
3 ( OLDNAME, HEADER( 13 ) ), ( REPEATS, SUBFIELD( 3 ) )

C
CALL FYOPT( 61, 0, 1, 0 )
CALL FYOPT( 85, 1, 1, 1 )
CALL FXALT( $470 )

```

INITIALIZE SUBROUTINE LINKAGES

```

1 CALL TENGHI( SCAN, ITC, COM, RECSIZE, HEADER,
DATA, DATA )
CALL READ( INPUT, COMMAND, SUBFIELD, COMMANDS, 2 )

```

GET DATE

```

CALL DATIME( DATE, MODE )
DECODE( DATE, 500 ) IDATE
WRITE( 42, 530 ) DATE
WRITE( 6, 505 )
GO TO 20

```

ERROR PROCESSING

```

010 WRITE( 6, 510 ) SUBFIELD( 1 ), SUBFIELD( 2 )
020 CALL READCHD

```

TRNGN154
 TRNGN155
 TRNGN156
 TRNGN157
 TRNGN158
 TRNGN159
 TRNGN160
 TRNGN161
 TRNGN162
 TRNGN163
 TRNGN164
 TRNGN165
 TRNGN166
 TRNGN167
 TRNGN168
 TRNGN169
 TRNGN170
 TRNGN171
 TRNGN172
 TRNGN173
 TRNGN174
 TRNGN175
 TRNGN176
 TRNGN177
 TRNGN178
 TRNGN179
 TRNGN180
 TRNGN181
 TRNGN182
 TRNGN183
 TRNGN184
 TRNGN185
 TRNGN186
 TRNGN187
 TRNGN188
 TRNGN189
 TRNGN190
 TRNGN191
 TRNGN192
 TRNGN193
 TRNGN194
 TRNGN195
 TRNGN196
 TRNGN197
 TRNGN198
 TRNGN199
 TRNGN200
 TRNGN201
 TRNGN202
 TRNGN203
 TRNGN204
 TRNGN205

C
C
CIE

END OF INPUT FILE REACHED

```
IF( EOF ) , 490.
```

INPUT DIRECTIVE CHECKED

```

030      DO 30 MATCH = 1, CMDS
          IF( COMMAND.EQ. COMMANDS( MATCH ) ) GO TO
            1      ( 1, 2, 3, 4 ), MATCH
          WRITE( 6, 520 )
          GO TO 20

```

TITLE DIRECTIVE PROCESSED

```
001      TITLE = INPUT
      GO TO 20
```

REVIEW COMMAND PROCESSED

002 REWIND 1
GO TO 20

RECORD SIZE PROCESSED

```
003      IF( SUBFIELD( 1 )) 10, 10,
```

TRNGN206
TRNGN207
TRNGN208
TRNGN209
TRNGN210
TRNGN211
TRNGN212
TRNGN213
TRNGN214
TRNGN215
TRNGN216
TRNGN217
TRNGN218
TRNGN219
TRNGN220
TRNGN221
TRNGN222
TRNGN223
TRNGN224
TRNGN225
TRNGN226
TRNGN227
TRNGN228
TRNGN229
TRNGN230
TRNGN231
TRNGN232
TRNGN233
TRNGN234
TRNGN235
TRNGN236
TRNGN237
TRNGN238
TRNGN239
TRNGN240
TRNGN241
TRNGN242
TRNGN243
TRNGN244
TRNGN245
TRNGN246
TRNGN247
TRNGN248
TRNGN249
TRNGN250
TRNGN251
TRNGN252
TRNGN253
TRNGN254
TRNGN255
TRNGN256
TRNGN257

TRNG 259
TRNG 259
TRNG 260
TRNG 261
TRNG 262
TRNG 263
TRNG 264
TRNG 265
TRNG 266
TRNG 267
TRNG 268
TRNG 269
TRNG 270
TRNG 271
TRNG 272
TRNG 273
TRNG 274
TRNG 275
TRNG 276
TRNG 277
TRNG 278
TRNG 279
TRNG 280
TRNG 281
TRNG 282
TRNG 283
TRNG 284
TRNG 285
TRNG 286
TRNG 287
TRNG 288
TRNG 289
TRNG 290
TRNG 291
TRNG 292
TRNG 293
TRNG 294
TRNG 295
TRNG 296
TRNG 297
TRNG 298
TRNG 299
TRNG 300
TRNG 301
TRNG 302
TRNG 303
TRNG 304
TRNG 305
TRNG 306
TRNG 307
TRNG 308
TRNG 309

C
C
C
CIF
C
C

10

C

10

C
C
C
C
CIF
C
C

10
11
12

C
C
C
C
CIF
C
C

C
C
C
C
C
C
C

13

13

C
C
C
C
C
C
C

14

C
C

T2NGN352
 T2NGN363
 T2NGN364
 T2NGN365
 T2NGN366
 T2NGN367
 T2NGN368
 T2NGN369
 T2NGN370
 T2NGN371
 T2NGN372
 T2NGN373
 T2NGN374
 T2NGN375
 T2NGN376
 T2NGN377
 T2NGN378
 T2NGN379
 T2NGN380
 T2NGN381
 T2NGN382
 T2NGN383
 T2NGN384
 T2NGN385
 T2NGN386
 T2NGN387
 T2NGN388
 T2NGN389
 T2NGN390
 T2NGN391
 T2NGN392
 T2NGN393
 T2NGN394
 T2NGN395
 T2NGN396
 T2NGN397
 T2NGN398
 T2NGN399
 T2NGN400
 T2NGN401
 T2NGN402
 T2NGN403
 T2NGN404
 T2NGN405
 T2NGN406
 T2NGN407
 T2NGN408
 T2NGN409
 T2NGN410
 T2NGN411
 T2NGN412
 T2NGN413

T2NGN414
T2NGN415
T2NGN416
T2NGN417
T2NGN418
T2NGN419
T2NGN420
T2NGN421
T2NGN422
T2NGN423
T2NGN424
T2NGN425
T2NGN426
T2NGN427
T2NGN428
T2NGN429
T2NGN430
T2NGN431
T2NGN432
T2NGN433
T2NGN434
T2NGN435
T2NGN436
T2NGN437
T2NGN438
T2NGN439
T2NGN440
T2NGN441
T2NGN442
T2NGN443
T2NGN444
T2NGN445
T2NGN446
T2NGN447
T2NGN448
T2NGN449
T2NGN450
T2NGN451
T2NGN452
T2NGN453
T2NGN454
T2NGN455
T2NGN456
T2NGN457
T2NGN458
T2NGN459
T2NGN460
T2NGN461
T2NGN462
T2NGN463
T2NGN464
T2NGN465

233


```

C          DO 165 CLEAR = INRECORD, RESIZE
165          DATA( CLEAR ) = 0
167          CONTINUE
          GO TO 160

C
C
C
C
C
C
C
C          PROCESS NON-STANDARD MODES

170          READ( 1, END = 90 ) ( DATA( I ), I = 1, INRECORD )
          COM = SERIAL / 10 ** 8
          ITC = ( SERIAL / 10 ** 7 ) - ( COM * 10 )
          SCAN = ( SERIAL / 10 ** 6 ) - ( ITC * 10 ** 3 ) -
1          ( COM * 10 ** 4 )
          RECORDS = RECORDS + 1
          CALL TPNGN2
          WRITE( 3 ) ( DATA( I ), I = 1, RESIZE )

C
C
C
C
C          CLEAR DATA RECORD AREA EXTENSION

180          DO 180 CLEAR = INRECORD, RESIZE
          DATA( CLEAR ) = 0
          GO TO 170

C
C
C
C
C
C
C
C          PROGRAM ABORT PROCESSED

470          ENDFILE 2
          ENDFILE 3
          WRITE( 42, 570 )
          IF( REPEATS - 1 ) , , 475
          WRITE( 6, 580 ) SUBFIELD( 1 ), SUBFIELD( 2 )
          GO TO 480
475          WRITE( 6, 590 ) SUBFIELD( 1 ), SUBFIELD( 2 ),
1          SUBFIELD( 3 ) - SKIP
480          CALL FXEM( 61, , )

C
C
C
C
C          NORMAL TERMINATION

```

TPNGN515
 TPNGN516
 TPNGN517
 TPNGN518
 TPNGN519
 TPNGN520
 TPNGN521
 TPNGN522
 TPNGN523
 TPNGN524
 TPNGN525
 TPNGN526
 TPNGN527
 TPNGN528
 TPNGN529
 TPNGN530
 TPNGN531
 TPNGN532
 TPNGN533
 TPNGN534
 TPNGN535
 TPNGN536
 TPNGN537
 TPNGN538
 TPNGN539
 TPNGN540
 TPNGN541
 TPNGN542
 TPNGN543
 TPNGN544
 TPNGN545
 TPNGN546
 TPNGN547
 TPNGN548
 TPNGN549
 TPNGN550
 TPNGN551
 TPNGN552
 TPNGN553
 TPNGN554
 TPNGN555
 TPNGN556
 TPNGN557
 TPNGN558
 TPNGN559
 TPNGN560
 TPNGN561
 TPNGN562
 TPNGN563
 TPNGN564
 TPNGN565
 TPNGN566
 TPNGN567

REPRODUCIBILITY OF THE
 ORIGINAL PAGE IS POOR

C
C

```

490  ENDFILE 2
      ENDFILE 3
      REWIND 1
      REWIND 2
      REWIND 3
      WRITE( 42, 570 )
      STOP *      END OF TRANS - GENERATOR ACTIVITY *
500  FORMAT( I2, I4, I2, I7, I2 )
505  FORMAT( '0', T47, 'TPANS - GENERATOR DIRECTIVE',
1    ' * REPORT', 5( / ) )
510  1  FORMAT( ' ', 5( '**' ), ' * F SUPFIELD - ', I4,
1    ' ', I1, I4, ' * ILLEGAL, IGNORED.', 3( / ) )
520  1  FORMAT( ' ', 5( '**' ), ' * F DIRECTIVE UNKNOWN.',
1    ' * IGNORED.', 3( / ) )
530  1  FORMAT( '0', T2, A4, T57, 'OUTPUT FILE DIRECTORY',
1    ' ', 3( / ), T2, 'RECORD', T15, 'FILE', T30, 'FILES' /
2    T2, 'SIZE', T15, 'TITLE', T30, 'MERGED', 3( / ) )
540  FORMAT( 2( / ), T2, I3, T15, A60, 3( / ) )
550  FORMAT( T11, I1 )
560  FORMAT( ' ' )
570  FORMAT( '0**' - EOF )
580  1  FORMAT( ' ', 5( '**' ), ' * T FILENAME ', I4, I3, '- ', I1,
1    ' 14', ' * WAS NOT FOUND' )
590  1  FORMAT( ' ', 5( '**' ), ' * T FILENAME ', I4, I3, '- ', I1,
1    ' 14', ' * WAS ONLY FOUND ', I1, ' * TIMES' )
600  1  FORMAT( '0', 5( '**' ), ' * W THERE WERE ONLY ', I5,
1    ' * RECORDS FOUND, EXPECTING ', I5, ' * RECORDS' )
610  1  FORMAT( '0', T30, 'THERE ARE ', I5, ' * DATA RECORDS IN THIS',
1    ' * FILE' )
      END

```

```

TRAN568
TRAN569
TRAN570
TRAN571
TRAN572
TRAN573
TRAN574
TRAN575
TRAN576
TRAN577
TRAN578
TRAN579
TRAN580
TRAN581
TRAN582
TRAN583
TRAN584
TRAN585
TRAN586
TRAN587
TRAN588
TRAN589
TRAN590
TRAN591
TRAN592
TRAN593
TRAN594
TRAN595
TRAN596
TRAN597
TRAN598
TRAN599

```

C2EAD PROGRAM DIRECTIVE INTERPRETER

LANGUAGE -- HONEYWELL'S SERIES 6000 FORTRAN
SYSTEM RELEASE A.

WRITTEN BY JAMES KAHN 27-JAN-75.

UPDATED TO HANDLE REAL NUMBERS BY JAMES KAHN 16-FEB-75.

PURPOSE

THIS ROUTINE SEARCHES FOR DIRECTIVES ON FILE CODE 5 PLUS THEIR VARIABLE FIELD AND RETURNS THE RESULTS TO ITS CALLING ROUTINE. THE 'ETC' DIRECTIVE IS PROCESSED EXCLUSIVELY BY THIS ROUTINE. THE DATA FORMAT IS A COMMAND DIRECTIVE(COLUMNS 8 - 13) AND OPTIONALLY FOLLOWED BY INFORMATION IN ITS VARIABLE FIELD(COLUMNS 15 - 72). EACH VARIABLE FIELD ON THE CARD IS SEPARATED BY A COMMA. A BLANK MARKS THE BEGINNING OF THE COMMENT FIELD ON THE DATA CARD. THERE ARE THREE SPECIAL CHARACTERS ALLOWED IN A VARIABLE FIELD. A '.' IN THE NUMBER MARKS IT AS A REAL NUMBER. OTHERWISE THE ASSUMED TYPE IS INTEGER. A '-' AND A '*' ARE THE REMAINING SPECIAL CHARACTERS. THEIR OPERATION IS IDENTICAL. THE NUMBER FOLLOWING THESE CHARACTERS IS STORED IN THE 'SUBFIELD' ARRAY. A MAXIMUM OF TWO WORDS ARE AVAILABLE FOR STORAGE. A PROVISION HAS BEEN MADE FOR SPECIAL PROCESSING BY THE USER OF CERTAIN COMMAND DIRECTIVES. THESE SIX CHARACTER DIRECTIVES ARE CONTAINED IN THE ARRAY 'SPECIAL' AND VARIABLY DIMENSIONED BY 'XSPECIAL'. IF NO SPECIAL PROCESSING IS DESIRED, IT MUST CONTAIN A ZERO.

READ0001
READ0002
READ0003
READ0003
READ0003
READ0004
READ0005
READ0006
READ0007
READ0008
READ0009
READ0010
READ0011
READ0012
READ0013
READ0014
READ0015
READ0016
READ0017
READ0018
READ0019
READ0020
READ0021
READ0022
READ0023
READ0024
READ0025
READ0026
READ0027
READ0028
READ0029
READ0030
READ0031
READ0032
READ0033
READ0034
READ0035
READ0036
READ0037
READ0038
READ0039
READ0040
READ0041
READ0042
READ0043
READ0044
READ0045
READ0046
READ0047
READ0048
READ0049
READ0050

ORIGINAL PAGE IS
OF POOR QUALITY

ENDLINE

NORMALLY SET TO -1, BUT SET TO 0 IF A BLANK
IS FOUND DURING A SCAN OF THE VARIABLE FIELDS
OR THE VARIABLE FIELDS ARE EXHAUSTED.
(INTEGER)

ENDREC

NORMALLY SET TO -1, BUT SET TO 0 IF A VARIABLE FIELD DOES NOT END IN A COMMA. (INTEGER)

EOF

NORMALLY SET TO -1, BUT SET TO 0 IF FILE
CODE 5 IS EXHAUSTED. (INTEGER)

REAL

NORMALLY SET TO -1, BUT SET TO 2 IF A SUBFIELD
ARRAY ELEMENT CONTAINS A REAL NUMBER.
(INTEGER)

PEAC0102
PEAC 0113
READ0104
READ0105
READ0106
READ0117
READ0108
READ0109
READ0110
READ0111
READ0112
READ0113
READ0114
READ0115
READ0116
READ0117
READ0118
READ0119
READ0120
READ0121
READ0122
READ0123
READ0124
READ0125
READ0126
READ0127
READ0128
READ0129
READ0130
READ0131
READ0132
PEAC0133
READ0134
PEAC0135
READ0136
PEAC0137
READ0138
PEAC0139
READ0140
PEAC0141
READ0142
PEAC0143
READ0144
PEAC0145
READ0146
PEAC0147
READ0148
PEAC0149
READ0150
PEAC0151
READ0152
PEAC0153
READ0154
PEAC0155
READ0156
PEAC0157
READ0158
PEAC0159
READ0160
PEAC0161
READ0162
PEAC0163
READ0164
PEAC0165
READ0166
PEAC0167
READ0168
PEAC0169
READ0170
PEAC0171
READ0172
PEAC0173
READ0174
PEAC0175
READ0176
PEAC0177
READ0178
PEAC0179
READ0180
PEAC0181
READ0182
PEAC0183
READ0184
PEAC0185
READ0186
PEAC0187
READ0188
PEAC0189
READ0190
PEAC0191
READ0192
PEAC0193
READ0194
PEAC0195
READ0196
PEAC0197
READ0198
PEAC0199
READ0200

ORIGINAL PAGE IS
OF POOR QUALITY

```

SUBROUTINE READ( INPUT, COMMAND, SUBFIELD, SPECIAL,
1 XSPECIAL )
1 IMPLICIT INTEGER( A - Z )
1 PARAMETER ( NWIDTH = 12, SUBSIZE = 3, DELIMIT = '-',
2 BLANK = ' ', COMMA = ',', ETC = 'ETC',
2 REPEAT = '**', PERIOD = '.' )
COMMON /READC/ ENDLIN, ENOREC, EOF, PEAL
1 CHARACTER INPUT * 60, COMMAND, TEMP1 / ' ' /, TEMP2 * 12,
2 SPECIAL( XSPECIAL ),
2 FORMAT * 11 / '( T , A1 )' /, IFORMAT * 6 / '( I )' /
INTEGER SUBFIELD( SUBSIZE )

SUBROUTINE LINKAGE SET-UP

EOF = -1
ENOREC = 0
ASSIGN 85 TO BYPASS3
005 RETURN

DIRECTIVE'S END-OF-FILE
PROCESSED

010 EOF = 0
ENOREC = 0
COMMAND = BLANK

ENTRY TO ECHO PRINT DIRECTIVE

020 ENTRY READECHO
IF( EOF ) , 5,
READ( 5, 510, END = 10 ) COMMAND, INPUT
WRITE( 6, 515 ) COMMAND, INPUT

INPUT IS A COMMENT,
NOT A COMMAND

IF( COMMAND .EQ. BLANK ) GO TO 20
GO TO 25

ENTRY TO SUPPRESS DIRECTIVE
ECHO

022 ENTRY READNEHO
IF( EOF ) , 5,
READ( 5, 510, END = 10 ) COMMAND, INPUT
IF( COMMAND .EQ. BLANK ) GO TO 22

```

```

READ0130
READ0131
READ0132
READ0133
READ0134
READ0135
READ0136
READ0137
READ0138
READ0139
READ0140
READ0141
READ0142
READ0143
READ0144
READ0145
READ0146
READ0147
READ0148
READ0149
READ0150
READ0151
READ0152
READ0153
READ0154
READ0155
READ0156
READ0157
READ0158
READ0159
READ0160
READ0161
READ0162
READ0163
READ0164
READ0165
READ0166
READ0167
READ0168
READ0169
READ0170
READ0171
READ0172
READ0173
READ0174
READ0175
READ0176
READ0177
READ0178
READ0179

```

[illegible]

ORIGINAL PAGE IS
OF POOR QUALITY

```

C      SORT DIRECTIVE'S VARIABLE
C      FIELD
C
C      DO 100 SEARCH = START, 57
C      ENCODE( FORMAT, 550 ) SEARCH
C      DECODE( INPUT, FORMAT ) TEMP1
C
C      CHARACTER IS A FIELD SCAN
C      TERMINATOR
C
C      IF( TEMP1 .EQ. BLANK ) GO TO 110
C
C      CHARACTER DELIMITS A REAL
C      NUMBER FIELD, NOT THE USUAL
C      INTEGER NUMBER FIELD
C
C      IF( TEMP1 .EQ. PERIOD ) REAL = 0
C
C      SCAN HAS REACHED AN END OF A
C      FIELD
C
C      IF( TEMP1 .EQ. COMMA ) GO TO BYPASS1
C
C      VARIABLE FIELD CONTAINS MORE
C      THAN ONE ENTRY
C
C      IF( TEMP1 .EQ. DELIMIT ) GO TO 50
C
C      VARIABLE FIELD CONTAINS A
C      REPEAT SPECIFICATION
C
C      IF( TEMP1 .EQ. REPEAT ) GO TO 90
C
C      DIRECTIVE'S VARIABLE FIELD
C      LOADED
C
C      IF( STOP ) , 100,
C
C      SAVE CHARACTER
C
C      STOP = STOP - 1
C      TALLY = TALLY + 1
C      ENCODE( FORMAT, 550 ) TALLY
C      ENCODE( TEMP2, FORMAT ) TEMP1

```

```

085      GO TO BYPASS3
        ASSIGN 120 TO BYPASS1
        ASSIGN 100 TO BYPASS3
        GO TO 100

C
C C I F
C
C
C 090      IF( REAL ) , 94,

C
C
C
C
C
C
C
C
C 094      DECODE( TEMP2, 570 ) SUBFIELD( INDEX )
        REAL = 2

C
C
C
C
C 096      INDEX = INDEX + 1
        TALLY = 0
        STOP = FWIDTH
        CONTINUE

C
C
C
C
C 100      DIRECTIVE'S VARIABLE FIELDS
        EXHAUSTED

C
C
C
C
C 105      ENOLINE = 0
        START = START + 1
        RETURN

C
C
C
C
C 110      ENCODE( FORMAT, 550 ) SEARCH = 1
        DECODE( INPUT, FORMAT ) TEMP1
        ENOLINE = 0
        ENDREC = 0
        IF( TEMP1.EQ. COMMA ) ENDREC = -1
        GO TO BYPASS1

```

VARIABLE FIELD CONTAINS
A REAL NUMBER

CONVERT CHARACTER STRING TO
INTEGER

CONVERT CHARACTER STRING TO
REAL

SET-UP FOR NEXT SUBFIELD
SEARCH

DIRECTIVE'S VARIABLE FIELDS
EXHAUSTED

IGNORE NULLED VARIABLE FIELD

READ0317
 READ0318
 READ0319
 READ0320
 READ0321
 READ0322
 READ0323
 READ0324
 READ0325
 READ0326
 READ0327
 READ0328
 READ0329
 READ0330
 READ0331
 READ0332
 READ0333
 READ0334
 READ0335
 READ0336
 READ0337
 READ0338
 READ0339
 READ0340
 READ0341
 READ0342
 READ0343
 READ0344
 READ0345
 READ0346
 READ0347
 READ0348
 READ0349
 READ0350
 READ0351
 READ0352
 READ0353
 READ0354
 READ0355
 READ0356
 READ0357
 READ0358
 READ0359
 READ0360
 READ0361

READ0256

C
C
C
C

120

START = SEARCH + 1
 ASSIGN 105 TO BYPASS1
 ASSIGN 85 TO BYPASS3

C
C
C
C
C
C

IF(REAL) . 130,

C
C
C
C
C

DIRECTIVE'S VARIABLE FIELDS
 NOT EXHAUSTED

VARIABLE FIELD CONTAINED A
 REAL NUMBER

CONVERT CHARACTER STRING TO
 INTEGER

ENCODE(IFORMAT, 550) TALLY
 DECODE(TEMP2, IFORMAT) SUBFIELD(INDEX)
 RETURN

C
C
C
C
C

130

510

515

520

1

530

540

1

550

560

570

DECODE(TEMP2, 570) SUBFIELD(INDEX)
 RETURN
 FORMAT(T9, A6, T16, A60)
 FORMAT(' ', T10, A6, T20, A60)
 FORMAT(' ', 5(' '), ' F ', A3,
 ' EXPECTING ETC DIRECTIVE, ')
 FORMAT(' ', T41, ' IGNORED, ', 3(/))
 FORMAT(' ', T41, ' TREAT AS END OF PREVIOUS ',
 ' DIRECTIVE, ', 3(/))
 FORMAT(T4, I2)
 FORMAT(I6)
 FORMAT(G12.6)
 END

PEAC0354
 PEAC0355
 PEAC0356
 PEAC0357
 PEAC0358
 PEAC0359
 PEAC0370

PEAC0371
 PEAC0372
 PEAC0373
 PEAC0374
 PEAC0375
 PEAC0376
 PEAC0377
 PEAC0378
 PEAC0379
 PEAC0380
 PEAC0381
 PEAC0382
 PEAC0383
 PEAC0384
 PEAC0385
 PEAC0386
 PEAC0387
 PEAC0388
 PEAC0389
 PEAC0390
 PEAC0391
 PEAC0392
 PEAC0393
 PEAC0394
 PEAC0395
 PEAC0396
 PEAC0397
 PEAC0398
 PEAC0399
 PEAC0400
 PEAC0401
 PEAC0402

CIMAGE

PROGRAM IMAGE

DATE 4/1/75

AUTHOR D CROOKS

PURPOSE (1) TO PRODUCE IMAGE(S) OF USER-SPECIFIED COMPONENTS OF THE DATA VECTORS OF CREATED DISK FILES USING THE PITCHR SUBROUTINE--FOR THIS PROGRAM, DATA RECORDS ARE READ FROM FILECODE 03, HEADER RECORDS FROM FILECODE 02.

(2) TO PRINT ADJACENT TO EACH IMAGE ROW THE NUMERICAL VALUE OF THE SPECIFIED COMPONENT FOR EACH COMMAND ANGLE OF THE SCAY ROW.

(3) TO PRODUCE HISTOGRAM(S) FOR USER-SPECIFIED COMPONENTS WHEN REQUESTED--IF REQUESTED, A HISTOGRAM IS PRODUCED FOR EACH DATA SEGMENT OF A CREATED DISK FILE.

DATA CARDS ONE OR MORE COMPONENT-IMAGE REQUESTS--
EACH REQUEST CONSISTS OF 1 - 3 CARDS. EACH OF A
DISTINCT TYPE. THE FIVE POSSIBLE CARD TYPES ARE--

COL.8 COL.16

- (1) MAX (MAXIMUM VALUE OF COMP.--F8.3)
- (2) MIN (MINIMUM VALUE OF COMP.--F8.3)
- (3) HISTOG (HISTOGRAM OPTION DESIRED--A4)

HISTOGRAM OPTIONS--

NO (NO HISTOGRAM PRODUCED)
 SAME (HISTOGRAM IS PRODUCED USING MAX-MIN
 VALUES ALREADY SPECIFIED)
 TRUE (HIST. IS PRODUCED USING ACTUAL MAX-MIN
 VALUES OF DATA SEGMENT)

- (4) TITLE (COMPONENT DESCRIPTION--A54)
- (5) COMP (2-DIGIT COMP, NUMBER--12)

INPUT VALUES FOR EACH CARD ARE LEFT-JUSTIFIED IN
COLUMNS 8, 16.

CARD TYPE (5) MUST APPEAR AS THE LAST CARD IN EACH

REQUEST.

IF FEWER THAN 5 CARDS APPEAR IN THE COMPONENT-IMAGE REQUEST, THOSE VARIABLES FOR WHICH CARDS DO NOT APPEAR ARE ASSUMED TO HAVE THE SAME VALUES AS SPECIFIED IN THE PRECEDING REQUEST.

DECK SET-UP

S IDENT 9999,USER

PRECEDING ACTIVITIES

S SELECT JYOUNG/IMAGE
S EXECUTE
S LIMITS 10,15K
S DATA 05

(DATA CARDS).

S DISK 02,X2R
S DISK 03,X3R
S PRMFL LB,R,S,PATTERN/GEE/LIB

OTHER ACTIVITIES
(OPTIONAL)

S ENDJGD

DECLARATIONS

DIMENSION MDATE(3),N1(4),N2(12)
DIMENSION DATAV(100)

IS A SINGLE DATA VECTOR READ FROM FILECODE 03 FROM WHICH THE APPROPRIATE COMPONENT VALUE WILL BE SELECTED

DIMENSION X(12)

IS AN ARRAY SENT TO THE PITCHR SUBROUTINE CONTAINING VALUES OF A SINGLE COMPONENT FOR A PARTICULAR SCAN ROW

DIMENSION XX(12)

IS AN ARRAY LIKE X, EXCEPT PRINTED INSTEAD OF BEING SENT TO PITCHR--MAY ALSO BE SENT TO HISTOGRAM SUBROUTINES.

CHARACTER ICMND=6,CPNAME=54

REFER TO INFORMATION TYPE OF AN INPUT VALUE (GIVEN IN COL. 8) AND TO THE COMPONENT NAME SPECIFIED BY USER

C CHARACTER HISTOG=4
C CHARACTER NTITLE=60,NTITLE=60

C NTITLE IS THE TITLE OF A PARTICULAR DATA SEGMENT
C NTITLE IS THE TITLE OF A CREATED DISK WORKING FILE.

C LOGICAL LEFTRT

C IS TRUE WHEN COMPONENT VALUES BEING COLLECTED IN X ARRAY AND
C XX ARRAY ARE FROM A LEFT-TO-RIGHT SATELLITE SCAN

C DATA DEFLT/037777777777/

C IS THE DEFAULT VALUE INDICATED FOR COMPONENTS ON DISC

C CALL FXOPT(85,1,1,1)
C CALL FXALT(920)

C READ USER-SPECIFIED COMPONENT INFORMATION--
C CARDS READ UNTIL COMP. NUMBER
C SPECIFICATION IS FOUND.
C XMAX,XMIN ARE MAXIMUM AND MINIMUM
C VALUES OF A PARTICULAR COMPONENT
C ICOMP IS COMP. NO. OF INTEREST TO USER

506 READ(5,500,END=509)ICMND

500 FORMAT(7X,A6)

BACKSPACE 5

IF(ICMND.EQ.'TITLE') GO TO 503

IF(ICMND.EQ.'COMP') GO TO 504

IF(ICMND.EQ.'MAX') GO TO 502

IF(ICMND.EQ.'MIN') GO TO 501

IF(ICMND.EQ.'HISTOG') GO TO 520

WRITE(6,510)

510 FORMAT('0','ILLEGAL COMMAND IN COL. 8 OF USER INPUT, '//)

GO TO 509

501 READ(5,505)XMIN

505 FORMAT(15X,F8,3)

GO TO 506

502 READ(5,505) XMAX

GO TO 506

503 READ(5,507)CPNAME

507 FORMAT(15X,A54)

GO TO 506

520 READ(5,522)HISTOG

522 FORMAT(15X,A4)

GO TO 506

504 READ(5,508)ICOMP

508 FORMAT(15X,I2)

C ECHO-PRINT USER'S COMPONENT SPECIFICATION

ORIGINAL PAGE IS
OF POOR QUALITY

```

C      WRITE(6,550)ICOMP,CPNAME,XMIN,XMAX
550 FORMAT('1',6X,'COMPONENT ',12,5X,A54,5X,'MINIMUM ',F8.3,5X,'MAXIMUM
      1M ',F8.3,5X,')
      WRITE(6,523)HISTOG
523 FORMAT('0',6X,'HISTOGRAM ',2A4,1X,'MAX-MIN VALUES')

```

```

      READ MASTER HEADER FROM DISK
      PROCESS REMAINDER OF DISK WORKING-FILE.
      MDSEG IS NO. OF DATA SEGMENTS IN CURRENT
      WORKING FILE
      MWPR IS NO. WORDS PER RECORD FOR THAT FILE

```

```

10 READ(02,END=20)MTITLE,MDATE,MUSEG,MWPR
   WRITE(6,39)MTITLE,MUSEG,MWPR
39 FORMAT('///1X,'MASTER HEADER',16X,A60/1X,'NO. DATA SEGMENTS',13/1X,'
      1WORDS/DATA RECORD',14)
   DO 30 L=1,MUSEG

```

```

      PROCESS SINGLE DATA SEGMENT IN WORKING-FILE
      READ HEADER RECORD
      NRECD IS NO. OF DATA RECORDS FOR THAT
      HEADER RECORD

```

```

      READ(02)N1,NRECD,N2,NTITLE

```

```

      CALL PITCHR SUBROUTINE

```

```

      NSNAP=2*NDROW
      CALL PITCHR(X,1,12,NSNAP,0,XMIN,XMAX,1,0,,129,1000000,3,,2,,)

```

```

      CALL HISTOGRAM INITIALIZING ROUTINE IF
      HIST. IS TO BE CALCULATED USING SAME
      MAX-MIN VALUES SENT TO PITCHR.

```

```

      IF(HISTOG.EQ.'SAME') CALL DFIN(12,NRECD,XMIN,XMAX)

```

```

      PROCESS REMAINDER OF DATA SEGMENT
      XXMIN, XXMAX GIVE CURRENT TRUE MIN. AND
      TRUE MAX. FOR THE DATA SEGMENT

```

```

      READ(03)(DATAV(I),I=1,MWPR)
      XXMIN=DATAV(1COMP)
      IF(XXMIN.EQ.DEFLT) XXMIN = (XMIN + XMAX)/2
      XXMAX=DATAV(1COMP)
      BACKSPACE 3
      INDEX=0

```

```

      LEFTRY=.FALSE.
      DO 50 J=1,NDROW

```

```
INDEX=INDEX+1
IF(LEFTRT)GO TO 60
```

COLLECTION OF ROW VALUES FOR RT-LEFT SCAN

```
DO 70 K=1,12
READ(03)(DATAV(I),I=1,MWPR)
XX(K)=DATAV(ICOMP)
IF(XX(K).LT.XXMIN.AND.XX(K).NE.DEFLT) XXMIN = XX(K)
IF(XX(K).GT.XXMAX) XXMAX=XX(K)
X(K)=DATAV(ICOMP)
70 IF(X(K).EQ. DEFLT)X(K)=XXMIN
```

DEFAULT VALUES FOR A COMPONENT ARE SET TO XXMIN BEFORE SCAN ROW
DATA IS SENT TO PITCHR,

```
LEFTRT=.TRUE.
GO TO 90
```

COLLECTION OF ROW VALUES FOR LEFT-RT SCAN

```
60 DO 80 K=1,12
READ(03)(DATAV(I),I=1,MWPR)
XX(13-K)=DATAV(ICOMP)
IF(XX(13-K).LT.XXMIN.AND.XX(13-K).NE.DEFLT) XXMIN = XX(13-K)
IF(XX(13-K).GT.XXMAX) XXMAX = XX(13-K)
X(13-K)=DATAV(ICOMP)
80 IF(X(13-K).EQ. DEFLT)X(13-K)=XXMIN
LEFTRT=.FALSE.
```

CALL SNAP FOR ROW IMAGE
WRITE COMPONENT VALUES NEXT TO IMAGE ROW
CALL DENSITY FUNCTION CALCULATING ROUTINE
IF 'SAME' OPTION WAS INDICATED.

```
90 CALL SNAP
WRITE(6,100) INDEX,(XX(M),M=1,12)
100 FORMAT(1H+,39X,I2,2X,12F7.2)
IF(HISTOG.EQ.'SAME') CALL DF(XX)
30 CALL SNAP
```

PRINT HEADER TITLE

```
WRITE(6,40)NTITLE
40 FORMAT(1H+,39X,A60)
WRITE(6,102)XXMIN,XXMAX
102 FORMAT(///1X,'TRUE MINIMUM VALUE IS ',F10.5/1X,'TRUE MAXIMUM VALUE
1 IS ',F10.5///)
IF(HISTOG.EQ.'SAME') CALL DFOUT(CPNAME)
IF(HISTOG.NE.'TRUE')GO TO 30
```

IF HISTOGRAM OPTION WAS TRUE, HISTOGRAM
FOR COMP. IS NOW CALCULATED USING TRUE
MAX-MIN VALUES

```
CALL DFIN(12,NRECRD,XXMIN,XXMAX)
DO 103 K=1,NRECRD
103 BACKSPACE 3
DO 530 J=1,NDROW
DO 531 K=1,12
READ(03)(DATAV(I),I=1,MWPR)
531 XX(K)=DATAV(ICOMP)
530 CALL DF(XX)
CALL DFOUT(CPNAME)
```

PROCESS NEXT DATA-SEGMENT OF WORKING-FILE

```
30 CONTINUE
```

CLOSE CURRENT WORKING-FILES-

```
CALL FCLOSE(02)
CALL FCLOSE(03)
GO TO 10
```

PREPARE TO HANDLE NEXT COMPONENT-REQUEST

```
20 REWIND 2
REWIND 1
GO TO 506
509 STOP
END
```



```

XMAX=XXMAX
RANGE=XMAX-XMIN
DANGE=(FLOAT(NG)-1,E-10)/RANGE
DO 1 I=1,NG
1  F(I)=0
RETURN
END

CSCF      D F O U T
C          DATE INFORMATION 7/22/72 RMH
C          THIS SUBROUTINE OUTPUTS A HISTOGRAM
C          SUBROUTINE DFOUT(NAME)
COMMON/DFB/PROB(50),NPPCAL,NTOTAL,START,END,NCALL,INTERS
COMMON /DFB/ DANGE,AMEAN,VAR
DIMENSION NAME(9),F(6),LINE(60)
DATA IBLANK,L1,ISTAR,IDASH,IONE/1H ,1H1,1H*,1H-,1H1/
LHIST = 40
INTER1=INTERS+1
XINTR=END-START
XDIV=XINTR/FLOAT(INTERS)

C          FIND MAXIMUM PROBABILITY
C
DO 3 I=1,INTERS
3 IF(PROB(I).GT,A) A=PROB(I)

C          SET B TO PROBABILITY INTERVAL SIZE
C
B = A / FLOAT(LHIST)

C          WRITE OUT HEADER FOR HISTOGRAM
C
DO 11 I=1,60
11 LINE(I)=IDASH
WRITE(6,106)
WRITE(6,107) (LINE(I),I=1,59)
WRITE(6,100) NAME,XDIV,START,END,INTERS
WRITE(6,105) AMEAN,VAR
LINE(INTERS+1)=IONE
DO 6 I=1,INTERS
6 LINE(I)=IBLANK

C          FILL STARS IN LINE ARRAY ACCORDING TO PRO
C
DO 4 I=1,LHIST
DO 5 J=1,INTERS
5 IF(PROB(J).GE,A) LINE(J)=ISTAR
WRITE(6,101) A,(LINE(L),L=1,INTER1)
4 A=A-B

C          WRITE OUT TRAILER

```

SCAT0024
SCAT0025
SCAT0026
SCAT0027
SCAT0028
SCAT0029
SCAT0030
SCAT0031
SCAT0032
SCAT0033
SCAT0034
SCAT0035
SCAT0036
SCAT0037
SCAT0038
SCAT0039
SCAT0040
SCAT0041
SCAT0042
SCAT0043
SCAT0044
SCAT0045
SCAT0046

ORIGINAL PAGE IS
OF POOR QUALITY


```

C
DO 7 I=1, INTERS
7 LINE(I)=LI
WRITE(6,102) (LINE(I), I=1, INTER1)
DO 8 I=1, INTERS
8 LINE(I)=IBLANK
DO 9 I=5, INTERS, 10
9 LINE(I)=LI
WRITE(6,104) (LINE(I), I=1, INTER1)
N=0
DO 10 I=5, INTERS, 10
N=N+1
10 F(N)=START.XDIV.FLOAT(I)
WRITE(6,103) (F(I), I=1, N)
WRITE(6,99)
DO 12 I=1, 60
12 LINE(I)=IDASH
WRITE(6,107) (LINE(I), I=1, 59)
106 FORMAT(1H1)
107 FORMAT(9X,1H1,59A1,1H1)
100 FORMAT(9X,1H1,11X,25HHISTOGRAM OF DISTRIBUTION,
123X,1H1/9X,1H1,2X,9A6,3X,1H1/9X,1H1,11X,
2 13HINTERVAL SIZE,F10.4,25X,1H1,/9X,1H1,11X,
314HDATA STARTS AT,F10.4,2X,11HAND ENDS AT,F10.4,
4 1X,1H1/9X,1H1,11X,25HNUMBER OF CLASS INTERVALS,
5 14,19X,1H1/9X,1H1,59X,1H1/9X,1H1,12H PROBABILITY,
647X,1H1)
105 FORMAT(9X,1H1,11X,5HMEAN=F10.3,4X,10H VARIANCE=,
1 F10.3,9X,1H1)
101 FORMAT(7X,2H1 ,F6.4,2H I:101A1)
102 FORMAT(9X,1H1,8X,1H1,101A1)
104 FORMAT(7X,1H1,9X,101A1)
103 FORMAT(9X,1H1,8X,5F10.4,1X,1H1)
99 FORMAT(9X,1H1,59X,1H1/9X,1H1,25X,15HRANDOM VARIABLE,
1 19X,1H1/2(9X,1H1,59X,1H1/))
RETURN
END

```

```

SCAT0047
SCAT0048
SCAT0049
SCAT0050
SCAT0051
SCAT0052
SCAT0053
SCAT0054
SCAT0055
SCAT0056
SCAT0057
SCAT0058
SCAT0059
SCAT0060
SCAT0061

```

```

SCAT0063
SCAT0064
SCAT0065
SCAT0066
SCAT0067
SCAT0068

```

```

SCAT0070
SCAT0071
SCAT0072
SCAT0073

```

```

SCAT0076
SCAT0077
SCAT0078

```

```

SCAT0080
SCAT0081
SCAT0082
SCAT0083

```

C-SCAT S C A T T E R G R A M

LANGUAGE -- HONEYWELL'S SERIES 6000 FORTRAN
SYSTEM RELEASE 8.

WRITTEN BY JAMES KAHN 14-JULY-75.

PURPOSE

THIS PROGRAM PRODUCES SCATTERGRAMS FROM DATA ON FILE CODES 2 AND 3, WHICH WERE GENERATED DURING THE PREVIOUS TRANS-GENERATOR ACTIVITY. SCATTERGRAMS ARE PRODUCED BY SUBROUTINE "SCAT" AND CONTROL INFORMATION IS INTERPRETED BY SUBROUTINE "READ" FROM FILE CODE 5. A CONTROL DIRECTIVE LISTING PLUS ERROR MESSAGES IS PRINTED OUT ON FILE CODE 6. THE SCATTERGRAMS ARE PRINTED OUT TO FILE CODE 42.

SCATTERGRAM DATA POINTS ARE COLLECTED FROM ALL FILES WITHIN FILE CODE 3 OR UNTIL THE DATA POINT VECTOR ARRAYS (XVECTOR AND YVECTOR) ARE FULL. NOTE ALSO THAT BETWEEN FILE SEARCHES WHEN THE DATA POINTS ARE BEING LISTED ON FILE CODE 42, THAT THE DEFAULT VALUES ARE REMOVED FROM THE ARRAYS THUS RESULTING IN LESS WASTAGE OF STORAGE SPACE. AN EOF ON THE DIRECTIVE INPUT FILE WILL RESULT IN SCATTERGRAM SKIPPING TO THE NEXT DATA FILE FOR SUBSEQUENT PROCESSING.

CONTENTS OF THE SCATTERGRAM PROGRAM

..... (MAIN LINE)
READ (DIRECTIVE INTERPRETER)
SCAT (PRODUCES THE SCATTERGRAM)

MSCAT001
MSCAT002
MSCAT003
MSCAT003
MSCAT003
MSCAT004
MSCAT005
MSCAT006
MSCAT007
MSCAT008
MSCAT009
MSCAT010
MSCAT011
MSCAT012
MSCAT013
MSCAT014
MSCAT015
MSCAT016
MSCAT017
MSCAT018
MSCAT019
MSCAT020
MSCAT021
MSCAT022
MSCAT023
MSCAT024
MSCAT025
MSCAT026
MSCAT027
MSCAT028
MSCAT029
MSCAT030
MSCAT031
MSCAT032
MSCAT033
MSCAT033
MSCAT034
MSCAT035
MSCAT035
MSCAT037
MSCAT038
MSCAT039
MSCAT040
MSCAT041
MSCAT042
MSCAT043
MSCAT044
MSCAT045
MSCAT046
MSCAT047
MSCAT048
MSCAT049

DIRECTIVES

CENTER

TWO REAL VALUES CONTAINING A DECIMAL POINT WHICH SPECIFY THE CENTER OF THE XAXIS AND THE CENTER OF THE YAXIS OF THE SCATTERGRAM. A NULL FIELD RESULTS IN AUTOMATIC CENTERING OF THE RESPECTIVE AXIS OF THE SCATTERGRAM.

RANGE

TWO REAL VARIABLES WHICH ARE COMMA SEPERATED DETERMINING THE RANGE OF THE XAXIS AND THE YAXIS OF THE SCATTERGRAM, RESPECTIVE. EACH VARIABLE MUST END WITH A PERIOD UNLESS IT IS TO BE NULLED. THIS WILL RESULT IN THE CURRENT RANGE FOR THAT AXIS BEING RETAINED.

RESCAT

NO VARIABLE FIELD. THIS DIRECTIVE RESULTS IN A SCATTERGRAM BEING PERFORMED USING THE DATA COLLECTED FROM THE LAST 'SCAT' DIRECTIVE.

SCAT

THREE VARIABLES IN THE VARIABLE FIELD(COLUMNS 16 - 72) WHICH DETERMINE THE COORDINATES OF OF THE POINTS OF THE XVECTOR AND THE YVECTOR ARRAYS WHICH ARE INPUT TO THE SCATTERGRAM SUBROUTINE. THE FORMAT OF EACH VARIABLE IS THE COMPONENT NUMBER WHICH IS SEPERATED BY A '-' FROM THE COMMAND ANGLE. THE THIRD FIELD IS OPTIONAL. IF USED IT CONTAINS THE COMPONENT LOCATION OF THE USER SUPPLIED GRAPH SYMBOLS. THESE THREE VARIABLES MUST BE COMMA SEPERATED.

TITLE

THE 60 CHARACTER VARIABLE FIELD(COLUMNS 16 - 76) IS USED AS THE TITLE OF THE SCATTERGRAMS UNTIL CHANGED BY A NEW 'TITLE' DIRECTIVE. THE DEFAULT TITLE IS THE TITLE FROM THE MASTER HEADER(ON FILE CODE 3).

XAXIS

THE 12-CHARACTER FIELD IS USED TO LABEL THE THE XAXIS OF THE SCATTERGRAM AND THE XVECTOR LISTING. THIS FIELD EXTENDS FROM COLUMNS 16 - 28.

YAXIS

THE 12-CHARACTER FIELD IS USED TO LABEL THE THE YAXIS OF THE SCATTERGRAM AND THE YVECTOR LISTING. THIS FIELD EXTENDS FROM COLUMNS 16 - 28.

MSCAT053
MSCAT054
MSCAT055
MSCAT056
MSCAT057
MSCAT058
MSCAT059
MSCAT060
MSCAT061
MSCAT062
MSCAT063
MSCAT064
MSCAT065
MSCAT066
MSCAT067
MSCAT068
MSCAT069
MSCAT070
MSCAT071
MSCAT072
MSCAT073
MSCAT074
MSCAT075
MSCAT076
MSCAT077
MSCAT078
MSCAT079
MSCAT080
MSCAT081
MSCAT082
MSCAT083
MSCAT084
MSCAT085
MSCAT086
MSCAT087
MSCAT088
MSCAT089
MSCAT090
MSCAT091
MSCAT092
MSCAT093
MSCAT094
MSCAT095
MSCAT096
MSCAT097
MSCAT098
MSCAT099
MSCAT100
MSCAT101
MSCAT102
MSCAT103
MSCAT104
MSCAT105
MSCAT106
MSCAT107
MSCAT108
MSCAT109
MSCAT110
MSCAT111

SAMPLE PROGRAM

```

TITLE      THIS A SAMPLE SCATTERGRAM PROGRAM
XAXIS      XAXIS TITLE
YAXIS      YAXIS TITLE
RANGE      10.0          USE DEFAULT FOR THE XAXIS RANGE
SCAT       17-1,15-3     THIS IS A COMMENT
RANGE      1.55          USE DEFAULT YAXIS RANGE VALUE
SCAT       14-5,11-3,10

```

EXPLANATION OF THE SAMPLE PROGRAM

BOTH SCATTERGRAMS ARE TITLED 'THIS IS A SAMPLE SCATTERGRAM PROGRAM'. THE XAXIS IS LABELED 'XAXIS TITLE' AND THE YAXIS IS LABELED 'YAXIS TITLE' AS WELL AS THE RESPECTIVE XVECTOR AND YVECTOR ARRAY LISTINGS. THE RANGE IS SET TO 10.0 FOR THE YAXIS AND THE XAXIS RANGE IS LEFT DEFAULT. THE SCATTERGRAM XAXIS POINTS CONSIST OF ALL POINTS FROM COMPONENT NUMBER 17 WHICH ARE PART OF COMMAND ANGLE 1. THE YAXIS POINTS OF THE SCATTERGRAM CONSIST OF ALL POINTS FROM COMPONENT 15 OF THE DATA RECORD WHICH IS PART OF COMMAND ANGLE 3. THE DEFAULT PLOT SYMBOL, '*', IS USED FOR THE SCATTERGRAM.

THE SECOND SCATTERGRAM ALTERS THE RANGE OF THE XAXIS TO 1.55, BUT USES THE CURRENT RANGE OF THE YAXIS, 10.0. THE XAXIS POINTS CONSIST OF POINTS FROM COMPONENT NUMBER 14 WHICH ARE PART OF COMMAND ANGLE 5. THE YAXIS POINTS COME FROM COMPONENT NUMBER 11 WHICH IS PART OF COMMAND ANGLE 3. USER SYMBOLS FROM COMMAND ANGLE 5 AND COMPONENT NUMBER 10 ARE USED INSTEAD OF THE DEFAULT PLOT SYMBOLS.

```

MSCAT111
MSCAT112
MSCAT113
MSCAT114
MSCAT115
MSCAT116
MSCAT117
MSCAT118
MSCAT119
MSCAT120
MSCAT121
MSCAT122
MSCAT123
MSCAT124
MSCAT125
MSCAT126
MSCAT127
MSCAT128
MSCAT129
MSCAT130
MSCAT131
MSCAT132
MSCAT133
MSCAT134
MSCAT135
MSCAT136
MSCAT137
MSCAT138
MSCAT139
MSCAT140
MSCAT141
MSCAT142
MSCAT143
MSCAT144
MSCAT145
MSCAT146
MSCAT147
MSCAT148
MSCAT149
MSCAT150
MSCAT151
MSCAT152
MSCAT153
MSCAT154
MSCAT155
MSCAT156
MSCAT157
MSCAT158
MSCAT159

```

ORIGINAL PAGE IS
OF POOR QUALITY

CC

```

PARAMETER CMUS = 7, DSEGS = 50, VMAX = 1092, XDATA = 50
IMPLICIT INTEGER ( A - Z )
COMMON /READG/ ENDLNE, ENOREC, EOF, REAL
REAL PANDEF ( 2 ) / 2 * 10.0 /, RCENTER ( 3 ), PFIELD
INTEGER BLANK / ' ' /, CENTER ( 2 ) / 2 * 037777777777 /,
1 COMANGLE ( 2 ), DATA ( XDATA ), DEFAULT / 037777777777 /,
2 MASTER ( 15 ), RANGE ( 2 ), RECORDJ ( 2 ),
3 SUBFIELD ( 3 ), SYMBOLS ( VMAX ), XREF ( VMAX ),
4 XVECTOR ( VMAX ), YVECTOR ( VMAX ), MFILES / 1 /
CHARACTER COMMAND, INPUT * 60, TITLE * 50 / ' ' /,
1 OLDITLE * 60, XAXIS * 12 / ' ' /, YAXIS * 12 / ' ' /,
2 COMMANDS ( CMDS ) / 'RESCAT', 'TITLE', 'XAXIS', 'YAXIS',
3 'CENTER', 'RANGE', 'SCAT' /, CSYMBOL ( VMAX ), RLABEL,
4 TOP * 12 / 'MASTER - 1' /, DATASEG ( DSEGS )
EQUIVALENCE ( XQOM, COMANGLE ( 1 ), ( YQOM, COMANGLE ( 2 ),
1 ( XREC, RECORDS ( 1 ), ( YREC, RECORDS ( 2 ),
2 ( OLDITLE, MASTER ( 1 ), ( RECSIZE, MASTER ( 15 ),
3 ( SERIAL, DATA ( 1 ), ( RANGE, RANGEF ),
4 ( SYMBOLS, CSYMBOL ), ( RCENTER, CENTER ),
5 ( RFIELD, SUBFIELD ( 2 ) )

```

CCCC

PRINT ACTIVITY BANNER

```
WRITE( 6, 500 )  
CALL READ( INPUT, COMMAND, SUBFIELD, COMMANDS, 4 )
```

333

LOAD MASTER HEADER

```

READ( 2, END = 490 ) MASTER
RECERROR = RECSIZE + 1
ASSIGN 150 TO OPEN
ASSIGN 250 TO CLOSE
GO TO 25

```

CCCC

ERROR PROCESSING RETURN

010

```
WRITE( 6, 510 ) SUBFIELD( 1 ), SUBFIELD( 2 )
```

הנהגה

NORMAL PROCESSING RETURN

020

CALL READECHO

22

CIF
C
C

IF A DIRECTIVE EOF OCCURS,
SKIP TO THE NEXT MASTER FILE
AND PROCESS IT.

MSCAT150
MSCAT151
MSCAT153
MSCAT152
MSCAT156
MSCAT155
MSCAT166
MSCAT167
MSCAT152
MSCAT169
MSCAT173
MSCAT171
MSCAT172
MSCAT173
MSCAT174
MSCAT175
MSCAT175
MSCAT177
MSCAT173
MSCAT179
MSCAT190
MSCAT191
MSCAT192
MSCAT193
MSCAT154
MSCAT185
MSCAT126
MSCAT187
MSCAT194
MSCAT199
MSCAT190
MSCAT191
MSCAT192
MSCAT193
MSCAT194
MSCAT195
MSCAT196
MSCAT197
MSCAT199
MSCAT199
MSCAT200
MSCAT201
MSCAT202
MSCAT203
MSCAT204
MSCAT205
MSCAT206
MSCAT207
MSCAT203
MSCAT209
MSCAT211
MSCAT211

MSCAT256
MSCAT265
MSCAT265
MSCAT267
MSCAT268
MSCAT269
MSCAT270
MSCAT271
MSCAT272
MSCAT273
MSCAT274
MSCAT275
MSCAT276
MSCAT277
MSCAT279
MSCAT279
MSCAT290
MSCAT291
MSCAT282
MSCAT283
MSCAT284
MSCAT295
MSCAT285
MSCAT287
MSCAT295
MSCAT299
MSCAT290
MSCAT291
MSCAT292
MSCAT293
MSCAT292
MSCAT295
MSCAT295
MSCAT297
MSCAT299
MSCAT299
MSCAT300
MSCAT301
MSCAT302
MSCAT303
MSCAT304
MSCAT305
MSCAT305
MSCAT307
MSCAT308
MSCAT309
MSCAT310
MSCAT311
MSCAT312
MSCAT313
MSCAT314
MSCAT315

```

070      RCENTER( LOAD ) = - PFIELD
02C      CALL SORT
          GO TO 20
C.....
C
C
C      RANGE DIRECTIVE PROCESSED
C.....
006      DO 90  LOAD = 1, 2
C
C
C      X,Y-RANGES MUST BE REAL
C      NUMBERS.
          IF( REAL ) 90, , 90
          RANGE( LOAD ) = SUBFIELD( 1 )
          CALL SORT
090      GO TO 20
C.....
C
C
C      SCAT DIRECTIVE PROCESSED
C.....
C
C
C      GET COMMAND ANGLE TO BE PROCESSED
C      AND COMPONENT LOCATIONS FROM
C      USER.
007      DO 110  LOAD = 1, 2
C
C
C
C
C      REAL NUMBERS AND NULL FIELDS
C      ARE NOT LEGAL.
          IF( REAL ) , 10, 10
          IF( SUBFIELD( 1 ) ) , 10,
C
C
C
C      THE COMPONENT NUMBER MUST NOT
C      BE GREATER THAN THE MAXIMUM
C      DATA RECORD SIZE TO BE LEGAL.
          IF( SUBFIELD( 1 ) .LT. RECDERROR ) GO TO 100
          WRITE( 6, 590 ) SUBFIELD( 1 ), SUBFIELD( 2 ), RECDERROR
          GO TO 20
100      RECORDS( LOAD ) = SUBFIELD( 1 )
          COMANGLE( LOAD ) = SUBFIELD( 2 )

```

```

MSCAT316
MSCAT317
MSCAT318
MSCAT319
MSCAT320
MSCAT321
MSCAT322
MSCAT323
MSCAT324
MSCAT325
MSCAT326
MSCAT327
MSCAT328
MSCAT329
MSCAT330
MSCAT331
MSCAT332
MSCAT333
MSCAT334
MSCAT335
MSCAT336
MSCAT337
MSCAT338
MSCAT339
MSCAT340
MSCAT341
MSCAT342
MSCAT343
MSCAT344
MSCAT345
MSCAT346
MSCAT347
MSCAT348
MSCAT349
MSCAT350
MSCAT351
MSCAT352
MSCAT353
MSCAT354
MSCAT355
MSCAT356
MSCAT357
MSCAT358
MSCAT359
MSCAT360
MSCAT361
MSCAT362
MSCAT363
MSCAT364
MSCAT365
MSCAT366
MSCAT367
MSCAT368

```



```

110      CALL SORT
          CONTINUE
          ASSIGN 200 TO BYPASS
          SREC = SUBFIELD( 1 )

C
C
C IF
C
C
C
C IF
C
C
C
C
C IF( UTITLE ) 120, . 120
  WRITE( 42, 570 ) CLDTITLE, TOP
  GO TO 130
120  WRITE( 42, 570 ) YTITLE, TOP
130  WRITE( 42, 600 ) XAXIS, YAXIS, XAXIS, YAXIS
      INDEX = 0
      XINDEX = 0
      YINDEX = 0
      DINDEX = 0
      START = 0
      XFULL = - VMAX
      YFULL = - VMAX
      REF = - VMAX
      ASSIGN 180 TO RETURN
      GO TO OPEN
140  READ( 3, END=230 ) ( DATA( I ), I = 1, RECSIZE )
150  WRITE( 4 ) ( DATA( I ), I = 1, RECSIZE )
      GO TO 170
160  READ( 4, END=230 ) ( DATA( I ), I = 1, RECSIZE )
170  COM = SERIAL / 10 ** 8
      ITC = ( SERIAL / 10 ** 7 ) - ( COM * 10 )
      SCAN = ( SERIAL / 10 ** 4 ) - ( ITC * 10 ** 3 ) -
1      ( COM * 10 ** 4 )

C
C
C IF
C
C
C
C
C IF
C
C
C
C
C IF THIS IS THE BEGINNING OF A
  NEW DATA SEGMENT, GO PRINT THE
  PREVIOUS ONE.

180  IF( SCAN .LT. REF ) GO TO 400
      REF = SCAN

C
C
C IF
C
C
C IF THIS IS THE SPECIFIED
  COMMAND ANGLE OF THE XVECTOR,
  SAVE THE SPECIFIED COMPONENT.

```

```

MSCAT359
MSCAT370
MSCAT371
MSCAT372
MSCAT373
MSCAT374
MSCAT375
MSCAT376
MSCAT377
MSCAT378
MSCAT379
MSCAT380
MSCAT381
MSCAT382
MSCAT383
MSCAT384
MSCAT385
MSCAT386
MSCAT387
MSCAT388
MSCAT389
MSCAT390
MSCAT391
MSCAT392
MSCAT393
MSCAT394
MSCAT395
MSCAT396
MSCAT397
MSCAT398
MSCAT399
MSCAT400
MSCAT401
MSCAT402
MSCAT403
MSCAT404
MSCAT405
MSCAT406
MSCAT407
MSCAT408
MSCAT409
MSCAT410
MSCAT411
MSCAT412
MSCAT413
MSCAT414
MSCAT415
MSCAT416
MSCAT417
MSCAT418
MSCAT419
MSCAT420
MSCAT421
MSCAT422

```

MSCAT423
MSCAT424
MSCAT425
MSCAT426
MSCAT427
MSCAT428
MSCAT429
MSCAT430
MSCAT431
MSCAT432
MSCAT433
MSCAT434
MSCAT435
MSCAT436
MSCAT437
MSCAT438
MSCAT439
MSCAT440
MSCAT441
MSCAT442
MSCAT443
MSCAT444
MSCAT445
MSCAT446
MSCAT447
MSCAT448
MSCAT449
MSCAT450
MSCAT451
MSCAT452
MSCAT453
MSCAT454
MSCAT455
MSCAT456
MSCAT457
MSCAT458
MSCAT459
MSCAT460
MSCAT461
MSCAT462
MSCAT463
MSCAT464
MSCAT465
MSCAT466
MSCAT467
MSCAT468
MSCAT469
MSCAT470
MSCAT471
MSCAT472
MSCAT473
MSCAT474

266

```

220 IF( XFULL + YFULL ) 140, , 140
    WRITE( 6, 610 )
230 ASSIGN 240 TO RETURN
    GO TO 400
240 GO TO CLOSE
250 ASSIGN 160 TO OPEN
    ASSIGN 260 TO CLOSE
    TOP = " "
    ENDFILE 4
    REWIND 4
260
C
C
C IF
C
    CHECK FOR ENOUGH POINTS TO GRAPH.
270 IF( INDEX - 4 ) , 280, 280
    WRITE( 6, 620 )
    ENDREC = 0
    GO TO 20
C
C
C IF
C
C
C
    IF THE USER TITLE IS NOT
    PRESENT, USE THE MASTER FILE
    HEADER TITLE.
280 IF( UTITLE ) 290, , 290
    WRITE( 42, 570 ) OLDTITLE, TOP
    GO TO 300
290 WRITE( 42, 570 ) TITLE, TOP
300 CALL SCAT( XVECTOR, YVECTOR, SYMBOLS, START, RANGE( 1 ),
1 RANGE( 2 ), CENTER( 1 ), CENTER( 2 ))
    WRITE( 42, 580 ) XAXIS, YAXIS
    GO TO 20
400 STOP = MIN( XINDEX, YINDEX )
    DINDEX = DINDEX + 1
    WRITE( 42, 630 ) DATASEG( DINDEX )
    START = START + 1
    PRINT = START - STOP
    RPRINT = PRINT / ( - 2 ) + START
C
C
C CDO
C
C
    COMPRESS DATA ARRAYS AND LIST
    THE DATA ACCUMULATED THUS FAR.
    DO 460 COMPACT = START, STOP
C
C
C IF
C
C
C
    DECIDE WHETHER TO PRINT BOTH
    SIDES, THE LEFT SIDE ONLY,
    OR FINISH COMPRESSION OF THE
    DATA ARRAYS.
    IF( PRINT ) , 420, 440

```

```

MSCAT475
MSCAT476
MSCAT477
MSCAT478
MSCAT479
MSCAT480
MSCAT481
MSCAT482
MSCAT483
MSCAT484
MSCAT485
MSCAT486
MSCAT487
MSCAT488
MSCAT489
MSCAT490
MSCAT491
MSCAT492
MSCAT493
MSCAT494
MSCAT495
MSCAT496
MSCAT497
MSCAT498
MSCAT499
MSCAT500
MSCAT501
MSCAT502
MSCAT503
MSCAT504
MSCAT505
MSCAT506
MSCAT507
MSCAT508
MSCAT509
MSCAT510
MSCAT511
MSCAT512
MSCAT513
MSCAT514
MSCAT515
MSCAT516
MSCAT517
MSCAT518
MSCAT519
MSCAT520
MSCAT521
MSCAT522
MSCAT523
MSCAT524
MSCAT525
MSCAT526

```

```

RLABEL = ' '
PRINT = PRINT + 2
RPRINT = RPRINT + 1

```

LABEL VALUES SUPPRESSED FROM THE
DATA ARRAYS ON THE RIGHT SIDE OF
THE LISTING.

```

IF( XVECTOR( RPRINT ) .EQ. DEFAULT .OR.  
YVECTOR( RPRINT ) .EQ. DEFAULT ) RLABEL = ' '

```

LABEL VALUES THAT ARE BEING
SUPPRESSED FROM THE DATA ARRAYS
WHICH ARE ON THE LEFT SIDE OF
THE LISTING.

```

IF( XVECTOR( COMPACT ) .EQ. DEFAULT .OR.  
YVECTOR( COMPACT ) .EQ. DEFAULT ) GO TO 410  
WRITE( 42, 640 ) XREF( COMPACT ), YVECTOR( COMPACT ),  
YVECTOR( COMPACT ), SYMBOLS( COMPACT ),  
XREF( RPRINT ), RLABEL, XVECTOR( RPRINT ),  
YVECTOR( RPRINT ), SYMBOLS( RPRINT )  
GO TO 450  
WRITE( 42, 650 ) XREF( COMPACT ), XVECTOR( COMPACT ),  
YVECTOR( COMPACT ), SYMEQLS( COMPACT ),  
XREF( RPRINT ), RLABEL, XVECTOR( RPRINT ),  
YVECTOR( RPRINT ), SYMBOLS( RPRINT )  
GO TO 460  
PRINT = PRINT + 1

```

LABEL VALUES THAT ARE BEING
SUPPRESSED FROM THE DATA ARRAYS
WHICH ARE ON THE LEFT SIDE.

```

IF( XVECTOR( COMPACT ) .EQ. DEFAULT .OR.  
YVECTOR( COMPACT ) .EQ. DEFAULT ) GO TO 430  
WRITE( 42, 660 ) XREF( COMPACT ), XVECTOR( COMPACT ),  
YVECTOR( COMPACT ), SYMBOLS( COMPACT )  
GO TO 450  
WRITE( 42, 670 ) XREF( COMPACT ), XVECTOR( COMPACT ),  
YVECTOR( COMPACT ), SYMBOLS( COMPACT )  
GO TO 460

```

FINISH CLEANING UP THE DATA
ARRAYS.

```

IF( XVECTOR( COMPACT ) .EQ. DEFAULT .OR.  
YVECTOR( COMPACT ) .EQ. DEFAULT ) GO TO 460

```

```

MSCAT527
MSCAT528
MSCAT529
MSCAT530
MSCAT531
MSCAT532
MSCAT533
MSCAT533
MSCAT534
MSCAT535
MSCAT535
MSCAT537
MSCAT538
MSCAT539
MSCAT540
MSCAT541
MSCAT541
MSCAT542
MSCAT543
MSCAT544
MSCAT545
MSCAT546
MSCAT547
MSCAT548
MSCAT549
MSCAT550
MSCAT551
MSCAT552
MSCAT553
MSCAT554
MSCAT555
MSCAT556
MSCAT557
MSCAT558
MSCAT559
MSCAT560
MSCAT561
MSCAT562
MSCAT563
MSCAT564
MSCAT565
MSCAT566
MSCAT567
MSCAT568
MSCAT569
MSCAT570
MSCAT570
MSCAT570
MSCAT570
MSCAT571

```

```

450      INDEX = INDEX + 1
      XVECTOR( INDEX ) = XVECTOR( COMPACT )
      YVECTOR( INDEX ) = YVECTOR( COMPACT )
      SYMBOLS( INDEX ) = SYMBOLS( COMPACT )
460      CONTINUE
      START = INDEX
      XINDEX = START
      YINDEX = XINDEX
      XFULL = YINDEX - VMAX
      YFULL = XFULL
      GO TO RETURN
490      STOP      *      END OF SCATTERGRAM ACTIVITY*
500      FORMAT( 50X, 'SCATTERGRAM ACTIVITY REPORT', 5( / ) )
510      FORMAT( ' ', 5( ' ' ), ' F SUBFIELD - ', 14', 14,
1      ' ', 11, 14', ' ILLEGAL, IGNORED.', 3( / ) )
520      FORMAT( 9( / ) )
530      FORMAT( 'MASTER -', 12 )
540      FORMAT( 13, ' ', 11 )
550      FORMAT( 5( ' ' ), ' W DATA SEGMENT TABLE OVERFLOW' )
560      FORMAT( ' ', 5( ' ' ), ' F UNRECOGNIZABLE DIRECTIVE.',
1      ' IGNORED.', 3( / ) )
570      FORMAT( '1', 32X, 460, 26X, A12 )
580      FORMAT( '0 THE X-AXIS IS ', A12, 70X, 'THE Y-AXIS IS ',
1      A12 )
590      FORMAT( ' ', 5( ' ' ), ' F SUBFIELD - ', 14', 14,
1      ' ', 11, 14', ' HAS COMPONENT NUMBER GREATER THAN ',
2      14, ' ', ' IGNORED DIRECTIVE' )
600      FORMAT( '0 DATA', 7X, 'INDEX', 3X, 'XVALUES', 10X, 'YVALUES',
1      8X, 'GRAPH', 13X, 'INDEX', 2X, 'XVALUES', 10X, 'YVALUES',
2      8X, 'GRAPH' / ' SEGMENT', 5X, '(SCAN)', 5X, A12, 5X,
3      A12, 5X, 'SYMBOL', 12X, '(SCAN)', 5X, A12, 5X, A12, 5X,
4      'SYMBOL' // )
610      FORMAT( 5( ' ' ), ' W DATA TABLE OVERFLOW, TERMINATING',
1      ' DATA ACQUISITION', 3( / ) )
620      FORMAT( ' ', 5( ' ' ), ' F INSUFFICIENT DATA POINTS FOR',
1      ' SCATTERGRAM' )
630      FORMAT( '0 ', A5 )
640      FORMAT( ' ', 14X, 13, 6X, F10.3, 7X, F10.3, 10X, A1, 16X,
1      13, 1X, A1, 4X, F10.3, 7X, F10.3, 10X, A1, // )
650      FORMAT( ' ', 14X, 13, ' ', 4X, F10.3, 7X, F10.3, 10X, A1,
1      16X, 13, 1X, A1, 4X, F10.3, 7X, F10.3, 10X, A1 // )
660      FORMAT( ' ', 14X, 13, 6X, F10.3, 7X, F10.3, 10X, A1 // )
670      FORMAT( ' ', 14X, 13, ' ', 4X, F10.3, 7X, F10.3, 10X, A1 // )
      END

```

```

MSCAT572
MSCAT573
MSCAT574
MSCAT575
MSCAT576
MSCAT577
MSCAT578
MSCAT579
MSCAT580
MSCAT581
MSCAT582
MSCAT583
MSCAT584
MSCAT585
MSCAT586
MSCAT587
MSCAT588
MSCAT589
MSCAT590
MSCAT591
MSCAT592
MSCAT593
MSCAT594
MSCAT595
MSCAT596
MSCAT597
MSCAT598
MSCAT599
MSCAT600
MSCAT601
MSCAT602
MSCAT603
MSCAT604
MSCAT605
MSCAT606
MSCAT607
MSCAT608
MSCAT609
MSCAT610
MSCAT611
MSCAT612
MSCAT613
MSCAT614
MSCAT615
MSCAT616

```

CSCAT

SCAT VERSION 2

LANGUAGE -- HONEYWELL'S SERIES 6000 FORTRAN
SYSTEM RELEASE 3.

WRITTEN BY JAMES KAHN 10-JULY-75.

PURPOSE

THIS SUBROUTINE PRODUCES A SCATTERGRAM OF THE INPUT VECTORS USING THE USER SUPPLIED VECTOR SYMBOLS TO DENOTE THE VECTOR'S POSITION ON THE GRAPH. IF MORE THAN ONE VECTOR SYMBOL OCCUPIES THE SAME POSITION ON THE SCATTERGRAM, SPECIAL INTERNAL SYMBOLS WILL BE SUBSTITUTED AT THIS POSITION. THIS SYMBOL WILL CORRESPOND TO THE DECIMAL NUMBER OF INTERSECTIONS AT THAT POSITION. IF THE NUMBER OF INTERSECTIONS EXCEEDS 9, THE SYMBOL '*' WILL REPLACE THE NUMERIC SYMBOL AT THAT POSITION. THIS SCATTERGRAM SUBROUTINE ALSO FEATURES OPTIONAL AUTOMATIC AXIS CENTERING. ON THE RIGHT SIDE OF THE SCATTERGRAM INFORMATION ON THE NUMBER OF DATA POINTS, GRAPH INTERVAL SIZES, AND STANDARD DEVIATION PERCENTAGES ARE LISTED FOR THE USER'S CONVIENCE.

SCAT0001
SCAT0002
SCAT0003
SCAT0004
SCAT0005
SCAT0006
SCAT0007
SCAT0008
SCAT0009
SCAT0010
SCAT0011
SCAT0012
SCAT0013
SCAT0014
SCAT0015
SCAT0016
SCAT0017
SCAT0018
SCAT0019
SCAT0020
SCAT0021
SCAT0022
SCAT0023
SCAT0024
SCAT0025
SCAT0026
SCAT0027
SCAT0028
SCAT0029
SCAT0030
SCAT0031
SCAT0032
SCAT0033
SCAT0034
SCAT0035
SCAT0036
SCAT0037
SCAT0038
SCAT0039
SCAT0040
SCAT0041
SCAT0042
SCAT0043
SCAT0044
SCAT0045
SCAT0046
SCAT0047
SCAT0048
SCAT0049
SCAT0050

ORIGINAL PAGE IS
OF POOR QUALITY

CALLING ARGUMENTS

XVECTOR AN ARRAY OF X-VECTORS DIMENSIONED BY VSIZE
 TO BE GRAPHED(REAL).
YVECTOR AN ARRAY OF Y-VECTORS DIMENSIONED BY VSIZE
 TO BE GRAPHED(REAL).
SYMBOLS AN ARRAY OF GRAPH SYMBOLS FOR THE
 CORRESPONDING VECTOR POINTS. IT IS DIMENSIONED
 BY VSIZE(CHARACTER).
VSIZE THE DIMENSION OF THE XVECTOR, YVECTOR, AND
 SYMBOLS ARRAYS(INTEGER).
RANGEX THE RANGE BETWEEN THE MINIMUM AND MAXIMUM
 VALUES OF THE XAXIS ON THE GRAPH(REAL).
RANGEY THE RANGE BETWEEN THE MINIMUM AND MAXIMUM
 VALUES OF THE YAXIS ON THE GRAPH(REAL).
CENTERX THE CENTER OF THE XAXIS. IF DEFAULT, THE
 MIDRANGE OR MEAN OF THE XAXIS WILL BE USED
 (REAL).
CENTERY THE CENTER OF THE YAXIS. IF DEFAULT,
 THE MIDRANGE OR MEAN OF THE YAXIS WILL BE USED
 (REAL).

SCAT0051
 SCAT0052
 SCAT0053
 SCAT0054
 SCAT0055
 SCAT0056
 SCAT0057
 SCAT0058
 SCAT0059
 SCAT0060
 SCAT0061
 SCAT0062
 SCAT0063
 SCAT0064
 SCAT0065
 SCAT0066
 SCAT0067
 SCAT0068
 SCAT0069
 SCAT0070
 SCAT0071
 SCAT0072
 SCAT0073
 SCAT0074
 SCAT0075
 SCAT0076
 SCAT0077
 SCAT0078
 SCAT0079
 SCAT0080
 SCAT0081
 SCAT0082
 SCAT0083
 SCAT0084
 SCAT0085
 SCAT0086
 SCAT0087
 SCAT0088
 SCAT0089
 SCAT0090
 SCAT0091
 SCAT0092
 SCAT0093
 SCAT0094
 SCAT0095
 SCAT0096
 SCAT0097
 SCAT0098
 SCAT0099
 SCAT0100
 SCAT0101
 SCAT0102

```

SUBROUTINE SCAT( VVECTOR, VSIZE, SYMBOLS, RANGE, RANGEY,
1  RANGEY, CENTERX, CENTERY )
  IMPLICIT INTEGER( I - P )
  INTEGER CALC, CHAF( 10 ), DUMMY( 3 ), FILL, LINE( 95 )
2  / 95 * 1 /, VSIZE, SYMBOLS( VSIZE ), XPOINTS( 3 ),
  YPOINTS( 3 )
  REAL POINTS, STAT( 51 ) / 51 * 03777777777777 /, VALUE( 51 )
1  / 51 * 03777777777777 /, VVECTOR( VSIZE ), VVECTOR( VSIZE )
  CHARACTER SOAP( 51 ) / 12 * 'I', 12 * 'I', 12 * 'I', 12 * 'I',
1  12 * 'I', 12 * 'I' /, CHARS( 10 )
2  / 12 * '2', 12 * '3', 12 * '4', 12 * '5', 12 * '6', 12 * '7', 12 * '8', 12 * '9' /
  CHARACTER INFO * 10( 51 ) / 4 * ' ', 4 * ' ', 4 * ' ', 4 * ' ', 4 * ' ', 4 * ' ', 4 * ' ', 4 * ' ', 4 * ' ', 4 * ' ' /
1  3 * ' ', 3 * ' ', 3 * ' ', 3 * ' ', 3 * ' ', 3 * ' ', 3 * ' ', 3 * ' ', 3 * ' ', 3 * ' ' /
2  3 * ' ', 3 * ' ', 3 * ' ', 3 * ' ', 3 * ' ', 3 * ' ', 3 * ' ', 3 * ' ', 3 * ' ', 3 * ' ' /
3  3 * ' ', 3 * ' ', 3 * ' ', 3 * ' ', 3 * ' ', 3 * ' ', 3 * ' ', 3 * ' ', 3 * ' ', 3 * ' ' /
4  3 * ' ', 3 * ' ', 3 * ' ', 3 * ' ', 3 * ' ', 3 * ' ', 3 * ' ', 3 * ' ', 3 * ' ', 3 * ' ' /
5  3 * ' ', 3 * ' ', 3 * ' ', 3 * ' ', 3 * ' ', 3 * ' ', 3 * ' ', 3 * ' ', 3 * ' ', 3 * ' ' /
6  3 * ' ', 3 * ' ', 3 * ' ', 3 * ' ', 3 * ' ', 3 * ' ', 3 * ' ', 3 * ' ', 3 * ' ', 3 * ' ' /
7  3 * ' ', 3 * ' ', 3 * ' ', 3 * ' ', 3 * ' ', 3 * ' ', 3 * ' ', 3 * ' ', 3 * ' ', 3 * ' ' /
8  3 * ' ', 3 * ' ', 3 * ' ', 3 * ' ', 3 * ' ', 3 * ' ', 3 * ' ', 3 * ' ', 3 * ' ', 3 * ' ' /
9  3 * ' ', 3 * ' ', 3 * ' ', 3 * ' ', 3 * ' ', 3 * ' ', 3 * ' ', 3 * ' ', 3 * ' ', 3 * ' ' /
  "X X WITHIN", " ", "X RANGE = ",
  "1 STEV = ", "2 STEV = ", "3 STEV = ",
  "MIN Y = ", "MAX Y = ", "MEAN Y = ",
  "STDEV Y = ", "2 ", "X Y WITHIN", " ",
  "Y RANGE = ", "1 STEV = ", "2 STEV = ",
  "3 STEV = ", "4 " /
  EQUIVALENCE ( TEMP, ITEMP ), ( DEFAULT, VALUE( 1 ) ),
1  ( CENTER, VALUE( 26 ) ), ( MIDX, DUMMY( 1 ) ),
2  ( MEANX, DUMMY( 2 ) ), ( MIDY, DUMMY( 3 ) ),
3  ( POINTS, STAT( 5 ) ), ( DX, STAT( 12 ) ),
4  ( DY, STAT( 13 ) ), ( XMIN, STAT( 18 ) ),
5  ( XMAX, STAT( 19 ) ), ( XMINH, STAT( 21 ) ),
6  ( XSD, STAT( 22 ) ), ( YMIN, STAT( 35 ) ),
7  ( YMAX, STAT( 36 ) ), ( YMEAN, STAT( 33 ) ),
8  ( YSD, STAT( 39 ) ), ( CHAR, CHARS )
  PCY( A, B ) = ( A / 3 ) * 120.
  NOSWITCH = 0

```

NOSWITCH = 0

NOSWITCH = 0

THE X,Y-VECTOR PAIRS PLUS THEIR
ACCOMPANYING GRAPH SYMBOLS ARE
SORTED IN DESCENDING ORDER OF
THE Y VECTOR.

```
00 20  ORDER1 = 1, VSIZE - 1
      00 20  ORDER2 = ORDER1 + 1, VSIZE
```

CHECK FOR DESCENDING ORDER OF THE
Y VECTOR ARRAY.

```
IF( YVECTOR( ORDER1 ) .GE. YVECTOR( ORDER2 ) )
  GO TO 20
```

SCAT0103
SCAT0104
SCAT0105
SCAT0106
SCAT0107
SCAT0108
SCAT0109
SCAT0110
SCAT0111
SCAT0112
SCAT0113
SCAT0114
SCAT0115
SCAT0116
SCAT0117
SCAT0118
SCAT0119
SCAT0120
SCAT0121
SCAT0123
SCAT0125
SCAT0126
SCAT0129
SCAT0130
SCAT0131
SCAT0132
SCAT0133
SCAT0134
SCAT0135
SCAT0136
SCAT0137
SCAT0139
SCAT0139
SCAT0140
SCAT0141
SCAT0142
SCAT0143
SCAT0144
SCAT0145
SCAT0146
SCAT0147
SCAT0148
SCAT0149
SCAT0150
SCAT0151
SCAT0152
SCAT0153
SCAT0154
SCAT0155
SCAT0156
SCAT0157
SCAT0159

SWAP X,Y-VECTOR PAIRS AND
ACCOMPANYING GRAPH SYMBOLS TO
ORDER Y VECTORS AND SET RESOPT
INDICATOR.

NOSWITCH = NOSWITCH + 1
TEMP = XVECTOR(ORDER1)
XVECTOR(ORDER1) = XVECTOR(ORDER2)
XVECTOR(ORDER2) = TEMP
TEMP = YVECTOR(ORDER1)
YVECTOR(ORDER1) = YVECTOR(ORDER2)
YVECTOR(ORDER2) = TEMP
ITEMP = SYMBOLS(ORDER1)
SYMBOLS(ORDER1) = SYMBOLS(ORDER2)
SYMBOLS(ORDER2) = ITEMP
CONTINUE

CHECK THE RESOPT INDICATOR AND
SORT THE Y VECTORS AGAIN IF IT
IS ON.

IF(NOSWITCH) 10, . 10
XMAX = XVECTOR(1)
XMIN = XMAX
YMAX = YVECTOR(1)
YMIN = YVECTOR(VSIZE)
XSUM = 0.
YSUM = 0.
XSS = 0.
YSS = 0.

CALCULATE THE MINIMUM AND
MAXIMUM OF THE X VECTORS.
CALCULATE THE SUM AND SUM OF
SQUARES OF THE X,Y-VECTOR PAIRS.

DO 30 CALC = 1, VSIZE
TEMP = XVECTOR(CALC)
XSUM = XSUM + TEMP
XMAX = AMAX1(XMAX, TEMP)
XMIN = AMIN1(XMIN, TEMP)
XSS = XSS + TEMP ** 2
YSUM = YSUM + YVECTOR(CALC)
YSS = YSS + YVECTOR(CALC) ** 2
CONTINUE
POINTS = VSIZE

SCAT0159
SCAT0160
SCAT0161
SCAT0162
SCAT0163
SCAT0164
SCAT0165
SCAT0166
SCAT0167
SCAT0168
SCAT0169
SCAT0170
SCAT0171
SCAT0172
SCAT0173
SCAT0174
SCAT0175
SCAT0176
SCAT0177
SCAT0178
SCAT0179
SCAT0180
SCAT0181
SCAT0182
SCAT0183
SCAT0184
SCAT0185
SCAT0186
SCAT0187
SCAT0188
SCAT0189
SCAT0190
SCAT0191
SCAT0192
SCAT0193
SCAT0194
SCAT0195
SCAT0196
SCAT0197
SCAT0198
SCAT0199
SCAT0200
SCAT0201
SCAT0202
SCAT0203
SCAT0204
SCAT0205
SCAT0206
SCAT0207
SCAT0208
SCAT0209
SCAT0210

COMPUTE THE MEAN AND STANDARD
DEVIATION OF THE X,Y-VECTOR
PAIRS.

```

XMEAN = XSUM / POINTS
TEMP = XSS / POINTS - XMEAN ** 2
IF( TEMP .LT. 0. ) TEMP = 0.
XSD = SQRT( TEMP )
YMEAN = YSUM / POINTS
TEMP = YSS / POINTS - YMEAN ** 2
IF( TEMP .LT. 0. ) TEMP = 0.
YSD = SQRT( TEMP )
ENTRY RESCAT

```

INITIALIZE COUNTERS FOR THE
FOLLOWING STANDARD DEVIATION
POINT COMPUTATION.

```

DO 40 INIT = 1, 3
  XPOINTS( INIT ) = 0
  YPOINTS( INIT ) = 0
  DUMMY( INIT ) = 0
  CONTINUE
MEANX = 0
XFRANGE = RANGE / 2.
DX = XFRANGE / 48.
XGRAPH = XFRANGE - DX / 2.
YFRANGE = RANGE / 2.
DY = YFRANGE / 26.
YGRAPH = YFRANGE - DY / 2.
XCENTER = CENTERX

```

IF THE USER DID NOT SUPPLY AN
XAXIS CENTER FOR THE GRAPH,
THEN USE THE DEFAULT XAXIS
CENTER.

```

IF( XCENTER .EQ. DEFAULT ) XCENTER = ( XMAX + XMIN ) / 2.
YCENTER = CENTERY

```

IF THE USER DID NOT SUPPLY A
YAXIS CENTER, THEN USE THE
DEFAULT YAXIS CENTER.

```

IF( YCENTER .EQ. DEFAULT ) YCENTER = ( YMAX + YMIN ) / 2.

```

COMPUTE THE NUMBER OF GRAPH
POINTS THAT ARE WITHIN ONE

SCAT0211
SCAT0212
SCAT0213
SCAT0214
SCAT0215
SCAT0216
SCAT0217
SCAT0218
SCAT0219
SCAT0220
SCAT0221
SCAT0222
SCAT0223
SCAT0224
SCAT0225
SCAT0226
SCAT0227
SCAT0228
SCAT0229
SCAT0230
SCAT0231
SCAT0232
SCAT0233
SCAT0234
SCAT0235
SCAT0236
SCAT0237
SCAT0238
SCAT0239
SCAT0240
SCAT0241
SCAT0242
SCAT0243
SCAT0244
SCAT0245
SCAT0246
SCAT0247
SCAT0248
SCAT0249
SCAT0250
SCAT0251
SCAT0252
SCAT0253
SCAT0254
SCAT0255
SCAT0256
SCAT0257
SCAT0258
SCAT0259
SCAT0260
SCAT0261
SCAT0262

ORIGINAL PAGE IS
OF POOR QUALITY

COUNT THE NUMBER OF GRAPH POINTS OF THE Y-AXIS THAT ARE WITHIN THE THREE STD. DEV. RANGES.

SCAT0265
SCAT0266
SCAT0267
SCAT0268
SCAT0269
SCAT0270
SCAT0271
SCAT0272
SCAT0273
SCAT0274
SCAT0275
SCAT0276
SCAT0277
SCAT0278
SCAT0279
SCAT0280
SCAT0281
SCAT0282
SCAT0283
SCAT0284
SCAT0285
SCAT0286
SCAT0287
SCAT0288
SCAT0289
SCAT0290
SCAT0291
SCAT0292
SCAT0293
SCAT0294
SCAT0295
SCAT0296
SCAT0297
SCAT0298
SCAT0299
SCAT0300
SCAT0301
SCAT0302
SCAT0303
SCAT0304
SCAT0305
SCAT0306
SCAT0307
SCAT0308
SCAT0309
SCAT0310
SCAT0311
SCAT0312
SCAT0313
SCAT0314

```

050      IF( ITEMP .LT. 4 ) YPOINTS( ITEMP ) =
          YPOINTS( ITEMP ) + 1
          CONTINUE

          CALCULATE THE FINAL TOTAL
          NUMBER OF POINTS WITHIN THE
          THREE STD. DEV. RANGES.

XPOINTS( 2 ) = XPOINTS( 2 ) + XPOINTS( 1 )
XPOINTS( 3 ) = XPOINTS( 3 ) + XPOINTS( 2 )
YPOINTS( 2 ) = YPOINTS( 2 ) + YPOINTS( 1 )
YPOINTS( 3 ) = YPOINTS( 3 ) + YPOINTS( 2 )

          CALCULATE THE PERCENTAGES OF
          GRAPH POINTS WITHIN ONE STD.
          DEV., TWO STD. DEV., AND THREE
          STD. DEV.

DO 60 CALC = 1, 3
  STAT( CALC + 27 ) = PCT( XPOINTS( CALC ), POINTS )
  STAT( CALC + 44 ) = PCT( YPOINTS( CALC ), POINTS )
  CONTINUE

060      IF THE USER SUPPLIED AN XAXIS
          CENTER FOR THE GRAPH, CENTER IT
          ABOUT THE XAXIS MIDRANGE.

          IF( CENTERX .NE. DEFAULT ) GO TO 70

          IF THERE ARE MORE POINTS ON THE
          GRAPH IF THE XAXIS IS CENTERED
          ON ITS MIDRANGE THAN ITS MEAN,
          CENTER IT ON ITS MIDRANGE.

          IF( MEANX .LT. MIDX ) GO TO 70

          CENTER THE XAXIS ON ITS MEAN.

XCENTER = XMEAN
STAT( 27 ) = PCT( MEANX, POINTS )
GO TO 80

          CENTER THE XAXIS ON ITS MIDRANGE.

STAT( 27 ) = PCT( MIDX, POINTS )
070

```

```

SCAT0315
SCAT0316
SCAT0317
SCAT0318
SCAT0319
SCAT0320
SCAT0321
SCAT0322
SCAT0323
SCAT0324
SCAT0325
SCAT0326
SCAT0327
SCAT0328
SCAT0329
SCAT0330
SCAT0331
SCAT0332
SCAT0333
SCAT0334
SCAT0335
SCAT0336
SCAT0337
SCAT0338
SCAT0339
SCAT0340
SCAT0341
SCAT0342
SCAT0343
SCAT0344
SCAT0345
SCAT0346
SCAT0347
SCAT0348
SCAT0349
SCAT0350
SCAT0351
SCAT0352
SCAT0353
SCAT0354
SCAT0355
SCAT0356
SCAT0357
SCAT0358
SCAT0359
SCAT0360
SCAT0361
SCAT0362
SCAT0363
SCAT0364
SCAT0365
SCAT0366

```

00000000

SCAT0417
SCAT0413

```

LASTX = 1
LASTY = 1
WRITE( 42, 600 ) Y0

```

```

PRINT OUT THE SCATTERGRAM ONE
LINE AT A TIME FOR ALL THE
POINTS.

```

```

DO 210 PRINT = 1, VSIZE

```

```

IF A POINT IS OUTSIDE THE
BOUNDARYS OF THE GRAPH, SKIP IT.

```

```

IF( YVECTOR( PRINT ) .GE. YTOP .OR.
1 XVECTOR( PRINT ) .LE. XBOTTOM .OR.
2 XVECTOR( PRINT ) .GE. XTOP ) GO TO 190

```

```

IF THE POINT LIES BELOW THE YAXIS
LOWER BOUNDARY, END THE GRAPH.

```

```

IF( YVECTOR( PRINT ) .LT. YBOTTOM ) GO TO 200

```

```

POSITION IS THE LOCATION OF THE
CURRENT POINT ON THE PRINT LINE.

```

```

POSITION = ( XVECTOR( PRINT ) - XLOC ) / CX
LINENUM = ( YLOC - YVECTOR( PRINT ) ) / CY

```

```

IF THE CURRENT LINE NUMBER IS
DIFFERENT THAN THE LAST LINE
NUMBER, PRINT A GRAPH LINE.

```

```

IF( LINENUM .EQ. LASTY ) GO TO 170

```

```

INSERT DUPLICATE POSITION
SYMBOLS AND BLANKS INTO THE
PRESENT LINE.

```

```

DO 140 FILL = 1, 95

```

```

IF A LINE ELEMENT IS NEGATIVE,
REPLACE IT WITH A BLANK. IF IT
IS ZERO, REPLACE IT WITH THE
DUPLICATE POSITION COUNTER
OVERFLOW SYMBOL.

```

```

SCAT0419
SCAT0420
SCAT0421
SCAT0422
SCAT0423
SCAT0424
SCAT0425
SCAT0426
SCAT0427
SCAT0428
SCAT0429
SCAT0430
SCAT0431
SCAT0432
SCAT0433
SCAT0434
SCAT0435
SCAT0436
SCAT0437
SCAT0438
SCAT0439
SCAT0440
SCAT0441
SCAT0442
SCAT0443
SCAT0444
SCAT0445
SCAT0446
SCAT0447
SCAT0448
SCAT0449
SCAT0450
SCAT0451
SCAT0452
SCAT0453
SCAT0454
SCAT0455
SCAT0456
SCAT0457
SCAT0458
SCAT0459
SCAT0460
SCAT0461
SCAT0462
SCAT0463
SCAT0464
SCAT0465
SCAT0466
SCAT0467
SCAT0468
SCAT0469

```

ORIGINAL PAGE IS
OF POOR QUALITY

SCAT0470
SCAT0471
SCAT0472
SCAT0473
SCAT0474
SCAT0475
SCATE475
SCAT0477
SCAT0478
SCAT0479
SCAT0480
SCAT0481
SCAT0482
SCATO-83
SCAT0484
SCAT0-85
SCAT0486
SCAT0487
SCAT0488
SCAT0489
SCAT0490
SCAT0491
SCAT0492
SCAT0493
SCAT0494
SCAT0495
SCATE495
SCAT0497
SCAT0499
SCAT0499
SCAT0500
SCAT0501
SCAT0502
SCAT0503
SCAT0504
SCAT0505
SCAT0506
SCATE507
SCAT0509
SCAT0509
SCAT0510
SCATE511
SCAT0512
SCAT0513
SCAT0514
SCATE515
SCAT0516
SCAT0517
SCAT0518
SCATE519
SCAT0520
SCAT0521

IF THERE IS NO POINT IN THIS
POSITION. INSERT THE USER SYMBOL
, OTHERWISE INCREMENT DUPLICATE
LOCATION COUNTER.

IF(LINE(POSITION) - 1) 180, , 180
LINE(POSITION) = SYMBOLS(PRINT)
GO TO 190

INITIALIZE THE DUPLICATE POINT
POSITION COUNTER.

IF(LINE(POSITION) .GE. 10 .OR. LINE(POSITION)
.LT. 2) LINE(POSITION) = 1
LINE(POSITION) = LINE(POSITION) + 1

IF THE DUPLICATE POSITION
COUNTER EXCEEDS 9, SET THE
COUNTER OVERFLOW INDICATOR.

IF(LINE(POSITION) .EQ. 10) LINE(POSITION) = 0

IF THIS IS THE LAST POINT,
FINISH THE GRAPH.

IF(PRINT .NE. VSTZF) GO TO 210

LINENUM = 52

GO TO 110

CONTINUE

WRITE(42, 600) YEND

WRITE(42, 620) X0, XCENTER - 24. * DX, XCENTER,

XCENTER + 24. * DX, XEND

RETURN

FORMAT(1X, F11.3, '++', 3(23('-'), 'I'), 23('-'), '++')

FORMAT(1X, F11.3, 97A1, 2X, A10, F11.3)

FORMAT(5X, 5(F11.3, 13X))

END

SCAT0522
SCAT0523
SCAT0524
SCAT0525
SCAT0526
SCAT0527
SCAT0528
SCAT0529
SCAT0530
SCAT0531
SCAT0532
SCAT0533
SCAT0534
SCAT0535
SCAT0536
SCAT0537
SCAT0538
SCAT0539
SCAT0540
SCAT0541
SCAT0542
SCAT0543
SCAT0544
SCAT0545
SCAT0546
SCAT0547
SCAT0548
SCAT0549
SCAT0550
SCAT0551
SCAT0552
SCAT0553
SCAT0554
SCAT0555
SCAT0556
SCAT0557
SCAT0558
SCAT0559
SCAT0560
SCAT0561
SCAT0562

CREGRES PROGRAM INTERFACE BETWEEN TRNGEN AND BMD02R

DATE 4/16/75 LAST MODIFICATION 6/20/75

PURPOSE

THIS PROGRAM INTERFACES TRNGEN (THE TRANS-GENERATOR MAIN LINE) WITH THE LIBRARY STEPWISE REGRESSION ANALYSIS PROGRAM (BMD02R). THE USER MUST SPECIFY AS DATA THE COMMAND ANGLES (COMANG(I)) AND THE COMPONENTS HE WISHES TO USE FOR REGRESSION ANALYSIS (COMPNT(I)), I<16. THE USER ALSO INCLUDES THE SET-UP CARDS FOR BMD02R AS EXPLAINED IN THE BMD WRITE-UP, EXCEPT LEAVE OUT:

- 1) 'PROBLEM' CARD
- 2) 'FORMAT' CARD
- 3) 'FINISH' CARD

THESE CARDS ARE GENERATED BY THIS PROGRAM AT RUN TIME.

DATA CARDS

- 1) COMMAND ANGLE CONTROL CARD
COL 8-13 COMANG
COL 16 (THE COMMAND ANGLE NUMBER(S); DIFFERENT ANGLES SHOULD BE SEPARATED BY COMMAS. BLANKS MAY BE FREELY USED TO FACILITATE EASY READING. DO NOT INCLUDE A COMMA AFTER THE LAST ANGLE. A MAXIMUM OF 5 ANGLES MAY BE SELECTED.)
- 2) COMPONENT SELECTOR CARD
COL 8-13 COMPNT
COL 16-80 THE COMPONENTS OF THE DATA VECTOR TO BE USED FOR REGRESSION ANALYSIS. DIFFERENT COMPONENTS SHOULD BE SEPARATED BY COMMAS. BLANKS MAY BE USED FREELY TO FACILITATE EASY READING. DO NOT INCLUDE A COMMA AFTER THE LAST COMPONENT #. THE COMPONENT #'S MUST BE LISTED TO CORRESPOND WITH THE APPROPRIATE VARIABLE ON THE 'LABELS' CARD. FOR EXAMPLE, THE FIRST COMPONENT SELECTED SHOULD BE THE VALUE OF VARIABLE 0001. A MAXIMUM OF 15 COMPONENTS MAY BE CHOSEN.
- 3) ZERO Y-INTERCEPT CARD (OPTIONAL)
COL 8-12 ZEROY
THIS CARD ALLOWS THE USER TO SELECT A ZERO Y-INTERCEPT. IT SHOULD BE USED FOR

WEIGHTED DATA, IF OMITTED, THE PROGRAM
ASSUMES A NON-ZERO Y-INTERCEPT

DECK SET-UP

DATA
CARDS

```

      S      SELECT  JYOUNG/REGRESS
      -----
      COMANG  (THE COMMAND ANGLE #'S)
      COMPNT  (COMPONENT #'S TO BE USED IN REGRESSION)

      BMD02R CONTROL CARDS, OMIT 'PROBLM', 'FORMAT' AND
      'FINISH' CARDS, THIS PROGRAM GENERATES THESE CARDS,
      ALL VARIABLES MUST BE LABELED,
      |
      |
      |
      S      SELECT  JYOUNG/BMD02R
  
```

TABLE OF IMPORTANT VARIABLES AND THEIR FUNCTION

NAME	FUNCTION
COMANG(I)	COMMAND ANGLE NUMBER(S)
COMPNT(I)	CONTAINS #'S OF COMPONENTS TO BE USED IN REGRESSION
DATVEC(I)	DATA VECTOR GENERATED BY TRNGN
FINDAT(I)	FINAL DATA VECTOR FOR REGRESSION ANALYSIS
NUMOBS	NUMBER OF DATA VECTORS ACTUALLY USED IN REGRESSION
NUMPRO	NUMBER OF PROBLEMS
NUMREC	NUMBER OF DATA RECORDS CORRESPONDING

ORIGINAL PAGE IS
OF POOR QUALITY

.....

.....

.....

.....

CCC

C

УГОЛОВНО-ПРОЦЕССУАЛЬНЫЙ КОДЕКС

CALL FREEFORM(1,CHECK,COMPNT,15,NUMVAR,NULL)

```

      IF(ICMPNT,EO,ICHECK) GO TO 8
      CALL FXEH(61,ICMPNT,10)
      WRITE(6,964)(CMPNT(I),I=1,NUMVAR)
8    964 FORMAT(///5X, 'THE COMPONENTS TO BE SELECTED FOR REGRESSION ANALYSIS
      1'S ARE #',3H'S)//5X,15(I3,2X))

C
C
C      CHECK FOR OPTIONAL ZERO Y-INTERCEPT CARD
C
20  READ(5,899) ZEROYINT
899 FORMAT(7X,A6)
      IF(ZEROYINT,NE,'ZEROY ') GO TO 22
      ZEROYINT=' YES '
      GO TO 25
22  ZEROYINT=' '
      BACKSPACE(5)

C
C
C      READ AND STORE LABELS FOR DATA HEADINGS
C
25  READ(5,902)(LABELS(I),I=1,NUMVAR)
902 FORMAT(6X,7(4X,A6))

C
C
C      SCAN '05' TO COUNT NUMBER OF SUBPROBLEMS
      (NUMSUB)
C
C
C      NUMSUB=0
30  READ(5,903,END=40) NAMCRD
903  FORMAT(A6)
      IF(NAMCRD,EQ,SUBPRO) NUMSUB=NUMSUB+1
      GO TO 30
40  CALL FCLOSE(05)
      NUMPRO=0

C
C
C      READ MASTER HEADER
      INCREMENT THE PROBLEM COUNTER(NUMPRO);
      WRITE OUT MASTER HEADER DATA
C
C
C
50  READ(2,END=300)(TITLE(I),I=1,10),(DATE(I),I=1,3),NUMHED,WDPRO
      NUMPRO=NUMPRO+1
      WRITE(6,950) NUMPRO
950  FORMAT(1H1, 'THIS IS THE DATA SET FOR PROBLEM #',I2)
      WRITE(6,951) TITLE,DATE
951  FORMAT(1H0,10A6,5X,I2,'/',I2,'/',I2)
      NUMOBS=0

C
C
C      PROCESS NEXT HEADER AND DATA

```

```

60 READ(2,END=200) DOY,DATSEG,MODE,NOLDWD,NUMREC,HEAD,TITLE
   COLHD='SCAN'
   IF(MODE.EQ.-2) COLHD='CELL'
   WRITE(6,952)DOY,DATSEG,TITLE,COLHD,(LABELS(I),I=1,NUMVAR)
952 FORMAT(1H0,5X,13,'-',11,10X,10'A6//','CASE ',A4,15(2X,A6))
   DO 120 IREC=1,NUMREC
   READ(3)SERIAL,(DATVEC(J),J=2,WDPRD)

```

```

PROCESS THIS DATA VECTOR IF IT HAS THE
CORRECT COMMAND ANGLE

```

```

IF(SERIAL/1000000000.NE.COMANG(ICOUNT)) GO TO 120
NSCAN=(SERIAL-SERIAL/100000000*10000000)/10000
IDFLT=0

```

```

PICK OUT THE PROPER COMPONENTS; CHECK
THEM FOR DEFAULT AND FLAG IF DEFAULT IS
FOUND, IDFLT=1

```

```

DO 80 J=1,NUMVAR
INDEX=COMPNT(J)
FINDAT(J)=DATVEC(INDEX)
80 IF(DATVEC(INDEX).EQ.DEFLT) IDFLT=1

```

```

SKIP PROCESSING THIS SCAN IF A DEFAULT
IS FOUND, IF NO DEFAULT, INCREMENT
OBSERVATION COUNTER(NUMOBS) AND WRITE
THIS SCAN IN FORMATTED STYLE FOR BMD02R

```

```

IF(IDFLT.NE.0) GO TO 100
NUMOBS=NUMOBS+1
WRITE(9,953)(FINDAT(I),I=1,NUMVAR)
953 FORMAT(7(E11,4))
WRITE(6,954) NUMOBS,NSCAN,(FINDAT(I),I=1,NUMVAR)
954 FORMAT(14,2X,14,15F8,3)
GO TO 120
100 WRITE(6,955)(FINDAT(I),I=1,NUMVAR)
955 FORMAT(6X,'####',15F8,3)
120 CONTINUE

```

```

GO AND PICK UP NEXT HEADER

```

```

GO TO 60

```

```

CLOSE DATA FILES FOR THIS PROBLEM(MASTER
HEADER); CREATE THE BMD02R CONTROL CARDS
FOR THIS PROBLEM ON FILE '08'

```

```

200 CALL FCLOSE(2)
205 READ(3,END=210)
210 CALL FCLOSE(3)
    WRITE(6,957)
957 FORMAT(1H0,'IF **** APPEARS FOR SCAN #, THIS SCAN HAS A DEFAULT')
    WRITE(6,956) NUMPRO
956 FORMAT(1H1,4X,'THESE ARE THE BMD02R CONTROL CARDS FOR PROBLEM #',1
12//5X,'COL NO',5X,'1234567890123456789012345678901234567
2890123456789012345678901234567890')

```

REWIND '05' AND POSITION AT FIRST BMD02R
CONTROL CARD IMAGE

```

REWIND(5)
READ(5)
READ(5)
IF(ZEROYINT,NE,' YES ') GO TO 215
READ(5)

```

CREATE 'PROBLEM' CARD

```

215 WRITE(8,958) DOY,DATSEG,NUMOBS,NUMVAR,NUMSUB,NUMVAR,ZEROYINT
958 FORMAT('PROBLM',3X,13,'-1,11,2X,14,3X,12,13X,'09',3X,12,2X,12,
1' YES YES YES',A6,'NO 01 ')
    WRITE(6,959) DOY,DATSEG,NUMOBS,NUMVAR,NUMSUB,NUMVAR,ZEROYINT
959 FORMAT(5X,'PROBLM',3X,13,'-1,11,2X,14,3X,12,13X,'09',3X,12,2X,12,
1' YES YES YES',A6,'NO 01 ')

```

READ 'LABELS' CARD, WRITE IT ON '08'

```

220 READ(5,904)(CARD(1),I=1,16)
904 FORMAT(8(A6,A4))
IF(CARD(1).NE,ILABEL) GO TO 230
    WRITE(8,904) CARD
    WRITE(6,905) CARD
905 FORMAT(5X,8(A6,A4))
GO TO 220

```

INSERT FORMAT CARD

```

230 WRITE(8,904) FERHAT
    WRITE(6,905) FERHAT

```

READ AND WRITE REST OF BMD02R CONTROL
CARDS, WHEN FINISHED TRANSFER TO PROCESS
NEXT MASTER HEADER(PROBLEM),

```

240 WRITE(8,904) CARD
    WRITE(6,905) CARD

```

```

READ(5,904,END=50) CARD
GO TO 240

```

REWIND '02' AND '03', IF THERE ARE MORE
COMMAND ANGLES, SKIP AND PROCESS, IF NOT,
WRITE 'FINISH', SET EOF'S, REWIND AND
STOP, THE ORIGINAL DATA IS READY FOR
BMD02R STEPWISE REGRESSION ANALYSIS,

```

300 REWIND(02)
    REWIND(03)
    ICOUNT=ICOUNT+1
    IF(ICOUNT,LE,NUMANG) GO TO 50
    WRITE(8,960)
960 FORMAT(80HFINISH
1
    WRITE(6,961)
961 FORMAT(5X,80HFINISH
1
    ENDFILE(09)
    ENDFILE(09)
    REWIND(08)
    REWIND(09)
340 STOP
    END

```

ORIGINAL PAGE IS
OF POOR QUALITY

CSTDV.M STANDARD DEVIATION MAINLINE

DATE 9/1/75

AUTHOR BIRRRER

PURPOSE

THIS PROGRAM ESTIMATE THE STANDARD DEVIATIONS OF DIFFERENT CATEGORIES OF DATA. THE ESTIMATE IS MADE BY COMPUTING THE R M S DEVIATION OF THE RESIDUALS FROM A LINEAR REGRESSION FIT. THIS PROGRAM PRESUPPOSES A TRANSGENERATION ACTIVITY DURING WHICH THE RESIDUALS FOR DIFFERENT COMPONENTS ARE COMPUTED AND STORED IN DIFFERENT WORDS OF THE DATA VECTORS. THE USER SUPPLIES DATA CARDS WHICH SPECIFY THE COMMAND ANGLE(S), THE LOCATION OF THE RESIDUAL(S), THE NUMBER OF CATEGORIES, AND THE LOCATION OF THE CATEGORY NUMBER WITHIN THE DATA VECTOR.

THIS MAINLINE HANDLES THE FILE MANIPULATION, DATA CARD PROCESSING, AND CALLS THE SUBROUTINE WHICH COMPUTES THE R M S DEVIATIONS.

NOTE A MISSING CATEGORY IN THE OUTPUT MEANS THAT THERE WERE NO POINTS IN THIS CLASS.

DATA CARDS

1) COMMAND ANGLE CONTROL CARD

COL 8-13

COL 16-80

COMANG

(THE COMMAND ANGLE NUMBER(S). THESE SHOULD BE FREE FORMAT INTEGERS WITH DIFFERENT ANGLES SEPARATED BY COMMAS. DO NOT INCLUDE A COMMA AFTER THE LAST ANGLE. A MAXIMUM OF 5 ANGLES ARE ALLOWED.)

2) RESIDUAL LOCATOR CARD

COL 8-12

COL 16-80

RESID

(THE LOCATIONS IN THE DATA VECTOR WHICH CONTAIN THE THE VALUES OF THE RESIDUALS. THESE SHOULD BE FREE FORMAT

INTEGERS WITH DIFFERENT LOCATIONS
SEPARATED BY COMMAS; DO NOT INCLUDE
A COMMA AFTER THE LAST LOCATION, A
MAXIMUM OF 4 RESIDUALS MAY BE CHOSEN.)

3) CATEGORY SPECIFICATION CARD

COL 8-13 CATGOR
COL 16-60
(TWO INTEGERS SEPARATED BY A COMMA,
THE FIRST INTEGER IS THE LOCATION OF
CATEGORY VALUE IN THE DATA VECTOR, THE
SECOND INTEGER IS THE MAXIMUM NUMBER
OF USER CATEGORIES, THIS MUST BE LESS
THAN 13.)

DECK SET-UP

(TRANSGENERATOR ACTIVITY TO PUT RESIDUALS AND CATEGORIES
INTO THE DATA VECTOR.)

```

S      OPTION  FORTRAN,NOMAP
      (OBJECT DECKS FOR STANDARD DEVIATION PROGRAM--
      MAINLINE, SPEEFORM, AND STANDARD DEVIATION SUBROUTINE)
S      EXECUTE
S      LIMITS  3,13K,,5K
S      FILE    02,02S
S      FILE    03,03S
      COMANG   X1,X2,...,X5
      RESID    Y1,Y2,Y3,Y4
      CATGOR    LOCATION,MAXNUM

```

(SUBSEQUENT ACTIVITIES)

```

IMPLICIT INTEGER(A-Z)
CHARACTER NAME*6
INTEGER NCASES(5,4,12), COMANG(5),RESIDUAL(4), TITLE(10),DATE(3),
1  CATGOR(2),IDATVEC(150),HEADER(13)
REAL MEAN(5,4,12), STDEV(5,4,12), DATVEC(150),DEFLT/0377777777777/
EQUIVALENCE (CATLOC,CATGOR(1)),(DATVEC,IDATVEC),

```



```

1      (NUMCAT,CATGOR(2)),(TITLE(1),HEADER(1)),(DATE(1),HEADER(11))
      SET-UP ERROR OVERFIDE TO PROCESS DOUBLE
      END OF FILE MARK

      CALL FXOPT(85,1,1,1)
      CALL FXALT(SAQ)

      REWIND DATA FILES TO TOP

      REWIND(02)
      REWIND(03)

      INPUT DATA CARDS FOR THIS PROGRAM

10     READ(5,901,END=40) NAME
901    FORMAT(7X,A6)
      BACKSPACE(5)

      PROCESS COMMAND ANGLE CARD

      IF(NAME.NE.,ICOMANG') GO TO 12
      CALL FREEFORM(NAME,COMANG,5,NUMANG,NULL)
      WRITE(42,800) COMANG
800    FORMAT(5I5)
      GO TO 10

      PROCESS RESIDUAL CARD

12     IF(NAME.NE.,IRESID') GO TO 14
      CALL FREEFORM(NAME,RESIDUAL,4,NUMRES,NULL)
      GO TO 10

      PROCESS CATEGORY CARD

14     IF(NAME.NE.,ICATGOR') GO TO 19
      CALL FREEFORM(NAME,CATGOR,2,NULL,EOF)
      GO TO 10

      IF YOU GET HERE, ABORT--THE DATA CARD
      IS NOT PROCESSIBLE

19     WRITE(6,951) NAME
951    FORMAT(4X,'***ERROR*** THE NAME ',1H',A6,1H', ' IS IMPROPER, EXEC
      UTION TERMINATED,')
      STOP

      INPUT NEXT MASTER HEADER

40     READ(02,END=80)TITLE,DATE,NUMHED,WDPRD

      CALL SUBROUTINE TO COMPUTE AND STORE ON
      '05'(IF REQUESTED) THE RESULT

      CALL STDV(CATGOR,COMANG,RESIDUAL,STDEV,MEAN,NCASES,5,4,12, NUMANG,

1      NUMRES,WDPRD,DATVEC,IDATVEC,HEADER)

      CLOSE'03' AND MOVE TO END AND CLOSE'02'
      SKIP TO PROCESS NEXT HEADER

      CALL FCLOSE(03)
90     READ(02,END=60)
      GO TO 50
60     CALL FCLOSE(02)
      GO TO 40
80     REWIND(02)
      REWIND(03)
      STOP
      END

```

```

SUBROUTINE STDV(CATGOR,COMANG,RESIDUAL,STDEV,MEAN,NCASES,MAXANG,
1  MAXRES,MAXCAT,NUMANG,NUMRES,WDPRD,DATVEC,IDATVEC,HEADER)

```

PURPOSE

THIS SUBROUTINE COMPUTES THE R M S DEVIATION AND THE MEAN FOR A SET OF RESIDUALS CORRESPONDING TO EACH COMMAND ANGLE COMPONENT PAIR. THE CALCULATIONS ARE DONE IN PARALLEL DURING ONE PASS THROUGH THE DATA.

INPUT ARGUMENTS

CATGOR A 2 ELEMENT VECTOR--CATGOR(1) = LOCATION OF CATEGORY INFORMATION IN DATA VECTOR, CATGOR(2) = NUMBER OF CATEGORIES FOR THIS RUN

COMANG VECTOR CONTAINING COMMAND ANGLES TO BE PROCESSED

RESIDUAL VECTOR CONTAINING LOCATIONS OF THE RESIDUALS IN THE DATA VECTOR

STDEV MATRIX USED TO COMPUTE STANDARD DEVIATION

MEAN MATRIX USED TO COMPUTE MEAN

NCASES MATRIX USED TO KEEP A RUNNING TOTAL OF USABLE CASES

MAXANG MAXIMUM ALLOWABLE NUMBERS OF COMMAND ANGLES

MAXRES MAXIMUM POSSIBLE RESIDUALS

MAXCAT MAXIMUM NUMBER OF CATEGORIES

NUMANG NUMBER OF ANGLES ACTUALLY USED

NUMRES NUMBER OF RESIDUALS ACTUALLY USED

WDPRD WORDS PER RECORD IN THE DATA VECTOR

DATVEC 150 WORD VECTOR FOR INPUTTING FROM DATA FILE

IDATVEC INTEGER EQUIVALENT OF DATVEC

HEADER ADDRESS OF THE HEADER RECORD

```

IMPLICIT INTEGER(A-Z)
INTEGER COMANG(MAXANG),RESIDUAL(MAXRES),CATGOR(2),HEADER(13),
1  IDATVEC(150),NCASES(MAXANG,MAXRES,MAXCAT)
REAL STDEV(MAXANG,MAXRES,MAXCAT),MEAN(MAXANG,MAXRES,MAXCAT),
1  DATVEC(150),DEFLT/0377777777777777/

```

ORIGINAL PAGE IS
OF POOR QUALITY

```

CATEGORY=CATGOR(1)
NUMCAT=CATGOR(2)

ZERO OUT MATRICES AND ARRAYS

DO 20 I=1,NUMANG
DO 20 J=1,NUMRES
DO 20 K=1,NUMCAT
STDEV(I,J,K)=0
MEAN(I,J,K)=0
NCASES(I,J,K)=0

READ IN NEXT DATA VECTOR

40 READ(03,END=100) SERIAL,(DATVEC(J),J=2,NDPRD)

CHECK AND SEE IF THIS IS A REQUESTED
COMMAND ANGLE, IF YES, SKIP TO CHECK FOR
DEFAULTIO/M SKIP TO READ

DO 50 I=1,NUMANG
IF(SERIAL/1000000000.EQ.COMANG(I)) GO TO 55
GO TO 40
55 ANGLE=COMANG(I)
CATEGORY= CATGOR(1) + I -1

IF DEFAULT, SKIP TO READ

DO 90 J=1,NUMRES
INDEX=RESIDUAL(J)
60 IF(DATVEC(INDEX).EQ.DEFLT) GO TO 90
CATPOINT=IDATVEC(CATEGORY)
II = II + 1
IF(II,LT,200) WRITE(42,900) HEADER(1), ANGLE, DATVEC(16),CATPOINT
900 FORMAT(14,12,F6.2,13)

ADD THE CONTRIBUTION OF THIS DATA
VECTOR TO 'STDEV', 'MEAN' AND 'NCASES'

STDEV(ANGLE,J,CATPOINT)=STDEV(ANGLE,J,CATPOINT)+DATVEC(INDEX)**2
MEAN(ANGLE,J,CATPOINT)=MEAN(ANGLE,J,CATPOINT)+DATVEC(INDEX)
80 NCASES(ANGLE,J,CATPOINT)=NCASES(ANGLE,J,CATPOINT)+1
90 CONTINUE
GO TO 40

COMPUTE AND PRINT OUT RESULTS

100 DO 120 I=1,NUMANG
WRITE(6,951) HEADER, COMANG(I)
951 FORMAT(1H1//4X,10A6,13X,12,1//,12,1//,12//4X,'THE COMMAND ANGLE M
NUMBER IS',12)
DO 120 J=1,NUMRES
WRITE(6,952) RESIDUAL(J)

952 FORMAT(1H0//T5,'THE COMPONENT NUMBER IS',13//T5,'CATEGORY',T24,
1 'R M S DEVIATION',T49,'MEAN',T62,'NUMBER OF CASES')
DO 120 K=1,NUMCAT
IF(NCASES(I,J,K).EQ.0) GO TO 120
STDEV(I,J,K)=SQRT(STDEV(I,J,K)/FLOAT(NCASES(I,J,K)))
MEAN(I,J,K)=MEAN(I,J,K)/FLOAT(NCASES(I,J,K))
WRITE(6,953) K,STDEV(I,J,K),MEAN(I,J,K),NCASES(I,J,K)
953 FORMAT(T8,12,T27,F8.5,T47,F8.5,T68,13)
120 CONTINUE
RETURN
END

```

SUBROUTINE FREEFORM(NAME,COMPNT,SIZE,NUMCMPT,EOF)

PURPOSE

TO READ IN FREE FORMAT INTEGER ARRAYS FROM DATA CARDS
AND CONVERT IT TO INTEGER ARRAYS.

DATA CARDS SHOULD BE PUNCHED AS FOLLOWS:

COL 8-13 6 CHARACTER NAME
COL 16-80 INTEGER VALUES SEPARATED BY COMMAS,
DO NOT INCLUDE A TRAILING COMMA,

INPUT ARGUMENTS

SIZE DIMENSIONED SIZE OF ARRAY

OUTPUT ARGUMENTS

NAME 6 CHARACTER ALPHANUMERIC NAME
COMPNT ARRAY CONTAINING THE INTEGER VALUES. THE VALUES
ARE STORED IN ORDER AS READ FROM LEFT TO RIGHT ON
THE DATA CARDS. THEY ARE STORED AT THE TOP OF THE
ARRAY.
EOF EOF=1, IF END OF FILE ENCOUNTERED; OTHERWISE EOF=0

1 INTEGER BLANK/' ',COMMA/',',ICHAR(65),SIZE,COMPNT(SIZE),
IFACT/010000000000/,EOF
CHARACTER NAME=6

INITIALIZE COUNTERS AND ARRAY TO ZERO,

IDIG=0
EOF=0
DO 5 I=1,SIZE
COMPNT(I)=0
NUMCMPT=SIZE

INPUT DATA CARD

901 READ(5,901,END=40) NAME, ICHAR
FORMAT(7X,A6,2X,65A1)

PROCESS THE CARD IMAGE BY SCANNING
FROM RIGHT TO LEFT,

DO 20 I=1,65
K=66-I

```

C      IGNORE BLANK
C
C      IF(ICHAR(K),EQ,BLANK) GO TO 20
C
C      IF NON-BLANK CHARACTER IS A COMMA, A FULL
C      INTEGER HAS BEEN SCANNED, MOVE POINTER
C      AND RESET IDIG,
C
C      IF(ICHAR(K),NE,COMMA) GO TO 10
C      NUMCHPT=NUMCHPT+1
C      IDIG=0
C      GO TO 20
C
C      IF NON-BLANK CHARACTER IS A NUMBER, ADD
C      THE CONTRIBUTION OF THIS DIGIT TO THE
C      CURRENT INTEGER, BUMP DIGIT COUNTER,
C
10  COMPNT(NUMCHPT)=COMPNT(NUMCHPT)+ICHAR(K)/IFACT*10**IDIG
    IDIG=IDIG+1
20  CONTINUE
C
C      COMPUTE NUMCHPT, IF NUMCHPT IS LESS
C      THAN SIZE, MOVE DATA TO TOP OF ARRAY,
C
    NUMCHPT=SIZE-NUMCHPT+1
    WRITE(42,800) COMPNT
800  FORMAT(5I5)
    IF(NUMCHPT,EQ,SIZE) RETURN
    DO 30 I=1,NUMCHPT
30  COMPNT(I)=COMPNT(I)+SIZE-NUMCHPT+1
    RETURN
C
C      IF END OF FILE FLAG, SET EOF=1
C
40  EOF=1
    RETURN
    END

```

CACOR.M AUTO-CORRELATION FUNCTION EVALUATION (MAINLINE)

DATE 6/1/75

AUTHOR BIRRE

PURPOSE

THIS PROGRAM PROVIDES THE ARGUMENTS FOR THE AUTO-CORRELATION SUBROUTINE(AUTCOR). THE USER PROVIDES AS DATA CARDS THE COMMAND ANGLE NUMBERS AND COMPONENT NUMBERS. THIS PROGRAM WILL CALL AUTCOR WITH EVERY ANGLE-COMPONENT COMBINATION POSSIBLE. IN ADDITION, THIS ROUTINE READS THE MASTER HEADER AND SUPPLIES THE NUMBER OF WORDS PER RECORD(WOPRD). THIS ROUTINE ASSUMES A TRANSEN ACTIVITY WHICH STORES THE RESIDUALS IN THE COMPONENTS SPECIFIED ON THE COMPONENT SELECTOR CARD.

DATA CARDS

- 1) COMMAND ANGLES CONTROL CARD
 COL 8-13 COMANG
 COL 16-80 (THE COMMAND ANGLE NUMBER(S), THESE SHOULD BE FREE FORMAT INTEGERS WITH DIFFERENT ANGLES SEPARATED BY COMMAS. DO NOT INCLUDE A COMMA AFTER THE LAST ANGLE, A MAXIMUM OF 5 ANGLES ARE ALLOWED.)
- 2) COMPONENT SELECTOR CARD
 COL 8-13 COMPNT
 COL 16-80 (THE COMPONENT NUMBER(S) SELECTED, THESE SHOULD BE FREE FORMAT INTEGERS WITH DIFFERENT COMPONENTS SEPARATED BY COMMAS. DO NOT INCLUDE A COMMA AFTER THE LAST COMPONENT NUMBER, A MAXIMUM OF 10 COMPONENTS ARE ALLOWED.)

NOTE THE COMMAND ANGLE CARD AND COMPONENT CARD SHOULD BE IN PAIRS. THE COMMAND ANGLE CARD MUST BE FIRST.

ORIGINAL PAGE IS
OF POOR QUALITY

DECK SET-UP

(TRANSGENERATION ACTIVITY TO STORE RESIDUALS)

```

$ OPTION FORTRAN,NOMAP
$ (OBJECT DECKS FOR AUTOCORRELATION EVALUATION--
$ ACOR,M(HAINLINE), FREEFORM, AND AUTOCOR SUBROUTINE)
$ EXECUTE
$ LIMITS 3,11K,,5K
$ FILE 02,02S
$ FILE 03,03S
$ COMANG X1,X2,...,X5
$ COMPNT Y1,Y2,Y3,...,Y15

```

(SUBSEQUENT ACTIVITIES)

```

CHARACTER NAME*4
INTEGER COMANG(5),COMPNT(10),NDPRD,TITLE(10),DATE(3),
1 SEQFLAG/0/,EOF

```

```

SET UP ERROR CVERRIDE FOR PROCESSING
DOUBLE EOF MARK, RE,IND FILES TO TOP,

```

```

CALL FXOPT(85,1,1,1)
CALL FXALT(9150)
REWIND(02)
REWIND(03)

```

IFILE=3

```

INPUT NEXT DATA CARD, LEAVE INTEGER
VALUES IN COMPNT(I);

```

10 CALL FREEFORM(NAME,COMPNT,10,NUMCOMPNT,EOF)

```

IF NO MORE COMANG ANGLE OR COMPONENT
CARDS, STOP,

```

IF(EOF,NE,0) STOP

```

C      IF THIS IS A 'COMANG' CARD, TRANSFER
C      VALUES TO COMANG(I), INCREMENT 'SEQFLAG',
C
C      IF (NAME,EQ,'COMPNT') GO TO 30
C      DO 20 I=1,5
20    COMANG(I)=COMPNT(I)
      NUMANG=NUMCMPT
      SEQFLAG=SEQFLAG+1
      GO TO 35
C
C      IF THIS IS A 'COMPNT' CARD, DECREMENT
C      'SEQFLAG',
C
30    SEQFLAG=SEQFLAG-1
C
C      TEST 'SEQFLAG'. IF THE VALUE IS NOT '0'
C      OR '1', THE DATA CARDS ARE IN AN ORDER
C      THAT IS NOT PROCESSIBLE. IF ERROR,
C      TRANSFER TO PRINT ERROR MESSAGE AND
C      TERMINATE EXECUTION,
C
35    IF (SEQFLAG,LT,0,OR,SEQFLAG,GT,1) GO TO 120
      PICK UP 'COMPNT', IF IT HAS NOT BEEN READ
      IF (SEQFLAG,EQ,1) GO TO 10
      PROCESS ANGLE-COMPONENT PAIRS
      I=1
      READ MASTER HEADER, STORE NUMBER OF WORDS
      PER RECORD IN WDPHD,
40    READ(02,END=100) TITLE,DATE,NUMHD,WDPHD
      WRITE(6,950) TITLE,DATE
950   FORMAT(1H1,10A6,10X,12,'/',12,'/',12//)
      COMPUTE AND EVALUATE AUTO-CORRELATION
      FUNCTION FOR THIS MASTER HEADER,
      CALL AUTCOR(COMANG(I),COMPNT,NUMCMPT,WDPHD,FILE)
      CALL FCLOSE(02)
      READ(03,END=80)
80    CALL FCLOSE(03)
      PROCESS NEXT MASTER HEADER (IF ANY)
      GO TO 60
      MOVE TO TOP OF FILES

```

```

C
C      100 REWIND(02)
C      REWIND(03)
C
C      PROCESS THE NEXT COMMAND ANGLE; IF ALL
C      ANGLES HAVE BEEN PROCESSED, STOP,
C
C      I=1
C      IF (I,LE,NUMANG) GO TO 60
C      GO TO 10
120   WRITE(6,952)
952   FORMAT('***ERROR*** IMPROPER DATA CARD SEQUENCE--EXECUTION TERMINA
1TED')
      STOP
      END

```


CALTCOR AUTO-CORRELATION FUNCTION EVALUATION ROUTINE
 SUBROUTINE AUTCOR(COMANG,COMPNT,NUMCHPT,WOPRD,IFILE)

PURPOSE

'AUTCOR' EVALUATES THE AUTO-CORRELATION FUNCTION OF THE REGRESSION RESIDUALS FOR A POOLED SAMPLE OF DATA SEGMENTS. 'AUTCOR' EXPECTS FILE '02' TO BE POSITIONED AT THE FIRST HEADER OF THE POOLED SAMPLE (MASTER HEADER SHOULD ALREADY HAVE BEEN PROCESSED).

INPUT ARGUMENTS

COMANG -- THE COMMAND ANGLE NUMBER TO BE SELECTED
 COMPNT -- THE ARRAY CONTAINING THE COMPONENTS TO BE SELECTED
 NUMCHPT -- NUMBER OF COMPONENTS TO BE USED
 WOPRD -- NUMBER OF WORDS PER RECORD OF THE DATA VECTORS. (MASTER HEADER -CRD 15)
 IFILE -- SPECIFIES INPUT FILE FOR DATA VECTORS

REAL RESIDUAL(10,35),DATVEC(150),RESPRO(10,16),MEAN(10),
 1 DEFLT/0377777777777777/
 1 INTEGER COMANG,COMPNT(10),WOPRD,POINT,SERIAL,HEAD(12),TITLE(10),
 1 N(10,16),DOY,DATSEG,CTNCLR
 EQUIVALENCE (TITLE(1),DATVEC(1)),(HEAD(1),DATVEC(11))

INITIALIZE RESPRO(I,J),N(I,J), AND
 MEAN(I) TO ZERO

DO 20 I=1,NUMCHPT
 MEAN(I)=0
 DO 20 J=1,16
 RESPRO(I,J)=0
 20 N(I,J)=0

INPUT NEXT HEADER. STORE THE NUMBER OF
 DATA RECORDS(NUMREC) CORRESPONDING TO
 THIS HEADER TO BE READ FROM '03'

40 READ(02,END=200) DOY,DATSEG,MODE,NOLDWD,NUMREC,HEAD,TITLE

BUILD THE RESIDUAL TABLE

NUMRES=0

ASSIGN CTNCLR TO 65 IF MODE=5(CTNCLR/R),
 OTHERWISE ASSIGN CTNCLR TO 62

ASSIGN 65 TO CTNCLR
 IF(MODE.EQ.5) ASSIGN 62 TO CTNCLR

DO 65 J=1,NUMREC

INPUT 1 DATA VECTOR, IF WRONG COMMAND
ANGLE NUMBER, SKIP PROCESSING THIS ANGLE.

```
READ(IFILE) SERIAL,(DATVEC(K),K=2,NDPRD)  
IF(SERIAL/100000000.NE.COMANG) GO TO 65
```

STORE RESIDUAL IN NEXT LOCATION OF
RESIDUAL TABLE.

```
NUMRES=NUMRES+1
DO 60 I=1,NUMCMPT
  INDEX=COMPNT(I)
  RESIDUAL(I,NUMRES)=DATVEC(INDEX)
```

IF NOT DEFAULT, ADD VALUE TO MEAN

```

        IF (DATVEC(INDEX), NE, DEFLT) MEAN(I) = MEAN(I) + DATVEC(INDEX)
60      CONTINUE
        GO TO CTNCLR, (62, 65)

```

ADD DEFAULT LINE FOR CTNC L/R

```

62 NUMRES=NUMRES+1
   DO 64 I=1,NUMCMPT
64 RESIDUAL(I,NUMRES)=DEFLT
65 CONTINUE

```

PROCESS THIS RESIDUAL TABLE,

DO 160 POINT=1.16

```

SET J EQUAL TO THE LAG DISTANCE TO BE
EVALUATED DURING THIS PASS;  MOVE TO TOP
OF TABLE

```

```

J=POINT-1
I=1

```

IF WE ARE STILL IN THE TABLE, PROCESS THIS PAIR, OTHERWISE, SKIP TO INCREMENT LAG DISTANCE.

```
100 IF(I+J-NUMRES) 120,120,160
120 DO 130 ICOMP=1,NUMCMP
```

DROP THIS PAIR IF DEFAULT

```
IF(RESIDUAL(ICOMP,I),EQ,DEFLT,OR;RESIDUAL(ICOMP,I+J),EQ,DEFLT)
1      GO TO 130
```

ORIGINAL PAGE IS
OF POOR QUALITY

```

      RESPRO(I,COMP,POINT)=RESPRO(I,COMP,POINT)+RESIDUAL(I,COMP,I)*
1      RESIDUAL(I,COMP,I+J)
      N(I,COMP,POINT)=N(I,COMP,POINT)+1
130 CONTINUE

```

```
140 I=I+1
    GO TO 100
160 CONTINUE
```

GO TO 40

```

200 DO 220 J=1,NUMCMPT
    WRITE(6,950) COMPANG,COMPNT(I)
950 FORMAT(1H0,'THE COMMAND ANGLE NUMBER IS ',I1//1X,'THE COMPONENT NU
    MBER IS ',I2)
    MEAN(I)=MEAN(I)/FLOAT(N(I,1))
    WRITE(6,951) MEAN(I)
951 FORMAT(1H1,'THE MEAN VALUE OF THE RESIDUAL IS ',F6,4///)
    WRITE(6,952)
952 FORMAT(1H0,'LAG DISTANCE',I20,'CORRELATION FUNCTION',I4,
    1 'CORRELATION COEFFICIENT',F77,'NUMBER OF CASES')
    DO 220 J=1,16
        CORFUNC=RESPRO(I,J)/FLOAT(N(I,J))
        IF(J.EQ.1) COEFFLAG=CORFUNC
        CORCOEF=CORFUNC/COEFFLAG
        LAGDIST=J-1
        WRITE(6,953) LAGDIST, CORFUNC, CORCOEF, N(I,J)
953 FORMAT(6X,I2,I27,F7,4,F55,57,4,T83,I3)
220 CONTINUE
    RETURN
    END

```

CHAXLIK MAXIMUM LIKELIHOOD ESTIMATOR FOR SKYLAB DATA

PURPOSE

THIS PROGRAM IS AN ADAPTATION OF THE NELDER AND RAEDE ALGORITHM FOUND ON PAGES 298-308 OF OPTIMIZATION TECHNIQUES IN FORTRAN. THIS TECHNIQUE IS USED TO FIND THE MAXIMUM LIKELIHOOD ESTIMATES OF REGRESSION COEFFICIENTS, STANDARD DEVIATIONS OF DIFFERENT CATEGORIES, AND CORRELATION COEFFICIENTS FOR A NON-LINEAR MODEL OF KIND ESTIMATES.

THE OPENING SECTION AND THE LAST 6 CARDS HAVE BEEN ADDED TO INTERFACE WITH THE STANDARD SKYLAB OCEANOGRAPHIC FILES. THIS PROGRAM PRESUPPOSES A TRANSGENERATION ACTIVITY.

DATA CARDS

- 1) COMMAND ANGLE CONTROL CARD
COL 8-13 COMANG
COL 16-80 (THE COMMAND ANGLE NUMBERS SEPARATED BY COMMAS, DO NOT INCLUDE A TRAILING COMMA, A MAXIMUM OF FIVE COMMAND ANGLES MAY BE SPECIFIED)
- 2) COMPONENT SELECTOR CARD
COL 8-13 COMPNT
COL 16-80 (THE COMPONENTS OF THE DATA VECTOR TO BE USED FOR THE REGRESSION MODEL, THESE SHOULD BE IN ORDER WITH THE ADDRESS OF LOG10(W) FIRST, THEN X1,X2,X3, THESE SHOULD BE SEPARATED BY COMMAS WITH NO TRAILING COMMA, A MAXIMUM OF 3 VARIABLES MAY BE USED IN ADDITION TO LOG10(W)
- 3) NUMBER OF CORRELATION COEFFICIENTS
COL 8-13 CORCOEF
COL 16-17 NUMBER OF CORRELATION COEFFICIENTS(12 FORMAT)
- 4) CATEGORY SPECIFICATION CARD
COL 8-13 CATGOR
COL 16-80 (TWO INTEGERS SEPARATED BY A COMMA, THE FIRST INTEGER IS THE ADDRESS OF THE CATEGORY INFORMATION IN THE DATA VECTOR, THE SECOND INTEGER IS THE NUMBER OF CATEGORIES IN THIS PROBLEM.
- 5) ONE CARD CONTAINING THE MAXIMUM NUMBER OF ITERATIONS AND THE NUMBER OF ITERATIONS TO BE SKIPPED BETWEEN PRINTING THE SIMPLEX--FORMAT 6110
- 6) THE REST OF THE DATA CARDS ARE EXACTLY AS DESCRIBED IN THE MANUAL FOR THIS ALGORITHM, THE FORMAT IS 8(2X,F8,5) THE VALUES FOR INITIAL ESTIMATES MUST BE INPUT IN THIS ORDER; REGRESSION VALUES, STANDARD DEVIATIONS IN

ASCENDING ORDER BY CATEGORY NUMBER), CORRELATION COEFFICIENT COEFFICIENTS (IN ORDER OF INCREASING LAG DISTANCE)

NOTE THE TOTAL NUMBER OF PARAMETERS (NUMBER OF REGRESSION
PARAMETERS + NUMBER OF CATEGORIES + NUMBER OF
CORRELATION COEFFICIENTS) MUST BE LESS THAN 21,
INTEGER COMANG(5), ANGCOUNT, COMPNT(4), TITLE(10), DATE(3),
WDPRD, CATEGORY(2)
REAL X(21,20), XCEN(21,20), XCON(21,20), XEX(21,20), Z(21), XREF(21,20)
EQUIVALENCE (CATLOC, CATEGORY(1)), (NUMCAT, CATEGORY(2))

SET-UP ERROR OVERRIDE TO PROCESS DOUBLE
END OF FILE MARK, REWIND WORKING FILES,

CALL FXOPT(85,1,1,1)
CALL FXALT(5100)
REWIND(02)
REWIND(03)

INPUT DATA CARDS

CALL FREEFORM(NAME, COMANG, 5, NUMANG, IEOF)
CALL FREEFORM(NAME, COMPNT, 4, NUMCMPT, IEOF)
READ(5, 901) NUMCOEF
901 FORMAT(15X, I2)
CALL FREEFORM(NAME, CATEGORY, 2, NULL, IEOF)
NREGPRAM=NUMCMPT
N=NREGPRAM+NUMCOEF+NUMCAT
NP1=N+1
20 ANGCOUNT=ANGCOUNT+1
NI=5
NO=6
READ(NI, 001) ITMAX, IPRINT
001 FORMAT (8I10)

INPUT MASTER HEADER

40 READ(02, END=100) TITLE, DATE, NUMHEAD, WDPRD

INITIAL CALL TO SUBROUTINE FUNC1
TO INPUT THE DATA FOR THIS PROBLEM AND
SET-UP NECESSARY DATA STRUCTURES

CALL FUNC1(COMANG(ANGCOUNT), COMPNT, NUMCMPT, CATLOC, NUMCAT,
1 NREGPRAM, NUMHEAD, NUMCOEF, WDPRD, N, NP1, X, Z)

MAINLINE FOR NELDER AND READ MINIMIZATION ROUTINE

READ (NI, 002) ALFA, BETA, GAM, ACC, A
002 FORMAT(8(2X, F8.5))
READ (NI, 002) (X(1,J), J=1,N)

PRECEDING PAGE BLANK NOT FILMED

```

C
Q=(A/N*(2.,5))*((N+1.)**5-1.)
P=(A/N*(2.,5))*((N+1.)**5-N-1.)
M=N+1
DO 130 I=2,M
AP=1.
DO 120 J=1,N
AP=AP+1.
IF(I.EQ.AP) GO TO 135
X(I,J)=X(1,J)+Q
GO TO 120
135 X(I,J)=X(1,J)+P
120 CONTINUE
130 CONTINUE

C
IF(ALFA.EQ.0.) ALFA=1.
IF(BETA.EQ.0.) BETA=.5
IF(GAM.EQ.0.) GAM=2.
IF(ACC.EQ.0.) ACC=.0001

C
WRITE (NO,003)
003 FORMAT (1H1,10X,28HNELDER AND HEAD OPTIMIZATION )
WRITE (NO,004)
004 FORMAT (/ ,2X,10HPARAMETERS )

C
WRITE (NO,005) N, ACC, ALFA, BETA, GAM, A
005 FORMAT (/ ,2X,4HN = ,12,4X,11HACCURACY = ,F7,4/ ,2X,8HALPHA = ,
1 F7,4,4X,7HBETA = ,F7,4, 4X,8HGAMMA = ,F7,4,4X,4HA = ,F7,4)
WRITE (NO,007)
007 FORMAT (/ ,10X,16HSTARTING SIMPLEX )
DO 140 I=1,NP1
WRITE (NO,006) (I,J,X(I,J),J=1,N)
006 FORMAT (/ ,2(1X,2HX(,12,1H,,12,2H)=,F8,5)/5(1X,2HX(,12,1H,,12,
1 2H)=,F8,5)/4(1X,2HX(,12,1H,,12,2H)=,F8,5))
140 CONTINUE
ITR=0
DO 155 I=1,NP1
CALL FUNC (I,X,Z,N,NP1)
155 CONTINUE
150 ITR=ITR+1
IF(ITR.GE.ITMAX) GO TO 149
IF (IPRINT) 156,152,156
156 IF (ITR-ITR/IPRINT=IPRINT) 162,158,162
158 WRITE (NO,008) ITR
008 FORMAT (/ ,2X,17HITERATION NUMBER ,13)
DO 160 J=1,NP1
160 WRITE (NO,006) (J,I,X(J,I),I=1,N)
WRITE (NO,009) (I,Z(I), I=1,NP1)
009 FORMAT (/ ,3(2X,2HF(,12,3H) =,F12,3))
162 ZHI=Z(1)
ZLO=Z(1)
DO 163 I=2,NP1

```

ORIGINAL PAGE IS
OF POOR QUALITY

```

      ZHI=AMAX1(Z(I),ZHI)
163  ZLO=AMIN1(Z(I),ZLO)
      DO 165 I=1,NP1
      IF (ZHI,EQ,Z(I)) GO TO 170
165  CONTINUE
C
C      LOCATE AND EVALUATE CENTROID
C
170  K=1
      EN=N
      DO 180 J=1,N
      SUM=0.
      DO 175 I=1,NP1
      IF (K,EQ,I) GO TO 175
      SUM= SUM+X(I,J)
175  CONTINUE
180  XCEN (K,J)=SUM/EN
      I=K
C  WRITE(42,920)(XCEN(K,J),J=1,N)
920  FORMAT('THE VALUES OF XCEN ARE'/10(F9,5,3X))
      CALL FUNC (I,XCEN,Z,N,NP1)
      ZCEN=Z(I)
      SUM=0.
      DO 185 I=1,NP1
      IF (K,EQ,I) GO TO 185
C
C      CHECK FOR CONVERGENCE, STOP IF CRITERIA
C      IS MET,
C
      SUM=SUM+(Z(I)-ZCEN)*(Z(I)-ZCEN)/EN
185  CONTINUE
      EJ=SQRT(SUM)
      IF (EJ.LT,ACC) GO TO 998
C
C      LOCATE AND EVALUATE REFLECTED POINT
C
      DO 190 J=1,N
      XREF(K,J)=XCEN(K,J)+ALFA*(XCEN(K,J)-X(K,J))
190  CONTINUE
      I=K
C
      CALL FUNC (I,XREF,Z,N,NP1)
      ZREF=Z(I)
      DO 200 I=1,NP1
      IF (ZLO,EQ,Z(I)) GO TO 205
200  CONTINUE
205  L=I
      IF (ZREF,LE,Z(I)) GO TO 240
      DO 207 I=1,N
      IF (ZREF,LT,Z(I)) GO TO 208
      GO TO 215
209  DO 210 J=1,N

```

```

210 X(K,J)=XREF(K,J)
    ZHI=ZREF
    IREF=1

```

C
C
C

LOCATE AND EVALUATE CONTRACTED POINT

```

215 DO 220 J=1,N
220 XCON(K,J)=XCON(K,J)+BETA*(X(K,J)-XCON(K,J))
    I=K
    CALL FUNC (I,XCON,Z,N,NP1)
    ZCON=Z(I)
    IF (ZCON.LT.ZHI) GO TO 230
    IF (IREF.EQ.0) GO TO 223
    IREF=0
    GO TO 150
223 DO 228 I=1,NP1
    IF (I.EQ.L) GO TO 228
    DO 225 J=1,N
225 X(I,J)=(X(I,J)+X(L,J))/2.
    CALL FUNC(I,X,Z,N,NP1)
228 CONTINUE
    GO TO 150
230 DO 235 J=1,N
235 X(K,J)=XCON(K,J)
    GO TO 150

```

C
C
C

LOCATE AND EVALUATE EXPANDED POINT

```

240 DO 245 J=1,N
245 XEX(K,J)=XCON(K,J)+GAM*(XREF(K,J)-XCON(K,J))
    I=K
    CALL FUNC (I,XEX,Z,N,NP1)
    ZEX=Z(I)
    IF (ZEX.LT.Z(L)) GO TO 255
    DO 250 J=1,N
250 X(K,J)=XREF(K,J)
    Z(K)=ZREF
    GO TO 150
255 DO 260 J=1,N
260 X(K,J)=XEX(K,J)
    GO TO 150
145 WRITE (NO,011) ITMAX
011 FORMAT (///,15X,20H DID NOT CONVERGE IN ,15,11H ITERATIONS, )
998 WRITE (NO,012) ZLO
012 FORMAT (///,2X,21H OPTIMUM VALUE OF F = ,E16,8)
    WRITE (NO,013)
013 FORMAT (///,2X,27H OPTIMUM VALUES OF VARIABLES )
    DO 300 I=1,N
300 WRITE (NO,014) I, X(NP1,I)
014 FORMAT (//,2X,24H ,12.4H) = ,1PE16,8)
    GO TO 40
100 REWIND(02)

```

```

REWIND(03)
IF (ANGCOUNT.NE.NUMANG) GO TO 20
STOP
END

```

ORIGINAL PAGE IS
OF POOR QUALITY

SUBROUTINE FUNC1(COMANG,COMPNT,NUMCMPT,CATLOC,NUMCAT,NREGPRAM,
1 NUMHEAD,NUMCOEF,WDPRD,NN,NP1,PARAM,Z)

PURPOSE

FUNC1 EVALUATES THE FUNCTION FOR A GIVEN POINT;
THIS EVALUATION IS DONE BY PARTITIONING THE COVARIANCE MATRIX
BY DATA SEGMENTS. THIS CAN BE DONE BECAUSE THERE IS NO
CORRELATION BETWEEN DATA SEGMENTS. THE VALUE OF THE
TOTAL FUNCTION IS THIS SUM ADDED TOGETHER FOR ALL OF THE
DATA SEGMENTS:(THE INVERSE OF THE VECTOR OF RESIDUALS)*
(THE INVERSE OF THE COVARIANCE MATRIX)*
(THE VECTOR OF RESIDUALS) + LOG10(OF THE DETERMINANT
OF THE COVARIANCE MATRIX)

THIS SUBROUTINE USES THE HIGH EFFICIENCY MATRIX PACKAGE(HEMP)
TO INVERT THE COVARIANCE MATRIX AND CALCULATE ITS DETERMINANT

THIS SUBROUTINE HAS TWO ENTRY POINTS; FUNC1 IS CALLED TO
INPUT THE DATA VECTORS AND BUILD Y(I) AND X(I,J). FUNC1
ALSO SETS OF DATA DESCRIPTOR VECTORS; SCAL, CATEGORY,N
ENTRY POINT FUNC IS THE NORMAL ENTRY POINT USED IN THE
MINIMIZATION TECHNIQUE.

INPUT ARGUMENTS

- COMANG • THE COMMAND ANGLE NUMBER
- COMPNT • AN ARRAY CONTAINING THE ADDRESSES IN THE DATA
VECTOR OF THE COMPONENTS USED FOR THE
REGRESSION PROBLEM. THESE MUST BE IN ORDER;
1) DEPENDENT VARIABLE, 2) CONSTANTS--A0, 3) COEFFI-
CIENTS--A1,A2,A3. A1 IS REQUIRED; A2 AND A3
ARE OPTIONAL TO BE USED IN LARGER MODELS.
- NUMCMPT • NUMBER OF COMPONENTS FROM THE DATA VECTOR
NEEDED FOR THIS MODEL.
- CATLOC • LOCATION OF THE CATEGORY WITHIN THE DATA VECTOR
- NUMCAT • NUMBER OF CATEGORIES
- NREGPRAM • NUMBER OF REGRESSION PARAMETERS (THIS IS EQUAL TO
NUMBER OF COMPONENTS)
- NUMHEAD • NUMBER OF HEADERS (DATA SEGMENTS) USED FOR THIS
PROBLEM
- NUMCOEF • NUMBER OF CORRELATION COEFFICIENTS
- WDPRD • NUMBER OF WORDS PER RECORD IN DATA VECTOR

NN • NUMBER OF PARAMETERS FOR EACH POINT IN THE
 SIMPLEX
 NP1 • NUMBER OF POINTS IN THE SIMPLEX(NN+1)
 PARAM • DATA SIMPLEX

OUTPUT ARGUMENT

Z(INP1) • FUNCTION EVALUATED AT CALLING POINT(ROW OF
 DATA SIMPLEX)

INTERNAL VARIABLES

CATEGORY • CATEGORY INFORMATION FOR EACH ROW OF X
 COVAR • COVARIANCE MATRIX
 DATVEC • INPUT DATA VECTOR OF SKYLAB DATA
 ENDHEAD • POINTER TO LAST ELEMENT OF PREVIOUS HEADER
 IDATVEC • INTEGER ADDRESS OF DATVEC
 N • VECTOR CONTAINING THE NUMBER OF USABLE SCANS
 IN EACH DATA SEGMENT
 RESIDUAL • VECTOR OF REGRESSION RESIDUALS
 SCAN • VECTOR OF THE SCAN NUMBERS CORRESPONDING TO
 TO EACH ROW OF X AND EACH ELEMENT OF Y
 X • MATRIX CONTAINING ONE COLUMN FOR EACH SCATTERING
 COEFFICIENT USED IN THE REGRESSION PROBLEM,
 Y • VECTOR OF GROUND TRUTH WIND ESTIMATES, THESE
 ESTIMATES SHOULD BE LOGIC AS THE RESULT OF A
 TRANSEN ACTIVITY

DESCRIPTION OF PARAM(I,J)

EACH ROW OF PARAM(I,J) CONTAINS THE VALUES FOR ALL OF THE
 PARAMETERS CORRESPONDING TO ONE POINT IN THE SIMPLEX. THE
 PARAMETERS ARE PACKED FROM THE LEFT END OF EACH ROW IN
 THIS ORDER: 1) REGRESSION PARAMETERS, 2) STANDARD DEVIATIONS,
 3) THE CORRELATION COEFFICIENTS. THE TOTAL NUMBER OF
 PARAMETERS MUST BE LESS THAN 21.

IMPLICIT INTEGER(A-Z)

[illegible]

```

N(NHEAD)=1-ENDHEAD
ENDHEAD=1
WRITE(42,980) N(NHEAD)

```

```

      SKIP TO LOAD DATA FROM NEXT SEGMENT

```

```

      GO TO 20

```

```

      CLOSE DATA FILES AND RETURN

```

```

100 CALL FCLOSE(02)
    READ(03,END=110)
110 CALL FCLOSE(03)
    RETURN

```

```

ENTRY FUNC(INP1,PARAM,Z,NN,NP1)

```

```

      THIS ENTRY POINT IS USED DURING THE ITERATION PROCESS.

```

```

      INPUT ARGUMENTS

```

```

      INP1  •   ROW OF PARAM TO BE EVALUATED
      PARAM •   ADDRESS OF SIMPLEX
      NN    •   NUMBER OF PARAMETERS
      NP1   •   NUMBER OF POINTS

```

```

      OUTPUT ARGUMENT

```

```

      Z(INP1) •   EVALUATED FUNCTION

```

```

      ENDHEAD=0
      Z(INP1)=0

```

```

      SCALE STANDARD DEVIATION TO AVOID
      UNDERFLOW

```

```

      DO 180 I=1,NUMCAT
180  PARAM(INP1,NREGPRAM+I)=PARAM(INP1,NREGPRAM+I)*.1,

```

```

      THIS LOOP HANDLES EACH DATA SEGMENT AS
      A PARTITION. EACH SEGMENT IS PROCESSED
      AND THEN ADDED TO THE RESULT OF PREVIOUS
      SEGMENTS. AT THE END OF THE LOOP ALL OF
      THE DATA HAS BEEN PROCESSED,

```

```

      DO 500 HEADCNT=1,NUMHEAD
      IF(N(HEADCNT).EQ.0) GO TO 500

```

ORIGINAL PAGE IS
OF POOR QUALITY

```

C
C
C      CALCULATE THE RESIDUALS, (THESE ARE ALSO
C      SCALED,)
C
DO 220 I=1,N(HEADCNT)
  RESIDUAL(I)=0
  TEMP=PARAM(INP1,1)
  DO 200 J=1,NUMCHPT-1
200  TEMP=TEMP+X(I+ENDHEAD,J)*PARAM(INP1,J+1)
220  RESIDUAL(I)=(Y(I+ENDHEAD)-TEMP)*10.

C
C      ZERO OUT COVARIANCE MATRIX
C
DO 260 I=1,N(HEADCNT)
  DO 260 J=1,N(HEADCNT)
260  COVAR(I,J)=0

C
C      BUILD UP THE COVARIANCE MATRIX
C
J=1
DO 320 I=1,N(HEADCNT)
  CATI=CATEGORY(I+ENDHEAD)

C
C      BUILD UP DIAGONAL ELEMENT
C
IF(I.EQ.J) COVAR(I,J)=PARAM(INP1,CATI+NREGPRAM)*.2
300  J=J+1
  IF(J.GT.N(HEADCNT)) GO TO 320

C
C      BUILD OFF DIAGONAL ELEMENTS
C
LAGDIST=SCAN(J+ENDHEAD)-SCAN(I+ENDHEAD)
IF(LAGDIST.GT.NUMCOEF) GO TO 320
CATJ=CATEGORY(J+ENDHEAD)
COVAR(I,J)=PARAM(INP1,LAGDIST+NREGPRAM+NUMCAT)*PARAM(INP1,
1  CATI+NREGPRAM)*PARAM(INP1,CATJ+NREGPRAM)
  COVAR(J,I)=COVAR(I,J)
  GO TO 300
320  J=J+1

C
C      CALL HEMP TO INVERT THE COVARIANCE
C      MATRIX AND EVALUATE ITS DETERMINANT
C
CALL HEMINV(COVAR,N(HEADCNT),SCRATCH,DETERM)

C
C      COMPUTE THE VECTOR TRIPLE PRODUCT
C
DO 420 J=1,N(HEADCNT)
  TEMP=0
  DO 400 I=1,N(HEADCNT)
400  TEMP=TEMP+RESIDUAL(I)*COVAR(I,J)
420  Z(INP1)=Z(INP1)+TEMP*RESIDUAL(J)

C
C      SUM PRODUCT AND LOG10 OF DETERMINANT
C
Z(INP1)=Z(INP1)+ALOG(DETERM)

C
C      PRINT WARNING MESSAGE IF DETERMINANT IS
C      LESS THAN OR EQUAL TO ZERO,
C
IF(DETERM.LE.0.) WRITE(6,950) Z(21), INP1, HEADCNT, DETERM
950  FORMAT('DETERMINANT ERROR**CALL ',F3.1,4X,'ROW ',I2,4X,'HEADER ',
: 12,4X,'VALUE ',1PE16.8)
999  ENHEAD=ENDHEAD+N(HEADCNT)

C
C      SCALE STANDARD DEVIATIONS DOWN TO
C      INPUT VALUES
C
DO 600 I=1,NUMCAT
600  PARAM(INP1,NREGPRAM+I)=PARAM(INP1,NREGPRAM+I)/10.
  RETURN
END

```

CINC

SUBROUTINE INCANG (SIGMA,THETA,ICOM,WS,SIGMAC,RSIGMA)

THIS SUBROUTINE CORRECTS THE SIGMA VALUES FROM INCIDENT ANGLE
VARIATIONS BY USING THE FOLLOWING EQUATION
$$\text{SIGMAC (B)} = (\text{COEFF(1,B,C)} + \text{COEFF(2,B,C)} * \text{LOG (WS)}) * (\text{ANGLE} - \text{THETA}) + \text{SIGMA (B)}$$

DEFINITION OF THE VARIABLES

COEFF(A,B,C) = A IS 1 FOR INTERCEPT TERM, 2 FOR SLOPE TERM,
B INDICATES POLARIZATION, 1 FOR VV, 2 FOR HH,
3 FOR VH, 4 FOR HV.
C INDICATES COMMAND ANGLE, 1 FOR 50, 2 FOR 43,
3 FOR 32, 4 FOR 17, AND 5 FOR 1 DEGREE.

SIGMAC(I) = CORRECTED SIGMA, SUBSCRIPT INDICATING THE
POLARIZATION AS DEFINED ABOVE

SIGMA (I) = UNCORRECTED SIGMA, SUBSCRIPT INDICATING THE
POLARIZATION AS DEFINED ABOVE

RSIGMA (I) = INCIDENT ANGLE CORRECTION, SUBSCRIPT INDICATING
POLARIZATION AS DEFINED ABOVE

WS = WIND SPEED

ANGLE = STANDARD ANGLES, SET EQUAL TO 50, 43, 32, 17, AND 1
DEGREE,

THETA = INCIDENT ANGLE

THE PROGRAM CALCULATES THE CORRECTED SCATTERING COEFFICIENTS,
SIGMAC(I), FOR THE GIVEN INCIDENT ANGLE(THETA), COMMAND
ANGLE(ICOM), AND THE SCATTERING COEFFICIENTS, SIGMA(I).

DIMENSION SIGMA(4), SIGMAC(4), COEFF(2,4,5), RSIGMA(4)

DATA COEFF /-0.3587,0.0817,-0.7646,0.1471,-0.3335,0.0946,
-0.3385,0.0946,-0.4628,0.1362,-0.8568,0.2343,-0.3333,0.1019,
-0.3333,0.1015,-0.5238,0.2016,-0.7363,0.2615,-0.3119,0.1207,
-0.3119,0.1207,-1.1874,0.1416,-1.1600,0.1244,0.0,0.0,0.0,0.0,
-0.1813,0.0917,-0.1819,0.0917,0.0,0.0,0.0,0.0/
DATA DEFLT/037777777777777777/

IF (THETA.EQ.DEFLT) GO TO 100

IF (WS.EQ.DEFLT) GO TO 100

IF (ICOM.LT.1.OR.ICOM.GT.5) GO TO 100

IF (ICOM.EQ.1) ANGLE=50,

IF (ICOM.EQ.2) ANGLE=43.

IF (ICOM.EQ.3) ANGLE=32.

IF (ICOM.EQ.4) ANGLE=17.

IF (ICOM.EQ.5) ANGLE=1.

IF (ABS(ANGLE-THETA).GT.2.) GO TO 100

DO 10 I=1,4

IF (SIGMA(I).EQ.DEFLT) GO TO 200

RSIGMA(I) = (ANGLE-THETA)*(COEFF(1,I,ICOM)+COEFF(2,I,ICOM)*
ALOG10(WS))

SIGMAC (I) = SIGMA(I) + RSIGMA(I)

GO TO 10

200 SIGMAC(I) = DEFLT

RSIGMA(I) = DEFLT

10 CONTINUE

GO TO 300

100 DO 20 I=1,4

RSIGMA(I) = DEFLT

20 SIGMAC (I) = DEFLT

300 RETURN

END

SUBROUTINE ASPCOR (SIGMA,ASPANG,WNDSPD,ICOM,SIGMAC,RSIGMA)

CASPCOR

THE SUBROUTINE ASPCOR CORRECTS SIGMA VALUES FROM ASPECT ANGLE VARIATIONS.

FOR GIVEN SCAN NUMBER, COMMAND ANGLE NUMBER(ICOM), AND WIND SPEED(WNDSPD), THE SIGMA IS CORRECTED BY FOLLOWING EQUATION

SIGMAC (I) = SIGMA (I) + 0 IF WNDSPD.LE.6.5 KNOTS
= SIGMA (I) + (COEFF(1,I,C)+COEFF(2,I,C)*LOG(WNDSPD))
*F(AANGLE)

WHERE

F(AANGLE) = 0.498-0.1916 COS(AANGLE)-0.4042 COS(2*AANGLE)
+0.0978 COS(4*AANGLE)

AANGLE = ASPECT ANGLE IN RADIANS

SIGMAC (I) = CORRECTED SIGMA, I=1 FOR VV, I=2 FOR HH.

SIGMA (I) = UNCORRECTED SIGMA, I=1 FOR VV, I=2 FOR HH.

RSIGMA (I) = INCIDENT ANGLE CORRECTION, SUBSCRIPT INDICATING POLARIZATION AS DEFINED ABOVE

COEFF(A,B,C) = COEFFICIENTS, A=1 FOR THE CONSTANT TERM,
A=2 FOR THE SLOPE TERM, B INDICATES THE
POLARIZATION (B=1 FOR VV, B=2 FOR HH,
B=3 FOR VH, B=4 FOR HV),
C INDICATES COMMAND ANGLE NUMBER, 1 FOR 50;
2 FOR 43, 3 FOR 32 DEGREES).

WNDSPD = WIND SPEED, KNOTS

DIMENSION SIGMA(4),SIGMAC(4),COEFF(2,4,3),RSIGMA(4)
DATA COEFF/-5.269,6.735,-4.985,6.879,-10.649,13.268,-10.649,
13.268,-5.106,6.585,-4.785,6.543,-10.627,13.209,-10.627,13.209,
-5.299,6.600,-5.257,6.615,-10.657,13.139,-10.657,13.139/
DATA DEFLT/0.3777777777777777/
IF (ASPANG.EQ.DEFLT) GO TO 100
IF (WNDSPD.EQ.DEFLT) GO TO 100
IF (ICOM.EQ.DEFLT) GO TO 100
IF (ICOM.LT.1.OR.ICOM.GT.3) GO TO 600

AANGLE = ASPANG*3.14159/180
F = 0.498-0.1916*COS(AANGLE)-0.4042*COS(2*AANGLE)
+0.0978*COS(4*AANGLE)

DO 10 I=1,4
IF (SIGMA(I).EQ.DEFLT) GO TO 200
IF (WNDSPD.LE.6.5) GO TO 300
RSIGMA (I) = (COEFF(1,I,ICOM)+COEFF(2,I,ICOM)*ALOG10(WNDSPD))*F
SIGMAC (I) = SIGMA(I)+RSIGMA(I)

GO TO 10
200 SIGMAC (I) = DEFLT
RSIGMA(I) = DEFLT
GO TO 10

300 SIGMAC(I) = SIGMA(I)
RSIGMA(I) = 0.0

10 CONTINUE
GO TO 400

100 DO 20 I=1,4
RSIGMA(I) = DEFLT
20 SIGMAC(I) = DEFLT

400 RETURN

600 DO 30 I=1,4
RSIGMA(I) = 0.0
30 SIGMAC(I) = SIGMA(I)
RETURN
END

SUBROUTINE ATM50(THETA,TW,TAPV,TAPH,SAL,EV,EH,ATTEN)

THIS ROUTINE COMPUTES THE POLARIZED EMISSIVITIES AND ATTENUATION AT 50 DEGREES INCIDENT ANGLE. THE INCIDENT ANGLE (THETA) AND WATER TEMPERATURE (TW) ARE CONVERTED FROM DEGREES TO RADIANS AND FROM DEGREES CENTIGRADE TO DEGREES KELVIN INTERNALLY. THE ROUTINE ALSO CHECKS THE INPUT ARGUMENTS FOR DEFAULT VALUES. SHOULD THERE EXIST ANY DEFAULTED INPUT PARAMETERS, THE ROUTINE WILL RETURN DEFAULT VALUES FOR THE CORRESPONDING OUTPUT PARAMETERS.

INPUT PARAMETERS

THETA = INCIDENT ANGLE (DEG)
TW = WATER TEMPERATURE (DEG C)
TAPV = VERTICAL APPARENT TEMPERATURE (DEG K)
TAPH = HORIZONTAL APPARENT TEMPERATURE (DEG K)
SAL = SALINITY IN PPM

OUTPUT PARAMETERS

EV = VERTICAL EMISSIVITY
EH = HORIZONTAL EMISSIVITY
ATTEN = ATTENUATION (DB)

INTERNAL PARAMETERS

I = A FLAG WHICH IS SET TO DETERMINE WHETHER OR NOT ALL THE OUTPUT PARAMETERS ARE DEFAULTED FOR THE 50 DEGREE CASE. WHEN I=0, ALL THE 50 DEGREE CASE PARAMETERS ARE DEFAULTED AND THERE IS NO NEED TO PERFORM THE CALCULATIONS AT THE ENTRY POINT ATM. WHEN I=1, ALL THE OUTPUT PARAMETER VALUES FOR THE 50 DEGREE CASE ARE NOT DEFAULT. I IS RESET TO 1 FOR EACH NEW SCAN.
RV,RH = POLARIZED FRESNEL COEFFICIENTS
GAMMA = TRANSMITTANCE AT 50 DEGREES INCIDENT ANGLE
GAMANG = TRANSMITTANCE AT OTHER INCIDENCE ANGLES
TABARV,TABARH = POLARIZED MEAN ATMOSPHERIC TEMP.
TVAT,THAT = POLARIZED ATMOSPHERIC TEMPERATURES
T = ATMOSPHERIC OPACITY

COMPLEX RV,RH

DATA DEFLT/0377777777777777/

DATA FREQ,1/13.9,1/

IF(THETA,EQ,DEFLT,OR,TW,EQ,DEFLT,OR,TAPV,EQ,DEFLT,OR,SAL,EQ,DEFLT)
160 TO 20

ANGRAD=THETA/57.3 CONVERT INCIDENT ANGLE IN DEG TO RADIANS

THK=TW+273.18 CONVERT WATER TEMPERATURE IN DEG C TO DEG K

CALL DIECO(FREQ,THK,SAL) CALCULATE THE VERTICAL EMISSIVITY FOR THE ZERO WIND CASE

CALL FRESNEL(ANGRAD,RV,RH)

RVH2=RV*CONJG(RV)

ORIGINAL PAGE IS
OF POOR QUALITY


```

EV=1.-RVH2
C      CALCULATE VERTICAL BRIGHTNESS TEMPERATURE
TBV=EV-TWK
C      CALCULATE VERTICAL EXCESS TEMPERATURE
TVEX=TAPV-TBV
CALL ATTENV(TVEX,THETA,GAMMA,ATTEN,T)
CALL TATH(TVEX,GAMMA,TWK,TAPV,TVAT,TABARV)
IF(TAPH.EQ.DEFLT) GO TO 10
CALL HEXCESS(TVEX,THEX)
C      CALCULATE HORIZONTAL BRIGHTNESS TEMPERATURE
TBH=TAPH-THEX
C      CALCULATE HORIZONTAL EMISSIVITY
EH=TBH/TWK
CALL TATH(THEX,GAMMA,TWK,TAPH,THAT,TABARH)
GO TO 30
10 EH=DEFLT
GO TO 30
20 EV=DEFLT
EH=DEFLT
ATTEN=DEFLT
I=0
30 RETURN
ENTRY ATH(THETA,TW,TAPV,TAPH,EV,EH,ATTEN)
THIS ENTRY POINT CALCULATES THE POLARIZED
EMISSIVITIES AND THE ATTENUATION FOR INCIDENT
ANGLES OTHER THAN 50 DEGREES. THE MAIN ROUTINE
IS CALLED ONCE TO DETERMINE THE POLARIZED MEAN
ATMOSPHERIC TEMPERATURES (TABARV AND TABARH) AND THE
ATMOSPHERIC OPACITY (T) FOR THE 50 DEGREE CASE AND
SINCE THESE ARGUMENTS ARE CONSTANT AT ALL OTHER
INCIDENCE ANGLES, THE EMISSIVITIES AND ATTENUATION
MAY BE DETERMINED FOR ANY INCIDENT ANGLE,

IF(I.EQ.0.OR.THETA.EQ.DEFLT) GO TO 70
ANGHAD=THETA/57.3
SECANG=1./COS(ANGRAD)
C      CALCULATE THE TRANSMITTANCE AND ATTENUATION
GAMANG=EXP(-SECANG*T)
ATTEN=-10.*ALOG10(GAMANG)
IF(TAPV.EQ.DEFLT.OR.TW.EQ.DEFLT) GO TO 40
TWK=TW+273.18
CALL EPS(TABARV,TAPV,GAMANG,TWK,EV)
GO TO 50
40 EV=DEFLT
50 IF(TAPH.EQ.DEFLT.OR.TW.EQ.DEFLT) GO TO 60
TWK=TW+273.18
CALL EPS(TABARH,TAPH,GAMANG,TWK,EH)
GO TO 80
60 EH=DEFLT
GO TO 80
70 EV=DEFLT
EH=DEFLT

```

```

ATTEN=DEFLT
80 RETURN
END

```

SUBROUTINE TRANSREF(TW,SAL,THETA,STDANG,EV,EH,TBVREF,TBHREF)

THIS ROUTINE CORRECTS THE RADIOMETER MEASUREMENTS
BY TRANSLATING THE BRIGHTNESS TEMPERATURE TO A
REFERENCE BRIGHTNESS TEMPERATURE BASED ON 290 DEGREE
KELVIN WATER TEMPERATURE AND THE STANDARD ANGLE
SPECIFIED.

INPUT PARAMETERS

TW = WATER TEMPERATURE (DEG C)
SAL = SALINITY IN PPM
THETA = INCIDENT ANGLE (DEG)
STDANG = STANDARD ANGLE (DEG)
EV = VERTICAL EMISSIVITY
EH = HORIZONTAL EMISSIVITY

OUTPUT PARAMETERS

TBVREF = VERTICAL REFERENCE TEMPERATURE (DEG K)
TBHREF = HORIZONTAL REFERENCE TEMPERATURE (DEG K)

DATA FREQ,TS/13.9,290,/
DATA DEFLT/0377777777777777/
COMPLEX RV,RH
IF(EV,EQ,DEFLT.AND,EH,EQ,DEFLT) GO TO 100
IF(TW,EQ,DEFLT.OR,SAL,EQ,DEFLT.OR,THETA,EQ,DEFLT.OR,STDANG,EQ,DEFLT
OR) GO TO 100

ANGRAD=THETA/57.3 CONVERT INCIDENT ANGLE IN DEG TO RADIANS
SAR=STDANG/57.3 CONVERT STANDARD INCIDENT ANGLE
IN DEGREES TO RADIANS
TWK=TW+273.15 CONVERT WATER TEMPERATURE IN DEG C TO DEG K
CALCULATE THE FRESNEL COEFFICIENTS AND
THE EMISSIVITIES AT THE CELL WATER
TEMPERATURE AND THE ACTUAL INCIDENT ANGLE

CALL DIECO(FREQ,TWK,SAL)
CALL FRESNEL(ANGRAD,RV,RH)
RVM2=RV*CONJG(RV)
RHM2=RH*CONJG(RH)
EPSLV=1.-RVM2
EPSLH=1.-RHM2

CALCULATE THE FRESNEL COEFFICIENTS AND
THE EMISSIVITIES AT THE STANDARD WATER
TEMPERATURE (290 DEG KELVIN) AND THE
STANDARD INCIDENT ANGLE

CALL DIECO(FREQ,TS,SAL)
CALL FRESNEL(SAR,RV,RH)
RVMG2=RV*CONJG(RV)
RHM2=RH*CONJG(RH)
EPSLVN=1.-RVMG2
EPSLHN=1.-RHM2

CALCULATE THE CHANGE IN EMISSIVITY BETWEEN

DELEV=EPSLVN-EPSLV THE STANDARD AND CELL WATER TEMPERATURES
DELEH=EPSLHN-EPSLH

IF(EV,EQ,DEFLT) GO TO 50 TRANSLATE TO THE REFERENCE WATER TEMP.

ESV=EV*DELEV
TBVREF=TS*ESV
GO TO 60

50 TBVREF=DEFLT

60 IF(EH,EQ,DEFLT) GO TO 80

ESH=EH*DELEH
TBHREF=TS*ESH
GO TO 200

80 TBHREF=DEFLT

GO TO 200

100 TBVREF=DEFLT

TBHREF=DEFLT

200 RETURN

END

```

SUBROUTINE EPS(TK,TAPP,GAMANG,TWK,E)
  THIS ROUTINE CALCULATES THE POLARIZED EMISSIVITY AT A
  GIVEN INCIDENT ANGLE OTHER THAN 50 DEGREES,

```

INPUT PARAMETERS

```

  TK = POLARIZED MEAN ATMOSPHERIC TEMPERATURE
  TAPP = POLARIZED APPARENT TEMPERATURE (DEG K)
  GAMANG = TRANSMITTANCE
  TWK = WATER TEMPERATURE (DEG K)

```

OUTPUT PARAMETER

```

  E = POLARIZED EMISSIVITY

```

```

  TATH=TK*(1.-GAMANG)
  A=TAPP
  B=GAMANG
  C=TATH
  D=TWK
  E=(A-C*(B+1.)-2.7*B*B)/(B*(D-C-2.7*B)-C)
  RETURN
  END

```

SUBROUTINE HEXCESS(V,H)

```

  THIS ROUTINE CALCULATES THE HORIZONTAL EXCESS TEMPERATURE
  AS A FUNCTION OF VERTICAL EXCESS TEMPERATURE.

```

INPUT PARAMETER

```

  V = VERTICAL EXCESS TEMPERATURE (DEG K)

```

OUTPUT PARAMETER

```

  H = HORIZONTAL EXCESS TEMPERATURE (DEG K)

```

```

  H=1.53102*V+.00447*V**2-.00008*V**3
  RETURN
  END

```

SUBROUTINE TATH(TEX50,GAMMA,TWK,TAPP,TATH50,TK)

```

  THIS ROUTINE CALCULATES THE POLARIZED ATMOSPHERIC
  TEMPERATURE AT 50 DEGREES AND MEAN ATMOSPHERIC TEMP.

```

INPUT PARAMETERS

```

  TEX50 = EXCESS TEMPERATURE FOR 50
          DEGREES INCIDENT ANGLE (DEG K)
  GAMMA = TRANSMITTANCE AT 50 DEGREES INCIDENT ANGLE
  TWK = WATER TEMPERATURE (DEG K)
  TAPP = POLARIZED APPARENT TEMPERATURE (DEG K)

```

OUTPUT PARAMETERS

```

  TATH50 = POLARIZED ATMOSPHERIC TEMPERATURE (DEG K)
  TK = POLARIZED MEAN ATMOSPHERIC TEMPERATURE

```

```

  E50=(TAPP-TEX50)/TWK
  A=TEX50
  B=GAMMA
  C=E50
  D=TWK
  TATH50=(A-(B-1.)*C*D-2.7*B*B*(1.-C))/(B*(1.-C)+1.)
  TK=TATH50/(1.-GAMMA)
  RETURN
  END

```

```

SUBROUTINE ATTENU (TVEX50,THETA,GAM50,ATTN50,T)
      THIS ROUTINE CALCULATES THE ATTENUATION,TRANSMITTANCE,
      AND OPACITY AT 50 DEGREES INCIDENT ANGLE.

      INPUT PARAMETERS
            TVEX50 = VERTICAL EXCESS TEMPERATURE
                      AT 50 DEGREES INCIDENT ANGLE (DEG K)
            THETA = INCIDENT ANGLE (DEG)

      OUTPUT PARAMETERS
            GAM50 = TRANSMITTANCE AT 50 DEGREES
            ATTN50 = ATTENUATION AT 50 DEGREES (DB)
            T = ATMOSPHERIC OPACITY

      X=TVEX50
      ATTN50=3.017950335*X-0.00005559*X**2+0.000004331*X**3
      GAM50=10.**(-ATTN50/10.)
      RAD=THETA/57.3
      SEC=1./COS(RAD)
      T=*(ALOG(GAM50))/SEC
      RETURN
      END

```

```

SUBROUTINE FRESNEL(THETA,RV,RH)
  THIS ROUTINE COMPUTES THE CLASSICAL
  FRESNEL REFLECTION COEFFICIENTS FOR SEA WATER.
  THIS SUBROUTINE MUST BE INITIALIZED BY
  CALLING THE SECONDARY ENTRY ROUTINE DIECO.
  THE COMPLEX PERMITTIVITY IS COMPUTED BY DIECO.
  ONCE HAVING COMPUTED THE PERMITTIVITY FOR A PARTICULAR
  FREQUENCY(FREQ), WATER TEMPERATURE(TEMP), AND
  SALINITY(SAL), FRESNEL MAY BE CALLED REPEATEDLY
  FOR DIFFERENT ANGLES(THETA),

INPUT PARAMETERS
  FREQ = FREQUENCY IN GHZ
  TEMP = TEMPERATURE(DEG K)
  SAL = SALINITY IN PP4
  THETA = INCIDENT ANGLE (RADIAN)

OUTPUT PARAMETERS
  RV = VERT. POL. FRESNEL COEFF. (COMPLEX)
  RH = HORT. POL. FRESNEL COEFF. (COMPLEX)

DIMENSION E(2)
EQUIVALENCE (E(1),ESP)
COMPLEX ESP,COST,SQ,RV,RH
DATA PID/0.0314159265/
COST=CMPLX(COS(THETA),0.0)
SQ=CSQRT(ESP-CMPLX(SIN(THETA)**2,0.0))
RV=(ESP-COST-SQ)/(ESP-COST+SQ)
RH=(COST-SQ)/(COST+SQ)
RETURN
ENTRY DIECO(FREQ,TEMP,SAL)
  THIS ENTRY POINT COMPUTES THE DIELECTRIC CONSTANT
  FOR SEA WATER. ALGO BASED ON PORTER'S WORK (1971).
  (SEE S.T. WU AND A.K. FUNG'S REPORT NASA CR 2329).

  CONVERT SALINITY TO NORMALITY (SEE STOGRYN IEEE
  MTT AUG, 1971)

  S = SAL
  S=((4.058E-09*S+1.205E-05)*S+1.707E-02)*S
  T=TEMP-273.18
  NORMALIZED WAVELENGTH
  R1=((0.00147*T-0.11)*T+3.38+(0.0173*T-0.52)*S)*FREQ/30.0
  R2=(R1)**1.96
  R1=R1**.98
  E(2)=83.0-15.3*S-0.363*T
  D=1.0+2.0*R1*PID*R2
  E(1)=4.8-E(2)*(1.0*R1*PID)/D
  SIG=(0.12*T+5.0)*S+0.04*T
  E(2)=18.0*SIG/FREQ+E(2)*R1/D
  RETURN
END

```

ORIGINAL PAGE IS
OF POOR QUALITY

```

SUBROUTINE CATGOR(HEADER,IX,RECSIZE,SCAN,COMANG,ICAT)
SUBROUTINE TO ASSIGN DIFFERENT CATEGORY DESIGNATIONS
CATGOR
AUTHOR BIRREP
PURPOSE
  THIS ROUTINE RETURNS THE CATEGORY FOR A GIVEN DATA VECTOR
INPUT ARGUMENTS
  HEADER • THE ADDRESS OF THE FIRST ELEMENT IN THE HEADER
           OF THIS DATA SEGMENT
  IX      • INTEGER DATA VECTOR
  RECSIZE • NEW RECORD SIZE
  SCAN    • SCAN NUMBER OF THIS DATA VECTOR
  COMANG  • COMMAND ANGLE NUMBER OF THIS DATA VECTOR
OUTPUT ARGUMENT
  ICAT    • THE INTEGER VALUE OF THE CATEGORY
           1, WEATHERSHIP OR AIRCRAFT
           2, SHIP WITH ANEMOMETER OF KNOWN HEIGHT
           3, SHIP WITH ANEMOMETER OF UNKNOWN HEIGHT
           4, VISUAL OBSERVATION
           5, NO SHIP REPORT
           6, HURRICANE
  INTEGER HEADER(27),RECSIZE,IX(RECSIZE),SCAN,COMANG
  IF(HEADER(4),LT,29) GO TO 30
  ICAT=5
  DO 20 I=29,50,3
  IF(IX(I),LT,2) GO TO 20
  IF(IX(I)-1,LT,ICAT) ICAT=IX(I)-1
20 CONTINUE
  RETURN
30 IF(HEADER(1),NE,157,AND,HEADER(1),NE,245) GO TO 40
  ICAT=6
  RETURN
40 IF(HEADER(1),NE,156) GO TO 80
  NCELL = SCAN*(5-COMANG)
  ICAT=5
  IF(NCELL,GT,5,AND,NCELL,LT,10) ICAT=1
  RETURN
80 IF(HEADER(1),NE,247) GO TO 100
  ICAT=3
  RETURN
100 IF(HEADER(1),NE,162) GO TO 120
  ICAT=5
  RETURN
120 WRITE(42,950) HEADER(1),HEADER(2)
950 FORMAT('***WARNING***NO CATEGORIES WERE ASSIGNED TO ',I3,'-',I1)
  RETURN
  END

```

```

CFFT
SUBROUTINE FFT(XR,XI,YR,YI,N)
C
C.....
C
C ARGUMENTS
C INPUT
C XR --- XR(N) CONTAINS THE REAL COMPONENTS OF THE SAMPLED
C       FUNCTION TO BE TRANSFORMED
C XI --- XI(N) CONTAINS THE IMAGINARY COMPONENTS OF THE
C       SAMPLED FUNCTION TO BE TRANSFORMED
C N --- NUMBER OF SAMPLE POINTS TO BE TRANSFORMED
C OUTPUT
C YR --- YR(N) CONTAINS THE REAL COMPONENTS OF THE FOLDED
C       FREQUENCY SPECTRUM
C YI --- YI(N) CONTAINS THE IMAGINARY COMPONENTS OF THE
C       FOLDED FREQUENCY SPECTRUM
C
C NOTE - XR AND XI HAVE BEEN DESTROYED UPON RETURN
C.....
C
C INTEGER P(15), PRIME, R(63), ADDRESS(15)
C DIMENSION XR(N),XI(N),YR(N),YI(N)
C
C SPECIFY PRIME NUMBERS AND 2*PI
C
C DATA R/2,3,5,7,11,13,17,19,23,29,31,37,41,43,47,53,59,61,67,71,73,
C       79,83,89,97,101,103,107,109,113,127,131,137,139,149,151,
C       157,163,167,173,179,181,191,193,197,199,211,223,227,229,
C       233,239,241,251,257,263,269,271,277,281,283,293,307/
C DATA TP/6.2831853/
C
C FIND THE M PRIME NUMBERS IN N AND STORE
C THEM IN P
C
11 I=0
M=0
N1=N
1 I=I+1
IF(I.EQ.64) GO TO 15
2 IF((N1/R(I))*R(I).NE.N1) GO TO 1
M=M+1
P(M)=R(I)
N1=N1/R(I)
IF(FLOAT(R(I)).GT.SQRT(FLOAT(N1))+0.001) GO TO 3
GO TO 2
3 IF(N1.EQ.1) GO TO 8
15 M=M+1
P(M)=N1
8 NDIV=1

```

ORIGINAL PAGE IS
OF POOR QUALITY

```

C      DO EACH LAYER
C
C      DO 4 LAYER=1,M
C      PRIME=P(LAYER)
C
C      DETERMINE NUMBER AND LENGTH OF TRANSFORMS
C      IN THE LAYER
C
C      NTRANS=NDIV
C      LTRANS=N/NTRANS
C
C      DETERMINE THE NUMBER AND LENGTH OF
C      DIVISIONS IN LAYER
C
C      NDIV=NDIV*P(LAYER)
C      LDIV=N/NDIV
C
C      DO EACH TRANSFORM
C
C      DO 4 I=1,NTRANS
C
C      DETERMINE LOCATION IMMEDIATELY BEFORE
C      TRANSFORM
C
C      LOC1=(I-1)*LTRANS
C
C      GO THROUGH EACH INDEPENDENT PART OF THE
C      TRANSFORM
C
C      DO 10 K=1,LDIV
C
C      DETERMINE FIRST LOCATION IN INDEPENDENT
C      PART
C
C      LOC2=LOC1+K
C
C      DETERMINE EACH TRANSFORM ELEMENT OF
C      INDEPENDENT PART
C
C      DO 6 J=1,PRIME
C      YR(J)=0
C      YI(J)=0
C
C      ADD COMPONENTS FORMING TRANSFORM ELEMENT
C
C      DO 6 L=1,PRIME
C
C      DETERMINE LOCATION OF COMPONENT
C
C      LOC4=LOC2+(L-1)*LDIV
C      THETA=PI*((FLOAT(L)-1.)*(FLOAT(J)-1.)/FLOAT(PRIME))
C      YR(J)=YR(J)+XR(LOC4)*COS(THETA)+XI(LOC4)*SIN(THETA)

```

```

      YI(J)=YI(J)+XI(LOC4)*COS(THETA)-XR(LOC4)*SIN(THETA)
6  CONTINUE

```

C
C
C

TWIDDLE INDEPENDENT PART

```

      DO 10 J=1,PRIME
      PHI = TPI*(FLOAT(K)-1.)*(FLOAT(J)-1.)/FLOAT(LTRANS)
      LOC3=LOC2+(J-1)*LDIV
      XR(LOC3)=YR(J)*COS(PHI)+YI(J)*SIN(PHI)
      XI(LOC3)=YI(J)*COS(PHI)-YR(J)*SIN(PHI)
10  CONTINUE
4  CONTINUE

```

C
C
C

UNSCRAMBLE OUTPUT IF N ISN'T PRIME

```

      IF(M.EQ.1) GO TO 5
      DO 12 K=1,N
      KK=K-1

```

C
C
C

GET BIT-REVERSED REPRESENTATION OF KK

```

      IVALUE=N
      DO 13 J=1,M
      JJ=M-J+1
      IVALUE=IVALUE/P(JJ)
      IDIGIT=KK/IVALUE
      KK=KK-IDIGIT*IVALUE
13  ADDRESS(J)=IDIGIT

```

C
C
C
C

FIND MAGNITUDE OF THIS BIT-REVERSED
NUMBER, ADDRESS(J)

```

      IVALUE=1
      MAG=ADDRESS(1)
      M1=M-1
      DO 14 J=1,M1
      JJ=M-J+1
      IVALUE=IVALUE*P(JJ)
14  MAG=MAG+ADDRESS(J+1)*IVALUE
      I=MAG+1
      YR(K)=XR(I)
      YI(K)=XI(I)
      XI(I)=0.
12  CONTINUE
      RETURN
5  DO 7 I=1,N
      YR(I)=XR(I)
      YI(I)=XI(I)
      XI(I)=0.
7  CONTINUE
      RETURN
      END

```


APPENDIX E

ADDITIONAL SCATTERGRAMS OF GROUND-TRUTH WIND SPEEDS AND MICROWAVE MEASUREMENTS FROM SL2 AND SL3

The symbols used in the following scattergrams indicate the data segments from which the observations came. The correspondence between symbols and the data segments are as follows:

<u>Symbol</u>	<u>Segment</u>	<u>Symbol</u>	<u>Segment</u>
A	156-1	G	220-2
B	157-1	H	220-3
C	162-1	I	220-4
D	216-1	J	245-2
E	216-2	K	247-1
F	220-1	L	252-1

Note: A numeral indicates the number of multiple observations for one location on a scattergram. The data-segment indication is lost in such cases.

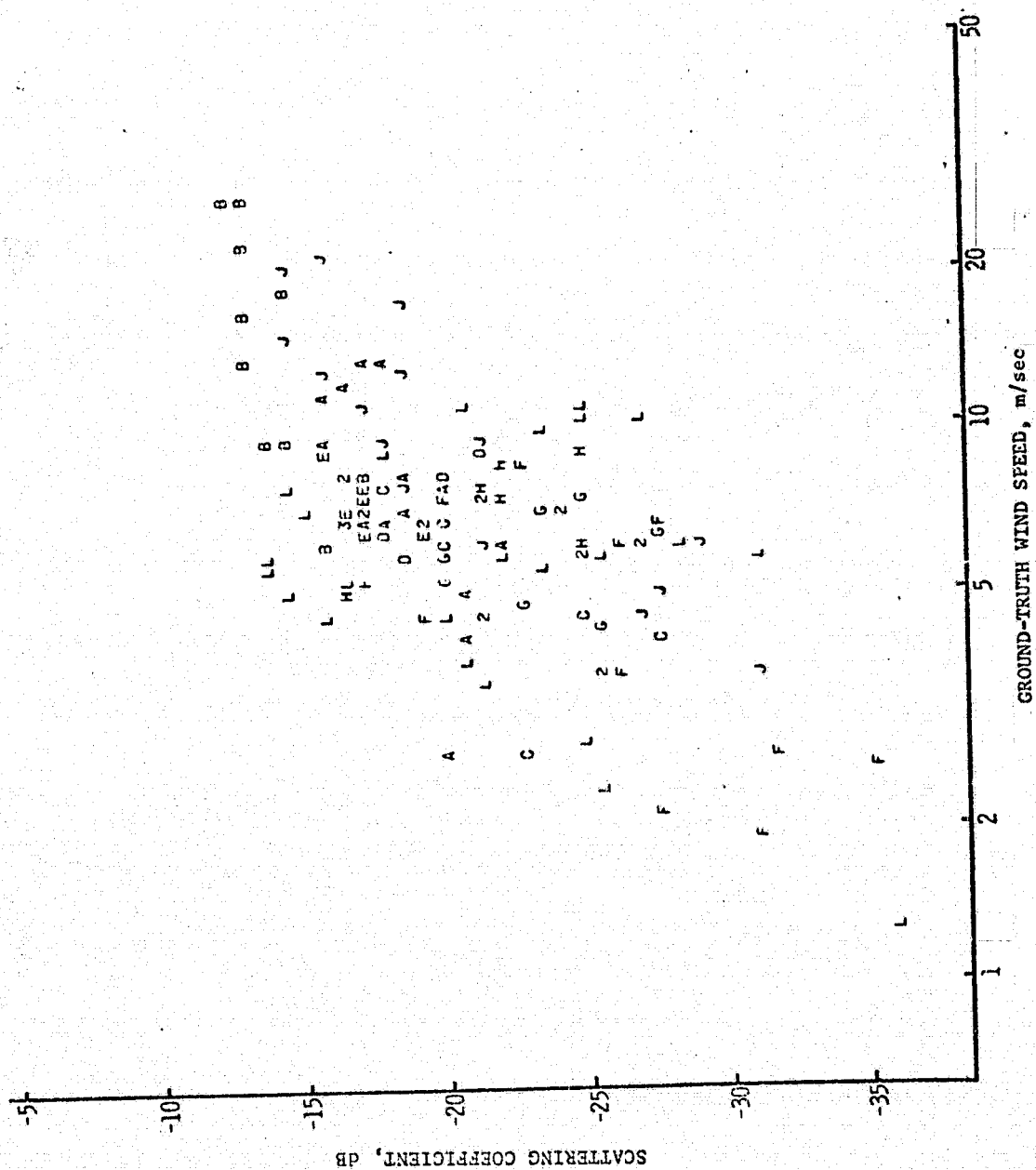


Figure E.1.1. Scattergram of σ_{VV}^0 at 50° incident angle versus ground truth wind speed using logarithmic scales. SL2 and 3 data.

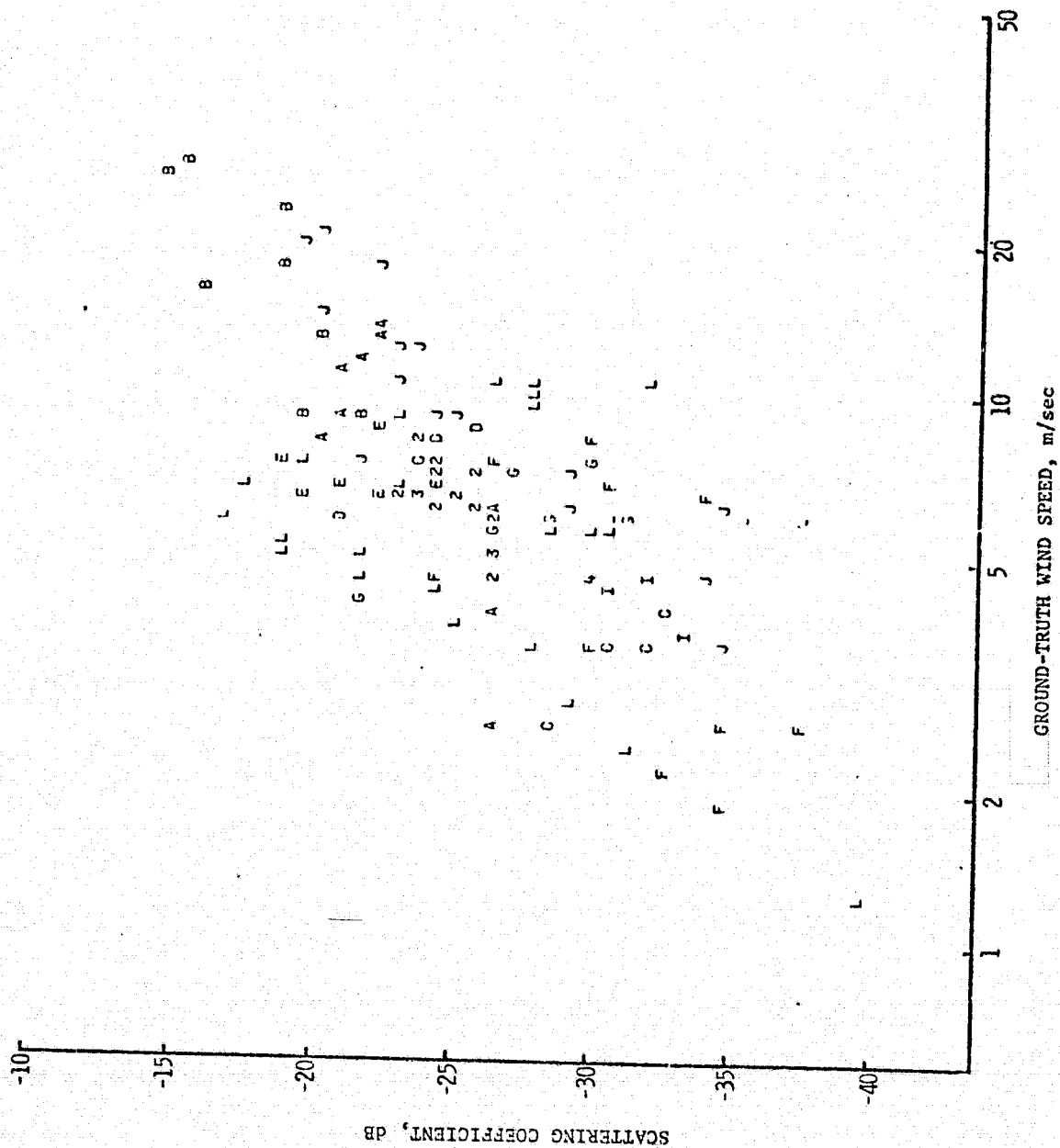


Figure E.1.2. Scattergram of σ^0_{HH} at 50° incident angle versus ground truth wind speed using logarithmic scales. SL2 and 3 data.

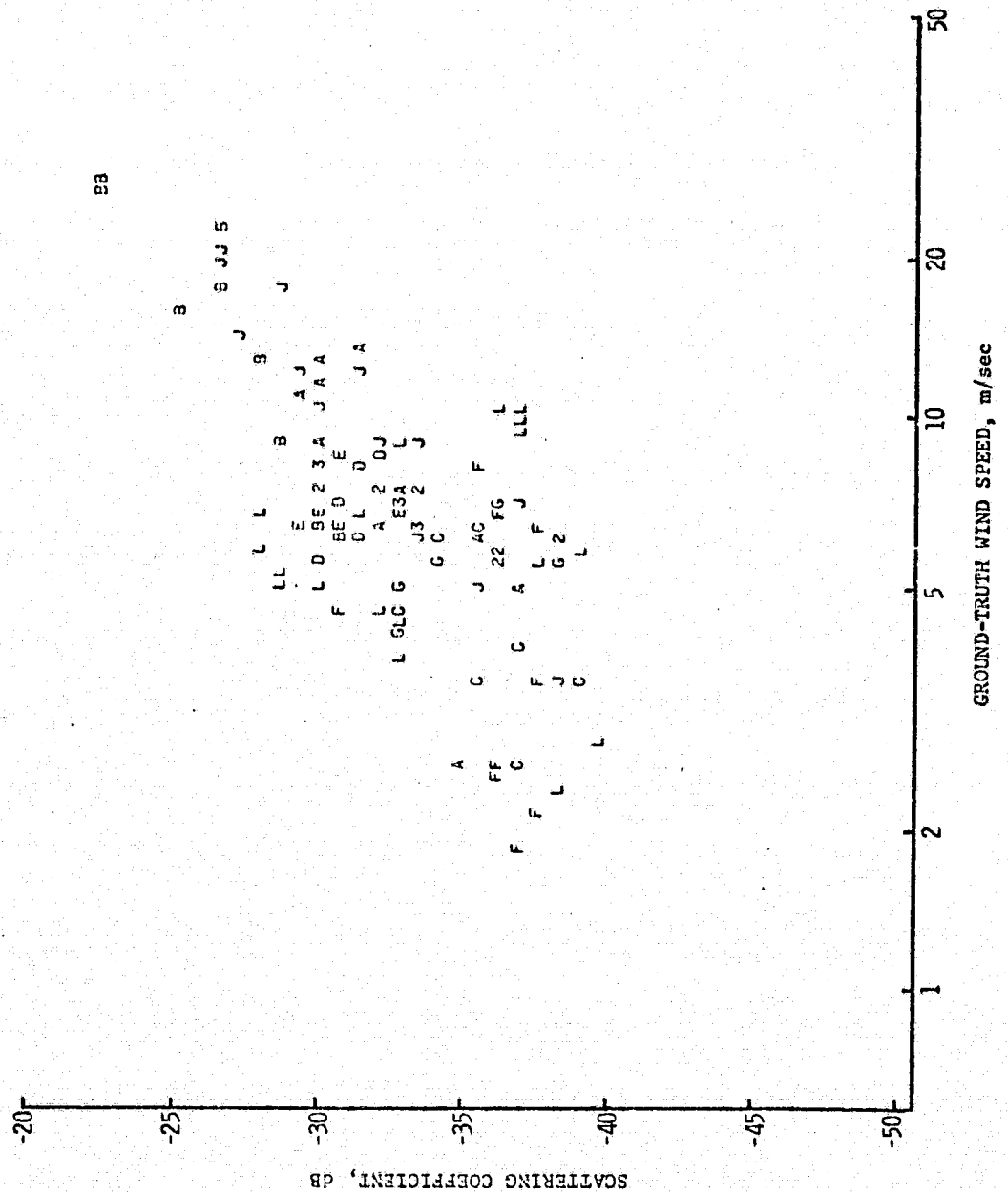


Figure E.1.3. Scattergram of σ_{VH}^0 at 50° incident angle versus ground truth wind speed using logarithmic scales. SL2 and 3 data.



326

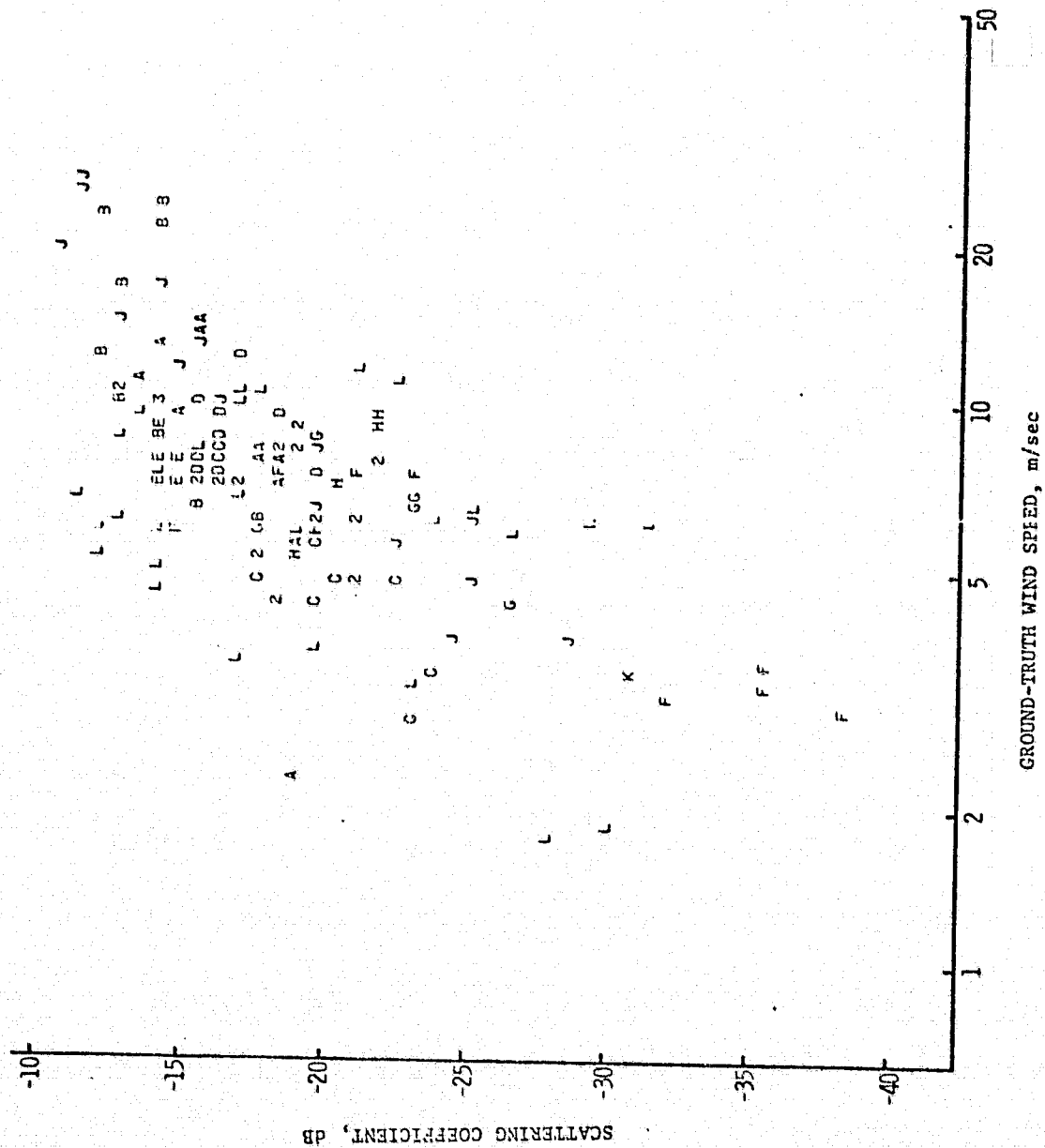


Figure E.1.5. Scattergram of σ_{VV}^0 at 43° incident angle versus ground truth wind speed using logarithmic scales. SL2 and 3 data.

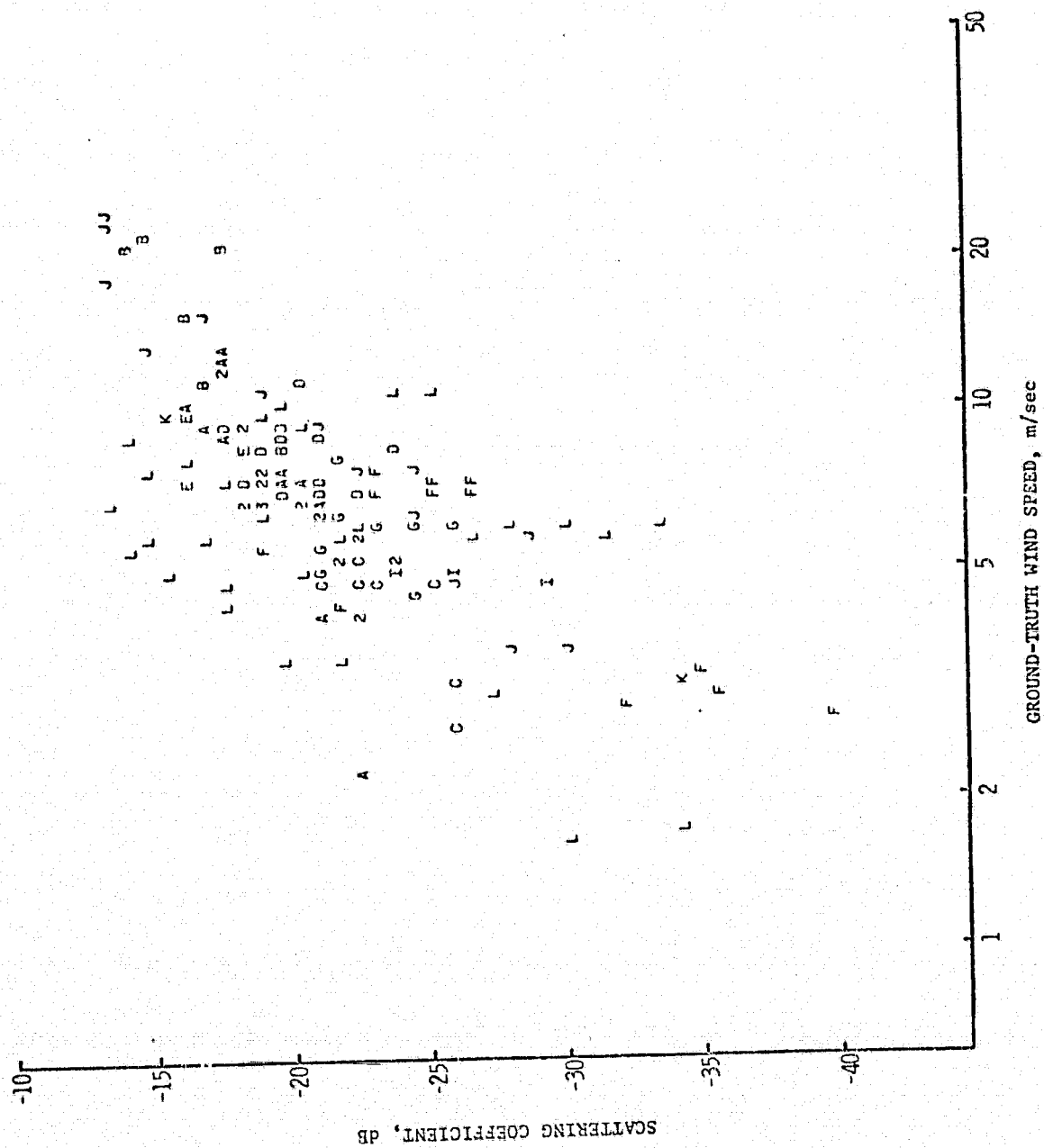


Figure E.1.6. Scattergram of σ_{HH}^0 at 43° incident angle versus ground truth wind speed using logarithmic scales. SL2 and 3 data.

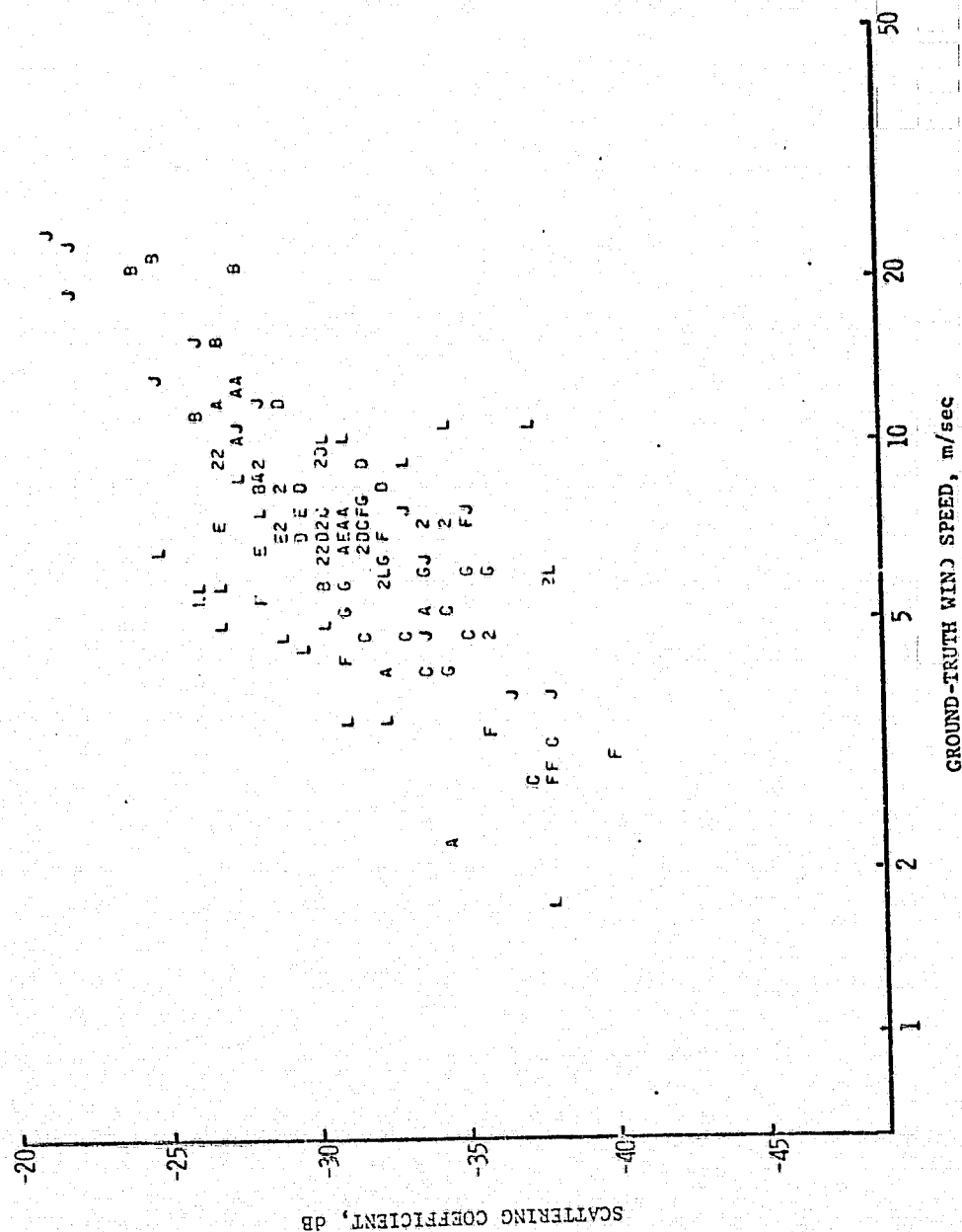


Figure E.1.7. Scattergram of σ^0_{VH} at 43° incident angle versus ground truth wind speed using logarithmic scales. SL2 and 3 data.

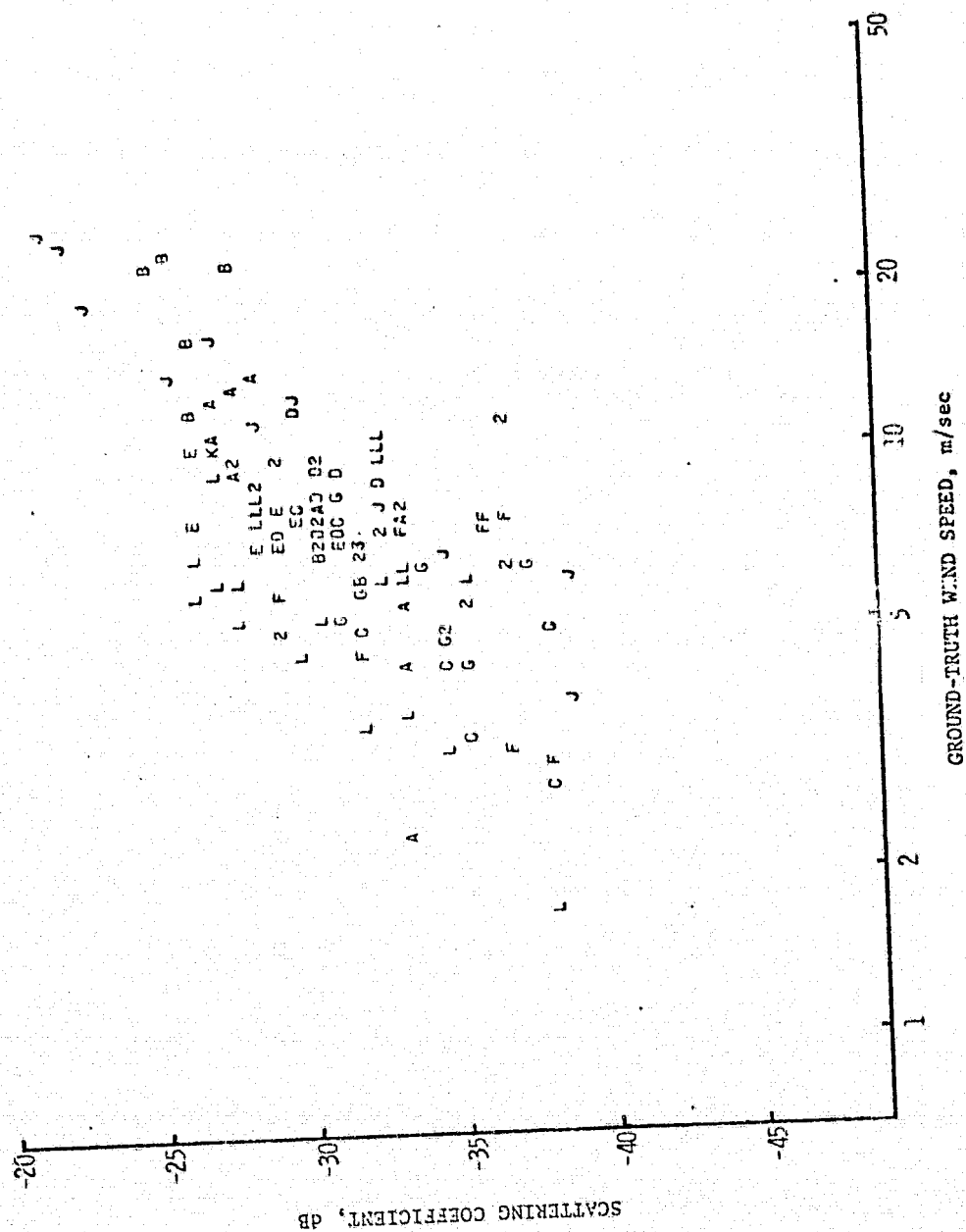


Figure E.1.8. Scatter-gram of σ_{HV}^0 at 43° incident angle versus ground truth wind speed using logarithmic scales. SL2 and 3 data.

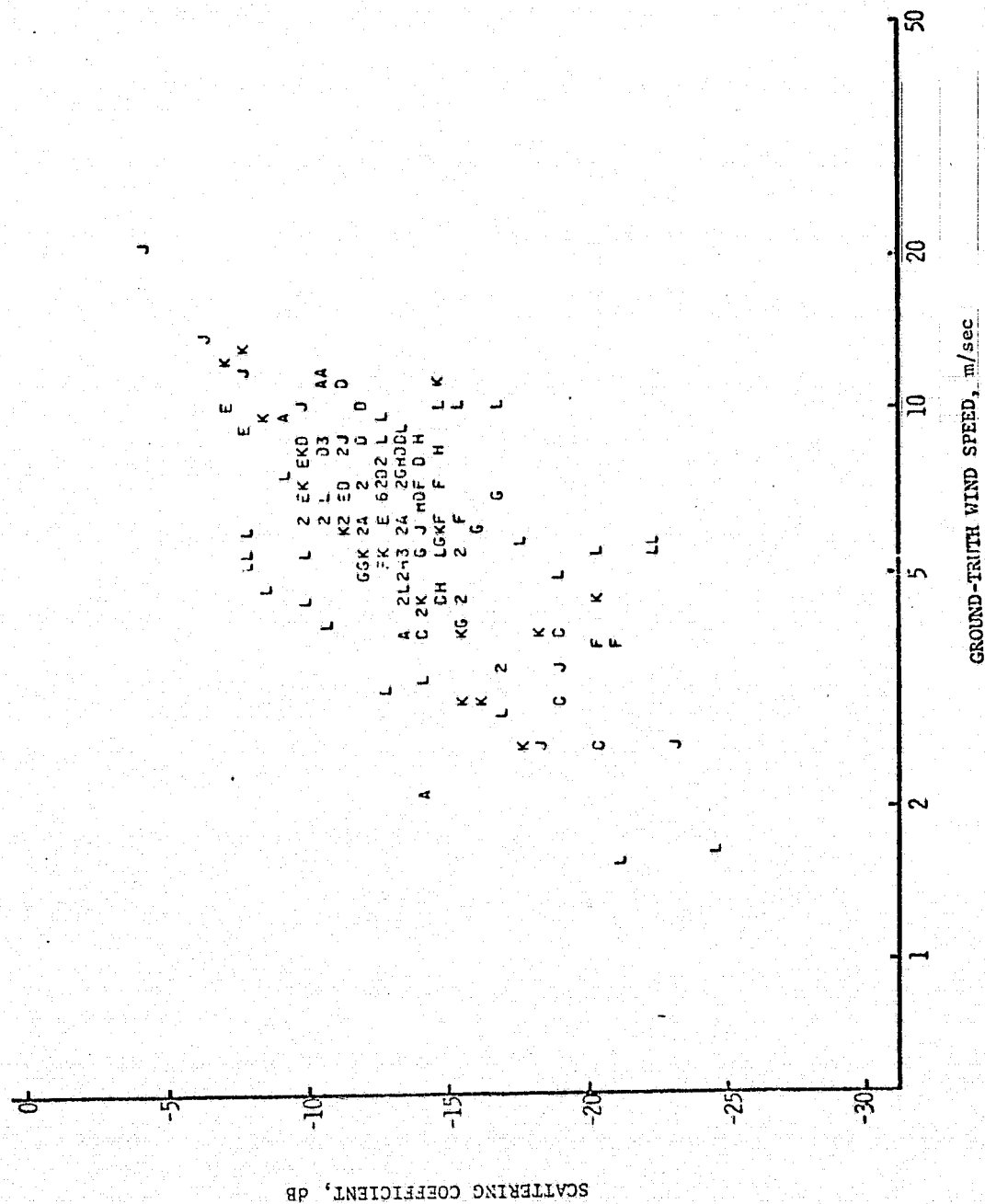


Figure E.1.9. Scattergram of σ_{vv} at 32° incident angle versus ground truth wind speed using logarithmic scales. SL2 and 3 data.



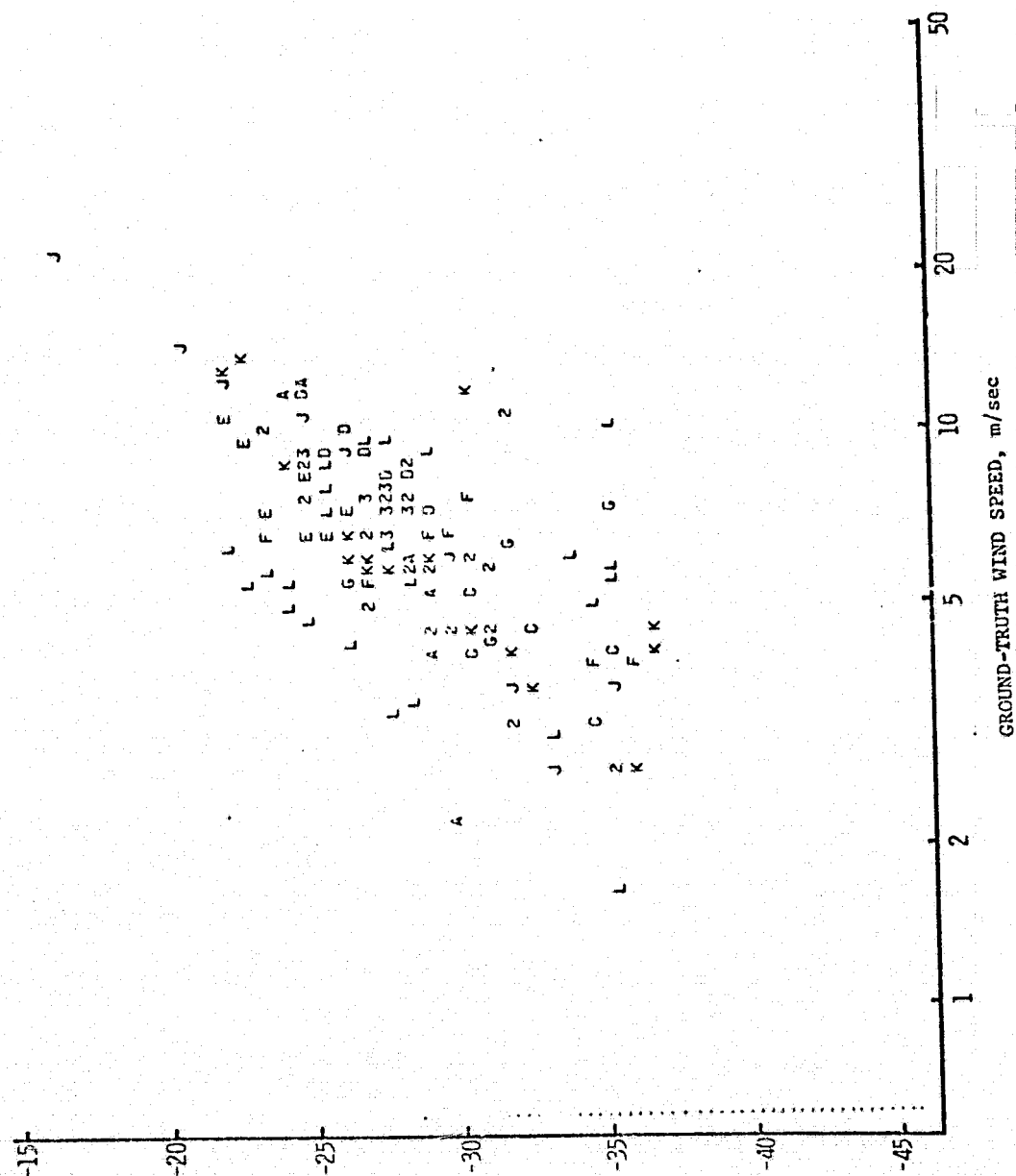


Figure E.1.11. Scattergram of σ^0_{VH} at 32° incident angle versus ground truth wind speed using logarithmic scales. SL 2 and 3 data.

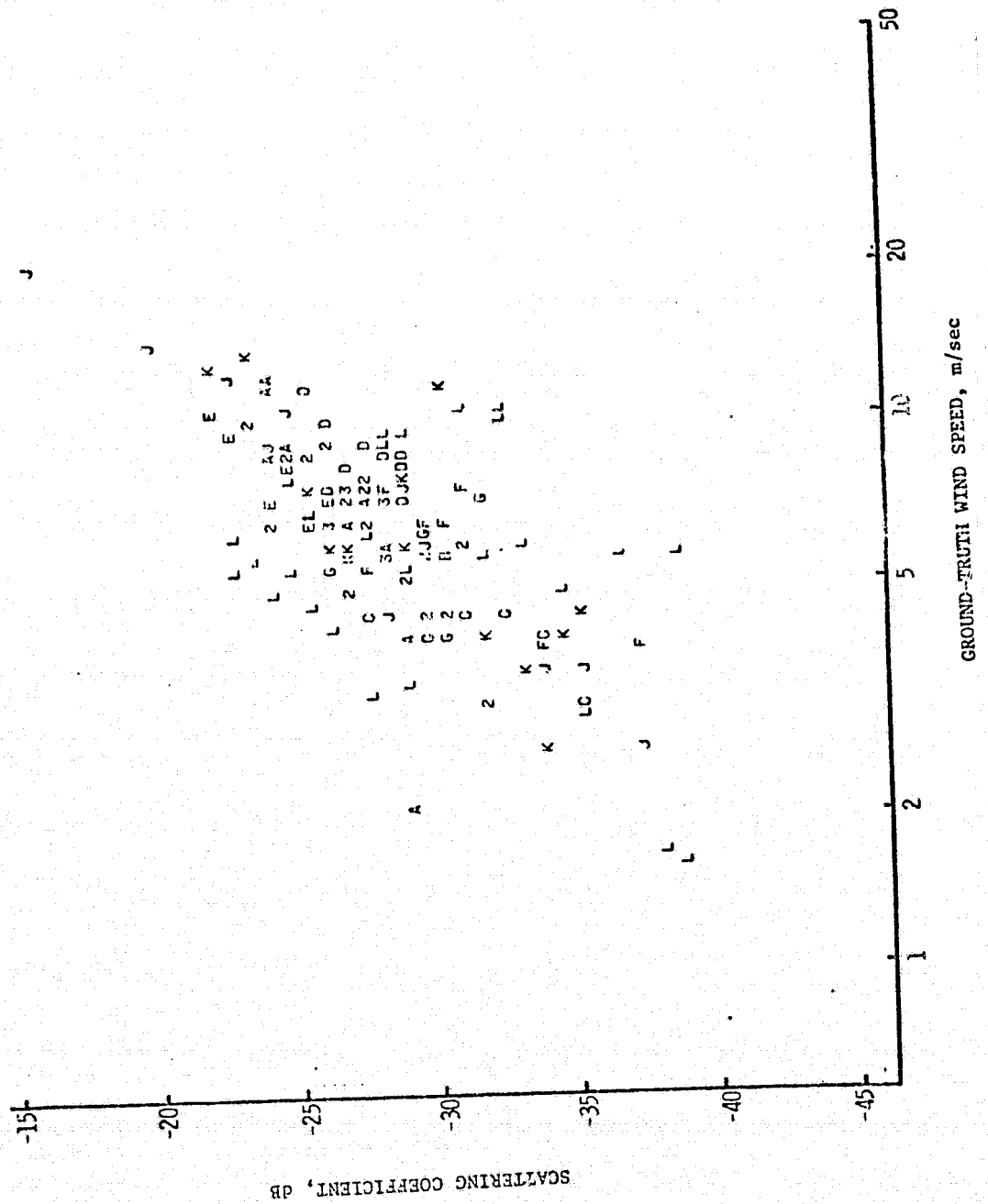


Figure E.1.12. Scattergram of σ_{H}^0 at 32° incident angle versus ground truth wind speed using logarithmic scales. SL2 and 3 data.

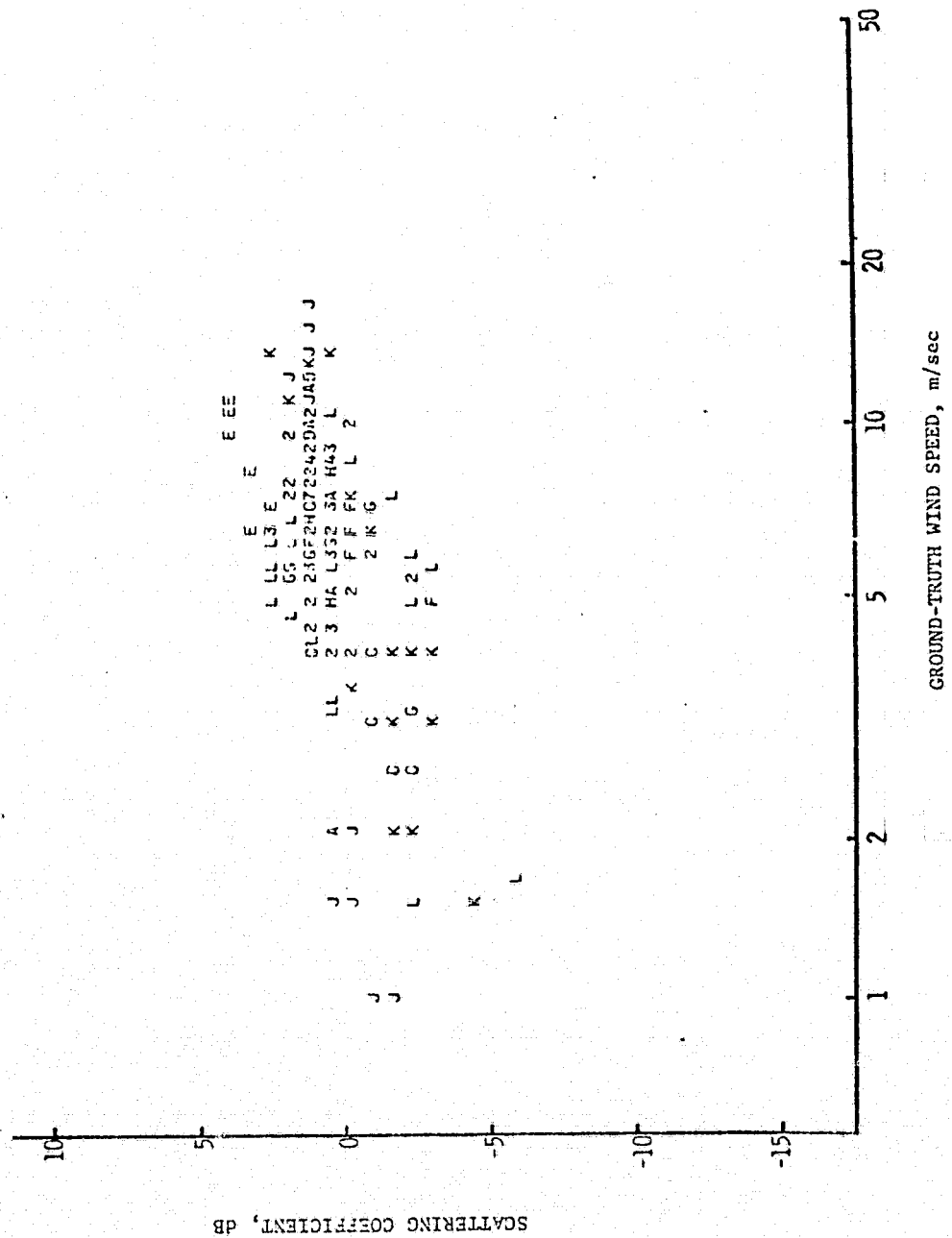


Figure E.1.13. Scattergram of σ_{VV}^0 at 17° incident angle versus ground truth wind speed using logarithmic scales. SL2 and 3 data.

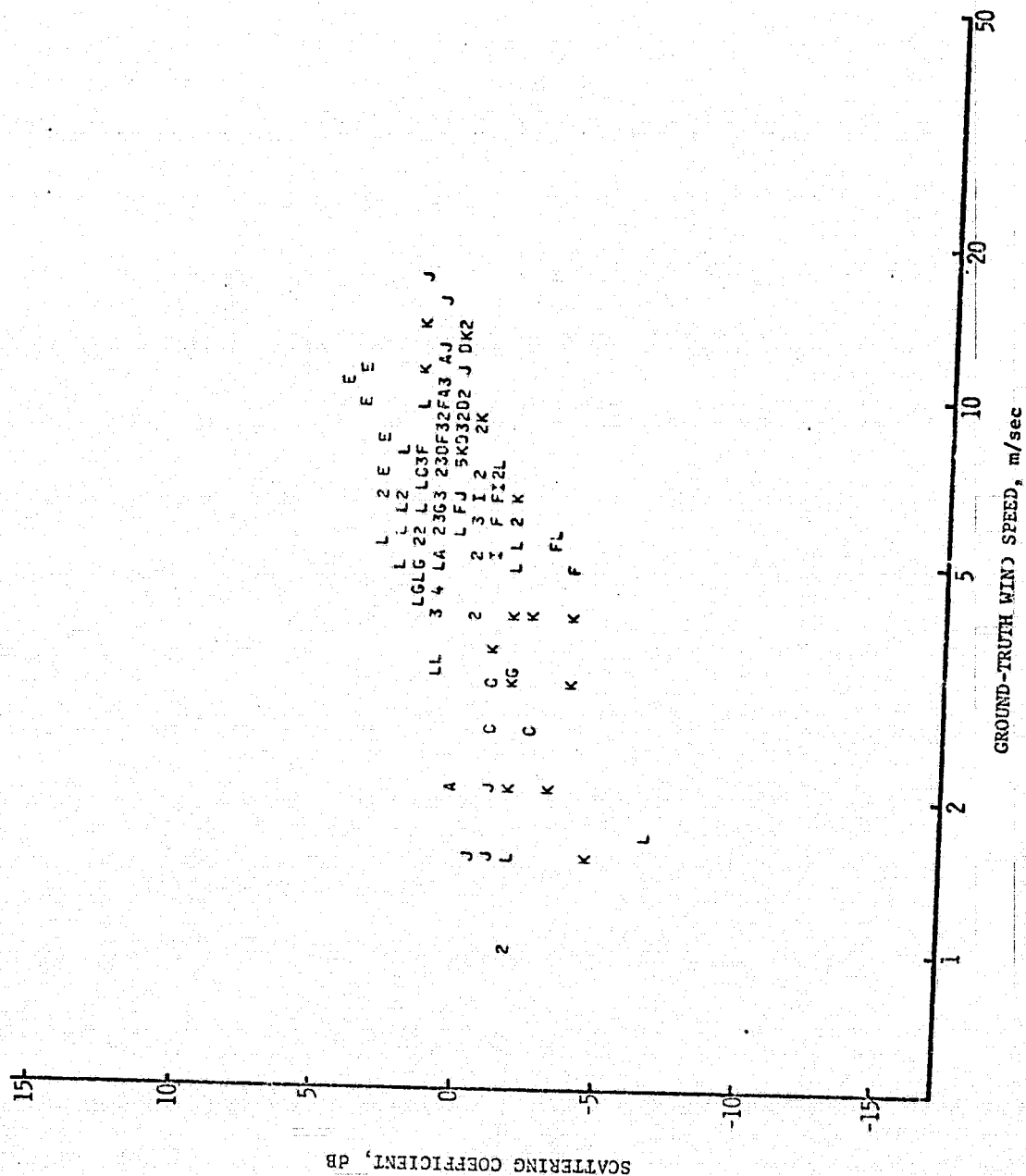
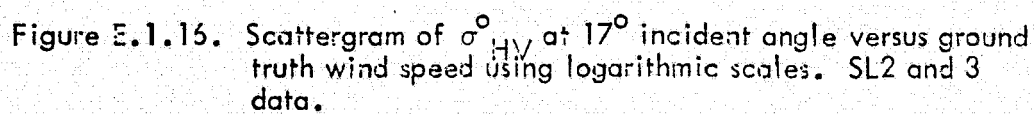


Figure E.1.14. Scattergram of σ_{HH} at 17° incident angle versus ground truth wind speed using logarithmic scales. SL2 and 3 data.

REPRODUCIBILITY OF THE
ORIGINAL PAGE IS POOR



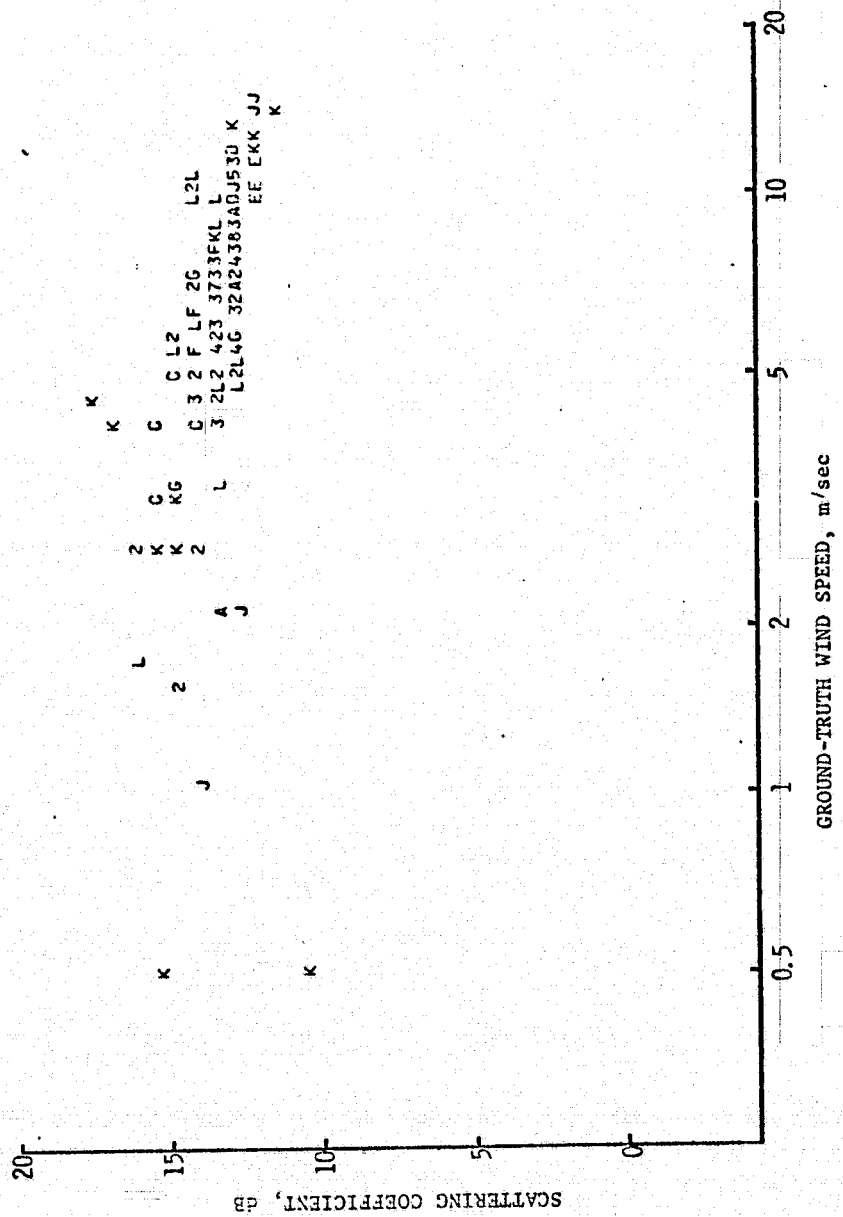
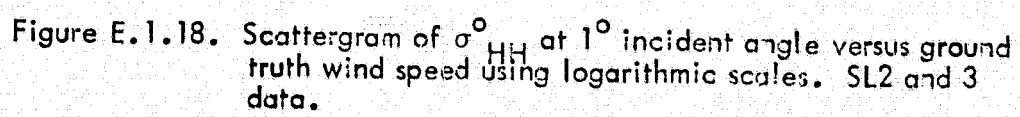
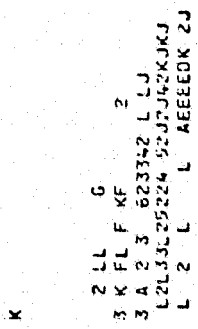


Figure E.1.17. Scattergram of σ_{VV}^0 at 1° incident angle versus ground truth wind speed using logarithmic scales. SL2 and 3 data.





341

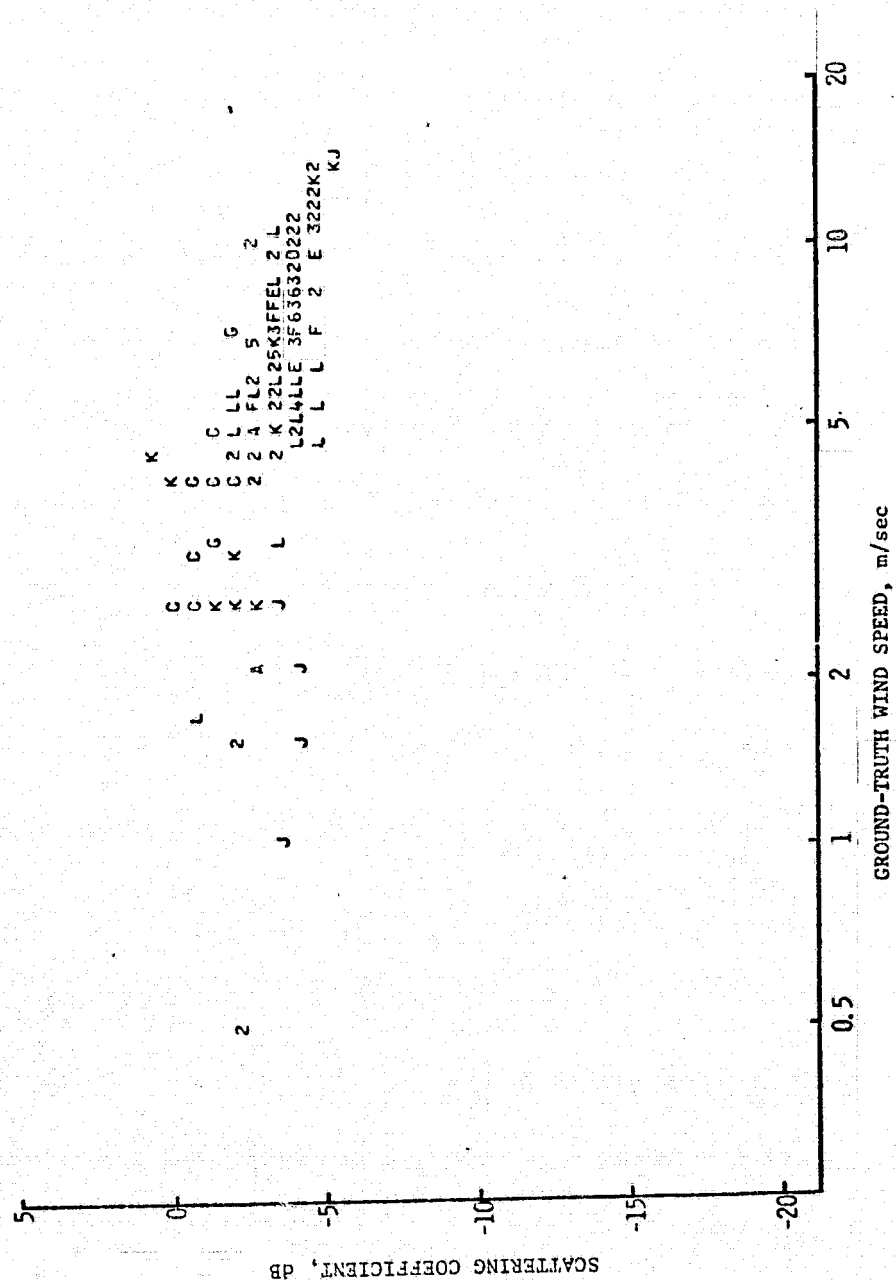


Figure E.1.20. Scattergram of σ_H^0 at 1° incident angle versus ground truth wind speed using logarithmic scales. SL2 and 3 data.

REPRODUCIBILITY OF THE
ORIGINAL PAGE IS POOR

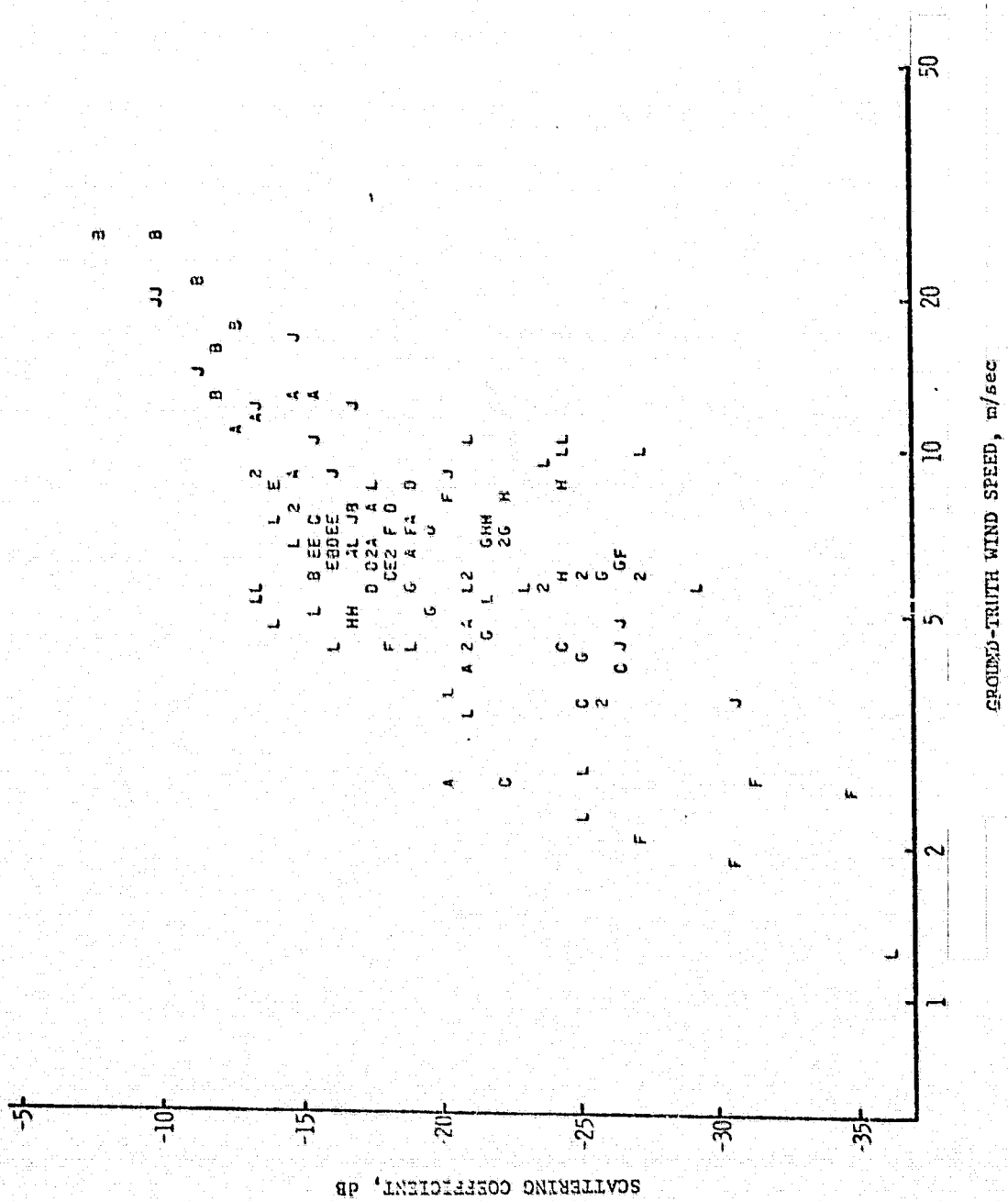


Figure E.2.1. Scattergram of σ_{vv} at 50° incident angle versus ground truth wind speed using logarithmic scales. The scattering coefficients are adjusted to upwind. SL2 and 3 data.

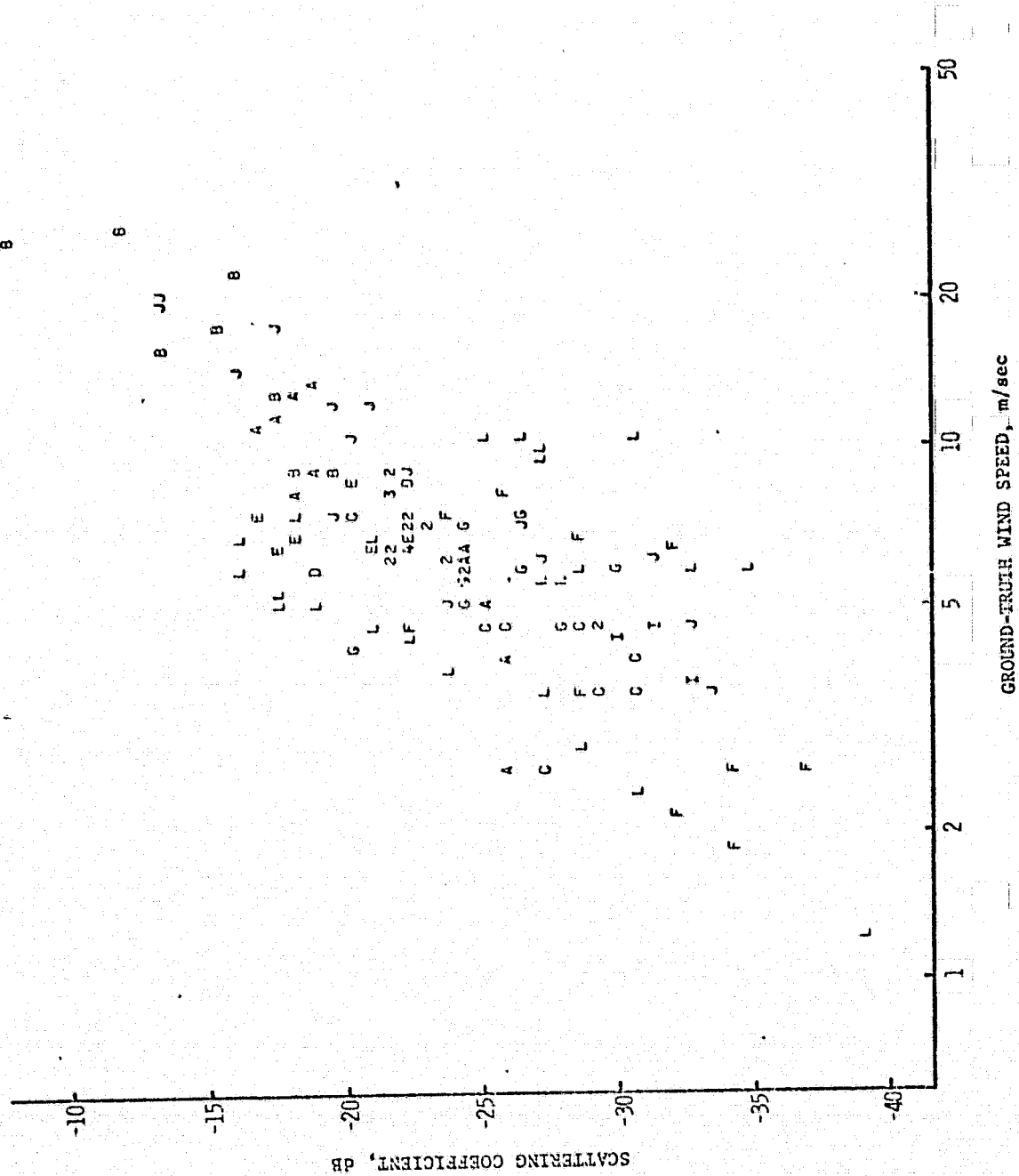


Figure E.2.2. Scattergram of σ_{LL} at 50° incident angle versus ground truth wind speed using logarithmic scales. The scattering coefficients are adjusted to upwind. SL2 and 3 data.

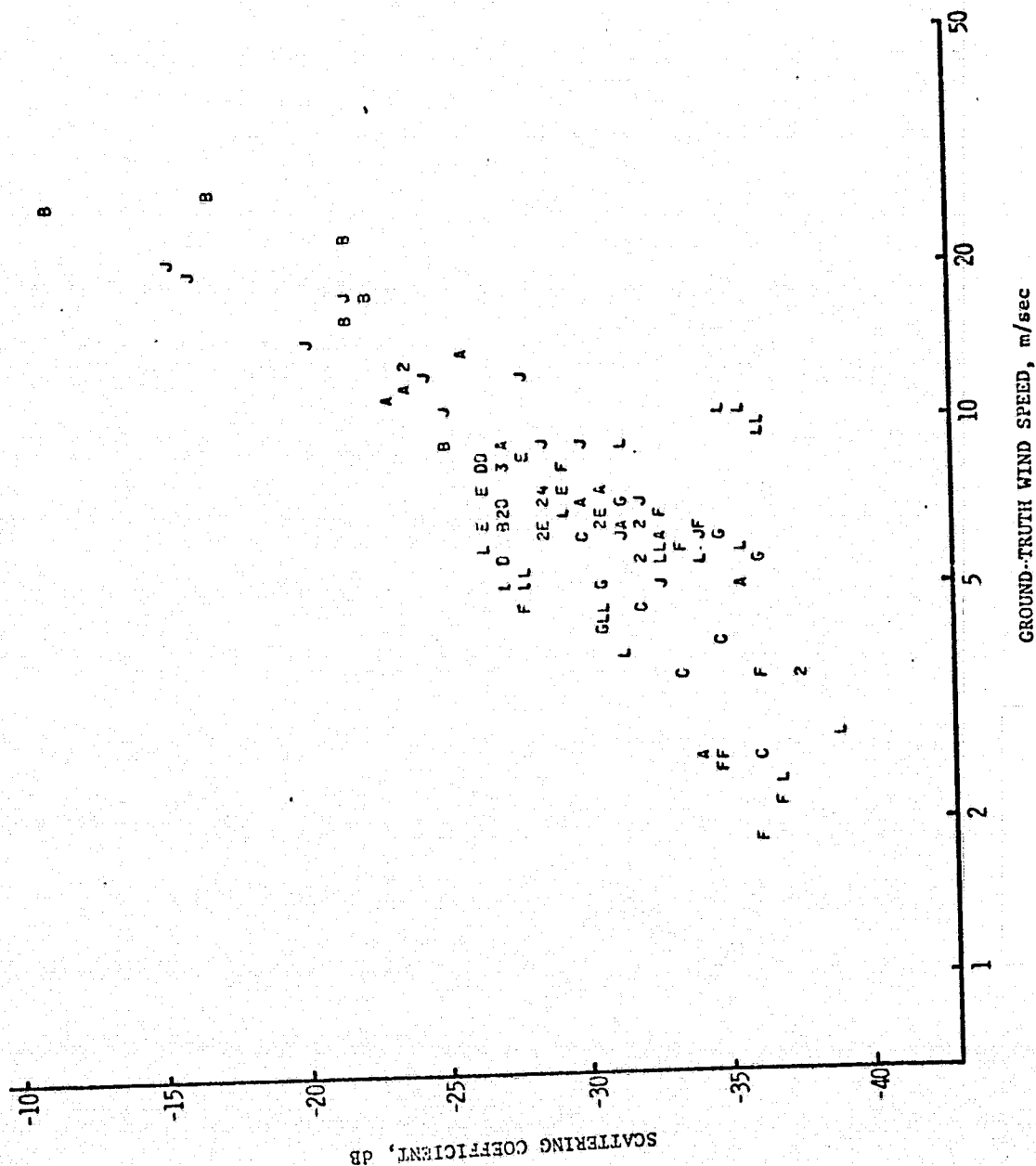


Figure E.2.3. Scattergram of σ_{VH}^{50} at 50° incident angle versus ground truth wind speed using logarithmic scales. The scattering coefficients are adjusted to upwind. SL2 and 3 data.

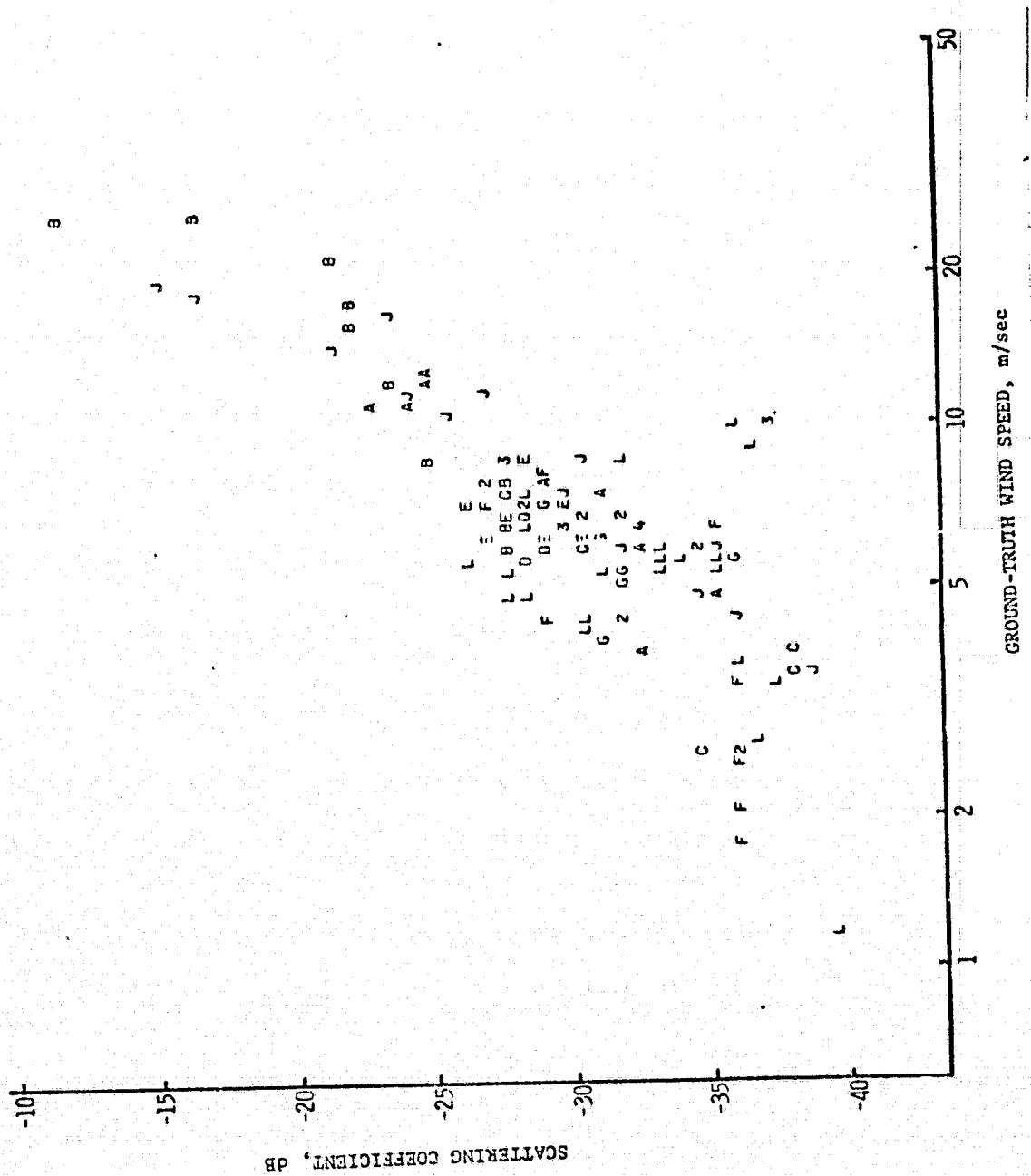


Figure E.2.4. Scattergram of σ_{HV}^0 at 50° incident angle versus ground truth wind speed using logarithmic scales. The scattering coefficients are adjusted to upwind. SL2 and 3 data.

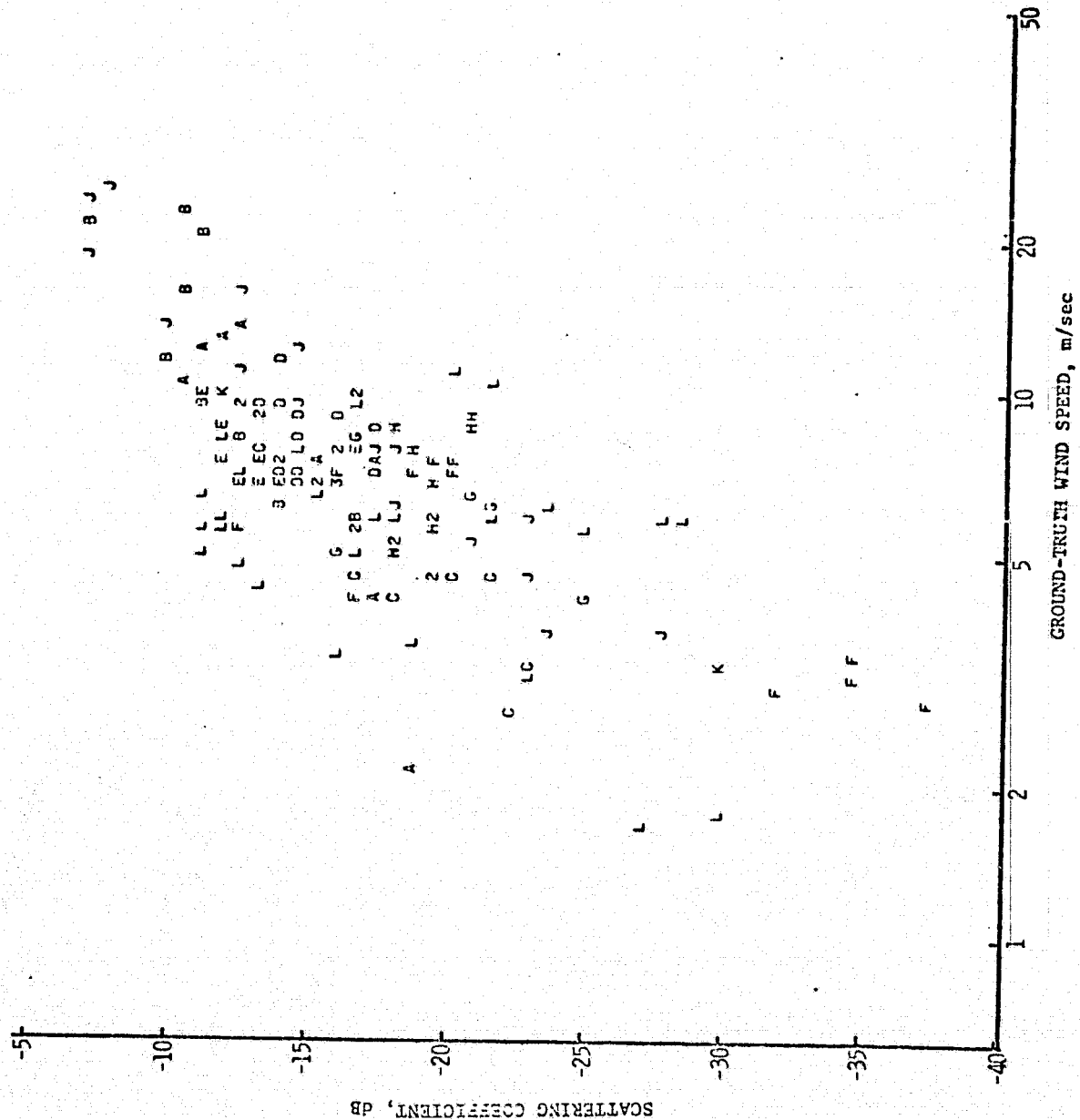


Figure E.2.5. Scattergram of $\sigma^0_{\sqrt{V}}$ at 43° incident angle versus ground truth wind speed using logarithmic scales. The scattering coefficients are adjusted to upwind. SL2 and 3 data.

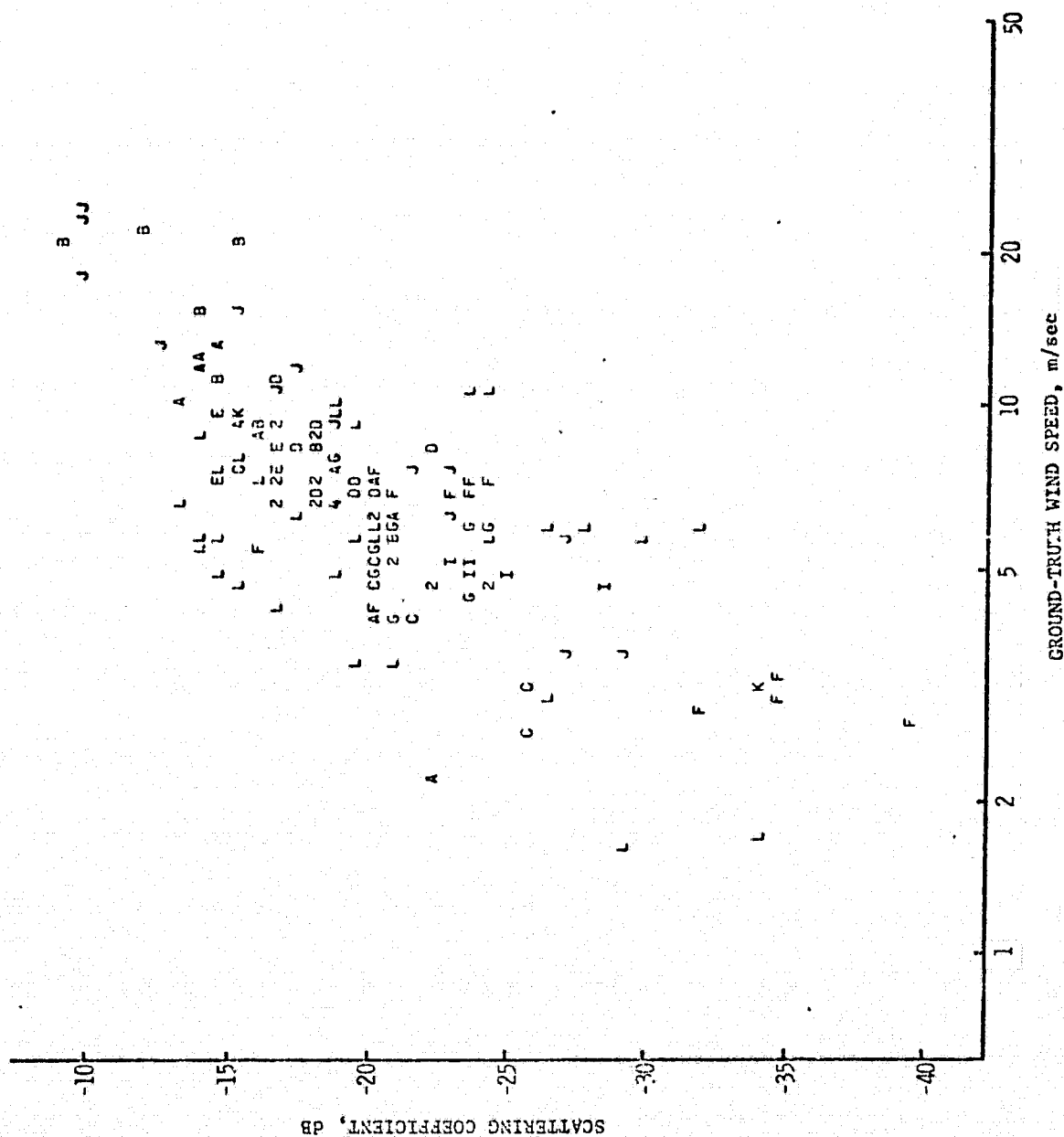


Figure E.2.6. Scattergram of σ^0_{UH} at 43° incident angle versus ground truth wind speed using logarithmic scales. The scattering coefficients are adjusted to upwind. SL 2 and 3 data.

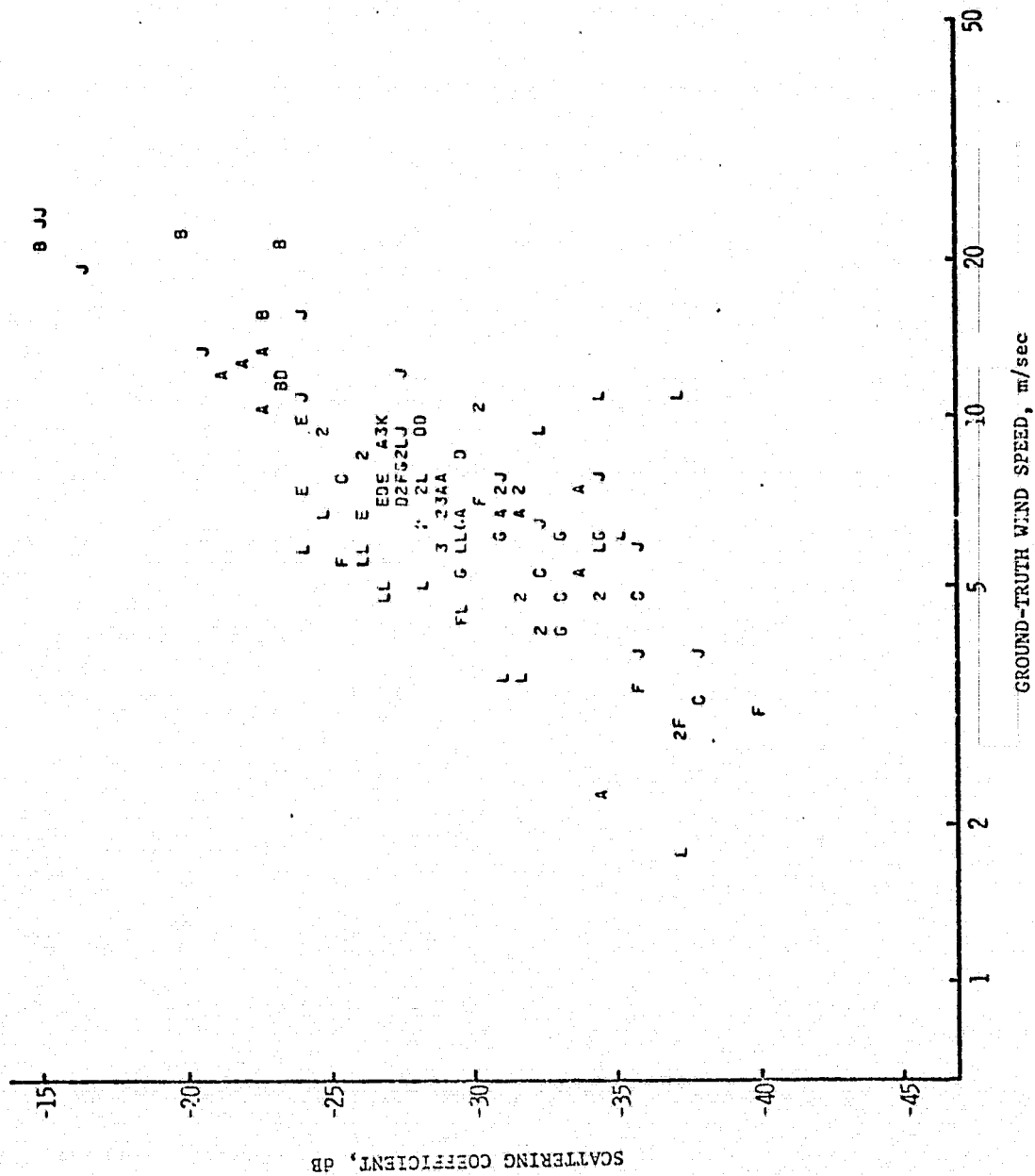


Figure E.2.7. Scattergram of σ^0_{VH} at 43° incident angle versus ground truth wind speed using logarithmic scales. The scattering coefficients are adjusted to upwind. SL2 and 3 data.

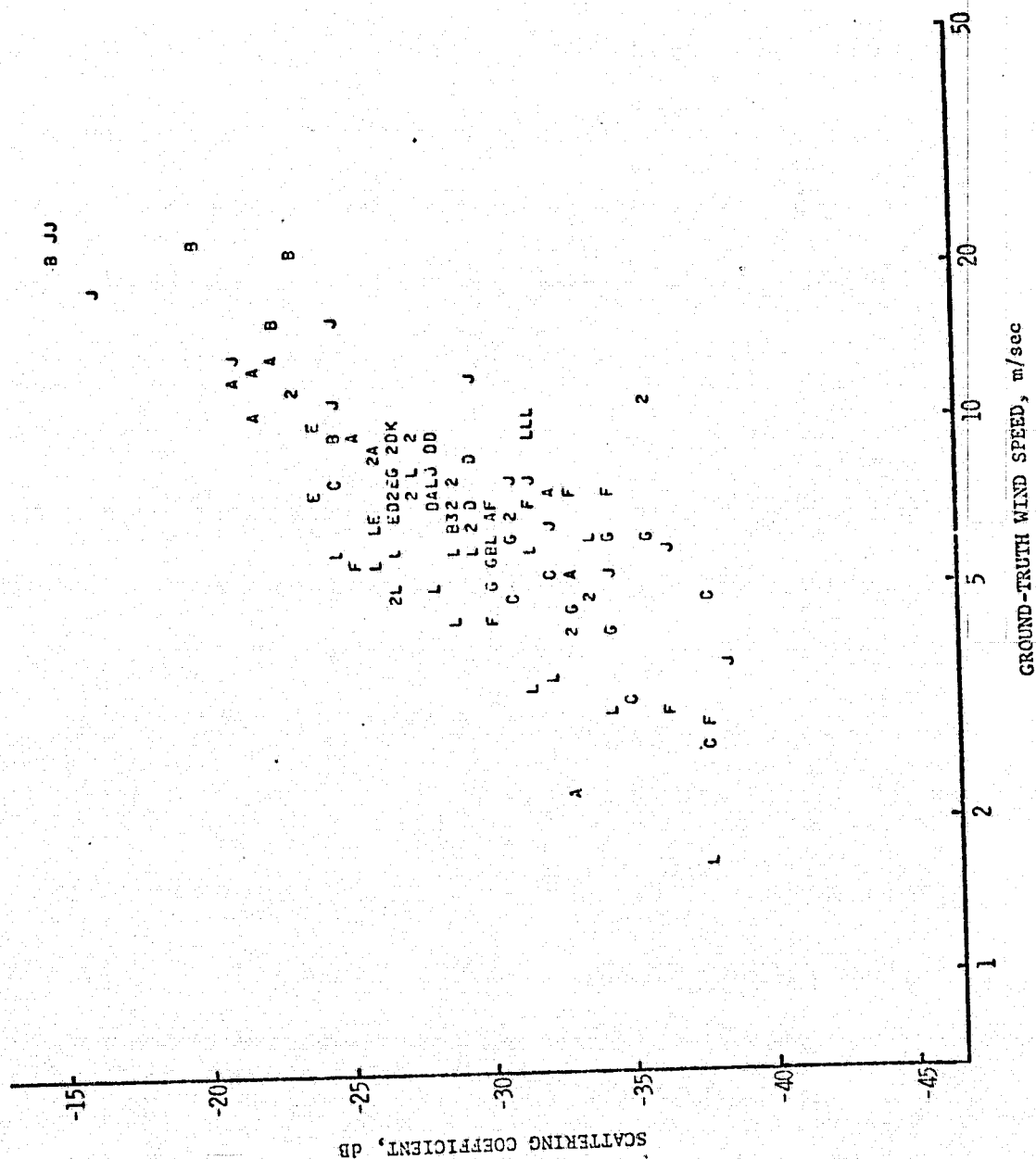


Figure E.2.8. Scattergram of σ_{HV}^0 at 43° incident angle versus ground truth wind speed using logarithmic scales. The scattering coefficients are adjusted to upwind. SL2 and 3 data.

REPRODUCIBILITY OF THE
ORIGINAL PAGE IS POOR

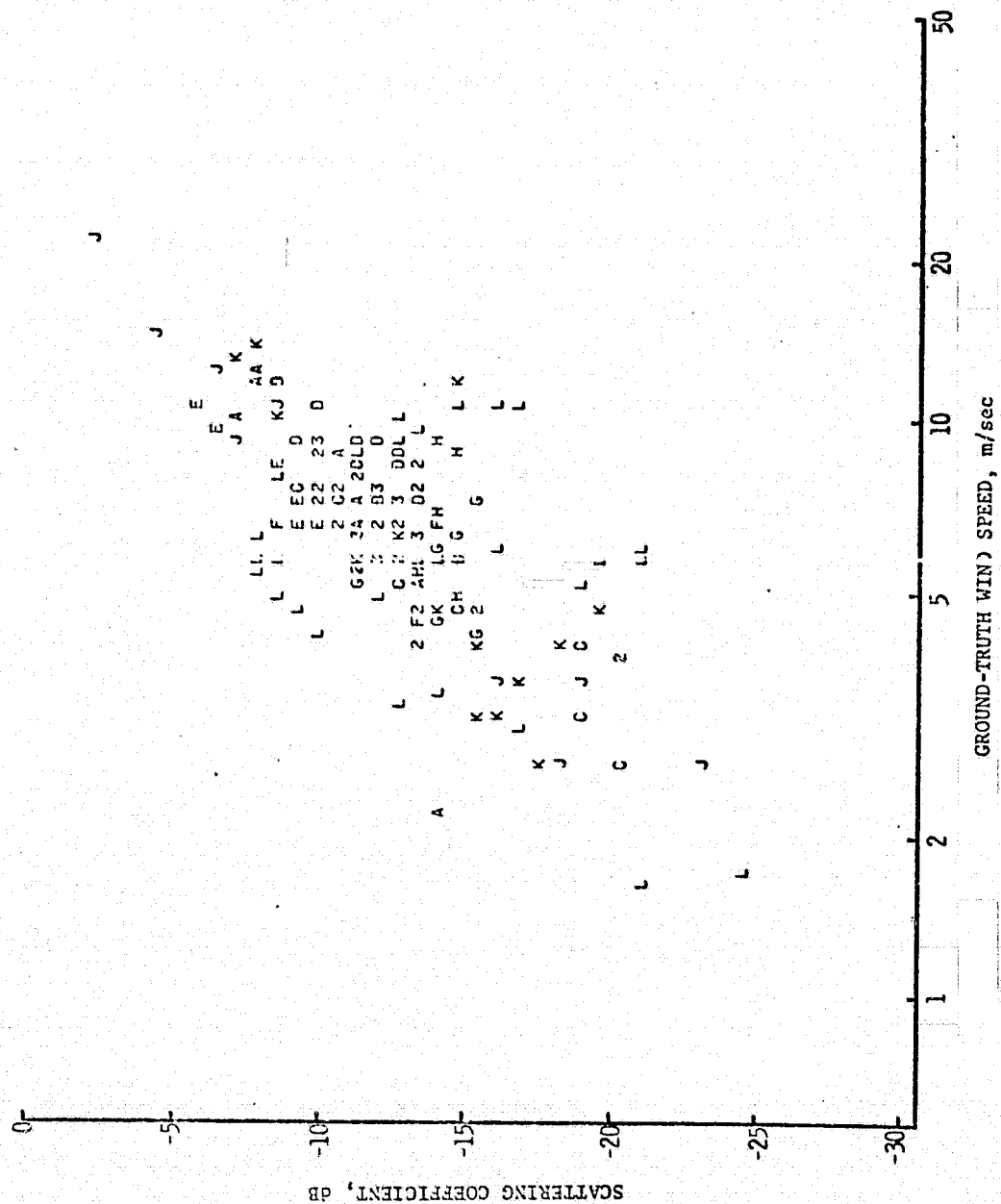
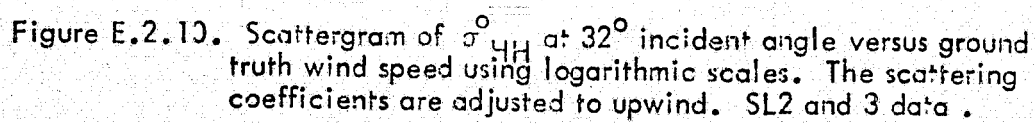
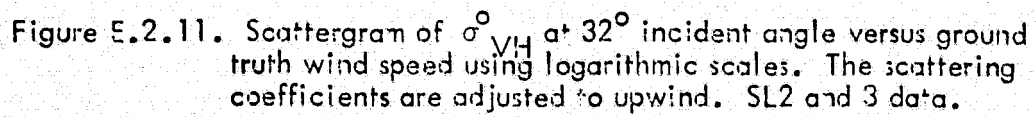


Figure E.2.9. Scattergram of σ_{VV}^0 at 32° incident angle versus ground truth wind speed using logarithmic scales. The scattering coefficients are adjusted to upwind. SL2 and 3 data.



352



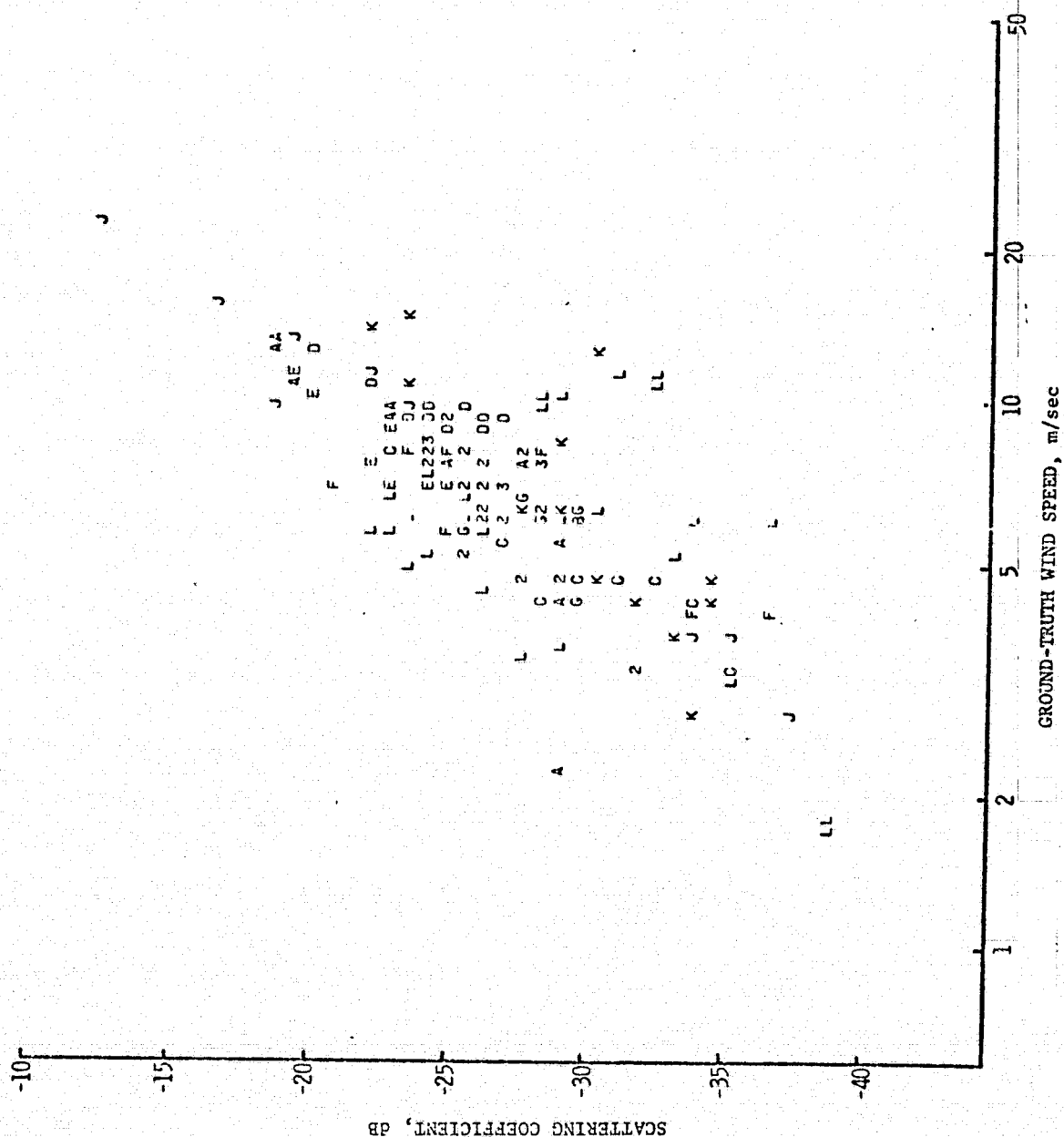


Figure E.2.12. Scattergram of σ^o_{HV} at 32° incident angle versus ground truth wind speed using logarithmic scales. The scattering coefficients are adjusted to upwind. SL2 and 3 data.

REPRODUCIBILITY OF THE
ORIGINAL PAGE IS POOR

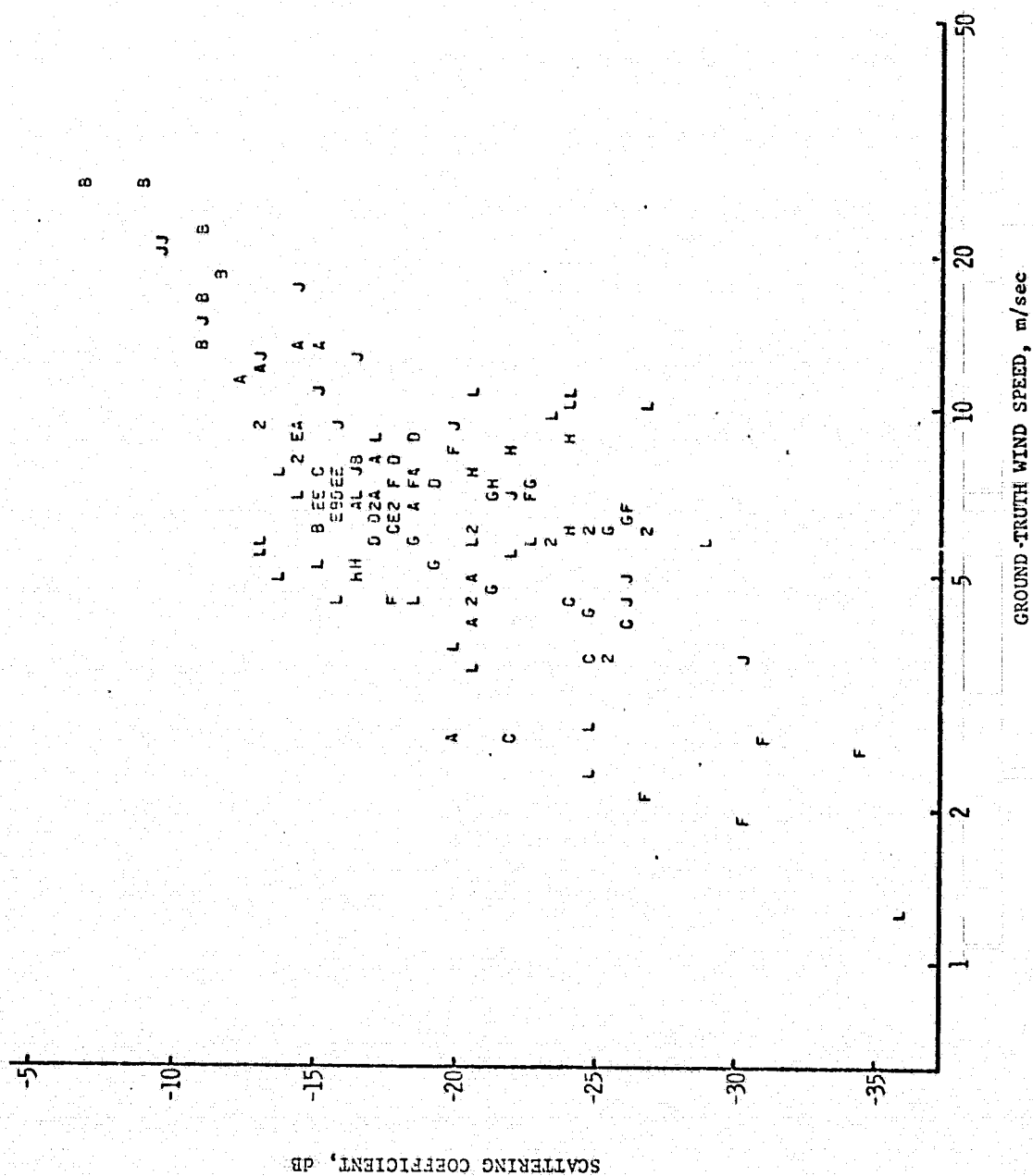


Figure E.3.1. Scattergram of σ_{VV}^0 at 50° incident angle versus ground truth wind speed using logarithmic scales. The scattering coefficients are adjusted to upwind and are corrected for atmospheric effects. SL2 and 3 data.

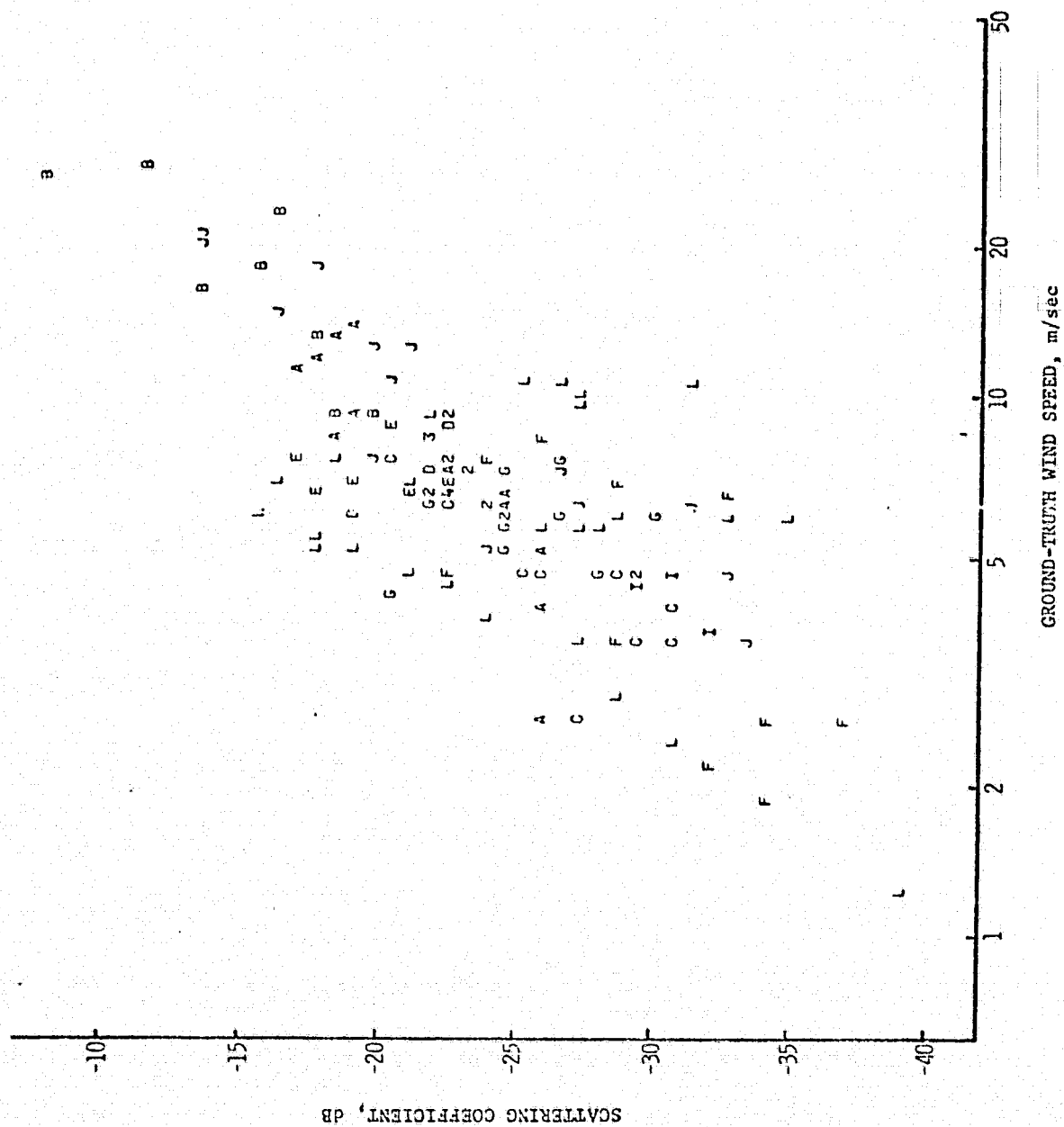


Figure E.3.2. Scattergram of σ^0_{HH} at 50° incident angle versus ground truth wind speed using logarithmic scales. The scattering coefficients are adjusted to upwind and are corrected for atmospheric effects. SL2 and 3 data.

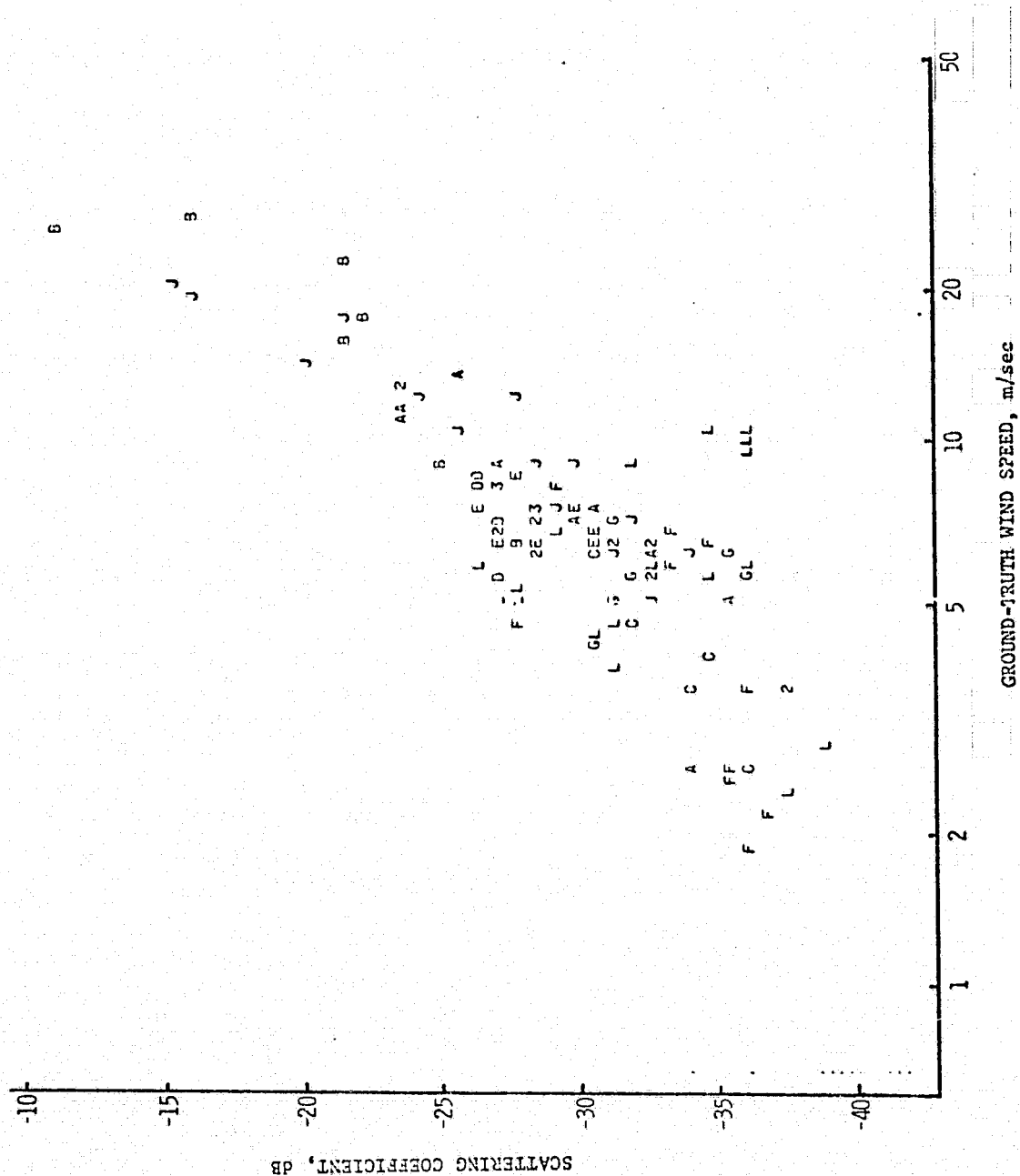
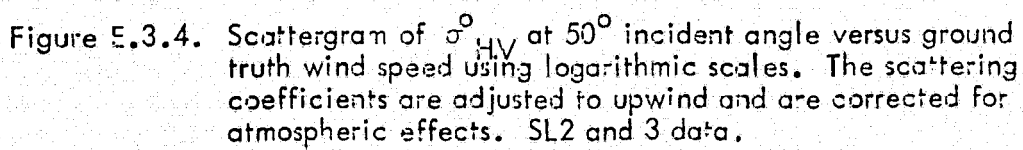


Figure E.3.3. Scattergram of σ_{VH}^0 at 50° incident angle versus ground truth wind speed using logarithmic scales. The scattering coefficients are adjusted to upwind and are corrected for atmospheric effects. SL2 and 3 data.



APPENDIX F

ADDITIONAL SCATTERGRAMS OF GROUND-TRUTH WIND SPEEDS AND MICROWAVE MEASUREMENTS FROM SL4

The symbols used in the following scattergrams indicate the data segments from which the observations came. The correspondence between symbols and data segments are as follows:

<u>Symbol</u>	<u>Segment</u>	<u>Symbol</u>	<u>Segment</u>
A	6-2	L	9-1
B	334-1 L	M	11-2
C	334-1 R	N	24-1
D	338-1 L	O	25-1
E	338-1 R	P	27-1
F	4-1 L	Q	29-1
G	4-1 R	R	29-2
H	7-1 L	S	30-1
I	7-1 R	T	30-2
J	8-1 L	U	32-1
K	8-1 R		

Note: A numeral indicates the number of multiple observations for one location on a scattergram. The data-segment indication is lost in such cases.

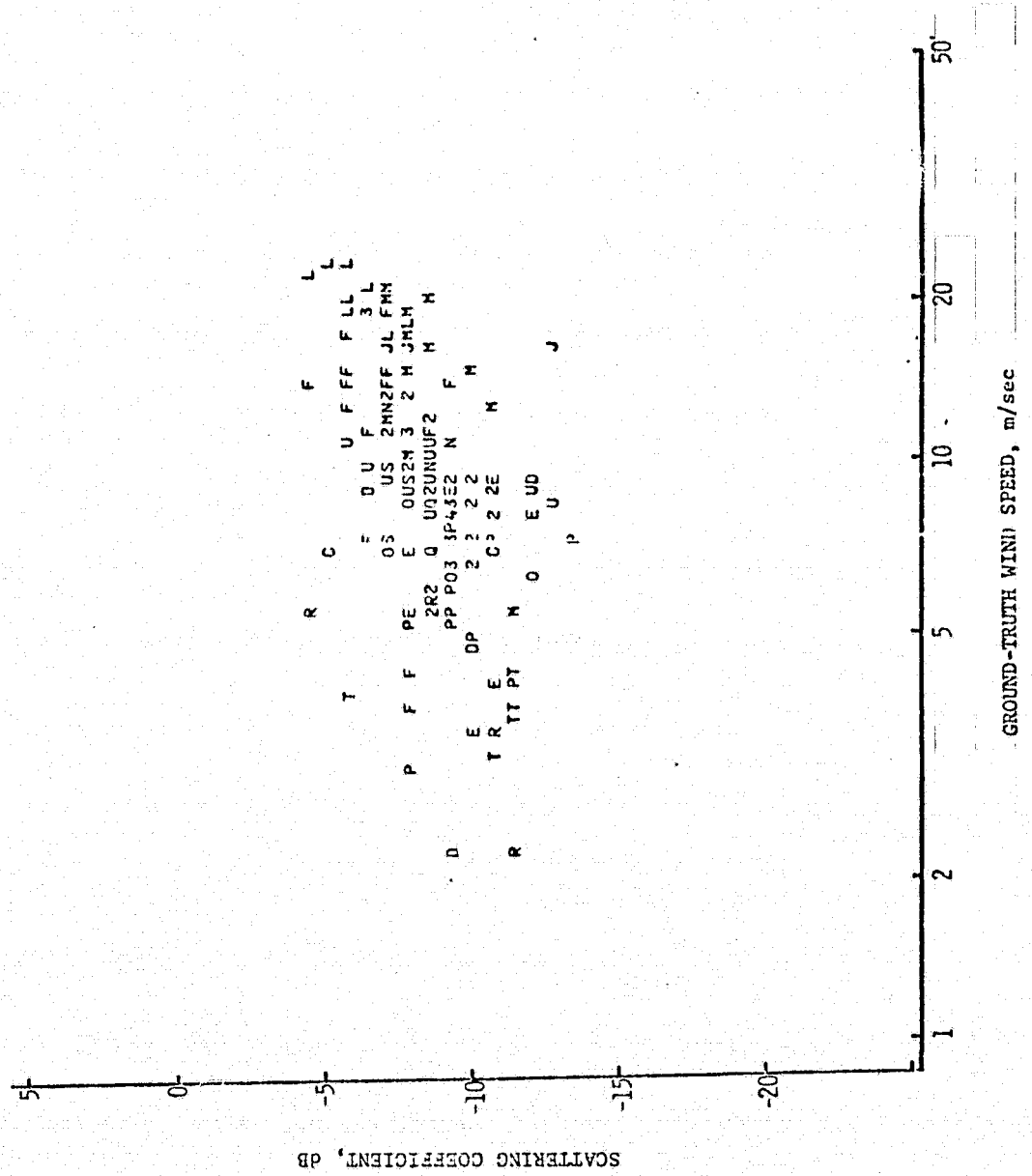


Figure F.1.1. Scattergram of σ_{VV}^0 at 50° incident angle versus ground truth wind speed using logarithmic scales. SL4 data.

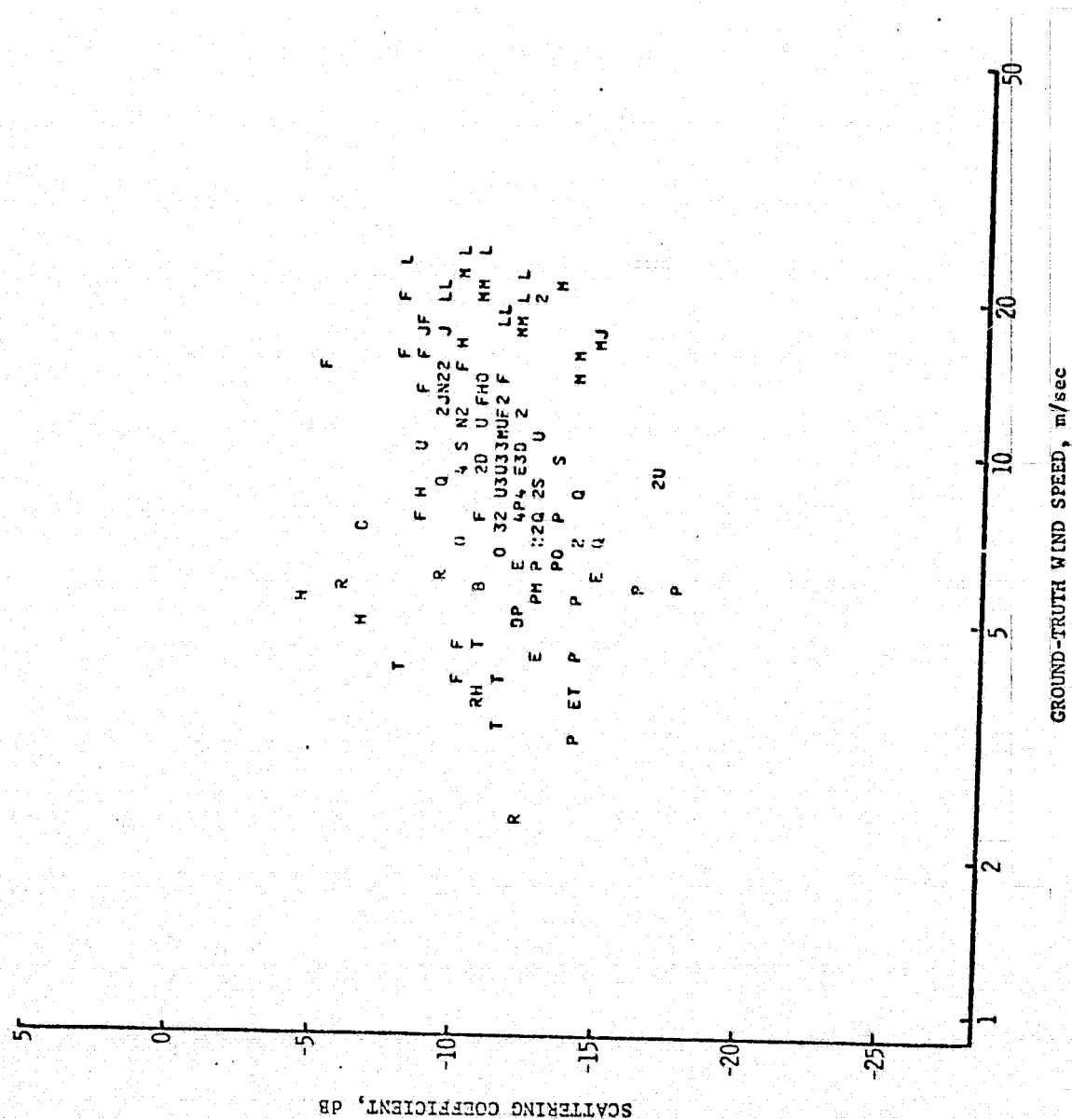


Figure F.1.2. Scattergram of σ_{HH}^0 at 50° incident angle versus ground truth wind speed using logarithmic scales, SL4 data.

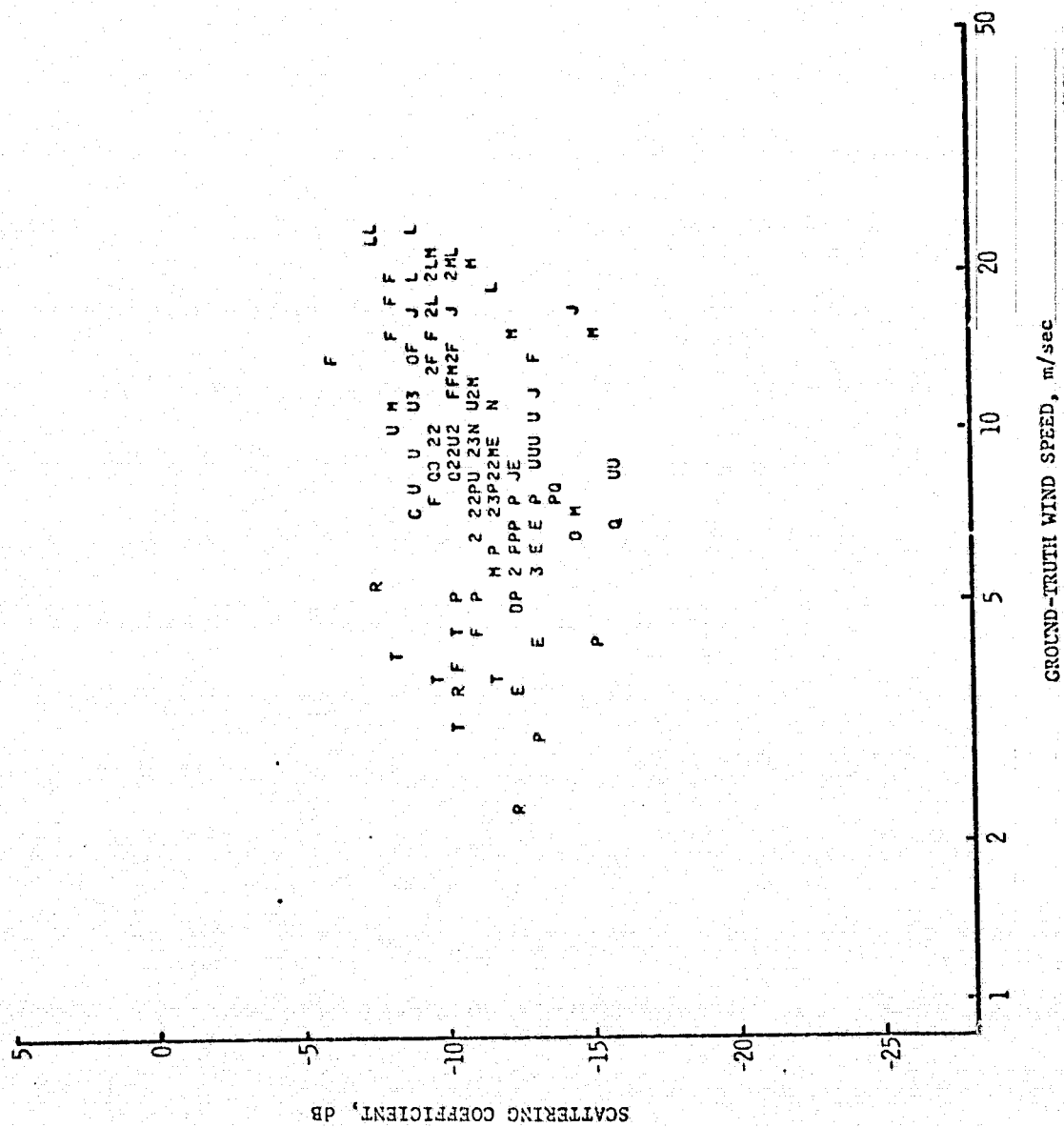


Figure F.1.3. Scattergram of σ_{VH}^0 at 50° incident angle versus ground truth wind speed using logarithmic scales. SL4 data.

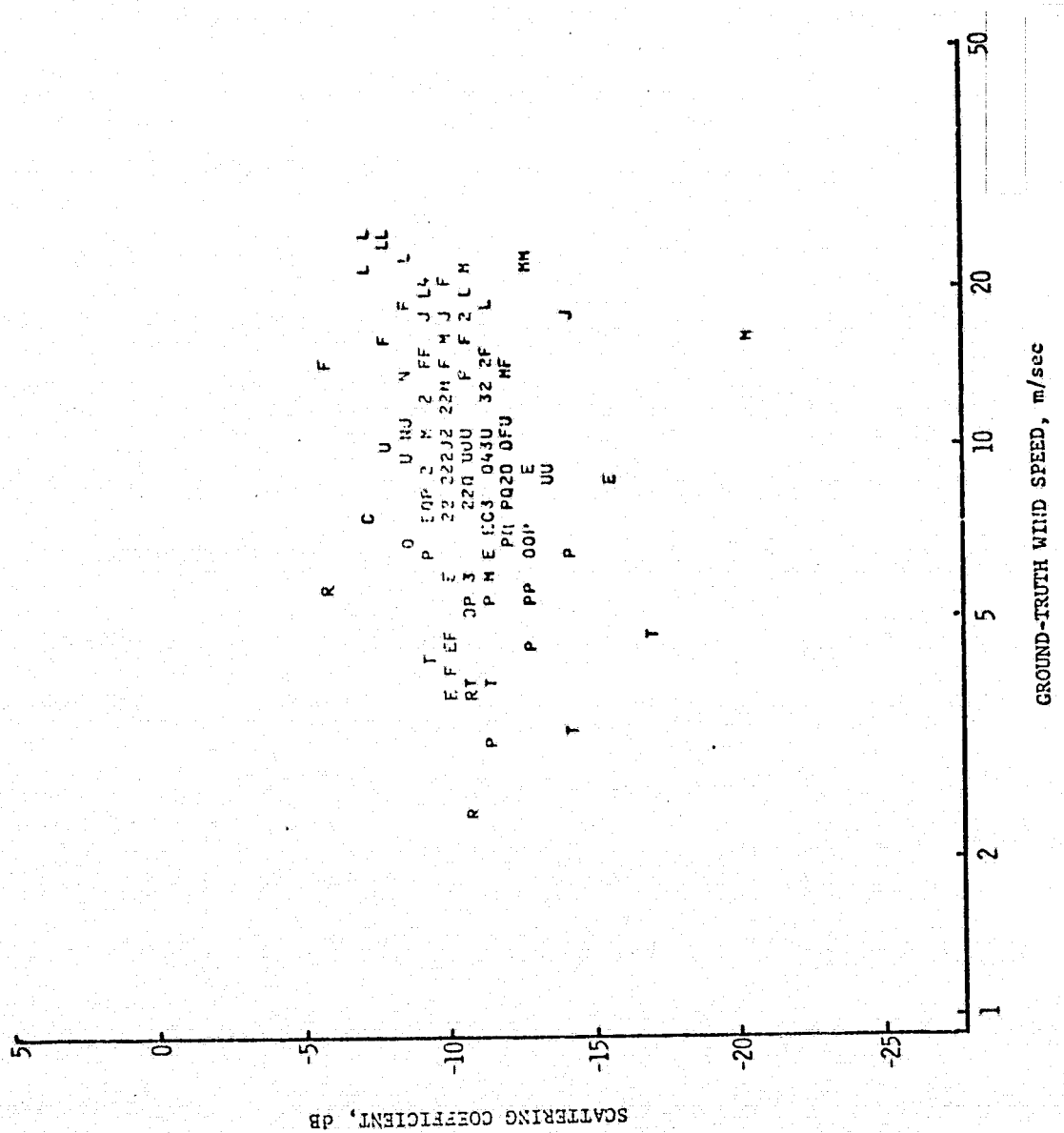


Figure F.1.4. Scattergram of σ_{HV}^0 at 50° incident angle versus ground truth wind speed using logarithmic scales. SL4 data.

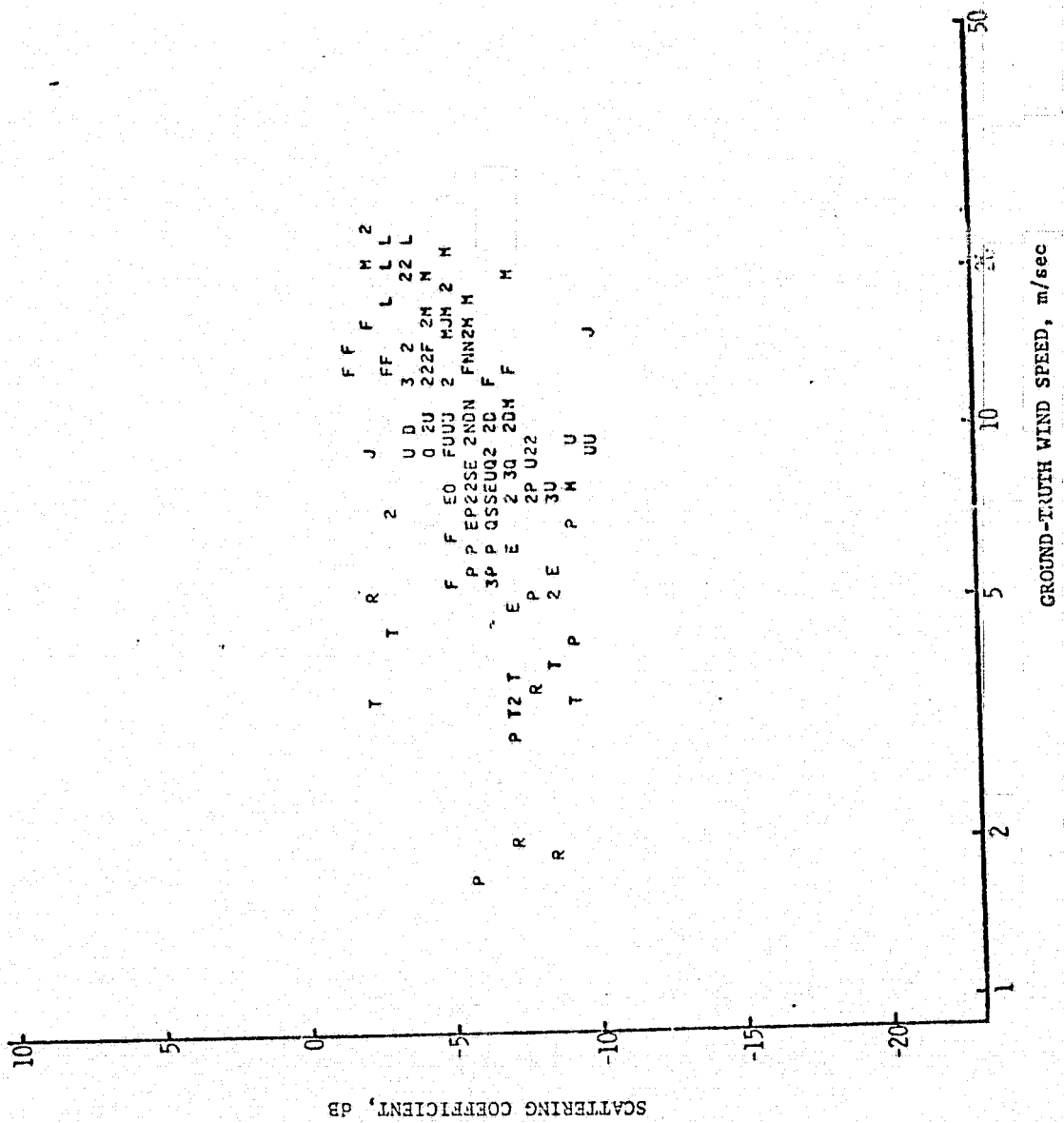


Figure F.1.5. Scattergram of σ^0_{VV} at 43° incident angle versus ground truth wind speed using logarithmic scales. SL4 data.

REPRODUCIBILITY OF THE
ORIGINAL PAGE IS POOR

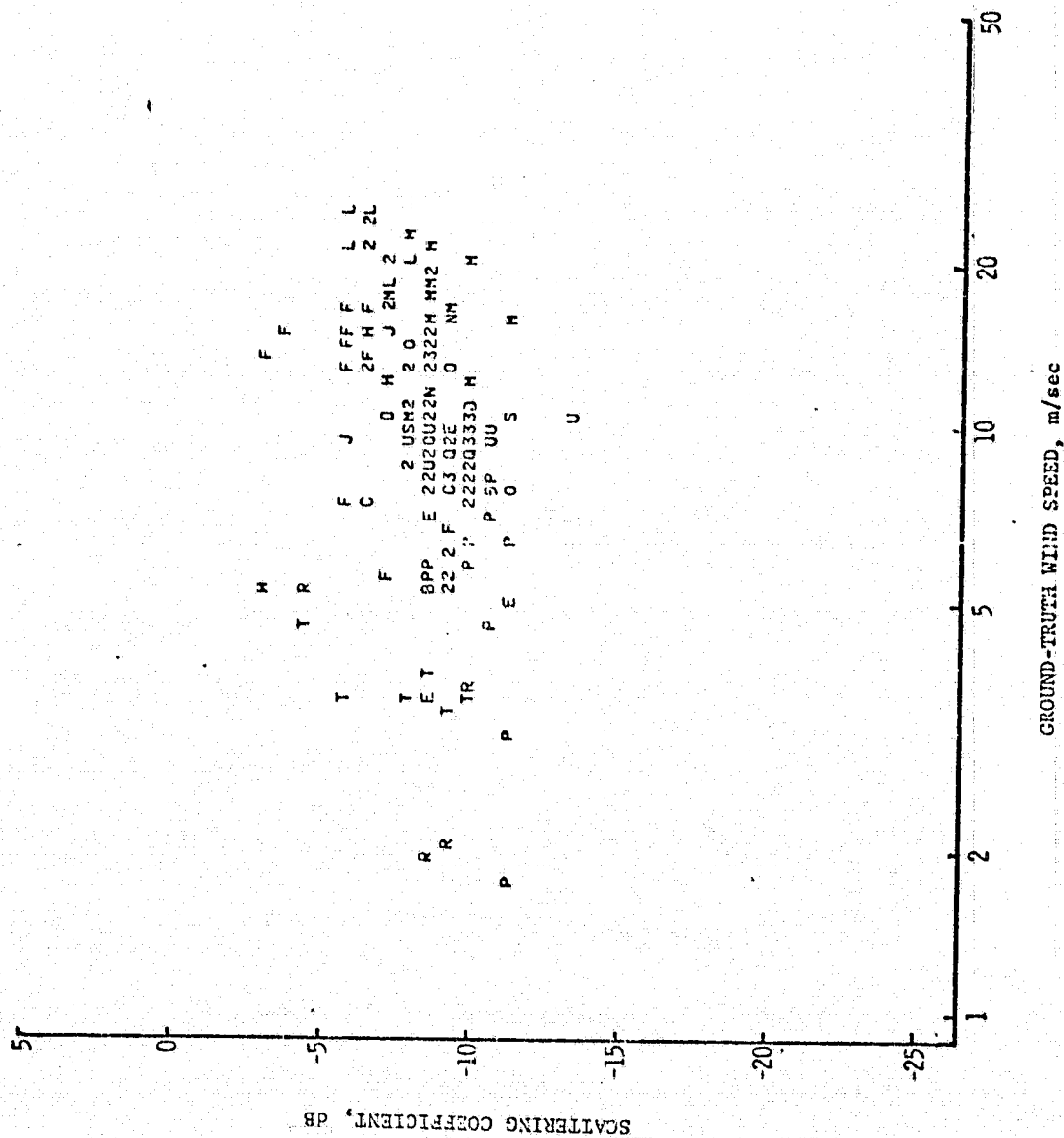


Figure F.1.6. Scattergram of σ_{LHH}^0 at 43° incident angle versus ground truth wind speed using logarithmic scales. SL4 data.

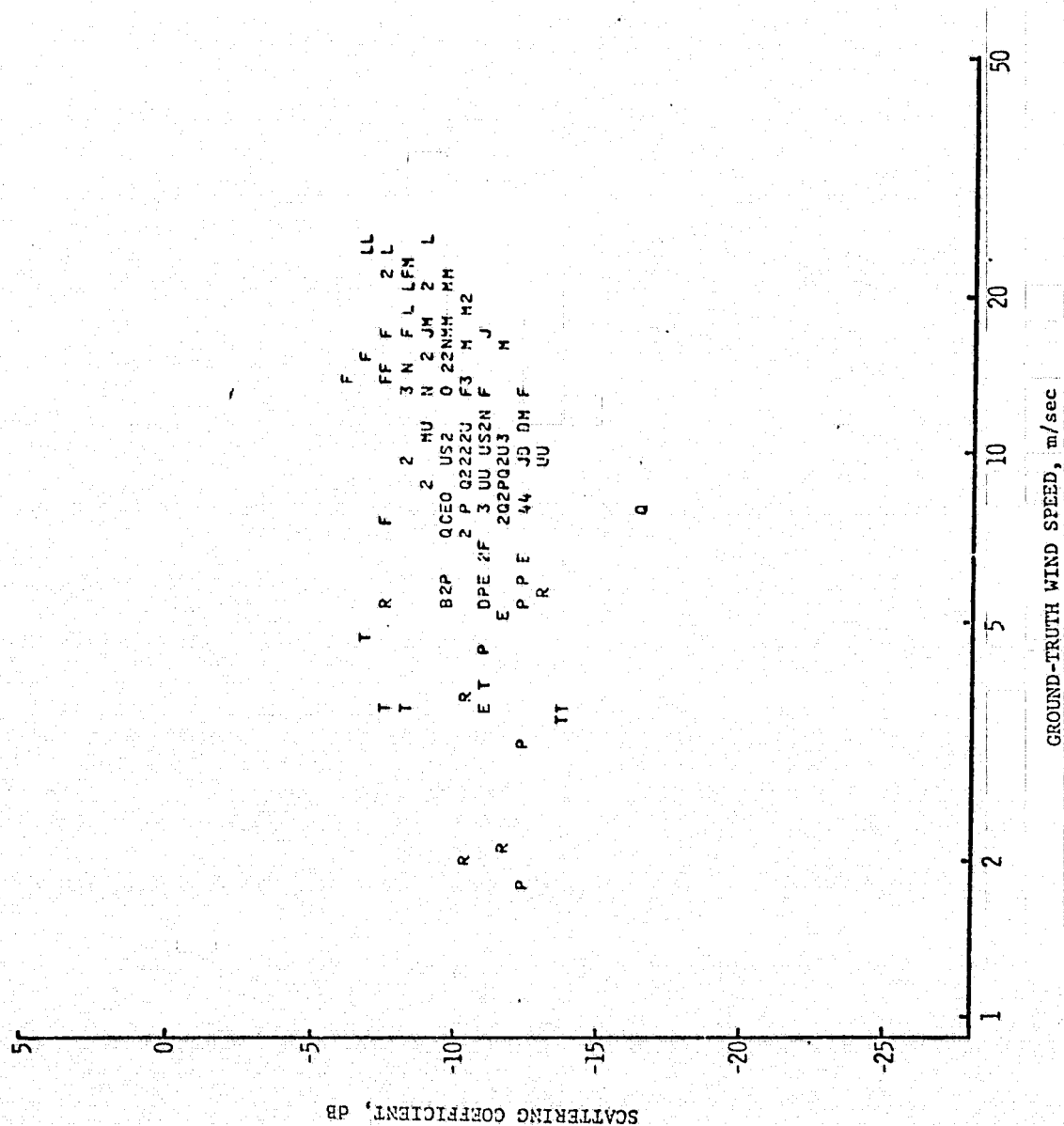


Figure F.1.7. Scattergram of α_{VH}^0 at 43° incident angle versus ground truth wind speed using logarithmic scales. SL4 data.

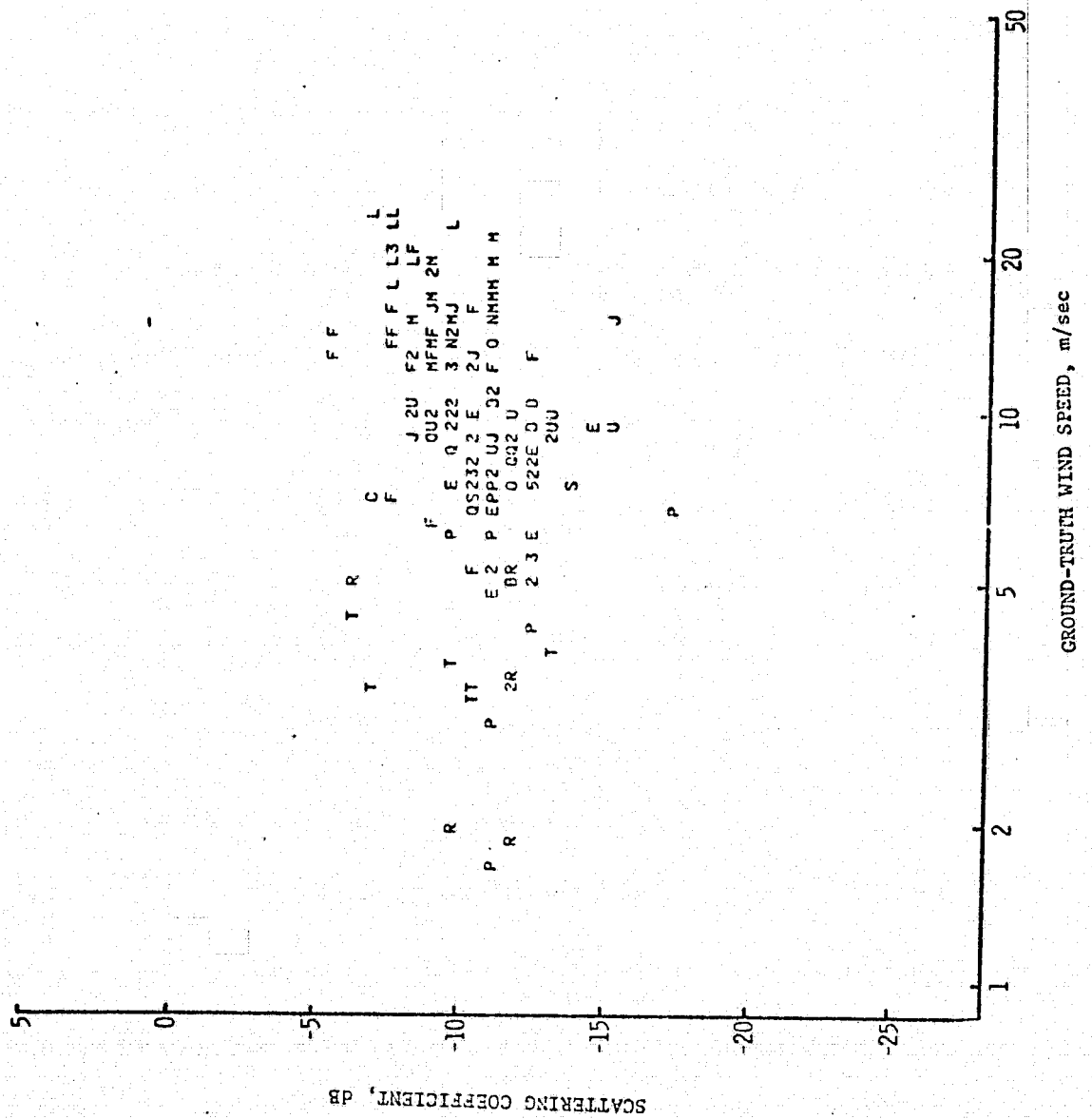


Figure F.1.8. Scattergram of σ_{HV}^0 at 43° incident angle versus ground truth wind speed using logarithmic scales. SL4 data.

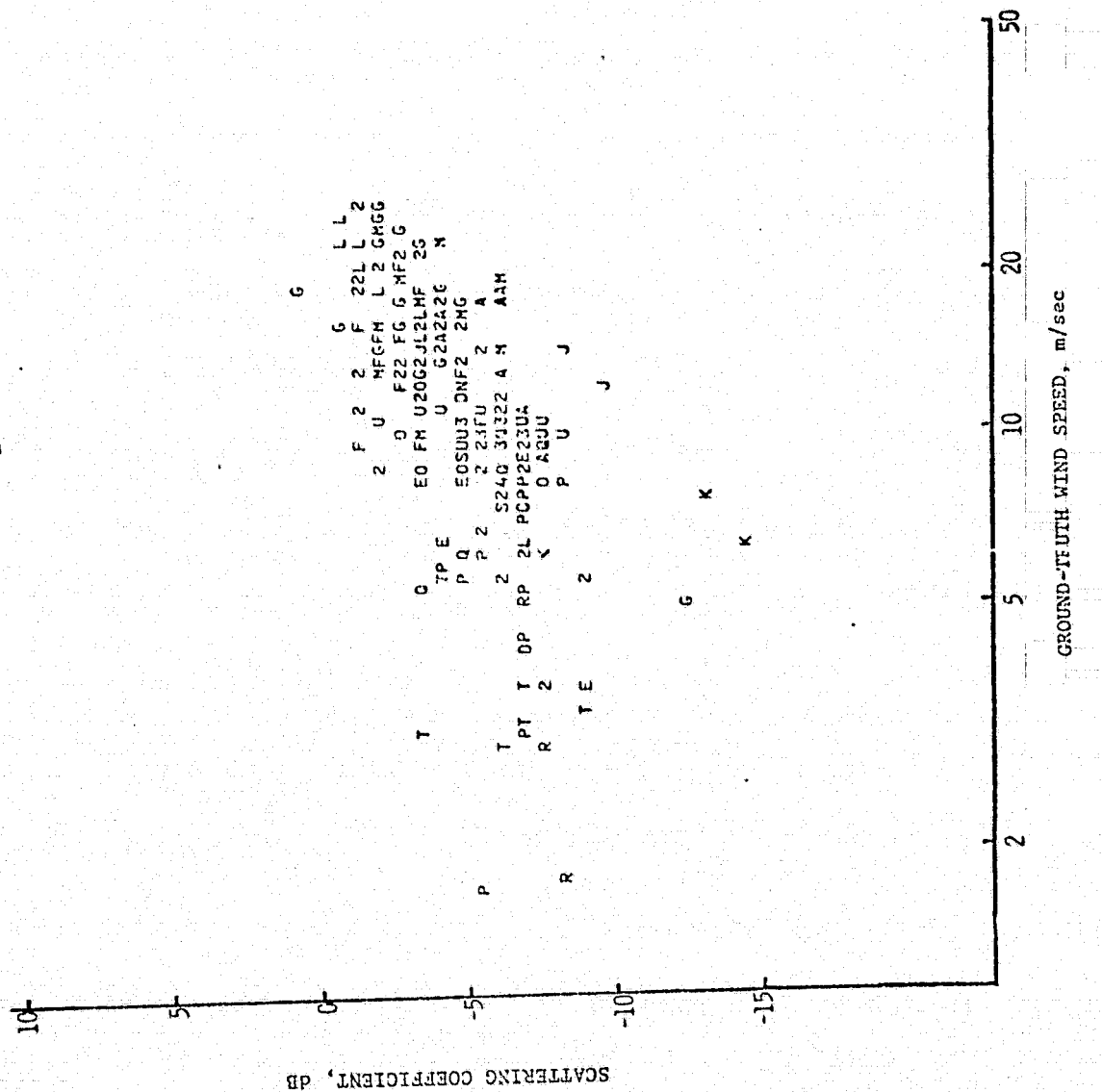


Figure F.1.9. Scattergram of σ_{VV}^0 at 32° incident angle versus ground truth wind speed using logarithmic scales. SL4 data.

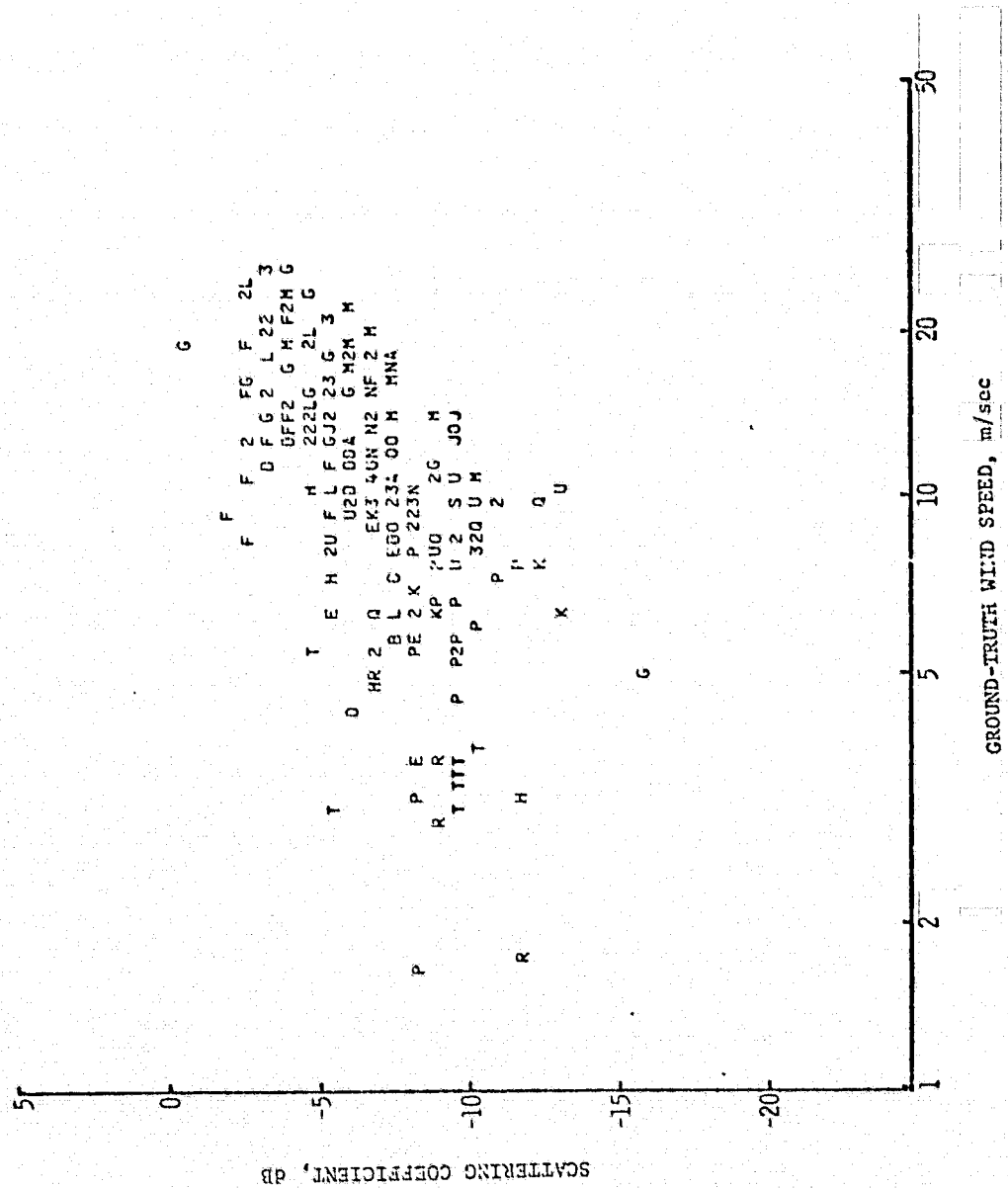
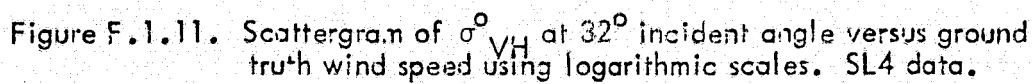


Figure F.1.10. Scattergram of σ_{HH}^0 at 32° incident angle versus ground truth wind speed using logarithmic scales. SL4 data.



370

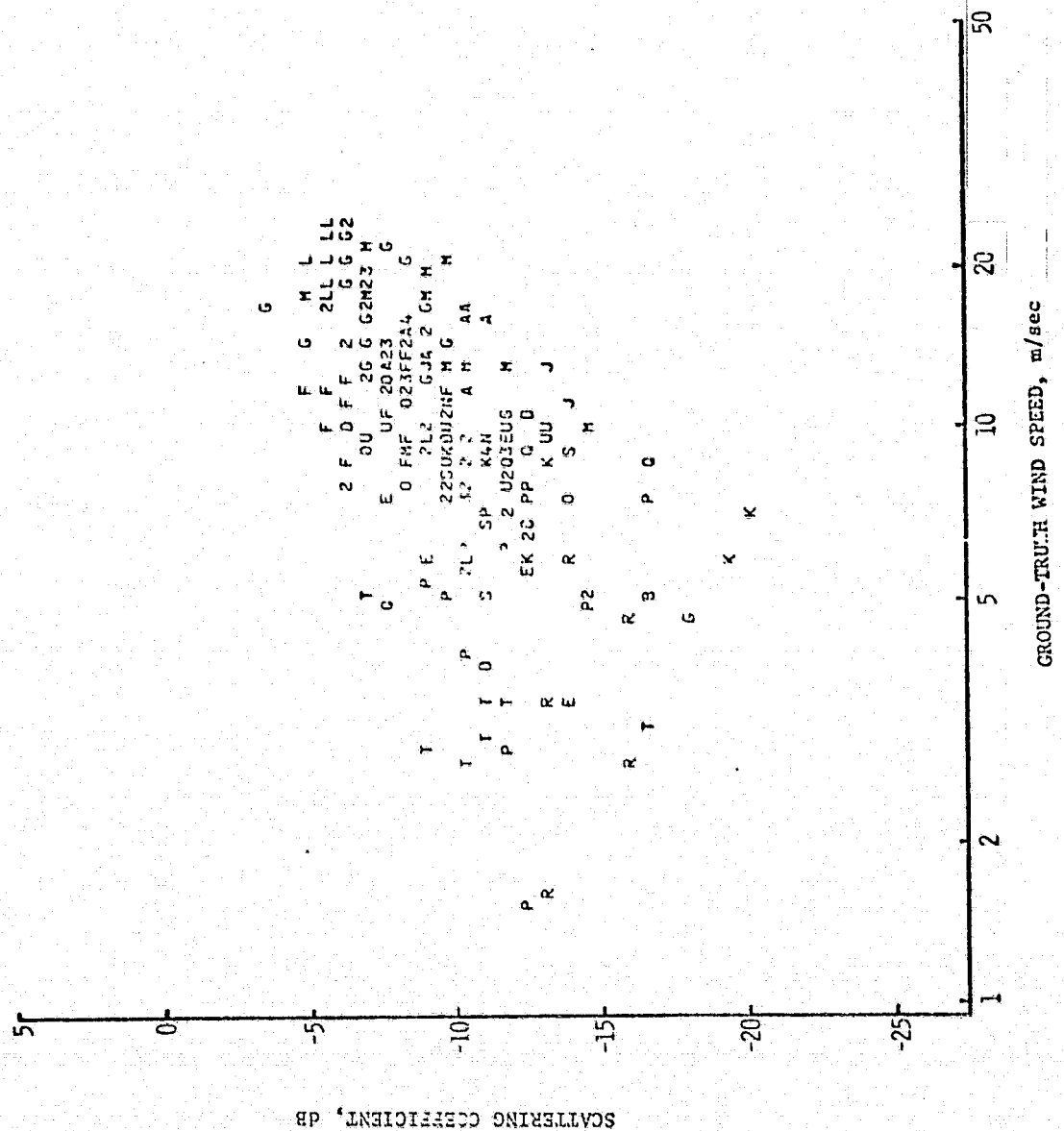


Figure F.1.12. Scattergram of σ^0_{HH} at 32° incident angle versus ground truth wind speed using logarithmic scales. SL4 data.

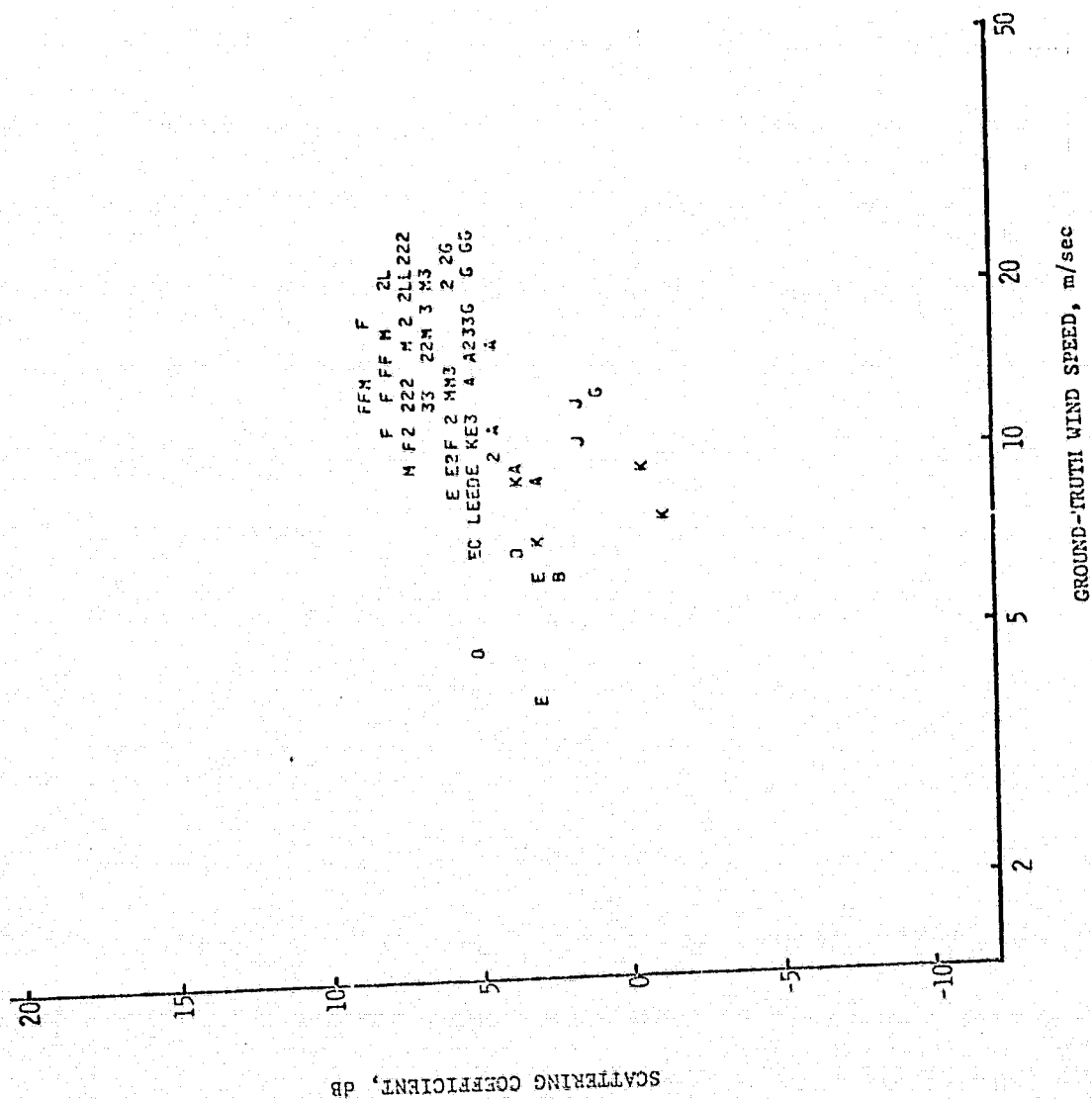


Figure F.1.13. Scattergram of σ_{VV}^0 at 17° incident angle versus ground truth wind speed using logarithmic scales. SL4 data.

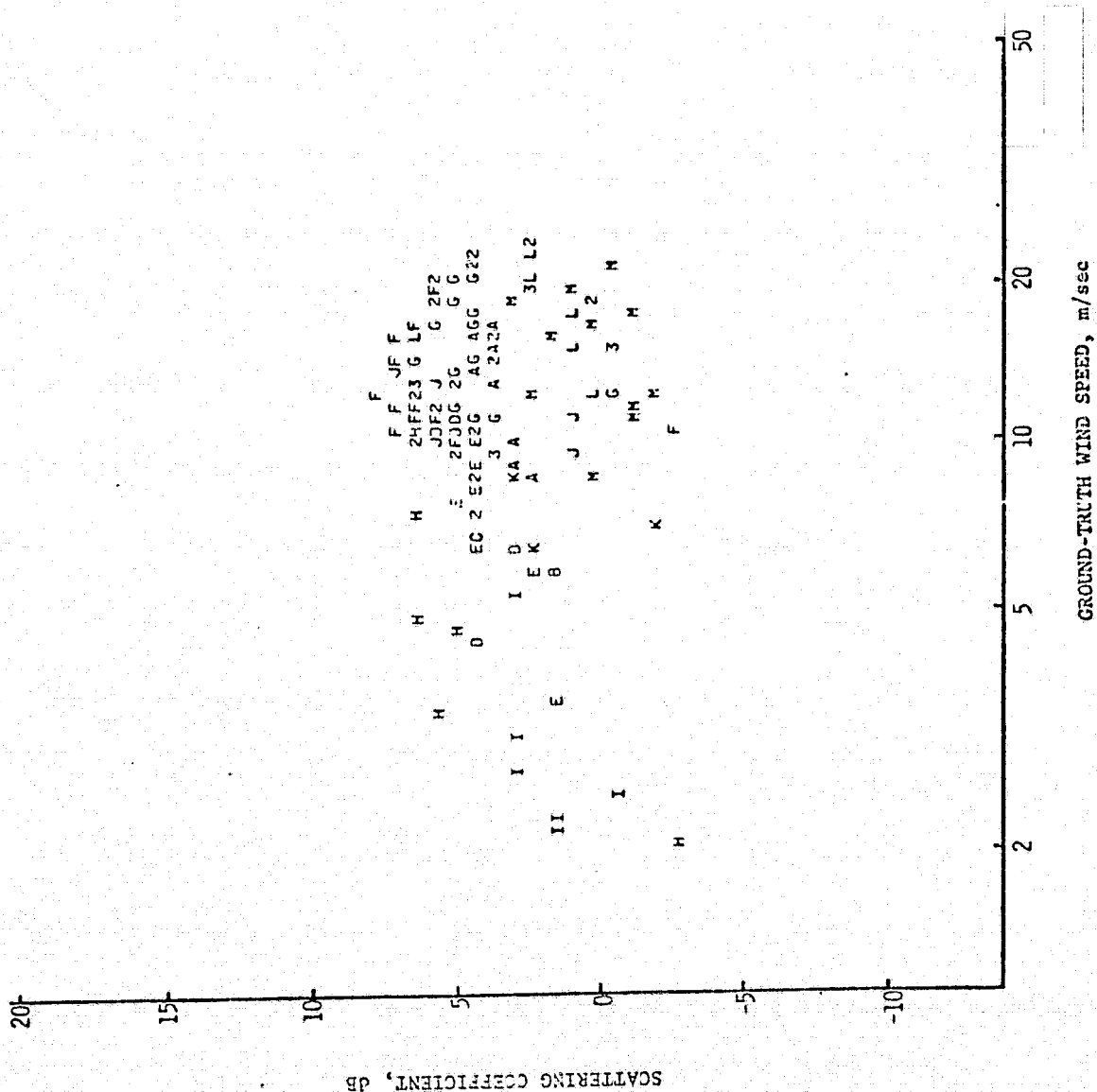


Figure F.1.14. Scattergram of σ_{HH}^0 at 17° incident angle versus ground truth wind speed using logarithmic scales. SL4 data.

REPRODUCIBILITY OF THE
ORIGINAL PAGE IS POOR

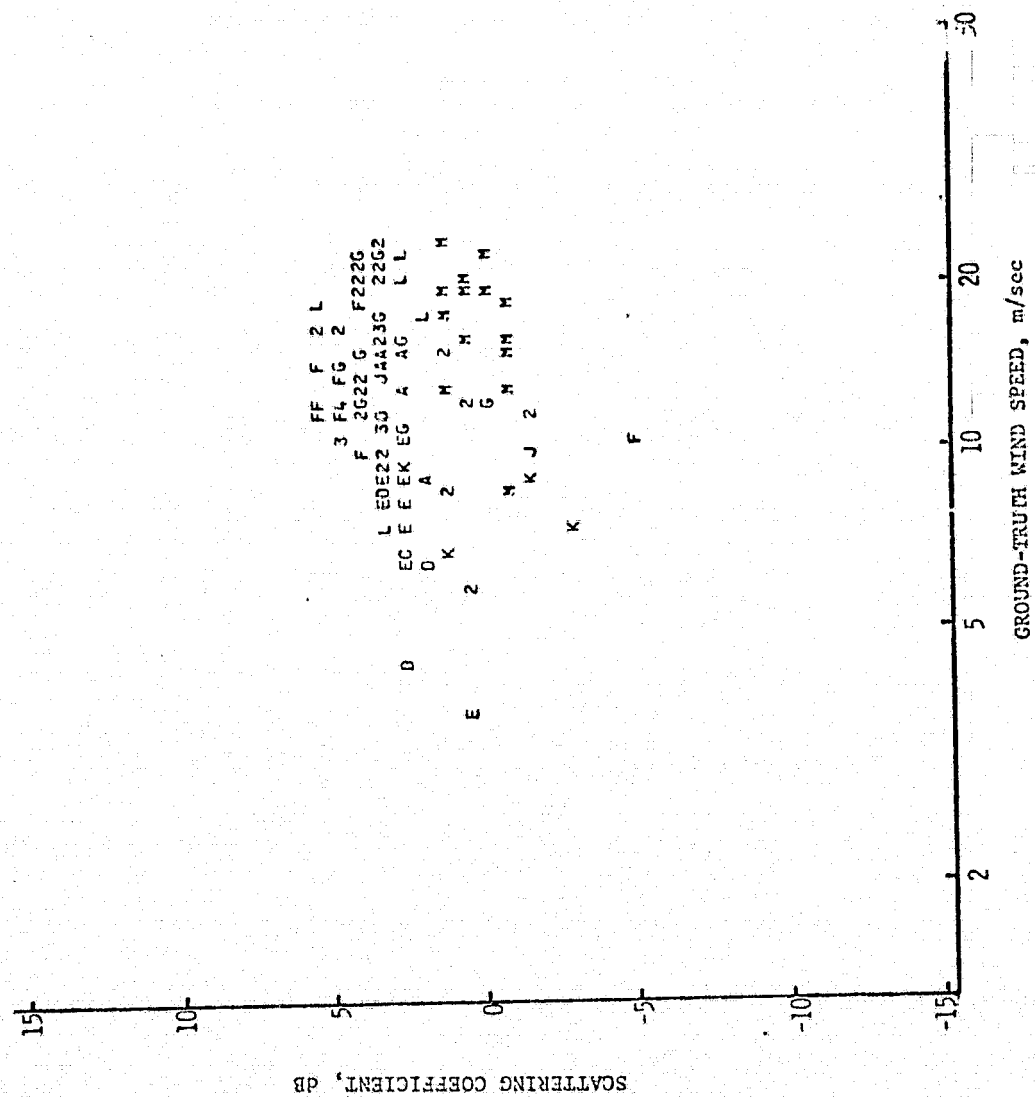


Figure F.1.15. Scattergram of σ_{VH}^0 at 17° incident angle versus ground truth wind speed using logarithmic scales. SL4 data.

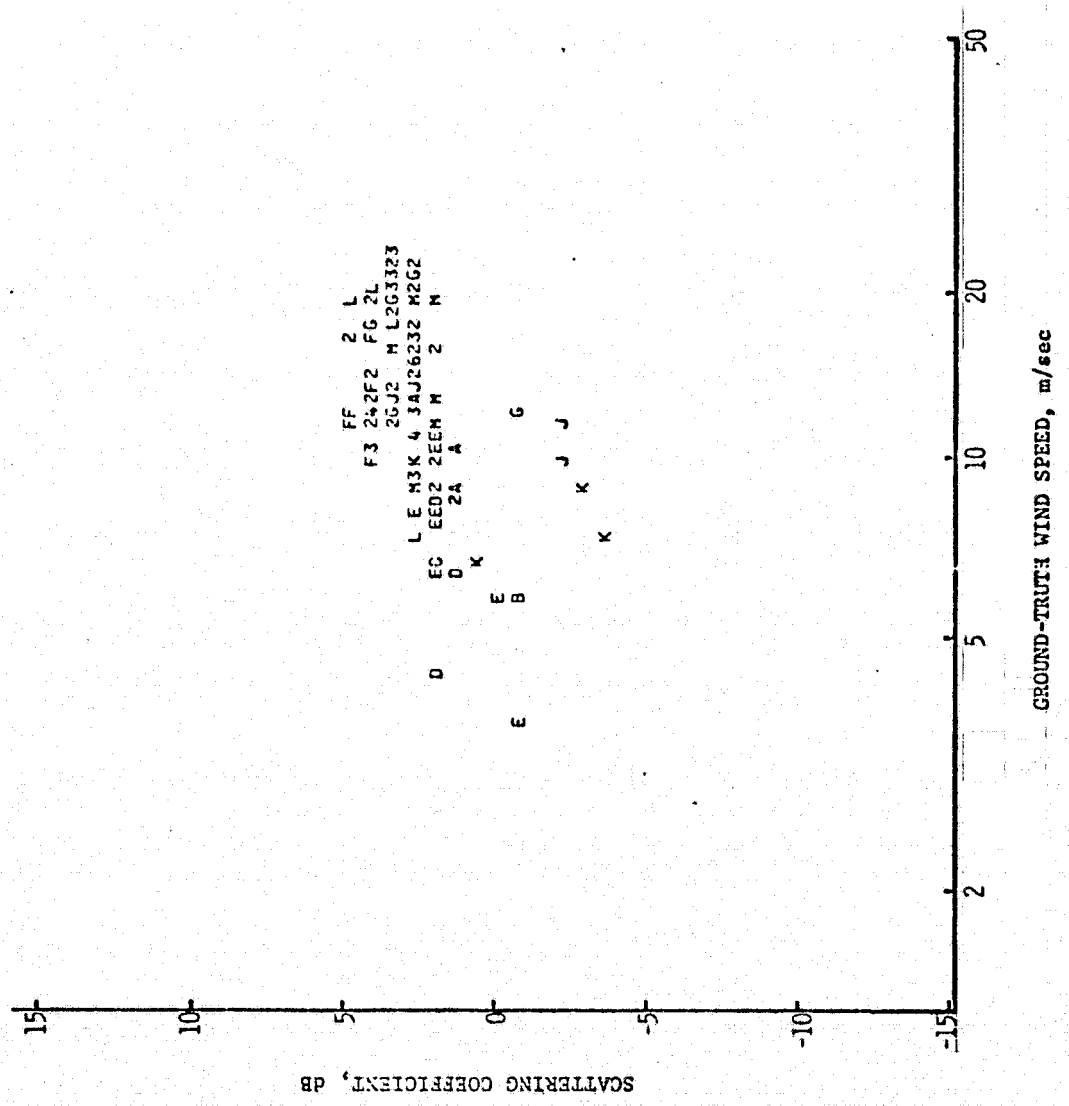


Figure F.1.16. Scattergram of σ_{HV}^0 at 17° incident angle versus ground truth wind speed using logarithmic scales. SL4 data.

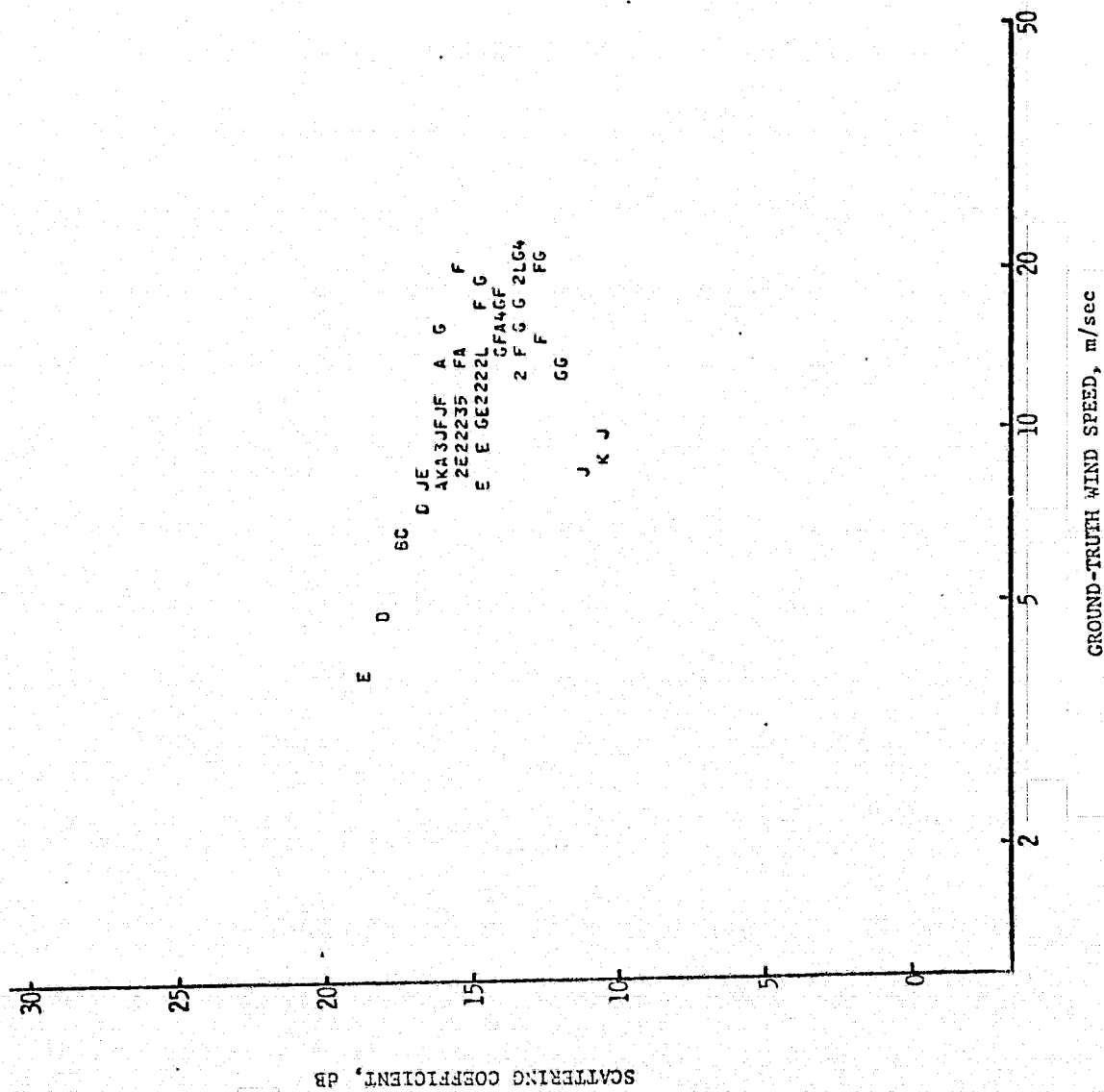


Figure F.1.17. Scattergram of σ_{vv}^0 at 1° incident angle versus ground truth wind speed using logarithmic scales. SL4 data.

REPRODUCIBILITY OF THE
ORIGINAL PAGE IS POOR

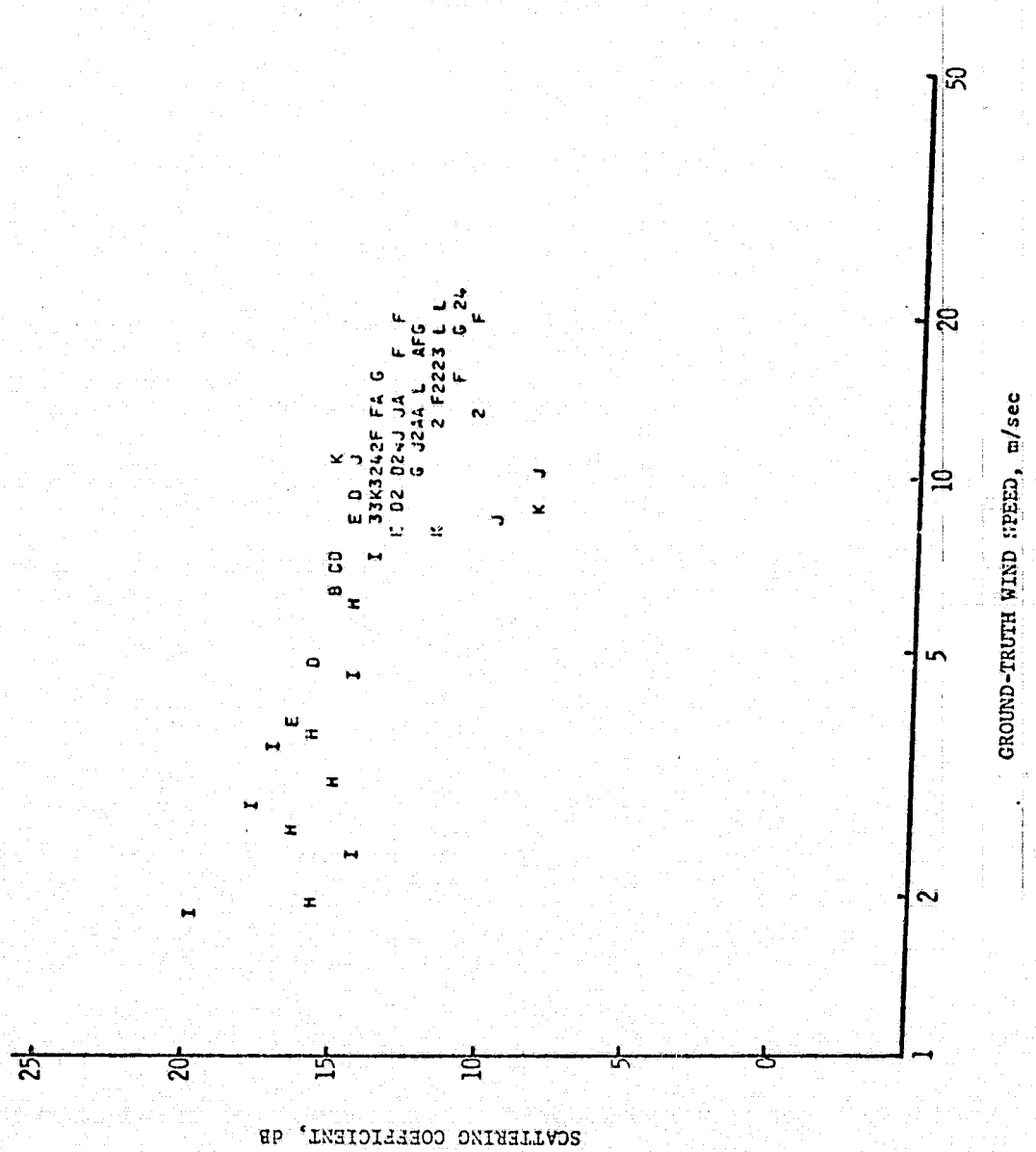


Figure F.1.18. Scattergram of σ_{HH}^0 at 1° incident angle versus ground truth wind speed using logarithmic scales. SL4 data.

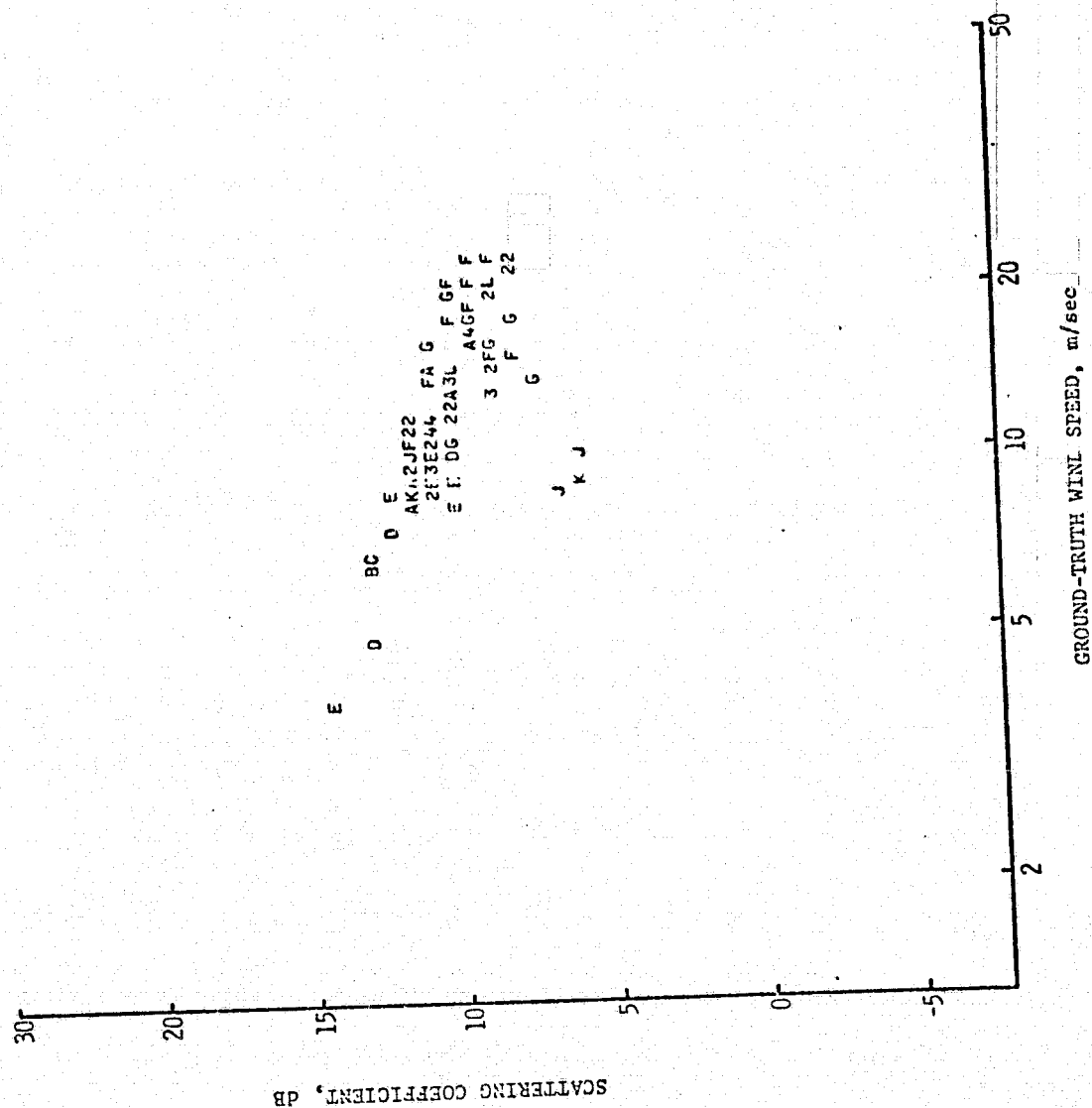


Figure F.1.19. Scattergram of σ_{VH}^0 at 1° incident angle versus ground truth wind speed using logarithmic scales. SL4 data.

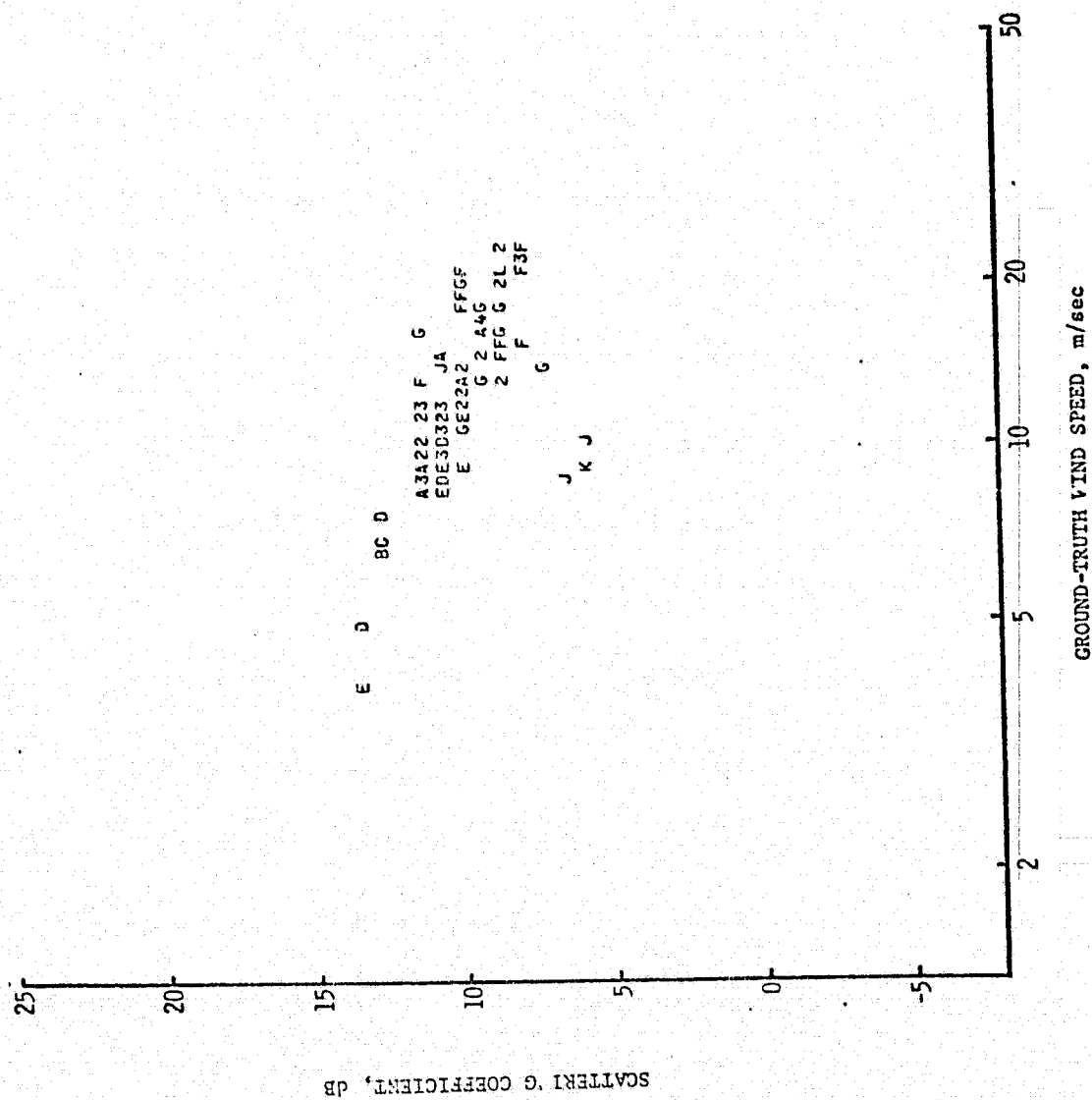


Figure F.1.20. Scattergram of σ_{HV}^0 at 1° incident angle versus ground truth wind speed using logarithmic scales. SL4 data.

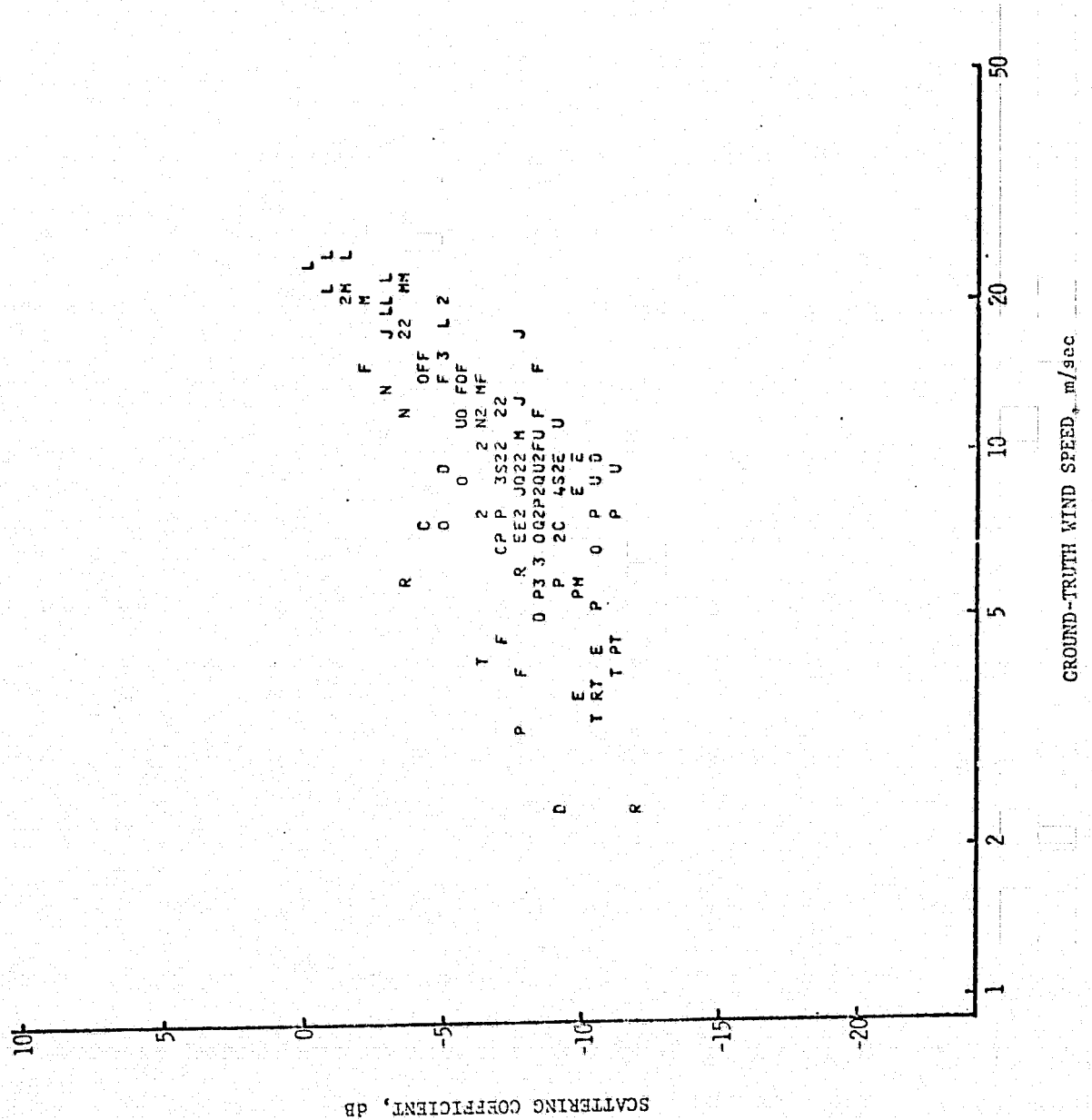


Figure F.2.1. Scattergram of σ_{vv}^0 at 50° incident angle versus ground truth wind speed V_w using logarithmic scales. The scattering coefficients are adjusted to upwind. SL4 data.

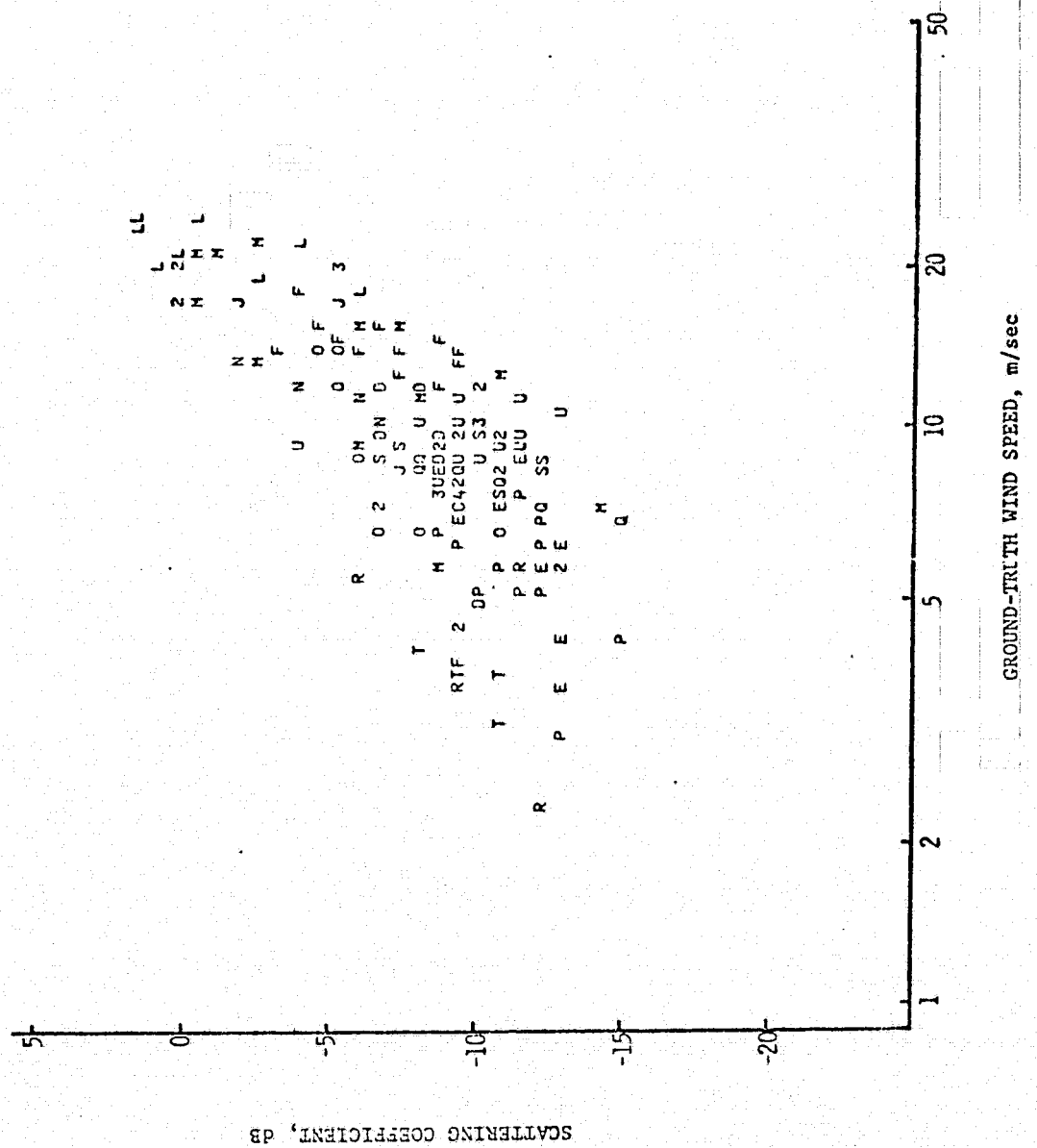


Figure F.2.3. Scattergram of σ_{VH}^0 at 50° incident angle versus ground truth wind speed using logarithmic scales. The scattering coefficients are adjusted to upwind. SL4 data.

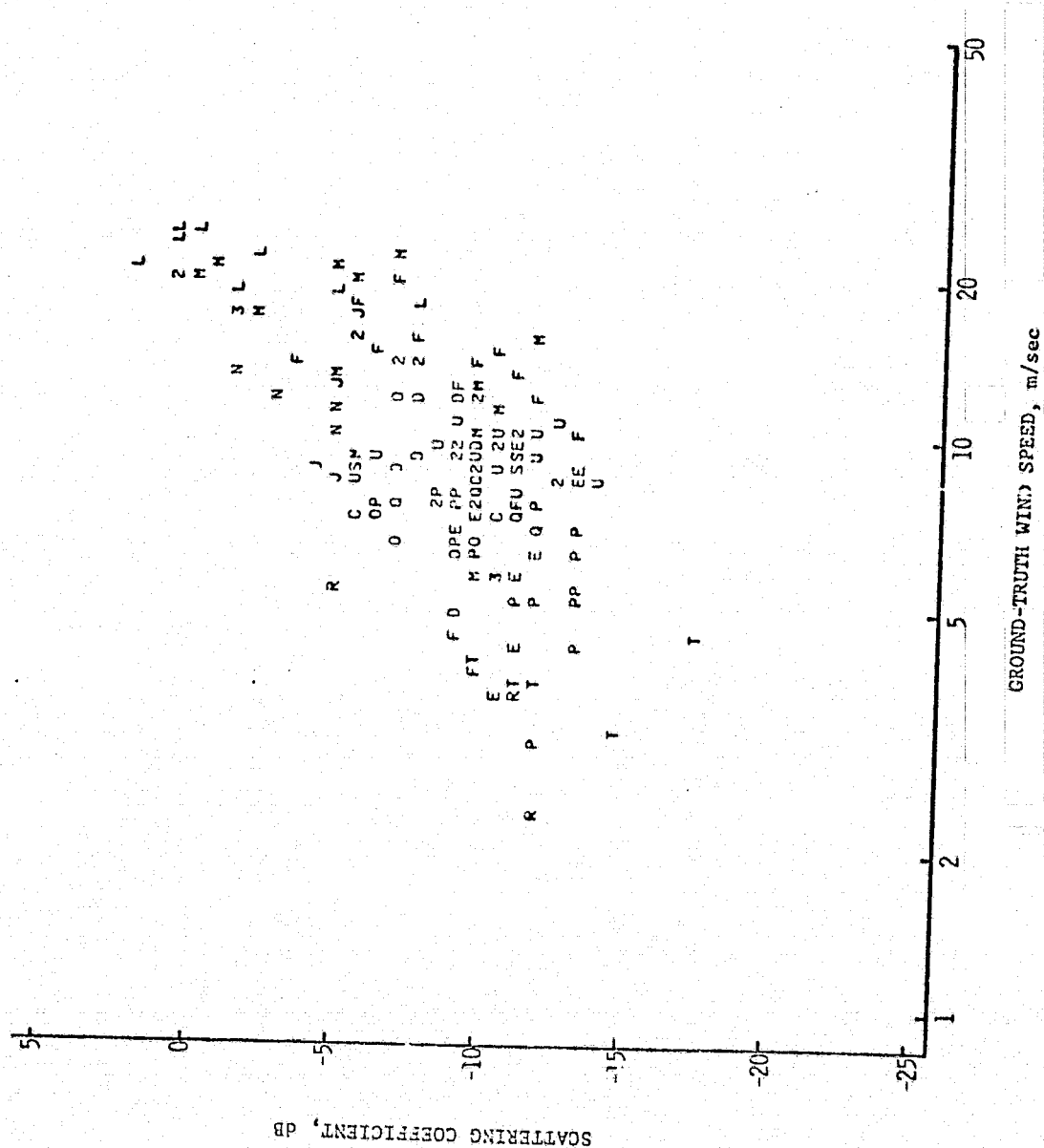


Figure F.2.4. Scattergram of σ^0_{HV} at 50° incident angle versus ground truth wind speed using logarithmic scales. The scattering coefficients are adjusted to upwind. SL4 data.

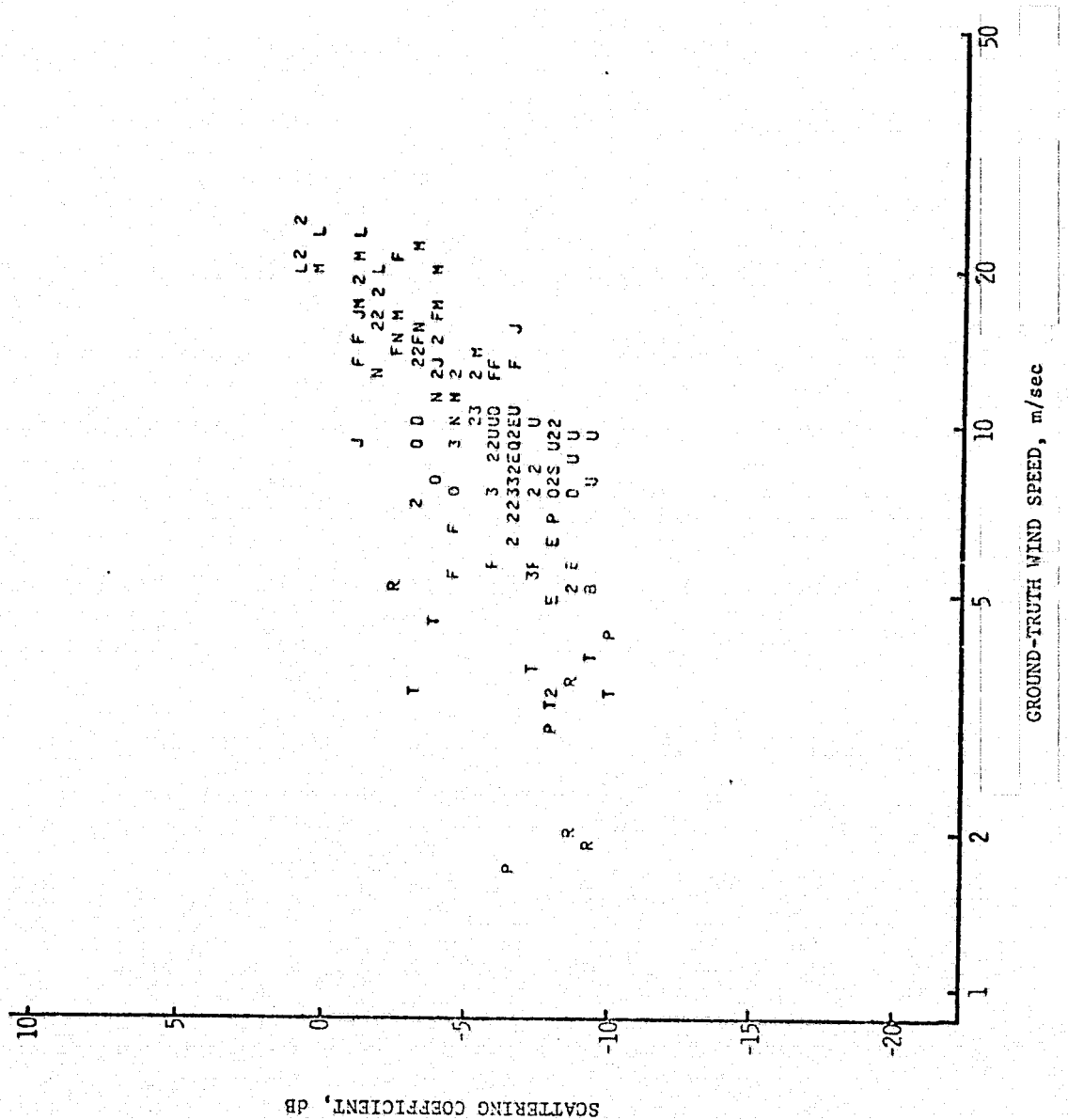


Figure F.2.5. Scattergram of σ_{VV}^0 at 43° incident angle versus ground truth wind speed using logarithmic scales. The scattering coefficients are adjusted to upwind. SL4 data.

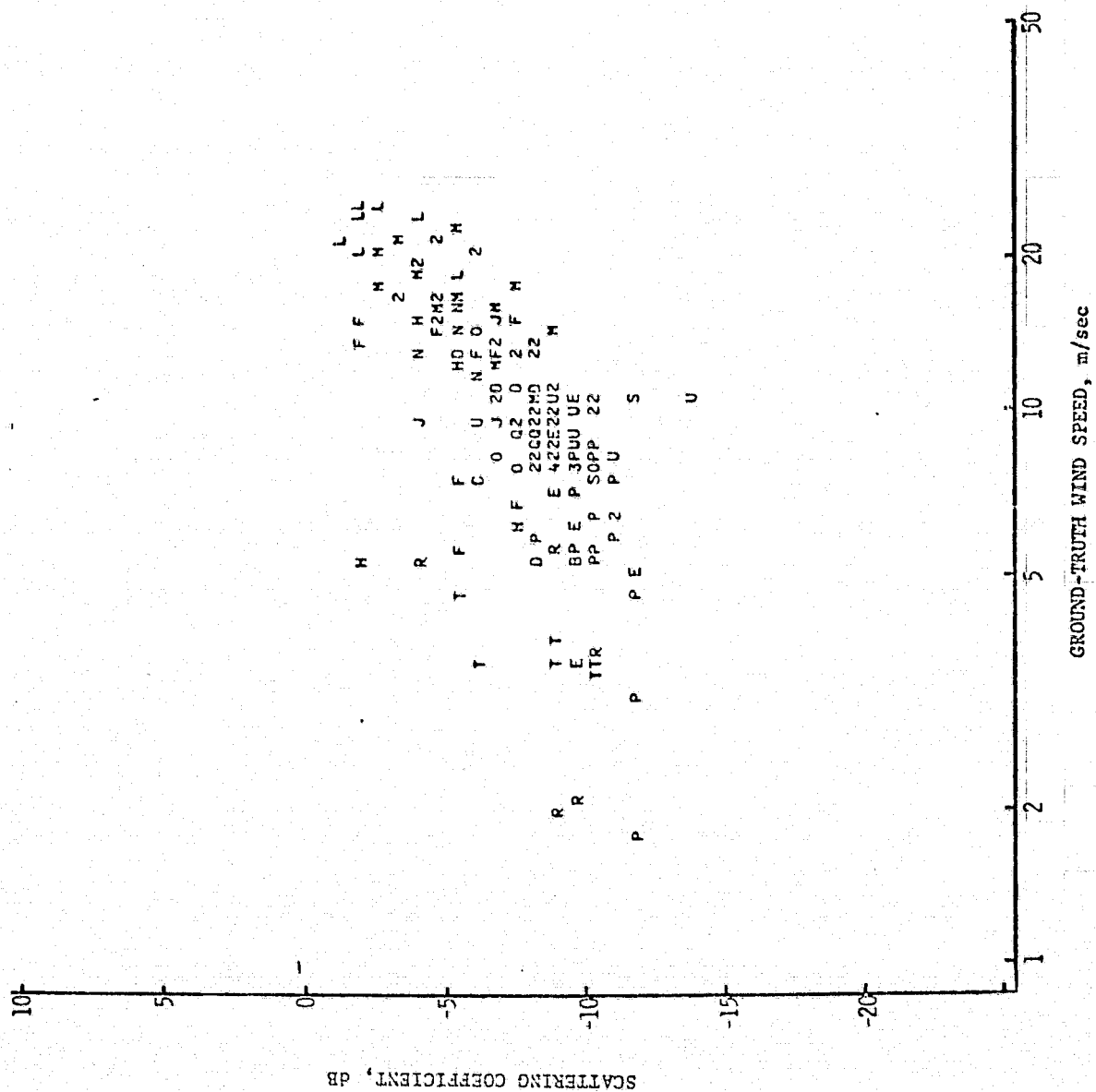


Figure F.2.6. Scattergram of σ^0_{LH} at 43° incident angle versus ground truth wind speed using logarithmic scales. The scattering coefficients are adjusted to upwind. SL4 data.

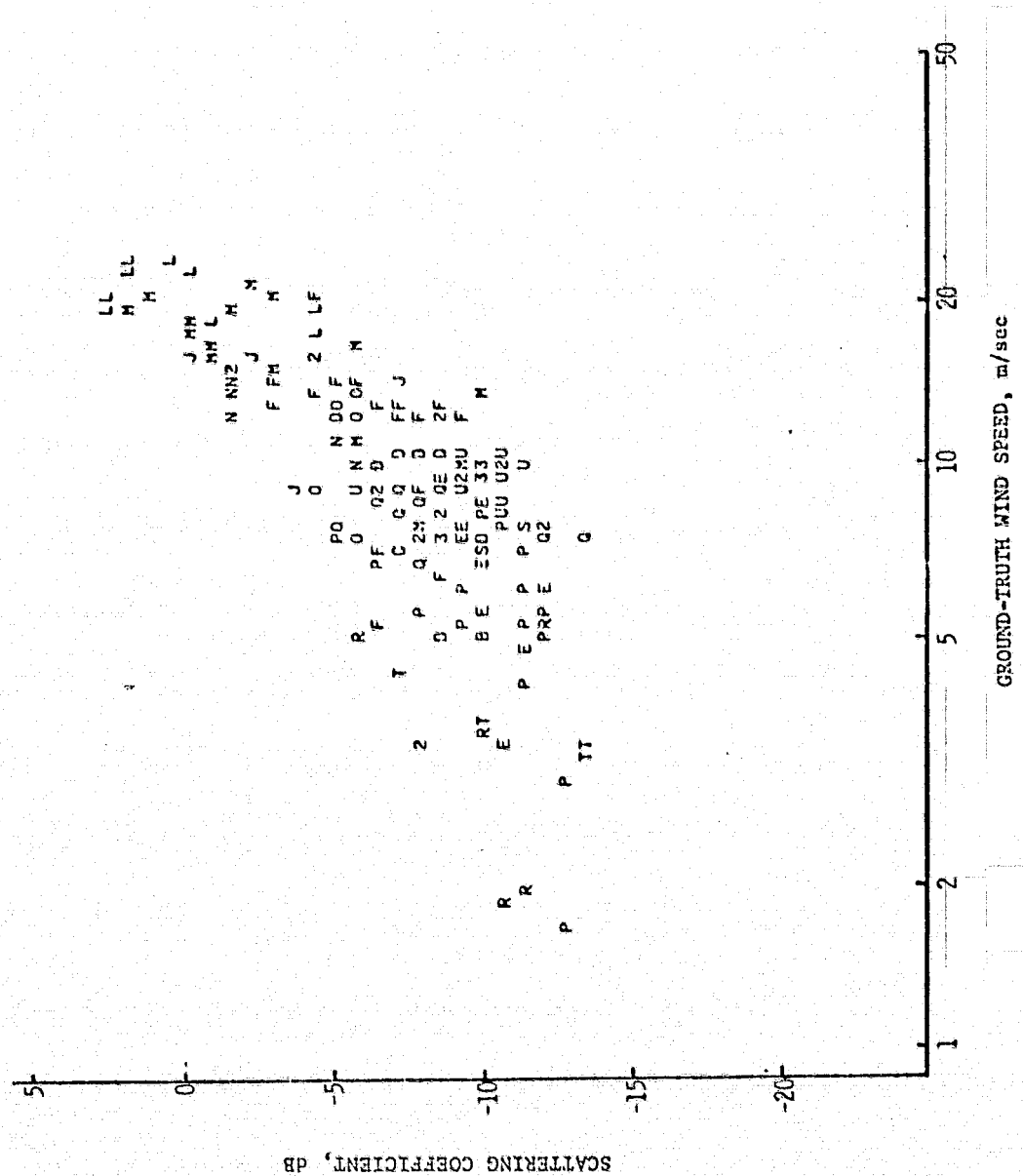


Figure F.2.7. Scattergram of σ_{VH}^0 at 45° incident angle versus ground truth wind speed using logarithmic scales. The scattering coefficients are adjusted to upwind. SL4 data.

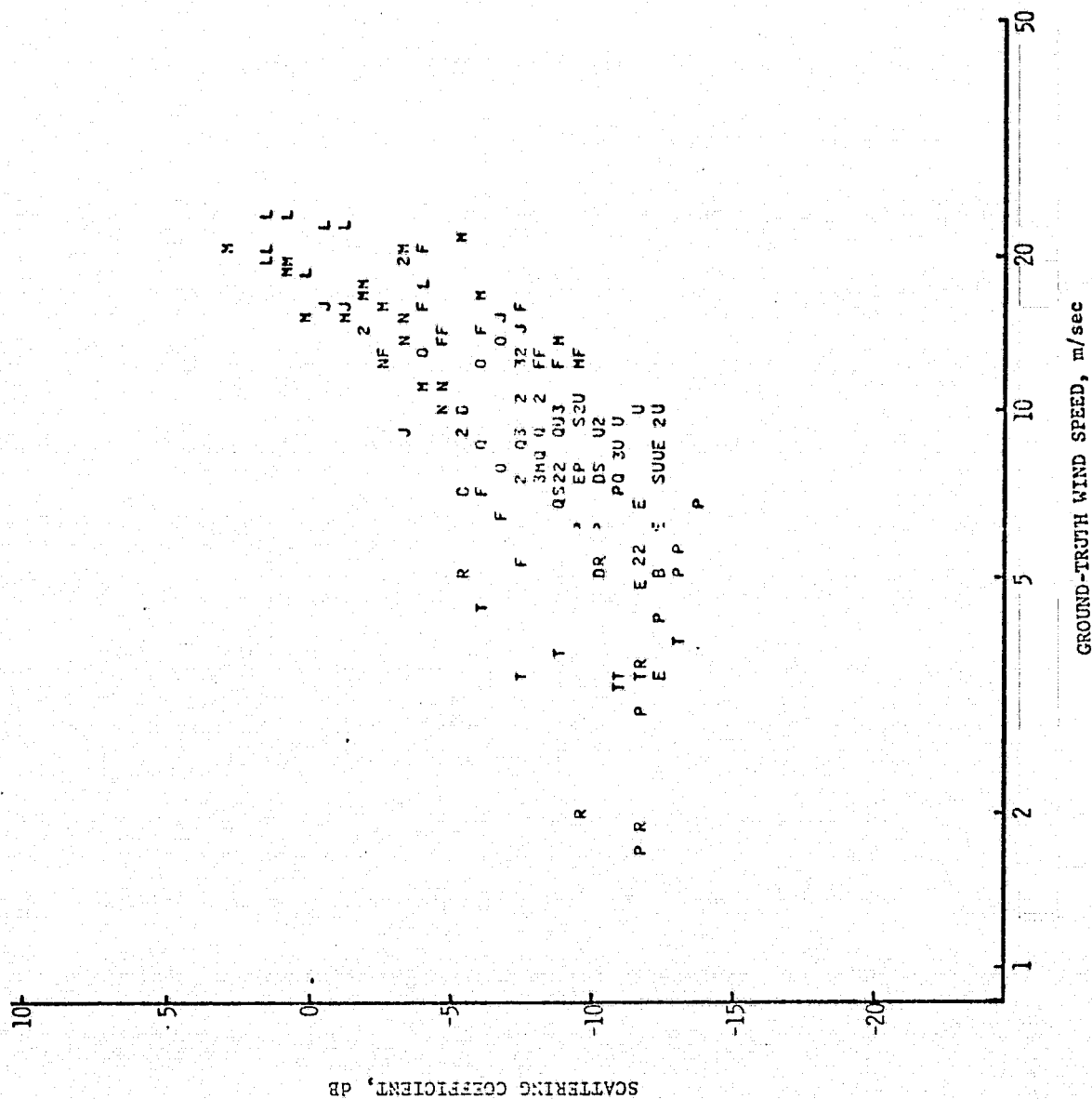


Figure F.2.8. Scattergram of σ^0_{HV} at 43° incident angle versus ground truth wind speed using logarithmic scales. The scattering coefficients are adjusted to upwind. SL4 data.

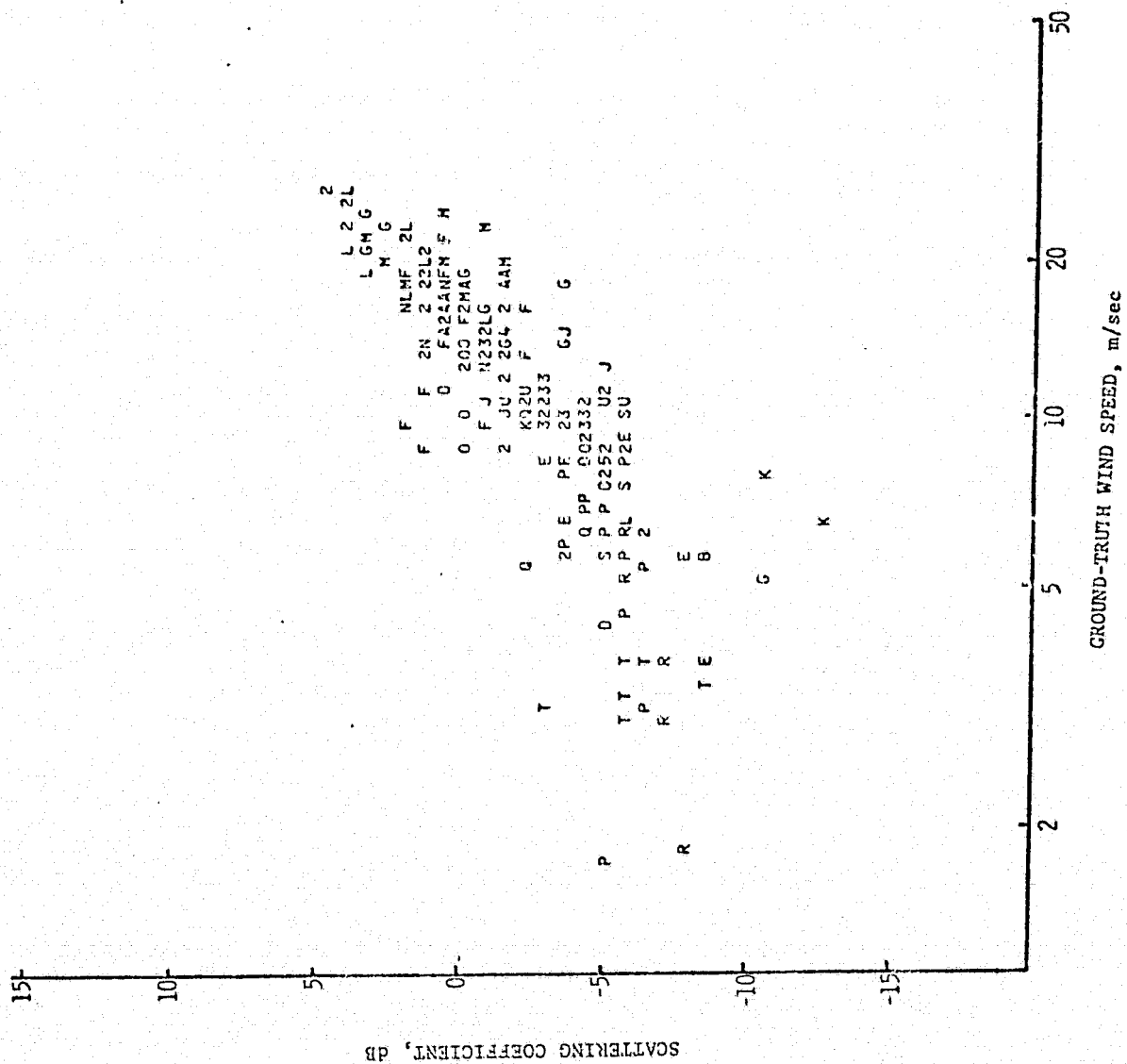


Figure F.2.9. Scattergram of σ_{VV}^0 at 32° incident angle versus ground truth wind speed using logarithmic scales. The scattering coefficients are adjusted to upwind. SL4 data.

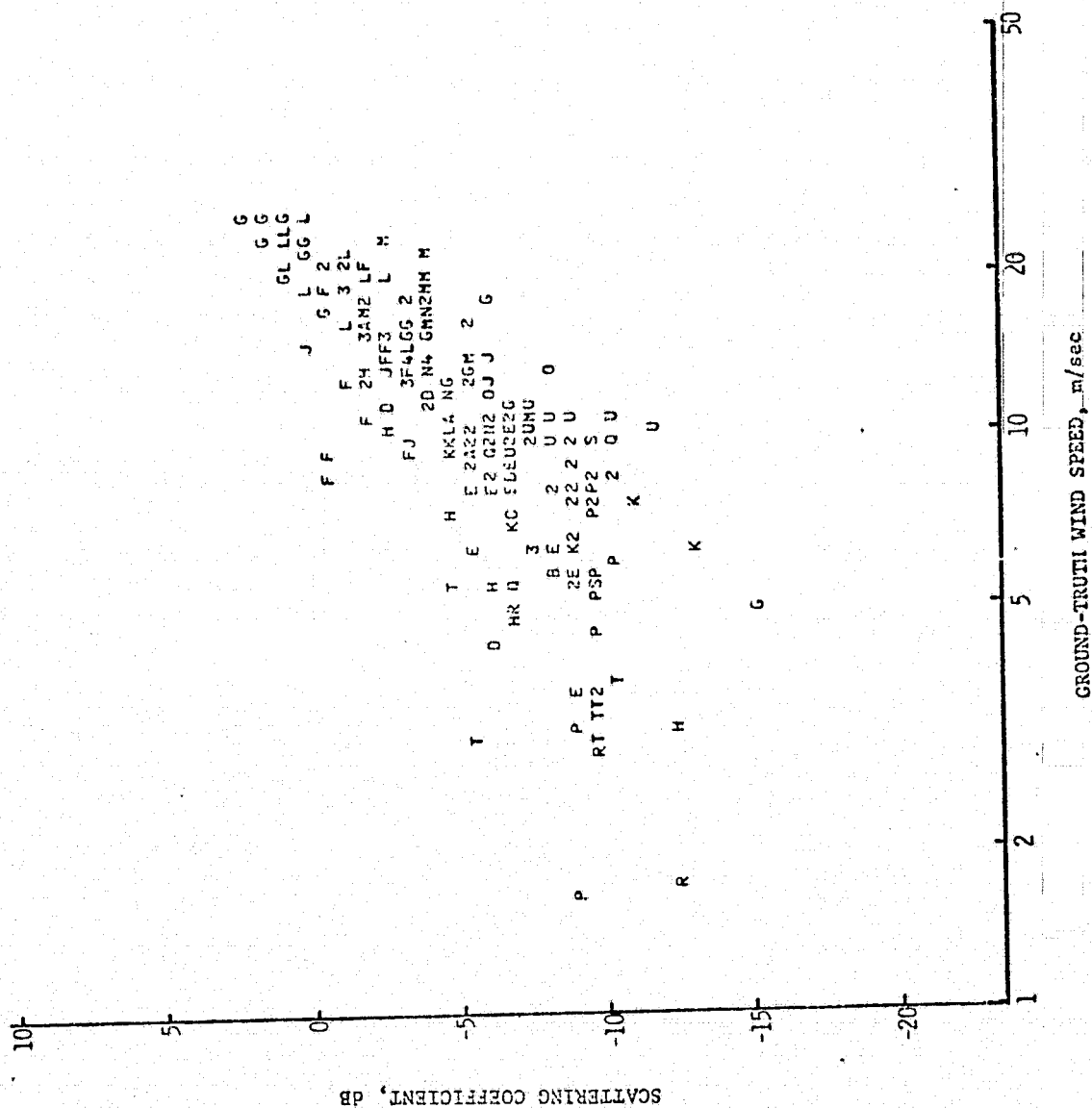


Figure F.2.10. Scattergram of σ_{HH}^0 at 32° incident angle versus ground truth wind speed using logarithmic scales. The scattering coefficients are adjusted to upwind. SL4 data.

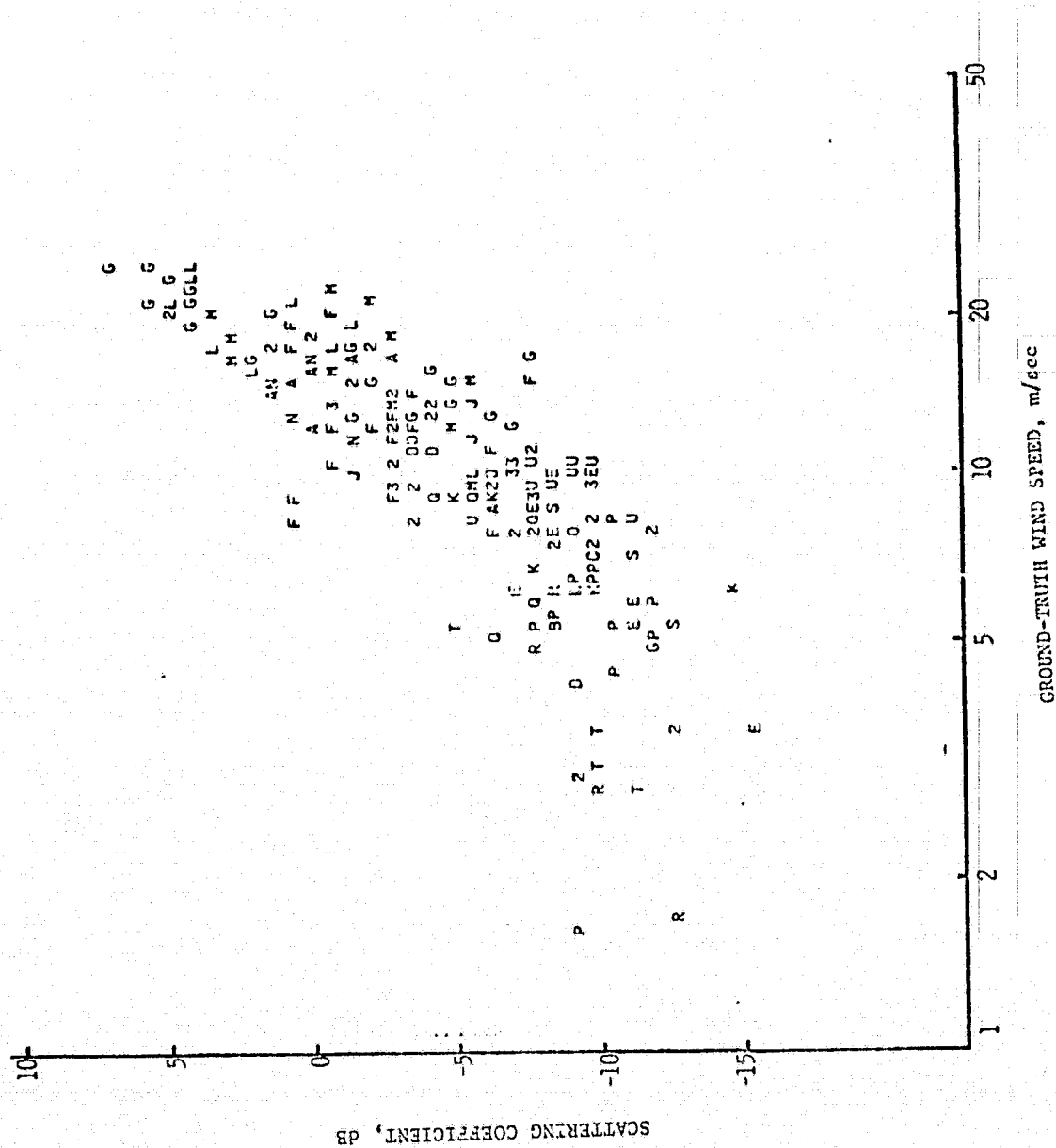


Figure F.2.11. Scattergram of σ_{VH}^0 at 32° incident angle versus ground truth wind speed using logarithmic scales. The scattering coefficients are adjusted to upwind. SL4 data.

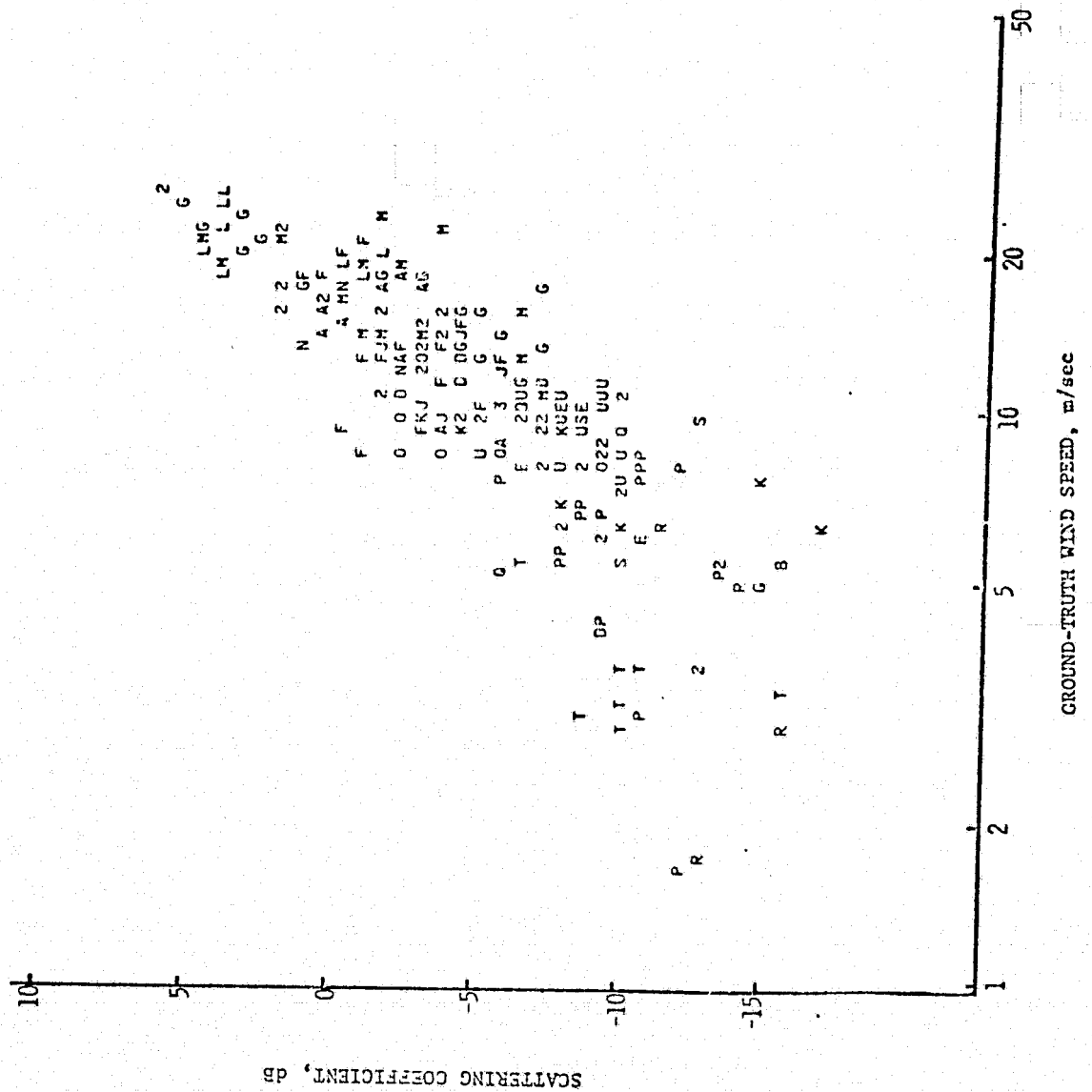


Figure F.2.12. Scattergram of σ_{HV}^0 at 32° incident angle versus ground truth wind speed using logarithmic scales. The scattering coefficients are adjusted to upwind. SL4 data.